Sun Grant Initiative Regional Biomass Feedstock Partnership
Competitive Grants Program

Final Technical Report

An Award from the:

US Department of Energy
Award Number DE-FC36-08GO88073

Report Submitted by:

Vance N. Owens, Director
North Central Regional Sun Grant Center
South Dakota State University

30 December 2016

Table of Contents

Executive Summary v

Introduction: The Sun Grant Initiative vi

Request for Applications vi

Outcomes and Outputs viii

Industry Involvement viii

Final Project Reports viii

2008 Nationwide Competitive Awards

Optimizing the Logistics of a Mobile Fast Pyrolysis System for Sustainable Bio-Crude Oil Production; *S. Capareda; Texas A&M University* P1:1-53

Evaluation of In-Field Corn Stover Densification and Interaction with Storage Quality, Logistics, and Production Costs; *M. Darr; Iowa State University* P2:1-207

Prioritizing Corn Harvest and Biomass Collection Activities; *C. Gustafson, North Dakota State University* P3:1-55

The Logistics of Herbaceous Crop Residue-based Ethanol Production Under Uncertainty; *D. Lambert; North Dakota State University and Kansas State University* P4:1-54

Strategies for Concurrent Wet Storage and Pretreatment of Corn Stover; *Y. Li; Ohio State University* P5:1-14

Improving Handling Characteristics of Herbaceous Biomass; *V. Morey; University of Minnesota* P6:1-70

Transforming and Densifying Biomass in Regional Biomass Processing Centers; *K Muthu; South Dakota State University* P7:1-29

In-Field Cubing of Cellulosic Biomass; *K. Shinners; University of Wisconsin* P8:1-26

2008 Capacity Building Internal Awards

Landscape Scale Lignocellulosic Biomass Production; *C. Johnson; South Dakota State University* P9:1-21

Biofuel Crops in Eastern South Dakota Establishment, Productivity, Biotic Impact, and Multiple Use Potential; *P. Johnson; South Dakota State University* P10:1-10

Interactions of Biochar/Bio-ash Source/Properties Impacts on Soil Properties, C Sequestration Potential, and Crop Management; *D. Malo; South Dakota State University* P11:1-6

Wind Resource Assessment Network; *D. Todey; South Dakota State University* P12:1-7

2009 Nationwide Competitive Awards

Seed Technologies to Secure Rapid and Complete Switchgrass Establishment; *B. Baldwin; Mississippi State University* P13:1-14

Barley Straw Fructanosic Ethanol for On-Farm Biofuel Production; *T. Blake; Montana State University* P14:1-7

Optimization of Biomass Productivity and Environmental Sustainability for Cellulosic Feedstocks: Land Capability and Life Cycle Analysis; *S. Brouder; Purdue University* P15:1-13

Do Nurse Crops Make Miscanthus Giganteus Establishment More Sustainable; *E. Heaton; Iowa State University* P16:1-11

Sustainable Biomass Production on Marginal Lands Using a Novel legume/Grass Mixture; *V. Owens; South Dakota State University* P17:1-8

Evaluation of Bioenergy Crop Production on Marginal Land in Wisconsin; *S. Ventura; University of Wisconsin-Madison* P18:1-10

2009 Capacity Building Internal Awards

Cup Plant as a Potential New Biomass Crop; *A. Boe; South Dakota State University* P19:1-12

Biofuel Feedstock Crops in Sub-Irrigated Lowlands; *C. Johnson; South Dakota State University* P20:1-17

Pyrolysis of Forest Residue; *L. Wei; South Dakota State University* P21:1-34

2010 Nationwide Competitive Awards

Using Second-Generation Biofuel Feedstocks to Improve the Carbon Economy of US Agriculture; *E. DeLucia; University of Illinois* P22:1-9

Improving Production, Resilience, and Biodiversity of Perennial Grass Mixtures and Monocultures as Biofuel Feedstocks Across Environmentally Heterogeneous Landscapes; *C. Johnson; South Dakota State University* P23:1-4

Production and Economics of Perennials-Based Woody and Herbaceous Biomass Crops Under Alley-Cropping Systems; *G. Johnson; University of Minnesota* P24:1-11

Intensifying the Corn-Soybean Rotation with the Use of Winter Rye Grown for Biomass Energy Production; *P. Sexton; South Dakota State University* P25:1-20

2010 Capacity Building Internal Awards

Beneficial Plant Microbe Interactions and Their Potential Application to Increase Biomass Production and Environmental Sustainability of Prairie Cordgrass; *H. Bucking; South Dakota State University* P26:1-13

Develop Solid-stem Triticale as a Feedstock for Biofuel Production; *W. Li; South Dakota State University*.....P27:1-5

2013 Capacity Building Proof of Concept Projects

Electrophoretic Deposition of Biochar Nanoparticle Based Films for Energy Storage; *Q. Fan; South Dakota State University*.....P28:1-15

Developing Gas Stripping-Absorption/Desorption Processes Based on Porous Carbon Adsorbents for Biofuel Purification from Bioreactors; *Z. Gu; South Dakota State Univ. ...*P29:1-6

Catalytic Fast Pyrolysis Conversion of Corn Stover to Drop-in Quality Hydrocarbons; *L. Wei; South Dakota State University*.....P30:1-20

2015 Capacity Building Proof of Concept Projects

Plasma Activation of Biochar for Supercapacitors; *Q. Fan; South Dakota State University*.P31:1-10

Engineering *Aurebasidium pullulans* to Produce and Secrete Beta Glucans and Poly-lysine; *J. Gibbons; South Dakota State University*.....P32:1-7

Optimize Multifunctional Catalysts for Efficiently Converting Lignocellulosic Biomass to Advanced Biofuels; *L. Wei; South Dakota State University*.....P33:1-39

Appendices

2008 Request for Applications.....A1:1-7

2009 Request for Applications.....A2:1-7

2010 Request for Applications.....A3:1-7

2013 Internal Proof of Concept Request for Applications.....A4:1-4

2015 Internal Proof of Concept Request for Applications.....A4:1-4

Executive Summary

The Sun Grant Initiative partnered with the US Department of Energy (DOE) in 2008 to create the Regional Biomass Feedstock Partnership Competitive Grants Program. The overall goal of this project was to utilize congressionally directed funds to leverage the North Central Regional Sun Grant's Competitive Grant program at South Dakota State University (SDSU) to address key issues and research gaps related to development of the bioeconomy. Specific objectives of this program were to:

1. Identify research projects through a Regional Competitive Grants program that were relevant to the sustainable production, harvest, transport, delivery, and processing/conversion of cost-competitive, domestically grown biomass.
2. Build local expertise and capacity at the North Central Regional Sun Grant Center at SDSU through an internal selection of key bioenergy research projects.

To achieve these, three nationwide Request for Applications (RFA) were developed: one each in 2008, 2009, and 2010. Internal, capacity building projects at SDSU were also selected during each one of these RFAs. In 2013 and 2015, two additional Proof of Concept RFAs were developed for internal SDSU projects. Priority areas for each RFA were 1) Biomass feedstock logistics including biomass harvesting, handling, transportation, storage, and densification; 2) Sustainable biomass feedstock production systems including biomass crop development, production, and life-cycle analysis; 3) Biomass production systems that optimize biomass feedstock yield and economic return across a diverse landscape while minimizing negative effects on the environment and food/feed production; and 4) Promotion of knowledge-based economic development in science and technology and to advance commercialization of inventions that meet the mission of the Sun Grant Initiative. A total of 33 projects were selected for funding through this program. Final reports for each of these diverse projects are included in this summary report.

Projects funded under this award have contributed significantly to and advanced the bioeconomy body of knowledge. Specifically, no fewer than 109 peer-reviewed publications, 2 patents, 4 invention disclosures, 5 book chapters, 30 conference papers, 224 professional presentations, 31 outreach publications, and 1 website have been generated. This contribution to the scientific community (peer-reviewed literature, presentations, etc.) and to the public (outreach publications, websites, etc.) has been significant.

In addition, a number of projects funded through this award included significant industry involvement and support both in terms of funding (both in-kind and direct) and input. Key industry stakeholders included AGCO, Alliant Energy, Applied Nanofilms, Archer Daniels Midland, ConocoPhillips, DuPont-Danisco Cellulosic Ethanol, EcoSun Prairie Farm, Federal Machine Co., Hawkeye Renewables, John Deere, Mendel, SD Innovation Partners, and Thermo-Ag.

Introduction: The Sun Grant Initiative

The Sun Grant Initiative (SGI) is a national network of land-grant universities and federally funded laboratories working together to further establish a biobased economy. These institutes are at the forefront of research and innovation involving bioenergy and biofuels production. They have the history, technology and resources available to lead the nation towards a renewable, sustainable, domestic energy industry. Sun Grant Centers are also charged with reviving America's farming communities by placing an emphasis on rural economic development through the production of biobased renewable energy feedstocks.

The mission of the Sun Grant Initiative is to:

1. Enhance national energy security through development, distribution, and implementation of biobased energy technologies.
2. Promote diversification in and the environmental sustainability of agricultural production in the United States through biobased energy and products technologies.
3. Promote economic diversification in rural areas of the United States through biobased energy and product technologies.
4. Enhance the efficiency of bioenergy and biomass research and development programs through improved coordination and collaboration between the US Department of Agriculture, the US Department of Energy, and land-grant colleges and universities.

In 2008, the Sun Grant Initiative partnered with the US Department of Energy (DOE) specifically to create the Regional Biomass Feedstock Partnership Competitive Grants Program. *The overall goal of this project was to utilize congressionally directed funds to leverage the North Central Regional Sun Grant's Competitive Grant program at South Dakota State University to address key issues and research gaps related to development of the bioeconomy.* To achieve this goal, specific objectives of this program were to:

1. Identify research projects through a Regional Competitive Grants program that were relevant to the sustainable production, harvest, transport, delivery, and processing/conversion of cost-competitive, domestically grown biomass.
2. Build local expertise and capacity at the North Central Regional Sun Grant Center at SDSU through an internal selection of key bioenergy research projects.

For the two objectives listed above, 75% of these congressionally directed funds were allocated to the Regional Competitive Grants Program and 25% were dedicated to building local expertise at strength at the North Central Sun Grant Regional Center at SDSU.

Request for Applications

To achieve the two objectives listed above, three nationwide Request for Applications (RFA) were developed: one each in 2008, 2009, and 2010. Internal, capacity building projects were also selected during each one of these RFAs. In 2013 and 2015, two additional Proof of Concept RFAs were developed for internal (SDSU) projects. For all awards, a minimum 20% cost share was required. A copy of each RFA is included in Appendix A of this report. A summary of priority area and submission data for each RFA is outlined in Table 1 below.

Table 1. Requests for Applications, number of full proposals submitted, and funded awards (externally and internally competitive) through the DOE congressionally directed funds administered by the North Central Sun Grant Regional Center at South Dakota State University.

RFA Year	Priority Area	Full proposals	Funded Competitive Projects	Funded Internal Projects
2008	Biomass feedstock logistics: biomass harvesting, handling, transportation, storage, and densification	20	8	4
2009	Sustainable biomass feedstock production systems including biomass crop development, production, and life-cycle analysis	19	6	3
2010	Biomass production systems that optimize biomass feedstock yield and economic return across a diverse landscape while minimizing negative effects on the environment and food/feed production	14	4	2
2013	Proof of Concept: Promote knowledge-based economic development in science and technology and to advance commercialization of inventions that meet the mission of the Sun Grant Initiative			3
2015	Proof of Concept: Promote knowledge-based economic development in science and technology and to advance commercialization of inventions that meet the mission of the Sun Grant Initiative			3

Outcomes and Outputs

The Project Investigator (PI) for each project funded under the RFAs shown in Table 1 submitted a final report. Specific outcomes and outputs for each of these projects are shown in their final report. In summary, projects funded under this award produced no fewer than:

- 109 peer-reviewed publications
- 2 patents
- 4 invention disclosures
- 5 book chapters
- 30 conference papers
- 224 professional presentations
- 31 outreach publications
- 1 website

Contribution to the scientific community (peer-reviewed literature, presentations, etc.) and to the public (outreach publications, websites, etc.) has been significant.

Industry Involvement

A number of projects funded through this award included significant industry involvement and support both in terms of funding (both in-kind and direct) and input. Several of the key industry stakeholders are listed below:

- AGCO
- Alliant Energy
- Applied Nanofilms
- Archer Daniels Midland
- ConocoPhillips
- DuPont-Danisco Cellulosic Ethanol
- EcoSun Prairie Farm
- Federal Machine Co.
- Hawkeye Renewables
- John Deere
- Mendel
- SD Innovation Partners
- Thermo-Ag

Final Reports by Project

Each of the projects awarded through the DOE-funded Sun Grant Initiative Regional Biomass Feedstock Partnership Competitive Grants Program are distinct in nature. Therefore, final reports submitted by each of the PIs are included in this Final Technical Report and follow in the sections below.

Back to Table of Contents

Sun Grant Initiative
DOE Final Progress Report

Project Title: Optimizing the Logistics of a Mobile Fast Pyrolysis System for Sustainable Bio-crude Oil Production

Project Director/Principal Investigator:
Sergio C. Capareda, Associate Professor
Department of Biological and Agricultural Engineering
Texas A&M University
College Station, TX

All Co-Principal/Other Investigators:
Clyde Munster, Professor
Department of Biological and Agricultural Engineering
Texas A&M University
College Station, TX

Tony Provin, Professor and Donald Vietor, Professor
Department of Soil and Crop Science
Texas A&M University
College Station, TX

Marco Palma, Associate Professor
Department of Agricultural Economics
Texas A&M University
College Station, TX

Collaborators:
Caroline Massiello, Associate Professor
Department of Chemistry
Rice University
Houston, TX

Sandun Fernando, Associate Professor
Department of Biological and Agricultural Engineering
Texas A&M University
College Station, TX

Period of Performance: 31 July 2009 - 31 December 2012

Funding Awarded: $700,000

Cost Share Amount: $214,020

Cost Share Sources: Time and effort from PIs and CoPIs; Indirect on time and effort; tuition remission at Texas A&M.

Executive Summary

This research developed a system for sustainable bio-crude oil production via mobile fast pyrolysis process. Biooil, as drop-in biofuel was optimized while investigating the logistics associated with the production. GIS studies were implemented to optimize the movement of the mobile fast pyrolyzer based on various factors and the delivery of drop-in fuels to nearby refineries. The biochar co-product was thoroughly investigated for possible nutrient recycling and soil amendment. Finally, a risk-based economic simulation model was developed for this conversion process to show how commercial crude oil prices and other risk factors affect the economic viability of the system. Thus, this research has contributed to various aspects of bio-crude oil production through various technical optimization procedures using various unique biomass resources readily available in the North Central Region of the US. The GIS research would help future commercial entities understand the logistics of the system, while the char research would help improve the sustainability of the agricultural land. The risk-based economic model establishes the various economic indicators for a viable commercial product.
The technical effectiveness and economic feasibility of the methods and techniques investigated or demonstrated.

The risk-based economic feasibility has provided a versatile technique to would-be users of the technology in terms of financial factors as it relate to actual risks associated with the operation of the system. Feedstock issues, crude, oil prices are just a few of the significant factors that would affect the overall viability of the system. Thus, the developed simulation model will assist the financial institution assess the overall economic feasibility of the process demonstrated.

How the project is of benefit to the public: The real benefit of the research to the public is the detailed technical analysis of the various aspects of the mobile fast pyrolysis process and the optimized production of biooil from various biomass resources. The comprehensive information was not readily available in previous studies. In addition, the inclusion of GIS studies aids to a clear understanding of logistics of the system. Agricultural land , where biomass will be produced, will also benefit from the recycling of the co-products of the process and return nutrients for sustainable. Finally, the project envisions a unique way of producing drop-in biofuels whereby the conversion facility is brought near areas where biomass is produced and thus limiting transport and other logistics costs.

Project Objectives

Project Objective 1: Development of Mobile Fast Pyrolysis System (Sergio Capareda)

Outcomes and Impacts: This part of the project investigated the development of a mobile fast pyrolysis system for biofuel production from corn stover, sorghum and switchgrass. Product yields and characteristics were determined to evaluate the potential of the process in producing the biofuels. Estimates of bio-oil yield and energy content were crucial in determining the economic feasibility of the process as well as future product application. Bio-char yield evaluation and preliminary characterization were performed to determine its fuel properties and energy content. Synthesis gas utilization as energy source was shown to be possible due to its high hydrogen and methane content.

Actual Versus Expected Accomplishments: Overall product yields were successfully determined and full product characterization was evaluated as planned to gain insights on biofuel production from corn stover, sorghum and switchgrass.

Project Objective 2: Geographic Information System Analysis (Clyde Munster)

Outcomes and Impacts: A Geographic Information System (GIS) program was developed to optimize the movement of mobile pyrolysis units based on an analysis of transportation networks, cropping patterns, feedstock production rates, and oil refinery locations in the NC region. The locations of existing corn, sorghum, and CRP fields (for switchgrass) in the NC region were obtained from the cropland data layer (CDL) database from the National Agricultural Statistics Service (NASS). Model builder was used to automate the GIS procedures. Network analyst, an extension of ArcGIS, was used to find the best route to move the mobile pyrolysis units to new locations and to identify the closest refinery to receive the bio-crude oil. The mobile pyrolysis unit feedstock input rate was assumed to be 40 tons/day. The GIS program was integrated with a stochastic economic model to assess bio-oil production costs. A sensitivity analysis of the economic model showed feedstock costs were reduced to $19.90/tons with 90% or higher probability of a positive net present value.

The GIS program was used to assess feedstock availability for mobile pyrolysis units in the North Central (NC) region. The feedstocks used for this study were corn stover, energy sorghum, and switchgrass. The GIS program identifies optimum locations for mobile pyrolysis stations based on feedstock availability and calculates the routes and distances between the optimum pyrolysis stations. The GIS program utilized a harvest grid concept with the mobile pyrolysis unit located in the center of the grid cell. It was assumed that the mobile pyrolysis units would move on discrete time steps of 1, 2, 4, 6, 8, 10 and 12 months (stationary). The harvest grid sizes ranged from 2.4 to 9.6 km for corn stover, from 5 to 23 km for energy sorghum, and 3.3 to 12 km for switchgrass, depending on move times. In the NC region, distances to move the mobile pyrolysis unit from one location to the next location varied from 2.1 to 138.7 km for corn stover, from 4.4 to 81.0 km for energy sorghum, and 3.0 to 60.7 km for switchgrass. Distances to transport the bio-oil to the closest oil refineries ranged from 81 to 195 km for corn stover, 365 to 522 km for energy sorghum, and 192 to 265 km for switchgrass. The GIS program was coupled with the economic model (SIMETAR) to calculate the total cost of producing and transporting the bio-oil to an oil refinery. The highest probability of success was a stationary model (the mobile pyrolysis unit stayed one location for 12 months). However, mobile pyrolysis units had more flexibility under constraints.

Actual Versus Expected Accomplishments: The deliverables for the GIS analyses were identified in the proposal as follows.

- Optimize the logistics required to establish networks of pyrolysis stations to produce bio-crude oil in a sustainable system using mobile pyrolysis units;
- Identify the most cost-effective routes for bio-crude oil transport using existing highways and railroad lines to existing oil refineries;
- Establish the locations of pyrolysis stations on the cost-effective transportation routes;
- Optimize the area surrounding pyrolysis stations needed for feedstock production;
- A real-time GIS model linked with crop production predictions, weather forecasts and economic models to optimize the deployment of the mobile pyrolysis units;
- The total bio-crude oil capacity of the North Central region using mobile pyrolysis units.

All of these objectives were accomplished except that the GIS model was not linked with crop production predictions or weather forecasts. It was determined that automatically linking the GIS model to crop production predictions and weather forecasts was not needed. It turned out that the GIS model can be easily adjusted manually for poor crop production or bad weather and seamless integration was not worth the added complexity to run the model.

It was expected at the start of the project that railroads and existing oil pipelines would be major factor in the feedstock logistics in the NC region. However the GIS analyses revealed that railroads and pipelines

were generally not useful in optimizing feedstock logistics. Instead, roads and highways were the preferred means of transportation.

Project Objective 3: Feedstock Evaluation and Char-by products Utilization (Tony Provin)

Outcomes and Impacts:The sustainability of the mobile pyrolysis units depends upon whether they can provide potential uses not only for the liquid and gaseous products but also for the solid product (bio-char) as well. One method to achieve this goal is to recycle biomass nutrients back to the soil by land application of bio-char. Although pyrolysis of biomass will result in loss of all plant available nitrogen, some plant available nutrients can be conserved, which will likely require environmental weathering prior to becoming plant available. Analysis of the nutrient recovery in bio-chars obtained from the pyrolysis of various feedstocks was performed. Moreover, bio-chars were incorporated and incubated into different soil types to evaluate the influence of bio-char application and bio-char type on soil pH, salinity and plant available nutrients. Finally bio-char was incorporated into soil to determine its influence on plant growth. Results provide detailed insights on the recovery of nutrients in the bio-char and the effect of utilizing bio-char from the pyrolysis system in land applications.

Actual Versus Expected Accomplishments: Investigations on the recovery of feedstock plant nutrients revealed that the recovery of macro nutrients (P, K, Ca, Mg) varies depending on the feedstock source and pyrolyzer operating conditions. In general, the recovery of plant macro and secondary nutrients was greatest in the bio-char, although significant losses of nutrients were observed across all species and platforms. For the slow, fixed-bed system, more than 90% of feedstock P and greater than 66% of feedstock Ca was recovered in HES co-products. The highest amount of feedstock Mg was recovered in corn stover co-products. Recovery of feedstock K was relatively low for co-products produced by slow pyrolysis. If the goal is to recycle soil P, Ca, Mg and minimal K, HES and corn stover bio-chars could be recycled back to production fields. For the fluidized-bed system, corn stover performed the best. More than 70% of feedstock P, 55% of feedstock K, 68% of feedstock Ca, and 65% of feedstock Mg was recovered.

Incorporating bio-char into soils resulted in lowering of pH levels in the clay Burleson soil while significant increase in soil pH was observed for the the acid sandy Boonville soil. Similar results were observed for salinity measurements. These affected the plant availabilty of major plant nutrients, thus yielding poor growing conditions for switchgrass. Bio-chars must be incorporated properly to prevent derogatory soil environment leading to limited root development or rapid migration of the bio-char to the roots or possible erosion that could impair local surface waters.

Project Objective 4: Feasibility and Economic Analysis (Marco Palma)

Outcomes and Impacts:The objective of the economic objective was to estimate the economic feasibility of a mobile vs. a stationary pyrolysis plant using alternative feedstocks. The feedstocks used for the analysis are corn stover in Illinois and Texas, and energy sorghum in Nebraska. A Monte Carlo financial simulation model was used to analyze the probability of economic viability of a pyrolysis system for alternative feedstocks, locations, and frequency of plant relocation.

The simulation model to analyze the mobile pyrolysis unit is an annual Monte Carlo financial statement model that incorporates multiple variables including historical prices and yields, estimated conversion ratios from feedstock inputs to bio-oil, biochar, and syngas outputs, and machine/labor/fuel costs. These variables, along with numerous other items that affect income and expense, are itemized in an easy-to-understand. The result is a distribution of key output variables such as profit, yields, and net present value (NPV). These visualizations are crucial for analyzing feasibility for future business decisions, since sales, prices or other market-driven aspects that make or break a business venture are often out of the business

owner's control. The results are based on risk assessments and forecasting using SIMETAR, a simulation and risk analysis software.

Actual Versus Expected Accomplishments**:** The final model incorporated 15 different scenarios, based on crop/location and moving times. There were 3 crop/locations and 5 moving time scenarios. The results of the final model show a very low probability of net present value (NPV) to be positive. Net present value is calculated using the formula (NPV = – beginning net worth + sum of the dividends + ending net worth). Generally speaking, NPV is a measure of the performance of the business from start to finish using a target rate of return. In finance, this value must be greater than zero in order for the business to be considered successful. Investors would typically consider investing in an enterprise with at least a 90% probability of positive NPV. These final results reflect a feedstock cost between $60 and $75. It is important to emphasize that the two products considered in the economic analysis are the bio-oil and char, but there is also economic value to the syngas not considered in the analysis yet that might increase the feasibility. Another possibility is for alternative feedstocks with lower cost. In a simulation analysis, it was shown that if feedstock cost were to be reduced to $10 to $30 dollars, then the feasibility will likely increase. Finally it is also noted that the highest probabilities of success (defined as a NPV greater than zero) occurred when the pyrolysis machine was stationary. The cost per gallon increased as moving times per year increased and the probability of success was reduced as the pyrolyzer moved more often.

Project Activities

Task 1: Development of Mobile Pyrolysis System (Sergio Capareda)

Original Hypothesis

Biofuels such as bio-char, bio-oil and synthesis gas can be produced from the pyrolysis of different biomass feedstocks such as corn stover, sorghum and switchgrass, with the product yields and proportions varying with temperature.

Approaches Used (Methodology)

Biomass characterization of the three feedstocks (corn stover, sorghum and switchgrass) was done through the analysis of their proximate and elemental composition, as well as heating value. Biomass pyrolysis at varying temperatures followed with the evaluation of product yields and composition.

Problems Encountered and Changes in Methodology

Initial problem encountered was the lack of standard methods for the analysis of bio-char and bio-oil. This was solved by adapting the standard methods for petroleum fuels and coal and development of procedures appropriate for the pyrolysis products.

Impact of Changes in Methodology on Project Results

No relevant changes in methodology were employed.

A. Switchgrass Characterization and Pyrolysis

Switchgrass was analyzed for its proximate and ultimate composition as shown in Table 1.1, and was found to contain high amount of volatile matter, low ash content. The oxygen content was high and almost comparable to the amount of carbon.

Table 1.1. Composition of switchgrass biomass.

Switch grass Biomass	Moisture Content	Volatile Combustible Matter		Ash Content	Fixed Carbon
Proximate Analysis	9.3%	84.2%		3.9%	11.9%
	N%	**C%**	**H%**	**S%**	**O%**
Ultimate Analysis	0.4	42.0	6.1	0.1	47.4

Product yields at the different pyrolysis temperatures were evaluated and are shown in Figures 1.1, 1.2 and 1.3 below. Bio-oiland synthesis gas or syngas yields were shown to increase with temperature while the bio-char yield decreased as the pyrolysis reactions that caused decomposition of the biomass became more severe at the higher temperatures.

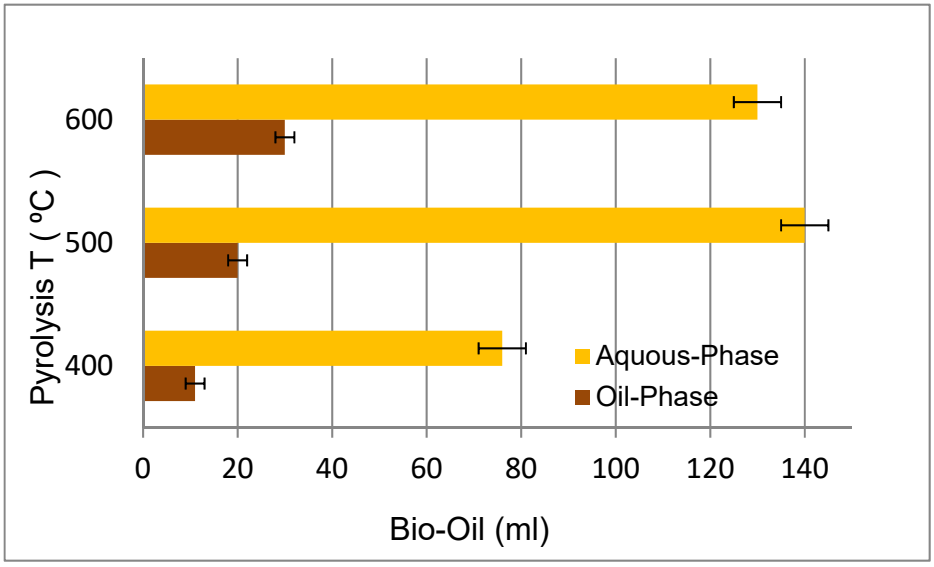

Figure 1.1. Bio-oil production at different pyrolysis temperatures.

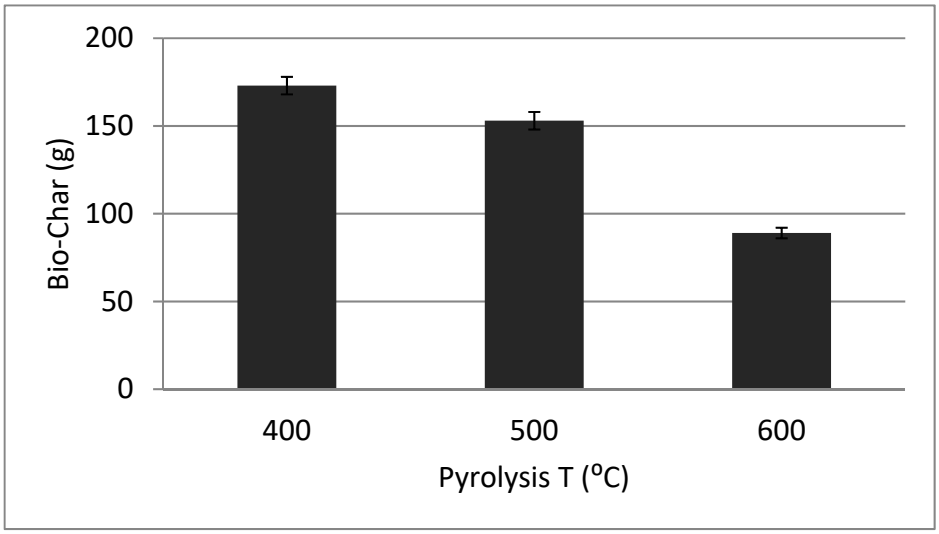

Figure 1.2. Bio-char production at different pyrolysis temperatures.

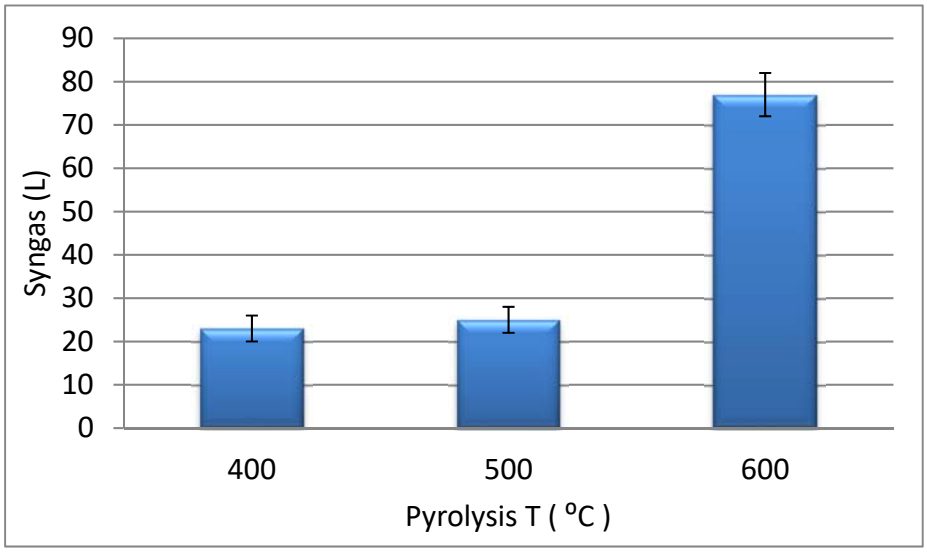

Figure 1.3. Syngas production at different pyrolysis temperatures.

Switchgrass bio-oil was analyzed for its properties and composition, as shown in Table 1.2, and indicates that it is a high energy product with high C and lower oxygen content as compared to the original feedstock.

Table 1.2. Elemental composition and heating value of switchgrass bio-oil.

Switch grass Bio-oil	**N%**	**C%**	**H%**	**S%**	**O%**
Ultimate Analysis	1.5	75.8	8.9	0.57	16.6
Heating Value	15,500 BTU/lb				

The chemical composition of the bio-oil was also analyzed by dissolving the bio-oil first in a ratio of 1:9 of the oil and solvent. They were mixed in a vortex at room temperature for 15 minutes. This mixture was then transferred to an Erlenmeyer flask and shaken for 16-24 hours in 10°C in an incubator shaker. Bio-oil dissolved in the solvents are then analyzed on GC-MS. Summary of the hydrocarbon mixture present in bio-oil together with a detailed analysis of the oil is presented.

A large majority of compounds found in chloroform dissolution are alkanes and phenols while phenols and benzene comprised most of those dissolved in dichloromethane. The table below (Table 1.3) shows the bio-oil composition when it was dissolved in chloroform.

Table 1.3. Different compounds found in switchgrass bio-oil dissolved in chloroform.

Compounds	% in Bio-Oil
Alkane	36.2
Phenol	20.5
Alkene	8.8
Acids	8.7
Alcohol	7.4
Ketone	5.1
Furan	3.5
Ester	2.4
Benzene	2.2
Naphthalene	1.7
Amide	1.5
Other solvents	2.1

Table 1.4 shows the bio-oil composition when it was dissolved in dichloromethane.

Table 1.4. Different compounds found in switchgrass bio-oil dissolved in dichloromethane.

Compounds	% in Bio-Oil
Alkane	9.1
Phenol	29.9
Alkene	5.0
Acids	9.8
Alcohol	3.1
Ketone	8.3
Xylene	3.8
Pyrazole	3.0
Benzene	11.8
Naphthalene	8.1
Amide	1.3
Other solvents	6.8

Pathway for Production of Gasoline from Switchgrass

The photo below (Figure 1.4) shows the resulting bio-oil from pyrolysis of switchgrass as well as the various fractionates and the chromatogram of the bio-oil fractionate and the gasoline standards.

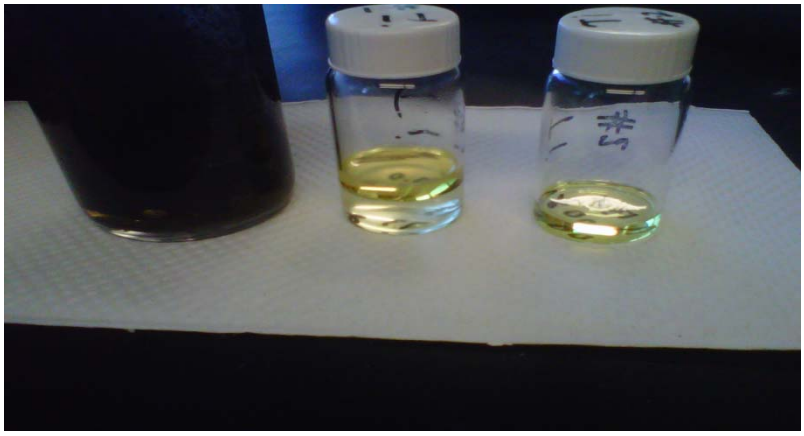

Figure 1.4. Switchgrass bio-oil and fractionates.

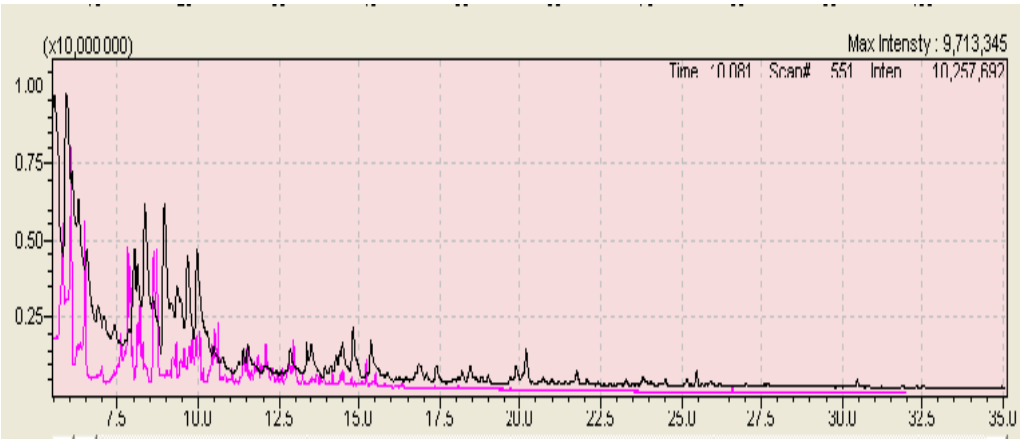

Figure 1.5. GC-MS chromatograms of switchgrass bio-oil fractionate and gasoline standards.

The figure below (Figure 1.6) shows the pathway for the production of light range of hydrocarbon from switchgrass bio-oil based on its compositional analysis.

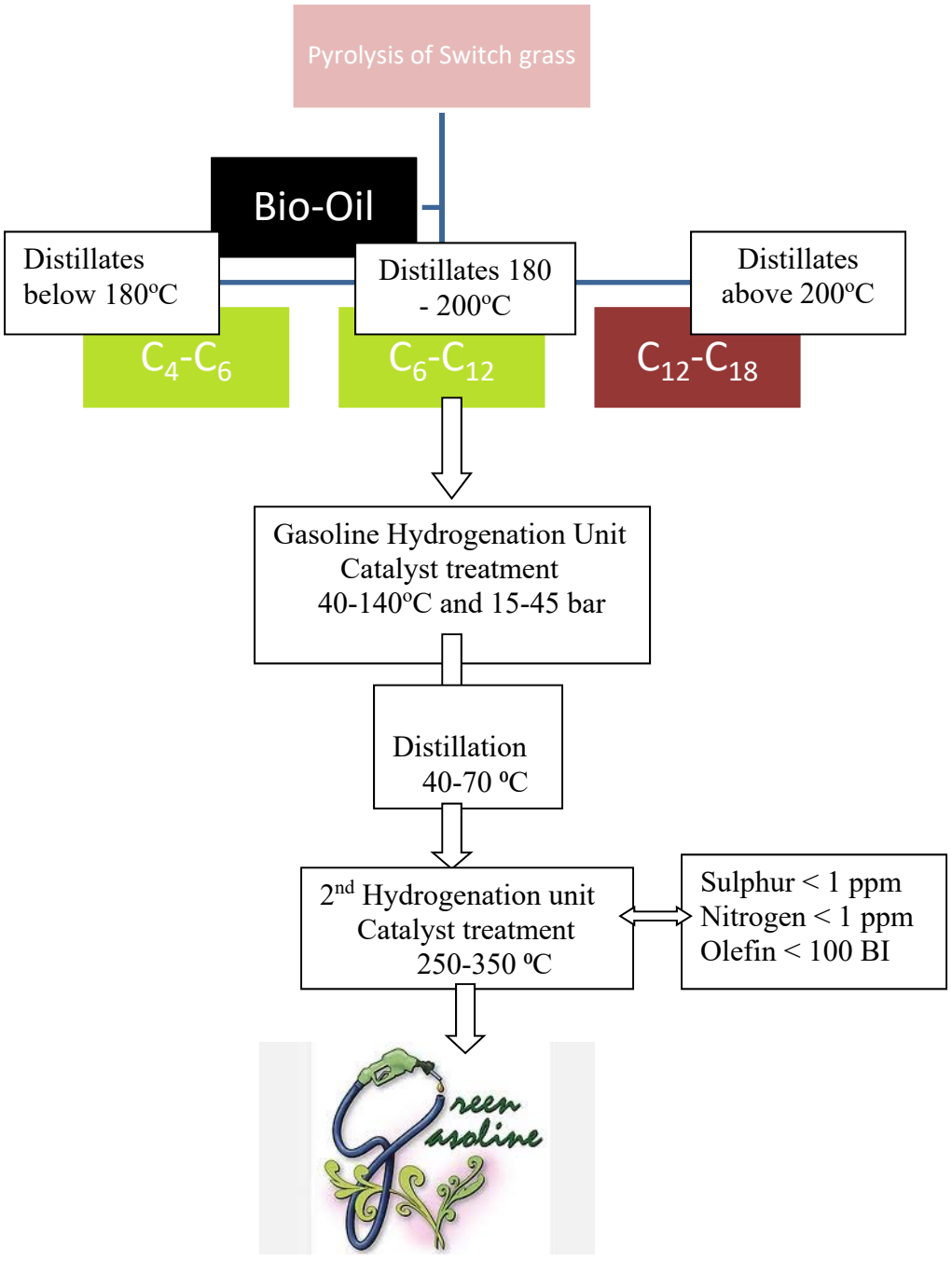

Figure 1.6. Pathway for the production of light hydrocarbons from switchgrass bio-oil.

The initial estimate for oil production is shown in Table 1.5 below.

Table 1.5. Yield of bio-oil from switchgrass.

Type of Oil	Yield (gal oil/ton of biomass)
Bio-oil	10 ± 0.5
Light oil (C_4-C_{12} range)	6 ± 0.4
Heavy oil (C_{12}-C_{18} range)	3 ± 0.2

B. Sorghum Characterization and Pyrolysis

Table 1.6 shows the characteristics of sorghum feedstock while Table 1.7 and Figure 1.7 give the yields of the different products of sorghum pyrolysis. Synthesis gas production increased as the pyrolysis temperature was increased while the char yield decreased and the bio-oil obtained its maximum yield at the middle temperature (500°C).

Table 1.6. Proximate, ultimate and HV analyses of high tonnage sorghum biomass.

	as received	**dry basis**	**dry ash free basis**
Proximate Analysis (wt. %)			
Moisture	12.80		
Ash	8.52	9.77	
Volatile Matter	74.95	85.95	95.26
Fixed Carbon (by difference)	3.73	4.28	4.74
Ultimate Analysis (wt. %)			
Moisture	12.80		
C	38.10	43.69	48.42
H	5.57	6.39	7.08
N	0.91	1.04	1.16
S	0.18	0.21	0.23
O (by difference)	33.92	38.90	43.11
Ash	8.52	9.77	
Gross heating value, Btu/lb	6394.68	7333.35	8127.45
Gross heating value, kJ·kg^{-1}	14842.05	17020.70	18863.82

Table 1.7. Product yields as a function of temperature in units of wt%/wt% for all products and by-products.

Temp., deg C	Bio-char, % wt	Bio-oil, % wt	Syngas, % wt	Losses, % wt
400	39.7 ± 5.5	30.2 ± 0.8	17.1 ± 0.13	13.0
500	36.9 ± 1.7	33 ± 2.5	21.8 ± 3.69	8.3
600	36.1 ± 0.9	31.2 ± 0.5	20.3 ± 3.36	12.4

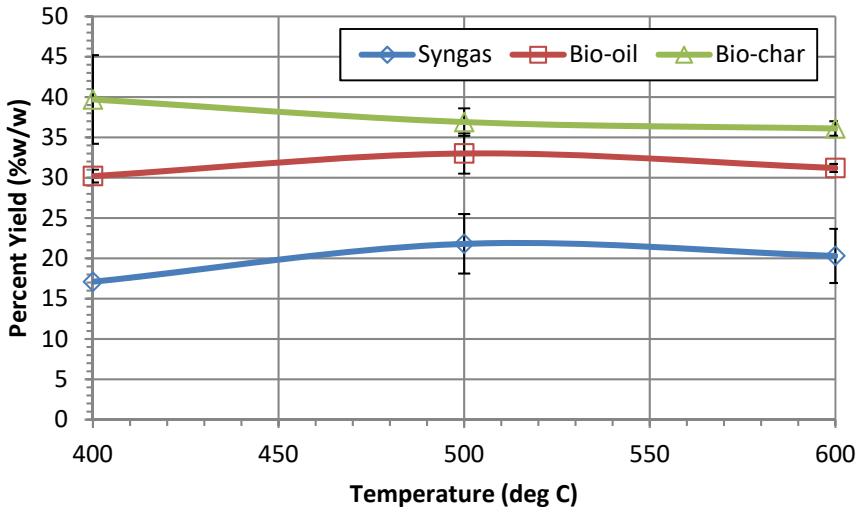

Figure 1.7. Sorghum pyrolysis product yields as a function of temperature.

The products were also characterized, particularly in terms of their heating values so as to evaluate their energy content for possible fuel use. The synthesis gas was first analyzed for its composition as shown in Table 1.8 and Figure 1.8. Methane and hydrogen production was highest at the 500°C while carbon monoxide and carbon dioxide were maximum at the lowest temperature (400°C). From the synthesis gas composition, the heating values were calculated and are presented in Table 1.9 and Figure 1.9.

Table 1.8. Syngas composition as a function of temperature broken down into individual gas components.

Temp., deg C	H2, % vol.	O2, % vol.	N2, % vol.	CH4, % vol.	CO, % vol.	C2H6, % vol.	CO2, % vol.
400	4.19 ± 0.86	6.06 ± 2.80	11.94 ± 4.62	14.38 ± 2.06	13.98 ± 1.90	2.62 ± 1.33	44.58 ± 1.79
500	12.36 ± 3.64	4.50 ± 2.81	8.19 ± 1.35	29.62 ± 3.70	8.15 ± 2.61	4.69 ± 1.40	23.67 ± 7.31
600	8.58 ± 0.26	2.50 ± 1.27	10.02 ± 1.94	18.04 ± 3.56	7.39 ± 2.70	3.61 ± 0.44	23.39 ± 9.59

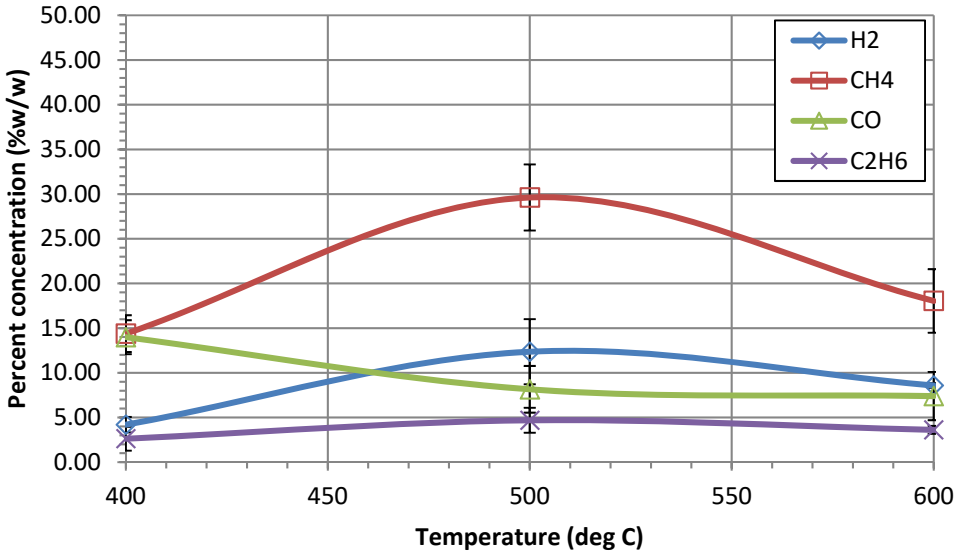

Figure 1.8. Synthesis gas composition as a function of temperature.

Table 1.9. Syngas production in cubic feet/ton of biomass at various temperatures.

Temp., deg C	Production, ft^3/ton		GHV, Btu/ft^3	GHV, MJ/m^3
400	4387	± 247	261.38	9.73
500	7872.7	± 221	468.62	17.45
600	8319.1	± 1575	310.50	11.56

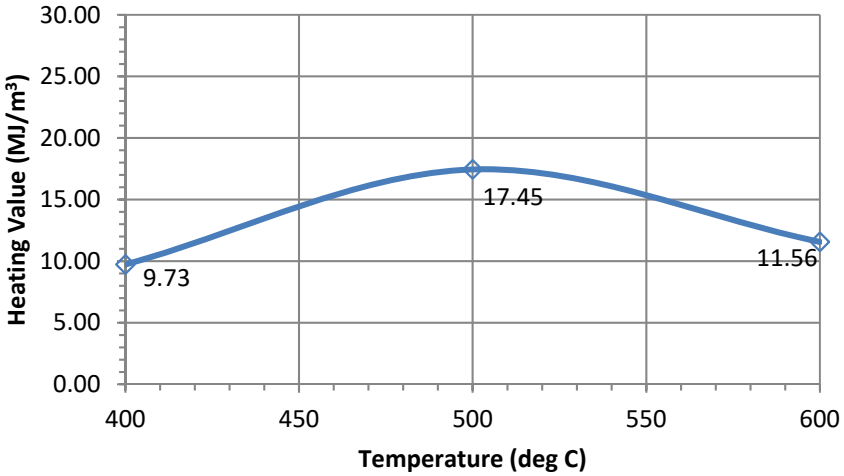

Figure 1.9. Heating value of syngas as a function of temperature.

The bio-char was also analyzed for its proximate composition, as shown in Table 1.10 and Figure 1.10. Increasing the pyrolysis temperature causes an increase in the fixed carbon content of the char and a decrease in its volatile combustible matter content (VCM). Increasing the pyrolysis temperature releases more volatile components in the biomass, thus the observed results.

Table 1.10. Proximate analysis of dry bio-char at various temperatures.

Temp., deg C	VCM, % wt	ASH, % wt	FC, % wt
400	23.8% ± 1.9%	37.8% ± 2.66%	38.4% ± 4.2%
500	14.9% ± 1.6%	33.4% ± 4.0%	51.8% ± 5.2%
600	9.4% ± 1.6%	35.3% ± 2.8%	55.3% ± 4.3%

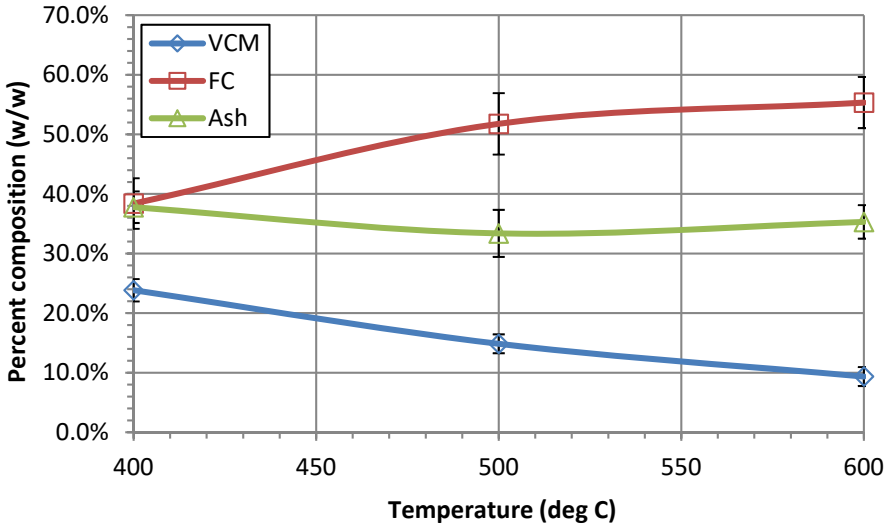

Figure 1.10. Proximate analysis of bio-char as a function of temperature.

Table 1.11 and Table 1.12 shows the bio-char and bio-oil production in lbs/dry ton and gal/ton, respectively and their corresponding heating values (plotted in Figure 1.11).

Table 1.11. Bio-char yields in lbs/ dry ton at various temperatures with corresponding heating value of bio-char at various temperatures.

Temp., deg C	Production, lbs/ton	GHV, Btu/lb	GHV, MJ/kg
400	911.3 ± 126	10,095 ± 254	23.43 ± 0.61
500	838.3 ± 32	10,388 ± 207	24.11 ± 0.49
600	824.3 ± 20	10,560 ± 108	24.51 ± 0.11

Table 1.12. Bio-oil yields in gallons/dry ton as a function of temperature with corresponding HV of bio-oil.

Temp., deg C	Production, gal/ton	GHV, Btu/lb	GHV, MJ/kg	GHV (Btu/gal)	GHV (MJ/L)
400	58 ± 2	12,454 ± 1664	28.91 ± 3.86	129,636 ± 17,315	36.13 ± 4.83
500	63 ± 5	12,988 ± 322	30.14 ± 0.75	135,186 ± 3,348	37.68 ± 0.93
600	60 ± 1	12,998 ± 369	30.17 ± 0.86	135,298 ± 3,837	37.71 ± 1.07

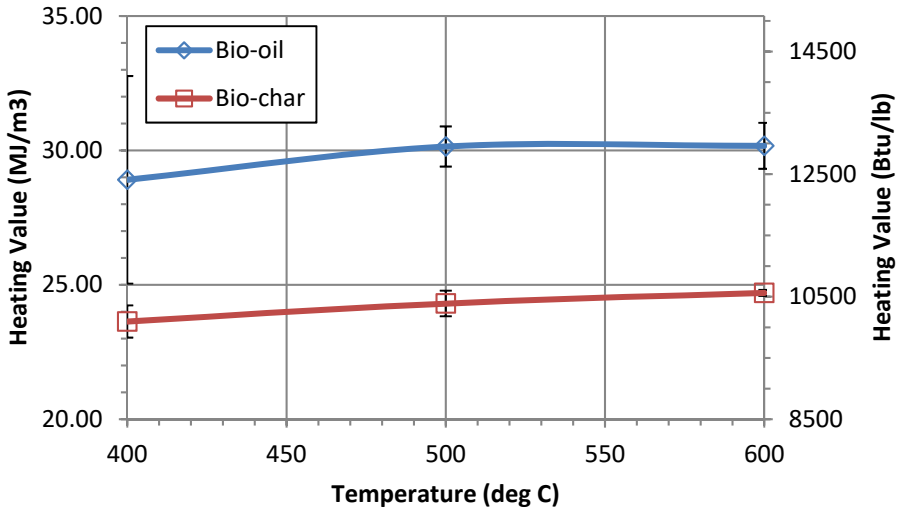

Figure 1.11. Heating value of bio-char and bio-oil as a function of temperature.

C. Corn Stover Characterization and Pyrolysis

Table 13 shows the composition of corn stover in terms of the proximate and elemental components as well as the lignin, extractives and structural carbohydrates. The heating value was similar to that of the other biomass (sorghum).

Table 1.13. Corn stover characteristics.

Biomass Characteristics	**Experimental Value**	**Biomass Characteristics**	**Experimental Value**
Proximate Analysis, % w/w, d.b.		*Compositional analysis, % w/w, d.b.*	
Ash	6.62 ± 0.27	Lignin	13.1 ± 0.1
Volatile Matter (VM)	78.7 ± 1.4	Extractives	18.1 ± 0.4
Fixed Carbon (FC)	14.7 ± 1.7	Glucan	31.9 ± 0.3
Moisture content, %w/w	6.18 ± 0.14	Xylan	19.6 ± 0.2
Ultimate Analysis, % w/w, d.b.		Galactan	1.0 ± 0.1
C	44.3 ± 0.4	Arabinan	2.3 ± 0.1
H	6.28 ± 0.09	Protein	5.8
N	0.80 ± 0.06	*Heating value, MJ kg^{-1}*	17.0 ± 0.7
S	0.23 ± 0.06		
O (by difference)	41.8 ± 0.6		

Figure 1.12 shows the different product yields during corn stover pyrolysis, and indicates maximum bio-char and lowest syngas production at the lowest temperature considered, which was 400°C.

Similar trends with sorghum and switchgrass pyrolysis were observed for the product yields at the different temperatures.

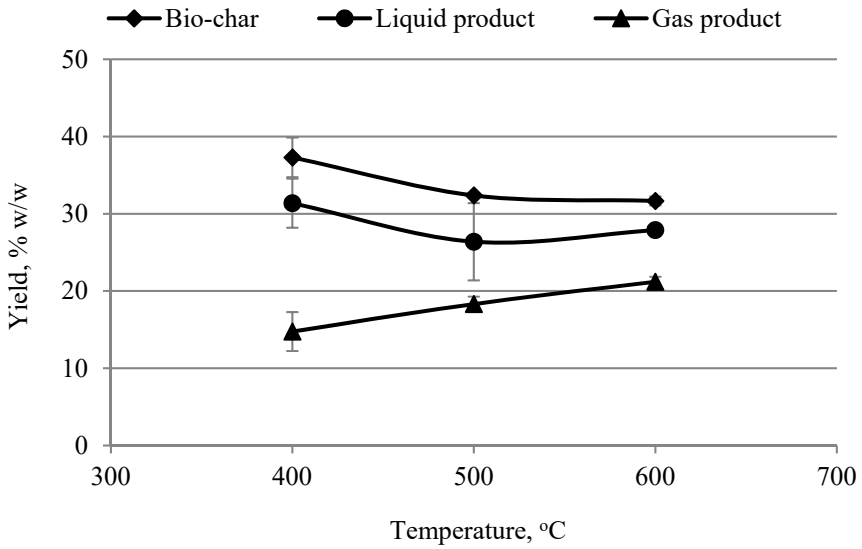

Figure 1.12. Bio-char, bio-oil & synthesis gas yields at different temperatures during batch pyrolysis of corn stover.

The pyrolysis products were analyzed for their composition, as shown in the following figures. Figure 1.13 shows the proximate analysis of the bio-char while Figure 1.14 shows its elemental analysis. The volatile matter was shown to decrease with increasing pyrolysis temperature due to the release of more volatiles at the higher temperatures while the fixed carbon was observed to increase, consistent with the observed increase in the carbon content in Figure 1.14. The oxygen content of the bio-char was significantly lower than that for the original biomass, which translates to an increase in the heating value of the bio-char as shown in Table 1.14.

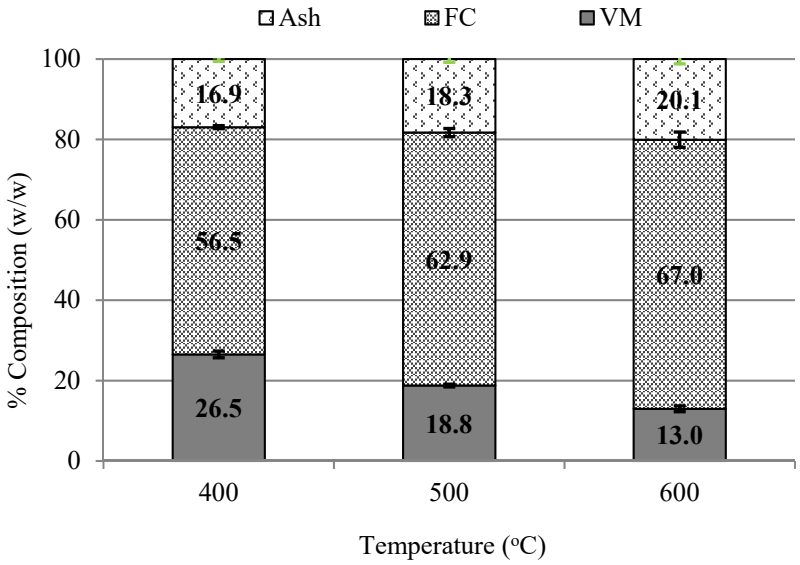

Figure 1.13. Proximate analysis of dry bio-char at the different pyrolysis temperatures.

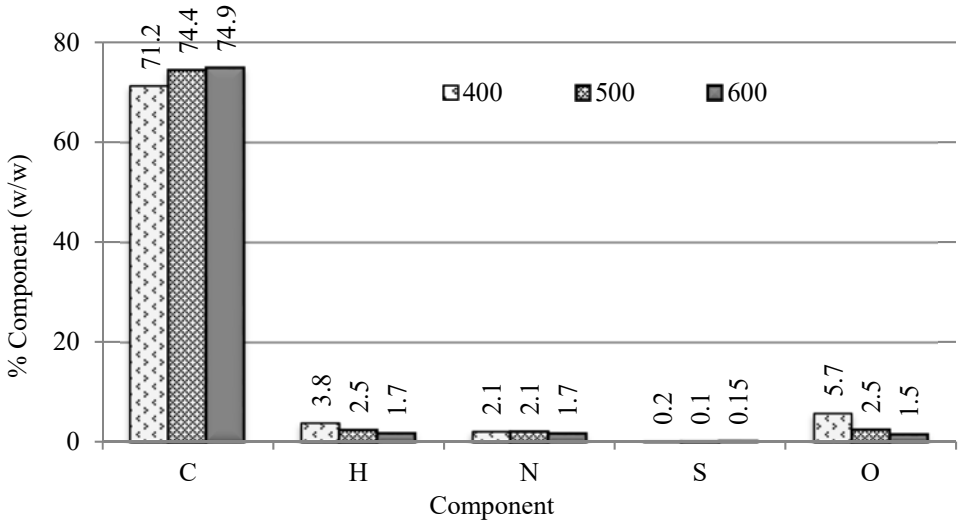

Figure 1.14. Elemental analysis of dry bio-char at the different pyrolysis temperatures.

Table 1.14. Energy yields from the different pyrolysis products at different temperatures.

Product	Char		Bio-oil				Gas			
Temp., °C	BTU/lb	MJ/kg	BTU/lb	BTU/gal	MJ/kg	MJ/liters	BTU/lb	BTU/ft^3	MJ/m^3	MJ/kg
400	11996	27.9	14519	120364	33.8	33.6	3137	272	10.12	7.3
500	9846	22.9	13999	116048	32.6	32.4	6225	386	14.38	14.5
600	9950	23.1	11979	99305	27.9	27.7	11026	582	21.69	25.6

The bio-oil produced was dark brown in color and has higher energy content as compared with the biomass and also higher carbon content and lower oxygen content (Table 1.15). The bio-oil has moisture content and acid number that fall within literature values.

Table 1.15. Some corn stover bio-oil properties.

Parameter	**Value**
Ultimate Analysis, %w/w	
C	78.0 ± 1.1
H	9.02 ± 0.12
N	1.86 ± 0.03
S	0.38 ± 0.10
Ash	0.18 ± 0.06
O (by diff.)	10.6 ± 1.4
H/C molar ratio	1.38
O/C molar ratio	0.10
Acid number, mg KOH/g	23.8 ± 3.7
Moisture content, %w/w	12.8 ± 0.8

The composition of the bio-oil was also determined by FTIR spectrometry and Gas Chromatography-Mass Spectrometry (GC-MS) analysis, with the results shown in Figure 1.15, Tables 1.16 and 1.17. The bio-oil was found to contain a variety of organic compounds that range from long-chain aliphatic hydrocarbons to substituted aromatics as well as oxygenated compounds such as ketones and alcohols. The major components were phenolics and benzene derivatives.

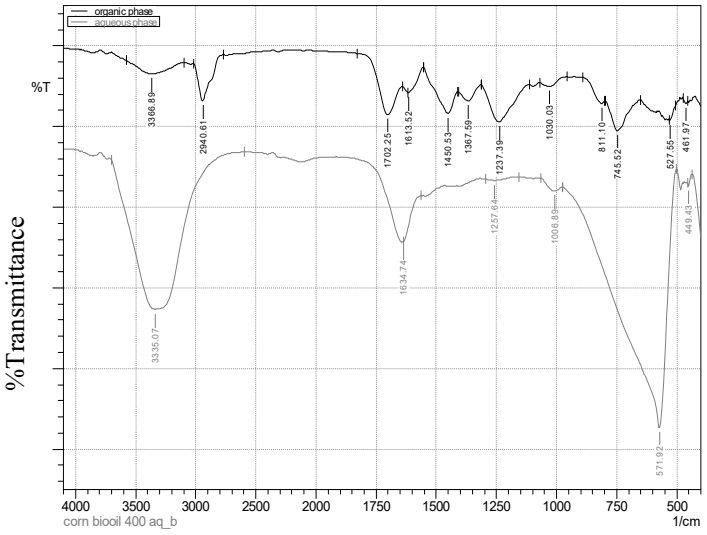

Figure 1.15. FTIR spectra of the corn stover bio-oil (top-bio-oil; bottom-water product).

Table 1.3. FTIR functional group composition of corn stover bio-oil.

Type of Functional Group	Class of Compound	Frequency range (cm^{-1})	Frequency (cm^{-1})	
			Organic phase	Aqueous phase
O-H stretching	phenols, polymeric O-H, water impurities	3600-3200	3367	3335
C-H stretching	Alkanes	3200-2800	2941	--
C=O stretching	Ketones, aldehydes, esters	1750-1650	1702	--
C=C stretching	Alkenes, aromatic compounds	1650 -1580	1614	1635
C-H deformation	Alkanes	1470-1350	1451, 1368	--
C-O stretching	primary, secondary, tertiary alcohols, phenols	1300-950	1237, 1030	1007
O-H bending	mono-, polycyclic, substituted aromatic rings	900-675	811, 746	--

Table 1.4. Compounds identified in the bio-oil sample and their relative composition.

Compounds	% Relative content	Compounds	% Relative content
Alkanes	11.9	*Phenols*	26.7
Nonane	1.1	Phenol	4.29
3-Chloro-3-ethylhexane	0.2	Phenol, 2-methyl-	4.1
3-Bromooctane	3.2	Phenol, 2-methoxy-	1.68
Dodecane	1.76	Phenol, 2,6-dimethyl-	2.92
Undecane, 3,6-dimethyl-	0.67	Phenol, 2-ethyl-	3.89
Octane, 3,6-dimethyl-	0.82	Phenol, 2,4-dimethyl-	1.34
Tridecane	1.1	Phenol, 3-(1-methylethyl)-, methylcarbamate	0.86
Dodecane, 2,6,10-trimethyl-	0.59	Phenol, 2,5-dimethyl-	1.49
Tetradecane	0.75	Phenol, 2,4,5-trimethyl-	0.55
Dodecane, 4,6-dimethyl-	0.29	Phenol, 3-(1-methylethyl)-	0.96
Pentadecane	0.66	Phenol, 2-ethyl-4-methyl-	1.38
Heptadecane	0.5	Phenol, 4-propyl-	0.21
Octadecane	0.14	Phenol, 3-ethyl-5-methyl-	0.41
Heneicosane	0.12	Phenol, 4-ethyl-2-methoxy-	1.47
Alkenes	8.66	Phenol, 5-methyl-2-(1-methylethyl)-, acetate	0.38
2,4-Hexadiene, 2,5-dimethyl-	2.94	2,5-Diethylphenol	0.54
1-Undecene	1.07	2-Ethyl-5-n-propylphenol	0.23
7-Tetradecene	1.1		
1-Tridecene	1.26	*Benzene and its derivatives*	20.24
2-Octene, 2,6-dimethyl-	0.66	Ethylbenzene	4.85
1-Tetradecene	0.61	p-Xylene	4.06
3-Hexadecene, (Z)-	0.32	Benzene, 1,3,5-trimethyl-	1.12
1-Pentadecene	0.46	Benzene, 1-ethyl-3-methyl-	1.05
5-Octadecene, (E)-	0.11	2-Octyl benzoate	1.97
1-Heptadecene	0.13	Benzene, 1,2,4-trimethyl-	4.16
Alcohols	3.06	Benzene, 1,3-diethyl-5-methyl-	0.21
Thymol	0.26	2,4-Dimethylstyrene	2.27
2,5-Cyclooctadien-1-ol, acetate	1.51	Benzene, 1-ethoxy-4-methoxy-	0.19
Cyclohexanol, 3,3,5-trimethyl-, cis-	0.33	Benzene, 1,2,3,4-tetramethyl-4-(1-methylethenyl)-	0.18
trans,cis-2,6-Nonadien-1-ol	0.17	Benzene, 2-(2-butenyl)-1,3,5-trimethyl-	0.18
(1-Benzyl-cyclopropyl)-methanol	0.22	*Furans*	1.55
Cholesta-4,6-dien-3-ol, (3.beta.)-	0.11	Ethyl-2-benzofuran	0.38
1-Phenyl-1-penten-5-ol	0.22	Benzofuran, 4,7-dimethyl-	1.17
1-Dodecanol, 3,7,11-trimethyl-	0.24		
		Other heterocyclic compounds	11.06
Ketones	13.41	Pyrazine, methyl-	0.1
Cyclopentanone, 2-methyl-	2.25	2,3-Diazabicyclo[2.2.1]hept-2-ene, 5-ethenyl-4,7,7-trimethyl-, (1.alpha.,4.alpha.,5.beta.)-	0.52
2-Heptanone	1.54	Indane	1.28

Cyclopentanone, 2,5-dimethyl-	0.61	Bicyclo[3.2.0]heptan-3-ol, 2-methylene-6,6-dimethyl-	0.65
Cyclopentanone, 2,3-dimethyl-	0.81	1H-Indene, 1-chloro-2,3-dihydro-	1.05
4-Cyclononen-1-one	2.32	Tetrahydro-2H-thiopyran-4-ylidenemalononitrile, 5,5-dioxide	0.94
2-Cyclopenten-1-one, 2,3-dimethyl-	3.11	2,3-Epoxycarane, (E)-	2.89
2-Cyclohexen-1-one, 3,4-dimethyl-	0.2	1H-Indene, 2,3-dihydro-5-methyl-	0.96
2-Cyclopenten-1-one, 2,3,4-trimethyl-	0.81	2-Ethyl-2,3-dihydro-1H-indene	0.45
Cyclopentanone, 2-(2-hexenyl)-	0.35	1H-Benzocycloheptene, 2,4a,5,6,7,8-hexahydro-3,5,5,9-tetramethyl-, (R)-	0.41
3-Buten-2-one, 4-phenyl-	0.39	1H-Indene, 2,3-dihydro-4,7-dimethyl-	0.5
3H-Naphtho[2,3-b]furan-2-one, 3-[(4-methoxybenzylamino)methyl]-5,8a-dimethyl-3a,7,8,8a,9,9a-hexahydro-	0.44	2,3-Diazabicyclo[2.2.1]hept-2-ene, 1-phenyl-	0.49
Ethanone, 1-[4-(1-methylethenyl)phenyl]-	0.58	1H-Indene, 2,3-dihydro-4,7-dimethyl-	0.23
		1H-Indene, 2,3-dihydro-1,1,5-trimethyl-	0.18
Acids	1.13	2,5,6-Trimethylbenzimidazole	0.14
Levo-menthoxyacetic acid	0.66	3-Cyclohexen-1-carboxaldehyde, 3-methyl-	0.12
2,4-Dimethoxyphenyl-.beta.-phenpropionic acid	0.47	1H-Indene, 1,1,3-trimethyl-	0.15
Naphthalenes	1.68	*Esters*	0.61
Naphthalene, 1-methyl-	1.07	Bis-(3,5,5-trimethylhexyl) phthalate	0.12
Naphthalene, 1,2,3,4-tetrahydro-1,6,8-trimethyl-	0.17	5-Chlorovaleric acid, undecyl ester	0.29
Naphthalene, 2,6-dimethyl-	0.17	Octanoic acid, nonyl ester	0.2
Naphthalene, 1,3-dimethyl-	0.13		
Naphthalene, 1,8-dimethyl-	0.14	TOTAL	100

The synthesis gas was also analyzed for its composition and was found to contain significant quantities of hydrogen and methane especially at the higher temperatures as shown in Figure 1.16, making it a valuable enegy source, as indicated by its high energy content (see Table 1.14 and Figure 1.17).

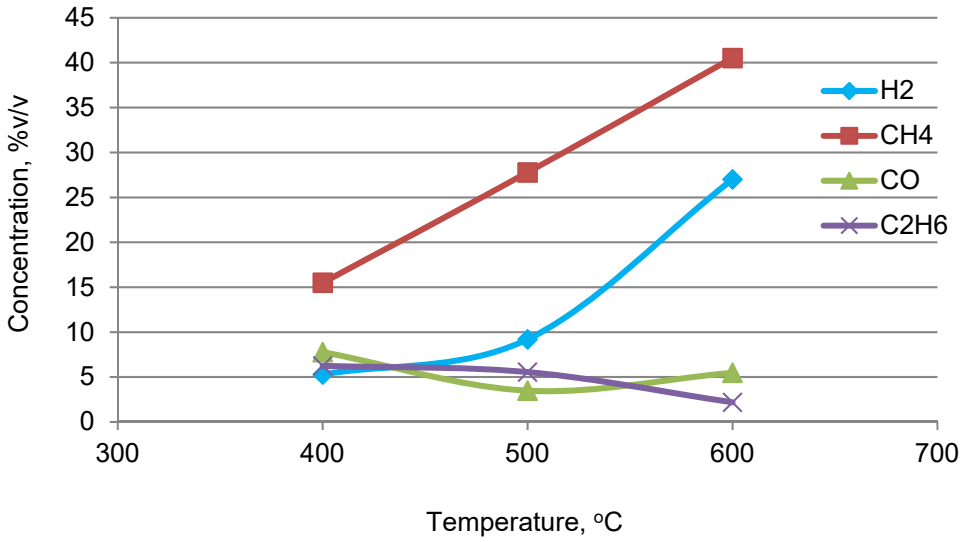

Figure 1.16. Components of synthesis gas product at the different pyrolysis temperatures.

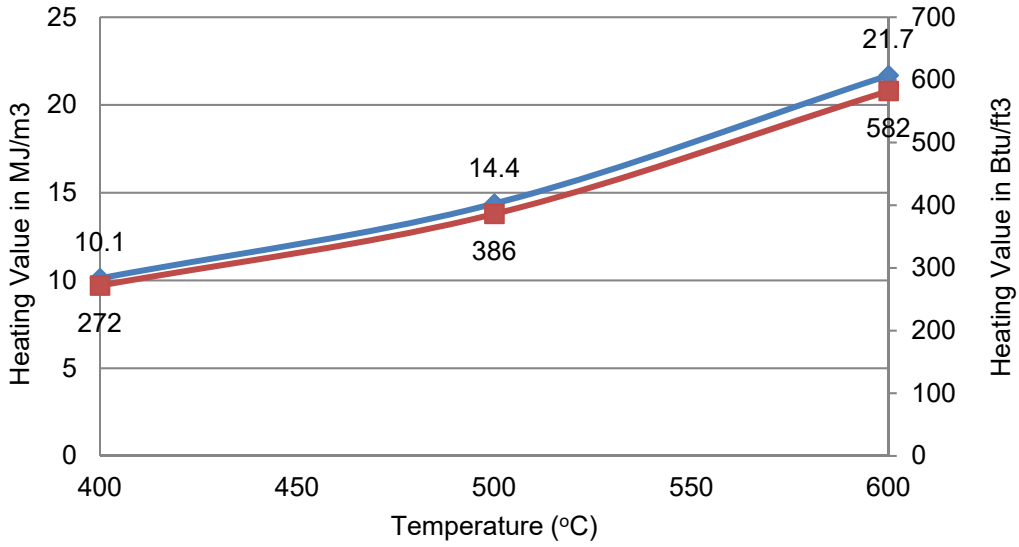

Figure 1.17. Energy content of synthesis gas product at the different pyrolysis temperatures.

Mass and energy balances are shown in Figures 1.18 and 1.19 and show an overall recovery of both around 80% of mass and energy in the products. Highest mass and energy recoveries were obtained in the bio-char due to higher yields for this product. Losses can be attributed to uncollected products and random losses during the pyrolysis process.

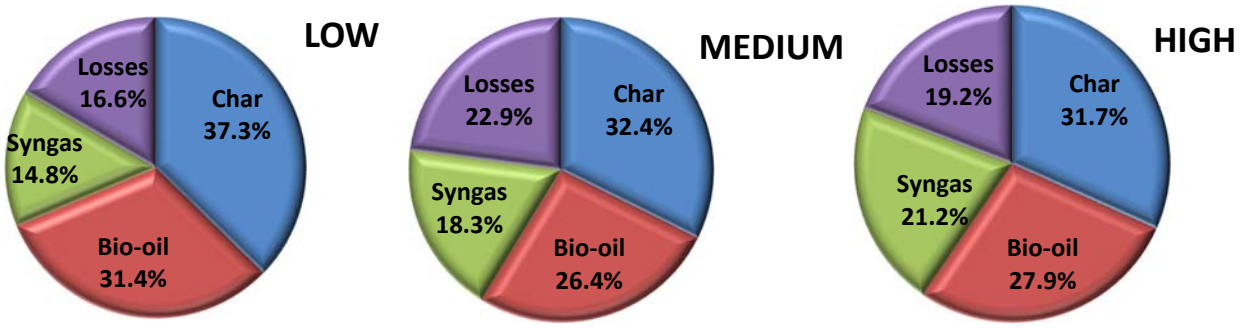

Figure 1.18. Mass balance for the pyrolysis of corn stover at the different pyrolysis temperatures.

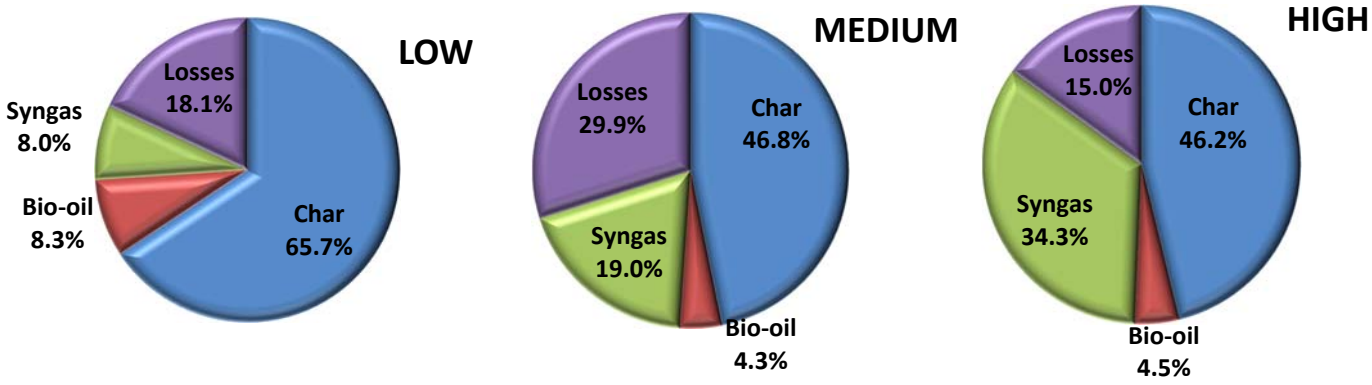

Figure 1.19. Energy balance for the pyrolysis of corn stover at the different pyrolysis temperatures.

Conclusions

Pyrolysis of the three feedstocks (corn stover, sorghum and switchgrass) at different temperatures (400, 500 and 600°C) resulted in variation in the distributions of product (bio-char, bio-oil and synthesis gas) yields. Increasing the reaction temperature lead to a decrease in char yield and an increase in gas yield. Maximum bio-char and liquid product yields were obtained at 400°C for corn stover, while maximum bio-oil yields were obtained at 500°C for switchgrass and sorghum. Syngas yield was maximum at the highest temperature for all the three feedstocks. The gross heating values and composition of the bio-char, liquid and gas products indicated the potential of these materials as energy sources. The composition of bio-char indicates that it is comparable in fuel characteristics with other solid fuels. Bio-oils from corn stover and switchgrass consist mostly of phenolic and oxygenated compounds with aliphatic compounds in significant amounts. For corn stover, majority of the feedstock's mass and energy were converted and transferred to the bio-char.

Task 2: Geographic Information System Analysis (Clyde Munster)

Original Hypothesis

The original hypothesis was that a GIS model could be developed for the analysis of land resources, feedstock production and transportation infrastructure to support networks of pyrolysis stations to produce bio-crude oil. These pyrolysis stations were to be located along major highways and railroad lines in close proximity to existing oil refineries. Locations of the pyrolysis stations would be based on feedstock availability. In addition, an assessment of total bio-crude oil production capacity using mobile pyrolysis units in the North Central region, based on *sustainable* feedstock production, would be made.

Approaches Used (Methodology)

An ArcGIS program was developed to optimize the movement of mobile pyrolysis units based primarily on an analysis of road/highway networks, feedstock production rates, and oil refinery locations in the NC region. The locations of existing corn, sorghum, and CRP fields (for switchgrass) in the NC region were utilized in the analysis. The 10-year average crop production values, on a county basis, were used to calculate biomass availability. A square grid was overlain over the entire NC region and feedstock availability was calculated for each grid. Grid sizes were adjusted based on feedstock availability and the mobile pyrolysis unit move times of 1, 2, 4, 6, 8, 10 and 12 months. It was assumed that the feedstock input rate for the mobile pyrolysis units was 40 tons/day and that bio-oil was produced at a rate of 50 gallons per ton of feedstock. It was assumed that the mobile pyrolysis unit would be placed in the center of the grid and therefore feedstock transportation distances were half the grid size. Network analyst, an extension of ArcGIS, was used to find the best route to move the mobile pyrolysis units to new locations and to identify the closest refinery to receive the bio-crude oil. Model builder, another ArcGIS utility, was used to automate the GIS procedures.

Problems Encountered and Changes in Methodology

No major problems were encountered in the GIS analysis although small issues had to be resolved. For instance, GIS procedures had to be developed when the grid lines bisected a feedstock field and the feedstock had to be allocated to two different grids.

Impact of Changes in Methodology on Project Results

Since there were no changes in methodology in the GIS analyses there were also no impact to the project results.

Analysis of Results (Tables and Figures)

(A) Grid (B) Feedstock locations (C) Merged grid and feedstock locations

Figure 2.1. The GIS methods that were used to calculate feedstock availability for mobile pyrolysis units using the following methods, (A) a square grid was developed, (B) planted feedstock fields as polygon shape (raster files converted to vector files) files from NASS were used, and (C) the grid and feedstock shape files were merged and shape files that overlapped multiple grid cells were subdivided into shape files that do not overlap multiple cells.

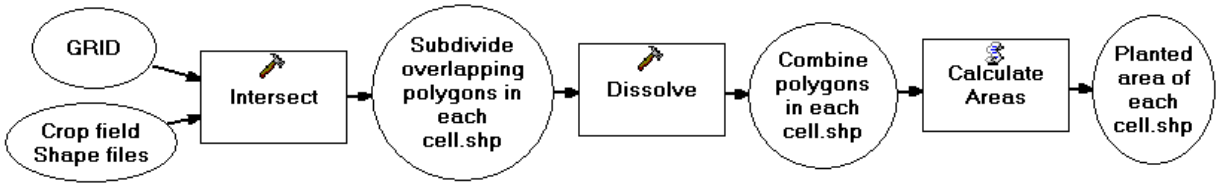

Figure 2.2. A flowchart of the Model Builder procedure used to determine feedstock availability for mobile pyrolysis units in the NC region.

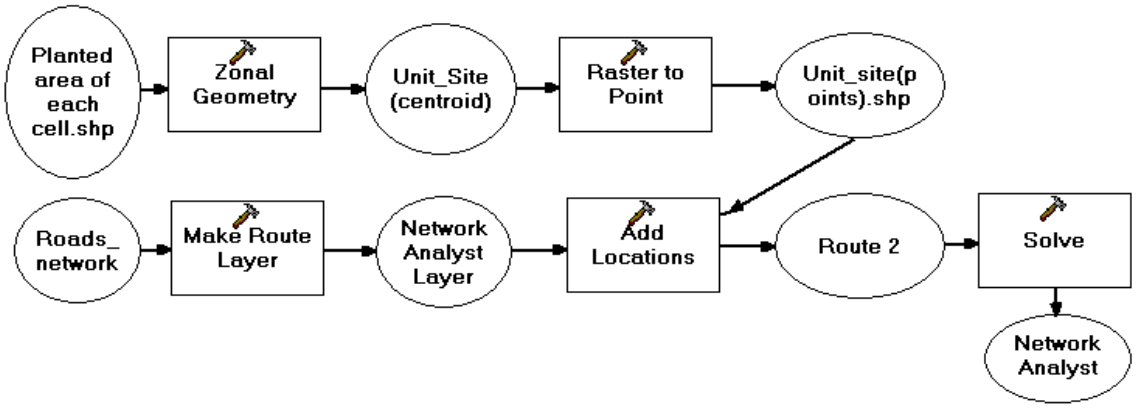

Figure 2.3. A flowchart of the Model Builder procedure used to route, 1) mobile pyrolysis units from one station to next station, and 2) distances from the mobile pyrolysis station to the closet oil refinery.

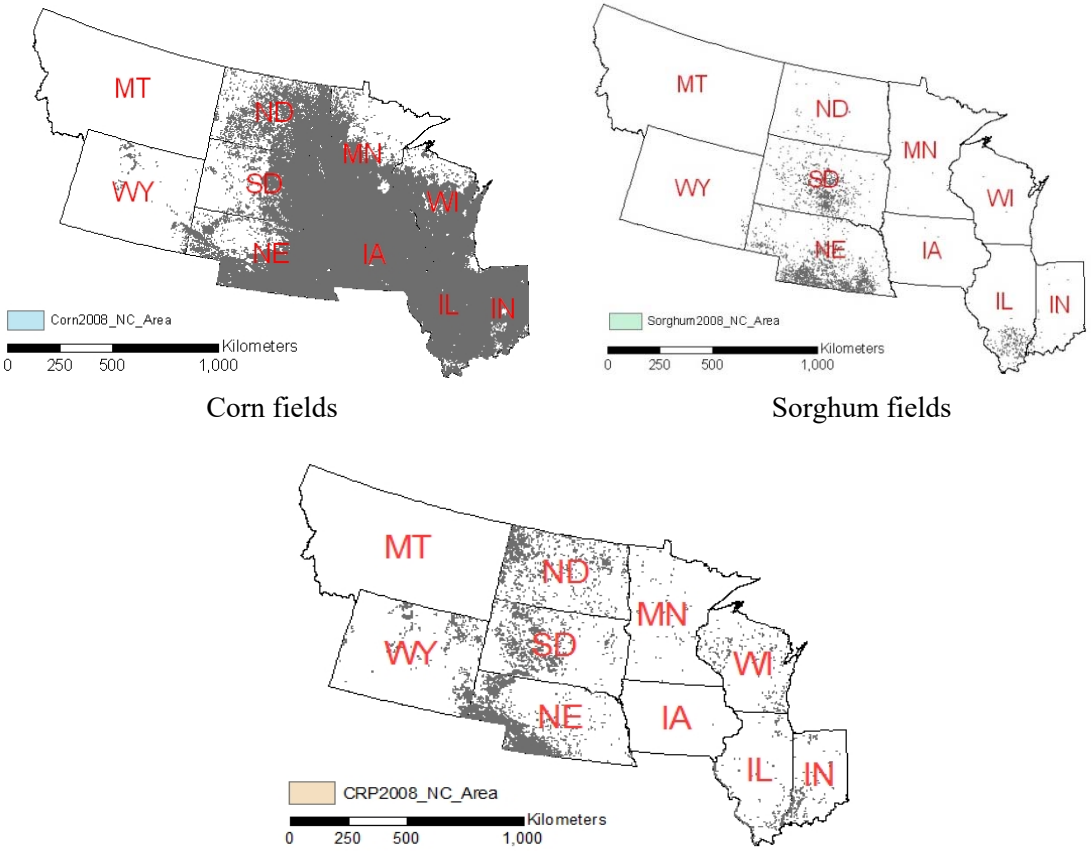

Corn fields

Sorghum fields

CRP lands

Figure 2.4. Location of corn and sorghum fields in the North Central United States in 2008.

Table 2.1. Feedstock hauling distances to transport from the fields to a mobile pyrolysis station for three feedstocks.

Move Time	Feedstock hauling distances (km)		
(month)	Corn Stover	Energy Sorghum	Switchgrass
1	1.2	2.5	1.65
2	1.75	4.05	2.5
4	2.25	6.0	3.5
6	3.1	7.5	4.25
8	3.65	9.5	4.9
10	4.05	11.0	5.5
12	4.8	11.5	6.0

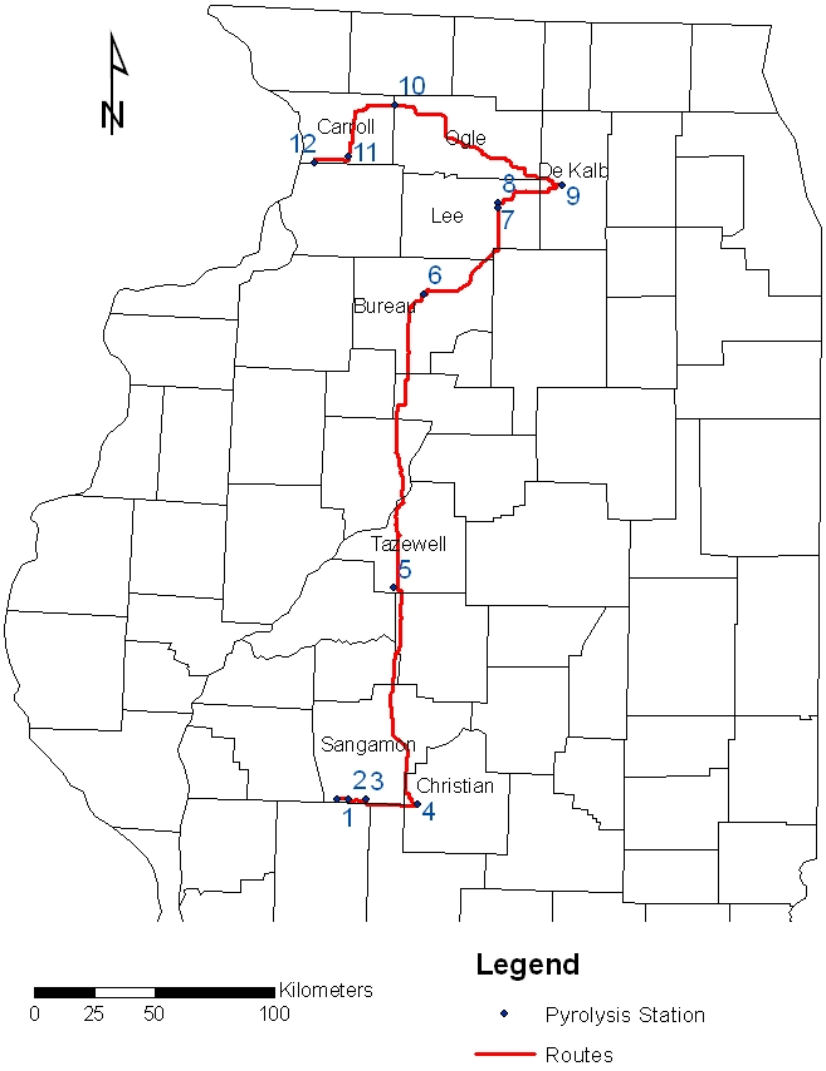

Figure 2.5. The optimized route map for a mobile pyrolysis unit to move to the top 12 corn stover feedstock sites in Illinois. This analysis was based on a squre havest grid (2,400 m) and one month move times.

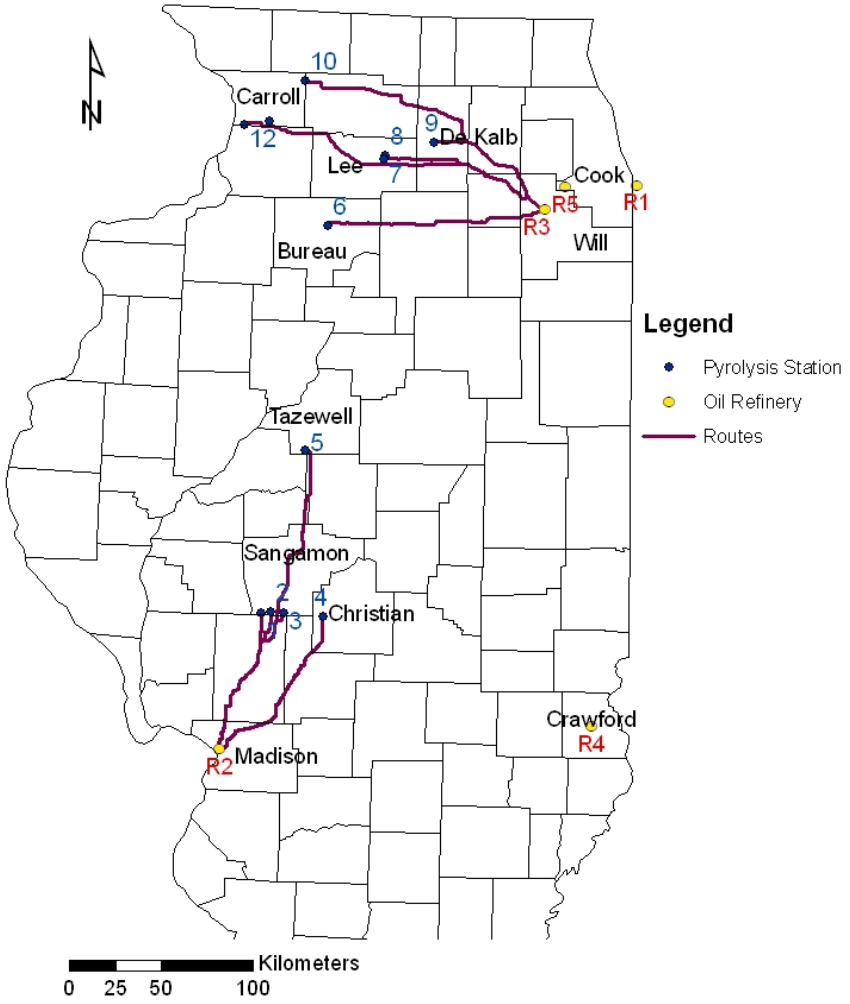

Figure 2.6. The optimized route map to transport bio-oil from mobile pyroysis stations to oil refineries for the top 12 corn production sites in Illinois. This analysis was based on a squre harvest grid (2,400 m) and one month move times.

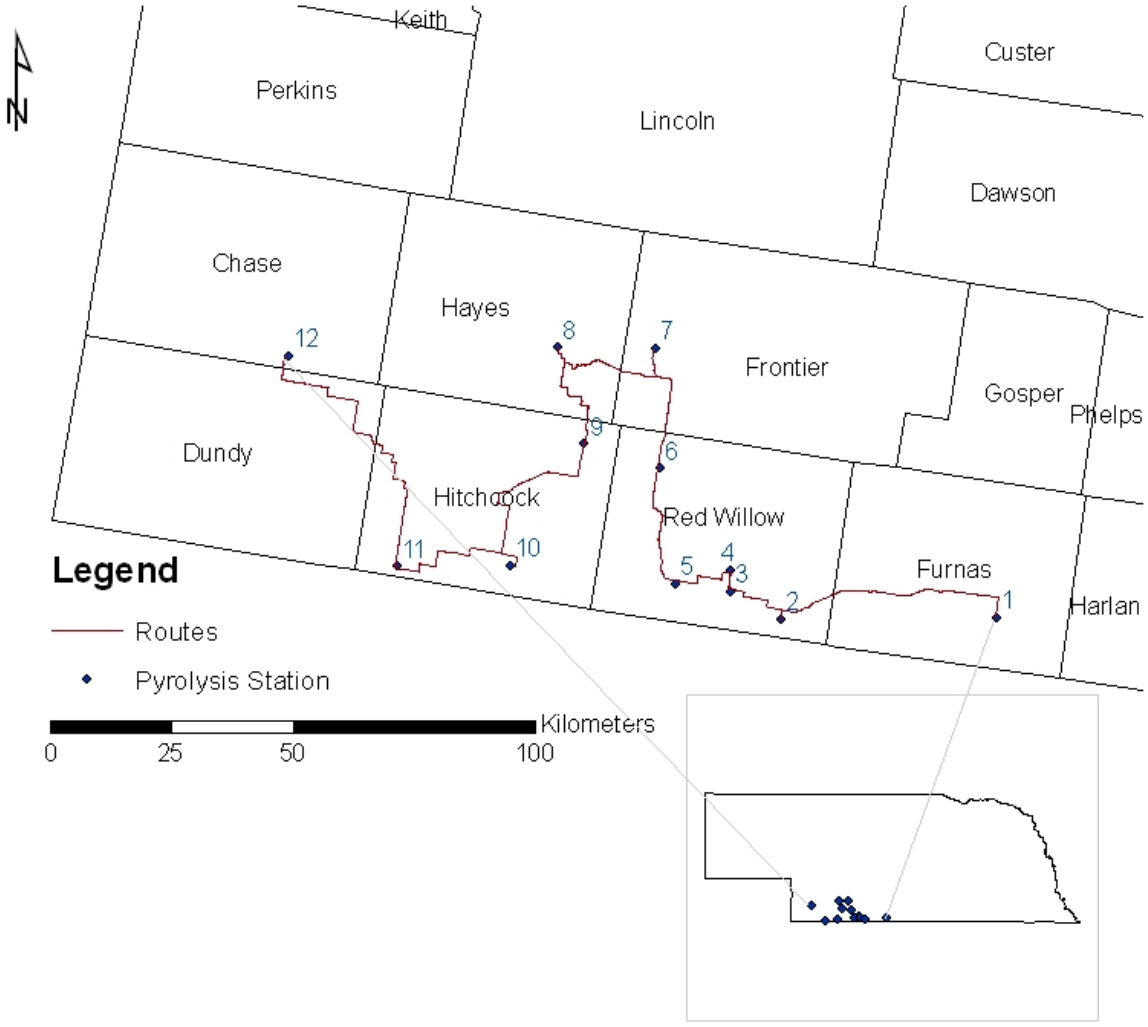

Figure 2.7. The optimized route map from a mobile pyrolysis unit to move to the top 12 sorghum production sites in Nebraska. This analysis was based on a squre havest grid (5.0 km) and one month move times.

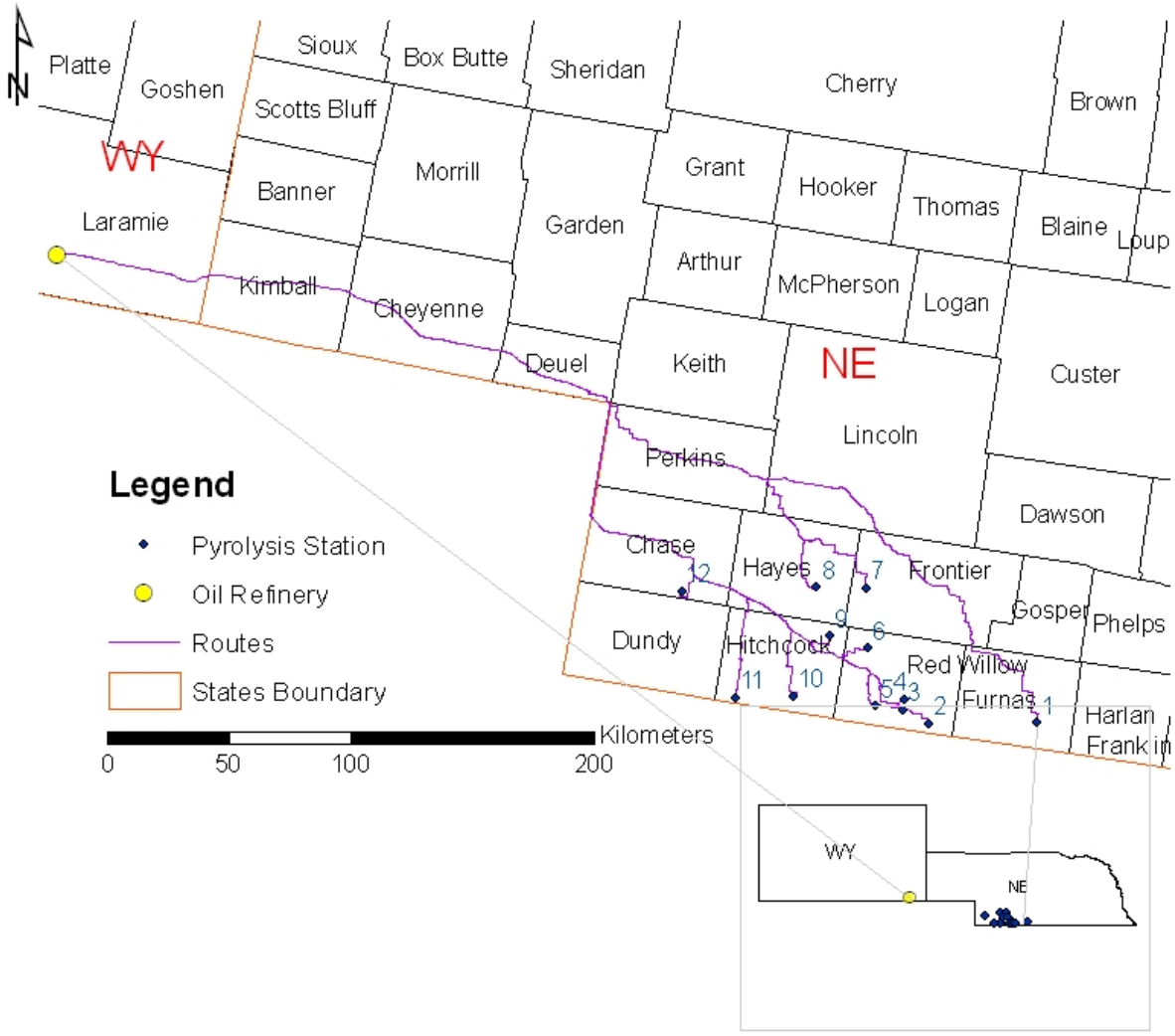

Figure 2.8. The optimized route map from mobile pyrolysis stations to the nearest oil refinery for the top 12 sorghum production sites in Nebraska. This analysis was based on a squre harvest grid (5.0 km) and a one month move time.

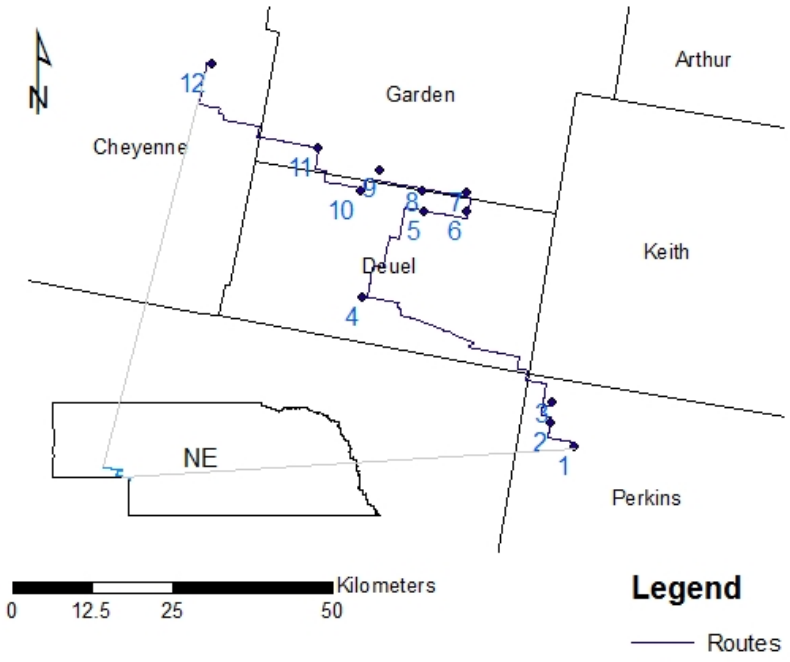

Figure 2.9. The optimized route map from a mobile pyrolysis unit to move to the top 12 switchgrass production sites in Nebraska. This analysis was based on a squre havest grid (3.3 km) and one month move times.

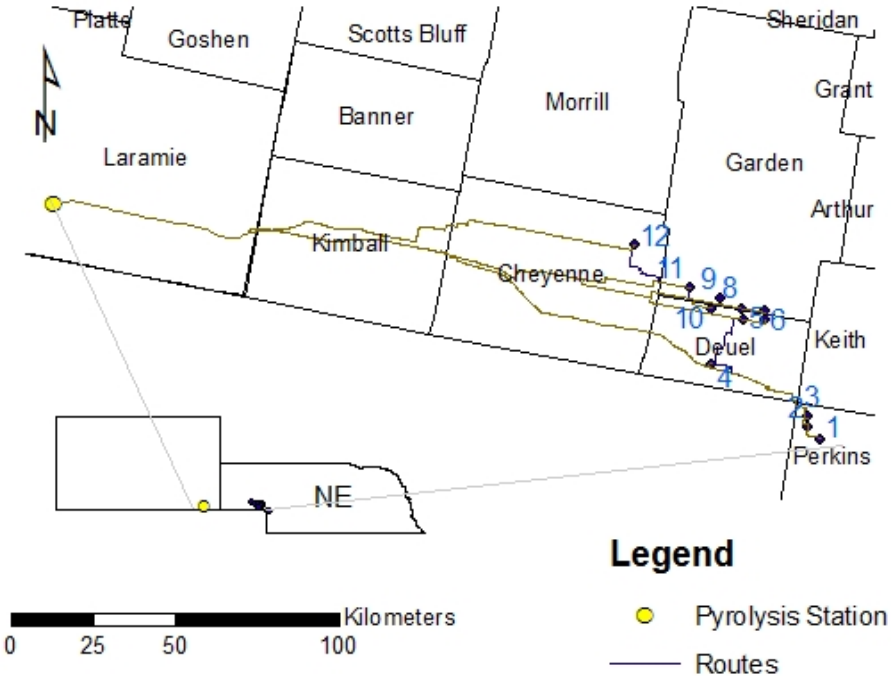

Figure 2.10. The optimized route map to transort bio-oil from mobile pyrolysis stations to the nearest oil refinery in Laramie, WY, for the top 12 switchgrass production sites in Nebraska. This analysis was based on a squre harvest grid (3.3 km) and a one month move time.

Table 2.2. The average, minimum, and maximum distances to transport from the mobile pyrolysis station to the next station for three feedstocks (corn stover, energy sorghum, and switchgrass) in IL or NE, based on one year scenarios (monthly, bi-monthly, quaterly, bi-annnual and stationary).

Feedstock	Corn stover (IL)			Energy sorghum (NE)			Switchgrass (NE)		
	Distance (km)			Distance (km)			Distance (km)		
Move time (mo.)	Avg.	Min.	Max.	Avg.	Min.	Max.	Avg.	Min.	Max.
1	48.4	2.1	138.7	31.7	4.4	68.6	13.4	3,0	41.9
2	60.8	8.5	139	27.6	5.6	45.3	17.2	4.8	38.4
4	31.5	8.2	54.7	33.4	13.1	53.6	19.8	18.1	21.5
6	78.6	-	-	18.3	-	-	16.1	-	-
8	27.9	-	-	57.9	-	-	60.7	-	-
10	77.4	-	-	81.0	-	-	22.6	-	-
12	Stationary			Stationary			Stationary		

Table 2.3. The average, minimum and maximum distances to transport bio-oil from mobile pyrolysis stations to the closest refinery for three feedstocks (corn stover, energy sorghum, and switchgrass) in IL or NE.

Feedstock	Corn stover (IL)			Energy sorghum (NE)			Switchgrass (NE)		
	Distance (km)			Distance (km)			Distance (km)		
Move time (mo.)	Avg.	Min.	Max.	Avg.	Min.	Max.	Avg.	Min.	Max.
1	128	81	194	438.1	365.3	521.7	227.5	192.1	265.0
2	137	105	195	437.2	393.1	475.0	217.0	195.2	235.2
4	111	102	125	443.6	416.2	461.1	218.5	203.3	234.1
6	139	102	177	470.4	461.6	479.2	222.4	217.8	227.0
8	93	84	102	439.5	412.0	467.0	242.9	224.6	261.1
10	143	107	178	440.0	405.5	474.5	227.2	221.5	232.9
12	102	-	-	474.3	-	-	218.5	-	-

Conclusions

A GIS system was developed to assess feedstock logistics. It was used to determine the optimum locations for mobile pyrolysis units in the NC region based on feedstock availability. The feedstocks evaluated were corn stover, energy sorghum, and switchgrass. Feedstock logistics were evaluated for move times of 1 to 12 months for the mobile pyrolysis units. The GIS program determined the distances required to move, 1) feedstock from production fields to the mobile pyrolysis station, 2) the mobile pyrolysis unit from one pyrolysis station to the next station, and 3) bio-oil from the pyrolysis stations to the nearest oil refinery.

The GIS analysis used a square harvest grid to calculate the biomass available at each pyrolysis station. The size of the harvest grid depends on both the move time of the mobile pyrolysis unit and the feedstock production rates. The GIS program used Model Builder to automate the feedstock logistics analysis. Network Analysis was used to calculate the shortest routes to move the mobile pyrolysis units from station to station as well as to move bio-oil to the nearest refinery. The GIS analysis was integrated with an economic model to calculate the total cost for bio-oil production using mobile pyrolysis units.

A major strength of the mobile pyrolysis unit is its flexibility to move processing to the feedstock production areas avoiding the need to move low-density feedstocks long distances to a central plant. The feedstock input rate for one mobile pyrolysis unit was assumed to be 40 tons/day. Therefore, a single mobile pyrolysis unit would be capable of producing 17,381 barrels of bio-oil per year. Using these assumptions then 853 mobile pyrolysis units would be needed to process all of the corn stover feedstock

(limited to only 25% of the total available) for Illinois at 2008 production rates. To process all of the energy sorghum feedstock (energy sorghum was assumed to replace grain sorghum) in Nebraska, 27 mobile pyrolysis units would be needed. And to process all of the switchgrass feedstock in Nebraska (switchgrass was assumed to be planted on all suitable CRP land), 56 mobile pyrolysis units would be needed. This would result in, 1) 14,825,993 barrels of bio-oil produced in Illinois from 25% of the corn stover, 2) 469,287 barrels of bio-oil produced in Nebraska from energy sorghum, and 3) 973,336 barrels of bio-oil produced in Nebraska from switchgrass. The total bio-oil produced would be 16,268,616 barrels of bio-oil per year.

Task 3: Biochar Characterization and Analysis (Tony Provin)

Original Hypothesis

The pyrolysis of biomass will result in loss of all plant available nitrogen, but will conserve plant available nutrients, although these nutrients will likely require environmental weathering prior to becoming plant available.

Approaches Used (Methodology)

Three methods were used to determine the impact of pyrolysis on the availability of plant nutrients. These approaches included 1) development of a mini-scale laboratory slow batch pyrolyzer for the evaluation of nutrient recovery from multiple feedstocks, 2) The same feedstocks were also analyzed using two different fluidized bed fast pyrolyis units, 3) incorporation and incubation of biochar into soil to measure the influence of biochar application and biochar type on soil pH, salinity, and plant available nutrients, and 4) broadcast and incorporate biochar into soil to determine the influence on plant growth.

Problems Encountered and Changes in Methodology

Initial problems with seedling emergence in an initial greenhouse study led to a more aggressive evaluation of soil salinity, modification of soil pH and the impact of residual oil on seedling emergence and development. No modifications were made to the growth studies, however separate laboratory studies were developed or modified to address and measure the relative impact of soluble salts, pH modification and residual oils.

During the development of the pyrolyzer, every attempt was made to construct an all stainless steel or polymer furnace and gas flow path to insure full recovery of all pyrolysis bi-products. Unfortunately, the full recovery of all combustion products following every individual run was determined too time-consuming and risked the probability of new gas leaks, therefore six individual runs, considered sub-replicates, were combusted and the all byproducts for all six runs were pooled as a single replication. Even the increased number of combustion events per recognized replication failed to full address the removal of all residues and as a result, some coke type residues were impossible to remove from the stainless steel tubing with normal non-high temperature or chemical means.

The mobility of the very low density biochar on the surface or within the soil created significant problems during runoff studies. The biochar quickly segregates from soil upon drying and soil pulverization. The soil/biochar mixes were required to be split multiple times with sample drifters, thereby eliminating errors associated with segregation of soil and biochar when conducting soil analyses.

Impact of Changes in Methodology on Project Results

The impact of methodology changes were implemented to improve data integrity, as well as, eliminate problems with analysis and interpretation of results. The most significant methodology change was the use of a sample drifter that required numerous laborious passes to reduce the sample sizes to the required range allowed for laboratory soil analyses. These changes only enhance the data integrity, however from a routine laboratory analyses perspective, these steps are far an above those that would ever be used by private or public soil testing laboratories. As a result, the ability for close accurate monitoring of soil nutrient status of biochar applied fields still remains limited.

Analysis of Results (Tables and Figures)

The recovery of nutrients in biochar were dependant on pyrolyzer conditions, nutrient and species/feedstock.

Table 3.1. Recovery of P, K, Ca, and Mg from Slow Pyrloysis system.

Species	P	Std Dev	K	Std Dev	Ca	Std Dev	Mg	Std Dev
%								
Bio-char co-product								
Corn stover	49.9c†	20.5	30.1a	12.8	60.8a	26.7	61.5b	26.1
Switchgrass	159.8a	64.9	10.7c	2.8	67.0a	8	83.1a	20.1
HES	90.5b	20.3	4.8d	1.8	55.9a	12.6	38.3c	12.2
Rice stover	52.1c	3.4	18.4b	0.9	40.7b	2.8	45.1c	2.5
Bio-oil co-product								
Corn stover	0.1b	0.1	0.1b	0	0.3b	0.1	1.7a	1.5
Switchgrass	0.3a	0.4	0.26a	0.16	4.5ab	8.8	3.0a	2.5
HES	0.2ab	0.2	0.1b	0	5.6a	5.7	2.8a	2
Rice stover	0.1b	0.1	0.1b	0.05	0.6b	0.4	2.4a	1.6
NCG co-product								
Corn stover	0.2b	0.1	0.1b	0	2.1b	0.6	0.1c	0
Switchgrass	3.4a	2.3	1.3a	0.9	6.5a	1.5	6.6a	1.1
HES	1.0b	1.2	0.1b	0.1	5.4a	3.2	2.9b	1.4
Rice stover	0.1b	0.1	0.1b	0	4.3ab	4.2	0.1c	0.1
Co-products combined								
Corn stover	50.1c	20.5	30.3a	12.8	63.2b	26.6	63.3b	25.4
Switchgrass	163.5a	64.5	12.3c	2.9	78.1a	8.2	92.8a	21.7
HES	91.6b	20	5.0d	1.8	66.9ab	11.3	44.0c	13.1
Rice stover	52.2c	3.4	18.6b	1	45.6c	5.7	47.6c	3.2

Table 3.2. Recovery of P, K, Ca, and Mg from Fast Fluized Bed Pyrolyzers

Species	P	Std Dev	K	Std Dev	Ca	Std Dev	Mg	Std Dev
			%					
Bio-char co-product (Wyndmoor, PA)								
Corn stover	65.4a†	16.8	53.1a	3.9	63.2a	10.6	57.8a	3
HES	56.5a	9.7	54.0a	8.3	57.9a	8.2	36.0b	5.3
Switchgrass	30.1b	6.7	8.9b	1.2	38.5b	5.8	14.3c	1.4
Bio-oil co-product (Wyndmoor, PA)								
Corn stover	5.2a	2	2.1a	0.7	5.3a	1.3	7.7a	2
HES	2.0a	2	0.9a	0.6	2.3a	1.9	3.3a	1.7
Switchgrass	5.5a	4.4	2.1a	1.5	6.1a	4.7	7.7a	4.5
Bio-char and bio-oil combined (Wyndmoor, PA)								
Corn stover	70.8a	14.8	55.1a	3.3	68.5a	17.7	65.5a	7.1
HES	58.6a	8.5	54.8a	8	60.2a	4.7	39.3b	3.6
Switchgrass	35.5b	5.5	11.0b	1.7	44.6b	5.7	22.0c	1
Bio-char co-product (College Station, TX)								
Corn stover	37.8a†	0.8	46.64a	1.4	61.1a	3.2	47.2a	2.6
HES	49.9a	19.1	46.48a	21.5	40.5a	18.4	38.9a	18.9
Switchgrass	47.6a	7.9	38.72a	3.8	41.6a	6.3	37.0a	5.4
Bio-oil co-product (College Station, TX)								
Corn stover	0.9a	0.2	0.75a	0.2	1.8a	0	1.0a	0.1
HES	0.8a	0.4	1.10a	0.8	1.8a	0.3	1.2a	0.4
Switchgrass	0.8a	0.7	0.96a	0.8	0.7a	0.3	1.0a	0.7
Bio-char and bio-oil combined (College Station, TX)								
Corn stover	38.6a	1	47.4a	1.5	62.9a	3.2	48.3a	2.7
HES	50.8a	19.5	47.6a	22.3	42.3a	18.2	40.0a	19.1
Switchgrass	48.4a	8.2	39.7a	3.8	42.3a	6.3	38.0a	5.4

Overall, the recovery of plant macro and secondary nutrients was greatest in the biochar, however significant losses of nutrients were observed across all species and platforms.

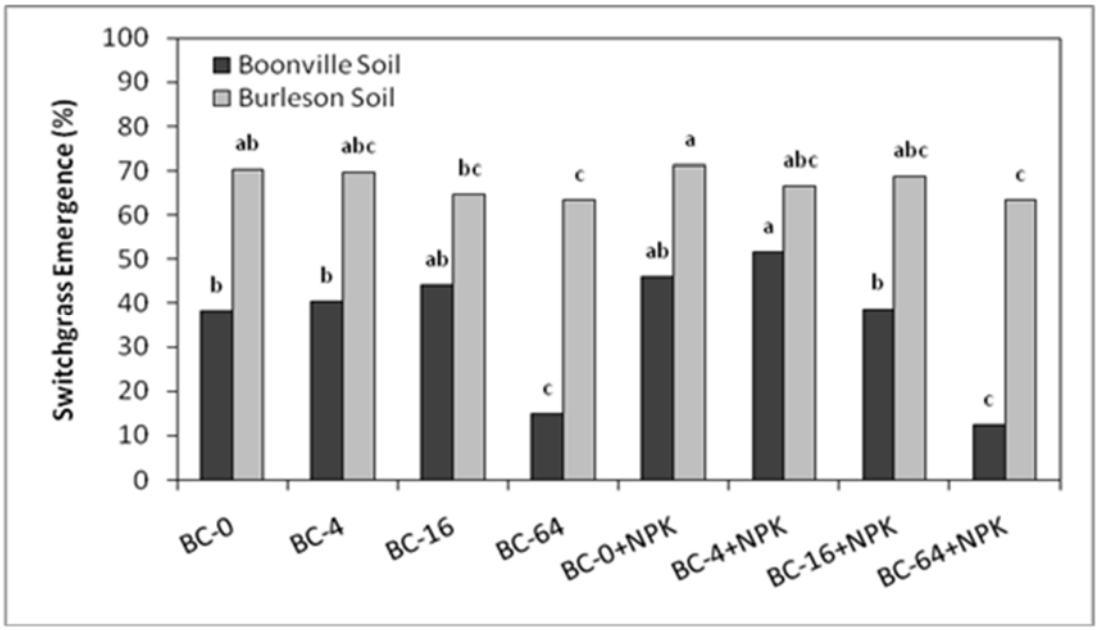

Figure 3.1. Seedling emergence of switchgrass with varying sorghum derived biochar applied at various rates on two soils. Switchgrass emergence for Boonville and Burleson soils alone and amended with 4, 16, and 64 Mg biochar (BC) ha^{-1}, with and without supplemental N-P-K fertilizer. Letters above bars indicate mean separation using LSD (P = 0.05).

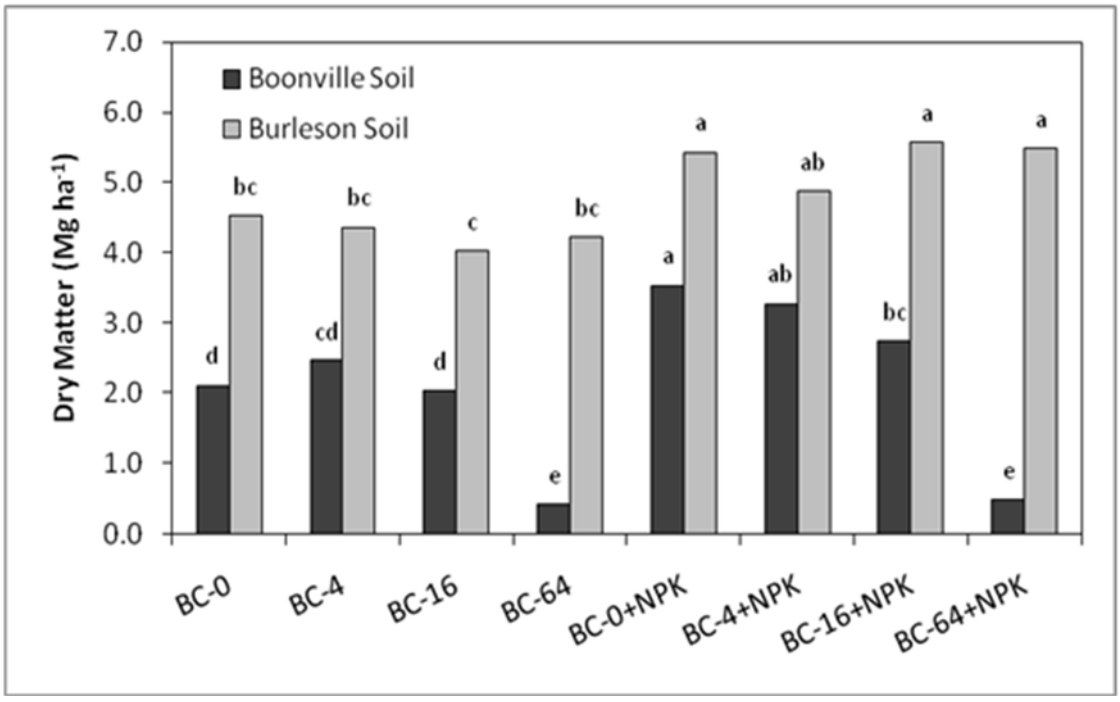

Figure 3.2. Mean dry matter production of switchgrass for Boonville and Burleson soils alone and amended with 4, 16, and 64 Mg biochar (BC) ha^{-1}, with and without supplemental N-P-K fertilizer. Letters above bars indicate mean separation using LSD (P = 0.05).

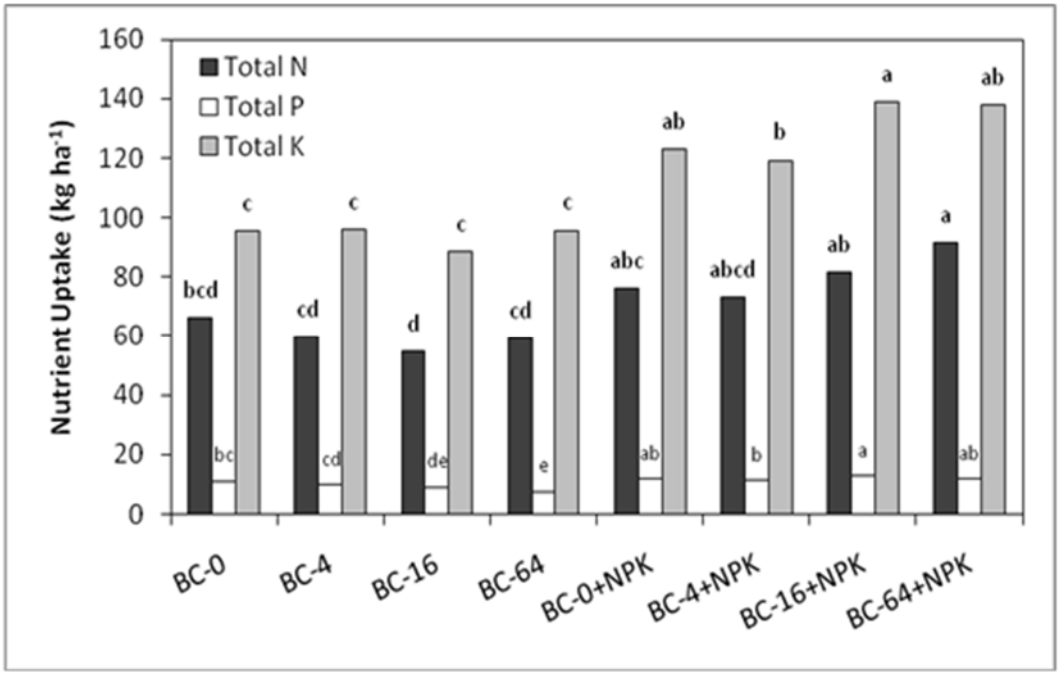

Figure 3.3. Uptake of total N, P, and K in aboveground switchgrass biomass for the Burleson soil alone and amended with 4, 16, and 64 Mg biochar (BC) ha^{-1}, with and without supplemental N-P-K fertilizer. Letters above bars indicate mean separation using LSD (P = 0.05).

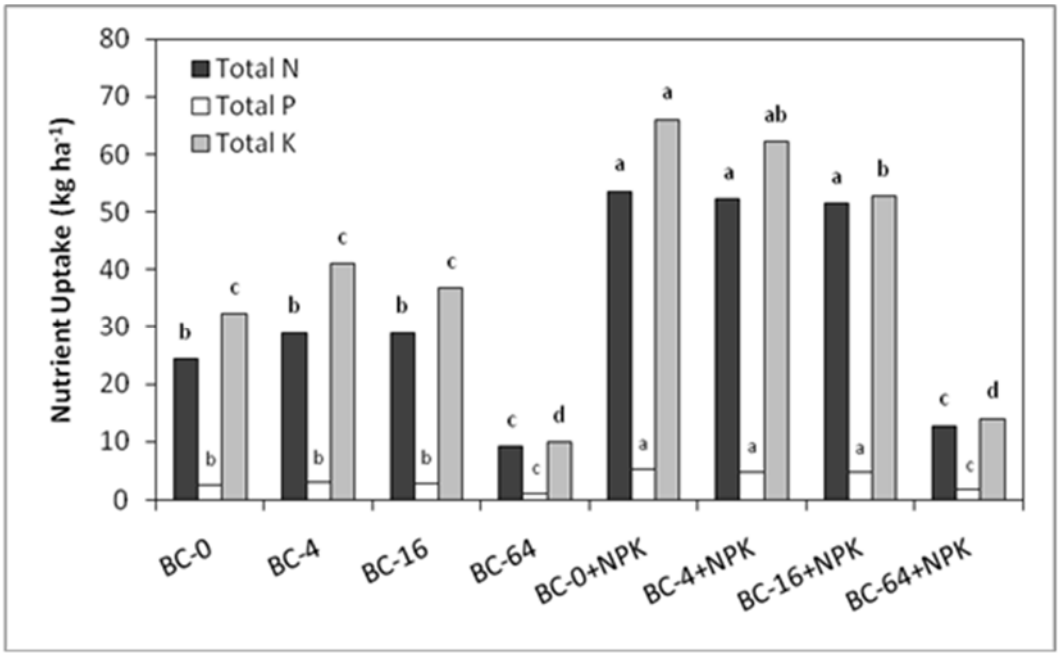

Figure 3.4. Uptake of total N, P, and K in aboveground switchgrass biomass for the Boonville soil alone and amended with 4, 16, and 64 Mg biochar (BC) ha^{-1}, with and without supplemental N-P-K fertilizer. Letters above bars indicate mean separation using LSD (P = 0.05).

Table 3.3. Percent N, P, and K applied as biochar at 4, 16, and 64 Mg biochar (BC) ha^{-1}, with and without supplemental N-P-K fertilizer, taken up by switchgrass in the Boonville soil. BC -N, -P, and -K taken up in switchgrass is calculated as the difference in plant uptake between control treatments (BC-0 or BC-0+NPK) and 4, 16, or 64 Mg BC ha^{-1} (with or without supplemental N-P-K fertilizer), divided by the N, P, and K rate applied as biochar.

	Total N			**Total P**			**Total K**		
	Applied as BC	Plant Uptake	BC-N Taken up in Switchgrass	Applied as BC	Plant Uptake	BC-P Taken up in Switchgrass	Applied as BC	Plant Uptake	BC-K Taken up in Switchgrass
Treat-ment	kg ha^{-1}	kg ha^{-1}	%	kg ha^{-1}	kg ha^{-1}	%	kg ha^{-1}	kg ha^{-1}	%
BC-0	0	24.3	0.0	0	2.6	0.0	0	32.3	0.0
BC-4	76	29.0	6.2	8	2.8	2.5	12	41.0	72.5
BC-16	300	28.9	1.5	33	2.8	0.6	49	36.7	9.0
BC-64	1198	9.1	-1.3	130	1.0	-1.2	196	10.0	-11.4
BC-0+NPK	0	53.6	0.0	0	5.3	0.0	0	66.1	0.0
BC-4+NPK	76	52.2	-1.8	8	4.7	-7.5	12	62.1	-33.3
BC-16+NPK	300	51.4	-0.7	33	4.6	-2.1	49	52.7	-27.3
BC-64+NPK	1198	12.7	-3.4	130	1.6	-2.8	196	14.0	-26.6

Table 3.4. Percent N, P, and K applied as biochar at 4, 16, and 64 Mg biochar (BC) ha^{-1}, with and without supplemental N-P-K fertilizer, taken up by switchgrass in the Burleson soil. BC -N, -P, and -K taken up in switchgrass is calculated as the difference in plant uptake between control treatments (BC-0 or BC-0+NPK) and 4, 16, or 64 Mg BC ha^{-1} (with or without supplemental N-P-K fertilizer), divided by the N, P, and K rate applied as biochar.

	Total N			**Total P**			**Total K**		
	Applied as BC	Plant Uptake	BC-N Taken up in Switchgrass	Applied as BC	Plant Uptake	BC-P Taken up in Switchgrass	Applied as BC	Plant Uptake	BC-K Taken up in Switchgrass
Treat-ment	kg ha^{-1}	kg ha^{-1}	%	kg ha^{-1}	kg ha^{-1}	%	kg ha^{-1}	kg ha^{-1}	%
BC-0	0	66.0	0.0	0	10.9	0.0	0	95.5	0.0
BC-4	76	59.5	-8.6	8	9.7	-15.0	12	96.0	4.2
BC-16	300	54.5	-3.8	33	8.9	-6.1	49	88.5	-14.3
BC-64	1198	59.1	-0.6	130	7.6	-2.5	196	95.8	0.2
BC-0+NPK	0	76.3	0.0	0	11.8	0.0	0	122.9	0.0
BC-4+NPK	76	73.3	-3.9	8	11.3	-6.3	12	119.1	-31.7
BC-16+NPK	300	81.4	1.7	33	12.8	3.0	49	139.0	32.9
BC-64+NPK	1198	91.4	1.3	130	11.7	-0.1	196	137.9	7.7

Little to no N, P or K was taken up by the switchgrass in either the sandy Boonville or Burleson clay soil, suggesting the application of biochar nutrients are either not in plant available forms or the biochar application resulted in poor growing conditions, thus limiting dry matter yields and nutrient uptake.

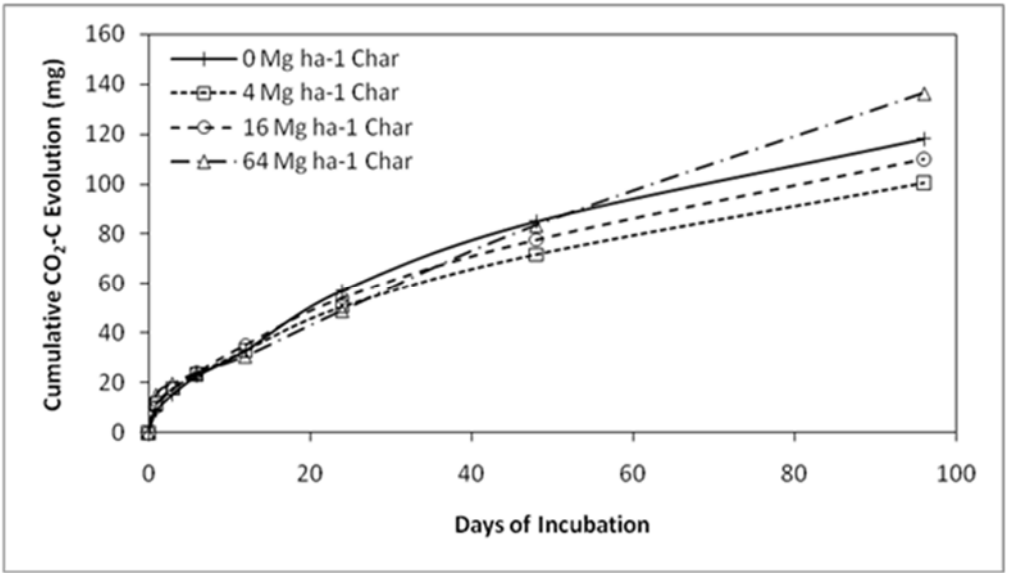

Figure 3.5. Mean cumulative CO_2-C evolution from Boonville soil alone and with 4, 16, and 64 Mg ha^{-1} of biochar during a 96-day incubation.

Limited to no net mineralization of carbon from the biochar was observed following 96 days of incubation and carbon dioxide trapping. This suggests that the carbon and nitrogen in the biochar is at least in the short-term considered extremely stable and not microbially available.

Back to Table of Contents

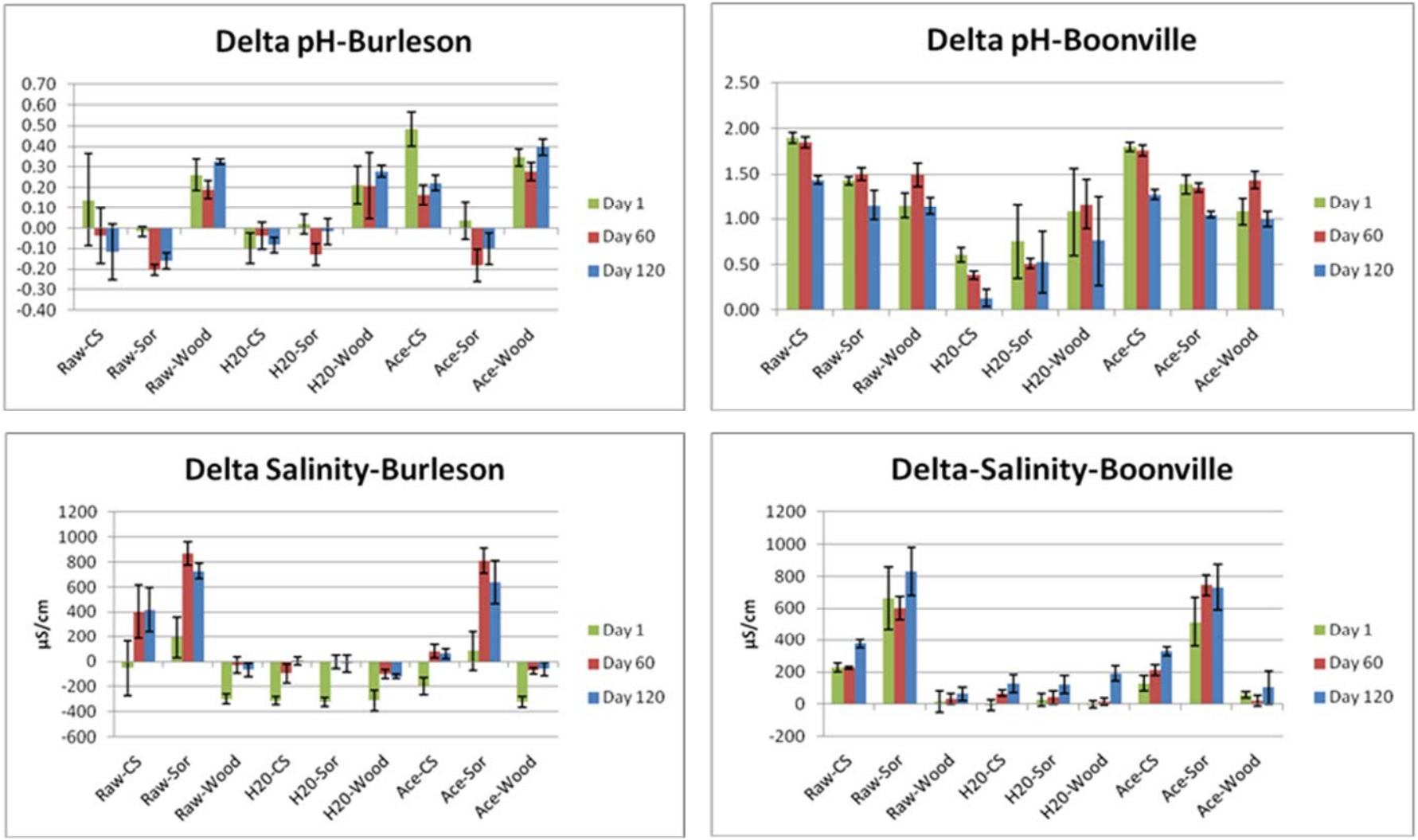

Figure 3.6. Influence of soil pH and salinity following addition of three biochars that have been unwashed, D.I. water washed and acetone washed to remove residual oils.

The influence of biochar, unwashed, washed or solvent washed was mixed, with some treatments resulting in lowering pH levels in the clay Burleson soil, while uniformly, the addition of biochar to the acid sandy Boonville soil resulted in significant increases in soil pH. Similar results were observed for salinity measurements.

Conclusions

Recovery of feedstock plant nutrients is highly dependent on feedstock source and pyrolyzer operating conditions. The plant availability of major plant nutrients by plants appear to be limited in the short-term by the relatively high increases in soil pH and soil salinity. Careful attention on the soil placement of these biochars to prevent a derogatory soil environment what may either limit root development, or result in rapid migration of the biochar to roots or be subject to erosion and thereby impair local surface waters.

Project Activities

Task 4: Feasibility and Economic Analysis (Marco Palma)

Original Hypothesis

- The cost per gallon of producing bio-oil varies depending on the feedstock source and also depending on the number of times the mobile unit needs to be moved.
- There is a threshold level that makes pyrolysis economically feasible in terms of either the cost of production or the price of oil.
- There may be additional processing that may add value to char and syngas.
- The mobile nature of the systems allows to look at historic data in terms of weather impacts.

Approaches Used (Methodology)

This project analyzed the economic feasibility of a mobile bioenergy pyrolysis system using a Monte Carlo simulation model. Pyrolysis transforms any cellulosic materials into i) a bio-oil similar to crude oil ii) a synthesis gas similar to natural gas, and iii) a bio-charcoal substance. The pyrolyzer machine is currently being manufactured and tested with various types of feedstocks including corn stover and energy sorghum. The economic analysis focused on creating an automated process that integrates a transportation logistics cost optimization model with geographic information system (GIS) data. The geographic data provides possible paths for the mobile bioenergy pyrolysis unit as it moves to and from each harvest area, depending on stochastic availability of feedstock (determined by historical crop yields) and distance to oil refineries. The results indicated that there is a low probability of a positive Net Present Value (NPV) with current economic conditions. In general, the NPV was highest with a stationary scenario and it decreased with additional moving times. A sensitivity analysis is presented to assess the potential probability of success of a mobile pyrolysis system under alternative oil prices and feedstock costs scenarios.

Problems Encountered and Changes in Methodology

A few issues of logistics were worked out with the GIS group to ensure enough feedstock supply to operate the pyrolizer. We also discovered a threshold level for the cost of feedstock that would make the system economically feasible.

Impact of Changes in Methodology on Project Results

We show differences in the results by different scenarios of operating alternative feedstock products and prices of oil.

Analysis of Results (Tables and Figures)

The most critical output variable from the model for evaluating the economics of pyrolysis is the net present value (NPV). The model calculates NPV as follows:

$$NPV = -\left(BeginningNetWorth\right) + \sum_{j=1}^{10} \frac{Dividends_j}{\left(1+i\right)^j} + \frac{EndingNetWorth}{\left(1+i\right)^{10}} \quad (1)$$

Equation 1 calculates NPV (assuming a discount rate of i = 5%) of dividends paid to investors and net worth over the life of the investment (ten years), and compares that value to the net worth at the beginning

of the investment. If the value of NPV is greater than zero, the business is considered an economic success (Richardson and Mapp 1976).

The major income-generating product is a bio-oil, equivalent to crude oil, which is transported to the nearest refinery, and sold at a 5% discount from the price of crude oil. The mean bio-oil price for 2011 was $78.54/barrel. The value for bio-char is determined based on the soil amendment value as a soil additive. According to Wise et al. (2011), char produced in 2011 can be sold for $24 per ton and it's value varies by feedstock. Syngas is assumed to be used as an energy source to sustain the pyrolysis unit and it is not generating revenue. Its production also varies with the level of moisture in the initial feedstock and by feedstock. Both the price of bio-oil (PO) and char (PC), along with the price of crude oil, are inflated annually and used to determine net income over the life of the business (Richardson et al., 2011). The model assumes a $1.00/gallon subsidy (S) for pyrolysis bio-oil offered as an incentive throughout the analysis period, as this is the current subsidy for second generation biofuels. Income is calculated as:

$$\text{Income}=(PO+S)*Q(\text{Bio oil})+PC*Q(\text{Char})+P*Q(\text{Syngas}) \quad (2)$$

Income is stochastic because prices are drawn at random from probability distributions estimated from historical series. Other random variables include feedstock yield and prices, as well as the inputs and outputs. Syngas revenue is included for eventual analysis of excess syngas production but not included in this analysis.

An input to the financial simulation model was output from a transportation logistics cost optimization model with geographic information system (GIS). The analysis includes 15 alternative scenarios, including 3 stations/sources of feedstocks, and 5 frequencies for moving the mobile pyrolysis unit. The three sources of feedstock are corn stover in Illinois and Texas, and energy sorghum in Nebraska; the unit can be moved monthly, bi-monthly, quarterly, bi-annually, or it can be stationary. Table 4.1 summarizes the model scenarios for pyrolysis bio-oil production.

In addition to the transportation costs, there are also other set up costs associated with moving the pyrolysis unit. A hard surface movable pad and access road is needed around the pyrolysis unit, as this is a high traffic area. A portable military-grade "matting system" from GFI Inc., is used with interlocking mats measuring 6 feet by 6 feet with a unit cost of $450. A ¾ acre area is used requiring 908 mats for a total cost of $408,600. This pad area includes set up of machinery and storage of feedstock area. The access road is a 120 feet by 12 feet with a cost of $18,000. The labor cost to dismantle and assemble the movable mats in a new location each time the mobile pyrolysis unit is moved is $2,500.

Table 4.1. Model Scenarios for Bio-oil Production

Scenario	Name	Source	Frequency of Moving
1	IL 12M	Corn stover, IL	Monthly
2	IL 6M	Corn stover, IL	Bi-Monthly
3	IL 4M	Corn stover, IL	Quarterly
4	IL 2M	Corn stover, IL	Bi-Annual
5	IL 0M	Corn stover, IL	Stationary
6	TX 12M	Corn stover, TX	Monthly
7	TX 6M	Corn stover, TX	Bi-Monthly
8	TX 4M	Corn stover, TX	Quarterly
9	TX 2M	Corn stover, TX	Bi-Annual
10	TX 0M	Corn stover, TX	Stationary
11	NE 12M	Energy sorghum, NE	Monthly
12	NE 6M	Energy sorghum, NE	Bi-Monthly
13	NE 4M	Energy sorghum, NE	Quarterly
14	NE 2M	Energy sorghum, NE	Bi-Annual
15	NE 0M	Energy sorghum, NE	Stationary

Drying the feedstock presents a logistics issue. Moisture content of the feedstock can be anywhere from 25%-50% depending on field and weather conditions. The maximum optimal moisture content for feedstock at the pyrolyzer is 10% (Capunitan and Capareda 2010). The pyrolysis unit operating at 40 tons of feedstock as is per day generates enough BTUs to dry the feedstock to the 10% acceptable level for efficient operation of the machine (Capunitan and Capareda 2010). Energy start-up costs to initially power (heat up) the unit as well as replacement of bed sand amount to $2,000. Syngas generates sufficient heat to dry and process the feedstock once the unit has reached steady state.

The pyrolyzer can produce an average of 50 gallons of bio-oil per ton of corn stover and 45 gallons of bio-oil per ton of energy sorghum across expected moisture levels ranging from 10-40% wet basis (Capareda 2010). The pyrolysis unit has the capacity to process 40 tons of feedstock as is per day for 290 to 326 days per year, for the 12M vs 0M scenarios, respectively. On average, producers are paid a price of $67.5 per ton of feedstock delivered to the edge of the field, with a range from $60-$75 per ton depending on moisture content. The model assumes 11% of wasted feedstock during the logistics of transporting, storage and processing. The price for the feedstock includes the opportunity costs associated with additional fertilizer applications needed to replace nutrients. It is assumed that one pound of corn grain is equal to one pound of available corn stover (Pordesimo et al. 2004); however, only 25% of the available biomass in the fields will be harvested, leaving the remaining 75% on the fields for erosion control and soil sustainability purposes (Nelson 2002). The mobile pyrolysis business will own all handling, processing, and transportation equipment.

Total capital assets (beginning net worth) for the mobile pyrolysis unit are $2,169,516 and will be financed with 50% equity and 50% debt at a 7% interest rate over a 10 year period. If net cash income is positive, investors receive a dividend equal to 15% of net cash income each year. The initial capital investment in assets includes the pyrolysis machine, movable pads, access road, storage and transportation of feedstock and bio-oil. Mobile pyrolysis model assumptions are presented in Table 4.2, and initial capital assets in Table 4.3.

Table 4.2. Mobile Pyrolysis Model Assumptions

Variable	Unit	Value
Corn stover cost	$/ton	GRKS(60,67.5,75)
Energy sorghum cost	$/ton	GRKS(60,67.5,75)
Corn stover to oil conversion	gal/ton	GRKS(40,50,60)
Energy sorghum to oil conversion	gal/ton	GRKS(35,45,55)
Corn stover to char conversion	ton/ton	0.237
Energy sorghum to char conversion	ton/ton	0.254
Operation processing	tons/day	GRKS(30,40,50)
Wasted feedstock per day	%	11.0
Processing bio-oil to crude equivalent	$/gal	GRKS(0.20,0.30,0.40)
Discount bio-oil from crude	%	5.0
Subsidy for bio-oil	$/gal	1.00
Costs of Mobile Unit		
Fraction of unit financed	fraction	0.5
Length of loan	years	10
Interest rate	%	5.0
Operating Loan Interest Rate	%	7.0
Dividend rate on equity borrowed	%	15.0

The projected mean values for the total cost of production per barrel of bio-oil from the mobile pyrolysis unit ranged from $142 to $167 depending on the production scenario. Costs were broken down by feedstock costs and other costs. Other costs include the transportation costs, processing costs and finance costs (Table 4.3).

The simulation results showed a negative mean NPV for all 15 scenarios. The NPV improves (less negative) as the number of moving times is decreased. For corn stover in Illinois, the mean NPVs go from -$2.2 million with a monthly moving schedule to -$1.4 million with a stationary pyrolysis unit. Corn stover in Texas had mean NPVs from -$2.1 million to -$1.4 million if the plant is moved monthly vs. a stationary pyrolyzer. For energy sorghum in Nebraska the NPV was -$7.7 million with monthly moves and -$4.9 million for a stationary machine. The stationary plants had higher NPVs due to the savings from not moving the plant that were higher than the extra cost of longer hauls for feedstock and biochar to and from the field.

Table 4.3. Mean Values for Estimated Costs of Production and Revenue of Pyrolysis Bio-oil Production for 15 Scenarios

Scenario	Cost Feed	Total Cost	Revenue	Net Revenue
	$/barrel	$/barrel	$/barrel	$/barrel
Illinois				
12 moves	63	151	122	-30
6 moves	63	146	122	-25
4 moves	63	144	122	-23
2 moves	63	144	122	-22
stationary	63	142	122	-21
Texas				
12 moves	63	151	122	-29
6 moves	63	146	122	-25
4 moves	63	144	122	-23
2 moves	63	143	122	-22
stationary	63	143	122	-21
Nebraska				
12 moves	70	167	122	-45
6 moves	70	163	122	-41
4 moves	70	160	122	-38
2 moves	70	159	122	-37
stationary	70	158	122	-36

A sensitivity analysis with changes in the level of crude oil prices, the costs of feedstock, and conversion efficiency of feedstock to bio-oil, and their impact on the economic feasibility of the mobile pyrolysis model was performed. NPV would improve if feedstocks could be obtained at a lower cost than the current mean of $67.5/ton. A 10% reduction of feedstock purchasing price, i.e. $60.8/ton would increase the probability of success from 16 to 29% for scenario IL 0M, from 15 to 27% for TX 2M and from 2 to 6% for NE 2M. In general, a probability of 90% or higher is typically regarded as a good chance of economic viability of a project as evaluated by investors. A 50% reduction in feedstock price, i.e. $33.8/ton, would increase the probability of success with 8 out of the 15 scenarios having a 90% or higher chance of success. With feedstock costs of about $16.9/ton all scenarios in all locations show a higher than 90% chance of economic success (Table 4.4).

Table 4.4. Sensitivity Analysis of the Impact of Cost of Feedstock to the Probability of Success of each Scenario (NPV>0)

	Baseline	**10%**	**25%**	**50%**	**75%**
	$67.5/ton	$60.8/ton	$50.6/ton	$33.8/ton	$16.9/ton
Illinois					
12M	5%	12%	27%	74%	100%
6M	10%	18%	42%	88%	100%
4M	14%	23%	48%	92%	100%
2M	15%	25%	50%	93%	100%
0M	16%	29%	55%	95%	100%
Texas					
12M	4%	11%	29%	76%	100%
6M	11%	21%	42%	87%	100%
4M	14%	25%	49%	91%	100%
2M	15%	27%	52%	93%	100%
0M	5%	17%	59%	99%	100%
Nebraska					
12M	0%	1%	6%	36%	88%
6M	1%	3%	12%	50%	97%
4M	2%	5%	15%	61%	99%
2M	2%	6%	16%	63%	99%
0M	0%	1%	8%	75%	100%

A sensitivity analysis on the price of oil was also conducted. An average increase of 10% in oil prices over the ten-year horizon, from $79.4 to $87.3 per barrel in 2011 would increase the range of probability of success from 0-16% to 2-37%, respectively. An average increase of 50% in oil prices ($119.1 in 2011) would increase the probability of success ranges to 59-100%, with 9 scenarios with a 90% or higher probability of economic success. With mean oil prices of $139.0/barrel in 2011 all scenarios in all locations show a greater than 90% chance of economic success (Table 4.5).

Table 4.5. Sensitivity Analysis on the Impact of Crude-oil prices ($/barrel) to the Probability of Success of each Scenario (NPV>0)

	Baseline	**10%**	**25%**	**50%**	**75%**
Illinois					
12M	5%	15%	46%	90%	99%
6M	10%	25%	58%	94%	100%
4M	14%	32%	63%	96%	100%
2M	15%	33%	66%	97%	100%
0M	16%	37%	70%	97%	100%
Texas					
12M	4%	17%	47%	90%	100%
6M	11%	27%	59%	94%	100%
4M	14%	32%	63%	96%	100%
2M	15%	33%	65%	96%	100%
0M	5%	30%	79%	100%	100%
Nebraska					
12M	0%	3%	15%	59%	92%
6M	1%	6%	23%	68%	95%
4M	2%	7%	28%	74%	97%
2M	2%	8%	29%	75%	98%
0M	0%	2%	24%	88%	100%

Conclusions

The results showed a low probability of economic success for all scenarios ranging from 0% to 16%. In Illinois, the probability of success increases as the number of moving times is decreased, with a stationary unit having the highest probability of success. In the case of corn stover from Texas and energy sorghum from Nebraska, the probabilities of success increased as the moving schedule is less frequent, except for a stationary unit. For a stationary unit located in Texas and Nebraska, the maximum and minimum receipts are higher than for the mobile scenarios. A stationary unit has higher production compared to mobile scenarios, hence, reducing downside risk and increasing net returns.

A sensitivity analysis of changes in the cost of feedstock showed that if feedstock cost were reduced to $16.9/ton, all scenarios in all locations would have a 90% or higher probability of a positive NPV. Similarly, if mean crude oil prices are greater than of $139 per barrel in 2011 over the ten-year planning horizon all scenarios in all locations show a higher than 90% chance of economic success. If the conversion efficiency of feedstock to bio-oil is increased to 70-90 gallons of bio-oil per ton of feedstock (Capareda et al., 2010; Wise et al., 2011) then the probability of success is higher than 99% for all scenarios in all locations.

Products developed under the award

Publications:

Refereed Journal Articles (Complete Citation)

1. **Capunitan, J.A. and S.C. Capareda.** 2012. Assessing the Potential for Biofuel Production of Corn Stover Pyrolysis Using a Pressurized Batch reactor. Fuel, Volume 95 (2012) 563-572. Elsevier Science Ltd., UK. England.

2. **Kane, E. S., Hockaday, W. C., Turetsky, M. R., Masiello, C. A., Valentine, D. W., Finney, B. P., & Baldock, J. A.** 2010. Topographic controls on black carbon accumulation in Alaskan black spruce forest soils: implications for organic matter dynamics. *Biogeochemistry*, *100*(1-3), 39–56. doi:10.1007/s10533-009-9403-z

3. **Kinney, T. J., Masiello, C.A., Dugan, B., Hockaday, W.C., Dean, M.R., Zygourakis S.K., & Barnes, R.T.** 2012. Hydrologic properties of biochars produced at different temperatures. *Biomass and Bioenergy*, 1–10. doi:10.1016/j.biombioe.2012.01.033

4. **LeCroy, C., Masiello, C. A., Rudgers, J. A., Hockaday, W. C., & Silberg, J. J.** 2013. Nitrogen, biochar, and mycorrhizae: Alteration of the symbiosis and oxidation of the char surface. *Soil Biology and Biochemistry*, *58*, 248–254. doi:10.1016/j.soilbio.2012.11.023

5. **Lehmann, J., Rillig, M. C., Thies, J., Masiello, C. A., Hockaday, W. C., & Crowley, D.** 2011. Biochar effects on soil biota – A review. *Soil Biology and Biochemistry*, *43*(9), 1812–1836. doi:10.1016/j.soilbio.2011.04.022

6. **Li, D., Hockaday, W. C., Masiello, C. A., & Alvarez, P. J. J.** 2011. Earthworm avoidance of biochar can be mitigated by wetting. *Soil Biology and Biochemistry*, 1–6. doi:10.1016/j.soilbio.2011.04.019

7. **Nguyen, B. T., Lehmann, J., Hockaday, W. C., Joseph, S., & Masiello, C. A.** 2010. Temperature Sensitivity of Black Carbon Decomposition and Oxidation. *Environmental Science and Technology*, *44*(9), 3324–3331. doi:10.1021/es903016y

8. **Palma, M.A., J.W. Richardson, B.E. Roberson, L.A. Ribera, J. Outlaw, C.L. Munster.** 2011. Economic feasibility of a mobile fast pyrolysis system for sustainable bio-crude oil production. International Food and Agribusiness Management Review, Vol. 14, Issue 3.

9. **Schnell R.W., D.M. Vietor, T.L. Provin, C.L. Munster and S.C. Capareda.** 2012. Capacity of Biochar Application to Maintain Energy Crop Productivity: Soil Chemistry, Sorghum Growth, and Runoff Water Qaulity Effects. J. Envion. Qual. 41: 1044-1051.
10. **Sun, H., Hockaday, W.C., Masiello, C.A., & Zygourakis, K.** 2012. Multiple Controls on the Chemical and Physical Structure of Biochars. *Industrial & Engineering Chemistry Research*, *51*(9), 3587–3597. doi:10.1021/ie201309r;

11. **Wise, J.T., D. Vietor, T. Provin, S. Capareda, C. Munster, and A. Boateng.** 2012. Mineral nutrient recovery from pyrolysis systems. Environ. Progress & Sustain. Energy. Vol 31-2. pg. 251-255.

Conference Papers (Complete Citation)

1. **Capunitan, J.A. and S.C.Capareda.** 2010. Corn Stover Pyrolysis in a High-Pressure/High-Temperature Batch Reactor: Evaluation of Product Yields and Conversion Efficiencies. Paper presented at the 2010 American Society of Agricultural and Biological Engineering (ASABE) Annual Meeting. ASABE Paper #100-9881. ASABE, St. Joseph, MI.

2. **Cook, W., A. Van Orshoven, C.L. Munster, T. Provin, and K. McInnes.** 2012. Soil property changes as a result of pyrolysis biochar applications. ASABE International Meeting, Dallas, TX, July.

3. **Ha, M., C. Munster, S. Capareda, D. Vietor, T. Provin, and M. Palma.** 2011. GIS program to optimize feedstock utilization for mobile pyrolysis units. Presented at the 2011 ASABE Annual International Meeting, Louisville, KY, 7 – 10 August.

4. **Hockaday W.C., S. Kim, P.G. Hatcher, and C.A. Masiello.** 2010. Comparing the Molecular Structures of Black Carbon in Soil and Water to Constrain Processes of Formation and Decomposition. American Chemical Society National Meeting, San Francisco, March 21-25, 2010.

5. **Husmoen, D., D. Vietor, C. Munster, and T. Provin.** 2011 ASA-CSSA-SSSA Annual Meetings in San Antonio, TX, Title of Presentation: "Biochar Effects On Switchgrass Establishment and Runoff Loss of Nutrients"

6. **Husmoen, D., S. Capareda, T.L. Provin, C.L. Munster, R.W. Schnell, J. Wise, and E.M. Vietor.** 2010. Biochar effects on switchgrass establishment and water quality. Paper 169-6, Poster 614, Div. A05, Annual ASA Meeting, Long Beach, CA.

7. **Husmoen, D., T. Provin, C. Munster, J. Wise, and M. Keough.** 2011. Biochar effects on switchgrass establishment and runoff loss of nutrients. ASA-CSSA-SSSA Int. Ann. Meetings. Oct. 16-19, 2011. 205-20.

8. **Keough, M., T. Provin, D. Vietor, C. Munster, and S. Capareda.** 2011. Post removal of oil/tar materials from biochar and subsequent impact on weathering. ASA-CSSA-SSSA Int. Ann. Meetings. Oct. 16-19, 2011. 137-13.

9. **Masiello C.A., W.C. Hockaday, K. Zygourakis, B. Dugan, J.A. Rudgers, P.J.J. Alvarez, T.W. Boutton, L.A. Pyle, T.J. Kinney, H. Sun, and D. Li.** 2010. Biochar Research at Rice University: An Overview. Geological Society of America, Denver, CO, 2010.

10. **Palma, M.A., Richardson, J., Roberson, B., Ribera, L., Outlaw, J., and C. Munster.** 2011. "Economic Feasibility of a Mobile Fast Pyrolysis System for Sustainable Bio-crude

Oil Production" Paper presented at the International Food and Agribusiness Management Association meeting. June 14, 2011. Frankfurt, Germany.

11. **Pyle L.A., W.C. Hockaday, C.A. Masiello, T.W. Boutton, and C. LeCroy.** 2010. Production and Isotopic Composition of Black Nitrogen Following Experimental Charring of Plant Materials. Fall American Geophysical Union Meeting, San Francisco, Dec. 13-18, 2010.

12. **Schnell, R.W., S. Capareda, T.L. Provin, C.L. Munster, D. Husmoen, J. Wise, and D.M. Vietor.** 2010. Cycling biochar affects crop production and water quality. Paper 166-1, Division A05, Annual ASA Meeting, Long Beach, CA.

13. **Sun H., W.C. Hockaday, C.A. Masiello, K. Zygourakis.** 2010. Physical and Chemical Structure Analysis of Biochars Produced from Different Feedstocks and Under a Variety of Pyrolysis Conditions. American Institute of Chemical Engineers Annual Meeting (AiChE), Salt Lake City, Nov 7-12, 2010.

14. **Vietor, D.M., S. Capareda, J. Wise, D. Husmoen, R. Schnell, B. Santos, J. Capunitan, T. Provin, C. Munster, and W. Rooney.** 2010. Biochar yield and composition from sorghum pyrolysis at varied temperature. Annual Meeting of Northeasten Branch of Agronomy, Crop, and Soil Societies. Ithaca, NY, June 28-30.

15. **Wise J, Provin T, Vietor D, Munster C, Capareda S, Boateng A.** 2011. Nutrient Recovery from Pyrolysis Systems. Presented at the TC Biomass 2011 International Conference on Thermochemical Conversion Sciences. Chicago, Illinois. September 29. (Placed 2nd in the graduate student competition).

16. **Wise J, Provin T, Vietor D, Munster C, Capareda S, Boateng A.** 2011. Nutrient Recovery from Pyrolysis Systems. Presented at the 2011 ASA-CSSA-SSSA Annual Meetings. San Antonio, Texas. October 16-19.

17. **Wise J, Provin T, Vietor D, Munster C, Capareda S, Husmoen D, Schnell R.** 2010. Mineral Nutrient Recovery in Pyrolysis Systems for Varied Feedstocks. Presented at the 2010 ASA-CSSA-SSSA Annual Meetings. Long Beach, California. October 31-November 3.

18. **Wise, J., D. Vietor, T. Provin, D. Husmoen, M. Keough, S. Capareda, C. Munster, and A. Boateng.** 2011. Mineral nutrient recovery from pyrolysis systems. ASA-CSSA-SSSA Int. Ann. Meetings. Oct. 16-19, 2011. 127-30.
19. **Wise, J., T. Provin, D. Vietor, D. Husmoen*, C. Munster, M. Keough, S. Capareda, A. Boateng.** Nutrient Recovery from Pyrolysis Systems. Poster presented at: TC Biomass 2011. The International Conference on Thermochemical Conversion Science; 2011 Sept 27; Chicago, Illinois.

20. **Wise, J., T.L. Provin, D. Husmoen, R.W. Schnell, D.M. Vietor, S. Capareda, and C.L. Munster.** 2010. Mineral nutrient recovery in co-products of pyrolysis for varied biomass feedstocks. Paper 56-17, Poster 731, Div. A10, Annual ASA Meetings, Long Beach, CA.

Other Presentations (Complete Citation)

21. **Bumguardner, M., M. Ha, and C. Munster.** 2011. Result of a GIS model developed to optimize feedstock logistics for production of bio-oil using mobile pyrolysis units. Poster presentation at the Energy Forum 2011: Energy Security and Sustainability – Global Challenges. Feb. 1 – 2, 2011. College Station, TX.

22. **Wise J, Provin T, Vietor D, Munster C, Capareda S, Husmoen D, Schnell R.** Mineral Nutrient Recovery in Pyrolysis Systems for Varied Feedstocks. Presented at the 2011 Hispanic Leaders in Agriculture and the Environment (HLAE) South Texas Symposium. Corpus Christi, TX. March 16.

23. **Wise J, Provin T, Vietor D, Munster C, Capareda S, Rooney B.** Relationship of Feedstock Composition and Pyrolysis Temperature to Bio-Char Yield. Presented at the 2010 AgriLife Conference. College Station, Texas. January 11-15.

24. **Wise J, Provin T, Vietor D, Munster C, Capareda S, Rooney B.** Relationship of Feedstock Composition and Pyrolysis Temperature to Bio-Char Yield. Presented at the 2010 Hispanic Leaders in Agriculture and the Environment (HLAE) Orientation. College Station, Texas. August 26.

a. Website or other Internet sites that reflect the results of this project.

Biochar.rice.edu: http://biochar.rice.edu/Rice_Biochar_Group_/Home.html

b. Networks or collaborations fostered.

Rice University, Houston, Texas (Caroline Massiello)
USDA-ARS Eastern Regional Research Center (Akwasi Boateng)

c. Technologies/techniques.

Mobile Fast Pyrolyzer (Developed at TAMU with Invention Disclosures)

d. Inventions/patent applications, licensing agreements.

Capareda, S. C., C. B. Parnell, Jr., D. Carney and W. A. LePori. Pyrolysis and Gasification System for Biomass Feedstock. Provisional Patent with Serial No. 61/302,001 (Issued February 5, 2010).

e. Other products, such as data or databases, physical collections, audio or video, software* or Netware, model, educational aid or curricula, instruments, or equipment.

None.

1. Academic

a. Courses developed (Complete description)

None.

b. M.S. students supported (Name: Thesis title: Department: Year Supported:)

Derek Husmeon, Effects of biochar recycling on switchgrass growth and soil and water quality in bioenergy production systems, Soil and Crop Sciences, 2009-2011

Matt Keough, Influence of biochar applications on soil chemical properties, Soil and Crop Sciences, 2010-2012.

c. M.S. degrees conferred(Name: Thesis title: Department: Year Conferred:)

Derek Husmeon, Effects of biochar recycling on switchgrass growth and soil and water quality in bioenergy production systems, Soil and Crop Sciences, 2011.

Matt Keough, Influence of biochar applications on soil chemical properties, Soil and Crop Sciences, 2010-2012.

d. Ph.D. students supported(Name: Thesis title: Department: Year Supported:)

Hao Sun, PhD Chemical Engineering, Rice University, 2011

Jewel Capunitan, Bio-fuels from Corn Stover: Pyrolytic Production and Catalytic Upgrading Studies, Department of Biological and Agricultural Engineering, 2009-2011

Jatara Wise, Mineral Nutrient Recovery from Pyrolysis Systems, 2012.

Miae Ha, Optimizing Feedstock Logistics and Assessment of Hydrologic Impacts for Sustainable Bio-energy Production, Biological and Agricultural Engineering Department, 2009 – 2012.

e. Ph.D. degrees conferred (Name: Thesis title: Department: Year Conferred:)

Jatara Wise, Mineral Nutrient Recovery from Pyrolysis Systems, 2010-2012.

Miae Ha, Optimizing Feedstock Logistics and Assessment of Hydrologic Impacts for Sustainable Bio-energy Production, Biological and Agricultural Engineering Department, December 2012.

Hao Sun, PhD Chemical Engineering, Rice University, 2011

f. Post-docs supported (Name: Thesis title: Department: Year Supported:)

Willam C. Hockaday, Rice University

ITEM	NUMBER	
Abstracts		
Peer Reviewed Publications	***11***	
Outreach Publications /Web Pages	***1***	
Presentations	***24***	
MS Degrees Conferred	***2***	
Ph.D. Degrees Conferred	***3***	
MS Students Supported	***2***	
Ph.D. Students Supported	***4***	
Disclosures	***1***	
Patents Filed	***0***	
Provisional Patents	***1***	
Patents Issued	***0***	
License Agreements	***0***	
Plant Variety Protection	***0***	
Investigators Supported	***6***	
Post-Docs Supported	***1***	
Graduate Students Supported	***6***	
Undergraduate Students Supported	***3***	
Start-Up Jobs Created	***0***	

Back to Table of Contents

DOE Final Progress Report

Project Title: Evaluation of In-field Corn Stover Densification and Interaction with Storage Quality, Logistics, and Production Costs

Project Director/Principal Investigator:
Matthew J. Darr, Assistant Professor, Agricultural and Biosystems Engineering Department, Iowa State University, Ames, IA 50011

All Co-Principal/Other Investigators:
Stuart J. Birrell, Associate Professor, Agricultural and Biosystems Engineering Department, Iowa State University, Ames, IA 50011

Robert P. Anex, Professor, Biological Systems Engineering Department, University of Wisconsin, Madison, WI 53706

Robert C. Brown, Mechanical Engineering Department, Iowa State University, Ames, IA 50011.

Collaborators:
Kyle Althoff, Supply Chain Manager, DuPont, Des Moines, IA

Maynard Herron, Engineering Manager, AGCO, Hesston, KS

Period of Performance: 1 January 2009 - 31 December 2011

Funding Awarded: $699,557

Cost Share Amount: $559,681

Cost Share Sources: Time and effort of PIs and CoPIs plus indirect charged to this; AGCO,

Dupont Cellulosic Ethanol, ConocoPhillips, Archer Daniels Midland, Hawkeye Renewables,

Alliant Energy, John Deere

ACKNOWLEDGEMENTS

This research was partly supported by funding from the North Central Regional Sun Grant Center at South Dakota State University through a grant provided by the U.S. Department of Energy Office of Biomass Programs under award number DE-FG36-08GO88073. Additional funding for this project was provided by AGCO, Dupont Cellulosic Ethanol, ConocoPhillips, Archer Daniels Midland, Hawkeye Renewables, Alliant Energy, John Deere, and Iowa State University.

We would also like to thank Andy Suby from BCRF (BioCentury Research Farm, Iowa State University, Ames, IA 50011) and Dustin Dalluge, Marjorie Rover, Patrick Johnston and Ryan Smith from CSET (Center for Sustainable Environmental Technologies, Iowa State University, Ames, IA 50011) for their contribution to this project.

EXECUTIVE SUMMARY

Densification of biomass early in the supply chain is a key component in developing a pathway for corn stover to become a viable commodity in the bioeconomy of the 21st century. This project addressed novel in-field densification methods and an investigation of the impact of densification on field logistics and long term storage quality as key components of an integrated corn stover supply systems. Deliverables from this project included: 1) experimental models for rapid in-field densification of corn stover under harvest conditions, 2) production-scale experiments and analysis of corn stover field logistics and total production cost under most likely harvest and transport methods, 3) evaluation of corn stover deterioration and chemical composition under storage scenarios designed for both biochemical and thermochemical conversion, and 4) identification of conversion parameters and economics of on-farm generation of high energy density corn stover products from torrefaction and pyrolysis oil production.

Experimental models for rapid in-field densification of corn stover under harvest conditions:

Novel densification bench to generate large, tapered and cylindrical, densified corn stover briquettes directly from raw corn stover was built and investigated. This product weighed between 0.9 and 2.0 kg, is 220-420 mm long, has a 127 mm large end diameter, and a 102 mm small end diameter. At optimized bench settings, corn stover was densified to a dry bulk density of 190 kg/m^3 at a specific energy requirement of 22.3 MJ/t. Moisture content was a significant impact factor on the densification characteristics of corn stover and results indicated that corn stover above 25%$_{wb}$ moisture content was not suitable for this method of bulk densification. Durability testing, utilizing a modified form of ASABE S269.4, was conducted to determine the overall product quality associated with these densified briquettes produced with different material types (corn stover, MOG, and pure cobs) and particle sizes (produced from a combine chopper, and a hammer mill with a 19 mm screen). The durability rating varied with each of the main effect test parameters and produced a maximum 46% durability rating using pure cobs directly from a combine without additional size reduction. Durability rating increased from corn stover and MOG to pure cobs. Biomass preprocessing in a hammer mill significantly reduced durability due to the lack of fiber interaction throughout the large briquette.

Production-scale experiments and analysis of corn stover field logistics and total production cost under most likely harvest and transport methods:

Commercial stover harvesting for ethanol and biofiber production is just starting to emerge as a new industry in Iowa and the United States. As more corn stover is demanded to supply plants more and more acres of corn will need to be harvested and baled. As the industry develops a better understanding of the impurities in material a market will develop for corn stover that is harvested with minimal soil contamination. Multi-pass harvesting is one option of harvesting corn stover but it comes with a penalty of increased soil contamination in the corn stover of greater than 6-8% ash. Single-pass harvesting has the preferred ash content of the stover of around 3.5%. The issue with single-pass harvesting is the problem of slowing the combine productivity in-field during harvest due to the additional draft loads of a baler and processing the corn stover. Research conducted at Iowa State University found a productivity

reduction of 11% when a combine towed a baler through the field and a 25-50% reduction in the combine's productivity in processing and separating the extra stover from the grain. There is a cost inherent to the reduction in productivity. Additionally there is a cost in the equipment required to support baling both on the grain harvest side and stover collection side of the harvest. A model developed at Iowa State University uses field collected data and current machinery cost to develop a cost analysis based upon harvest cost from the 2010 fall harvest. Cost of harvesting stover ranged from $20-$30 per ton based on a range of stover collection rates from .5 ton to 1.75 tons per acre.

Evaluation of corn stover deterioration and chemical composition under storage scenarios designed for both biochemical and thermochemical conversion:

Short annual harvest window (≤1-2 months) but year-round demand of corn (*Zea mays*) stover necessitates continuous exploration to identify its cost-effective and quality-preserving storage methods, especially in the principal corn growing Midwestern states. The effects of the interactions of storage conditions and durations on the quality of single-pass large square corn stover bales stored outdoors in different ways in Iowa were investigated. Different storage types included storing with either tarp or breathable film cover or within a tube-wrap or inside a metal building. Additionally, a 120-bales pilot-scale stack was tube-wrapped and stored. Qualities of stored bales were characterized by dry matter loss (DML), temperature profiles, and changes in moisture and biomass compositions, as determined by fiber and ultimate analyses. DML for different storage treatments were between 3 and 17%. More than half of the total DML occurred early during the storage. There were measurable differences in carbon, hydrogen, nitrogen, sulfur, oxygen, cellulose, hemi-cellulose and acid detergent lignin for the different storage treatments.

Identification of conversion parameters and economics of on-farm generation of high energy density corn stover products from torrefaction and pyrolysis oil production:

Low bulk density, high moisture content, dry matter degradation during storage and low energy density of raw lignocellulosic biomass are all significant challenges in supplying agricultural residues as a cellulosic feedstock. Torrefaction and pyrolysis can be employed to efficiently solve some of these problems facing the cellulosic feedstocks supply chain. Torrefaction process parameters were investigated to improve biomass energy density and reduce moisture content. The biomass of choice (corn stover) was torrefied at three moisture content levels (30, 45 and 50%), three different temperatures (200, 250 and 300°C), and three unique reaction times (10, 20 and 30 min). Solid, gaseous, and liquid products were analyzed, and the mass and energy balance of the reaction was quantified. An overall increase in energy density (2-19%) and decrease in mass and energy yield (3-45% and 1-35%, respectively) was observed with the increase in process temperature. Mass and energy losses also increased with an increase in the initial biomass moisture content. Additionally, the equilibrium moisture content (EMC) of torrefied corn stover was investigated. The EMC of raw corn stover, along with corn stover thermally pretreated at three temperatures, was measured using the static gravimetric method at equilibrium relative humidity (ERH) and temperature ranging from 10 to 98% and from 10 to 40°C, respectively. Five isotherms were fitted to the experimental data to obtain the prediction equation which best describes the relationship between the ERH and the EMC of

lignocellulosic biomass. Microbial degradation of the samples was tested at 97% ERH and 30°C. Fiber analyses were conducted on all samples. In general, torrefied biomass showed an EMC lower than that of raw biomass, which implied an increase in hydrophobicity. The modified Oswin model performed best in describing the correlation between ERH and EMC. Corn stover torrefied at 250 and 300°C had negligible dry matter mass loss due to microbial degradation. Fiber analysis showed a significant decrease in hemicellulose content with the increase in pretreatment temperature, which might be the reason for the hydrophobic nature of torrefied biomass. The outcomes of this work can be used for torrefaction process optimization, and decision-making regarding raw and torrefied biomass storage and downstream processing.

Results obtained from the process optimization experiments were used to analyze the mass and energy balance, assess the techno-economic feasibility of a production-scale torrefaction system, and to quantify the sensitivity of energy and cost results to changes in initial feedstock moisture content, torrefaction process temperature, plant operating window and initial capital investment. The output from this analysis provides clear guidance on the opportunities and costs associated with production-scale torrefaction of biomass as a feedstock intermediate. Analysis of energy results indicated the net external energy required for the torrefaction process increased and energy efficiency of the torrefaction system decreased with increasing moisture contents. However, both of these energy metrics exhibited decreasing trend with increasing process temperatures. In addition to the energy results, unit torrefaction process cost exhibited decreasing trend with decreasing initial moisture contents of feedstock and decreasing torrefaction process temperatures. For the typical moisture content of 30%$_{wb}$, process temperature of 240°C, plant operating window of 6 mo.yr^{-1} and initial capital investment of \$7.5M for the system with rated capacity of 25 Tton.hr^{-1}, unit torrefaction process cost was estimated to be 17.5 \$-Tton^{-1}. Additional system improvements through capital cost reduction and wider operating windows can yield a torrefaction product cost of ~12 \$-Tton^{-1}.

Fast pyrolysis is the next thermochemical technique to convert biomass into liquid fuel. Although researchers are heavily involved in investigating multifarious aspects of fast pyrolysis of different cellulosic feedstock, attention is lacking towards the exploration of the fast pyrolysis characteristics of stored biomass. This study investigated the yields and the physiochemical properties of the fast pyrolysis products obtained from single-pass corn (*Zea mays*) stover and cobs stored in different ways. For comparison, stored multi-pass stover, and stored and torrefied single-pass stover were also pyrolyzed. Five different biomass samples were pyrolyzed in a 183 cm long and 2.1 cm inner diameter free-fall fast pyrolysis reactor. The physiochemical properties of bio-oil and biochar from different biomass were characterized with their moisture, ash, volatile matters, carbon, hydrogen, nitrogen and oxygen contents. In addition to these, higher heating values were determined for both bio-oil and biochar, and the acidity was measured for bio-oil. Yields of bio-oil, biochar and non-condensable gases from different biomass samples were in the ranges of 40-55, 25-36 and 11-22 wt.%, respectively, with the highest bio-oil yield from the ensiled single-pass corn stover and the lowest from the torrefied single-pass stover. Moisture and ash contents of bio-oils from different samples were in the ranges of 34-52 and 0.1-0.2 wt.%, respectively, and were not significantly different at 95% confidence interval. Bio-oils generated from ensiled single-pass cobs and torrefied single-pass stover were respectively the most and the least acidic with the modified acid numbers of 95.0 and 57.1 mg g^{-1}, respectively.

CHAPTER 1

INTRODUCTION

1.1 Background

The revised Renewable Fuel Standard (RFS2) authorized under the Energy Independence and Security Act (EISA) of 2007 mandates the production of 16 billion gallons of cellulosic biofuels by 2022. Feedstock supply and quality are the key issues that must be addressed to ensure the success of the cellulosic feedstock industry (DOE, 2007). Crop residues are the most viable and immediate feedstock option for the North Central Region because they are readily available and are the co-products of high value grain. Current estimates of corn stover feedstock availability within the US are 75 million dry tons with the potential for 170 million dry tons under moderate yearly yield increases (DOE, 2005). Over two-thirds of this available corn stover is produced within the North Central Sun Grant region (NASS, 2008). The high value grain fraction provides producers an additional income stream and reduces the societal impact of cellulosic ethanol production by maintaining grain (i.e. food) producing acreage. These natural advantages make it likely that corn stover will play a leading role in defining the biofuel future of the North Central Region.

The development of a viable corn stover cellulosic biofuel pathway requires systems for the harvest and collection of corn residues as well as methods to densify, transport, and store stover biomass in a cost effective, quality-preserving or quality-enhancing manner (DOE, 2007). In a recent study by Hess et al. (2007) it was noted that "logistical costs exceeding 25% of the total biomass value leaves very little profit margin for biomass producers and biorefinery operators." Systems level efficiency improvements are needed to hit this target on a repeatable, widespread basis. Additionally, Fales et al. (2007) stated that "improvements in feedstock density and flow characteristics are crucial to optimize collection and handling activities, decrease supply-system energy use, standardize biomass format, and maximize revenue in the biomass ethanol production system." Bulk density has been shown to have a major impact on in-field collection equipment requirements, transportation costs, harvest and transportation labor requirements, capital costs in storage systems, and capital cost and complexity in material handling at biorefineries (Hess et al., 2007; Sokhansanj and Turhollow, 2002). Idaho National Labs have estimated that dry matter losses in storage must be less than 5% in order to achieve the feedstock cost targets set by government and private sector industries.

A comprehensive analysis of wet and dry corn stover storage systems is required to identify the key impact variables and conditions which promote excessive dry matter loss and biomass quality degradation and to understand how these storage conditions are impacted by harvest and densification processes. Advanced methods of energy densification and value added processing should also be included in the analysis of biomass feedstock logistics to provide insight into opportunities for future technologies and production strategies that could transform our current understanding of the physical and economic factors limiting biomass feedstock logistics.

1.2 Project Objectives

The primary objective of this project was to determine the optimal processes to continuously densify corn stover during single pass harvesting and to quantify the interaction of in-field densification, field logistics and long term storage quality. Four specific objectives were identified to accomplish the primary objective of this project:

1. Identify new in-field densification methods for bulk handled material based on variable moisture content and typical cut length for biomass harvested in a single pass system.

2. Determine the optimal biomass feedstock harvesting pathway based on quantified field scale logistics for harvest, densification, and transportation to a storage facility.

3. Quantify optimal wet and dry biomass storage conditions to minimize material degradation and storage costs.

4. Quantify the techno-economic and logistical benefits of generating high energy density biomass products from torrefaction and pyrolysis oil production at satellite pre-conversion facilities.

1.3 Journal Publications

Published

1. Medic, D., M. Darr, A. Shah, B. Potter and J. Zimmerman. 2012. Effects of torrefaction process parameters on biomass feedstock upgrading. *Fuel*. 91: 147-154.
2. Shah, A., M. Darr, D. Medic, R. Anex, S. Khanal and D. Maski. 2012. Techno-economic analysis of a production-scale torrefaction system for cellulosic biomass upgrading. *Biofuels Bioproducts & Biorefining*. 6: 45-57.
3. Shah, A., M. Darr, K. Webster and C. Hoffman. 2011. Outdoor storage characteristics of single-pass large square corn stover bales in Iowa. *Energies*. 4: 1687-1695.
4. Thoreson, C. and M. Darr. 2011. Durability analysis of large corn stover briquettes. *Applied Engineering in Agriculture*.

Submitted

5. Medic, D., M. Darr, A. Shah and S. Rahn. Water vapor adsorption of thermally treated lignocellulosic biomass. Submitted to: *Energy & Fuels*.

Under Internal Review

6. Shah, A., M. Darr, K. Webster, K. Peyton, B. Schon and A. Kissel. Outdoor storage characteristics of tube-wrapped large square single-pass corn stover bales in Iowa. *Under Internal Review*.

7. Shah, A., M. Darr, D. Medic, B. Schon, K. Webster, K. Peyton and J. Brue. Physicochemical properties of bio-oil and biochar produced by fast pyrolysis of different stored and torrefied single-pass corn stover and cobs. *Under Internal Review*.
8. Thoreson, C., M. Darr, K. Webster and A. Shah. Investigation of process variables on the densification characteristics of corn stover. *Under Internal Review*.
9. Webster, K., M. Darr, C. Thoreson and W. Edwards. Single-pass corn stover baling economics analysis. *Under Internal Review*.
10. Webster, K., M. Darr, C. Thoreson, and W. Edwards. Single-pass corn stover harvesting system productivity analysis. *Under Internal Review.*

1.4 Conference Proceedings

1. Shah, A., M. Darr, K. Webster, B. Schon, K. Peyton and A. Kissel. 2012. Outdoor storage characteristics of tube-wrapped single-pass corn stover bales in Iowa *[Poster]*. To be presented in ASABE Annual International Meeting 2012, July 29-August 1, Dallas, TX.
2. Webster, K., M. Darr and K. Peyton. 2012. Analysis of the effects of grain logistics on single-pass harvesting productivity. To be presented in ASABE Annual International Meeting 2012, July 29-August 1, Dallas, TX.
3. Shah, A., M. Darr, K. Webster and C. Hoffman. 2011. Dry storage characteristics of single-pass harvested large rectangular corn stover bales in the Midwestern United States *[Poster]*. ASABE Annual International Meeting 2011, August 7-10, Louisville, KY.
4. Thorseson, C., M. Darr and K. Webster. 2010. Corn stover densification methods and their impacts on large scale biomass production preliminary analysis. ASABE Annual International Meeting 2010, June 20-23, Pittsburgh, PA.
5. Webster, K., M. Darr, C. Thoreson and M. Zucchelli. 2010. Productivity and logistical analysis of single-pass stover collection harvest systems. ASABE Annual International Meeting 2010, June 20-23, Pittsburgh, PA.

1.5 Public Releases or Outreach of Results

- **M. J. Darr** and A. Heggenstaller**.** 2012. Sustainable Corn Stover Production and Supply Chain Management. Ames, IA. February 2, 2012. 65 participants
- **M. J. Darr.** 2011. Biomass Supply Chain Systems. Ames, IA. October 11, 2011. 25 participants
- **M. J. Darr.** 2011. Corn Stover Production Systems. Ames, IA. September 27, 2011. 28 participants
- **M. J. Darr.** 2010. Impact of Crop Residue Collection on Machinery Capacity and Biomass Cost. Agricultural Equipment Technology Conference. Orlando, FL. January 12, 2010.
- **M. J. Darr** and S. Birrell**.** 2009. Corn Stover Harvesting. Iowa Corn Growers Association. Boone, IA. August 6, 2009. 40 participants
- **M. J. Darr.** 2009. Harvesting and Storage Challenges of a Cellulosic Biomass. Agricultural Machinery Conference. Cedar Rapids, IA. May 6, 2009. 30 participants
- **M. J. Darr.** 2009. Soil Quality and Production Challenges of a Cellulosic Biomass Crop. Conservation Tillage and Technology Conference. Ada, OH. February 27, 2009. 120 participants

- **M. J. Darr.** 2009. Advanced Biofuels. Ohio Top Farmer Conference. Columbus, OH. January 24, 2009. 65 participants

- **M. J. Darr.** 2009. Agriculture's Role in the Bioeconomy. Ohio Corn Growers Association Board Retreat. Newark, OH. January 19, 2009. 25 participants

1.6 Network or Collaborations fostered

DDCE
Powerstock

1.7 Technologies/techniques

None applicable

1.8 Inventions/Patent applications, licensing agreements

None applicable

1.9 Report Organization

This report contains five chapters. Chapter 1 includes a brief background and objectives of this study. Chapters 2-5 respectively address objectives 1-4 of this study. First three sections of each of the chapters 2-5 contain some background information, statement of objective and the specific tasks for their accomplishment, and their overall impact. Their fourth and subsequent sections include details on different tasks performed to accomplish different objectives. Fourth and subsequent sections of each of the chapters 2-5 are drafted in the journal article format and are either published or submitted to the journal or being internally reviewed.

References

DOE. 2005. Biomass as a Feedstock for Bioenergy and Bioproducts Industry: The Technical Feasibility of a Billion-Tom Annual Supply. Oak Ridge, TN: U.S. Department of Energy, Biomass Research and Development Initiative.

DOE. 2007. Roadmap for Bioenergy and Biobased Products in the United States. Oak Ridge, TN: U.S. Department of Energy, Biomass Research and Development Initiative.

Fales, S. L., J. R. Hess, and W. W. Wilhelm. 2007. Convergence of Agriculture and Energy: II. Producing Cellulosic Biomass for Biofuels. CAST Commentary. QTA2007-2

Hess, J.R., , C. T. Wright, K. L. Kenney. 2007. Cellulosic biomass feedstocks and logistics for ethanol production. Biofuels, Bioproducts and Biorefining. 1(3): 181 – 190.

NASS. 2008. USDA National Agricultural Statistics Service: 2008 State Crop Production Statistics. Washington, DC: National Agricultural Statistics Service.

Sokhansanj, S. and A. Turhollow. 2002. Baseline Cost for Corn Stover Collection. Applied Engineering in Agriculture. 18(5), pp. 525–530.

CHAPTER 2
NOVEL IN-FIELD DENSIFICATION METHODS FOR BULK-HANDLED MATERIAL HARVESTED IN A SINGLE-PASS SYSTEM

2.1 Background

Corn stover is a widely available biomass resource for use as a feedstock for biofuel production. In 2005, the USDA estimated that approximately 75 million dry tons of corn stover were available annually for a biomass industry (DOE, 2005). Depending on the agricultural setting and feedstock use, corn stover can be harvested in various fractions and amounts to minimize negative soil impacts and material moisture content, and maximize feedstock potential for processing. The low bulk density of corn stover poses a major obstruction to its large scale acceptance as a biomass feedstock. The loose bulk density of chopped corn stover ranges from 40 to 80 kg/m^3 (2.5-5 lb/ft^3) (Knutson & Miller, 1982) which is low enough to create large inefficiencies during the harvest, transport, and storage phases of production. These inefficiencies are created because transportation vehicles loaded with corn stover are restricted by volume capacity rather than weight capacity. A cost-effective means of increasing corn stover bulk density during the harvest phase will be critical to the feasibility of large-scale production.

2.2 Objective and Specific Tasks

This chapter addresses the first objective of this project which was to identify new in-field densification methods for bulk handled material based on variable moisture content and typical cut length for biomass harvested in a single pass system. This objective was accomplished through a set of tasks:

1. Identify fundamental densification models for increasing the bulk density of field harvest corn stover with variable moisture content and cut length.
    a. A test briquette densifacation bench was developed to determine the requirements for in-field densification based upon the energy requirements and the material characteristics. This looked at compression ratio, volume, speed, stover particle size, stover fraction, moisture content, stover elasticity, and cohesion.

2. Evaluate in-field mechanisms for increasing density of bulk flowable corn stover utilizing available collection wagon power sources.
    a. The feasibility of commercial development of an in-field briquetter was determined to be unobtainable in the timeframe of the research. Instead the more feasibly produced large square baler was substituted to look at the collection and transport characteristics of corn stover collection to the field edge.
    b. Briquettes produced from bench testing were created and tested for their durability according to stover fraction and moisture content. This information provided guidance on how briquettes and bales would need to be formed in order to survive transport and storage from the field to the processing plant.
    c. Knowledge taken from in-field single-pass baling testing and from the bench top briquette densification test apparatus was used to determine the energy

requirements and material factors that would need to be achieved produce an in-field mobile briquetting machine.

2.3 Overall Impacts of study

This research differentiates itself from previous densification work in many ways. Focusing on testing densification characteristics of corn stover produced from real harvesting scenarios involving chopped particle sizes and field-harvested moisture contents allows this work to produce a better indication of the feasibility of this method for in-field densification systems. Testing this process under energy and power requirements which are feasible for traditional agricultural equipment allows this process to be scaled for in-field operation. Only corn stover fractions that can be produced using harvesting technology currently available are tested in this research. All of these factors combine to produce research that is well aligned with current corn stover crop and harvesting systems.

2.4 Investigation of process variables on the densification characteristics of corn stover

Curtis P. Thoreson, Matthew J. Darr, Keith E. Webster and Ajay Shah

(to be submitted to a peer-reviewed journal)

ABSTRACT

The bulk density of raw corn stover is a major obstruction to its large scale viability as a biomass feedstock. Raw corn stover has a low bulk density of 50 kg/m^3 which induces significant transportation costs and limits optimization of transport logistics. Producing a densified corn stover product directly at the point of harvest would reduce harvest and transportation costs and lead to viable pathways for corn stover as a biomass feedstock. This research investigated a densification method that generates a large, tapered and cylindrical, densified stover product directly from raw corn stover. This product weighs between 0.9 and 2.0 kg is 220-420 mm long, has a 127 mm large end diameter, and a 102 mm small end diameter. This research differentiates itself from previous briquetting and pelleting work because these briquettes are produced at field harvested particle sizes and low compression pressures which are achievable in a continuous in-field system. At optimized bench settings, corn stover was densified to a dry bulk density of 190 kg/m^3 at a specific energy requirement of 22.3 MJ/t. Moisture content was a significant impact factor on the densification characteristics of corn stover and results indicated that corn stover above 25%$_{wb}$ moisture content was not suitable for this method of bulk densification.

Keywords: Corn, Stover, Densification, Density, Briquette, Pellet

2.4.1 INTRODUCTION

Corn stover is a widely available biomass resource in the United States and particularly in the Mid-west where corn is the predominant food grain product. In 2005, the USDA estimated approximately 75 million dry tons of corn stover were available annually to support a biomass industry [1]. The low bulk density of corn stover poses a major obstruction to its large scale acceptance as a biomass feedstock. The loose bulk density of chopped corn stover ranges from 40 to 80 kg/m^3 [2], which creates large inefficiencies during the harvest, transport, and storage phases of production. These inefficiencies are created because transportation vehicles loaded with corn stover are restricted by volume capacity rather than weight capacity due to the low product density. A cost-effective means of increasing corn stover bulk density during the harvest phase will be critical to the feasibility of large-scale production. Ideally, a densification system would densify the material in-field to minimize in-field transport wagons and trips, and maximize over-the-road truck hauling potential. Current self-unloading trailers suitable for over the road transportation of densified biomass have volumes of 65 to 90 m^3 . The minimum bulk density of a briquetted biomass to fully load these trailers ranges from 270 to 370 kg/m^3 based on common legal weight restrictions of 36,290 kg for tractor-trailer combinations and accounting for the base weight of the tractor and trailer.

Several methods have been used to densify corn stover including grinding, baling, briquetting, and pelleting. Often used as a pre-processing operation for other densification systems, grinding operations involve reducing the particle size of a material which increases bulk density. Hammer mill performance with corn stover has been quantified with the output bulk

density ranging from 130 to 160 kg/m^3 at a specific energy requirement range of 25 to 122 MJ/t [3]. While grinding operations can increase the bulk density of stover, grinding alone does not provide enough density gain to maximize hauling efficiency. Grinding operations are also energy intensive, so an engineered densification system should attempt to minimize the amount of grinding used within the process. Square baling operations utilize a reciprocating plunger to compress material into a chamber and then wrap the compressed material with strings to hold it in a densified form. A study of single-pass large square baled corn stover at the Agricultural Engineering Farm at Iowa State University in Ames, IA was conducted over the 2009 and 2010 harvest seasons. These tests showed baled corn stover wet bulk densities of 207 kg/m^3 (156 kg/m^3 dry bulk density) [4] are possible at a specific energy requirement of approximately 11.2 MJ/t. While baling offers an increased bulk density over loose stover, it requires an additional unit handling operation which complicates transportation logistics and drives up unit production costs.

Briquetting and pelleting operations apply extreme pressure, and in many cases, heat energy to the input material to compress it into a specific shape that can be retained without additional binding mechanisms. Densification studies on both instrumented testing machines and ring-die pelleting mills were conducted over the past several years. Output corn stover particle density was 1220 kg/m^3 at a specific energy requirement of 44 MJ/t on an instrumented single axis densification testing machine [5]. Ring-die pellet mill tests produced bulk densities of 550 to 610 kg/m^3 at a specific energy requirement of 189 to 262 MJ/t [6]. While these systems offer great density compared to baling and grinding systems, they require a high energy input to complete, and are not feasible to accomplish at common harvesting rates. These factors drive up the production cost of densified corn stover.

Current briquetting and pelleting methods require large amounts of energy and sub-millimeter particle sizes to complete the process. This research sought to significantly reduce the specific energy and particle size reduction requirements of densification compared with other conventional briquetting and pelleting operations. The objective of this work was to study the effects of important densification process variables; including compression pressure, die taper angle, material particle size, material moisture content, and material type on the output density and specific energy requirements of large densified briquettes. The requirements that drove these densification experiments were as follows:

- The corn stover materials tested in this research must represent the variable range of settings that can be harvested in common Midwest corn harvesting setups. This includes different material moisture contents, particle sizes, and corn stover material fractions.

- The densification apparatus must be capable of applying a variable compression pressure from 0-17 MPa . Previous research indicated this compression pressure range could produce feasible energy and power requirements for scaled up densification processes, so this work focused on determining the capabilities of a densification system within this compression pressure range.

To accomplish this, a bench-scale, instrumented, densification apparatus was designed to test different inputs with respect to the output densification characteristics. The inputs were varied to test different forms of stover available from different harvesting setups, and to produce feasible energy requirements for a large scale system (based on field capacities and engine sizes

of common harvesting equipment). The tested variables in these experiments included compression pressure, material particle size, material moisture content, and material type (the specific corn stover material fraction). Specific experiments were designed around various combinations and levels of these four variables to determine the effects of each.

2.4.2 MATERIALS AND METHODS

2.4.2.1 Densification Bench Development

A custom designed, bench-scale densification system was used to conduct the experiments required to address the objectives of this research, details of which are included in Thoreson [7]. Figure 1 shows the bench and a cross-section of the densification region on the bench. Material was fed in through the inlet on the top of the 127 mm cylindrical chamber. A tapered cylindrical die (203 mm long, variable taper angle) was attached to the end of the chamber, and a plunger pressed the material from the chamber into the tapered die. This process was repeated with additional material added until the target briquette compression pressure was reached. The end cap and die were then removed and the briquette was extracted using a separate ejection press. The densification bench was capable of applying compression pressures at the plunger head up to 17 MPa. It was controlled by a Microsoft Excel based macro-embedded worksheet on a personal computer (PC). The PC was connected to a Measurement Computing 1408-FS data acquisition card which controlled bench functions and read data from two load cells and a string potentiometer to control and log compression pressure and plunger position, and to log cap force data.

Figure 1: Bench-based densification system

The free body diagram of the die region of the densification bench is shown in figure 2. A tapered die was selected because it distributed a larger amount of axial force (resistance) to the material than a straight, cylindrical die. An instrumented die cap was installed to stop material flow and measure the cap force to quantify the process variable effects on force distribution.

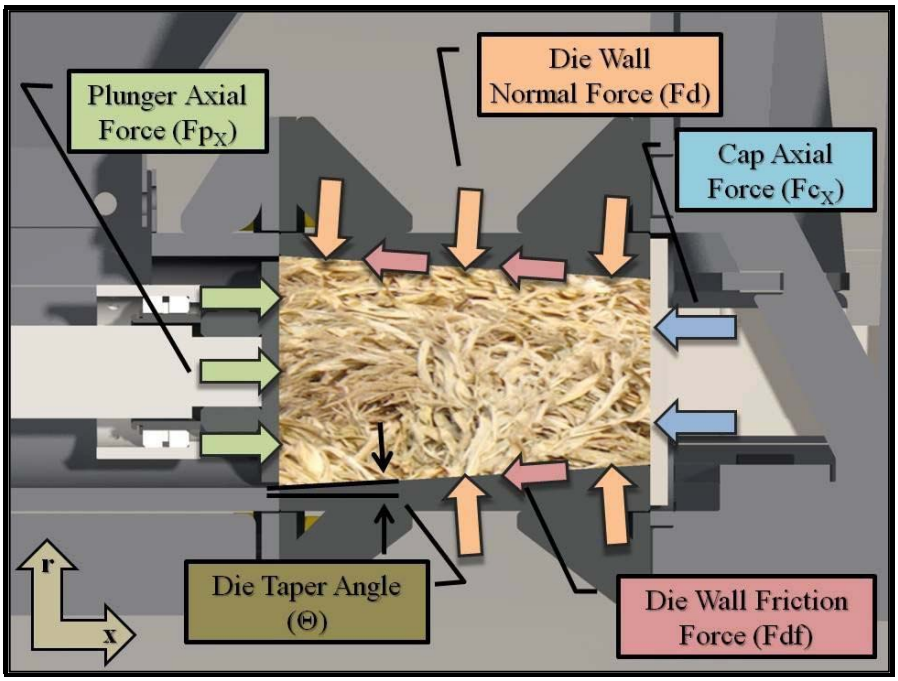

Figure 2: Free Body Diagram of Material under Compression Cycle

2.4.2.2 Input Materials

Corn stover utilized in this research was collected from the fall 2009 and 2010 grain harvest seasons in the Ames, IA area. A range of different corn stover moisture contents were generated by using stover samples from multiple harvest dates, or if necessary, by moisture conditioning the material. The observed moisture content for each sample is listed with each experiment description. Particle size influence on densification was evaluated for three different methods which are reported numerically throughout the results and discussion sections. The actual geometric mean particle sizes are reported for each experiment in the section 2.4. The particle size reduction methods include:

- 1: 'As Received' This material had passed through an integrated chopper on a combine, but saw no further size reduction.

- 2: 'Vermeer HG200' This material was the same as that from category 1, but had been size reduced using a Vermeer HG200 wood chipper with dual parallel screens set at 70 and 111 mm respectively.

- 3: 'Hammer mill' This material was the same as that from category 1, but had been size reduced using an Arts-Way 60HP stationary hammer mill with a 19 mm round-hole screen.

Different fractions of corn stover components were also used as a treatment factor in these experiments. These fractions were generated using different corn stover harvesting systems. A description of each material type is listed below:

- Corn Stover: This material was harvested with a standard 'all crop' header which cuts the plant just below the corn ear and harvests all material above the cut point. The output material consists of significant amounts of stalk and leaf, with smaller amounts of cob and husk.

- MOG (Material other than grain): This material was harvested using a conventional corn header which generally harvests just the ear and husk. Output material consists mostly of leaf, husk, and cob.

- Pure Cobs: This material was harvested using a conventional corn header and combine with a secondary attachment for output material processing. This output material consists of mostly cob with small amounts of leaf, husk, and stalk.

2.4.2.3 Material Properties

Input material properties were determined using the ASABE standard procedures for determining particle size and moisture content. Material particle size was quantified using the screening procedure outlined in ASABE S424.1 [8]. Material moisture content was determined using the drying procedure from ASABE S358.2 [9]. Stover input samples were dried at 60^{O} C for 72 hr, and final weights were measured immediately following drying. All moisture contents are reported on a wet basis.

Physical briquette properties were measured by the operator and mechanical data was measured by the densification bench data acquisition system. Particle density was determined by manually measuring the volume of a briquette and measuring the weight using a digital scale. Density was reported on a dry material basis in the results sections. Energy was calculated on a mechanical basis using the instrumentation on the bench that measured plunger force and position at a rate of 10 Hz. This energy was scaled based on the briquette dry weight to determine the dry specific energy.

2.4.2.4 Experiment Design

2.4.2.4.1 3-Way Interaction Experiment

Previous literature regarding biomass densification [5, 6, and 10] suggested densification characteristics are highly sensitive to compression pressure, material moisture content, and material particle size. The objective of the 3-way interaction experiment was to determine the main and interaction effects of these three densification process variables with respect to the dry particle density and dry specific energy. Three levels of compression pressure (7.0, 10.5, 14.0 MPa), two levels of material moisture content (8.3, 54.5%$_{wb}$), and three levels of material particle size (methods 1, 2, 3) were tested together in a full factorial experiment. The material tested in this experiment for particle size reduction methods 1, 2, and 3 had mean particle sizes

of 19-23 mm, 22-35 mm, and 40-42 mm, respectively. This created 18 individual treatments (briquettes) that were replicated three times.

2.4.2.4.2 Moisture Effects Experiment

The moisture effects experiment was developed to study the effects of moisture content observed during the 3-way interaction experiment more closely. More specifically, the objective of this experiment was to determine the main and interaction effects of material moisture content, compression pressure, and die taper angle (θ in figure 2) with respect to dry particle density and dry specific energy. Three levels of material moisture content (13.0, 24.8, 47.6%$_{wb}$), two levels of compression pressure (8.8, 14.0 MPa), and two levels of die taper angle (3.6, 7.2^{o}) were tested together in a full factorial experiment, and replicated three times for a total of 36 briquettes produced. The increased minimum compression pressure was chosen based on the poor performance of the low (7.0 MPa) compression pressure during the 3-way interaction experiment. Because this experiment was not targeting the effect of material particle size, the mean particle size of the corn stover was held constant at 40 mm throughout this experiment.

2.4.2.4.3Material Types Experiment

Different fractions of corn stover components could produce different densification characteristics, so the material types experiment was developed to test the effect of corn stover material type. Three different corn stover material types (corn stover, MOG, pure cobs), two levels of compression pressure (7.0, 14.0 MPa), and two levels of material particle sizes (methods 1 and 3) were tested together in a full factorial experiment and replicated three times for a total of 37 briquettes produced. The material tested in this experiment for particle size reduction methods 1 and 3 had mean particle sizes of 2-17 mm and 31-39 mm, respectively. For timing reasons, the material for this experiment was densified directly from harvest, so the material moisture content of the samples was not controlled and ranged from 10-20%$_{wb}$.

2.4.2.4.4 Bulk Density Experiment

In order to understand the bulk density of these briquettes, an experiment was designed to determine the bulk density of the material for different material moisture contents. Bulk density measures the density of several combined briquettes rather than the density of a single briquette. Briquettes were produced at a specified treatment and loaded into 0.19 m^3 cylindrical barrels until the barrels were approximately 60% full. Briquette bulk sample volume and weight were then measured to determine the characteristics of the briquetted stover. This method was used over an alternative standardized method [11] for measuring the briquetted bulk density because the standard method uses a 0.028 m^3 volume for density measurement. This volume was too small to efficiently fill with these briquettes, so the larger volume was selected. The experiment was designed with two levels of material moisture content (8.3, 54.5%$_{wb}$) and was replicated three times for a total of 6 barrels of briquettes. All other process variables were set at optimal levels for briquette density based on results from the previous experiments.

2.4.3 Data Analysis

All statistical tests were conducted using Minitab software. All experiments discussed utilized full-factorial experiment designs which allowed the use of the factorial analysis tool (ANOVA) to determine the variation caused by each treatment factor. Factorial ANOVA was

used to determine the significance of each treatment variable on the selected output factor. Confidence interval plots were used to determine if significant differences were present between treatment variable levels. The confidence intervals assume a normal distribution of the data and use critical values following a t-distribution. Treatments were reported to be significantly different if the confidence intervals between treatment combinations did not overlap.
The factorial ANOVA output tables shown in section 3 provide values that indicate the significance of each potential source of variation from each experiment. The tables provides values for the source's degrees of freedom (DF), sequential sum of squares (Seq SS), adjusted sum of squares (Adj SS), adjusted mean squares (Adj MS), the F-statistic (F), and the P-value (P). The degrees of freedom indicate the number of values in a potential source of variation that are free to vary. The adjusted sum of squares provides the sum of square metric for the ANOVA that is adjusted to any unbalance in the experiment design (a missing or extra observation). The P-value indicates the probability a potential source of variation is not significant.

2.4.4 RESULTS AND DISCUSSION

2.4.4.1 Three-Way Interaction Experiment

2.4.4.1.1 Dry Particle Density

During this experiment, briquettes were produced with dry particle densities between 170 and 470 kg/m^3. Based on the P-values in the factorial ANOVA, data from the 3-way interaction experiment rejected the hypothesis of no effect from all three treatment factors and an interaction effect from moisture content and compression pressure on dry particle density (table 1). The adjusted mean squares indicated that material moisture content was responsible for the greatest variability with the other three effects accounting for smaller amounts of variation on the outputs.

Dry Particle Density (kg/m^3)						
Source	DF	Seq SS	Adj SS	Adj MS	F	P
Compression Pressure (MPa)	2	37913	37692	18846	54.5	0.000
Particle Size Reduction Method	2	3826	2346	1173	3.39	0.045
Material Moisture Content (%wb)	1	373961	373578	373578	1080.3	0.000
Compression Pressure (MPa) * Particle Size Reduction Method	4	1658	1706	427	1.23	0.314
Compression Pressure (MPa) * Material Moisture Content (%wb)	2	15323	15304	7652	22.13	0.000
Particle Size Reduction Method * Material Moisture Content (%wb)	2	1809	1853	926	2.68	0.083
Compression Pressure (MPa) * Particle Size Reduction Method * Material Moisture Content (%wb)	4	4234	4234	1058	3.06	0.029
Error	35	12103	12103	346		
Total	52	450827				

Table 1: Factorial ANOVA for dry particle density (3-way interaction experiment)

Figure 3 shows the effects of compression pressure and moisture content averaged over all particle sizes on dry particle density. At 8.3%$_{wb}$ moisture content, compression pressure showed a significant and positive with output particle density ranging from 330 – 430 kg/m^3 across 7.0-14.0 MPa. This was caused by an increase in briquette weight (from the additional compression cycles with added material) with no significant increase in briquette axial expansion. No significant differences were found between the compression pressure treatment levels at 54.5%$_{wb}$ moisture content on dry particle density ($\alpha = 0.05$). While the factorial ANOVA showed a potential relationship between the particle size reduction method and dry particle density, only two isolated significant treatment differences were observed between particle size treatments levels during the experiment ($\alpha = 0.05$).

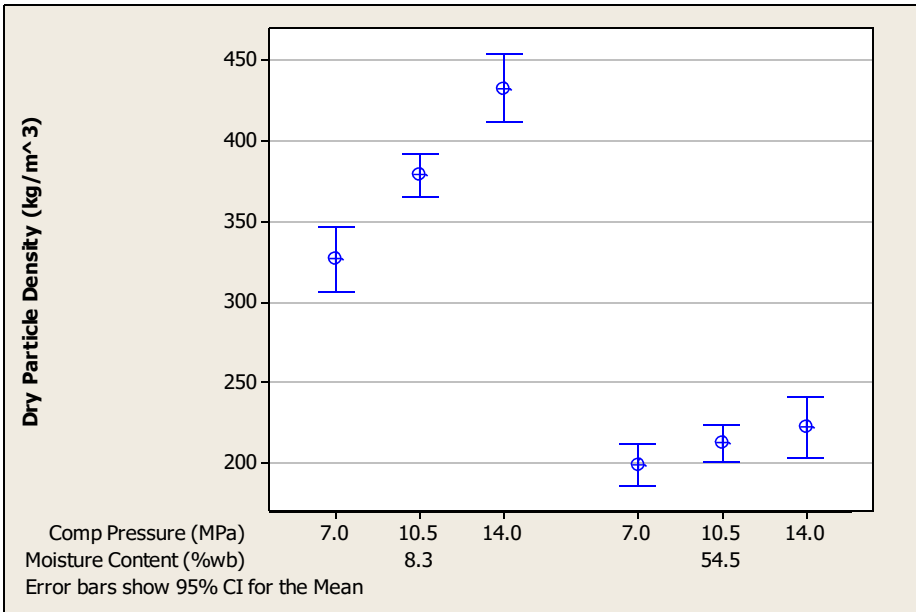

Figure 3: Treatment factor effects on dry particle density (3-way interaction experiment)

The most significant effect on dry particle density was caused by material moisture content. Increasing moisture content from 8.3 to 54.5%$_{wb}$ decreased the mean dry particle density by about 45% from 380 to 210 kg/m^3 (averaged over all levels of compression pressure and material particle size treatments). This significant decrease in dry particle density caused by material moisture content can be attributed to two main factors that were observed during this experiment; briquette dry weight and briquette axial expansion. While increasing moisture content increased the wet weight of a briquette, the weight was offset by the large amount of moisture present in the briquette, so the overall dry briquette weight was reduced. The elastic behavior of the briquette was also altered with increased moisture content, as evidenced by the significant increase in briquette axial expansion (the amount the briquette expands after ejection from the die) over increasing moisture content. Both of these factors directly contributed to a significant reduction in dry particle density at increased material moisture contents.

2.4.4.1.2 Dry Specific Energy

During the 3-way interaction experiment, briquettes were produced with a dry specific energy requirement range of 12-52 MJ/t. Based on P-values less than 0.05, the factorial ANOVA for this experiment on dry specific energy could not reject the hypothesis of no main effect caused by any of the treatment factors (table 2). Similar to dry particle density, material moisture content was responsible for the most variation on dry specific energy (based on the adjusted mean square), and compression pressure and particle size had a small amount of potentially significant variation.

Dry Specific Energy (MJ/t)						
Source	DF	Seq SS	Adj SS	Adj MS	F	P
Compression Pressure (MPa)	2	466.33	462.8	231.4	14.17	0.000
Particle Size Reduction Method	2	155.18	110.75	55.38	3.39	0.045
Material Moisture Content (%wb)	1	3852.26	3843.4	3843.4	235.34	0.000
Compression Pressure (MPa) * Particle Size Reduction Method	4	75.78	68.49	17.12	1.05	0.396
Compression Pressure (MPa) * Material Moisture Content (%wb)	2	14.56	15.4	7.7	0.47	0.628
Particle Size Reduction Method * Material Moisture Content (%wb)	2	41.89	36.35	18.17	1.11	0.340
Compression Pressure (MPa) * Particle Size Reduction Method * Material Moisture Content (%wb)	4	43.63	43.63	10.91	0.67	0.619
Error	35	571.6	571.6	16.33		
Total	52	5221.22				

Table 2: Factorial ANOVA for dry specific energy (3-way interaction experiment)

Based on 95% confidence interval plots ($\alpha = 0.05$) of each treatment variable combination (figure 4), all material particle size treatment levels demonstrated no significant differences in the dry specific energy. Averaging the effects of compression pressure and material moisture content over all levels of material particle size produces the interval plot shown in figure 5. Similar to dry particle density, compression pressure had a significant effect on dry specific energy at 8.3%wb moisture content, but not at 54.5%$_{wb}$. At 8.3%$_{wb}$ moisture content, the mean dry specific energy requirement increased by approximately 40% (15.6 to 22.2 MJ/t) from 7.0-14.0 MPa. As expected, this increase was caused by a significant increase in the amount of compression cycles required to reach a desired compression pressure.

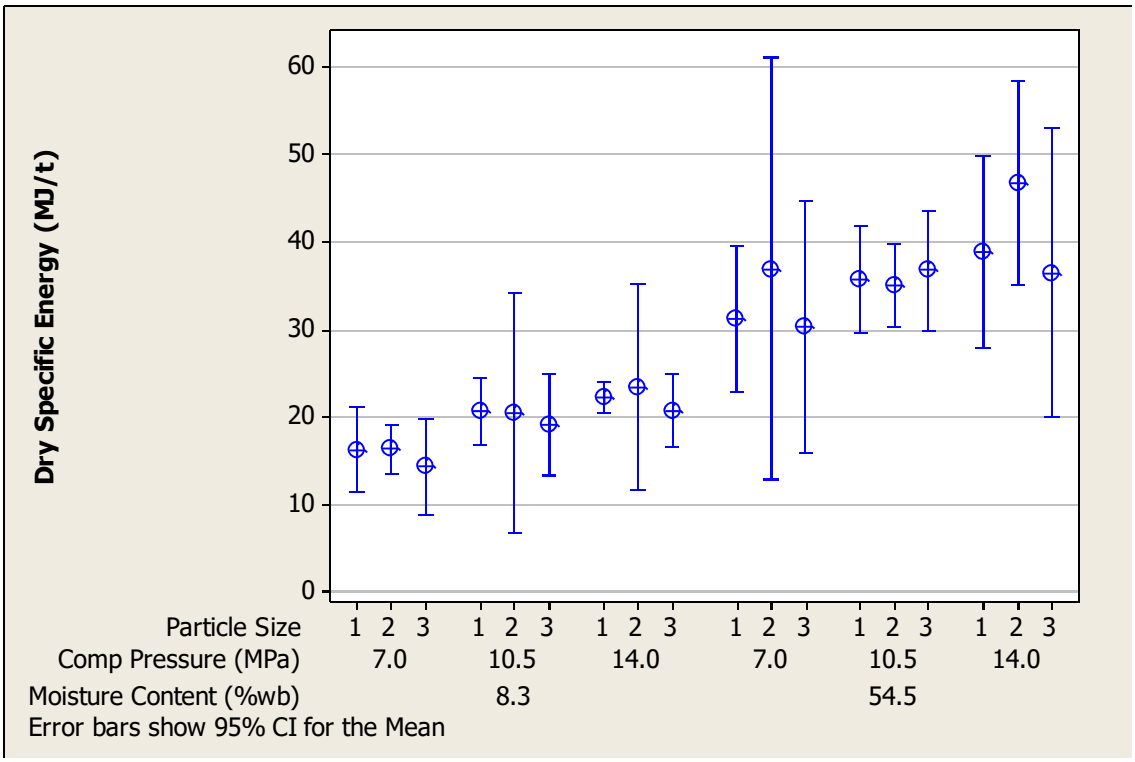

Figure 4: Treatment factor effects on dry specific energy (3-way interaction experiment)

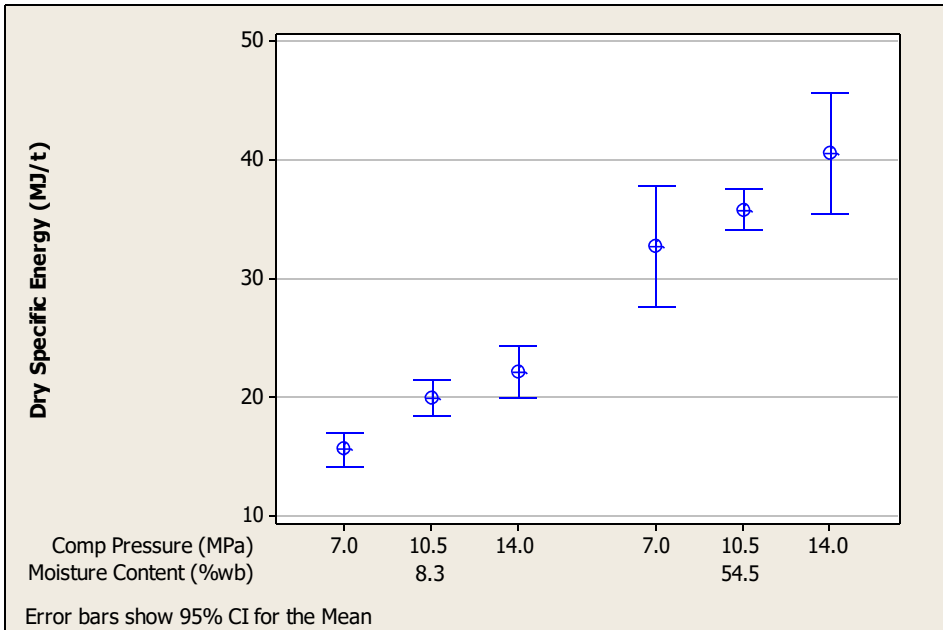

Figure 5: Treatment factor effects on dry specific energy (3-way interaction experiment)

Moisture content showed a very strong positive trend with respect to dry specific energy. From 8.3 to 54.5%$_{wb}$, the dry specific energy requirement increased approximately 90% (19.2 to 36.4 MJ/t) (averaged over all levels of compression pressure and material particle size). This increase can be partially attributed to the same factors that negatively affected dry particle density. As mentioned in section 3.1.1, the dry briquette weight significantly dropped as

moisture content increased which negatively impacted the dry specific energy. The second factor that affected the dry specific energy was the number of compression cycles required to reach the desired compression pressure. Averaged over all levels of compression pressure and material particle size, briquettes with a 54.5%$_{wb}$ moisture content averaged 4.5 more compression cycles than briquettes at 8.3%wb. Each additional compression cycle required more energy, therefore, adding 4.5 more compression cycles led to significant increases in the energy requirement.

2.4.4.1.3 Qualitative Effects

The effect of compression pressure on the output briquette quality can be observed by visual inspection. Figure 6 shows a briquette produced at 7.0 MPa, while figure 7 shows one produced at 14.0 MPa. While the overall size and shape of the briquettes was about the same, the surface texture of the high pressure briquette was much smoother than the low pressure version. The individual flakes tended to hold together better on the high pressure briquettes than the low pressure versions. The difference between the tested particle size reduction methods was also visually noticeable. The hammer milled briquette (figure 8) shows a bit more flake separation, whereas the previous two briquettes (figure 6 and 7) appear to be more uniform across the briquette length. Briquette surface stiffness was also significantly reduced for smaller particle sizes. The apparent flake separation and reduced stiffness will likely have a negative effect on briquette durability. Briquette fracturing over handling processes will reduce the bulk density of the product making it likely that the hammer milled briquettes will not maintain the same density as the 'as received' briquettes would.

Figure 6: Briquette produced at 7.0 MPa with 42 mm (as received) corn stover (3-way interaction experiment)

Figure 7: Briquette produced at 14.0 MPa with 42 mm (as received) corn stover (3-way interaction experiment)

Figure 8: Briquette produced using hammer milled (19 mm) corn stover (3-way interaction experiment)

2.4.4.2 Moisture Effects Experiment

2.4.4.2.1 Dry Particle Density

This experiment produced briquettes ranging in dry particle density from 170-400 kg/m^3. Based on the P-values in the factorial ANOVA for dry particle density, no significant mean differences were found for the die taper angle main or interaction effects (table 3). That hypothesis, however, for compression pressure and material moisture content was rejected. The p-values indicated potentially significant main effects caused by compression pressure and material moisture content.

Dry Particle Density (kg/m^3)						
Source	DF	Seq SS	Adj SS	Adj MS	F	P
Material Moisture Content (%wb)	2	76654.8	78633.1	39316.6	44.53	0.000
Compression Pressure (MPa)	1	15945.2	16026.6	16026.6	18.15	0.000
Die Taper Angle (deg)	1	1033.7	1021.4	1021.4	1.16	0.293
Material Moisture Content (%wb) * Compression Pressure (MPa)	2	8684.6	7515	3757.5	4.26	0.027
Material Moisture Content (%wb) * Die Taper Angle (deg)	2	1423.2	1669	834.5	0.95	0.403
Compression Pressure (MPa) * Die Taper Angle (deg)	1	119.5	64.3	64.3	0.07	0.790
Material Moisture Content (%wb) * Compression Pressure (MPa) * Die Taper Angle (deg)	2	2882.8	2882.8	1441.4	1.63	0.217
Error	23	20305.4	20305.4	882.8		
Total	34	127049				

Table 3: Factorial ANOVA for dry particle density (moisture effects experiment)

Compression pressure demonstrated similar effects to those observed during the 3-way interaction experiment. Increasing levels of compression pressure produced significant dry particle density gains at moisture contents at and below 24.8%$_{wb}$ moisture content (figure 9), however, this trend was not significant at increased moisture contents (47.6%wb).

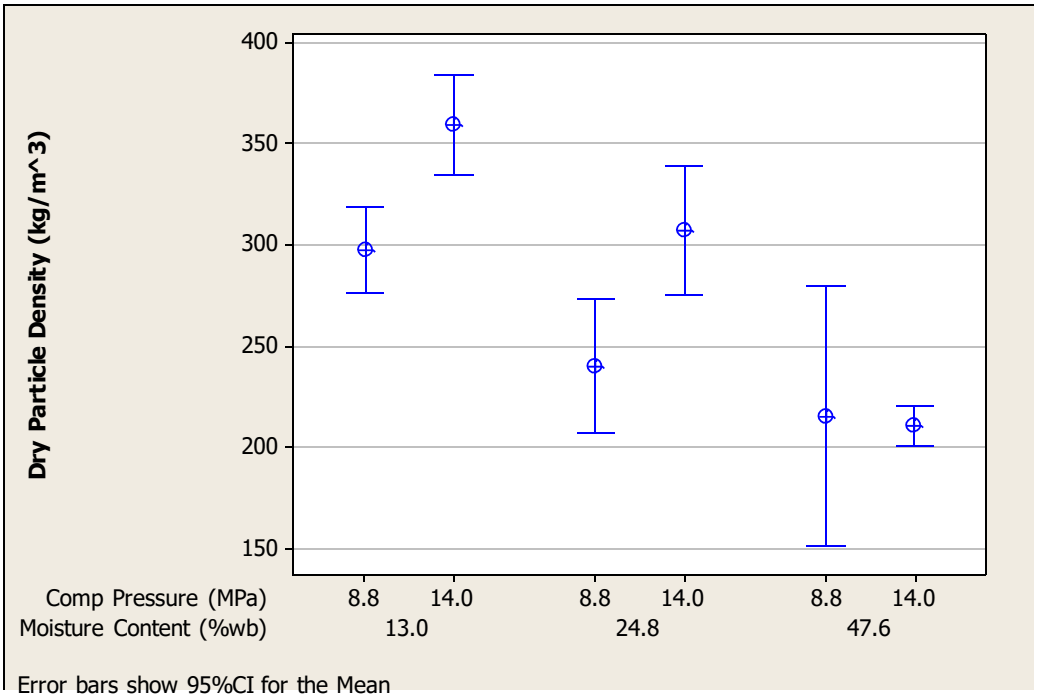

Figure 9: Treatment factor effects on dry particle density (moisture effects experiment)

Following a similar trend displayed during the 3-way interaction experiment, material moisture content had a significant negative effect on dry particle density. Averaged over all levels of compression pressure and die taper angle, material moisture content demonstrated a negative, linear relationship. From 13.0 to 47.6%$_{wb}$ moisture content, dry particle density decreased by approximately 35% (figure 10). While the final relationship between moisture content and dry particle density was similar between the 3-way interaction and moisture effect experiments, the reasoning behind the relationship was different. During the 3-way interaction experiment, increased moisture content led to decreased briquette dry weight and increased axial expansion, leading to significantly reduced dry particle density values. During the moisture effects experiment, the relationship was slightly different (figure 11). An increase in dry briquette weight was observed between 13.0 and 24.8%$_{wb}$ moisture content, followed by an insignificant change to 47.6%$_{wb}$. The weight increases were small (33% increase between 13.0 and 24.8%$_{wb}$) in comparison to the changes in briquette axial expansion over different moisture contents. A sharp trend was observed between 13.0 and 47.6%$_{wb}$ moisture content, where axial expansion increased by 360% which completely negated the density gains the increased dry particle weight offered. This indicates while certain moisture content levels might allow for more dry material weight to be densified, any density gained in that manner will be lost upon ejection due to the increased elasticity of briquettes made at increased moisture content.

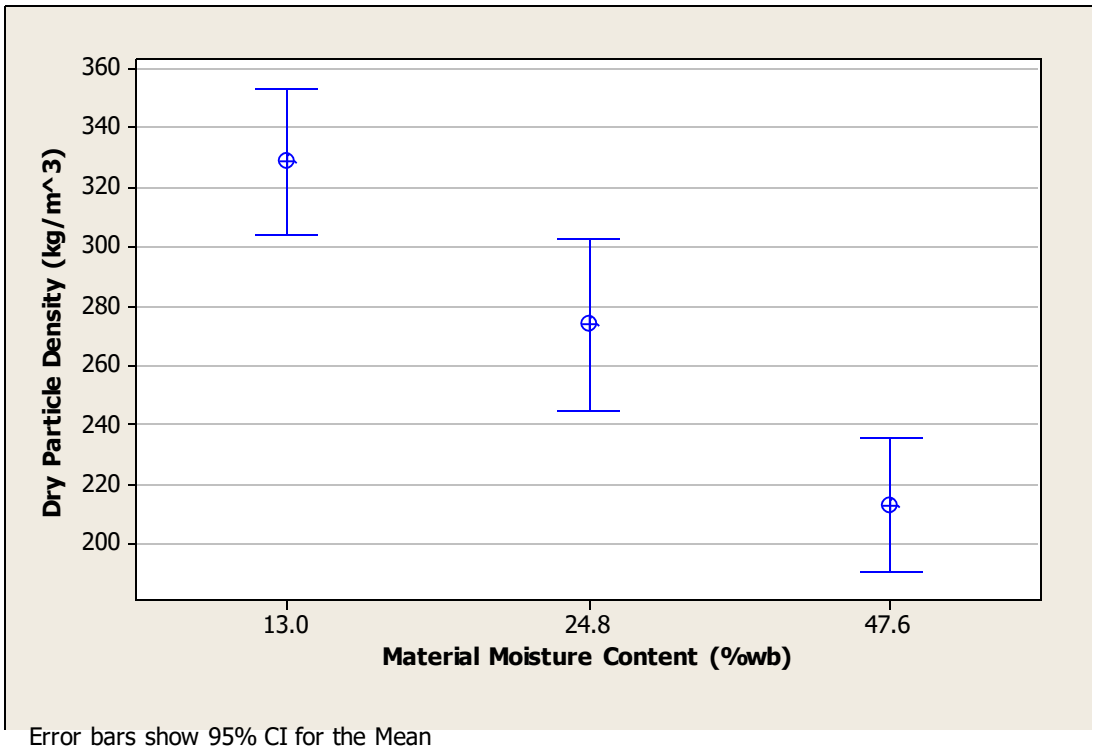

Figure 10: Moisture content main effect on dry particle density (moisture effects experiment)

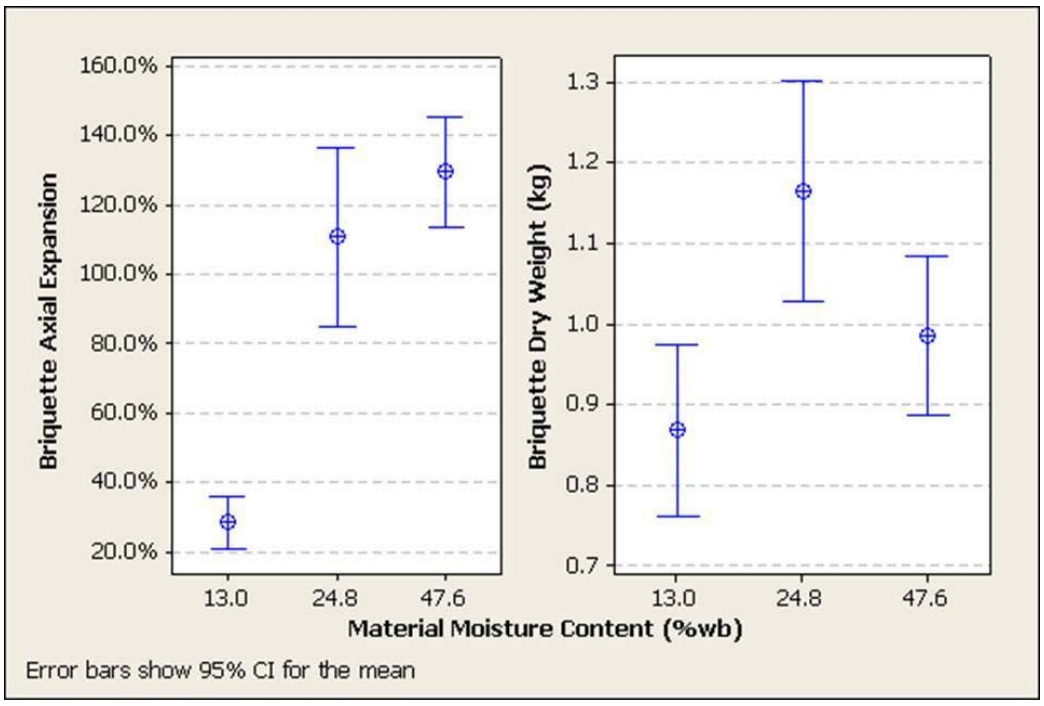

Figure 11: Moisture content effects on axial expansion and dry briquette weight (moisture effects experiment)

2.4.4.2.2 Dry Specific Energy

Briquettes were produced with a dry specific energy requirement of 16-37 MJ/t during the moisture effects experiment. Based on the p-values, the factorial ANOVA rejected the

hypothesis that compression pressure and material moisture content had no difference in group means (table 4) and accepted the hypothesis of no change in dry specific energy from die taper angle or any interaction factors.

Dry Specific Energy (MJ/t)						
Source	DF	Seq SS	Adj SS	Adj MS	F	P
Material Moisture Content (%wb)	2	175.089	156.99	78.495	8.55	0.002
Compression Pressure (MPa)	1	432.81	419.45	419.45	45.71	0.000
Die Taper Angle (deg)	1	0.327	0.594	0.594	0.06	0.801
Material Moisture Content (%wb) * Compression Pressure (MPa)	2	9.595	7.307	3.654	0.4	0.676
Material Moisture Content (%wb) * Die Taper Angle (deg)	2	20.315	21.432	10.716	1.17	0.329
Compression Pressure (MPa) * Die Taper Angle (deg)	1	17.381	16.897	16.897	1.84	0.188
Material Moisture Content (%wb) * Compression Pressure (MPa) * Die Taper Angle (deg)	2	21.187	21.187	10.593	1.15	0.333
Error	23	211.042	211.042	9.176		
Total	34	887.744				

Table 4: Factorial ANOVA for dry specific energy (moisture effects experiment)

As expected, compression pressure demonstrated a significant and positive main effect on the dry specific energy requirement (figure 12). Increasing the compression pressure from 9.0 to 14.0 MPa significantly increased the dry specific energy at 24.8 and 47.6%$_{wb}$ moisture content. At these higher moisture content treatments, a 60% increase in compression pressure added about 40% to the specific energy requirement (which increased dry particle density by about 0-30%). The ratio was not 1:1 because the extra compression pressure allowed more material weight to be briquetted as well. The mechanical energy requirement was increased by about 55% to increase the compression pressure, but the individual briquette weight was increased by about 15%. Based on the data means and confidence intervals, moisture content did not have a significant effect on dry specific energy (α=0.05).

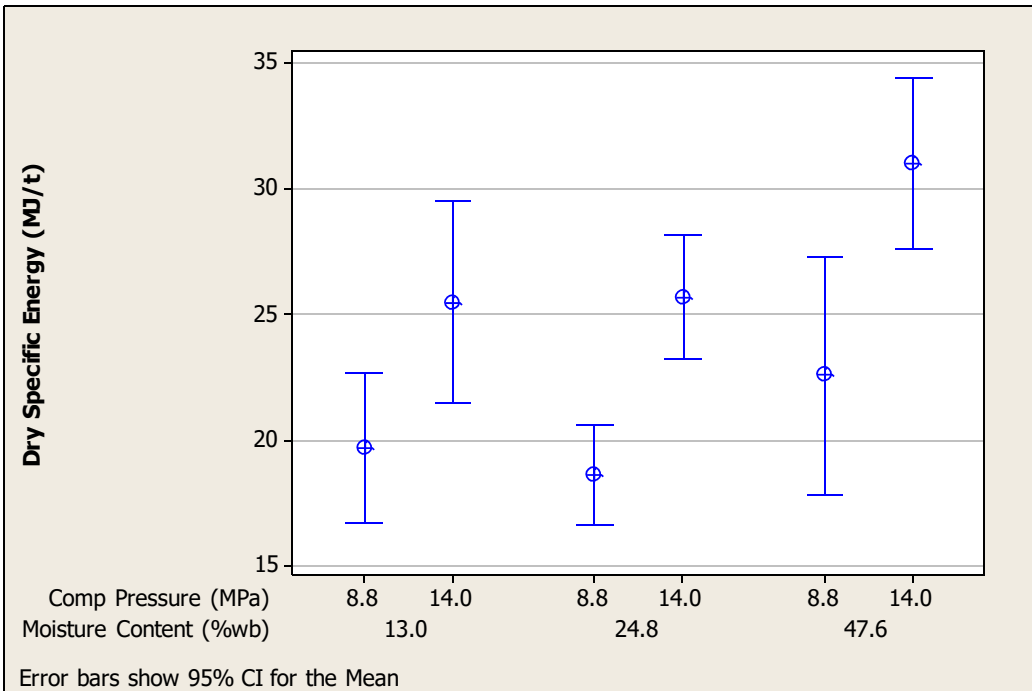

Figure 12: Treatment factor effects on dry specific energy (moisture effects experiment)

2.4.4.2.3 Qualitative Effects

The effect of material moisture content on briquette quality can easily be observed visually. Figures 7 and 13 show briquettes produced at 13.0 and 47.6%$_{wb}$ moisture content, respectively (all other treatment variables are equal). The obvious visual difference was the amount of axial expansion observed on the high moisture briquette. Dry briquettes can be easily handled (by hand) as a single unit, while wet briquettes cannot be moved without completely supporting the briquette. Without support, the wet briquette completely falls apart and handles like loose corn stover.

Figure 13: Briquette produced at 47.6%wb moisture content (moisture effects experiment)

2.4.4.3 Material Types Experiment

2.4.4.3.1 Dry Particle Density

This experiment produced briquettes ranging in dry particle density from 300-500 kg/m^3. The p-value in the factorial ANOVA showed no significant main effect from material type on dry particle density, however, it rejected the hypothesis of no difference from the interaction effect of material type and material particle size (table 5). The largest amount of variation was caused by compression pressure which was expected because compression pressure was always the second highest source of variation behind material moisture content in all of the other experiments with respect to dry particle density.

Dry Particle Density (kg/m^3)						
Source	DF	Seq SS	Adj SS	Adj MS	F	P
Material Type	2	3732	1371	686	2.01	0.154
Compression Pressure (MPa)	1	103604	102011	102011	298.66	0.000
Particle Size Reduction Method	1	4556	3790	3790	11.09	0.003
Material Type * Compression Pressure (MPa)	2	391	467	234	0.68	0.513
Material Type * Particle Size Reduction Method	2	3198	3032	1516	4.44	0.022
Compression Pressure (MPa) * Particle Size Reduction Method	1	27	40	40	0.12	0.734
Material Type * Compression Pressure (MPa) * Particle Size Reduction Method	2	7696	7696	3848	11.27	0.000
Error	27	9222	9222	342		
Total	38	132426				

Table 5: Factorial ANOVA for dry particle density (material types experiment)

Figure 14 shows a plot of the data means and confidence intervals of the dry particle density for each treatment variable combination during this experiment. No significant dry particle density differences were caused by material type ($\alpha = 0.05$). Similar to the previous experiments, the effect of material particle size was not consistent across each material type and compression pressure treatment, however, particle size did have a significant effect on pure cob materials at 14.0 MPa compression pressures. At this treatment, hammer milling the cobs resulted in an 11% increase in dry particle density.

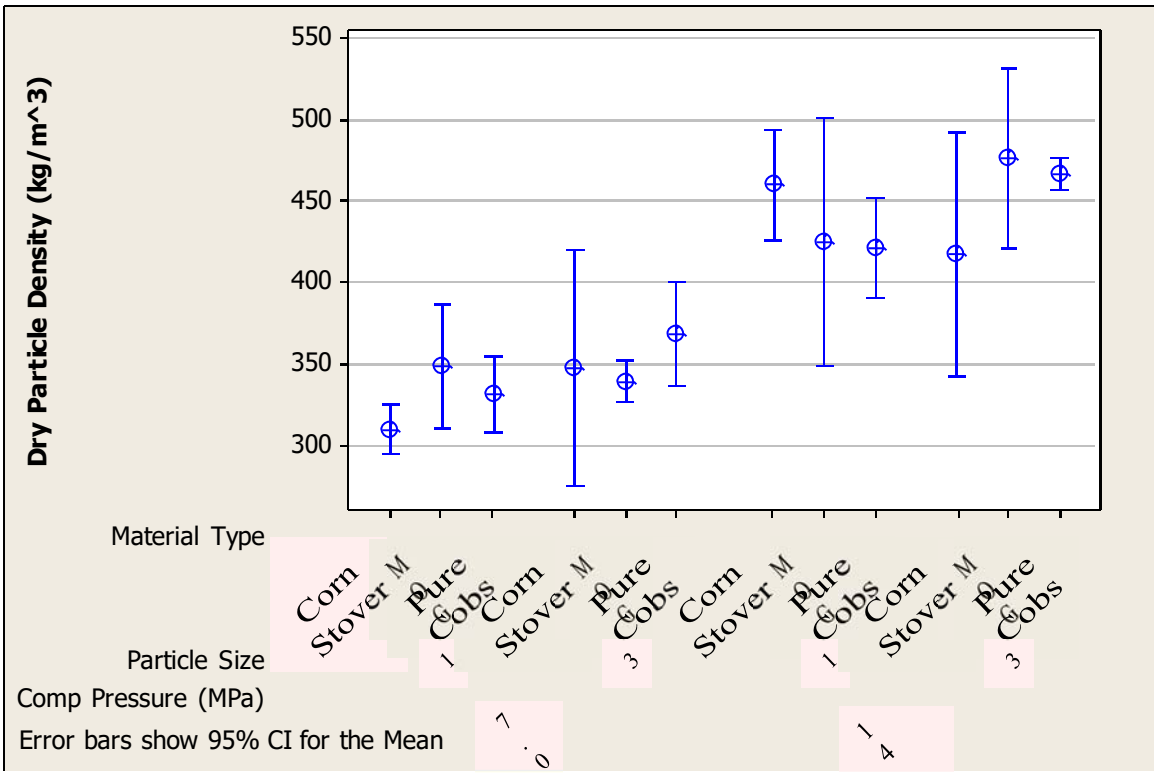

Figure 14: Treatment factor effects on dry particle density (material types experiment)

Compression pressure was the only variable that demonstrated consistently significant differences between treatment levels (for $\alpha = 0.05$) on dry particle density. Averaged across every material type and particle size reduction method, increasing compression pressure from 7.0 to 14.0 MPa increased the dry particle density by 30%. This can be directly attributed to a 30% increase in briquette weight with essentially no change in the briquette axial expansion. This is expected because all materials tested in this experiment were between 5 and 15%wb moisture content, which showed very little axial expansion in previous experiments.

2.4.4.3.2 Dry Specific Energy

Briquettes were produced with a dry specific energy range of 11-39 MJ/t during the material types experiment. The factorial ANOVA table for dry specific energy is shown in table 6. While material type showed a potentially significant effect based on 5% probability, there was only isolated significant treatment differences based on 95% confidence intervals (figure 15). For briquettes produced using an 'as received' particle size at 14.0 MPa compression pressure, pure cobs had approximately a 27% higher specific energy requirement than corn stover. No other treatment variable combinations demonstrated significant differences based on material type, indicating a weak relationship overall between material type and dry specific energy.

Dry Specific Energy (MJ/t)						
Source	DF	Seq SS	Adj SS	Adj MS	F	P
Material Type	2	39.49	35.99	17.99	5.19	0.012
Compression Pressure (MPa)	1	876.47	881.45	881.45	254.25	0.000
Particle Size Reduction Method	1	192.85	173.35	173.35	50	0.000
Material Type * Compression Pressure (MPa)	2	53.12	54.24	27.12	7.82	0.002
Material Type * Particle Size Reduction Method	2	33.01	30.2	15.1	4.36	0.023
Compression Pressure (MPa) * Particle Size Reduction Method	1	14.42	13.6	13.6	3.92	0.058
Material Type * Compression Pressure (MPa) * Particle Size Reduction Method	2	9.45	9.45	4.72	1.36	0.273
Error	27	93.61	93.61	3.47		
Total	38	1312.4				

Table 6: Factorial ANOVA for dry specific energy (material types experiment)

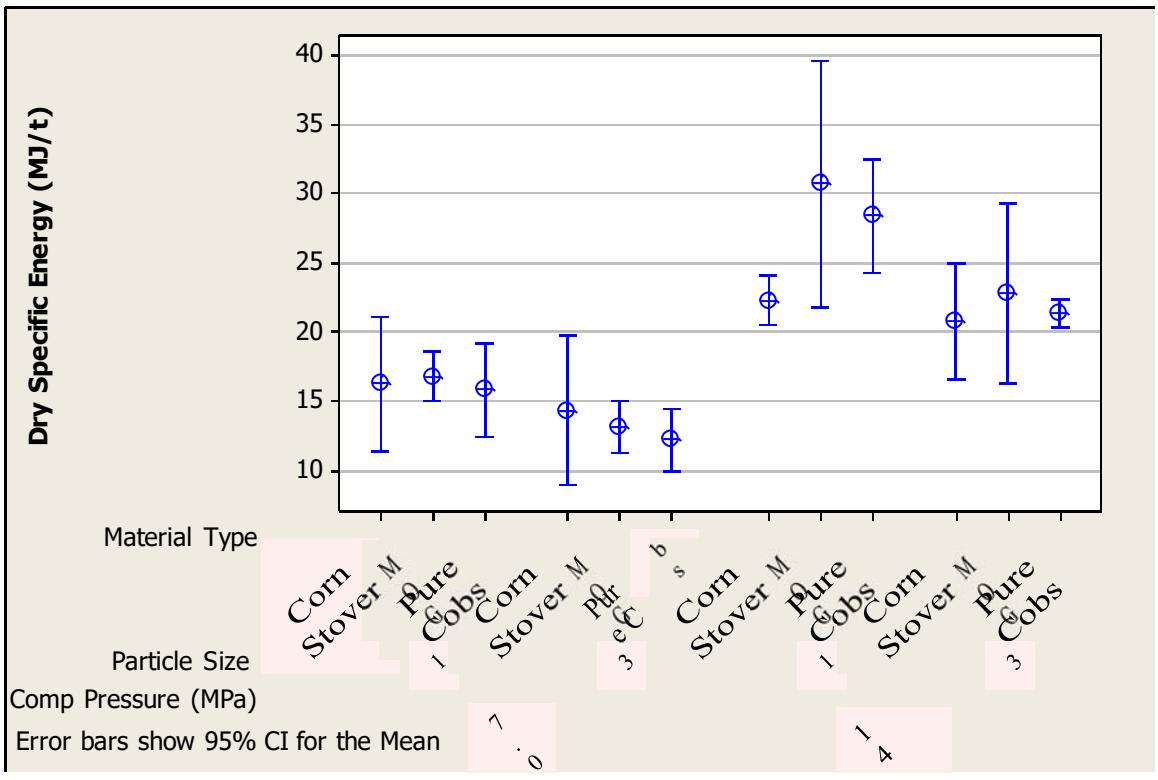

Figure 15: Treatment factor effects on dry specific energy (material types experiment)

Similar to the effect of material type, particle size reduction method also had only isolated significant effects on dry specific energy. MOG briquettes produced at 7.0 MPa, and pure cob briquettes produced at 14.0 MPa had similar significant effects caused by the particle size reduction method. In both of those treatments, 'as received' particle sizes had approximately a 30% higher specific energy requirement than hammer milled treatments.

Compression pressure demonstrated approximately the same trend on dry specific energy it showed during the moisture effects experiment. Averaged over all particle size reduction methods and material types, increasing the compression pressure from 7.0-14.0 MPa increased the dry specific energy by about 65% (14.7-24.3 MJ/t). The extra energy offsets the briquette weight gain at increased compression pressure, which led to an increased dry specific energy.

2.4.4.3.3 Qualitative Effects

Figures 7, 16, and 17 show briquettes made from corn stover, MOG, and pure cobs, respectively. The surface texture of MOG and pure cobs was significantly smoother and stiffer than the surface of the corn stover product. In every corn stover briquette produced the flake divisions were clearly visible, however, that visibility was reduced with MOG and nearly impossible to identify with the pure cob briquettes. MOG and pure cobs formed more of a single unit briquette compared with corn stover. Based on these observations, increasing cob content improved the overall briquette quality.

Figure 16: Briquette produced using MOG (material types experiment)

Figure 17: Briquette produced using pure cobs (material types experiment)

2.4.4.4 Bulk Density Experiment

As expected from previously presented results, the bulk density experiment demonstrated a highly significant effect from material moisture content on dry bulk density. Figure 18 shows the dry bulk density results from the two treatments of the bulk density experiment alongside the average dry particle density values for the same treatments. As expected, a large decrease was observed between particle density and overall bulk density. For 54.5%$_{wb}$ moisture content stover, the dry density decreased approximately 70% going from particle to bulk density while the 8.3%$_{wb}$ moisture content stover had a decrease of approximately 60%. The low moisture material had a mean dry bulk density of 190 kg/m^3 while the high moisture material had a dry bulk density of 64 kg/m^3, marginally improved from a non-densified material sample. This inefficiency in translating particle density to bulk density was created by large void spaces between the particles, creating a large amount of storage space taken by air.

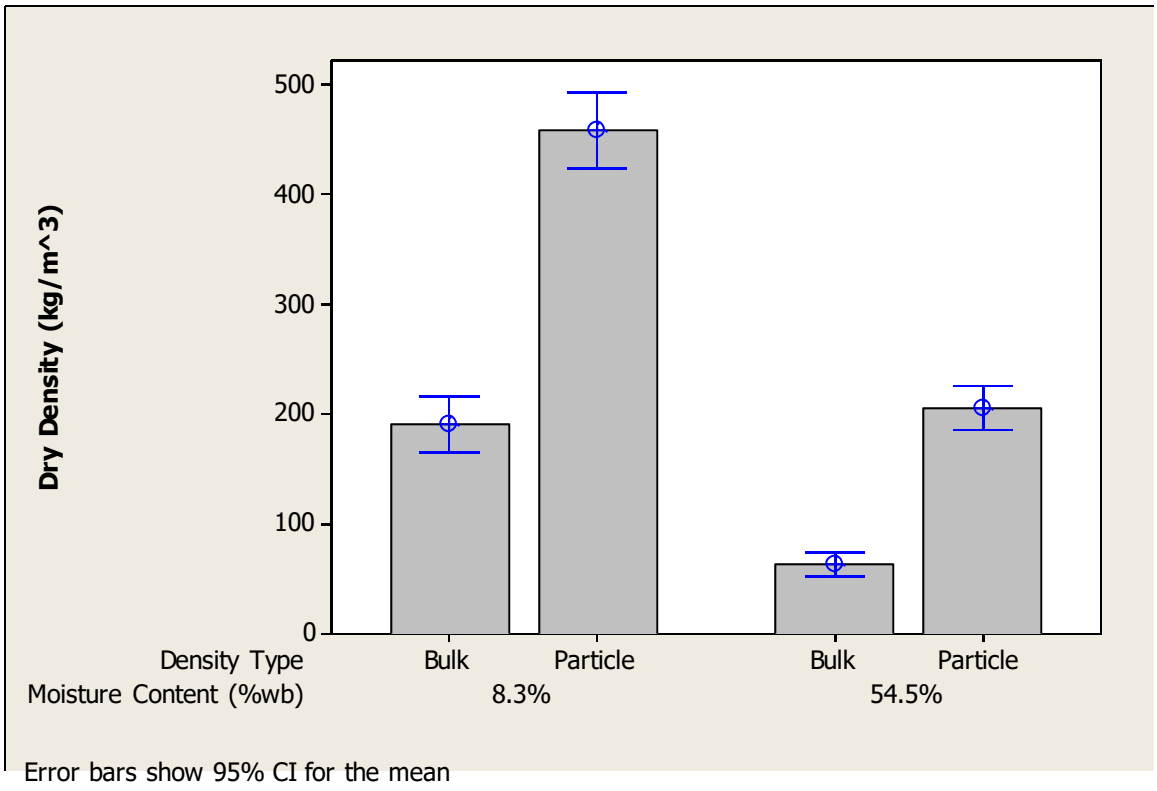

Figure 18: Material moisture content effect on density (bulk density experiment)

2.4.4.5 Summary

Compression pressure demonstrated significant and predictable effects on the output factors. Compression pressure was tested from 7.0-14.0 MPa and positive, fairly linear trends were demonstrated with respect to dry particle density and dry specific energy. At optimized treatment variables, dry particle density increased 50% (310 to 460 kg/m^3) when increasing compression pressure from 7.0-14.0 MPa. In that same range, dry specific energy increased by approximately 37% (16.3 to 22.3 MJ/t).

The experiments showed the most important effects on all of the output factors were caused by material moisture content. Material moisture content was tested on corn stover ranging from approximately 8-55%$_{wb}$ throughout the testing period and between 8 and 25%$_{wb}$ the briquette quality would translate from good to unacceptable. At optimized treatment variables, dry particle density decreased from 368 to 214 kg/m^3 (42%) when increasing material moisture content from 13.0 to 47.6%$_{wb}$. While dry particle density was significantly affected, dry specific energy was not consistently affected by material moisture content. Material bulk density would significantly decrease due to extreme amount of briquette expansion at moisture contents greater than 25%$_{wb}$, indicating future in-field densification systems based from this research will require materials dryer than 25%$_{wb}$.

Material particle size was not identified in any of the experiments for having consistently significant effects on particle density or specific energy. Qualitatively, decreasing particle size led to a greater number of flake divisions and a softer briquette. Based on the energy data demonstrated in the literature review, particle size reduction processes have very significant energy requirements. For this type of densification, any particle size reduction beyond the integrated chopper on the combine is not recommended.

While material type had minimal effects on dry particle density and dry specific energy, obvious qualitative differences were noted between treatments. Based on briquette stiffness and flake divisions, the overall briquette quality was significantly improved with increased cob content, therefore, harvesting systems that can increase cob content would be advantageous to this type of densification system. Further extrapolation of these advantages can be found in Thoreson, 2011 [7].

2.4.5 CONCLUSIONS

Based on briquette density and visual briquette quality, the following process variable settings should be used to maximize densified product quality.

- Only 'as received' material particle sizes (passed through an integrated combine chopper only) should be used to reduce briquette flake divisions.
- Maximum compression pressure (14.0 MPa) should be used to maximize particle density.
- Only moisture contents below 25%$_{wb}$ should be used to maximize briquette density and quality.
- Corn stover fractions with a greater cob content will improve briquette quality.
- Die geometry did not show any effects on density or specific energy.

While this densification method didn't increase the corn stover density enough to optimize over the road transportation, the improved bulk density was competitive with baled corn stover densities. Depending on the type and moisture of corn stover harvested, material can be continuously densified to approximately 190 kg/m^3 dry bulk density (210 kg/m^3 wet bulk density). Based on maximum legal trailer dimensions (without a specialized permit), this densified corn stover product allows over the road trucks to theoretically haul approximately 18-19.5 metric tons using a single, 16.1 m (53 foot), live bottom trailer. By comparison, up to 18-20 metric tons of large square bales (0.9 m x 1.2 m x 2.4 m) can be hauled using a single, 16.1 m (53 foot) flatbed or drop deck trailer.

The specific energy of optimal densification treatments was significantly reduced when compared with the alternative briquetting/pelleting densification systems. When compared with densification treatments that utilize 100-150 MPa compression pressures and 0.8 mm corn stover particle sizes, the specific energy requirement was reduced by approximately 40-55% while density was reduced by approximately 60%. This process can also be accomplished without any additional particle size reduction processes beyond the combine and proved to be a viable option for continuous densification of a large briquette.

REFERENCES

[1] DOE-USDA. 2005. Biomass as a Feedstock for a Bioenergy and Bioproducts Industry: The Technical Feasibility of a Billion-ton Annual Supply. Oak Ridge, TN.: U.S. DOE Office of Scientific and Technical Information.

[2] Knutson, J. and G. E. Miller. 1982. Agricultural residues in California – factors affecting utilization. Leaflet No. 21303, Cooperative Extension, Berkeley, CA: University of California.

[3] Mani, S., L. G. Tabil, and S. Sokhansanj. 2002. Grinding Performance and Physical Properties of Selected Biomass. ASABE Paper No. 026175. St. Joseph, MI.: ASABE

[4] Webster, K. 2010. Productivity and Logistical Analysis of Single-Pass Stover Collection Harvest Systems. ASABE Paper No. 1008567. St. Joseph, MI.: ASABE

[5] Kaliyan, N. and V. R. Morey. 2006. Densification Characteristics of Corn Stover and Switchgrass. ASABE Paper No. 066174. St. Joseph, MI.: ASABE

[6] Kaliyan, N., V. R. Morey, M.D. White, and A. Doering. 2009. Roll Press Briquetting and Pelleting of Corn Stover and Switchgrass. Transactions of the ASABE 52(2): 543-555

[7] Thoreson, C. P. 2011. Characterization of the Impact of Process Variables on the Densification of Corn Stover. MS thesis. Ames, Iowa: Iowa State University, Department of Agricultural and Biosystems Engineering.

[8] ASABE Standards. 2007. S424.1 – Method of Determining and Expressing Particle Size of Chopped Forage Materials by Screening. 663-665. St. Joseph, MI.: ASABE

[9] ASABE Standards. 2008. S358.2 - Moisture Measurement-Forages. 1. St. Joseph, MI.: ASABE

[10] Mani, S., S. Sokhansanj, and B. Xiaotao. 2004. Compaction of Corn Stover. ASABE Paper No. 041160. St. Joseph, MI.: ASABE

[11] ASTM Standards. 2006. E873 – 82: Standard Test Method for Bulk Density of Densified Particle Biomass Fuels. West Conschohocken, PA.: ASTM

2.5 Durability analysis of large corn stover briquettes

Curtis P. Thoreson and Matthew J. Darr

(published in: *Applied Engineering in Agriculture*)

ABSTRACT

Densification of agricultural residues is a key step in a cost-effective, large-scale, biomass feedstock supply system. Lab-scale densification systems exist which can produce large-scale densified corn stover briquettes that measure between 220 and 420 mm in length and with an average bulk density of 190 kg/m^3 (dry particle density of 460 kg/m^3). MOG (material other than grain) and pure cob briquettes produced similar lengths and dry particle densities of 424 kg/m^3 and 421 kg/m^3, respectively. Durability testing, utilizing a modified form of ASABE S269.4 (ASABE Standards, 2007) was conducted to determine the overall product quality associated with these densified briquettes. This publication describes experiments which quantified the durability or briquettes produced with different material types (corn stover, MOG, the chaff from a conventional corn harvest, and pure cobs) and material particle sizes (produced from a combine chopper, MOG, and a hammer mill with a 19-mm screen opening size). The durability rating varied with each of the main effect test parameters and produced a maximum 46% durability rating using pure cobs directly from a combine without additional size reduction. The durability rating was quite low for corn stover and MOG briquettes, and it was improved for pure cob briquettes. Biomass preprocessing in a hammermill significantly reduced durability due to a lack of fiber interaction throughout the large briquette.

2.5.1 INTRODUCTION

A new method of densification was developed which resulted in large agricultural residue briquettes (Thoreson, 2011). The densification system produced corn stover briquettes at low compression pressures (14 MPa) and coarse particle sizes (30-50 mm particle length). The briquettes (fig. 1) weighed between 0.9 and 2.0 kg, and they were approximately 220 to 420 mm long. They follow a tapered, cylindrical shape with a large diameter of about 127 mm, and a 3.6° taper angle. The production method for these briquettes was developed to determine if a densified biomass product can be produced at a reduced energy requirement. The energy requirement is reduced by utilizing lower compression pressures and larger particle sizes (eliminate intermediate fine grinding operations).

Figure 1. Example corn stover briquette produced during low compression pressure and coarse particle densification.

This densification method was tested at different levels of important material and mechanical process variables, including moisture content, particle size, material type, compression pressure, and die geometry. These variables were tested at multiple levels across several experiments to determine the main and interaction effects of each. During these experiments, briquettes were produced with dry particle densities up to 460 kg/m^3 with a specific energy requirement of approximately 22.3 MJ/t, depending on the combination of variables chosen. The experiments demonstrated that, for the given ranges tested, material moisture content had the largest impact on the output product density, while compression pressure also demonstrated significant effects.

Briquette durability is an important factor to indicate the feasibility of a densified biomass product. Product damage and density loss throughout handling processes after densification will reduce product consistency and increase handling costs. If a briquette can only tolerate a single handling operation before falling apart, the benefits of the densification process are very limited. Physical testing was required to quantify the effect of each treatment variable on briquette durability. ASABE standard S269.4 (*ASABE Standards*, 2007) contains procedures for measuring the physical properties (including durability) of densified materials like pellets and cubes. While no references were located that utilized the portion of the standard for determining durability of 'cubes,' several studies were identified that utilize the portion of the standard for quantifying the durability of pellets. Mani et al. (2004) utilized the pellet durability procedure to quantify the durability of corn stover briquettes, with output durability ratings ranging from 88 to 90. Kaliyan et al. (2009) utilized the same portion of the standard to test the durability of roll-press briquettes and ring-die corn stover pellets (durability rating ranged from 67 to 95). Based on the portion of the standard for determining the durability of a sample of 'cubes,' research objectives were developed to determine the effect of material particle size and material type on briquette durability, and express the outputs as Durability Rating and Size Distribution Index of the Durability. These variables were chosen for the analysis because during the briquette production the durability was not immediately obvious between different treatment levels. This analysis will provide numerical data to indicate the durability differences between these treatments.

2.5.2 MATERIALS AND METHODS

ASABE Standard S269.4 outlines a procedure for determining the durability of 'cubes,' which are defined as "An agglomeration of unground ingredients in which some of the fibers are equal to or greater than the length of the minimum cross-sectional dimension of the agglomeration. The configuration of the agglomeration may take any form." The usage of this procedure for measuring the durability of large agricultural briquettes was appropriate because many of the briquettes produced include particles exceeding 102 mm, which is the smallest cross-section of a briquette produced using the 3.6° die.

The S269.4 procedure for determining the durability of cubes involves tumbling the briquettes at a specified rate and period of time in a defined rotating tumbler box. After tumbling, the remaining particles are sorted based on final weight into discrete weight classes. The weight of all materials in each weight class was used in calculating the durability rating and size distribution index of the durability. Particles with a mass 20% greater than the original particle mass are designated 'CSM' (cube size material). If a sample does not produce any CSM in the

output sample, the durability rating is zero. Equations 1 and 2 show the calculations used to determine the durability rating (DR), and the size distribution index of the durability (SDI)

Equation 1. Durability Rating for Cubes

$$DR = \frac{M_{CSM}}{M_{INPUT}} \times 100$$

where

DR	=	durability rating
M_{CSM}	=	weight of cube sized material (particles weighing more than 20% of the average initial briquette weight)
M_{INPUT}	=	weight of input material

Equation 2. Size Distribution Index for Cubes

$$SDI = 4 \times M_{80-100\%} + 3 \times M_{60-80\%} + 2 \times M_{40-60\%} + 1 \times M_{20-40\%}$$

where

SDI	=	size distribution index
$M_{80\text{-}100\%}$	=	percent of total particles weighing 80% to 100% of the average initial cube weight
$M_{60\text{-}80\%}$	=	percent of total particles weighing 60% to 80% of the average initial cube weight
$M_{40\text{-}60\%}$	=	percent of total particles weighing 40% to 60% of the average initial cube weight
$M_{20\text{-}40\%}$	=	percent of total particles weighing 20% to 40% of the average initial cube weight

Material moisture content was determined using ASABE S358.2 (*ASABE Standards*, 2008). Samples were dried at 60°C for 72 h, and final weights were measured immediately following drying. Moisture content values for each treatment combination are shown in table 1 and are reported on a wet basis.

2.5.2.1 Durability Tumbler Development

2.5.2.1.1 Tumbler Capacity

The S269.4 standard does not describe the target volume range of a cube or offer any indication of the maximum volume the cubes should fill inside the tumbler box. The standard does mention that a sample of ten cubes should be utilized for durability testing. The standardized box volume was 0.042 m^3, and the average volume of ten large agricultural briquettes produced as part of this work was about 0.039 m^3 (91% of the standardized box capacity). The tumbling test defined in ASABE S269.4 was not suitable because the briquettes produced on the densification bench likely have a much larger volume than the cubes used to develop the standard.

To provide a more balanced volume ratio, the number of briquettes used in the box was reduced, and the S269.4 standard box dimensions were modified to increase the overall volume

capacity. The box dimensions were increased to 457 × 457 × 610 mm, which increased the volume to 0.127 m^3. The number of briquettes per test was reduced to three, which used only 9% of the new tumbler volume capacity.

2.5.2.1.2 Tumbler Speed

Due to the increase in overall size, the rotational radius of the tumbler box was modified. This required a change in rotational speed to maintain equal outside velocities between the test defined in the S269.4 standard and the enlarged tumbler box. The radius was assumed to be the width dimension of the box (305 mm on the standard box, 457 mm on the new box), and the tangential velocity at that radius was set equal between the two boxes. Based on these assumptions, the necessary shaft speed to drive the larger box at the same outside velocity as the standard box was 27 rpm. This speed was used for all durability experiments conducted in this project.

2.5.2.1.3 Tumbler Design

The modified, enlarged durability tumbler is shown in figure 2. The catch pan for any materials that fell from the tumbler box was removable for quick mass determination and cleaning. A chain drive powered by a hydraulic gear motor was used to power the drive system. Material was added and removed from the tumbler box through a hinged door. The tumbler was powered by an external hydraulic power supply with adjustable flow control to control the rotational speed. Rotational speed was calibrated before each experimental treatment.

Figure 2. Enlarged rotating tumbler used for durability testing.

2.5.2.1.4 Durability Testing Method

While the mechanical design of the durability tumbler was altered, the procedure for determining the durability of cubes was not modified. With the exception of operating the tumbler at 27 rev/min, as opposed to 40 rev/min, the procedure from sections 5.1.1-5.1.6 in ASABE Standard S269.4 was followed to quantify the durability of the large briquettes. The briquettes were tumbled for 3 min, and the mesh hole size was 12.7 mm, as stated in the standard.

2.5.2.1.5 Statistical Analysis

All statistical tests were conducted using Minitab software. This durability experiment utilized full-factorial experiment design with three replicates of each treatment, which allowed the use of the factorial analysis tool (ANOVA) to determine the variation caused by each

treatment factor. Factorial ANOVA was used to determine the significance of each treatment variable on the selected output factor. Confidence interval plots were used to determine if significant differences were present between treatment variable levels. The confidence intervals assume a normal distribution of the data and use critical values following a t-distribution. Treatments were reported to be significantly different if the confidence intervals do not overlap for $\alpha = 0.05$.

2.5.2.2 Durability Experiments

The objective of these experiments was to determine the effects of corn stover material type and particle size on the durability rating and size distribution index of the output briquettes. The material types represented different fractions of corn stover that could be harvested using different header and corn stover processing attachments. Corn stover was harvested using an 'all crop' header which cuts the corn stalk just below the ear and harvests all material above that point. Material other than grain (MOG) was harvested using a conventional ear-snapping corn header which harvests mostly the corn cob and husk. Pure cobs are produced in the same manner as MOG, but are processed using a secondary cleaning attachment to clean the husk and leaf material from the MOG, leaving mostly cobs. The material particle size treatments represented different particle size reduction methods. The 'as received' particle size treatment (method 1 in table 1) was material that had passed through an integrated chopper on a combine harvester, but saw no further size reduction. The hammer milled material (method 3 in table 1) had passed through both the combine chopper and a hammer mill with a 19-mm screen hole size.

A factorial experiment was developed which tested the three material types and both material particle size reduction methods. Due to the different nature of each corn stover fraction, each material type did not have the same particle sizes for the same size reduction treatment, or the same moisture content. Table 1 shows all treatment combinations tested in this experiment, along with the actual particle size and moisture content of each treatment. Each treatment was replicated three times for a total observation count of 18. All durability tests were conducted within 24 h of briquette production. Corn stover for this experiment was sourced from multiple dates in various locations around the Ames, Iowa region during the fall 2010 harvest. Since these materials were collected from production scale corn stover harvesting operations, the exact corn varieties, harvest dates, and locations for these materials are not known.

Table 1. Treatment design for the durability experiment.

Durability Experiment						
		Particle Size Reduction Method[a]		Moisture Content[c]	Average Initial Briquette Mass	Initial Briquette Dry Particle Density
Treatment	Material Type	(method)	(mm)[b]	(%wb)	(kg)	(kg/m^3)
1	Corn stover	3	17	8.3	1.49	460
2	MOG[d]	3	12	12.0	1.45	424
3	Pure cobs	3	2	10.0	1.26	421
4	Corn stover	1	42	8.3	1.28	417
5	MOG[d]	1	31	11.0	1.30	386
6	Pure cobs	1	39	10.0	1.09	372

[a] Particle size reduction method 1 indicates hammer milled material, while reduction method 3 indicates 'as received' material from a combine harvester.

[b] Geometric mean particle length as defined by ASABE Standard S424.1 (*ASABE Standards*, 2007).

[c] Wet basis moisture content as determined using ASABE Standard S358.2 (*ASABE Standards*, 2008).

[d] MOG indicates 'material other than grain,' the resulting chaff from corn harvesting using a conventional ear-snapping corn header.

2.5.3 RESULTS

Factorial ANOVA was used to determine the significance of each treatment factor on both durability rating and size distribution index. The tumbler experiments revealed strong main and interaction effects from both material type and particle size on the durability rating and size distribution index. Table 2 shows the ANOVA results for both the durability rating and size distribution index of the durability. The near-zero p-values show that both particle size control and material type demonstrate potentially significant main and interaction effects. Particle size was responsible for the most variation, and the same variation was seen between the main effect of material type and the interaction of the two variables. This was caused by the extreme effects of material particle size on both output factors.

Table 2. Durability experiment factorial ANOVA for durability rating and size distribution index.

Durability Rating

Source	F	Seq SS	Adj SS	Adj MS	F	P
Material type (name)	4	717.44	717.44	358.72	15.83	0.000
Particle size reduction method	42	3556.42	3556.42	3556.42	156.98	0.000
Material type (name)* particle size reduction method	4	717.44	717.44	358.72	15.83	0.000
Error	26	271.86	271.86	22.66		
Total	77	5263.15				

Size Distribution Index of the Durability

Source	F	Seq SS	Adj SS	Adj MS	F	P
Material type (name)	5	2179.58	2179.58	1089.8	32.36	0.000
Particle size reduction method	8	5432.8	5432.8	5432.8	161.31	0.000
Material type (name)* particle size reduction method	5	2179.58	2179.58	1089.8	32.36	0.000
Error	26	404.1	404.1	33.7		
Total	77	10196				

Based on the differences between the 95% confidence intervals, the plots of durability rating and size distribution index show strong main effects from both material type and material particle size, and a significant interaction effect between the two (fig. 3). Any briquette made from material that was hammer milled had a zero durability rating. While no significant differences were observed between corn stover and MOG, significant durability improvements were quantified for pure cobs. As indicated by the low values of the size distribution index of the durability, the remaining particles from any of the tests were much lighter than the original briquette, indicating significant breakage occurred during the test regardless of the combination. The plots also show the confidence interval for chopped MOG briquettes having a range below zero for both durability rating and size distribution index of the durability. This is not physically possible, as zero durability is the minimum possible value from this test. This was not accounted for in the statistical calculations (based on a t-distribution) and it indicates the data was not normally distributed, which was assumed when calculating the confidence intervals.

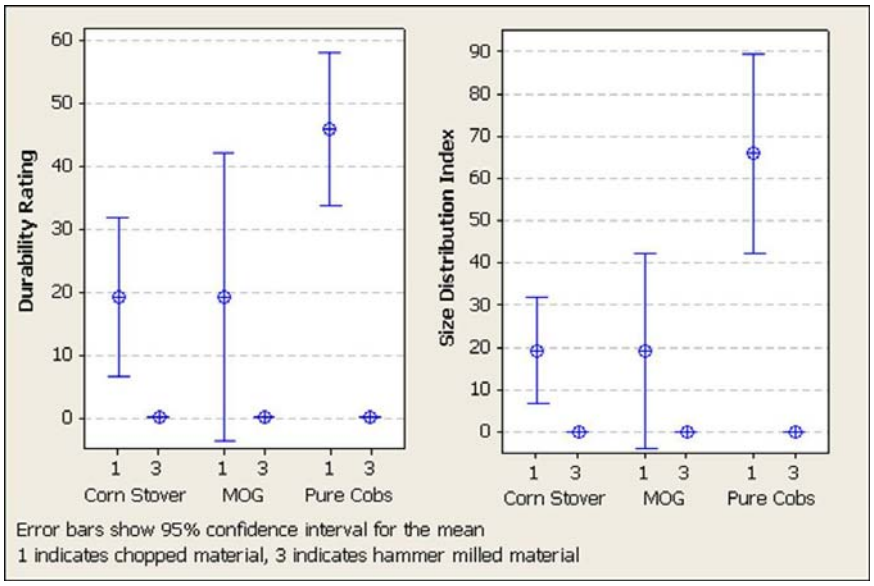

Figure 3. Interval plots for treatment variable effects on durability rating and size distribution index.

The durability improvement when moving from corn stover and MOG to pure cobs indicates either adding cob content to the briquetted material positively affects durability, or adding stalk, leaf, and husk content to the material negatively impacts durability. Shifting across those materials from corn stover, to MOG, to pure cobs reduces the stalk and leaf content, and increases the cob content.

Tests that resulted in zero durability ratings had the same appearance after tumbling as the input product to the densification system. Figure 4 shows a representative sample from a zero durability rating trial of hammer milled corn stover. All of the trials that resulted in a zero durability rating had a very similar appearance. Briquettes produced with hammer milled material all felt noticeably softer after densification when compared with the briquettes from chopped material. During basic handling after densification, the hammer milled briquettes tended to begin separating at the flakes, while the chopped briquettes held together much more readily. The chopped briquettes tended to have longer pieces of material stretching across multiple flakes, which may improve the strength between them, whereas on the hammer milled briquettes, the particles are too small to provide much structure to the flake joints.

Figure 4. Output product from a hammer milled corn stover durability test.

The chopped MOG briquette treatments showed improved durability ratings compared with the hammer milled samples, and this can be observed from the output sample from the tumbler (fig. 5). This material was able to retain a small amount of the original briquette mass and shape with three remaining particles that were 20% to 40% of the original briquette weight in this particular test. The remainder of the material either completely fractured back to loose material or remained in single briquette flakes that were less than 20% of the original average briquette weight.

Figure 5. Output product from a chopped MOG durability test.

The chopped pure cob briquettes demonstrated the best durability based on the output values, and this can also be seen in the output material (fig. 6). This material was able to retain particles that weighed into the 20% to 40% and 40% to 60% mass class, and had very little product that was completely loose after the tumbling. The majority of the material that did not qualify as CSM was still in a densified form.

Figure 6. Output product from a chopped pure cobs durability test.

2.5.4 CONCLUSIONS

This modified durability tumbling apparatus facilitated the durability analysis of a larger densified corn stover product. While the machine was altered, the same procedure and durability grading system was used as prescribed in ASABE S269.4. Overall, the durability rating of all of the process variable treatments tested was quite low. Materials conditioned on a hammer mill to reduce particle size all had zero durability during tumbler testing. Significant durability improvements were observed between corn stover, MOG, and pure cobs. Pure cob briquettes produced the best durability of all combinations, with a durability rating of 46%. Even though the durability rating of this densified material was quite low, a densified corn stover feedstock produced at these settings could still provide benefits to in-field, single-pass harvesting systems. The handling operations required to get the material harvested, densified, transported, and stored would likely be less intense and frequent than those simulated using this apparatus. Defining the durability requirements for a densified product produced using in-field biomass harvesting systems to deliver a feedstock to an upgrading or processing plant would provide a better indication of the potential of this type of briquetting for large scale biomass production.

Acknowledgements

This research was supported by funding from the North Central Regional Sun Grant Center at South Dakota State University through a grant provided by the U.S. Department of Energy Office of Biomass Programs under award number DE-FG36-08GO88073.

REFERENCES

ASABE Standards. 2007. S269.4: Cubes, pellets, and crumbles-definitions and methods for determining density, durability, and moisture content. St. Joseph, Mich.: ASABE.

ASABE Standards. 2007. S424.1: Method of determining and expressing particle size of chopped forage materials by screening. St. Joseph, Mich.: ASABE.

ASABE Standards. 2008. S358.2: Moisture measurement-forages. St. Joseph, Mich.: ASABE.

Kaliyan, N., V. R. Morey, M. D. White, and A. Doering. 2009. Roll press briquetting and pelleting of corn stover and switchgrass. *Trans. ASABE* 52(2): 543-555.

Mani, S., S. Sokhansanj, and B. Xiaotao. 2004. Compaction of corn stover. ASABE Paper No. 041160. St. Joseph, Mich.: ASAE.

Thoreson, C. P. 2011. Characterization of the impact of process variables on the densification of corn stover. MS thesis. Ames, Iowa: Iowa State University, Department of Agricultural and Biosystems Engineering.

CHAPTER 3
OPTIMAL BIOMASS FEEDSTOCK HARVESTING PATHWAY BASED ON QUANTIFIED FIELD SCALE LOGISTICS FOR HARVEST, DENSIFICATION, AND TRANSPORTATION

3.1 Background

Single-pass corn stover harvesting is a novel approach to corn stover harvesting that will produce a clean and high quality product that many end users (ethanol and fibrous plant material) will ultimately benefit from using. Single-pass harvesting with a combine designed for corn harvest today will slow a combine because of the increase material flow through the combine. Development of two separate systems have begun one concentrating mainly on collecting stover in a loose bulk material and another system concentrating on baling the material behind the combine. The two different systems have different effects on the productivity of the combine in the field but also have can affect the cost of harvesting corn stover based upon the amount of equipment needed to adequately support the corn stover harvest collection process.

3.2 Objective and Specific Tasks

This chapter addresses the second objective of this project which was to determine the optimal biomass feedstock harvesting pathway based on quantified field scale logistics for harvest, densification, and transportation to a storage facility. This objective was accomplished through a set of tasks:

1. Generate field scale experimental data for total energy and logistical requirements of corn stover harvest and delivery to the field edge for most likely harvest scenarios.
    a. This was completed by harvesting over 1000 acres of corn over a period of two years. The test factors analyzed were the baseline combine harvesting grain, the combine configure to harvest loose bulk stover, and the combine using a single-pass baler. The combine and stover collection equipment was instrumented to capture fuel consumption, speed, and stover weight in either a cart or in a bale.
    b. Year three of the data collection strictly tested a single-pass baling combine in a production setting which harvested over 1000 acres itself. This tested the combine in baseline grain harvesting as well using a single-pass baler.
    c. The data was analyzed to determine the productivity loss of the combine from harvesting the increase material flow of the corn stover through the combine and the impact of the stover harvest system on the productivity as well.
    d. Over the course of the experimentation the feasibility of near future commercial development of a stover briquetting machine for the efficient transport of corn stover was low. This was then removed from the test plan.
    e. Commercial demonstration of a cob-only harvest machine was achieved at the start of this project. However, as the development of future stover cellulosic ethanol plants progressed the ability to process cobs and stover lessened the demand for cob-only harvest equipment and increased the demand for machines that could collect the whole plant. Testing the cob-only equipment was removed from the test plan.

2. Determine least cost harvest and transportation methods for corn stover delivery to the field edge.
    a. Development of a model from in-field data was used to determine the least cost method for harvesting and transporting corn stover to the field edge. This data was collected for the bulk harvest configuration of a combine and the single-pass baling platform.
    b. It was determined that the most easily adapted equipment was the single-pass baling platform. A report was completed that detailed the least cost method of harvesting (baling) and transport to the field edge. An article is currently under internal review for future publication in peer reviewed journal.
    c. Due to the movement of the industry from exploration of commercial scale bulk harvest equipment to scaling up of baling

3.3 Overall Impacts of study

Data collected during testing is unique to previous research because of the implementation of real-time data logging of vehicle performance and logistics in the field during the harvest season. The completion of this analysis allows producers to make rational decisions on whether to collect stover in a single-pass operation or in a multi-pass system. This data also helps agricultural equipment companies set performance goals to meet for equipment in single-pass harvest systems.

3.4 Single-pass corn stover harvesting system productivity analysis

Keith Webster, Matthew J. Darr, Curt Thoreson, and W. Edwards

(to be submitted to a peer-reviewed journal)

ABSTRACT

Commercial stover harvesting for ethanol and biofiber production is just starting to emerge as a new industry in Iowa and the United States. As more corn stover is demanded to supply plants more and more acres of corn will need to be harvested and baled. As the industry develops a better understanding of the impurities in material a market will develop for corn stover that is harvested with minimal soil contamination. Multi-pass harvesting is one option of harvesting corn stover but it comes with a penalty of increased soil contamination in the corn stover of greater than 6-8% ash. Single-pass harvesting has the preferred ash content of the stover of around 3.5% ash. The issue with single-pass harvesting is the problem of slowing the combine productivity in-field during harvest due to the additional draft loads of a baler and processing the corn stover. Reaseach conducted at Iowa State University show a productivity reduction of 11% when a combine towed a baler through the field and a 25-50% reduction in the combine's productivity in processing and separating the extra stover from the grain.

3.4.1 INTRODUCTION

Corn grain ethanol has been a staple in the renewable energy portfolio of the United States for many years. From its initial start to present it has undertaken a long and tenuous process of trial and error with the rapid development of the industry only coming in the last 10 years since 2000. The Energy Independence and Security Act of 2007 (EISA, 2007) mandated that advanced biofuels such as cellulosic ethanol be produced at a rate of 79.38 billion liters (21 billion gallons) per year by 2022. In 2011, renewable fuels including corn grain ethanol were only mandated to produce 52.9 billion liters (13.95 billion gallons) of fuel. Of this amount, advanced biofuels including cellulosic biofuels were to produce 5.1 billion liters (1.35 billion gallons) of that total. Cellulosic biofuels were mandated to produce .95 billion liters (.25 billion gallons) of fuel. Cellulosic biofuels must develop methods and build up infrastructure that will support the production of 60.5 billion liters (16 billion gallons) of the 136 billion liters (36 billion gallons) of total renewable fuels made in the United States by 2022 or in the next 11 years. Compare this to corn grain ethanol which has been subsidized since the start of the National Energy and Conservation Act of 1978 (California Energy Commission, 2004). It was produced on a smaller scale initially which allowed it to develop a supply infrastructure. Cellulosic biofuel infrastructure development will need to be much more rapid. Cellulosic biofuels while not a new idea have had far less time to perfect its supply infrastructure with movement to large scale production only beginning to be developed. Not only do feedstocks need to be identified that can produce biofuels efficiently, but systems must be developed to

harvest the feedstock, transport the feedstock to the plant, and process the feedstock into a convertible product. One feedstock, corn stover, has been identified as a potential feedstock in the Midwest United States due to its wide availability (Hettenhaus & Wooley, 2000).

Most plant material is returned to the soil in current corn cropping systems. While it is the least labor intensive method of getting rid of the excess material it does present challenges. Development of higher yielding and more resistant varieties of corn to disease and insects has in many producers' opinions made it more difficult to breakdown the remaining plant residue over the winter period and hampers new crop planting in the spring. Now some producers will take additional passes over the field with extra tillage or shredders in order to enhance material breakdown either in the fall or spring (Hanna & Al-Kaisi, 2008).

The current design of the multi-pass collection systems for livestock systems emphasizes quantity rather than quality of material harvested. However, for the renewable energy future this thinking must be changed to improve quality and to address sustainability concerns. New constraints to harvesting will be introduced such as moisture content and quality much like corn grain is currently subjected to. One way to improve material quality is to use a single-pass harvest and collection system. Single-pass systems take the higher portion, which has less nutrient value and more stable moisture content than other sections of the plant (Karlen, 2008). Multi-pass system will harvest almost all of the lowest part of the plant that has the highest moisture and nutrient levels (Johnson, et al., 2010). Single-pass harvest systems have a selectable height and therefore infinite harvest rate with the typical harvest height of within one foot below the ear as shown in Figure 1. Single-pass harvest systems have been under development for many years now. The initial single-pass harvester was developed (Rosenthal, 1950) and continues in development today. The two systems that have emerged as possible solutions to maximize collection and harvest of corn are a bulk harvest system and a baling harvest system.

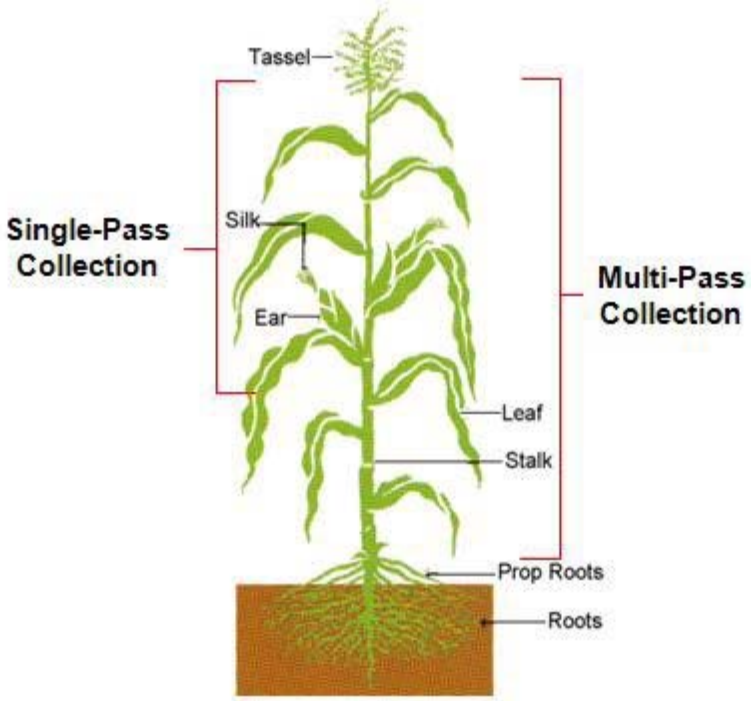

Figure 1: A comparison of the cut height for a single-pass and the multi-pass harvest.

Today there are two single-pass corn stover harvesting concepts that are being investigated within the industry, a bulk harvest system and a baling harvest system. Vermeer manufacturing and a collaboration between John Deere, Hillco Technologies, and Iowa State University each have produced a bulk cob harvester. The single-pass bulk stover harvesting system and the single-pass baling harvest system. The dual stream single-pass corn stover harvest systems that exist, beyond the current cob harvest systems. At Iowa State University development of an attachment that will attach to the back of a combine that will convey stover into a wagon that is towed by a tractor is currently being investigated (Schlesser, 2007). The implementation of the single-pass baling harvesting system originated in Western Australia in order to catch weed seed that had become hard to control in the fields (Glenvar Bale Direct, 2007). These systems are being used to produce anywhere from 0.9 - 3.2 Mg (1 – 3.5 ton) of wheat straw per acre. These are now entering the corn stover harvesting market in the Midwest and marketing to corn cob producers (Mud Hog, 2011) (AGCO Corporation, 2010).

Some of the first analysis of performance of modern single-pass combines set to collect stover was performed by Shinners et al. (2005). Results from this test showed that overall, harvesting stover with the whole crop head at its lowest height could reduce combine productivity by 50%. Shinners et al. (2009) followed up this research by modifying the current combine design and also testing new header concepts. Similar results were seen in performance between the new header concepts. Very little published work has been completed to provide a database on actual single-pass baling machine performance. Earlier analysis of data from the 2009 harvest at Iowa State University suggests a 15% drop in combine productivity while towing a baler during harvest (Webster et al. (2010)).

The objective of this work is to quantify the productivity loss in a combine due to the additional power needed to process and separate the corn grain and additional corn stover. Data collected from a combine modified to harvest additional corn stover and to either bale it or convey it into a catch wagon in a loose bulk form. Corn stover was harvested from 500 acres over two years in order to collect the data necessary for determining this.

3.4.2 MATERIALS AND METHODS

3.4.2.1 COMBINE AND HEADER

A John Deere STS combine was selected to perform all tests for the 2010 harvest season. The combine was outfitted with a 12.5 L engine, four wheel drive, and a twelve row corn head with selectable row configurations for stover collection. The combine was classified as a Class 8 (279+ kW; 375+ hp) machine with an engine horsepower output ranging from 360 – 380 kW (480 – 514 hp).

By switching any of the twelve rows of the header to either a conventional harvest system or a stover harvest setting, the rate of stover collected by the combine was varied. These row configurations corresponded to the varying rates of collection dependent upon crop conditions and the crop year, about 1.1 Mg/ha (.5 tn/ac) for zero row, 2.5 Mg/ha (1 tn/ac) for six row collection and 4 Mg/ha (1.75 tn/ac) for twelve row collection. These rates were variable, mainly dependent on overall crop conditions such as plant height.

3.4.2.2 HARVEST SYSTEM TESTING CONFIGURATIONS

3.4.2.2.1 CONVENTIONAL HARVEST SYSTEM

To collect baseline performance data, the combine was configured to the normal (conventional) operating system. This entailed disabling power to the blower section of the bulk harvest system which was attached to the back of the combine by means of removing the drive belt between the chopper and blower. Once the blower was disabled, the straw spreaders were re-attached to the back of the machine and powered hydraulically. The spreaders kept residue from windrowing as it came out the back of the machine and preventing interference with standard tillage practices.

The conventional harvest system used the corn head to strip as much biomass material away from the ear of corn prior to gathering the ear for threshing inside of the combine. Most stalk and plant residue was processed by the head and left on the ground to deteriorate or be harvested for stover in a multi-pass harvest system. The combine then threshed and separated the grain from the material other than grain (MOG) and elevated the grain to the combine's hopper. The MOG was then conveyed by the chopper out the back of the machine onto the spreaders to be returned to the soil.

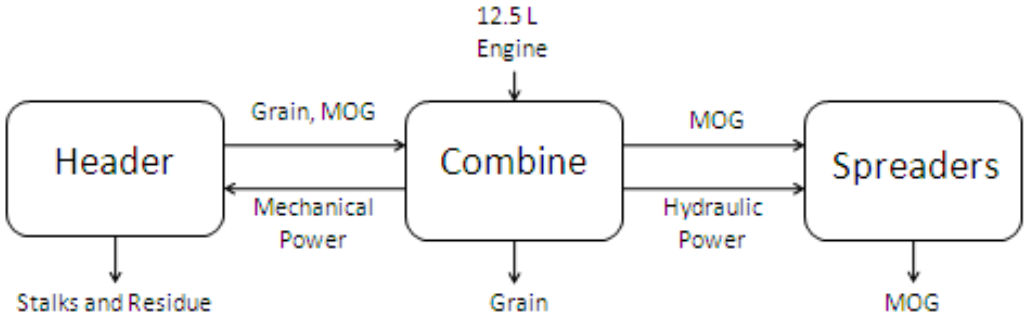

Figure 2: Detailed pathway of corn plant pathway through the combine, stalks and residue are left on the ground at the header and grain and MOG are passed through the separator.

3.4.2.2.2. SINGLE-PASS BULK HARVEST SYSTEM

The single-pass bulk harvest system that was tested consisted of the John Deere combine with the bulk stover attachment and an Oxbo model 1516 hydraulic side dump cart towed by a John Deere 8245R tractor. The 30 cu m (1100 cu ft) cart was outfitted with digital scales in order to track the weight of corn stover being removed from the field during a test.

Figure 3: Combine in bulk stover collection configuration conveying stover into the Oxbo 1516 cart being towed by a John Deere tractor. This was one of the configurations tested.

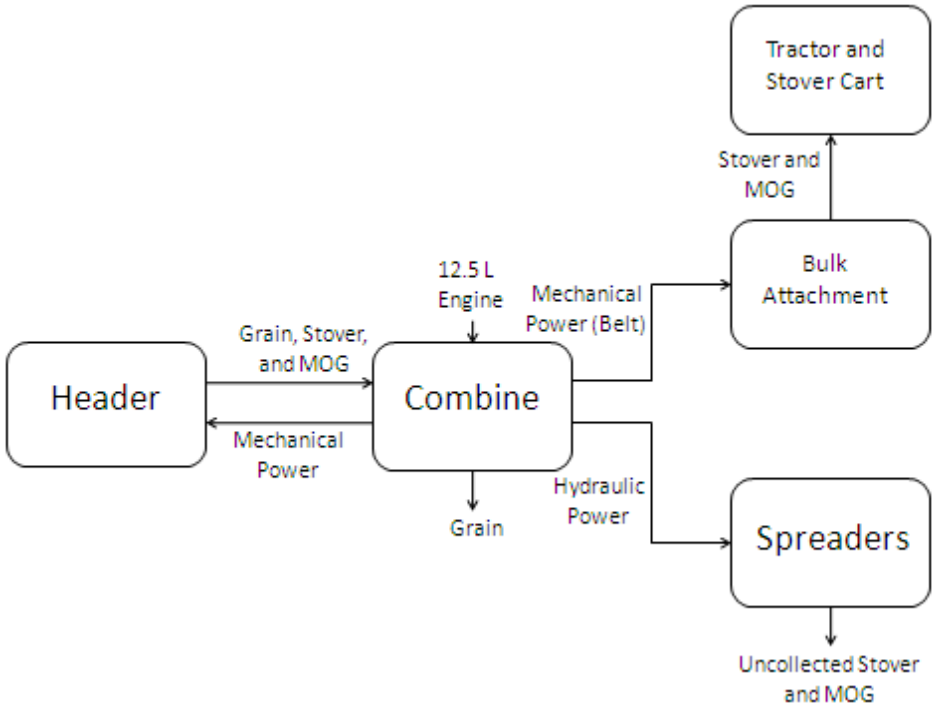

Figure 4: Detail diagram of the power distribution and pathway for the corn stover through the combine and the bulk harvest attachment.

3.4.2.2.3 SINGLE-PASS BALING HARVEST SYSTEM

The single-pass baling system consisted of the John Deere STS combine and an AGCO Hesston single-pass baler. The combine was outfitted with a custom built hitch that allowed it to tow the baler through the field during harvest. Typical bale chamber pressures of 6,900 – 13,800 kpa (1000 - 2000 psi) were used with a plunger force of 2100 kpa (300 psi) max desired.

The baler was powered by an integrated Perkins diesel 4 cylinder, 4.4 L turbocharged diesel engine. The baler was controlled over a dedicated CAN system with displays and controls in the combine cab to allow the operator to control and monitor both the combine and baler simultaneously during harvesting operations.

Figure 5: A combine and single-pass baler harvesting corn grain and stover during fall harvest testing.

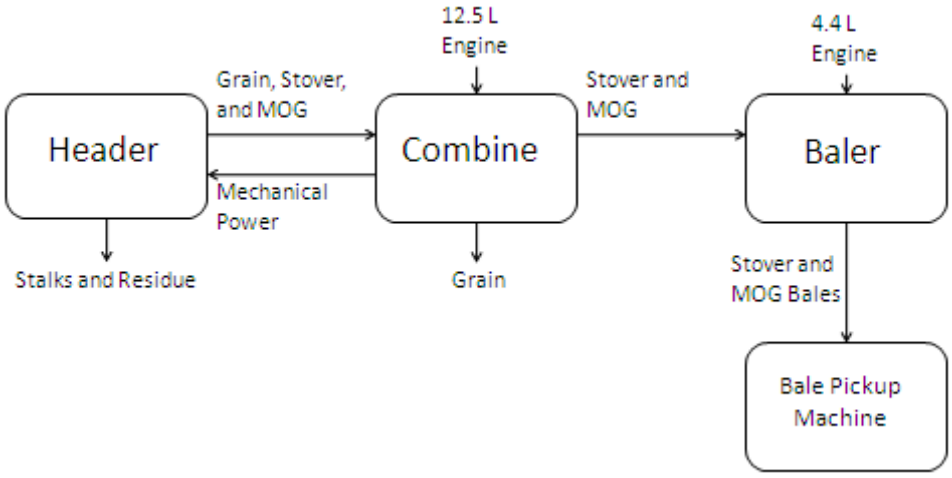

Figure 6: Block diagram showing the power distribution through the combine from the combine engine and baler engine along with showing the pathway of the stover and grain through the combine and baler.

3.4.2.3 DATA LOGGING

Data logging was conducted throughout each trial using the CyCAN loggers. CyCAN loggers were developed at Iowa State University for the purpose of collecting CAN messages broadcasted on an ISOBUS compatible machine. The data collected contained information such as fuel consumption, engine load, and other tractor functions. The logger also collected information over digital and analog signals along with GPS data to connect the data spatially as the machine operated in the field environment. Loggers for the combine and baler were placed inside the cab to allow the operator to monitor the loggers during each test. In bulk harvest

system tests an additional data logger was placed in the tractor's cab that towed the Oxbo 1516 cart. The data logger was also configured to read the cart scale output that was displayed in the tractor cab from the Oxbo cart

3.4.2.4 IN-FIELD TEST PROCEDURE

Two calibrations were performed during the testing season once beginning of the harvest to setup the machine with the correct values for higher moisture grain and then once again in the middle of season when drier crop conditions were experienced. Calibrations were not performed daily due to varying configurations that were used in the testing, limited crop area for testing, and in the interest of time during harvesting.

The combine separator and header were started along with the baler if it was being used. Once the machines were at high idle, 2300 rpm for the combine and 2500 rpm for the baler, the test began. The combine's forward speed was varied according to its engine rpm to maintain an engine rpm between 2200 rpm and 2250 rpm. This engine rpm range was selected to maximize the engine loading of the combine and to minimize variation amongst the data from factors other than the increased corn stover processed by the combine.

Type of Harvest	Rows of Collection	Condtions	Number of Passes	Total Passes per Configuration
Baling				
	0	Tough	4	10
		Normal	6	
	50	Tough	2	
		Hill	2	8
		Normal	4	
	100	Tough	4	
		Hill	2	12
		Normal	6	
Bulk				
	0	Tough	4	11
		Normal	7	
	50	Tough	2	8
		Normal	6	
	100	Tough	4	10
		Normal	6	
Conventional				
	0	Tough	4	
		High Moisture	5	15
		Hill	2	
		Normal	4	
	50	Tough	4	
		High Moisture	5	13
		Hill	2	
		Normal	2	
	100	Tough	4	
		High Moisture	4	12
		Hill	1	
		Normal	3	

Table 1: Final summary of the total test passes harvested by the harvest configuration and amount of stover collected based upon header setting.

Machine Configurations and Settings		
Conventional System		
Combine		
Cleaning Fan Speed (RPM)		800 - 1000
Chaffer Setting		13 - 15
Sieve Setting		7 -10
Chopper Speed (RPM)		1600 RPM
Header Backshaft Speed (RPM)		600 - 700
Bulk System		
Combine		
Cleaning Fan Speed (RPM)		1300
Chaffer Setting		15 - 18
Sieve Setting		5-8
Chopper Speed (RPM)		1600 RPM
Header Backshaft Speed (RPM)		700
Blower Speed (RPM)		900
Baling System		
Combine		
Cleaning Fan Speed (RPM)		1300
Chaffer Setting		15 - 18
Sieve Setting		5-8
Chopper Speed (RPM)		1600 RPM
Header Backshaft Speed (RPM)		700
Baler		
Baler Engine (RPM)		2500
Operational Temperature degrees F		180 - 210
Baler PTO (RPM)		1000
Baler Auto Pressure Setting		
MOG		210-250
1 - 2.5 tons		240 - 295
Chamber Operational Pressure Ranges (PSI)		1000 -2500
Plunger Force	ideal	less than 300
Plunges per flake	ideal	1 - 3
Flakes per bale	dependent on bale length	20-30

Table 2: List of machine configurations and settings for the systems used during the testing of the machines.

3.4.2.5 DATA PROCESSING

The Ag Leader SMS Advanced spatial management software was chosen for data processing due to previous working experience with the software and its ability to import custom files with non-traditional data such as data from the biomass harvesting experiments.

Yield monitor data was also imported into SMS Advanced software. This data was logged by the yield monitoring system on the combine and recorded to the GreenStar 2 Display located in the combine cab. Data was removed from the display via a compact flashcard at the conclusion of harvest testing. The data from this was uploaded to a computer and then processed by the SMS Advanced software using preset data templates provided by Ag Leader specifically for the John Deere GreenStar 2 data format.

3.4.2.6 PRODUCTIVITY STATISTICAL ANALYSIS

The data which was averaged and recorded from the SMS Advanced program was scaled to adjust for the varying yields throughout the fields and compensate for different engine loading conditions which were due to the unique operation configurations and conditions.

Equation 1: Productivity Index Equation.

$$Productivity\ Index = \frac{CF}{Y_{norm}\ x\ E}$$

Where as

CF	=	Crop Flow (Grain) (kg/sec)
Y_{norm}	=	Yield of Pass as a percentage (%) of max yield of the testing areas.
E	=	Percent of engine load (out of 100%) at current speed

Since no prior method to quantify this data was in place, a new formula was developed that factored variables such as grain yield, crop flow, and engine loading. These were selected as the main variables due to the requirements of the testing to remain at an engine loading of 100% or near that level without stalling the engine and the need to factor out variations in the yield across the field. The formula displayed Equation 1 a productivity index was determined by compensating for the three major factors affecting combine productivity. These factors were crop flow, percent of maximum yield, and percent of load on the engine. Crop flow was determined from the amount of grain hitting the impact sensor at the top of the clean grain elevator in the combine before entering the grain tank. The percent of maximum yield is determined after harvest in the SMS Advanced software program, the highest yield is benchmarked at 100% and subsequent yields determine as a percent of the maximum yield. Percent engine load is the ratio of actual engine percent torque to maximum indicated torque available at the current engine speed (SAE, 1998).

To determine the productivity index, overall crop flow was used. However, since crop flow was inconsistent due to varying crop conditions across the field it had to be scaled by the percent of maximum yield and the percent engine load used in the field section. This formula was determined by looking at a comparison of the raw crop flow data recorded from the actual test runs and the speed of the combine. Results of the raw data are shown Figure 7 and Figure 8.

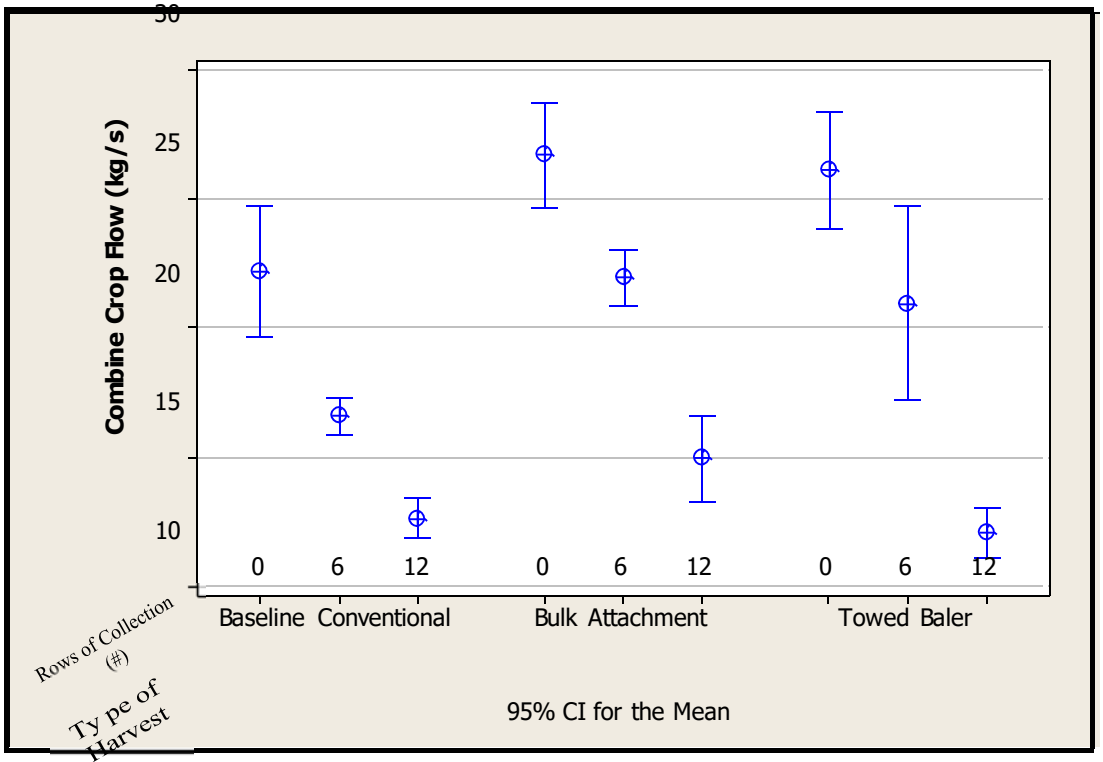

Figure 7: Average crop flow data recorded by the combine's yield monitoring system during testing. The conventional test shows a decreased crop flow compared to the bulk and baling configurations which was not a predicted outcome.

In Figure 7, the crop flow for the conventional harvest system was lower in all cases. If solely determining productivity from the crop flow, then the baseline conventional configuration had the lowest productivity. However, looking at the overall speed of the combine in Figure 8, the conventional configuration speed was greater than each of the corn stover harvest systems.

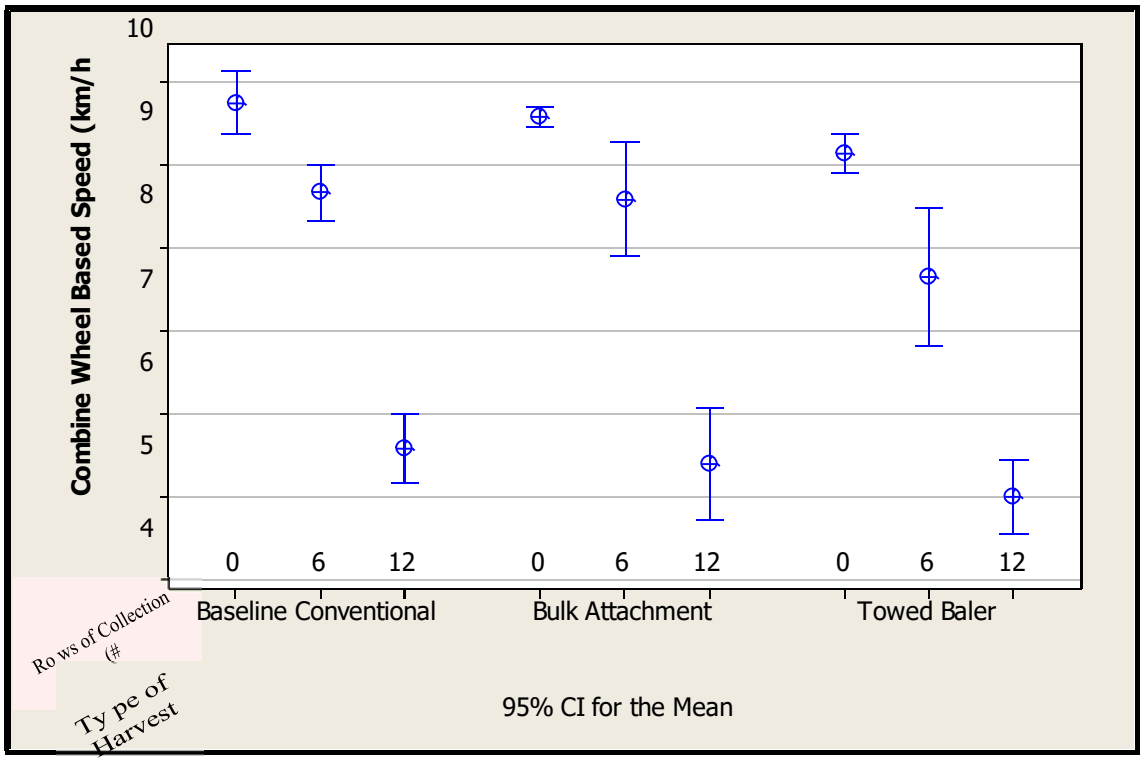

Figure 8: Average speed of the combine during the test from the combine. Speed is more consistent across the configurations and shows a predicted drop off as more stover is harvested.

Yield was also determined to be a factor in the low crop flow values in the conventional harvest system due to the highly variable yield experienced in the test fields. Low yielding test passes also had low crop flow values and showed less productivity. By determining the highest yield in the test passes and normalizing the rest of the yields to that value a scalable number was created that would eliminate the variation in the yield. The raw yield data is shown in Figure 9.

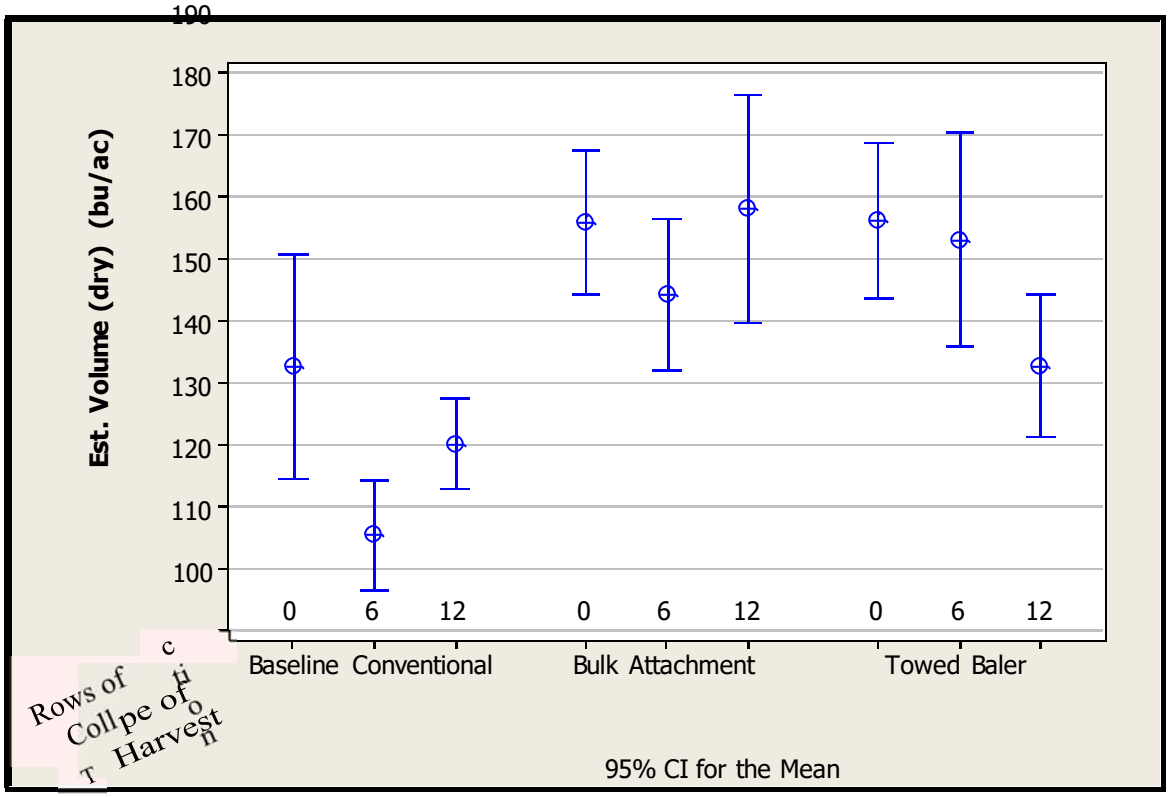

Figure 9: Estimated average yield of the test passes from the combine's yield monitoring system. The conventionally harvested passes are lower than the bulk and baling configurations.

Finally, the percent of load applied to the engine was also used to scale the crop flow data. It was determined that this was needed in order to compensate for test cases in which the engine was not required to be fully loaded, 100%. As shown in Figure 10, the raw engine percent loading data showed that in zero row collection the engine for the combine still had available power, but it was variable amongst the configurations. By eliminating this variation in the data all test configurations had the same engine power output.

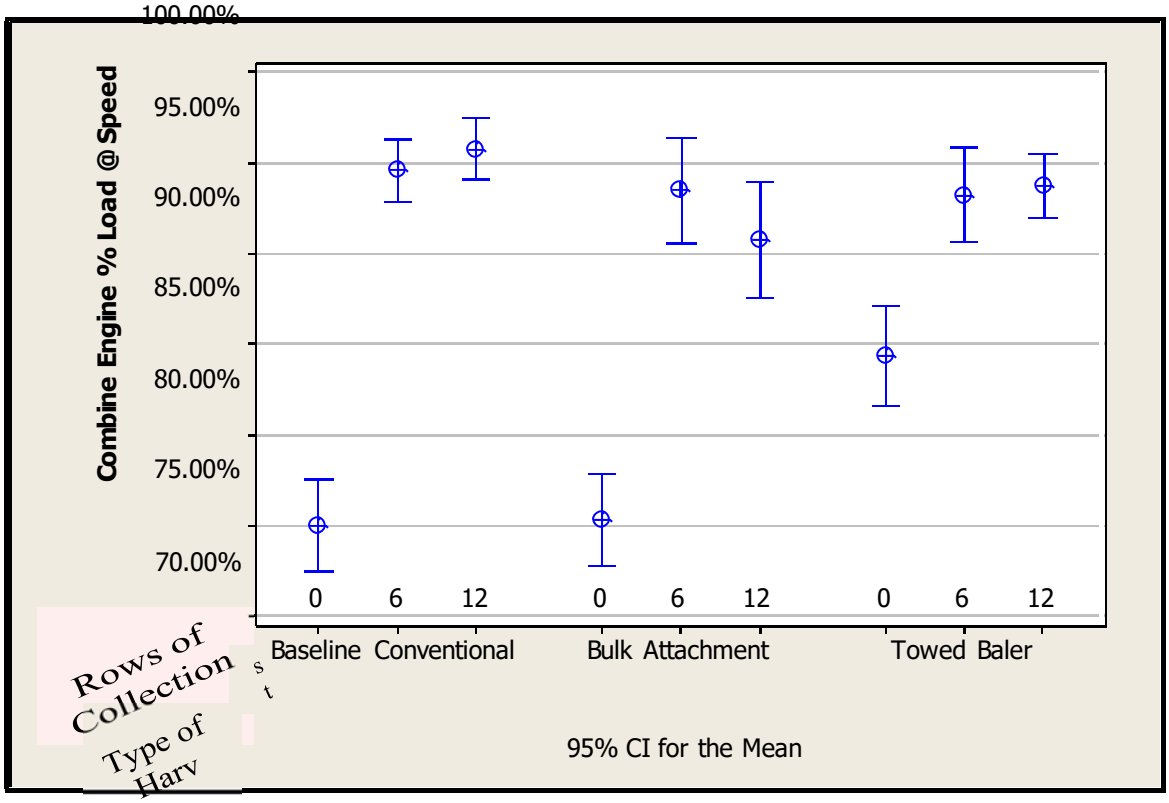

Figure 10: Combine engine loading % @ speed (engine rpm), for the test passes the lower harvest rates show that the engine is not loaded fully until more stover is introduced. The engine loading also increases when the baler is being towed by the combine.

By dividing the crop flow by the percent of maximum yield and percent of load applied to the engine the reductions in these two factors were eliminated from biasing the data. This potential maximum productivity was expressed by each configuration with the assumption that the yield and the engine load were both maximized. The final adjustment to the productivity index was to normalize the output of the equation on a scale of 1-100%.

3.4.3 RESULTS

3.4.3.1 SYSTEM PRODUCTIVITY ANALYSIS

During the tests there were two treatment factors that provided significant shifts in overall productivity loss. The effects that each type of harvest system, bulk attachment or towed baler, had on the combine's productivity will be discussed first.

Entering the testing phase it was known that because of the differences in harvest system equipment configuration there was an inherent drag on the productivity for some systems. It was also known that the single-pass baler had an overall mass of 10,000 kg (22,000 lbs) and had a disadvantage in productivity versus single-pass bulk attachment due to the large draft load the

single-pass baler induced on the combine. It was also assumed that the single-pass bulk attachment would have some effect on overall productivity. What was not known was the magnitude of the impact on productivity that each system would have on the combine.

Figure 11, shows the overall effect of both the collection systems and rates collected. Concentrating on the overall system effect first and comparing this to the baseline conventional data indicates that the single-pass bulk harvest has little effect on the overall productivity of the combine. As seen in Figure 11, there was no statistical difference in the overall confidence interval of the data under these conditions. The predicted means also were within 1-2% of each other and most variation can be accounted for by the overall variation in speed throughout the trials. Overall, the single-pass bulk harvest attachment had no statistical effect on the combine's productivity.

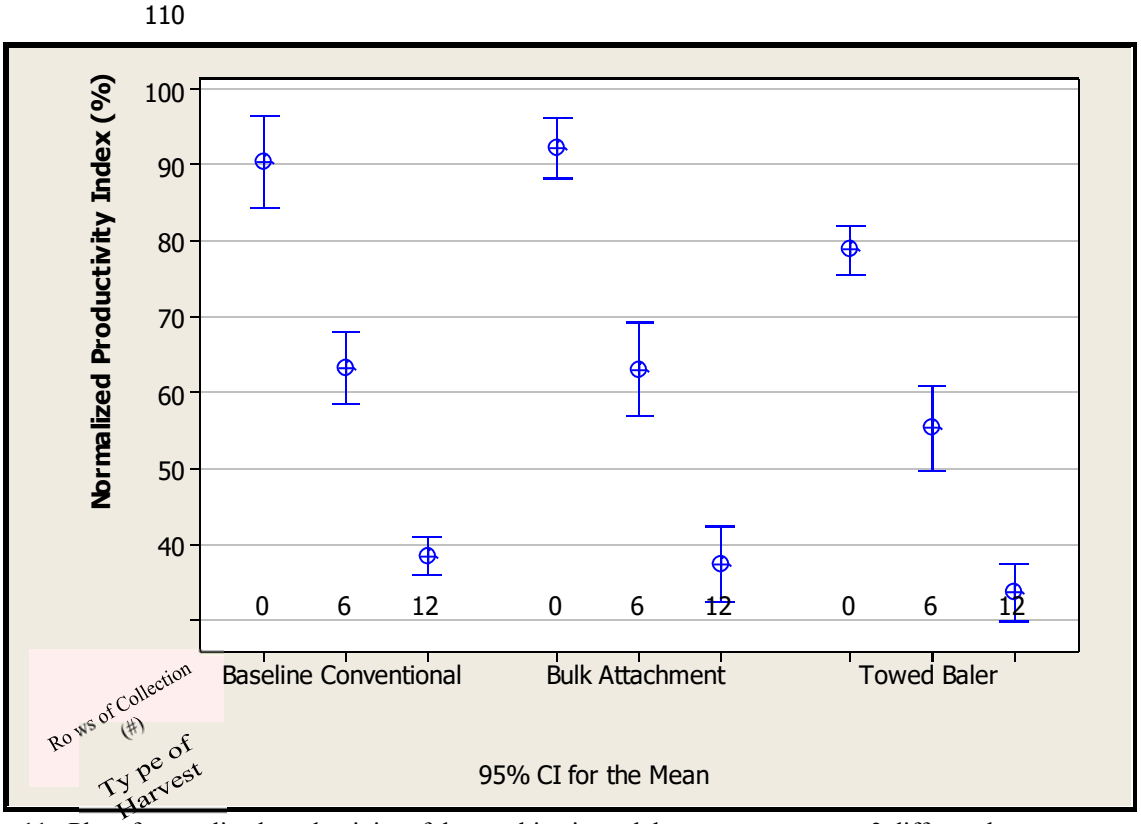

Figure 11: Plot of normalized productivity of the combine in each harvest system over 3 different harvest rates. This shows the combine's productivity is reduced as the amount of corn stover is increased and when the baler is towed behind the combine.

The single-pass baling harvest system showed more productivity loss than the baseline or bulk collection system. Only one interval was statistically different, which will be discussed later in the section. The predicted means as shown in Figure 11 tend to trend lower than either the baseline conventional harvest system or single-pass bulk harvest system. Analysis of the predicted means of the data shows an average loss in productivity of 10-12% for the single-pass baling harvest system.

3.4.3.2 AMOUNT HARVESTED ANALYSIS

What had more effect on productivity was the total amount of material that was harvested and processed through the combine. Figure 11 shows the overall effects of increased rates of corn stover that was collected and processed by the combine in an interval plot. In the plot there was a statistical difference in the loss of productivity between the different rates of stover harvested in each stover harvest system. The rates of stover harvested were the main drivers for the productivity loss. This was shown by concentrating on the baseline conventional data which shows about a 27% loss in productivity seen in each increase in the rate of stover collected determined by the amount of harvested rows of corn stover. Collecting all twelve rows of stover will yield about a 52% drop in overall productivity to just the combine.

Further analysis of Figure 11 showed a rather large interval in the zero collection row units between the towed baling system versus the baseline conventional harvest system and the single-pass bulk harvest system. This was explained by two different factors.

The first factor was that towing the single-pass baler, the overall speed of the combine was slower, especially the top end speeds of the zero row collection setting. As the amount of rows that were set to collect stover increased, the rate of the corn stover increased, the combine speed was slowed to process the extra corn stover being harvested. The affect that the 11% productivity loss from the single-pass baling system was minor when compared to this major productivity loss associated with increasing stover collection rates. This was why in Figure 11 the intervals for the six row collection and twelve row collection harvest rates, begin to group together and become statistically indifferent.

The second factor was that the engine of the combine was also loaded more as it towed the baler. In the productivity index, Equation 1, the influence of varying engine loading was minimized by using the loading percent as a scaling factor for the crop flow. The engine loading percent for all cases was factored out by doing this. The potential productivity was factored into the data instead of expressing the actual productivity calculated during testing. The single-pass baler harvest system had less potential productivity because the engine of the combine was already loaded more and it maximized the use of its power production quicker than either the conventional harvest system or the single-pass bulk harvest system.

Additionally, this data indicates that at the zero row collection configuration the combine was not limited by power or speed. When analyzing the speeds, none were statistically different from each other and all were within one kph. This was due primarily to the intake limitation in the header. At forward speeds higher than 11 kph (6.8 mph) the header started to ‘push’ the stalks over prior to fully stripping the ear away from the plant. This was caused by the head not being able to pull the stalk through the stripper plates prior to reaching the back end of the row units. When this happened the ear was still pulled off the stalk, but the stalk was not fully processed as it would be in normal operation. This also caused ear shatter which was when the ear of corn broke apart in the header, leaving corn in the field instead of the ear reaching the

combine separator. Ear shatter was determined through visual inspection during and after the test pass. Adjustments to the speed and stripper plate width were made to combat this problem.

3.4.3.3 PRODUCTIVITY PREDICTION EQUATION

A regression curve was formulated from the harvest data to further analyze the productivity index data. Not all factors tested were chosen to be included in the equation. The high moisture grain and terrain factors each had p-values that were out of range of the acceptable limit which was $\alpha = .05$. After removing these two factors the regression analysis produced Equation 2.

Equation 2: Regression equation for predicted Productivity Index

$$PI = 99.4 - 4.23\ HR - 7.99\ Ba + .29\ Bu$$

Where as

PI = Percent of productivity based on the maximum productivity of a conventional harvest system

HR = Header rows set to collect stover. (# Header Rows)

Ba = If using the single-pass baling harvest system use (1) if not use (0).

Bu = If using the single-pass bulk harvest system use (1) if not use (0).

The regression equation produced an r^2 value of 90.9%.

The productivity index regression equation showed a reasonably placed average could be determined for how much the combine productivity would be impacted depending on the system chosen to collect stover with and the amount of stover collected. In the equation 99.4% was the highest confidence interval mean percentage of machine productivity. The stover rate factor was scalable based upon the amount of rows of stover collected. This would help predict productivity for a header up to 12 rows wide because it was indifferent to the amount of conventional rows was used. The only requirement in this calculation was that it was assumed that the combine size was the same. Additional reductions were seen for each stover collection system. Only an 8% reduction was seen when baling according to the regression equation, this was shown in the corresponding coefficient listed in the equation, however in the raw data analysis a larger reduction of 11% was seen. The difference here can be attributed to two factors; the first being that the r^2 value for the curve is only 90% so there was some variation from the curve that could account for this, also the wide variation of crop conditions were not all accounted for in the treatment factors or by the productivity equation. This was only a predictive equation and will not fully fit the curve. The final term in the equation showed less than .3% reduction in productivity for bulk harvest. This value was representative of the values seen from the bulk productivity analysis.

3.4.4 CONCLUSTIONS

Data that was collected from the in-field testing that occurred in the fall of 2010 tested five different factors. The factors: collection system and collection rate were tested, collected data, and produced statistically significant results. The data collected was processed and combined with yield monitoring files in the Ag Leader SMS Advanced software, then was averaged for each trial pass, and then analyzed in Minitab. Little statistical difference was seen between a conventional harvest system and single-pass bulk harvest system. Between the conventional harvest system and single-pass baling harvest system there were statistical differences at the lower rates of collection in the 0 row collection header configuration. The difference seen between the two systems was 11%. Other statistically different data was seen in the different harvest collection rates of 0, 6, and 12 rows. The increased stover rates lowered combine productivity by about 27% for each increase in the rate of collection. The lower productivity was a result of slower forward travel speed in the combine as well. The slower forward travel speed of the combine, removed the statistical significance from the differences in the harvest systems but there was still about a 10-11% difference between single-pass baling harvest systems and the conventional system.

REFERENCES

Mud Hog. (2011). Retrieved June 21, 2011, from Tuthill Drive Systems: www.mudhog.com

AGCO Corporation. (2010). *Challenger Biomass Baler*. Retrieved February 15, 2011, from Challenger-Ag/AGCO: http://www.challenger-ag.com/NA/EN/products/harvesting/1379.htm

California Energy Commission. (2004, January). Retrieved June 20, 2011, from http://www.energy.ca.gov/reports/2004-02-03_600-04-001.PDF

CLAAS. (2011). *CLAAS Jaguar*. Retrieved February 16, 2011, from CLAAS: http://www.claas.com/countries/generator/cl-pw/en/products/forage_harvester/jaguar_980-930/tech-data/start,lang=en_UK.html

Dupont Danisco Cellulosic Ethanol LLC. (2011, June 27). DDCE enters agreement to purchase land in Iowa for commercial biorefinery to make fuel from corn stover. Itasca, Il, United States of America: DDCE.

EISA. (2007, January 4). Energy Independence and Security Act of 2007. (110 Congress). United States: United States Senate. Retrieved February 12, 2011, from http://energy.senate.gov/public/_files/getdoc1.pdf

Glenvar Bale Direct. (2007). Retrieved February 16, 2011, from ASABE: http://www.asabe.org/standards/ICCHP2007DirectBaler.pdf

Gray, W. H. (1898). Corn Harvester and Binder. U.S. Patent No. 602659.

Hanna, M., & Al-Kaisi, M. (2008, 4 9). *Managing Residue for a Good Stand*. Retrieved June 20, 2011, from Integrated Crop Management News: http://www.extension.iastate.edu/CropNews/2008/0402AlKaisiHanna.htm

Hettenhaus, J. R., & Wooley, R. (2000, October). Biomass commercialization prospects in the next two to five years. *BIOMASS COLLOQUIES 2000*. National Renewable Energy Laboratory.

Hillco Technologies. (2010). *Cob Collection Attachment.* Retrieved February 15, 2011, from Hillco Technologies: http://www.hillcotechnologies.com/cob-collection-attachment.html

Johnson, J. M., Wilhelm, W. W., Karlen, D. L., Archer, D. W., Wienhold, B., Lightle, D. T., et al. (2010). Nutrient Removal as a Function of Corn Stover Cutting Height and Cob Harvest. *Bioenergy Resources*, 342-352.

Karlen, D. (2008, October). Cellulosic Ethanol From Corn Stover: Calculating—and Improving—the Bottom Line. *Agricultural Research*.

POET Biorefining. (2011). *Project Liberty.* Retrieved February 16, 2011, from POET Biorefining: http://poet.com/innovation/cellulosic/projectliberty/index.asp

Rosenthal, H. (1950). Corn harvester. *U.S. Patent No. 2524603*.

SAE. (1998, Octobor). J1939-71 Rev Oct 1998. Pennsylvania, United States: SAE.

Schlesser, B. (2007). *Development and evaluation of a single pass, dual stream corn stover harvester*. Retrieved June 20, 2011

Shinners, K. J., Binversie, B. N., & Phillippe, S. (2003, July 27-30). WHOLE-PLANT CORN HARVESTING FOR BIOMASS: COMPARISON OF SINGLE-PASS AND MULTIPLE-PASS HARVEST SYSTEMS. Las Vegas, Nevada, United States: ASABE.

Shinners, K. J., Binversie, B. N., Digman, M. F., Muck, R. E., & Weimer, P. J. (2005, January). SINGLE-PASS, SPLIT-STREAM HARVEST OF CORN GRAIN AND STOVER. ASABE.

Shinners, K. J., Boettcher, G. C., Hoffman, D. S., Munk, J. T., Muck, R. E., & Weimer, P. J. (2009). Single-Pass Harvest of Corn Grain and Stover: Performance of Three Harvester Configurations. *ASABE.* ASABE.

Vermeer Manufacturing. (2009). *Vermeer CCX770 Cob Harvester.* Retrieved February 15, 2011, from Vermeer Manufacturing: http://www2.vermeer.com/vermeer/NA/en/N/equipment/cob_harvester/ccx770

Webster, K. E., Darr, M. D., Thoreson, C. P., & Zuchelli, M. (2010). Productivity and Logistical Analysis of Single-Pass Stover Collection Systems. *ASABE.* Pittsburgh: ASABE.

3.5 Single-pass corn stover baling economics analysis

Keith Webster, Matthew J. Darr, Curt Thoreson, and W. Edwards

(to be submitted to a peer-reviewed journal)

ABSTRACT

Baling has become the most commercially feasible method for collecting and transporting corn stover in the near future. Single-pass corn stover harvesting provides a product that is the cleanest available to meet end-users needs today. The additional stover and a baler in tow behind a combine will slow the combine down. In doing so there is inherent cost associated with this, additionally there is a cost in the equipment required to support baling both on the grain harvest side and stover collection side of the harvest. A model developed at Iowa State University uses field collected data and current machinery cost to develop a cost analysis based upon harvest cost from the 2010 fall harvest. Cost of harvesting stover ranged from $20-$30 per ton based on a range of stover collection rates from .5 ton to 1.75 tons per acre.

3.5.1 INTRODUCTION

Corn grain ethanol has been a staple in the renewable energy portfolio of the United States for many years. From its initial start to present it has undertaken a long and tenuous process of trial and error with the rapid development of the industry only coming in the last 10 years since 2000. The Energy Independence and Security Act of 2007 (EISA, 2007) mandated that advanced biofuels such as cellulosic ethanol be produced at a rate of 79.38 billion liters (21 billion gallons) per year by 2022. In 2011, renewable fuels including corn grain ethanol were only mandated to produce 52.9 billion liters (13.95 billion gallons) of fuel. Of this amount, advanced biofuels including cellulosic biofuels were to produce 5.1 billion liters (1.35 billion gallons) of that total. Cellulosic biofuels were mandated to produce .95 billion liters (.25 billion gallons) of fuel. Cellulosic biofuels must develop methods and build up infrastructure that will support the production of 60.5 billion liters (16 billion gallons) of the 136 billion liters (36 billion gallons) of total renewable fuels made in the United States by 2022 or in the next 11 years. Compare this to corn grain ethanol which has been subsidized since the start of the National Energy and Conservation Act of 1978 (California Energy Commission, 2004). It was produced on a smaller scale initially which allowed it to develop a supply infrastructure. Cellulosic biofuel infrastructure development will need to be much more rapid. Cellulosic biofuels while not a new idea have had far less time to perfect its supply infrastructure with movement to large scale production only beginning to be developed. Not only do feedstocks need to be identified that can produce biofuels efficiently, but systems must be developed to harvest the feedstock, transport the feedstock to the plant, and process the feedstock into a convertible product. One feedstock, corn stover, has been identified as a potential feedstock in the Midwest United States due to its wide availability (Hettenhaus & Wooley, 2000). Research is now under way to efficiently collect, transport and process corn stover.

Corn stover has been mainly relegated to ground fodder in current harvest systems. Harvesting technology has evolved since removing the plant and ear from the field using a corn binder in the early 1900s and storing the bundles (Gray, 1898). The next method for harvest was using an ear corn harvester for harvesting the ear of corn. Now current combines harvest and separate the kernels of corn from the cob. Once, the corn grain is harvested the leftover corn stover is either returned to the ground and allowed to deteriorate for next year's planting or collected in small multi-pass systems for use as animal feed and bedding.

Most plant material is returned to the soil in current corn cropping systems. While it is the least labor intensive method of getting rid of the excess material it does present challenges. Development of higher yielding and more resistant varieties of corn to disease and insects has in many producers' opinions made it more difficult to breakdown the remaining plant residue over the winter period and hampers new crop planting in the spring. Now some producers will take

additional passes over the field with extra tillage or shredders in order to enhance material breakdown either in the fall or spring (Hanna & Al-Kaisi, 2008).

The current design of the multi-pass collection systems for livestock systems emphasizes quantity rather than quality of material harvested. However, for the renewable energy future this thinking must be changed to improve quality and to address sustainability concerns. New constraints to harvesting will be introduced such as moisture content and quality much like corn grain is currently subjected to. One way to improve material quality is to use a single-pass harvest and collection system. Single-pass systems take the higher portion, which has less nutrient value and more stable moisture content than other sections of the plant (Karlen, 2008). Multi-pass system will harvest almost all of the lowest part of the plant that has the highest moisture and nutrient levels (Johnson, et al., 2010). Single-pass harvest systems have a selectable height and therefore infinite harvest rate with the typical harvest height of within one foot below the ear as shown in Figure 1. Single-pass harvest systems have been under development for many years now. The initial single-pass harvester was developed (Rosenthal, 1950) and continues in development today. The two systems that have emerged as possible solutions to maximize collection and harvest of corn are a bulk harvest system and a baling harvest system.

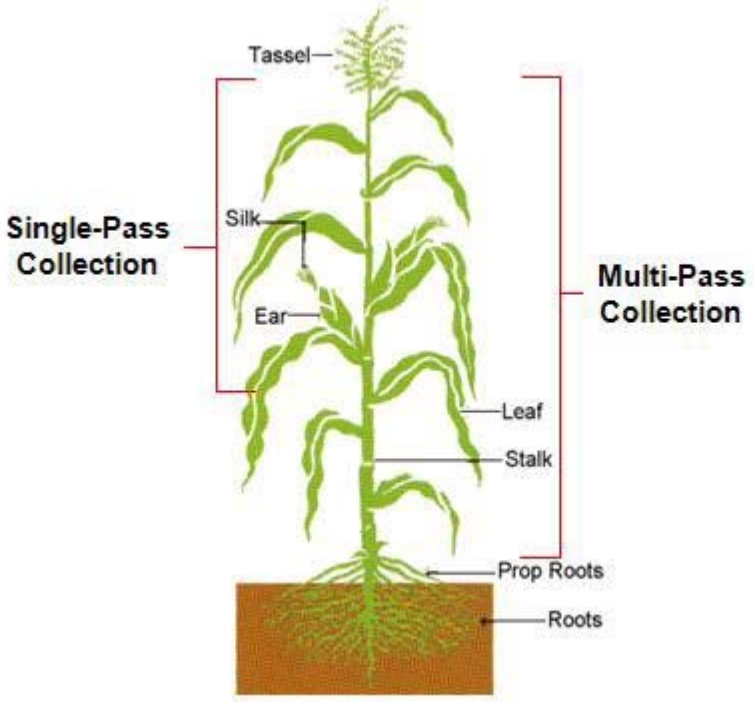

Figure 1: A comparison of the cut height for a single-pass and the multi-pass harvest.

The towed bale system or singe-pass baling harvest system has been analyzed but no production scale economic studies have been produced that can be used by the producer or end user to determine the applicability of this technology. Production scale economic and productivity data will help establish the predicted economic value of corn stover to the producer to ensure a profit for the extra work that will come along with collecting corn stover. There was also very little data collected to evaluate the effects of the additional stover harvested, weather conditions, and collection systems on the productivity of the combine. The lack of this

information can lead to inaccurate predictions of collection costs. It can also hinder further investigation into systems which can improve harvesting.

Some of these questions and lack of knowledge was addressed by quantifying performance data from prototype single-pass harvest machines, productivity of bale collection machinery, and cost to harvest and collect corn stover to the field edge. The testing conducted at the BioCentury Research Farm, Agricultural Engineering and Agronomy Farm, Iowa State Research and Demonstration Farms, and Iowa State Agricultural and Biosystems Engineering Department produced a comprehensive dataset of machine performance factors which provided a basis to make these quantifications. This data along with a predictive model will attempt to quantify reduction in overall machine performance, cost of the performance reduction, cost of stover collection, and the significant factors for improvements in machine performance.

3.5.1.1 Single-Pass Bale Harvesting Systems

The implementation of the single-pass baling harvest system started in the 2000's on the Glenvar Farm in Western Australia. The Glenvar Farm was originally looking for a way to collect wheat straw from the back of the combine in order to catch weed seed that had become hard to control in their fields. The first single-pass baler developed was a small square baler which worked successfully but was limited by the overall throughput of the machine and collection logistics. Later the farm moved to a large square baler in order to achieve the desired throughput, higher bale densities, and bigger bales (Glenvar Bale Direct, 2007). A partner company, Tuthill Drive Systems, has now started marketing and selling the balers in the United States for the same purposes. These systems are being used to produce anywhere from 0.9 - 3.2 Mg (1 – 3.5 ton) of wheat straw per acre. The baler draws its power completely from the combine's engine and chopper drive system while material is conveyed from the rear of the combine into the baler by a conveyor system. Tuthill Drive System has now started to enter the corn stover harvesting market by using the same configuration in the Midwest and marketing to corn cob producers (Mud Hog, 2011). Other companies in the U.S. have begun to work on these as well. The AGCO Challenger combine and single-pass baler has been debuted at recent farm shows and is under current development (AGCO Corporation)

Economic analysis of single-pass harvesting system is difficult due to a lack of true machine performance data under production scale conditions. Shinners et al. (2003) found that corn harvest alone cost $7.80 per dry Mg ($7 per dry ton) to harvest compared to $7.50 per dry Mg ($6.75 per dry ton) for both an integrated single-pass baler and for a chopper unit to be attached to a combine. To harvest and transport corn grain and stover to a storage site cost $106 per ha ($42.40 per acre), $182 per ha ($72.80 per acre), and $219 per ha ($87.60 per acre) for a conventional grain combine, a single-pass bulk harvest system, and a single-pass baling harvest system respectively. While the single-pass bulk harvest system did provide a cheaper method of harvest and initial transport from the field it was found that long-term storage for bulk material was more expensive than storing bales.

Numerous commercial scale multi-pass harvest systems have been tested in the past 15 years in order to develop a working knowledge of the system. An analysis of current custom harvest practices showed a cost of $21.60 per dry Mg ($19.44 per dry ton) for square bales and $23.60 per dry Mg ($21.24 per dry ton) for a round bale system (Sokhansanj & Turhollow, 2002). This included a transport cost for 8 km (5 miles) of travel which was responsible for part of the cost assigned to the transport cost in their research of $6.10 and $8.60 for round and

square baling respectively. The cost was analyzed using shredding, raking, and baling passes separately.

Perlack and Turhollow (2002) analyzed four systems similar to current production practices. The systems were divided into multi-pass bulk and multi-pass baling. The multi-pass bulk system consisted of a forage harvester towed by a tractor and a tractor mounted blower that left the stover unprocessed. Each of these systems would convey stover into a 31.2 cu m (1092 cu ft) or 62 cu m (1935 cu ft) wagon that would compress the stover to double the packing density. The bulk system cost ranged from about $27.5 - $42.90 per dry Mg ($25 - $39 per dry ton) delivered to a processing facility that used between 454.5 – 3636 dry Mg (500 – 4000 dry tons) per day. The range of the biomass cost was dependent on the hauling system. The unprocessed system was from $22 – $38.5 per dry Mg ($20 - $35 per dry ton) delivered which mainly was attributed to the lower capital equipment cost associated with the blower. The other system analyzed was a baling system consisting of square baling and round baling. When hauled to a similar facility large round bales cost $24.20 - $27.50 per dry Mg ($22 - $25 per dry ton) to bale and transport while large square bales had a higher cost from $26.4 – $30.8 per dry Mg ($24 - $28 per dry ton).

Work completed at the Oak Ridge National Laboratory developed a cost analysis model using many of the American Society of Agriculture and Biological Engineers and American Agricultural Economics Association adapted standards for equipment costing. This analysis took into account all fixed and variable costs associated with biomass collection. The model was tied into the Integrated Biomass Supply Analysis and Logistics model (IBSAL) which allowed for estimation of equipment needs and optimization of equipment for herbaceous crops and agricultural residues (Turhollow, (2009)). The model included assumptions and calculations to provide estimates for machine productivity and provided a breakdown of supply chain costs. This work clearly highlighted the need for improved estimates on actual machine productivity associated collection and transportation of biomass feedstock.

Previous work completed at Iowa State University quantified combine productivity with the combine harvesting in a conventional harvest configuration and in the single-pass baling harvest configuration. A key application of the single-pass collection system productivity data was to develop reasonable economic conclusions for potential adopters. The conclusions could be used to assess the value of corn stover when selling it by quantifying the cost to harvest the corn stover with a single-pass system. An economic model was developed for this research that specifically used the data collected during in-field testing. The model was used to determine the cost of the single-pass baling system with the goal of developing a cost database for various system parameters. Cost was developed in units of dollars per acre, dollars per ton, and dollars per hour basis. The model had the capability to create databases for the conventional, single-pass bulk, and single-pass baling systems. The conventional system was used to create a baseline cost for grain harvest.

Only the single-pass baling system was analyzed for this analysis. This was chosen over the single-pass bulk harvest system because the industry trend was moving towards a baling solution for stover harvesting and transportation logistics. The two cellulosic ethanol plants that are being constructed in Iowa will be using round and square bales. One plant will exclusively use 3 ft x 4 ft square bales. The single-pass bulk harvest system provides challenges in the movement of material from the field and in storing the material in a protected environment. The baling solution has more efficient solutions in both of these situations that make it the more preferred method of harvest.

3.5.2 MATERIALS AND METHODS

3.5.2.1 Data Analysis Methods

An Excel-based macro was developed that used performance data collected from fall harvest to develop economic outcomes. The data used in the model removed many of the assumptions that previous economic models have used to develop fiscal values for corn stover harvesting. There were two variables looked at in the model stover yield and combine productivity. Constant inputs which mainly were taken from in-field data collected from the fall 2010 harvest also were used in the model. Some cost data such as fuel prices, machinery capital cost and lease rates, and machinery repair cost analysis were taken from various sources.

The inputs listed in Table 2 were selected to be constant through the analysis. Some of the constant inputs dealt with an economic aspect of the data which required the use of a long term average for prices of corn and fuel. Another constant was the rental rates of machinery which had set prices that came from outside vendors who supplied equipment for the harvest tests. Fuel consumption was also a constant during each run of the model. Values for consumption for the model were taken straight from the harvest testing dataset and statistical analysis discussed earlier. There were three different fuel consumption levels used, a rate in the conventional configuration, a consumption rate was determined when baling behind the combine set with a conventional harvesting head (.5 ton/ac), and a consumption rate was determined at a high stover harvest rate seen in the fall 2010 harvest (2 ton/ac).

Variable Inputs				
Variable Name	Units	Minimum	Maximum	Interval
Stover Yield	Tons/Acre	0.5	4	0.5
Single-Pass Baling Productivity	%	5	100	5

Table 1: Variables into the economic model used to analyze single-pass baling. Data from the 2010 harvest was used to set the boundaries of this model but not tied directly to the output of the model.

Constant Inputs		
Variable	Units	Value
Machine operating hours per day	Hours	11
Machine operating days in season	Days	27
Fuel Price	$/Gal	3.04
Labor Cost	$/hour	13.45
Self Propelled Bale Collector Rental Cost	$/hour	45
Tractor Rental Cost	$/hour	72
Corn Price (5-year average)	$/bushel	3.8
Unloading while harvesting	%	75
Crop Flow	lbs/sec	60
Header Width	Feet	30

Table 2: Inputs factored into the economic model for the determination of the single-pass baling system harvest cost. These inputs were based off of typical machines industry today or in field data from the 2010 harvest.

Constant Inputs		
Variable	Units	Value
Grain Yield	Bushels	173
Grain Unload Rate	Bushels/Second	3.3
Grain Cart Capacity	Bushels	1000
Grain Cart Unload Rate	Bushels/Minute	500
Grain Cart Tractor Speed(estimated)	mph	7.5
Average Grain Cart Travel Distance	Feet	1300
Bale Density	lbs/cubic feet	10
Bale Length	Feet	8
Bale Width	Feet	4
Bale Height	Feet	3

Table 3: Inputs factored into the economic model for the determination of the single-pass baling system harvest cost. These inputs were based off of typical machines industry today or in field data from the 2010 harvest.

Constant Inputs		
Variable	Units	Value
Baler Average Fuel Consumption	gal/hr	4
Combine Conventional Configuration Fuel	gal/hr	16.25
Combine Single-pass baling Configuration	gal/hr	18.5
Combine Single-pass baling Configuration Fuel Consumption - 1.5 and 2.5 ton per acre	gal/hr	20.5
Bale Collection Vehicle average fuel consumption	gal/hr	8.24
Grain Cart Tractor Average Fuel Consumption Waiting	gal/hr	3
Grain Cart Tractor Average Fuel Consumption Loaded	gal/hr	11.7
Grain Cart Tractor Average Fuel Consumption Unloaded	gal/hr	11.7

Table 4: List of fuel consumption inputs into the economic model for analysis.

The fuel consumption and speed values were taken directly from field data. The grain cart and tractor were not instrumented to log data during harvest. It was assumed that fuel consumption from the tractor with the stover carts had similar fuel consumption. The speed of the cart traveling by itself in the field was estimated from previous experience of in-field operation of machinery. The knowledge base from operation of the machines in field provide a reasonable basis for any assumptions made and provide many statistically analyzed data values for input into the model. Fuel consumption data for the bale collection machine was taken from the Nebraska OECD tests. The tractor used for the bale collector was the Case IH MX 240 with a Cummins 8.2 L engine. Productivity was also provided from bale collection data collected from other 2010 corn stover harvest research activities.

The analysis was bounded by some assumptions to limit the scope. The analysis was determined to be used for a single operator working in the Iowa fall harvesting corn. The single operator in Iowa had a set operational time in two factors, operational days in season and operational hours per day. The operational days per year was determined from data that was extracted from the United States Department of Agriculture National Agricultural Statistics Service (USDA-NASS) weekly reports of working days and percent of corn harvested in the United States. Data for the State of Iowa was extracted for the entire harvest window for the years 1999 – 2010 (USDA - National Agriculture Statistics Service). The window of analysis spanned from the middle of August to the end of the reporting period which was when the corn harvest reached 95% complete for the United States. The completion percentage was chosen for the entire United States instead of just Iowa because it intended to cover the entire Midwest harvest timeline. In Figure 2, the last eleven years of harvest progress was calculated in order to determine the average time span for harvesting 80% of the crop with the 10% fringe areas of the

dataset being disregarded. This data suggests that the typical harvest window in Iowa for a harvest is around 27 days.

The number of operational hours was determined to be 11 hours according to research conducted by Edwards (1979). This determination came from participants in the CROP-OPT program. The initial assumption for hours worked was 11 hours with a low assumption of 6.5 hours per day and high assumption of hours worked per day of 15.5 hours per day.

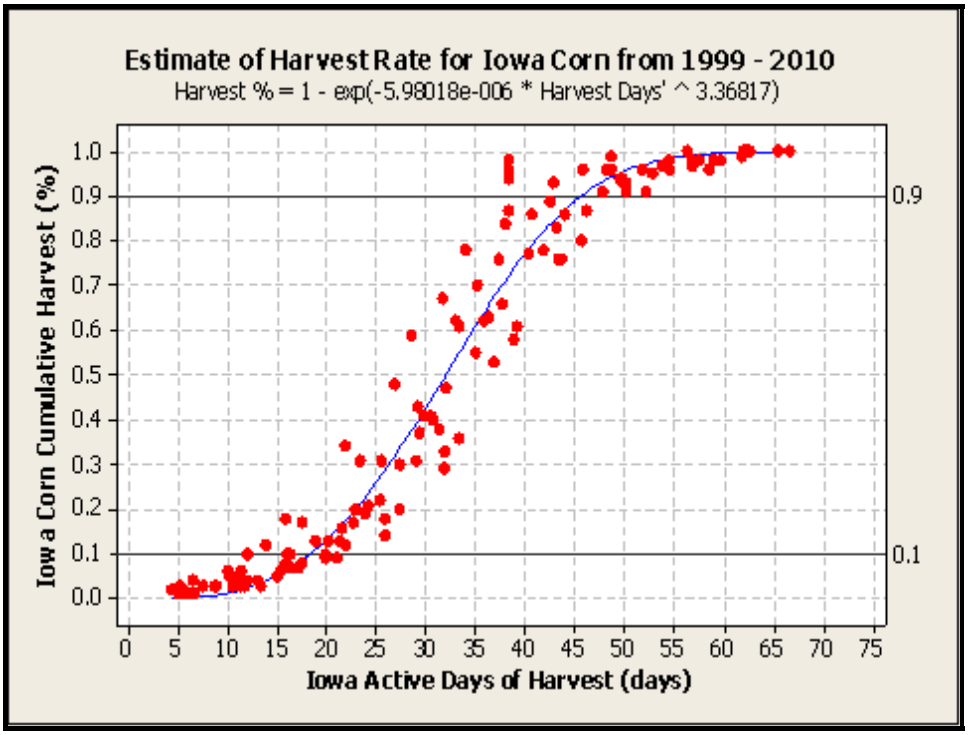

Figure 2: The average trend in harvest progress for Iowa for the last 11 years based upon cumulative progress of the corn harvest. Markers are placed 10% for early harvest progress and 90% for late harvest progress. 80% of the crop is removed in under 30 days.

The salvage value for each machine was one factor used in the model that determined the depreciation cost. The salvage value for a particular piece of equipment was determined from the formula from the ASABE standard D497.7 (ASABE, 2011). Further detailed in Equation 3, the salvage value was factored from the capital cost for the equipment listed in Table 7 and given coefficients for various types of machines from the ASABE standard listed in Table 5. Capital costs were acquired from industry contacts, equipment sales literature, and equipment dealers.

Equation 3: Salvage Value Equation based upon ASABE factors salvage values (ASABE, 2011)

$$RV_n = 100(C_1 - C_2 n^5 - C_3 h_a^5)^2$$

Where as

RV_n	= Remaining percent of list value of a machine after n years and h hours of use per year (%)
C_1, C_2, C_3	= Coefficient for various equipment types, Table 5
h_a	= Average annual usage (hours/year)
n	= Years of usage (years)

Salvage Value Coefficents			
Equipment	C1	C2	C3
Combine & Header	1.13	0.17	0.01
Baler	0.85	0.10	-
Grain Cart	0.79	0.09	-

Table 5: Coefficients for determine machine salvage value from the ASABE Standard 497.7. (ASABE, 2011)

The ASABE Standard D497.7 also provided an estimated life for the equipment which was further detailed in Table 6. An estimation of the yearly usage of a machine was determined to get the total number of years of use. This number was dependent upon the window for harvest and the hours worked per day for the stover harvest machines and average yearly use for the tractors.

Estimated Lifespan	
Equipment	Hours
Combine & Header	3000
Baler	3000
Grain Cart	2000

Table 6: Estimated lifespan of purchased equipment for harvest. Based upon the average lifespan of equipment from the ASABE Standard D497.7. (ASABE, 2011)

Equation 4: Calculation for determining the salvage value price for a machine based upon the ASABE Salvage Value Equation and capital value of a machine for the 2010 harvest.

$$RV_p = RV_n \, x \, P_c$$

Where as

RV_p = Remaining value ($, dollars)
P_c = Capital Cost of Machine ($, dollars)
RV_n = Remaining percent of list value of a machine at a certain level of use ($, dollars)

Machine Capital Cost	
Equipment	Cost
Combine & 12 Row Header	$466,800
Baler	$140,000
Grain Cart	$39,750

Table 7: Capital prices for machinery for determining capital costs based upon the 2010 harvest.

Depreciation and interest were factored into the cost by using the straight line depreciation and interest calculations. These produced hourly depreciation and interest costs for the machine which could be converted to a yearly basis. The equations are further detailed in Equation 5 and Equation 6.

Equation 5: Calculation for determining the depreciation for a machine Turhollow et al (2009).

$$Cap_d = \left(\frac{PP - SV}{h_1}\right)$$

Where as

Cap_d	=	Capital Cost (depreciation), Table 7, ($ per hour)
PP	=	Purchase price, ($, dollars)
SV	=	Salvage value (RV_p), ($, dollars)
h_l	=	Lifetime usage, Table 8 (hours)

Equation 6: Calculation for determining interest for a machine Turhollow et al (2009).

$$Cap_i = \frac{i(PP + SV)}{(2)(h_a)}$$

Where as

Cap_i	=	Capital Cost (interest) ($/h)
PP	=	Purchase price, ($, dollars)
SV	=	Salvage value (RV_p), ($, dollars)
h_a	=	Annual usage, (hours)
i	=	Operating rate interest rate (6.64%; (Mellert, 2011))

Machines like a tractor, which can be used year round, had the cost applied through a rental rate versus charging the full cost of the tractor for the year. The rental rate that was charged for the fall 2010 harvest was 27 cents per horsepower hour (Hawbaker, 2010). For this analysis it was assumed that tractors of similar size to the ones used in the fall 2010 testing would be used. The John Deere 8230 was used for to pull the grain cart in the field tests. The tractor was 265 horsepower which equated to $71.55 per hour of operation. The self-propelled bale collector rental rate was determined to be $45 per hour (Matlack, 2010). The rental cost was used because of the unknown maintenance and repair factors along with the unknown salvage value factors for the bale collector and other use of the tractor. The rental cost covered all ownership costs besides the fuel and labor in the rental price. Overall cost was divided into the cost per acre, cost per hour, and cost per ton. The rental cost was derived to determine the total cost per acre, total cost per hour, and total cost per ton of stover harvested.

Machine Rental Cost	
Equipment	Cost per Hour
Tractor	$72
Self Propelled Bale Collector	$45

Table 8: Rental cost for tractors which were considered a multi-use machine over the year besides harvesting and the self-propelled bale collector which was could be used to move bales at different times of the year.

The stover harvest rate and the combine productivity rates were incrementally changed independent of each other through the model analysis. This demonstrated either an improvement or reduction in the productivity of the combine. The modeled cost for the

conventional combine system and then the model cost for the single-pass baling system were compared in which an economic conclusion was able to be developed. The conventional combine system in theory harvested a minimal rate of stover between 1.12-1.6 Mg/ha (.5-.7 tn/ac).

3.5.2.2 Other Operational Characteristics

The dataset which this data was developed from was collected from a 12 row or 30 ft header. To validate the model at other header width data would have to be collected with the same machine and different headers. The additional data collected with the smaller header would provide a broader set of data with which to compare the combine performance curves.

Operational times of the grain cart and tractor in field were also factored into the cost of harvesting stover. Additional time or cost associated with stover harvesting for the tractor and grain cart were applied to the cost of the stover. Most of this was associated with the lower productivity of the combine in the field and the additional cost in labor and operational costs of the tractor.

Data collected from the baler provided. The fuel consumption was considered to be constant and from the previous data it was determined to be 4 gph. Bale length, width, and height were 2.4, 1.2 and .9 m (8, 4, and 3 ft) which were considered maximized for current over the road transport logistics and remained constant throughout the model. String to tie the bales off was priced at $20 per roll of 4000 ft. Bale density was consistent in this year's dataset and represented in the model as .13 kg per cu meter (10 lbs per cu ft).

In the model, a self-propelled bale collection unit was used throughout the analysis. Machine productivity was determined from the analysis of the 2010 fall harvest using a Stinger LTD 6500 Stacker. This machine collected and transported up to 12 bales per time to the field edge at a collection rate of 55.4 bales per hour.

3.5.2.3 Output: Combine

Field data that was used in the model helped bound the scope of the analysis to within actual machine performance and productivity values versus any theoretical performance and productivity calculations. These values were also used in the model for predicting the economic costs of harvesting. There were six data types that were analyzed for the combine that provided a basis for economic and performance calculations in other sections. These data types were area covered, grain and material throughput, fuel consumption, repair and maintenance cost, and event timing for the combine.

The model for the combine distinguished between the active time harvesting versus non-active harvesting events. For this model it was assumed that there were three major non harvesting events: turning on headlands, unloading grain while not harvesting, and miscellaneous delays. These were used to predict the maximum theoretical area covered by a combine conventionally harvesting corn or single-pass harvesting. In order to predict the amount of time spent harvesting on a per hour basis Equation 7 was developed.

Equation 7: Time per hour spent harvesting based upon time for turning machine, unloading grain while harvesting, and miscellaneous stops.

$$T_t = \left(1 - P_h - P_{ug} - P_m\right) * 60$$

Where as

T_t = Total time per hour spent harvesting (minutes per hour)
P_h = Percent of hour spent turning around on headlands (%)
P_{ug} = Percent of hour spent unloading grain while not harvesting calculated in Equation 8 (%)
P_m = Percent of hour stop for miscellaneous reasons (%)

This equation factored in the various non-harvesting time that a combine would experience during the day: unloading while stopped, turn time, and miscellaneous stoppages. In this the miscellaneous stoppages and turned times were assumed to be zero and the productivity reduction would account for these. It also factored the percent of the hour used for unloading grain while the combine was stopped was also determined as shown in Equation 8. This used a ratio that factored the amount of grain unloaded while harvesting versus the amount of grain being harvested by the combine.

Equation 8: Calculation for determining the percent of the hour used for grain unloading based upon the ratio of grain entering the combine and the amount of grain being unloaded and percent of time the combine is stopped to unload.

$$P_{ug} = 100 * \left(\frac{\frac{U}{1-G}}{\frac{C_f}{56} + \frac{U}{1-G}}\right)$$

Where as
P_{ug} = Percent of hour spent unloading grain (%)
U = Unload rate (bushels per second)
G = Percent of unloading while harvesting (%)
C = Crop flow (lbs per second)

The total time spent harvesting value allowed for the total bushels per hour to be calculated as shown in Equation 9.

Equation 9: Calculation for determining bushels per hour harvested by the combine based upon the total time per hour spent harvesting and crop flow into the combine.

$$B_h = T_t x \frac{C_f}{56}$$

Where as
B_h = Bushels of grain harvested per hour (bushels per hour)
T_t = Time per hour spent harvesting (minutes per hour)
C_f = Maximum crop flow (lbs per second)

The bushels per hour harvested and the average yield of the field produced the total acres per hour as shown in Equation 10. By using the acres per hour and the average working hours per day from the input page, the total acres per day was determined as shown in Equation 11. An average harvest window of 27 days to remove 80% of the crop was determined for Iowa. Using this average the acres per year per combine was determined in = Hours per day working (hours) Equation 12.

Equation 10: Calculation for determination of acres per hour harvested by the combine based upon the total bushels per hour harvested and the average yield inputted into the model.

$$A_h = \frac{B_h}{Y_a}$$

Where as

A_h	=	Acres per hour harvested by the combine (ac/h)
B_h	=	Bushels of grain harvested per hour (bushels per hour)
Y_a	=	Average yield of the field (bushels per acre)

Equation 11: Calculation for the determination of acres per day harvested by the combine based upon the average working hours per day and the acres per hour harvested.

$$A_d = A_h x\, H_d$$

Where as

A_d	=	Acres per day harvested by the combine (acres per day)
A_h	=	Acres per hour harvested by the combine (ac/h)
H_d	=	Hours per day working (hours)

Equation 12: Calculation for the determination of acres per year harvested by the combine based upon the average working days in Iowa for corn harvest and the average acres per day harvested**.**

$$A_y = A_d x\, D_y$$

Where as

A_y	=	Acres per year harvested by the combine (acres per year)
A_d	=	Acres per day harvested by the combine (acres per day)
D_y	=	Average working days in harvest per year (days per year)

Fuel consumption was determined by taking the known consumption from previous analysis of the fall 2010 harvest data. The gallons per acre consumption were determined as further detailed in Equation 13.

Equation 13: Calculation for the determination of fuel consumption on a per acre basis based upon the estimated fuel per hour consumed and the acres per hour harvested.

$$F_a = \frac{F_h}{A_h}$$

Where as

F_a	=	Fuel consumption (gallons per acre)
F_h	=	Fuel consumption (gph)
A_h	=	Acres per hour covered by a machine (ac/h)

The predicted repair and maintenance costs were determined by ASABE standard D496.3 (ASABE, 2006) for the combine and are listed in Equation 14. The repair and maintenance costs were derived to reflect a cost per hour basis which was found by calculating the total cost of repairs over the lifetime of the machine and then breaking that cost down by the number of hours in the life of the machine as shown in Equation 14.

Equation 14: Repair and maintenance cost equation from the ASABE standard D496.3. (ASABE, 2006)

$$C_{rm} = (RF_1)P\ x\ [\frac{h}{1000}]^{(RF_2)}$$

Where as

C_{rm}	=	Accumulated repair and maintenance cost (dollars)
RF1, RF2	=	Repair and maintenance factors, Table 9 (from ASABE 497)
P	=	Machine list price, Table 7 (current dollars)
H	=	Accumulated use of machine, Table 9 (hours)

	Repair Factors			
	RF1	RF2	Total RM %	Est Life (h)
Small Tractor	0.007	2	100	12000
Large Tractor	0.003	2	80	16000
Combine	0.04	2.1	40	3000
Large Square baler	0.1	1.8	75	3000

Table 9: Repair factors and estimated life expectancy of machine for calculating machine repair cost based upon ASABE standard D496.3 (ASABE, 2006). Repair factors were used with no adjustment for corn stover harvest.

3.5.2.4 Output: Grain Cart and Tractor

While the combine and baler were instrumented with data collection devices to capture performance data of the machines a tractor and grain cart were not accessible to capture data from. To capture the differences of the cart performance during a conventional harvest versus a single-pass baling harvest a series of equations were developed to determine travel time between the combine and field edge, unload time, fill time, and waiting time for the grain cart and tractor. This provided a comparison of the activity of the grain cart during in-field operation. To calculate the time spent per hour filling the grain cart from the combine, Equation 15 was used.

Equation 15: Calculation for the amount of time spent filling the grain cart based upon the unload capacity of the combine and the total bushels per hour harvested by the combine.

$$T_f = \frac{B_h}{U} x \frac{1}{60}$$

Where as

T_f = Amount of time per hour spent filling grain cart (minutes per hour)
B_h = Bushels per hour harvested (bushels per hour)
U = Unloading rate for the combine (bushels per second)

Equation 16 determined the total cycles per hour that the cart would have to make in order to carry away the predicted bushels per hour from the combine. The values produced from this equation were rounded up and assumed that there could not be a partial travel cycle for a round trip in the field to the combine and back.

Equation 16: Calculation for the determination of the number of cycles the grain cart would make in one hour based upon the amount of grain harvested and the grain cart capacity.

$$N_c = \frac{B_h}{C_c}$$

Where as

N_c = Number of cycles per hour needed (cycle per hour)
B_h = Bushels per hour harvested (bushels per hour)
C_c = Grain Cart Capacity (bushels)

Field travel time was calculated by using taking the average distance traveled in the field and dividing by the average speed of the tractor while at field speed was determined in Equation 17.

Equation 17: Calculation for the determination of travel time in-field for the grain cart and tractor based upon in-field travel speed of the grain cart and tractor to and from the combine and the dump site.

$$T_{gc} = \frac{D_a}{S_a} x N_c x 2$$

Where as

T_{gc} = Travel time for the grain cart in-field (minutes per hour)
D_a = Average field distance traveled to or from the combine (ft)
S_a = Average in-field speed (mph)
N_c = Number of cycles per hour needed (cycle per hour)

To determine the unloading time for the cart the total bushels harvested per hour was determined by using Equation 18.

Equation 18: Calculation for the determination of time to unload the grain cart based upon the grain cart's capacity, unload rate and the number of time per hour it will need to unload.

$$T_u = \frac{C_c}{C_u} x\, N_c$$

Where as

T_u	=	Grain cart unload time (minutes/hour)
C_c	=	Grain cart capacity (bushels)
C_u	=	Grain cart unload rate (bushels per minute)
N_c	=	Number of cycles per hour needed (cycle per hour)

Total wait time was determined by calculating the total operational time of the tractor and grain cart which used the number of cycles, the time for the trips to and from the combine, the total time being loaded, and the total time unloading. The remaining time left in the hour was the predicted waiting time further detailed in Equation 19.

Equation 19: Calculation for determining the total amount of time spent waiting by the grain cart and tractor per hour for the combine to be ready to unload based upon the grain cart unload time, time for the combine to fill the cart, and the travel time of the grain cart.

$$T_w = 60 - (T_u + T_f + T_t)$$

Where as

T_w	=	Time waiting per hour (minutes per hour)
T_u	=	Grain cart unload time (minutes per hour)
T_f	=	Time to fill grain cart (minutes per hour)
T_t	=	Time traveling to and from combine (minutes per hour)

3.5.2.5 Outputs: Baler and Collection

The baler fuel consumption was determined by using Equation 13. This equation used the average fuel consumption determined earlier and then the predicted acres per hour harvested by the combine. The bale collection machine's fuel consumption was determined by using the estimated consumption and the predicted acres per hour covered by the collector.

Equation 20: Calculation for determining the number of bales per acre made by the baler based upon the density, size, and tons per acre of stover harvested.

$$B_a = \frac{T_a}{B_{de}} x \frac{K}{l\, x\, w\, x\, h}$$

Where as

B_a	=	Bales per acre made by the baler (bales per acre)
B_{de}	=	Bale density (lbs per cu ft)
T_a	=	Tons per acre harvested by the combine (tn/ac)
l	=	Length of bale (ft)
w	=	Width of bale (ft)
h	=	Height of bale (ft)
K	=	Constant (2000 lbs/ton)

Equation 21: Calculation for determining the number of bales per hour being produced based upon the average bales per acre produced and the acres per hour harvested.

$$B_h = B_a x\, A_h$$

Where as

B_h = Bales per hour made by the baler during harvest (bales per hour)

B_a = Bales per acre produced while harvesting (bales per acre)

A_h = Acres per hour harvested

The final baler data value calculated was the cost of the string. This was calculated at on a cost per bale and cost per acre value. It was assumed that it was a normal baler and it used six strings. The length and height of the bale were used to determine its circumference. It was also assumed that the rolls of string that were placed in the baler were 4000 ft in length. To determine the cost per bale the cost per foot of string was determined by using Equation 22. The cost per acre value was then extrapolated from the cost per bale by simply multiplying by the bales per acre value.

Equation 22: Calculation for determining the cost of the string per bale based upon the string cost, length of string used on the bale and in the roll, and bale size.

$$C_{bs} = \frac{C_r}{D_r} x\, B_c\, x\, N_s$$

Where as

C_{bs} = Cost of string per bale ($ per ft)

C_r = Cost of roll of string ($)

D_r = Length of string on roll (ft)

B_c = Bale circumference (ft)

N_s = Number of strings per bale

To determine the cost and some performance metrics of a bale collection machine using data from the 2010 harvest, bales per hour collected was determined. The collection rate was then transformed to the number of acres per hour collected. This was determined in Equation 23.

Equation 23: Calculation for the determination of acres per hour covered by the bale collector based upon the average amount of bales per hour collected and the bales per acre produced by the baler.

$$A_h = \frac{BC_h}{B_a}$$

Where as

A_h = Acres per hour by the bale collector (ac/h)

BC_h = Bales per hour collected by the collection machine (bales per hour)

B_a = Bales per acre produced by the baler (bales per acre)

3.5.2.6 Output: Cumulative Costs

Total costs were broken down in each system to differentiate the cost of harvesting the grain versus harvesting the stover. Within each system seven different cost categories were present: fuel, labor, maintenance, depreciation, rental cost, interest, and taxes, insurance, and housing (TIH). Depending upon how the system was configured or how costs were treated for certain machines these categories had varying amounts of machinery assigned to them as shown in Table 10.

Machine Cost Breakdown	
Cost Category	Equipment
Fuel	Combine
	Grain Cart Tractor
	Baler
	Bale Pickup Machine
Labor	Combine
	Grain Cart Tractor
	Bale Pickup Machine
Maintenance	Combine
	Baler
	Grain Cart
	String
Depreciation	Combine
	Baler
	Grain Cart
Interest	Combine
	Baler
	Grain Cart
Rental Cost	Grain Cart Tractor
	Bale Pickup Machine
Taxes Interest Housing	Combine
	Baler
	Grain Cart

Table 10: The assigned cost categories that each machine was analyzed for based upon how they were factored for cost either rental cost or capital purchase cost.

Assessing the fuel cost for each machine was done by calculating the cost per hour of the fuel use which was calculated by Equation 24.

Equation 24: Calculation for determining the cost per hour of fuel consumption based upon the average fuel consumption per hour, fuel cost, and the surcharge for lubrication based upon ASABE standards.

$$C_h = F_c \, x \, P \, x \, (1 + L)$$

Where as

C_h = Cost of fuel per hour for each machine (dollars per hour)
F_c = Fuel Consumption (gph)
P = Price of fuel per gallon (over a 5 year average) ($, dollars)
L = Lubrication charge (15%) (ASABE, 2006)

This was then broken down further into calculations for cost per acre and cost per ton basis by using Equation 25 and Equation 26.

Equation 25: Calculation for determining cost per acre of the stover harvest machines for fuel as based in Equation 27 and for other hourly costs as well.

$$C_a = \frac{C_h}{A_h}$$

Where as

C_a = Cost per acre ($/ac)
C_h = Cost per hour from Equation 24 ($/h)
A_h = Acres per hour covered by a machine (acres per hour)

Equation 26: Calculation for determining cost per ton of the stover harvest machines based off of the cost per hour in Equation 27 and the tons per hour of stover harvested.

$$C_t = \frac{C_h}{T_a \, x \, A_h}$$

Where as

C_t = Cost per ton (dollars per ton)
C_h = Cost per hour from Equation 24 ($/h)
T_a = Harvest rate (tn/ac)
A_h = Acres per hour covered by the machine (acres per hour)

The labor cost was figured to be at $13.45 per hour. To determine the amount of hours worked a factor of 1.2 labor hours for every 1 machine hour was used to determine the labor cost as recommended by Turhollow et al. (2009). From this the cost per ton and cost per acre were derived by again using Equation 25 and Equation 26. The cost was only assigned to the machines with operators in them and again the cost per acre and cost per ton were based off of the combine and bale collector acres per hour as in the fuel consumption.

The final cost characteristic analyzed was the ownership cost of the machine. This was partially covered by the use of depreciation and interest calculations. The second part of the ownership cost was the expense associated with taxes, insurance and housing. ASABE standard EP 496.3 stated that the method for determining the estimated cost of these was at 2% of the total capital cost of the machines.

3.5.2.7 Output: Total Gross Loss

To determine the total cost to harvest the corn stover in the single-pass baling system the cost to harvest the grain was subtracted. Equation 27 and Equation 28 determined the cost of harvesting the grain included the combine and grain cart. To determine the cost of stover harvest in the model, the analysis was operated concurrently with the single-pass baling system to determine the cost of the baseline grain harvest. The seven cost characteristics for the conventional harvest were then subtracted from the single-pass baling system. The difference between these two values was determined to be from the influence of the single-pass baling system on the combine or the extra capital equipment needed to operate a successful harvest as shown in Equation 29.

Equation 27: Calculation for determining the stover harvest cost of the combine found by taking the cost to operate a normal harvest from the additional cost to harvest stover.

$$D_c = C_{stover} - C_{conv}$$

Where as

D_c = Combine cost difference ($/ac or $/ton)
C_{stover} = Single-pass Baling Combine Cost ($/ac or $/ton)
C_{conv} = Conventional Combine Cost ($/ac or $/ton)

Equation 28: Calculation for determining the stover harvest cost of the grain cart and tractor which was found by taking the cost to operate a grain cart under normal harvested condition and subtracting it from the cost to operate when harvesting stover.

$$D_{gc} = GC_{stover} - GC_{conv}$$

Where as

D_{gc} = Grain cart and tractor cost difference ($/ac or $/ton)
GC_{stover} = Single-pass Baling Combine Cost ($/ac or $/ton)
GC_{conv} = Conventional Combine Cost ($/ac or $/ton)

Equation 29: Calculation for determining the stover harvest cost of the grain cart and tractor which was found by adding the cost difference of the operation of the combine, baler, bale collection machine, and grain cart.

$$SHC = D_{gc} + D_c + B_c + BC_c$$

Where as

D_{gc} = Grain cart and tractor cost difference ($/ac or $/ton)
D_c = Combine cost difference ($/ac or $/ton)
BC_c = Bale Collection Cost ($/ac or $/ton)
B_c = Baler Cost ($/ac or $/ton)
SHC = Stover Harvest Cost ($/ac or $/ton)

3.5.3 RESULTS

3.5.3.1 Cumulative Costs

The model was configured to the aforementioned settings and operated. The output produced results that were analyzed further in Excel. The first analysis investigated was the cumulative cost to harvest the grain and stover. The initial outcome from the data was that the cost to harvest corn was the same throughout all the scenarios as shown in Figure 3and Figure 4. The cost associated with harvesting the grain was determined to be $45 per ton and $22.52 per acre for the combine and grain cart and tractor systems. The cost of stover harvest varied depending on other factors that will be discussed later on in the section. The total cumulative cost to harvest stover and grain averages between $50 - $60 per ton of stover harvested and $30 - $60 per acre. This was dependent on the productivity level of the combine and the harvest rate both of which were affected by the configuration for stover collection and the amount of stover being harvested.

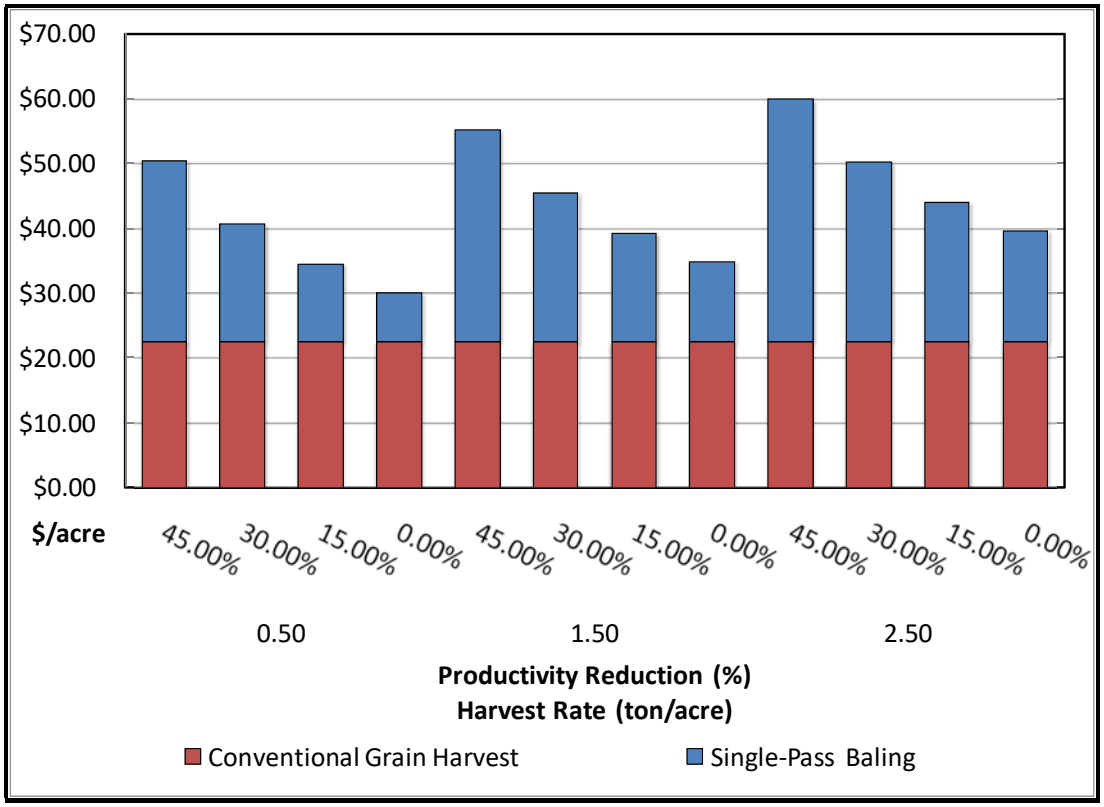

Figure 3: Total cumulative cost per acre for grain and stover harvest in the conventional configuration. The cost to normally harvest corn remains steady while the cost to harvest the stover varies according to the productivity of the combine.

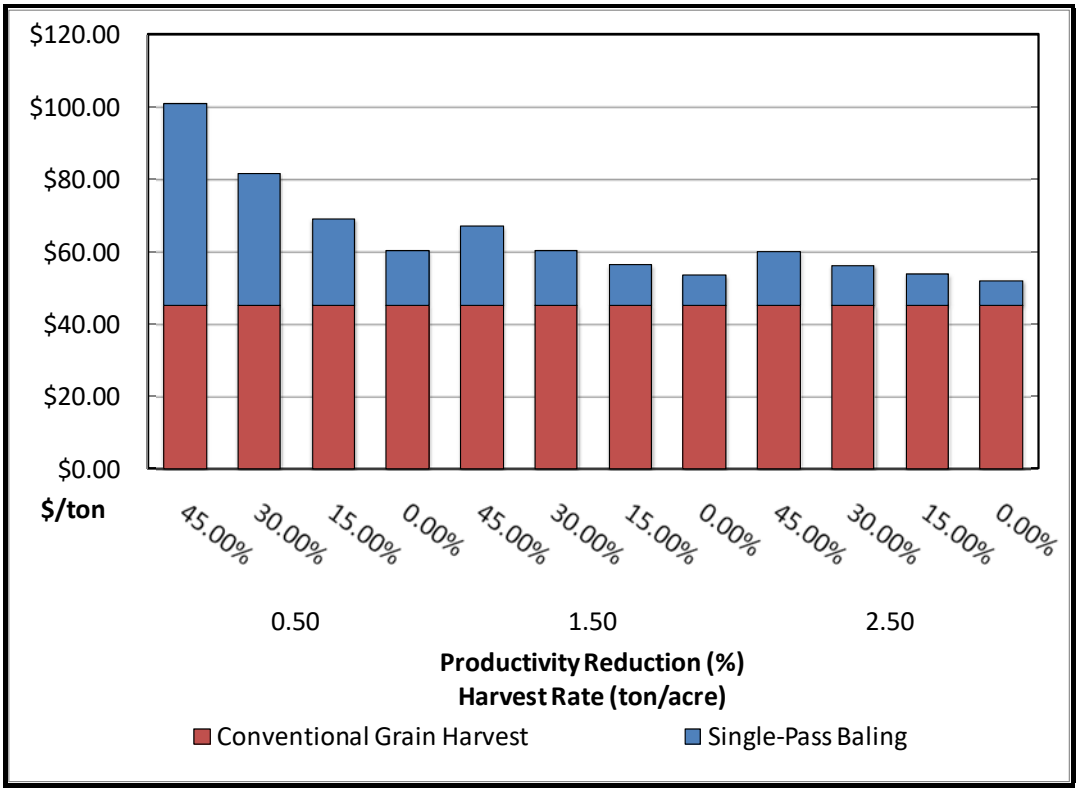

Figure 4: Total cumulative cost per ton for grain and stover harvest in the conventional configuration. As the harvest rate increases (ton/acre) the cost to harvest decreases as more cost was distributed amongst the higher rates of stover.

The model was used to figure the cost from the 2010 fall harvest. The fall stover harvest rates were .5, 1.1, and 1.75 tons per acre and the productivity reduction intervals of the three harvest rates were 11%, 45%, and 56.5% which were taken from the analysis completed in chapter 5. At these rates and percentages the cumulative cost for single-pass harvesting was $65.62, $52.73, and $43.33 per ton and $32.81, $52.73, and $65 per acre for the respective harvest rate and productivity reduction percentage respectively.

3.5.3.2 Stover Removal System Costs

Removing the cost to harvest the grain provides a direct assessment of the total cost of removing the stover and what expenses an end user will have to pay a producer to cover harvest costs. Figure 5 and Figure 6 show the general trend of the cost across four of the most likely harvest rates; .5, 1.5 and 2.5 tons per acre along with varying productivity responses. The two figures show that as the productivity of a machine was decreased the cost to operate the machine increased. Additionally, as the rate of harvest increased the cost per ton decreased but the overall cost per acre was higher. When using the harvest data from of 2010 as a baseline for cost, the stover harvest which had harvest rates of .5, 1.1, and 1.75 tons per acre and productivity intervals at 11%, 45%, and 56.5% had a cost per acre of $10.29, $30.22, and $42.48 per acre and $20.06, $30.39, and $28.46 per ton respectively.

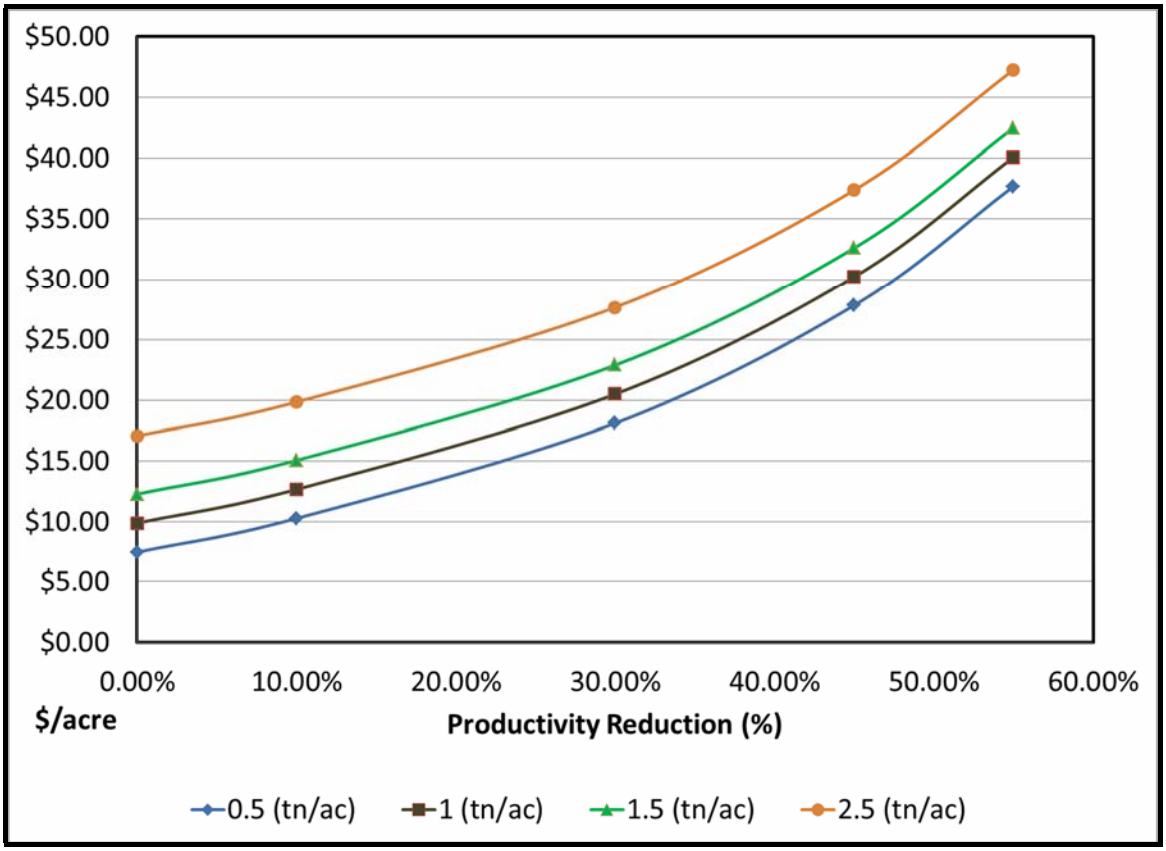

Figure 5: Cost per acre for harvesting stover at harvest rates between .5 tn/ac and 2.5 tn/ac with the factor of productivity reduction on the combine. Productivity reductions are not tied to a specific combine.

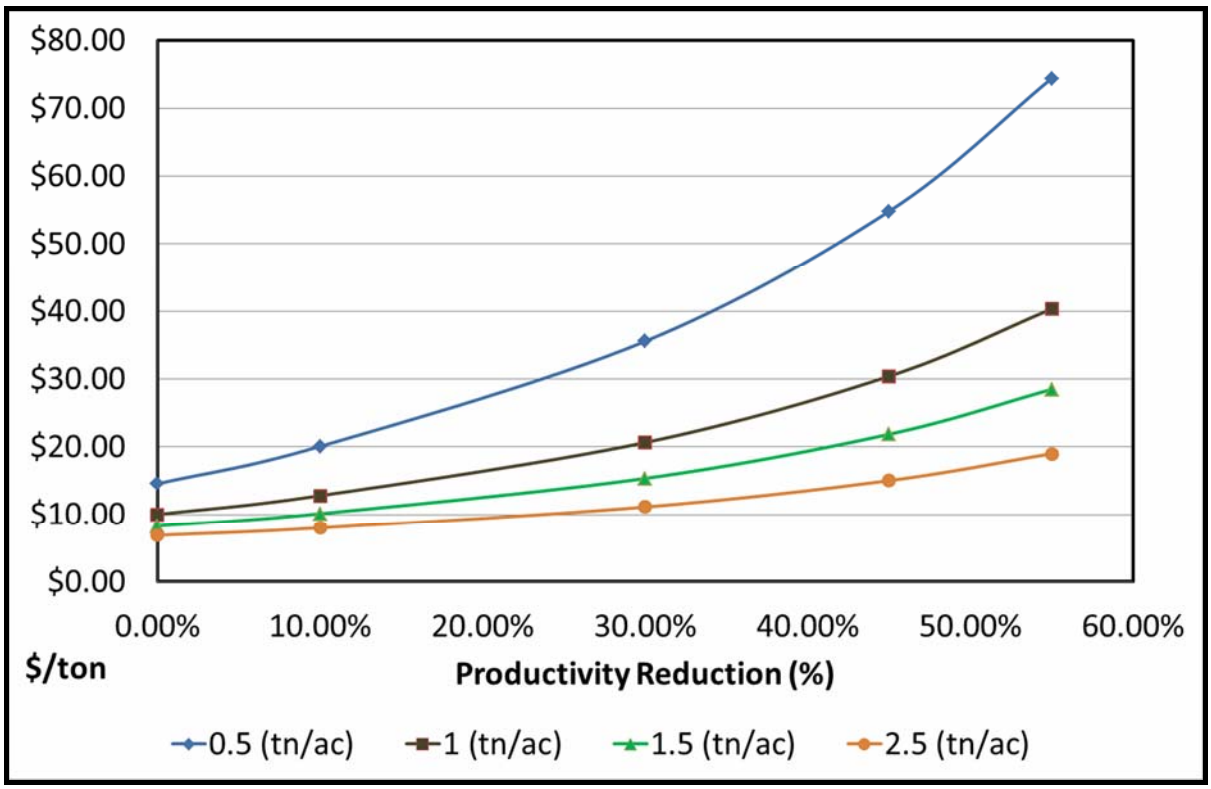

Figure 6: Cost per ton for harvesting stover at harvest rates between .5 tn/ac and 2.5 tn/ac with the factor of productivity reduction on the combine. Productivity reductions are not tied to a specific combine.

There are a couple of outcomes that can be drawn from these results. The first was that the reduction in the productivity loss in the system will reduce cost both in cost per ton and cost per acre. The other outcome was the cost per ton of stover decreases at the higher harvest rates but the cost per acre to harvest increases which was a tradeoff.

The next step in the analysis was to break the overall cost of the stover harvest into the cost applied to the harvest from each machine in the system. The five machines analyzed in this system were the combine, baler, bale collection machine, and the grain cart and tractor system. Figure 7 and Figure 8 show that the productivity reduction affects the cost of each machine differently. For example on a per ton basis the baler and the bale collection machine costs which were solely applied to the corn stover harvest cost remained level or relatively stagnant over the different productivity reduction levels. Through each increase in the harvest rate the cost per ton decreased. Meanwhile, the combine and grain cart had different responses. Through the increases in the harvest rates the cost remained stable at the same productivity reduction rates. However, when the productivity reduction was improved the cost for these was driven lower for both the cost per ton and cost per acre. The main driver for this was the area harvested by the combine.

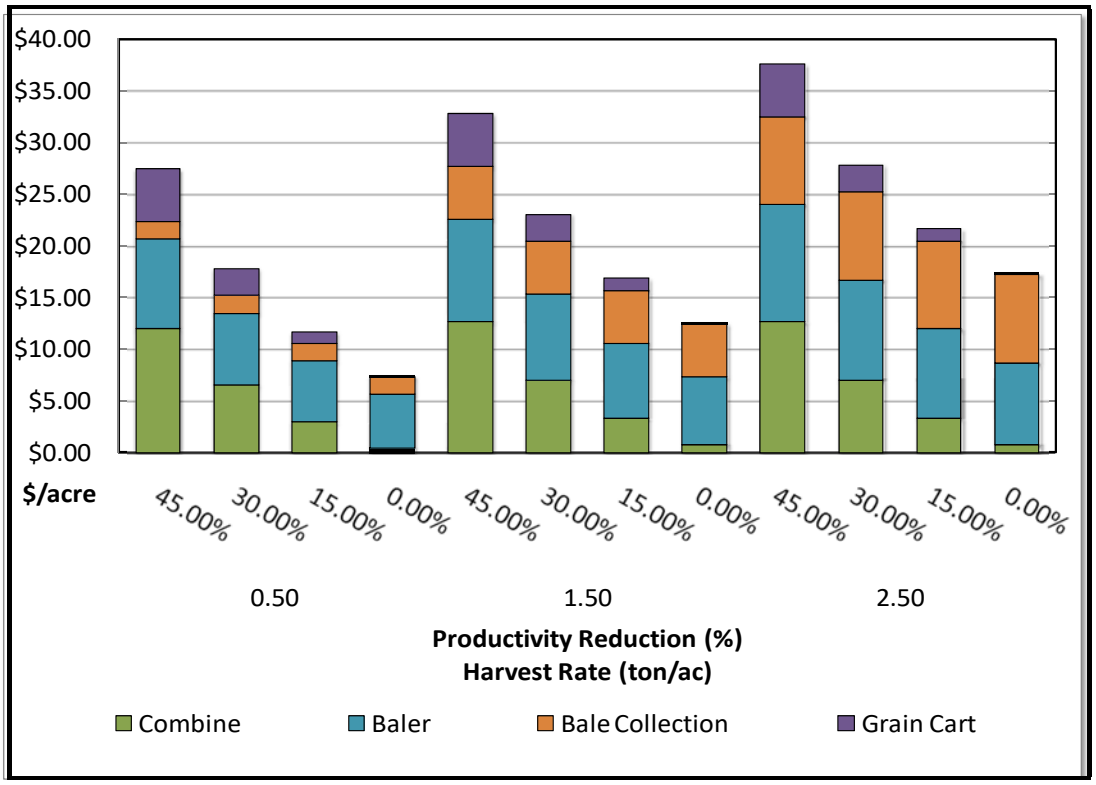

Figure 7: Total cost per acre for each machine system based upon the amount of stover harvested (tn/ac) and the reduction in productivity (%) for a combine harvesting stover.

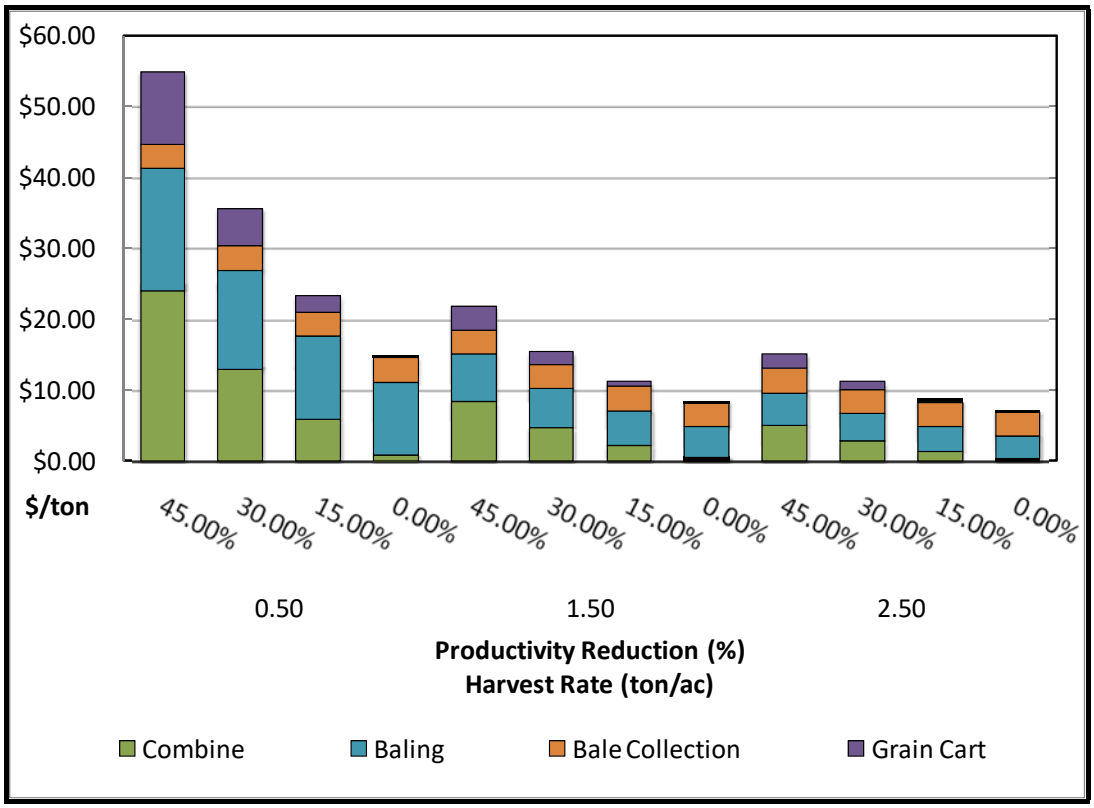

Figure 8: Total cost per ton for each machine system based upon the amount of stover harvested (tn/ac) and the reduction in productivity (%) for a combine harvesting stover.

3.5.3.3 Machine Cost Breakdown

As mentioned earlier, for most machines there are seven major cost categories that were used for this analysis. Further detailed in Figure 9, the seven major cost categories are distributed differently across each system and scenario. The breakdown of the combine cost the dominate cost category was the depreciation cost that was applied to the stover. As more acres are harvested per hour the productivity improved the added depreciation cost applied to stover became less because it was applied back to the cost of the grain harvest. As the productivity reduction got to 0% reduction the cost applied to the stover harvest was removed. This was the same case for the TIH, interest, maintenance, and labor costs.

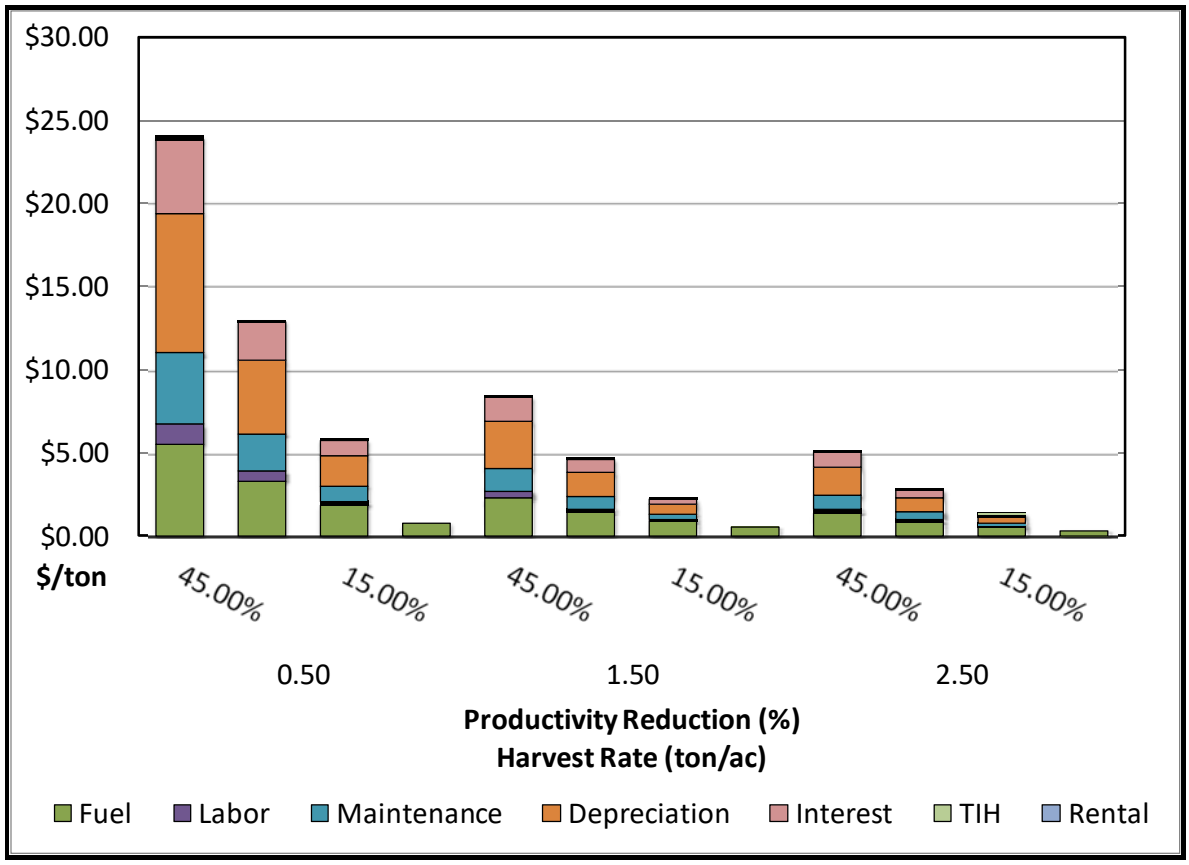

Figure 9: Total cost per ton for the combine to harvest stover broken down into seven cost categories for analysis based upon cost data from the ASABE D497 standard and current machine prices.

A main driver behind the large depreciation, interest, TIH, and maintenance cost for the combine was the high initial capital cost of the combine and header. As the price for a combine and header ranged from $300,000 -$500,000 and typical salvage value for a system like this was around $100,000. Which means $200,000 - $400,000 of the capital cost must be distributed between the grain and stover harvest. Each of the cost categories was determined from a total cost. For the combine used in 2010 the total maintenance cost was $176,820, interest costs were $180,390, depreciation costs were $342,270, and TIH costs were $8,790 over the life of the machine, which was 3000 hours.

Fuel cost was different from the ownership costs because there was an additional fuel cost penalty for pulling the baler through the field at all productivity reduction rates. The fuel cost from the combine was fairly moderate with the largest cost coming at the 45% reduction rate. While most of the fuel cost could be placed back onto the grain harvest at the 0% reduction rate there was still a fuel cost that ranged from $.29 to $.76 per ton.

The other machine system that had cost applied to both the grain harvest and stover harvest was the grain cart and tractor. The costs for the two tractors and grain cart were split evenly. As the productivity reduction improved the rental cost of the tractor also became slightly lower. Costs for the grain cart and tractor system were just as responsive to productivity as the combine cost. One difference between the grain cart and tractor system and the combine was that at the 0% reduction rate all costs were shifted to the grain harvest because there was no

slowdown in harvest. Having no slowdown in the harvest meant that the grain cart and tractor system became a non-factor in the total cost for harvesting corn stover.

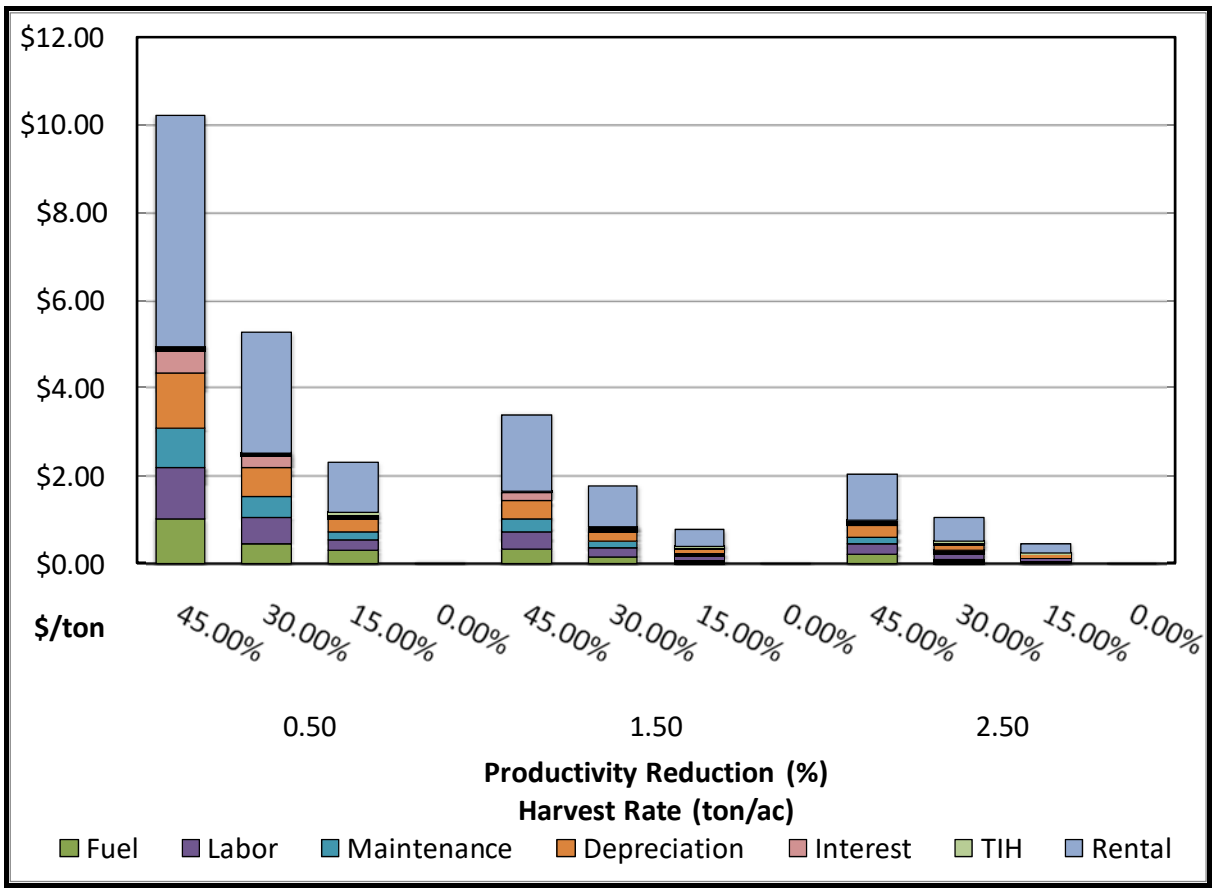

Figure 10: Total cost per ton for the grain cart and tractor to harvest stover broken down into seven cost categories for analysis based upon cost data from the ASABE D497 standard and current machine prices.

The lower capital cost of the grain cart in this system was the main reason that most costs were lower for the system. Another reason was that the tractor was treated as a multi-use machine and used the hourly rental rate which meant that not all of the total ownership costs were applied to harvesting grain or stover. This inherently drove down the cost of the tractor.

The grain cart and tractor system and the combine each had costs for stover harvest and grain harvest, the baler and bale collection machine did not. The costs associated with the baler and bale collection machine were strictly for the harvest of the corn stover.

The cost breakdown for the baler shown in Figure 11 had an eighth category, which was the cost of string for the baler. The baler had similar cost trends to that of the combine. It had relatively high capital cost with limited usage outside of fall harvest. This drove costs for interest, depreciation, maintenance, and TIH higher. In each scenario the costs associated with these four costs categories were roughly 60% -80% of the total cost of operation. String cost also was a large cost of harvest. It cost $1.38 per ton of the total cost to supply the string for the bales.

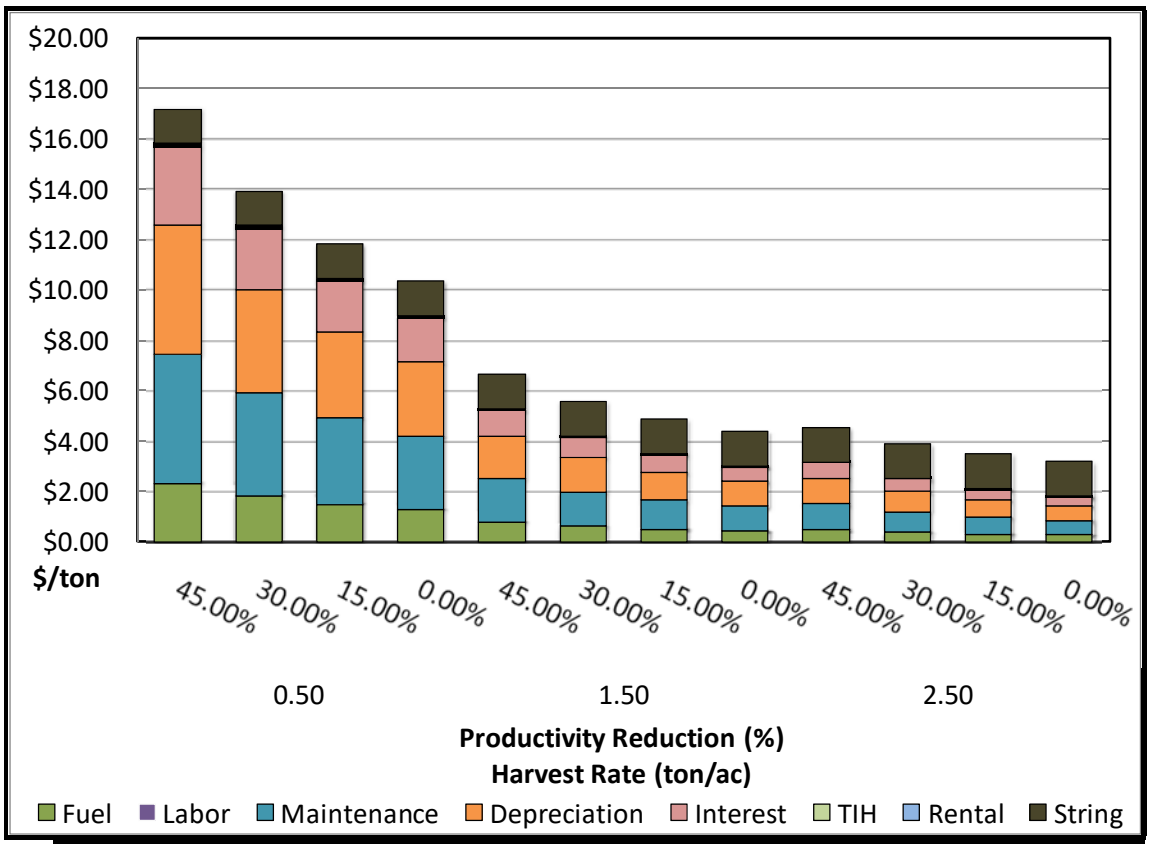

Figure 11: Total cost per ton for the single-pass baler to harvest stover broken down into eight cost categories for analysis based upon cost data from the ASABE D497 standard and current machine prices.

Fuel costs improved as the collection rates were increased and the productivity improved. At any rate of collection the extra fuel to operate the baler in the field behind the combine was about 10% or less of the total cost per ton of stover depending upon the productivity reduction interval.

Labor cost was completely removed from the baler. Since the combine operator could monitor and control the functions of the baler as well as the combine there was no additional labor cost associated with the baler.

The final machine system to break down in cost was the bale collection machine. Looking at the cost per ton of the machine it was similar across all scenarios. The reason behind this was that the bale collection machine was not tied to the productivity of the single-pass baler and could freely pick up bales as necessary which meant that it could pick the bales up after harvest of the field was complete. There were three major costs that were associated to the bale collection machine. These were the rental cost, labor cost, and fuel cost. The total cost for operation of the bale collector was $3.41 per ton. Of the three costs the highest cost was the rental cost. The rental cost was 50% of the total cost. The rental cost was used because it was assumed that the bale collection machine would get some use away from the fall harvest season and that cost would lower the capital cost assigned to the collection machine. Also, this analysis only determined the cost to the field edge for bale hauling. The next step in the transport logistics cycle would be moving bales from the field to the next point in the bale supply chain. Potentially this machine could be used to move bales to that next step in the supply chain.

Additional use would distribute the capital cost of the machine which would result in lower costs.

One other outcome to analyze for the bale collection vehicle to discuss was the cost per acre increase as the harvest rate increases. As the harvest rate increased, more bales were going to be produced per acre. Having more bales per acre caused the bale collection machine to stay within an acre longer in order to collect all of the bales present. This drove cost per acre higher, as shown in Figure 13.

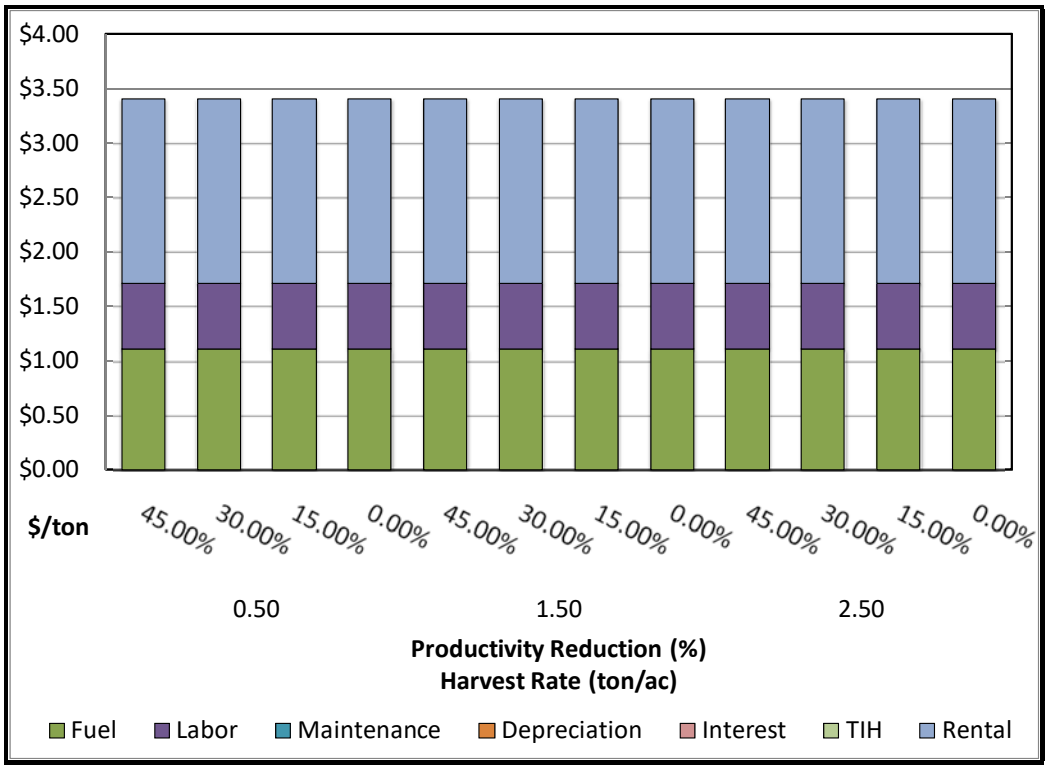

Figure 12: Total cost per ton for the single-pass baler to harvest stover broken down into eight cost categories for analysis based upon cost data from the ASABE D497 standard and current machine prices.

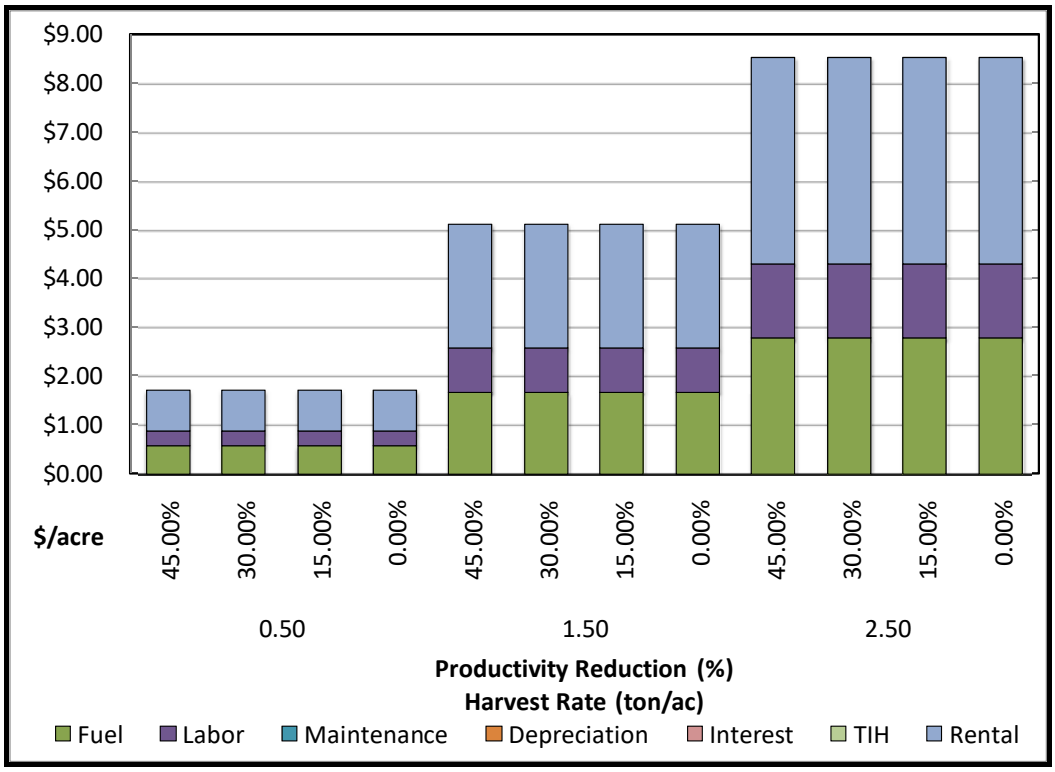

Figure 13: Total cost per acre for the single-pass baler to harvest stover broken down into eight cost categories for analysis based upon cost data from the ASABE D497 standard and current machine prices.

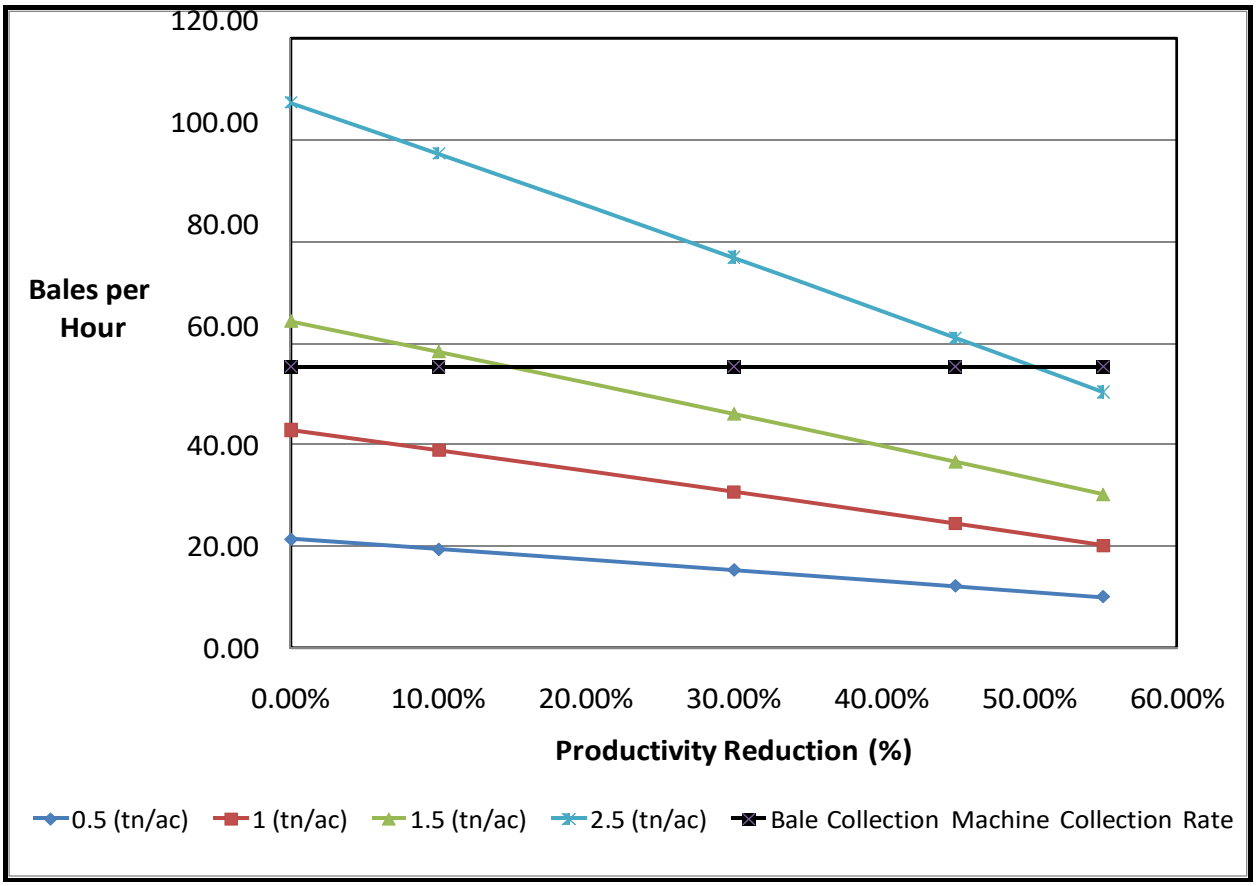

Figure 14: Comparison of the average amount of bales per hour collected versus the average amount of bales per hour produced by the baler by harvest rate and productivity reduction interval.

Comparing the capacity of the bale collection vehicle to the output of the baler, as shown in Figure 14, showed that the bale collection vehicle should be able to keep up with one single-pass baler bale output up to 1.5 tons per acre and 10% productivity reduction. What this meant was that at current harvest rates and productivity reduction levels one collection machine should be able to collect all of the daily output of the single-pass baler.

CONCLUSIONS

A model was developed and implemented that calculated the cost for single-pass baling of corn stover with delivery of the grain and stover to the field edge. The corresponding harvest rates for 2010 for the 0, 6, and 12 row collections were .5, 1.1, and 1.75 tons per acre with productivity reduction levels of 11%, 45%, and 56.5% respectively that were from the fall 2010 harvest. At these harvest rates and productivity reductions the total cost for stover harvest was determined to be $20.06, $30.39, and $28.46 per ton and $10.29, $30.22, and $42.48 per acre for each scenario respectively.

The model accounted for a variety of fixed and variable inputs such as fuel consumption, speed, crop flow, fuel cost, labor cost, and machinery cost. It also accounted for machine logistical variables like the unloading time, baled stover output, and time to collect the bales from the field.

The cost of single-pass baling harvest was broken into seven general cost categories: Fuel costs, labor costs, maintenance costs, depreciation costs, interest costs, taxes, insurance, and housing costs, and rental costs. An additional cost that was added for the baler was the cost of the string for the baler. Many of these cost categories were derived from ASABE machinery management standards and adapted for use in this model.

In addition to modeling the actual costs of the fall 2010 harvest the model was also used to predict costs for varying harvest and productivity rates of the harvest systems. Three harvest rates (.5, 1.5, 2.5 tn/ac) and four productivity reduction rates (0%, 15%, 30%, and 45%) were selected to determine cost to harvest grain and stover. Costs were also determined on machine system level, and individual cost categories level within each machine system. Outputs of the model were cost per ton of stover harvested and cost per acre of corn harvested.

The outcomes from the analysis of the modeled data were that the baseline total cost for the grain harvesting system (combine and grain cart) was $45 per ton and $22.52 per acre. The cumulative total cost for harvesting corn stover and grain was between $50-$60 per ton and $30-$60 per acre (combine, baler, bale collector, grain cart). The cost to harvest the stover was determined to be between $7.50 - $35 per acre and about $10-$35 per ton for the harvest scenarios most likely to be met in the analysis. The combine and grain cart costs diminished as the productivity of the single-pass baling system was improved. At the lowest productivity reduction (0%) the grain cart and combine costs were minimized. The cost per acre indicated that as more stover was harvested the cost increased. The cost per ton to harvest more stover decreased because as more stover was harvested the cost was distributed further by more stover. Dividing the cost into the seven cost categories illustrated that the major costs of the machinery for stover harvest was the ownership cost, mainly depreciation and maintenance cost for the combine, grain cart, and baler. Rental cost for machines was also a significant influence for the bale collection machine and the tractors.

REFERENCES

Mud Hog. (2011). Retrieved June 21, 2011, from Tuthill Drive Systems: www.mudhog.com

AGCO Corporation. (n.d.). *Challenger Biomass Baler. Retrieved.* Retrieved February 15, 2011, from Challenger-Ag/AGCO: http://www.challenger-ag.com/NA/EN/products/harvesting/1379.htm

ASABE. (2006, February). Agricultural Machinery Management, ASAE EP496.3. St. Joseph, Michigan: ASABE.

ASABE. (2011, Mar). 497.7. St. Joseph, Mi, United States: ASABE.

California Energy Commission. (2004, January). Retrieved June 20, 2011, from http://www.energy.ca.gov/reports/2004-02-03_600-04-001.PDF

Edwards, W. M. (1979). Farm Machinery Selection Under Condtions of Uncertainity. *Dissertation*. Ames, Iowa, United States of America: Iowa State University.

EISA. (2007, January 4). Energy Independence and Security Act of 2007. (110 Congress). United States: United States Senate. Retrieved February 12, 2011, from http://energy.senate.gov/public/_files/getdoc1.pdf

Glenvar Bale Direct. (2007). Retrieved February 16, 2011, from ASABE: http://www.asabe.org/standards/ICCHP2007DirectBaler.pdf

Gray, W. H. (1898). Corn Harvester and Binder. U.S. Patent No. 602659.

Hanna, M., & Al-Kaisi, M. (2008, 4 9). *Managing Residue for a Good Stand*. Retrieved June 20, 2011, from Integrated Crop Management News: http://www.extension.iastate.edu/CropNews/2008/0402AlKaisiHanna.htm

Hawbaker, R. (2010). Store Manager. (M. Darr, Interviewer)

Hettenhaus, J. R., & Wooley, R. (2000, October). Biomass commercialization prospects in the next two to five years. *BIOMASS COLLOQUIES 2000*. National Renewable Energy Laboratory.

Johnson, J. M., Wilhelm, W. W., Karlen, D. L., Archer, D. W., Wienhold, B., Lightle, D. T., et al. (2010). Nutrient Removal as a Function of Corn Stover Cutting Height and Cob Harvest. *Bioenergy Resources*, 342-352.

Karlen, D. (2008, October). Cellulosic Ethanol From Corn Stover: Calculating—and Improving—the Bottom Line. *Agricultural Research*.

Matlack, J. (2010, August). (K. Webster, Interviewer)

Mellert, K. (2011, 6 27). Edwards, Il.

Perlack, R. D., & Turhollow, A. F. (2002, September). *Assessment of Options for the Collection, Handling, and Transport of Corn Stover.* Environment Sciences Division. Oak Ridge : Oak Ridge National Laboratory.

Rosenthal, H. (1950). Corn harvester. *U.S. Patent No. 2524603*.

Shinners, K. J., Binversie, B. N., & Phillippe, S. (2003, July 27-30). WHOLE-PLANT CORN HARVESTING FOR BIOMASS: COMPARISON OF SINGLE-PASS AND MULTIPLE-PASS HARVEST SYSTEMS. Las Vegas, Nevada, United States: ASABE.

Sokhansanj, S., & Turhollow, A. F. (2002). Baseline Cost for Corn Stover Collection. *Applied Engineering in Agriculture*, 525-530.

Turhollow, A., Wilkerson, E., & Sokhansanj, S. (2009, December). *Cost Methodology for Biomass Feedstocks: Herbaceous Crops and Agricultural Residues.* Oak Ridge National Laboratory.

USDA - National Agriculture Statistics Service. (n.d.). Weekly Weather-State Stories & Crop Progress Report. United States: USDA.

CHAPTER 4

OPTIMAL BIOMASS STORAGE CONDITIONS TO MINIMIZE MATERIAL DEGRADATION AND STORAGE COSTS

4.1 Background

Achievement of the target set by the Energy Independence and Security Act (EISA) of 2007 to produce 60 billion liters (16 billion gallons) of cellulosic biofuels annually in the United States by 2022 will require around 200 million tons (dry) of cellulosic feedstocks each year. The fact that the majority of cellulosic feedstocks, including corn stover, are harvested within a short span of time, usually between 1–2 months, and are required by the biorefineries over the whole year necessitates their effective and efficient storage. A comprehensive analysis of wet and dry storage systems is required to identify the key impact variables and conditions which promote excessive dry matter loss and biomass quality degradation and to understand how these storage conditions are impacted by harvest and densification processes.

4.2 Objective and Specific Tasks

This chapter addresses the third specific objective of this project which was to quantify optimal wet and dry biomass storage conditions to minimize material degradation and storage costs. This specific objective was accomplished through a set of tasks:

1. Quantify the interaction of corn stover harvest and densification systems on storage characteristics and biomass deterioration during wet storage.
    a. Ensiling method for wet storage of bulk corn stover was employed in 55 gal test cells. However, the investigators found that 55 gal test cells were not large enough to simulate the real storage situations. Thus, the results obtained from those storage trials are not included in the final report.
    b. For the accomplishment of this task, initial plan was modified and single-pass corn stover bales were tube-wrapped for wet storage. Details of these tests are included in Section 4.4 of this chapter, which is drafted in the form of a journal article and is currently under internal review.

2. Quantify the interaction of corn stover harvest and densification systems on storage characteristics and biomass deterioration during dry storage.
    a. Field drying was not the possible option with single-pass baling, which was the choice for baling in this project, and, thus, was not implemented in this project.
    b. Supplemental and self-heat aeration drying methods were employed for bulk corn stover during storage in 55 gal test cells. However, the investigators found that 55 gal test cells were not large enough to simulate the real storage situations. Thus, the results obtained from those storage trials are not included in the final report.
    c. For the accomplishment of this task, initial plan was modified and single-pass corn stover bales were stored by allowing self-heat aeration drying method. Details of these tests are included in section 4.5, which has been published in a peer-reviewed journal-‘*Energies*’.

4.3 Overall Impacts of study

Updated Billion-Ton study of the Department of Energy estimated the 2012 and 2030 annual U.S. potential for corn stover at 60 $\$\text{-ton}^{-1}$ farmgate feedstock price to be around 85 and 140 million ton (dry) under normal scenario; and around 153 and 271 million ton (dry) under more aggressive agricultural practices. Moreover, analysis of USDA-NASS data for corn production in 2010, with the assumption that the corn stover removal rate would be same throughout the U.S., shows around 87% of total U.S. corn stover will be produced in 12 Midwestern states and 20% of this corn will be produced in Iowa alone. Thus, identification of better storage strategy for corn stover in Iowa will help reduce storage dry matter loss and preserve biomass qualities during storage.

4.4 Outdoor storage characteristics of tube-wrapped large square single-pass corn stover bales in Iowa

Ajay Shah, Matthew J. Darr, Keith Webster, Kevin Peyton, Brittany Schon, Andrew Kissel

(to be submitted to peer-review journal)

ABSTRACT

Short annual harvest window (≤1-2 months) but year-round demand of corn (*Zea mays*) stover necessitates continuous exploration to identify its cost-effective and quality-preserving storage methods, especially in the principal corn growing Midwestern states. The main objective of this study was to investigate the effects of the interactions of storage conditions and durations (~4.5 and 8.5 months) on the quality of single-pass corn stover bales tube-wrapped and stored outdoors in Iowa. Different storage conditions were based on some of the most-likely situations, such as storage of bales on the same day or after delaying for few days or when rainfall occurs after harvest. Additionally, a 120-bales pilot-scale stack was tube-wrapped and stored for 8.5 months. Qualities of stored bales were characterized by dry matter loss (DML), temperature profiles, and changes in moisture and biomass compositions, as determined by fiber and ultimate analyses. DML for different storage treatments were between 3 and 12%.

Keywords: Single-pass corn stover large square bales, tube-wrapping storage, drying matter loss (DML), outdoor storage

4.4.1 INTRODUCTION

Updated Billion-Ton study (DOE, 2011) estimated the 2012 and 2030 annual U.S. potential for corn stover at 60 \$-ton^{-1} farmgate feedstock price to be around 85 and 140 million ton (dry) under normal scenario; and around 153 and 271 million ton (dry) under more aggressive agricultural practices. Moreover, analysis of USDA data for corn production in 2010 (USDA-NASS, 2010), with the assumption that the corn stover removal rate would be same throughout the U.S., shows around 87% of total U.S. corn stover will be produced in 12 Midwestern states. 20% of this corn will be produced in Iowa alone. The fact that stover is harvested only once a year necessitates its effective and efficient storage in a quality-preserving manner to fulfill year round demands of corn stover based cellulosic biorefineries. Corn stover can be collected in bulk form or as bales either in a single pass or in multiple passes; however, the single-pass collection method has an advantage over multi-pass due to reduced ash content in collected biomass, and bales have an advantage over bulk stover due to their enhanced bulk density. Despite some of these notable advantages, single-pass collection method has some limitations, mainly the inability to control moisture content prior to harvest. Additionally, bales can be stored in different ways, including outdoors with individual plastic wrap, continuous plastic wrap, or a tarp cover, and indoors within a hoop barn or metal building. Among different biomass formats and storage types, this study focused on the outdoor storage of single-pass corn stover bales with plastic tube wrap.

In the past, several studies (Harrigan and Rotz, 1994; Huhnke, 1990; Sanderson et al., 1997; Shinners, 2000; Shinners et al., 2007, 2009a, 2009b, 2010) were focused on the

investigation of different storage characteristics, including dry matter loss (DML), of large round and square multi-pass bales formed of different biomass types and stored under different conditions at different geographic locations across U. S. Their reported storage DML values were in the range 0-19.5%, with indoor storage having the least amount of loss. Further analysis of DML values reported in different aforementioned studies indicated that for outdoor storage, bales with individual or tube plastic wraps suffered the least amount of dry matter degradation. For instance, Harrigan and Rotz (1994) reported DML for indoor stored twine wrapped large round alfalfa hay bales to be 6.0%, whereas for outdoor storage, they reported DML values for plastic, net and twine wrapped bales to be 9.6%, 16.3%, and 16.5%, respectively. Likewise, Shinners et al. (2009b) reported DML for indoor stored large round alfalfa bales to be 2.0%, whereas for outdoor storage, they reported DML values for plastic wrap as 5.9%. Other wrap types, including sisal twine, plastic twine and net wrap, were between 7.3-19.5%. The DML values reported by Shinners et al. (2010) were even more interesting. For outdoor stored large round perennial grasses bales, they reported DML values for bales wrapped with different wrap types, including breathable film, net wrap, plastic twine and sisal twine, to be in the range 4.8-14.9%; however, for bales wrapped individually and in tube with plastic wraps, their reported values were 3.8 and 1.1%, respectively.

Aforementioned studies indicate that outdoor storage of multi-pass bales with plastic wraps (individual or in tube) can preserve biomass better than other storage methods. Also, all of the aforementioned studies were based on the storage of multi-pass bales, but due to the advantage of single-pass collection method in obtaining cleaner biomass, it would be worthwhile to conduct a study to investigate the storage properties of single-pass bales. So far, only few studies (Shah et al., 2011; Shinners et al., 2011) have investigated the storage characteristics of corn stover collected in a single pass. Shah et al. (2011) stored single-pass large square corn stover bales outdoors with tarp and breathable film covers in Iowa for 3 and 9 months, and found the storage DML to be in the range of 5-17%. Shinners et al. (2011) stored different stover fractions harvested in a single pass in 2008 and 2009 for 183-237 days in aerobic piles (covered and uncovered), anaerobic silo bags or ventilated bags. They found the storage DML for different storage treatments to be in the range of 0.2-21.5%, with the stover stored under anaerobic conditions having the least amount of loss. Moreover, despite Iowa's potential to supply the majority of corn stover for cellulosic biofuels production in U. S., only few studies (Shah et al., 2011) have been focused on investigating the storage behavior of corn stover in Iowa. Thus, there is a need to explore the storage behavior of single-pass corn stover bales with individual or tube plastic wraps to see the effect of the changes in the parameters, such as initial feedstock moisture and storage durations, in biomass quality during storage in Iowa. The main objective of this study was to investigate the interactions of storage conditions and durations on the quality of single-pass large square corn stover bales tube-wrapped and stored outdoors above the bare ground in Iowa. For comparison, bales were also stored indoors within a metal building with concrete floor. Initial moisture contents of different treatment bales were around 10 and 20%$_{wb}$ and were stored for short (4.5 months) and long (8.5 months) term storage durations. Different storage conditions were based on some of the most-likely situations: storage of bales on the same day as harvest, left in field for some days following harvest, and when rainfall occurred before storage. Furthermore, to assess the effect of the stack heights on storage performance of different tube-wrapped bales, they were stored 2 or 3 bales high. In addition to these experimental-scale field storage tests, a stack of bales with initial moisture of around 10%$_{wb}$ was tube-wrapped and stored in a pilot-scale to study the characteristics of likely

industrial-scale storage. The qualities of stored bales were characterized by DML, temperature profiles of bales, and changes in moisture and biomass compositions, as determined by fiber and ultimate analyses, during storage.

4.4.2 MATERIALS AND METHODS

4.4.2.1 Corn stover bales used for storage

Corn (*Zea mays*) stover used in this study was harvested in the fall of 2010 with a John Deere Class 8 combine with a 12 row corn head, and was collected in a single pass from the fields located in Iowa State University research farms in Story County. The collected stover was then baled using a single pass AGCO baler. The baler was configured to make large square bales with dimensions 0.9 m high x 1.2 m wide x 2.4 m long (i.e., 3 ft high x 4 ft wide x 8 ft long); the term "bale(s)" shall indicate those dimensions throughout this paper. Biomass was harvested at two different moisture levels, with the typical values around 10 and 20%$_{wb}$. Specific values of initial moisture content for bales stored under different treatment combinations are included in table 2.

4.4.2.2 Storage of bales

Bales were stored under five different categories in this study: (1) control/baseline, (2) pre-aerated, (3) pre-wetted, (4) 3 bales high, and (5) inside a metal building. Distinguishing characteristics of each storage category are included in table 1. Bales under categories 1-4 were stored as tube-wrapped, whereas those under category 5 were stored as a stack inside a metal building. Bales were stored under these different categories within 10 days between 6 and 15 October 2010 and were sampled after short and long term storage durations. Both short and long term storage were completed within two days between 25 and 26 March 2011, and 22 and 23 June 2011, respectively. Short and long term storage durations were approximately 4.5 and 8.5 months, respectively. Total bales stored and sampled under different categories are included in table 1. It should be noted that all the stored bales were not sampled, as some were sacrificial bales and some could not be sampled due to the technical difficulties.

Table 1: Summary of different bale storage treatments investigated in this study.

Treatment ID	Initial Moisture Content ($\%_{wb}$)	#Storage Duration	Total Stored Bales	*Total Sampled Bales	Storage Categories	Description
TC 1	~20	Short	20 (2 stacks)	8	1 (Control/ Baseline)	Tube-wrapped immediately after harvest
TC 2	~20	Long	20 (2 stacks)	12		
TC 3	~20	Short	10 (1 stack)	4	2 (Pre-aerated)	Tube-wrapped after allowing to aerate in open atmosphere for 2 days after harvest
TC 4	~20	Long	10 (1 stack)	5		
TC 5	~10 (originally), ~33 (after drenching)	Long	10 (1 stack)	6	3 (Pre-wetted)	Tube-wrapped after drenching with water to simulate 60 mm rainfall immediately after harvest
TC 6	~20	Long	27 (1 stack)	5	4 (3 bales high)	Tube-wrapped 3-bales high immediately after harvest
TC 7	~20	Long	9 (1 stack)	4	5 (Inside metal building)	Stacked 3-bales high and 3-bales wide inside the metal building immediately after harvest

'Short' and 'Long' term storage durations are characterized by ~4.5 and 8.5 months, respectively
* Some bales were sacrificial bales and some could not be sampled due to technical difficulties

Under categories 1-3, bales at ~20%$_{wb}$ moisture were wrapped 2-bales high and 5-bales wide with 10 layers of 2.5×10^{-5} m (1 mil) thick plastic and were stored outdoors above the ground at Iowa State University research fields located in Boone and Story Counties for different (short and long term) storage durations. Ends of the stacks under categories 1-3 were sealed with 10.2×10^{-5} m (4 mil) thick plastic to prevent the flow of external air inside the stacks. For each stack, a vertical row of bales at each end were the sacrificial bales, leaving 6 bales in the central three vertical rows as treatment bales.

Under storage category 1, four stacks of ~20%$_{wb}$ initial moisture content bales were tube-wrapped immediately after harvest and stored for different storage durations. Storage category 1 bales were considered as the control storage treatments and were used as baseline storage scenario in this study. Among four stacks, two were sampled after short and long term storage durations and were used as stack-wise replications. The short and long term control storage stacks were designated as treatment combinations “TC 1” and “TC 2”, respectively (Table 1). Different results obtained from this storage category, as explained in section 2.3, were used as

the baseline results for the comparison of the results obtained from other storage categories. Under storage category 2, two stacks of bales at ~20%$_{wb}$ initial moisture content were tube-wrapped after allowing them to aerate in open atmosphere in research fields for 2 days after harvest. Out of two stacks, one was sampled after short term and the other after long term storage, and were designated as treatment combinations “TC 3”, “TC 4”, respectively (Table 1). This category was considered the pre-aerated bales storage treatment in this study. Bales were

pre-aerated to simulate the situations when bales could not be tube-wrapped immediately after harvest, thus, requiring temporary field-edge storage in dry (without rain) condition. Under storage category 3, six ~10%$_{wb}$ initial moisture content bales were drenched with water equivalent to 60 mm of rainfall immediately after harvest to simulate the situations when rainfall occurs before storing bales. Quantity of water was estimated based on the assumption that 60 mm rainfall will occur on the bales' surface with 2.4 m length and 1.2 m width. After drenching, average moisture contents of the bales were ~33%$_{wb}$. A stack of six drenched bales were then tube-wrapped and stored for long term and were designated as treatment combination "TC 5" (Table 1).

Under storage category 4, a stack of ~20%$_{wb}$ initial moisture content bales was tube-wrapped 3 bales high immediately after harvest and stored for long term storage duration. The main objective of this bale storage treatment was to examine the effect of stack height during tube-wrapped storage on different storage metrics. This treatment combination was designated as "TC 6" (Table 1). Category 4 bales were tube-wrapped in a similar way as in categories 1-3; however, stack size was 3 bales high and 9 bales wide. Ends of category 4 bales' stack were not sealed with extra plastic considering the three vertical rows of bales on both the sides of the stack would prevent ambient air from entering the stack. Thus, 9 bales in the central 3 vertical rows were the treatment bales, and 9 bales in 3 vertical rows at each end of the stack were the sacrificial bales.

Under storage category 5, a 3 bales high and 3 bales wide stack of ~20%$_{wb}$ initial moisture content bales was stored inside a non-insulated metal building with concrete floor immediately after harvest for long term storage duration, and was designated as "TC 7" (Table 1). All 9 bales in the stack were the treatment bales. Unlike storage categories 1-4, bales under this category were not tube-wrapped. The main objective of this bale storage treatment was to compare storage characteristics of outdoor stored tube-wrapped bales with indoor stored bales.

4.4.2.3 Pilot-scale storage of bales

A, 3 bales high and 40 bales wide, pilot-scale stack of ~10%$_{wb}$ initial moisture content bales were tube-wrapped and stored for long term. The main purpose of storing 120 bales in a pilot scale was to investigate the storage characteristics, mainly DML, during large-scale bale storage. Out of 40, 9 vertical rows of bales, beginning at the 4th and ending at the 36th row from one end of the stack, were sampled. Thus, 27 bales, in total, were sampled as treatment bales to quantify the overall storage DML for the pilot scale tube-wrapped bale storage and the variation in DML along the length of the pilot stack.

4.4.2.4 Measurements

All treatment bales were directly weighed before and after the storage using a hayrack equipped with weighing balance (Model: 640, Avery Weight-Tronix, Fairmont, MN) to determine their wet weights. The capacity of the balance was 9000 kg with tolerance of 1 kg. The dry weights of the bales were then estimated as the function of their moisture contents (wet basis) and wet weights. Additionally, initial dry densities of the stored bales were determined as the ratio of their dry weights and volumes. Volumes of the bales were determined through the physical measurements of their length, breadth and height. After weighing bales, remote single channel USB temperature data loggers (Model: USB-501, Measurement Computing, Contoocook, NH) were inserted in all the bales in central vertical row of each stack to determine

their temperature profiles throughout the storage duration. Data loggers were configured to continuously sample temperature at intervals of 20 min throughout the storage duration. After the completion of storage, collected temperature data was processed to yield daily averages.

For moisture measurement and other compositional analyses of the bales, sampling procedures were different before and after storage. For the moisture measurement before storage, around 1 kg of sample was grabbed from the end of the combine before making each bale. For other properties analyses of bales, small sample was collected from the combine in a similar way and were mixed together. After storage, a core sampler of .05 m diameter and 1 m length was used to collect three samples from top, middle and bottom of each bale. Two of the collected samples were used to determine the moisture content of each bale and one was used to determine the moisture and ash contents. For other post-storage properties analyses, samples used for moisture measurement of different bales of each treatment type (TCs 1-7, Table 1) were mixed together. After the collection of samples, moisture contents of the bales were determined as "wet basis" at the beginning and the end of feedstocks storage following the procedures of ASAE S358.2 (ASAE, 2008). Storage DML of the bales was quantified as the function of their pre and post storage weights and moisture contents.

A complete set of compositional/properties analyses were performed on the pre- and post-storage bales to fully understand the effect of storage on feedstocks properties. Different analyses included: (1) Short proximate analysis on pre-storage biomass to yield total moisture using ASTM D3173 (ASTM, 2008), ash using ASTM D3174 (ASTM, 2008) and sulfur using ASTM D4239 (ASTM, 2008), (2) Ash contents of the post-storage biomass using the National Renewable Energy Laboratory (NREL) laboratory analytical procedure (LAP) for the determination of ash in biomass (NREL, 2005), (3) ultimate analysis on pre- and post-storage biomass to yield carbon (C), hydrogen (H), nitrogen (N), total sulfur (S) and oxygen (O) (by difference) using ASTM D5373 (ASTM, 2008), and (4) chemical characterization on pre- and post- storage biomass to yield fractions of neutral detergent fiber (NDF) using AOAC 2002.04 (AOAC, 2002), and acid detergent fiber (ADF) and acid detergent lignin (ADL) using AOAC 973.18 (AOAC, 1990). The contents of cellulose and hemi-cellulose were then obtained from the values of NDF, ADF and ADL. All compositional analyses, except determination of ash content of post-storage biomass, were performed at Minnesota Valley Testing Laboratories, Inc., New Bismarck, ND. Ash contents of post-storage biomass were determined in the analytical lab in Iowa State University. Higher heating values (HHV, $MJ.kg^{-1}$) of pre- and post-stored biomass were estimated from the results of ultimate analyses using relation 1 (Sheng and Azevedo, 2005). In equation 1, C, H and O are respectively the percentages (dry basis) of carbon, hydrogen and oxygen in biomass, as determined by the ultimate analysis of the samples.

$$HHV = -1.3675 + 0.3137 \times C + 0.7009 \times H + 0.0318 \times O \quad \text{.....(1)}$$

4.4.2.5 Statistical Analysis

Statistical analysis was performed to employ Tukey-Kramer method for multiple comparisons for the simultaneous estimation of all pairwise differences of means (average DML and changes in moisture content for different bale storage treatments) in an imbalanced one-way ANOVA design at the 95% confidence interval. The analysis was done in JMP software. Statistical analysis was not performed on compositional analyses results as these tests were conducted and certified by an external lab, but were not replicated due to cost.

4.4.3 RESULTS

4.4.3.1 Physical characteristics (change in moisture content, DML and temperature profiles) of different bale storage categories

Physical characteristics of TCs 1-7 bales, including range of bale-wise dry matter stored, average initial dry densities of bales, average initial, final and changes in moisture contents of stored bales, and their average DML are summarized in table 2. Main findings for different storage categories are discussed in sections 3.1.1-3.1.5.

4.4.3.1.1 Storage Category 1: Control bale storage treatment-Bales tube-wrapped immediately after harvest (Baseline storage scenario)

For short and long term stored TC 1 and TC 2 bales, average increase in moisture contents were 5 and 8%s, respectively, and average DML were 9 and 12%, respectively (Table 2). The only difference between TCs 1 and 2 bales was their storage durations; the effect of which is reflected by an increase in the average change in moisture and DML for long term stored TC 2 bales; however, statistical multiple comparisons show that these results are not significantly different, primarily due to existing variability across the replicates of the same treatment, which was uncontrollable during field storage experiments. The initial DML (i.e., as obtained for short term stored TC 1 bales) must be pre-dominantly caused by the presence of trapped oxygen within the plastic while wrapping the bales. The presence of oxygen might have favored respiration by living cells of stored corn stover causing degradation of carbohydrates mainly into carbon dioxide, water and heat (Steele et al., 1969; Rees, 1982; McGechan, 1989; Wilcke et al., 2000). And, the increase in moisture content during storage should be due to the trapped water formed during the degradation of dry matter. Observations of temperature profiles showed that the initial temperatures of different treatment bales were around 40°C higher than the ambient temperature (Figures 1 and 2), which should be due to the heat generated during initial respiration. Furthermore, heat and water added due to the respiration might have favored fermentation and microbial activities, causing further degradation of stored dry matter (Rees, 1982; McGechan, 1989; McGechan, 1990).

Table 2: Summary of different physical properties of bales during storage

[+]Treatment ID	[^]Range of stored dry matter (kg)	[^,#]Initial bale densities (kg m^{-3}, d.b.)	[^,#]Moisture contents (%$_{wb}$)			[^,#,V]DML (%)
			Initial	Final	[*,V]Change	
TC 1	342-437	162 (10)	19 (3)	24 (4)	5 (4)^{a,b,c,d}	9 (5)^{a,b}
TC 2	330-420	165 (9)	21 (3)	29 (5)	8 (5)^{a,b}	12 (5)^{a}
TC 3	373-473	167 (18)	17 (4)	26 (1)	9 (5)^{a,b,c}	8 (8)^{a,b}
TC 4	372-457	163 (9)	18 (2)	30 (10)	12 (9)^{a}	10 (5)^{a,b}
TC 5	340-435	165 (13)	33 (4)	33 (6)	-1 (7)^{c,d}	8 (8)^{a,b}
TC 6	317-331	137 (4)	20 (2)	21 (3)	1 (2)^{b,c,d}	3 (2)^{b}
TC 7	346-368	151 (7)	17 (3)	13 (1)	-4 (3)^{d}	6 (2)^{a,b}

[+] Descriptions of different treatment IDs are included in table 1
[^] All the values are rounded to the nearest whole number
[#] Values are the average over all the sampled replications, with standard deviation in parentheses
[*] Positive values signify increase in moisture content of bales during storage
[*] Values followed by dissimilar letters are significantly different ($p<0.05$).

Further observation of the temperature profile indicated that for both TCs 1 and 2, bale temperature remained almost constantly around 40°C higher than ambient during the first month (till around mid-November 2010) and then, started to decline gradually over the next 1 month (till around mid-December 2010). After that, temperature profiles followed the ambient temperature trend over the winter months (between December 2010 and April 2011). The ambient and bales' temperatures for that duration were fluctuating between -10 and +10°C, with majority of time around and below the freezing point (0°C). Ambient temperature started to increase after short term sampling in March 2011. TC 2 bales' closely followed the ambient temperature until around 20°C, and, then the bale temperature continued to increase at a higher rate. TC 2 bales' temperature remained roughly 10°C above the ambient temperature until the completion of long term storage (Figure 2). Rees (1982) has suggested that microbial activities begin in humid storage conditions when temperature is usually about 20°C. Thus, the return of warm and humid storage conditions in the spring might have favored microbial activities within the long term stored TC 2 bales, and led to further degradation of dry matter, releasing carbon dioxide, heat and water.

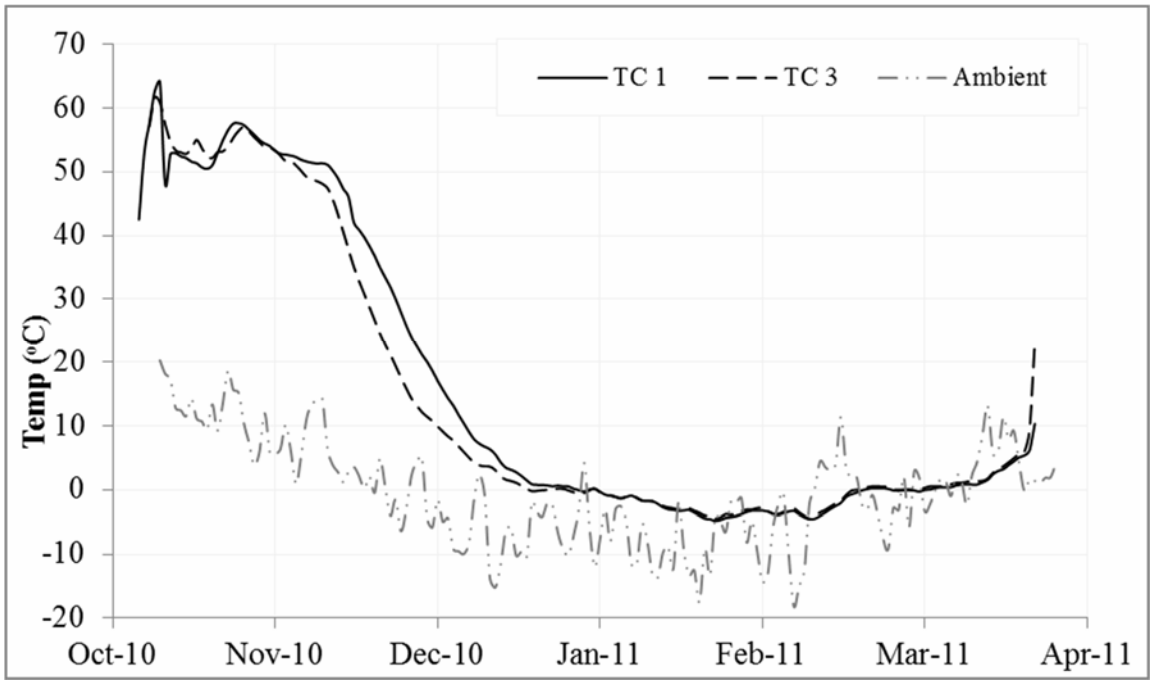

Figure 1: Temperature profiles for bales under treatment combinations TCs 1 and 3.

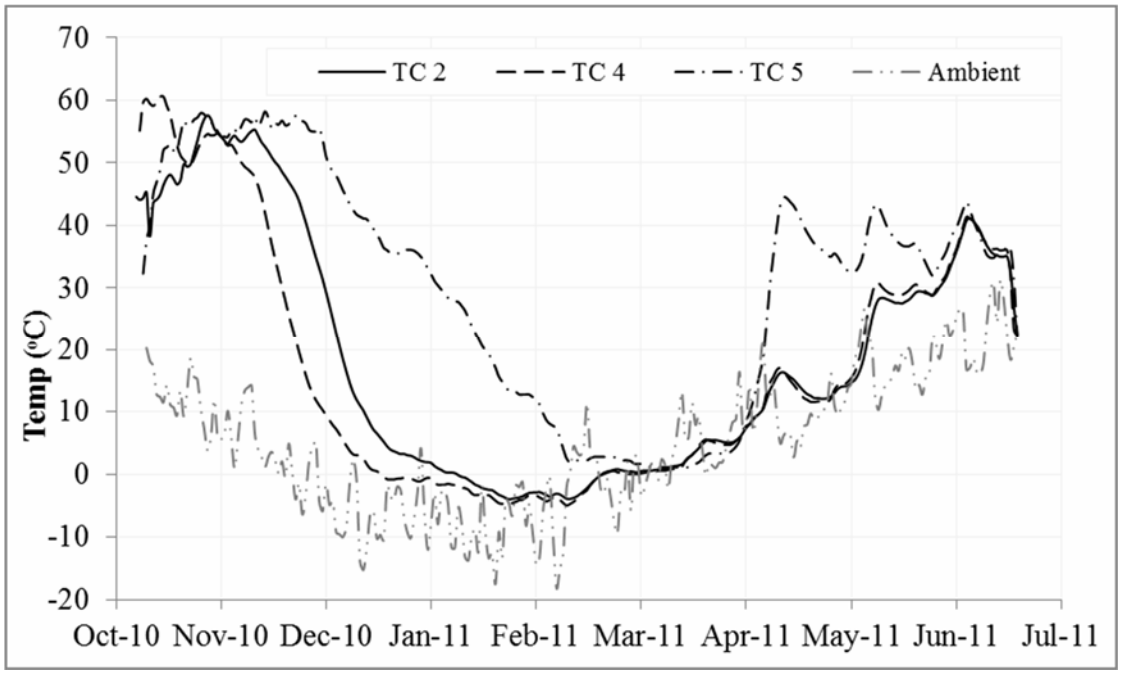

Figure 2: Temperature profiles for bales under treatment combinations TCs 2, 4 and 5.

4.4.3.1.2 Storage category 2: Pre-aerated bale storage treatment-Bales tube-wrapped after allowing them to aerate in open atmosphere for 2 days after harvest

Average DML of ~20% initial moisture bales stored for short term as TC 3 and for long term as TC 4 were 8 and 10%, respectively. In addition to DML, average moisture content of bales stored under TCs 3 and 4 increased respectively by 9 and 12%s from their initial values (Table 2). Comparing results for pre-aerated bales storage treatments (TCs 3 and 4) with non-

aerated baseline storage treatments (TCs 1 and 2) with similar initial moisture contents and storage durations show that the average DML for aerated bales storage treatment was lower by around 2% than that for non-aerated storage during both the short and long term storage; however, average increase in moisture content during storage was higher for aerated bales by around 4%. Statistically, all these results were not significantly different, due to the existing variability across replicate bales, as discussed in section 3.1.1. Earlier it was mentioned that the increase in moisture content for TCs 1 and 2 might be due to trapped water released during dry matter degradation, but in this case, in addition to the former reason, the increased moisture content might also be due to the atmospheric water absorbed and adsorbed by bales during aeration.

Observation of the final moisture content of stored bales for different treatment combinations (TCs 1-4) indicated that for this study's test conditions, tube-wrapped bales attained stability when the final moisture content of ~25 and ~30%$_{wb}$ were reached for short and long term storage durations, respectively. In addition, DML results indicated that as in control bale storage treatments (TCs 1 and 2), more than half of the total DML of aerated bales (TCs 3-4) occurred during initial phase of storage (i.e., before short term sampling) and changed slightly in the period after short term sampling. For these storage treatments, there was no statistically significant difference in DML for short and long term storage (Table 2). Shah et al. (2011) observed the similar storage DML trend for different tarp and breathable film covered single-pass corn stover bale storage tests.

Temperature profiles of short term stored pre-aerated TC 3 bales were similar to the trend of short term stored non-aerated TC 1 bales, except that after initial phase of constant temperature, rates of decline of temperature of TC 3 bales were slightly higher than those of TC 1 bales (Figure 1). The temperature profiles for long term stored pre-aerated TC 4 bales followed a similar trend as long term stored non-aerated TC 2 bales, except that temperature of TC 4 bales started to decline earlier after the initial phase of constant higher temperature (Figure 2).

4.4.3.1.3 Storage category 3: Pre-wetted bale storage treatment-Bales tube-wrapped after drenching them with water to simulate 60 mm of rain after harvest and before storage

Within storage category 3, 10%$_{wb}$ average initial moisture content bales were wetted with water to simulate around 60 mm rainfall, and were tube-wrapped and stored for long term storage duration. This bale storage treatment was designated as TC 5. After wetting, average moisture contents of TC 5 bales were 33%$_{wb}$ (Table 2). Average DML of TC 5 bales were 8%, and average post-storage moisture contents of bales were 33%$_{wb}$. Statistically, DML of pre-wetted tube-wrapped TC 5 bales were not significantly different when compared to those of long term stored control TC 2 and pre-aerated TC 4 bales; however, it should not be implied that it is always good to wet the bales before storage. Wetting bales might create a humid environment and result in higher DML (Rees, 1982). In this case, after wetting, bale moisture was around 30%$_{wb}$, which was earlier discussed to be the stabilization moisture content for different tube-wrapped bales considered in this study. This might be the reason for obtaining comparable DML for this case.

Observation of temperature profiles of TC 5 bales (Figure 2) shows that initial rise in bale temperature was similar to other bale storage treatments (TCs 1-4); however, TC 5 bales remained at an initial high temperature (~60°C) for a longer duration (~1.5 months) than other storage types, probably due to the higher heat retention capacity of wet biomass. After that, the temperature of TC 5 bales started to decline from around beginning of December 2010 when

atmospheric temperature started to fall below 0°C. Temperature declining rate for TC 5 was lower than TCs 1-4 and only followed ambient temperature between early February to late March, when the temperature was almost constantly between 0 and 5°C. After April, the temperature of bales increased to around 40°C and remained almost constant until the end of the storage duration. As bales were not stored for short term under pre-wetted storage treatment, it is hard to explain the dynamics of DML during storage.

4.4.3.1.4 Storage category 4: Three-bale high stack treatment-Tube-wrapped bales stored in higher stacks

It should be noted that all the treatments described so far (TCs 1-5) were stored in stacks 2 bales high. Storage DML and increase in moisture content for TC 6 bales were 3% and 1%s, respectively. DML for TC 6 bales were lower than the other storage treatments with equal storage durations by a magnitude of around 2 to 4 times. Only a small change in moisture content during storage indicates the reduced degradation of stored dry matter. The main reason of lower DML for TC 6 bales might be higher stack-wide compaction due to an extra height-wise layer of bales when compared to TCs 1-5. This extra layer of bale on the top might have eliminated more oxygen, creating unfavorable environment for stored biomass respiration and causing early cessation of oxygen-instigated microbial activities.

Temperature profiles for TC 6 bales (Figure 3) showed that initially the temperature increased to around 60°C (i.e., around 40°C higher than the ambient temperature), but, unlike other treatments discussed so far (TCs 1-5), temperature started to decline immediately and followed the ambient temperature within a month of the start of storage. This indicates that there might not have been a prolonged session of dry matter degradation in the start of the storage generating heat. From further observation, it can be seen that after following ambient temperature until around beginning of May 2011, temperature trends of TC 6 bales were similar to those of TC 2 bales. Some dry matter degradation might have occurred towards the end of storage during the period after May 2011 when ambient temperature started to warm up, favoring microbial activities.

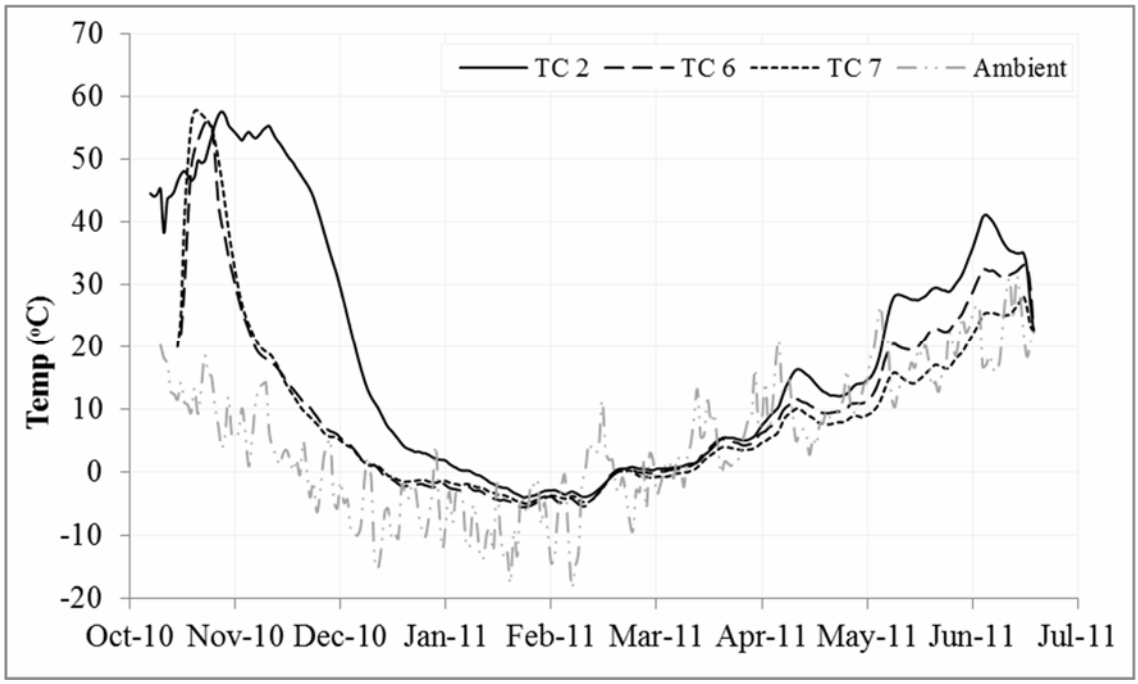

Figure 3: Temperature profiles for bales under treatment combinations TCs 2, 6 and 7.

4.4.3.1.5 Storage category 5: Indoor storage of bales

It should be noted that unlike all the treatments described so far, TC 7 bales were not tube-wrapped. Average storage DML and change in moisture content during storage were 6% and 4%s (decrease). The average DML for TC 7 was better than TCs 1-5 and comparable with TC 8; however, storage inside a metal building might not be the most economical storage option due to the higher cost of infrastructure. In contrast to different treatments discussed so far, moisture content decreased during storage for TC 7. This was due to TC 7 bales being open to the atmosphere, thus allowing originally present water in bales and water formed due to dry matter degradation to escape depending upon the surrounding and bales temperatures. Temperature profiles for TC 7 bales (Figure 3) between the start of storage and the beginning of April 2011 were similar to TC 6 bales. After April 2011, unlike TCs 1-6, TC 7 bales followed ambient temperature profile, probably due to minimal DML towards the end of storage, and more dissipation of generated heat to the ambient environment.

4.4.3.2 Pilot-scale storage of bales

Average long-term DML for all the treatment bales in the pilot stack were 4%, with standard deviation of 2%. During storage, average moisture contents of treatment bales increased by 5%s from average initial moisture of 7%$_{wb}$. DML result was comparable to that obtained for the 3 bales high storage treatment TC 6. The final moisture content of the pilot stack bales were slightly lower than the TC 6 bales, probably due to different initial moisture content of stored bales. In addition to this, range of average DML for treatment bales in different rows in the stack were 2-5%, and statistically were not significantly different. This indicates that the position of bales in the stack doesn't influence dry matter degradation during tube-wrapped storage.

4.4.3.3 Chemical characteristics (change in compositional properties) of different bale storage categories

Chemical properties of pre- and selected post-storage biomass were assessed through fiber and ultimate analyses to fully understand the effect of storage on feedstocks composition and the results are summarized in table 3. Among different bale storage treatments, post-storage chemical analyses were conducted only on TC 1, TC 2, TC 3, TC 4, and TC 7 due to cost. In originally stored biomass, dry weight percentages of cellulose, hemicellulose and ADL were 46.1, 30.3 and 6.4%, respectively. For different bales stored for long term, cellulose and hemicellulose contents decreased by around 1.1-3.6% and 2.1-5.3%, respectively; whereas ADL increased by 0.0-1.6%. Possible reasons for these changes in the contents of structural carbohydrates during storage are discussed by Shinners et al. (2009) and Wiselogel et al. (1996). Among different storage treatments, change in cellulose content was the lowest and the changes in hemi-cellulose and ADL contents were the highest for long term stored baseline scenario.

Average ash content of originally stored single-pass corn stover bales was 5.7%, which is lower than the ash content of multi-pass bales. For multi-pass bales, ash content is more than 11 wt.% (DOE, 2006). Under different long term storage treatments, ash contents of stored biomass decreased by around 0.8-1.3 wt.%. In addition to this, analysis of ultimate analysis results show that the weight percentages of C, H, N, S and O in originally stored bales were 47.1, 5.5, 0.3, 0.1 and 41.4%, respectively. Under different long term storage treatments, C decreased by 4.5-5.1 wt.%, probably due to the loss of organic matters as DML during storage (Blunk et al., 2003); however, H, N and S contents increased by less than 1 wt.%, and O content increased by 4.5-5.3 wt.%. The changes in these components did not largely differ depending upon the storage types. The HHV of originally stored biomass was 18.6 MJ kg^{-1}, and under different long term storage scenarios, it decreased by around 1.1 MJ kg^{-1}.

Back to Table of Contents

Table 3: Summary of different chemical properties of bales under investigation in this study

Bale Storage Treatments	Storage Phase	*Fiber Analysis Results (wt.%)			*Ultimate Analysis Results (wt.%)						- *HHV (MJ.kg^{-1})
		Cellulose	Hemi-Cellulose	Acid Detergent Lignin	Ash Content	C	H	N	S	O	
†Originally Stored Biomass	Before	46.1 (0.1)	30.3 (0.2)	6.4 (1.0)	5.7 (0.1)	47.1 (0.7)	5.5 (0.0)	0.3 (0.1)	0.1 (0.0)	41.4 (0.8)	18.6 (0.2)
TC1	After	42.9	26.9	6.7	5.0	43.6	6.3	0.5	0.2	44.5	18.1
	#Change	-3.2	-3.4	0.3	-0.7	-3.5	0.8	0.2	0.1	3.1	-0.5
TC 2	After	45.0	25.0	8.0	4.4	42.1	5.9	0.8	0.3	46.6	17.4
	#Change	-1.1	-5.3	1.6	-1.3	-5.0	0.4	0.4	0.2	5.3	-1.1
TC 3	After	44.3	28.5	5.3	4.6	44.5	6.4	0.5	0.2	43.8	18.5
	#Change	-1.8	-1.8	-1.1	-1.0	-2.6	0.9	0.1	0.1	2.5	-0.1
TC 4	After	43.6	28.2	7.0	4.5	42.0	6.0	0.6	0.3	46.7	17.5
	#Change	-2.5	-2.1	0.6	-1.2	-5.1	0.5	0.3	0.3	5.3	-1.1
TC 7	After	42.5	27.7	6.4	4.9	42.6	5.8	0.6	0.3	45.8	17.5
	#Change	-3.6	-2.6	0.0	-0.8	-4.5	0.3	0.2	0.3	4.5	-1.1

* All values are in dry basis

† Values are the average of two replications with standard deviation in parenthesis.

'Negative' sign indicates decrease in respective values and vice versa

4.4.4 Conclusion

Fall 2010 harvested single-pass large square corn stover bales were tube-wrapped and stored under four different storage categories for 4.5 and 8.5 months in Iowa. In addition to this, bales were stored within a metal building and in a pilot scale tube-wrapped stack for 8.5 months. Effects of different storage treatments on physical and chemical characteristics of stored bales were investigated. It was found that the average DML for different storage categories were between 3 and 12%, and was the least for outdoors stored 3-bales high tube-wrapped stack. For the pilot-scale storage, average DML of treatment bales was 4%.

Acknowledgments

This research was supported by funding from the North Central Regional Sun Grant Center at South Dakota State University through a grant provided by the US Department of Energy Office of Biomass Programs under award number DE-FG36-08GO88073.

References

AOAC Standard Methods, 1990. AOAC 973.18: Fiber (acid detergent) and lignin in animal feeds. Association of Official Analytical Chemists, Gaithersburg, Maryland.

AOAC Standard Methods, 2002. AOAC 2002.04: Gravimetric determination of amylase-treated neutral detergent fiber in feeds using refluxing in beaker or crucibles. Association of Official Analytical Chemists, Gaithersburg, Maryland.

ASAE Standards,2008. ASAE S358.2: Moisture measurement-Forages. American Society of Agricultural Engineers, St. Joseph, Michigan.

ASTM Standards, 2008. ASTM D3173: Standard test method for moisture in the analysis sample of coal and coke. ASTM International, West Conshohocken, Pennsylvania.

ASTM Standards, 2008. ASTM D3174: Standard test method for ash in the analysis sample of coal and coke from coal. ASTM International, West Conshohocken, Pennsylvania.

ASTM Standards, 2008. ASTM D4239: Standard test methods for sulfur in the analysis sample of coal and coke using high-temperature tube furnace combustion methods. ASTM International, West Conshohocken, Pennsylvania.

ASTM Standards, 2008. ASTM D5373: Standard test methods for instrumental determination of carbon, hydrogen, and nitrogen in laboratory samples of coal. ASTM International, West Conshohocken, Pennsylvania.

DOE, 2006. Biomass feedstock composition and property database. Department of Energy- Energy Efficiency and Renewable Energy, Office of the Biomass Program. Available at: http://www.afdc.energy.gov/biomass/progs/search1.cgi. Accessed online on: 12 March 2011.

DOE, 2011. U.S. Billion-Ton Update: Biomass supply for a bioenergy and bioproducts industry. R.D. Perlack and B.J. Stokes (Leads), ORNL/TM-2011/224, Oak Ridge National Laboratory, Oak Ridge, TN. 227p.

Harrigan, T.M., Rotz, C.A., 1994. Net, plastic, and twine-wrapped large round bale storage loss. Applied Engineering in Agriculture 10, 188-194.

Huhnke, R.L., 1990. Round bale wheat hay storage losses. Applied Engineering in Agriculture 6, 569-574.

McGechan, M.B., 1989. A review of losses arising during conservation of grass forage: Part 1, field losses. Journal of Agricultural Engineering Research 44, 1-21.

McGechan, M.B., 1990. A review of losses arising during conservation of grass forage: Part 2, storage losses. Journal of Agricultural Engineering Research 45, 1-30.

NREL Laboratory Analytical Procedures, 2005. NREL LAP: Determination of ash in biomass. National Renewable Energy Laboratory, Golden, Colorado.

Rees, D.V.H., 1982. A discussion of sources of dry matter loss during the process of haymaking. Journal of Agricultural Engineering Research 27, 469-479.

Sanderson, M.A., Egg, R.P., Wiselogel, A.E., 1997. Biomass losses during harvest and storage of switchgrass. Biomass and Bioenergy 12,107-114.

Shah, A., Darr, M.J., Webster, K., Hoffman, C., 2011. Outdoor storage characteristics of single-pass large square corn stover bales in Iowa. Energies 4, 1687-1695.

Sheng, C., Azevedo, J.L.T., 2005. Estimating the higher heating value of biomass fuels from basic analysis data. Biomass and Bioenergy 28, 499-507.

Shinners, K.J., 2000. Evaluation of methods to improve storage characteristics of large square bales in a humid climate. Applied Engineering in Agriculture 16, 341-350.

Shinners, K.J., Binversie, B.N., Muck, R.E., Weimer, P.J., 2007. Comparison of wet and dry corn stover harvest and storage. Biomass and Bioenergy 31, 211-221.

Shinners, K.J., Huenink, B.M., Muck, R.E., Albrecht, K.A., 2009a. Storage characteristics of large round and square alfalfa bales: Low-moisture wrapped bales. Transactions of the ASABE 52, 401-407.

Shinners, K.J., Huenink, B.M., Muck, R.E., Albrecht, K.A., 2009b. Storage characteristics of large round alfalfa bales: Dry hay. Transactions of the ASABE 52, 409-418.

Shinners, K.J., Boettcher, G.C., Muck, R.E., Weimer, P.J., Casler, M.D., 2010. Harvest and storage of two perennial grasses as biomass feedstocks. Transactions of the ASABE 53, 359-370.

Shinners, K.J., Wepner, A.D., Muck, R.E., Weimer, P.J., 2011. Aerobic and anaerobic storage of single-pass, chopped corn stover. Bioenergy Research 4, 61-75.

Steele, J.L., Saul, R.A., Hukill, W.V., 1969. Deterioration of shelled corn as measured by carbon dioxide production. Transactions of ASAE 12, 0685-0689.

USDA, 2010. Data and statistics/quick stats. United States Department of Agriculture-National Agricultural Statistics Service. Available at: http://www.nass.usda.gov/QuickStats/PullData_US.jsp. Accessed online on: 5 May 2011.

Wilcke, W.F., Gupta, P., Meronuck, R.A., Morey, R.V., 2000. Effect of changing temperature on deterioraiton of shelled corn. Transactions of the ASAE 43, 1195-1201.

Wiselogel, A.E., Agblevor, F.A., Johnson, D.K., Deutch, S., Fannell, J.A., Sanderson, M.A., 1996. Compositional changes during storage of large round switchgrass bales. Bioresource Technology 56, 103-109.

4.5 Outdoor storage characteristics of single-pass large square corn stover bales in Iowa

Ajay Shah, Matthew J. Darr, Keith Webster, and Chris Hoffman

(published in: *Energies*)

ABSTRACT

Year-round operation of biorefineries can be possible only if the continuous flow of cellulosic biomass is guaranteed. If corn (*Zea mays*) stover is the primary cellulosic biomass, it is essential to recognize that this feedstock has a short annual harvest window (≤1–2 months) and therefore cost effective storage techniques that preserve feedstock quality must be identified. This study evaluated two outdoor and one indoor storage strategies for corn stover bales in Iowa. High- and low-moisture stover bales were prepared in the fall of 2009, and stored either outdoors with two different types of cover (tarp and breathable film) or within a building for 3 or 9 months. Dry matter loss (DML), changes in moisture and biomass compositions (fiber and ultimate analyses) were determined. DML for bales stored outdoor with tarp and breathable film covers were in the ranges of 5–11 and 14–17%, respectively. More than half of the total DML occurred early during the storage. There were measurable differences in carbon, hydrogen, nitrogen, sulfur, oxygen, cellulose, hemi-cellulose and acid detergent lignin for the different storage treatments, but the changes were small and within a narrow range. For the bale storage treatments investigated, cellulose content increased by as much as 4% from an initial level of ~41%, hemicellulose content changed by −2 to 1% from ~34%, and acid detergent lignin contents increased by as much as 3% from an initial value of ~5%. Tarp covered bales stored the best in this study, but other methods, such as tube-wrapping, and economics need further investigation.

Keywords: single-pass corn stover large square bales; dry matter loss (DML); outside storage characteristics

4.5.1 INTRODUCTION

Achievement of the target set by the Energy Independence and Security Act (EISA) of 2007 to produce 60 billion liters (16 billion gallons) of cellulosic biofuels annually in the United States by 2022 will require around 200 million tons (dry) of cellulosic feedstocks each year [1]. The fact that the cellulosic feedstocks are harvested within a short span of time, usually between 1–2 months, and are required by the biorefineries over the whole year necessitates their effective and efficient storage. Different types of cellulosic feedstocks, including agricultural residues, such as corn stover and soybean (*Glycine max* L. Merr.) straw, and energy crops, such as switchgrass (*Panicum virgatum*) and miscanthus (*Miscanthus* × *giganteus*), are being stored in different ways, such as bales, piles and silos, in different parts of the United States. Collection of cellulosic biomass as bales in a single-pass is one of the options for in-field biomass collection. The single-pass collection method is advantageous compared to the multi-pass method due to their reduced ash content, and the biomass collection as bales has advantage over bulk collection due to their enhanced bulk density. In addition to these notable advantages, single-pass bales have some disadvantages, primarily the inability to control moisture content prior to harvest. This may adversely affect the bale storage characteristics. Therefore, this study focuses on the storage characteristics of large square single-pass corn stover bales in Iowa, one of the principal, Midwestern corn growing states.

Most related previous studies [2–8] were based on the storage of multi-pass bales formed with different types of biomass under different conditions and at different geographical locations. Blunk *et al.* [2] found the dry matter loss (DML) of large square rice straw bales stored under different indoor and outdoor storage treatments for a year to be in the range of 10 to 60%. Huhnke [3] found the DML of large round multi-pass wheat hay bales stored under different conditions (storage inside barn and several combinations of outdoor storage) for 10 months in Chickasha, Oklahoma to be in the range of 6.4 to 19.3%. Sanderson *et al.* [4] found the storage DML of large round bales of switchgrass stored

either outdoor unprotected above grass sod or gravel pad, or indoor above concrete for 6 and 12 months in Stephenville, Texas to be in the range of 0 to 13%. Shinners [5] investigated the storage characteristics of large square alfalfa bales under treatments with propionic acid, bacterial inoculant and formation of 0.08 or 0.12 m diameter vent hole through the bale center, and found that the storage DML didn't significantly change under any treatment, when compared to the control bales. Shinners *et al.* [6] studied the wet and dry storage characteristics of corn stover bales stored for around 9 months, at the University of Wisconsin Arlington Agricultural Research Station. They found the storage DML for wet tube-wrapped, and dry indoor and outdoor stored bales to be 2.4, 3.3 and 18.1%, respectively. Shinners *et al.* [7] investigated the storage characteristics, including DML, of large round and square alfalfa bales stored as individually and tube-wrapped. They found that the average DML of bales with initial moisture in the ranges of 30 to 40 and 40 to 55%$_{wb}$ were 3.5 and 2.3%, respectively. Shinners *et al.* [8] studied the effects of wrap types and storage methods on the preservation of large round alfalfa bales stored for 5 to 11 months, and found the DML for outdoor stored bales with different wrap types to be between 7.2 and 19.5%. Additionally, they found the DML of outdoor stored plastic covered and indoor stored bales to be 4.5 and 1.9%, respectively.

All of the studies discussed so far were based on the storage of multi-pass bales, but to meet the biorefineries' quality demands, alternative methods for feedstock storage need to be evaluated. Single-pass bales have advantages over multi-pass bales in that they have significantly lower ash levels, but to date, storage characteristics of single-pass bales have not been determined. The objective of this study was to investigate the storage characteristics of low and high moisture, single-pass corn stover bales stored either outdoors on wooden pallets and under two different types of cover [tarp or a breathable film (brand name Tyvek) through which water vapor can pass, but which does not allow liquid water to penetrate], or on a concrete floor within a metal building for short (3 months) or long (9 months) durations. The DML, changes in moisture, biomass composition (as determined by fiber and ultimate analyses and heating values during storage were investigated.

4.5.2 MATERIALS AND METHODS

4.5.2.1 Bales Used for Storage

Corn stover used in this study was harvested in the fall of 2009 with a John Deere Class 8 combine with a 12 row corn head, and was collected in a single-pass from the fields located in Iowa State University research farms in Story County. Collected stover was then baled using a single-pass AGCO baler configured to make square bales of dimensions 0.91 m high × 1.22 m wide × 2.44 m long. Bales were harvested at two moisture levels, designated as low and high, and were characterized with the typical values around 15–20 and 30–35%$_{wb}$, respectively. High and low moisture level bales were harvested and stored between 4–6 November 2009 and 14–16 November 2009, respectively.

4.5.2.2. Storage of Bales

The low- and high-moisture bales were stored for short (~3 months) and long (~9 months) time periods in three different ways: (1) outdoors covered with a tarp, (2) outdoors covered with a breathable film, or (3) indoors in a metal building. This created seven different treatment combinations (TC) as briefly described in Table 1. For TC 1 through TC 4, tarps were used to restrain the flow of water across the bales. This technique is widely used to protect biomass during outdoor storage. For TC 5 and TC 6, a breathable film, which allows for the outflow of water vapor while restraining water inflow, was used to protect the bales. This material is widely used to protect buildings during construction. Finally, for TC 7, low moisture bales were stored on a concrete floor inside a non-insulated metal building. Bales were stored in stacks of 4 (2 wide × 2 high) and 6 (3 wide × 2 high) bales; but, some of the long term stored treatment bales could not be sampled for DML determination due to the technical difficulties (Table 1). However, all bales were sampled for moisture measurement.

Table 1. Summary of different bale storage treatments

Storage Types	[#] Storage Moisture Content (%$_{wb}$)	* Storage Durations	Treatment Combination ID	Total Stored Bales	Total Sampled Bales
Storage Type 1: Outside storage with tarp cover	Low	Short	TC 1	6 (1 stack)	6
		Long	TC 2	12 (2 stacks)	9
	High	Short	TC 3	6 (1 stack)	5
		Long	TC 4	6 (1 stack)	6
Storage Type 2: Outside storage with breathable film cover	Low	Short	TC 5	6 (1 stack)	6
		Long	TC 6	12 (2 stacks)	7
Storage Type 3: Inside storage within a metal building	Low	Long	TC 7	8 (2 stacks)	7

[#] "Low" and "High" are characterized with ~15–20 and 30–35%$_{wb}$ moisture contents, respectively.
* "Short" and "Long" term storage durations are characterized by ~3 and 9 months, respectively.

4.5.2.3. Measurements

Each bale was weighed before and after storage by placing it on a hayrack equipped with a weighing balance (Avery Weigh-Tronix, LLC, Fairmont, MN, USA). The capacity of the balance was 9000 kg with tolerance of 1 kg. Dry matter loss (DML) was determined as a percentage based on the difference of the initial and final dry matter weights. Bale densities were computed by dividing the dry weight by bale volume. Following the designated storage period, bales were sampled for moisture content and compositional analyses. Approximately 1 kg of bulk stover was collected before making each bale and dried to determine moisture content [9]. For compositional analyses, small sample was collected before each bale was made and mixed together to provide approximately 10 kg of sample, in total. After each storage period, bales were torn apart, and approximately 1 kg of sample from each bale was used to determine moisture content [9]. Another kg was collected from each test bale and mixed together to provide 6 to 9 kg of sample of each treatment combination.

Storage effects on feedstock properties were evaluated using: (1) short proximate analysis to yield total moisture, ash and sulfur [10–12], (2) ultimate analysis to yield carbon (C), hydrogen (H), nitrogen (N), total sulfur (S) and oxygen (O) (by difference) [13], and (3) chemical characterization to yield fractions of neutral detergent fiber (NDF), acid detergent fiber (ADF), and acid detergent lignin (ADL) [14,15]. The contents of cellulose and hemi-cellulose were then obtained from the values of NDF, ADF and ADL. The analyses were performed at Minnesota Valley Testing Laboratories, Inc., New Bismarck, ND. Higher heating values (*HHV*) of pre- and post-stored biomass were estimated from the results of ultimate analyses using Equation 1 [16]:

$$HHV = -1.3675 + 0.3137 \times C + 0.7009 \times H + 0.0318 \times O \quad (1)$$

where, *HHV* (MJ kg^{-1}) is the higher heating value of the biomass; *C*, *H* and *O* are respectively the percentages (dry basis) of carbon, hydrogen and oxygen in biomass, as determined by ultimate analysis of the samples.

4.5.2.4. Statistical Analysis

Statistical analysis was performed to determine the least significant differences between average DML and average change in moisture contents of different treatments at the 95% confidence interval. This analysis was done using "One-Way Analysis of Variance (ANOVA)" multiple comparison method in Minitab. Statistical analysis was not performed on compositional results as these tests were conducted and certified by an external lab, but were not replicated because of cost.

4.5.3 RESULTS

4.5.3.1 Physical Characteristics of Bales Stored under Different Treatment Combinations

4.5.3.1.1. Outdoor Storage of Bales with Tarp Cover

Low moisture bales stored outdoors for short- and long-term periods with tarp cover (*i.e.*, TCs 1 and 2) had an average DML of 6 and 11%, respectively (Table 2). Comparing the average DML for the two storage treatments indicates that most of the loss occurred early, as DML for the short term (3 months) treatment (TC 1) was more than half that measured with long term (9 months) storage (TC 2) even though the short term storage duration was only 33% of long term duration. High initial dry matter degradation was pre-dominantly due to initial respiration of stored biomass [17]. Variability in DML and biomass moisture, across the replicates of same treatment was uncontrollable during field storage experiments. Therefore, statistical multiple comparison results show that average DML values were not significantly different. However, the average change in moisture was negligible for TC 1, whereas it increased by around 9 percentage units for TC 2 bales.

Table 2. Summary of physical properties of bales stored under different treatment combinations.

[+] Treatment Combination ID	[‡] Range of dry matter stored (kg)	[#,‡] Initial dry densities of stored bales (kg m^{-3})	[#,‡] Moisture Content (%$_{wb}$)			[#,‡,†] DML (%)
			Initial	Final	[*,†] Change	
TC 1	373–424	134(6)	18(4)	18(1)	−0(4) [abc]	6(2) [a]
TC 2	400–463	141(8)	15(4)	24(11)	9(14) [c]	11(4) [ab]
TC 3	369–468	134(9)	33(3)	24(1)	−10(2) [ab]	5(3) [a]
TC 4	384–437	129(7)	31(5)	17(1)	−14(5) [a]	8(5) [ab]
TC 5	392–466	137(10)	22(3)	22(3)	1(4) [bc]	14(7) [bc]
TC 6	414–574	146(9)	19(5)	29(11)	11(12) [c]	17(5) [c]
TC 7	365–458	135(9)	19(6)	16(2)	−3(6) [ab]	8(4) [ab]

[+] Descriptions of different treatment IDs included in Table 1; [‡] All values are rounded to the nearest whole number; [#] Values are the average over all the replications, with standard deviation in parentheses; * Positive values signify increase in moisture content of bales during storage; [†] Means followed by dissimilar letters are significantly different ($p < 0.05$).

High moisture bales stored under tarp cover for either short or long periods, (*i.e.*, TCs 3 and 4), had an average DML of around 5 and 8% respectively (Table 2). Statistically, these changes were not different from TC 1 and TC 2 bales. More than half the DML for high moisture, tarped bales also occurred during the first 3 months of storage. Furthermore, in contrast to low initial moisture tarped bales, high initial moisture tarped bales lost water during storage (10 and 14 percentage units, respectively), probably due to a higher rate of heating. The final moisture content of all bales stored within TCs 1–4 were in the range of 17 to 24%$_{wb}$, suggesting that for this region, that may be equilibrium moisture content for bales stored outdoors under tarp.

4.5.3.1.2. Outdoor Storage of Bales with Breathable Film Cover

Low moisture bales stored for short and long terms with breathable film cover (*i.e.*, TCs 5 and 6) had an average DML of 14 and 17%, respectively (Table 2). Like TCs 1–4, comparisons of average DML for TC 5 and 6 indicate that most dry matter degradation occurred early during storage. Average DML for low initial moisture breathable film covered bales was significantly higher than tarp covered low moisture bales stored for same storage duration. Furthermore, average changes in bale moisture for TCs 5 and 6 were similar to TC 1 and 2. Average change in bale moisture during short term storage was negligible for TC 5, whereas it increased by around 11 percentage units for TC 6 bales. Interestingly, for both TCs 5 and 6, the final bale moisture was in the range of 22 to 29%$_{wb}$, which was close to the range observed for TCs 1–4 bales.

4.5.3.1.3. Indoor Storage of Bales within Metal Building

Low initial moisture bales stored indoors for 9 months (TC 7) had an average DML of 8%, which was numerically lower than for bales with similar initial moisture content when stored outdoors under tarp or breathable film cover for same duration (TCs 2 and 6). Statistically, average DML for TC 2 and TC 7 bales was not different, but average DML for indoor storage may have been slightly lower due to enhanced protection from ambient conditions. During storage, moisture content for TC 7 bales decreased by around 3 percentage units. Furthermore, bales stored indoors had a final moisture content of 16%$_{wb}$.

4.5.3.2. Chemical Characteristics of Bales Stored under Different Treatment Combinations

Ultimate and fiber analyses based chemical properties of bales stored under different treatment combinations are summarized in Table 3. It should be noted that chemical characterization tests were performed only on different long term stored samples, and ash contents of stored biomass were not determined. However, for quantifying oxygen content in stored biomass, their ash contents were assumed to be equal to that of original biomass. Ash contents of low and high initial moisture single-pass bales were 3.1 and 2.7 wt.% (dry basis), respectively (Table 3), which are lower than ash content of multi-pass bales. Ash content of multi-pass bales can be more than 11 wt.% (dry basis) [18].

Percentage of C, H, N, S and O in originally stored low and high initial moisture bales were almost same, and were around 46, 5.8, 0.5, 0.06 and 44.7 wt.%, respectively (Table 3). For bales stored under different treatment combinations, changes in different ultimate analytes were almost the same. For different treatment combinations, changes in C, H, N, S and O were 3.3–3.7% (decrease), 0.3–0.4% (increase), 0.1–0.4% (increase), 0.06% (decrease), and 2.7–3.2% (increase).

Back to Table of Contents

Table 3. Summary of chemical properties of bales stored under different treatment combinations.

Storage Type	Storage Phase	* Ultimate Analysis Results (wt.%)						* HHV (MJ kg^{-1})	* Fiber Analysis Results (wt.%)		
		Ash Content	C	H	N	S	$^{\Delta}$O		Cellulose	Hemi-Cellulose	Lignin
Originally stored, Low moisture biomass	~~Before~~	~~3.1~~	~~45.8~~	~~5.8~~	~~0.5~~	~~0.06~~	~~44.7~~	~~18.5~~	~~41.9~~	~~35.1~~	~~3.7~~
Originally stored, High moisture biomass	~~Before~~	~~2.7~~	~~46.4~~	~~5.8~~	~~0.5~~	~~0.06~~	~~44.6~~	~~18.7~~	~~41.5~~	~~32.9~~	~~5.3~~
	After	† ND	42.2	6.2	0.7	0.00	47.8	17.7	41.3	35.9	5.3
Tarp-covered, low moisture, long term stored	$^{\#}$ Change	-	−3.7	0.4	0.2	−0.06	3.1	−0.8	−0.5	0.8	1.5
	After	ND	42.8	6.1	0.7	0.00	47.6	17.8	45.4	32.7	6.9
Tarp-covered, high moisture, long term stored	$^{\#}$ Change	-	−3.6	0.3	0.1	−0.06	3.1	−0.9	3.9	−0.1	1.6
	After	ND	42.1	6.1	0.8	0.00	47.8	17.6	42.3	33.7	6.5
Breathable film-covered, low moisture, long term stored	$^{\#}$ Change	-	−3.7	0.3	0.4	−0.06	3.2	−0.9	0.4	−1.4	2.8
	After	ND	42.5	6.2	0.8	0.00	47.4	17.8	42.1	35.1	5.3
Indoor storage, low moisture, long term stored	$^{\#}$ Change	-	−3.3	0.4	0.3	−0.06	2.7	−0.7	0.3	0.0	1.6

* All values are in dry basis; $^{\#}$ "Negative" sign indicates decrease in respective values and *vice versa*; † "ND" refers to "Not Determined"; $^{\Delta}$ Although ash content was not determined for stored bales, for the estimation of oxygen content by difference in post storage biomass, ash content of stored biomass was taken same as the original biomass.

Furthermore, the initial HHVs for low and high initial moisture bales were 18.5 and 18.7 MJ kg^{-1}, respectively (Table 3). For bales stored under different treatment combinations, cellulose increased by around 4 wt.% for high initial moisture bales whereas changed negligibly for low moisture bales. Hemicellulose content changed in either direction, and ranged between increase by 0.8 wt.% to decrease by 1.4 wt.%. For different storage treatments, ADL content increased by 1.5–2.8 wt.%, probably due to their higher resistance to biological degradation. HHV of stored biomass decreased by 0.7–0.9 MJ kg^{-1}.

4.5.4. CONCLUSIONS

Interactions between initial moisture content, and type and duration of storage on physical and chemical characteristics of corn stover bales were investigated. Covering with tarp preserved bales better than breathable film during outdoor storage in Iowa. For investigated storage treatments, more than half of total dry matter degradation occurred early in the storage. Additionally, changes in biomass compositions (ultimate and fiber analyses) were within a narrow range for different storage treatments. Although tarp preserved bales stored well in this study, other methods for outdoor bale storage, such as tube-wrapping, should be investigated. Furthermore, for the overall success of baled corn stover supply chain, economic feasibility of different storage methods should be evaluated.

ACKNOWLEGEMENTS

This research was supported by funding from the North Central Regional Sun Grant Center at South Dakota State University through a grant provided by the US Department of Energy Office of Biomass Programs under award number DE-FG36-08GO88073.

REFERENCES

1. Biomass Research and Development Initiative. *Increasing Feedstock Production for Biofuels: Economic Drivers, Environmental Implications, and the Role of Research*; Biomass Research and Development Board: Washington, DC, USA, 2003.
2. Blunk, S.L.; Yore, M.W.; Summers, M.D.; Lau, G.K.; Tang, S.T.; Jenkins, B.M. *Quality and Property Changes in Rice Straw during Long Term Storage*; ASAE Paper No. 036091; American Society of Agricultural and Biological Engineers: St. Joseph, MI, USA, 2003.
3. Huhnke, R.L. Round bale wheat hay storage losses. *Appl. Eng. Agric.* **1990**, *6*, 569–574.
4. Sanderson, M.A.; Egg, R.P.; Wiselogel, A.E. Biomass losses during harvest and storage of switchgrass. *Biomass Bioenergy* **1997**, *12*, 107–114.
5. Shinners, K.J. Evaluation of methods to improve storage characteristics of large square bales in a humid climate. *Appl. Eng. Agric.* **2000**, *16*, 341–350.
6. Shinners, K.J.; Binversie, B.N.; Muck, R.E.; Weimer, P.J. Comparison of wet and dry corn stover harvest and storage. *Biomass Bioenergy* **2007**, *31*, 211–221.
7. Shinners, K.J.; Binversie, B.N.; Muck, R.E.; Albrecht, K.A. Storage characteristics of large round and square alfalfa bales: Low-moisture wrapped bales. *Trans. ASABE* **2009**, *52*, 401–407.
8. Shinners, K.J.; Binversie, B.N.; Muck, R.E.; Albrecht, K.A. Storage characteristics of large round alfalfa bales: Dry hay. *Trans. ASABE* **2009**, *52*, 409–418.

9. ASAE Standard S358.2. *Moisture Measurement-Forages*; American Society of Agricultural Engineers: St. Joseph, MI, USA, 2008.
10. ASTM Standard D3173. *Standard Test Method for Moisture in the Analysis Sample of Coal and Coke*; ASTM International: West Conshohocken, PA, USA, 2008.
11. ASTM Standard D3174. *Standard Test Method for Ash in the Analysis Sample of Coal and Coke from Coal*; ASTM International: West Conshohocken, PA, USA, 2008.
12. ASTM Standard D4239. *Standard Test Methods for Sulfur in the Analysis Sample of Coal and Coke Using High-Temperature Tube Furnace Combustion Methods*; ASTM International: West Conshohocken, PA, USA, 2008.
13. ASTM Standard D5373. *Standard Test Methods for Instrumental Determination of Carbon, Hydrogen, and Nitrogen in Laboratory Samples of Coal*; ASTM International: West Conshohocken, PA, USA, 2008.
14. AOAC Standard 973.18. *Fiber (Acid Detergent) and Lignin in Animal Feeds*; Association of Official Analytical Chemists: Gaithersburg, MD, USA, 1990.
15. AOAC Standard 2002.04. *Gravimetric Determination of Amylase-Treated Neutral Detergent Fiber in Feeds Using Refluxing in Beaker or Crucibles*; Association of Official Analytical Chemists: Gaithersburg, MD, USA, 2002.
16. Sheng, C.; Azevedo, J.L.T. Estimating the higher heating value of biomass fuels from basic analysis data. *Biomass Bioenergy* **2005**, *28*, 499–507.
17. Rees, D.V.H. A discussion of sources of dry matter loss during the process of haymaking. *J. Agric. Eng. Res.* **1982**, *27*, 469–479.
18. U.S. Department of Energy (DOE). *Biomass Feedstock Composition and Property Database*; Technical Report from U.S. Department of Energy, Office of Energy Efficiency and
Renewable Energy, Biomass Program, 2006. DOE: Washington, DC, USA. Available online: http://www.afdc.energy.gov/biomass/progs/search1.cgi (accessed on 12 March 2011).

© 2011 by the authors; licensee MDPI, Basel, Switzerland. This article is an open access article distributed under the terms and conditions of the Creative Commons Attribution license (http://creativecommons.org/licenses/by/3.0/).

CHAPTER 5

TECHNO-ECONOMIC AND LOGISTICAL BENEFITS OF UPGRADING BIOMASS VIA TORREFACTION AND PYROLYSIS

5.1 Background

Short harvest windows, variable initial moisture contents, storage dry matter loss (DML), low bulk and energy densities, low bulk flowability, and non-uniformity among the feedstock types are several of the main impeding factors in the establishment of a sustainable biomass feedstock supply system. Among other options, torrefaction and fast pyrolysis are the two methods of upgrading biomass to manage some of the logistical issues of raw biomass. Torrefaction, also referred to as mild-pyrolysis, is a thermochemical pretreatment of biomass, where hemicellulose degrades to form volatiles, mainly permanent gases and condensables. During the torrefaction process, biomass is retained in an inert atmosphere at some pre-defined temperature (usually 200 to 300°C) for a specific duration (usually 5 to 120 min) to yield solid torrefied biomass, mainly composed of cellulose and lignin with reduced moisture content, enhanced energy density, improved hydrophobicity and microbial degradation resistance, and increased brittleness. Fast pyrolysis is the rapid thermal decomposition of organic compounds in the absence of oxygen and at moderate temperatures (400-600°C) to produce liquids (bio-oil), solids (biochar) and non-condensable gases. Residence times for fast pyrolysis of biomass is shorter (0.5-2 s) which is followed by rapid cooling and condensation of the formed pyrolysis vapors.

5.2 Objective and Specific Tasks

This chapter addresses the fourth specific objective of this project which was to quantify the techno-economic and logistical benefits of generating high energy density biomass products from torrefaction and pyrolysis oil production at satellite pre-conversion facilities. This specific objective was accomplished through a set of tasks:

1. Determine the optimal torrefaction temperature and residence times for corn stover biomass based on moisture content and corn stover fraction as measured by energy density gains.
    a. Details of this task is addressed in Sections 5.4-5.6 of this chapter. Sections 5.4 and 5.6 have been published in the peer-reviewed journals '*Fuel*' and '*Biofuels Bioproducts & Biorefining*', respectively. Section 5.5 has been submitted for peer-review and publication to a journal.

2. Determine the impact of post storage biomass chemical composition on bio-oil yield from fast pyrolysis.
    a. Details of this task are addressed in Section 5.7 of this chapter which is drafted in the form of a peer-reviewed journal article and is currently under internal review.

5.3 Overall Impacts of study

Two thermochemical processes, torrefaction and pyrolysis, show particularly high potential for on-farm densification of biomass energy. Although both increase processing energy

use at the point of biomass production, they offer the potential to recoup this energy through reduced storage infrastructure, reduced transportation energy and reduced preprocessing energy use at the biorefinery. Optimizing the process variables for torrefaction and pyrolysis oil development will lead to insight into the key characteristics affecting the scalability of torrefaction and pyrolysis to on-farm practice at typical harvest throughput rates.

5.4 Effects of torrefaction process parameters on biomass feedstock upgrading

Dorde Medic, Matthew J. Darr, Ajay Shah, Benjamin Potter and Jeffrey Zimmerman

(published in: *Fuel*)

ABSTRACT

Biomass is a primary source of renewable carbon that can be utilized as a feedstock for biofuels or biochemicals production in order to achieve energy independence. The low bulk density, high moisture content, degradation during storage and low energy density of raw lignocellulosic biomass are all significant challenges in supplying agricultural residues as a cellulosic feedstock. Torrefaction is a thermochemical process conducted in the temperature range between 200 and 300°C under an inert atmosphere which is currently being considered as a biomass pretreatment. Competitiveness and quality of biofuels and biochemicals may be significantly increased by incorporating torrefaction early in the production chain while further optimization of the process might enable its autothermal operation. In this study, torrefaction process parameters were investigated in order to improve biomass energy density and reduce its moisture content. The biomass of choice (corn stover) was torrefied at three moisture content levels (30, 45 and 50%), three different temperatures (200, 250 and 300°C), and three unique reaction times (10, 20 and 30min). Solid, gaseous, and liquid products were analyzed, and the mass and energy balance of the reaction was quantified. An overall increase in energy density (2-19%) and decrease in mass and energy yield (3-45% and 1-35% respectively) was observed with the increase in process temperature. Mass and energy losses also increased with an increase in the initial biomass moisture content.

Keywords. Biomass; corn stover; torrefaction; pretreatment.

5.4.1 INTRODUCTION

Energy has always played an important role in life, survival, and the development of mankind. Even though it has been superseded by other more potent fossil energy sources during the last 200 years, biomass has played a major role in supplying energy since the beginning of civilization and still plays an important role in economies of developing countries. Biomass recently has received renewed attention worldwide, mainly as a consequence of high and volatile oil prices and global climate changes caused by increased fossil fuel consumption. Moreover, rapid economic growth in developing countries, high dependence on global and local transportation, pollution, depletion of sources, and endangered national security of energy importing countries have raised the awareness of the need for non-fossil based renewable energy sources [1-3]. Among renewable energy sources, such as wind, solar, geothermal, wave, tidal and ocean thermal, biomass is the most likely short term energy source with mature and readily applicable conversion technologies for the production of transportation compatible liquid fuels. Although in the long term other forms of renewable energy may supersede biomass it will still remain as the only source of renewable carbon needed for chemicals and synthetic materials production.

According to the Renewable Fuel Standard (RFS) from the Energy Independence and Security Act of 2007, the minimum annual quantity of renewable fuel in the US transportation sector should be increased from 9 billion in 2008 to 36 billion in 2022, where after 2016 most of

renewable fuel must be advanced biofuel derived from cellulosic feedstocks instead of food crops [4]. In order to sustain production demanded by the RFS significant amounts of lignocellulosic biomass has to be collected, stored, and converted into biofuels.

The low bulk density, high moisture content, and low energy density of biomass feedstocks have a negative effect on the feasibility of long distance feedstock transportation. Moreover, in order to supply a feedstock for continuous operation of biorefineries year round, biomass has to be collected from large and often distant areas and hauled either to local storage facilities or to a refinery where it would be stored until conversion. Unfavorable physical properties of biomass dictate utilization of large storage facilities, which would further compromise economical use of biomass feedstock. In addition, storing such large amount of wet biomass will further increase expenses through the high rate of dry matter loss due to microbial activity and the hazard of self-heating/combustion [5-8].

Thermochemical conversion technologies, such as pyrolysis, gasification and hydrothermal processing, along with biomass co-firing in existing coal power plants, might have an important role in the production of heat energy, advanced energy carriers, chemicals, solvents, and materials. However, all aforementioned technologies have strict demands regarding the physical condition of biomass feedstocks such as particle size and shape which are conducive to optimal processing. Additionally the final end product characteristics and yield are also influenced by feedstock quality and composition [2]. Moreover, due to the recalcitrant nature of biomass it is difficult to grind in a continuous and cost effective manner [7]. Heterogeneity of feedstocks can also influence refinery operation considering not only different types of biomass, for example demolition wood, agricultural residues, and dedicated energy crops, or different plant species, but also the same plant species grown in different areas [9, 10].

Torrefaction, sometimes also referred to as mild-pyrolysis, is a thermochemical process conducted in the temperature range between 200 and 300°C under an inert atmosphere and low heating rate. Torrefaction is currently being considered as a biomass feedstock pretreatment particularly for thermal conversion systems. During torrefaction various permanent gases and condensables, with high oxygen content, are formed mainly due to hemicellulose degradation. As a consequence the final solid product, so called torrefied biomass, will be composed mainly of cellulose and lignin and characterized by increased brittleness, hydrophobicity, microbial degradation resistance, and energy density. Thus torrefaction can play a significant role in decreasing transportation and storage costs of biomass in the large quantities needed to sustain biofuels production. In addition, torrefaction may have positive effect on pyrolysis, gasification, and co-firing units operation by lowering power consumption and cost for biomass grinding, eliminating compounds responsible for high acidity of pyrolysis oil, and by increasing the uniformity of biomass feedstocks [9-12].

About 30 years ago, the process of torrefaction was first utilized and operated commercially for the production of a reducing agent for the metallurgical industry, but since then it has received little attention. There have been several studies that investigated the effects of torrefaction on biomass properties and the composition of different fractions released during the process, but the majority of these have focused on dry woody biomass which was finely ground before torrefaction. These experiments were conducted by utilizing either thermogravimetric analysis equipment (TGA) or small scale reactors [7, 10, 13, 14]. Since agricultural residues will play an important role in the production of advanced biofuels more research is needed to investigate the optimum torrefaction conditions for such feedstock.

The potential for torrefaction of agricultural residues immediately after harvest without drying and before significant size reduction should be investigated in order to incorporate torrefaction early in the supply chain and maximize the benefit of the physical property changes induced through torrefaction. In this research the influence of torrefaction reaction time, temperature, and moisture content on the quantity and composition of torrefied corn stover was investigated. Quantitative and qualitative data from the analysis of solids, permanent gases, and condensable volatiles were used to investigate mass and energy flows in the torrefaction process. A Box-Behnken design of experiments was utilized in this research in order to statistically model the torrefaction process in terms of mass and energy yields and evaluate the significance of temperature, time, and untreated corn stover moisture content as predictors of response variables. The results from this work will provide knowledge not only related to the influence of process parameters (time and temperature) but also the effect of moisture content of an untreated feedstock on the torrefied biomass characteristics.

5.4.2 MATERIALS AND METHODS

5.4.2.1 Samples

Corn stover samples, harvested during the fall 2009, were obtained from Department of Agricultural and Biosystems Engineering at Iowa State University, Ames, Iowa. Corn stover biomass is a highly available agricultural residue in the Midwest and has been proposed as a feedstock for advanced biofuels production. After harvest samples were stored in a cooling chamber at 3-5°C to prevent feedstock degradation and minimize moisture loss.

Field harvested corn stover at 22 and 41% moisture content were selected as the medium and high test moisture levels. Additional corn stover was dried to provide a suitable low moisture test level. The size of samples was reduced in a hammer mill equipped with 25 mm screen.

5.4.2.2 Torrefaction Reactor

Torrefaction experiments were conducted in 2 liters stainless steel fixed bed reactor with 0.1m diameter and 0.25m height, heated by three ceramic heaters in close contact with the reactor wall and separately controlled by PID controllers. This setup was used for coarse control of temperature, while fine temperature management was performed through circulation of preheated nitrogen gas. Figure 1 shows the position of four thermocouples inside the torrefaction reactor used for the temperature control. Thermocouples were immersed in the biomass at four different heights (0.05, 0.1, 0.15 and 0.2m from the bottom of reactor). They were positioned along the circumference (diameter of 0.08m and origin at the axis of reactor) and shifted by 90° as shown in Figure 1, top view. Nitrogen purge gas was used for maintaining an inert atmosphere during the experiments. For each experiment 4.5 L min^{-1} (0.000075 m^3 s^{-1}) of nitrogen was purged through the reactor. Outlet tubing was maintained at an elevated temperature of about 200°C to prevent condensation of released volatiles.

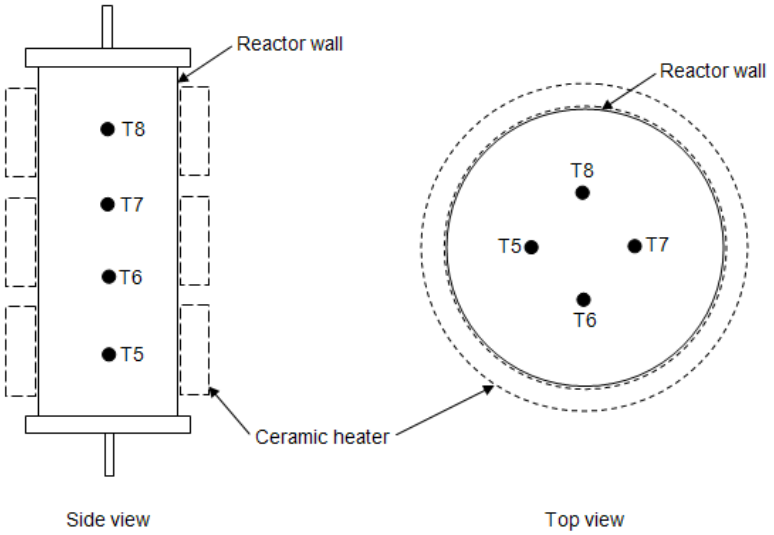

Figure 1. Position of four thermocouples (T5, T6, T7 and T8) utilized for controlling the temperature inside the reactor (not to scale)

For the purpose of comprehensively characterizing the torrefaction of corn stover the final torrefied solid product was recovered from the process and analyzed while the volatiles released during the process as torrefaction gas were first separated into permanent gases and condensable volatiles (liquid) and then analyzed separately.

5.4.2.3 Gas Analysis

Volatiles and permanent gases released from the process were cooled immediately following release from the reactor by means of glass impingers submerged in an ice bath. This facilitated removing the majority of the condensables and water from the gas sample. The remaining permanent gasses were then passed through desiccant columns before they were analyzed by a Varian 490-GC micro-gas chromatograph (Varian, Palo Alto, CA) equipped with a Molsieve 5A and Poraplot U columns.

5.4.2.4 Liquids Analysis

Liquid fractions developed during the torrefaction process and collected in glass impingers were stored in the cooling chamber at 3-5°C until they were analyzed. The water content in the condensed phase was analyzed according to the Karl-Fischer method by a moisture titrator (KEM MKS-500, Kyoto Electronics, Tokyo, Japan) and ASTM E 203–08 standard method [15]. Quantitative and qualitative analysis of organics present in condensed phase was conducted by a gas chromatograph equipped with Restek Stabilwax-DA column (Varian, Palo Alto, CA).

5.4.2.5 Proximate Analysis

Torrefied biomass samples were analyzed in a thermogravimetric analyzer TGA/DSC Star System (Mettler Toledo) according to a modified ASTM D 5142–04 method, in order to

determine the content of moisture, volatiles, ash and fixed carbon [16]. Analysis was done under an inert atmosphere, obtained by purging nitrogen gas at flow rate of 100mL/min. Initially samples were heated to 105°C at the heating rate of 10°C/min. After retaining the samples at 105°C for 40min, these were further heated at the rate of 10°C/min to 900°C, and maintained at this temperature for 20min. Subsequently the environment was changed to oxidative by purging 100mL/min of air for 30min. The moisture content is determined by the mass loss after the heating period at 105°C. Mass evolved between 105°C and 900°C represented volatile content, while the remaining was the fixed carbon content. The remaining after heating the sample in oxidative atmosphere at 900°C was considered to be ash.

5.4.2.6 Ultimate Analysis

Ultimate analysis of the solid fraction was done with PerkinElmer 2400 Series II CHNS/O Analyzer (PerkinElmer, Waltham, MA), according to ASTM D 5373–08 method [17]. Biomass samples were dried in an oven at 103°C for 24 h before the ultimate analysis was conducted. Combustion was conducted at 925°C under a helium atmosphere, while reduction was conducted at 650°C.

5.4.2.7 High Heating Value Determination

The higher heating value of raw and torrefied biomass samples was computed using Equation 1 developed by Sheng and Azevedo [18].

$$HHV\ (MJ/kg) = -1.3675 + 0.3137 * C + 0.7009 * H + 0.0318 * O \quad (1)$$

Where: C=percentage of carbon in biomass as determined by ultimate analysis; H= percentage of hydrogen in biomass as determined by ultimate analysis; O=percentage of oxygen determined by difference on dry and ash free basis, i.e. O (db, ash free)=100-C-H-N.

5.4.2.8 Design of Experiments

The set of torrefaction experiments conducted to meet the objectives of this project were based on a Box-Behnken experimental design, which is a three level design based on the combination of a two level factorial design and incomplete block design. It is useful for statistical modeling and optimization of a response variable of interest, which is a function of three or more independent variables. Moreover, Box Behnken designs allow estimating coefficients in a second degree polynomial regression and modeling of a quadratic response surface. The response surface can be further used for process optimization, identification of maximum or minimum responses, and significance of each involved factor or their combination. Furthermore, response surfaces can be used for calculating responses not only at experimentally investigated points, but also at any point on the surface [19-21]. Three factor-three level Box Behnken design, with 5 replicates at the center point and 17 runs in total was used in the experiments (Table 1). JMP statistical package from SAS (SAS Institute, Cary, NC) was used for the statistical analysis of experimental data.

Table 1. Box Behnken experimental design matrix generated by JMP

No.	Pattern	Moisture	Temperature	Time
1	− −0	3	200	20
2	− 0−	3	250	10
3	− 0 +	3	250	30
4	− + 0	3	300	20
5	0 − −	22	200	10
6	0 − +	22	200	30
7	0 0 0	22	250	20
8	0 0 0	22	250	20
9	0 0 0	22	250	20
10	0 0 0	22	250	20
11	0 0 0	22	250	20
12	0 + −	22	300	10
13	0 + +	22	300	30
14	+ − 0	41	200	20
15	+ 0 −	41	250	10
16	+ 0 +	41	250	30
17	+ + 0	41	300	20

5.4.3 RESUTLS AND DISCUSSION

Process time and temperature were defined such that the torrefaction process temperature was the average of temperatures measured by four thermocouples within the torrefaction reactor during the experiment. The torrefaction start time was measured from the point when the temperature first reached the temperature proposed by the experimental design. Figure 2 depicts an average temperature profile for one of the experiments at 250°C.

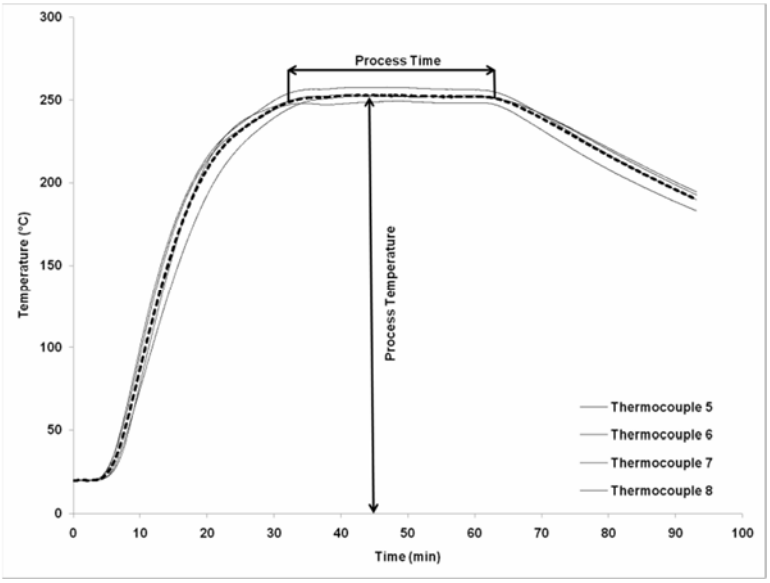

Figure 2. Temperature profiles for four thermocouples and average temperature profile (denoted by dashed line) used to determine process temperature and time

Mass balances for the torrefaction process were computed based on the results from the solid, liquid and gas analysis, and expressed on dry basis in the Table 2. Mass balances for torrefaction experiments conducted at low temperatures proved accurate regardless of moisture content and time. However, at 300°C errors in mass balance occurred mainly due to the lower yield of directly weighable torrefied solids, and an increased yield of volatiles that condensed throughout the exhaust system and were hard to recover completely. Additionally, a high amount of aerosols formed at this temperature would require either electrostatic precipitators or filters to accurately account for their mass.

Table 2. Total mass balance for torrefaction experiments

Sample ID	Raw Biomass	Process Parameters		Torrefied Biomass	Yield of Condensables	Yield of Permanent
	Moisture Content (%)	Temp. (°C)	Time (min)	Yield (%)	(%)	Gases (%)
3-200-20	3.2	200	20	97.1	0.02	0.4
3-250-10	3.2	250	10	86.6	1.79	1.1
3-250-30	3.2	250	30	84.4	4.07	1.4
3-300-20	3.2	300	20	57.4	13.30	2.7
22-200-10	22.1	200	10	98.1	0.39	0.5
22-200-30	22.1	200	30	98.4	0.40	0.6
22-250-20	22.1	250	20	86.2	4.32	1.3
22-250-20	22.1	250	20	85.3	4.37	1.3
22-250-20	22.1	250	20	83.4	4.39	1.5
22-250-20	22.1	250	20	83.5	4.26	1.4
22-250-20	22.1	250	20	83.4	4.09	1.4
22-300-10	22.1	300	10	58.0	11.52	2.0
22-300-30	22.1	300	30	53.9	18.39	3.3
41-200-20	41.0	200	20	91.2	0.66	0.6
41-250-10	41.0	250	10	80.0	3.79	1.2
41-250-30	41.0	250	30	78.7	6.11	1.3
41-300-20	41.0	300	20	56.3	18.59	2.9

There was an overall trend towards a decrease in yield of solids and increase in yield of permanent gases and condensable products as both temperature and reaction time increased (Table 2). Loss in solids was much more pronounced between 250 and 300°C, than between 200 and 250°C, regardless of moisture content of samples. This was likely due to higher reactivity or more extensive devolatilization and decarbonization of hemicellulose fraction above 250°C. Along with degradation of hemicellulose, initial reactions of cellulose decomposition might occur in this temperature regime, as proposed in other research [22]. The same trend was observed for the yield of condensables and permanent gases. However, at 300°C, regardless of moisture content in raw feedstock, yield of condensables was much higher than yield of permanent gases, which might be evidence of more intensive decomposition of not only hemicellulose, but also other polymer fractions. This would support the production of heavier compounds responsible for tar formation observed in condensed phase during the experiments. There was an evident influence of moisture content on loss in mass yield at 250°C and especially

at 200°C, where mass loss of samples with 45% moisture content was 3 times higher than that of samples with 3 and 22% moisture content in raw biomass (Figure 3).

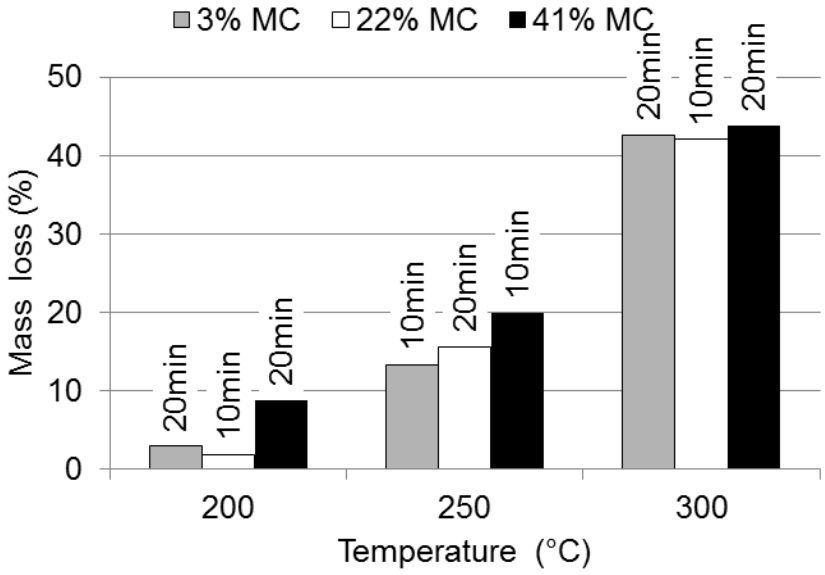

Figure 3. The effect of untreated biomass moisture content on mass loss of torrefied samples.

This interaction of mass loss and moisture content of the feedstock has not previously been reported in scientific journals and is of high importance for designing a commercial scale torrefaction system. A possible reason for this might be the expansion of water vapor inside the plant polymer matrix during the ramping stage of biomass heating. This expansion will loosen the material and make it less resistive to heat transfer. Since water has a higher heat conduction coefficient than both air and nitrogen it will enhance heat transfer in samples with high moisture content. Prins [23] has proposed that at heating rates lower than 50°C/min the parameter that restricts torrefaction reaction is reaction kinetics rather than heat transfer through the particle. Nevertheless, this might not be true since the particle size in these experiments were relatively large and representative of a real agricultural residue feedstock.

Moreover, since a packed bed reactor was used in this project a higher specific heat of water vapor than nitrogen gas might increase the amount of heat delivered to the zones closer to the top of reactor and enhance degradation of biomass. Another cause might be probability of close contact between released acids with biomass structural polymers, especially hemicellulose, as a result of increased specific area caused by expansion of water vapor. According to Huber et al. [24], short chain organic acids may act as a catalyst, thus promoting mainly hemicellulose degradation at this reaction condition, but also to a lesser extent, degradation of other polymers. As a consequence of a more aggressive environment during the processing of high moisture biomass, milder conditions (temperature/time) might be used to achieve the same effect as in the case of lower moisture content biomass torrefied at more extreme conditions. Nevertheless, there was almost no difference between mass losses of different samples at the most extreme time/temperature combinations regardless of sample moisture content. This might be due to accelerated thermal degradation of cellulose and lignin, in this temperature zone, after the total amount of hemicellulose was decomposed at lower temperatures, which would ultimately eliminate any initial difference between the samples.

Experimentally obtained mass loss data were analyzed using JMP statistical software and fitted into response surface quadratic model. The reduced model, containing only significant terms is shown in Equation 2.

$$\text{Predicted Mass Loss} = 95.68 - 1.0396*\text{Temperature} + 0.2491*\text{Moisture} + 0.00284*(\text{Temperature})^2 \quad (2)$$

Where: Temperature = °C and Moisture = wt%db.

The summary of fit and analysis of variance are included in Table 3 and Table 4 respectively. As can be seen from Table 3 the mass loss response surface model is in good agreement with actual data obtained in experiments.

Table 3. Summary statistics for the mass loss response surface model with three predictors: moisture, temperature and time

R^2	0.993
R^2 adjusted	0.985
Root Mean Square Error	1.807

Table 4. ANOVA for the mass loss response surface model with three predictors: moisture, temperature and time

Source	DF	Sum of	Mean	F Ratio	Prob. > F
Model	9	3465.10	385.01	117.82	<0.0001*
Error	7	22.87	3.268		
Corrected	16	3487.97			

* Significant

According to the model, temperature, moisture, and temperature squared were the only significant parameters (Table 5). The strength of effect of two significant process parameters on the dry matter mass loss is better revealed by surface plot in Figure 4. The effect of the moisture content of the raw biomass on dry matter loss is depicted in the plot by the more pronounced curvature in the temperature region below approximately 260°C and moisture content above about 20%.

Table 5. List of all terms used to obtain mass loss and energy yield models and their respective *p*– values

	Mass loss model	Energy yield model
Term	Prob.>|t|	Prob.>|t|
Intercept	< 0.0001*	< 0.0001*
Time	0.1964	0.3783
Temperature	< 0.0001*	< 0.0001*
Moisture	0.0069*	0.0025*
Time*Temperature	0.2630	0.4481
Time*Moisture	0.8106	0.8937
Temperature*Moisture	0.2260	0.4481
$(Time)^2$	0.8546	0.6227
$(Temperature)^2$	< 0.0001*	0.0002*
$(Moisture)^2$	0.0848	0.0211*

*Significant terms (as determined by JMP statistical package)

As revealed by Figure 5, water represents the largest portion of condensables released during the torrefaction process, followed by acetic acid, furfural, methanol, and hydroxyacetone in much smaller quantities. The water represented in Figure 5 is only reaction water and does not include water associated with the initial moisture content of the biomass. Water is formed in the process of polymer dehydration through the release of hydroxyl groups while acetic acid and methanol are formed from acetoxy and methoxy groups attached to hemicellulose sugar monomers and lignin. Other compounds are generated at high temperatures by thermal decomposition of plant polymer monomers [11].

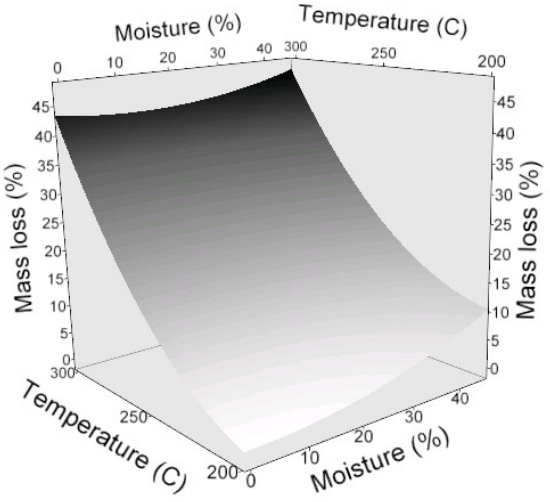

Figure 4. Surface plot of the effect of temperature and moisture content of raw biomass on predicted mass loss (time = 20min)

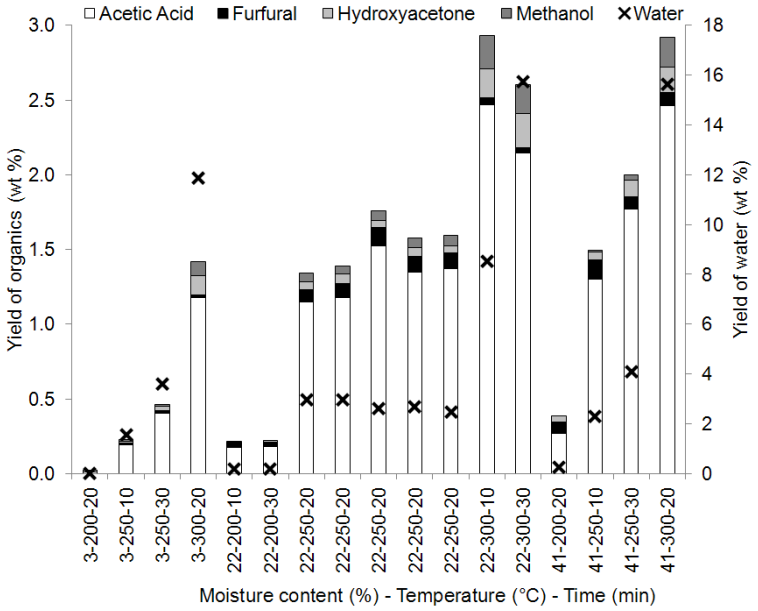

Figure 5. Composition of condensable volatiles released during torrefaction (The amount of water produced in torrefaction reaction and condensed together with organics was determined as a difference between the total water content in condensable phase and initial biomass moisture content. Only the reaction water is shown in Figure 5.)

As can be seen in Figure 5, the amount of condensables released during torrefaction of biomass samples with initial moisture content of 22 and 41% are not significantly different. However, they are two times higher than in the case of torrefaction of samples with 3% initial moisture content.

Figure 6 shows the composition of permanent gas phase released during the torrefaction of biomass with different initial moisture contents and at various combinations of process parameters. In Figure 6, only carbon monoxide and carbon dioxide are shown, since these are the main gas components even though traces of methane and hydrogen are present at high reaction temperature.

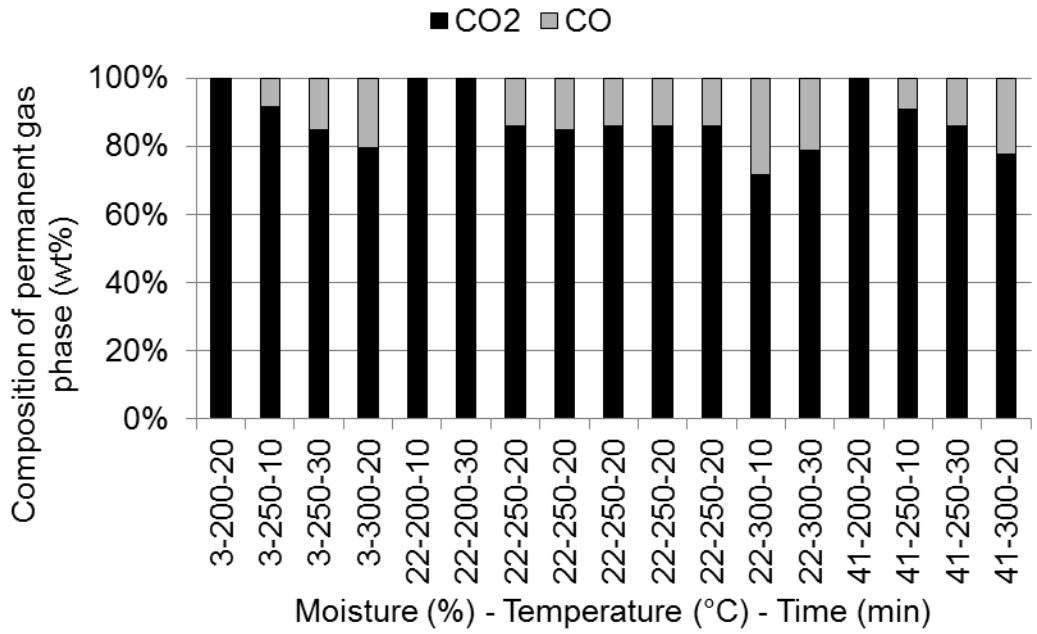

Figure 6. Change in permanent gas composition with process parameters and raw biomass moisture content

As can be seen in Figure 6, the ratio of carbon monoxide and carbon dioxide increases with the increase in both temperature and time. This is different from the influence of time on mass yield which does not have a significant effect. The composition of the permanent gas phase is not affected significantly by moisture content in raw feedstock. Production of carbon dioxide during the process might be explained by decarboxilation of acid groups attached to hemicellulose, while carbon monoxide may be produced in the reaction of carbon dioxide and steam with char at high temperatures [25].

Figure 7 shows the results of the proximate analysis of corn stover torrefied at different treatment conditions. As can be seen in Figure 7, temperature has the strongest effect on torrefied biomass composition. Moreover, as the temperature increases the amount of fixed carbon follows the same trend and rises from about 1.5 up to 3 times, at 250°C and 300°C respectively, relative to untreated biomass. This is a consequence of the more extensive removal of hydrogen and oxygen from biomass, although some carbon will be released in the form of hydrocarbons. There is a trend in the reduction of volatiles content by about 30% at the highest temperature as a result of aforementioned changes in biomass composition. This torrefied material will produce less organic compounds and aerosols during combustion and has a higher heating value. Water content of torrefied corn stover determined during proximate analysis was water adsorbed by biomass while it was waiting for the analysis in the TGA's auto-sampler.

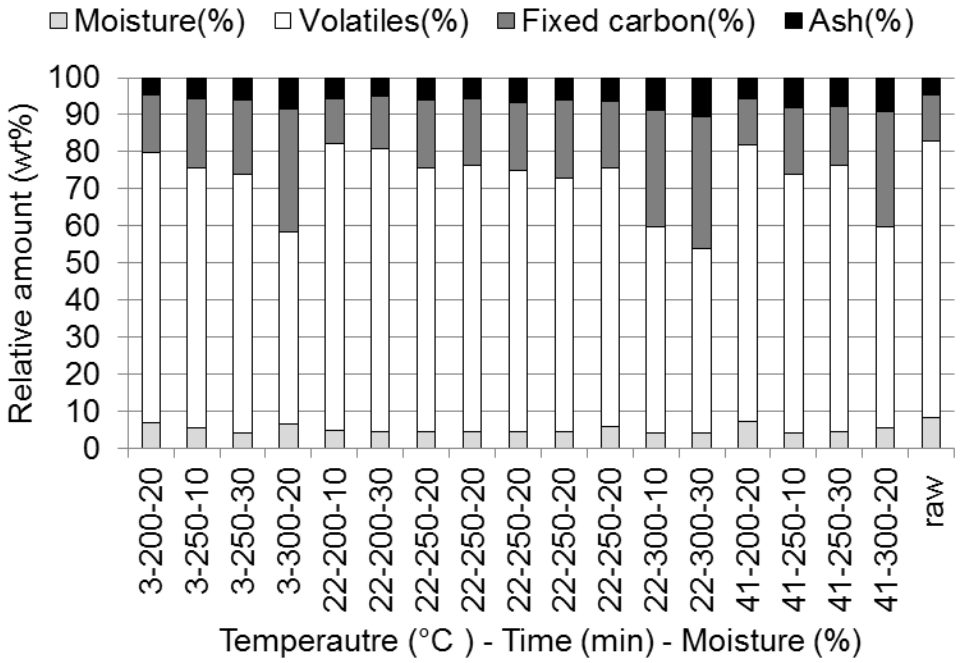

Figure 7. Proximate analysis of torrefied and raw corn stover

Torrefaction increases the amount of atomic carbon while decreasing the amount of atomic hydrogen and oxygen as shown in Table 6. A consequence of this change in the chemical composition was a decrease in the atomic O/C and H/C ratio of torrefied biomass in comparison to raw biomass. This is due to the release of volatiles rich in hydrogen and oxygen, such as water and carbon dioxide. The decrease in O/C, regardless of the moisture content in the raw biomass, can be up to about 7, 15 and 45% at 200, 250 and 300°C respectively. This change in the chemical composition of biomass will improve its quality as an energy source through an increase in energy density since more oxygen than carbon is lost in the form of volatiles.

Table 6. Ultimate analysis and computed energy density of torrefied samples[a]

Sample	C	H	N	O[b]	HHV[c]
3-200-20	45.8	5.5	0.5	48.2	18.4
3-250-10	47.7	5.3	0.6	46.4	18.8
3-250-30	49.1	5.4	0.6	45.0	19.2
3-300-20	58.7	4.7	0.7	35.8	21.5
22-200-10	45.7	5.7	0.7	47.9	18.5
22-200-30	45.8	5.5	0.6	48.1	18.4
22-250-20	49.1	5.4	0.7	44.8	19.2
22-250-20	48.3	5.5	0.6	45.6	19.1
22-250-20	49.2	5.4	0.7	44.7	19.3
22-250-20	49.4	5.4	0.6	44.5	19.3
22-250-20	48.7	5.4	0.6	45.3	19.1
22-300-10	56.6	4.9	0.9	37.6	21.0
22-300-30	59.0	4.7	1.0	35.4	21.6
41-200-20	45.6	5.4	1.0	48.0	18.2
41-250-10	48.2	5.3	0.9	45.6	18.9
41-250-30	48.8	5.2	0.9	45.1	19.0
41-300-20	55.8	4.8	1.1	38.2	20.8
Raw	44.2	5.8	0.5	49.5	18.2

[a]Sulfur levels for all analyzed samples were at levels lower than analyzer's precision level and were discarded as uncertain.
[b]Determined by difference
[c] Calculated

Another important characteristic of torrefied corn stover is its increase in energy density when compared to raw biomass. This is the result of a decrease in mass of torrefied samples through the release of compounds rich in oxygen and hydrogen. It can be seen in Figure 8 that temperature has strongest impact on energy density of torrefied biomass, while the effect of time and moisture is much less expressed.

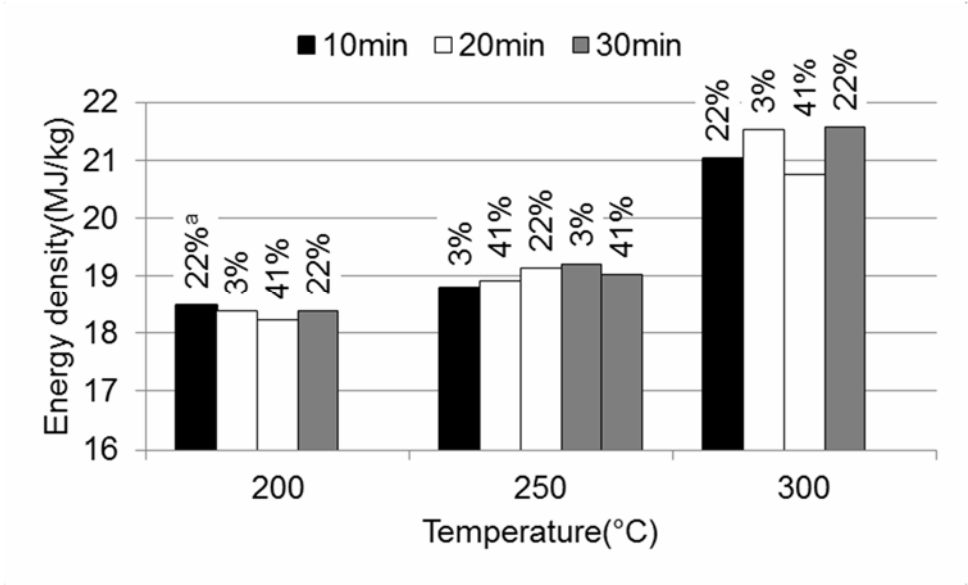

Figure 8. Effect of process parameters and raw biomass moisture content on energy density of torrefied material

Energy yield per dry raw biomass indicates the total energy preserved in the torrefied biomass. It was computed from mass yield and higher heating values using Equation 3 and expressed as a percentage of energy content of untreated dry biomass.

$$E_{yield}\ (\%) = (m_{torrefied} / m_{initial})_{dry\ basis} \times (E_{torrefied} / E_{initial})_{dry\ basis} \quad (3)$$

Where: $m_{torrefied}$ = mass of biomass feedstock measured after torrefaction expressed on dry basis; $m_{initial}$ = mass of untreated (raw) biomass feedstock measured before torrefaction expressed on dry basis; $E_{torrefied}$ = specific energy content of biomass feedstock after torrefaction expressed on dry basis; $E_{initial\text{-}dry\ basis}$ = specific energy content of biomass feedstock before torrefaction expressed on dry basis

Energy yields computed using Equation 3 are shown in Figure 9.

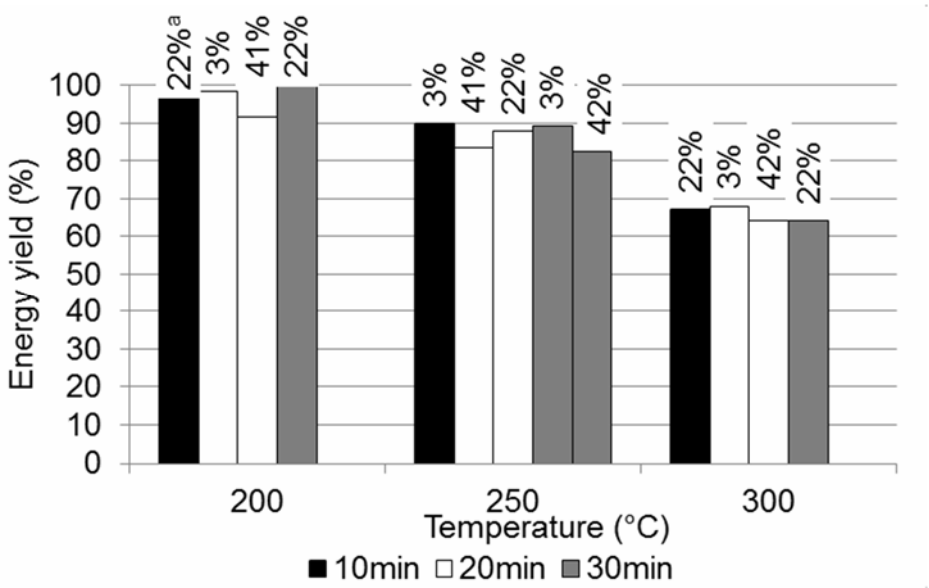

Figure 9. Effect of process parameters and initial moisture content of untreated biomass on energy yield ([a]raw biomass moisture content on a wet basis)

These values were fitted to response surface model represented by Equation 4, in order to analyze the effect of process parameters on energy yield.

$$\text{Predicted Energy Yield} = 10.0379 - 0.0144*\text{Moisture} + 0.9278*\text{Temperature} - 0.00721*(\text{Moisture})^2 - 0.002461*(\text{Temperature})^2 \quad (4)$$

Where: Temperature = °C and Moisture = wt%db.

As shown in Table 7 and Table 8, the model (Equation 4) was in good correlation with the actual data as justified by relatively high R^2 values (a measure of the amount of deviation around mean explained by the model). The small p-value in the ANOVA indicates high model significance.

Table 7. Summary statistics for the energy yield response surface model with three predictors: moisture, temperature and time

R^2	0.989
R^2 adjusted	0.977
Root Mean Square Error	1.804

Table 8. ANOVA for the for the energy yield response surface model with three predictors: moisture, temperature, and time

Source	DF	Sum of	Mean Square	F Ratio	Prob. > F
Model	9	2253.06	250.341	76.88	< 0.0001*
Error	7	22.79	3.256		
Corrected	16	2275.86			

*Significant

In this model (Equation 4) the significant parameters are temperature, temperature squared, moisture and moisture squared (Table 5). As revealed in Figure 10, biomass torrefied at

lower temperatures has the highest energy yield, which was expected since this parameter was strongly dependant on mass yield which was significantly affected by process temperature. Moisture has much less influence on energy yield than temperature as seen in Figure 10.

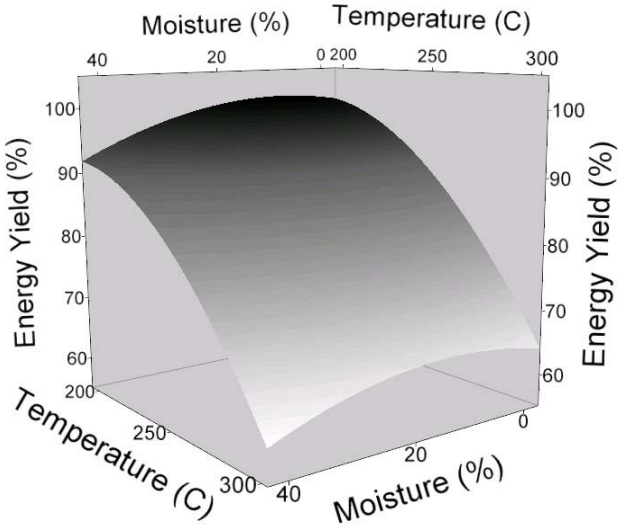

Figure 10. Surface plot of the effect of temperature and moisture content of raw biomass on predicted energy yield (time = 20min)

However, the initial moisture content induced up to 10% more energy loss at temperatures below 220°C and raw biomass moisture content higher than 20%. This was correlated with mass loss and was justified by the similar contour plot curvature in Figure 4. Moreover, as displayed in Figure 10, moisture had a stronger influence on energy yield than on mass loss, even at 300°C. This might be due to the loosening effect of water on fibrous matrix, its role in polymer hydrolysis, and formation of organic acids that promotes more extensive cellulose and lignin degradation through high energy volatile compounds, such as tar.

5.4.4 CONCLUSIONS

Corn stover undergoes changes in chemical composition, mass, and energy content during the torrefaction process. As expected these changes were more extensive at high temperatures and characterized by mass loss of up to 45% as well as a decrease in the O/C ratio from 1.11 to 0.6 and an increase in the energy density of about 19%. However, high mass loss offset gain in energy density and significantly reduced overall energy yield. Moisture content had a significant effect on energy density, mass and energy yield, and generally induced a reduction in each of these parameters. Moreover, the effect of moisture is more pronounced at lower temperatures, where if moisture content in raw biomass is increased from 22% to 44%, energy yield could be reduced by about 10%. Nevertheless, there is a raw biomass moisture content window between 3% and approximately 20% that can allow for the use of corn stover feedstock directly from the field without any negative effect on energy yield.

Despite inevitable losses in energy yield during the process, additional research in the future might justify the use of torrefaction as a biomass pretreatment or upgrading step, by obtaining data that will prove savings in torrefied biomass particle size reduction, improvements

in storage stability, hydrophobicity, and chemical properties important for thermochemical processes, such as pyrolysis, gasification, and co-firing.

ACKNOWLEDGEMENTS

Funding for this project was provided by the ConocoPhillips Company. Additional technical support was provided by CSET (Center for Sustainable Energy, Iowa State University, Ames) and BCRF (Biocentury Research Farm, Iowa State University, Ames). We would like to thank Andy Suby, Samuel Jones, Patrick Johnston and Marge Rover for their contribution to this work.

REFERENCES

1. Demirbas A. Biofuels. London: Springer; 2009.
2. Klass D. L. Biomass for Renewable Energy, Fuels and Chemicals. San Diego: Academic Press; 1998.
3. WEC, World Energy and Climate Policy: 2009 Assessment. 2009, World Energy Council: London, UK.
4. The Energy Independence and Security Act of 2007, Pub. L. No. 110-40 H.R. 6, 121 Stat. 1492 (January 7. 2007)
5. BRDI, Roadmap for Bioenergy and Biobased Products in the United States. Biomass Research and Development Initiative, October 2007.
6. Bridgeman T. G., Jones J. M., Shield I., Williams P.T. Torrefaction of reed canary grass, wheat straw and willow to enhance solid fuel qualities and combustion properties. Fuel 2008;87:844-56.
7. Arias B., Pevida C., Fermoso J., Plaza M. G., Rubeira F., Pis J. J. Influence of torrefaction on the grindability and reactivity of woody biomass. Fuel Processing Technology 2008;89:169-75.
8. Lipinsky E. S., Arcate J. R., Reed T. B. Enhanced Wood Fuels via Torrefaction. Inovative Thinking, Inc.: Fuel Chemistry Division Preprints 2002;47:408-10.
9. Yan W., Acharjee T. C., Coronella C. J., Vaquez R. V. Thermal Pretreatment of Lignocellulosic Biomass. Environmental Progress and Sustainable Energy 2009;28:435-40.
10. Bergman P. C. A., Boersma A. R., Zwart R. W. R., Kiel J.H.A. Torrefaction for Biomass Co-firing in Existing Coal-Fired Power Stations, The Netherlands: ECN: Petten; 2005.
11. Prins M. J., Ptasinski K. J., Janssen F. J. J.G. Torrefaction of wood. Part 2. Analysis of products, J Anal Appl Pyrol 2006;77:35-40.
12. Bergman P. C. A. Combined Torrefaction and Pelletization: The TOP Process, The Netherlands: ECN: Petten; 2005.
13. Couhert C., Salvador S., Commandre J-M. Impact of torrefaction on sygas production from wood. Fuel 2009;88:2286-90.
14. Prins M. J., Ptasinski K. J., Janssen F. J. J.G. Torrefaction of wood. Part 1. Weight Loss Kinetics, J Anal Appl Pyrol 2006;77:28-34.
15. ASTM E 203 – 08: Standard Test Method for Water Using Volumetric Karl Fischer Titration. 2008, ASTM Standards, Vol. 15.05.
16. ASTM D 5142 – 04: Standard Test Method for Proximate Analysis of the Analysis Sample of Coal And Coke by Instrumental Procedures. 2008, ASTM Standards, Vol. 05.06.

17. ASTM D 5373 – 08: Standard Test Method for Instrumental Determination of Carbon, Hydrogen and Nitrogen in Laboratory samples of Coal. 2008, ASTM Standards, Vol. 05.06.
18. Sheng C., Azevedo J. L. T. Estimating the higher heating value of biomass fuels from basic analysis data. Biomass Bioenerg 2005;28:499-507.
19. Box G. E. P., Behnken D. W. Some New Three Level Design for the Study of Quantitative Variables. Tehcnometrics 1960;2:455-75.
20. Carlborn K., Matuana L. M. Modeling and Optimization of Formaldehyde-Free Wood Composites Using a Box-Behnken Design. Polym Composites 2006;27:497-503.
21. Muthukumar M., Mohan D., Rajendran M. Optimization of Mix Properties of Mineral Aggregates Using Box Behnken Design of Experiments. Cement Concrete Comp 2003;25:751-8.
22. Koukious E. G., Mavrokoukoulakis J., Abatzoglou N. Energy densification of biomass. Proceedings of 1st. National Conference on Soft Energy Forms; 1982; Thessaloniki, Greece.
23. Prins M. J. Thermodynamic analysis of biomass gasification and torrefaction. The Netherlands: Technische Universiteit Eindhoven: Eindhoven; 2005
24. Huber G. W., Iborra S., Corma A. Synthesis of Transportation Fuels from Biomass: Chemistry, Catalysis and Engineering. Chem Rev 2006;106:4044-98.
25. White R. H., Dietenberger M. A. Wood Products: thermal degradation and fire. In: Buchow K. H. J., Cahn R. W., Flemings M. C., Ilschner B., Kramer E. J., Mahajan S. ,editors. The Encyclopedia of Materials: Science and Technology. Amsterdam, the Netherlands: Elsevier; 2001.

5.5 Water vapor adsorption of thermally treated lignocellulosic biomass

Dorde Medic, Matthew J. Darr, Ajay Shah and Sarah Rahn

(submitted for peer-review and publication to a journal)

ABSTRACT

The equilibrium moisture content (EMC) of biomass affects transportation, storage, downstream feedstock processing, and the overall economy of biorenewables production. Torrefaction is a thermochemical process conducted in the temperature regime between 200 and 300°C under an inert atmosphere that, among other benefits, aims to reduce the innate hydrophilicity and susceptibility to microbial degradation of biomass. The objective of this study was to examine water sorption properties of torrefied corn stover. The EMC of raw corn stover, along with corn stover thermally pretreated at three temperatures, was measured using the static gravimetric method at equilibrium relative humidity (ERH) and temperature ranging from 10 to 98% and from 10 to 40°C, respectively. Five isotherms were fitted to the experimental data to obtain the prediction equation which best describes the relationship between the ERH and the EMC of lignocellulosic biomass. Microbial degradation of the samples was tested at 97% ERH and 30°C. Fiber analyses were conducted on all samples. In general, torrefied biomass showed an EMC lower than that of raw biomass, which implied an increase in hydrophobicity. The modified Oswin model performed best in describing the correlation between ERH and EMC. Corn stover torrefied at 250 and 300°C had negligible dry matter mass loss due to microbial degradation. Fiber analysis showed a significant decrease in hemicellulose content with the increase in pretreatment temperature, which might be the reason for the hydrophobic nature of torrefied biomass. The outcomes of this work can be used for torrefaction process optimization, and decision-making regarding raw and torrefied biomass storage and downstream processing.

Keywords: equilibrium moisture content, torrefaction, microbial degradation, corn stover, hydrophobicity

5.5.1 INTRODUCTION

Lignocellulosic biomass has recently gained renewed attention in developed countries as a sustainable, abundant, and readily available energy and carbon source. Furthermore, public concern about the negative environmental impacts of fossil fuels use, energy dependence on foreign petroleum, and volatile oil prices have promoted the use of biomass feedstock in energy, fuel, and chemical production. Biomass has characteristics distinct from traditional, fossil energy/carbon sources that make its application more costly and complex than traditional fossil fuels. A number of factors increase the cost of biorenewables production, including the high oxygen content of biomass and products derived from it, the low energy and bulk density of biomass, a recalcitrant and heterogeneous nature, and high moisture content[1]. Unlike other unfavorable biomass characteristics, high moisture content is the parameter that affects multiple steps in a biorenewables production chain, such as transportation, storage, and upgrading of lignocellulosic biomass. Moisture increases the cost of transportation by increasing the amount of superfluous material that has to be transported[2]. Dry matter loss of wet biomass can be up to 30% depending on pretreatment and storage type, which increases overall production cost[1,3]. Furthermore, storage of large quantities of high moisture biomass represents a fire hazard due to

spontaneous ignition[4,5]. The energy requirement for size reduction increases significantly as a consequence of the increase in moisture content of biomass[6,7]. Gasification of high moisture feedstock causes an increase in tar yield, a decrease in thermal efficiency of the system, and a decrease in operation temperature[8]. Moisture increases char yield and has a mixed effect on bio-oil yield and composition, depending on temperature and mineral matter content[9]. Moreover, the high water content decreases the heating value of biomass, causes ignition issues, demands large process equipment to handle large flue gas volume, and affects the overall combustion quality[10].

Equilibrium moisture content (EMC) is established when the moisture content of material in question is in thermodynamic equilibrium with the relative humidity of the surrounding atmosphere at a particular temperature and pressure[11]. Therefore, change in the relative humidity of the environment affects the moisture content of any biological material at constant pressure and temperature[7]. The relationship between the EMC and the equilibrium relative humidity (ERH) at a constant temperature is expressed by moisture sorption isotherms[12]. The shape of isotherms gives insight into the mechanism of water sorption and depends on structure and composition of material, in addition to pressure and temperature[13]. Understanding the relationship between EMC and ERH helps in designing drying, combustion, and thermochemical conversion systems; making decisions regarding storage methods for different biomass types; and improving product quality in general[14].

More than 270 models have been used in the literature to predict water vapor sorption characteristics in materials of biological origin. According to Van der Berg and Bruin[15], these models can be broadly classified into three categories: theoretical, semi-empirical, and empirical. Theoretical models are based on a monolayer/multilayer sorption and a condensed film, and employ constants that have physical meaning. This is the opposite of empirical models, whose constants are not related to material properties[16]. Moreover, there is no single model that is capable of representing sorption behavior of every biological material over a wide range of temperatures and relative humidity levels[17]. Five isotherm equations: modified Henderson, modified Chung-Pfost, modified Halsey, modified Oswin and Guggenheim-Anderson-deBoer (GAB) are accepted by the American Society of Agricultural and Biological engineers as standard models for describing the relationship between the ERH and the EMC of agricultural products[18].

Torrefaction is a thermochemical process conducted in the temperature range between 200 and 300°C under an inert atmosphere and low heating rate. It is currently being considered as a biomass feedstock pretreatment, particularly for thermal conversion systems. The final solid product, referred to as torrefied biomass, is composed mainly of cellulose and lignin. It is characterized by increased brittleness, hydrophobicity, microbial degradation resistance, and energy density. Thus, torrefaction can play a significant role in decreasing the costs of transportation and storage of biomass in the large quantities needed to sustain biofuels production[6,19].

A lot of research on the EMC-ERH relationship has been dedicated to fruits and vegetables, dairy, forage, grain, agricultural residues, and wood[20-25]. Several researchers investigated the water sorption of charcoal, coals, and activated carbon[26-28]. However, there have been only a few studies that investigated water adsorption properties of torrefied biomass[19,29].

The objective of this work was to assess the hydrophobic nature of thermally treated biomass. Therefore, water adsorption characteristics of raw and torrefied corn stover were determined experimentally at four temperatures and five relative humidity levels. In addition, the suitability of five models for fitting ASABE accepted isotherms was evaluated. A microbial

degradation test was conducted to assess dry matter loss due to microbial growth at high ERH. Furthermore, fiber analysis test was performed to explain the lower water vapor adsorption onto torrefied corn stover.

5.5.2 MATERIALS AND METHODS

5.5.2.1 Sample preparation

Corn stover biomass was harvested in the fall 2010 from Iowa State University research fields located in Story County, IA. The bulk wet samples were stored in a cooling chamber at a temperature below 5°C to preserve their original qualities and to prevent the microbial degradation.

Subsamples of the wet material were dried at 60°C for 72h and stored in a desiccator until torrefaction or water vapor sorption experiments were conducted. The moisture content of samples before and after experiments was determined according to the ASAE standard for forage moisture measurement D358.2[30]. All samples were ground and sifted before experiments to obtain physically uniform samples with a particle size less than 2mm. Ground corn stover biomass was torrefied at 200, 250 and 300°C according to the method employed by Medic and co-workers[31] with the modifications that all samples were dried before the processing and were torrefied for 20 minutes.

5.5.2.2 Water vapor adsorption experiments

The EMC of biomass was determined at 10, 20, 30 and 40°C using the static gravimetric method[32]. For this, 2g (0.0001g resolution) of samples were spread in a thin layer in Petri dishes and placed in hygrostats, which were sealed plastic containers. Duplicates of raw corn stover, and corn stover samples torrefied at 200, 250 and 300°C were set in each hygrostat. Five saturated solutions of inorganic salts were used to control the ERH in the hygrostats as shown in Table 1[33].

Table 1. ERH of saturated solutions at four temperature levels

		ERH (decimal)			
Salt	Chemical formula	10°C	20°C	30°C	40°C
Lithium chloride	LiCl	0.113	0.113	0.113	0.112
Magnesium chloride	$MgCl_2$	0.335	0.331	0.324	0.316
Magnesium nitrate	$Mg(NO_3)_2$	0.574	0.544	0.514	0.484
Sodium chloride	NaCl	0.757	0.755	0.751	0.747
Potassium sulfate	K_2SO_4	0.982	0.976	0.970	0.964

All salts were reagent grade (Fischer Scientific, Pittsburgh, PA). Solutions were prepared at 50°C with excess salt to ensure a saturation condition. Remote data loggers to continuously measure and record temperature and relative humidity (HOBO U23 Pro v2, Onset Computer Corporation, Pocasset, MA) were placed in each hygrostat. An incubator with refrigeration capability (Isotemp incubator, Fischer Scientific, Pittsburgh, PA) was utilized to maintain different temperature levels (± 1°C) during experiments. Samples EMC were assumed to be in equilibrium with the ERH when there was no difference (≤ 0.001g) in three subsequent weight measurements. Tukey-Kramer Honestly Significant Difference procedure, available in JMP pro

9 statistical package (SAS Institute, Cary, CA) was used for pairwise comparison of all EMC means.

5.5.2.3 Adsorption modeling

Relationships between ERH and EMC of raw and torrefied corn stover at four different temperatures and five different ERH levels were determined by fitting the experimental data using five isotherm models (Equations 1-5) suggested in ASAE standard D245.6[18]. The GAB model is used in its adapted form to account for temperature influence[34,11].

1. Modified Henderson model:

$$EMC = \left[\frac{\ln(1-ERH)}{-A\cdot(t+B)}\right]^{\frac{1}{C}} \quad \text{.....(1)}$$

2. Modified Chung-Pfost model:

$$EMC = -\frac{1}{C}\ln\left[\frac{\ln(ERH)\,(t+B)}{-A}\right] \quad \text{.....(2)}$$

3. Modified Halsey model:

$$EMC = \left[\frac{-\exp(A+B\cdot t)}{\ln(ERH)}\right]^{\frac{1}{C}} \quad \text{.....(3)}$$

4. Modified Oswin model:

$$EMC = (A + B\cdot t)\left[\frac{ERH}{1-ERH}\right]^{\frac{1}{C}} \quad \text{.....(4)}$$

5. Modified GAB (Guggenheim-Anderson-deBoer) model:

$$EMC = \frac{A\cdot B_0\cdot C_0\cdot ERH}{(1-B_0\cdot ERH)(1-B_0\cdot ERH+B_0\cdot C_0\cdot ERH)} \quad \text{.....(5)}$$

$$B_0 = B\cdot\exp\left(\frac{H_1}{R\cdot T}\right)$$

$$C_0 = C\cdot\exp\left(\frac{H_2}{R\cdot T}\right)$$

where:

EMC = equilibrium moisture content ($\%_{db}$)
ERH = equilibrium relative humidity (decimal)
A, B, C, B_0, C_0, H_1, H_2 = empirical constants (Note: Their values are specific to particular model.)
t = temperature (°C)
T = absolute temperature (K)
R = universal gas constant (kJ $kmol^{-1}$ K^{-1})

Non-linear regression was used to fit the aforementioned models into experimental results and obtain unknown coefficients. Regression analysis was done using JMP pro 9 statistical package (SAS Institute, Cary, CA). The procedure employed the Gauss-Newton algorithm to minimize the residual sum of squares between predicted and observed data in an iterative way. The adequacy of tested models was evaluated using different statistical criteria, including mean percent relative error (MRE), residual sum of squares (RSS), root mean square error (RMSE), coefficient of determination (R^2), and plot of residuals[17,35]. Relations 6-8 were used to determine MRE, RSS RMSE, and residuals, respectively.

$$MRE = \frac{100}{n}\sum_{i=1}^{n}\frac{|EMC_{exp.}-EMC_{pred.}|}{EMC_{exp.}} \quad (6)$$

$$RSS = \sum_{i=1}^{n}(EMC_{exp.} - EMC_{pred.})^2 \quad (7)$$

$$RMSE = \sqrt{\frac{RSS}{df}} \quad (8)$$

$$Residual = EMC_{exp.} - EMC_{pred.} \quad (9)$$

where:

n = number of observations
$EMC_{exp.}$ = experimentally obtained equilibrium moisture content
$EMC_{pred.}$ = equilibrium moisture content predicted by the model
df = degree of freedom

The model with the smallest values of MRE, RMSE and RSS, as well as the largest value of R^2 was considered to be the best fit for the experimental data, and the most accurate description for the relationship between sample's EMC and ERH. Furthermore, a model was considered acceptable only if its plot of residual vs. predicted EMC showed no systematic spread or pattern[17].

5.5.2.4 Microbial degradation experiment

The microbial degradation test was conducted using the same equipment and experimental set up that was used for water vapor adsorption tests. The duration of the test was 30 days. During the experiment, temperature was maintained at 30°C with the help of incubator. Relative humidity was maintained at 97% (saturated solution of K_2SO_4 salt). These parameters were chosen to promote natural microbial growth without any attempt to inoculate material by specific fungi species. Dry matter content of samples was determined before and after the experiment, according to ASAE standard method D358.2[30].

5.5.2.5 Fiber analysis

Fiber analysis was done according to the National Renewable Energy Laboratory procedure[36]. In short, carbohydrates present in the biomass were dissolved in two stage sulfuric acid hydrolysis and the resulting monomers were analyzed by means of high performance liquid chromatography with refractive index detector (Varian ProStar 355/356, Varian Inc., Palo Alto, CA) and a column (Bio-Rad Aminex HPX-87P, Hercules, CA). Solid residual was weighed and considered to be acid insoluble lignin, while acid soluble lignin in hydrolysate was determined spectrometrically.

5.5.3 RESULTS AND DISCUSSION

5.5.3.1 Experimental results

The EMCs of raw and corn stover torrefied at 200 (T200), 250 (T250) and 300°C (T300) are included in Table 2. EMC of all four types of biomass decreased with an increase in temperature. The minimum and maximum EMC, with temperature in parentheses, of raw, T200, T250 and T300 were 1.77 (40°C) and 45.38 (10°C) $\%_{db}$; 1.63 (40°C) and 42.88 (10°C) $\%_{db}$; 1.18 (40°C) and 25.68 (10°C) $\%_{db}$; and 1.54 (40°C) and 30.44 (20°C) $\%_{db}$; respectively. This phenomenon is typical for biological products and might be a consequence of the enhanced excitation states of water molecules at higher temperatures, which lowers cohesive forces between them[34]. As expected, EMC of biomass increased with an increase in ERH and, with no exception, samples exposed to the lowest and highest ERH also respectively had the lowest and highest EMC, regardless of pretreatment temperature. Dry raw corn stover had the highest EMC values at all temperatures for ERH above 0.4. There was no significant difference between samples below 0.4, according to Tukey-Kramer HSD test, regardless of environmental temperature. Furthermore, EMC of thermally treated samples decreased with the increase in torrefaction process temperature. This is mainly a consequence of a decrease in the number of water adsorption sites and changes in the material structure due to cleavage of hydroxyl groups from biomass polymers and the formation of non-polar unsaturated structures[6]. Moreover, hemicellulose fraction in biomass is degraded to different extents during torrefaction, depending on temperature[19]. Since the main mechanism of water adsorption onto biomass is binding to polar sites, such as hydroxyl groups in sugar molecules, elimination of hemicellulose also increases hydrophobicity[37]. The difference between hydrophobicity of corn stover torrefied at 250 and 300°C is not statistically significant. Tukey-Kramer HSD test revealed that differences between ERH levels for the same sample and environmental temperature are all significant (not shown in Table 2). This is true regardless of sample type. If the samples of the same kind and ERH, but different environmental temperature, are compared to each other no straightforward conclusion could be established. Moreover, the only exception is the highest ERH value at which all samples were significantly different. Therefore, hydrophobicity of thermally treated material was clearly expressed only at the highest ERH level, regardless of environmental temperature, with raw and samples torrefied at 250°C having highest and lowest EMC, respectively.

Growth of fungi colonies was observed at the highest ERH values on raw samples at 20°C and 30°C, and on T200 and T250 samples only at 30°C. This might affect EMC of the samples. However, samples with mold contamination did not show any abnormally high EMC values caused by dry matter loss due to microbial degradation. Hence, the aforementioned samples were also included in the statistical analysis and fitting of water adsorption isotherms.

Back to Table of Contents

Table 2. EMC of raw and torrefied corn stover

RH (decimal)	T (°C)	Sample	EMC (%db)	S.D. (%db)	Sample	EMC (%db)	S.D. (%db)	Sample	EMC (%db)	S.D. (%db)	Sample	EMC (%db)	S.D. (%db)
0.113	10	Raw	2.35	0.02	T200	2.13	0.19	T250	1.73	0.16	T300	1.86	0.04
0.335	10	Raw	5.75	0.10	T200	4.98	0.14	T250	3.84	0.21	T300	4.34	0.04
0.574	10	Raw	9.93	0.00	T200	8.53	0.16	T250	6.80	0.14	T300	6.84	0.13
0.757	10	Raw	15.50	1.07	T200	12.35	0.45	T250	9.95	0.04	T300	9.76	0.01
0.982	10	Raw	45.38	1.53	T200	42.88	0.91	T250	25.68	0.10	T300	26.13	0.86
0.113	20	Raw	2.06	0.05	T200	2.03	0.04	T250	1.51	0.14	T300	1.67	0.19
0.331	20	Raw	5.04	0.13	T200	4.31	0.05	T250	3.32	0.07	T300	3.90	0.01
0.544	20	Raw	8.04	0.02	T200	6.76	0.14	T250	5.20	0.08	T300	5.87	0.02
0.755	20	Raw	13.11	0.03	T200	11.20	0.04	T250	8.62	0.00	T300	8.90	0.06
0.976	20	Raw[F]	41.48	0.94	T200	33.14	0.02	T250	24.00	1.03	T300	30.34	0.27
0.113	30	Raw	1.99	0.02	T200	2.00	0.02	T250	1.70	0.09	T300	1.82	0.20
0.324	30	Raw	4.86	0.00	T200	4.01	0.03	T250	3.25	0.03	T300	3.66	0.09
0.514	30	Raw	7.41	0.05	T200	6.23	0.05	T250	4.84	0.01	T300	5.44	0.03
0.751	30	Raw	12.22	0.10	T200	10.68	0.05	T250	8.34	0.13	T300	8.65	0.01
0.97	30	Raw[F]	24.81	0.44	T200[F]	23.24	1.45	T250[F]	16.44	0.12	T300	15.57	0.06
0.112	40	Raw	1.77	0.27	T200	1.63	0.13	T250	1.18	0.00	T300	1.54	0.06
0.316	40	Raw	4.66	0.26	T200	3.79	0.25	T250	2.92	0.05	T300	3.62	0.06
0.484	40	Raw	6.41	0.08	T200	5.35	0.05	T250	4.07	0.00	T300	4.74	0.21
0.747	40	Raw	10.94	0.40	T200	9.25	0.15	T250	7.30	0.09	T300	7.99	0.09
0.964	40	Raw	18.17	2.38	T200	13.78	0.21	T250	10.16	0.47	T300	11.06	0.27

[F] – fungi growth observed

5.5.3.2 Fitting sorption models to experimental results

Five water sorption isotherms, selected according to the ASABE standards, were used to fit experimental data presented in Table 2. Non-linear regression was used for fitting yielded unknown model parameters that are shown in Table 3. Statistical criteria for model performance characterization (MRE, RMSE, RSS, and R^2) are also given in Table 3. These were used for the selection of the model that described the relationship between ERH and EMC most accurately. Lowest MRE, RMSE and RSS values are used to indicate the best model for fitting experimental data. The modified Oswin model represented the best model for fitting raw and torrefied biomass, as with this model lowest values of the aforementioned three parameters were obtained. The modified Henderson was the second best performing model.

In addition to previously discussed statistical parameters used for model performance characterization, a residual plot is often used as a main criterion for model acceptance or rejection. Residual plots for all five selected models are shown in Figure 1. As can be seen in the figure, modified Chung-Pfost, modified Henderson, and modified GAB models show a systematic distribution of residuals. Therefore, these were poor models for describing the correlation of ERH and EMC of corn stover and had to be rejected. Modified Oswin and Halsey models had a random distribution of residuals, but since the former one has better statistical parameters it has been accepted as the best among five investigated models. The modified Oswin model provided the best fit not only for raw corn stover, but also for torrefied corn stover. Igathinathane and co-workers[25] investigated the EMC of three corn stover components and concluded that the modified Oswin and Halsey isotherm models performed best based on prediction capabilities and randomized residuals.

Table 3. Water vapor adsorption parameters for the raw and torrefied corn stover

Sample	Model	A	B	C	H_1	H_2	R^2	MRE (%)	RSS	RMSE
Raw	Modified Chung-Pfost	80.3430	12.9223	0.1395			0.8942	44.01	3.028	0.0422
	Modified Halsey	4.7831	-0.0358	2.1794			0.9645	31.39	1.017	0.0245
	Modified Oswin	10.6784	-0.1340	2.4557			0.9766	20.02	0.671	0.0199
	Modified Henderson	0.0018	26.4117	1.0734			0.9686	17.99	0.899	0.0230
	GAB	3.8848	0.3849	47.3216	2090.335	45000	0.9594	30.14	1.162	0.0278
T200	Modified Chung-Pfost	70.4461	9.3173	0.1601			0.8740	48.19	2.835	0.0408
	Modified Halsey	4.4186	-0.0420	2.1203			0.9783	25.45	0.489	0.0170
	Modified Oswin	9.3512	-0.1311	2.3795			0.9875	15.44	0.281	0.0129
	Modified Henderson	0.0027	20.9265	1.0297			0.9748	22.72	0.568	0.0183
	GAB	3.2719	0.3362	47.6590	2427.192	42356.11	0.9749	25.37	0.565	0.0194
T250	Modified Chung-Pfost	93.4331	13.4685	0.2416			0.9106	32.11	0.836	0.0222
	Modified Halsey	4.1963	-0.0353	2.3710			0.9548	29.51	0.423	0.0158
	Modified Oswin	6.9828	-0.0826	2.6851			0.9712	18.92	0.270	0.0126
	Modified Henderson	0.0022	26.6979	1.1954			0.9661	14.32	0.317	0.0137
	GAB	2.6351	0.3527	61.0000	2256.327	41223.2	0.9529	27.73	0.440	0.0171
T300	Modified Chung-Pfost	107.560	18.4000	0.2239			0.8551	31.15	1.663	0.0313
	Modified Halsey	4.2505	-0.0321	2.3463			0.9076	27.49	1.060	0.0250
	Modified Oswin	7.3975	-0.0848	2.6590			0.9223	18.38	0.891	0.0229
	Modified Henderson	0.0019	32.5443	1.1756			0.9072	19.47	1.064	0.0250
	GAB	2.7887	0.3993	39.1527	1965.523	44322	0.9016	24.27	1.129	0.0274

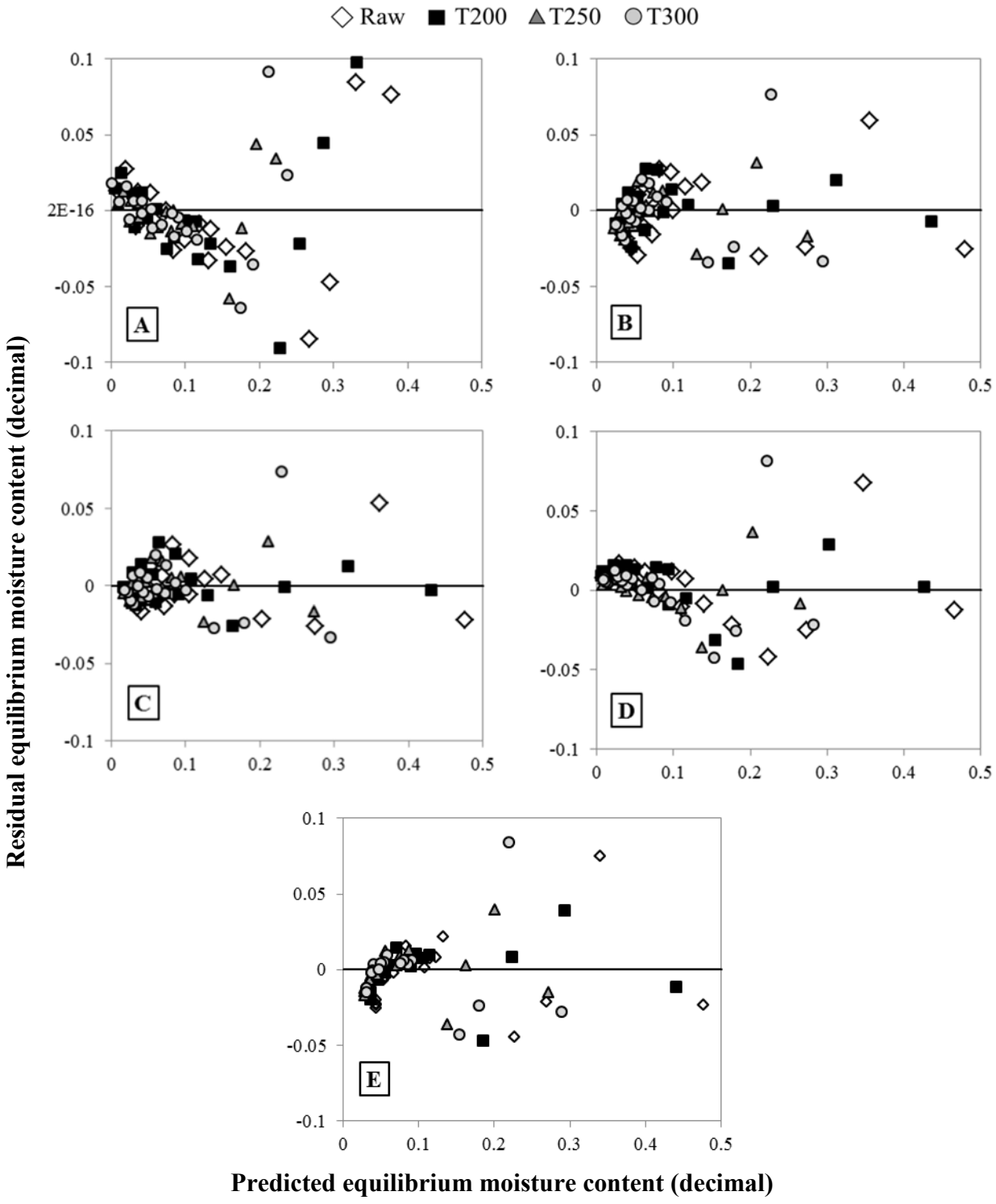

Figure 1. Residual plots of the water vapor adsorption isotherms for raw and torrefied corn stover (A – Modified Chung-Pfost, B – Modified Halsey, C - Modified Oswin, D - Modified Henderson, E – GAB)

As can be seen in Figure 2, 3, 4, and 5, the fitted modified Oswin equation shows that EMC data of raw and torrefied corn stover follow a sigmoidal curve, typical for the most

agricultural products[38]. This type of curve represents a type II isotherm, according to Brunauer and Emmet's classification[39]. This family of isotherms describes multilayer adsorption with an asymptotic trend as water activity approaches 1.0. The previously discussed trend of decrease in EMC with increase in environmental temperature, regardless of sample type, is clearly depicted in these figures. However, this trend is less expressed in the case of corn stover torrefied at 250 (T250) and 300°C (T300). It can be seen in the figures that increase in ERH causes increase in EMC of all samples. This is especially pronounced at ERH values above 0.9. The abrupt increase in EMC at ERH above 0.9 is larger for raw (45% db) and T200 (40% db) than for T250 (25% db) and T300 (25% db). As already stated, the difference between raw and corn stover torrefied at higher temperatures may be due to degradation of hemicellulose. Moreover, the elimination of hemicellulose leads to the elimination of monosaccharides and hydroxyl moieties that served as water binding sites. Curves show a sharp increase at about 0.8-0.9 ERH, which is characteristic for type II isotherms.

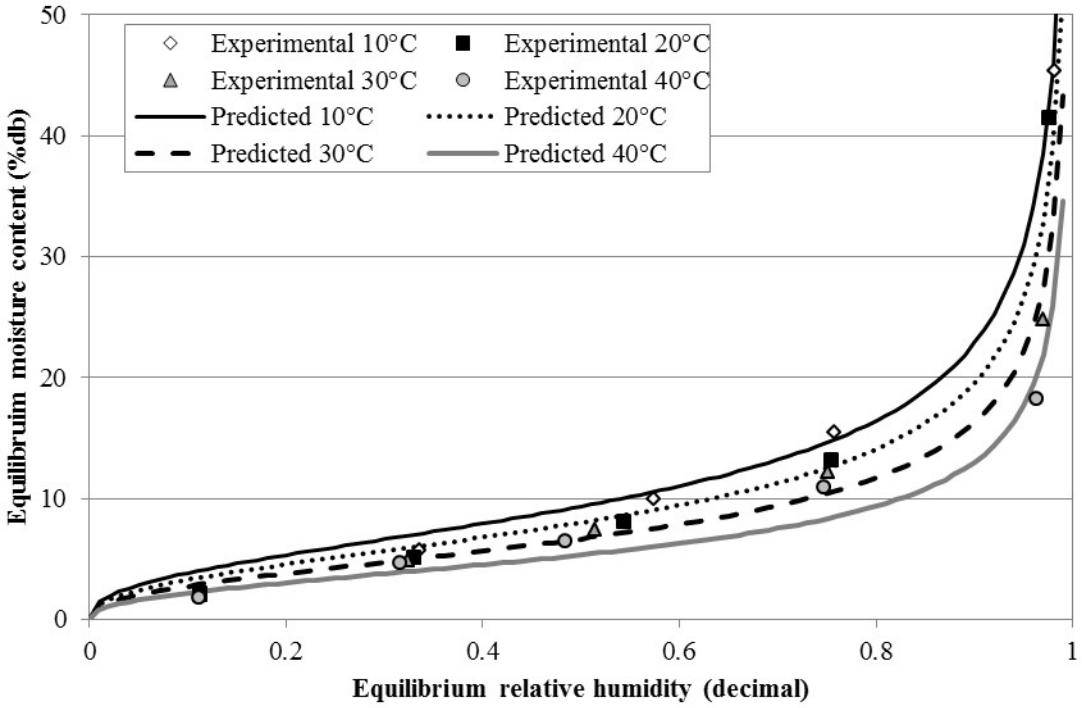

Figure 2. Experimental and isotherms predicted by Modified Oswin model of raw corn stover

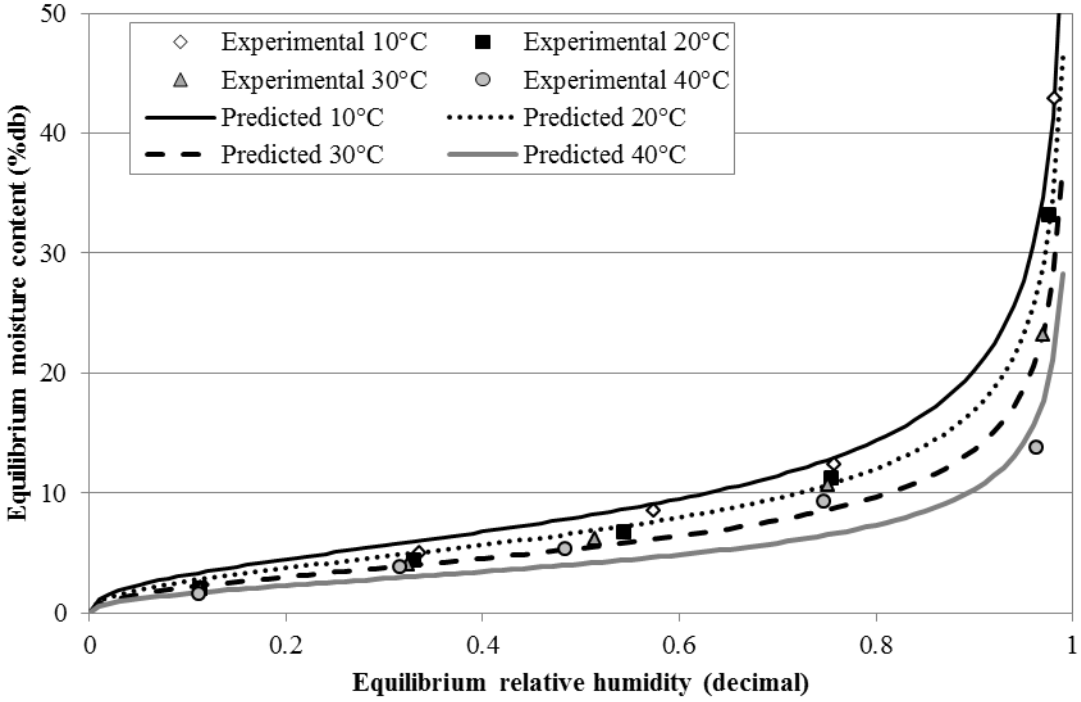

Figure 3. Experimental and isotherms predicted by Modified Oswin model of corn stover torrefied at 200°C

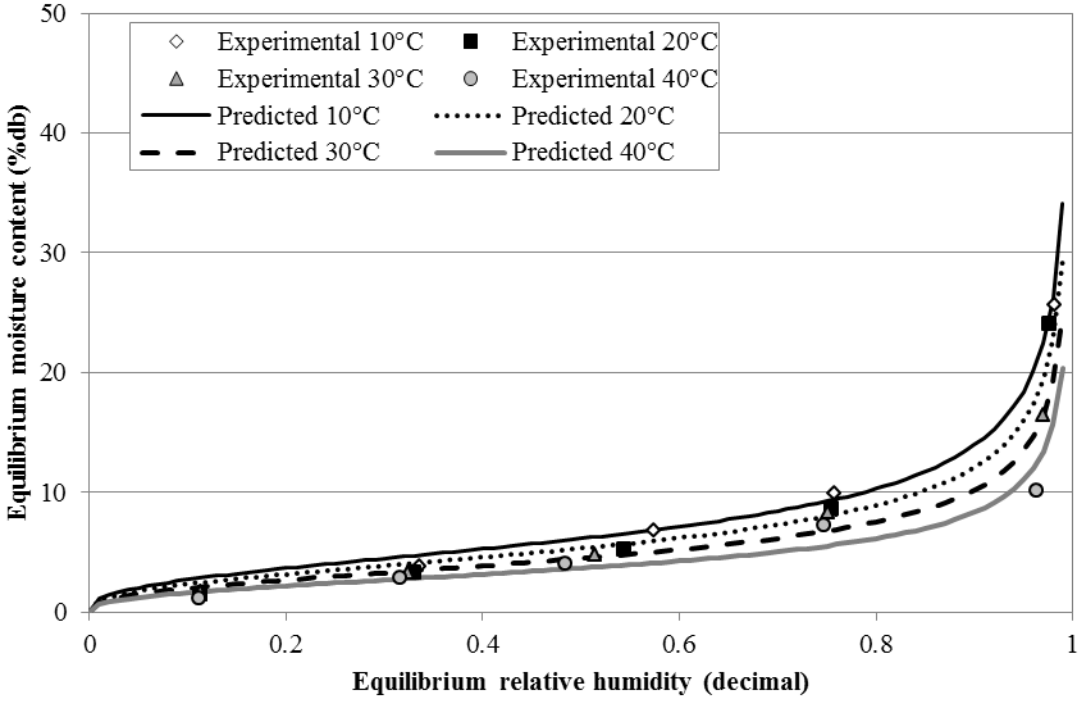

Figure 4. Experimental and isotherms predicted by Modified Oswin model of corn stover torrefied at 250°C

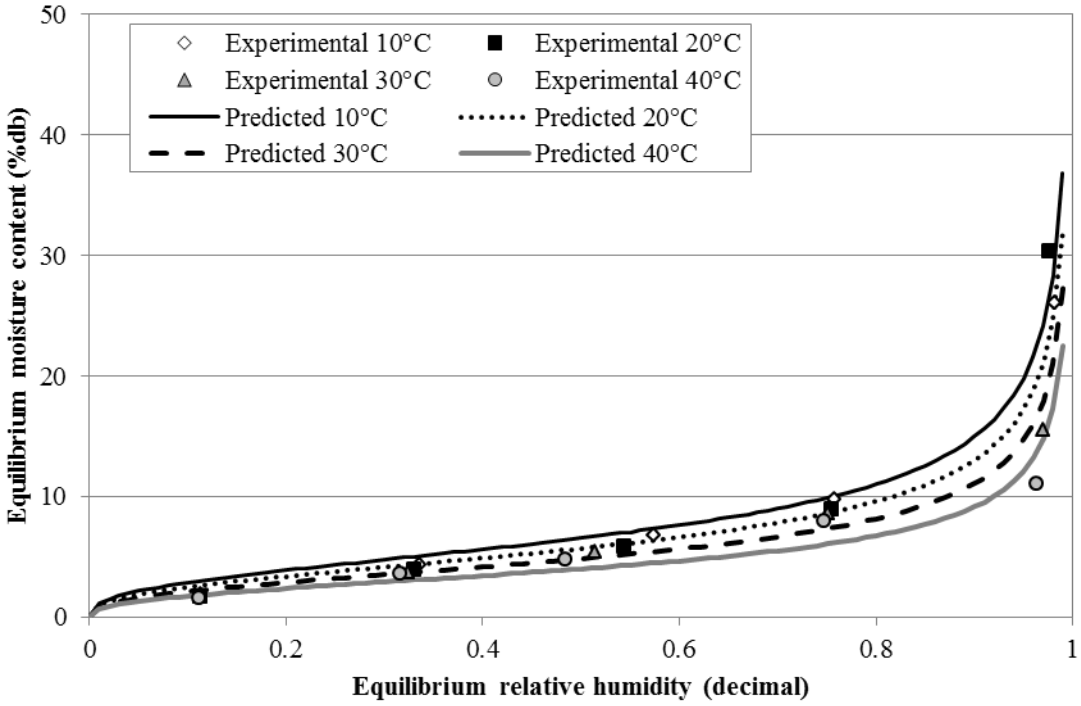

Figure 5. Experimental and isotherms predicted by Modified Oswin model of corn stover torrefied at 300°C

As can be seen in Figure 6, torrefied biomass has distinct water vapor adsorption properties from raw biomass. Therefore, all predicted isotherms of torrefied samples are grouped together at 40°C. However, raw corn stover at 10°C and corn stover torrefied at 200°C had a similar predicted EMC, but they were significantly different from samples torrefied at 250 and 300°C, which had similar behavior at this environmental temperature.

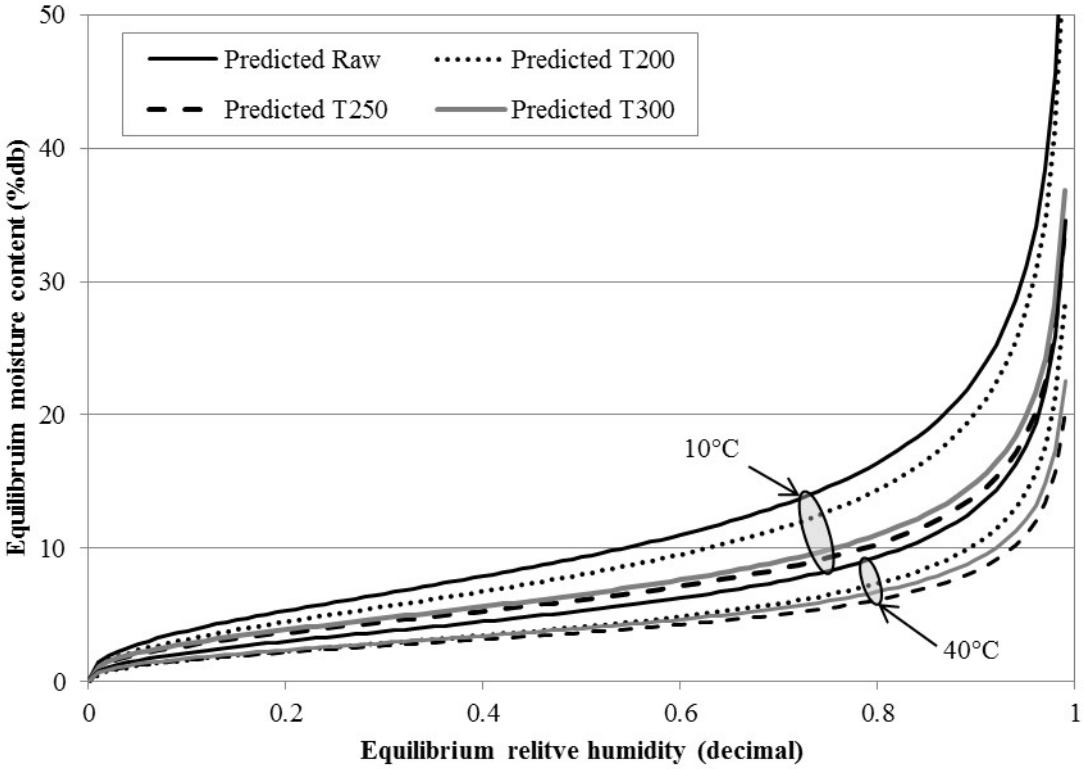

Figure 6. Comparison of raw and torrefied corn stover isotherms at 10 and 40°C

5.5.3.3 Microbial degradation results

Microbial degradation tests were conducted for the conditions when temperature was 30°C and ERH was 0.97 as there was not any mold growth at other conditions. The results are presented in Figure 7. Dry matter loss (DML) of the raw corn stover sample was about 17% after 30 days, and was the highest among all samples (Figure 7). This value was about 3 times higher than the dry matter mass loss of T200 sample. DML for corn stover torrefied at 250 and 300°C were less than 1%.

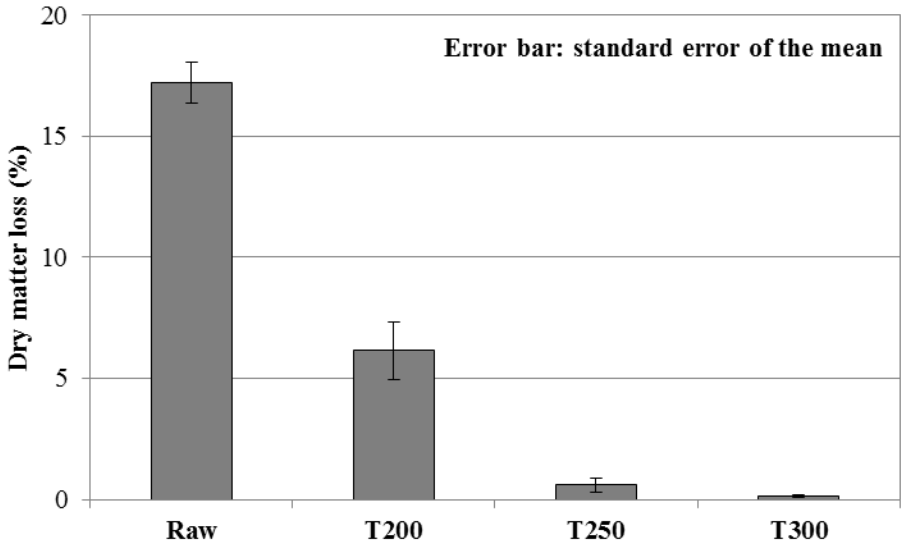

Figure 7. Dry matter loss due to microbial degradation at 0.97 ERH and 30°C

As discussed in the section 3.1 and 3.2, even though torrefied biomass is comparatively more hydrophobic in nature than raw biomass, it still adsorbs a relatively significant amount of water vapor. At the temperature and ERH used in the microbial degradation experiment, raw and T200, and T250 and T300 samples had EMC values of about 25 and 15%$_{db}$, respectively. However, DML was significantly lower in the case of corn stover torrefied at 250°C and 300°C than in the case of raw biomass. This might be not only due to the elimination of hemicellulose and an increase in hydrophobicity, but also the formation of sugar and lignin degradation products toxic to microorganisms, such as furan and phenol derivatives that are trapped in the pores of torrefied material.

5.5.3.4 Fiber analysis results

Results of the fiber analysis are shown in Table 4. There was an overall trend of decrease in both xylan and arabinan quantity with increase in torrefaction temperature. These two compounds represent the hemicellulose fraction of corn stover. As expected, raw and biomass pretreated at 300°C had respectively the highest (28%) and the lowest (4%) amount of hemicellulose. Similar trend was also observed by several other researchers[6,19]. Increase in the torrefaction temperature from 250 to 300°C caused cellulose degradation and decrease in its contents from about 45 to 20%, respectively. Nevertheless, there was no significant difference between raw, T200, and T250 in regards to cellulose content, which was expressed as a glucan percentage. Relative total lignin content increased from 20 to 75% with the temperature increase, probably due to carbohydrate elimination and conversion to acid insoluble products during the thermal pretreatment.

Table 4. Fiber analysis of raw and torrefied corn stover

Sample	ASL (%)	AIL (%)	Glucan (%)	Xylan (%)	Arabinan (%)
Raw	2.6 ± 0.14 [a]	19.4 ± 0.37[a]	45.7 ± 0.14[a]	27.8 ± 0.07[a]	4.6 ± 0.01[a]
T200	2.6 ± 0.14[a]	22.9 ± 0.25[b]	44.9 ± 0.31[a]	25.5 ± 0.04[b]	4.0 ± 0.23[b]
T250	2.7 ± 0.21[a]	33.3 ± 0.55 [c]	46.0 ± 0.41[a]	15.8 ± 0.70[c]	2.3 ± 0.05[c]
T300	1.0 ± 0.04[b]	75.1 ± 0.49 [d]	19.9 ± 0.27[b]	3.6 ± 0.27[d]	0.4 ± 0.01[d]

ASL = acid soluble lignin
AIL = acid insoluble lignin
Note: Values are given as mean ± standard deviation of two measurements. Samples marked with different letters in superscript are significantly different at $\alpha = 0.05$ according to the Tukey-Kramer pair-wise mean comparison test. Different fiber categories were not compared to each other.

5.5.4 CONCLUSIONS

The EMC of raw and thermally pretreated corn stover was measured at ERH and temperature ranging from 10 to 98% and 10 to 40°C, respectively. Except at the highest ERH value, sample torrefied at 200°C did not have water adsorption properties different from the raw biomass. However, the adsorption properties of samples torrefied at 250 and 300°C were significantly different from the raw biomass. Torrefaction may have increased hydrophobicity of biomass through the elimination of the hydrophilic carbohydrate fraction and its partial conversion into non-polar, hydrophobic degradation products. Five isotherms were fitted to the experimental data to obtain the EMC-ERH prediction equations. Isotherms of all samples belong to type II. Modified Oswin model, followed by modified Halsey model, showed the best performances and were recommended for the characterization of water vapor sorption behavior of raw and torrefied corn stover. Modified Chung-Pfost, modified Henderson and GAB models were not recommended since their residual plots were systematic. Degradation test at highest ERH and 30°C showed that raw biomass had about 17% dry matter loss due to microbial degradation. Samples torrefied at 250 and 300°C had negligible dry matter loss when compared to raw and samples torrefied at 200°C. This might be predominantly due to higher hydrophobicity and probably the formation of degradation products toxic to fungi. Fiber analysis showed a significant decrease in hemicellulose content and a relative increase in the lignin content of torrefied corn stover.

ACKNOWLEDGEMENTS

Funding for this project was provided by the ConocoPhillips Company. Additional technical support was provided by Center for Sustainable Energy (CSET) and Biocentury Research Farm (BCRF) of Iowa State University, Ames, IA. We would also like to thank Andy Suby and Patrick Johnston for their contribution to this work.

REFERENCES

(1) Brown, R. C. *Biorenewable Resources: Engineering New Products from Agriculture,* 1th ed.; Blackwell Publishing Professional: Ames, IA, 2003; pp 3-12.
(2) Jenkins, B. M.; Sumner, H. R. Harvesting and Handling Agricultural Residues. *T. ASABE* **1986**, 29 (3), 824-836.

(3) Shinners, J. K.; Binversie, J. B.; Muck, E. R.; Weimer, J. P. Comparison of wet and dry corn stover harvest and storage. *Biomass Bioenerg.* **2007**, 31, 211-221.
(4) Nurmi, J. The storage of logging residue for fuel. *Biomass Bioenerg.* **1999**, 17, 41-47.
(5) Wadsö, L. Measuring chemical heat production rates of biofuels by isothermal calorimetry for hazardous evaluation modeling. *Fire Mater.* **2007**, 31, 241-255.
(6) Bergman, P. C.; Boersma, A. R.; Zwart, R. W. R.; Kiel, J. H. A. *Torrefaction for biomass co-firing in existing coal-fired power stations (Biocoal);* ECN-C--05-013; Energy Research Centre of the Netherlands: Petten, NL, July 2005.
(7) Igathinathane, C.; Womac, A. R.; Sokhanasanj, S.; Narayan, S. Size Reduction of High- and Low-Moisture Content Corn Stalks by Linear Grid System. *Biomass Bioenerg.* **2009**, 33, 547-557.
(8) Neathery, J. K. Biomass gasification. In *Thermochemical Conversion of Biomass to Liquid Fuels and Chemicals,* 1st ed.; Crocker, M., Ed.; Royal Society of Chemistry: Cambridge, UK, 2010; pp 67-94.
(9) Gray, M. R.; Corcoran, W. H.; Gavalas, G. R. Pyrolysis of Wood-Derived Material. Effect of Moisture and Ash Content. *Ind. Eng. Chem., Process Des. Dev.* **1985**, 24, 646-651.
(10) Khan, A. A.; De Jong, W.; Jansens, P. J.; Spliethoff, H. Biomass Combustion in Fluidized Bed Boilers: Potential and Remedies. *Fuel Process. Technol.* **2009**, 98, 21-58.
(11) Cordeiro, D. D.; Raghavan, G. S. V.; Oliveira, W. P. Equilibrium Moisture Content Models for *Maytenus Ilicifolia* Leaves. *Biosyst. Eng.* **2006**, 94 (2), 221-228.
(12) Nurhan A.; Hasan T. The fitting of various models to water sorption isotherms of tea stored in a chamber under controlled temperature and humidity. *J. Stored Prod. Res.* **2006**, 42, 112-135.
(13) Mayor L.; Moreira R.; Chenlo F.; Sereno A. Water sorption isotherms of fresh and partially osmotic dehydrated pumpkin parenchyma and seed at several temperatures. *Eur. Food Res. Technol.* **2005**, 220, 163-167.
(14) Singh, R. N. Equilibrium moisture content of biomass briquettes. *Biomass Bioenerg.* **2004**, 26, 251-253.
(15) Van der Berg, C.; Bruin, S. Water Activity and Its Estimation in Food Systems: Theoretical Aspects. In *Water activity: Influences on Food Quality;* Rockland, L. B., Steward, G. F., Eds.; Academic Press: New York, NY, 1981; pp 1-61.
(16) Labuza T. P.; Altunakar B. Water Activity Prediction and Moisture Sorption Isotherms. In *Water Activity in Foods: Fundamentals and Application,* 1st ed.; Barbosa-Canovas, G. V., Fontana, A. J., Jr., Schmidt, S. J., Labuza, T. P., Eds.; Blackwell Publishing Professional: Ames, IA, 2007; pp 109-154.
(17) Chen, C. C.; Morey, R. V. Comparison of Four EMC/ERH Equations. *T. ASAE* 1989, 32, 983-990.
(18) ASAE standard D245.6. Moisture Relationships of Plant-Based Agricultural Products. St. Joseph, MI, 2007.
(19) Yan, W.; Acharjee, T. C.; Coronella, C. J.; Vasquez, V. R. Thermal Pretreatment of Lignocellulosic Biomass. *Environ. Prog. Sustainable Energy* **2009**, 28 (3), 435-440.
(20) Greig, S. J.; Sing, K. S. *Adsorption, Surface Area and Porosity,* 2nd ed., Academic Press: New York, NY, 1982.
(21) Chirife, J.; Fontan F. C.. Water activity of fresh food. *J. Food Sci.* **1982**, 47, 661-663.
(22) Rüegg, M. Water in Dairy Products Related to Quality, with Special Reference to Cheese. In *Properties of water in foods in relation to quality and stability;* Simatos, D.,

Multon J. L., Eds.; NATO ASI Series E 90; Martinus Nijhoff Publishers: Dordrecht, NL, 1985; pp 603-625.
(23) Sakaar, C. *Wood-Water Relations,* 1st ed.; Springer-Verlag: Berlin, DE, 1988.
(24) Fasina, O. O.; Sokhansanj, S. Equilibrium Moisture Relations and Heat of Sorption of Alfalfa Pellets. *J. Agr. Eng. Res.* **1993**, 55, 51-63.
(25) Igathinathane, C.; Womac, A. R.; Sokhansanj, S.; Pordesimo, L. O. Sorption Equilibrium Moisture Characteristics of Selected Corn Stover Components. *T. ASAE* **2005**, 48 (4), 1449-1460.
(26) Wiig, E. O.; Juhola A. J. The Adsorption of Water Vapor on Activated Charcoal. *J. Am. Chem. Soc.* **1949**, 71, 516-568.
(27) Monzam, E. R.; Shadle, L. J.; Evans, R.; Schroeder, K. Water Adsorption and Desorption by Coals and Chars. *Energy Fuels* **1998**, 12, 1299-1304.
(28) Bedia J.; Rodriguez-Mirasol J.; Cordero T. Water vapor sorption on lignin-based activated carbons. *J. Chem. Technol. Biotechnol.* **2007**, 82, 548-557.
(29) Acharjee , T. C.; Coronella , C. J.; Vasquez , V. R. Effect of thermal pretreatment on equilibrium moisture content of lignocellulosic biomass. *Bioresour. Technol*. **2011**, 102, 4849-4854.
(30) ASAE standard D358.2 (R2008). Moisture Measurement - Forages. St. Joseph, MI, 1998.
(31) Medic, D.; Darr, M.; Shah, A.; Potter, B.; Zimmerrnan, J. Effects of torrefaction process parameters on biomass feedstock upgrading. *Fuel* **2011**, 91, 147-154.
(32) Spiess, W. E. L.; Wolf, W. Water activity. In *Water Activity: Theory and Application to Food;* Rockland, L. B., Beuchat, L. R., Eds.; IFT Basic Symposium Series 664; Marcel Dekker: New York, NY, 1987; pp 215-233.
(33) Greenspan, L. Humidity Fixed Points of Binary Saturated Aqueous Solutions. *J. Res. Natl. Bur. Stand. Sec. A* **1977**, 81, 89-96.
(34) Mohamed, L. A.; Kouhila, M.; Jamali, A.; Lahsani, S.; Mahrouz, M. Moisture sorption isotherms and heat of adsorption of bitter orange leaves (*Citrus aurantium). J. Food Eng.* **2005**, 67, 491-498.
(35) Osborn, G. S.; White, G. M.; Sulaiman, A. H.; Walton, L. R. Predicting Equilibrium Moisture Properties of Soybeans. *T. ASAE* **1989**, 32, 2109-2113.
(36) Sluiter, J.; Hames, B.; Ruiz, R.; Scarlata, C.; Sluiter, J.; Tempelton, D.; Croker, D. *Determination of Structural Carbohydrates and Lignin in Biomass;* Technical report NREL/TP-510-42618; National Renewable Energy Laboratory: Golden, CO, July 2011.
(37) Bjork, H.; Rasmunson, A. Moisture equilibrium of wood and bark chips in superheated steam. *Fuel* **1995**, 74, 1887-1890.
(38) Lewicki, P. P. Data and Models of Water Activity. II: Solid Foods. In *Food properties handbook,* 2nd ed.*;* Shafiur, R., M., Ed.; CRC Press: Boca Raton, FL, 2009; pp 66-151.
(39) Brunauer, S.; Deming, L. S.; Dming W. E.; Troller, E. On the Theory of Van der Waal's Adsorption of Gases. *J. Am. Chem. Soc.* **1940**, 62, 1723-1732.

5.6 Techno-economic analysis of a production-scale torrefaction system for cellulosic biomass upgrading

Ajay Shah, Matthew J. Darr, Dorde Medic, Robert P. Anex, Sami Khanal and Dev Maski

(published in: *Biofuels Bioproducts & Biorefining*)

ABSTRACT

Torrefaction of biomass early in the supply chain is one method to enhance or preserve biomass quality during storage; to reduce storage and transportation costs; to attain uniformity among different feedstock types; and to meet biorefineries' quality and quantity demands for feedstock in a cost effective and sustainable manner. The main objectives of this study were to analyze the mass and energy balance, assess the techno-economic feasibility of a production-scale torrefaction system, and to quantify the sensitivity of energy and cost results to changes in initial feedstock moisture content, torrefaction process temperature, plant operating window and initial capital investment. The output from this analysis provides clear guidance on the opportunities and costs associated with production scale torrefaction of biomass as a feedstock intermediate. Analysis of energy results indicated the net external energy required for the torrefaction process increased and energy efficiency of the torrefaction system decreased with increasing moisture contents. However, both of these energy metrics exhibited decreasing trend with increasing process temperatures. In addition to the energy results, unit torrefaction process cost exhibited decreasing trend with decreasing initial moisture contents of feedstock and decreasing torrefaction process temperatures. For the typical moisture content of 30%$_{wb}$, process temperature of 240°C, plant operating window of 6 mo.yr^{-1} and initial capital investment of \$7.5M for the system with rated capacity of 25 Tton.hr^{-1}, unit torrefaction process cost was estimated to be 17.5 \$-Tton^{-1}. Additional system improvements through capital cost reduction and wider operating windows can yield a torrefaction product cost of ~12 \$-Tton^{-1}.

KEYWORDS: upgrading, torrefaction, techno-economics, cellulosic biomass.

5.6.1 INTRODUCTION

Achievement of the national biofuels production target set by the revised renewable fuel standard (RFS2) authorized under the Energy Independence and Security Act (EISA) of 2007 mandating the production of 36 billion gal (136.3 million m^3) of renewable biofuels, including 16 billion gal (60.6 million m^3) of cellulosic biofuels, by 2022, will require around 200 million dry tons of cellulosic feedstock delivered to the biorefineries annually.[1] Short harvest windows, variable initial moisture contents, storage dry matter loss (DML), low bulk and energy densities, low bulk flowability, and non-uniformity among the feedstock types are several of the main impeding factors in the establishment of a sustainable biomass feedstock supply system. One option for preserving and enhancing biomass quality during storage, reducing storage and transportation costs, attaining uniformity among different feedstock types, and meeting biorefineries' quality and quantity demands for feedstock in a cost effective and sustainable manner would be torrefying biomass early in the supply chain at a central location, preferably nearby large scale storage infrastructure.

Torrefaction, also referred to as mild-pyrolysis, is a thermochemical pretreatment of biomass, where hemicellulose degrades to form volatiles, mainly permanent gases and condensables. During the torrefaction process, biomass is retained in an inert atmosphere at some pre-defined temperature (usually 200 to 300°C) for a specific duration (usually 5 to 120 min) to yield solid torrefied biomass, mainly composed of cellulose and lignin with reduced moisture content, enhanced energy density, improved hydrophobicity and microbial degradation resistance, and increased brittleness.[2-12] Torrefaction is currently being considered as a biomass feedstock pretreatment process particularly for thermal conversion systems, such as pyrolysis, gasification and co-firing due to its potential to reduce power consumption and cost for biomass grinding. In addition to enhanced brittleness, torrefied biomass also improves uniformity in properties among different biomass feedstock types, eliminates volatile acids responsible for high acidity of bio-oil and improves fluidization properties of biomass.[5, 10, 13-17]

Earlier studies were mostly focused on the experimental aspects of torrefaction of wood or forest residues to determine the effects of different torrefaction process parameters on biomass properties and dry matter, and compositional analyses of different by-products released during the process.[2-5, 8, 10, 12-14, 16-20] Relatively few earlier studies have focused directly on torrefaction of agricultural residues and energy crops.[6, 9, 11, 12, 15] Regardless of the feedstock types, some of their main findings included enhanced energy density, reduced dry matter yield due to loss of hemicellulose as volatiles, improved grindability due to enhancement in brittleness, improved stability and reduced dry matter deterioration due to a reduction in moisture content, and a reduced acidity due to loss of acids as volatiles.

Pools of information obtained from all of the aforementioned studies have sufficiently identified the potential of torrefaction to be developed at a commercial scale to improve overall supply chain logistics. However, there is a lack in knowledge to understand the production-scale torrefaction system completely. The main objective of this study was to perform the techno-economic analysis of a large-scale torrefaction system for cellulosic feedstock upgrading. This work was based on a central hypothesis that upgrading technologies, like torrefaction, which convert biomass from a highly-variable low-density feedstock into a consistent high-energy-density commodity, can serve as transformative technologies to break the current production barriers imposed due to low density and instability of materials during storage, and to substantially reduce the production cost of biomass. The main objective of this study was accomplished through the following specific objectives: (1) analyze the mass and energy balance of production scale torrefaction system with exhaust heat recovery, (2) evaluate production cost of torrefied biomass, and (3) assess the influences of variability in torrefaction process parameters on overall energy and cost metrics of the system.

5.6.2 MATERIALS AND METHODS

5.6.2.1 Overview of the mass and energy balance model

A model was developed to simulate the mass and energy balance and the techno-economic aspects of a production-scale continuous-flow torrefaction system under different initial conditions. Model input parameters included initial moisture content of biomass, torrefaction process temperature, torrefaction plant operating periods, and initial capital investment. The model was developed in Matlab using Simulink dynamic modeling tools and consisted of several unique operational modules. The functional arrangement of different

processes and equipment of the conceived production-scale torrefaction system is schematically depicted in figure 1, and the key inputs and outputs of the model are summarized in table 1.

Table 1: Summary of different inputs and outputs of the large-scale torrefaction system model:

Inputs to the model	**Outputs from the model**
• Initial moisture content of feedstock ($\%_{wb}$) • Torrefaction process temperature (°C) • Torrefaction plant operating window ($mo.yr^{-1}$) • Initial capital investment for the large scale torrefaction plant ($\$-(Tton.hr^{-1})^{-1}$)	• Torrefaction process dry matter loss (%) • Net energy required for torrefaction process ($MJ.Tton^{-1}$) • Energy contained within torrefied biomass ($MJ.Tton^{-1}$) • Torrefaction cost ($\$-Tton^{-1}$) • Torrefaction system sub-costs (energy, labor, DML costs) ($\$-Tton^{-1}$)

The developed production-scale torrefaction system model accounted for all the required operations, from feeding cellulosic feedstock into the large-scale torrefaction chamber to obtaining the partly cooled torrefied biomass (Figure 1). In the conceived system, cellulosic feedstock (at a particular moisture level) would be fed into the torrefaction chamber and passed through a pre-drying system to remove the majority of the moisture from the biomass. Upon the completion of the pre-drying phase, feedstocks enter the torrefaction chamber with a defined process temperature (usually between 200-300°C) and remain inside the chamber for a specific duration (usually between 10-30 min, optimal retention time based on Medic *et al.*) until the biomass is completely torrefied.[9] The energy required for the complete torrefaction process was conceived to be obtained from three sources: (1) combusting volatiles from the torrefaction process and extracting heat energy with the help of heat exchangers, (2) extracting heat energy from the hot torrefied biomass and steam with the help of heat exchanger, and (3) supplying additional energy required for the overall torrefaction process by combusting compressed natural gas (CNG). This model was configured to assess the mass and energy balance during the overall torrefaction process and to estimate different costs associated with the establishment and operation of such systems. The model was comprised of five different functional modules, each representing a unique task or process of the overall torrefaction system, and a cost module for estimating the costs associated with the establishment and operation of the production-scale torrefaction system. The detailed explanation of each module is included in the following sections.

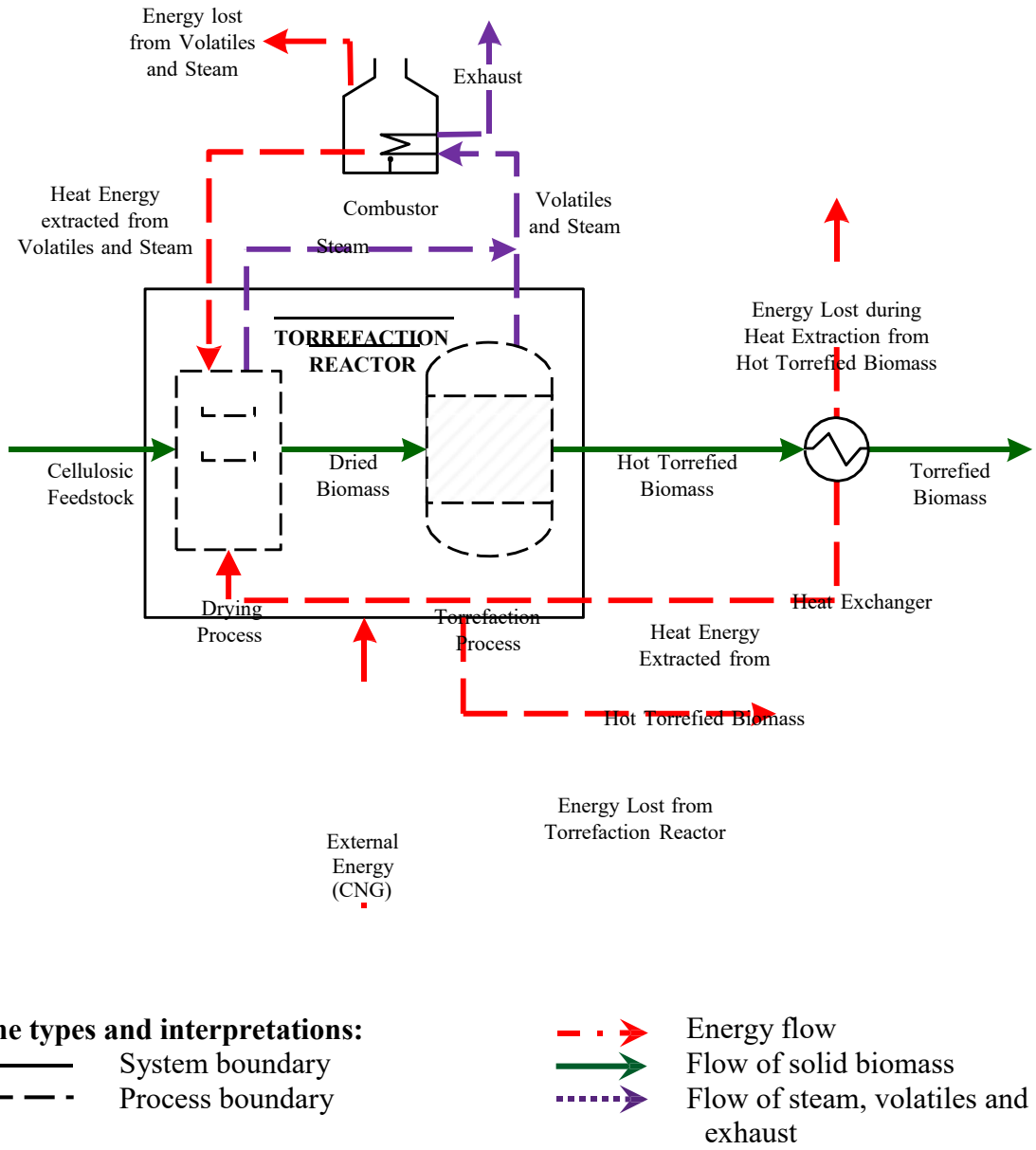

Figure 1: Schematic of a production-scale torrefaction system showing required equipment, processes, and mass and energy flow routes.

5.6.2.2 Biomass feeding and drying within torrefier

Biomass to be torrefied is first fed into the torrefier. Masses of dry matter and water in wet feedstocks received into the torrefaction facility were quantified based on their wet mass and initial moisture content (wet basis). Biomass fed into the torrefier is then dried. Drying is the first stage of torrefaction, where the temperature of wet biomass is raised to 100°C, followed by the vaporization of water contained in wet biomass. The drying process module was used for estimating the total drying energy required in the torrefaction system. Theoretical energy required for feedstock drying was estimated as the sum of sensible heat required to raise the

temperature of wet biomass to 100°C from its initial temperature, and the latent heat required for the liquid to gaseous phase transition of contained water. For the estimation of sensible heat energy required to raise the temperature of wet biomass, specific heat capacity of biomass was taken as 0.002 $MJ.kg^{-1}.K^{-1}$.[21, 22] Combustion efficiency of natural gas operated dryers is reported

up to 97%.[23] However, in this study, drying efficiency was taken as 65% for the estimation of actual drying energy, and the energy lost during the drying process.

The required drying energy was supplied from a variety of sources depending on the operating conditions of the torrefier. Initial energy was modeled as both heat recovery from hot torrefied biomass and steam as well as from heat energy recovered from the combustion of torrefaction off-gas volatiles. Supplemental heat from CNG was provided to the model when heat recovery did not provide sufficient process heat. The estimation of practically recoverable heat energy from volatiles and steam is explained in section 2.4, and that from hot torrefied biomass is included in section 2.5. The final energy content of dried biomass was estimated as the product of the average energy densities of different cellulosic biomass, which is 18.2 MJ.kg^{-1},[24] and the total mass of dry matter.

5.6.2.3 Biomass torrefaction phase within torrefier

After drying, the biomass is torrefied by retaining feedstock at some fixed temperature, usually in the range of 200-300°C in an inert environment which results in the partial decomposition of hemi-cellulose and the transformation to a torrefied material. Previous studies have reported the retention in the range 5-120 min; however, some researchers, as Medic *et al.*,[9] have shown that cellulosic biomass can be well torrefied in 10-30 min. Torrefied biomass and exhaust volatiles are the two main categories of products obtained during the torrefaction process. Volatiles include condensables like acetic acid, methanol, furfural, and water, and permanent gases like carbon dioxide, carbon monoxide, methane, hydrogen, etc.[9] The torrefaction module accounted for the change in mass and energy associated with the torrefaction process. Theoretical energy required for torrefying biomass was estimated as the sensible heat energy required to raise the temperature of hot dried biomass to the torrefaction process temperature. For the estimation of the actual energy required for torrefying biomass, torrefaction process energy efficiency was taken as 60%.[4] And, the energy lost during torrefaction process was estimated as the difference between the actual and theoretical energies required to torrefy the biomass. In addition to this, DML during torrefaction process ($ML\%_{Tor}$, %) and the energy density of the torrefied biomass ($EDen_{TDM}$, MJ.kg^{-1}) were estimated as the functions of torrefaction process temperature (T_{Tor}, K) and moisture content (MC %) using relations 1 and 2, respectively.[9] The final mass of torrefied biomass was estimated as the ($1 - ML\%_{Tor}$) fraction of initial dry matter. And, the total energy content of the torrefied biomass was estimated as the product of energy density and mass of torrefied biomass.

$$ML\%_{Tor} = f\left(T_{Tor}, MC(\%), {T_{Tor}}^2\right)$$
$$= 98.4 - 1.08 \times T_{Tor} + 0.133 \times MC + 0.00295 \times {T_{Tor}}^2 \quad \text{.....(1)}$$
$$EDen_{TDM} = f\left(T_{Tor}, MC(\%), {T_{Tor}}^2\right)$$
$$= 29.4 - 0.109 \times T_{Tor} + 0.00812 \times MC + 0.000275 \times {T_{Tor}}^2 \quad \text{.....(2)}$$

5.6.2.4 Volatiles combustor

Volatiles, including permanent gases and condensables, are formed as the by-product during torrefaction process, mainly due to the degradation of hemicellulose, and possess energy

density of 7.8 MJ.kg^{-1}.[25] The volatiles can be further combusted to generate heat.[6] The volatiles

combustor module was created to estimate the practical recoverable sensible heat energy available in steam and the combusted volatiles. The extracted heat energy was conceived to be used for pre-drying of biomass, as explained in section 2.2. The theoretical heat energy available in hot steam was estimated based on the assumption that the water lost during the drying phase changed completely to steam. Furthermore, it was assumed that the dry matter lost during the torrefaction process was completely transformed to the volatiles. The maximum energy available in volatiles was estimated as the product of their mass, measured by torrefaction DML, and energy density of 7.8 MJ.kg^{-1}. For the estimation of actual recoverable heat energy available in steam and combusted volatiles, process efficiency was taken as 60%.[26] And, the loss in extractable steam and volatiles energy was estimated as the difference in the theoretically maximum and practically extractable heat energies available in the steam and combusted volatiles.

5.6.2.5 Torrefaction solids heat exchanger

The sensible heat extracted from hot torrefied biomass using a heat exchanger could be used to supply process heat for pre-drying wet biomass, as explained in section 2.3. It was assumed that the temperature of the hot torrefied biomass, immediately after torrefaction, would be equal to the torrefaction process temperature, and the heat could be recovered from hot torrefied biomass until the temperature of the solid fraction drops below 50°C. For the estimation of actual recoverable heat energy from hot torrefied biomass, heat exchanger efficiency of 60% was used.[26]

5.6.2.6 Energy balance

The energy balance for the overall torrefaction system was based on the initial energy content (dry basis) of biomass (EC_{dm}, MJ), total energy lost during different processes in the conceived torrefaction system (EL_{TS}, MJ) and the final energy content (dry basis) of torrefied biomass (EC_{TDM}, MJ). The total external energy required by the torrefaction system ($ER_{(CNG-TS)}$, MJ), total input energy to the torrefaction system (EI_{TS}, MJ), total output energy from the torrefaction system (EO_{TS}, MJ), and energy efficiency of the torrefaction system ($\eta_{(EBC-TS)}$, %) were the outputs of this module.

-the total input energy to the torrefaction system, constituted the original energy content of the dry matter (EC_{dm}) and the total external energy supplied to the torrefaction system in the form of CNG ($ER_{(CNG-TS)}$) (Relation 3).

$$EI_{TS} = EC_{dm} + ER_{(CNG-TS)} \quad \text{.....(3)}$$

EO_{TS}-the total energy output from the torrefaction system, constituted the final energy content of the torrefied biomass (EC_{TDM}) and the overall energy loss in the torrefaction system (EL_{TS}) (Relation 4).

$$EO_{TS} = EC_{TDM} + EL_{TS} \quad \text{.....(4)}$$

Although EO_{TS} was the total output energy, only EC_{TDM} was the useful form of energy as its EL_{TS} component was the total energy loss from the system. Thus, the energy efficiency of the overall torrefaction system ($\eta_{(ER-TS)}$, %) was estimated using relation 6.

$$\eta_{(ER-TS)} = \frac{EC_{TDM}}{EO_{TS}} \quad \text{.....(6)}$$

5.6.2.7 Cost estimation

A cost module was developed to account for different costs associated with the establishment and the operation of the conceived large-scale torrefaction system. Costs were broadly classified as capital and operating costs.

Capital cost estimation

Costs associated with purchasing the required equipment for a production scale torrefaction system, such as the torrefaction chamber, combustor, heat exchanger, and building infrastructures to house and operate those equipments were categorized as capital costs. Currently production-scale torrefaction systems, similar to the one conceived in this study, are not commercially available. However, ballpark estimates are being made. For instance, Sklar has suggested the costs for torrefaction plants capable of processing between 1,500 and 2,000 ton.d^{-1} of wood waste or 750 to 1,000 ton.d^{-1} of dry chips to be in between $10M and 16M, [27] depending on the technology used. In this study, estimates for capital costs of production-scale torrefaction systems were made based on suggested values in the literature and discussions with potential suppliers. Sensitivity analysis was performed to determine the variability of unit torrefaction cost for a specific range of capital costs. Capital cost for the complete torrefaction system with rated production capacity of 25 Tton.hr^{-1} was considered to be in the range $2.5-7.5 million. On a unit capacity (Tton.hr^{-1}) basis, capital cost would deduce to $0.1-0.3 million per (Tton.hr^{-1}) per useful life of the system. Useful life of the torrefaction system was taken as 30 years,[28] and the interest rate of investment as 8%. Based on the aforementioned values, amortized capital cost ($-yr^{-1}) of the system was estimated.

The assumption was made that the torrefied biomass would be produced at the use efficiency (η_{use}, %) of 80%. This signifies the torrefaction system would operate for 80% of the total designated time, with 20% of the designated time being designated for maintenance. Total designated time comprised of daily operation duration (OD_{hpd}, hr.d^{-1}) of 24 hr.d^{-1}, monthly operation duration (OD_{dpm}, d.mo^{-1}) of 30 d.mo^{-1}, and yearly operation duration (OD_{mpy}, mo.yr^{-1}) of 2-10 mo.yr^{-1}. Thus, for the rated production capacity ($Cap_{(TS-Tph)}$, Tton.hr^{-1}) of 25 Tton.hr^{-1}, actually produced annual quantity of torrefied biomass ($Cap_{(TS-Tpy)}$, Tton.yr^{-1}) was estimated using relation 7.

$$Cap_{(TS-Tpy)} = (\eta_{use} \times Cap_{(TS-Tph)}) \times OD_{hpd} \times OD_{dpm} \times OD_{mpy} \quad \text{.....(7)}$$

Lastly, the unit capital cost of the conceived large-scale torrefaction system ($-Tton^{-1})

was estimated as the ratio of amortized capital cost and annual actual production capacity of the torrefaction system.

Operating cost estimation

Costs associated with the operation of the torrefaction system were categorized as operating costs. Operating costs included energy and labor costs, ownership costs (costs of insurance, repair and maintenance, and taxes), and costs associated with torrefaction DML (i.e., effect of torrefaction DML on harvest cost). The unit energy cost ($\$\text{-Tton}^{-1}$) was estimated as the product of external energy required to torrefy each ton of biomass and the unit cost of CNG of 0.0038 $\$\text{-MJ}^{-1}$.[29] The external energy supply required to produce each ton of torrefied biomass was estimated as the ratio of total external energy required by the torrefaction system (Section 2.8) and the total mass of torrefied biomass. For the continual operation of the conceived torrefaction system, a staff of five people for the rated duration was considered and the labor cost including benefits was estimated at the rate of 20 $\$\text{-person-hour}^{-1}$.

The next important category of the operating cost was the cost associated with torrefaction DML, which has a direct impact on the harvest and collection cost as physical loss of harvested biomass occurs during torrefaction. The cost of torrefaction DML was estimated as the product of torrefaction DML and unit harvest and collection costs. Harvest and collection costs were taken as 30 $\$\text{-ton}^{-1}$.[30] In addition to this, unit ownership costs, including costs for repair and maintenance, insurance and taxes on the equipment and infrastructure, were estimated at 2% of the total capital cost, as suggested by Gay and Grisso.[31] Finally, the unit operating costs for different operations were estimated as the sum of unit energy, labor, DML, and ownership costs.

Unit torrefaction system process cost

Unit cost for producing torrefied biomass ($\$\text{-Tton}^{-1}$) was estimated as the sum of unit capital and operating costs, and the unit torrefaction cost, based on energy contained in torrefied biomass ($\$\text{-MJ}^{-1}$), was estimated as the ratio of unit torrefaction cost and unit energy density of torrefied biomass.

5.6.2.8 Sensitivity analysis

Sensitivity analysis was performed to ascertain the influence of different input parameters, including the initial moisture content of biomass, torrefaction process temperatures, operating windows and initial capital investment, on different energy and cost results of the production-scale torrefaction system. Some of the main output parameters included torrefaction process DML, net energy required for the torrefaction of feedstock within the conceived system, energy efficiency of the torrefaction system or the energy available in torrefied biomass as a fraction of total external energy supplied to the conceived system, unit torrefaction cost, and unit energy and DML costs. Sensitivity analysis was performed by varying single input parameters at a time, while keeping all other variables fixed at their typical values. Typical values and the ranges of different input parameters for sensitivity analysis were based on the most likely operating conditions (explained in sections 2.1-2.7), and are summarized in table 2.

Table 2: Input parameters for sensitivity analysis, their typical values and anticipated ranges of variability:

Parameters	Typical Values	Variations Considered
Initial Moisture Content ($\%_{wb}$)	30	0, 10, 20, 30, 40, 50, 60
Torrefaction Temperature (°C)	240	200, 220, 240, 260, 280 300
Use Period ($mo.yr^{-1}$)	6	2, 4, 6, 8, 10
Capital Cost ($M\$-(Tton.hr^{-1})^{-1}.Useful\ life^{-1}$)	0.3	0.1, 0.2, 0.3

5.6.3 RESULTS AND DISCUSSIONS

5.6.3.1 Torrefaction process dry matter yield

Torrefaction process dry matter yield (Section 2.4) decreased with increasing initial moisture content of biomass and increasing torrefaction process temperatures (Figure 2). For initial moisture contents of biomass in the range 0-60%$_{wb}$, torrefaction process dry matter yields were in the ranges 91-99% and 52-60%, respectively for the process temperatures of 200 and 300°C. Dry matter yield results obtained from the model had similar trends as the experimentally obtained results by previous studies.[2, 6, 8-12, 15, 16] These studies were based on the torrefaction of a vast range of cellulosic biomass, including energy crops, agricultural residues and forest products, at different process temperatures.

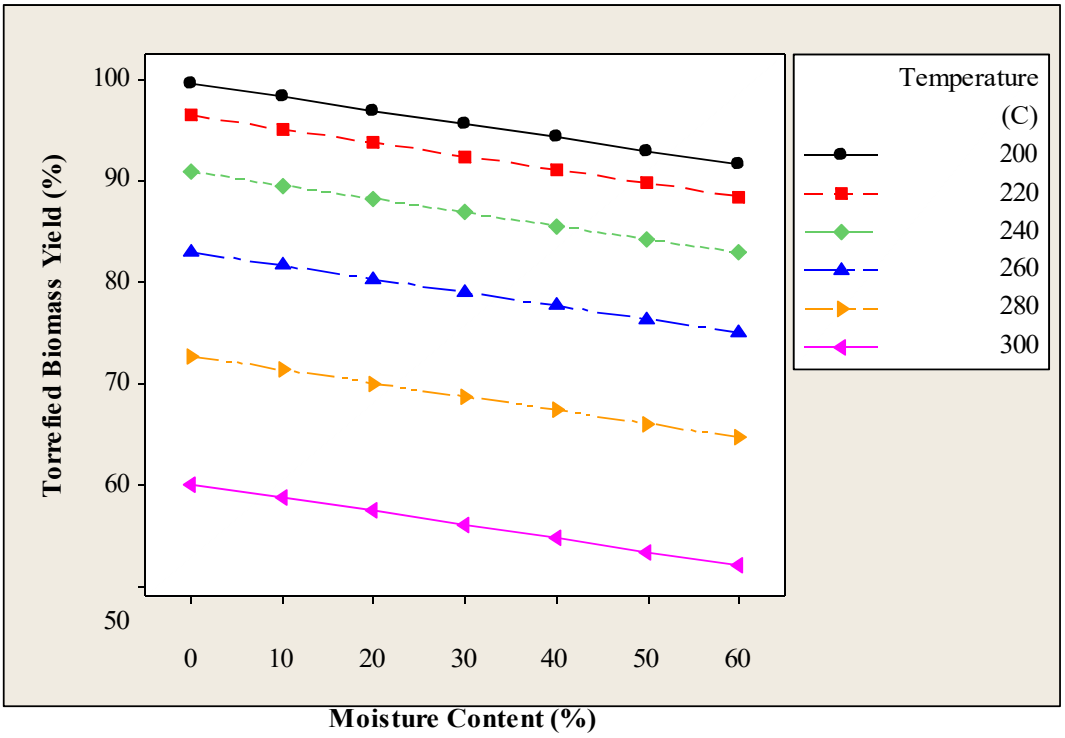

Figure 2: Dry matter yield from the torrefaction of biomass with different initial moisture contents at different process temperatures.

5.6.3.2 Torrefaction process energy results

Net external energy required to complete the torrefaction process and the fraction of total input energy contained in final torrefied biomass are included as the torrefaction process energy results, and are presented in graphical forms in figures 3 and 4, respectively. For the analysis, initial moisture contents of biomass were considered to be in the range 0-60%$_{wb}$, and the range of torrefaction process temperatures were taken as 200-300°C. Net external energy required is the total external energy (CNG) supplied to obtain each ton of torrefied biomass, and the fraction of energy available in torrefied biomass is the energy efficiency of the torrefaction system (Section 2.8).

With the increase in initial moisture content of the biomass, net external energy required to torrefy biomass at different process temperatures increased (Figure 3), and the energy efficiency of the torrefaction system decreased (Figure 4). These torrefaction energy trends were primarily due to the need to supply higher amounts of energy to dry biomass with higher initial moisture contents. Thus, for biomass with higher initial moisture content, a comparatively lower fraction of total energy supplied was utilized for the actual torrefaction process when compared to the same wet mass of biomass with lower initial moisture content. This resulted in the requirement of higher net energy to produce unit mass of torrefied biomass and lower fraction of net energy contained within torrefied biomass for higher initial moisture content feedstock.

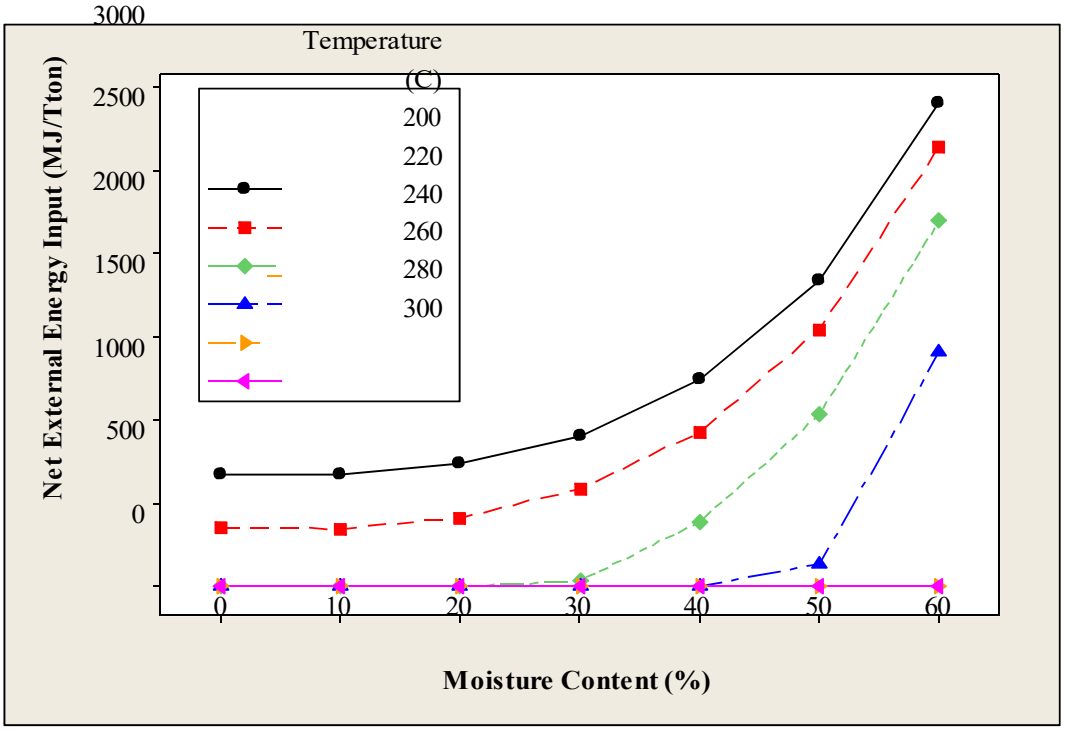

Figure 3: Net external energy required to complete the torrefaction process for biomass with different initial moisture contents at different torrefaction process temperatures.

Further observation of the torrefaction process energy results showed the net energy required to torrefy biomass at different initial moisture contents decreased with the increase in the torrefaction process temperatures (Figure 3). This was due to the availability of a higher

quantity of heat energy in torrefaction system products and by-products, including hot torrefied

biomass and combustible volatiles and steam, produced at higher process temperatures. Moreover, heat energy contained in the torrefaction system products and by-products were recovered, resulting in the reduction of overall external heat energy required for the process. In addition to this, some conditions existed when recovered heat was sufficient to operate the torrefaction system, eliminating the need to supply external heat. Such conditions were classified as "auto-thermal operating conditions". All the operating conditions at and below 0 $MJ.ton^{-1}$ "net energy input"-line (Figure 3) were auto-thermal operating conditions for the conceived large-scale torrefaction system. Any operation below the auto-thermal energy line would internally recover more energy than actually required and the additional waste heat would be lost in the system. The auto-thermal operating conditions existed at higher initial moisture contents for higher torrefaction process temperatures (Figure 3). This was due to higher quantity of heat energy recovered in processes occurring at higher temperatures. However, auto-thermal operation of the torrefaction system cannot always be considered as the best operating scenario as auto-thermal operating points exist at higher process temperatures where torrefaction DML is also higher. For 300°C, torrefaction system operated auto-thermally for all considered moisture levels (i.e., 0-60%$_{wb}$); however, for 200-220°C, auto-thermal conditions didn't exist. For the typical process temperature of 240°C, auto-thermal operation was possible at feedstock moisture contents of 20%$_{wb}$ and below.

Net energy contained in torrefied biomass exhibited decreasing trends with increasing torrefaction process temperatures for biomass with different initial moisture contents (Figure 4). This was due to higher mass loss at higher process temperatures, as explained earlier. It was assumed the lost fraction of mass would be completely converted to volatiles. Furthermore, it was considered that heat energy was recovered from the volatiles by combusting them at 60% efficiency. Thus, some energy was used for converting biomass to volatiles and some energy loss occurred during energy recovery from the volatiles, resulting in the decrease in energy efficiency at higher torrefaction process temperatures. Results for energy efficiency obtained from the model had similar trend to the experimentally obtained results by previous studies.[2, 6, 12, 15, 16, 19]

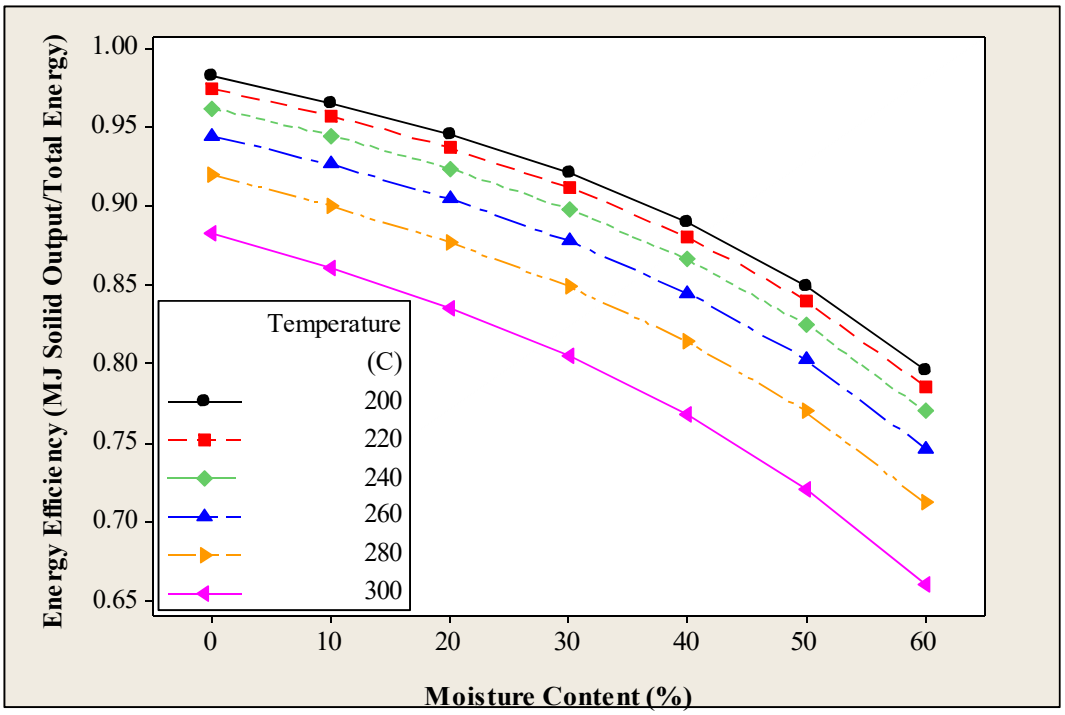

Figure 4: Fraction of total input energy contained within torrefied biomass obtained from the torrefaction of biomass with different initial moisture contents at different process temperatures.

5.6.3.3 Torrefaction process cost results

Unit costs and sub-costs for torrefying biomass with different initial moisture contents at different process temperatures for different operating windows and different initial capital investments are presented as torrefaction process cost results in figures 5-8. Typical values of input parameters for different analyses are included in table 2. For the typical feedstock moisture content of 30%$_{wb}$, process temperature of 240°C, plant operating window of 6 mo.yr^{-1} and initial capital investment of 0.3M \$-(Tton.hr^{-1})$^{-1}$.(Useful Life)$^{-1}$, unit torrefaction process cost was estimated to be nearly 17.5 \$-Tton^{-1} (Figure 5).

Unit torrefaction cost, and energy and DML sub-costs for the torrefaction of biomass with different initial moisture contents at different process temperatures are presented in figures 5 and 6, respectively. For different torrefaction process temperatures, all three costs increased with the increment in the initial moisture content of the biomass. However, energy costs for torrefying the feedstocks at and below auto-thermal operating conditions, as discussed in section 3.3, were 0 \$-Tton^{-1} because external energy was not required for operating the system under such conditions. Moreover, in this study, energy "credit" was not allocated to the excess heat at and below auto-thermal operating conditions that could be recovered and further utilized for other processes. In addition to this, energy costs increased with the increment in the initial moisture content of the feedstock as more energy was required for drying higher initial moisture feedstocks (Figure 6). Torrefaction DML costs also increased with the increment in the initial moisture content of the biomass (Figure 6) as torrefied dry matter yield decreased with increasing moisture content (Figure 2), resulting in increased DML. As energy and DML costs increased with increasing feedstock moisture content, and other capital and operating costs were

not dependent on feedstock's moisture contents, total torrefaction costs exhibited increasing trends with the increasing initial moisture content of the biomass.

For the biomass with initial moisture contents in the range 0-60%$_{wb}$, unit torrefaction process costs were in the range 16-27 \$-Tton^{-1} at the typical process temperature of 240°C. This signifies the unit torrefaction costs increased by 69% as the moisture content increased from 0 to 60%$_{wb}$. Thus, moisture content is one of the most influential parameters in the torrefaction process and will play an important role for the ultimate deployment, commercialization and overall success of large-scale torrefaction systems. There exists the need to determine optimal techniques for reducing the moisture content of the feedstocks before torrefying them and to perform the techno-economic analyses to assess the best option for moisture reduction before torrefaction. Some techniques for the moisture reduction might include harvesting at lower moisture contents and pre-drying biomass in alternative systems before torrefaction.

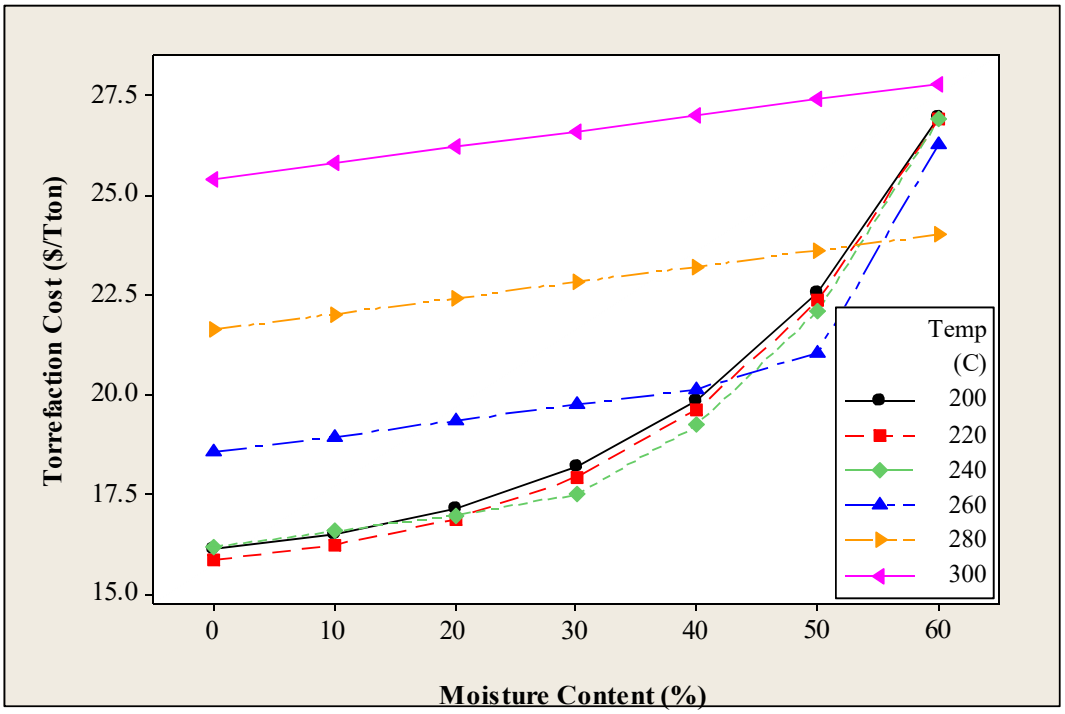

Figure 5: Unit torrefaction costs for biomass with different initial moisture contents torrefied at different process temperatures (initial capital costs were taken as 0.3M \$-Tton.hr^{-1})$^{-1}$.(useful life)$^{-1}$ and plant operating period as 6 mo.yr^{-1}).

For different initial moisture contents of the biomass, torrefaction DML costs increased and the energy costs decreased with the increase in the torrefaction process temperatures (Figure 6). As discussed in section 3.2, net energy required for the torrefaction process decreased with the increase in the process temperature, hence, the energy costs decreased for torrefaction at higher process temperatures. But, as discussed in section 3.1, torrefaction dry matter yield decreased for higher process temperatures, thus, resulting in the increase in DML and associated costs. Other operating and capital costs were independent of torrefaction process temperatures, and the unit torrefaction costs were higher for higher process temperatures (Figure 5). This signifies that DML costs had a higher impact than energy costs on the overall torrefaction process cost, as the overall cost followed DML cost trends, for the conceived production-scale torrefaction system. This emphasizes the need to operate at optimal process temperature rather

than very high temperatures in an attempt to achieve auto-thermal operating conditions at the expense of increased torrefaction DML.

For the feedstock with typical initial moisture content of 30%$_{wb}$ and the torrefaction process temperatures in the range 200-300°C, estimated unit torrefaction process costs were in the range 17-27 \$-Tton^{-1}. The unit torrefaction cost decreased from 18 to 17.5 \$-Tton^{-1} for the increase in process temperature from 200 to 240°C, and then increased to 27 \$-Tton^{-1} for the process temperature of 300°C. Unit torrefaction cost changed by 59% for the process temperature in the range 200-300°C. Thus, studies to predict the optimal torrefaction process temperature with regards to the cost and quality would be one of the major steps towards the sustainability and overall success of conceived production-scale torrefaction systems.

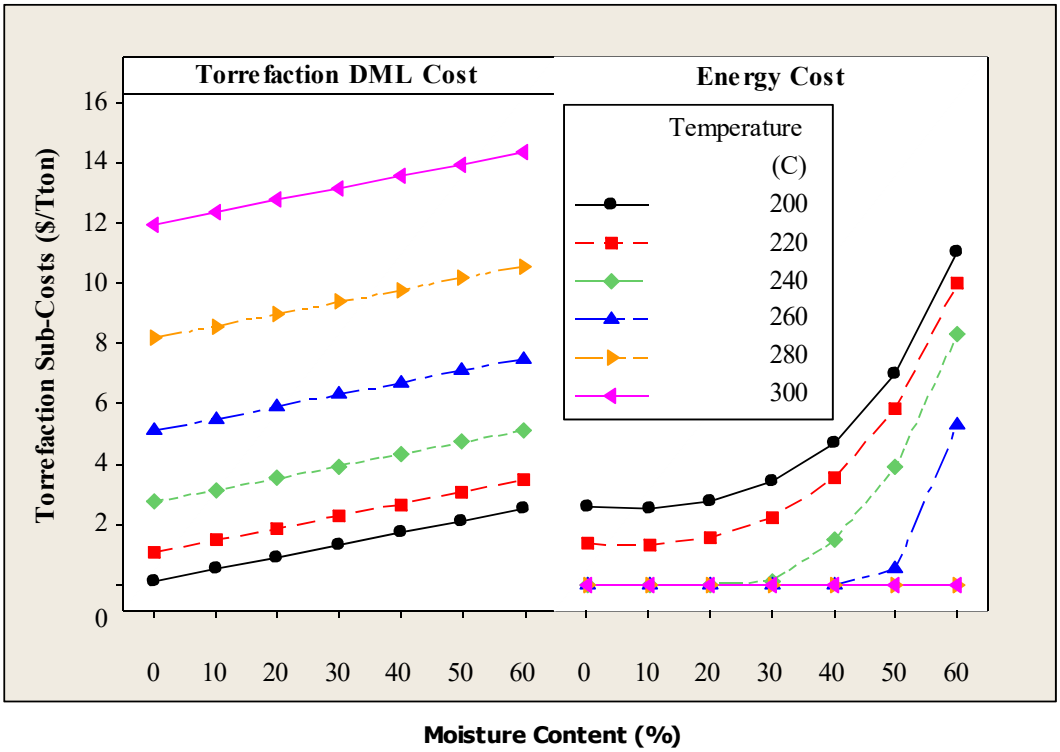

Figure 6: Unit torrefaction sub-costs (energy and DML costs) of biomass with different initial moisture contents torrefied at different process temperatures (initial capital cost was taken as 0.3M \$-(Tton.hr^{-1})$^{-1}$. (useful life)$^{-1}$ and plant operating period as 6 mo.yr^{-1}).

Unit torrefaction process cost increased with the decrease in the operating window (mo.yr^{-1}) (Figure 7). This was due to lower overall torrefied material throughput for shorter operating periods when compared to the extended operating periods for the torrefaction systems with the same capacities and ratings. For plant operating windows in the range 2-10 mo.yr^{-1}, unit process costs for torrefying biomass with 30%$_{wb}$ moisture at 240°C in plant with initial capital investment of 0.3M \$-(Tton.hr^{-1})$^{-1}$ were in the range 13-37 \$-Tton^{-1}; with higher costs being attributed to the shorter operating durations. This shows the unit torrefaction cost increased by 185% for the decrease in the operation window from 10 to 2 mo.yr^{-1}. Thus, operating window is the other most important metric for the sustainability of conceived large-scale system, and there exists the need to decide the optimal operating window of such systems with regards to preserving the feedstock qualities and meeting the biorefineries continuous feedstock demand, while reducing the overall cost. This might be accomplished by making such systems accessible

to sites where feedstock with different harvest seasons are grown and storage sites capable of accommodating multiple feedstock types are available.

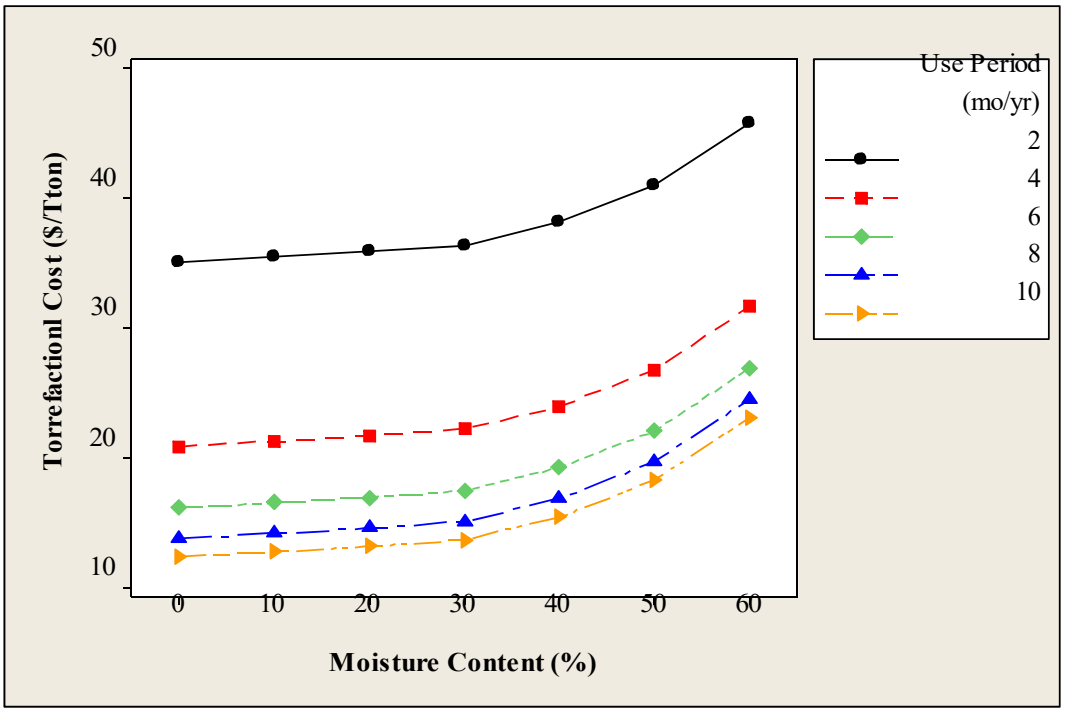

Figure 7: Unit torrefaction cost of biomass with different initial moisture contents torrefied at 240°C for different plant operating periods (initial capital cost was taken as 0.3M $\$\text{-}(\text{Tton.hr}^{-1})^{-1}.(\text{useful life})^{-1}$).

Unit torrefaction process costs increased with the increase in the initial capital costs ($\$\text{-}(\text{Tton.hr}^{-1})^{-1}.(\text{useful life})^{-1}$) for purchasing the torrefaction system (Figure 8). For torrefaction plant with initial capital investment in the range 0.1-0.3M $\$\text{-}(\text{Tton.hr}^{-1})^{-1}$, unit process costs for torrefying biomass with $30\%_{wb}$ moisture at 240°C over the operating window of 6 mo.yr^{-1} were in the range 11-18 $\$\text{-Tton}^{-1}$. This shows the unit torrefaction cost increased by 64% with the increase in the capital investment from 0.1M to 0.3M $\$\text{-}(\text{Tton.hr}^{-1})^{-1}$. Initial capital cost is one of the other most important metrics for the economic sustainability of production-scale torrefaction systems; similar to the one conceived in this study. Thus, the need exists for research towards developing systems with higher efficiency and lower capital costs.

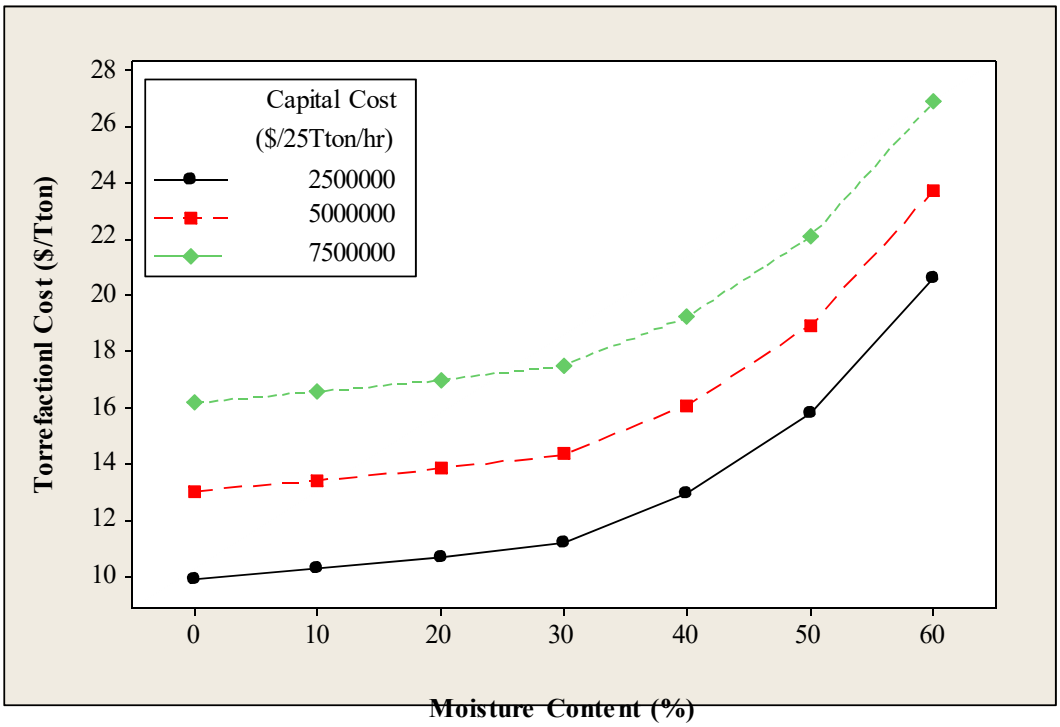

Figure 8: Sensitivity of unit torrefaction cost of feedstocks, with different initial moisture contents torrefied at 240°C, on different initial capital costs of torrefaction system (plant operating period was taken as 6 mo.yr^{-1}).

5.6.4 CONCLUSIONS

A model to simulate the mass and energy balance, and the techno-economic aspects of a production-scale torrefaction system was successfully developed and executed to trace the effects of variability in the system's input parameters, including the initial moisture content of biomass, torrefaction process temperatures, plant operating windows and initial capital investments, on system's output parameters, including net energy requirements, energy recovery potentials, dry matter changes, and different torrefaction process costs. Main findings of this study include:

- Torrefied dry matter yield decreased with the increase in torrefaction process temperatures and the initial moisture content of biomass.
- Analyses of energy results revealed the net energy required for the torrefaction process increased and the energy efficiency of the torrefaction system decreased with the increase in initial moisture content of the biomass. However, both of these energy metrics exhibited a decreasing trend with the increasing process temperatures.
- In the conceived system, some auto-thermal operating conditions existed, especially for biomass with lower initial moisture contents torrefied at higher process temperatures. Although external energy was not required to operate the system under auto-thermal conditions, torrefaction DML was higher. For the typical moisture content of 30%$_{wb}$, process temperature of 240°C, plant operating window of 6 mo.yr^{-1} and initial capital investment of 0.3M \$-(Tton.hr^{-1})$^{-1}$, estimated unit torrefaction process cost was 17.5 \$-Tton^{-1}.

- Sensitivity analyses on the cost results showed the unit torrefaction process cost had increasing trends with increasing initial moisture content of the biomass, increasing torrefaction process temperatures, decreasing plant operating windows and increasing initial capital investments.

The performances of large-scale torrefaction systems can be further enhanced by optimizing the torrefaction process temperatures, evaluating cost-effective pre-drying technologies to reduce initial moisture contents of biomass, designing systems capable of handling multiple feedstock types to widen the plant operating windows, and advancing technology to reduce the initial capital investment. Lastly, to form the sustainable and cost-effective feedstock supply chain, a production-scale torrefaction system needs to be integrated with other large-scale biomass preprocessing or upgrading processes, including drying, grinding, pelletization, and briquetting, at the central facilities.

ACKNOWLEDGEMENTS

This research was supported by Iowa State University's Biobased Industry Center (BIC).

REFERENCES

1. BRDI, *Increasing feedstock production for biofuels: Economic drivers, environmental implications, and the role of research*. Biomass Research and Development Board, Washington, DC (2008).
2. Arias B, Pevida C, Fermoso J, Plaza MG, Rubiera F and Pis J, Influence of torrefaction on the grindability and reactivity of woody biomass. *Fuel Process Technol* **89**:169–175 (2008).
3. Bergman PCA, *Combined torrefaction and pelletization: The TOP Process*. ECN Project Report ECN-C-05-073. ECN, Petten, the Netherlands (2005).
4. Bergman PCA and Kiel JHA, Torrefaction for Biomass Upgrading. In *Proceedings of 14th European Biomass Conference and Exhibition*. Paris, October 17–21 (2005).
5. Bergman PCA, Boersma AR, Zwart RWR and Kiel JHA, *Torrefaction for biomass co-firing in existing coal-fired power stations 'BIOCOAL'*. ECN Project Report ECN-C-05-013. ECN, Petten, the Netherlands (2005).
6. Bridgeman TG, Jones JM, Shield I and Williams PT, Torrefaction of reed canary grass, wheat straw and willow to enhance solid fuel qualities and combustion properties. *Fuel* **87**:844–856 (2008).
7. Kiel JHA, Verhoeff F, Gerhauser H, Daalen W and Meuleman B, *BO_2-Technology for biomass upgrading into solid fuel-an enabling technology for IGCC and gasification-based BtL*. ECN Project Report ECN-M-09-058. ECN, Petten, the Netherlands (2009).
8. Mani S, Integrating biomass torrefaction with thermo-chemical conversion processes. Paper 160229. In *Proceedings of the 2009 AIChE Annual Meeting*, Nashville, TN, November 8-13 (2009).
9. Medic D, Darr M, Potter B and Shah A, *Effect of torrefaction process parameters on biomass feedstock upgrading*. Paper 1009316. Annual International Meeting of the ASABE, Pittsburgh, PA, June 20-23 (2010).
10. Prins MJ, Ptasinski KJ and Janssen FJJG, Torrefaction of wood part 1: weight loss kinetics. *J Anal Appl Pyrol* **77**:28-34 (2006a).

11. Sadaka S and Negi S, Improvements of biomass physical and thermochemical characteristics via torrefaction process. *Environmental Progress & Sustainable Energy* **28**(3):427-434 (2009).
12. Zanzi R, Ferro DT, Torres A, Soler PB and Bjornbom E, Biomass torrefaction. In *6th Asia-Pacific International Symposium on Combustion and Energy Utilization*. Kuala Lumpur, Malaysia (2002).
13. Bergman PCA, Boersma AR, Kiel JHA, Prins MJ, Ptasinski KJ and Janssen FJJG, *Torrefaction for entrained-flow gasification of biomass*. ECN Project Report ECN-RX-04-046. ECN, Petten, The Netherlands (2004).
14. Couhert C, Salvador S and Commandre J, Impact of torrefaction on syngas production from wood. *Fuel* **88**:2286-2290 (2009).
15. Pimchuai A, Dutta A and Basu P, Torref action of agriculture residue to enhance combustible properties. *Energ Fuel* **24**:4638-4645 (2010).
16. Yan W, Acharjee TC, Coronella CJ and Vasquez RV, Thermal pretreatment of lignocellulosic biomass. *Environmental Progress & Sustainable Energy* **28**(3): 435-440.
17. Yan W, Hastings JT, Acharjee TC, Coronella CJ and Vasquez RV, Mass and energy balances of wet torrefaction of lignocellulosic biomass. *Energ Fuel* **24**(9):4738–4742 (2010).
18. Felfili FF, Luengo CA, Suarez JA and Beaton PA, Wood briquette torrefaction. *Energy for Sustainable Development* **9**(3): 19-22.
19. Prins MJ, Ptasinski KJ and Janssen FJJG, Torrefaction of wood part 2: analysis of products. *J Anal Appl Pyrol* **77**:35-40 (2006b).
20. Repellin V, Govin A, Rolland M and Guyonnet R, Energy requirement for fine grinding of torrefied wood. *Biomass Bioenerg* **34**:923-930 (2010).
21. Janse AMC, Westerhout RWJ and Prins W, Modeling of flash pyrolysis of a single wood particle. *Chem Eng Process* **39**:239-252 (2000).
22. Lathouwers D and Bellan J, Modeling of biomass pyrolysis for hydrogen production: the fluidized bed reactor. In *Proceedings of the 2001 DOE Hydrogen Program Review*, Baltimore, MD (2001).
23. Bennett AS, Bern CJ, Richard TL and Anex RP, Corn grain drying using corn stover combustion and CHP systems. *T ASABE* **50**(6): 2161-2170 (2007).
24. Scurlock J, *Bioenergy feedstock characteristics-Fact Sheet*. Bioenergy Feedstock Development Program, ORNL, Oak Ridge, TN (2001).
25. Prins MJ, Ptasinski KJ and Janssen FJJG, More efficient biomass gasification via torrefaction. *Energy* **31**: 3458-3470 (2006c).
26. Ulrich GD, *A guide to chemical engineering process design and economics*. John Wiley and Sons, New York, NY (1984).
27. Sklar T, *Torrefied wood, a bio-energy option that is ready to go: A Biomass Digest Special Report*. [Online]. Biomass Digest-31 December 2009 Issue. Available at: http://biomassdigest.net [8 June 2010].
28. Bepex, *Torrefaction and densification of biomass fuels for generating electricity*. Contract RD3-4. Bepex International LLC, Minneapolis, MN (2010).
29. US EIA, *Natural gas weekly update*. [Online]. US Energy Information Administration. Available at: www.eia.doe.gov [10 February 2011].
30. Hess JR, Wright CT and Kenney KL, Cellulosic biomass feedstocks and logistics for ethanol production. *Biofpr* **1**:181-190 (2007).

31. Gay SW and Grisso R, *Planning for a farm storage building*. Publication 442-760. Virginia Cooperative Extension, Blacksburg, VA (2009).

Notations

$Cap_{(TS-Tph)}$	rated production capacity, Tton.hr^{-1}
$Cap_{(TS-Tpy)}$	actual annual production of torrefied biomass, Tton.yr^{-1}
EC_{dm}	energy content of dried biomass, MJ
EC_{TDM}	energy content of torrefied biomass, MJ
$EDen_{TDM}$	energy density of torrefied biomass, MJ.kg^{-1}
EI_{TS}	total input energy to the torrefaction system, MJ
EL_{TS}	total energy loss within the torrefaction system, MJ
EO_{TS}	total output energy from the torrefaction system, MJ
$ER_{(CNG-TS)}$	total external energy (in form of CNG) required for the completion of all operations within the torrefaction system, MJ
MC	initial moisture content of biomass (wet basis), $\%_{wb}$
$ML\%_{Tor}$	torrefaction DML, %
OD_{hpd}	daily operation duration, hr.day^{-1}
OD_{dpm}	monthly operation duration, day.month^{-1}
OD_{mpy}	yearly operating window, month.yr^{-1}
T_{Tor}	torrefaction process temperature, °C

Greek Letters

$\eta_{(ER-TS)}$	energy efficiency of the torrefaction system, %
η_{use}	use efficiency of the torrefaction system, %

Abbreviations

CNG	compressed natural gas
DML	dry matter loss
M	million
Tton	metric ton of torrefied biomass

5.7 Physicochemical properties of bio-oil and biochar produced by fast pyrolysis of different stored and torrefied single-pass corn stover and cobs

Ajay Shah, Matthew J. Darr, Dorde Medic, Brittany Schon, Keith Webster, Kevin Peyton and Jeremy Brue

(to be published in a peer-review journal)

ABSTRACT

Renewed interest in biomass based energy necessitates the evaluation of fast pyrolysis technique as a mean to convert biomass into liquid fuel. Although researchers are heavily involved in investigating multifarious aspects of fast pyrolysis of different cellulosic feedstock, attention is lacking towards the exploration of the fast pyrolysis characteristics of stored biomass. This study investigated the yields and the physiochemical properties of the fast pyrolysis products obtained from single-pass corn (*Zea mays*) stover and cobs stored in different ways. For comparison, stored multi-pass stover, and stored and torrefied single-pass stover were also pyrolyzed. Five different biomass samples were pyrolyzed in a 183 cm long and 2.1 cm inner diameter free-fall fast pyrolysis reactor. The physiochemical properties of bio-oil and biochar from different biomass were characterized with their moisture, ash, volatile matters, carbon, hydrogen, nitrogen and oxygen contents. In addition to these, higher heating values were determined for both bio-oil and biochar, and the acidity was measured for bio-oil. Yields of bio-oil, biochar and non-condensable gases from different biomass samples were in the ranges of 40-55, 25-36 and 11-22 wt.%, respectively, with the highest bio-oil yield from the ensiled single-pass corn stover and the lowest from the torrefied single-pass stover. Moisture and ash contents of bio-oils from different samples were in the ranges of 34-52 and 0.1-0.2 wt.%, respectively, and were not significantly different at 95% confidence interval. Bio-oil generated from ensiled single-pass cobs and torrefied single-pass stover were respectively the most and the least acidic with the modified acid numbers of 95.0 and 57.1 mg g^{-1}, respectively.

Keywords: fast pyrolysis, free fall pyrolyzer, bio-oil, corn stover and cobs, physiochemical properties.

5.7.1 INTRODUCTION

In recent years, biorenewable energy sources are being promoted in different nations across the globe to reduce their reliance on imported fossil fuels and to mitigate the environmental impacts associated with the fossil fuels utilizations. Moreover, the potential to convert biomass directly to the liquid fuel, the presence of excess agricultural production capacity in many countries, and the importance of rural development in improving economies of many agricultural regions favor the utilization of biorenewable resources. In the United States, Energy Independence and Security Act (EISA) of 2007 has mandated the production of 136.3 million m^3 (36 billion gal) of renewable biofuels, including 60.6 million m^3 (16 billion gal) of cellulosic biofuels by 2022; and the corn stover is the most abundant agriculture residue and primary feedstock for cellulosic biofuels production in the Midwestern United States. Corn stover is annually harvested within a short window (typically 1-3 months); thus, requiring storage to fulfill year-round demand of biorefineries. Additionally, corn stover has low bulk density and bulk flowability; thus, it is advantageous to convert it to the liquid form before

transportation, and one of the techniques to do so, which is also the subject of this study, is fast pyrolysis.

Fast pyrolysis is the rapid thermal decomposition of organic compounds in the absence of oxygen and at moderate temperatures (400-600°C) to produce liquids (bio-oil), solids (biochar) and non-condensable gases. Residence times for fast pyrolysis of biomass is shorter (0.5-2 s) which is followed by rapid cooling and condensation of the formed pyrolysis vapors (Bridgwater et al., 1999; Brown, 2003; Venderbosch and Prins, 2011). Detailed discussions on the fundamentals and the state-of-the-art of fast pyrolysis, different pyrolysis reactor types, properties of pyrolysis products and their potential end-uses are explained elsewhere (Bridgwater, 2011; Laird et al., 2009; Mohan et al., 2006; Oasmaa and Czernik, 1999). Additionally, different researchers have successfully investigated different important aspects of fast pyrolysis of different biomass types.

This study focuses on the fast pyrolysis of stored corn (*Zea mays*) stover and cobs with the vision that pyrolyzing stover early in the supply chain would be advantageous in that each pyrolysis product can be separately delivered to their potential end-use sites. For instance, bio-oil can be transported to biorefineries for further processing and upgrading whereas biochar can be transported to fields for their potential soil-application and carbon sequestration. It can be argued that the corn stover can be pyrolyzed before storage; however, the potential issues like phase separation and aging of bio-oil during storage (Bridgwater et al., 2011; Mohan et al., 2006; Oasmaa and Czernik, 1999; Yu et al., 2007) as well as the need of higher throughput pyrolyzer to pyrolyze all biomass upon receipt at the storage site, thus, increasing the unit conversion price due to the increased capital and operating cost of the pyrolyzer would make it advantageous to store the biomass first, followed by the pyrolysis before transportation of different pyrolysis products to their respective end-use locations.

As per author's best knowledge, only Agblevor et al. (1995) has investigated the properties of the pyrolysis products from stored biomass feedstocks. They pyrolyzed fresh, and 26 and 52 weeks outside stored corn stover feedstock and found the increase in bio-oil yield for stover stored for longer durations. There is a need to investigate more into the fast pyrolysis behavior of different stored biomass. Thus, in this study single and multi-pass corn stover and cobs were stored in different ways and/or upgraded via torrefaction before pyrolysis. Details of the storage characteristics and torrefaction of cellulosic biomass has been discussed elsewhere (Medic et al., 2012; Shah et al., 2011a, 2011b; Shinners et al., 2007). The main objective of this study was to investigate the effects of different storage methods for single-pass corn stover and cobs on the physiochemical properties of different pyrolysis products. In addition to these, stored multi-pass stover and stored and torrefied single-pass stover were also pyrolyzed to see the differences in properties of pyrolysis products obtained from them when compared to those obtained from single-pass stover and cobs. Yields of different pyrolysis products for different biomass were determined, and the physiochemical properties of bio-oil and biochar from different biomass were characterized with their moisture, ash, volatile matters, carbon, hydrogen, nitrogen and oxygen contents. In addition to these, higher heating values were determined for both bio-oil and biochar, and acidity was measured for bio-oil.

5.7.2 MATERIALS AND METHODS

5.7.2.1 Biomass preparation

Corn stover and cobs used in this study were harvested as: (1) single-pass corn stover bales, (2) multi-pass corn stover bales, and (3) single-pass bulk corn cobs, within 10 days between 6 and 15 October 2010 at Iowa State University research farms located in Boone and Story counties. The collected stover and cobs were stored for 4.5 months and/or upgraded for the pyrolysis test in five different ways: (1) multi-pass corn stover bales stored inside a metal building, (2) single-pass corn stover bales stored inside a metal building, (3) single-pass corn stover bales stored outdoor in a plastic tube-wrap, (4) single-pass corn cobs stored in a plastic bag, and (5) single-pass corn stover bales stored inside a metal building followed by torrefying at 250°C for 30 min. In different tables of this paper, these five different biomass samples will respectively be designated as: (1) multi-pass corn stover (inside), (2) single-pass corn stover (inside), (3) single-pass corn stover (ensiled), (4) single-pass corn cobs (ensiled), and (5) single-pass corn stover (torrefied). Different samples were then dried down to less than 5%$_{wb}$ moisture content and were ground and sieved to 300-750 microns particle size range.

5.7.2.2 Pyrolysis

Pyrolysis tests were conducted using a free-fall pyrolyzer as described by Ellens and Brown (2011). The 183 cm long and 2.1 cm inner diameter free fall pyrolyzer provides a residence time of approximately 1.5 s. Watlow® ceramic heaters along the length of the reactor set are used to radiatively heat the reactor for its isothermal operation. To provide a reaction temperature of approximately 500°C, the heaters were set at 550°C. Ground and sieved samples were fed to the pyrolyzer at 1 kg hr^{-1} with a Tecweigh® CR5 volumetric feeder. To purge the vapors from the reactor tube and decrease the residence time of the vapors in the reactor, nitrogen carrier gas was introduced at the top of the reactor at 3 SLPM. Each biomass sample was pyrolyzed in triplicates, and each run took 45 to 60 minutes depending on the fed amount of the sample.

The char was collected at the bottom of the drop tube in a catch bin. And, any residual char was removed by passing the pyrolysate/carrier gas mixture through a cyclone. The bio-oil was collected in four stages, each referred to as a separate ‘stage fraction’. Bio-oil collected in the two condensers operated at 60 and 10°C were referred to as ‘stage fraction 1’ and ‘stage fraction 2’, and were followed by bio-oil resulting from the collection of aerosols in electrostatic precipitator (ESP) referred to as the ‘stage fraction 3’. Bio-oil from any vapors remaining after the ESP were collected in a stainless steel coil submerged in an ice bath, and were referred to as ‘stage fraction 4’.

Yields of bio-oil and biochar were measured gravimetrically by weighing the char catch bin and each component of the bio-oil collection system individually before and after the run. The volumetric flow rate through the system was measured using a Ritter® TG5/4-ER-1 bar drum type gas meter with water as the packing liquid. After the completion of each run, the average concentration of each gaseous component and the overall volumetric flow through the reactor were used to calculate the mass of each calibrated gaseous component. Overall mass closures were then estimated as ratio of the sum of the masses of different pyrolysis products and the total biomass mass fed during the experiment.

5.7.2.3 Characterization of biomass and pyrolysis products (bio-oil and biochar)

Biomass samples and the obtained biochar were characterized with their moisture, ash, volatile matters and fixed carbon contents as determined by proximate analysis using a thermogravimetric analyzer (TGA) (Model: TGA 1, Mettler-Toledo International Inc., Columbus, OH); and carbon, hydrogen and oxygen contents as determined by ultimate analysis using an elemental determinator (LECO Corporation, St. Joseph, MI). Biochar produced from three pyrolysis runs were mixed together and proximate and ultimate analyses on mixed biochar samples were performed in duplicates. For biomass samples also, these analyses were replicated twice. The oxygen contents of the biomass samples and biochar were estimated as difference, and their higher heating values (HHV) were estimated using Sheng and Azevedo (2005)'s correlation, as below:

$$HHV = -1.3675 + 0.3137 \times C + 0.7009 \times H + 0.0318 \times O$$

For bio-oil, TGA results yielded combined water and total volatiles contents in addition to ash and fixed carbon contents. Water or moisture contents of bio-oil were determined by Karl-Fischer (KF) titration using a KF Titrator MKS 500. For KF titration, hydranal composite 5K was used as titrant and hydranal working medium K was used as solvent. Water content obtained through KF titration was deducted to obtain the total volatiles contents. Carbon, hydrogen, nitrogen and oxygen contents of bio-oil were determined in a similar way as explained for biomass samples and biochar. HHV of bio-oil was determined using an oxygen bomb calorimeter (Model: 6400, Parr Instrument Company, Moline, Il). In addition to these, acidity of bio-oil samples were measured in terms of modified acid number (MAN) which is the mg of potassium hydroxide (KOH) needed to neutralize inorganic acids and carboxylic acids in each gram (g) of the sample when 0.1 M KOH in 2-propanol is titrated against 75 mL methanol and 5 mL dimethylformamide (DMF) solvent. Two, out of three, bio-oil samples obtained from the pyrolysis of each biomass type were randomly chosen, and different tests to assess the quality of each bio-oil sample were duplicated forming 4 replications, in total.

5.7.2.4 Statistical Analysis

Average and standard deviation of different parameters (i.e., pyrolysis products yields, and different properties of biomass, bio-oil and biochar) were computed for reporting the results. Additionally, one-way ANOVA was performed to test the null hypothesis that the average values for different parameters are the same at 95% confidence interval. P-values > 0.05, as obtained from the ANOVA test, signify that the null hypothesis is true and p-value < 0.05 indicates that the average values of at least two parameters are different. To identify the parameters with significantly different means, Tukey-Kramer multiple comparisons method was employed which simultaneously estimated all the pairwise differences of means of different parameters. The statistical analyses were done in JMP software.

5.7.3 RESULTS AND DISCUSSION

5.7.3.1 Stored and upgraded corn stover samples characterization

Different corn stover samples pyrolyzed in this study were characterized with their elemental compositions as obtained from ultimate analysis; moisture, ash, volatile matters and fixed carbon contents as obtained from proximate analysis; and their higher heating values (Table 1). Moisture content of torrefied stover was lower than other sample types. The ash contents of the single-pass inside-stored corn stover and ensiled cobs were lower than the other sample types. Volatile matter was the least for the torrefied stover. Carbon, hydrogen, nitrogen and oxygen contents, and higher heating values of different samples were within a narrow range although statistically there were some differences.

Table 1: Properties of different corn stover samples

*, ^, @ Parameters	Multi-Pass Corn Stover (Inside)	Single-Pass Corn Stover (Inside)	Single-Pass Corn Cobs (Ensiled)	Single-Pass Corn Stover (Ensiled)	Single-Pass Corn Stover (Torrefied)	ᵛ P-Value from ANOVA
Moisture Content (wt.%)	8.0 (0.0)^{a}	6.4 (0.1)^{a,b}	7.1 (0.8)^{a}	7.3 (0.0)^{a}	5.1 (0.5)^{b}	0.0043
Ash Content (wt.%)	5.5 (1.7)^{a}	2.6 (0.3)^{a,b}	1.6 (0.1)^{b}	5 (0.2)^{a}	5.6 (0.7)^{a}	0.0143
Total Volatiles (wt.%)	79.7 (2.6)^{a}	80.1 (0.0)^{a}	82.2 (0.5)^{a}	78.4 (0.4)^{a}	73.3 (0.2)^{b}	0.0059
Fixed Carbon (wt.%)	14.8 (1.0)^{c}	17.3 (0.2)^{b}	16.2 (0.4)^{b,c}	16.6 (0.2)^{b,c}	21.2 (0.1)^{a}	0.0004
Elemental Composition (wt.%)						
Carbon	46.2 (0.7)^{c}	48.3 (0.2)^{a,b}	48.5 (0.7)^{a,b}	47.5 (0.1)^{b,c}	49.6 (0.1)^{a}	0.0045
Hydrogen	6.7 (0.1)^{a}	6.8 (0.0)^{a}	6.8 (0.1)^{a}	6.7 (0.0)^{a}	6.2 (0.0)^{b}	0.0004
Nitrogen	0.4 (0.0)^{a,b}	0.4 (0.0)^{b}	0.5 (0.0)^{a}	0.3 (0.0)^{b}	0.4 (0.0)^{a,b}	0.0108
Oxygen (by difference)	41.2 (0.8)^{a}	41.9 (0.2)^{a}	42.6 (0.8)^{a}	40.6 (0.1)^{a}	38.2 (0.1)^{b}	0.0029
# **Higher Heating Value (MJ kg^{-1})**	19.1 (0.3)^{b}	19.9 (0.1)^{a}	20.0 (0.2)^{a}	19.5 (0.0)^{a,b}	19.7 (0.0)^{a,b}	0.0138

* All the values are the average of 2 replications with standard deviation in parentheses.
^ All wt.%s', and HHV values are in dry basis; moisture content (wt.%) is in wet basis
@ Values with same letter(s) in subscript in each row are not significantly different at 95% confidence interval.
ᵛ P-value less than 0.05 signify that at least two treatments are significantly different at 95% confidence interval
HHV estimated using Sheng and Azevedo (2005)'s correlation

5.7.3.2 Pyrolysis product yield

Yields of different pyrolysis products, including bio-oil, biochar and gases, from different corn stover samples are reported in table 2. Bio-oil yield was the highest for the ensiled single-

pass stover and the least for the torrefied corn stover. Bio-oil yield from the other samples were in between these two extremes. Bio-oil yield from the torrefied corn stover was the least as most of the hemicellulose fraction is lost during the torrefaction process (Medic et al., 2012); and during pyrolysis, hemicellulose fractions also convert to bio-oil (Mohan et al., 2006; Yang et al., 2007). The bio-oil yields from different stored stover and cobs samples were slightly lower than, but closer to, that obtained by Agblevor et al. (1995) for stored corn stover; whilst bio-oil yield from torrefied corn stover is significantly less.

Table 2: Pyrolysis products yield for different corn stover samples

*,@ Yield (wt.%)	Multi-Pass Corn Stover (Inside)	Single-Pass Corn Stover (Inside)	Single-Pass Corn Cobs (Ensiled)	Single-Pass Corn Stover (Ensiled)	Single-Pass Corn Stover (Torrefied)	ᵛP-value from ANOVA
Bio-oil (Liquid)	48.7 (2.0)^{a,b}	45.0 (1.7)^{b,c}	49.7 (2.4)^{a,b}	55.0 (1.0)^{a}	40.0 (5.4)^{c}	0.0011
Biochar (Solid)	32.1 (0.9)^{a}	36.1 (1.4)^{a}	31.6 (4.3)^{a}	25.5 (1.0)^{b}	32.6 (1.0)^{a}	0.0020
Gases	15.1 (3.2)	15.2 (2.3)	11.8 (6.3)	16.2 (2.6)	21.7 (5.5)	0.1552

* All the values are the average of 3 replications with standard deviation in parentheses.
ᵛ P-value less than 0.05 signify that at least two treatments are significantly different at 95% confidence interval
@ Values with same letter(s) in subscript in each row are not significantly different at 95% confidence interval.

Biochar yield was the least for ensiled single-pass stover, whereas there was no significant difference in biochar yield from the other biomass samples. In addition to this, the non-condensable gases yield was not significantly different for different sample types at 95% confidence interval.

5.7.3.3 Physiochemical properties of bio-oil

Physiochemical properties of bio-oil obtained from different corn stover samples pyrolyzed in this study were characterized with their moisture content as obtained from volumetric KF titration; elemental compositions as obtained from ultimate analysis; ash, volatile matters and fixed carbon contents as obtained from proximate analysis; HHV as determined by bomb calorimeter; and acidity in terms of MAN (Table 3). Statistically, moisture contents, ash contents, volatile matters and fixed carbons of bio-oil from different corn stover samples were not significantly different. Moisture contents of bio-oil from different corn stover samples were in the range of 34-52 wt.%, and were higher than those reported in other studies (Agblevor et al., 1995; Mullen et al., 2010; Yu et al., 2007). Ash contents of bio-oil produced from different samples were less than 0.2 wt.%, and were similar as the values reported in other literatures (Mullen et al., 2010; Yu et al., 2007).

Table 3: Properties of bio-oil produced from different corn stover samples

*, ^, @ Parameters	Multi-Pass Corn Stover (Inside)	Single-Pass Corn Stover (Inside)	Single-Pass Corn Cobs (Ensiled)	Single-Pass Corn Stover (Ensiled)	Single-Pass Corn Stover (Torrefied)	ᵛP-value from ANOVA
Moisture Content (wt.%)	39.3 (11.0)	48.3 (1.5)	34.4 (1.1)	39.0 (7.1)	51.3 (13.1)	0.0602
Ash Content (wt.%)	0.1 (0.0)	0.2 (0.0)	0.2 (0.1)	0.1 (0.1)	0.1 (0.1)	0.1219
Total Volatiles (wt.%)	82.0 (7.1)	79.2 (5.3)	83.6 (1.3)	79.8 (7.5)	89.8 (1.3)	0.0798
Fixed Carbon (wt.%)	19.2 (8.8)	20.6 (5.3)	16.2 (1.2)	20.2 (7.4)	10.1 (1.2)	0.1054
Elemental Composition (wt.%)						
Carbon	44.9 (0.7)^{b}	53.3 (0.6)^{a}	49.9 (4.4)^{a,b}	46.7 (3.7)^{a,b}	43.5 (4.8)^{b}	0.0061
Hydrogen	14.3 (0.4)^{c}	17.0 (0.1)^{b}	12.7 (0.1)^{d}	14.7 (0.6)^{c}	18.4 (0.3)^{a}	<.0001
Nitrogen	0.6 (0.1)	0.5 (0.3)	0.6 (0.0)	0.5 (0.1)	0.6 (0.1)	0.6218
Oxygen (by difference)	40.1 (0.5)^{a}	29.0 (0.8)^{b}	36.6 (4.4)^{a}	38.1 (3.6)^{a}	37.3 (4.5)^{a}	0.0024
Higher Heating Value (MJ kg^{-1})	19.2 (0.7)^{b}	23.0 (0.1)^{a}	22.2 (0.2)^{a}	19.1 (2.2)^{b}	18.3 (1.1)^{b}	<.0001
Modified Acid Number (mg g^{-1})	70.5 (3.3)^{b}	70.3 (6.6)^{b}	95.0 (0.4)^{a}	65.2 (2.3)^{b,c}	57.1 (4.5)^{c}	<.0001

* All the values are the average of 4 replications with standard deviation in parentheses. 2, out of 3, bio-oil samples were randomly chosen, and different tests to assess the bio-oil quality were duplicated on each bio-oil sample forming 4 replications, in total.

^ All wt.%s', and HHV values are in dry basis; moisture content (wt.%) is in wet basis

ᵛ P-value less than 0.05 signify that at least two treatments are significantly different at 95% confidence interval

@ Values with same letter(s) in subscript in each row are not significantly different at 95% confidence interval.

Elemental compositions of bio-oil produced from different corn stover samples showed that the oxygen content of bio-oil produced from inside stored single-pass corn stover was significantly lower than those produced from the other samples. Consequently, the higher heating value of bio-oil produced from this sample was the highest, as the presence of oxygen adversely affects the higher heating values of fuels (Brown, 2003). In addition to this, the higher content of carbon in bio-oil generated from inside stored single-pass stover might have resulted in its enhanced HHV. The oxygen contents and HHV of bio-oils in this study were close to those reported for corn stover by Agblevor et al. (1995) and Mullen et al. (2010). There was no significant different between the HHVs of bio-oil from ensiled cobs and inside stored single-pass stover; however, these were significantly higher than the HHVs of bio-oils produced from other samples. MAN of bio-oil from the torrefied corn stover was significantly less when compared to the bio-oil produced from other samples, probably due to losing acidic components of biomass during torrefaction (Medic et al., 2012). Bio-oil from ensiled cobs was the most acidic, and there was no significant difference between the acidity of bio-oil produced from other stored samples.

5.7.3.4 Physiochemical properties of biochar

The physiochemical properties of biochar produced form different corn stover samples pyrolyzed in this study were characterized with their moisture, ash, volatile matters and fixed carbon contents as obtained from proximate analysis; elemental compositions as obtained from ultimate analysis; and their higher heating values (Table 4). Although the moisture contents of biochar from different samples were within a narrow range of 2.8-5.0%$_{wb}$, moisture content of biochar produced from torrefied corn stover was the highest and significantly different than those produced form other samples. Ash content of biochar from torrefied corn stover was significantly higher and those from single-pass inside stored stover and ensiled cobs were significantly lower than biochar from other samples. The HHV of biochar from inside stored multi-pass corn stover was the least, and significantly different than the HHVs of biochar from other samples. Statistically, there was no significant difference in HHV of biochar generated from other samples. Biochar generated from pyrolysis can be applied to the agricultural lands to improve their fertility and sequester greenhouse gases (Laird et al., 2009). Additionally, biochar has a potential to be used as feedstock for energy production (Thangalazhy-Gopakumar et al., 2010).

Table 4: Properties of biochar produced from different corn stover samples

*, ^, @ Parameters	Multi-Pass Corn Stover (Inside)	Single-Pass Corn Stover (Inside)	Single-Pass Corn Cobs (Ensiled)	Single-Pass Corn Stover (Ensiled)	Single-Pass Corn Stover (Torrefied)	ᵛP-value from ANOVA
Moisture Content (wt.%)	4.1 (0.0)^{b}	2.8 (0.1)^{d}	3.1 (0.0)^{c,d}	3.8 (0.1)^{b,c}	5.0 (0.4)^{a}	0.0005
Ash Content (wt.%)	15.1 (1.8)^{a,b}	5.0 (0.1)^{c}	5.2 (0.0)^{c}	13.8 (0.1)^{b}	17.2 (0.4)^{a}	<.0001
Total Volatiles (wt.%)	41.7 (1.3)^{c}	60.3 (0.7)^{a}	55.5 (0.0)^{b}	38.3 (0.3)^{d}	28.8 (0.6)^{e}	<.0001
Fixed Carbon (wt.%)	43.2 (0.4)^{c}	34.7 (0.5)^{e}	39.3 (0.0)^{d}	48.0 (0.3)^{b}	54.0 (0.6)^{a}	<.0001
Elemental Composition (wt.%)						
Carbon	52.3 (0.2)^{d}	58.4 (0.2)^{c}	60.2 (1.3)^{b,c}	61.5 (0.2)^{b}	64.8 (0.1)^{a}	<.0001
Hydrogen	4.0 (0.0)^{b}	5.2 (0.0)^{a}	5.2 (0.1)^{a}	4.1 (0.0)^{b}	4.0 (0.0)^{b}	<.0001
Nitrogen	0.6 (0.0)^{a,b}	0.5 (0.0)^{b}	0.8 (0.0)^{a}	0.6 (0.0)^{a,b}	0.6 (0.0)^{a,b}	0.0199
Oxygen (by difference)	28.1 (0.3)^{a}	30.9 (0.2)^{a}	31.3 (2.4)^{a}	20.0 (0.1)^{b}	13.4 (0.1)^{c}	<.0001
#Higher Heating Value (MJ kg^{-1})	18.7 (0.1)^{b}	21.6 (0.0)^{a}	22.1 (0.4)^{a}	21.5 (0.0)^{a}	22.2 (0.0)^{a}	<.0001

* All the values are the average of 2 replications with standard deviation in parentheses. Biochar produced from the three pyrolysis runs were mixed together and were analyzed for the properties characterization in duplicates.

^ All wt.%s', and HHV values are in dry basis; moisture content (wt.%) is in wet basis

ᵛ P-value less than 0.05 signify that at least two treatments are significantly different at 95% confidence interval

@ Values with same letter(s) in subscript in each row are not significantly different at 95% confidence interval.

HHV estimated using Sheng and Azevedo (2005)'s correlation

5.7.4 CONCLUSIONS

Stored single-pass corn stover and cobs, stored multi-pass stover, and stored and torrefied single-pass stover were pyrolyzed in a free-fall fast pyrolysis reactor. Yields and physiochemical properties of different pyrolysis products were determined. The physiochemical properties of bio-oil and biochar from different biomass were characterized with their moisture, ash, volatile matters, carbon, hydrogen, nitrogen and oxygen contents. In addition to these, higher heating values were determined for both bio-oil and biochar, and the acidity was measured for bio-oil. Bio-oil yield from the ensiled single-pass corn stover was the highest and that from the torrefied single-pass stover was the least. Bio-oil generated from ensiled single-pass cobs and torrefied single-pass stover were respectively the most and the least acidic. There is further need to investigate the fast pyrolysis behaviors of different biomass types stored in different ways for different durations, and to compare the yields and properties of bio-oil from biomass stored for different durations with those obtained from fresh biomass.

ACKNOWLEDGEMENTS

Thanks to Dustin Dalluge, Marjorie Rover and Patrick Johnston from Iowa State University's Center for Sustainable Environmental Technologies (CSET) for pyrolyzing different biomass samples, and conducting different tests to characterize physiochemical properties of original biomass and pyrolysis products (bio-oil and biochar). This research was supported by funding from the North Central Regional Sun Grant Center at South Dakota State University through a grant provided by the US Department of Energy Office of Biomass Programs under award number DE-FG36-08GO88073.

REFERENCES

Agblevor, F. A., Besler, S., & Wiselogel, A. E. (1995). Fast pyrolysis of stored biomass feedstocks. *Energy & Fuels, 9*, 635-640.

Bridgwater, A. V. (2011). Review of fast pyrolysis of biomass and product upgrading. *Biomass and Bioenergy*, 1-27.

Bridgwater, A. V., Meier, D., & Radlein, D. (1999). An overview of fast pyrolysis of biomass. *Organic Geochemistry, 30*, 1479-1493.

Brown, R. C. (2003). *Biorenewable resources: Engineering new products from agriculture* (1st ed.). Ames, Iowa, United State of America: Blackwell Publishing.

Ellens, C. J., & Brown, R. C. (2012). Optimization of a free-fall reactor for the production of fast pyrolysis bio-oil. *Bioresource Technology, 103*, 374-380.

Laird, D. A., Brown, R. C., Amonette, J. E., & Lehmann, J. (2009). Review of the pyrolysis platform for coproducing bio-oil and biochar. *Biofuels Bioproducts & Biorefining, 3*, 547-562.

Medic, D., Darr, M. J., Shah, A., Potter, B., & Zimmerman, J. (2012). Effects of torrefaction process parameters on biomass feedstock upgrading. *Fuel, 91*, 147-154.

Mohan, D., Pittman, Jr., C. U., & Steele, P. H. (2006). Pyrolysis of wood/biomass for bio-oil: A critical review. *Energy & Fuels, 20*, 848-889.

Mullen, C. A., Boateng, A. A., Goldberg, N. M., Lima, I. M., Laird, D. A., & Hicks, K. B. (2010). Bio-oil and bio-char production from corn cobs and stover by fast pyrolysis. *Biomass and Bioenergy, 34*, 67-74.

Oasmaa, A., & Czernik, S. (1999). Fuel oil quality of biomass pyrolysis oils-State of the art for the end users. *Energy & Fuels, 13*, 914-921.

Shah, A., Darr, M. J., Medic, D., Anex, R., Khanal, S., & Maski, D. (2011a). Techno-economic analysis of a production-scale torrefaction system for cellulosic biomass upgrading. *Biofuels Bioproducts & Biorefining*, In press.

Shah, A., Darr, M. J., Webster, K. E., & Hoffman, C. (2011b). Outdoor storage characteristics of single-pass large square corn stover bales in Iowa. *Energies, 4*, 1686-1694.

Sheng, C., & Azevedo, J. (2005). EStimating the higher heating value of biomass fuels from basic analysis data. *Biomass and Bioenergy, 28*, 499-507.

Shinners, K. J., Binversie, B. N., Muck, R. E., & Weimer, P. J. (2007). Comparison of wet and dry corn stover harvest and storage. *Biomass & Bioenergy, 31*, 211-221.

Thangalazhy-Gopakumar, S., Adhikari, S., Ravindran, H., Gupta, R. B., Fasina, O., Tu, M., et al. (2010). Physiochemical properties of bio-oil produced at various temperatures from pine wood using an auger reactor. *Bioresource Technology, 101*, 8389-8395.

Venderbosch, R. H., & Prins, W. (2011). Fast Pyrolysis. In R. C. Brown (Ed.), *Thermochemical processing of biomass: Conversion into fuels, chemicals and power* (1st ed., pp. 124-156). Chichester, West Sussex, United Kingdom: John Wiley & Sons, Ltd.

Yang, H., Yan, R., Chen, H., Lee, D. H., & Zheng, C. (2007). Characteristics of hemicellulose, cellulose and lignin pyrolysis. *Fuel, 86*, 1781-1788.

Yu, F., Deng, S., Chen, P., Liu, Y., Wan, Y., Olson, A., et al. (2007). Physical and chemical properties of bio-oils from microwave pyrolysis of corn stover. *Applied Biochemistry and biotechnology, 136-140*, 957-970.

Please complete the following table to reflect your project at completion or time of report submission:

ITEM	NUMBER
Abstracts	**15 (*10 Journal; 5 Conference*)**
Peer Reviewed Publications	**10 (*6 Published; 4 Under Review*)**
Outreach Publications/Web Pages	**0**
Professional Presentations	**5**
MS Degrees Conferred	**4 (*Peyton; Schon; Thoreson; Webster*)**
Ph.D. Degrees Conferred	**1 (*Medic*)**
MS Students Supported	**4 (*Peyton; Schon; Thoreson; Webster*)**
Ph.D. Students Supported	**2 (*Medic; Shah*)**
Post-Docs Supported	**1 (*Maski*)**
Undergraduate Students Supported	**10**
Investigators Supported	**2 (*Shah; Webster*)**
Start-Up Jobs Created	**0**
Disclosures	**0**
Patents Filed	**0**
Provisional Patents	**0**
Patents Issued	**0**
License Agreements	**0**
Plant Variety Protection	**0**

Back to Table of Contents

Sun Grant Initiative
DOE Final Progress Report

Project Title: Prioritizing Corn Harvest and Biomass Collection Activities in North Dakota - A Weather Risk Analysis

Project Director/Principal Investigator: Cole R. Gustafson, Professor and Chair, Department of Agribusiness and Applied Economics, North Dakota State University, Fargo, ND 58108

All Co-Principal/Other Investigators: Thein A. Maung, Research Assistant Professor
Department of Agribusiness and Applied Economics, North Dakota State University,
Fargo, ND 58108

Collaborators: None

Project Location: Fargo, North Dakota

Period of Performance: 1 April 2009 - 31 December 2011

Funding Awarded: $80,000

Cost Share Amount: $20,040

Cost Share Sources: Time and effort from PIs and CoPIs; Indirect on time and effort.

Executive Summary

The overall objective of this project is to develop an economic stochastic simulation model of corn harvest timeliness and apply it to selected North Dakota corn grain farms to assist them in delineating the impact a new corn stover harvest activity would have on their operation. To achieve our goal, we use three stochastic linear programming models to analyze farmers' harvest activities under 1) corn grain only harvest option, 2) simultaneous corn grain and cob harvest "one-pass" option and 3) separate corn grain and stover harvest "two-pass" option. Under the corn grain only option, our findings show that farmers are able to complete harvesting corn grain and achieve profit maximization in a fairly short amount of time with existing combine harvest capacity.

Under the corn grain and cob one-pass harvest option, corn grain harvest capacity diminishes due to the attachment of cob harvester to the back of combine which results in harvest slowdown. Because of limited availability of harvest field time due to adverse weather, this reduction in harvest capacity results in some corn acres being left unharvested. This in turn can reduce corn grain revenue generated by farmers. Our findings indicate that the slowdown in combine harvest capacity causes farmers' net returns from harvesting both grain and cob to be lower than the net returns from harvesting corn grain only.

Time allocation will be the main challenge when farmers consider the third option of a two-pass harvest system. With limited availability of harvest field time, not enough field days exist to both collect grain and stover in two separate operations on all corn acres. Our results show that farmers may find it optimal to allocate most of their time to harvesting grain, and then proceed to bale stover if time permits at the end of the harvest season.

Farmers are especially challenged in finding time to harvest both corn grain and stover as farm size increases. This suggests that farmers need to expand not only the capacity of their combine, but the capacity of their stover collection equipment as well. Our evidence shows that under the two-pass harvest option, farmers with relatively small land acreage would have potential to harvest more quantities of stover than their counterparts with comparatively large land tracts. This is because relatively small farms can complete harvesting grain early and allocate more time to harvesting stover. In addition, our results indicate that farmers find it more valuable to harvest corn grain than stover when their harvest field time is limited.

Differences in the use of soil tillage practices among farms can result in differences in corn yields and production costs. We show that a small decrease in corn yield due to changes in tillage practice can result in a large decline in the net profit of harvesting corn grain and stover. As a result of changes in tillage practice, the decrease in corn yield must be more than offset by the decrease in production cost in order for net farm profit to remain unaffected.

This study suggests that the availability of harvest field time is the main factor that dictates

farmers' interest in harvesting corn cob or stover. Because harvest field time is very limited in North Dakota, a frequent suggestion is for farmers to hire additional labor to operate the farm machinery. However, additional farm labor is difficult to find in rural areas of North Dakota. At present, the state has the lowest unemployment rate in the nation. Moreover, large tractors and new stover collection equipment are highly sophisticated. Any new farm laborer would need extensive training and oversight, again burdening farmers who are already busy. Furthermore, farmers are unwilling to take any risk of holding a large inventory of corn cob or stover and prefer to have an external party bale, store and transport the goods.

1 Introduction and Research Objective

Following gasoline shortages in the 1970's, interest in biofuels was primarily motivated by rising crude oil prices. This interest waned following oil price declines in the mid 80's. Today, interest in biofuels has rebounded, especially cellulosic biofuels. In addition to rising oil prices, rural development (Leistritz and Nancy, 2008), risks associated with oil exploration in the Gulf of Mexico and political instability in the Middle East, and climate change are additional motivating considerations. Growing evidence suggests that combustion of fossil fuels which emit large amounts of greenhouse gases (GHG), are a causal factor behind climate change (IPCC, 2007). Research studies (Schneider and McCarl 2003; McCarl et al. 2009) have shown that cellulosic biofuel has higher GHG offset rates than grain-based biofuel. Hence, comparatively more GHG can be reduced through the use of cellulosic feedstock such as corn stover (which is comprised of stalk, leaves, husks and cobs) than corn grain to produce biofuel. However, greater reliance on corn stover as a bioenergy feedstock poses a logistical challenge for farmers who face limited fall harvest field time. Harvest in fall 2009 was especially difficult in the northern plains as cool temperatures and wet conditions resulted in sizeable acreage that had to be left unharvested. According to O'Brien (2010), about 68.7 million bushels of corn in North Dakota were reported to be left unharvested in 2009.

U.S. ethanol demand has been steadily increasing following passage of Renewable Fuel Standard (RFS) and the Energy Independence and Security Act of 2007 (EISA). Most domestic ethanol production utilizes corn grain as feedstock. Rising corn prices are encouraging current and potential ethanol producers to seek alternative feedstocks, especially cellulosic sources. EISA defines three classes of biofuels, conventional, advanced, and cellulosic. These classes are differentiated based on potential reduction of greenhouse gas (GHG) emissions of 20, 50, and 60 percent respectively. Because of its potential in reducing GHG emissions, corn-cob-based ethanol would be qualified as cellulosic biofuel per the federally mandated renewable fuels standard. By 2022, cellulosic ethanol production of 21 billion gallons per year will be required, creating a niche market opportunity. Existing biofuel producers are striving to develop cellulosic biofuels that qualify under EISA. For example, POET, an ethanol company, is expected to begin commercial operation of its cellulosic ethanol facility based on corn cobs in 2011, producing 25 million gallons per year which will require at least 700 tons of corn cobs per day to fuel the plant.

Collecting corn cobs can be a challenge while trying to get the grain harvest done on time because of the limitation in available harvest field days. In addition, corn producers do not have sufficient information to evaluate the economic investment returns from producing corn cob. The overall goal of this project is to develop an economic stochastic simulation model of corn harvest timeliness and apply it to selected North Dakota corn grain farms to assist them in delineating the impact a new corn stover

harvest activity would have on their operation. Specific objectives of this project are to: 1) quantify available fall corn harvest field days in North Dakota and estimate on-farm costs of producing corn cob and stover, 2) construct stochastic simulation models to assess the viability of farmers' investment in corn cob and stover harvesting business under different harvest options, and 3) use the simulation model to examine economic tradeoffs between corn grain, cob and stover harvest activities in the region.

In order to achieve our research objectives and explain project activities and outcomes in sequential steps, we organized our study in the following logical order. First related literatures in this research area are reviewed in section 2. Section 3 estimates the amount of corn cob/stover available for biofuel production in North Dakota. Section 4 presents currently available corn cob/stover harvest technologies. Farm level corn grain, cob and stover harvest costs are estimated in section 5. Section 6 develops economic stochastic simulation models for corn grain, cob and stover harvest scenarios. Section 7 presents empirical data, assumptions, results and their interpretations. Finally, section 8 concludes our study.

2 Literature Review

Many studies (Sokhansanj and Turhollow 2002; Gallagher et al. 2003; Perlack and Turhollow 2003, Petrolia 2008, and Turhollow and Sokhansanj 2007) have examined the economics of corn stover supply for biofuel production. While these studies have focused on estimating costs of harvesting corn stover as whole, only a few studies have particularly given emphasis on examining costs of supplying corn cob as a potential biofeedstock using up-to-date harvesting technologies. Chippewa Valley Ethanol Company (CVEC, 2009) has published a feasibility report on the use of corn cob as a sustainable source of biomass for providing thermal energy for its corn grain ethanol process. The company utilized two different cob harvest systems to demonstrate cob harvesting on 3,200 acres of land. The cost of harvesting and delivering corn cob to CVEC was evaluated to be at $33 per acre or $66 per ton. The CVEC's report did not provide details on how cob harvest costs were computed. Zych (2008) estimated potential U.S.

corn cob production and reviewed logistical issues associated with collection and storage of corn cobs. However, no cost estimates for cobs were provided in his study.

The aforementioned studies mainly focused on estimating supply costs of corn cob and stover and did not take into account the viability and profitability of farmers' investment in cob and stover harvesting machinery. Using the stochastic linear programming model, Bouzaher and Offutt (1992) investigated the feasibility and profitability of farm residue collection. Weather conditions can cause variations in the availability of field days as well as in grain and residue yields, and these variations can affect the feedstock supply and render uncertainties to both farmers and biofuel producers. Thus, in their model, they considered the sensitivity of grain and residue collection to the availability of days suitable for field work at harvest time. In addition, they considered the three harvesting alternatives: own baling, custom baling and simultaneous cob collection and grain harvest. Overall, they found that the custom baling alternative yielded higher net returns than the other two alternatives. Apland et al. (1981) employed the discrete stochastic programming model to examine the impact of production process, sequential decision making and fall field time availability on crop residue supply in mid-western US grain farms. The authors showed that crop residue production would be price responsive and that the development of new harvest techniques and storage were important to the economic viability of crop residues as energy sources. Using their Farm Plan Model, Erickson and Tyner (2010) examined the economics of harvesting corn cobs for energy generation. They showed that, in general, harvesting corn cobs could become feasible only if the cob price reaches at about $100 per ton. The authors also showed that corn cob operation is more attractive for relatively large farms (greater than or equal to 2000 corn acres) because their per unit cob harvest costs are lower.

3 Corn Stover and Cob Availability in North Dakota

The amount of corn stover available for collection is partially a function of residue levels needed to be maintained for soil health. Excess removal of corn residues from the agricultural fields can have negative impacts on soil productivity. Some residue must remain in the field for soil erosion control, maintenance of soil organic matter, maintenance/enhancement of soil carbon and wildlife habitat. Moreover, surface crop residues reflect light and protect soil from high temperatures and evaporative losses (Sauer et al., 1996). The maximum amount of crop residue that can be removed without affecting soil erosion depends on many site specific factors such as soil type and fertility level, slope characteristics, tillage system, climate and crops. Generally, USDA, National Resources Conservation Service (NRCS) recommends that about 30 percent residue cover is adequate to control soil erosion. Many studies (see Hall et al. 1993; Nelson 2002; McAloon et al. 2000; Perlack et al. 2005) have investigated the impact of removing corn stover on soil fertility. These studies have examined the amount of corn residues needed to remain in the field in order to bring erosion below the soil loss tolerance level.

3.1 Estimation of Corn Stover Yield

Crop residue cover is very important for preventing water and wind erosion during the winter months following harvest. Wind erosion is a serious problem in North Dakota, especially in the eastern part of the state (Cihacek et al., 1993; Van Donk et al., 2008). In order to prevent wind erosion from becoming a threat to soil productivity, this study follows the literature (see Hall et al. 1993) and assumes that on average 35 percent of corn stover can be removed from farm fields throughout the state. The quantities of stover that can be removed for biofuel production can be computed as,

$$Rstover = Grain\ Yield \times Weight \times SGR \times Removal\% \times [1\text{-}Moisture\%] \quad (1)$$

Rstover is the quantities of stover in dry ton that can be removed for biofuel production. Grain yield is the weighted average yield of grain crop in bushels per acre. Weight is the weight of grain in short tons per bushel converted by dividing bushel weight of 56 pounds per bushel with 2,000 pounds per short tons. SGR is defined as a stover-to-grain ratio and it is assumed to be 1:1 based on Lal (2005). *Removal%*, the percent of stover that can be removed for biofuel production considering soil erosion protection, is assumed to be 35 percent. *Moisture%*, the percent of moisture content contained in stover, is assumed to be 20 percent. Grain yield data were obtained from the USDA National Agricultural Statistics Service[1]. The yield data are based on the five-year (2005 to 2009) average data by county in North Dakota. Estimated results for corn stover availability in dry ton in North Dakota are reported in Table 3.1 by climatic region. Details of estimated yield data for corn stover (and cob described below) by county and climatic region map are given in Appendix I & II.

[1] See: http://www.nass.usda.gov/Data_and_Statistics/Quick_Stats/

3.2 Estimation of Corn Cob Yield

Corn cobs are desirable as a sustainable biofeedstock because they represent about 12 percent of corn stover remaining on the field, their removal has negligible impact on soil carbon and they have limited nutrient value to the soil (CVEC, 2009; Roberts, 2009). The availability of corn cob can be estimated as,

$$Rcob = Grain\ Yield \times Weight \times CGR \times Removal\% \times [1\text{-}Moisture\%] \quad (2)$$

where *Rcob* is the quantities of corn cobs that can be removed for biofuel production. CGR is defined as a cob-to-grain ratio and it is calculated as 1:5.6 based on Wiselogel et al. (1996)[2]. Since literature suggests that removal of corn cobs may have little impact on soil productivity, *Removal%* in equation (2) defined as percent of cobs that must be retained in farm fields each year to protect soil erosion is assumed to be one or 100 percent. Similar to stover, the moisture content of corn cob is assumed to be 20 percent. Estimated results for corn cob availability in dry ton in North Dakota are reported in Table 3.1 by climatic region.

Table 3.1 Estimated Corn Stover and Cob Yield by Climatic Division (2005-2009 Average)

	Harvested Acres	Land Area	Density	Stover Availability		Cob Availability	
Region	**(acre)**	**(acre)**	**(%)**	**(ton/acre)**	**(ton)**	**(ton/acre)**	**(ton)**
Northwest	13,538	5,852,864	0.23	0.44	5,917	0.22	3,019
North Central	72,434	4,379,872	1.65	0.61	43,981	0.31	22,439
North East	190,637	5,451,379	3.50	0.75	143,355	0.38	73,140
West Central	36,781	5,523,571	0.67	0.61	22,467	0.31	11,463
Central	206,691	4,531,546	4.56	0.79	163,703	0.40	83,522
East Central	493,067	3,545,363	13.91	0.99	486,232	0.50	248,078
Southwest	29,792	5,114,694	0.58	0.33	9,964	0.17	5,083
South Central	92,891	5,006,605	1.86	0.57	52,689	0.29	26,882
Southeast	684,987	4,738,701	14.46	1.03	704,635	0.52	359,508
State Total	**1,820,818**	**44,144,595**	**4.60***	**0.68***	**1,632,943**	**0.35***	**833,134**

Note: Harvested acres are weighted by yield. ***** represents state average.

4 Corn Cob and Stover Harvesting Technology

Corn growers currently have the following options for harvesting cobs:

4.1 Whole Cob Harvest Option

Under this option, different types of machineries are being developed to collect corn cobs. They are described in detail as follows:

[2] In Wiselogel et al. (1996), CGR was assumed to be 10 pounds/ bushel.

(1) Vermeer Cob Harvester

Vermeer Corporation's cob caddy is a wagon-style cob harvester pulled behind the combine (see related pictures in Appendix III). Since it has its own diesel-powered unit to power hydraulics, the caddy does not pull any power off the combine. The design has a separation process that distributes husks, leaves and stalks back into the field and cobs into the harvester wagon. Harvested cobs in the caddy can be directly dumped into a truck and transported to a nearby processing plant. This method of harvesting cob enables the operator to easily attach/detach the harvester to/from the combine and to transfer cobs to a grain wagon in the field during harvest or dump them in piles at the end of the field (Davidson, 2008; Bernick, 2009; and Wehrspann, 2009).

(2) Redekop and Case IH Cob Harvester

Redekop Manufacturing, a Canadian company, has been testing its corncob cart with farmers (see pictures in Appendix III). The company's H165 Cob Harvester features on-the-go unloading, light weight and is powered off the combine chopper drive. The matching C180 Cart, built exclusively for cobs, features fast conveyor unloading. The cart's conveyor unloads cobs from the cart to create tapered piles of cobs. The merit of using the cart is that it requires only a low horsepower tractor and is powered by the tractor's PTO and hydraulics (Grooms, 2010). Similar to the cob harvester of Vermeer and Redekop, another type of cob harvesting system involves a Case IH combine with cart.

(3) Residue Recovery System

Developed by the Stukenholtz brothers in Nebraska, the Residue Recovery System consists of the Clean Boot mounted on the top of the combine to separate corn cobs from leaves and stalks and the Top Tank (see Appendix III). The Clean Boot includes a sieve and two blowers. Corn cobs are captured through suction as they fall through while leaves and stalks are ejected. Corn cobs are then blown into the Top Tank as shown in the figure in the appendix. The merit of this method is that it requires no modification to the combine and virtually no slowdown during harvest. For unloading purpose, the Top Tank can move laterally past the harvesting head and a conveyor chain unloads corn cobs into a truck (Davidson, 2008; Johnson, 2008).

4.2 Corn Cob Mix Harvest Option

Through combine modifications, John Deere developed a prototype harvesting system that keeps grain and chopped cobs in a single comingled mix in the grain tank. The mixture collected in the combine grain tank needs to be separated. The merit of this option is that it permits farmers to use their existing combine to collect cobs by modifying just a few internal parts in the combine separator for efficient threshing and separating. The use of a separation machine (either attached to the back of combine or located separately on the field side as illustrated in figures in Appendix
III) will be required to screen corn grain from cobs. The John Deere prototype equipment is a one pass, two stream cob collection system. The attachment on the back of its combine allows the grain to be separated from the cobs which flow out of the attachment. A tractor-pulled wagon moves alongside the combine to collect the cobs. Other manufacturers involved in this technique include CNH America LLC with its Case IH combines, Claas of America Inc. with its Lexion combines, Wildcat: a manufacturer of trammel screen systems for cob separation and Feterl Manufacturing Corporation, preparing to market its commercial separator (Christiansen, 2009; Davidson, 2008; Bernick, 2009; Wehrspann, 2009; Neeley, 2007).

4.3 Stover Baling Option

Since corncobs cannot be baled alone, they need to be collected along with non-cob stover and packaged into either a round or rectangular shape bale. At present, technology such as the Challenger LB baling machine pulled behind a combine allows farmers to compact cob and stover discharged from the back of the combine into a square bale as depicted in the figure in Appendix III. The square bale will be free of dirt and other soil particles because cob and stover do not touch the ground during the baling process. Another type of baling machine involved in square baling is the Case IH LB pulled behind a tractor (see Appendix III). However, this type of machine may not be rid of soil particles since baling can only be done after harvesting grain. Bales can be transported to a road-side storage or stacking area using a bale handling equipment.

5 Farm Level Corn Grain, Cob and Stover Harvest Cost Estimation

5.1 Cost Estimation for Corn Grain Harvesting

Corn grain is assumed to be harvested using a 275 HP combine. Combine horse power, corn head width, life, annual hours of use, speed, field efficiency, fuel price, list price (includes corn and grain head prices) and labor costs listed in Table 5.1 were obtained from Lazarus and Smale

(2010). Fuel consumption, capacity of combine, fixed and repair costs are computed based on the method and formulas illustrated in Edwards (2009) (see Appendix IV). Fuel cost is obtained by multiplying fuel consumption with fuel price. Lubrication cost is assumed to be 15% of fuel cost. Variable cost is calculated by adding up repair, fuel, lubrication and labor costs. The total harvest cost for corn grain using a 275 HP combine is estimated to be $28.71 per acre as can be seen in the table below. The dollar per acre harvest cost was obtained by dividing dollar per hour total harvest cost ($194.9 /hr) with corn combine harvest capacity of 6.79 acre per hour.

Table 5.1 Estimated Corn Grain Harvest Cost

Variable	Corn Combine
Horse Power (hp)	275.00
Corn Head Width (ft)	20.00
Life (year)	12.00
Annual Hours of Use	300.00
Fuel Consumption (gal/hr)	12.10
Speed (mph)	4.00
Field Efficiency (%)	0.70
Capacity (acre/hr)	6.79
Fuel Price ($/gal)	$ 2.60
List Price ($)	$ 334,795.32
Fixed Cost ($/hr)	$ 104.02
Repair Cost ($/hr)	$ 37.20
Fuel Cost ($/hr)	$ 31.46
Lubrication Cost ($/hr)	$ 4.72
Labor Cost ($/hr)	$ 17.50
Variable Cost ($/hr)	$ 90.88
Total Cost ($/hr)	$ 194.90
Total Cost ($/acre)	$ 28.71

5.2 Cost Estimation for Simultaneous Corn Grain and Cob Harvesting

Harvest cost for corn cob is estimated using whole cob harvest option. According to Shirek (2008) and Wehrspann (2009), a one-pass cob harvester like Cob Caddy as described above involves little modification to the combine and uses equipment available commercially to harvest whole cob. Due to its simplicity, efficiency and commercial availability, the one-pass cob harvest method is employed to estimate corn cob harvest cost. We assume that the one-pass cob harvest method requires farmers to use a self-propelled 275 HP corn combine harvester and a pull- behind wagon-style cob harvester. Table 5.2 describes the machinery operation and estimated cost information for the cob collection operation. The method of cost estimation for using corn combine in Table 5.2 is exactly the same as that in Table 5.1 above. The main difference between the two tables in corn combine usage is the speed traveled and the capacity of combine.

Harvesting corn cob requires an attachment of cob harvester to the back of corn combine.

According to CVEC (2009), this can slow down the corn grain harvest time by as much as half. In Table 5.2 below, the speed of corn combine is assumed to reduce by 50 percent (i.e. from 4 mph to 2 mph) because of the use of cob harvester. This would result in the corn combine capacity being reduced by half (from 6.79 acre/hour to 3.39 acre/hour) as compared to the combine capacity in corn grain only harvest option. As a result of this reduction in corn combine speed and capacity, total harvest cost for corn grain harvest would increase (from $28.71/acre to $57.43/acre). Using the procedures described in Edwards (2009) as explained, similar cost computations are implemented for the cob harvester as shown in Table 5.2. The data for the cob harvester were obtained by personal communication with Jan Van Roekel of Vermeer Corporation and based on the specifications of the Vermeer CCX770 Cob Harvester. Since the cob harvester is attached to the back of the corn combine, no additional labor would be required to operate the machine and its capacity would be dependent on the capacity of the corn combine. As shown in the table, cost of harvesting corn cob is estimated to be $19.36. Table 5.3 reports the scenarios for the impact of changes in corn combine speed/capacity due to the use of cob harvester on corn grain and cob harvest costs. The table clearly shows that the impact of corn combine speed/capacity on grain and cob harvest costs can be significant.

Table 5.2 Estimated Grain and Cob Harvest Cost Using Cob Caddy Harvest Method

Variable	Corn Combine	Cob Harvester	Total
Horse Power (hp)	275.00	115.00	
Corn Head Width (ft)	20.00		
Life (year)	12.00	10.00	
Annual Hours of Use	300.00	300.00	
Fuel Consumption (gal/hr)	12.10	2.50	
Speed (mph)	2.00	2.00	
Field Efficiency (%)	0.70	0.70	
Capacity (acre/hr)	3.39	3.39	
Fuel Price ($/gal)	$ 2.60	$ 2.60	
List Price ($)	$ 334,795.32	$ 120,000.00	
Fixed Cost ($/hr)	$ 104.02	$ 40.24	$ 144.26
Repair Cost ($/hr)	$ 37.20	$ 18.00	$ 55.20
Fuel Cost ($/hr)	$ 31.46	$ 6.50	$ 37.96
Lubrication Cost ($/hr)	$ 4.72	$ 0.98	$ 5.69
Labor Cost ($/hr)	$ 17.50		$ 17.50
Variable Cost ($/hr)	$ 90.88	$ 25.48	$ 116.35
Total Cost ($/hr)	$ 194.90	$ 65.72	$ 260.61
Total Cost ($/acre)	$ 57.43	$ 19.36	$ 76.79

Table 5.3 Impact of Corn Combine Speed/Capacity on Grain and Cob Harvest Cost

	Corn Grain Harvest Cost	Corn Cob Harvest Cost	Total
Scenario	**$ per Acre**		
50% Speed/Capacity Reduction (Base)	57.43	19.36	76.79
25% Speed/Capacity Reduction	38.28	12.91	51.19
No Speed/Capacity Reduction	28.71	9.68	38.39

5.3 Cost Estimation for Separate Corn Grain and Stover Harvesting

At present, farmers may be able to use tractor-pulled balers that they own for hay and forage collection to gather corn stover. Under this two-pass harvest option, stovers are harvested using a tractor and a baler. Similar to above, corn grain is assumed to be harvested using a self-propelled 275 HP corn combine. Because corn grain and stover are harvested separately, there will be no slowdown in corn combine speed/capacity. Thus, corn grain harvest cost per acre will be identical to Table 5.1. It is assumed that a 130 HP MFWD Tractor is used along with 3x3 Large Rectangular Baler to harvest stover. Specifications and data for the tractor and baler obtained from Lazarus and Smale (2010) are given in Table 5.4. Following Edwards (2009), total variable and fixed costs for the tractor and baler are estimated to be $10.76 per acre. In addition, stover shredding and raking costs would need to be included. Shredding of stover may be necessary because some of them will be in stalks anchored to the ground after grain harvesting. The anchored pieces of biomass are difficult to cut and bale in a single operation. Large pieces of biomass would make better bales but shredding followed by raking or windrowing will accelerate field drying (Sokhansanj and Turhollow, 2002). Based on the Petrolia's (2008) estimation, total shredding and raking cost of $12.02 per acre is added to total variable and fixed costs to come up with total harvest cost of $22.78 per acre (or $33.53 per ton converted using stover yield of 0.68 ton per acre).

Table 5.4 Estimated Stover Harvest Cost

		Tractor		Baler
Horse Power (hp)		130.00		
Baler Width (ft)				20.00
Bale Weight (ton)				
Life (year)		12.00		12.00
Annual Hours of Use		450.00		250.00
Fuel Use (gal/hr)		5.72		
Speed (mph)		5.00		5.00
Field Efficiency (%)		0.80		0.80
Capacity (acre/hr)				9.70
Fuel Price ($/gal)	$	2.60		
List Price ($)	$	118,889.00	$	96,667.00
Fixed Cost ($/hr)	$	21.96	$	34.34
Repair Cost ($/hr)	$	2.20	$	11.28
Fuel Cost ($/hr)	$	14.87		
Lubrication Cost ($/hr)	$	2.23		
Labor Cost ($/hr)	$	17.50		
Variable Cost ($/hr)	$	36.80	$	11.28
Total Cost ($/hr)	$	58.77	$	45.61
Total Cost ($/acre)	$	6.06	$	4.70

6 Methodology

This section starts with the description corn grain harvest methodology and then followed by the descriptions of simultaneous corn grain and cob harvesting (one-pass harvest method) and separate corn grain and stover harvesting (two-pass harvest method).

6.1 Corn Grain Harvesting

The following linear programming model which maximizes net income is used to examine the production of corn grain.

Max $\pi = P_C \cdot Q_C - \sum_{j=1}^{4} C_j X_j$ (1)

s.t. $-\sum_{j=1}^{4} Yld_{c,j} X_j + Q_c \le 0$ (2)

$a_j X_j \le A_j$ (3)

$b_j X_j \ge L_j$ (4)

$\sum_{j=1}^{4} X_j \le L$ (5)

$Q_C \ge 0;\ X_j \ge 0,\ j = 1,\ldots,4$

Based on Apland (1990) and Bouzaher and Offutt (1992), we assume that $j = 1, \ldots, 4$ represent four two-week harvest periods which run from the end of September till the end of November. P_c is the price of corn grain in dollar per short ton. Q_c is denoted as the quantity of corn grain sold in tons. C_j is defined as corn grain harvest and production costs in dollar per acre. X_j is denoted as acres of corn grain harvested. $Yld_{c,j}$ represents per acre corn grain yield in each harvest period j. a_j and b_j are respectively denoted as labor and combine time required per acre to harvest corn grain in each harvest period. Both combine and labor time is respectively constrained by $\tilde{CT}_j$ and $\tilde{LT}_j$ which represent stochastic combine and labor harvest field time expressed in hours available in each period. L is defined as total farm land acres that are available for corn grain harvest.

The objective function (Equation (1)) of the optimization problem is to quantify the net return of corn grain harvesting at the farm level. Equation (2) balances corn grain sales with production. Equations (3) and (4) constrain the total amount of combine and labor time available for harvesting corn grain. Equation (5) limits the amount of land available for corn grain farming.

6.2 Simultaneous Corn Grain and Cob Harvesting

The following linear programming model is used to examine the viability of producing corn grain and cob simultaneously.

$$\text{Max} \quad \pi = P_c \cdot Q_c + P_{cb} \cdot Q_{cb} - \sum_{j=1}^{4} C_j X_j - \sum_{j=1}^{4} D_j X_j \quad (1.1)$$

$$\text{s.t} \quad -\sum_{j=1}^{4} Yld_{c,j} X_j + Q_c \leq 0 \quad (2.1)$$

$$-\sum_{j=1}^{4} Yld_{cb,j} X_j + Q_{cb} \leq 0 \quad (3.1)$$

$$e_j X_j \leq \tilde{CT}_j \quad (4.1)$$

$$f_j X_j \leq \tilde{LT}_j \quad (5.1)$$

$$\sum_{j=1}^{4} X_j \leq L \quad (6.1)$$

$$Q_c \geq 0; \; Q_{cb} \geq 0; \; X_j \geq 0, \; j = 1, \ldots, 4$$

P_{cb} is the price of corn cob in dollars per short ton. Q_{cb} is denoted as the quantity of corn cob sold in tons. D_j is defined as corn cob harvest cost in dollars per acre. X_j is denoted as acres of

corn grain or cob harvested. $Yld_{cb,j}$ represents per acre corn cob yield in each harvest period j. e_j is denoted as combine and cob harvester time required per acre to harvest corn grain and cob in each harvest period and is constrained by available combine harvest field time. Similarly f_j is denoted as labor time required per acre to harvest corn grain and cob and is restricted by available labor harvest field time. L is defined as total farm land acres that are available for corn grain and cob harvest.

The objective function (Equation 1.1) of the optimization problem is to quantify the net return potential associated with the adoption of corn cob harvesting technology. The adoption of corn cob harvesting technology into a grain farm is analyzed to determine the crop acres needed to maximize net returns. Equation (3.1) balances corn cob sales with production. Equations (4.1) and (5.1) constrain the total amount of machine and labor time available for harvesting corn grain and cob simultaneously. Equation (6.1) limits the amount of land available for corn grain and cob farming.

6.3 Separate Corn Grain and Stover Harvesting

Following Bouzaher and Offutt (1992), the linear programming model which maximizes net return is used to investigate the profitability of producing corn grain and stover separately during harvest time. The model is written as follows,

$$\text{Max} \quad \pi = P_c \cdot Q_c + P_{cs} \cdot Q_{cs} - \sum_{j=1}^{4} C_j X_j - \sum_{i=2}^{4} \sum_{j=1}^{3} G_{i,j} Y_{i,j} \quad (1.2)$$

$$\text{s.t} \quad - \sum_{j=1}^{4} Yld_{c,j} X_j + Q_c \leq 0 \quad (2.2)$$

$$\sum_{i=2}^{4} \sum_{j=1}^{3} Y_{i,j} + Q_{cs} \leq 0 \quad (3.2)$$

$$a_j X_j \leq CT_j \quad j = 1, \ldots, 3 \quad (4.2)$$

$$b_1 X_1 \leq LT_1 \quad (5.2)$$

$$b_i X_i + \sum_{j=1}^{3} a_{i,j} Y_{i,j} \leq LT_i \quad i = 2, 3 \quad (6.2)$$

$$\sum_{j=1}^{3} a_{4,j} Y_{4,j} \leq LT_4 \quad (7.2)$$

$$\sum_{j=1}^{3} a_{i,j} Y_{i,j} \leq BT_i \quad i = 2, \ldots, 4 \quad (8.2)$$

$$\sum_{j=1}^{3} X_j \quad : : ; L \quad (9.2)$$

$$\sum_{i=j+1}^{4} Y \quad - m X \quad : : ; 0 \quad j = 1, \ldots, 3 \quad (10.2)$$

$Q_c \geq 0;\ Q_{cs} \geq 0;\ X_j \geq 0;\ Y_{i,j} \geq 0;$

P_{cs} is the price of corn stover in dollar per ton. Q_{cs} is denoted as the quantity of corn stover sold in tons. $Y_{i,j}$ is denoted as tons of corn stover harvested in period i of corn grain harvested in period j with i > j. $G_{i,j}$ is defined as corn stover harvest cost in dollars per ton. b_i is denoted as labor time required per acre to harvest corn grain in period i. $h_{i,j}$ is denoted as labor time required per ton to harvest corn stover in period i of corn grain harvested in period j. $k_{i,j}$ is defined as baling time required per ton to bale corn stover in period i of corn grain harvested in period j. $B\tilde{T}_i$ represents stochastic baling field time expressed in hours available in each period i. L is defined as total farm land acres that are available for corn grain harvest. m_j represents stover yield in tons per acre of grain harvested in period j.

The objective function (Equation 1.2) of the optimization problem is to quantify the net return potential associated with harvesting corn grain and stover separately using conventional technology. Equation (3.2) balances corn stover sales with production. Since corn grain and stover are harvested separately, in the first period only corn grain can be harvested. All grain harvests are assumed to be completed by the end of the third period (i.e. $j = 1, \ldots, 3$). Stover baling starts in the second period and ends in the final period (i.e. $i = 2, \ldots, 4$). Equation (5.2) limits the total amount of labor time available for harvesting corn grain in the first period. Equation (6.2) constrains the total amount of labor time available for harvesting both corn grain and stover. Equation (7.2) restricts the total amount of labor time available for harvesting and baling corn stover in the final period. Equation (8.2) prohibits stover baling time from exceeding the limits. Equation (9.2) limits the total land acres available for corn grain harvesting. Equation (10.2) restricts the total corn stover harvested in future period i to not exceed the total current supply availability in period j.

7 Empirical Results and Discussions

7.1 Corn Grain Harvesting

7.1.1 Assumptions and Data

Assumptions and data used to analyze the grain model are described in the following Table 7.1. Corn price and production cost are respectively assumed to be $142.86 per ton (or $4 per bushel) and $356.92 per acre. The production cost of corn will vary depending on the size of farm. In

this particular case, the size of farm is assumed to be 2,000 acres. Production cost includes cost of using seed, fertilizer, chemicals, insurance, land, machinery, building etc. Corn yield is assumed to be 4.04 tons per acre (or 144.27 bushels per acre). Cost and yield data are based on five-year (2005-2009) average North Dakota data and obtained from FINBIN Farm Financial Database. Corn harvest cost of $28.71 per acre is based on our estimated results in Table 3.1. Corn combine and labor have harvest capacity of 6.79 and 5.43 acres per hour respectively. The combine capacity data is based on Lazarus and Smale (2010) and labor capacity data is determined based on a factor of 1.25. Harvest field day data (Table 7.2) for the state were collected from Crop Progress and Condition Report of USDA National Agricultural Statistics Service. As mentioned above, each period of harvest field day is assumed to last for two weeks**.**

Table 7.1 Assumptions Used in Corn Grain Harvest Model

Corn Price ($/ton)	142.86
Production Costs ($/ac)	356.92
Corn Harvest Cost ($/ac)	28.71
Corn Yield (ton/ac)	4.04
Combine Capacity (ac/hr)	6.79
Labor Capacity (ac/hr)	5.43
Total Corn Acres	2,000.00

Table 7.2 Harvest Field Day Data

	From	To	2005	2006	2007	2008	2009	Mean Average
Period 1	24-Sep	7-Oct	9.90	11.60	11.70	11.10	9.30	**10.72**
Period 2	8-Oct	21-Oct	10.70	10.30	9.60	8.20	4.30	**8.62**
Period 3	22-Oct	5-Nov	11.90	10.90	13.10	10.20	5.40	**10.30**
Period 4	6-Nov	19-Nov	9.00	-	12.70	6.40	12.90	**10.25**

7.1.2 Deterministic Results

Results can be deterministic or stochastic as a farmer's net return will change if corn price, yield and field time fluctuate. Deterministic results are the results that contain no risk or random component. On the other hand, stochastic results are estimated using a random component (in this case random harvest field time) to generate a sample of outcomes. By incorporating data assumptions into the corn grain only harvest optimization model, deterministic optimal outcomes for net farm profit, corn grain sold, and harvested acres are generated and shown in the following Table 7.3 for two scenarios with differing harvest field time expressed in hours in each period. For each period, the table shows the positive correlation between corn acres harvested and harvest field time. With more harvest field hours available in each period in scenario one, more corn grain acres can be harvested until farmers finish harvesting all corn acres in the final period. In scenario one, the shadow price of $191.52 suggests that farmers are able to complete harvesting all 2000 corn acres and if an additional corn acre is available for harvesting,

farmers can increase their net profit by $191.52. In scenario two, about 106 corn acres are left unharvested due to harvest time limit, and the shadow price of $1,040.89 suggests that if corn combine time can be increased by an additional hour, then farmers can benefit from their net profit increase from $362,783 to $363,823.

Table 7.3 Deterministic Results for Corn Grain Production

	Scenario 1	Shadow Price ($)	Scenario 2	Shadow Price ($)
Net Profit ($)	383,048.80		362,782.60	
Corn Grain Sold (Tons)	8,080.00		7,652.51	
Corn Harvested Acres				
Period 1	699.13		697.07	
Period 2	562.17		307.66	
Period 3	671.74		461.79	
Period 4	66.96		427.66	
Total Corn Harvested Acres	2,000.00	191.52	1,894.18	0.00
Harvest Field Time (Hours)				
Period 1	128.64	0.00	128.26	1,040.89
Period 2	103.44	0.00	56.61	1,040.89
Period 3	123.60	0.00	84.97	1,040.89
Period 4	123.00	0.00	78.69	1,040.89
Total Harvest Field Time	478.68		348.53	

7.1.3 Stochastic Results

Corn harvest field days can be limited in North Dakota due to the rainfall and early frost. Deterministic outcomes do not describe how farmers would likely change their harvesting priorities or to what degree profitability is affected when faced with harvest time risk and limited field days. Using historical field day data and @Risk simulation software (Palisade Corporation, 2009), 1,000 random numbers of field days (or hours) are generated based on a uniform distribution. These random field days (or hours) are incorporated into the corn grain only harvest model to estimate random outcomes which show the impact of harvest field time variations on the net farm income, corn grain sold and corn acres harvested (assuming that all other variables such as corn price, yield and cost are unchanged). GAMS software (GAMS Development Corporation) is used to simulate these random outcomes.

Simulated results are reported in the following table and figures. Table 7.4 indicates that variations in harvest field time will have an impact on the net farm profit. Maximum net income that a farmer can obtain is $383,048.80 with all 2,000 farm acres harvested as can be seen in the table and Figure 7.1 below. The figure implies that harvest field time and net profit are positively correlated until all farm acres are harvested (i.e. until profit maximization is achieved). As shown in the figure, a farmer in North Dakota would need a total of 31 harvest field days with 12 working hours each day to finish harvesting 2000 corn acres.

Figure 7.2 depicts distribution histograms for total harvest field days available and net farm

income. It shows that with 90% confidence total harvest field days range from 30.91 to 42.69 days. Similarly, it shows that with 90% confidence the net farm profit would range from $379,870 to $384,210 given that all other variables remain unchanged. Table 7.4

Table 7.4. Simulated Stochastic Results for Corn Grain Harvesting

Variable	Mean	Std. Dev.	Minimum	Maximum
Net Profit ($)	382,338.10	4,232.43	329,838.33	383,048.80
Corn Grain Sold (Tons)	8,065.01	89.28	6,957.58	8,080.00
Corn Harvested Acres				
Period 1	684.79	45.21	358.88	451.42
Period 2	489.13	120.55	166.05	412.73
Period 3	591.74	134.63	208.39	505.21
Period 4	230.64	170.93	179.55	496.59
Harvest Field Time (Hours)				
Period 1	126.00	0.69	111.60	140.40
Period 2	90.00	1.85	51.60	128.40
Period 3	111.00	2.22	64.80	157.08
Period 4	115.80	1.88	76.80	154.68

Figure 7.1 Relationship between Corn Grain Harvested Acre and Availability of Harvest Field Days

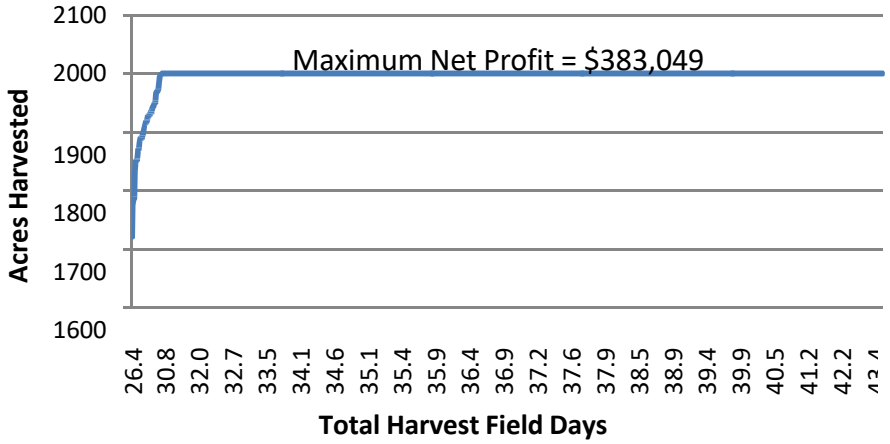

Figure 7.2 Histograms for Harvest Field Days and Corn Grain Net Farm Profit

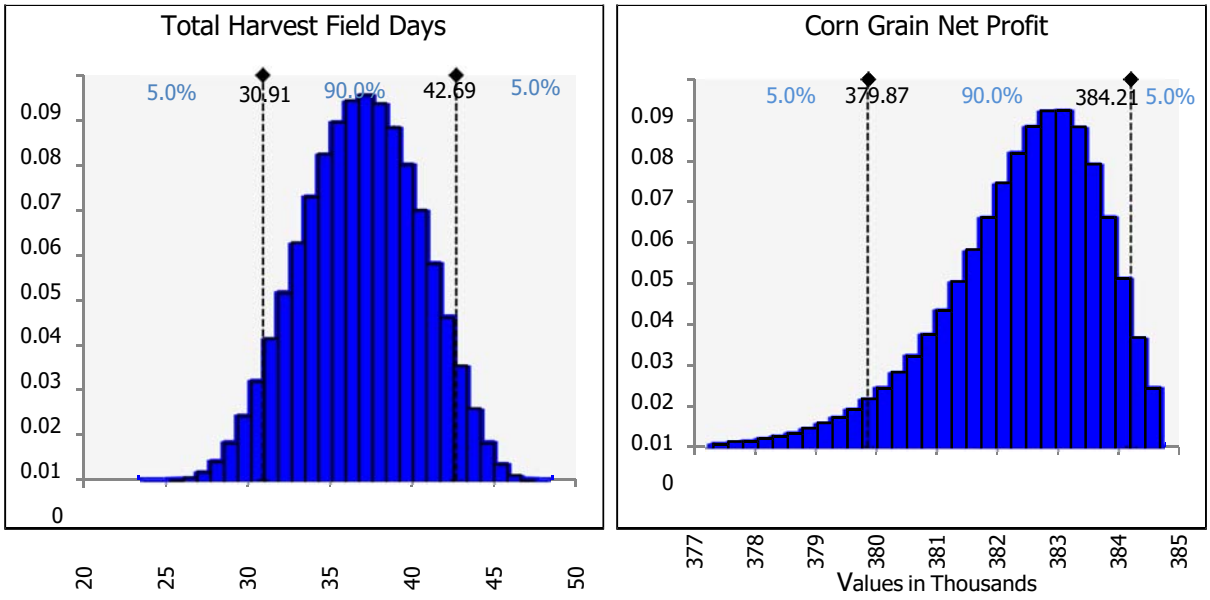

Distribution: Beta General

Weibull

7.1.4 *Impact of Farm Size on Corn Grain Harvesting*

Assuming that combine harvest capacity remains the same, as farm size increases farmers would need more harvest field time to cover additional land acres. Figure 7.3 reports the simulated results for different farm sizes ranging from 1,000 to 3,000 acres. During the simulation, it was assumed that all other variables such as price, yield, combine harvest capacity and production cost remain constant and the only variables changing are the farm size and stochastic harvest field time. The figure shows that for 1000- to 2000-acre farm sizes, farmers would be able to finish harvesting in a short amount of time and maximize their profit potential. However, as farm size increases to 3,000 acres, farmers would require more harvest field time to complete harvesting corn grain. Given limited harvest field time, the figure suggests that as farm size increases to 3,000 acres and above, farmers would be required to invest in additional labor and combine capacities in order to finish harvest early.

Figure 7.3 Impact of Farm Size on Net Farm Profit for Corn Grain Harvesting

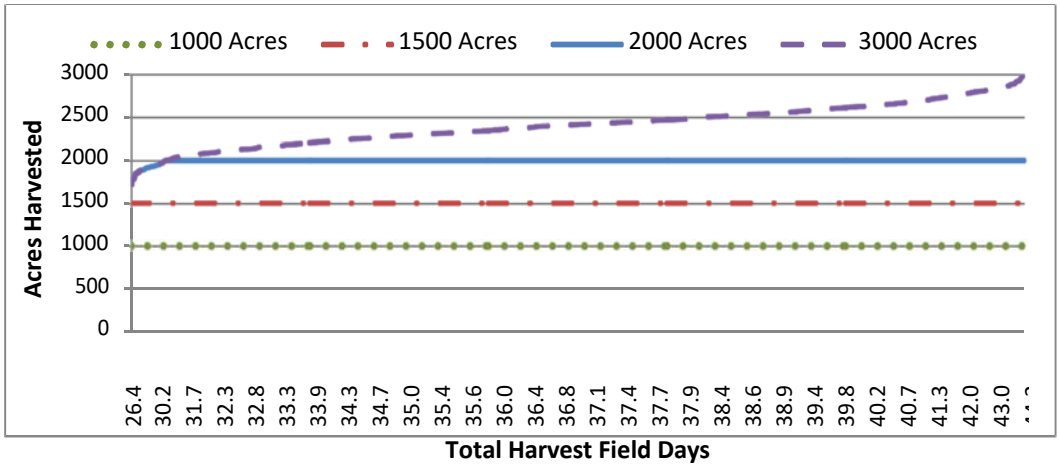

7.1.5 *Impact of Tillage Practice on Corn Grain Harvesting*

Tillage practices common in North Dakota can be grouped into two classes: conservation tillage (no tillage or reduced tillage) and conventional tillage. Conservation tillage reduces the frequency and intensity of tillage, retains crop residues as mulch on soil surface, reduces the risks of runoff and soil erosion, increases the soil organic carbon content of the surface soil, and reduces carbon dioxide emissions (Lal and Kimble, 1997; Reicosky, 1999; Al-Kaisi and Yin, 2005). Moreover, conservation tillage with residue cover usually results in less soil erosion than conventional tillage (Benoit and Lindstrom, 1987; Andrews, 2006).

Historically conventional tillage systems were more common, although conservation tillage systems have recently been found to have an advantage over conventional tillage systems (Uri, 1999). This could be due to the uncertainties associated with adopting a conservation tillage practice which requires investment in physical and human capital. In addition, conservation tillage usually leads to lower yields in early years before soil nutrients build up (Kurkalova et al., 2006). In Table 7.5 below, the yield and cost of corn grain are compared under different tillage systems for North Dakota. Yield and cost data for conventional tillage system were not specifically available but included in "All" tillage system in the table. Most farmers in the state use conventional tillage system for growing corn. Hence, "All" tillage system in the table may likely reflect conventional tillage system. The table shows that yield and cost per acre are lower with no till and reduced till than with other tillage systems.

Employment of different soil tillage practices results in different corn yields and production costs across farms with different soil types and climates (Harper 1996; Weersink et al. 1992; Mueller et al. 1985). Changes in both yields and costs will have an impact on the net farm profit of harvesting corn grain. Figure 7.4 illustrates scenarios for the impact of decrease in yield and production cost on the net farm profit of corn grain production. The figure shows that a small rate of decrease in corn yield (5% decrease) can have a negative impact on the net profit of harvesting corn grain. In addition, the figure shows that a decrease in corn yield followed by a decrease in production cost would have a positive impact on net farm profit only if the rate of decrease in corn production cost is much higher than the rate of decrease in corn yield.

Table 7.5 Five Year Average (2005-2009) Yield and Production Cost of Corn Grain by Tillage Practice (Include All Different Types of Farm/Enterprise Size)

Yield/Cost	No Till	Chisel/Reduced Till	All
Yield (bu/ac)	101.77	83.11	114.2
Variable Cost ($/ac)	204.01	210.07	262.42
Fixed Cost ($/ac)	55.71	42.02	57.13
Total Cost ($/ac)	259.72	252.09	319.55

Source: FINBIN Farm Financial Database

Figure 7.4 Scenarios for Impact of Yield and Production Cost on Net Farm Profit for Corn Grain (assumed 2000 acre farm size)

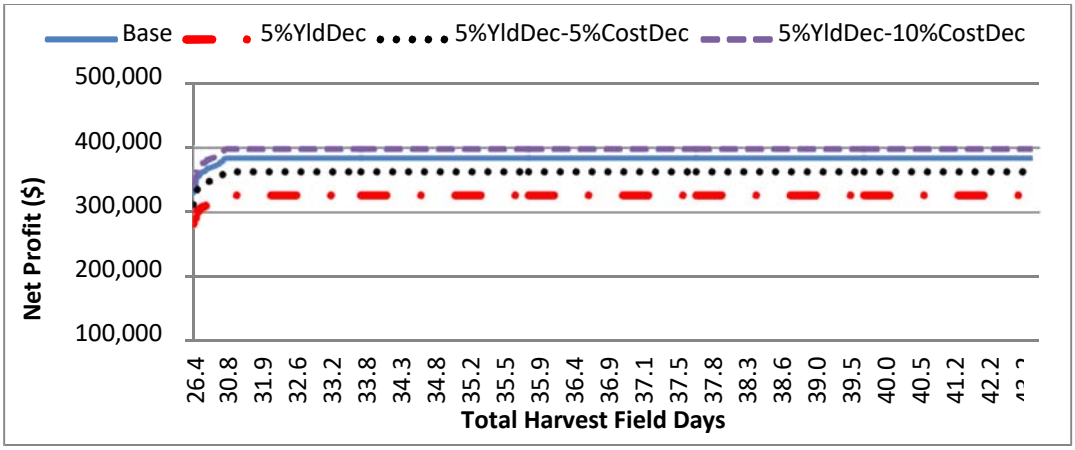

7.2 Simultaneous Corn Grain and Cob Harvesting

7.2.1 Assumptions and Data

Assumptions (see Table 7.6) for corn price, corn production cost, corn yield, and harvest field time remain the same as corn grain only harvest option. Cob price is based on the current biofuel industry offer price of $55 per ton. Corn grain harvest cost increases from $28.71 to $57.43 per acre due to an additional use of cob harvester attached to the back of combine assumed to slow down grain harvest capacity by half. Cob harvest cost of $19.36 per acre is based on our estimated result in Table 5.2. Corn cob yield of 0.35 ton per acre is based on the estimated average cob yield in North Dakota (see Table 5.1). Because of the additional use of cob harvester, corn combine capacity is assumed to reduce by half (from 6.79 acre/hour to 3.39 acre/hour).

Table 7.6 Assumptions Used in Simultaneous Corn Grain and Cob Harvest Model

Corn Price ($/ton)	142.86
Cob Price ($/ton)	55.00
Production Costs ($/ac)	356.92
Corn Harvest Cost ($/ac)	57.43
Cob Harvest Cost ($/ac)	19.36
Corn Yield (ton/ac)	4.04
Cob Yield (ton/ac)	0.35
Combine Capacity (ac/hr)	3.39
Labor Capacity (ac/hr)	5.43
Total Corn/Cob Acres	2,000.00

7.2.2 Deterministic Results

Deterministic results for simultaneous corn grain and cob harvesting are generated and reported in the following Table 7.7 (a & b). As can be seen in the table, results are generated based on three different corn combine capacity slowdown scenarios. If we assume that additional cob harvesting would not reduce corn combine harvest capacity, then farmers can generate additional revenue of $19,140 ($402,188.80 minus $383,048.80) from selling 700 tons of corn cobs in addition to selling 8,080 tons of corn grain. However, if additional cob harvesting results in the slowdown of corn combine harvest capacity, then farmers can incur a loss of $6,460 for 25% capacity reduction scenario or a loss of $119,054 for 50% capacity reduction scenario. The loss in revenue is mainly due to the slowdown in harvest capacity as a result of cob harvesting. Given that corn harvest time is constrained by the limited availability of harvest field days (expressed in hours in the table) in each period, farmers would not be able to maximize their net returns because of the slowdown. The 25% combine capacity reduction scenario in Table 7.7 (a) shows that all 2,000 acres of grain and cob can be harvested but net profit is reduced compared with no capacity reduction scenario. This is because the 25% slowdown in combine harvest capacity results in an

increase in corn grain and cob harvest costs which decrease net profit. The table also shows that about 377 corn acres are left unharvested if combine capacity slows down by 50%. Either the availability of harvest field time would have to increase or farmers would have to invest in additional harvest equipment and labor to finish all the harvesting to achieve maximum profit potential. Shadow prices correspond to the three scenarios are given in Table 7.7 (b). They can be interpreted in a similar manner as was done for the corn grain only harvest case.

Table 7.7 (a) Deterministic Results for Simultaneous Corn Grain and Cob Production

	50% Speed/Capacity Reduction	**25% Speed/Capacity Reduction**	**No Speed/Capacity Reduction**
Net Profit ($)	263,995.10	376,588.80	402,188.80
Corn Grain Sold (Tons)	6,555.48	8,080.00	8,080.00
Corn Cob Sold (Tons)	567.93	700.00	700.00
Corn Grain/Cob Harvested Acres			
Period 1	436.07	656.33	699.13
Period 2	350.64	527.76	562.17
Period 3	418.98	630.61	671.74
Period 4	416.95	185.31	66.96
Total Corn Grain/Cob Harvested Acres	1,622.64	2,000.00	2,000.00
Harvest Field Time (Hours)			
Period 1	128.64	128.64	128.64
Period 2	103.44	103.44	103.44
Period 3	123.60	123.60	123.60
Period 4	123.00	123.00	123.00

(b) Correspondent Shadow Price

	Shadow Price ($)		
	50% Speed/Capacity Reduction	**25% Speed/Capacity Reduction**	**No Speed/Capacity Reduction**
Total Corn Grain/Cob Harvested Acres	0.00	188.29	201.09
Harvest Field Time (Hours)			
Period 1	551.51	0.00	0.00
Period 2	551.51	0.00	0.00
Period 3	551.51	0.00	0.00
Period 4	551.51	0.00	0.00

7.2.3 Stochastic Results

Assuming that other variables such as corn grain and cob prices, costs and yields remain unchanged, variations in harvest field time will change the net farm income of producing corn grain and cob as indicated in the tables below for two different slowdown scenarios (Table 7.8 a & b). Increase in the availability of harvest field time would increase the amount of corn grain and cobs harvested and thus increase the net farm profit. Correlations between harvest field time, corn grain/cob acres harvested and net farm profit across different scenarios are examined in Figure 7.5 (a & b). For a 2000-acre farm, all grains and cobs can be harvested within 33 harvest field days for all the scenarios except the 50% harvest capacity reduction scenario (Figure 7.5 a). Harvest field time and net farm profits are positively correlated until all farm acres are harvested (Figure 7.5 b). For the 50% harvest capacity reduction scenario, more harvest field days will be needed to finish all the harvesting and achieve profit maximization. Results in the figure do not favor the simultaneous corn grain and cob harvesting if it causes corn combine to reduce its maximum potential harvest capacity. So, in that sense corn grain harvesting alone might be a better option. Figure 7.6 shows that with 90% confidence the net farm profit generated from corn grain and cob sales ranges from $204,600 to $282,500 for the 50% capacity reduction scenario, and from $398,850 to $403,410 for no capacity reduction scenario respectively.

Table 7.8 Simulated Stochastic Results for Simultaneous Corn Grain and Cob Harvesting

(a) 50% Capacity Reduction

Variable	Mean	Std. Dev.	Minimum	Maximum
Net Profit ($)	244,208.08	23,607.72	174,761.36	303,510.54
Corn Grain Sold (Tons)	6,064.13	586.22	4,339.65	7,536.72
Corn Cob Sold (Tons)	525.36	50.79	375.96	652.93
Corn Grain/Cob Harvested Acres				
Period 1	427.12	28.20	378.34	475.90
Period 2	305.08	75.19	175.05	435.12
Period 3	376.27	90.47	219.70	532.61
Period 4	392.55	76.37	260.51	524.51
Harvest Field Time (Hours)				
Period 1	126.00	0.69	111.60	140.40
Period 2	90.00	1.85	51.60	128.40
Period 3	111.00	2.22	64.80	157.08
Period 4	115.80	1.88	76.80	154.68

(b) No Capacity Reduction

Variable	Mean	Std. Dev.	Minimum	Maximum
Net Profit ($)	401,442.59	4,443.91	346,319.53	402,188.80
Corn Grain Sold (Tons)	8,065.01	89.28	6,957.58	8,080.00
Corn Cob Sold (Tons)	698.70	7.73	602.76	700.00
Corn Grain/Cob Harvested Acres				
Period 1	684.79	45.21	606.58	762.99
Period 2	489.13	120.55	280.65	697.61
Period 3	591.74	134.63	352.23	853.91
Period 4	230.64	170.93	0.00	738.15
Harvest Field Time (Hours)				
Period 1	126.00	0.69	111.60	140.40
Period 2	90.00	1.85	51.60	128.40
Period 3	111.00	2.22	64.80	157.08
Period 4	115.80	1.88	76.80	154.68

Figure 7.5 Comparison of Simulated Stochastic Scenario Results

(a) Correlation between Harvest Field Time and Acres Harvested

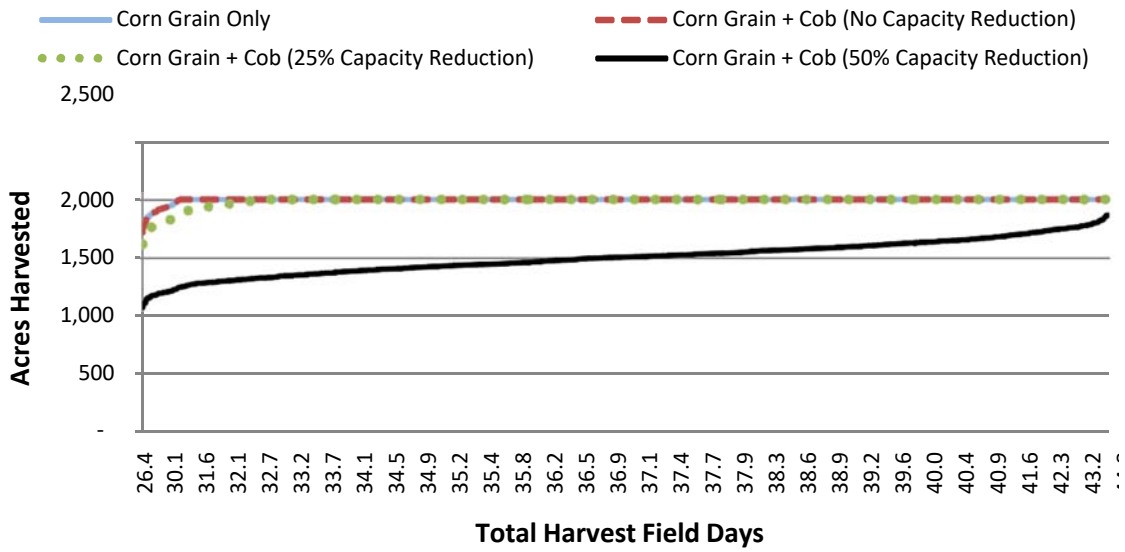

(b) Correlation between Harvest Field Time and Net Farm Profit

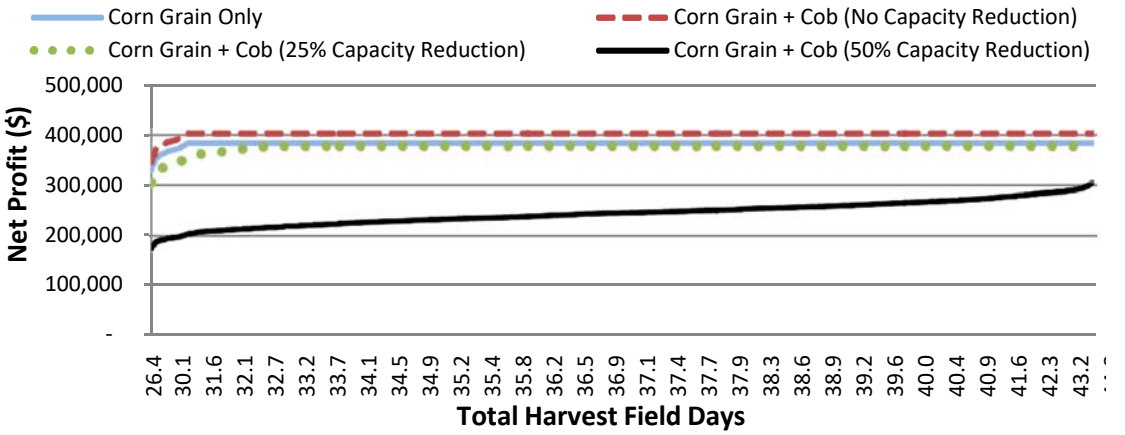

Figure 7.6 Histograms for Net Farm Profit of Corn Grain and Cob Production

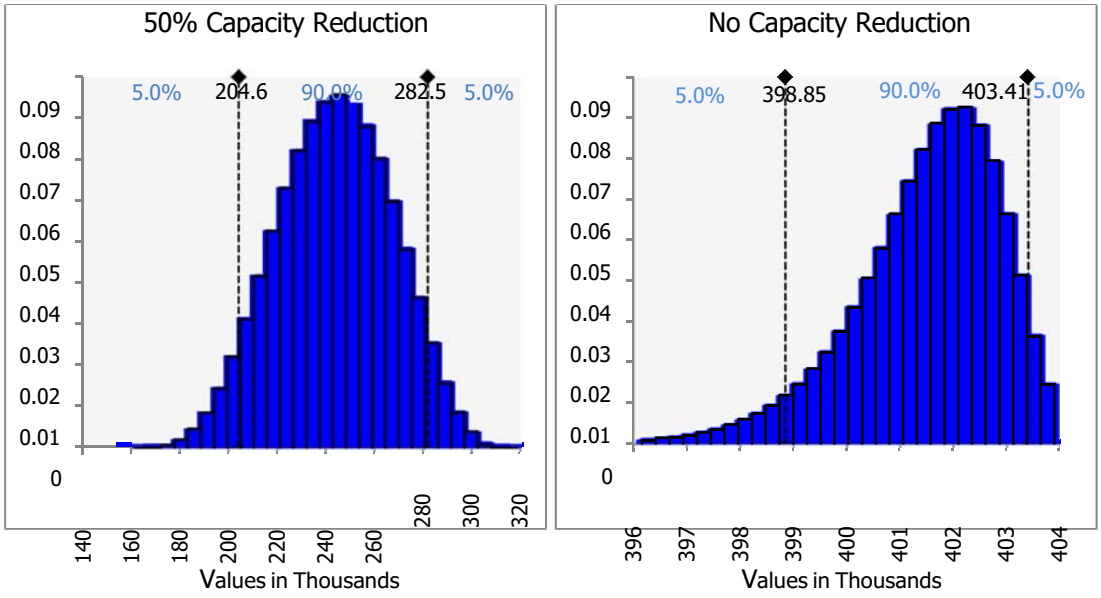

Distribution: Beta General Weibull

7.2.4 Impact of Farm Size on Simultaneous Corn Grain and Cob Harvesting

This analysis assumes that all other variables such as price, yield and production cost remain constant and the only variables changing are the farm size and harvest field time. Figure 7.7 (a, b & c) reports the simulated results for three different capacity reduction scenarios with different farm sizes ranging from 1,000 to 3,000 acres. All three scenarios indicate that harvesting both corn grain and cob in a relatively small 1000-acre farm is not constrained by limited harvest time and capacity. Farmers with a 1000-acre farm would be able to finish harvesting in a short amount of time and achieve profit maximization. However, when farm size increases, harvest time and capacity factors come into play. For example, with 50% harvest capacity slowdown because of cob harvesting, farmers with 1,500 acres of farm land would require more harvest field time to complete harvesting and reach their profit maximizing potential. As the assumption of harvest capacity slowdown decreases from 50% to 0%, harvest field time factor would become less relevant for farmers with 1,500 acres of land to achieve harvesting and profit maximizing goals. For comparatively large 2000- and 3000-acre farms, both harvest field time and capacity factors become very relevant. For example, farmers with 3000-acre farm land would not be able to maximize their profit potential if cob harvesting slowdown corn grain harvest capacity as shown in Figure 7.7 (a & b). Given limited harvest field time, the figure indicates that as farm size increases farmers would be required to expand their harvest capacity for both corn grain and cob

(i.e. invest in additional capital and labor) to finish all their harvesting activities and achieve profit maximizing potential. Our results suggest that as farm size increases the opportunity costs of harvesting corn cobs would become increasingly high such that if farmers' opportunity costs of harvesting cobs cannot be offset by revenues generated by harvesting those cobs then the farmers would be better off not harvesting any cobs at all.

Figure 7.7 Scenarios for Impact of Farm Size on Net Farm Profit for Simultaneous Corn Grain and Cob Harvesting

(a) 50% Reduction in Capacity Due to Cob Harvesting

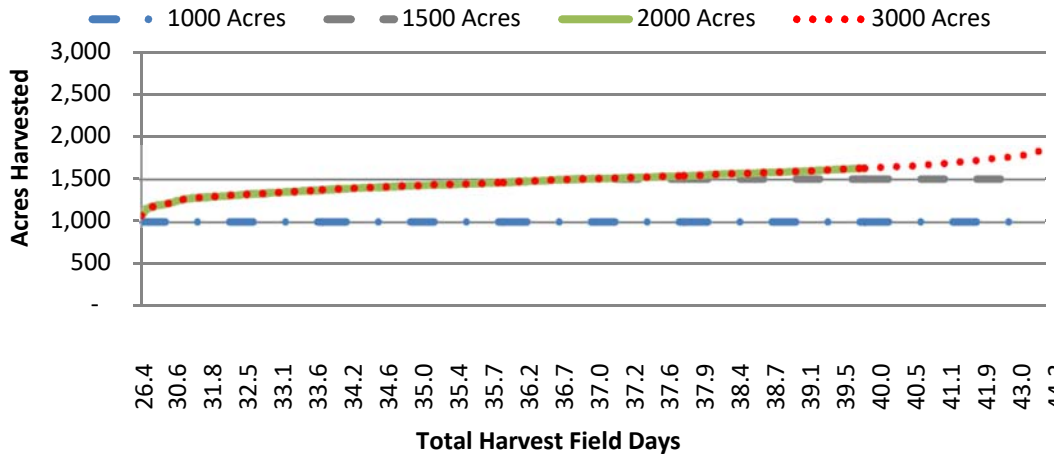

(b) 25% Reduction in Capacity Due to Cob Harvesting

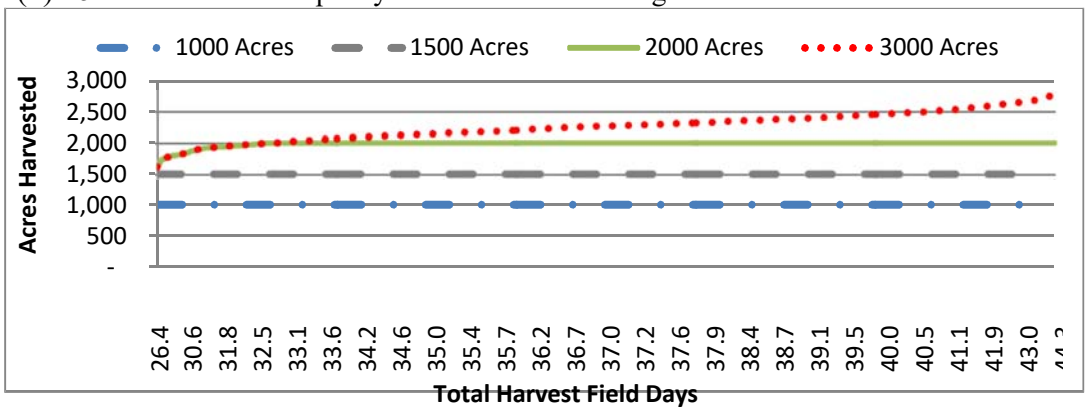

(c) No Reduction in Capacity Due to Cob Harvesting

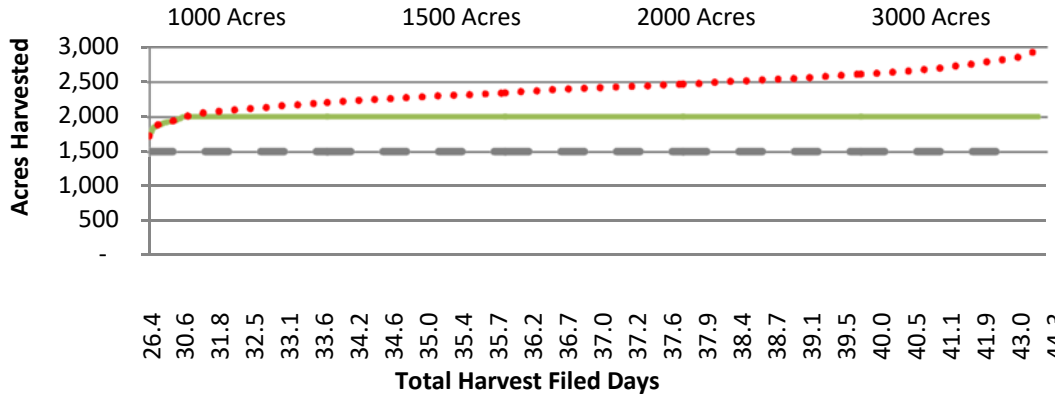

7.2.5 Impact of Tillage Practice on Simultaneous Corn Grain and Cob Harvesting

As we have mentioned, the use of different soil tillage practices would result in different yields and production costs across farms with different soil types and climates. This would have an impact on net farm profit of harvesting corn grain and cob. Figure 7.8 illustrates scenarios for the impact of decrease in yield and production cost on net farm profit for simultaneous corn grain and cob harvesting. Similar to corn grain only harvest option, the figure shows that a small rate of decrease in corn yield can have a significant negative impact on the net profit of harvesting corn grain and cob. Additionally, the figure shows that a decrease in corn yield followed by a decrease in production cost can have a positive on net farm profit only if the rate of the rate of decrease in corn yield is more than offset by the rate of decrease in corn production cost. Overall, the figure shows the volatility of simultaneous corn grain and cob harvest business because changes in yield and production cost (due to changes in tillage practice system) can result in fluctuations in net farm profits.

Figure 7.8 Scenarios for Impact of Changes in Yield and Production Cost on Net Farm Profit for Simultaneous Corn Grain and Cob Harvesting (assumed 50% capacity reduction)

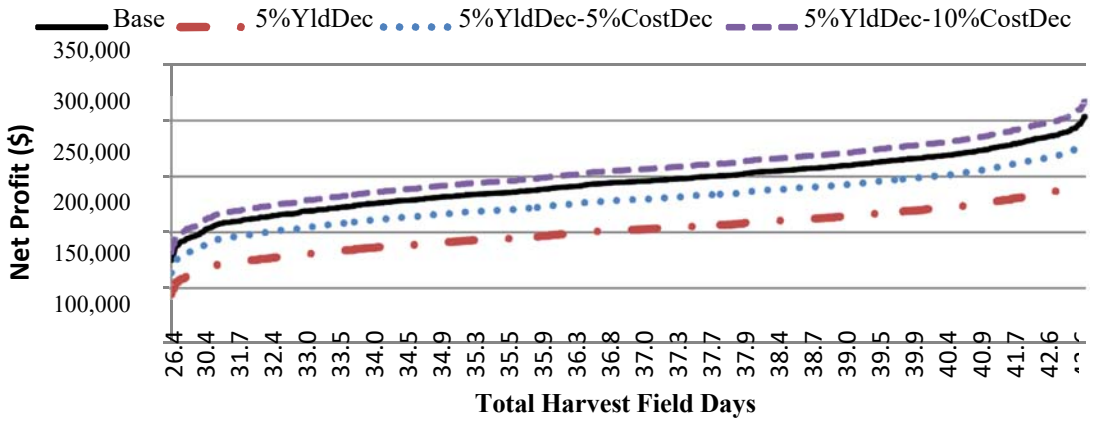

7.3 Separate Corn Grain and Stover Harvesting

7.3.1 Assumptions and Data

Corn grain and stover are assumed to be harvested separately and stover can be harvested only after grains are harvested. Stovers are assumed to be harvested using a tractor and a square baler. Table 7.9 describes the data assumptions used. Since, corn grain and stover are harvested separately there will be no slowdown in combine capacity. Corn price, production and harvest costs, corn yield, combine and labor harvest capacities are identical to the assumptions used in corn grain only harvest model. Stover price is assumed to be $45 per ton based on the current biofuel industry offer price. Stover harvest cost and state-average yield are computed to be

$33.53 per ton and 0.68 tons per acre (Table 5.4 & Table 3.1). Similarly, baler and labor baling capacities are respectively calculated to be 9.7 and 7.76 acres per hour. Labor baling capacity data is determined based on a factor of 1.25.

Table 7.9 Assumptions Used in Separate Corn Grain and Stover Harvest Model

Corn Price ($/ton)	142.86
Stover Price ($/ton)	45.00
Production Costs ($/ac)	356.92
Corn Harvest Cost ($/ac)	28.71
Stover Harvest Cost ($/ton)	33.53
Corn Yield (ton/ac)	4.04
Stover Yield (ton/ac)	0.68
Combine Capacity (ac/hr)	6.79
Labor Capacity for Grain Harvest (ac/hr)	5.43
Baler Capacity (ac/hr)	9.70
Labor Capacity for Baling (ac/hr)	7.76
Total Corn/Stover Acres	2,000.00

7.3.2 Deterministic Results

Table 7.10 below reports the deterministic results for corn grain and stover harvested separately. Results in the table are generated based on two different field time scenarios. In both scenarios we assume that farmers can spend 12 hours per day harvesting and baling stover using available harvest field time. As described in the methodology section, there are a total of four harvest periods and corn grain harvest must be completed within the first three periods. Stover harvesting and baling can take place only when corn grain harvest is completed. Hence, no stover can be harvested and baled in the first period and no corn grain can be harvested in the final period. All grain and stover harvest activities need to be completed within four harvest periods. In scenario one, the total acres of corn grain harvested (1,933 acres) fell short of the maximum 2,000 acres. This is because part of the farmers' time has been allocated to harvesting and baling stover in the final period and some acres of corn would be left unharvested.

The first scenario in the table also shows that no stover is harvested in the second and third periods. This is due to the fact that farmers find it optimal to allocate all of their time to harvest corn grain instead of stover during these two periods. The negative shadow price of $186.3 in the first scenario implies that if farmers were to attempt to harvest corn stover in either the second or third harvest period their net profit would decrease by $186.3 per ton of stover harvested. As suggested in the table, all stover harvest time is optimally allocated to the final period since no grain can be harvested during this final period. The shadow prices of $1,040.89 (for grain) and $60.37 (for stover) in the first scenario indicate that it would be much more valuable for farmers to harvest corn grain than stover if an additional harvest field hour is available.

In the second scenario as compared to the first scenario, we assume that the more harvest field time is available in each period. As can be seen in the table, farmers are able to finish harvesting all 2,000 corn acres in this second scenario as more time is available. The shadow price of $60.37 in the second scenario suggests that if an extra harvest field hour is available, farmers are better off harvesting stover since they are assumed to have perfect information and expect to complete harvesting all corn grain acres on time. The maximum amount of stover harvested for the first scenario is about 647 tons and for the second scenario is 960 tons. The difference in net profit between the first and second scenarios can be explained by the difference in corn stover sold or harvested.

Table 7.10 Deterministic Results for Corn Grain and Stover Production

	Scenario 1	Shadow Price ($)	Scenario 2	Shadow Price ($)
Net Profit ($)	377,650.31		394,060.00	
Corn Grain Sold (Tons)	7,809.50		8,080.00	
Corn Stover Sold (Tons)	647.37		959.64	
Corn Grain Acres Harvested				
Period 1	699.13		733.70	
Period 2	562.17		690.00	
Period 3	671.74		576.30	
Total Corn Grain Acres Harvested	1,933.04	0.00	2,000.00	180.42
Corn Stover Harvested in Tons				
Period 2	0.00	-186.30	0.00	0.00
Period 3	0.00	-186.30	201.21	0.00
Period 4	647.37	0.00	758.43	0.00
Harvest Field Time (Hours)				
Period 1	128.64	1,040.89	135.00	60.37
Period 2	103.44	1,040.89	126.96	60.37
Period 3	123.60	1,040.89	144.27	60.37
Period 4	123.00	60.37	144.10	60.37
Total Harvest Field Time	478.68		550.33	

7.3.3 Stochastic Results

Fluctuations in harvest field time will have an impact on the amount of corn grain and stover harvested which in turn will have an effect upon the net farm income as indicated in Table 7.11 below. Results in the table were simulated under the assumption that all other variables remain constant except harvest field time. The table suggests that as the availability of harvest field time increases, farmers are willing to allocate a little more of their time to harvest stover in the second and third periods although the final period remains the critical period when farmers spend most of their time on harvesting and baling stover.

Figure 7.9 analyzes the relationship between corn grain and stover harvested in tons as the availability of harvest field time increases. The figure shows that for a 2000-acre farm the amount of corn grain and stover harvested can fluctuate depending on the harvest field time availability in each period. The fluctuations of corn grain and stover harvested as available field time changes in each period can be explained numerically using Table 7.12. For example, if we compare the scenarios 1, 2 and 3 in the table, the differences in stover harvested in tons can be explained by the differences in harvest field time in the final period 4 when most stover harvesting and baling take place. In the table, harvest field time in the final period for the scenario 3 is higher than that of the scenario 1 or 2, and consequently total stover harvested in

the third scenario would be higher. Given the limited availability of harvest time, as more (less) labor time is allocated to harvesting stover less (more) would be available for harvesting corn grain and this would have an impact on net farm profit as illustrated in the first three scenarios in the table.

When overall total availability of harvest field time increases to above 40 days as shown in the table (scenario 5-8), farmers would be able to finish harvesting all 2000 corn grain acres within the first three periods and allocate their remaining time on harvesting stover. From the table (scenario 5-8), we can see that once farmers realize that they can finish harvesting corn grain on time, they are willing to increase their time and effort on harvesting and baling stover as the availability of harvest field time increases. This results in an increase in tons of stover harvested and consequently in net profit. This explains why grain and stover lines in Figure 7.9 are getting smoother rather than fluctuating up and down once total harvest field days exceed above 40. Generally, the figure shows that as harvest field time increases the quantities of corn grain and stover harvested tend to trend upward gradually.

Table 7.11 Simulated Stochastic Results for Corn Grain and Stover Harvesting

Variable	**Mean**	**Std. Dev.**	**Minimum**	**Maximum**
Net Profit ($)	345,284.50	34,234.02	248,631.24	394,055.77
Corn Grain Sold (Tons)	7,133.24	717.34	5,097.87	8,080.00
Corn Stover Sold (Tons)	620.64	123.44	404.47	959.63
Corn Grain Acres Harvested				
Period 1	684.79	45.21	606.58	762.99
Period 2	488.82	120.44	280.65	697.61
Period 3	592.04	134.98	352.23	853.91
Corn Stover Harvested in Tons				
Period 2	0.30	5.64	0.00	160.74
Period 3	10.87	34.74	0.00	224.53
Period 4	609.48	118.57	404.47	814.37
Harvest Field Time (Hours)				
Period 1	126.00	0.69	111.60	140.40
Period 2	90.00	1.85	51.60	128.40
Period 3	111.00	2.22	64.80	157.08
Period 4	115.80	1.88	76.80	154.68

Figure 7.9 Relationships between Corn Grain and Stover Harvest

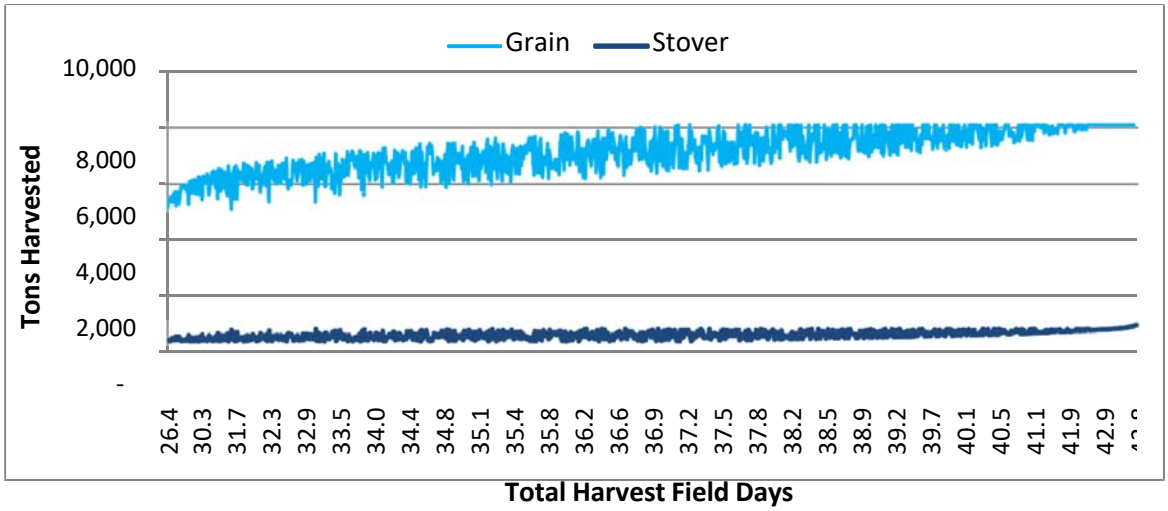

Table 7.12 Simulated Stochastic Results for Corn Grain and Stover Harvesting

	Harvest Field Time (Days)								
Scenario	Period1	Period2	Period3	Period4	Total	Stover (Tons)	Grain (Tons)	Acres Harvested	Net Profit ($)
1	9.32	4.56	5.63	6.90	26.41	435.90	5,139.14	1,272.07	248,631.24
2	9.49	6.14	8.09	6.44	30.15	406.42	6,247.95	1,546.52	300,858.30
3	9.87	6.62	6.31	12.30	35.10	776.95	6,005.55	1,486.52	293,616.77
4	9.35	10.22	10.34	10.09	40.00	637.26	7,881.73	1,950.92	380,958.94
5	11.29	10.55	11.66	11.57	45.08	910.00	8,080.00	2,000.00	393,486.50
6	10.56	10.40	11.84	12.55	45.34	926.74	8,080.00	2,000.00	393,678.47
7	10.74	10.46	12.94	11.35	45.48	935.53	8,080.00	2,000.00	393,779.29
8	10.65	9.81	12.68	12.71	45.84	958.53	8,080.00	2,000.00	394,043.10

7.3.4 Impact of Farm Size and Corn Yield on Separate Corn Grain and Stover Harvesting

Figure 7.10 (a & b) reports the simulated results for different farm sizes ranging from 1,000 to 3,000 acres. During the simulation, it was assumed that all other variables remain constant except the size of farm and harvest field time. The figure indicates that farmers with 1000-acre farm land would be able to finish harvesting both grain and stover within a short period of time. As farm size increases to 1,500 acres, farmers would require a longer period of time to complete harvesting both grain and stover. For relatively large 2000- and 3000-acre farms, harvest field time could become a limited factor and farmers would find it difficult to allocate time for harvesting both grain and stover. Given limited harvest field time, Figure 7.10 (b) indicates that farmers with 1500-acre land would have the potential to harvest more quantities of corn stover than those of their counterparts with comparatively large 2000- and 3000-acre lands. This is because for a relatively small farm, grain harvest can be completed within a short amount of time

and hence more time can be allocated to harvesting stover. Our findings suggest that as farm size increases (assuming that harvest capacity and other variables remain constant), farmers would find less amounts of time allocated to harvesting stover. Similar to the simulated results shown in the simultaneous corn grain and cob harvesting case, a small rate of decrease in corn yield due to changes in tillage practice systems can have a large negative impact on the net profit of harvesting corn grain and stover (not reported).

Figure 7.10 Impact of Farm Size on Corn Grain and Stover Harvesting

(a) Corn Grain

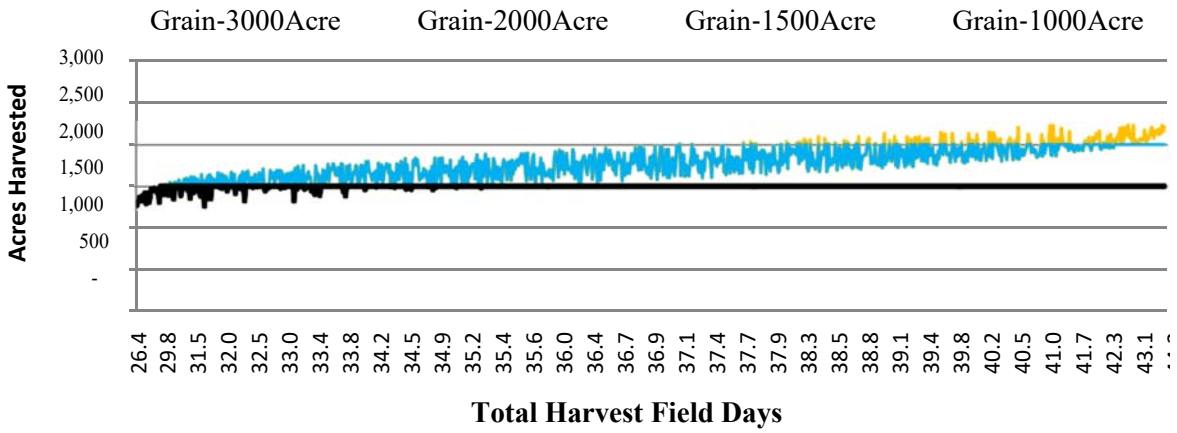

(b) Corn Stover

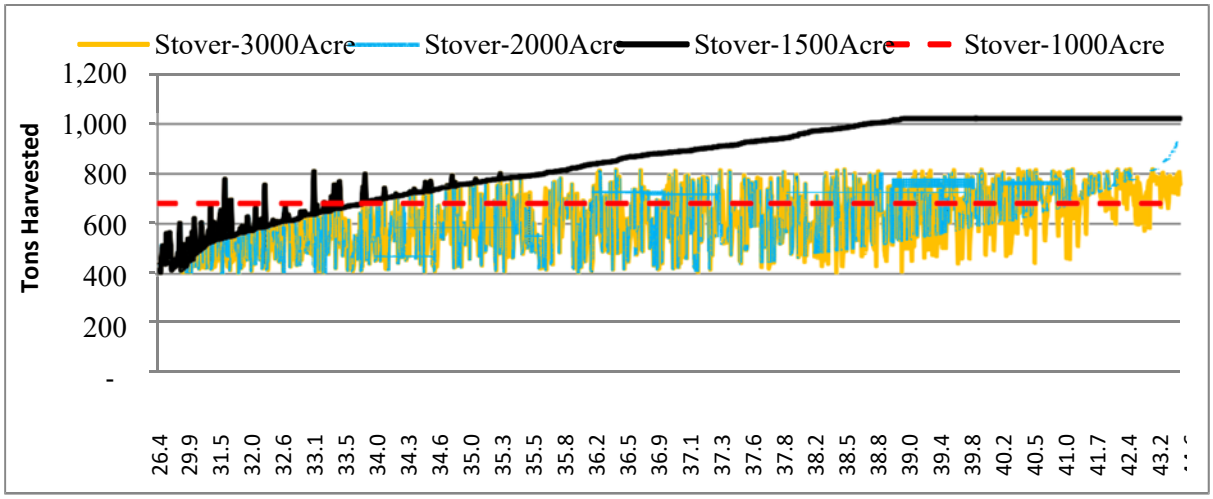

8 Summary and Conclusions

In this study, corn cob and stover availability in North Dakota were first estimated on a per acre basis. In addition, currently available cob and stover harvesting technologies were described and harvest costs for corn grain, cob and stover were estimated using machinery cost estimation procedures. In order to gain insights into the economic tradeoffs between corn grain and residue harvest activities in the region, we analyzed net farm returns under changing harvest field time using stochastic linear programming models with different corn grain and residue harvest options. Emphasis was placed on understanding the impact of harvest field time, cob and stover harvest technologies, farm sizes and tillage practice on profit maximizing potential of corn farmers. Harvest field time can be very limited in North Dakota because of rainfall and early frost. Randomized fall harvest field days were incorporated into our models to create stochastic outcomes which show that variations in the availability of field time can have a great impact on net farm profits. Harvest field time and net farm returns were found to be positively correlated until all farm acres were harvested and farmers reached their profit maximizing goals.

Under the corn grain only harvest option, farmers were able to complete harvesting corn grain and achieve profit maximization in a fairly short amount of time. However, when the corn cob harvest option was added to our model, corn grain harvest capacity would be reduced due to the attachment of a cob harvester to the back of the combine. Given the limited amount of harvest field time available, this reduction in harvest capacity would result in some corn acres being left unharvested and consequently may cause a loss in net farm revenue. Our findings indicate that if additional corn cob harvesting does not interfere with grain harvest capacity then farmers' net returns from producing both grain and cob would be higher as compared to the net returns from producing only corn grain. In reality this scenario would not likely happen because under the simultaneous corn grain and cob (one-pass) harvest option, farmers' harvest activities are not only constrained by the slowdown in harvest capacity but also by the limited availability of harvest field time. This calls into question the viability of using a cob harvester to harvest corn cobs for energy production.

Another major problem associated with harvesting corn stover is the time allocation when farmers choose the option of harvesting corn grain and stover separately (two-pass harvest method). If more labor time is allocated to harvesting stover, less would be available for harvesting corn grain and this would have an impact on farmers' net profits. Because part of the

farmers' time has to be allocated to harvesting and baling stover, with limited availability of harvest field time some acres of corn grain could be left unharvested. Our results show that farmers may find it optimal to allocate most of their time to harvesting stover during the last harvest period when corn grain harvests were completed or nearly completed. In general, as the total availability of harvest field time increases, the quantities of corn grain and stover harvested tend to increase gradually.

Changes in farm sizes can also have an impact on the amount of corn grain and cob/stover harvested. Our findings suggest that an increase in the size of farm would require farmers to expand their harvest capacity for both corn grain and cob/stover. For example, given limited harvest field time as farm size increases farmers would need more harvest capacity to finish harvesting both grain and cob under the one-pass harvest option (as compared to the corn grain only harvest option) since additional use of cob harvester attached to the back of corn combine would slowdown the grain harvest capacity. Comparatively, this suggests that an increase in farm size would require farmers to invest in additional labor and machinery equipment to increase their harvest capacities and complete harvesting both grain and cob.

Under the two-pass grain and stover harvest option, as farm size increases (assuming that all other variables remain unchanged) the availability of harvest field time could become a very limited factor. With given harvest capacity and field time, farmers would increasingly find it difficult to allocate time for harvesting both grain and stover as farm size increases. Our results indicate that farmers with relatively small acres of land would have the potential to harvest more quantities of corn stover than those of their counterparts with comparatively large land tracts. This is due to the fact that small farm owners can afford to allocate more of their time to harvesting stover since they have less amounts of land to cover for harvesting grain. Our findings suggest that as farm size increases, farmers would find less amounts of time allocated to harvesting stover.

Variations in the use of soil tillage systems would result in changes in corn yields and production costs among farms with different soil types. This would have an impact on farmers' net returns of harvesting corn grain and cob/stover. Our evidence shows that a small decrease in corn yield due to changes in tillage practices can result in a large decline in the net profit of harvesting corn grain and cob/stover. As a consequence of changes in tillage practices, the rate of decrease in yield must be more than offset by the rate of decrease in production cost in order for

net farm profit to remain unaffected. Overall, the findings in this paper show the volatility of the corn grain and cob/stover harvest business not only because of changes in yield but because of issues related to harvest capacity slowdown, time allocation and unpredictability in the availability of harvest field time.

To summarize, the simultaneous corn grain and cob one-pass harvest system may not be an optimal choice for biofeedstock production unless farmers are compensated for their potential losses due to harvest capacity slowdown. On the other hand, under the corn grain and stover two-pass harvest system, farmers may find it challenging on how to allocate time between harvesting grain and stover. Harvest field time could become very limited as the size of farm land needed to be harvested increases. Based on our evidence in this paper, we believe that it would be more efficient economically to allow a second party (either a biofuel firm or a firm that specializes in collecting crop residues and other biomass sources) to participate in the stover harvesting and baling business.

References

Al-Kaisi, M. M., and X. Yin. 2005. "Tillage and Crop Residue Effects on Soil Carbon and Carbon Dioxide Emission in Corn-Soybean Rotations." *Journal of Environmental Quality* 34: 437-445.

Andrews, S. S. 2006. "Crop Residue Removal for Biomass Energy Production: Effects on Soil and Recommendations." U.S. Department of Agriculture-Natural Resource Conservation Service. Available at: http://soils.usda.gov/sqi/files/AgForum_Residue_White_Paper.pdf.

Apland, J., B. A. McCarl, and T. G. Baker. 1981. "Crop Residue Supply for Energy Generation: A Prototype Application to Midwestern U.S.A. Grain Farms." *Energy in Agriculture*, 1: 55-70.

Apland, J. 1990. "Incorporating Field Time Risk into a Stochastic Programming Model of Farm Production." Staff Paper P90-11, Department of Agricultural and Applied Economics, University of Minnesota.

Benoit, G. R., and M. J. Lindstrom. 1987. "Interpreting Tillage-residue Management Effects." *Journal of Soil and Water Conservation* 42:87-90.

Bouzaher, A. and S. Offutt. 1992. "A Stochastic Linear Programming Model for Corn Residue Production." *Journal of Operational Research Society*, 43: 843-57.

Bernick, J. 2009. "Cob Harvest Makes Strides." Available at: http://www.agweb.com/Farm Journal/current/Article.aspx?id=154884.

Cihacek, L. J., M. D. Sweeney, and E. J. Deibert. 1993. "Characterization of Wind Erosion Sediments in the Red River Valley of North Dakota." *Journal of Environmental Quality*, 22: 305-10.

Chippewa Valley Ethanol Company (CVEC). 2009. "Corn Cobs as Sustainable Biomass for Renewable Energy, a Field-to-Facility Demonstration and Feasibility Study." Final Report to the Minnesota Department of Commerce Office of Energy Security. Available at: http://www.cvec.com/ main.asp?SectionID=21&SubSectionID=57&FileID=30&UID=578499.

Christiansen, R. C. 2009. "Craving Corn and the Cob." Available at: http://www.biomass magazine.com/article.jsp?article_id=2307&q=&page=all.

Davidson, D. 2008. "A Look at Some Biomass Harvest Options in Corn." Available at: http://www. agecon.purdue.edu/topfarmer/newsletter/TFCW1_2008.pdf.

Edwards, W. 2009. "Estimating Farm Machinery Costs." Available at: http://www.extension. iastate.edu/agdm/crops/pdf/a3-29.pdf.

Erickson, M. J. and W. E. Tyner. 2010. "The Economics of Harvesting Corn Cobs for Energy." Purdue Extension ID-417-W, Purdue University. Available at: http://www.agecon.purdue.edu/papers/biofuels/ID_417_W.pdf.

FINBIN Farm Financial Database. Crop Summary Reports. Available at: http://www.finbin.umn.edu/CropEnterpriseAnalysis/Default.aspx.

Gallagher, P. W., M. Dikeman, J. Fritz, E. Wailes, W. Gauthier, and H. Shapouri. 2003. "Supply and Social Cost Estimates for Biomass from Crop residues in the United States." *Environmental and Resource Economics*, 24:335-58.

GAMS Development Corporation. Available at: http://www.gams.com/

Grooms, L. 2010. "Equipment Manufacturers Demonstrate Their Biomass Harvesters at a POET Field Day." Available at: http://farmindustrynews.com/farm-equipment/0101-poet-biomass- plant/.

Hall, D. O., F. Rosillo-Calle, R. H. Williams, and J. Woods. 1993. "Biomass for Energy: Supply Prospects." In T. B. Johansson, H. Kelly, A. K. Reddy, and R. H. Williams, eds. *Renewable Energy: Sources for Fuels and Electricity*. Washington, DC: Island Press, pp. 593- 651.

Harper, J. K. 1996. "Economics of conservation tillage." Pennsylvania State University: College of Agricultural Sciences Cooperative Extension. Available at: http://cropsoil.psu.edu/extension/ct/uc130.pdf.

Intergovernmental Panel on Climate Change (IPCC), 2007. "IPCC Fourth Assessment Report: Climate Change 2007." Available at : http://www.ipcc.ch/publications_and_data/publications_and_data_reports.shtml#1.

Johnson, A. 2008. "Demonstration Shows Two Ways to Collect Corncobs." Available at: http://www.farmandranchguide.com/articles/2008/11/05/ag_news/production_news/prods00.txt.

Kurkalova, L. A., C. L. Kling, and J. Zhao. 2006. "Green subsidies in agriculture: Estimating the Adoption Costs of Conservation Tillage from Observed Behavior." *Canadian Journal of Agricultural Economics* 54:247–267.

Lal, R. 2005. "World Crop Residues Production and Implications of Its Use As a Biofuel." *Environment International* 31(4):575-584.

Lal, R., and J. M. Kimble. 1997. "Conservation Tillage for Carbon Sequestration." *Nutrient Cycling in Agroecosystems* 49:243–253.

Lazarus, W. F. and A. Smale. 2010. "Farm Machinery Cost Estimation Spreadsheet (MACHDATA.XLS)." Available at: http://www.apec.umn.edu/faculty/wlazarus/tools.html.

Leistritz, L. and N. Hodur. 2008. "Local and Regional Economic Impacts of Biofuel Development." Available at: http://ageconsearch.umn.edu/bitstream/53503/2/LeistritzLarry.pdf.

McCarl, B. A., T. A. Maung and K. T. Szulczyk. 2009. "Could Bioenergy be used to Harvest the Greenhouse: An Economic Investigation of Bioenergy and Climate Change?" In Madhu Khanna, Jurgen Scheffran and David Zilberman, eds. *Handbook of Bioenergy Economics and Policy*. New York, NY: Springer, pp. 195-218.

McAloon, A., F. Taylor, W. Yee, K. Ibsen, and R. Wooley. 2000. "*Determining the Cost of Producing Ethanol from Cornstarch and Lignocellulosic Feedstocks*." Report No. NREL/TP- 580-28893, National Renewable Energy Laboratory, Golden, Colorado.

Mueller, D. H., R. M. Klemme, and T. C. Daniel. 1985. "Short- and Long-term Cost Comparisons of Conventional and Conservation Tillage Systems in Corn Production." *Journal of Soil and Water Conservation*, 40: 466-470.

Nelson, R.G. 2002. "Resource Assessment and Removal Analysis for Corn Stover and Wheat Straw in the Eastern and Midwestern U.S.—Rainfall and Wind-induced Soil Erosion Methodology." *Biomass and Bioenergy* 22:349-63.

Neeley, T. 2007. "Cobs: The Future of Cellulosic Ethanol." Available at: http://www.dtnethanol.com/ index.cfm?show=10&mid=66&pid=41.

O'Brien, D. 2010. "Corn Market Supply Questions for Late Winter-Spring 2010." Available at: http://www.agmanager.info/marketing/outlook/newletters/archives/GRAIN-OUTLOOK_01-27- 10.pdf.

Palisade Corporation. 2009. @Risk 4.5 - Professional Edition. Software. New York, NY. Perlack, R. D.,

A. F. Turhollow. 2003. "Feedstock Cost Analysis of Corn Stover Residues for Further Processing." *Energy*, 28: 1395-1403.

Perlack, R. D., L. L. Wright, A. F. Turhollow, R. L. Graham, B. J. Stokes, and D. C. Erbach. 2005. "*Biomass as Feedstock for a Bioenergy and Bioproducts Industry: the Technical Feasibility of a Billion-ton Annual Supply*." Oak Ridge National Laboratory, Oak Ridge, Tennessee. Available at: http://feedstockreview.ornl.gov/pdf/billion_ton_vision.pdf.

Petrolia, D. R. 2008. "The Economics of Harvesting and Transporting Corn Stover for Conversion to Fuel Ethanol: A Case Study for Minnesota." *Biomass and Bioenergy*, 32:603-12. Petrolia, D.R. 2008. "The Economics of Harvesting and Transporting Corn Stover for Conversion to Fuel Ethanol: A Case Study for Minnesota." *Biomass and Bioenergy*, 32: 603-12.

Reicosky, D. C. 1999. "Effects of Conservation Tillage on Soil Organic Carbon Dynamics: Field Experiments in the U.S. Corn Belt." Available at http://topsoil.nserl.purdue.edu/nserlweb-old/isco99/pdf/iscodisc/Sustaining%20the%20Global%20Farm/P002-Reicosky.pdf.

Roberts, M. C. 2009. "Biomass Availability in Northwest Ohio." Available at: http://ohioline.osu .edu/aex-fact/pdf/0541.pdf.

Sauer, T. J., J. L. Hartfield, and J. H. Prueger. 1996. "Corn Residue Age and Placement Effects on Evaporation and Soil Thermal Regime." *Soil Science Society of American Journal* 60:1558- 64.

Schneider, U. A., and B. A. McCarl. 2003. "Economic potential of biomass based fuels for greenhouse gas emission mitigation." *Environ. & Res. Econ.* 24, 291–312.

Shirek, M. 2008. "Going Beyond the Corn Kernel." Available at: http://www.ethanolproducer. com/article.jsp?article_id=3626&q=&page=1.

Sokhansanj, S. and A. F. Turhollow. 2002. "Baseline Cost for Corn Stover Collection." *Applied Engineering in Agriculture*. 18: 525–530

Turhollow, A. F. and S. Sokhansanj. 2007. "Costs of Harvesting, Storing in a Large Pile, and Transporting Corn Stover in a Wet Form." *Applied Engineering in Agriculture*, 23: 439-48.

USDA National Agricultural Statistics Service. Progress and Condition Report. Available at: http://www.nass.usda.gov/Statistics_by_State/North_Dakota/Publications/Crop_Progress_&_Co ndition/index.asp.

Uri, N. D. 1999. "Factors Affecting the Use of Conservation Tillage in the United States." *Water, Air, and Soil Pollution* 116:621-638.

Van Donk, S. J., S. D. Merrill, D. L. Tanaka, J. M. Krupinsky. 2008. "Crop Residue in North Dakota: Measured and Simulated by the Wind Erosion Prediction System." *American Society of Agricultural and Biological Engineers*, 51(5): 1623-32.

Weersink, A., M. Walker, C. Swanton, and J. E. Shaw. 1992. "Costs of Conventional and Conservation Tillage Systems." *Journal of Soil and Water Conservation*, 47: 328-334.

Wehrspann, J. 2009. "Concept Cob Collectors." Available at: http://farmindustrynews.com/farm-equipment/0201-concept-cob-collectors/.

Wiselogel, A., S. Tyson, and D. Johnson. 1996. "Biomass Feedstock Resources and Composition." In C. E. Wyman, eds. *Handbook of Bioethanol: Production and Utilization*. Washington, DC: Taylor and Francis Press, pp. 105-116.

Zych, D. 2008. "The Viability of Corn Cobs as a Bioenergy Feedstock." Available at: http://renewables.morris.umn.edu/biomass/documents/Zych-TheViabilityOfCornCobsAsA BioenergyFeedstock.pdf.

Back to Table of Contents

Appendix I

Estimated Corn Stover and Cob Yield by Climatic Region and County (2005-2009 Average)

Region/County	Harvested Acres (acre)	Land Area (acre)	Density (%)	Stover Availability (ton/acre)	Stover Availability (ton)	Cob Availability (ton/acre)	Cob Availability (ton)
Northwest	**13,538.23**	**5,852,864.00**	**0.23**	**0.44**	**5,917.46**	**0.22**	**3,019.11**
Burke	-	706,259.20	-	-	-	-	-
Divide	1,580.33	806,099.20	0.20	0.25	388.05	0.13	197.98
Mountrail	-	1,167,315.20	-	-	-	-	-
Renville	2,400.00	559,852.80	0.43	0.10	243.10	0.05	124.03
Ward	7,713.47	1,288,243.20	0.60	0.54	4,183.57	0.28	2,134.47
Williams	1,844.43	1,325,094.40	0.14	0.60	1,102.74	0.31	562.62
North Central	**72,433.62**	**4,379,872.00**	**1.65**	**0.61**	**43,980.83**	**0.31**	**22,439.20**
Benson	36,071.75	883,584.00	4.08	0.72	25,825.52	0.37	13,176.29
Bottineau	2,997.22	1,067,897.60	0.28	0.21	625.99	0.11	319.38
McHenry	19,781.36	1,199,417.60	1.65	0.55	10,964.57	0.28	5,594.17
Pierce	11,591.11	651,404.80	1.78	0.50	5,845.03	0.26	2,982.16
Rolette	1,992.19	577,568.00	0.34	0.36	719.71	0.18	367.20
North East	**190,636.60**	**5,451,379.20**	**3.50**	**0.75**	**143,355.09**	**0.38**	**73,140.35**
Cavalier	2,011.63	952,614.40	0.21	0.27	542.53	0.14	276.80
Grand Forks	60,446.61	920,198.40	6.57	0.90	54,432.32	0.46	27,771.59
Nelson	20,197.40	628,236.80	3.21	0.62	12,423.95	0.31	6,338.75
Pembina	25,576.10	716,000.00	3.57	0.72	18,439.51	0.37	9,407.91
Towner	9,474.17	655,712.00	1.44	0.31	2,916.14	0.16	1,487.82
Ramsey	48,346.61	758,304.00	6.38	0.77	37,115.34	0.39	18,936.40
Walsh	24,584.08	820,313.60	3.00	0.71	17,485.30	0.36	8,921.07
West Central	**36,781.47**	**5,523,571.20**	**0.67**	**0.61**	**22,467.28**	**0.31**	**11,462.90**
Dunn	6,133.08	1,286,144.00	0.48	0.45	2,776.33	0.23	1,416.50
McKenzie	1,948.64	1,754,892.80	0.11	0.51	998.22	0.26	509.30
McLean	15,984.63	1,350,368.00	1.18	0.58	9,261.11	0.30	4,725.06
Mercer	4,265.20	669,113.60	0.64	0.66	2,805.54	0.34	1,431.40
Oliver	8,449.93	463,052.80	1.82	0.78	6,626.07	0.40	3,380.65
Central	**206,690.92**	**4,531,545.60**	**4.56**	**0.79**	**163,702.87**	**0.40**	**83,521.87**
Eddy	11,960.17	403,276.80	2.97	0.64	7,660.82	0.33	3,908.58
Foster	30,234.60	406,528.00	7.44	0.67	20,115.15	0.34	10,262.83
Kidder	11,346.42	864,505.60	1.31	0.73	8,281.80	0.37	4,225.41
Sheridan	5,400.36	621,920.00	0.87	0.31	1,652.06	0.16	842.89
Stutsman	104,165.66	1,421,696.00	7.33	0.89	92,233.44	0.45	47,057.88
Wells	43,583.70	813,619.20	5.36	0.77	33,759.59	0.40	17,224.28
East Central	**493,067.30**	**3,545,363.20**	**13.91**	**0.99**	**486,232.02**	**0.50**	**248,077.56**
Barnes	107,852.14	954,656.00	11.30	0.96	103,276.79	0.49	52,692.24
Cass	189,400.55	1,129,747.20	16.76	1.03	194,848.62	0.52	99,412.56
Griggs	23,688.20	453,440.00	5.22	0.90	21,305.28	0.46	10,870.04
Steele	63,595.05	455,910.40	13.95	0.94	59,640.76	0.48	30,428.96
Traill	108,531.36	551,609.60	19.68	0.99	107,160.57	0.50	54,673.76
Southwest	**29,792.44**	**5,114,694.40**	**0.58**	**0.33**	**9,963.62**	**0.17**	**5,083.48**
Adams	3,554.42	632,262.40	0.56	0.28	995.40	0.14	507.86
Billings	1,216.68	736,902.40	0.17	0.24	287.12	0.12	146.49
Bowman	2,977.19	743,712.00	0.40	0.37	1,104.97	0.19	563.76
Golden Valley	4,468.76	641,273.60	0.70	0.33	1,464.46	0.17	747.18
Hettinger	9,751.40	724,640.00	1.35	0.35	3,397.48	0.18	1,733.41
Slope	1,563.92	779,481.60	0.20	0.33	523.30	0.17	266.99
Stark	6,260.08	856,422.40	0.73	0.35	2,190.89	0.18	1,117.80

Appendix I (continued)

Region/County	Harvested Acres (acre)	Land Area (acre)	Density (%)	Stover Availability		Cob Availability	
				(ton/acre)	(ton)	(ton/acre)	(ton)
South Central	**92,890.85**	**5,006,604.80**	**1.86**	**0.57**	**52,688.55**	**0.29**	**26,881.91**
Burleigh	18,052.32	1,045,177.60	1.73	0.52	9,462.71	0.27	4,827.91
Emmons	44,563.46	966,323.20	4.61	0.72	31,989.00	0.37	16,320.92
Grant	13,595.46	1,062,054.40	1.28	0.21	2,914.13	0.11	1,486.80
Morton	12,579.62	1,232,812.80	1.02	0.61	7,692.69	0.31	3,924.84
Sioux	4,100.00	700,236.80	0.59	0.15	630.02	0.08	321.44
Southeast	**684,986.69**	**4,738,700.80**	**14.46**	**1.03**	**704,634.80**	**0.52**	**359,507.55**
Dickey	116,634.18	723,840.00	16.11	1.06	123,482.20	0.54	63,001.12
La Moure	121,380.71	734,195.20	16.53	1.04	126,280.60	0.53	64,428.88
Logan	19,518.50	635,289.60	3.07	0.72	13,958.95	0.36	7,121.91
McIntosh	18,889.97	624,121.60	3.03	0.77	14,469.11	0.39	7,382.20
Ransom	69,962.12	552,160.00	12.67	1.07	75,002.30	0.55	38,266.48
Richland	241,653.62	919,494.40	26.28	1.03	248,756.30	0.53	126,916.48
Sargent	96,947.59	549,600.00	17.64	1.06	102,685.34	0.54	52,390.48

Appendix II

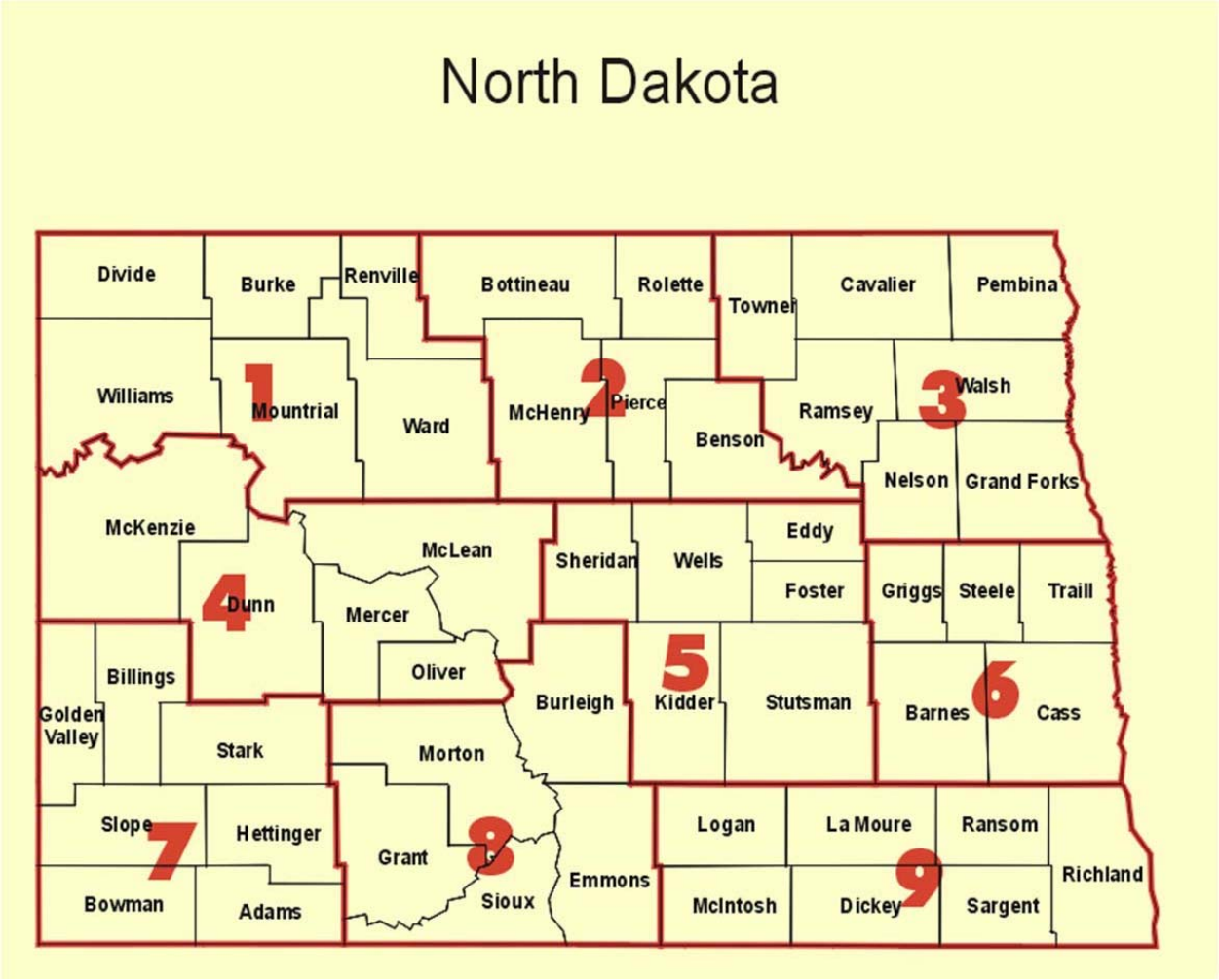

1 Northwest
2 North Central
3 Northeast
4 West Central
5 Central
6 East Central
7 Southwest
8 South Central
9 Southeast

Source: http://www.cpc.noaa.gov/products/analysis_monitoring/regional_monitoring/CLIM_DIVS/states_counties_climate-divisions.shtml.

Appendix III

A. Whole Cob Harvest Option

(1) Vermeer Cob Harvester

(2) Redekop and Case IH Cob Harvester

H165 Cob Harvester

C180 Cart

Case IH

Appendix III

Whole Cob Harvest Option Continued

(3) Residue Recovery System

Source: http://www.cvec.com/SiteImages/FileGallery/CVEC_Final_Report_to_Office_of_Energy_Security_30.pdf

Appendix III

B. Corn Cob Mix Harvest Option

Source: http://www.bioeconomyconference.org/08%20Presentations%20approved/Breakouts/Feeding%20the%20Dragon/McGrew.pdf

Appendix III

C. Stover Baling Option

Challenger LB

Case IH LB

Appendix IV

Assumptions and Formulas

Fuel Consumption = 0.044 x horsepower

For cob harvester, fuel consumption (2.5 gal/hr) is directly obtained by personal communication with Vermeer Corporation.

Capacity = (Width × Speed × Field Efficiency) / 8.25

Description and explanation details can be seen in Edwards (2009). Fixed

Cost = Capital Recovery + Taxes, Insurance and Housing

Capital Recovery = [Total Depreciation × Capital Recovery Factor] + [Salvage Value × Real Interest Rate]

Taxes, Insurance and Housing = 1% of Purchase Price

Total Depreciation = Purchase Price – Salvage Value

Salvage Value = List Price × Remaining Value Factor

Remaining Value Factor is obtained from Table 1 in Edwards (2009) (18% for corn combine and 23% for cob harvester). 23% is based on the value of forage harvester, since no data for cob harvester is currently available.

Purchase price and real interest rate are assumed to be 85% of list price and 5% respectively. Capital

Recovery Factor is assumed to be 11.3% for corn combine and 13% for cob harvester
based on Table 2 in Edwards (2009).

Repair Cost = Accumulated Repair Cost / Economic Life

Accumulated Repair Cost = 40% of List Price for corn combine (45% of List Price for Cob Harvester) (Based on Table 3 in Edwards (2009)). 45% is based on the value of forage harvester, since no data for cob harvester is currently available.

Variable Cost = Repair Cost + Fuel Cost + Lubrication Cost + Labor Cost

Results Validation through Panel Meeting

Summary

We invited four panelists to join our discussions. But one panelist could not make it to the meeting due to a time conflict. Our three panelists were Dr. Joel Ransom, Joe Breker and Paul Anderson. Dr. Joel Ransom is a professor and extension agronomist at the department of Plant Sciences in NDSU. Joe Breker is a North Dakota Corn Grower Association board member and also a farmer. Mr. Breker has many years of experience harvesting stover on his crop livestock operation near Havanna, ND. Paul Anderson is a farmer located in Harvey, North Dakota. He grows corn, pinto beans, soybeans, sunflowers, wheat and peas.

The session began with a presentation of our research findings. Our panelists enthusiastically participated in an open discussion and provided a number of thoughtful comments including their views on corn cob/stover harvesting for biofuel production during and after the presentation. The information and feedback obtained from our panelists are summarized as follows.

Farmers are busy during harvest time. The window for harvesting corn can be very limited in North Dakota due to weather constraints. According to our panelists, depending on the weather, it would take about two weeks to a couple of months to finish harvesting corn. Generally, soybeans and corn grains are not competing for harvest time since soybean harvests are completed earlier than corn in North Dakota. As indicated by our panelists, farmers may spend 10 hours of combine time each day to harvest corn during the harvest season. There are times when some corn acres are left unharvested because of unfavorable weather.

Our empirical results are consistent with current farm practices, i.e. the use of a corn cob harvester would slow down corn grain harvesting and thereby affect farmers' profits. The panelists indicated that they would prefer to harvest corn stover instead of cobs because corn cob harvesting would interfere with their grain harvesting activities. The most important factor in farmers' decision to harvest corn cob/stover is the price paid to farmers by biofuel producers as mentioned by our panel members. Considering all factors such as soil erosion, nutrient losses, and slowdown in grain harvesting, farmers might not be willing to get involved in cob/stover harvest business unless they are compensated with a high cob/stover contract price.

Corn stovers have some soil nutrient values and farmers would need to replenish the loss in nutrients if too much stover is removed. As the price of fertilizer rises, farmers' willingness to harvest stover diminishes. The best time to harvest stover in North Dakota would be at the end of November or early December when grain harvests were completed. Spring is not a good time to harvest stover because our panelists pointed out that soils are saturated from winter snow and heavy harvesting machines would damage fragile soils. Due to harvest field time constraints,

farmers prefer to let somebody else harvest stovers for them. The method that farmers prefer to use to harvest stover is the two-pass harvest method. Farmers are already familiar with the method and it does not slow down grain harvesting.

The majority of farmers would likely use reduced tillage with a chisel plow to grow corn in North Dakota. As our panelists pointed out, farmers switching to a no-till system from a reduced or conventional till system must go through the learning curve of knowing how much corn yield they will get and how much production costs they can save as a result of converting to a no-till system. Thus, it will take a while before farmers realize their profit potential of employing a no- till system. Overall, the research findings are consistent with what our panelists believe.

Questions for Panel Meeting Discussions

1) In addition to the alternatives we have presented, is there any other way to harvest stover?
2) How much time do you generally need to complete harvesting corn?
   a) Two weeks
   b) Four weeks
   c) Eight Weeks
   d) More than eight weeks
3) Would employing no-till system to grow corn result in higher net returns than utilizing conventional-till system?
4) How many hours do you work on field each day during the harvest season?
5) Are there any chances of corn acres being left unharvested because of limited availability of harvest field time?
6) Do you prefer to harvest corn cobs or stover?
7) What would be the most important factor in your decision to harvest corn cobs/stover?
   a) Price paid
   b) Harvest field time
   c) Farm size
   d) Soil erosion and carbon organic matter
   e) Other
8) Would you be willing to remove corn cobs/stover from your field for biofuel production considering soil erosion and nutrient issues?
9) Is spring a good time to harvest cobs/stover?
10) Would you prefer to harvest corn cobs/stover on your own or let somebody else do it?
11) Which method would you prefer to use to harvest corn cobs?
   a) One-pass harvest method using cob harvester
   b) Two-pass harvest method using tractor and baler
   c) Neither

12) Do you have to worry about concentrating on harvesting another crop like soybeans when harvesting corn grain?

13) What type of tillage practice do you think most farmers in North Dakota employ to grow corn?
   a) No Till
   b) Reduced Till
   c) Conventional Till

Please complete the following table to reflect your project at completion or time of report submission:

ITEM	NUMBER
Abstracts	**2**
Peer Reviewed Publications	**In progress**
Outreach Publications/Web Pages	**http://www.ethanolproducer.com/articles/8063/harvesting-both-corn-grain-and-stover-in-adverse-weather**
Professional Presentations	**2**
MS Degrees Conferred	**0**
Ph.D. Degrees Conferred	**0**
MS Students Supported	**0**
Ph.D. Students Supported	**0**
Post-Docs Supported	**1**
Undergraduate Students Supported	**0**
Investigators Supported	**0**
Start-Up Jobs Created	**0**
Disclosures	**0**
Patents Filed	**0**
Provisional Patents	**0**
Patents Issued	**0**
License Agreements	**0**
Plant Variety Protection	**0**

Back to Table of Contents

Sun Grant Initiative

DOE Final Progress Report

Project Title: The Logistics of Herbaceous Crop Residue-Based Ethanol Production under Uncertainty

Project Director/Principal Investigator: David K. Lambert, Department of Agricultural Economics; Kansas State University, Manhattan, KS

Period of Performance: 1 January 2009 - 30 June 2011

Funding Awarded: $116,063

Cost Share Amount: $29,027

Cost Share Sources: Time and effort from PIs and CoPIs; Indirect on time and effort.

Project Summary

Technical advances are expected to result in commercialization of the lignocellulosic conversion of biomass to fuels and other products in the near future. Although other feedstocks will be used, herbaceous crop residues will be one important input to this new industry. Logistical network design to service this new industry will in part determine the rates of return to investments in harvest, storage, pretreatment, and biorefineries to convert biomass to fuels, feed, and industrial products. As recent experience in the corn-based ethanol system demonstrates, however, risk and uncertainty regarding input and output prices and technical aspects of the conversion process can negatively affect investment returns. The proposed research project will develop a logistical system model of an emerging HCR-based industry in Minnesota, North, and South Dakota to identify optimal harvest, storage, distribution of pretreatment facilities, and location and scale of biorefineries strategies. Sensitivity analysis will incorporate uncertainty surrounding costs of harvest, transportation, feed values, prices of biofuels and other potential industrial products, in addition to the uncertainty regarding engineering aspects of the yet to be developed conversion facilities. The results indicate optimal system design under uncertainty.

Summary Results

The objective of the current research is to characterize potential HCR supplies in North and South Dakota and Minnesota and to determine the feasibility of developing HCR-based facilities under a range of potential production, price, and cost assumptions.

The results indicate HCR-based cellulosic ethanol production is profitable under the cost, price, and technical assumptions used to model plant investment decisions. Results further identify necessary site characteristics for the location of a cellulosic processing complex, and include:

- Output prices, input costs, and pretreatment and biorefinery investment costs influence the feasibility and location of local plants;
- Local cropping patterns, with subsequent impacts on corn stover and small grain residues, influence likely locations for locating pretreatment and refinery operations;
- Potential crop residue-based ethanol plants favor the more productive agricultural areas of the three states that now produce higher output levels of corn and small grains, especially

southern and western Minnesota, the eastern counties of South Dakota, and the southeastern counties of North Dakota;

- Scale economies in both pretreatment facilities and in biorefineries mitigate against a decentralized pretreatment pattern, with large pretreatment plants co-located with large biorefineries; and
- Ammonium Fiber Expansion pretreatment (AFEX) yields feedstock for ethanol production yet also can provide high value cattle feed for local feedlots.

Introduction

American response to increasing energy costs includes conservation and the promotion of energy production from renewable resources. A major thrust in President George Bush's State of the Union addresses of 2006 and 2007, and mandated in the Energy Policy Act (EPA) of 2005 and the Energy Independence and Security Act (EISA) of 2007, calls for the production of ethanol as a substitute for petroleum-based transportation fuels. In response to both federal mandate and local, state, and federal subsidy, corn-based annual ethanol production in the United States increased from 6 billion liters (1.6 billion gallons) in 2000 to forecast levels of 51 billion liters (13.5 billion gallons) in 2011 (Renewable Fuels Association).

Despite widespread investment in corn-based ethanol production facilities, the sustainability of the corn-based ethanol industry has been questioned. Swenson (2007) addresses the technical aspects of corn-based biofuels while de Gorter and Just (2010) question the social welfare affects of renewable fuels policy. Limited potential for further conversion of land to corn production, perceptions of negative impacts of increasing industrial use of corn on food and feed markets, limited reductions in greenhouse gas production from reliance on a corn-based industry, and low efficiency of conversion of corn to ethanol reduce the long run potential of a corn-based ethanol expansion (Carolan, Joshi, and Dale 2007).

In light of these perceived constraints, as well as recognizing the cost-effectiveness of ethanol production from feedstocks other than corn, the EISA established goals of 45 percent of ethanol (60 billion liters) to be derived from lignocellulosic and other advanced processes by 2022. Consequently, alternative ethanol production technologies are under study. One major focus explores the technical and economic feasibility of herbaceous crop residues (HCR) as a feedstock for ethanol production. There are many advantages of using HCR for ethanol

production. The technical yield of energy produced from lignocellulosic conversion may be as high as 11.31 BTUs produced per BTU used in production, comparing well with sugar cane and far exceeding the relatively low yield of corn-based ethanol of 1.40 to 1 (Vadas, Barnett, and Undersander, 2008). In addition, global policy attention has focused on problems of converting grains from meeting food to meeting energy demand. Cellulosic ethanol production based on HCR feedstocks can result in a joint agricultural production function: grains that can be used for food or feed and crop residues available for biofuels, combined heat and power, animal feed, industrial products, and other joint products.

Although potentially more profitable than corn-based ethanol production, economic analyses of the logistics of production, biomass harvesting, transportation, storage of feedstock, decentralized versus centralized pre-treatment operations, biorefinery scale and location, and transportation of product to wholesale fuel blenders is essential for determining if commercial investment in the new industry will occur. Several authors have addressed specific logistical systems of cellulosic ethanol production: Petrolia in Minnesota (2008); Kang et al. in Illinois (2010); Perkis, Tyner, Preckel and Brechbill in Indiana (2008); and Lambert and Middleton (2010) in North Dakota. This research uses county estimates of HCR supplies from corn and small grains in North and South Dakota and Minnesota to identify locations of possible pretreatment facilities and biorefineries. Results are illustrative, yet sensitivity analysis provides estimates of system feasibility under economic, agronomic, and engineering uncertainty inherent in the system.

Literature Review

Much past research has focused on specific components of the HCR production system. Thorsell et al. (2004) considered alternative harvesting approaches to determine equipment complements essential for timely residue harvest. Optimal machinery complements estimated mowing, raking, baling, gathering, and stacking costs would be within $11.26 and $14.01 per metric ton. Carolan, Joshi, and Dale (2007) analyzed scale economies from separating pretreatment facilities from ethanol refineries. Their analysis considered dispersed AFEX treatment facilities ranging in daily feedstock capacity from 604 to 4032 metric tons, with the necessary number of distributed pretreatment plants determined to meet the needs of a one billion liter per year biorefinery. The authors found pretreatment costs decreased by 52% when

the pretreatment facilities increased from 604 to 4032 MTPD throughput, signifying considerable economies of scale associated with the larger pretreatment plants. Wright and Brown (2007) used engineering cost formulas to analyze optimal biorefinery scale based on alternative feedstocks and pretreatment and refining processes. Optimal scale for biochemical cellulosic plants in Wright and Brown's study were very large plants with ethanol capacities of approximately 1.3 billion liters of gasoline equivalent ethanol produced per year. Leistritz et al. (2006) estimated costs of a hypothetical system from harvest of wheat straw through commercial production of ethanol and industrial products. Assuming a centralized AFEX pretreatment process co-located with a 206 million liter biorefinery, estimated return on investment ranged from 7.06% to 7.33%, indicating potential profitability of the wheatstraw-based cellulosic system. In a preliminary study for the current project, Lambert and Middleton (2010) analyzed the potential system characteristics of distributed pretreatment plants and cellulosic ethanol refineries in seven counties of northeastern North Dakota. Minimum ethanol selling prices (MESP) to justify development of a wheatstraw-based ethanol industry was $0.45 per liter ($1.70 per gallon) under their baseline scenario.

Interest in HCR-based ethanol systems is growing as feasible conversion technologies approach commercialization. State and regional level models are cited in the introduction (Petrolia (2008); Kang et al. (2010); Perkis, Tyner, Preckel and Brechbill (2008); Lambert and Middleton (2010)). All of these authors reported the potential feasibility of cellulosic ethanol plants under their base assumptions regarding costs and output prices. Tembo, Epplin, and Huhnke (2003) developed a mixed integer programming model to determine the feasibility of harvesting herbaceous crop residues, native forages, biomass harvested from improved pastures, and dedicated energy crops. An ethanol selling price of $0.24 per liter resulted in six ethanol refineries being constructed in Oklahoma under their base scenario. This early model was refined to consider biomass harvest from Conservation Reserve lands in Mapemba, Epplin, Taliaferro, and Huhnke (2007). It is interesting that all of these studies find cellulosic ethanol production to be feasible, based on cost estimates from a technology that did not exist at the time of the research.

Modeling Approach

The objective of the research project is to identify optimal location and scale of the

multiple activities underlying the production of HCR-based ethanol and byproducts. Research methods incorporate agronomic, engineering, and economic characteristics of the activities in a mixed integer programming (MIP) model determining optimal activity location and scale. Given recent experience of the effects of variability in both input and product prices in the corn-based ethanol industry, sensitivity analysis is conducted to incorporate uncertainty regarding input and output prices, feedstock yields, and the technology of HCR-based ethanol production. The advantage of the detailed MIP approach allows prediction of changes in plant location and scale, production of feed and industrial byproducts of the pretreatment and biorefining process, and HCR harvest in response to changes in the agronomic, economic, and technical variables underlying the system.

The study area encompasses Minnesota, North Dakota, and South Dakota. Two factors underlie selection of these three states. First, a thorough analysis of the HCR-based bioprocessing sector can be completed for this three state area given the time and budget allocated to the proposed research project. Second, these three states are representative of the

Table 1. Small Grain and Corn Production in the North Central Sun Grant Region, 2009

State	All Wheat	Other Small Grains[a]	Corn
		(Thousands of metric tons)	
Illinois	1081	20	44070
Indiana	710	6	20040
Iowa	23	77	52346
Minnesota	1982	242	26703
Montana	4158	786	85
Nebraska	1808	26	33812
North Dakota	8880	1613	4470
South Dakota	3040	104	15435
Wisconsin	504	193	9622
Wyoming	118	133	135
Total	22,304	3,199	206,719

a. Other small grain production reported by NASS includes oats and barley

variety of HCR supplies in the North Central Sun Grant Region (table 1). North Dakota leads the region in wheat and other small grain production. HCR supplies from Minnesota will primarily be corn stover. South Dakota has significant, though intermediate, supplies of wheat and other small grains, as well as significant corn acreage.

Great potential for HCR-based biorefining exists in the North Central Sun Grant Region (table 1). Combining all wheat and other small grain production in 2009, small grain baled straw production from the 10-state region could total 9.5 million metric tons (mmt) on a dry weight basis assuming an upper limit of straw removal of 43%. In addition, the 206 mmt of corn produced in the region in 2009 would yield approximately 72 mmt of corn stover potentially available for processing based on a 35% removal rate. Based on a conservative conversion ratio of approximately 250 liters of ethanol produced per metric ton of feedstock, the 10-state region could potentially produce approximately 20.3 billion liters of ethanol from small grain and corn residues, or one third of the 60 billion liter goal of ethanol produced from lignocellulosic feedstocks established in EISA.

As discussed in Carolan, Joshi, and Dale (2007), an advantage of the HCR technology is the variety of feedstocks that can be used for fuel, feed, or industrial product production. This feedstock variety reduces dependency upon a single crop, such as wheat, and lengthens the time period for HCR harvest, storage, and pretreatment based on the characteristics of the different feedstock sources.

Overview of the Logistical Model

The mixed integer programming (MIP) model is an effective workhorse in analyzing the optimal location of economic activity. The traditional framework identifies a large number of potential sites of economic activity, termed nodes, and incorporates arcs defining transportation networks joining the nodes. The permissible direction of movements along the arcs maintain sequential characteristics of the system (for example, ethanol cannot be produced until feedstock has been pretreated). Plant location and scale decisions are modeled as integer variables. These integer variables represent decisions to build a plant of a certain scale in a certain location. The structure of the logistics model of HCR-based ethanol production in the study area is:

1. Farm production regions

   a. Potential crop residue production will depend upon historical wheat, other small grain, and corn plantings and harvest of straw and stover following grain harvest. Grain yield potential is based on historical county crop yield data rather than future land use changes should local markets for crop residue or energy crops arise.

2. Straw Storage nodes
   a. Following HCR harvest, storage is assumed to occur either locally or at centralized locations adjacent to pretreatment facilities. Ending HCR inventory in each period at each location equals carry-in supplies (including harvest), minus HCR that is pretreated during the period.
3. Pretreatment nodes
   a. Because of the high daily feedstock requirements of HCR-based ethanol processing, decentralized pre-treatment sites have been proposed to minimize storage constraints at biorefineries. Carolan, Joshi, and Dale (2007) provide preliminary cost estimates of pretreatment facility capital and operating costs. Output from the pretreatment facilities can be stored or used for animal feeds, electricity generation, or production of ethanol or industrial chemicals.
   b. Pretreatment can occur at a site only if fixed costs of building the facility are incurred. Once a plant is built, pretreatment occurs at a constant marginal cost. Choice of plant size is endogenous in the model to permit balancing of transportation costs of straw and pretreated feedstocks with increasing returns to scale. Fewer, larger pretreatment facilities can realize economies of scale, but incur higher costs associated with longer hauls from farm to pretreatment facility for the raw biomass.
   c. Output of the pretreatment process can be used for ethanol yet also may be used as animal feed. Consequently, feeding of the AFEX-treated biomass is included as a decision variable in alternative formulations of the basic logistical model.
4. Ethanol production nodes
   a. Although commercial scale processes to convert HCR to ethanol and other industrial products have not yet been developed, Leistritz et al. (2006) have characterized the technical and economic characteristics projected for the production nodes.
   b. Similar to the pretreatment nodes, processing plants of different scale can be built. Plant location and scale are modeled as special ordered sets of type 2 (SOS2)

variables, allowing explicit consideration of increasing returns to scale as plants get larger. Plants that are built incur fixed construction and investment costs and constant marginal costs of producing output.

5. Final markets
    a. Plant-specific ethanol prices would consider transportation costs to final demand. However, the model is simplified by parameterizing ethanol prices rather than adjusting ethanol prices by location of the biorefineries relative to final markets. The simplification allows sensitivity of the model solution to output price variability. In addition, model complexity required smaller representations of the study area, thus preventing solution of the large scale model in which localized output prices would affect the distribution of biorefineries.
    b. However, necessary breakeven ethanol prices for biorefineries more distant from wholesale blenders and final demand regions would probably increase to account for the added ethanol transportation costs.

HCR Supplies

Supplies of herbaceous crop residues were based on county data collected by the National Agricultural Statistics Service of the U.S. Department of Agriculture. Mean grain production combines wheat, barley, oats, and grain corn output based on 10-year production averages for each county. Conversion rates from bushels to pounds are provided in table 2. Metric tons per hectare multiply pounds per acre times 2.471/2204.623, the ratio of acres per hectare to pounds per metric ton. Mean grain yield per hectare is an average of grain yields, weighted by crop mix, on total county harvested hectares. The county average per hectare supply of harvestable crop residues results from adjusting crop residue production on each harvested acre by the total number of land hectares in the county. Potential county supplies are thus a function of agricultural productivity and the county's land base devoted to wheat, small grains, and corn. The final adjustment constrains crop residue removal to 43% of available supply for small grains (based on Lundstrom, 1994) and 35% (based on Petrolia, 2008) for corn in order to retain erosion, nutrient, and organic matter benefits of crop residues remaining on the fields.

Table 2. Conversion of Grain Yields to Common Weights

Crop	Conversion Rates (pounds per bushel)
Wheat	51.90
Barley	41.04
Oats	27.52
Corn for Grain	47.32

Source: NDSU Extension Service (http://www.ag.ndsu.edu/pubs/ageng/machine/ae945w.htm

As an example, Chippewa County in southern Minnesota has a productive agricultural economy. Weighted average grain and corn yields on harvested hectares are 7.765 mt/ha. Based on removal constraints, HCR supplies are limited in the model to 2.723 mt/ha on the harvested hectares. Finally, we consider harvestable HCR to be uniformly distributed across each county. Since 38.72% of Chippewa County produces wheat, barley, oats, and corn (though mostly corn), available HCR supplies if distributed uniformly over the county would be 1.054 mt/ha.

Estimating site specific crop supplies over the three state study area, although necessary for actual investment decisions for plant locations, was beyond the objectives of the current research. Hence, production of the small grain and corn crops was assumed to be uniformly distributed across each county. The density of crop residue production within each county was assumed to match county average residue production levels, the last columns of appendix tables A1-A3. Figure 1 illustrates the potential harvestable herbaceous crop residues from corn and small grains per harvested hectare in each of the three states, adjusted by county acres planted to grains. Unsurprisingly, the farming regions of southern Minnesota and southeastern South Dakota have the highest potential supplies of crop residues. Lesser potential supplies exist following the Red River north from southeastern North Dakota to the counties above the Fargo-Moorhead metropolitan area. Although productive, much of this northern land is planted to crops such as soybeans not currently considered for ethanol production.

Given five-year average corn, wheat, and other small grain production data, potential supplies of county biofuel feedstocks are depicted in Table 3.

Table 3. Potential Maximum HCR-Based Ethanol Production in MN, ND, and SD

	Potential Harvestable HCR (Million tons of HCR)	Potential Cellulosic Ethanol From HCR (Millions of liters)	2011 Operating Capacity of Corn-based Ethanol (MLY)
Minnesota	5.839	1,460	4,234
North Dakota	4.425	1,106	1,317
South Dakota	3.061	765	3,846
Three State Total	13.325	3,331	9,398

If all herbaceous crop residue were harvested from each state's corn, wheat, and small grain harvested lands, the three states could potentially provide 13.325 million metric tons of cellulosic feedstocks. If all of this HCR were used in ethanol production, a total of 3,331 million liters (880 million gallons) could be produced. In comparison, the estimated operating capacity for traditional, corn-based ethanol plants in these three states was 9,398 million liters (2,483 million gallons) in early 2011 (Nebraska). Figure 1 illustrates that the potential supplies of HCR are not uniformly spread across the three states, but are concentrated in southern Minnesota and through portions of the lands bordering Minnesota on the east and portions of South Dakota and North Dakota.

Bales of harvested crop residue could be stored either on farm or transported to centralized locations. In either case, distances were required to calculate transportation costs from farms to storage or pretreatment facilities. The study areas are divided into 20x20 km cells. The center of each of the cells was designated as a potential location for biomass storage and/or pretreatment. Distance needed to transport biomass from farms to each cell's center was calculated by generating locations for 100,000 uniformly distributed points ("farms") within each cell and calculating the straightline distance to the center of each cell. Since storage and pretreatment facilities need not be built in each cell, distances from the generated farm locations to the centers of all other cells were also calculated. To reduce model size, it was assumed that costs of transporting straw bales beyond about 240 kilometers would be prohibitive.

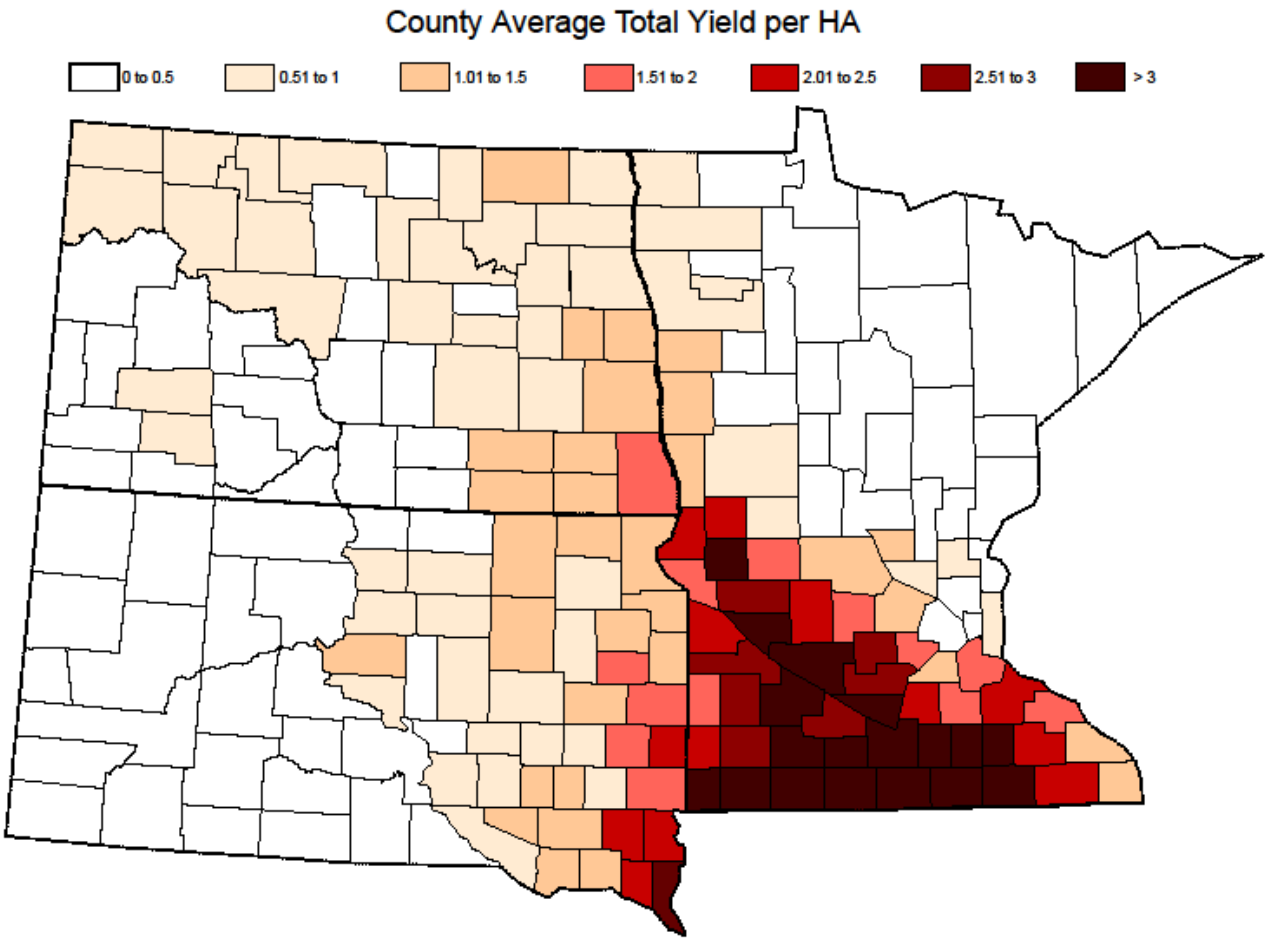

Figure 1. Average corn and grain harvestable grain yields per county.

Consequently, the model considered a planning area of approximately 200 by 200 kilometers. The GAUSS routine and a description of the calculations underlying the procedure to calculate farm to storage or pretreatment center is attached as appendix I.

Bales of harvested crop residue could be stored either on farm or transported to centralized locations. In either case, distances were required to calculate transportation costs from farms to storage or pretreatment facilities. The study areas are divided into 20x20 km cells. The center of each of the cells was designated as a potential location for biomass storage and/or

pretreatment. Distance needed to transport biomass from farms to each cell's center was calculated by generating locations for 100,000 uniformly distributed points ("farms") within each cell and calculating the straightline distance to the center of each cell. Since storage and pretreatment facilities need not be built in each cell, distances from the generated farm locations to the centers of all other cells were also calculated. To reduce model size, it was assumed that costs of transporting straw bales beyond about 240 kilometers would be prohibitive. Consequently, the model considered a planning area of approximately 200 by 200 kilometers. The GAUSS routine and a description of the calculations underlying the procedure to calculate farm to storage or pretreatment center is attached as appendix I.

Distances from centralized storage and pretreatment facilities to refineries, both assumed to be in the center of cells, were also based on straightline distances. For cells lying along the same latitude or longitude, distances were just equal to the cell size (20 km) times the number of cells the baled HCR or pretreated feedstock travelled from the centers of the origin and destination cells. Distances to cells lying off the vertical or horizontal grid lines of the cell under consideration were calculated as the hypotenuse of the triangle formed by the horizontal and vertical distances to nearby cells. Rather than employing an arbitrary fudge factor (such as the "tortuosity" factor used in Wright ad Brown), inaccuracies in the calculation of distances from assuming straightline transportation routes were retained. Calculated transportation distances are thus lower bounds on transporting feedstock to either pretreatment or biorefining facilities.

Transportation Costs

Farms are assumed to be distributed uniformly across each 20x20 km cell. Harvested straw is transported to centralized storage and pretreatment locations, assumed located at the center of each cell. Given weight limits on many of the rural roads necessary for transporting crop residues, truckloads were limited to 15.4 MT loads. Trucking costs were assessed $2.78 per loaded km per truck, or about $0.18 per mt per km.

Treatment of biomass, such as crop residue, woody feedstock, or switchgrass, can entail extensive transportation loads on rural infrastructure. For the four sizes of pretreatment plants considered in the model (annual capacities of 220,590, 441,511, 883,022, and 1,471,924 mt of biomass), truck deliveries would be approximately 40, 80, 160, and 267 every day, respectively.

Ignored in this study are any public costs arising from such increased usage of rural roads and other infrastructure, as well as possible public opposition to increasing rural truck traffic.

Pretreatment and Processing Costs

Although small-scale plants, such as Iogen's Ottawa facility with 2009 production of about 0.6 million liters, are in operation, no commercial scale facilities for processing cellulosic feedstock into fuel and other products currently exist. Fixed and variable cost estimates for pretreatment and for feedstock processing are thus tentative and are based on technologies current at the time of this analysis. Rough estimates indicate current cellulosic technologies result in costs of approximately $0.70 per liter of ethanol produced, higher than the $0.44 per liter costs of corn-based ethanol. Technological advances could, however, result in lowering costs to the $0.29 per liter target set by the Department of Energy for cellulosic ethanol production in the 2010-2012 period (Collins, 2007).

Fixed and operating costs for pretreatment facilities were derived from values reported in Carolan, Joshi and Dale (2007). Their analysis confirms the existence of economies of scale in pretreatment facilities. However, cost advantages of building fewer, larger plants may be offset by higher transportation costs of delivering unprocessed straw from more distant fields. The higher transportation cost of untreated crop residue to the pretreatment plants may, however, be offset by closer proximity of a few large pretreatment plants to the biorefineries. Location and scale of pretreatment plants will thus be sensitive to the fixed and variable costs of the plants, as well as to the transportation costs of shipping crop residues from farmer fields to the pretreatment plants and pretreated feedstock to the biorefineries.

Table 4 provides fixed and variable cost estimates for pretreatment plants of five different capacities. Fixed costs represent annualized costs assuming 10-year straightline depreciation of capital equipment and facilities (CJD, 2007). Since straw value is endogenous in the mathematical programming model, straw procurement costs assumed in CJD are subtracted from the reported facility operating costs.

The average total costs reported in table 4 are nearly identical to the estimates of stand-alone AFEX pretreatment plants extracted from Sendich et al.'s (2008) analysis and further reported in Bals et al. (2010). Bals et al. estimate AFEX pretreatment costs of $14 to $21 per ton

of dry matter.

Table 4. Pretreatment costs per metric ton of crop residue treated (cost estimates adjusted to 2008 dollars)

Daily Throughput (mt)	Capital Cost	Operating Cost	Administrative Cost	Total Cost / mt
604	$3.85	$14.57	$2.23	$20.65
806	$3.55	$13.44	$1.76	$18.75
1210	$3.19	$12.29	$1.29	$16.78
2419	$2.66	$11.13	$0.79	$14.59
4033	$2.34	$10.61	$0.59	$13.53

Source: Carolan, Joshi and Dale (2007)

Refinery Costs

Capital and operating costs from refining pretreated HCR feedstock into ethanol were derived from NREL estimates (Aden et al., 2002). The NREL contract report combines costs of AFEX pretreatment and ethanol production. To isolate just the refining process, pretreatment costs reported in Carolan, Joshi and Dale were subtracted from the total costs reported in NREL. Table 5 reports total costs (Aden et al., 2002), CJD pretreatment costs, adjusted for the scale of the plant underlying the NREL estimates, and costs representative of the ethanol refining process net of pretreatment. For both the Aden et al. 2002 estimates and the CJD 2007 estimates, current values resulted from inflating the reported costs to 2008 values using the producer price index for total manufacturing industries (BLS series PCUOMFG-OMFG).

Table 5. Ethanol facility costs for a 206,000,000 liter/year refinery (2008 dollars)

	NREL Total Costs	CJD Pretreatment Costs	Net Refining Costs
Annual Capital Costs	$18,191,613	$3,052,547	$15,139,066
Production Costs (Net of Feedstock)	$37,375,284	$9,932,140	$27,443,144
Total	$55,566,897	$12,884,687	$42,682,210

The net refining costs reported in table 5 imply a $48.44/MT cost in terms of refining pretreated feedstock into ethanol, or $0.19 per liter of ethanol produced under an assumption of 250 liters mt^{-1}.

CJD cite refinery economies of scale as a motivating force underlying a system of decentralized pretreatment locations. The cost estimates provided by NREL were used to approximate capital and operating costs for different scale refineries. Production costs in table 5 were assumed constant regardless of scale. Capital costs were adjusted by a factor equal to the production capacity of the plant raised to a factor of 0.6. A returns to capital exponent of 0.6 is commonly used in projecting capital costs associated with plants of different size (CJD, page 5).

Pretreatment and refining cost estimates based on tables 4 and 5 indicate per liter annualized costs of approximately $0.36 for the largest 206 MMLY plant. Adding an estimated $44 per metric ton of crop residue delivered to the pretreatment plant (Leistritz et al., 2006) would increase costs for the largest scale plant to approximately $0.58 per liter, higher than current corn-based costs but below the cellulosic ethanol estimates reported in Collins (2007).

Modeling Fixed and Variable Pretreatment and Refining Costs

Location decisions where facilities reflect increasing returns to scale pose a modeling problem. Misspecified models in which increasing returns to scale are present yet ignored typically select building the most efficient (i.e., largest) plant, yet operate the plant at less than full capacity to take advantage of the lower average costs of the largest-scale plants. Two common options to ensure average fixed and variable costs accurately reflect plant scale include lower and upper bounds on capacity utilization (Lambert and Middleton) or specification of plant size as special ordered sets of type 2 (Williams; Broek et al.). The latter approach, SOS2, is adopted in the current analysis.

Consider a plant decision at one location. A set of variables identifies the construction of plants of increasing size at a particular location. The SOS2 variables include building a plant of zero capacity, indicating no plant is built. An SOS2 restriction specifies that no more than two of the variables can be non-zero. In addition, if two variables are non-zero, they must be adjacent in the ordered set. For example, let λ_i and λ_{i+1} represent two non-zero solution values, and $\lambda_i + \lambda_{i+1} = 1$. If the scale of the plant associated with element *i* (*i+1*) of the special ordered

set equals S_i (S_{i+1}) and associated average total costs are C_i (C_{i+1}), facility capacity will be $\lambda_i S_i + \lambda_{i+1} S_{i+1}$ and total costs will be $\lambda_i C_i + \lambda_{i+1} C_{i+1}$. If average costs are falling over the range of plant sizes reflected in the special ordered set (i.e., $C_i > C_{i+1}$), optimal solutions will ensure that a plant represented by the convex combination of plant scales at *i* and at *i+1* will be selected, rather than perhaps selecting the largest plant with the lowest average cost and using it at a capacity less than full, thus incorrectly calculating the actual costs of producing a lower quantity at an underutilized plant.

Based on the average fixed and variable costs reported in tables 4 and 5, adjusted as necessary using the capital cost adjustment factor of 0.6 reported in CJD, the following special ordered sets of type 2 were defined to reflect facility siting decisions within each cell of the model:

Table 6. Average total costs for pretreatment and refining for plants of different scale (2008 dollars)

Associated SOS2 Variable	Annual Straw Throughput (MT)	Pretreatment Facility		Refinery	
		Total Cost	Average Total Cost per MT	Total Cost	Average Total Cost per MT
λ_0	0	$0	$0	$0	$0
λ_1	1	$100000	$100000	$100000	$100000
λ_2	220,590	$4,555,184	$20.65	$12,697,160	$57.56
λ_3	441,511	$7,408,555	$16.78	$23,651,744	53.57
λ_4	883,022	$12,883,291	$14.59	$43,780,231	49.58
λ_5	1,471924	$19,915,132	$13.53	$65,029,602	$44.18

For any location, $\lambda_0 = 1$ implies no facility is built. Solutions including nonzero values for λ_1 allow plants of less than 220,590 MT of straw per year to be built. However, the artificially high average total costs for λ_1 will likely limit solutions to either construct no plant at the location (i.e., $\lambda_0 = 1$) or to build plants larger than 220,590 mt of crop residue throughput per year. If solutions for the pretreatment plants, for example, are $\lambda_4 = \lambda_5 = 0.5$, a pretreatment plant with an annual capacity of 1,177,473 MT will be built, total costs will be $16,399,211, and

average costs per metric ton of processed crop reside will be $14.06.

Figure 2 graphs the average total costs for the pretreatment and refining facilities. Increasing returns to scale are evident in the decreasing average costs as HCR throughput increases.

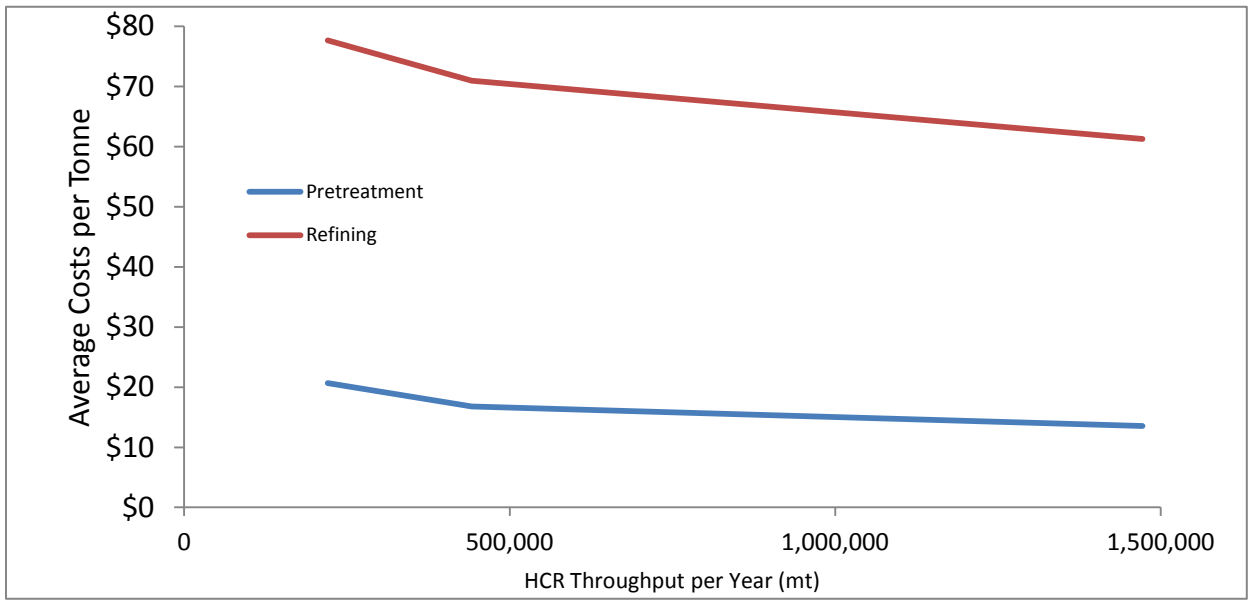

Figure 2. Average total costs of pretreatment and refining.

Procedures

A mixed integer programming model with SOS2 variables representing plant location and scale decisions formed the basis for determining optimal harvest, pretreatment, and ethanol refining decisions. The production year was divided into three periods of four months each. Period one corresponded to straw harvest. The model activities are presumed to begin in period one, so investment, construction, any HCR contractual arrangements, and other activities necessary to support an operational HCR-based ethanol complex are assumed to have been made in earlier periods and are available for operation in period one. Period two modeled optimal storage, transportation, pretreatment, and refining activities. Period three continued pretreatment and refining activities, with ending conditions stipulating depletion of any crop residue harvested in period one.[1]

[1] As a result of preliminary model results, subsequent model simulations reduce the model to two time periods as

The MIP model is described below:

$$Maximize\, Z = \; Eprice * Ethanol \; + \; FeedVal \sum_t \sum_i Feed_{ti}$$
$$- \; (\; (SoilVal + Harvest) \sum_j \sum_i x_{t1,ij} \; + \sum_t \sum_i \sum_j SCost_{ij} \, SS_{tij} \; + \sum_t \sum_i \sum_j PPCost_{ij} \, PPS_{tij}$$
$$+ \sum_t \sum_i SSCost \, SStore_{ti} \; + \sum_t \sum_i PPSCost \, PPStore_{ti} \; + \; \sum_i \sum_{size} PPATC_{size} \, BuildPP_{i,size}$$
$$+ \sum_i \sum_{size} RATC_{size} \, BuildR_{i,size} \;)$$

Objective function: Revenues derive from sales of ethanol and animal feed produced during the AFEX pretreatment process. Costs accrue from harvest costs and replacement nutrient costs from removal of crop residue, from transportation and storage of HCR and pretreated biomass, and from the amortized investment costs and operating costs of pretreatment plants and refineries.

Subject to the following constraints:

Straw Harvest and Handling

1. $\sum_j SS_{t1,ij} \; \leq Supply_i$

   Constraint 1: For all locations *i*, the quantity of herbaceous crop residue shipped from site *i* to site *j* in time period one is equal to the total supply of straw/stover produced at site *i*.

2. $\sum_i SS_{tij} = SupStraw_{tj}$

   Constraint 2: For all locations *j*, the sum of all HCR shipped from sites *i* to *j* in each time period t equals HCR supplies at site *j*.

3. $SupStraw_{ti} - PP_{ti} - SStore_{ti} = 0$

   Constraint 3: For each site *i* and time period *t*, the supply of HCR is either pretreated or stored.

4. $SupStraw_{t2,i} - PP_{t2,i} = 0$

   Constraint 4: Any remaining HCR at site *i* in the second (terminal) time period must be pretreated.

5. $SStore_{ti} - \sum_j SS_{t+1,ij} = 0$

   Constraint 5: For all locations *i* and time periods one and two, all stored HCR at site *i* is

well as combine the pretreatment and biorefinery investments.

shipped in the next period (could just remain as stored HCR if $i=j$).

Pretreatment and Refining

6. $PP_{t1,i} - \sum_j PPS_{t1,ij} = 0$

Constraint 6: For all locations i in time period one, all pretreated biomass at site i is shipped to j.

7. $\sum_i PPS_{tij} - R_{tj} - PPStore_{tj} - Feed_{tj} = 0$

Constraint 7: For all time periods and locations j, all pretreated biomass at time t is either refined, stored, or used as animal feed.

8. $\sum_i PPS_{t2,ij} - R_{t2,j} - Feed_{t2,j} = 0$

Constraint 8: For time period two and locations j, all pretreated biomass is either refined or used as animal feed.

9. $PPStore_{ti} + \sum_i PP_{t+1,i} - \sum_j PPS_{t+1,ij} = 0$

Constraint 9: For all locations i and time periods one and two, all pretreated stored biomass in period t plus pretreated biomass in period $t+1$ is shipped in period $t+1$.

10. $Ethanol_{ti} - 250\,R_{ti} \le 0$

Constraint 10: Refined biomass yields 250 liters per metric ton of ethanol.

Plant Construction and Use

11. $\sum_{size} BuildPP_{i,size} = 1$

Constraint 11: One of the pretreatment plants of capacity *size* (including *size* = 0) will be built at each location i.

12. $\sum_{size} BuildR_{i,size} = 1$

Constraint 12: One of the refineries of capacity *size* (including *size* = 0) will be built at each location i.

13. $\sum_t PP_{ti} = \sum_{size} CapPP_{size}\, BuildPP_{i,size}$

Constraint 13: For each location i, the quantity of HCR pretreated over all three periods equals the convex combination of pretreatment plant capacities times the SOS2 plant investment variables.

14. $\sum_t R_{ti} = \sum_{size} CapR_{size}\, Build_{i,size}$

Constraint 14: For each location *i*, the quantity of pretreated biomass that is refined into ethanol over all three periods equals the convex combination of refinery capacities times the SOS2 plant investment variables.

15. $0.5R_{ti} - 0.5\sum_{tt \neq t} R_{tt,i} \leq 0$

Constraint 15: For each location *i*, conversion of pretreated biomass is equalized across both time periods.

In addition to the above constraints, the base model was constrained so that the refinery could only be built in the central cell of the 200x200 km study area. Allowing both pretreatment plant and refinery locations and scale decisions to be solved simultaneously resulted in an unsolvable model. This problem likely resulted from the assumptions of homogeneous HCR yields over the entire study area, no differences in pretreatment and refining costs among plant locations, and assumptions that transportation follows straightline distances across featureless land areas rather than accounting for existing road systems. Failure to reach an optimal solution without limiting refinery construction to a central location likely caused the model to cycle through solutions yielding identical objective function values and differing only in placement of pretreatment and refining plants.

Decision variables are defined in table 7.

Table 7. MIP Decision Variables

Label	Description
$BuildPP_{i,size}$	Build a pretreatment facility with capacity *size* at location *i* (SOS2 variables)
$BuildR_{i,size}$	Build an ethanol refinery with capacity *size* at location *i* (SOS2 variables)
Ethanol	Liters of ethanol produced
$Feed_{ti}$	Metric tons of animal feed sold
PPS_{tij}	Shipments of pretreated biomass shipped from *i* to *j* at time *t*
$PPStore_{ti}$	MT of pretreated biomass stored at *i* in period *t*
PP_{ti}	MT of pretreated biomass produced at i in period t
R_{tj}	MT of pretreated biomass refined at j in period t
SS_{tij}	Shipments of baled HCR shipped from *i* to *j*
$SStore_{ti}$	MT of HCR stored at *i* in period *t*
$SupStraw_{tj}$	MT of baled HCR at *j* in period *t*
$x_{t1,ij}$	MT of HCR harvested in *i* and shipped to *j* in period 1

Base Scenario

Table 8 presents the initial parameter variables for the base case scenario. Using these parameter values, the breakeven price of ethanol was $0.38 per liter.

Table 8. Model Parameters and Base Values

Parameters	Description	Base Values
$CapPP_{size}$	Pretreatment plant capacity of scale *size* (mt yr^{-1})	See table x
$CapR_{size}$	Ethanol plant capacity of scale *size* (mt yr^{-1})	See table x
Eprice	Ethanol price ($ lit^{-1})	0.60
FeedVal	AFEX-Treated biomass value as animal feed ($ mt^{-1})	0.0
Harvest	Cost to harvest and bale straw ($ mt^{-1})	11.79
$PPATC_{size}$	Average total cost of AFEX pretreatment in plant of scale *size* (smallest to largest scale) ($ mt^{-1})	See table x
$PPCost_{ij}$	Cost to transport pretreated biomass straw from *i* to *j* ($ mt^{-1} km^{-1}) (assumes 25% reduction in feedstock bulk)	0.135
PPSCost	Cost to store pretreated biomass from period to period ($ mt^{-1})	4.27
$RATC_{size}$	Average total cost of ethanol refining plant of scale *size* (smallest to largest scale) ($ mt^{-1})	See table x
$SCost_{ij}$	Cost to transport straw from *i* to *j* ($ mt^{-1} km^{-1})	0.181
SoilVal	Soil nutrient value of unharvested straw ($ mt^{-1})	14.824
SSCost	Cost to store straw from period to period ($ mt^{-1})	4.86
$Supply_i$	Initial harvestable HCR in area *i* (mt ha^{-1})	2.00

Base Scenario – Optimal Solution

Crop residue is harvested and shipped to one centralized pretreatment facility and co-located refinery. The maximum scale plant is built (1.47 mmt of biomass pretreated and refined to produce 368 million liters of ethanol per year).

Total revenue from sales of 367,981,000 liters of ethanol at $0.60/liter equal $220,778,600. Total costs derived from the model's objective function equal $127,416,500. Cost items are: harvest and soil nutrient replacement, $30,497,972 (24%), HCR shipment cost, $8,831,203 (7%), pretreated biomass storage, $735,962 (0.6%), amortized pretreatment facility

investment and operating costs, $19,915,130 (16%), and amortized refinery investment and operating costs, $67,105,020 (51%).

Table 9. Base Scenario Solution Values

Activity	Total	Dollars per mt of HCR	Dollars per Liter
Ethanol Revenue	$220,788,600	$150.00	$0.6000
Harvest Cost	$8,678,022	$5.90	$0.0236
Soil Nutrient Loss	$21,819,950	$14.82	$0.0593
Straw Ship Cost	$8,831,203	$6.00	$0.0240
Store PP Cost	$3,142,558	$2.14	$0.0085
PP_Plant Cost	$19,915,130	$13.53	$0.0541
Plant Cost	$65,029,600	$44.18	$0.1767
Total Cost	$127,416,500	$86.56	$0.3463
Ethanol (Liters)	367,981,000		
Straw Harvest (mt)	1,471,924		
Pretreatment (mt)	1,471,924		
Store PP (mt)	735,962		

Under the base assumption of 2 mt per ha of harvestable crop residue, in order to provide 1.47 mmt of HCR, straw and stover must be harvested from 0.735 million ha of cropland. Because the planning area is split into 40,000 hectare cells, HCR is harvested from 18.4 of the cells distributed symmetrically around the central cell of the planning area in which the refinery was constrained to be located. The farthest HCR haul was 45.1 km, incurring a transportation

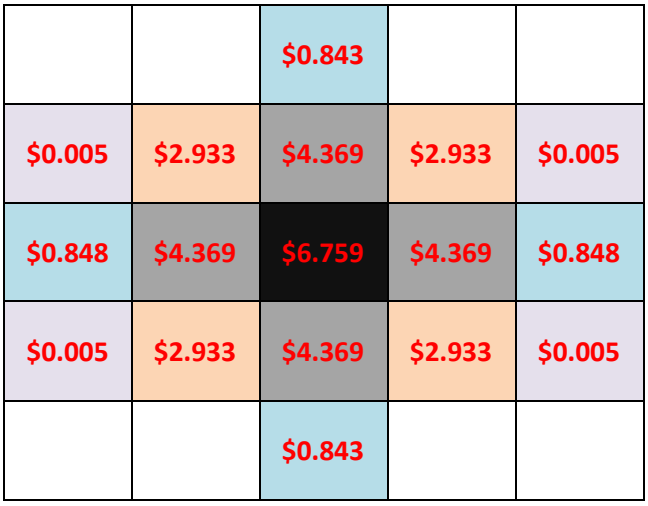

Figure 3. Marginal values of an additional mt of HCR by location relative to central processing plant, base scenario.

cost of $8.14 per mt. Conversely, farms located in the central cell where the pretreatment and refineries are located, incurred an average haul distance of 7.65 km, with an average transportation cost of $1.38 per mt.

Contractual arrangements will determine the distribution of costs between farmers and refiners. However, costs associated with delivery of HCR to the pretreatment location are $26.61 for harvest and nutrient replacement plus the transportation costs (ranging from the average of $1.38 per mt in the central cell to $8.14 for the cells on the fringe of the supply area).

Because of the transportation cost differential, the marginal value of the HCR feedstock varies by distance from the pretreatment and refinery facilities. The geographic distribution of HCR marginal values are presented in figure 3. In order to maintain the plant at its full capacity of 1.47 mt of feedstock, refiners would be willing to pay an additional $6.76 per mt for HCR from the central cell (i.e., the location of the plant with the 7.65 km average haul distance). By sourcing a ton of biomass from the central cell, processors would eliminate the need to buy biomass from the most distant cells, thus saving transportation costs. This savings is $6.76, or the difference between HCR biomass delivery from the farthest distance ($8.14) and from farms located in the same cell as the processor ($1.38). The total value of this local supply of HCR is thus $34.75 per mt (the $26.61 necessary to cover harvest and soil nutrient replacement costs, the $1.38 transportation cost, and the $6.76 marginal value of local versus the most distant sources of biomass). Conversely, the negligible marginal value of an additional mt of HCR from the fringes of the supply area indicate a willingness on the part of the refiner to also pay an additional $34.75 per mt for HCR from this location, where the total value derives from harvest and actual transportation costs incurred. Thus, assuming harvest cost and HCR quality are identical, the refiner would be willing to pay $34.75 per mt of HCR at an ethanol price of $0.60 per liter, with transportation cost and marginal values derived from the MIP solution moving in equal and opposite directions as distance from the central plant changes (e.g., as distance increases, transportation costs go up and marginal values for additional crop residues go down equally). This estimated value of $34.75 per mt compares favorably with the $40 per ton (or about $44 per mt) often assumed as the delivered price of farm HCR (Leistritz 2007).

The marginal value of an additional ton of crop residue within the same cell as the

pretreatment plant increases as potential crop residue supplies decrease. For example, if potential residue yields are halved, to one metric ton per hectare, the value of an additional ton of feedstock within the same cell as the pretreatment plant rises from $6.76 to $10.08. This increase in local feedstock value results from substituting a nearby ton of feedstock for a ton from the most distant cell necessary to maintain the 1.47 ton facility, which would be 63.51 km from the plant when yields are 1 mt/ha.

The breakeven price for ethanol under the base scenario parameters is $0.35 per liter, below the 10-year average price of $0.60 per liter, the average 2009 price of about $0.47 per liter, or current (March 2011) nearby future price of $0.66/liter. Using published harvest, transport, storage, pretreatment and refining costs, assuming an refinery price of $0.60 per liter of ethanol, and ignoring the final costs of transporting ethanol to wholesalers, cellulosic ethanol production appears to be profitable.

Scenario Analysis

Changes are made in the base parameters to assess sensitivity of the results to changing economic and agronomic conditions. Changes considered are:

1. Changing Herbaceous Crop Residue Densities
2. Changes in Pretreatment and Refinery Average Total Costs
3. Forced Decentralization of Pretreatment Plants
4. Livestock Feeding Option

1. Changing Herbaceous Crop Residue Densities

The base scenario assumed 2 mt per ha as the potential source of HCR feedstock for the ethanol complex. From tables x-y and the maps of crop and HCR yields, HCR varies considerably over the three state area. The tables report both harvestable residues (constrained by removal limits) on just the harvested hectares (i.e., not adjusted by percentage of total county land area) and county average supplies when distributed uniformly over a county's total land area.

The area needed to provide 1.47 million mt of biomass to supply the largest scale biorefinery assumed in the model will decrease as the density of available feedstocks increase.

Table 10 illustrates a simple model of distances and hauling costs to a central pretreatment facility and refinery with an annual throughput of 1.47 million mt.

Table 10. Simulated transportation variables for increasing crop residue yields

HCR Density (mt/ha)	Maximum Supply Radius (km)	Average Haul Distance (km)	HCR Haul Costs (Millions)
0.25	136.9	94.6	$25.144
0.5	96.8	66.9	$17.780
0.75	79.0	54.6	$14.517
1	68.4	47.3	$12.572
1.25	61.2	42.3	$11.245
1.5	55.9	38.6	$10.265
1.75	51.7	35.8	$9.504
2	48.4	33.5	$8.890
2.25	45.6	31.5	$8.381
2.5	43.3	29.9	$7.951
2.75	41.3	28.5	$7.581
3	39.5	27.3	$7.259

As the harvestable herbaceous crop residue density increases, supply area and average haul distance to the pretreatment and refinery plants decreases. Hauling costs from more distant farms when HCR density is low increase the costs, with the best fit resulting from the power form of the cost function, Haul Cost = 12.5722 ($Density^{-0.5}$), with haul costs expressed in millions of dollars. As HCR density increases by one percent, hauling costs fall by 0.5% in this simple simulation.

Results from solving the MIP model are similar to the simulated values in table 10. Under all parameterized values of the HCR density, the largest refinery is built and the largest pretreatment plant is located next to the refinery. Total biomass harvested remains at 1.47 million metric tons, 368 million liters of ethanol are produced, and revenues at $0.60 per liter remain at $221 million. As harvestable yields decline, however, the supply area naturally increases, requiring longer hauls for the baled crop residues to be transported to the centralized pretreatment facility. Increasing total costs from the production of 368 million liters of ethanol arise solely from the increasing cost of transporting the HCR to the central plant.

Given the assumption of uniform density of HCR over the region, total hectares to supply the centralized plant range linearly from 490,641 ha when harvestable supplies are 3.0 mt per ha

to 2,943,848 ha under the 0.5 mt/ha parameter value. The longest haul when yields are 3.0 mt per ha is 40.4 km and is 100.2 km under the less dense, 0.5 mt per ha assumption. Average cost per mt of shipped HCR ranges, again linearly, from $11.73 to $4.98 for yields ranging from 0.5 to 3.0 mt/ha.

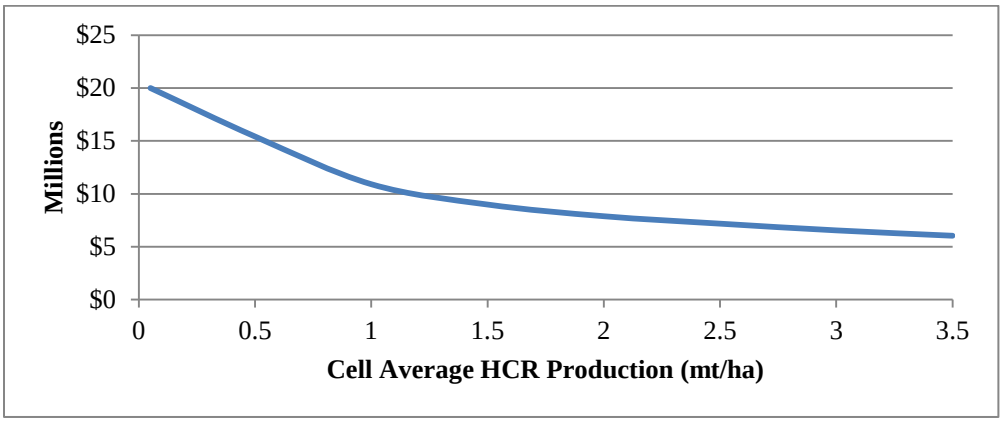

Figure 4. Total HCR Transportation Cost to Centralized Pretreatment Facility.

Shadow prices of additional HCR supplies are affected by changing HCR densities. When HCR density is high, the shadow price of additional supplies adjacent to the pretreatment plant is less than under lower density production. Since supplies do not need to be shipped from as far away when HCR densities are high, and thus the supply area for a 1.472 mmt plant is smaller, the substitution effect of replacing a nearby ton of biomass for a ton coming from farther away, though still within the plant's supply area, is smaller. Thus, the shadow price from the base scenario was $6.759 per mt when crop densities were 2 mt/ha. When density is 3 mt/ha, the shadow price on a ton of biomass from a farm co-located in the cell with the processing plants is $5.916. Conversely, when density falls to 0.5 mt/ha, the value of an additional ton of biomass located in the same cell as the pretreatment plant increases to $16.698 to save the cost of shipping the feedstock from the most distant farms. A nearby increase in supply saves the transportation cost of shipping from the most distant fields, about 100 kilometers distant when yields are 0.5 mt/ha.

The shadow prices quantify the higher cost of biomass delivery to the centralized pretreatment and processing plants in regions having lower HCR yields per hectare. The sensitivity of shadow prices to HCR densities confirm the benefits of locating pretreatment and refining operations in areas having relatively higher supplies of biomass feedstocks. Figure 4

provides an illustration useful for investors considering feedstock transportation costs for areas such as Bowman county in southwestern North Dakota (county average HCR supplies of 0.12 mt/ha) or more productive Chippewa county in southern Minnesota (county average HCR supplies of 1.05 mt/ha).

2. Changes in Pretreatment and Refinery Average Total Costs

Since commercial cellulosic refineries of the scale considered here have yet to be built, there is uncertainty over the eventual investment and operation costs for both pretreatment and refinery facilities. Cost assumptions used are based on engineering studies conducted several years ago (Carolan, Joshi and Dale, 2007; Aden et al., 2002). Cost uncertainty has not been resolved since no commercial scale HCR-based ethanol refineries are operational. Because of this uncertainty, impacts on plant investment and profitability were assessed under a range of average total costs for the pretreatment and refining plants (i.e., the parameters PPCost and RCost).

Solution decisions do not change. Ethanol production remains at 368 million liters, and annual net revenues (assuming $0.60 per liter) remain at $221 million. Figure 5 illustrates revenues from ethanol sales net of processing costs and the amortized investment costs at pretreatment and refining plant costs ranging from 50% through 150% of the costs used for the base analysis. Optimal harvest quantities and transportation schedules and ethanol production do not change when pretreatment and refining costs change from the base scenario. What does change is the potential net revenue from development of the HCR-based complex. Consequently, the breakeven ethanol price (exclusive of feedstock purchase cost) for supporting feasibility of the HCR based system falls from $0.23 per liter under the 50% drop in facility operating and amortized investment costs to $0.46 per liter for costs equaling 150% of the base costs.

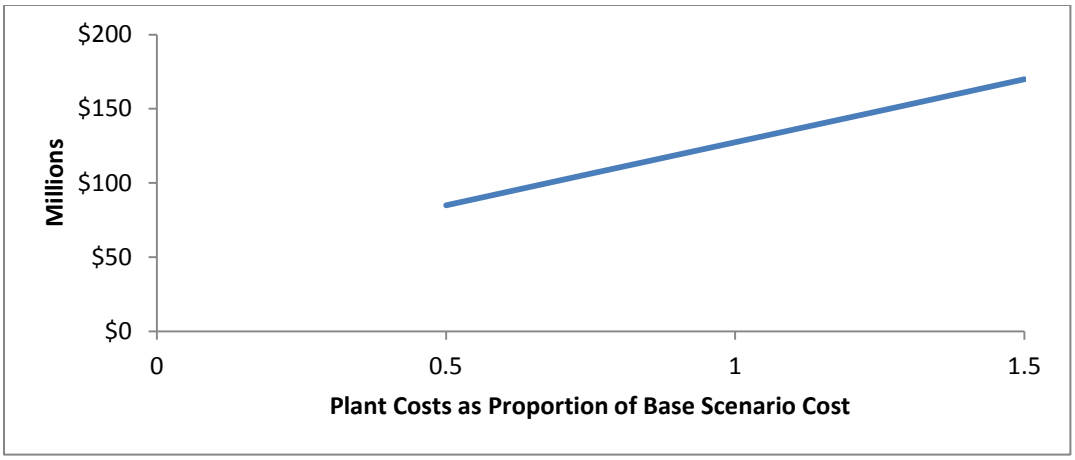

Figure 5. Total costs as variable and amortized plant costs vary from base scenario.

3. Forced Decentralization of Pretreatment Plants

A potential advantage of the AFEX pretreatment process (or most of the other processes to reduce the raw HCR biomass to the cellulose, hemicelluloses, and other components necessary for sacharification and fermentation) is the possibility to separate pretreatment from refining operations. Possible advantages from this process separation might arise from densification of the raw biomass harvested from the fields, thus reducing handling, storage, and transportation costs of the biomass to the final refining location. The assumption of the base model is that densification reduces biomass volume, thus resulting in a reduction in storage and transportation costs for pretreated biomass versus the bales of harvested crop residues. However, under the base scenario, even this high level of densification fails to result in decentralized pretreatment plants, with the optimal solution being to build one pretreatment plant with the capacity to process all of the HCR for use by the co-located ethanol refinery.

A series of alternative models were solved in which only smaller scaled pretreatment plants could be built. Constraining pretreatment plant capacities to be smaller than the maximum assumed in the base scenario eliminates the lower average variable costs possible through economies of scale associated with larger plants. Optimal solutions thus balance transportation and storage costs of the raw crop residues and the pretreated biomass with the higher per unit processing costs of using smaller pretreatment facilities. Models were constructed such that pretreatment plants could have no larger annual capacities than 220,590 mt, 441,511 mt, 883,022 mt, and 1,471,924 mt (the latter plant capacity being the base scenario).

In all cases, the optimal solution was to build the large centralized ethanol plant with pretreated feedstock requirements of 1.47 mmt and ethanol production of 368 million liters. Sources of supply of the 1.47 mmt of feedstock depended upon constraints imposed on pretreatment plant size. Results are in table 11.

With an upper capacity of 220,590 mt per year, fifteen distributed pretreatment plants were built to pretreat the 1.47 mmt of feedstock needed by the large biorefinery. Only one of the plants was of the maximum allowed size, or 220,590 mt. Fourteen smaller scale plants were built, ranging from 80,075 to 159,928 mt capacity. Because pretreatment plants were built closer to the farm sources of HCR, results in table 11 indicate that transportation costs for HCR bales were lowest with the smaller, distributed network of pretreatment plants. However, shipments of the pretreated feedstock to the central refinery were highest under this scenario. Similarly, the total cost of pretreatment (amortized investment and operating costs) was highest with the smaller scale plants. Total costs were highest when pretreatment plants were constrained to be less than or equal to 220,590 mt annual throughput, being about 7.8% or $10.0 million higher than under the base scenario in which the large, 1,471,924 mt pretreatment plant could be built adjacent to the biorefinery.

Table 11. Cost Results from Changing Pretreatment Plant Scale

	Maximum Allowable Scale			
	220590	441511	883022	1471924
Pretreatment Plants Built	15	4	2	1
Average PT Plant Scale	98178	366,951	735,778	1,471,924
Straw Shipment Cost	$3,133,535	$5,492,294	$7,166,549	$8,831,203
Pretreated Shipment Cost	$5,192,657	$3,586,536	$2,254,799	$0
Total Feedstock Shipment Cost	$8,326,192	$9,078,830	$9,421,348	$8,831,203
Total PP Plant Cost	$30,395,890	$25,835,420	$22,119,490	$19,915,130
Total Cost	$137,392,200	$133,584,400	$130,211,000	$127,416,500

As allowable scale increases, total shipment costs of the baled crop residues increases as HCR needs to be transported farther distances to more distant pretreatment facilities. The increasing HCR transportation costs are somewhat, though not completely, offset by shorter hauls and resulting lower transportation costs for the pretreated feedstock. The net effect,

however, is to decrease total feedstock transportation costs when fewer, larger pretreatment plants are built.

Transportation cost savings with the larger scale pretreatment plants are further magnified as the economies of scale resulting from the larger plants are realized. Total costs continue to decline as larger pretreatment plants are built until the optimal solution obtained under the unconstrained base scenario occurs (i.e., allowing the largest pretreatment plant to be built adjacent to the refinery).

As a test of the importance of increasing returns to scale in the pretreatment facilities, restrictions on pretreatment plant scale were removed and constant average total costs were assumed, regardless of plant size. Under this constant returns to scale assumption, the optimal solution was to build a small scale pretreatment plant of approximately 80,074 mt annual capacity in 18 of the cells surrounding the centralized ethanol refinery. With constant returns to scale in pretreatment, there are no investment and operating cost advantages from building larger plants. Transportation costs for the pretreated feedstock are lower than for the baled crop residues, so costs are reduced by shipping the raw crop residues shorter distances to smaller, nearby pretreatment facilities.

The model results indicate the importance of logistical network design that is sensitive to scale economies in the construction and placement of a distributed pretreatment plant system. When significant economies of scale exist, results indicate pretreatment costs dominate transportation cost considerations, and a large pretreatment facility should be co-located with the biorefinery.

4. Livestock Feeding Option

Nutrient value of AFEX treated herbaceous crop residue is comparable to grains and other livestock feeds. Bals et al. (2010) recently analyzed protein availability and digestibility by ruminant animals of both traditional and nontraditional (including corn stover and wheat straw) feed sources. Bals et al. found the primary advantage of AFEX treatment was to decrease the amount of indigestible aNDFom (48-h neutral detergent fiber) prevalent in nontreated feedstuffs considered. In particular, AFEX treatment improved the digestibility of corn stover and late harvested switchgrass by 52% and 128%, respectively, over untreated samples. Crude protein

content of all of the treated feedstuffs, including wheat straw, also increased with AFEX treatment, increasing to over 100 g/kg (i.e., 10%) dry forage. Although based on traditional ammoniation processes, shown by Bals et al. to be inferior to the potential feed value improvements resulting from the AFEX process, Oosting, Vlemmix, and Van Bruchem (1994) provide supporting evidence of the gains from ammoniation in the feed value of wheat straw.

In the base scenario analyses of this research, no livestock feeding of AFEX treated HCR was permitted. This constraint was relaxed, and feeding was permitted. Other authors have allowed animal feeding as fixed proportions of pretreated crop residues usable for animal feeding. Carolan, Joshi and Dale (2007) restricted upper limits of 25% of feedstock that could be used as animal feed at a feed value of $108.54 per metric ton. Our analysis assumed investors consider either feed or refining options based on relative rates of financial returns. Feed was thus not constrained to 25% of the total pretreated supply as in, for example, CJD.

Due to model size and assumptions of homogeneity regarding residue production and transportation networks (i.e., all cells were identical with respect to residue density and transportation networks), solutions to the integer programming model did not converge. The model was thus reformulated to approximate the decision relying on continuous variables bounded between zero and one for the pretreatment and refinery investments. The price of ethanol was fixed at the observed average price of $0.60/liter. AFEX-treated feed price was parameterized from a lower bound of $30/mt. Leistritz et al. estimated the value of animal feed to be approximately $100/mt based on nutrient composition of AFEX treated feed.

Based on the assumed harvest, transportation, storage, and pretreatment costs, considerable value potentially exists for AFEX-treated crop residue. Using the parameter values from the base scenario, with the exception of allowing animal feeding, no residue was harvested for feed at AFEX-treated feed prices below $33.50/mt.

When feed values increased to $35.50/ton, all residue in the 200x200 km modeled region was harvested. The refinery producing 368 million liters of ethanol and continued to use 1.472 million mt of treated feedstock produced within a maximum supply area of about 45 km from the centralized biorefinery. The remainder of the residue throughout the study area was harvested, treated, and became available to livestock.

Changes in the solution occurred again as feed values increased above $117.50/mt. All available crop residue continued to be harvested over the study area, but a decreasing portion of the AFEX-treated feedstock was converted to ethanol. At a feed value above about $125/mt, no treated crop residue was used for ethanol production. All residue supplies were harvested and converted to AFEX-treated livestock feed.

Addition of the feeding option demonstrates that a potential market for AFEX-treated crop residues exists, with or without a biomass ethanol industry. Although investment decisions were necessarily continuous variables in order to attain a solution, indepth analysis of the potential for investing in dispersed pretreatment facilities might indicate an alternative market for agricultural crop residues. Combining feeding operations with cellulosic ethanol production appears feasible when feed value exceeds about $35.50/mt. Above this value, and below about $117.50/mt, HCR can be harvested for both feed and as feedstock for ethanol production. Since the nutrient value of AFEX-treated feed may be as high as $108/mt based on Carolan, Joshi, and Dale's estimates, opportunities exist to develop commercial pretreatment facilities, design long term contracts to ensure the delivery of pretreated feedstock to biofuel refineries, while maintaining local markets for animal feed to provide some risk protection to farmers and investors through diversification of crop residue markets.

Conclusions

There are currently no large scale commercial plants in the United States converting biomass to ethanol. A small, 1.4 million gallon demonstration plant operated by Verenium was scheduled to open in Jennings, LA in 2008. A biorefinery operated by Poet at Emmetsburg, IA will combine existing starch-based refining with refining of ethanol based on corn cobs, with plans to produce 25 million gallons of ethanol per year from cobs by the end of 2011. An unofficial list reported on the website *Gas2.org*, listed seven commercial scale plants with anticipated combined capacity of 183 million gallons planned as of March 5, 2009 (Cornell, 2009). Although targets for advanced biofuels established in the 2007 EISA may not be achievable, it appears that public policies still research and possibly development of cellulosic ethanol refineries.

Our results indicate that ethanol production based on herbaceous crop residues can be

profitable. With annualized pretreatment investment and operating costs of approximately $13.53 per ton, refining costs of $0.20 per liter, and estimated HCR harvest and soil nutrient replacement costs of $22.34, optimal plans include jointly located pretreatment and processing facilities at the largest scale assumed in the current model, 368 million liters per year. Unsurprisingly, net returns favor plants located in areas of high crop production due to reductions in the haul distances of feedstock to the centralized processing facilities. In the three state area analyzed, higher potential crop residues are found in southern Minnesota, and along the border of Minnesota and both North and South Dakota.

The research focused on the feasibility of dedicated facilities for the production of ethanol from herbaceous crop residues. Given current investment in corn-based ethanol plants throughout the Midwest, an alternative consideration might be the joint siting of corn-based and crop residue based ethanol facilities. For example, the Poet investment in their Liberty plant in Emmetsburg, Iowa, may realize scope economies from producing ethanol from corn and from corn cobs at the same location. Average fixed costs might be reduced by combination of unloading facilities and mixing of output from the two ethanol production processes in shipping of product. The current research did not consider either related production processes or another potential use of crop residues, such as use of residue in combined heat and power generation at existing corn-based ethanol plants. In this case, joint unloading facilities might reduce costs, and use of crop residues in supplying the heat and power to the corn-based refinery might reduce reliance and costs of outside purchases of power and heat (Perrin).

In summary, it does appear that HCR use in cellulosic ethanol production is feasible. Greater gains are possible with use of some AFEX treated residues as animal feed. Additional gains may be attainable with joint location of starch and cellulosic based ethanol production facilities, or by use of HCR in combined heat and power generation. Based on current crop production patterns, if commercial-scale conversion technology is developed and reflects the annualized costs used on this research, and if markets for ethanol remain strong, then areas of southern Minnesota and eastern North and South Dakota may support a profitable cellulosic ethanol industry.

References

Aden, A., M. Ruth, K. Ibsen, J. Jechura, K. Neeves, J. Sheehan, B. Wallace, L. Montague, A. Slayton, and J. Likas. 2002. "Lignocellulosic Biomass to Ethanol Process Design and Economics Utilizing Co-Current Dilute Acid Prehydrolysis and Enzymatic Hydrolysis for Corn Stover." NREL/TP-510-32438, Golden, CO.

Bals, Bryan, Hannah Murnen, Micahel Allen, and Bruce Dale. 2010. "Ammonia fiber expansion (AFEX) treatment of eleven different forages: Improvements to fiber digestibility *in vitro*." *Animal Feed Science and Technology* 155:147-155.

Collins, Keith. 2007. "The new world of biofuels: Implications for agriculture and energy." Slide –Presentation, EIA Energy Outlook, Modeling, and Data Conference. March 28, 2007.
Available at: http://www.eia.doe.gov/oiaf/aeo/conf/handouts.html

Carolan, J.E., S.V. Joshi, and B.E. Dale. 2007. "Technical and Financial Feasibility Analysis of Distributed Bioprocessing Using Regional Biomass Preprocessing Centers." *Journal of Agricultural and Food Industrial Organization* 5(2):1-27.

Cornell, Clayton B. 2010. "Complete List of Cellulosic Ethanol Plants Operating or Under-Construction in the US." *Gas2.org*. Accessed April 8, 2010: http://gas2.org/2009/03/05/complete-list-of-cellulosic-ethanol-plants-operating-or-under-construction-in-the-us/

De Gorter, Harry and David R. Just. 2010. "The Social Costs and benefits of Biofuels: The Intersection of Environmental, Energy and Agricultural Policy." *Applied Economic Perspectives and Policy* 32(1):4-32.

Kang, Seungmo, Hayri Önal, Yenfeng Ouyang, Jürgen Scheffran, and Ü. Deniz Tursun. 2010. "Optimizing the Biofuels Infrastructure: Transporation Networks and Biorefincery Locations in Illinois." Ch. 10 in Handbook of Bioenergy Economics and Policy, eds. Madhu Khana, Jürgen Scheffran, and David Zilberman. Springer Verlag,

Lambert, David K. and Jason Middleton. 2010. "Logistical Design of a Regional Herbaceous Crop Residue-Based Ethanol Production Complex," *Biomass and Bioenergy* 34: 91-100.

Leistritz, F.L., D.M. Senechal, M.D. Stowers, W.F. McDonald, C.M. Saffron, and N.M. Hodur. 2006. *Preliminary Feasibility Analysis for an Integrated Biomaterials and Ethanol Biorefinery Using Wheat Straw Feedstock.* Agribusiness & Applied Economics Report No. 509. 37 pp. Available at: http://ageconsearch.umn.edu/handle/23500

Lundstrom, Darnell. 1994. *Response to Steele County Job Development Authority in Straw Board Grower Questions*. Fargo: North Dakota State University, Extension Service, Agricultural and Natural Resources.

Mapemba, L. D., Epplin, F. M., Taliaferro, C. M., & Huhnke, R. L. (2007). Biorefinery feedstock production on Conservation Reserve Program land. *Review of Agricultural Economics, 29* (2), 227-246.

Nebraska. 2011. "Ethanol Facilities' Capacity by State." Nebraska State Government Website. Accessed April 7, 2011: http://www.neo.ne.gov/statshtml/121.htm

Oosting SJ, P.J.M. Vlemmix, and J. Van Bruchem. 1994. "Effect of ammonia treatment of wheat straw with or without supplementation of potato protein on intake, digestion and kinetics of comminution, rumen degradation and passage in steers." *British Journal of Nutrition* 72:147–65.

Perkis, David, Wallace Tyner, Paul Preckel, and Sarah Brechbill. 2008. "Spatial Optimization and Economies of Scale for Cellulose to Ethanol Facilities in Indiana." In *Risk, Infrastructure and Industry Evolution*, eds. B.C. English, R.J. Menard, and K. Jensen, a conference sponsored by the Farm Foundation. Berkeley, CA. June 24-25, 2008.

Petrolia, Daniel Ryan. 2008. "The Economics of harvesting and Transporting Corn Stover fro Conversion to Fuel Ethanol: A Case Study for Minnesota." *Biomass and Bioenergy* 32:603-612.

Renewable Fuels Association. 2011. *Global Ethanol Production to Reach 88.7 Billion Litres in 2011*. News Release, February 14, 2011. Available at http://www.ethanolrfa.org/news/entry/global-ethanol-production-to-reach-88.7-billion-litres-in-2011/ (acessed February 15, 2011).

Sendich, E., M. Laser, S. Kim, H. Alizadeh, L. Laureno-Perez, B. Dale, and L. Lynd. 2008. Recent process improvements for the ammonia fiber expansion (AFEX) process and resulting reductions in minimum ethanol selling price." *Bioresources Technology* 99:8429-8435.

Tembo, Gelson, Epplin Francis M, Huhnke, Raymond L. 2003. "Integrative investment appraisal of a lignocellulosic biomass-to-ethanol industry." *Journal of Agricultural and Resource Economics* 28, 3:611–33.

Thorsell, S., Epplin, F. M., Huhnke, R. L., & Taliaferro, C. M. 2004. Economics of a coordinated biorefinery feedstock harvest system: lignocellulosic biomass harvest cost. *Biomass and Bioenergy , 27* (4), 327-337.

Wright, M. and R.C. Brown. (2007) "Establishing the Optimal Sizes of Different kinds of Biorefineries." *Biofuels, Bioproducts, & Biorefining* 1:191-200.

Back to Table of Contents

Table A1. Minnesota small grain and corn production (MT)

County	Mean Grain Production (mt)	Mean Grain Yields per Ha	Mean Ha Harvested	County Ha (Land area)	% of County Land Harvested	Mean Harvestable HCR	County-wide Mean HCR
Aitkin	1572	3.659	567	471195	0.12%	1.335	0.002
Anoka	17243	5.021	3367	109714	3.07%	1.76	0.054
Becker	98514	3.167	31249	339396	9.21%	1.276	0.118
Beltrami	6377	2.276	2752	648860	0.42%	0.961	0.004
Benton	112368	5.638	19643	105744	18.58%	1.976	0.367
Big Stone	248968	5.817	42803	128709	33.26%	2.108	0.701
Blue Earth	588094	8.068	72802	194860	37.36%	2.824	1.055
Brown	474391	7.883	60119	158212	38.00%	2.762	1.049
Carlton	604	4.848	121	222824	0.05%	1.697	0.001
Carver	174718	7.659	22820	92473	24.68%	2.686	0.663
Cass	5817	4.978	1128	522554	0.22%	1.765	0.004
Chippewa	453367	7.765	58440	150944	38.72%	2.723	1.054
Chisago	52855	5.683	9271	108165	8.57%	1.99	0.171
Clay	278426	3.449	81381	270715	30.06%	1.38	0.415
Clearwater	7867	2.767	2804	257628	1.09%	1.115	0.012
Cottonwood	549972	7.794	70374	165756	42.46%	2.729	1.159
Crow Wing	9565	4.446	2137	258110	0.83%	1.556	0.013
Dakota	274228	7.694	35608	147520	24.14%	2.694	0.65
Dodge	353877	8.276	42661	113830	37.48%	2.897	1.086
Douglas	138204	5.304	26069	164288	15.87%	1.919	0.304
Faribault	663796	8.197	80677	184829	43.65%	2.869	1.252
Fillmore	480775	8.043	59573	223062	26.71%	2.816	0.752
Freeborn	580273	8.092	71551	183277	39.04%	2.832	1.106
Goodhue	428948	8.121	52685	196390	26.83%	2.844	0.763
Grant	298473	5.644	53005	141519	37.45%	2.062	0.772
Hennepin	39640	6.761	5880	144163	4.08%	2.366	0.097
Houston	164839	7.826	21015	144627	14.53%	2.74	0.398
Hubbard	25677	5.997	4254	238915	1.78%	2.115	0.038
Isanti	72940	5.418	13403	113718	11.79%	1.898	0.224
Itasca	555	4.570	121	690245	0.02%	1.6	0.0003
Jackson	568528	7.745	73307	181736	40.34%	2.711	1.093
Kanabec	26227	4.714	5516	135956	4.06%	1.674	0.068
Kandiyohi	439854	7.555	58201	206178	28.23%	2.652	0.749
Kittson	174796	2.591	65829	284142	23.17%	1.108	0.257
Koochiching	1184	2.203	516	803505	0.06%	0.947	0.0006
Lac qui Parle	472777	6.812	69301	198100	34.98%	2.402	0.84
Lake of the Woods	11715	2.120	5034	335843	1.50%	0.912	0.014
Le Sueur	280462	7.638	36676	116161	31.57%	2.677	0.845
Lincoln	278532	6.710	41293	139090	29.69%	2.374	0.705
Lyon	536604	7.418	72231	184969	39.05%	2.602	1.016
McLeod	320698	7.737	41451	127404	32.54%	2.715	0.883

Back to Table of Contents

Mahnomen	70576	3.354	20970	144039	14.56%	1.325	0.193
Marshall	258210	2.524	101655	459007	22.15%	1.078	0.239
Martin	729848	8.271	87965	183718	47.88%	2.895	1.386
Meeker	310382	6.867	45190	157611	28.67%	2.413	0.692
Mille Lacs	40264	5.309	7511	148787	5.05%	1.859	0.094
Morrison	146553	5.142	28125	291243	9.66%	1.805	0.174
Mower	569148	7.933	71434	184277	38.76%	2.777	1.076
Murray	528781	7.522	70135	182446	38.44%	2.633	1.012
Nicollet	374203	8.072	46348	117142	39.57%	2.827	1.119
Nobles	580828	7.466	77536	185285	41.85%	2.613	1.094
Norman	250580	3.126	80345	226952	35.40%	1.272	0.45
Olmsted	344601	8.160	42143	169128	24.92%	2.856	0.712
Otter Tail	373354	5.003	74610	512741	14.55%	1.827	0.266
Pennington	74563	2.437	30282	159683	18.96%	1.037	0.197
Pine	25907	5.189	4937	365457	1.35%	1.82	0.025
Pipestone	277658	7.034	39404	120665	32.66%	2.468	0.806
Polk	420509	2.983	141480	510322	27.72%	1.25	0.347
Pope	273134	6.696	40840	173565	23.53%	2.368	0.557
Red Lake	68710	2.775	24718	111999	22.07%	1.161	0.256
Redwood	744812	7.870	94504	227848	41.48%	2.757	1.144
Renville	815505	7.957	102586	254574	40.30%	2.79	1.124
Rice	244568	7.821	31322	128870	24.31%	2.737	0.665
Rock	395525	7.730	51002	124995	40.80%	2.705	1.104
Roseau	111127	2.239	47210	430587	10.96%	0.955	0.105
Scott	109266	7.465	14621	92379	15.83%	2.613	0.414
Sherburne	69898	6.468	10789	113001	9.55%	2.264	0.216
Sibley	440353	8.073	54538	152459	35.77%	2.83	1.012
Stearns	424942	6.154	68735	348228	19.74%	2.169	0.428
Steele	337820	8.064	41783	111253	37.56%	2.823	1.06
Stevens	445722	6.978	63911	145572	43.90%	2.477	1.087
Swift	496312	7.317	67901	192573	35.26%	2.576	0.908
Todd	119159	4.959	23953	243981	9.82%	1.762	0.173
Traverse	355819	5.832	61131	148688	41.11%	2.112	0.868
Wabasha	249733	8.194	30416	135977	22.37%	2.871	0.642
Wadena	35795	5.308	6693	138569	4.83%	1.871	0.09
Waseca	385621	8.157	47214	109621	43.07%	2.855	1.23
Washington	56981	6.925	8166	101450	8.05%	2.424	0.195
Watonwan	410709	8.217	49925	112537	44.36%	2.876	1.276
Wilkin	280615	3.567	78904	194619	40.54%	1.409	0.571
Winona	230954	8.077	28558	162210	17.61%	2.83	0.498
Wright	187693	6.419	29230	171133	17.08%	2.257	0.386
Yellow Medicine	551927	7.144	77196	196310	39.32%	2.515	0.989

Back to Table of Contents

Table A2. South Dakota small grain and corn production (MT)

County	Mean Grain Production (mt)	Mean Grain Yields per Ha	Mean Ha Harvested	County Ha (Land area)	% of County Land Harvested	County Average Yield per Total Ha	Mean Harvestable HCR	County-wide Mean HCR
Aurora	116473	3.679	30501	183417	16.63%	0.612	1.345	0.224
Beadle	319919	4.243	73299	326001	22.48%	0.954	1.54	0.346
Bennett	55609	2.155	25070	306988	8.17%	0.176	0.876	0.072
Bon Homme	170721	4.575	36745	145904	25.18%	1.152	1.623	0.409
Brookings	318002	6.181	51224	205764	24.90%	1.539	2.188	0.545
Brown	643512	5.218	122816	443682	27.68%	1.445	1.888	0.523
Brule	118681	3.131	35927	212109	16.94%	0.530	1.192	0.202
Buffalo	26899	3.316	7798	121882	6.40%	0.212	1.258	0.08
Butte	17577	2.622	6544	582360	1.12%	0.029	1.012	0.011
Campbell	89118	2.557	32366	190568	16.98%	0.434	0.994	0.169
Charles Mix	260233	3.917	66230	284268	23.30%	0.913	1.442	0.336
Clark	225136	4.555	48853	248099	19.69%	0.897	1.668	0.328
Clay	232121	6.432	36089	106604	33.85%	2.177	2.254	0.763
Codington	198778	4.812	40970	178105	23.00%	1.107	1.774	0.408
Corson	60561	1.446	37975	640484	5.93%	0.086	0.606	0.036
Custer	4007	2.281	1659	403439	0.41%	0.009	0.94	0.004
Davison	138196	4.397	31019	112778	27.50%	1.209	1.583	0.435
Day	216045	4.124	51892	266398	19.48%	0.803	1.566	0.305
Deuel	178174	5.516	31994	161498	19.81%	1.093	1.983	0.393
Dewey	33346	1.820	16721	596379	2.80%	0.051	0.747	0.021
Douglas	136802	4.224	32091	112283	28.58%	1.207	1.532	0.438
Edmunds	248657	3.460	69095	296703	23.29%	0.806	1.315	0.306
Fall River	11662	2.628	4546	450620	1.01%	0.027	1.034	0.01
Faulk	170902	3.444	48230	259034	18.62%	0.641	1.324	0.247
Grant	200549	4.885	40824	176769	23.10%	1.128	1.791	0.414
Gregory	71980	2.814	24815	263124	9.43%	0.265	1.043	0.098
Haakon	106432	1.982	51131	469556	10.89%	0.216	0.842	0.092
Hamlin	228864	6.024	37947	131276	28.91%	1.741	2.148	0.621
Hand	233138	3.077	72899	372071	19.59%	0.603	1.18	0.231
Hanson	153850	4.891	31193	112602	27.70%	1.355	1.738	0.481
Harding	17530	1.284	12666	691654	1.83%	0.024	0.551	0.01
Hughes	112302	2.637	41411	191897	21.58%	0.569	1.065	0.23
Hutchinson	308540	4.995	61742	210519	29.33%	1.465	1.771	0.519
Hyde	82437	2.540	31128	222990	13.96%	0.355	1.019	0.142
Jackson	20444	1.652	11412	484101	2.36%	0.039	0.687	0.016
Jerauld	73801	3.374	21254	137246	15.49%	0.523	1.256	0.195
Jones	47961	2.121	22205	251363	8.83%	0.187	0.886	0.078
Kingsbury	282897	5.198	53996	217136	24.87%	1.292	1.867	0.464
Lake	271667	6.412	42220	145875	28.94%	1.856	2.249	0.651
Lawrence	427	1.906	220	207209	0.11%	0.002	0.82	0.0009
Lincoln	371013	6.627	55829	149724	37.29%	2.471	2.32	0.865
Lyman	138209	2.631	52155	424746	12.28%	0.323	1.066	0.131

McCook	278327	6.167	45097	148800	15.32%	0.945	2.16	0.331
McPherson	88894	2.834	30080	294465	13.86%	0.393	1.105	0.153
Marshall	202581	5.314	38368	216965	25.79%	1.370	1.915	0.494
Meade	42431	1.778	22771	898886	2.53%	0.045	0.757	0.019
Mellette	22492	1.998	10898	338378	3.22%	0.064	0.833	0.027
Miner	134243	4.803	27814	147717	18.83%	0.904	1.711	0.322
Minnehaha	413026	6.862	60034	209703	28.63%	1.965	2.403	0.688
Moody	332936	7.190	45858	134593	34.07%	2.450	2.521	0.859
Pennington	50550	1.888	25956	719017	3.61%	0.068	0.804	0.029
Perkins	60182	1.531	36874	743744	4.96%	0.076	0.647	0.032
Potter	218175	2.966	70382	224419	31.36%	0.930	1.179	0.37
Roberts	301657	4.802	62733	285229	21.99%	1.056	1.783	0.392
Sanborn	111373	4.442	24455	147372	16.59%	0.737	1.579	0.262
Shannon	17117	1.805	8656	542311	1.60%	0.029	0.764	0.012
Spink	492676	4.536	108025	389499	27.73%	1.258	1.667	0.462
Stanley	76437	1.896	38849	373807	10.39%	0.197	0.811	0.084
Sully	287408	2.710	101955	260785	39.10%	1.060	1.091	0.427
Todd	20572	3.549	5840	359520	1.62%	0.058	1.324	0.022
Tripp	126730	2.414	51463	417898	12.32%	0.297	0.936	0.115
Turner	357485	6.181	57663	159755	36.09%	2.231	2.169	0.783
Union	317728	6.825	46404	119237	38.92%	2.656	2.389	0.93
Walworth	111894	2.706	39622	183321	21.61%	0.585	1.064	0.23
Yankton	191492	5.667	33600	135080	24.87%	1.410	1.99	0.495
Ziebach	35737	1.758	19586	508240	3.85%	0.068	0.752	0.029

Back to Table of Contents

Table A3. North Dakota small grain and corn production (MT)

County	Mean Grain Production (mt)	Mean Grain Yields per Ha	Mean Ha Harvested	County Ha (Land area)	% of County Land Harvested	County Average Yield per Total Ha	Mean Harvestable HCR	County-wide Mean HCR
Adams	88893	1.420	61491	255867	24.03%	0.341	0.606	0.146
Barnes	368418	2.997	125535	386334	32.49%	0.974	1.206	0.392
Benson	211386	2.148	98118	357573	27.44%	0.589	0.899	0.247
Billings	16691	1.550	10627	298213	3.56%	0.055	0.662	0.024
Bottineau	293816	2.087	137874	432161	31.90%	0.666	0.896	0.286
Bowman	87766	1.597	54142	300969	17.99%	0.287	0.681	0.123
Burke	152703	1.700	90474	285812	31.66%	0.538	0.731	0.231
Burleigh	112868	1.905	58011	422967	13.72%	0.261	0.793	0.109
Cass	575226	3.580	162401	457191	35.52%	1.272	1.402	0.498
Cavalier	388048	2.265	171033	385508	44.37%	1.005	0.973	0.432
Dickey	295375	4.393	67201	292927	22.94%	1.008	1.622	0.372
Divide	180554	1.708	106442	326216	32.63%	0.557	0.734	0.24
Dunn	113909	1.673	67986	520482	13.06%	0.219	0.714	0.093
Eddy	72146	2.226	32358	163200	19.83%	0.441	0.937	0.186
Emmons	163376	2.079	74169	391056	18.97%	0.394	0.852	0.162
Foster	135555	2.534	53041	164516	32.24%	0.817	1.048	0.338
Golden Valley	50177	1.697	29363	259513	11.32%	0.192	0.719	0.081
Grand Forks	315154	2.778	113346	372390	30.44%	0.846	1.147	0.349
Grant	88612	1.421	59524	429797	13.85%	0.197	0.604	0.084
Griggs	126927	2.620	48861	183500	26.63%	0.698	1.084	0.289
Hettinger	232381	1.838	126502	293250	43.14%	0.793	0.787	0.34
Kidder	66120	2.253	28837	349852	8.24%	0.186	0.909	0.075
La Moure	307000	3.565	87597	297117	29.48%	1.051	1.364	0.402
Logan	85721	1.956	42297	257092	16.45%	0.322	0.813	0.134
McHenry	173825	1.928	89474	485386	18.43%	0.355	0.814	0.15
McIntosh	97471	2.090	45603	252572	18.06%	0.377	0.859	0.155
McKenzie	142690	1.710	83752	710178	11.79%	0.202	0.733	0.086
McLean	341975	1.968	173631	546473	31.77%	0.625	0.84	0.267
Mercer	79321	1.786	44268	270780	16.35%	0.292	0.762	0.125
Morton	138905	1.577	85990	498900	17.24%	0.272	0.667	0.115
Mountrail	236390	1.713	138125	472394	29.24%	0.501	0.736	0.215
Nelson	154300	2.299	67310	254238	26.48%	0.609	0.968	0.256
Oliver	63441	1.922	32949	187390	17.58%	0.338	0.81	0.142
Pembina	281481	2.664	105018	289754	36.24%	0.966	1.127	0.409
Pierce	143832	2.031	70572	263613	26.77%	0.544	0.862	0.231
Ramsey	231840	2.282	104209	306874	33.96%	0.775	0.944	0.32
Ransom	230741	4.167	55546	223451	24.86%	1.036	1.576	0.392
Renville	219230	2.004	109384	226564	48.28%	0.968	0.861	0.416
Richland	691522	4.822	143539	372105	38.58%	1.860	1.77	0.683
Rolette	107460	2.181	48663	233733	20.82%	0.454	0.934	0.194
Sargent	267059	4.371	61151	222415	27.49%	1.202	1.628	0.448
Sheridan	107293	1.911	56044	251681	22.27%	0.426	0.816	0.182

Back to Table of Contents

Sioux	17386	1.285	11962	283375	4.22%	0.054	0.541	0.023
Slope	95107	1.741	53960	315444	17.11%	0.298	0.747	0.128
Stark	176860	1.735	101412	346581	29.26%	0.508	0.743	0.217
Steele	205997	3.155	65752	184500	35.64%	1.124	1.259	0.449
Stutsman	329585	2.602	128016	575338	22.25%	0.579	1.053	0.234
Towner	198539	2.058	95083	265356	35.83%	0.738	0.88	0.315
Traill	316047	3.716	84513	223228	37.86%	1.407	1.434	0.543
Walsh	286371	2.594	110639	331968	33.33%	0.865	1.097	0.366
Ward	383872	2.049	187520	521332	35.97%	0.737	0.878	0.316
Wells	253167	2.251	111987	329259	34.01%	0.766	0.943	0.321
Williams	289151	1.700	170333	536245	31.76%	0.540	0.73	0.232

Appendix 1. GAUSS input file.

GAUSS input file for calculating distances from farms to centers of each cell. The example problem solves for both straw and pretreated feedstock transportation among cells in a 5x5 grid.

As an example of the calculations, consider the distance from a farm to the center of the cell in which it lies. The farm's location would be represented by a random draw of horizontal and vertical distances from the cell's center. Each farm will be α km from the cell's center in a horizontal direction and β km in a vertical direction. Both α and β are randomly drawn from a uniform distribution between 0 (the farm lies at the cell's center) and 10 km (the distance from the cell's center to an edge moving in either a horizontal or a vertical direction). The distance from the farm is then calculated as the hypotenuse formed by the horizontal (α) and vertical (β) distance of the randomly drawn coordinates to the cell's center. Pairs of (α,β) were drawn 100,000 times, resulting distances to the center were calculated, and the 100,000 calculated distances were averaged to represent the average distance of farms to the center of its cell. Similar procedures were used to derive distances from a farm in one cell to the centers of all cells within the outer boundary considered for transporting bales of crop residue. For example, for two cells sharing a common vertical border, say cells A and B, the distance from a farm in B to the center of cell A will equal the hypotenuse of a triangle formed from a value of α between 10 and 30 km (i.e., the horizontal distance of the farm in B to the center of A) and a value of β between 0 and 10 km (the vertical distance of the farm in B to the center of cell A).

File: DistanceJune.e
Creation date: December 15, 2009

```
/*
Generation of new distance table from i to j
First task, generate table of distances, then put in full matrix form

   Straw Hauling Distances  */

rx=5;
r1 = Distances(rx);
R = zeros((2*rx-1),(2*rx-1));
rr1=(rev(r1'))';
R[rx:(2*rx-1),1:(2*rx-1)] = rr1[.,1:(rx-1)]~r1;
rr=rev(r);
rnew=rr[1:(rx-1),.]|r[rx:(2*rx-1),.];
/*
```

```
Creation of i to j table for GAMS pivots on middle of rnew, making new site i correspond to midpoint
  of rnew.  Vectorization of rnew from the pivots around the central cell of rnew creates GAMS table
*/
rc = zeros(rx^2,rx^2);
i=1;j=0;k=0;
do while i .le rx^2;
do while j .lt rx;
do while k .lt rx;
   rc[i,.] = vec(rnew[(rx-j):(2*rx-1-j),(rx-k):(2*rx-1-k)]')';
   i = i + 1;
   k = k + 1;
endo;
   k = 0;
   j = j + 1;
endo;
   j = 0;
endo;
ret1 = xlswrite(rc,"strawdist","b2",1,"");
/*   Pretreated feedstock Hauling Distances  */

r1 = PPDist(rx);
R = zeros((2*rx-1),(2*rx-1));
rr1=(rev(r1'))';
R[rx:(2*rx-1),1:(2*rx-1)] = rr1[.,1:(rx-1)]~r1;
rr=rev(r);
rnew=rr[1:(rx-1),.]|r[rx:(2*rx-1),.];
/*
Creation of i to j table for GAMS pivots on middle of rnew, making new site i correspond to midpoint
  of rnew.  Vectorization of rnew from the pivot cell creates GAMS table
*/
prc = zeros(rx^2,rx^2);
i=1;j=0;k=0;
do while i .le rx^2;
do while j .lt rx;
do while k .lt rx;
   prc[i,.] = vec(rnew[(rx-j):(2*rx-1-j),(rx-k):(2*rx-1-k)]')';
   i = i + 1;
   k = k + 1;
endo;
   k = 0;
   j = j + 1;
endo;
   j = 0;
endo;
ret2 = xlswrite(prc,"PPdist","b2",1,"");

proc Distances(cell);
  local c2, sq, n, dist, outt,i,j,k,b,h;
/*
Calculation of distances between plant locations.
Based on squares of 20 km per side.
```

Farms (crop residue origins) are assumed to be distributed uniformly within each square.

Potential locations of pretreatment and refining facilities are assumed to be in the center of each square.

Distances from farms to the centers of squares are calculated as the straightline distance based on the hypotenuse of a right triangle of base b and height h.
*/

```
c2=cell^2;
sq=20;     /* Side of each square (in kms.) */
n=100000;     /* Number of calculated distances from farm to square centers */
dist=zeros(cell,cell);
outt=zeros(c2,3);
i=1;j=1;k=1;
do while i .le cell;
do while j .le cell;
b=(sq/2)*rndu(n,1);
if i .eq 1;
b=(sq/2)*rndu(n,1);
else;
b=(sq/2+(i-2)*sq)+((sq/2+(i-1)*sq)-(sq/2+(i-2)*sq))*rndu(n,1); /* Random number generation for height
of each triangle */
endif;
if j .eq 1;
h=(sq/2)*rndu(n,1);
else;
h=(sq/2+(j-2)*sq)+((sq/2+(j-1)*sq)-(sq/2+(j-2)*sq))*rndu(n,1); /* Random number generation for height
of each triangle */
endif;
dist[i,j] = meanc(sqrt(b^2+h^2));
outt[k,.]=i~j~dist[i,j];
j=j+1;k=k+1;
endo;
j=1;i=i+1;
endo;
retp(dist);
endp;

proc PPDist(cell);
  local d, p1;
/*
```

Calculation of distances between plant locations.
Based on squares of of 20 km miles per side.

Potential locations of pretreatment and refining facilities are assumed to be in the center of each square.

Distances from center to center of squares are calculated as the straightline distance based on the hypotenuse of a right triangle of base b and height h.
*/

```
d=20;
/*  5 cells to the side  */
p1 = 0~d~2*d~3*d~4*d|
(d~sqrt(d^2+d^2)~sqrt(d^2+(2*d)^2)~sqrt(d^2+(3*d)^2)~sqrt(d^2+(4*d)^2))|
(2*d~sqrt((2*d)^2+d^2)~sqrt((2*d)^2+(2*d)^2)~sqrt((2*d)^2+(3*d)^2)~sqrt((2*d)^2+(4*d)^2))|
(3*d~sqrt((3*d)^2+d^2)~sqrt((3*d)^2+(2*d)^2)~sqrt((3*d)^2+(3*d)^2)~sqrt((3*d)^2+(4*d)^2))|
(4*d~sqrt((4*d)^2+d^2)~sqrt((4*d)^2+(2*d)^2)~sqrt((4*d)^2+(3*d)^2)~sqrt((4*d)^2+(4*d)^2));
;

retp(p1);
endp;
```

Appendix II. GAMS Mixed Integer Programming Model

```
Options limrow=0,limcol=0,solprint=off;
Options iterlim = 500000, reslim = 100000, optcr = 0.0250;
SETS
     I    / R1C1*R1C10, R2C1*R2C10, R3C1*R3C10, R4C1*R4C10,
            R5C1*R5C10, R6C1*R6C10, R7C1*R7C10, R8C1*R8C10,
            R9C1*R9C10, R10C1*R10C10 /
     Breaks / k0*k6 /
     Plant(I) / R5C5 /
     Time    Production schedule        / T1*T2 /
     Till  / Notill, Conv /
     CROP  / Corn, Grains /
     RNS   / Runs1 / ;

Alias(I, J);

SCALAR
       EPrice  Ethanol price per liter - Five year average is $0.60 per liter
              / 0.60 /
       EthMT   Ethanol yield per metric ton (equal to 60 gallons per ton)
              / 250 /
       Plants   Limit on number of refining plants to build
              / 1 /
       LatDeg  Width of cells in km
              / 20 /
       LongDeg Heighth of cells
              / 20 /
       FeedVal  Value of preprocessed straw as animal feed
                 (98.47 - Carolan 2007)
              / 0 /
       MTonnes Convert tons to metric tonnes
              / 1.102 /
       SCost   Dollars per loaded km for 15.4 mt truck
              / 2.78 /
       Dense   Pretreatment transportation cost as percent of straw cost
              / 0.75 /
       LoadL   Metric tonnes per truck - 17 US tons
              / 15.4 /
       Area    Area of each cell
       HarvCost Cost per ton of harvest (Brechbill et al 2008)
            / 10.7 /
       SoilVal Value of nutrients in harvested straw
             /13.452/
       Count   Counter for looping through solve statements
              / 1 /
       EnvValue  Environmental benefits per ton of leaving residues
             / 15 /
       Carbon   Carbon values of left residues
             / 1 /
       TCCut Reduce ATC for pretreat and refining
             / 1. / ;
$ontext
   Conversion factors:
     US tons to metric tonnes is 1.102 US to 1 mt
```

```
     1 km equals 0.62137 miles
$offtext

Area = 100*LatDeg*LongDeg;
HarvCost=HarvCost*MTonnes;
EnvValue = SoilVal*MTonnes;

*  Model fixing HCR supplies to regional "averages"
Parameter Yields(*,*) Crop residue yields
          Land(*,*)   Proportion of land in each crop and practice
          Limits(*)   HCR limits based on tillage;
   Yields(TILL,Crop) = 2.0;
   Land(TILL,Crop) = 0.0;
   Land('Conv','Corn') = 1.0;
   Limits(TILL) = 1.0;

Parameter
    StorCost(Time) StorCost Per month straw bale storage cost
       / T1 4.86, T2 9.98 /
    PPStorCost(Time) Per month cost of preprocessed residue storage as a
function of StorCost
       / T1 4.27, T2 0 / ;

$ontext
Model allowing multiple production practices and differential limits on HCR
removal
Table Yields(*,*)  Crop residue yields
         Corn    Grains
Notill    10       8
Conv      3       2.5    ;

Table Land(*,*)   Proportion of land in each crop and practice
          Corn    Grains
Notill    .4        .3
Conv      .1        .2    ;

PARAMETER   Limits     "HCR limits based on tillage";
      Limits('Notill') = 0.35;
      Limits('Conv')   = 0.50;
$offtext

* Load in distance data from external files
$include C:\Documents and Settings\lambertd\My Documents\D-
Documents\Research\SunGrant\Data\StrawDist.prn
$include C:\Documents and Settings\lambertd\My Documents\D-
Documents\Research\SunGrant\Data\PPDist.prn

Table Data(*,*)    Final cost estimates based on CJD paper Table 4 2008
dollars
         Size        ATC
K0         0         0.0
K1         1     10000.0
K2       80100     22.27
K3      220590     20.65
K4      441511     16.78
K5      883022     14.59
K6     1471924     13.53  ;
```

```
*Data(Breaks,'ATC')$(ord(breaks) gt 2) = 13.53;

Table EData(*,*)   Final cost estimates derived from MBI report to NDSU
         Size        ATC
K0          0         0.0
K1          1     1000000
K2          2     1000000
K3     220590       78.21
K4     441511       70.35
K5     883022       64.17
K6    1471924       57.71  ;

*  Reduce EData by pretreatment cots:
EData(Breaks, 'ATC') = EData(Breaks, 'ATC') - Data(Breaks, 'ATC');

Variables Z;
Positive Variables
   Harvest    Harvest CROP under practice TILL in region I
   EnvBen     Value of nutrients removed with HCR harvest
   Supply     Total HCR supply in region I
   ShipStraw   'Shipments of baled HCR from origin Lat/Long to Lat1/Long1'
   Store
   SupStraw
   PPStore
   Feed      Use of preprocessed straw as animal feed
   PProc     'Preprocessing of HCR at Lat/Long'
   Refine    Refine the pretreated biomass into ethanol
   Raw
   Demand    Total liters of ethanol produced at all loactions in both time
periods
   ShipPP    Ship pretreated biomass ;
SOS2 Variables
   BuildPP    'Build the refinery plant at Site'
   Build    'Build the refinery plant at Site';

Equations
   Obj    Objective function
   ConA
   ConB
   ConC
   Con1   Potential supply of crop residues at origins
   Con2   Transshipment points period 1
   Con3  Total pretreatment is shipped
   Con4   Total supply exceeds system demand
   Con5
   Con5
   Con6  All pretreated shipments must be processed first
   Con7
   Con8  All ethanol must be refined
   Con9
   Con10
   Con11
   Con12
   Con13
   Con14
   Con15
```

```
   Con16
   Con17
;

* Scenario analyses by fixing/unfixing variable levels
*BuildPP.FX(I,'K0')$(Not Plant(I)) = 1;
*BuildPP.FX(I,Breaks)$(Ord(Breaks) gt 3) = 0;
*BuildPP.FX(I,'K5')$(Plant(I)) = 1;
Build.FX(I,'K0')$(Not Plant(I)) = 1;
*Build.FX(I,'K5')$(Plant(I)) = 1;
*Feed.fx(Time,I) = 0;

Obj .. Z =E= EPrice * Demand + Sum((Time,I), FeedVal*Feed(Time,I))
         - ( EnvValue*Sum(I, EnvBen(I) )
         +   Sum((I,Till,Crop), HarvCost*Harvest(I,Till,Crop))
         +   Sum((Time,I,J),
             (SCost/LoadL)*MILES(I,J)*ShipStraw(Time,I,J))
         +   Sum((Time,I,J),
             Dense*(SCost/LoadL)*PPMiles(I,J)*ShipPP(Time,I,J))
         +   Sum((Time,I),StorCost(Time)*Store(Time,I))
         +   Sum((Time,I),PPStorCost(Time)*PPStore(Time,I))
         +   SUM((I,BREAKS),
             TCCut*DATA(BREAKS,"ATC")*DATA(BREAKS,"Size")*BuildPP(I,BREAKS) +

TCCut*EDATA(BREAKS,"ATC")*EDATA(BREAKS,"Size")*Build(I,BREAKS)));

*  In each time period, shipments from fields located at Lat,Long to
Lat1,Long1 is less than
*  or equal to total crop residue supply at Lat,Long

ConA(I) .. Supply(I) =L=
           Sum((Till,Crop),
           Limits(Till)*Yields(Till,Crop)*Harvest(I,Till,Crop));

ConB(I,Till,Crop) .. Harvest(I,Till,Crop) =L= Area*Land(Till,Crop);

ConC(I) .. EnvBen(I) =E= Carbon*Sum((Till,Crop),
        Yields(Till,Crop)*Limits(Till)*Harvest(I,Till,Crop) );

Con1(I) .. Sum(J, ShipStraw('T1',I,J)) =E= Supply(I);

Con2(J) .. Sum(I, ShipStraw('T1',I,J)) =E= SupStraw('T1',J);

Con3(J) .. SupStraw('T1',J) =E= PProc('T1',J) + Store('T1',J);

Con4(I) .. Store('T1',I) =e= Sum(J, ShipStraw('T2',I,J));

Con5(J) .. Sum(I, ShipStraw('T2',I,J)) =E= SupStraw('T2',J);

Con6(J) .. SupStraw('T2',J) =E= PProc('T2',J);

Con7(J) .. PProc('T1',J) =E= Sum(I,ShipPP('T1',J,I));

Con8(J) .. PProc('T2',J) + PPStore('T1',J) =E= Sum(I,ShipPP('T2',J,I));

Con9(Time,I) .. Sum(J,ShipPP('T1',J,I)) =e= Refine('T1',I) + PPStore('T1',I)
            + FEED('T1',I);
```

```
Con10(Time,I) .. Sum(J,ShipPP('T2',J,I)) =e= Refine('T2',I) + FEED('T2',I);

Con11(Time,I) ..
    Raw(Time,I) =L= EthMT * Refine(Time,I);

*  EthMT is yield in ethanol liters per metric ton of feedstock (Leistritz et
al.)

Con12 .. Sum((Time,I), Raw(Time,I)) =E= Demand;

CON13(I) .. SUM(BREAKS, BuildPP(I,BREAKS)) =E= 1;

CON14(I) .. Sum(Time, PProc(Time,I)) =E=
                  SUM(BREAKS, BuildPP(I,BREAKS)*DATA(BREAKS,"SIZE"))  ;

CON15(I) .. SUM(BREAKS, Build(I,BREAKS)) =E= 1;

CON16(I) .. Sum(Time, Refine(Time,I)) =E=
                  SUM(BREAKS, Build(I,BREAKS)*EDATA(BREAKS,"SIZE"))  ;

Con17(I) .. (1/2)*Raw('T1',I) -
    (1/2)*Raw('T2',I)  =L= 0;


Model Transport / All /;
Option MIP=CoinCbc;
Parameter  Res1, Pretreat, Ref, ShipS, ShipP, LandVal, Hauling;

Loop (RNS,
Solve Transport using MIP Maximizing Z;
*$ontext
  Res1('Total Costs',RNS)$(Ord(RNS) = Count) =  TCCut;
  Res1('Ethanol Price',RNS)$(Ord(RNS) = Count) =  EPrice;
  Res1('Feed Price',RNS)$(Ord(RNS) = Count) =  FeedVal;
  Res1('RegProd',rns)$(Ord(RNS) = Count) =
           Sum((I,Till,Crop),
           Limits(Till)*Yields(Till,Crop)*Harvest.L(I,Till,Crop))
           / Sum((I,Till,Crop), Harvest.L(I,Till,Crop));
  Res1('Ethanol Revenue',RNS)$(Ord(RNS) = Count) =  EPrice * Demand.L;
  Res1('Feed Revenue',RNS)$(Ord(RNS) = Count) = Sum((Time,I),
FeedVal*Feed.L(Time,I));
  Res1('Harvest Cost',RNS)$(Ord(RNS) = Count) =Sum((I,Till,Crop),
              (HarvCost)*Harvest.L(I,Till,Crop));
  Res1('Environ Cost',RNS)$(Ord(RNS) = Count) = EnvValue*Sum(I, EnvBen.L(I)
);
  Res1('Straw Ship Cost',RNS)$(Ord(RNS) = Count) = Sum((Time,I,J),
            (SCost/LoadL)*Miles(I,J)*ShipStraw.L(Time,I,J)) ;
  Res1('Max Dist',RNS)$(Ord(RNS) = Count) =
       Smax((Time,I,J)$(ShipStraw.L(Time,I,J)),Miles(I,J)) ;
  Res1('Max Cost per mt',RNS)$(Ord(RNS) = Count) =
             Res1('Max Dist',RNS)*(SCost/LoadL);
  Res1('Pretreat Ship Cost',RNS)$(Ord(RNS) = Count) = Sum((Time,I,J),
             Dense*(SCost/LoadL)*PPMiles(I,J)*ShipPP.L(Time,I,J));
  Res1('Store Straw Cost',RNS)$(Ord(RNS) = Count) =
            Sum((Time,I),StorCost(Time)*Store.L(Time,I));
  Res1('Store PP Cost',RNS)$(Ord(RNS) = Count) =
```

```
            Sum((Time,I),PPStorCost(Time)*PPStore.L(Time,I));
  Res1('PP_Plant Cost',RNS)$(Ord(RNS) = Count) = SUM((I,BREAKS),
DATA(BREAKS,"ATC")*DATA(BREAKS,"Size")
                *BuildPP.L(I,BREAKS)*TCCut);
  Res1('Plant Cost',RNS)$(Ord(RNS) = Count) = SUM((I,BREAKS),
EDATA(BREAKS,"ATC")*EDATA(BREAKS,"Size")
                *Build.L(I,BREAKS)*TCCut);
  Res1('Total Cost',RNS)$(Ord(RNS) = Count) = Res1('Harvest Cost',RNS)
    + Res1('Environ Cost',RNS)
    + Res1('Straw Ship Cost',RNS) + Res1('Pretreat Ship Cost',RNS)
    + Res1('Store Straw Cost',RNS) + Res1('Store PP Cost',RNS)
    + Res1('Plant Cost',RNS) + Res1('PP_Plant Cost',RNS);

  Res1('Ethanol Liters',RNS)$(Ord(RNS) = Count) =  Demand.L;
  Res1('Feed',RNS)$(Ord(RNS) = Count) = Sum((Time,I), Feed.L(Time,I));
  Res1('Straw Harvest',RNS)$(Ord(RNS) = Count)
=Sum((I,J),ShipStraw.L('T1',I,J));
  Res1('Pretreatment',RNS)$(Ord(RNS) = Count) =Sum((Time,I),PProc.L(Time,I));
  Res1('Store Straw',RNS)$(Ord(RNS) = Count) = Sum((Time,I),Store.L(Time,I));
  Res1('Store PP',RNS)$(Ord(RNS) = Count) = Sum((Time,I),PPStore.L(Time,I));

  Ref('Pretreat',I,Breaks,RNS)$(Ord(RNS) = Count and BuildPP.l(I,'k0') ne 1)
= BuildPP.L(I,BREAKS);
  Ref('Refine',I,Breaks,RNS)$(Ord(RNS) = Count and Build.l(I,'k0') ne 1) =
Build.L(I,BREAKS);
  ShipS(i,RNS)$(Ord(RNS) = Count) = Sum(J,shipstraw.l('t1',i,j));
  Hauling(i,j) = MILES(I,J)$ShipStraw.L('T1',I,J);
  LandVal('MC',I,rns)$(Ord(RNS) = Count) =
             ConB.M(I,'Conv','Corn')/(Limits('Conv')*Yields('Conv','Corn'));
*$offtext
*  TCCut = TCCut + .25;
  Eprice = Eprice - .025;
*  FeedVal = FeedVal + 2.5;
  Count = Count + 1;
*  Yields(TILL,Crop) = Yields(TILL,Crop) + 0.5;

*$offtext
);

Display Res1, Ref;
```

Back to Table of Contents

Sun Grant Initiative

DOE Final Progress Report

Project Title: Strategies for Concurrent Wet Storage and Pretreatment of Corn Stover

Project Director/Principal Investigator: Yebo Li, Assistant Professor, Department of Food, Agricultural and Biological Engineering

Collaborators: N/A

Project Performance Period: 1 January 2009 – 31 March 2012

Funding Awarded: $79,688

Cost Share Amount: $25,194

Cost Share Sources: Time and effort from PI; Indirect on time and effort; Tuition remission

Executive summary

Storage of feedstock is necessary to supply biorefinery industry with year-round feedstocks. Drying, baling, and densification of corn stover have been widely investigated recently. A cost effective concurrent wet storage and pretreatment technology was developed in this study to provide homogeneous delignified cellulosic feedstock to biorefinery. NaOH or fungal assisted concurrent treatment and wet storage of corn stover showed enhanced enzymatic digestibility and reduced loss of carbohydrates. *C. subvermispora* selectively degraded lignin by as much as 39.2% while the cellulose loss was less than 5% during 42 d of wet storage. However, hemicellulose loss of up to 27.0% was concomitant with the lignin degradation. The enzymatic hydrolysis yield of corn stover delignified by *C. subvermispora* was remarkably improved, reaching about 57-67% overall glucose yield after 18-42d of pretreatment, while the glucose yield of the untreated was only 22%. At 50-g/kg DM NaOH loading, the glucose and xylose yields were 2.9 and 3.9 fold higher, respectively, than those of the control after 90 d of wet storage. The lignin and xylan degradation of corn stover was significantly influenced by NaOH loading and moisture content. A preliminary economic analysis conducted based the lab scale results demonstrated the economic feasibility of this technology. However this needs to be validated through the pilot scale testing.

This project can benefit the farmers by value added processing of corn stover. Delignified corn stover will be sold to the biorefinery industry at higher price than the unprocessed corn stover. As this technology has the potential to reduce the cost for the biofuel production from corn stover, which will benefit the general public with biofuels produced domestically at a lower cost.

Objectives

Objective 1: Study and optimize the concurrent wet storage and alkali pretreatment for high sugar recovery and low inhibitor formation;
The concurrent alkali pretreatment and wet-storage of corn stover during a 90-d period was studied. Compared with ensilage, adding NaOH significantly enhanced the enzymatic degradability of corn stover by 2-3 fold after 90-d wet storage. Lignin and xylan removal during NaOH pretreatment and wet-storage were influenced by NaOH loading and moisture. NaOH pretreatment retarded the production of organic acids during storage and the acetate release correlated with lignin and xylan removal. The actual accomplishment meets the expected one.

Objective 2: Screen selective white-rot fungi and optimize the concurrent wet storage and microbial pretreatment for high lignin degradation with minimum holocellulose loss.
Lignin degradation and enzymatic hydrolysis yield were significantly affected by the particle size and moisture content of corn stover, as well as the time and temperature of the microbial pretreatment. This environmentally friendly fungal pretreatment shows great potential to be a cost-effective pretreatment process for ethanol production from corn stover. Considering the ambient temperature, the relatively long pretreatment time, and the limited amount of cellulose loss, it is feasible to apply fungal treatment concurrently with on-farm wet storage for ethanol production. The actual accomplishment meets the expected one.

Objective 3: Study the effect of homogenization on the enzymatic hydrolysis sugar yield, flowability, microstructure, and surface area of the alkali/microbial treated materials;

Short-term microbial pretreated corn stover was subjected to mechanical dispersion using a homogenizer. The glucose yield was improved by about 8-12% for 14-18d pretreated samples. However, when the pretreatment/wet storage time extended 4 weeks or longer, the effect of homogenization was not significant. The actual accomplishment meets the expected one.

Objective 4: Evaluate the economic impacts of the concurrent wet storage and pretreatment processes.
A preliminary economic analysis was conducted based on the lab scale results. The ethanol production cost based on the proposed technology has the potential to reduce the ethanol production cost from corn stover by up to 5-13% by eliminating the pretreatment and conditioning steps in the biorefining plants.

Original hypothesis: During the long wet storage period, low severity alkali /selective white-rot fungi could effectively decompose lignin at ambient condition. After homogenization of the delignified cellulosic material, we expect to obtain sugar yield in enzymatic hydrolysis compatible to the current leading pretreatment technologies. Replacing the high severity (high temperature/ high chemical uses) pretreatment process with the low severity alkali /microbial pretreatment during the wet storage process will not only reduce the processing and waste stream treatment cost, but also produce high quality homogeneous substrate with less or no inhibitor.

Approach:
Alkaline Assisted Wet-Storage of Corn Stover
Twenty grams of corn stover (dry basis) was mixed with NaOH stock solution (20 wt.%) and deionized (DI) water to obtain NaOH loadings of 0, 10, 20, 35 and 50 g/kg dry corn stover, with moisture contents of 45%, 60% and 75% for each. NaOH soaked corn stover was placed in heavy-duty Ziploc plastic bags and the air was pressed out. Sealed wet-storage bags were incubated at ambient temperature (23±0.5 °C) for different durations. Bags were sampled at 6 h, 5 d, 12 d, 35 d and 90 d for analysis of dry matter loss, pH, and composition, and subjected to enzymatic hydrolysis for measuring sugar yields. All tests were run in duplicate.

Fungi- Assisted Wet-Storage of Corn Stover
The white rot fungus *C. subvermispora* (ATCC 96608) was purchased from American Type Culture Collection (Manassas, VA, USA) and kept on 2% (w/v) malt extract agar (MEA) plates at 4 °C. The fungus was firstly revived on 2% MEA at 28°C for 5 d, then transferred to 2% (w/v) malt extract liquid medium in a 500-ml cotton-plugged Erlenmeyer flask and incubated at 28 °C statically for 7 d. Harvested culture was aseptically homogenized in a blender for three 15-s cycles for inoculation.

Ten gram samples of ground corn stover for each of the three particle sizes were placed in 250 ml Erlenmeyer flasks and then conditioned with different amounts of DI water to obtain moisture contents of 45, 60, 75, and 85 % (wet basis), respectively. Flasks containing wet corn stover were autoclaved (121 ºC, 30 min) and cooled prior to inoculation. A homogeneous liquid culture of 2 ml was inoculated on the top of the substrate in each flask. Pretreatment was carried out in a refrigerated incubator at 28 ºC in static conditions for 35 d. The subsamples were taken at predetermined time periods (18, 28, and 35 d) for compositional analysis. Corn stover (5 mm) with a moisture content of 75 % was pretreated by *C. subvermispora* at seven levels of temperature (4, 19, 24, 28, 32, 34, and 37 ºC) for 18 d. Fungal pretreatment of corn stover

fraction at a moisture content of 75%, particle size of 5mm were tested and 28 ºC for 35 d. All samples were subjected to enzymatic hydrolysis to evaluate saccharification rate. Samples without fungal inoculation were used as controls. All tests were performed in triplicate.

Homogenization

Mechanical homogenizing was conducted using a rotor-stator homogenizer (IKA-Werke, Staufen Breisgau, Germany). The substrate was mixed with distilled water to obtain a solid concentration of 5%. The slurry was dispersed at room temperature with a rotation rate of 28,000 rpm for 0.5-2 min to obtain a homogeneous watery mash. The homogeneous mash was diluted for enzymatic hydrolysis.

Enzymatic hydrolysis

Enzymatic hydrolysis was carried out following NREL Laboratory Analytical Procedure (LAP)-008 (Dowe and McMillan, 2001). Cellulase (Spezyme CP) was obtained from Genencor (Palo Alto, CA). Corn stover was loaded at a solid concentration of 2.5 % (w/w) in a 50 mM citrate buffer (pH 4.8) and cellulase was loaded at 10 FPU/g solid. The hydrolysis was carried out at 50 ºC and 130 rpm on a rotary shaker for 72 h. The hydrolyzed slurry was boiled to inactivate cellulase. After cooling to room temperature, the slurry was filtered through 0.2 µm nylon membrane filter for sugar analysis by high performance liquid chromatography (HPLC).

Simultaneous saccharification and fermentation (SSF)

SSF was carried out using Spezyme CP and Saccharomyces cerevisiae (ATCC 248585) following NREL LAP-008 (Dowe and McMillan, 2001). Corn stover with 5 mm particle size and 75% moisture content pretreated at 28 °C was added to a 125 ml flask containing 50 mM citrate buffer (pH 4.8) with a solid loading of 5% (w/w). Some samples were washed with 250 ml deionized water twice and filtered while other samples were directly used for hydrolysis and SSF tests without washing. Spezyme CP was added at a loading of 5 FPU/g solid. S. cerevisiae stock culture was revived in YM medium (yeast extract 3 g/L, malts extract 3 g/L, peptone 3 g/L and glucose 50 g/L) at 37 ºC and 120 rpm on a rotary shaker for 12 h. The cells were harvested, washed with DI water twice by centrifugation (5000 rpm for 5 min) and used for inculcating SSF flasks (the starting optical density (OD) was around 0.5 in a SSF flask). The flasks were equipped with water traps to vent CO2. The SSF was conducted at 37 ºC and 120 rpm for 72 h. The samples were taken at predetermined intervals (0, 6, 12, 24, 48, and 72 h) and filtered through a 0.2 um nylon membrane filter for ethanol analysis by HPLC.

Analytical methods

The structural carbohydrate (cellulose and hemicellulose) and lignin contents of untreated and pretreated corn stover were determined following NREL LAP (Sluiter et al., 2008) using two-step acid hydrolysis. Lignin is the sum of acid-soluble and acid-insoluble lignin. The acid insoluble lignin was measured by gravimetric analysis and the acid soluble lignin was measured by UV-Vis spectroscopy. Cellulose and hemicellulose were acid-hydrolyzed into monomeric sugars, which were measured by HPLC. The content of cellulose was calculated from glucose while hemicellulose was calculated from the sum of xylose, arabinose, galactose, and mannose, using an anhydro correction of 0.90 for C-6 sugars and 0.88 for C-5 sugars, respectively (Sluiter et al., 2008).

High Performance Liquid Chromatography (HPLC) (Agilent 1200 series, MN, USA) equipped with an online degasser, isocratic pump, autosampler, thermostated column compartment, and refractive index detector (RID) was used in this study. Biorad Aminex HPX-87P column was used for sugar analysis and the mobile phase was HPLC grade water eluting at 0.6 ml/min. The temperature of the column and RID was maintained at 80 ºC and 55 ºC, respectively. Phenomenex Rezex RFQ-Fast Fruit H+ column (Phenomenex Inc., CA) was used for the analysis of ethanol and sugar-degraded products (e.g. HMF, furfural). The mobile phase for this column was 5 mM H2SO4 at a flow rate of 0.6 ml/min. The temperature of the column and the RID was maintained at 55 ºC and 45 ºC, respectively. Guard columns (Micro-Guard Refill Cartridge, Biorad, CA, USA) were installed with the analytical columns.

Dry matter loss was calculated as the percentage of total solid loss during pretreatment. Lignin degradation, cellulose loss and hemicellulose loss were defined as the percentage of total lignin, total glucan and total hemicellulose reduced during pretreatment, respectively. Overall glucose and xylose yields were defined as the percentage of theoretical glucose and xylose yield of untreated corn stover, respectively. Overall ethanol yield was calculated as the percentage of theoretical ethanol yield on the basis of total cellulose in untreated corn stover.

Results and Conclusions

Alkaline Assisted Wet-Storage of Corn Stover

NaOH or fungal assisted concurrent treatment and wet storage of corn stover showed enhanced enzymatic digestibility and reduced loss of carbohydrates. At 50-g/kg DM NaOH loading, the glucose and xylose yields were 2.9 and 3.9 fold higher, respectively, than those of the control after 90 d of wet storage. The lignin and xylan degradation of corn stover was significantly influenced by NaOH loading and moisture content. The results are shown in Figures 1-3.

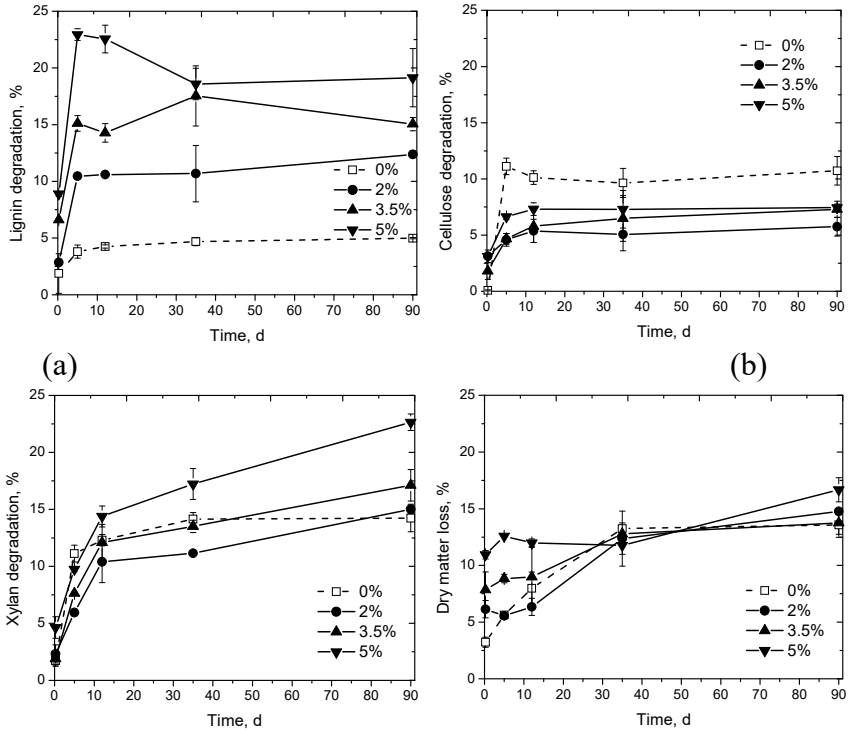

Figure 1 Effect of NaOH loading on structural degradation during wet storage of corn stover: **a)** lignin degradation, **b)** cellulose degradation, **c)** xylan degradation, and **d)** dry matter loss.

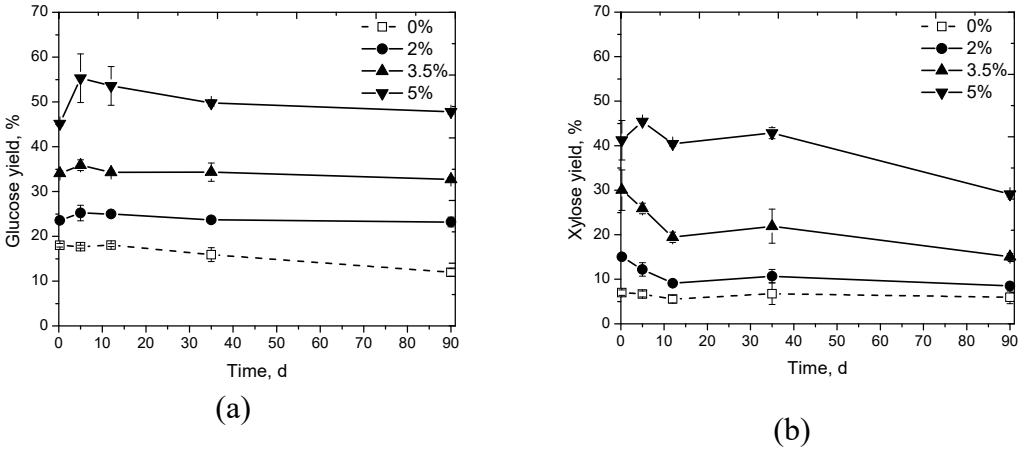

Figure 2 Effect of NaOH loading on sugar yield during wet storage of corn stover: **a)** glucose yield and **b)** xylose yield.

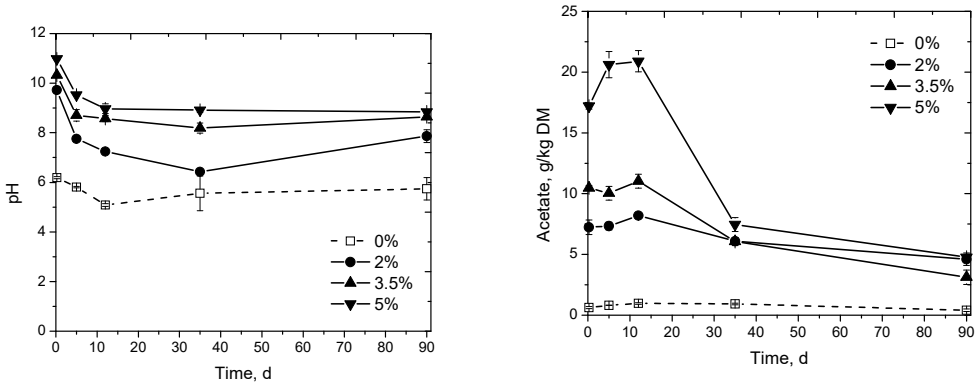

(a) (b)

Figure 3 Changes of **a)** pH, and **b)** acetate concentration during 90 d wet storage at different NaOH loadings.

Fungi- Assisted Wet-Storage of Corn Stover

C. subvermispora can effectively reduce recalcitrance of corn stover with high selectivity of lignin degradation and minimal cellulose loss. When 5 mm corn stover was pretreated at 28 °C with 75% moisture content, overall glucose yields of 57.67%, 62.21% and 66.61% were obtained with 18, 28-, and 35-d microbial pretreated corn stover, respectively. For the above condition, the highest overall ethanol yield of 57.80% was obtained with 35-d pretreated corn stover. Enzymatic hydrolysis yield was highly related to the lignin removal during microbial pretreatment. The results are shown in Figures 4-5.

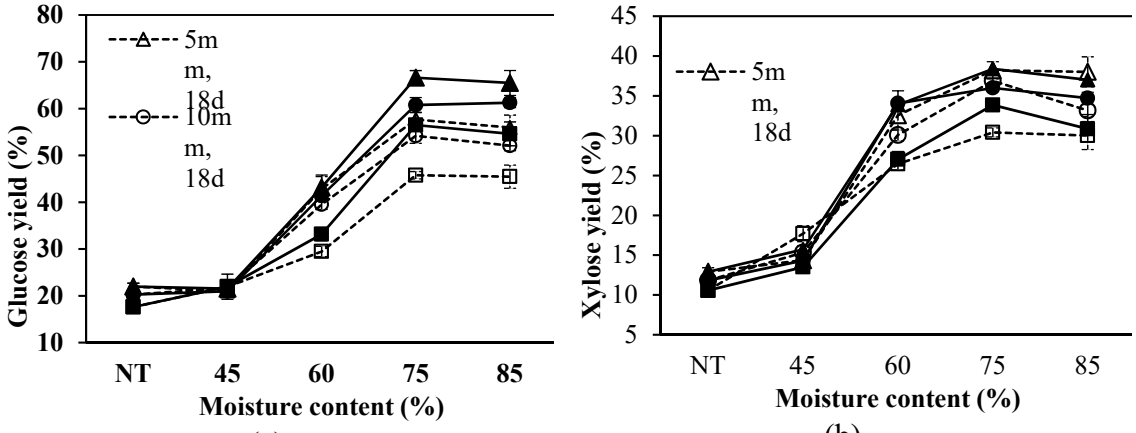

(a) (b)

Figure 4 Sugar yield of corn stover pretreated by *C. subvermispora* (pretreatment conditions: 28 °C): (a) Overall glucose yield and (b) Overall xylose yield.

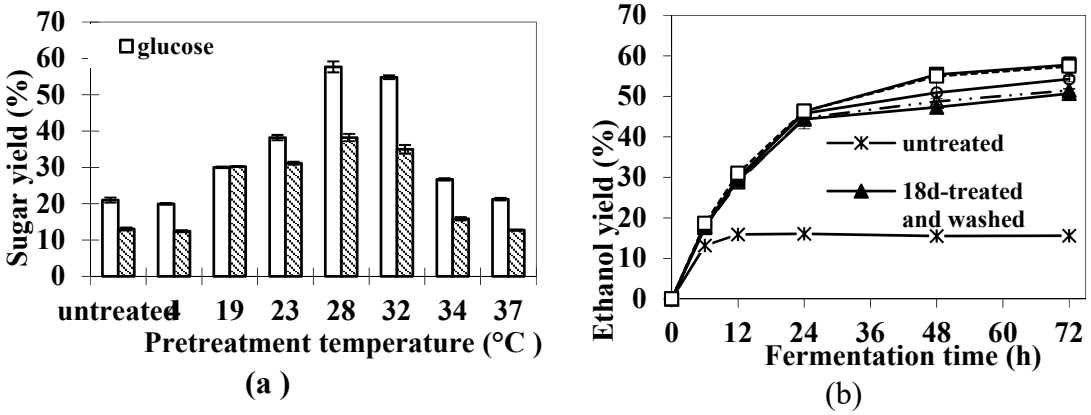

Figure 5. Sugar and ethanol yields of corn stover pretreated by *C. subvermispora* (a) effect of temperature on sugar yield glucose yield and (b) ethanol yields.

C. subvermispora selectively degraded lignin by as much as 39.2% while the cellulose loss was less than 5% during 42 d of cultivation. However, hemicellulose loss of up to 27.0% was concomitant with the lignin degradation. Ligninolytic enzymes – MnP and laccase were detected during degradation of corn stover by *C. subvermispora*. For major hydrolytic enzymes, xylanase was the only enzyme detected. The enzymatic hydrolysis yield of corn stover delignified by *C. subvermispora* was remarkably improved, reaching about 57-67% overall glucose yield after 18-42 d of pretreatment, while the glucose yield of the untreated was only 22%. A higher overall glucose yield of about 72% was obtained when the enzymatic hydrolysis of the 18 d-treated corn stover was supplemented with an accessory xylanase/cellulase enzyme complex. The results are shown in Figure 6.

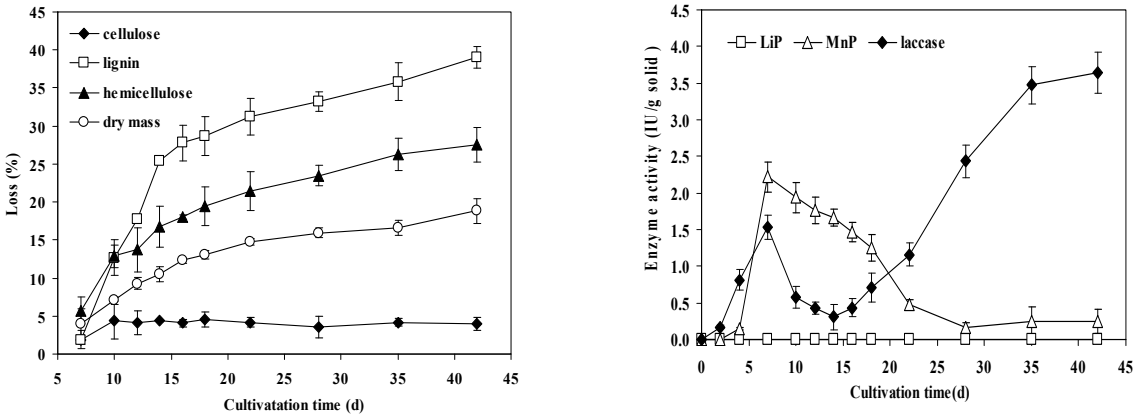

Figure 6. Dry mass loss and degradation of cell wall components (a) and ligninolytic enzymes production of corn stover during 42-d cultivation by *C. subvermispora*.

Corn stover fractions (leaves, cobs, and stalks) were studied for enzymatic digestibility after pretreatment with a white rot fungus, *C. subvermispora*. Among the three fractions, leaves had the least recalcitrance to fungal pretreatment and the lignin degradation reached 45% after 30 days of pretreatment. The lignin degradation of stalks and cobs were similar to each other but was lower than that of leaves. For all fractions, xylan and glucan degradation followed a similar

pattern as lignin degradation, with leaves having a higher percentage of degradation. Enzyme activity was higher in leaves than in cobs and stalks during fungal pretreatment, contributing to the higher degradation in leaves. However, the highest sugar yield was obtained with corn cobs.

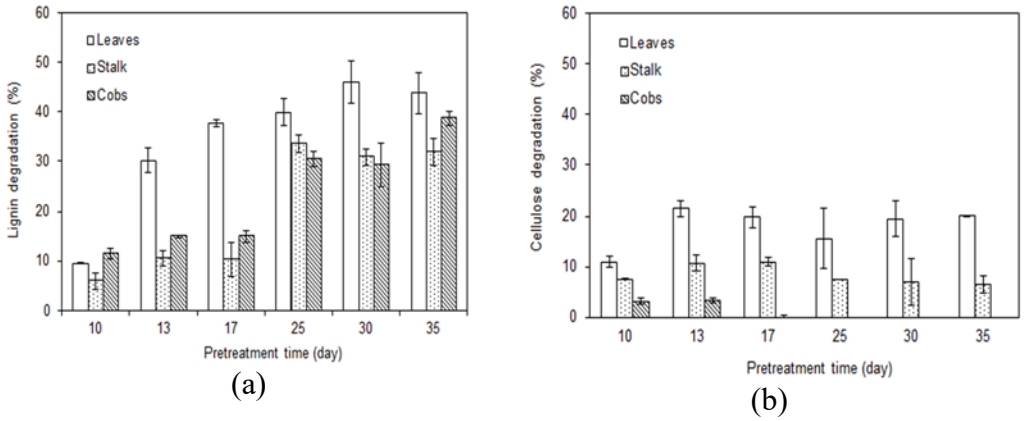

Figure 7. Degradation of fractions of corn stover by *C. subvermispora*: (a) lignin degradation, (b) cellulose degradation, and (c)xylan degradation.

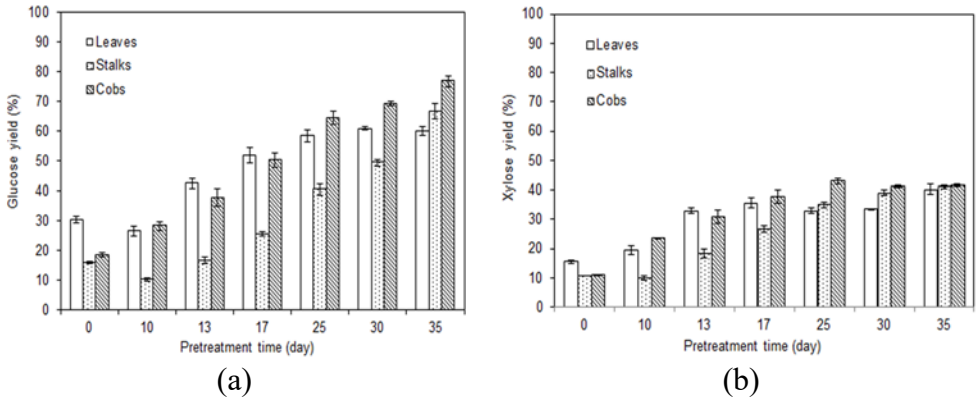

Figure 8. Sugar yields of fractions of corn stover pretreated by *C. subvermispora*: (a) glucose yield, and (b) xylose yield.

Homogenization

Short-term microbial pretreated corn stover was subjected to mechanical dispersion using a homogenizer. The glucose yield was improved by about 8-12% for 14-18 pretreated samples. The preliminary test showed that mechanical dispersion had a synergistic effect on microbial pretreatment. Therefore, a higher glucose yield could be obtained for short-term microbial pretreated materials when the mechanical dispersion was combined.

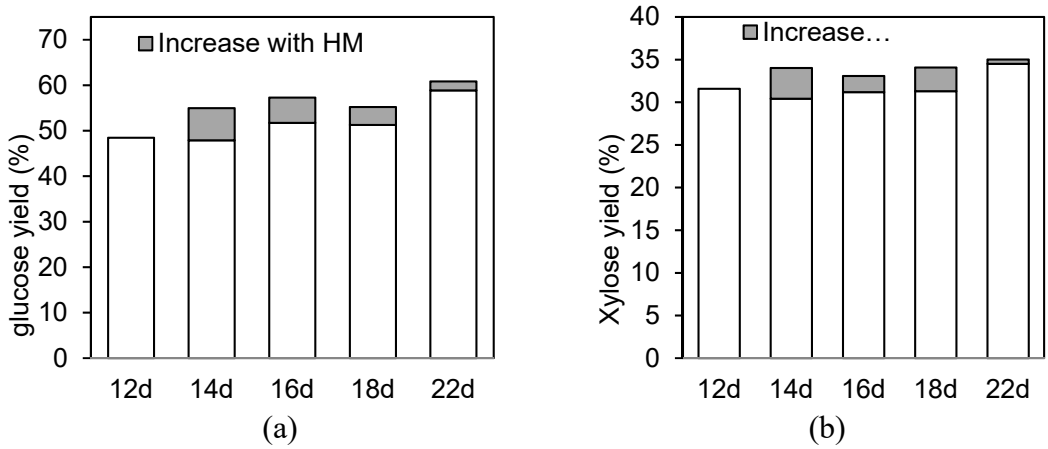

Figure 9. Effect of homogenization on glucose (a) and xylose (b) yields of fungal treated corn stover.

Economic Analysis

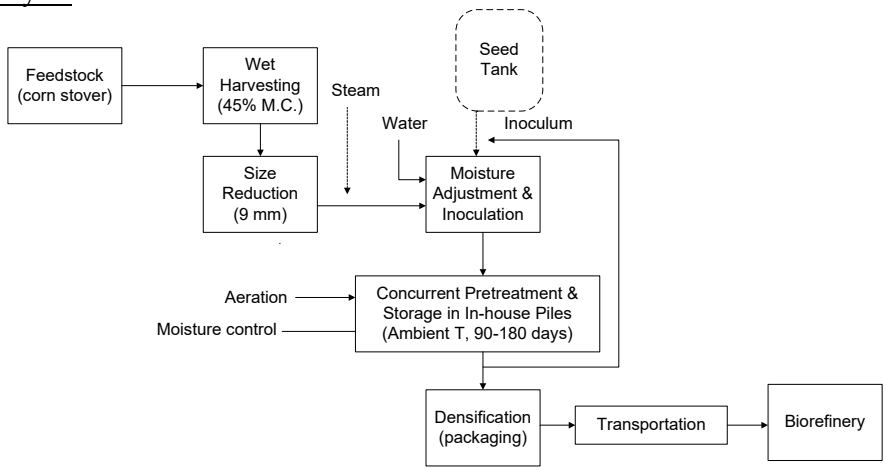

Figure 10 On farm Concurrent Pretreatment and Wet-Storage of Corn Stover

Stover is harvested wet (>45% moisture). In a typical harvesting scenario, the shredder typically follows right behind the combine harvester, shredding and windrowing in a single pass. A forage harvester with windrow pickup is used to house gather and size-reduce the stover prior to wet-storage. After size reduction, corn stover is belted to a concurrent pretreatment and wet-storage (CPWS) facility. Steam may be introduced to corn stover for disinfection purpose (10 seconds, 120 °C) prior to inoculation. Small portion of corn stover (10%) is recycled as inoculum. Inoculum can also be provided by an optional seed tank. Inoculation of white rot fungi is preferably carried out in-line, and applied as a liquid spray to the passing corn stover.

After inoculation, corn stover is piled in-house with temperature and humidity control. The temperature is controlled at 27-32°C and the humidity is controlled at 75-80%. A typical CPWS pile has dimensions about 10m high, 25m wide and any length. A 100 m long pile can accommodate a biorefinery utilizing about 200 tons of corn stover daily. CPWS typically lasts 90-180 days; however, 3-week period can give optimal performance. After CPWS, corn stover is densified by pelleting or other options and transport to a biorefinery.

Figure 11 gives two saccharification scenarios using different enzyme doses/cocktails. In scenario 1, glucose and xylose yield reach 66.3% and 57.8%, respectively, at a minimal enzyme use of 0.15g/g biomass. However, increasing enzyme dose to 0.19g/g biomass with supplementing xylanse (Scenario 2), glucose and xylose yield increase to 71.8% and 57.8%, respectively. Nevertheless, compared with the NREL biochemical conversion design (90% cellulose to glucose), sugar yield from CPWS corn stover is low.

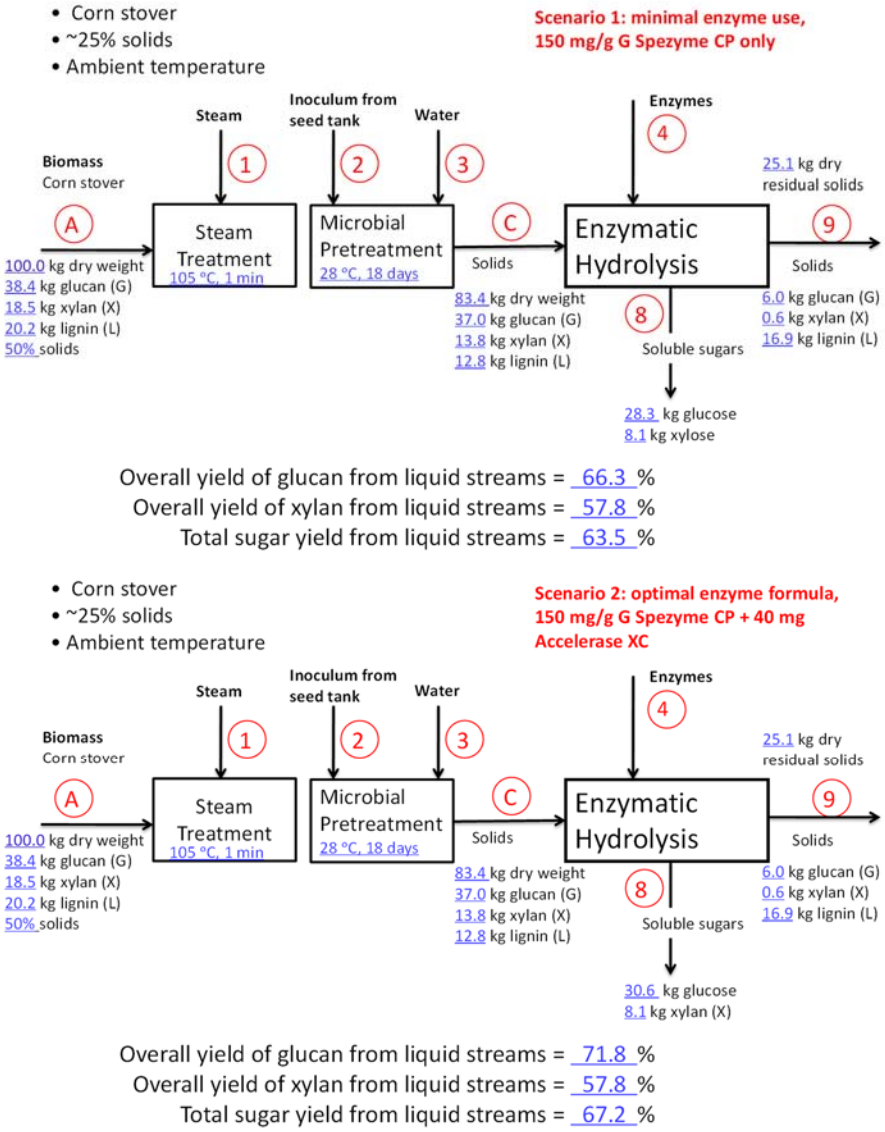

Figure 11 Material balance for microbial pretreatment: **a)** scenario 1: minimal enzyme use, 150 mg/g G Spezyme CP only; **b)** scenario 2: optimal enzyme formula, 150 mg/g G Spezyme CP + 40 mg Accelerase XC.

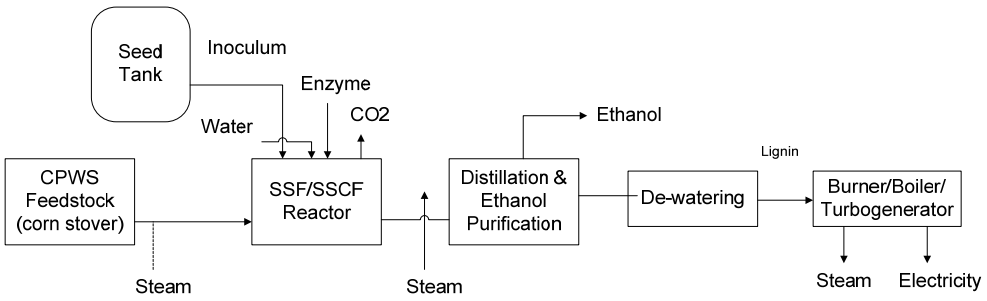

Figure 12. Simplified Biorefinery Process Design Utilizing CPWS Corn Stover.

Compared with NREL design (Aden 2002&2009), Biorefinery utilizing CPWS corn stover is simplified by eliminating pretreatment and subsequent neutralization/conditioning and S/L separation operations. Steam may be introduced to CPWS corn stover for disinfection.

We estimated that the add-on cost for inoculation, aeration and humidification off-set the reduced cost compared to the conventional three-pass large square baler, covered dry storage scenario. It is assumed that the proposed CPWS produced a feedstock cost at $110/Mg, equitable to the conventional three-pass LSB, covered dry storage scenario. Based on the most recent breakdown of minimum ethanol selling price (MSEP) (Table 1), pretreatment and conditioning (A200) constitute $0.29 (ca. 13.4%) of the total MSEP of $2.15/gal ethanol. Thus, by taking off pretreatment and conditioning (A200), a biorefinery process design utilizing CPWS corn stover could reduce the total MSEP to $1.86/gal ethanol assuming the same saccharification and fermentation efficiency achieved using CPWS corn stover. As the sugar yield of CPWS is lower than the thermochemical process, the MSEP of CPWS may be 5-13% lower than the thermochemical process. However, a comprehensive economic analysis needs to be conducted based on the pilot scale data.

Table 1. Breakdown of MESP for each cost in each area (Aden, 2009)

Area	Description	Area cost, %	Area cost, $	Modified Area cost, $
A700	Storage	1.07%	$0.02	$0.02
A900	Utilities	2.93%	$0.06	$0.06
A800	Boiler/Turbogenerator	2.00%	$0.04	$0.04
A600	Wastewater Treatment	15.56%	$0.34	$0.34
A500	Distillation and Solids Recovery	5.62%	$0.12	$0.12
A400	Cellulase	15.70%	$0.34	$0.34
A300	Saccharification and Fermentation	9.38%	$0.20	$0.20
A200	Pretreatment / Conditioning	13.38%	$0.29	**$0.00**
A100	Feedstock + Handling	34.37%	$0.74	$0.74
Total	MESP	100.00%	$2.15	$1.86

Outputs

Journal Publications

- Cui, Z. F., Wan, C. X., Sykes, R., Li, Y. B. 2012. Enzymatic digestibility of corn stover fractions in response to fungal pretreatment. *Industrial & Engineering Chemistry Research.* Under revision.
- Wan, C. X., Li, Y. B. 2011. Fungal pretreatment of lignocellulosic biomass. *Biotechnology Advances.* Accepted.
- Cui, Z.F, Shi, J., Wan, C. X., Li, Y. B. 2012. Comparison of alkaline- and fungi- assisted wet-Storage of corn Stover. *Bioresource Technology.* 109:98-104.
- Wan, C. X., Li, Y. B. 2011. Effect of hot water extraction and liquid hot water pretreatment on the fungal degradation of biomass feedstocks. *Bioresource Technology* 102: 9788-9793.
- Wan, C. X., Li, Y. B. 2011. Effectiveness of microbial pretreatment by *Ceriporiopsis subvermispora* on different biomass feedstocks. *Bioresource Technology. 102: 7507–7512*
- Wan, C. X., Zhou. Y. G. , Li, Y. B. 2011. Liquid hot water and alkaline pretreatment of soybean straw for improving cellulose digestibility. *Bioresource Technology 102:6254-6259.*
- Wan, C. X., Li, Y. B. 2010. Microbial pretreatment of corn stover with *Ceriporiopsis subvermispora* for enzymatic hydrolysis and ethanol production. *Bioresource Technology*. 101:6398-6403.
- Wan, C. X., Li, Y. B. 2010. Microbial delignification of corn stover by *Ceriporiopsis subvermispora* for improving cellulose digestibility. *Enzyme and Microbial Technology*. 47: 31–36.

Conference Presentations

- Cui, Z. F., Wan, C. X., Fu, G. M., **Li, Y. B**, 2011. Concurrent NaOH pretreatment and ensilage of corn stover. Presented at 2011 ASABE Annual International Meeting. Louisville, KY. (August 7 - 11)
- **Li, Y. B.**, Wan, C. X., Racharaks, S. 2010. The selection of microbial-pretreated lignocellulosic feedstocks for ethanol production. 2010 Annual ASABE Meeting, Pittsburgh, PA, June 21-23, 2010. ASABE Paper No. 1009438.
- Wan, C. X., **Li, Y. B.** 2010. In-storage Microbial Pretreatment of Corn Stover for Improving Sugar Yields. 2010 Annual ASABE Meeting, Pittsburgh, PA, June 21-23, 2010. ASABE Paper No. 1009435.
- Wan, C. X., **Li, Y. B.** 2009. Microbial pretreatment of corn stover for improved enzymatic saccharification and ethanol production. 31th Symposium of Biotechnology for Fuels and Chemicals, San Francisco, CS, May 3-6, 2009.
- Zhou, Y. G., **Li, Y. B.**, Wan, C. X., Li, D., Mao, Z. H. 2009. Application of hot water and homogenization treatment for ethanol production from corn stover. 2009 Annual ASABE Meeting, Reno, NV. June 21-23, 2009.
- Wan, C. X., **Li, Y. B.** 2009. Microbial Pretreatment of Corn Stover by Solid State Fermentation for Bioethanol Production. 2009 Annual ASABE Meeting, Reno, NV. June 21-23, 2009

Please complete the following table to reflect your project at completion or time of report submission:

ITEM	NUMBER
Abstracts	
Peer Reviewed Publications	**9**
Outreach Publications/Web Pages	**1**
Professional Presentations	**6**
MS Degrees Conferred	
Ph.D. Degrees Conferred	**1**
MS Students Supported	
Ph.D. Students Supported	**1**
Post-Docs Supported	**2**
Undergraduate Students Supported	**1**
Investigators Supported	**1**
Start-Up Jobs Created	
Disclosures	**1**
Patents Filed	
Provisional Patents	
Patents Issued	
License Agreements	
Plant Variety Protection	

Sun Grant Initiative

DOE Final Progress Report

Project Title: Improving Handling Characteristics of Herbaceous Biomass

Project Director/Principal Investigator:
R. Vance Morey, Professor, Department of Bioproducts and Biosystems Engineering, University of Minnesota, St. Paul, MN

All Co-Principal/Other Investigators:
Lowell Rasmussen, Vice Chancellor for Finance and Facilities, University of Minnesota – Morris, Morris, MN

Mike Reese, Renewable Energy Director, University of Minnesota West Central Research and Outreach Center, Morris, MN

Collaborators:
Douglas G. Tiffany, Assistant Extension Professor, Department of Applied Economics, University of Minnesota, St. Paul, MN
Nalladurai Kaliyan, Research Associate, Department of Bioproducts and Biosystems Engineering, University of Minnesota, St. Paul, MN
Jim Barbour, Emissions Specialist, Biomass Gasification Project, University of Minnesota – Morris, Morris, MN
Mike White, Director of Marketing, Bepex International, LLC, Minneapolis, MN

Period of Performance: 1 July 2009 – 31 December 2012

Funding Awarded: $154,242

Cost Share Amount: $51,413

Cost Share Sources: Time and effort from PIs and CoPIs; Indirect on time and effort; University of Minnesota – Morris, Morris, Minnesota; West Central Research and Outreach Center, University of Minnesota, Morris, Minnesota Initiative for Renewable Energy and the Environment, University of Minnesota

Executive Summary

Corn stover and perennial grasses are potential biomass feedstocks that could be used for producing fuel ethanol and combined heat and power (CHP) to replace fossil fuels in order to curb the greenhouse gas (GHG) emissions. Industrial users of biomass need a consistent supply throughout the year. Collection/harvesting occurs on an agricultural cycle (late summer or fall time frame), whereas the user operates on an industrial cycle (year around time frame). Thus, a system is needed to collect, store, accumulate, process, densify, and deliver consistent, dense, free-flowing material to the users throughout the year. A key component requiring new approaches is the step involving accumulation of biomass stored at numerous field or farm sites and delivery to a processing facility or end user throughout the year in a form that is easy to handle and efficient to transport. Thus, the overall goal of this project was to evaluate the concept of a portable system that would take bales stored at individual farm sites, coarsely grind the biomass, then compact it to a bulk density of at least 240 kg/m^3 (15 lb/ft^3), and load it on trucks for delivery as a bulk product. The project activities include coarse-grinding, pilot-scale roll press compaction, demonstration-scale roll press compaction, lab-scale compaction, validation of roll press compactor design equations, and evaluation of a biomass supply logistics system including coarse-grinding/roll-press compaction in terms of cost, life-cycle fossil energy consumption, and life-cycle GHG emissions. Key project results and conclusions are given below.

We studied coarse-grinding of round bales [1.8 m (6 ft) diameter × 1.5 m (5 ft) width] of corn stover and native perennial grasses using a Mighty Giant tub-grinder powered by a diesel engine of 463 kW (630 HP). A typical perennial grass bale contained about 60% (by mass) of brome grass and the remaining was native prairie mix including fescue, foxtail, and weeds. Three round-hole screens with opening sizes of 25.4 mm (1.0 in.), 76.2 mm (3.0 in.), and 127.0 mm (5.0 in.) were tested in the tub-grinder. The bulk density of ground biomass ranged from 69 to 207 kg/m^3 (4.3 to 12.9 lb/ft^3) with the moisture content of particles ranging from 14% to 39% (w.b.). Mighty Giant tub-grinder achieved the highest throughput of 24 t/h (26.5 ton/h). The specific energy consumption for the Mighty Giant tub-grinder with screen opening sizes of 76.2 to 127.0 mm (3.0 to 5.0 in.) was 212 to 347 MJ/t for grinding corn stover bales, and was 93 to 123 MJ/t for grinding native perennial grass bales. High moisture bales (≥ 25% w.b.) decreased the performance of the grinder.

Pilot-scale roll press compaction experiments were conducted for coarsely ground corn stover and perennial grasses. The goal of the roll press compaction study was to increase the bulk density of the coarsely ground biomass materials to a target bulk density of at least 240 kg/m^3 (15 lb/ft^3). A 44.8 kW (60 HP) roll press compaction machine was used for the study. The diameter and width of the rolls were 0.52 m (20.5 in.), and 0.13 m (5.0 in.), respectively. Bulk density of compacted materials ranged from 265 to 365 kg/m^3 (16 to 23 lb/ft^3). The roll press throughput ranged from 0.13 to 0.62 t/h (0.15 to 0.68 ton/h). Roll forces of 356 and 534 kN (40 and 60 ton) or the three particle sizes obtained from the tub-grinder screen opening sizes of 25.4, 76.2, and 127.0 mm (1.0, 3.0, and 5.0 in.) resulted in similar bulk density and durability of compacted materials. Durability (ASABE tumbling can test) and angle of repose of roll press compacted products were 61% to 92%, and 21° to 27°, respectively. Based on our experience, roll press compacted biomass products can be handled with belt conveyors.

A 44.8 kW (60 HP) roll press compaction machine was used to demonstrate the concept of coarse-grinding followed by roll-press compaction of biomass feedstock to produce a bulk compacted product with a bulk density of at least 240 kg/m^3 (15 lb/ft^3) for efficient truck transport . The diameter and width of the rolls were 0.52 m (20.5 inch), and 0.33 m (13.0 inch), respectively. For both corn stover and corn cobs, the bulk density of compacted materials was near 240 kg/m^3 (15 lb/ft^3) or higher. The maximum throughput of the roll press was 2.6 t/h (2.9 ton/h) for corn cobs. The measured energy consumption for the roll press compaction was 168 MJ/t for corn stover and 33 MJ/t for corn cobs.

The roll press design equations given by Johanson (1965) and Blake et al. (1963) were validated using the data collected from roll press compaction studies, and the data collected from a laboratory compaction study. The validated roll press design equations will be used for deriving design specifications for a production scale roll press compactor. From the tub-grinding experimental results, specific energy consumption for a production scale tub-grinder with a capacity of 25 ton/h was estimated at 227 MJ/t (1.509 gal diesel/ton). From the pilot-scale and demonstration-scale roll-press compaction experiments, specific energy consumption for a production scale roll press compactor with a capacity of 25 ton/h was estimated at 227 MJ/t (1.509 gal diesel/ton).

We modeled a 25 ton/h production scale system for the coarse-grinding and roll-press compaction of corn stover (15% wet basis moisture content), and its overall impact on the total cost, life-cycle energy consumption, and life-cycle GHG emissions for a proposed “field to facility” corn stover logistics system. The logistics system included collection and transport by round bales to local storages within 3.2 km (2 mile) of the field during the fall harvest period followed by processing at the local storage sites throughout the year using mobile units which converted the bales to bulk material by tub-grinding and roll-press compacting (i.e., bale to bulk processing) to 240 kg/m^3 (15 lb/ft^3) to achieve 22.7 t (25 ton) loads for truck delivery to an end user within a 48 km (30 mile) radius.

The cost (i.e., fixed cost + operating cost) of tub-grinding of corn stover was $9.33/t ($8.46/ton). The fixed cost of the tub-grinder was $2.14/t ($1.95/ton). The cost (i.e., fixed cost + operating cost) of roll-press compaction of corn stover was $10.90/t ($9.88/ton). The fixed cost of the roll-press compactor was $3.29/t ($2.99/ton). The cost, life-cycle fossil energy consumption, and life-cycle GHG emissions for tub-grinding followed by roll-press compaction (i.e., bale to bulk processing) of corn stover at a local storage were $26.79 ($24.30), 562 MJ/t, and 43 g CO_2e/t, respectively. The total logistics cost, life-cycle fossil energy consumption, and life-cycle GHG emissions for delivering the bulk corn stover to end users were $99.49/t ($90.26/ton), 1264 MJ/t, and 139 kg CO_2e/t at 15% moisture or 10 g CO_2e/MJ of dry matter including emissions for logistics and combustion, but excluding those associated with soil organic carbon (SOC) loss, respectively. Thus, the percentage contribution of the bale to bulk processing on the total logistics cost, life-cycle fossil energy consumption, and life-cycle GHG emissions is 26.9%, 44.4%, and 31.0%, respectively. The total fossil energy consumption for the corn stover logistics was equivalent to approximately 8.9% of the energy content of corn stover. Our estimates show that as a fuel for heat and power applications, corn stover reduced life-cycle GHG emissions by factors of approximately 7 and 11 compared to natural gas and coal, respectively.

Project Objectives

Users of biomass need a consistent supply throughout the year. However, collection/harvesting of herbaceous biomass is limited to certain times of the year, usually late summer or fall. A system is needed to collect, store, accumulate, process, densify, and deliver consistent, dense, free-flowing material to the users throughout the year. Collection/harvesting occurs on an agricultural cycle (late summer or fall time frame). The user operates on an industrial cycle (year around time frame). A key component requiring new approaches is the step involving accumulation of biomass stored at numerous field or farm sites and delivery to a processing facility or end user throughout the year in a form that is easy to handle and efficient to transport.

The overall goal of this project was to evaluate the concept of a portable system that would take bales stored at individual farm sites, coarsely grind the biomass, then compact it to a bulk density of at least 240 kg/m^3 (15 lb/ft^3), and load it on trucks for delivery as a bulk product.

The outcomes and impacts including comparing actual versus expected accomplishments for each project objectives are discussed below.

Objective 1: Determine optimum conditions for coarse grinding of biomass followed by roll compaction to produce a compacted product with bulk density of at least 240 kg/m^3 (15 lb/ft^3).

Outcome: A Mighty Giant tub-grinder powered by a diesel engine of 463 kW (630 HP) was used to study the effect of tub-grinder screen opening size on the particle size, bulk density, throughput, and specific energy consumption. Three round-hole screens with opening sizes of 25.4 mm (1.0 in.), 76.2 mm (3.0 in.), and 127.0 mm (5.0 in.) were tested. Two biomass feedstocks (corn stover and native perennial grasses) were studied. A typical perennial grass bale contained about 60% (by mass) of brome grass and the remaining was native prairie mix including fescue, foxtail, and weeds. The bulk density of ground biomass ranged from 69 to 207 kg/m^3 (4.3 to 12.9 lb/ft^3) with the moisture content of particles ranging from 14% to 39% (w.b.). Mighty Giant grinder achieved the highest throughput of 24 t/h (26.5 ton/h). The specific energy consumption for the Mighty Giant with screen opening sizes of 76.2 to 127.0 mm (3.0 to 5.0 in.) was 212 to 347 MJ/t for grinding corn stover bales, and was 93 to 123 MJ/t for grinding native perennial grass bales. Increasing the grinder screen opening size increased the ground particle size and throughput, but decreased the bulk density of ground biomass, specific energy consumption, and cost of grinding. High moisture bales (≥ 25% w.b.) decreased the performance of the grinder.

Pilot-scale roll press compaction experiments were conducted for coarsely ground corn stover and native grasses. The goal of the roll press compaction study was to increase the bulk density of the coarsely ground biomass materials to a target bulk density of at least 240 kg/m^3 (15 lb/ft^3). A 44.8 kW (60 HP) roll press compaction machine was used for the study. The diameter and width of the rolls were 0.52 m (20.5 in.), and 0.13 m (5.0 in.), respectively. Effects of biomass feedstock (corn stover and perennial grasses), particle size [obtained from Mighty Giant tub-grinder with three screen opening sizes of 25.4, 76.2, and 127.0 mm (1.0, 3.0, and 5.0 in.)], and roll force [214, 356, and 534 kN (24, 40, and 60 ton)] on the bulk density and durability of roll

press compacted products and on the throughput and specific energy consumption of the roll press compactor were investigated. Bulk density of compacted materials ranged from 265 to 365 kg/m^3 (16 to 23 lb/ft^3). The roll press throughput ranged from 0.13 to 0.62 t/h (0.15 to 0.68 ton/h). The specific energy consumption (excluding no-load machine operation energy) for the rolls ranged from 16 to 304 MJ/t, and for the screw feeder ranged from 3 to 37 MJ/t. Roll forces of 356 and 534 kN (40 and 60 ton) or the three particle sizes obtained from the tub-grinder screen opening sizes of 25.4, 76.2, and 127.0 mm (1.0, 3.0, and 5.0 in.) resulted in similar bulk density and durability of compacts (i.e., compacted biomass products).

Impact: Optimum tub-grinding and roll press compaction variables were obtained to produce compacted biomass materials with a bulk density of at least 240 kg/m^3 (15 lb/ft^3). Specific energy consumption for tub-grinding and roll press compaction of corn stover and perennial grasses were measured. Our research team collaborated with Kolbeck, Inc., Le Mars, Iowa to conduct tub-grinding experiments, and with Bepex International LLC, Minneapolis, MN to conduct roll press compaction experiments.

Objective 2: Evaluate handling properties of the compacted biomass products (durability and angle of repose).

Outcome: Durability (ASABE tumbling can test) and angle of repose of roll press compacted biomass products were 61% to 92%, and 21° to 27°, respectively. For the roll forces of 356 and 534 kN (40 and 60 ton), the three particle sizes obtained from the tub-grinder screen opening sizes of 25.4, 76.2, and 127.0 mm (1.0, 3.0, and 5.0 in.) resulted in durability of 87% to 92% for corn stover compacts, and 79% to 91% for perennial grass compacts. Durability is a measure of dusting potential of compacts during handling. For designing handling and storage systems, data on angle of repose of compacts would be required. Also, the angle of repose is a measure of flowability of compacts. The angle of repose values of roll press compacts were in the range of angle of repose values reported in the literature for feed pellets.

Impact: The durability and angle of repose values of roll press compacted materials indicate that roll press compacts may be handled in belt conveyors without much dust formation during operation.

Objective 3: Evaluate the concept of coarse grinding and roll compaction on a demonstration scale at the University of Minnesota – Morris Campus and West Central Research and Outreach Center.

Outcome: A 44.8 kW (60 HP) demonstration-scale roll press compaction machine was used to compress corn stover and corn cobs. The maximum throughput of the roll press was 2.6 t/h (2.9 ton/h) for corn cobs. For both corn stover and corn cobs, the bulk density of compacted materials was near 240 kg/m^3 (15 lb/ft^3) or higher. The measured energy consumption for the roll press compaction was 168 MJ/t for corn stover and 33 MJ/t for corn cobs.

Impact: The concept of coarse-grinding followed by roll-press compaction of biomass feedstock to produce a bulk compacted product with a bulk density of at least 240 kg/m^3 (15 lb/ft^3) for efficient truck transport was demonstrated. Using belt conveyors, ground materials were fed to

the screw feeder, and compacted materials exiting the roll press were conveyed to a weighing truck-trailer. Thus, based on our experience, roll press compacted biomass products can be handled with belt conveyors.

Objective 4: Specify design conditions for a production scale (20 to 40 tons/hour) coarse grinding and roll compaction system.

Outcome: The roll press design equations given by Johanson (1965) and Blake et al. (1963) were validated using the data collected from the pilot-scale roll press compaction study (Objective 1), and the data collected from laboratory compaction study. The validated roll press design equations will be used for deriving design specifications for a production scale roll press compactor.

Lab scale compaction tests were conducted to derive a relationship between compaction pressure and density of the compacted biomass. The variables studied were three compaction pressures of about 15, 30, and 60 MPa, and three particle sizes of corn stover and perennial grasses (initial moisture contents were < 20% w.b.) obtained from Mighty Giant tub-grinder with three different round-hole screen opening sizes [25.4 mm (1.0 in.), 76.2 mm (3.0 in.), and 127.0 mm (5.0 in.)]. The unit density of lab compacts (measured immediately after making) ranged from 421 to 773 kg/m^3 (26 to 48 lb/ft^3). The unit densities of compacts made in the lab compaction experiments and pilot-scale roll-press compaction experiments (Objective 1) were similar. This may be due to the use of similar biomass feedstocks and similar compression pressures for both the lab and roll press experiments. The average compressibility factors for corn stover and native perennial grasses are 3.87 and 4.88, respectively. The compressibility factors were used for the validation of roll press design equations. The compressibility factors show that corn stover is easier to compress than perennial grasses.

Johanson (1965) model predicts the roll force with a mean relative percent error of 47% to 61%. Blake et al. (1963) model calculates the unit density of compacts (measured after curing) with a mean relative percent error of 18% to 30%. The mean relative percent error for the prediction of specific energy consumption for rolls is 48% to 83% for Johanson (1965) model, and 37% to 71% for Blake et al. (1963) model. Including a motor efficiency, the roll press design models may result in reasonable estimates for roll motor power requirement and specific energy consumption for rolls.

Impact: From the tub-grinding experimental results (Objective 1), specific energy consumption for a production scale tub-grinder with a capacity of 25 ton/h was estimated at 227 MJ/t (1.509 gal diesel/ton). From the pilot-scale and demonstration-scale roll-press compaction experiments (Objectives 1 and 3), specific energy consumption for a production scale roll press compactor with a capacity of 25 ton/h was estimated at 227 MJ/t (1.509 gal diesel/ton). The validated roll press design equations given by Johanson (1965) and Blake et al. (1963) can be used for obtaining roll press design specifications. The results are scalable to other system capacities such as 20 ton/h or 40 ton/h.

Objective 5: Estimate the cost of a coarse grinding/roll compaction system and its overall economic impact on the biomass logistics system described above.

Outcome: For this objective, corn stover (15% wet basis moisture content) was chosen as the model biomass feedstock to be analyzed for the biomass supply logistics system. The cost (i.e., fixed cost + operating cost) of tub-grinding [76.2 mm (3.0 in.) screen size] was $9.33/t ($8.46/ton). The fixed cost of tub-grinder was $2.14/t ($1.95/ton). The cost (i.e., fixed cost + operating cost) of roll-press compaction was $10.90/t ($9.88/ton). The fixed cost of roll-press compactor was $3.29/t ($2.99/ton). For the tub-grinding energy of 226 MJ/t (1.509 gal diesel/ton) and roll-press compaction energy of 226 MJ/t (1.509 gal diesel/ton), life-cycle GHG emissions for coarse-grinding and roll-press compaction are 20.69 and 20.69 kg CO_2e/t, respectively.

We evaluated the economics, energy inputs, and greenhouse gas (GHG) emissions for a proposed "field to facility" corn stover logistics system. The system included collection and transport by round bales to local storages within 3.2 km (2 mile) of the field during the fall harvest period followed by processing at the local storage sites throughout the year using mobile units which converted the bales to bulk material by tub-grinding and roll-press compacting to 240 kg/m^3 (15 lb/ft^3) to achieve 22.7 t (25 ton) loads for truck delivery to an end user within a 48 km (30 mile) radius. The total cost and fossil energy consumption for delivering the bulk corn stover (15% moisture) to end users were $99.49/t ($90.26/ton) and 1264 MJ/t, respectively. The total fossil energy consumption was equivalent to approximately 8.9% of the energy content of corn stover. The life-cycle GHG emission for heat and power applications was approximately 139 kg CO_2e/t at 15% moisture or 10 g CO_2e/MJ of dry matter including emissions for logistics and combustion, but excluding those associated with soil organic carbon (SOC) loss. Our estimates show that as a fuel for heat and power applications, corn stover reduced life-cycle GHG emissions by factors of approximately 7 and 11 compared to natural gas and coal, respectively.

Impact: We modeled a 25 ton/h production scale system for the coarse-grinding and roll-press compaction (i.e., bale to bulk processing), and its overall impact on the total cost, life-cycle energy consumption, and life-cycle GHG emissions for corn stover supply logistics system. The percentage contribution of the bale to bulk processing on the total logistics cost, life-cycle energy consumption, and life-cycle GHG emissions is 26.9%, 44.4%, and 31.0%, respectively. The results are scalable to other system capacities such as 20 ton/h or 40 ton/h.

Project Activities

Project activities for each objective of this project are discussed in separate chapters as indicated below.

Objective 1: Determine optimum conditions for coarse grinding of biomass followed by roll compaction to produce a compacted product with bulk density of at least 240 kg/m^3 (15 lb/ft^3).

Chapter 1 - Commercial Scale Tub Grinding of Corn Stover and Perennial Grasses

Chapter 2 - Roll Press Compaction of Corn Stover and Perennial Grasses

Objective 2: Evaluate handling properties of the compacted biomass products (durability and angle of repose).

Chapter 2 - Roll Press Compaction of Corn Stover and Perennial Grasses

Objective 3: Evaluate the concept of coarse grinding and roll compaction on a demonstration scale at the University of Minnesota – Morris Campus and West Central Research and Outreach Center.

Chapter 3 - Demonstration Scale Roll Press Compaction of Corn Stover and Corn Cobs

Objective 4: Specify design conditions for a production scale (20 to 40 tons/hour) coarse grinding and roll compaction system.

Chapter 4 - Compaction Characteristics of Coarsely Ground Corn Stover and Perennial Grasses

Chapter 5 - Validation of Roll Press Design Equations for Compaction of Corn Stover and Perennial Grasses

Objective 5: Estimate the cost of a coarse grinding/roll compaction system and its overall economic impact on the biomass logistics system described above.

Chapter 6 - A Biomass Supply Logistics System Involving Coarse Grinding/Roll Press Compaction

Back to Table of Contents

Chapter 1

Commercial Scale Tub Grinding of Corn Stover and Perennial Grasses

Abstract

Performance of a commercial mobile tub-grinder [463 kW (630 HP)] was studied to produce coarsely ground particles from round-baled, plastic net-wrapped corn stover and native perennial grasses. The effects of grinder screen opening size [25.4 to 127.0 mm (1.0 to 5.0 in.)] and feedstock type on ground particle size, bulk density of ground biomass, throughput, specific energy consumption, and cost of grinding were studied. The bulk density of ground biomass ranged from 69 to 207 kg/m^3 with the moisture content of particles ranging from 14% to 39% (w.b.). The throughput of the grinder ranged from 6 to 45 t/h. The specific energy consumption ranged from 93 to 661 MJ/t. The estimated cost of grinding ranged from $4.39/t to $31.23/t. Increasing the grinder screen opening size increased the ground particle size and throughput, but decreased the bulk density of ground biomass, specific energy consumption, and cost of grinding. High moisture bales (≥ 25% w.b.) decreased the performance of the grinder. The results from this study would be useful for developing a biomass supply logistics system involving mobile grinding.

1. Objectives

The objective of this study is to evaluate the effects of grinder screen opening size and feedstock type on ground particle size, bulk density of ground biomass, throughput, specific energy consumption, and cost for coarse-grinding of round-baled, plastic net-wrapped corn stover and native perennial grasses using a commercial scale grinder.

2. Materials and Methods

2.1 Tub Grinder

All coarse grinding experiments were conducted at Kolbeck, Inc., Le Mars, Iowa. The grinding tests were conducted using a commercial mobile grinder, Mighty Giant (Model 5000 Hydrafork; Jones Mfg., Beemer, Iowa; www.mightygiant.com), owned by Kolbeck, Inc., Le Mars, Iowa (fig. 1). The Mighty Giant is a tub-grinder with swinging hammers on the grinding rotor and is similar to a conventional hammer mill. It was powered by a 463 kW (630 HP) diesel engine. Round-hole screens were used in the grinder to separate ground particles. Biomass bales, with plastic net-wrap, were fed vertically downward into the grinder-tub. The tub speed was automatically controlled by a hydraulic governor to assist feeding of biomass over the hammer mill, which is located directly below an opening in the bottom of the tub. The grinder discharged the ground material on the ground through an auger (0.4 m diameter) situated below the hammer mill and then a belt conveyor (8.2 m length × 0.5 m width). The belt conveyor can be adjusted for any angle of elevation and is used for loading the ground biomass on to a truck. It was observed that dust (i.e., fines) was released to the environment from the ground material exiting the grinder, but the dust can probably be controlled by covering the conveyor and transfer points.

2.2 Grinding Experiments

2.2.1 November 2009 Tests

Testing in November 2009 was conducted for two round-hole screens with opening sizes of 25.4 mm (1.0 in.) and 76.2 mm (3.0 in.) in the Mighty Giant. These grinder screen opening sizes were selected based on a preliminary study on coarse-grinding followed by roll press compaction of corn stover and perennial grasses (Kaliyan et al., 2009). Tests were conducted on round bales [1.8 m (6 ft) diameter × 1.5 m (5 ft) width] of corn stover from fall 2008 and fall 2009 harvests, and native perennial grasses from fall 2009 harvest. All biomass feedstocks used in this study were grown in Northwest Iowa. According to the grinder operator (Kolbeck, Inc.), a typical perennial grass bale contained about 60% (by mass) of brome grass and the remaining was native prairie mix including fescue, foxtail, and weeds. All bales had 2.5 wraps of plastic net-wrap and were stored outdoors. The net-wrap was ground along with the biomass. A total of six grinding tests were conducted for different combinations of grinder screen opening size (2) and biomass feedstock type [i.e., corn stover (2) and native perennial grasses (1)]. It is noted that corn stover bales from fall 2008 and fall 2009 were tested to understand the effect of outdoor storage on the grinding performance.

2.2.2 March 2010 Tests

Additional coarse grinding studies were conducted in March 2010. Three round-hole screens with opening sizes of 25.4 mm (1.0 in.), 76.2 mm (3.0 in.), and 127.0 mm (5.0 in.) were tested in the Mighty Giant. Tests were conducted using round bales of corn stover and native perennial grasses collected from the fall 2009 harvest. All bales had 2.5 wraps of plastic net-wrap and were stored outdoors until used for the grinding study in March 2010. The net-wrap was ground along with the biomass. Six grinding tests were conducted for different combinations of grinder screen opening size (3) and biomass feedstock type [i.e., corn stover (1) and native perennial grasses (1)].

2.3 Procedures

Each grinding test was performed for 10 to 15 minutes, processing 3 to 12 bales (about 454 kg/bale) per test. The number of bales ground during the test period was a function of the throughput of the grinder. The grinder was fed continuously to operate at the maximum capacity. Each test was concluded with the complete grinding of the last bale fed. The mass of each bale was weighed using the electronic scale attached to the boom-grapple loader of the Mighty Giant. Throughput (t/h) of the grinder was calculated based on the total weight of bales ground and the grinding time.

Prior to each test, the diesel fuel tank was filled to the top of the neck of the fuel tank. After the test, the fuel tank was refilled and the mass of the fuel added was recorded. Specific energy (MJ/t) for grinding was calculated from the diesel fuel consumption and the mass of material ground.

Immediately after grinding, bulk density of the ground materials was measured according to ASTM (2009). A cubical box of 305 × 305 × 305 mm was filled by pouring the ground biomass materials from a height of 610 mm above the top edge of the box. The box was dropped five times from a height of 150 mm on to the ground to allow settling. Additional materials were added and the excess was struck off level with a top edge. The mass of the sample along with the box was measured using a Taylor 7344 lithium electronic scale with an accuracy of 45 g (Taylor Precision Products, Las Cruces, New Mexico). The bulk density of the sample was calculated by dividing the mass of sample in the box by the volume of the box.

Ground samples (about 10 kg/test) were randomly collected from different locations in the pile of ground biomass to gather representative samples, packed in large sealed (neck-tied) plastic bags, and transported to the lab to measure particle size and moisture content. Moisture content of the ground materials was measured within 12 h of grinding based on ASABE Standards (2009a). Bagged samples were stored in a walk-in freezer at -10°C. Particle size analysis was performed on the stored samples within one week of grinding following procedures developed for forage materials by Heinrichs and Kononoff (2010). This procedure uses a stack of sieves [three round-hole sieves with hole-diameters of 38.1, 19.1, and 7.9 mm, a square-hole sieve with hole-diagonal length of 1.8 mm, and a pan]. The top sieve was filled with approximately 200 g of ground corn stover or 100 g of ground native perennial grasses, and the stack was shaken manually for 40 times (i.e., 40 shakes) on a flat bench using a horizontal shaking pattern that involves rotating the stack 90 degrees after each 5 shakes. The geometric mean length (GML) and standard deviation of the ground particles were estimated by following the calculation procedure given in ASABE Standards (2009b). Although this study follows the particle size analysis procedure from Heinrichs and Kononoff (2010), it is suggested that the future researches may follow the ASABE Standards (2009b). Three replicates were made for measuring bulk density, moisture content, and particle size.

During the March 2010 tests, the temperatures of ambient air and ground biomass piles were measured using a handheld thermocouple temperature recorder (Digi-Sense, Model 91100-40, Cole-Parmer Instruments Co., Vernon Hills, Ill.).

2.4 Cost of Grinding

Cost of grinding was estimated by summing the costs for overhead (fixed), labor, fuel, and management and profit. The overhead costs included depreciation, interest, insurance, housing, and annual repair costs. These overhead costs were calculated based on procedures from Lazarus and Smale (2010) with the following tub-grinder data (Morey et al., 2010): initial cost = $390,000; salvage value = 10% of initial cost; life = 5 years; operating hours = 1800 h/year; interest rate = 6%; insurance rate = 0.85%; housing = $0.67 per square foot per year; shelter space required for the tub-grinder = 3.4 m (11 ft) width × 12.5 m (41 ft) length; and annual repair costs = 3% of initial cost. Labor cost was calculated for two labors based on a $17.50/h skilled-labor charge (Lazarus and Smale, 2010). One person operates the tub-grinder from the operator control cabin and loads the bales to the grinder using the grapple loader (i.e., hydraulic fork) attached to the tub-grinder, while the other transports the biomass bales closer to the grinder using a tractor mounted front-end loader. The overhead and fuel costs for the tractor mounted front-end loader were not included in this study. Fuel costs included diesel fuel cost and lubrication cost. The price of farm diesel fuel was assumed to be $0.69/L ($2.60/gal), and

lubrication cost was assumed to be 10% of diesel fuel cost (Lazarus and Smale, 2010). Cost for management and profit was assumed to be 20% of overhead plus labor costs.

3. Results and Discussion

The high variability of moisture content of the biomass bales used for the grinding experiments obscured interpretation of some of the results, but likely reflects true conditions in the field as the variability in the bale moisture contents was the result of the way the bales were stored outdoors. Despite this variability in moisture content and its impact on our experimental results, we believe that important conclusions can be drawn from the experimental data. In addition, grinding performances (e.g., grinding process and specific energy consumption) between net-wrapped and string-wound round bales may be similar as confirmed from the experience of the grinder operator (Kolbeck, Inc.). Thus, the grinding results of net-wrapped round bales given in this study may be applicable to string-wound round bales.

3.1 Effect of Grinder Screen Opening Size

Increasing the screen opening size used in the Mighty Giant tub-grinder increased the geometric mean length of ground particles and throughput, but decreased the bulk density of ground particles and specific energy consumption (tables 1 and 2). Similar findings were reported in the literature where mobile hammer mill type tub-grinders with screen opening sizes of 12.7 to 203.2 mm were used to coarsely grind bales of corn stover, wheat straw, rice straw, and barley straw (Arthur et al., 1982; Wright et al., 2006; Kaliyan et al., 2009).

For the grinder screen opening sizes of 25.4 to 127.0 mm, the geometric mean length of the ground particles ranged from 5.8 to 10.3 mm for corn stover 2009 samples, and from 2.6 to 9.0 mm for native perennial grasses from the 2009 samples. Bulk density of ground biomass ranged from 69 to 207 kg/m^3 with the moisture content of particles ranging from 14% to 39% (w.b.). The highest throughput achieved was 24 t/h for corn stover and 44.6 t/h for native perennial grasses. Specific energy consumption ranged from 170 to 251 MJ/t for grinding 2009 corn stover bales and from 93 to 451 MJ/t for grinding 2009 bales of native perennial grasses. The energy consumption for operating the empty (i.e., no load) tub-grinder was averaged 4.2 MJ/t, which is very small compared to the energy expended to grind biomass bales (table 2).

3.2 Effect of Biomass Feedstock

Generally, bales of 2009 corn stover ground in November 2009 had larger ground particle size, higher throughput, and lower specific energy consumption than for 2008 corn stover bales (table 1). This difference is likely due to the deterioration of 2008 corn stover bales during the one year outdoor storage and due to the higher bale moisture content at the time of grinding. There were small differences in the grinding results for 2009 corn stover bales between November 2009 and March 2010 tests. This may be due to the fact that the 2009 corn stover bales ground in March 2010 had higher moisture content (> 25% w.b.) than for 2009 corn stover bales ground in November 2009 (tables 1 and 2). The increase in bale moisture contents may have been due to the snow melting and rain events during November 2009 to March 2010 in Le Mars, Iowa. The

specific energy consumption values measured in November 2009 and March 2010 were comparable for grinding 2009 corn stover bales.

The bulk density of ground corn stover ranged from 68.9 to 207.2 kg/m^3 with moisture content of particles ranging from 14.1% to 38.7% (w.b.). The bulk density of ground native perennial grasses ranged from 101.5 to 168.7 kg/m^3 with moisture content of particles ranging from 16.0% to 25.1% (w.b.). For a given grinder screen opening size, corn stover resulted in larger ground particle size than the native perennial grasses. In general, the native perennial grass bales ground in November 2009 resulted in larger ground particle size, lower throughput, and higher specific energy consumption than the native perennial grass bales ground in March 2010 (tables 1 and 2). The differences in the grinding results for native perennial grasses ground in November 2009 and March 2010 were likely due to the differences in the harvested perennial grasses (e.g., type and mixture of grass species in the bales) used at these two times. Differences in grinding characteristics between biomass feedstocks have been well documented (Arthur et al., 1982; Yu et al., 2003; Mani et al., 2004; Bitra et al., 2009a and 2009b; Bitra et al., 2010). These differences in grinding behaviors among the biomass feedstocks are typically attributed to fundamental differences in the structural, compositional, or mechanical properties of biomass feedstocks.

In this study, the effect of individual bale moisture content, prior to grinding, was not determined. However, it is likely that the average, post grinding, moisture content measured in this study may be slightly lower than the average moisture content of the individual bales due to the increase in biomass temperatures during grinding and subsequent loss of moisture through evaporation. Table 2 shows that the average temperature of the ground materials was higher than ambient air temperature by 7 to 24°C. This rise in biomass temperature may have caused loss of some moisture. In addition to the temperature rise, breaking of biomass tissues and exposure of new surface area generated to environment may contribute to moisture loss. The smaller the grinder screen opening size, the larger the grinding effort (friction and heat production). Thus, the smaller grinder screen opening size may have caused higher moisture loss from the ground particles than the larger grinder screen opening size. In general, the results from this study show that bale moisture content of more than 25% (w.b.) decreases grinder performance (e.g., lower throughput and higher specific energy consumption).

3.3 Particle Size Distribution

Figures 2 and 3 show the particle size distribution curves for corn stover and native perennial grasses, respectively. For both corn stover and native perennial grasses, nearly 100% of ground particles from the grinder screen opening size of 25.4 mm passed through the top sieve (i.e., sieve opening size of 38.1 mm) during the particle size analysis, but certain percentages of ground particles retained on the top sieve for the grinder screen opening sizes of 76.2 and 127.0 mm because of production of ground particles longer than 38.1 mm for these two grinder screen opening sizes. For example, the average lengths of the longest particles (manually measured) for 2009 corn stover bales ground in March 2010 for the grinder screen opening sizes of 76.2 and 127.0 mm were 81.7 and 116.6 mm, respectively. Average lengths of the longest particles (manually measured) for native perennial grasses 2009 bales ground in March 2010 for the grinder screen opening sizes of 76.2 and 127.0 mm were 94.7 and 107.9 mm, respectively. In

general, a larger grinder screen opening size resulted in a lower mass of particles that retained in the pan (i.e., particle length <1.8 mm) during the particle size analysis (figs. 2 and 3).

Particle size distributions showed that 2009 corn stover bales ground in November 2009 had slightly larger ground particle sizes than 2008 corn stover bales ground in November 2009 and 2009 corn stover bales ground in March 2010 (fig. 2). This may be due to the deterioration of corn stover during the outdoor storage caused by increased bale moisture and adverse weather conditions such as snow melting and rain events. The differences in particle size distribution of native perennial grasses ground in November 2009 and March 2010 were likely due to the differences in the harvested perennial grasses (e.g., type and mixture of grass species in the bales) used at these two times (fig. 3).

3.4 Cost of Grinding and Logistics

The estimated cost for grinding 2009 corn stover bales ranged from $8.98/t to $15.55/t, and for grinding 2009 bales of native perennial grasses ranged from $4.39/t to $20.08/t (tables 1 and 2). The cost of grinding was higher for 2008 corn stover bales than for 2009 corn stover bales ground in November 2009 (table 1). This is perhaps due to the higher moisture content of 2008 corn stover bales (i.e., about 23 to 32% w.b.) than for 2009 corn stover bales (i.e., about 14 to 16% w.b.). A larger grinder screen opening size or higher grinder throughput resulted in a lower cost of grinding because of more efficient use of costs associated with overhead, labor, and management and profit, and lower fuel cost (tables 1 and 2). This trend was also reported by Arthur et al. (1982) for grinding corn stover, wheat straw, rice straw, and forest residues.

Comparing the results of Mighty Giant tub-grinder at different screen opening sizes, the screen opening size of 25.4 mm resulted in finer particle sizes than for the screen opening sizes of 76.2 mm and 127.0 mm (tables 1 and 2). Morey (2010) reported that pilot-scale roll press compaction of corn stover and native perennial grasses obtained from the Mighty Giant with screen opening sizes of 76.2 mm and 127.0 mm resulted in compacted products with bulk densities of 273 to 360 kg/m^3. No significant difference in the compacted product bulk densities was found between the ground particle sizes obtained from the Mighty Giant screen opening sizes of 76.2 mm and 127.0 mm (Morey, 2010). Thus, for the biomass supply logistics system described in Morey et al. (2010), the Mighty Giant with a screen opening size of 76.2 to 127.0 mm would be preferable for coarse grinding of biomass before roll press compaction to increase the bulk density further to 240 kg/m^3. The specific energy consumption for the Mighty Giant with screen opening sizes of 76.2 to 127.0 mm was 212 to 347 MJ/t for grinding corn stover bales with moisture contents of 16 to 39% (w.b.). Native perennial grass bales with moisture contents of 17 to 25% (w.b.) required 93 to 123 MJ/t for grinding (tables 1 and 2). The corresponding estimated costs of grinding were $8.98/t to $12.97/t for corn stover bales, and $4.39/t to $6.23/t for native perennial grass bales.

Morey et al. (2010) estimated the cost for operation of a tub-grinder [403 kW (540 HP)] with a capacity of 22.7 t/h at $5.18/t for coarse grinding of corn stover. Thus, the results from our study show similar costs for grinding native perennial grasses, but higher costs for grinding corn stover.

4. Conclusions

The following conclusions were drawn from the results of grinding experiments involving the Mighty Giant tub-grinder [463 kW (630 HP)] to produce coarsely ground materials from the round-baled, plastic net-wrapped corn stover and native perennial grasses.

- Increasing the screen opening size used in the tub-grinder increased the geometric mean length of ground particles and throughput of the grinder, but decreased the bulk density of the ground particles, specific energy consumption of the grinder, and cost of grinding.
- The biomass feedstock type (corn stover versus native perennial grasses), bale moisture content, and outdoor storage time after collection of bales affected the geometric mean length and bulk density of ground particles, grinder throughput, specific energy consumption, and cost of grinding. Bales with high moisture content (> 25% w.b.) considerably decreased the throughput, which consequently increased the specific energy consumption of the grinder.
- For the biomass supply logistics system described in Morey et al. (2010), a tub-grinder similar to the Mighty Giant with a screen opening size of 76.2 to 127.0 mm could be adopted to produce coarsely ground biomass with bulk density of about 100 kg/m^3 at a capacity of 22.7 t/h. The specific energy consumption for the Mighty Giant with screen opening sizes of 76.2 to 127.0 mm was 212 to 347 MJ/t for grinding corn stover bales, and was 93 to 123 MJ/t for grinding native perennial grass bales. The corresponding costs of grinding were estimated to be $8.98/t to $12.97/t for corn stover bales, and $4.39/t to $6.23/t for native perennial grass bales.

REFERENCES

Arthur, J.F., R.A. Kepner, J.B. Dobie, G.E. Miller, and P.S. Parsons. 1982. Tub grinder performance with crop and forest residues. *Trans. ASAE* 25(6): 1488-1494.

ASABE Standards. 2009a. ASAE S358.2 DEC1998 (R2008): Moisture measurement – forages. St. Joseph, Mich.: ASABE.

ASABE Standards. 2009b. ANSI/ASAE S424.1 MAR1992 (R2007). Method of determining and expressing particle size of chopped forage materials by screening. St. Joseph, Mich.: ASABE.

ASTM. 2009. E 873-82 (Reapproved 2006): Standard test method for bulk density of densified particulate biomass fuels. West Conshohocken, PA: ASTM International.

Bitra, V.S.P., A.R. Womac, C. Igathinathane, P.I. Miu, Y.T. Yang, D.R. Smith, N. Chevanan, and S. Sokhansanj. 2009a. Direct measures of mechanical energy for knife mill size reduction of switchgrass, wheat straw, and corn stover. *Biores. Tech.* 100(24): 6578-6585.

Bitra, V.S.P., A.R. Womac, N. Chevanan, P.I. Miu, C. Igathinathane, S. Sokhansanj, and D.R. Smith. 2009b. Direct mechanical energy measures of hammer mill comminution of switchgrass, wheat straw, and corn stover and analysis of their particle size distributions. *Powder Technol.* 193(1): 32-45.

Bitra, V.S.P., A.R. Womac, C. Igathinathane, and S. Sokhansanj. 2010. Knife mill comminution energy analysis of switchgrass, wheat straw, and corn stover and characterization of particle size distributions. *Trans. ASABE* 53(5): 1639-1651.

Heinrichs, J., and P. Kononoff. 2010. Evaluating particle size of forages and TMRs using the New Penn State Forage Particle Separator. University Park, PA: Department of Dairy and Animal Science, The Pennsylvania State University. Available at: http://www.das.psu.edu/research-extension/dairy/nutrition/pdf/evaluating-particle-size-of-forages.pdf. Accessed 6 January 2010.

Kaliyan, N., R.V. Morey, M.D. White, and D.G. Tiffany. 2009. A tub-grinding/roll-press compaction system to increase biomass bulk density: preliminary study. ASABE Paper No. 096658. St. Joseph, Mich.: ASABE.

Lazarus, W.F., and A. Smale. 2010. Machinery cost estimates. St. Paul, Minn.: University of Minnesota Extension Service. Available at: http://www.apec.umn.edu/faculty/wlazarus/documents/machdata.pdf. Accessed 10 December 2010.

Mani, S., L.G. Tabil, and S. Sokhansanj. 2004. Grinding performance and physical properties of wheat and barley straws, corn stover and switchgrass. *Biomass and Bioenergy* 27(4): 339-352.

Morey, R.V. 2010. Biomass Electricity Generation at Ethanol Plants – Achieving Maximum Impact. Milestone 5 Report of Xcel Energy Renewable Development Fund Project RD3-23. St. Paul, Minn.: Department of Bioproducts and Biosystems Engineering, University of Minnesota. Available at: http://www.biomasschpethanol.umn.edu/Project2/reports.html. Accessed 15 December 2010.

Morey, R.V., N. Kaliyan, D.G. Tiffany, and D.R. Schmidt. 2010. A corn stover supply logistics system. *Applied Eng. in Agric.* 26(3): 455-461.

Wright, C.T., P.A. Pryfogle, N.A. Stevens, J.R. Hess, and C.W. Radtke. 2006. Value of distributed preprocessing of biomass feedstocks to a bioenergy industry. ASABE Paper No. 066151. St. Joseph, Mich.: ASABE.

Yu, M., A.R. Womac, and L.O. Pordesimo. 2003. Review of biomass size reduction technology. ASAE Paper No. 036077. St. Joseph, Mich.: ASABE.

Figure 1. Mighty Giant tub-grinder [463 kW (630 HP)] used for the study.

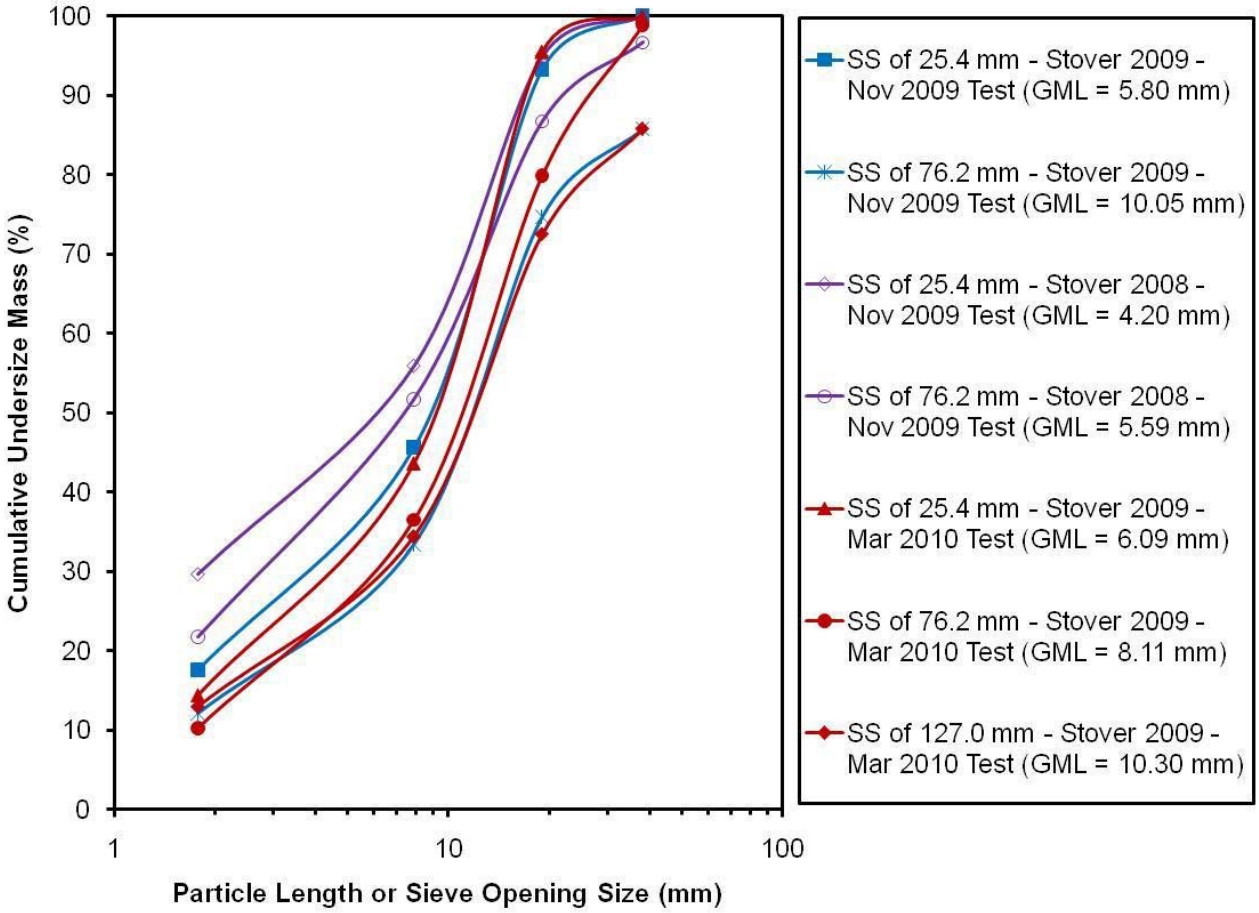

Figure 2. Particle size distributions for corn stover bales ground in Mighty Giant tub-grinder in November 2009 and March 2010. Each curve is an average of three replications. (SS = screen size used in the grinder; GML = geometric mean length of ground particles).

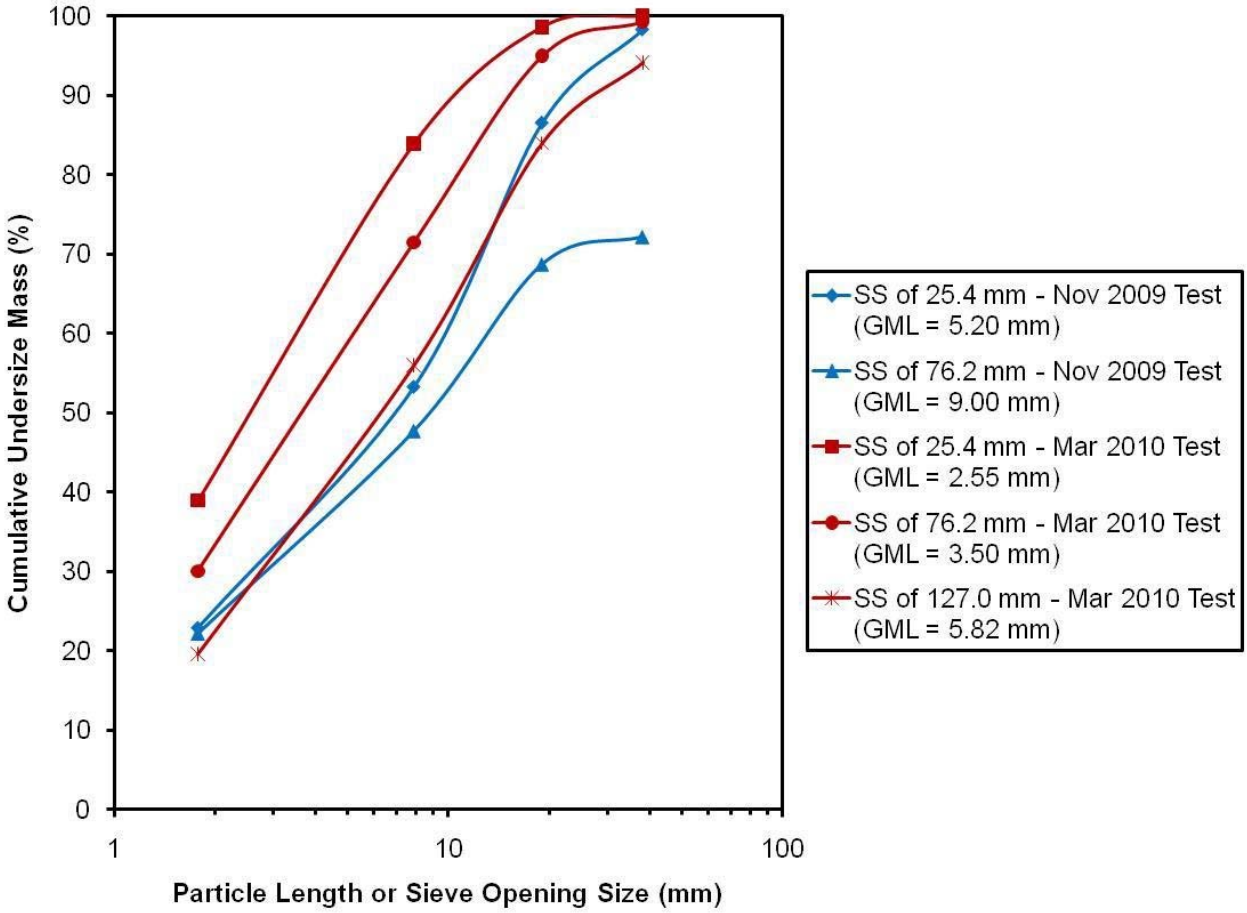

Figure 3. Particle size distributions for native perennial grass bales ground in Mighty Giant tub-grinder in November 2009 and March 2010. Each curve is an average of three replications. (SS = screen size used in the grinder; GML = geometric mean length of ground particles).

Table 1. Particle size, bulk density, throughput, specific energy consumption, and cost for biomass bales ground in Mighty Giant tub-grinder in November 2009.

Biomass Feedstock Type	Grinder Screen Opening Size, mm	Ground Particle Size, mm (n = 3) [a]	Moisture Content of Ground Particles, % w.b. (n = 3)	Bulk Density of Ground Particles, kg/m^3 (n = 3)	Throughput, t/h (n = 1)	Specific Energy Consumption, MJ/t [b] (n = 1)	Estimated Cost of Grinding, $/t	
							Fuel Cost [c]	Total Cost [d]
Corn stover 2009	25.4	5.80 ± 2.90	14.1 ± 0.5	117.5 ± 1.8	14.0	235.7	4.98	12.73
	76.2	10.05 ± 3.74	16.4 ± 0.2	92.9 ± 5.5	24.0	211.8	4.47	8.98
Corn stover 2008	25.4 [e]	4.20 ± 3.27	23.1 ± 0.5	147.4 ± 5.5	6.3	660.8	13.96	31.23
	76.2	5.59 ± 3.54	31.7 ± 2.1	207.2 ± 20.3	19.1	346.7	7.32	12.97
Native perennial grasses 2009	25.4	5.20 ± 3.29	19.9 ± 2.3	112.1 ± 5.5	10.3	451.1	9.53	20.08
	76.2	9.00 ± 5.38	16.7 ± 1.1	101.5 ± 1.8	20.4	NA [f]	NA	NA

[a] Ground particle size denotes geometric mean length ± geometric standard deviation. n = number of replications.

[b] Specific energy consumption values include energy for grinder operation (i.e., no-load energy consumption). The lower heating value (LHV) of diesel fuel was assumed to be 35.9 MJ/L (Morey et al., 2010).

[c] Fuel cost is the sum of diesel fuel cost and lubrication cost. The price of farm diesel fuel was assumed to be $0.69/L ($2.60/gal), and lubrication cost was assumed to be 10% of diesel fuel cost (Lazarus and Smale, 2010).

[d] Total cost is the sum of the costs for overhead (fixed), labor, fuel, and management and profit. The overhead cost ($55.17/h) is the sum of depreciation ($39.00/h), interest ($8.32/h), insurance ($1.18/h), housing ($0.17/h), and annual repair ($6.50/h) costs. Labor cost is $35.00/h. Cost for management and profit is $18.03/h. Dividing $/h by t/h, $/t was calculated.

[e] When grinding 2008 corn stover bales with a grinder screen opening size of 25.4 mm, it was noted that one of the bales used for the test appeared to be very wet and took a longer time to grind, which may be the reasons for lower throughput and higher specific energy consumption for this test.

[f] NA = measurements were not made.

Table 2. Particle size, bulk density, throughput, specific energy consumption, and cost for biomass bales ground in Mighty Giant tub-grinder in March 2010.

Grinder Screen Opening Size, mm	Ground Particle Size, mm (n = 3) [a]	Moisture Content of Ground Particles, % w.b. (n = 3)	Ambient Air Temperature, C	Temperature of Ground Biomass Pile Measured at 0.5 m Depth, C (n = 3)	Bulk Density of Ground Particles, kg/m^3 (n = 3)	Throughput, t/h (n = 1)	Specific Energy Consumption, MJ/t [b] (n = 1)		Estimated Cost of Grinding, $/t	
							Including Energy for Grinder Operation	Excluding Energy for Grinder Operation [c]	Fuel Cost [d]	Total Cost [e]
Corn Stover 2009										
25.4	6.09 ± 2.71	27.1 ± 0.4	4.7	29.1 ± 1.4 (Max = 30.0 C)	108.9 ± 11.1	9.1	170.4	163.8	3.60	15.55
76.2	8.11 ± 2.84	38.7 ± 10.5	7.2	21.4 ± 1.3 (Max = 22.3 C)	118.5 ± 33.4	16.9 [f]	239.9 [f]	234.9 [f]	5.07	11.50
127.0	10.30 ± 4.11	26.8 ± 2.4	11.6	27.6 ± 0.1 (Max = 27.7 C)	68.9 ± 2.3	19.8 [f]	251.3	247.4	5.31	10.90
Native Perennial Grasses 2009										
25.4	2.55 ± 2.72	16.0 ± 0.3	4.6	22.4 ± 2.1 (Max = 25.0 C)	168.7 ± 10.3	18.9	133.6	129.1	2.82	8.56
76.2	3.50 ± 3.06	25.1 ± 2.8	7.2	14.8 ± 3.2 (Max = 18.3 C)	137.8 ± 3.2	29.8	123.0	120.4	2.60	6.23
127.0	5.82 ± 3.68	25.1 ± 2.1	11.6	18.4 ± 2.4 (Max = 19.8 C)	122.8 ± 8.1	44.6	92.8	91.0	1.96	4.39

[a] Ground particle size denotes geometric mean length ± geometric standard deviation. n = number of replications.

[b] Diesel consumption for operating empty (i.e., no load) Mighty Giant tub-grinder was 2.44 L/h. The lower heating value (LHV) of diesel fuel was assumed to be 35.9 MJ/L (Morey et al., 2010).

[c] This is the energy expended for grinding the biomass bales alone. It excludes the energy consumed for operating the empty Mighty Giant tub-grinder.

[d] Fuel cost is the sum of diesel fuel cost and lubrication cost. The price of farm diesel fuel was assumed to be $0.69/L ($2.60/gal), and lubrication cost was assumed to be 10% of diesel fuel cost (Lazarus and Smale, 2010).

[e] Total cost is the sum of the costs for overhead (fixed), labor, fuel, and management and profit. The overhead cost ($55.17/h) is the sum of depreciation ($39.00/h), interest ($8.32/h), insurance ($1.18/h), housing ($0.17/h), and annual repair ($6.50/h) costs. Labor cost is $35.00/h. Cost for management and profit is $18.03/h. Dividing $/h by t/h, $/t was calculated.

[f] This value is an average of two replications.

Chapter 2

Roll Press Compaction of Corn Stover and Perennial Grasses

Abstract

The objective of this study was to investigate roll press compaction of coarsely-ground corn stover and native perennial grasses to produce compacted products with a bulk density of at least 240 kg/m^3 (15 lb/ft^3). A 44.8 kW (60 HP) pilot-scale roll press compaction machine was used to compress corn stover and native perennial grasses (initial moisture contents of < 20% w.b.) ground in a tub-grinder with three different round-hole screen opening sizes [25.4, 76.2, and 127.0 mm (1.0, 3.0, and 5.0 in.)]. Unit density of individual compacts [133.7 mm (5.3 in.) length × 25.8 mm (1.0 in.) width × 20.0 mm (0.8 in.) depth] ranged from 325 to 725 kg/m^3 (20 to 45 lb/ft^3). Bulk density of compacted materials ranged from 265 to 365 kg/m^3 (16 to 23 lb/ft^3) for the roll compaction forces of 214 to 534 kN (24 to 60 ton). Durability (ASABE tumbling test) of compacts ranged from 61% to 92%. Throughput of roll press ranged from 0.1 to 0.6 t/h (0.2 to 0.7 ton/h). Roll forces of 356 and 534 kN (40 and 60 ton) or the three particle sizes obtained from the tub-grinder screen opening sizes of 25.4, 76.2, and 127.0 mm (1.0, 3.0, and 5.0 in.) resulted in similar unit density, bulk density, and durability of compacts. Specific energy consumption (excluding no-load energy consumption) for the operation of rolls and screw feeder ranged from 19 to 339 MJ/t (i.e., 0.1% to 2.3% of energy in the biomass material).

1. Objectives

The overall goal of this study is to investigate roll press compaction of coarsely ground corn stover and native perennial grasses to obtain compacted products with a target bulk density of at least 240 kg/m^3 (15 lb/ft^3). The sub-objective is to study the effects of biomass feedstock (corn stover and perennial grasses), particle size, and roll force on the bulk density and durability of roll press compacted products and on the throughput and specific energy consumption of the roll press compactor.

2. Materials and Methods

Roll press compaction experiments were conducted at Bepex International LLC (Minneapolis, MN) pilot plant in April 2010. A 37.3 kW (50 HP) roll press compaction machine (MS 75 Roll Compactor, Bepex International LLC, Minneapolis, MN) that had two counter rotating rolls with 520.7 mm (20.5-in.) diameter and 127.0 mm (5.0-in.) width was used (Fig. 1). The rolls had 72 “stick” pockets per roll. The size of one pocket on one of the rolls was 114.3 mm (4.5 in.) width x 20.3 mm (0.8 in.) height x 5.1 mm (0.2 in.) depth. The stick pocketed rolls were used to assist the feeding. The gap between the rolls was set at about 2.03 mm (0.08 in.). The force was applied to the one of the rolls by a hydraulic pressure system. This roll was floating during the compaction (i.e., the roll was separating to slightly increase the roll gap to allow for compaction of particles). The force applied between the rolls was a variable in this study. Three roll forces, 214, 356, and 534 kN (24, 40, and 60 ton) were studied.

Roll press compaction tests were conducted for corn stover and native perennial grasses ground in Mighty Giant tub-grinder [463 kW (630 HP); Jones Mfg., Beemer, Iowa; www.mightygiant.com) with three round-hole screen opening sizes [25.4, 76.2, and 127.0 mm (1.0, 3.0, and 5.0 in.)] in March 2010 at Kolbeck, Inc., Le Mars, Iowa (Kaliyan et al., 2012). Corn stover and native grasses (hay) bales collected from 2009 were stored outdoors until used for the grinding study in March 2010. The native perennial grasses contained about 60% (by mass) of brome grass and the remaining was native prairie mix including fescue, foxtail, and weeds. All bales had 2.5 wraps of plastic net-wrap. The net-wrap was ground along with the biomass. Tub-ground corn stover and perennial grasses were bagged (2 biomass materials × 3 screen opening sizes × 23 kg per plastic bag × 10 plastic bags) and transported to St. Paul, MN for use in pilot scale roll press compaction study at Bepex International LLC, Minneapolis, MN.

The tub-ground biomass materials had moisture contents of more than 20% (w.b.). Thus, the ground materials were dried in an unheated building (room temperature of 18 to 24 °C, and relative humidity of 31% to 66%) in St. Paul, MN to adjust moisture contents to 15% to 20% (w.b.) before using the materials for the roll press compaction study. The particle size analysis procedure developed for forage materials by Heinrichs and Kononoff (2012) was followed to determine the geometric mean particle length of ground biomass materials. Geometric mean length and standard deviation of the particles were estimated by following the calculation procedure given in ASABE Standards (2009a).

Preliminary roll press compaction experiments showed that a gravity feeder box located above the rolls did not satisfactorily feed the ground materials to the rolls. Ground materials bridged inside the gravity box. Thus, a conical hopper with a screw feeder [7.46 kW (10 HP)] was used for consistent feeding (vertically downwards) to the rolls. In addition, a separate horizontal screw feeder [1.04 kW (1.4 HP); Acrison 1015Z-K] with mixing paddles was used to control the feeding to the screw feeder located above the rolls. This set up avoided overfeeding to the screw feeder that occurred when the screw feeder was manually hand-fed. The screw feeder partially removed the air entrained in the ground material and partially densified the material before feeding the material to the rolls. The roll speed and screw feeder speed were adjusted for each test such that the material caught between the rolls separate (i.e., float) the pressurized roll. At the exit of the rolls, the compacted biomass materials separated into shorter lengths due to the natural breaking points along the width of the compacted sheet. This resulted in a bulk compacted product (Fig. 1).

For each compaction test, the mass of compacted materials collected for 2 to 6 min was weighed to determine the roll press throughput. The current consumed by the roll motor and screw feeder motor was recorded for estimating the specific energy consumption by the rolls and screw feeder. The energy consumption by the 1.04 kW (1.4 HP) horizontal screw feeder was not measured and was ignored in the calculation of specific energy consumption for the roll press compaction process. The bulk density of compacted materials was measured immediately after forming by following the procedure given in ASTM (2009). A cubical box of 305 × 305 × 305 mm was filled by dropping the compacted materials from a height of 610 mm above the top edge of the box. The box was dropped five times (i.e., five taps) from a height of 150 mm on to the ground to allow settling. Additional compacts were added and the excess was struck off level with a top edge. The bulk density of the sample was calculated by dividing the mass of sample in

the box by the volume of the box. The same ASTM (2009) procedure was followed to measure the bulk density of tub-ground materials.

Unit density, durability, and angle of repose of compacts were measured after one week of storage of compacts in large sealed (neck-tied) plastic bags at room temperature (about 25 °C) (i.e., curing process). Unit density of compacts was measured by water displacement method (ASABE Standards, 2009b). A piece of compact formed between a pair of stick pockets was carefully separated and was sealed inside a plastic film (Food Saver® VacLoc® Roll; Item No. 01-0028; Heavy duty 3-ply material) using a vacuum sealer (Food Saver® Vac 300, Tilia International, Inc., San Francisco, CA; www.foodsaver.com). A typical size of the individual piece of compacts formed between a pair of stick pockets was 133.7 mm (5.3 in.) length × 25.8 mm (1.0 in.) width × 20.0 mm (0.8 in.) depth. The sealed compact was immersed in a graduated cylinder (accuracy of 5 mL) filled with water to measure the volume of the compact plus the plastic film. To detect the volume of the plastic film covering the compact, the volume of the plastic film was measured by immersing the plastic film in a graduated cylinder (accuracy of 1 mL) filled with water. The unit density of the compact was calculated from the measured mass and the volume of the compact (excluding the volume of the plastic film).

Durability of compacts was measured according to ASABE Standards (2009b). Durability is a measure of dusting potential of compacts during handling (Kaliyan and Morey, 2009). About 500 g of compacted materials was tumbled for 2.4 min at 50 rpm (i.e., 120 revolutions) in the ASABE tumbling can durability tester. Durability (%) = [Mass of compacted materials retained on 19.1 mm (0.75 in.) screen after tumbling × 100 / Mass of compacted materials used for tumbling].

Angle of repose of bulk sample of compacts (about 1000 g) on a galvanized steel surface was measured using a tilted-plane angle of repose apparatus (Mohsenin, 1986). Moisture contents of the ground materials and compacted materials were measured based on ASABE Standards (2009c).

3. Results and Discussion

Tables 1 and 2 provide the bulk density, throughput, and specific energy consumption for the roll press compaction of corn stover and native perennial grasses, respectively. Tables 3 and 4 give the unit density, durability, and angle of repose of compacted corn stover and native perennial grasses, respectively, measured after one week of curing at room temperature. The bulk density of bulk compacted materials ranged from 262 to 365 kg/m^3 (16.4 to 22.8 lb/ft^3) (Tables 1 and 2). Thus, the bulk density of compacts produced is more than the target bulk density of 240 kg/m^3 (15 lb/ft^3). The roll press compactor increased the bulk density of coarsely ground materials by 2.9 to 5.1 fold for corn stover, and by 1.7 to 3.8 fold for perennial grasses. Bulk density of compacts increased with increasing the roll force from 214 to 356 kN (24 to 40 ton); however, the roll forces of 356 and 534 kN (40 and 60 ton) resulted in compacts with similar bulk densities (Tables 1 and 2). The three particle sizes obtained from the tub-grinder with screen opening sizes of 25.4, 76.2, and 127.0 mm (1.0, 3.0, and 5.0 in.) did not affect the bulk density of compacts.

Roll speed ranged from 1.1 to 3.3 rpm and screw feeder speed ranged from 49.0 to 66.8 rpm (Tables 1 and 2). The roll press throughput ranged from 0.13 to 0.62 t/h (0.15 to 0.68 ton/h). Throughput of the roll press compactor was influenced by the ability of screw feeder to feed the rolls without creating roll starvation. It was observed that smaller particle size had better feeding properties, and perennial grasses were easier to feed compared to corn stover. Results show that the type of biomass material (corn stover or perennial grasses) and the initial bulk density of the ground material affected the throughput of the roll press compactor (Tables 1 and 2). Perennial grasses resulted in higher throughput than corn stover.

Specific energy consumption increased with increasing the roll force from 214 to 534 kN (24 to 60 ton) (Tables 1 and 2). The specific energy consumed by the rolls ranged from 16.4 to 304.1 MJ/t excluding the no-load operation energy (i.e., 0.11 % to 2.03% of energy in the biomass material, assuming a lower heating value of 15 MJ/kg of biomass at 15% w.b. moisture content). The specific energy consumed by the screw feeder ranged from 2.5 to 37.4 MJ/t excluding the no-load operation energy (i.e., 0.02 % to 0.25% of energy in the biomass material, assuming a lower heating value of 15 MJ/kg of biomass at 15% w.b. moisture content). Also, the measured specific energy consumption data showed that about 50% to 87% of the total energy input was required to operate the empty (i.e., no-load) roll press and screw feeder. This may be due to the fact that the pilot scale roll press compactor used in this study was not optimized to compact corn stover and perennial grasses, but they were designed for compacting a variety of particulate materials such as coal and fertilizers. The speed of the rolls was controlled by a frequency controller which may contribute to roll press compaction system inefficiency. The general trend was that corn stover consumed a higher specific energy than perennial grasses per tonne of biomass compacted (Tables 1 and 2).

The unit density and durability of cured compacts were 325 to 724 kg/m^3 (20 to 45 lb/ft^3) and 61% to 92%, respectively (Tables 3 and 4). Unit density and durability of compacts increased with increasing the roll force from 214 to 356 kN (24 to 40 ton). The roll forces of 356 and 534 kN (40 and 60 ton) resulted in similar unit density and durability of compacts made from both the biomass materials. The three particle sizes obtained from the tub-grinder with three different screen opening sizes of 25.4, 76.2, and 127.0 mm (1.0, 3.0, and 5.0 in.) did not affect the unit density and durability of compacts. In general, corn stover produced higher durability compacts than perennial grasses. The difference in the compaction results between corn stover and perennial grasses may be due to fundamental differences in the structural, compositional, or mechanical properties of these two biomass feedstocks. Moreover, roll force appears to be a more dominant factor than particle size affecting the unit density and durability of compacts.

During the roll press compaction of biomass particles, densification mechanisms were air removal from the individual biomass particles (i.e., intra-particle air) as well as from the inter-particles, and elastic- and plastic-deformation of particles due to the application of pressure by the rolls. The dominant binding mechanism was solid bridges created by mechanical interlocking of particles. The mechanical interlocking may occur due to the folding of particles with each other and due to the diffusion of molecules from one fiber to another at the contact points. The biomass particles may also bind to one another due to the natural binding components such as water soluble carbohydrates, protein, and lignin available in the biomass materials (Kaliyan and Morey, 2009 and 2010).

The angle of repose values of cured compacts ranged from 21° to 27° (Tables 3 and 4). For comparison, typical feed pellets have angle repose values of 27° to 40° (White and Jayas, 2001). For designing handling and storage systems, data on angle of repose of compacts would be required. Also, the angle of repose is a measure of flowability of compacts (Mohsenin, 1986). The durability and angle of repose values of roll press compacted materials indicate that roll press compacts may be handled in belt conveyors without much dust formation during operation.

4. Conclusions

The following conclusions were obtained from the pilot-scale roll press compaction of corn stover and perennial grasses.

- Compacts with bulk density of more than the target bulk density of 240 kg/m^3 (15 lb/ft^3) were produced.
- Bulk density of compacted materials ranged from 265 to 365 kg/m^3 (16 to 23 lb/ft^3). Bulk density of ground materials was increased by 3 to 5 fold for corn stover, and 2 to 4 fold for perennial grasses.
- Unit density of individual compacts ranged from 325 to 725 kg/m^3 (20 to 45 lb/ft^3).
- Durability of compacts ranged from 61% to 92%.
- Roll press compaction performances for roll forces of 356 and 534 kN (40 and 60 ton) were similar. These roll forces resulted in similar unit density, bulk density, and durability of compacts; however, the roll force of 534 kN (60 ton) consumed slightly higher specific energy than for the roll force of 356 kN (40 ton).
- Roll press compaction performances for biomass particles produced from tub-grinder screen opening sizes of 25.4 to 127.0 mm (1.0 to 5.0 in.) were similar. These particle sizes resulted in similar unit density, bulk density, and durability of compacts.
- Compared to corn stover, perennial grasses resulted in higher roll press throughput and consumed lower specific energy for the roll press operation.

REFERENCES

ASABE Standards. 2009a. ANSI/ASAE S424.1 MAR1992 (R2007). Method of determining and expressing particle size of chopped forage materials by screening. St. Joseph, Mich.: ASABE.

ASABE Standards. 2009b. S269.4: Cubes, pellets, and crumbles – Definitions and methods for determining density, durability, and moisture content. St. Joseph, Mich.: ASABE.

ASABE Standards. 2009c. ASAE S358.2 DEC1998 (R2008): Moisture measurement – forages. St. Joseph, Mich.: ASABE.

ASTM. 2009. E 873-82 (Reapproved 2006): Standard test method for bulk density of densified particulate biomass fuels. West Conshohocken, PA: ASTM International.

Heinrichs, J., and P. Kononoff. 2012. Evaluating particle size of forages and TMRs using the New Penn State Forage Particle Separator. University Park, PA: Department of Dairy and Animal Science, The Pennsylvania State University. Available at:

http://extension.psu.edu/animals/dairy/health/nutrition/forages/forage-quality-physical/separator/manual-and-spreadsheet-tool/evaluating-particle-size-of-forages-and-tmrs-using-the-new-penn-state-forage-particle-separator/view. Accessed 26 July 2012.

Kaliyan, N., and R.V. Morey. 2009. Factors affecting strength and durability of densified biomass products. *Biomass and Bioenergy* 33(3): 337-359.

Kaliyan, N., and R.V. Morey. 2010. Natural binders and solid bridge type binding mechanisms in briquettes and pellets made from corn stover and switchgrass. *Bioresource Tech.* 101(3): 1082-1090.

Kaliyan, N., D.R. Schmidt, R.V. Morey, and D.G. Tiffany. 2012. Commercial scale tub grinding of corn stover and perennial grasses. *Applied Eng. in Agric.* 28(1): 79-85.

Mohsenin, N.N. 1986. *Physical Properties of Plant and Animal Materials*. New York, NY: Gordon and Breach Science Publishers.

White, N.D.G., and D.S. Jayas. 2001. Physical properties of canola and sunflower meal pellets. *Canadian Biosystems Eng.* 43(3): 3.49-3.51.

Roll Press Compactor at Bepex International LLC

Top View of the Two Rolls Below a Gravity Feeder Box

One of the Rolls Showing the "Stick" Pockets

Roll Compacted Corn Stover (Individual Compacts)

A Bulk Product of Compacted Corn Stover Collected from the Roll Press Compactor

Measurement of Bulk Density of Compacted Materials Based on ASTM (2009)

Figure 1. Roll press compaction at Bepex International LLC (Minneapolis, MN) pilot plant.

Table 1. Bulk density, throughput, and specific energy consumption for roll press compaction of corn stover.

Roll force, kN (ton)	Roll speed (rpm)	Screw feeder speed (rpm)	Room temperature (°C)	Temperature of compacted materials (C) (n = 1 or 2)	Bulk density of compacted materials, kg/m^3 (lb/ft^3) (n = 1 or 2)	Roll press throughput, t/h (ton/h) (n = 1)	Specific energy consumption (MJ/t) [#] (n = 1)	
							Roll motor	Screw feeder motor
Mighty Giant grinder screen size = 25.4 mm (1.0 in.); Particle size [&] = 6.09 ± 2.71 mm (0.24 ± 0.11 in.); Moisture content of particles = 17.9 ± 0.7% w.b.; Bulk density of particles with five taps = 91.8 ± 4.9 kg/m^3 (5.7 ± 0.3 lb/ft^3)								
214 (24)	1.6	49.1	18.8	20.3	262.7 ± 0.0 (16.4 ± 0.0)	0.18 (0.20)	304.8 (40.4)	38.9 (7.8)
356 (40)	1.1	51.5	19.8	22.1	325.2 (20.3)	0.20 (0.22)	410.2 (170.7)	52.8 (24.7)
534 (60)	1.2	51.7	18.8	26.2 ± 4.4	330.0 ± 6.8 (20.6 ± 0.4)	0.18 (0.20)	510.7 (237.8)	60.2 (28.1)
Mighty Giant grinder screen size = 76.2 mm (3.0 in.); Particle size [&] = 8.11 ± 2.84 mm (0.32 ± 0.11 in.); Moisture content of particles = 10.2 ± 0.2% w.b.; Bulk density of particles with five taps = 65.1 ± 1.8 kg/m^3 (4.1 ± 0.1 lb/ft^3)								
214 (24)	1.2	49.0	--	--	301.1 (18.8)	0.18 (0.20)	375.7 (101.2)	60.6 (28.3)
356 (40)	1.2	39.9	18.8	27.0 ± 0.0	338.0 (21.1)	0.16 (0.18)	485.3 (188.2)	65.5 (30.6)
534 (60)	1.2	45.5	17.6	30.6 ± 0.1	331.6 ± 18.1 (20.7 ± 1.1)	0.15 (0.16)	638.1 (304.1)	73.7 (34.4)
Mighty Giant grinder screen size = 127.0 mm (5.0 in.); Particle size [&] = 10.30 ± 4.11 mm (0.41 ± 0.16 in.); Moisture content of particles = 14.6 ± 2.7% w.b.; Bulk density of particles with five taps = 75.8 ± 3.7 kg/m^3 (4.7 ± 0.2 lb/ft^3)								
214 (24)	1.2	49.0	--	--	275.5 ± 4.5 (17.2 ± 0.3)	0.13 (0.15)	506.4 (142.6)	80.2 (37.4)
356 (40)	1.2	49.1	17.6	23.2	317.2 (19.8)	0.17 (0.19)	482.7 (203.6)	61.6 (28.7)
534 (60)	1.2	55.4	--	--	320.4 (20.0)	0.14 (0.15)	507.2 (158.7)	76.9 (35.9)

[#] Specific energy consumption includes no-load machine operation energy. The value inside the parenthesis is specific energy consumption excluding no-load machine operation energy.

[&] Geometric mean particle length ± geometric standard deviation.

Table 2. Bulk density, throughput, and specific energy consumption for roll press compaction of native perennial grasses.

Roll force, kN (ton)	Roll speed (rpm)	Screw feeder speed (rpm)	Room temperature (°C) (n = 1)	Temperature of compacted materials (C)	Bulk density of compacted materials, kg/m^3 (lb/ft^3) (n = 2)	Roll press throughput, t/h (ton/h) (n = 1)	Specific energy consumption (MJ/t) # (n = 1)	
							Roll motor	Screw feeder motor
Mighty Giant grinder screen size = 25.4 mm (1.0 in.); Particle size & = 2.55 ± 2.72 mm (0.10 ± 0.11 in.); Moisture content of particles = 17.1 ± 0.7% w.b.; Bulk density of particles with five taps = 169.8 ± 11.6 kg/m^3 (10.6 ± 0.7 lb/ft^3)								
214 (24)	3.3	49.3	--	--	292.3 ± 3.4 (18.3 ± 0.2)	0.58 (0.64)	100.7 (16.4)	12.4 (2.5)
356 (40)	3.2	53.1	--	--	341.2 ± 0.0 (21.3 ± 0.0)	0.62 (0.68)	124.1 (44.8)	12.8 (3.5)
534 (60)	3.2	55.5	20.3	20.7	365.2 ± 4.5 (22.8 ± 0.3)	0.57 (0.63)	145.6 (60.6)	20.0 (10.0)
Mighty Giant grinder screen size = 76.2 mm (3.0 in.); Particle size & = 3.50 ± 3.06 mm (0.14 ± 0.12 in.); Moisture content of particles = 17.4 ± 2.6% w.b.; Bulk density of particles with five taps = 116.4 ± 3.7 kg/m^3 (7.3 ± 0.2 lb/ft^3)								
214 (24)	2.1	49.2	--	--	290.7 ± 7.9 (18.2 ± 0.5)	0.36 (0.39)	158.0 (20.7)	20.2 (4.0)
356 (40)	1.9	62.7	19.7	24.0	308.4 ± 14.7 (19.3 ± 0.9)	0.32 (0.36)	216.3 (66.0)	28.7 (11.1)
534 (60)	1.8	64.8	20.5	25.0	355.6 ± 9.1 (22.2 ± 0.6)	0.33 (0.37)	255.2 (109.1)	30.1 (12.9)
Mighty Giant grinder screen size = 127.0 mm (5.0 in.); Particle size & = 5.82 ± 3.68 mm (0.23 ± 0.15 in.); Moisture content of particles = 16.5 ± 1.7% w.b.; Bulk density of particles with five taps = 96.1 ± 3.2 kg/m^3 (6.0 ± 0.2 lb/ft^3)								
214 (24)	1.6	49.1	--	--	273.1 ± 7.9 (17.1 ± 0.5)	0.22 (0.25)	260.2 (43.5)	31.9 (6.4)
356 (40)	1.5	64.7	20.5	20.7	323.6 ± 2.3 (20.2 ± 0.1)	0.26 (0.29)	315.6 (128.4)	41.3 (19.3)
534 (60)	1.5	66.8	20.5	22.0	359.6 ± 10.2 (22.5 ± 0.6)	0.24 (0.26)	335.0 (129.1)	33.3 (9.1)

Specific energy consumption includes no-load machine operation energy. The value inside the parenthesis is specific energy consumption excluding no-load machine operation energy.

& Geometric mean particle length ± geometric standard deviation.

Table 3. Properties of roll press compacted corn stover measured after one week of curing at room temperature.

Roll press conditions			Properties of cured compacted corn stover (n = 3)			
Roll force, kN (ton)	Roll speed, rpm	Screw feeder speed, rpm	Moisture content, % w.b.	Unit density based on water displacement method, kg/m^3 (lb/ft^3)	Durability, %	Angle of repose, deg
Mighty Giant grinder screen size = 25.4 mm (1.0 in.); Particle size [&] = 6.09 ± 2.71 mm (0.24 ± 0.11 in.); Moisture content of particles = 17.9 ± 0.7% w.b.; Bulk density of particles with five taps = 91.8 ± 4.9 kg/m^3 (5.7 ± 0.3 lb/ft^3)						
214 (24)	1.6	49.1	15.8 ± 0.4	394.6 ± 31.8 (24.6 ± 2.0)	81.7 ± 1.1	26.3 ± 0.6
356 (40)	1.1	51.5	14.9 ± 0.6	508.4 ± 102.1 (31.7 ± 6.4)	88.9 ± 3.3	27.0 ± 2.6
534 (60)	1.2	51.7	18.2 ± 0.5	489.9 ± 28.7 (30.6 ± 1.8)	91.9 ± 1.6	25.7 ± 0.6
Mighty Giant grinder screen size = 76.2 mm (3.0 in.); Particle size [&] = 8.11 ± 2.84 mm (0.32 ± 0.11 in.); Moisture content of particles = 10.2 ± 0.2% w.b.; Bulk density of particles with five taps = 65.1 ± 1.8 kg/m^3 (4.1 ± 0.1 lb/ft^3)						
214 (24)	1.2	49.0	10.3 ± 0.1	420.9 ± 22.5 (26.3 ± 1.4)	85.1 ± 3.0	24.3 ± 0.6
356 (40)	1.2	39.9	9.8 ± 0.1	627.9 ± 72.4 (39.2 ± 4.5)	87.4 ± 4.0	21.0 ± 0.0
534 (60)	1.2	45.5	9.7 ± 0.1	724.4 ± 139.4 (45.2 ± 8.7)	88.0 ± 2.4	23.0 ± 1.0
Mighty Giant grinder screen size = 127.0 mm (5.0 in.); Particle size [&] = 10.30 ± 4.11 mm (0.41 ± 0.16 in.); Moisture content of particles = 14.6 ± 2.7% w.b.; Bulk density of particles with five taps = 75.8 ± 3.7 kg/m^3 (4.7 ± 0.2 lb/ft^3)						
214 (24)	1.2	49.0	13.2 ± 0.1	399.1 ± 17.8 (24.9 ± 1.1)	82.8 ± 1.8	21.7 ± 0.6
356 (40)	1.2	49.1	13.3 ± 0.1	488.1 ± 27.2 (30.5 ± 1.7)	90.2 ± 3.3	24.0 ± 0.0
534 (60)	1.2	55.4	13.5 ± 0.2	637.2 ± 105.8 (39.8 ± 6.6)	91.5 ± 0.6	25.0 ± 1.0

[&] Geometric mean particle length ± geometric standard deviation.

Table 4. Properties of roll press compacted native perennial grasses measured after one week of curing at room temperature.

Roll press conditions			Properties of cured compacted native perennial grasses (n = 3)			
Roll force, kN (ton)	Roll speed, rpm	Screw feeder speed, rpm	Moisture content, % w.b.	Unit density based on water displacement method, kg/m^3 (lb/ft^3)	Durability, %	Angle of repose, deg
Mighty Giant grinder screen size = 25.4 mm (1.0 in.); Particle size [&] = 2.55 ± 2.72 mm (0.10 ± 0.11 in.); Moisture content of particles = 17.1 ± 0.7% w.b.; Bulk density of particles with five taps = 169.8 ± 11.6 kg/m^3 (10.6 ± 0.7 lb/ft^3)						
214 (24)	3.3	49.3	14.8 ± 0.4	374.9 ± 51.5 (23.4 ± 3.2)	60.8 ± 4.3	25.7 ± 0.6
356 (40)	3.2	53.1	15.2 ± 0.3	498.0 ± 12.4 (31.1 ± 0.8)	79.0 ± 1.2	23.0 ± 1.0
534 (60)	3.2	55.5	13.9 ± 0.3	510.2 ± 54.7 (31.9 ± 3.4)	90.7 ± 4.4	23.3 ± 2.1
Mighty Giant grinder screen size = 76.2 mm (3.0 in.); Particle size [&] = 3.50 ± 3.06 mm (0.14 ± 0.12 in.); Moisture content of particles = 17.4 ± 2.6% w.b.; Bulk density of particles with five taps = 116.4 ± 3.7 kg/m^3 (7.3 ± 0.2 lb/ft^3)						
214 (24)	2.1	49.2	15.7 ± 0.1	347.4 ± 23.6 (21.7 ± 1.5)	65.0 ± 3.8	23.7 ± 2.5
356 (40)	1.9	62.7	15.4 ± 0.1	456.5 ± 43.0 (28.5 ± 2.7)	81.1 ± 0.8	21.7 ± 0.6
534 (60)	1.8	64.8	16.2 ± 0.1	461.9 ± 46.9 (28.8 ± 2.9)	88.0 ± 1.8	23.7 ± 1.2
Mighty Giant grinder screen size = 127.0 mm (5.0 in.); Particle size [&] = 5.82 ± 3.68 mm (0.23 ± 0.15 in.); Moisture content of particles = 16.5 ± 1.7% w.b.; Bulk density of particles with five taps = 96.1 ± 3.2 kg/m^3 (6.0 ± 0.2 lb/ft^3)						
214 (24)	1.6	49.1	15.8 ± 0.2	325.2 ± 55.2 (20.3 ± 3.4)	66.3 ± 3.9	24.3 ± 1.5
356 (40)	1.5	64.7	12.0 ± 0.2	488.9 ± 64.1 (30.5 ± 4.0)	85.9 ± 1.2	22.0 ± 1.0
534 (60)	1.5	66.8	14.7 ± 0.6	472.9 ± 68.3 (29.5 ± 4.3)	86.3 ± 2.1	24.3 ± 1.2

[&] Geometric mean particle length ± geometric standard deviation.

Chapter 3

Demonstration Scale Roll Press Compaction of Corn Stover and Corn Cobs

Abstract

A 44.8 kW (60 HP) demonstration-scale roll press compaction machine was used to compress corn stover and corn cobs. The maximum throughput of the roll press was 2.6 t/h (2.9 ton/h) for corn cobs. For both corn stover and corn cobs, the bulk density of compacted materials was near 240 kg/m^3 (15 lb/ft^3) or higher. The measured energy consumption for the roll press compaction was 168 MJ/t for corn stover and 33 MJ/t for corn cobs.

1. Objectives

The objective of the study was to demonstrate roll press compaction of coarsely-ground biomass feedstocks to obtain compacted products with a bulk density of at least 240 kg/m^3 (15 lb/ft^3). We have studied roll press compaction of corn stover and corn cobs using the demo-scale roll press compactor. It is noted that we did not have access to perennial grasses at the time of testing with the demo-scale roll press compactor so we could not study roll press compaction of perennial grasses.

2. Materials and Methods

2.1 Roll Press Compactor

A 60 hp (44.8 kW) demonstration scale roll press compaction machine was purchased from Bepex International LLC (Minneapolis, MN) and was located at the University of Minnesota – Morris Campus and West Central Research and Outreach Center (Fig. 1). Table 1 provides the specification of the demonstration scale roll press compactor. The compactor is a prototype unit.

2.2 Procedures

During operation of the roll press compactor, hydraulic pressure (roll pressure) is set to a specific value, screw feeder hopper is continuously fed with the biomass feedstock using a belt conveyor, and roll speed and screw feeder speed are synchronized so that the top roll "float" indicating that the pre-set roll pressure is experienced by the biomass at the roll nip. A belt conveyor located at the exit of the rolls loaded the compacted materials into a truck. An electrical panel controls and displays the roll speed and screw feeder speed. A kWh meter attached to the electrical panel gauges and displays the electricity consumption during roll press operation.

There was a delay in initially receiving the prototype unit. It was first tested on January 5, 2012. Several mechanical issues were identified during this testing which required that the unit be sent back to the manufacturer for modifications. The modified unit was tested again on April 24, 2012 and May 14, 2012. Further mechanical issues were identified, so the unit was sent back to the manufacturer for additional modifications.

Roll press compaction tests were conducted on the modified unit on September 5, 2012 and October 24, 2012 for corn stover, corn cobs, and wood chips. Each roll press compaction test was performed for about 2 to 3 minutes. Throughput (t/h) of the roll press was calculated based on the mass of compacted materials collected and the compaction time. Energy consumption (MJ/t) of the roll press (machine plus compaction energy) was calculated from the total kWh consumption for the operation of roll motor plus screw feeder motor. Bulk densities of biomass feedstock (before compaction) and compacted materials (immediately after compaction) were measured according to ASTM (2009). A cubical box of 305 × 305 × 305 mm (1 × 1 × 1 ft) was filled by pouring the materials from a height of 610 mm (2 ft) above the top edge of the box. The box was dropped five times from a height of 150 mm (0.5 ft) on to the ground to allow settling. Additional materials were added and the excess was struck off level with a top edge. The mass of the sample along with the box was measured using a Taylor 7344 lithium electronic scale with an accuracy of 45 g (Taylor Precision Products, Las Cruces, New Mexico). The bulk density of the sample was calculated by dividing the mass of sample in the box by the volume of the box. Moisture content of biomass feedstock was measured based on ASABE Standards (2009).

During September 2012 tests, corn stover was difficult to feed, which resulted in slugging and then plugging of the compactor rolls. Thus, the feed mechanism was modified by tapering the auger near the end where it pushes the material into the rolls. The goal is to provide a more uniform feed so that is does not build up and then suddenly pull in a large amount (slug) which stops the machine. Compaction tests were conducted with this feed screw auger modification in October 2012.

3. Results and Discussion

Figure 2 presents samples of roll press compacted corn stover and corn cobs.

3.1 September 2012 Tests

We conducted preliminary tests with corn cobs, corn stover, and wood chips on September 5, 2012. The results are summarized in Table 2.

The corn cobs had been broken up (ground) for use in a gasifier/generator set, so they fed well and produced a nice sheet of material. We ran a test for almost 3 minutes and measured 279 lbs of compacted material throughput, which is about 97.2 lb/min or about 2.6 t/h (2.9 ton/h). This is close to our specification of 3 tons per hour. The corn cobs started at 128 kg/m^3 (8 lb/ft^3) and were 256 to 272 kg/m^3 (16 to 17 lb/ft^3) after compaction.

Although we did not obtain throughput data, we got some limited bulk density data for the other materials. For corn stover the uncompacted material was about 72 kg/m^3 (4.5 lb/ft^3) and compacted material was about 192 to 224 kg/m^3 (12 to 14 lb/ft^3). The wood chips started at about 240 kg/m^3 (15 lb/ft^3) and were about 368 kg/m^3 (23 lb/ft^3) after compaction.

3.2 October 2012 Tests

In October 2012, roll press compaction tests were conducted with the modified feed screw auger. The compaction results for corn stover (ground with 3.0 inch screen), ground corn cobs (≤ 3.0 inch particle sizes), and whole corn cobs are given in Table 3. The modified auger design improved feeding of the materials, but there were still some problems with the corn stover.

The roll press compaction increased the bulk density of corn stover from 72 kg/m^3 (4.5 lb/ft^3) to 231 kg/m^3 (14.4 lb/ft^3). We ran the test for 2.1 minutes and measured 74.3 lbs of compacted material throughput, which is 1.0 t/h (1.1 ton/h). The electrical energy consumption was 1.57 kWh, which is equivalent to 167.7 MJ/t. It was observed that a consistent compacted sheet was not made for the corn stover due to the longer stringy particles causing inconsistent feeding to the roll nip area.

It appears that better preparation of the feedstock is important for improved performance with corn stover. Some suggestions include: 1) smaller and more uniform particle size, especially reduction in long, stringy materials, 2) control of stover moisture content in the 14% to 18% range (because of several delays due to mechanical problems, the corn stover feedstock was around 10% moisture), and 3) coupled with item 2, grinding the materials immediately before they are fed into the compactor to capture some of the heat produced in grinding and the potential advantages that this might provide to enhance uniformity of feeding. Because of the physical location of the compactor and limited materials handling equipment available, we were not able to grind the material and feed it directly into the compactor. We believe attention to these issues will greatly improve performance with corn stover. Because of the significant delays in obtaining a working compactor, we were not able to pursue this additional testing as part of this project. However, we think it holds promise for future work.

The ground corn cobs were fed well to the rolls and produced a nice sheet of compacted material. We ran the test for 1.43 minutes and measured 132 lbs of compacted material throughput, which is about 2.5 t/h (2.8 ton/h). The corn cobs started at 144 kg/m^3 (9 lb/ft^3) and were 256 kg/m^3 (16 lb/ft^3) after compaction. The electrical energy consumption was 0.55 kWh, which is equivalent to 33.1 MJ/t.

A test with whole corn cobs showed that roll press compaction increased the bulk density from 141 kg/m^3 (8.8 lb/ft^3) to 221 kg/m^3 (13.8 lb/ft^3). However, throughput and energy consumption were not measured for this run.

4. Conclusions

A 44.8 kW (60 HP) roll press compaction machine was used to demonstrate the concept of coarse-grinding followed by roll-press compaction of biomass feedstock to produce a bulk compacted product with a bulk density of at least 240 kg/m^3 (15 lb/ft^3) for efficient truck transport. The maximum throughput of the demonstration-scale roll press was 2.6 t/h (2.9 ton/h) for corn cobs. For both corn stover and corn cobs, the bulk density of compacted materials was

near 240 kg/m^3 (15 lb/ft^3) or higher. The measured energy consumption for the roll press compaction was 168 MJ/t for corn stover and 33 MJ/t for corn cobs.

Future work is required to study the effects of roll pressure, biomass species, particle size, and moisture content, and to optimize the demo-scale roll press compactor.

REFERENCES

ASABE Standards. 2009. ASAE S358.2 DEC1998 (R2008): Moisture measurement – forages. St. Joseph, Mich.: ASABE.

ASTM. 2009. E 873-82 (Reapproved 2006): Standard test method for bulk density of densified particulate biomass fuels. West Conshohocken, PA: ASTM International.

Back to Table of Contents

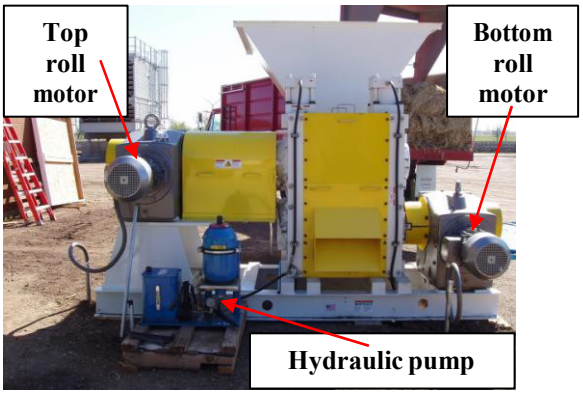

1a. Front view.

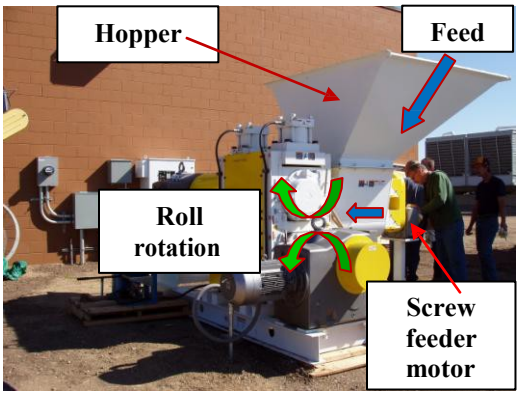

1b. Side view.

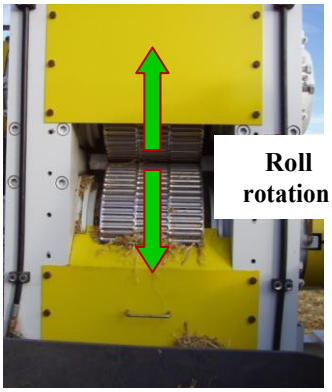

1c. Two counter-rotating rolls with pockets.

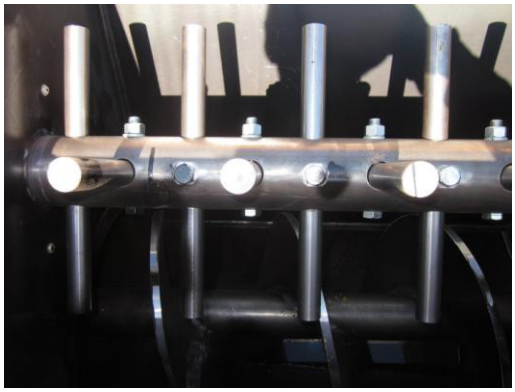

1d. Screw feeder system (paddle and auger).

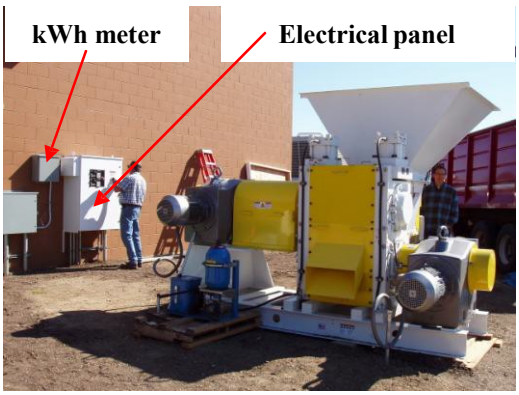

1e. Electrical control panel and kWh meter.

1f. Roll press operation.
A belt conveyor feeds ground biomass into roll press hopper, and another belt conveyor discharges roll press compacted materials into a truck.

Figure 1. Components of demonstration scale roll press compactor.

2a. Sample of ground corn stover (ground with 3.0 inch screen) fed to screw feeder hopper.

2b. Continuous output of compacted corn stover.

2c. Sample of ground corn cobs (≤ 3.0 inch particle sizes) fed to screw feeder hopper.

2d. Continuous output of compacted corn cobs.

2e. Sample of whole corn cobs fed to screw feeder hopper.

2f. Continuous output of compacted corn cobs.

Figure 2. Roll press compacted corn stover and corn cobs.

Table 1. Specifications of the demonstration scale roll press compactor.

Item	Value
Model	MS R/R 150 Compactor, Bepex International LLC
Roll diameter	0.52 m (20.5 in.)
Roll width	0.33 m (13.0 in.)
Roll gap	1.27 mm (0.05 in.)
Roll motor power	25 HP (per roll)
Roll pressure, max.	3000 psi (150 ton of roll force)
Roll speed, max.	12 RPM
Screw feeder motor power	10 HP
Screw feeder speed, max.	62 RPM
Total machine horse power	60 HP [i.e., (25 × 2) + 10]

Table 2. Results from preliminary testing of demo-scale roll press compactor at University of Minnesota-Morris on September 5, 2012.

Material	Moisture Content	Bulk Density, kg/m^3 (lb/ft^3)		Throughput,
	% w.b.	Before Compaction	After Compaction	t/h (ton/h)
Corn stover	10.1	72.1 (4.5)	192.2-224.3 (12.0-14.0)	--
Corn cobs	14.1	128.1 (8.0)	256.3-272.3 (16.0-17.0)	2.6 (2.9)
Wood chips	9.0	240.3 (15.0)	368.4 (23.0)	--

Table 3. Results from demo-scale roll press compaction at University of Minnesota-Morris on October 24, 2012.

Biomass Feedstock	Moisture Content, % w.b.	Roll Press Variables			Bulk Density, kg/m^3 (lb/ft^3)		Throughput, t/h (ton/h)	Energy Consumption (Machine plus Compaction Energy), MJ/t
		Roll Pressure (psi)	Roll Speed (rpm)	Screw Feeder Speed (rpm)	Before Compaction	After Compaction		
Corn stover (ground with 3.0 inch screen)	10.1	1150	12	20	72.1 (4.5)	230.7 (14.4) [a]	1.0 (1.1)	167.7
Ground corn cobs (≤ 3.0 inch particle size)	10.1	1150	12	40	144.2 (9.0)	256.3 (16.0) [b]	2.5 (2.8)	33.1
Whole corn cobs	--	1150	--	--	141.0 (8.8)	221.1 (13.8) [c]	--	--

[a] Feeding of corn stover was improved due to modified screw feeder; however, consistent compacted sheet was not made for this run. The bulk density of selectively chosen good compacted sheet was measured.

[b] Feeding of ground corn cobs was easier and consistent compacted sheet was made for this run.

[c] Feeding of whole cobs was easier, but consistent compacted sheet was not made for this run. The bulk density of agglomerated cobs was measured.

Chapter 4

Compaction Characteristics of Coarsely Ground Corn Stover and Perennial Grasses

Abstract

Compaction characteristics of coarsely ground corn stover and native perennial grasses were investigated using a piston-cylinder compaction apparatus. The inner diameter and height of the cylinder used were 88.7 mm (3.5 in.) and 143.8 mm (5.7 in.), respectively. Three compaction pressures of about 15, 30, and 60 MPa were studied. Corn stover and perennial grasses were coarsely ground using Mighty Giant tub-grinder with three different round-hole screen opening sizes [25.4 mm (1.0 in.), 76.2 mm (3.0 in.), and 127.0 mm (5.0 in.)] to obtain coarsely ground materials with three particle sizes (initial moisture contents were < 20% w.b.). A typical size of compacts produced was 90.2 mm (3.6 in.) diameter × 16.6 mm (0.7 in.) thickness. The unit density of individual compacts (measured after one week of curing at room temperature) ranged from 309 to 670 kg/m^3 (19 to 42 lb/ft^3). Higher pressure and smaller particle size resulted in higher density of compacts. Corn stover produced higher density compacts with lower volume expansion after one week of curing at room temperature than perennial grasses. Compressibility factors derived from compaction pressure-density relationships showed that corn stover was easier to compress than perennial grasses.

1. Objectives

The objectives of this study are (1) to study the compaction characteristics of coarsely ground corn stover and native perennial grasses, and (2) to estimate compressibility factors from compaction pressure-density relationships for coarsely ground corn stover and native perennial grasses. Compressibility factor is an important input for the design of roll press compactor (Johanson, 1965; Kaliyan and Morey, 2011).

2. Materials and Methods

We used a newly constructed piston-cylinder compaction apparatus for the tests (Fig. 1). The inner diameter and height of the cylinder (die) are 88.7 mm (3.49 in.) and 143.8 mm (5.66 in.), respectively. The thickness of the cylinder is 13.0 mm (0.51 in.). The diameter and height of the piston are 88.4 mm (3.48 in.) and 156.3 mm (6.15 in.), respectively. The gap between the cylinder and the piston is 0.13 mm (0.005 in.).

Corn stover and native perennial grasses were coarsely ground using Mighty Giant tub-grinder in March 2010 at Kolbeck, Inc., Le Mars, Iowa (Kaliyan et al., 2012). The native perennial grasses contained about 60% (by mass) of brome grass and the remaining was native prairie mix including fescue, foxtail, and weeds. Three round-hole screen opening sizes of 25.4 mm (1.0 in.), 76.2 mm (3.0 in.), and 127.0 mm (5.0 in.) were used in the Mighty Giant tub-grinder to obtain ground materials with three different particle sizes. The particle size analysis procedure developed for forage materials by Heinrichs and Kononoff (2012) was followed to determine the

geometric mean particle length of ground biomass materials. Geometric mean length and standard deviation of the particles were estimated by following the calculation procedure given in ASABE Standards (2009a). The moisture content of the particles ranged from 10% to 20% wet basis (w.b.). We did not attempt to adjust the moisture content of the tub-ground materials because it appeared that it would be difficult to arrive at uniform final moisture contents because of larger particle sizes.

Three compaction forces of 89.0, 177.9, and 355.9 kN (20,000, 40,000, and 80,000 lbf), corresponding compaction pressures of 14.4, 28.8, and 57.6 MPa, were studied. The compression forces were applied by Baldwin hydraulic universal testing machine (SATEC Systems Inc., Grove City, PA). About 60.0 g of biomass particles were filled inside the cylinder and then the piston was inserted into the cylinder. The cross-head of the Baldwin hydraulic universal testing machine was operated (downward movement) to apply compression force to the piston. After reaching a target compression force, the cross-head was retracted from the top of the piston. It was noted that the cross-head could not be stopped at exact target force because of inertia of the cross-head; thus, the cross-head was stopped as close as to the target compression force. Finally, the compact was pushed out of the cylinder manually using the piston.

A sample size of 60 g used for this compaction study was determined based on preliminary experiments which showed that either 60 g or 100 g of biomass sample used for the compaction tests resulted in similar compaction results (Table 1). No preheating or binders/additives were involved in this study.

During compression of biomass particles, the compression force (automatic display on the Baldwin controller) and displacement of the piston (MiniMag Height Gauge, Model IP54, www.iGaging.com) were recorded. It was noted that the force application was non-linear with respect to time. Typical time to reach 44.5, 177.9, and 355.9 kN (10,000, 40,000, and 80,000 lbf) was 27, 31, and 34 s, respectively. The force and displacement data were converted to pressure and in-die density of compacts, respectively. Out of-the die unit density (immediately after making) and cured unit density (after one week of making) were calculated based on the mass and volume of the compact. The volume of the compact was estimated from the diameter and thickness of the compacts measured using a digital caliper. The compacts were cured by storing the compacts in zip-lock plastic bags at room temperature (about 24 °C) for one week.

The measured compression data on applied pressure (P, MPa) and cured compact density (ρ, kg/m^3) were fitted to the equation (Johanson, 1965):

$$\text{Log}(\rho) = [(1/K)\ \log(P)] + C$$

Where, K is the compressibility factor (i.e., 1/slope), and C is the fitting constant (i.e., intercept of the model line).

The moisture content of the particles and compacts were measured based on ASABE Standards (2009b).

3. Results and Discussion

Figure 1 shows pictures of select compacted biomass. Tables 1 and 2 present the diameter, thickness, unit density, and expansion of compacted materials made at different combinations of compression force (pressure) and particle size.

In general, increasing compaction pressure or decreasing the particle size increased the unit density of compacts. Immediately after compaction, the out of-the die unit density of lab compacts ranged from 421 to 773 kg/m^3 (26 to 48 lb/ft^3) for the compaction pressures of about 15 to 60 MPa (Tables 1 and 2). The unit densities of compacts made in the lab compaction experiments and pilot-scale roll press compaction experiments (Kaliyan et al., 2011) were found to be similar. This may be due to the use of similar biomass feedstocks and similar compression forces (pressure) for both the lab and roll press experiments. It was found that more than 50% reduction in the in-die unit density compared to the out of-the die unit density of compacts (Tables 1 and 2). This may be due to the stress relaxation and elastic expansion of particles after the compact has been removed from the cylinder.

Unit density of individual compacts (measured after one week of curing at room temperature) ranged from 309 to 670 kg/m^3 (19 to 42 lb/ft^3) for the compaction pressures of about 15 to 60 MPa (Tables 1 and 2). The decrease in the unit density of cured compacts compared to the out of-the die unit density of compacts may have been due to continued elastic expansion of particles and loosening of some of the particle bonding. Loss of moisture (drying) during curing may have also contributed to the decrease in the unit density of cured compacts (Tables 1 and 2). During curing, the volume of the compacts increased by 17% to 47% (Tables 1 and 2). Corn stover resulted in a lower volume expansion than perennial grasses. Therefore, when trucking un-cured compacts made from coarsely ground corn stover and native perennial grasses, such as during a mobile compaction process, enough free-board (headroom) should be made available in the truck-trailer to account for the volume expansion of compacts.

Table 3 provides the compressibility factors for corn stover and native perennial grasses. The average compressibility factor (K) is 3.87 and 4.48 for corn stover and native perennial grasses, respectively. The lower K value for corn stover indicates that corn stover is easier to compress than perennial grasses (Johanson, 1965). The difference in compressibility between corn stover and perennial grasses may be due to fundamental differences in the structural, compositional, or mechanical properties of these two biomass feedstocks. The compressibility factors are used for the design of roll press compactor (Kaliyan and Morey, 2011).

4. Conclusions

In this study, compaction characteristics of coarsely ground corn stover and native perennial grasses [particles obtained from Mighty Giant tub-grinder with 25.4 to 127.0 mm (1.0 to 5.0 in.) screen opening sizes] were studied at compaction pressures of about 15 to 60 MPa. Key findings are:

- Unit density of individual compacts (measured after one week of curing at room temperature) ranged from 309 to 670 kg/m^3 (19 to 42 lb/ft^3).

- Higher compaction pressure and smaller particle size resulted in higher density of compacts.
- Corn stover produced higher density compacts with lower volume expansion than perennial grasses.
- Compressibility factors of corn stover and perennial grasses are 3.87 and 4.48, respectively. The compressibility factors show that corn stover is easier to compress than perennial grasses.

REFERENCES

ASABE Standards. 2009a. ANSI/ASAE S424.1 MAR1992 (R2007). Method of determining and expressing particle size of chopped forage materials by screening. St. Joseph, Mich.: ASABE.

ASABE Standards. 2009b. ASAE S358.2 DEC1998 (R2008): Moisture measurement – forages. St. Joseph, Mich.: ASABE.

Heinrichs, J., and P. Kononoff. 2012. Evaluating particle size of forages and TMRs using the New Penn State Forage Particle Separator. University Park, PA: Department of Dairy and Animal Science, The Pennsylvania State University. Available at: http://extension.psu.edu/animals/dairy/health/nutrition/forages/forage-quality-physical/separator/manual-and-spreadsheet-tool/evaluating-particle-size-of-forages-and-tmrs- using-the-new-penn-state-forage-particle-separator/view. Accessed 26 July 2012.

Johanson, J.R. 1965. A rolling theory for granular solids. *Trans. ASME J. Applied Mechanics* 32(4): 842-848.

Kaliyan, N., and R.V. Morey. 2011. Validation of roll press design equations for compaction of corn stover and perennial grasses. ASABE Paper No. 1110568. St. Joseph, Mich.: ASABE.

Kaliyan, N., R.V. Morey, and D.R. Schmidt. 2011. Roll press compaction of corn stover and perennial grasses. ASABE Paper No. 1110564. St. Joseph, Mich.: ASABE.

Kaliyan, N., D.R. Schmidt, R.V. Morey, and D.G. Tiffany. 2012. Commercial scale tub grinding of corn stover and perennial grasses. *Applied Eng. in Agric.* 28(1): 79-85.

Piston-Cylinder Compaction Apparatus

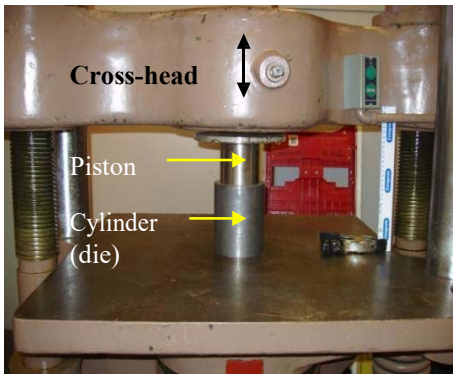

Compression of Biomass in Baldwin Testing Machine

Compacted Corn Stover Made at 14.5 MPa

Compacted Corn Stover Made at 59.5 MPa

Compacted Native Perennial Grasses Made at 14.7 MPa

Compacted Native Perennial Grasses Made at 59.7 MPa

Figure 1. Pictures of lab compaction apparatus, and compacted corn stover and native perennial grasses. These compacts were made using the ground corn stover and native perennial grasses obtained from Mighy Giant tub-grinder with 76.2 mm (3.0 in.) screen.

Table 1. Properties of compacted corn stover made in the laboratory.

Compaction force, kN (lbf) (n = 3)	Compaction pressure (MPa) (n = 3)	Properties of the compacts immediately after compaction (n = 3) *				Properties of the compacts after one week of curing at room temperature (n = 2)				
		Diameter (mm)	Thickness (mm)	Unit density, kg/m^3 (lb/ft^3)		Unit density, kg/m^3 (lb/ft^3)	Moisture content (% w.b.)	Expansion (%)		
				In-die density	Out of-the die density			Diameter	Thickness	Volume
Mighty Giant grinder screen size of 25.4 mm (1.0 in.); Particle size [&] = 6.09 ± 2.71 mm (0.24 ± 0.11 in.); Moisture content of particles 19.5 ± 1.8% w.b.										
91.2 ± 3.1 (20500 ± 693)	14.8 ± 0.5	90.1 ± 0.2	18.3 ± 0.8	1080.8 ± 21.0 (67.5 ± 1.3)	517.5 ± 12.6 (32.3 ± 0.8)	414.0 ± 17.7 (25.8 ± 1.1)	15.3 ± 0.1	1.3 ± 0.2	21.7 ± 6.3	25.0 ± 6.1
191.6 ± 9.8 (43067 ± 2203)	31.0 ± 1.6	90.2 ± 0.2	14.1 ± 0.9	1341.9 ± 67.0 (83.8 ± 4.2)	668.5 ± 34.6 (41.7 ± 2.2)	505.2 ± 3.5 (31.5 ± 0.2)	16.0 ± 0.1	1.2 ± 0.3	23.1 ± 1.9	26.0 ± 1.2
359.0 ± 1.9 (80700 ± 436)	58.1 ± 0.3	90.1 ± 0.1	13.5 ± 0.4	1522.4 ± 15.9 (95.0 ± 1.0)	699.2 ± 26.9 (43.7 ± 1.7)	559.5 ± 24.3 (34.9 ± 1.5)	15.8 ± 0.1	1.1 ± 0.1	22.4 ± 0.8	25.1 ± 0.7
Mighty Giant grinder screen size of 76.2 mm (3.0 in.); Particle size [&] = 8.11 ± 2.84 mm (0.32 ± 0.11 in.); Moisture content of particles 10.0 ± 3.1% w.b.										
89.9 ± 0.4 (20200 ± 100)	14.5 ± 0.1	90.1 ± 0.1	17.9 ± 0.4	969.6 ± 5.9 (60.5 ± 0.4)	525.7 ± 7.3 (32.8 ± 0.5)	425.0 ± 4.1 (26.5 ± 0.3)	10.5 ± 0.2	0.8 ± 0.1	18.7 ± 0.6	20.6 ± 0.4
186.7 ± 6.1 (41967 ± 1365)	30.2 ± 1.0	89.9 ± 0.2	14.2 ± 0.3	1164.3 ± 34.4 (72.7 ± 2.1)	656.9 ± 23.3 (41.0 ± 1.5)	531.5 ± 28.3 (33.2 ± 1.8)	11.1 ± 0.2	1.0 ± 0.1	17.8 ± 1.8	20.2 ± 1.6
367.6 ± 14.0 (82633 ± 3156) [#]	59.5 ± 2.3	89.6 ± 0.1	12.4 ± 0.4	1471.2 ± 24.1 (91.8 ± 1.5)	772.6 ± 30.2 (48.2 ± 1.9)	669.7 ± 25.5 (41.8 ± 1.6)	10.6 ± 0.1	1.1 ± 0.1	14.0 ± 3.8	16.6 ± 3.7
Mighty Giant grinder screen size of 127.0 mm (5.0 in.); Particle size [&] = 10.30 ± 4.11 mm (0.41 ± 0.16 in.); Moisture content of particles 16.7 ± 2.6% w.b.										
91.6 ± 1.3 (20600 ± 300)	14.8 ± 0.2	90.5 ± 0.1	19.4 ± 1.4	1031.2 ± 44.1 (64.4 ± 2.8)	481.7 ± 30.8 (30.1 ± 1.9)	381.9 ± 48.8 (23.8 ± 3.0)	13.7 ± 0.1	2.7 ± 0.2	15.6 ± 5.0	22.0 ± 5.7
187.7 ± 6.7 (42200 ± 1513)	30.4 ± 1.1	90.2 ± 0.1	16.0 ± 1.3	1235.3 ± 77.8 (77.1 ± 4.9)	584.7 ± 43.6 (36.5 ± 2.7)	478.0 ± 73.0 (29.8 ± 4.6)	13.3 ± 0.3	1.5 ± 0.04	16.2 ± 5.1	19.6 ± 5.1
355.6 ± 2.5 (79933 ± 551)	57.5 ± 0.4	90.3 ± 0.4	14.2 ± 0.9	1485.6 ± 43.5 (92.7 ± 2.7)	664.7 ± 43.9 (41.5 ± 2.7)	536.7 ± 10.3 (33.5 ± 0.6)	14.8 ± 0.2	1.3 ± 0.04	23.1 ± 0.5	26.2 ± 0.4

***** The mass of individual compacts is about 60.0 g.

[&] Geometric mean particle length ± geometric standard deviation.

[#] For corn stover (from Mighty Giant tub-grinder with 76.2 mm screen) with a mass of 98.7 g compressed at 82,200 lbf (41.1 ton or 59.2 MPa) resulted in compact diameter of 90.1 mm, thickness of 20.0 mm, in-die density of 1353.0 kg/m^3 (84.5 lb/ft^3), and out-of-the die density of 773.4 kg/m^3 (48.3 lb/ft^3). After one week of curing, the results were unit density of 680.1 kg/m^3 (42.5 lb/ft^3), moisture content of 10.6 ± 0.004% (w.b.), expansion in diameter of 1.1%, expansion in thickness of 9.8%, and expansion in volume of 12.2%.

Table 2. Properties of compacted native perennial grasses made in the laboratory.

Compaction force, kN (lbf) (n = 3)	Compaction pressure (MPa) (n = 3)	Properties of the compacts immediately after compaction (n = 3) *				Properties of the compacts after one week of curing at room temperature (n = 2)				
		Diameter (mm)	Thickness (mm)	Unit density, kg/m^3 (lb/ft^3)		Unit density, kg/m^3 (lb/ft^3)	Moisture content (% w.b.)	Expansion (%)		
				In-die density	Out of-the die density			Diameter	Thickness	Volume
Mighty Giant grinder screen size of 25.4 mm (1.0 in.); Particle size & = 2.55 ± 2.72 mm (0.10 ± 0.11 in.); Moisture content of particles 17.1 ± 0.6% w.b.										
93.9 ± 9.8 (21100 ± 2193)	15.2 ± 1.6	90.6 ± 0.2	19.4 ± 1.1	1146.1 ± 40.0 (71.6 ± 2.5)	481.4 ± 26.4 (30.1 ± 1.6)	386.5 ± 22.5 (24.1 ± 1.4)	15.0 ± 0.1	1.0 ± 0.1	22.3 ± 1.7	24.8 ± 1.9
181.3 ± 4.4 (40767 ± 981)	29.3 ± 0.7	90.1 ± 0.3	16.1 ± 0.2	1346.9 ± 2.0 (84.1 ± 0.1)	587.1 ± 6.0 (36.7 ± 0.4)	468.1 ± 7.2 (29.2 ± 0.4)	15.0 ± 0.4	1.2 ± 0.2	21.1 ± 0.4	23.9 ± 0.1
361.3 ± 4.9 (81233 ± 1102)	58.5 ± 0.8	90.1 ± 0.2	14.0 ± 0.8	1496.9 ± 56.0 (93.4 ± 3.5)	667.5 ± 46.0 (41.7 ± 2.9)	500.5 ± 44.4 (31.2 ± 2.8)	16.1 ± 0.2	1.3 ± 0.1	24.3 ± 4.0	27.5 ± 4.2
Mighty Giant grinder screen size of 76.2 mm (3.0 in.); Particle size & = 3.50 ± 3.06 mm (0.14 ± 0.12 in.); Moisture content of particles 17.9 ± 1.3% w.b.										
90.7 ± 0.4 (20400 ± 100)	14.7 ± 0.1	90.7 ± 0.5	22.2 ± 1.5	1056.1 ± 13.4 (65.9 ± 0.8)	420.6 ± 33.4 (26.3 ± 2.1)	324.3 ± 7.6 (20.2 ± 0.5)	16.4 ± 0.2	1.8 ± 0.8	25.0 ± 10.2	29.6 ± 12.5
180.2 ± 3.6 (40500 ± 819)	29.2 ± 0.6	90.2 ± 0.2	17.0 ± 1.8	1275.7 ± 29.5 (79.6 ± 1.8)	559.8 ± 52.8 (34.9 ± 3.3)	457.0 ± 2.0 (28.5 ± 0.1)	17.2 ± 0.2	1.4 ± 0.3	22.8 ± 1.7	26.4 ± 1.1
368.9 ± 9.8 (82933 ± 2194)	59.7 ± 1.6	90.3 ± 0.1	14.9 ± 0.4	1477.5 ± 25.1 (92.2 ± 1.6)	626.3 ± 15.5 (39.1 ± 1.0)	485.1 ± 1.0 (30.3 ± 0.1)	17.9 ± 0.1	1.5 ± 0.3	23.8 ± 2.5	27.7 ± 1.8
Mighty Giant grinder screen size of 127.0 mm (5.0 in.) ; Particle size & = 5.82 ± 3.68 mm (0.23 ± 0.15 in.); Moisture content of particles 20.1 ± 0.8% w.b.										
90.7 ± 4.0 (20400 ± 889)	14.7 ± 0.6	90.5 ± 0.4	21.8 ± 1.3	1027.3 ± 14.1 (64.1 ± 0.9)	432.6 ± 25.9 (27.0 ± 1.6)	308.5 ± 12.3 (19.3 ± 0.8)	15.1 ± 0.4	2.8 ± 1.1	24.9 ± 3.4	32.0 ± 0.7
180.9 ± 2.7 (40667 ± 603)	29.3 ± 0.4	90.5 ± 0.3	18.0 ± 1.6	1238.4 ± 22.9 (77.3 ± 1.4)	521.2 ± 48.2 (32.5 ± 3.0)	365.4 ± 24.8 (22.8 ± 1.5)	15.0 ± 1.5	2.9 ± 0.5	38.8 ± 5.4	46.9 ± 4.1
356.0 ± 3.0 (80033 ± 666)	57.6 ± 0.5	90.4 ± 0.04	16.0 ± 1.2	1421.8 ± 2.3 (88.8 ± 0.1)	589.3 ± 47.0 (36.8 ± 2.9)	414.4 ± 48.9 (25.9 ± 3.1)	15.4 ± 0.2	2.4 ± 1.3	37.9 ± 3.9	44.6 ± 7.7

* The mass of individual compacts is about 60.0 g.

& Geometric mean particle length ± geometric standard deviation.

Table 3. Compressibility factors for corn stover and native perennial grasses.

Mighty Giant grinder screen size, mm (in.)	Moisture content of particles (% w.b.)	Maximum pressure range (MPa)	Cured compact density range (kg/m^3)	Compression model *	Compressibility factor (K)
Corn Stover					
25.4 (1.0)	19.5 ± 1.8	14.5 to 58.5	401.4 to 576.7	Log(ρ) = 0.2208 log(P) + 2.3637 (R^2 = 0.9538)	4.53
76.2 (3.0)	10.0 ± 3.1	14.5 to 61.8	422.0 to 687.8	Log(ρ) = 0.3230 log(P) + 2.2509 (R^2 = 0.9894)	3.10
127.0 (5.0)	16.7 ± 2.6	14.6 to 57.8	347.4 to 544.0	Log(ρ) = 0.2512 log(P) + 2.2932 (R^2 = 0.7853)	3.98
Native Perennial Grasses					
25.4 (1.0)	17.1 ± 0.6	14.0 to 59.2	370.6 to 531.9	Log(ρ) = 0.1884 log(P) + 2.3748 (R^2 = 0.8235)	5.31
76.2 (3.0)	17.9 ± 1.3	14.6 to 60.6	318.9 to 485.8	Log(ρ) = 0.2855 log(P) + 2.1993 (R^2 = 0.8468)	3.50
127.0 (5.0)	20.1 ± 0.8	14.2 to 58.0	299.8 to 449.0	Log(ρ) = 0.2156 log(P) + 2.2403 (R^2 = 0.8695)	4.64

* The compression data on applied pressure (P, MPa) and cured compact density (ρ, kg/m^3) were fitted to the equation: Log(ρ) = [(1/K) log(P)] + C, where K is the compressibility factor (i.e., 1/slope) and C is the fitting constant (i.e., intercept of the model line).

Chapter 5

Validation of Roll Press Design Equations for Compaction of Corn Stover and Perennial Grasses

Abstract

The objective of this study was to validate roll press design equations given by Johanson (1965) and Blake et al. (1963). The roll press design equations were validated for pilot-scale roll press compaction data collected for corn stover and native perennial grasses (initial moisture contents of < 20% w.b.) ground using three Mighty Giant tub-grinder round-hole screen opening sizes (25.4, 76.2, and 127.0 mm), three roll forces (24, 40, and 60 ton), and two roll gap sizes (0.012 and 0.022 m). Laboratory compaction data collected for three compression pressures of about 15, 30, and 60 MPa were used to obtain input parameters (compressibility factor, and pressure-deformation relationship) needed by the roll press design equations. Johanson (1965) model predicted the roll force with a mean relative percent error of 47% to 61%. Blake et al. (1963) model calculated the unit density of compacts (measured after curing) with a mean relative percent error of 18% to 30%. The mean relative percent error in prediction of specific energy consumption for rolls (excluding no-load roll motor energy consumption) was 48% to 83% for Johanson (1965) model, and 37% to 71% for Blake et al. (1963) model. The validated roll press design equations will be used for deriving design specifications for a production scale roll press compactor.

1. Objectives

The objective of this study was to validate the roll press design equations given by Johanson (1965) and Blake et al. (1963) using data collected from a pilot-scale roll press compaction of corn stover and native perennial grasses, and data collected from a laboratory compaction study. The validated roll press design equations will be used for deriving design specifications for a production scale (25 ton/h) roll press compactor.

2. Materials and Methods

2.1 Roll Press Compactor Design Equations

2.1.1 Johanson (1965) Model

Johanson (1965) established relationships for roll force (R_f) and roll torque (R_t) as functions of roll pressure (P), roll diameter (D), roll width (W), roll gap (R_g), and compressibility factor (K) (Fig. 1). The roll gap (R_g) is the sum of two times the depth of pockets on one of the rolls (d/2) plus the pre-set roll gap (S) [i.e., $R_g = d + S$]. It is noted that the pre-set roll gap (S) varied during the pilot-scale roll press experiments due to the floating of one of the rolls.

The equation for roll force is (Johanson, 1965):

$$R_f = P\ W\ D\ F_f / 2 \quad (1)$$

Where, R_f = roll separating force (MN); P = applied pressure that may produce the required density of compact (obtained from the uniaxial lab compression test) (MPa); W = roll width (m); D = roll diameter (m); and F_f = force factor, estimated as a function of D, d, S, and K using Eq. 2 (Johanson, 1965).

$$F_f = \frac{\pi}{180}\int_{\theta=0}^{\theta=\alpha}\left[\frac{(d+S)/D}{\frac{d}{D}+[(1+\frac{S}{D}\cos\theta)\cos\theta]}\right]^K \cos\theta\, d\theta \quad (2)$$

The equation for roll torque is (Johanson, 1965):

$$R_t = P\ W\ D^2\ T_f / 8 \quad (3)$$

Where, T_f = torque factor, estimated as a function of D, d, S, and K using Eq. 4 (Johanson, 1965).

$$T_f = \frac{\pi}{180}\int_{\theta=0}^{\theta=\alpha}\left[\frac{(d+S)/D}{\frac{d}{D}+[(1+\frac{S}{D}\cos\theta)\cos\theta]}\right]^K \sin 2\theta\, d\theta \quad (4)$$

The force factor and torque factor integrals were evaluated numerically using trapezoidal rule (Cheney and Kincaid, 1985). In this study, these integrals were evaluated for a maximum angle of θ where P is about zero (i.e., $\theta = \alpha = 60^\circ$).

Johanson (1965) derived the following relationship between the pressure and density for compaction of powdered materials during uniaxial compression in laboratory compaction apparatus.

$$(\rho/\rho_o) = (P/P_o)^{(1/K)} \quad (5)$$

Where, ρ is compact density (out-of-the die density after curing one week at room temperature) at pressure P, and K is the compressibility factor of powdered material. Using the above relationship, the roll pressure required to produce a compact with a prescribed compact density is estimated.

2.1.2 Blake et al. (1963) Model

Blake et al. (1963) modeled the force between the rolls (R_f) as a function of the diameter (D) of the rolls, the width of the rolls (W), the angle θ subtended at the center of the roll by a particular position of an element of powdered material and the horizontal, and the actual pressure P on the element of material at angle θ.

The force between the rolls (R_f) is (Blake et al., 1963):

$$R_f = \frac{\pi DW}{360}\int_{p=0,\ \theta}^{Pmax,\ \theta=0} P(\theta)\ \cos\theta\, d\theta \quad (6)$$

From the roll force, the torque on each roll (R_t) can be calculated as:

$$R_t = \frac{\pi D^2 W}{720} \int_{P=0,\ \theta}^{Pmax,\ \theta=0} P(\theta)\ cos\ \theta\ sin\ \theta\ d\theta \quad (7)$$

Where, P is the actual pressure on an element of material at an angle θ measured upward from the center of the rolls. The angle θ is zero at the horizontal line connecting the centers of the rolls. The roll force and roll torque integrals can be evaluated if P is known as a function of θ. The integrals were evaluated numerically using trapezoidal rule (Cheney and Kincaid, 1985). In this study, the integrals were evaluated for a maximum angle of θ where P is about zero.

To get the relation between P and θ, it is first necessary to assume a maximum pressure (P_{max}). For this assumed maximum pressure, laboratory compaction test is conducted to get a compression curve between P and Δ L/L. Where, L is the thickness of the compact (in-die) at the maximum pressure, and Δ L is the difference between the compact thickness (in-die) at the maximum pressure and the compact thickness (in-die) at any other pressure. For the assumed maximum compression pressure, a polynomial relationship between P and Δ L/L is established.

If L is the minimum roll gap (i.e., the thickness of compact at the minimum roll gap = R_g = d + S), then, from the geometry of the rolls, Δ L/L = D/L [1 – cos θ]. The expressions for Δ L/L for the roll press and the lab compaction can be equated, and they provide the relation between P and θ. While numerical integration of the roll force and torque equations, a value for θ is chosen and Δ L/L for the roll press is calculated; using this Δ L/L value, the corresponding pressure is obtained from the polynomial relationship between P and Δ L/L for the lab compaction data. With the integrals evaluated, the roll force and torque corresponding to the assumed maximum pressure is readily calculated. In this manner, a linear relationship between the roll force or torque and the maximum compaction pressure can be derived for a given roll press compactor specifications (D, W, and L).

2.1.3 Throughput, Power, and Specific Energy Consumption

The theoretical relationships for calculating throughput of roll press compactor, roll motor power, and specific energy consumption for operation of the rolls are given below.

$$\text{Throughput of roll press compactor } (C_c) = 60\ \rho_g \pi\ D\ W\ R_g\ R_s / 1000 \quad (8)$$

Where, C_c = throughput of roll compactor (t/h), ρ_g = density of roll press compacts at the minimum roll gap before exiting the rolls (kg m^{-3}), D = roll diameter (m), W = roll width (m), R_g = roll gap (m) (two half-pocket depths plus gap between rolls), and R_s = roll speed (rpm). ρ_g is calculated based on the mass of biomass compacted per unit time (i.e., throughput) and the theoretical volume of the roll press compactor that caused this throughput. The volume is calculated as a function of D, W, R_g, and R_s.

$$\text{Roll motor power required for operating two rolls } (R_p) = 2\ R_t\ \omega \quad (9)$$

Where, R_p = roll power (MW), R_t = roll torque (MN-m) estimated based on Johanson (1965) model or Blake et al. (1963) model, $\omega = (2 \pi R_s / 60)$, ω = angular velocity of rolls (s^{-1}), and R_s = roll speed (rpm). Please note that 1 MW = 1340.483 hp.

Specific energy consumption (MJ/t) for operating two rolls (R_{se}) = $3600 R_p / C_c$ (10)

Where, R_p = roll power (MW), and C_c = throughput of roll compactor (t/h)

2.2 Experimental Data

The roll press design equations were validated using pilot-scale roll press compaction data given in Kaliyan et al. (2011a). From Kaliyan et al. (2011a), we have collected data on roll diameter (D = 0.521 m), roll width (W = 0.127 m), roll gap (R_g = L = 0.012 m or 0.022 m), roll speed (R_s), throughput (C_c), and specific energy consumption (R_{se}) for roll press compaction of corn stover and native perennial grasses. The native perennial grasses contained about 60% (by mass) of brome grass and the remaining was native prairie mix including fescue, foxtail, and weeds. According to the roll pocket dimension (d = 2 x 5.1 mm) and set roll gap (2.03 mm), the minimum roll gap (R_g or L) is 0.012 m. However, the minimum roll gap increased during the roll press operation due to the floating of one of the rolls. Thus, assuming a maximum floating roll displacement of 10.0 mm, modeling results were calculated for another minimum roll gap (R_g or L) of 0.022 m.

The roll press design equations were validated for two biomass materials (corn stover and native perennial grasses) ground using three Mighty Giant tub-grinder round-hole screen opening sizes (25.4, 76.2, and 127.0 mm), three roll forces (24, 40, and 60 ton), and two minimum roll gap sizes (R_g = L = 0.012 m or 0.022 m).

From Kaliyan et al. (2011b), lab compaction experimental results were obtained for three maximum compression pressures of about 15, 30, and 60 MPa for corn stover and perennial grass particles obtained from three Mighty Giant tub-grinder round-hole screen opening sizes (25.4, 76.2, and 127.0 mm). From the lab compaction data, compressibility factors (K) for corn stover and perennial grasses were estimated (Table 1). The compressibility factors are used in the Johanson (1965) model. Also, polynomial relationships between maximum compaction pressure P and Δ L/L for lab compaction data were obtained to use in Blake et al. (1963) model. An example calculation involved for Blake et al. (1963) model is given in Table 2.

No binders (additives) or preheating was involved for pilot-scale roll press and lab compaction experiments. The particle size analysis procedure developed for forage materials by Heinrichs and Kononoff (2012) was followed to determine the geometric mean particle length of ground biomass materials. Geometric mean length and standard deviation of the particles were estimated by following the calculation procedure given in ASABE Standards (2009a). Moisture content of the ground materials was measured based on ASABE Standards (2009b).

2.3 Validation of Johanson (1965) Model

To validate the roll force calculated using Johanson (1965) model, first it is assumed that the maximum pressure required to produce compacts with a given unit density (measured after curing one-week at room temperature) is the same for roll press compaction and lab compaction. Using the lab compaction data, a relationship between maximum pressure and unit density of compacts (cured) is established (Eq. 5). From this relationship between pressure and cured density, for each pilot-scale roll press experiment, the maximum roll pressure (P) that may have been applied to the rolls is calculated for the measured (cured) unit density of roll press compacts. Then, the roll force is calculated using Johanson (1965) model (Eq. 1) by inputting the maximum roll pressure (P) to the Eq. 1. Finally, this calculated roll force and the actual roll force applied to the rolls during the pilot-scale roll press experiments are compared.

Similarly, for a given maximum roll pressure (P), the roll torque is calculated using Eq. 3. The calculated roll torque is used to estimate the roll power (Eq. 9) and specific energy consumption for the rolls (Eq. 10). Then, the calculated and measured specific energy consumption (excluding no-load roll motor energy consumption) values are compared.

The throughput of the roll press compactor is calculated using Eq. 8 and compared with the measured data.

2.4 Validation of Blake et al. (1963) Model

To validate the Blake et al. (1963) model, first it is assumed that the maximum pressure required to produce compacts with a given unit density (measured after curing one-week at room temperature) is the same for roll press compaction and lab compaction. Using the lab compaction data, a relationship between maximum pressure and unit density of compacts (cured) is established (Eq. 5). Then, using the linear relationship established between the roll force [calculated using Blake et al. (1963) model] and the maximum pressure, the maximum pressure experienced by the rolls is calculated for an applied roll force. Applied roll force is used to calculate the roll pressure due to the fact that the material experiences the applied roll force during the roll press operation as indicated by floating of one of the rolls. From the relationship between pressure and cured density (Eq. 5), for each pilot-scale roll press experiment, the cured density of compact is calculated by inputting the calculated maximum roll pressure (due to the applied force). Finally, the calculated and measured (cured) unit densities of roll press compacts are compared.

The roll torque is calculated using the linear relationship established between the roll torque [calculated using Blake et al. (1963) model] and the maximum roll pressure. The calculated roll torque is used to estimate the roll power (Eq. 9) and specific energy consumption for the rolls (Eq. 10). Then, the calculated and measured specific energy consumption (excluding no-load roll motor energy consumption) values are compared.

The throughput of the roll press compactor is calculated using Eq. 8 and compared with the measured data.

3. Results and Discussion

Tables 3 and 4 provide example results for Johanson (1965) model validation for corn stover and native perennial grasses, respectively. Tables 5 and 6 provide example results for Blake et al. (1963) model validation for corn stover and native perennial grasses, respectively. The throughput of the roll press was calculated with 1.1% to 2.0% of mean relative percent error by using the at-the-minimum-gap unit density of roll press compacts in the throughput model (Eq. 8). The predicted maximum pressure created between the rolls ranged from 11 to 153 MPa for the applied roll forces of 24 to 60 ton.

For validation of both models, increasing the minimum roll gap (R_g or L) from 0.012 m to 0.022 m decreased the mean relative percent errors for the prediction of roll force, cured unit density of compacts, and specific energy consumption for rolls (Table 7). This indicates that the minimum roll gap during operation of the roll press may have been larger than the pre-set roll gap (i.e., 1.12 m). The measured thickness of compacts (after curing) ranged from 20.0 to 27.7 mm for corn stover and from 25.1 to 37.0 mm for perennial grasses. Thus, the measured thicknesses of compacts also suggest that the roll gap varied during the operation of roll press. The variation in roll gap may be affected by the screw feeder operation. Therefore, the minimum roll gap needs to be measured accurately for better validation of roll press design equations.

The average compressibility factor (K) is 3.87 and 4.48 for corn stover and native perennial grasses, respectively (Table 1). The lower K value for corn stover indicates that corn stover is easier to compress than perennial grasses (Johanson, 1965). Johanson (1965) model predicts the roll force with a mean relative percent error of 46.5% to 60.9% (Table 7). One reason for predicting the roll force with a higher mean relative percent error is that Johanson (1965) model considers only the densification effect on the roll force and neglects the effect of elastic spring-back of compacts on the roll force.

Peter et al. (2010) reported that the roll force due to elastic spring-back of compacts in the roll press can be as much as 30% of the total roll force. Yusof et al. (2005) found that Johanson (1965) model predicted the roll force and roll torque with an accuracy of 20% for maize powder with compressibility factor of 9.0. Dec et al. (2003) concluded that Johanson (1965) model predicts the roll force and roll torque with larger errors (as much as 50%) for materials with low compressibility factors.

Blake et al. (1963) model predicts the (cured) unit density of roll press compacts with a mean relative percent error of 18.3% to 30.0% (Table 7). Although it appears Blake et al. (1963) model is more accurate than Johanson (1965) model, it should be noted that both models ignore the effect of shear forces that would occur during the roll press compaction. Also, modeling results may be affected by the possible measurement errors that may have happened during roll press compaction and lab compaction studies.

Johanson (1965) model calculates the maximum roll power requirement of 5.4 hp. Blake et al. (1963) model predicts the maximum roll power requirement of 12.2 hp. The mean relative percent error in prediction of specific energy consumption for rolls (excluding no-load roll motor energy consumption) is 47.6% to 83.1% for Johanson (1965) model and 36.6% to 71.4% for

Blake et al. (1963) model (Table 7). Both models resulted in lower relative percent errors for native perennial grasses than for corn stover (Table 7). It is noted that these two theoretical models do not include efficiency of the roll press components such as motor and speed reduction systems. The pilot-scale roll press was operated with a 50 hp motor and was designed to operate as high as 20 rpm whereas the maximum roll speed involved in our study was 3.3 rpm. Also, the measured specific energy consumption data showed that about 52% to 87% of the total energy input was required to operate the empty (i.e., no-load) roll press (Kaliyan et al., 2011a). Thus, including a motor efficiency, the roll press design models may result in reasonable estimates for roll motor power requirement and specific energy consumption for rolls.

4. Conclusions

The following conclusions were drawn from validation of roll press design equations given by Johanson (1965) and Blake et al. (1963) for roll press compaction of corn stover and native perennial grasses.

- Johanson (1965) model predicts the roll force with a mean relative percent error of 47% to 61%.
- Blake et al. (1963) model calculates the unit density of compacts (measured after curing) with a mean relative percent error of 18% to 30%.
- The mean relative percent error in prediction of specific energy consumption for rolls (excluding no-load roll motor energy consumption) is 48% to 83% for Johanson (1965) model and 37% to 71% for Blake et al. (1963) model. Both Johanson (1965) and Blake et al. (1963) models may be used to obtain reasonable estimates on the roll power requirement and specific energy consumption for the operation of rolls.

REFERENCES

ASABE Standards. 2009a. ANSI/ASAE S424.1 MAR1992 (R2007). Method of determining and expressing particle size of chopped forage materials by screening. St. Joseph, Mich.: ASABE.

ASABE Standards. 2009b. ASAE S358.2 DEC1998 (R2008): Moisture measurement – forages. St. Joseph, Mich.: ASABE.

Blake, J.H., R.G. Minet, and W.P. Steen. 1963. Pressure developed in a roll-type briquet press. Proceedings of the 8th IBA Biennial Briquetting Conference. pp. 38-48.

Cheney, W., and D. Kincaid. 1985. *Numerical Mathematics and Computing*. Monterey, Cal.: Brooks/Cole Publishing.

Dec, R.T., A. Zavaliangos, and J.C. Cunningham. 2003. Comparison of various methods for analysis of powder compaction in roller press. *Powder Tech.* 130(1-3): 265-271.

Heinrichs, J., and P. Kononoff. 2012. Evaluating particle size of forages and TMRs using the New Penn State Forage Particle Separator. University Park, PA: Department of Dairy and Animal Science, The Pennsylvania State University. Available at: http://extension.psu.edu/animals/dairy/health/nutrition/forages/forage-quality-physical/separator/manual-and-spreadsheet-tool/evaluating-particle-size-of-forages-and-tmrs-using-the-new-penn-state-forage-particle-separator/view. Accessed 26 July 2012.

Johanson, J.R. 1965. A rolling theory for granular solids. *Trans. ASME J. Applied Mechanics* 32(4): 842-848.

Kaliyan, N., R.V. Morey, and D.R. Schmidt. 2011a. Roll press compaction of corn stover and perennial grasses. ASABE Paper No. 1110564. St. Joseph, Mich.: ASABE.

Kaliyan, N., D.R. Schmidt, and R.V. Morey. 2011b. Compaction characteristics of coarsely ground corn stover and perennial grasses. ASABE Paper No. 1110566. St. Joseph, Mich.: ASABE.

Peter, S., R.F. Lammens, and K.J. Steffens. 2010. Roller compaction/dry granulation: Use of the thin layer model for predicting densities and forces during roller compaction. *Powder Tech.* 199(2): 165-175.

Yusof, Y.A., A.C. Smith, and B.J. Briscoe. 2005. Roll compaction of maize powder. *Chemical Eng. Sci.* 60(14): 3919-3931.

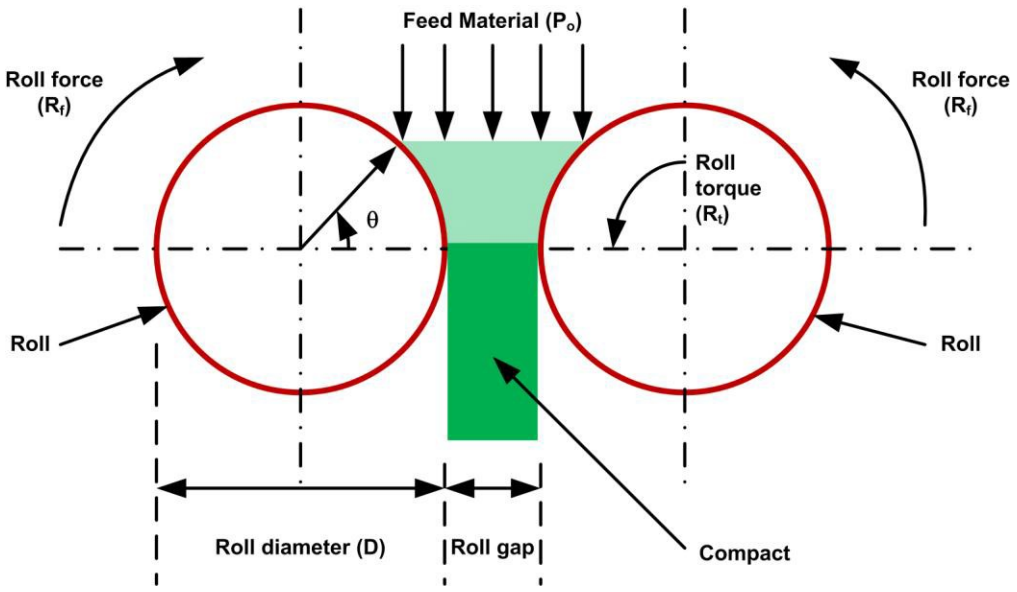

Figure 1. Schematic of a roll press compaction process.

Table 1. Compressibility factors for corn stover and native perennial grasses obtained from lab compaction study (Kaliyan et al., 2011b).

Mighty Giant grinder screen size, mm (in.)	Moisture content of particles (% w.b.)	Maximum pressure range (MPa)	Cured compact density range (kg/m^3)	Compression model (Eq. 5) *	Compressibility factor (K)
Corn Stover					
25.4 (1.0)	19.5 ± 1.8	14.5 to 58.5	401.4 to 576.7	Log(ρ) = 0.2208 log(P) + 2.3637 (R^2 = 0.9538)	4.53
76.2 (3.0)	10.0 ± 3.1	14.5 to 61.8	422.0 to 687.8	Log(ρ) = 0.3230 log(P) + 2.2509 (R^2 = 0.9894)	3.10
127.0 (5.0)	16.7 ± 2.6	14.6 to 57.8	347.4 to 544.0	Log(ρ) = 0.2512 log(P) + 2.2932 (R^2 = 0.7853)	3.98
Native Perennial Grasses					
25.4 (1.0)	17.1 ± 0.6	14.0 to 59.2	370.6 to 531.9	Log(ρ) = 0.1884 log(P) + 2.3748 (R^2 = 0.8235)	5.31
76.2 (3.0)	17.9 ± 1.3	14.6 to 60.6	318.9 to 485.8	Log(ρ) = 0.2855 log(P) + 2.1993 (R^2 = 0.8468)	3.50
127.0 (5.0)	20.1 ± 0.8	14.2 to 58.0	299.8 to 449.0	Log(ρ) = 0.2156 log(P) + 2.2403 (R^2 = 0.8695)	4.64

* The compression data on applied pressure (P, MPa) and cured compact density (ρ, kg/m^3) were fitted to the equation: Log(ρ) = [(1/K) log(P)] + C, where K is the compressibility factor (i.e., 1/slope) and C is the fitting constant (i.e., intercept of the model line).

Table 2. Input and outputs for Blake et al. (1963) model for an example case for corn stover with moisture content of 10.0% (w.b.) ground using Mighty Giant grinder screen opening size of 76.2 mm (3.0 in.).

Lab compaction maximum pressure (MPa)	Polynomial relationship between compaction pressure P in MPa (= Y) and ΔL/L (= x) for lab compaction data	Maximum pressure (P, MPa) and cured unit density of compacts (ρ, kg m^{-3}) relationship for lab compaction data	Roll force (R_f, ton) and maximum roll pressure (P, MPa) relationship from Blake et al. (1963) model for D = 0.521 m, W = 0.127 m, and L = 0.012 m	Roll force (R_f, ton) and maximum roll pressure (P, MPa) relationship from Blake et al. (1963) model for D = 0.521 m, W = 0.127 m, and L = 0.022 m	Roll torque (R_t, MN-m) and maximum roll pressure (P, MPa) relationship from Blake et al. (1963) model for D = 0.521 m, W = 0.127 m, and L = 0.012 m	Roll torque (R_t, MN-m) and maximum roll pressure (P, MPa) relationship from Blake et al. (1963) model for D = 0.521 m, W = 0.127 m, and L = 0.022 m
14.5	$Y = 0.1311 x^6 - 1.8971 x^5 + 10.72 x^4 - 30.181 x^3 + 45.206 x^2 - 36.205 x + 14.427$ ($R^2 = 0.9992$)	$\text{Log}(\rho) = 0.3230 \log(P) + 2.2509$ ($R^2 = 0.9894$)	$P = 2.1129 R_f - 0.0644$ ($R^2 = 0.9982$)	$P = 1.5677 R_f - 0.0625$ ($R^2 = 0.9982$)	$R_t = 9.4912E-05 P + 5.8766E-05$ ($R^2 = 0.9912$)	$R_t = 1.7154E-04 P + 1.0957E-04$ ($R^2 = 0.9918$)
30.2	$Y = 0.188 x^6 - 3.1132 x^5 + 19.977 x^4 - 62.78 x^3 + 101.23 x^2 - 81.419 x + 29.566$ ($R^2 = 0.9934$)					
59.5	$Y = 0.0452 x^6 - 1.112 x^5 + 10.58 x^4 - 49.041 x^3 + 114.93 x^2 - 128.55 x + 57.459$ ($R^2 = 0.9931$)					

Notes: L = thickness of the compact (in-die) at the maximum pressure (P, MPa); ΔL= difference between the compact thickness (in-die) at the maximum pressure (P, MPa) and the compact thickness (in-die) at any other pressure (P_i, MPa); D = roll diameter (m); W = roll width (m); L = minimum roll gap (m).

Table 3. Results for corn stover with Johanson (1965) model (D = 0.521 m, W = 0.127 m, and R_g = 0.012 m).

Measured data from pilot-scale roll press compaction (Kaliyan et al., 2011a)						Calculated values using Johanson (1965) model					Relative percent error (%) *		
R_f (ton)	R_s (rpm)	ρ_g (kg m^{-3})	ρ_c (kg m^{-3})	C_c (t/h)	R_{se} (MJ/t)	C_c (t/h)	P (MPa)	R_f (ton)	R_p (hp)	R_{se} (MJ/t)	C_c	R_f	R_{se}
Mighty Giant grinder screen size = 25.4 mm (1.0 in.); Particle size & = 6.09 ± 2.71 mm (0.24 ± 0.11 in.); Moisture content of particles = 17.9 ± 0.7% w.b.													
24	1.6	755.5	394.6	0.18	40.4	0.18	11.3	4.2	0.29	8.2	2.4	82.6	79.7
40	1.1	1213.3	508.4	0.20	170.7	0.20	35.6	13.1	0.64	20.0	1.8	67.2	88.3
60	1.2	975.9	489.9	0.18	237.8	0.18	30.1	11.1	0.59	17.6	0.8	81.5	92.6
Mighty Giant grinder screen size = 76.2 mm (3.0 in.); Particle size & = 8.11 ± 2.84 mm (0.32 ± 0.11 in.); Moisture content of particles = 10.2 ± 0.2% w.b.													
24	1.2	970.2	420.9	0.18	101.2	0.18	14.3	6.7	0.48	16.6	1.3	72.1	83.6
40	1.2	896.7	627.9	0.16	188.2	0.16	49.4	23.1	1.64	38.4	2.6	42.1	79.6
60	1.2	797.5	724.4	0.15	304.1	0.15	76.9	36.0	2.56	51.8	2.7	40.0	83.0
Mighty Giant grinder screen size = 127.0 mm (5.0 in.); Particle size & = 10.30 ± 4.11 mm (0.41 ± 0.16 in.); Moisture content of particles = 14.6 ± 2.7% w.b.													
24	1.2	732.3	399.1	0.13	142.6	0.13	16.8	6.7	0.39	14.3	3.1	72.0	90.0
40	1.2	954.6	488.1	0.17	203.6	0.17	37.5	15.0	0.87	26.1	2.8	62.6	87.2
60	1.2	764.2	637.2	0.14	158.7	0.14	108.3	43.2	2.51	57.8	0.1	28.0	63.6
										Average:	2.0	60.9	83.1

Notes: D = roll diameter (m); W = roll width (m); R_g = minimum roll gap; R_f = roll force (ton); R_s = roll speed (rpm); ρ_g = unit density of roll press compacts at the minimum roll gap (kg m^{-3}), calculated based on the mass of biomass compacted per unit time (i.e., throughput) and the theoretical volume of the roll press compactor that caused this throughput (i.e., π D W R_g R_s); ρ_c = unit density of roll press compacts after curing one week at room temperature (kg m^{-3}); C_c = throughput of roll press compactor (t/h); P = maximum pressure applied between the rolls (MPa); R_p = roll motor power (hp); and R_{se} = specific energy consumption for rolls, excluding no-load roll motor energy consumption (MJ/t).

* Relative percent error (%) = |measured value – calculated value| × 100 / measured value.

& Geometric mean particle length ± geometric standard deviation.

Table 4. Results for native perennial grasses with Johanson (1965) model (D = 0.521 m, W = 0.127 m, and R_g = 0.022 m).

Measured data from pilot-scale roll press compaction (Kaliyan et al., 2011a)						Calculated values using Johanson (1965) model					Relative percent error (%) *		
R_f (ton)	R_s (rpm)	ρ_g (kg m^{-3})	ρ_c (kg m^{-3})	C_c (t/h)	R_{se} (MJ/t)	C_c (t/h)	P (MPa)	R_f (ton)	R_p (hp)	R_{se} (MJ/t)	C_c	R_f	R_{se}
Mighty Giant grinder screen size = 25.4 mm (1.0 in.); Particle size & = 2.55 ± 2.72 mm (0.10 ± 0.11 in.); Moisture content of particles = 17.1 ± 0.7% w.b.													
24	3.3	632.1	374.9	0.58	16.4	0.58	11.4	5.2	0.9	7.3	0.3	78.2	55.4
40	3.2	693.3	498.0	0.62	44.8	0.62	51.5	23.6	4.1	24.9	0.8	41.1	44.5
60	3.2	647.2	510.2	0.57	60.6	0.57	58.5	26.8	4.7	27.6	0.7	55.3	54.5
Mighty Giant grinder screen size = 76.2 mm (3.0 in.); Particle size & = 3.50 ± 3.06 mm (0.14 ± 0.12 in.); Moisture content of particles = 17.4 ± 2.6% w.b.													
24	2.1	610.0	347.4	0.36	20.7	0.36	15.7	9.3	1.4	19.1	1.3	61.3	7.8
40	1.9	615.8	456.5	0.32	66.0	0.32	40.9	24.2	3.4	37.8	1.4	39.5	42.7
60	1.8	668.9	461.9	0.33	109.1	0.33	42.6	25.2	3.3	38.9	1.2	58.0	64.3
Mighty Giant grinder screen size = 127.0 mm (5.0 in.); Particle size & = 5.82 ± 3.68 mm (0.23 ± 0.15 in.); Moisture content of particles = 16.5 ± 1.7% w.b.													
24	1.6	507.2	325.2	0.22	43.5	0.22	18.2	9.1	0.9	16.1	2.3	62.3	63.1
40	1.5	626.0	488.9	0.26	128.4	0.26	120.8	60.0	5.4	70.8	0.1	50.0	44.9
60	1.5	569.3	472.9	0.24	129.1	0.24	103.6	51.4	4.6	62.7	1.3	14.3	51.4
										Average:	1.1	51.1	47.6

Notes: D = roll diameter (m); W = roll width (m); R_g = minimum roll gap; R_f = roll force (ton); R_s = roll speed (rpm); ρ_g = unit density of roll press compacts at the minimum roll gap (kg m^{-3}), calculated based on the mass of biomass compacted per unit time (i.e., throughput) and the theoretical volume of the roll press compactor that caused this throughput (i.e., π D W R_g R_s); ρ_c = unit density of roll press compacts after curing one week at room temperature (kg m^{-3}); C_c = throughput of roll press compactor (t/h); P = maximum pressure applied between the rolls (MPa); R_p = roll motor power (hp); and R_{se} = specific energy consumption for rolls, excluding no-load roll motor energy consumption (MJ/t).

* Relative percent error (%) = |measured value – calculated value| × 100 / measured value.

& Geometric mean particle length ± geometric standard deviation.

Table 5. Results for corn stover with Blake et al. (1963) model (D = 0.521 m, W = 0.127 m, and L = 0.012 m).

Measured data from pilot-scale roll press compaction (Kaliyan et al., 2011a)						Calculated values using Blake et al. (1963) model					Relative percent error (%) *		
R_f (ton)	R_s (rpm)	ρ_g (kg m^{-3})	ρ_c (kg m^{-3})	C_c (t/h)	R_{se} (MJ/t)	C_c (t/h)	P (MPa)	ρ_c (kg m^{-3})	R_p (hp)	R_{se} (MJ/t)	C_c	ρ_c	R_{se}
Mighty Giant grinder screen size = 25.4 mm (1.0 in.); Particle size [&] = 6.09 ± 2.71 mm (0.24 ± 0.11 in.); Moisture content of particles = 17.9 ± 0.7% w.b.													
24	1.6	755.5	394.6	0.18	40.4	0.18	59.9	570.4	1.8	26.9	2.4	44.6	33.4
40	1.1	1213.3	508.4	0.20	170.7	0.20	101.3	640.6	2.1	27.2	1.8	26.0	84.1
60	1.2	975.9	489.9	0.18	237.8	0.18	153.1	701.7	3.3	50.0	0.8	43.2	79.0
Mighty Giant grinder screen size = 76.2 mm (3.0 in.); Particle size [&] = 8.11 ± 2.84 mm (0.32 ± 0.11 in.); Moisture content of particles = 10.2 ± 0.2% w.b.													
24	1.2	970.2	420.9	0.18	101.2	0.18	50.8	633.6	1.6	24.9	1.3	50.5	75.4
40	1.2	896.7	627.9	0.16	188.2	0.16	84.6	747.2	2.7	44.6	2.6	19.0	76.3
60	1.2	797.5	724.4	0.15	304.1	0.15	126.8	851.6	4.1	75.0	2.7	17.6	75.3
Mighty Giant grinder screen size = 127.0 mm (5.0 in.); Particle size [&] = 10.30 ± 4.11 mm (0.41 ± 0.16 in.); Moisture content of particles = 14.6 ± 2.7% w.b.													
24	1.2	732.3	399.1	0.13	142.6	0.13	56.1	540.1	1.5	29.4	3.1	35.3	79.4
40	1.2	954.6	488.1	0.17	203.6	0.17	95.0	616.6	2.4	36.3	2.8	26.3	82.2
60	1.2	764.2	637.2	0.14	158.7	0.14	143.7	684.2	3.5	66.9	0.1	7.4	57.9
										Average:	2.0	30.0	71.4

Notes: D = roll diameter (m); W = roll width (m); L = minimum roll gap; R_f = roll force (ton); R_s = roll speed (rpm); ρ_g = unit density of roll press compacts at the minimum roll gap (kg m^{-3}), calculated based on the mass of biomass compacted per unit time (i.e., throughput) and the theoretical volume of the roll press compactor that caused this throughput (i.e., π D W R_g R_s); ρ_c = unit density of roll press compacts after curing one week at room temperature (kg m^{-3}); C_c = throughput of roll press compactor (t/h); P = maximum pressure applied between the rolls (MPa); R_p = roll motor power (hp); and R_{se} = specific energy consumption for rolls, excluding no-load roll motor energy consumption (MJ/t).

* Relative percent error (%) = $|$measured value – calculated value$|$ × 100 / measured value.

[&] Geometric mean particle length ± geometric standard deviation.

Table 6. Results for native perennial grasses with Blake et al. (1963) model (D = 0.521 m, W = 0.127 m, and L = 0.022 m).

Measured data from pilot-scale roll press compaction (Kaliyan et al., 2011a)						Calculated values using Blake et al. (1963) model					Relative percent error (%) *		
R_f (ton)	R_s (rpm)	ρ_g (kg m^{-3})	ρ_c (kg m^{-3})	C_c (t/h)	R_{se} (MJ/t)	C_c (t/h)	P (MPa)	ρ_c (kg m^{-3})	R_p (hp)	R_{se} (MJ/t)	C_c	ρ_c	R_{se}
Mighty Giant grinder screen size = 25.4 mm (1.0 in.); Particle size [&] = 2.55 ± 2.72 mm (0.10 ± 0.11 in.); Moisture content of particles = 17.1 ± 0.7% w.b.													
24	3.3	632.1	374.9	0.58	16.4	0.58	44.5	484.6	5.2	24.0	0.3	29.3	46.4
40	3.2	693.3	498.0	0.62	44.8	0.62	76.0	536.0	8.2	35.8	0.8	7.6	20.1
60	3.2	647.2	510.2	0.57	60.6	0.57	115.4	579.9	12.2	56.9	0.7	13.7	6.1
Mighty Giant grinder screen size = 76.2 mm (3.0 in.); Particle size [&] = 3.50 ± 3.06 mm (0.14 ± 0.12 in.); Moisture content of particles = 17.4 ± 2.6% w.b.													
24	2.1	610.0	347.4	0.36	20.7	0.36	43.1	463.2	3.4	26.0	1.3	33.3	25.7
40	1.9	615.8	456.5	0.32	66.0	0.32	73.6	539.9	4.8	40.1	1.4	18.3	39.2
60	1.8	668.9	461.9	0.33	109.1	0.33	111.8	608.3	6.6	53.5	1.2	31.7	51.0
Mighty Giant grinder screen size = 127.0 mm (5.0 in.); Particle size [&] = 5.82 ± 3.68 mm (0.23 ± 0.15 in.); Moisture content of particles = 16.5 ± 1.7% w.b.													
24	1.6	507.2	325.2	0.22	43.5	0.22	41.8	389.0	2.6	31.2	2.3	19.6	28.2
40	1.5	626.0	488.9	0.26	128.4	0.26	69.5	433.9	4.1	42.3	0.1	11.2	67.1
60	1.5	569.3	472.9	0.24	129.1	0.24	104.0	473.3	6.2	69.9	1.3	0.1	45.9
										Average:	1.1	18.3	36.6

Notes: D = roll diameter (m); W = roll width (m); L = minimum roll gap; R_f = roll force (ton); R_s = roll speed (rpm); ρ_g = unit density of roll press compacts at the minimum roll gap (kg m^{-3}), calculated based on the mass of biomass compacted per unit time (i.e., throughput) and the theoretical volume of the roll press compactor that caused this throughput (i.e., π D W R_g R_s); ρ_c = unit density of roll press compacts after curing one week at room temperature (kg m^{-3}); C_c = throughput of roll press compactor (t/h); P = maximum pressure applied between the rolls (MPa); R_p = roll motor power (hp); and R_{se} = specific energy consumption for rolls, excluding no-load roll motor energy consumption (MJ/t).

* Relative percent error (%) = $|$measured value – calculated value$|$ × 100 / measured value.

[&] Geometric mean particle length ± geometric standard deviation.

Table 7. Effect of roll gap on the prediction of throughput, compact density, roll force, and specific energy for rolls.

Biomass feedstock	Roll gap (m)	Average relative percent error (%) (n = 9) *			
		C_c	ρ_c	R_f	R_{se}
Johanson (1965) model					
Corn stover	0.012	2.0	-	60.9	83.1
	0.022	2.0	-	46.5	82.5
Native perennial grasses	0.012	1.1	-	58.3	49.3
	0.022	1.1	-	51.1	47.6
Blake et al. (1963) model					
Corn stover	0.012	2.0	30.0	-	71.4
	0.022	2.0	20.0	-	61.0
Native perennial grasses	0.012	1.1	25.6	-	43.7
	0.022	1.1	18.3	-	36.6

Notes: C_c = throughput of roll press compactor (t/h); ρ_c = unit density of roll press compacts after curing one week at room temperature (kg m^{-3}); R_f = roll force (ton); and R_{se} = specific energy consumption for rolls, excluding no-load roll motor energy consumption (MJ/t).

* Relative percent error (%) = |measured value – calculated value| × 100 / measured value.

Chapter 6

A Biomass Supply Logistics System Involving Coarse Grinding/Roll Press Compaction

Abstract

We evaluated the economics, energy inputs, and greenhouse gas (GHG) emissions for a proposed "field to facility" corn stover logistics system. The system included collection and transport by round bales to local storages within 3.2 km (2 mile) of the field during the fall harvest period followed by processing at the local storage sites throughout the year using mobile units which converted the bales to bulk material by tub-grinding and roll-press compacting to 240 kg/m^3 (15 lb/ft^3) to achieve 22.7 t (25 ton) loads for truck delivery to an end user within a 48 km (30 mile) radius. The total cost and fossil energy consumption for delivering the bulk corn stover (15% moisture) to end users were $99.49/t ($90.26/ton) and 1264 MJ/t, respectively. The cost (i.e., fixed cost + operating cost) of tub-grinding was $9.33/t ($8.46/ton). The cost (i.e., fixed cost + operating cost) of roll-press compaction was $10.90/t ($9.88/ton).The total fossil energy consumption for the logistics system was equivalent to approximately 8.9% of the energy content of corn stover. The life-cycle GHG emission for heat and power applications was approximately 139 kg CO_2e/t at 15% moisture or 10 g CO_2e/MJ of dry matter including emissions for logistics and combustion, but excluding those associated with soil organic carbon (SOC) loss. Our estimates show that as a fuel for heat and power applications, corn stover reduced life-cycle GHG emissions by factors of approximately 7 and 11 compared to natural gas and coal, respectively.

1. Objectives

The objective of this study is to evaluate economic, fossil energy, and greenhouse gas (GHG) emission impacts of a corn stover logistics system including: 1) collection and delivery to local storages within 3.2 km (2 mile) of the field in the fall, and 2) bale to bulk processing (i.e., coarse grinding followed by roll press compaction) at the local storages followed by truck transport to a large end user within a 48 km (30 mile) radius throughout the year.

2. Materials and Methods

Morey et al. (2010) proposed a "field to facility" corn stover supply logistics system. The system includes collection/harvesting of corn stover after harvest of the corn grain. It involves stalk shredding to increase the amount of harvestable stover and to facilitate drying to the target moisture content of 15%. The stover is then raked, baled (round), and transported to local storages within 3.2 km (2 mile) of the field in the fall. Drawing stover from a 3.2 km (2 mile) radius for local storage is intended to strike a balance between the distance to move bales from the field at harvest and the desire to accumulate sufficient biomass [at least 181 t (200 ton)] for a minimum of one full day of bale to bulk processing at each site. At the local storage sites, mobile units which convert the bales to bulk material by tub-grinding and roll-press compacting to 240

kg/m^3 (15 lb/ft^3) to achieve 22.7 t (25 ton) loads for truck delivery to an end user within a 48 km (30 mile) radius.

Using the tub-grinding and roll-press compaction data obtained from this project, we updated the total cost, energy consumption, and life-cycle GHG emission for the corn stover supply logistics system given by Morey et al. (2010). Detailed calculation procedures for the biomass logistics system can be found in Morey at al. (2010). Some of the key parameters/assumptions of the Morey et al. (2010) corn stover logistics system are as follows. It is assumed that 70% corn stover is removed per unit land area with collection every other year that corn is grown resulting in an average removal rate of 35% per year. This leads to more efficient, less costly collection with less compaction than harvesting 35% of the stover each year. In this study, we did not quantify soil organic carbon (SOC) changes from stover removal, but the system is based on sustainable removal rates of an average of 35% per year. Corn stover removal rate is 7.4 t dry matter/ha (3.3 ton dry matter/acre) [8.7 t/ha (3.9 ton/acre) at 15% wet basis moisture content].

We considered nutrient replacement for the material removed from the field. Nitrogen, phosphorus, and potassium fertilizers are applied at a rate of 7.4, 2.9, and 12.7 kg/t dry matter (14.8, 5.9, and 25.4 lb/ton dry matter), respectively (Sawyer and Mallarino, 2007). The price per pound of nitrogen, phosphorus, and potassium fertilizer is $0.413, $0.541, and $0.489, respectively (2012 southwest Minnesota prices).

From the results of this project, tub-grinding energy of 226 MJ/t (1.509 gal diesel/ton) and roll-press compaction energy of 226 MJ/t (1.509 gal diesel/ton) are derived for a capacity of 22.7 t/h (25 ton/h) of corn stover (15% wet basis moisture content) processing. It is assumed that tub-grinder is powered by a diesel engine with of 403 kW (540 hp). Similarly, roll-press compactor is assumed to be powered by a diesel engine of 403 kW (540 hp).

Cost of coarse-grinding [tub-grinder with a round-hole screen opening size of 76.2 mm (3.0 in.)] of biomass particles was calculated by assuming the following: tub-grinder [403 kW (540 hp)] capacity = 22.7 t/h (25 ton/h); diesel fuel consumption = 6.296 L/t (1.509 gal/ton); first cost = $390,000; salvage value = 10% of first cost; operating hours = 1800 h/year; life = 5 years; interest rate = 6%; and annual repair costs = 3% of first cost. The cost for insurance and housing was calculated based on procedures from Lazarus (2012).

Cost of roll press compaction of coarsely ground biomass particles [to obtain a compacted product with bulk density of 240 kg/m^3 (15 lb/ft^3)] was calculated by assuming the following: roll press compactor [403 kW (540 hp)] capacity = 22.7 t/h (25 ton/h); diesel fuel consumption = 6.296 L/t (1.509 gal/ton); first cost = $600,000; salvage value = 10% of first cost; operating hours = 1800 h/year; life = 5 years; interest rate = 6%; and annual repair costs = 3% of first cost. The cost for insurance and housing was calculated based on procedures from Lazarus (2012).

Price of diesel fuel is assumed to be $3.25/gallon.

3. Results and Discussion

The cost, life-cycle energy, and life-cycle GHG emissions for tub-grinding followed by roll-press compaction (i.e., bale to bulk processing) of corn stover (15% wet basis moisture content) at a local storage are $26.79 ($24.30), 562 MJ/t, and 43 g CO_2e/t, respectively (Tables 1 and 2). The cost (i.e., fixed cost + operating cost) of tub-grinding was $9.33/t ($8.46/ton). The fixed cost of tub-grinder was $2.14/t ($1.95/ton). The cost (i.e., fixed cost + operating cost) of roll-press compaction was $10.90/t ($9.88/ton). The fixed cost of roll-press compactor was $3.29/t ($2.99/ton).

The total cost and fossil energy consumption for delivering the bulk compacted corn stover (15% wet basis moisture content) to end users are $99.49/t ($90.26/ton) and 1264 MJ/t, respectively (Table 2). The total fossil energy consumption for nutrient replacement, collection, processing at the local storage, and transport to the end user is equivalent to approximately 8.9% of the energy content of the biomass. The lower heating value (LHV) of corn stover is taken to be 16.7 MJ/kg of dry matter (Morey et al., 2009).

The total life-cycle GHG emission is 9.8 g CO_2e/MJ of dry matter including combustion. The life-cycle GHG emission value does not include any contribution for reduction in soil organic carbon (SOC) loss because of our restrictions on corn stover annual removal of 35%. While there is uncertainty related to allowable removal levels on particular soils, we believe our 35% removal assumption is reasonable. The life-cycle GHG emissions for corn stover, natural gas, and coal as fuels for heat and power applications are compared in figure 1. These estimates show that for heat and power applications, corn stover reduces life-cycle fossil GHG emissions by factors of approximately 7 and 11 compared to natural gas and coal, respectively.

4. Conclusions

In this study, we evaluated a proposed corn stover logistics system that included collection and transport of corn stover (15% moisture) as net-wrapped round bales to local storages within 3.2 km (2 mile) of the field in the fall. This stage was followed by processing at the local storage sites throughout the year using mobile units which converted the bales to bulk material by tub-grinding and roll-press compacting to 240 kg/m^3 (15 lb/ft^3). Bulk compacted corn stover is then loaded on trucks and delivered as 22.7 t (25 ton) loads to an end user within a 48 km (30 mile) radius. Other components of the logistics system were payment to the farmer for participation, nutrient replacement, and local storage loss. For the assumptions made for the proposed corn stover logistics system, we found the following:

- The total cost for delivering the bulk corn stover (15% moisture) to end users is $99.49/t ($90.26/ton). The cost (i.e., fixed cost + operating cost) for tub-grinding is $9.33/t ($8.46/ton), and for roll-press compaction is $10.90/t ($9.88/ton).
- Fossil energy input is about 9% of energy in corn stover.
- Life-cycle GHG emissions are about 139 kg of CO_2e/tonne including combustion, but excluding soil organic carbon loss.

- For heat and power applications, life-cycle GHG emissions for corn stover fuel are approximately 10 g CO_2e/MJ of dry matter, which amounts to a 7 or 11 times reduction in GHG emissions compared to natural gas or coal fuels, respectively.

REFERENCES

ASBAE Standards. 2009. ASAE D497.5 FEB2006 Agricultural Machinery Management Data. St. Joseph, Mich.: ASABE.

GREET. 2009. *The Greenhouse Gases, Regulated Emissions, and Energy Use in Transportation (GREET) Model*. Ver. GREET 1.8c.0. Argonne, IL: Center for Transportation Research, Energy Systems Division, Argonne National Laboratory. Available at: http://www.transportation.anl.gov/modeling_simulation/GREET/index.html.

Lazarus, W.F. 2012. Machinery cost estimates. St. Paul, Minn.: University of Minnesota Extension Service. Available at: http://www.apec.umn.edu/faculty/wlazarus/documents/machdata.pdf. Accessed 28 July 2012.

Morey, R.V., D.L. Hatfield, R. Sears, D. Haak, D.G. Tiffany, and N. Kaliyan. 2009. Fuel properties of biomass feed streams at ethanol plants. *Applied Eng. in Agric.* 25(1): 57-64.

Morey, R.V., N. Kaliyan, D.G. Tiffany, and D.R. Schmidt. 2010. A corn stover supply logistics system. *Applied Eng. in Agric.* 26(3): 455-461.

Sawyer, J., and A. Mallarino. 2007. Nutrient removal when harvesting corn stover. Integrated Crop Management IC-498(22), August 6, 2007. Ames, IA: Iowa State University Extension. Available at: http://www.ipm.iastate.edu/ipm/icm/2007/8-6/nutrients.html. Accessed 28 July 2012.

Table 1. Cost, life-cycle energy consumption, and life-cycle greenhouse gas (GHG) emissions for coarse-grinding and roll-press compaction.▲

Operation	Tractor/Power Unit Size, kW (hp)	Machine Capacity, t/h (ton/h)	Fuel Diesel Use, L/t (gal/ton)	Lubricant Oil Use, L/t (gal/ton) [&]	Cost, $/t ($/ton)	Life-Cycle Energy, MJ/t [#]	Life-Cycle GHG Emission, kg CO_2e/t
Feeding bales into tub-grinder with a tractor and front-end loader	97 (130)	22.7 (25)	0.477 (0.114) *	0.006 (0.0013)	$2.81 ($2.55)	20.69	1.58
Coarse-grinding of biomass bales	403 (540) [Ψ]	22.7 (25)	6.296 (1.509) **	0.020 (0.0048)	$9.33 ($8.46)	270.64	20.69
Roll-press compaction	403 (540) **	22.7 (25)	6.296 (1.509) **	0.020 (0.0048)	$10.90 ($9.88)	270.64	20.69
Total	--	--	--	--	$26.79 ($24.30)	561.97	42.95

▲Mass or weight is defined at 15% (wet basis) moisture content unless otherwise indicated.

[&] Oil consumption was estimated according to ASABE Standards (2009).

[#] Life-cycle energy (MJ/t) = [gal of diesel plus oil (i.e., fossil fuel)/ton of corn stover × 135.89 MJ/gal of fossil fuel] / [0.9072 × fossil fuel efficiency]. GREET (2009) provides a fossil fuel efficiency of 0.8377 to account for upstream energy consumption for fossil fuel production and distribution.

[∀] Life-cycle GHG emission (kg CO_2e/t) = [gal of diesel plus oil (i.e., fossil fuel)/ton of corn stover × 135.89 MJ/gal of fossil fuel × 0.0913 kg CO_2e/MJ of fossil fuel] / 0.9072. GREET (2009) suggests an upstream (i.e., fuel production and distribution) emission factor and combustion emission factor of 17.23 and 74.02 g CO_2e/MJ of diesel fuel, respectively, for stationary reciprocating engines (tub-grinder and roll-press compactor). The GHG emission factors suggested for farm tractors were used to estimate the life-cycle GHG emission for the bale-feeding tractor (GREET, 2009).

* Diesel consumption was assumed to be 0.223 L of diesel per PTO kW per hour (0.044 gallons of diesel per PTO horsepower-hour) on average for each implement type (Lazarus, 2012).

[Ψ] Data from Vermeer TG5000 tub-grinder (Vermeer Corporation, Pella, IA; www.vermeer.com).

** Derived from tub-grinding and roll-press compaction experiments conducted in this project.

Table 2. Cost, life-cycle fossil energy consumption, and life-cycle greenhouse gas (GHG) emissions for corn stover supply logistics system. ▲

Operation	Cost		Life-Cycle Energy		Life-Cycle GHG Emission
	$/t ($/ton)	%	MJ/t	%	kg CO_2e/t
Payment to farmer for participation	7.50 (6.80)	7.5	--	--	--
Nutrient replacement (N-P-K)	20.36 (18.47)	20.5	412.7	32.6	31.0
Collection/transport to local storage	33.91 (30.76)	34.1	196.9	15.6	13.1
Local storage cost/local storage loss [#]	3.45 (3.13)	3.5	30.5	2.4	2.2
Tub-grinding/roll-press compaction	26.79 (24.30)	26.9	562.0	44.4	42.9
Truck transport of compacted corn stover	7.50 (6.80)	7.5	62.4	4.9	4.8
Combustion of corn stover *	--	--	--	--	44.5
Total	99.49 (90.26)	100.0	1264.4	100.0	138.6

▲Mass or weight is defined at 15% (wet basis) moisture content unless otherwise indicated.

[#] Average dry matter loss during storage was assumed to be 5%. The cost due to the storage and storage loss is equal to the sum of 36¢/t (33¢/ton) for the land rent charge, plus 5% of the costs for payment to farmer for participation, nutrient replacement, and collection/transport to local storage. The energy or GHG emission due to storage loss is equal to the sum of 5% of the corresponding values for nutrient replacement, and collection/transport to local storage.

* Combustion of corn stover in industrial boilers emits 0.0036 g of CH_4/MJ and 0.0102 g of N_2O/MJ of dry matter (GREET, 2009).

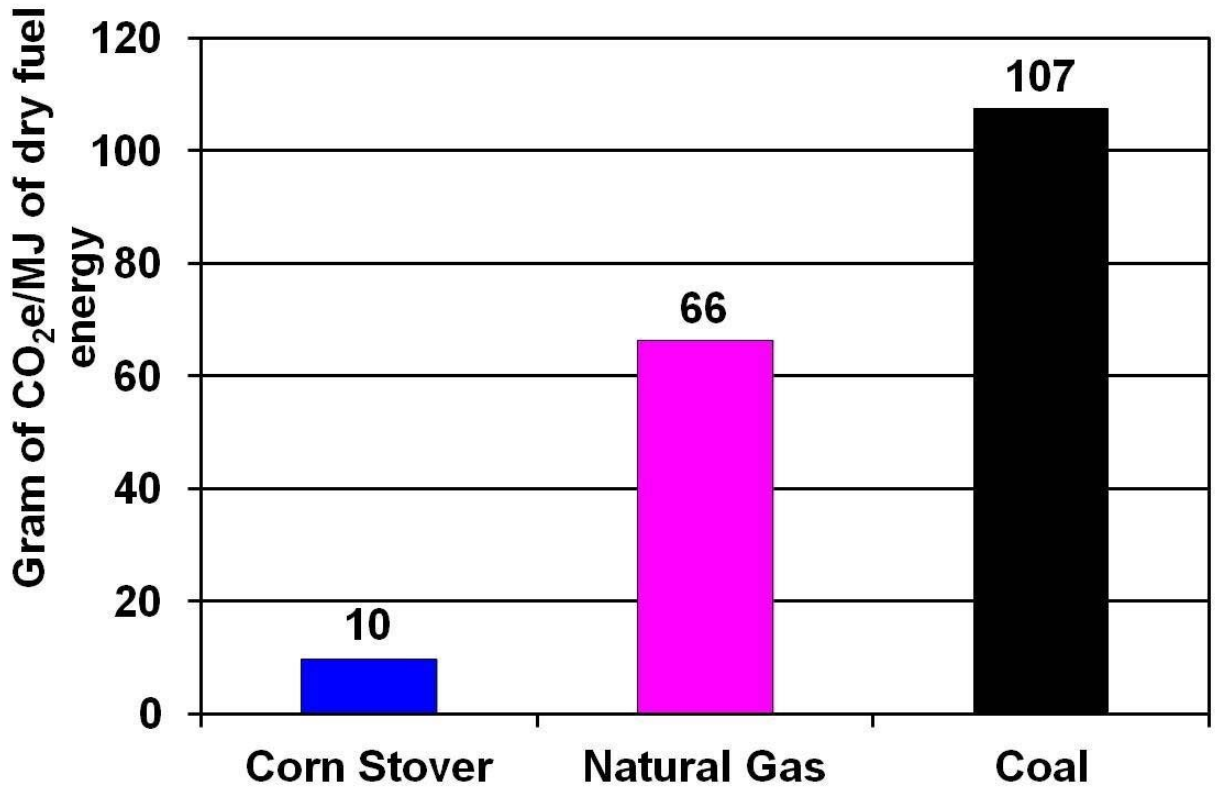

Figure 1. Life-cycle greenhouse gas emissions for heat and power applications. The GHG data for natural gas and coal include upstream (i.e., fuel production and distribution) and combustion emissions as fuels in industrial boilers (GREET, 2009).

Back to Table of Contents

Journal Publications

Morey, R.V., N. Kaliyan, D.G. Tiffany, and D. R. Schmidt. 2010. A corn stover supply logistics system. *Applied Engineering in Agriculture* 26(3): 455-461.

Kaliyan, N., D.R. Schmidt, R.V. Morey, and D.G. Tiffany. 2012. Commercial scale tub grinding of corn stover and perennial grasses. *Applied Engineering in Agriculture* 28(1): 79-85.

Conference Papers

Morey, R.V. 2010. Biomass densification. A presentation made at the Biomass Conversion to Heat & Electricity Workshop, Heartland Community College, Normal, Illinois, March 11, 2010.

Kaliyan, N., R.V. Morey, and D.R. Schmidt. 2011. Roll press compaction of corn stover and perennial grasses. ASABE Paper No. 1110564. St. Joseph, Mich.: ASABE. A paper presented at the 2011 American Society of Agricultural and Biological Engineers (ASABE) Annual International Meeting Sponsored by ASABE, Louisville, Kentucky, August 7-10, 2011.

Kaliyan, N., D.R. Schmidt, and R.V. Morey. 2011. Compaction characteristics of coarsely ground corn stover and perennial grasses. ASABE Paper No. 1110566. St. Joseph, Mich.: ASABE. A paper presented at the 2011 American Society of Agricultural and Biological Engineers (ASABE) Annual International Meeting Sponsored by ASABE, Louisville, Kentucky, August 7-10, 2011.

Kaliyan, N., and R.V. Morey. 2011. Validation of roll press design equations for compaction of corn stover and perennial grasses. ASABE Paper No. 1110568. St. Joseph, Mich.: ASABE. A paper presented at the 2011 American Society of Agricultural and Biological Engineers (ASABE) Annual International Meeting Sponsored by ASABE, Louisville, Kentucky, August 7-10, 2011.

North Central Region Sun Grant Annual Meeting Presentations

Morey, R.V. 2010. Improving handling characteristics of herbaceous biomass. Presentation at North Central Region Sun Grant Annual Meeting. Reno, Nevada, January 12-13, 2010.

Morey, R.V. 2011. Improving handling characteristics of herbaceous biomass. Presentation at North Central Region Sun Grant Annual Meeting. Orlando, Florida, January 11-12, 2011.

Morey, R.V. 2012. Improving handling characteristics of herbaceous biomass. Presentation at North Central Region Sun Grant Annual Meeting. Indianapolis, Indiana, January 10-11, 2012.

Back to Table of Contents

Networks/Collaborations

Kolbeck, Inc., Le Mars, Iowa.

Bepex International LLC, Minneapolis, Minnesota.

University of Minnesota-Morris campus and West Central Research and Outreach Center, Morris, Minnesota.

David R. Schmidt, Research Engineer, Department of Bioproducts and Biosystems Engineering, University of Minnesota, St. Paul, Minnesota.

Troy Schaar, Junior Scientist, Department of Bioproducts and Biosystems Engineering, University of Minnesota, St. Paul, Minnesota.

Academic, Post-docs Supported

Nalladurai Kaliyan, Research Associate, Department of Bioproducts and Biosystems Engineering, University of Minnesota, St. Paul, Minnesota.

Back to Table of Contents

Please complete the following table to reflect your project at completion or time of report submission:

University of Minnesota -- USDOE DE-FG36-08GO88073

ITEM	NUMBER
Abstracts	**3**
Peer Reviewed Publications	**2 plus 1 submitted**
Outreach Publications/Web Pages	**0**
Professional Presentations	**3**
MS Degrees Conferred	**0**
Ph.D. Degrees Conferred	**0**
MS Students Supported	**0**
Ph.D. Students Supported	**0**
Disclosures	**0**
Patents Filed	**0**
Provisional Patents	**0**
Patents Issued	**0**
License Agreements	**0**
Plant Variety Protection	**0**
Investigators Supported	**0**
Post-Docs Supported	**1**
Graduate Students Supported	**0**
Undergraduate Students Supported	**0**
Start-Up Jobs Created	**?**

Back to Table of Contents

Sun Grant Initiative
DOE Final Report

Project Title: Transforming and Densifying Biomass in Regional Biomass Processing Centers (RBPC)

Project Director/Principal Investigator: Kasiviswanathan Muthukumarappan PhD, Distinguished Professor/Graduate Coordinator, Department of Agricultural and Biosystems Engineering, South Dakota State University, Brookings, SD, 57007

All Co-Principal/Other Investigators:
Bruce E. Dale, PhD, Professor and Associate Director of Biobased Technologies and Venkatesh Balan, PhD, Associate Professor; Department of Chemical Engineering and Material Science, Michigan State University, East Lansing, MI

Chris Saffron, PhD, Assistant Professor; Department of Biosystems and Agricultural Engineering, Michigan State University, East Lansing, MI

James Julson, PhD, Professor, South Dakota State University, Brookings, SD

Lew P Christopher, PhD, Associate Professor, South Dakota School of Mines and Technology, Rapid City, SD

Michael Twedt, Program Engineer, Mechanical Engineering Department, South Dakota State University, Brookings, SD

Michael Flaherty, Federal Machine Inc., Fargo, ND

Scott W Pryor, PhD, Department of Agricultural and Biosystems Engineering, North Dakota State University, Fargo, ND

William Gibbons, Department of Biology and Microbiology, South Dakota State University, Brookings, SD

Collaborators: N/A

Period of Performance: 1 January 2009 – 31 December 2013

Funding Awarded: $689,553

Cost Share Amount: $366,447

Cost Share Sources: Time and effort from PIs and CoPIs; Indirect on time and effort; Tuition remission; Federal Machine Co.

Executive Summary

This collaborative project led by Dr. Kasi Muthukumarappan of South Dakota State University (SDSU) had collaborators from, SDSU, Michigan State University (MSU), North Dakota State University (NDSU), and South Dakota School of Mines and Technology (SDSMT). This project had five different objectives: 1) Optimize AFEX pretreatment conditions for switchgrass, corn stover and prairie cord grass; 2) Determine optimal ComPAKco operating conditions; 3) Evaluate the effects of storage on PAKS physical characteristics; 4) Determine the effects of densification and storage on hydrolysis and fermentation characteristics; 5) Conduct economic and energy analyses of process to determine optimal and minimal scale. Different collaborators have been responsible in accomplishing the tasks and sub-tasks and in the sections below, the summary and outcome of the each objective and accomplished the tasks by the responsible committee has been reported.

Objective 1: Optimize AFEX pretreatment conditions for switchgrass, corn stover and prairie cord grass
Recipient: Bruce Dale, Venkat Balan
Collaborators: NA

MSU, as a subcontracting collaborator, was primarily responsible for three research activities in the project: 1) optimizing AFEX™ pretreatment conditions for different biomass materials, 2) providing adequate quantities of AFEX treated biomass to collaborators for pelletization research and 3) supporting the conceptual design of regional biomass processing centers (RBPCs) based on the AFEX pretreatment. The first two activities were carried out in the laboratory of Professor Bruce Dale and the third activity was primarily centered in the laboratory of Professor Chris Saffron, with input from the Dale laboratory. This final report briefly describes all three activities.

Research Activity #1: Optimize AFEX pretreatment conditions for switchgrass, corn stover and prairie cord grass
The laboratory of Professor Bruce Dale completed all of this AFEX pretreatment work on three different biomasses: corn stover (CS), switchgrass (SWG) and prairie cord grass samples (PCG). AFEX conditions were optimized for all three feedstocks at various level of moisture and particle size of 2, 4 and 8 mm. Results showed that all of these residues and prairie grasses can be effectively pretreated by AFEX under somewhat different operating conditions.

Research Activity #2: Provide AFEX treated biomass for ComPAKCo Pelletization
Professor Bruce Dale's laboratory provided sufficient AFEX treated biomass for the different biomass materials to allow pelletization studies by the industrial collaborator, ComPAKCo.

Research Activity #3: Development of AFEX process model
This work has been performed under the direction of Professor Chris Saffron of MSU, with input from the laboratory of Professor Bruce Dale. A process model of AFEX was developed in order to assess the costs and profitability associated with this biomass pretreatment method. Details of this activity have been emphasized in the objective 5, a section below in the report.

Key outcomes & impacts:

- Designed and developed a 2L AFEX batch reactor (Figure 1A) and a 5 gallon AFEX batch reactor with stirring option (Figure 1B)
- Optimized AFEX pretreatment conditions for effective bioethanol production from three different feedstocks. They are:

i) AFEX pretreatment conditions of corn stover were: 1:1 ratio of ammonia to biomass, 60% moisture, 100°C and 15 minute residence time.
ii) AFEX pretreatment conditions of switchgrass were: 1:2 ratio of ammonia to biomass, 50% moisture, 100°C and 30 minute residence time.
iii) AFEX pretreatment conditions of prairie cord grass were: 1:2 ratio of ammonia to biomass, 40% moisture, 100°C and 30 minute residence time.

A B

Figure 1. Pictures of AFEX reactors. Here A, 2L AFEX batch reactor; B, 5 gallon AFEX batch reactor with stirring option

Objective 2**:** Determine optimal ComPAKco operating conditions
Recipient: Michael Flaherty
Collaborators: NA

A novel compaction process called ComPAKco densification developed by Federal Machine in Fargo, ND was used to compress biomass through a tapering channel between adjacent gear teeth and to produce densified pellets. Physical properties and storage characteristics of densified biomass (PAKS) were studied. The quality (durability, bulk density, compressibility, etc.) of AFEX treated pellets is very good. AFEX pretreatment appears to permit effective pelletization at lower temperatures and pressures than is possible for untreated biomass.

Key outcomes & impacts:

- Designed and developed a lab scale ComPAKco densification system (Figure 2A) and a pilot scale ComPAKco densification system (Figure 2B)
- Produced ComPAKed feedstocks using the pilot scale densification system (Figure Figure 2C and 2D)

Figure 2A

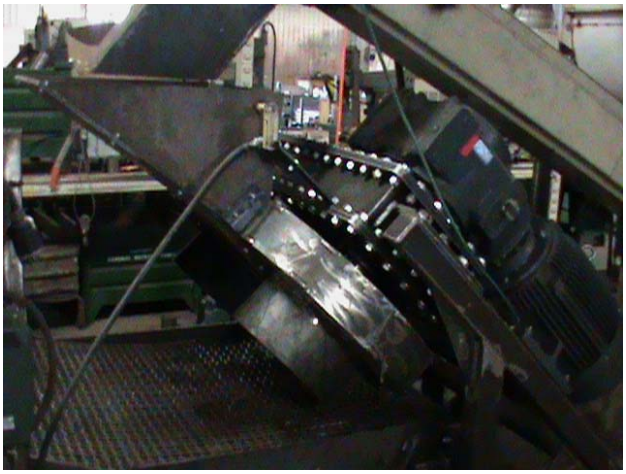

Figure 2B

Figure 2C

Figure 2D

Objective 3: Evaluate the effects of storage on PAKS physical characteristics
Recipient: Kasi Muthukumarappan, James Julson
Collaborators: NA

Research Activity # 1: Evaluation of physical characteristics of control, AFEX pretreated, and PAKs of Switchgrass, corns stover and prairie cord grass samples before and after storage

Results (Table 3.1) showed that no significant differences exist between thermal properties of switchgrass before and after storage. The water activity significantly decreased after being stored for 6 months for both AFEX treated and PAKs of switchgrass. Also, the durability shows significant increase after storage. Decrease in moisture content and water activity at this storage condition (20C and 70% RH) shows that chance for mold/fungus growth is less. True density, bulk density, WAI and WSI shows mixed trends.

Table 3.1. The properties of AFEX and packed switchgrass before and after storage

	Switchgrass (AFEX)		Switchgrass (paked)	
	before storage	After storage	before storage	After storage
Thermal conductivity(w/m^{o}c)	0.04^{a}	0.04^{a}	0.09^{a}	0.09^{a}
Thermal resistivity(m^{0}c/w)	25.1^{a}	25.4^{a}	11.8^{a}	11.4^{a}
Thermal diffusivity(mm^{2}/s)	0.26^{a}	0.255^{a}	0.12^{a}	0.11^{a}
Water activity	0.323^{a}	0.19^{b}	0.312^{a}	0.197^{b}
AOR(^{O})	55.97^{a}	57.5^{a}	74.6^{a}	77.4^{a}
Moisture content(%,db)	6.41^{a}	5.24^{b}	6.8^{a}	5.14^{b}
Aerated bulk density(kg/m^{3})	131^{a}	131^{a}	430^{a}	414^{a}
Packed bulk density(kg/m^{3})	159^{a}	159^{a}	460^{a}	451^{a}
Compressibility	17.6^{a}	17.2^{a}	6.6^{b}	8.1^{a}
True density(kg/m^{3})	1463^{a}	1293^{b}	1434^{a}	1403^{a}
Bulk density(kg/m^{3})	125^{b}	157^{a}	368^{a}	363^{a}
Porosity	0.914^{a}	0.878^{b}	0.785^{a}	0.742^{b}
Specific gravity	1.463^{a}	1.293^{b}	1.434^{a}	1.403^{a}
Water Absorption Index(-)	5.09^{a}	4.55^{b}	5.35^{a}	5.2^{a}
Water Solubility Index (%)	10.08^{a}	9.07^{a}	10.93^{a}	7.96^{b}
Tg(^{o}C)	78.2^{a}	69.31^{b}	69.6^{a}	68.45^{a}
Durability (%)			78.2^{b}	91.7^{a}

Different letters means significant difference between the properties of switchgrass before and after storage.

Similarly, no significant differences observed between thermal properties of both AFEX treated and packed corn stover before and after storage. Water activity and moisture content showed significant decrease after being stored for 6 months for both AFEX treated and packed corn stover. Glass transition temperature of AFEX treated and packed corn stover decrease after storage, too. WAI and WSI shows mix trends. Results are shown in Table 3.2.

Table 3.2. The properties of AFEX and packed corn stover before and after storage.

	Corn stover (AFEX)		Corn stover (paked)	
	before storage	After storage	before storage	After storage
Thermal conductivity(w/m^{o}c)	0.04^a	0.04^a	0.09^a	0.09^a
Thermal resistivity(m^{0}c/w)	25.1^a	26.1^a	11.3^a	11.6^a
Thermal diffusivity(mm^2/s)	0.253^a	0.257^a	0.1^a	0.11^a
Water activity	0.359^a	0.192^b	0.376^a	0.191^b
AOR(^{O})	54.0^b	64.4^a	70.7^a	74.2^a
Moisture content(%,db)	6.16^a	3.76^b	7.1^a	4.45^b
Aerated bulk density(kg/m^3)	270^a	173^b	355^a	357^a
Packed bulk density(kg/m^3)	296^a	191^b	382^a	397^a
Compressibility	8.83^a	9.2^a	7.2^b	10.1^a
True density(kg/m^3)	1329^a	1082^b	1429^a	1424^a
Bulk density(kg/m^3)	93^b	125^a	420^a	358^b
Porosity	0.910^a	0.885^a	0.796^a	0.748^a
Specific gravity	1.329^a	1.082^b	1.429^a	1.424^a
Water Absorption Index(-)	4.64^a	4.09^a	5.58^a	4.64^b
Water Solubility Index(%)	11.16^a	9.07^b	8.6^b	9.37^a
Tg(^{o}C)	79.4^a	66.23^b	73.5^a	66.91^b
Durability (%)			92.8^a	93.9^a

Different letters means significant difference between the properties of corn stover before and after storage.

From Table 3.3, no significant differences exist between thermal properties of both AFEX treated and packed prairie cord grass before and after storage. But water activity, moisture content and glass transition temperature significantly decreased after storage for both AFEX treated and packed prairie cord grass. Compressibility shows mix trends.

Table 3.3 The properties of AFEX and packed prairie cord grass before and after storage.

	Prairie cord grass (AFEX)		Prairie cord grass (paked)	
	before storage	After storage	before storage	After storage
Thermal conductivity(w/m^{o}c)	0.04^{a}	0.04^{a}	0.11^{a}	0.1^{a}
Thermal resistivity(m^{0}c/w)	27.13^{a}	25.8^{a}	9.09^{a}	9.8^{a}
Thermal diffusivity(mm^{2}/s)	0.267^{a}	0.254^{a}	0.097^{a}	0.102^{a}
Water activity	0.329^{a}	0.198^{b}	0.329^{a}	0.189^{b}
AOR(^{O})	47.6^{b}	59^{a}	70.6^{a}	73.6^{a}
Moisture content(%,db)	6.21^{a}	4.9^{b}	6.3^{a}	4.33^{b}
Aerated bulk density(kg/m^{3})	133^{a}	121^{a}	315^{a}	397^{a}
Packed bulk density(kg/m^{3})	156 ^{a}	137^{a}	330^{b}	424^{a}
Compressibility	14.9^{a}	11.7^{b}	4.5^{b}	6.5^{a}
True density(kg/m^{3})	1401^{a}	1309^{a}	1545^{a}	1460^{a}
Bulk density(kg/m^{3})	106^{a}	124^{a}	408^{a}	432^{a}
Porosity	0.924^{a}	0.905^{a}	0.736^{a}	0.704^{a}
Specific gravity	1.401^{a}	1.309^{a}	1.545^{a}	1.460^{a}
Water Absorption Index(-)	5.03^{a}	4.9^{a}	3.69^{a}	2.38^{b}
Water Solubility Index(%)	16.85^{a}	16.49^{a}	9.28^{a}	4.8^{b}
Tg(^{o}C)	74.24^{a}	66.09^{b}	75.6^{a}	66.42^{b}
Durability (%)			97.3^{a}	97.1^{a}

Different letters means significant difference between the properties of prairie cord grass before and after storage.

To study the effect of storage conditions on the physical properties of control, AFEX, and PAKed prairie cord grass samples, small experimental set-up was established at three different levels of relative humidity (RH), i.e., 70%, 80% and 90% at 40ºC. The prairie cord grass samples that were previously stored at 80% and 90% RH appeared to have fungal growth after 6 weeks and 2 weeks of storage, respectively. The samples that were stored at 70% RH did not have any microbial contamination during the storage. The samples were evaluated for their physical properties [true density, bulk density, porosity, water absorption index (WAI), water solubility index (WSI), angle of repose, water activity, moisture content, thermal properties, and pellet durability index (PDI)] to determine the effects of storage. The true and bulk density, porosity, WAI and thermal properties of all three forms of samples remain unchanged before and after storage. PDI was determined only for AFEX-PAKS samples and that remained unchanged due to storage. However, significant differences ($P<0.05$) were observed for moisture content, water activity and WSI samples. Moisture content and water activity increased slightly for all the samples while water solubility index decreased for control and AFEX-PAK samples by approximately 9%. But the WSI of AFEX sample remains unaffected.

Research Activity # 2: Evaluation of compaction behavior of AFEX pretreated corn stover, prairie cord grass and switch grass

The study involved compression of untreated and Ammonia Fiber Explosion (AFEX) pretreated samples in a single pelleter unit under different loading conditions (1000, 2000, 3000, 4000, 5000 N) with different biomass particle sizes (2, 4, 8 mm) and moisture contents (8, 12, 16, 20% wb). Single pelleter unit consists of a piston and cylinder assembly with a base plate. The internal diameter and the height of the cylinder were 6.35 and 76.2 mm respectively. The cylinder was wrapped with a heating element to maintain the temperature of 100°C mimicking commercial densification process. Compression was carried out by attaching the piston to the crosshead of texture analyzer (TA HD plus, Texture technologies Corp, New York). Samples loaded in the cylinder were allowed to compress in a single stroke of piston. Five replications were produced in each combination. Unit density of the pellet was calculated by measuring the dimensions and the mass of the pellets. The effect of different parameters selected on pellet density was carried using statistical analysis and the data obtained were fitted with Jones, Walker and Kawakita compaction models to understand the compaction mechanisms to obtain quality densified products.

Key Outcomes & Impacts:

- Increase in particle size caused decrease in pellet density and increase in moisture and applied load increased the pellet density of AFEX treated biomass.
- Moisture content increase reduced the application of load to obtain high compacted pellets.
- From the Kawakita - Ludde model parameters, AFEX treated biomasses at high moisture content leads to onset of deformation at relatively low pressure.

Pellets produced under different conditions were subjected to enzymatic hydrolysis using enzyme mixtures of cellulase (NS50013), β-glucosidase (NS50010) and Xylanase (Htec2). Fermentable sugar yield was estimated using HPLC. The saccharification result obtained showed the enzymatic conversion of cellulose (ECC) was in the range of 69-93%. Increase in load and decrease in particle size showed the increase in sugar yield of all the biomass. For AFEX treated corn stover, the maximum ECC of 93.4% was obtained (2 mm, 8% wb and 5000 N), for the prairie cord grass the ECC value was 92.6% (2 mm, 14% wb and 3000 N) and for the switch grass 91.4 % ECC was obtained (2 mm, 20% wb and 5000 N).

Objective 4 - Determine the effects of densification and storage on hydrolysis and fermentation characteristics
Recipient: William Gibbons, Scott Pryor, Lew Christopher
Collaborators: NA

Research Activity 4.1 (William Gibbons, SDSU): Determine the effects of densification and storage on control, AFEX pretreated, and PAKs of switchgrass, corn stover, prairie cord grass using simultaneous saccharification and fermentation (SHF) process.

For SHF experiments using PAKs from corn stover, switchgrass, and prairie cordgrass, major findings were as follows:

- Pretreatment significantly improved glucose and ethanol production for each substrate. Comparing substrates to the control groups at low and high enzyme dose rates respectively found increases as follows; corn stover at 4 and 6 times more ethanol production, switchgrass at 4 and 9 times and prairie cordgrass at 2 and 2 times compared to non-pretreated controls. At the high dose rate, untreated prairie cordgrass performed relatively well. Other control group substrates showed no significant difference from low to high dose, with prairie cordgrass performance increasing by a

factor of 4 from low to high dose. This may indicate a natural amenability to degradation. Another indicator that this substrate may be easier to degrade was the fact that pretreated prairie cordgrass performed best among substrates regarding ethanol production with a 41% and 18% increase over corn stover and switchgrass respectively.

- Densification of AFEX-treated biomass had an adverse impact on SHF glucose production and ethanol yields in some cases. The results were more highly variable from PAK materials overall with prairie cordgrass results revealing the most variability of the substrate groups. The prairie cordgrass PAKS were most difficult to break up.
- Higher enzyme loadings of 15 FPU/g glucan produced significantly higher glucose and ethanol production than using enzyme loadings of 5 FPU/g glucan for SHF experiments.
- 6-month storage of PAKs did not appear to have a significant negative impact on SHF ethanol yields.

A common set of experimental hydrolysis and fermentation conditions were first agreed upon by researchers collaborating at NDSU and SDSU. The proposal indicated the use of solid loading rates of 24% but that was later deemed too high at this stage. This was also echoed in the initial grant review. SHF glucan loadings were set at 1% w/v. This would mean that solid loadings may be slightly different based on material composition but results could be compared more easily for the three biomass feedstocks.

The sampling regime was reduced from the original proposal so as not to impact the effective solid loading rate when removing liquid samples in the first 24 hr. Only 2 samples were taken in the first 24 hour rather than the 7 proposed.

Proposed hydrolysis and fermentation with a pH 4.3 phosphate buffer was changed to pH 4.8 citrate buffer for closer agreement with standard NREL protocols. Agitation rates were also reduced to 150 rpm from the 250 rpm proposed rate to align more closely with established NREL procedures.

Our task was to determine the impact of material (corn stover, switchgrass, cordgrass), initial particle size (2-mm, 4-mm, 8-mm), enzyme loading (5 and 15 FPU/g glucan), and storage (6 month) on both SSF and SHF ethanol yields. Testing all combinations of factors would not be feasible or efficient for time or resources. Particle size was initially tested using corn stover PAKs in an SHF system. Those results suggested we should do further tests using only 8-mm (initial grind) material.

The effects of densification on all three materials were tested by comparing controls (no pretreatment), AFEX pretreatment, and AFEX pretreatment with subsequent densification. These experiments were done with all three feedstocks. Experiments were repeated including both high and low enzyme loadings.

The impact of storage was also studied using AFEX-treated biomass and AFEX-treated PAKs that had been stored for approximately 6 months. One difficulty in carrying out these tests is that the "non-stored" materials also had some level of storage because material needed to be pretreated, sent to another location for densification, sent to another location for compositional analysis, and then sent to additional locations for hydrolysis and fermentation experiments. Each stage of this process took some amount of time at the delay might not have been the same for each feedstock depending on scheduling restrictions when materials were received. Stored PAKs were stored for 6 months prior to being sent for hydrolysis and fermentation but actual storage for fresh and stored PAKs were likely longer than originally planned and may have led to some disparity between SSF and SHF results.

Research Activity # 2 (Scott Pryor, NDSU): Determine the effects of densification and storage on control, AFEX pretreated, and PAKs of switchgrass, corn stover, prairie cordgrass using simultaneous saccharification and fermentation (SSF) process.

For SSF experiments using PAKS from corn stover, switchgrass, and prairie cordgrass, major findings were as follows:

- Initial particle size had an impact on final SSF ethanol yields from corn stover PAKS. Final (144-hr) ethanol yields were 4-5% higher for material with an initial grind size of 2-mm than for material ground to 4-mm or 8-mm. Smaller initial particle size contributes to higher front-end costs and increased difficulty in PAK formation, however. Intermediate (72-hr) ethanol yields were also more than 90% of final yields for all treatments and no significant differences were seen at this time point. Initial grind size of 8-mm was recommended for future work.
- Densification of AFEX-treated biomass had no adverse impact on SSF ethanol yields from corn stover or switchgrass, while yields from cordgrass PAKS were more variable and lower than nondensified AFEX-treated material. Cordgrass PAKS were noticeable harder than other PAKs and did not break up as easily when mixed in buffer. Grinding of cordgrass PAKs reduced the high level of variability seen in SSF ethanol yields but yields were approximately 40% lower than for nondensified, AFEX-treated cordgrass. Additional grinding of corn stover PAKs had no effect on ethanol yields or rates.
- Higher enzyme loadings of 15 FPU/g glucan produced 15-20% more ethanol than using enzyme loadings of 5 FPU/g glucan for SSF experiments.
- 6-month storage of PAKs did not appear to have a significant on SSF ethanol yields.

A common set of experimental hydrolysis and fermentation conditions were first agreed upon by researchers collaborating at NDSU and SDSU. The proposal indicated the use of solid loading rates of 24% but that was later deemed too high at this stage. This was also echoed in the initial grant review. SSF glucan loadings were set at 4% w/v. This would mean that solid loadings may be slightly different based on material composition but results could be compared more easily for the three biomass feedstocks.

The sampling regime was reduced from the original proposal so as not to impact the effective solid loading rate when removing liquid samples in the first 24 hr. Only 2 samples were taken in the first 24 hr rather than the 7 proposed.

Proposed hydrolysis and fermentation with a pH 4.3 phosphate buffer was changed to pH 4.8 citrate buffer for closer agreement with standard NREL protocols. Agitation rates were also reduced to 150 rpm from the 250 rpm proposed rate to align more closely with established NREL procedures.

Our task was to determine the impact of material (stover, switchgrass, cordgrass), initial particle size (2-mm, 4-mm, 8-mm), enzyme loading (5 and 15 FPU/g glucan), and storage (6 month) on both SSF and SHF ethanol yields. Testing all combinations of factors would not be feasible or efficient for time or resources. Particle size was initially tested using corn stover PAKs in an SSF system. Those results suggested we should do further tests using only 8-mm (initial grind) material.

The effects of densification on all three materials were tested by comparing controls (no pretreatment), AFEX pretreatment, and AFEX pretreatment with subsequent densification. These experiments were done with all three feedstocks. Experiments were repeated including both high and low enzyme loadings.

The impact of storage was also studied using AFEX-treated biomass and AFEX-treated PAKs that had been stored for approximately 6 months. One difficulty in carrying out these tests is that the "non-stored" materials also had some level of storage because material needed to be pretreated, sent to another location for densification, sent to another location for compositional analysis, and then sent to additional locations for hydrolysis and fermentation experiments. Each stage of this process took some amount of time at the delay might not have been the same for each feedstock depending on scheduling restrictions when

materials were received. Stored PAKs were stored for 6 months prior to being sent for hydrolysis and fermentation but actual storage for fresh and stored PAKs were likely longer than originally planned and may have led to some disparity between SSF and SHF results.

Research Activity # 3 (Lew Christopher, SDSMT): Determine the effects of densification and storage on control, AFEX pretreated, and PAKs of switchgrass, corn stover, prairie cordgrass using SHF and SSF processes.

For SHF experiments using untreated, AFEX treated and PAKs of switchgrass, prairie cordgrass and corn stover, the major findings were as follows:

- From all pretreatments used, the AFEX pretreatment of stored biomass produced the greatest amounts of fermentable sugars and ethanol.
- In comparison, the AFEX pretreatment of stored biomass more than doubled the ethanol yields compared to untreated biomass.
- Biomass storage had a positive impact on AFEX pretreatment improving ethanol yield by approximately 30%.
- Enzymatic hydrolysis declined in the following descending order: 1) AFEX PAKs of stored corn stover; 2) AFEX of stored switchgrass; 3) AFEX of stored prairie cordgrass. This suggests that densification had no adverse impact on enzymatic hydrolysis.
- Switchgrass produced more fermentable sugars and ethanol than corn stover and prairie cordgrass.
- Overall, in most instances, the use of greater enzyme loadings (15 FPU/g) improved sugar and ethanol yields by 30-50% in comparison to the use of lower enzyme loadings (5 FPU/g).
- The greatest ethanol yield of 9.5 g/l was produced on AFEX of stored switchgrass.

For SSF experiments using untreated, AFEX treated loose, PAKS from switchgrass, prairie cordgrass, and corn stover, the major findings were as follows:

- With the use of greater enzyme loadings (15 FPU/g), the ethanol yields increased up to 2-fold compared to the use of lower enzyme loadings (5 FPU/g).
- The greatest ethanol yield of 5.6 g/l was observed in the stored AFEX PAKS sample at 15 FPU/g. This represents a 62-72% increase in the ethanol yield when compared to 5 FPU/g glucan.
- Overall, SSF produced lower ethanol yields compared to SHF which is probably due to the use of a lower temperature of 37^{o}C for the fermentation process that is suboptimum for the enzymatic hydrolysis step with thermophilic enzymes.

A common set of experimental hydrolysis, fermentation conditions and protocols were first agreed upon by collaborating researchers. We obtained samples for analysis from SDSU with a predetermined optimum particle size of 8 mm which was used in our studies. We obtained two sets of samples – fresh and 6-months stored samples of switchgrass, prairie cordgrass and corn stover that were subjected to the following pretreatment: 1) none (untreated or control); 2) AFEX pretreatment (AFEX); 3) AFEX pretreatment followed by densification (AFEX PAKs). The stored samples were in fact older than 6 months due to transportation and additional storage after shipment prior to use. Our task at SDSM&T was to evaluate the effects of densification and storage on untreated, AFEX pretreated, and AFEX PAKs treated samples of switchgrass, corn stover, prairie cordgrass in the SHF and SSF process configurations employing thermostable enzymes produced in-house. We experienced some difficulties producing sufficient enzyme quantities due to the fact that 1) the extremophilic strain we used produced low enzyme yields, and 2) we used a small lab fermentor for this purpose. The enzymes were partially purified and concentrated by ammonium sulfate precipitation and their FPU and CBU were determined. Due to the lack of sufficient CBU activity in the crude enzymes, their CBU/FPU ratio had to be adjusted to match that of the commercial

enzyme by supplementing the thermophilic crude cellulase with additional CBU activity. We used NZ 188 as a source of CBU activity and a CBU/FPU ratio of 4.3 in our experiments. Hence, we used two crude enzyme preparations: one with 5 FPU thermophilic cellulase supplemented with 21.3 CBU from NZ 188/g glucan, called "low enzyme loading" (5 FPU+21.3 CBU/g glucan), and another called "high enzyme loading" (15 FPU+64 CBU/g glucan). As the crude thermophilic enzyme preparation was used at 70ºC in the SHF experiments, some of the CBU of the NZ 188 with a temperature optimum of 50ºC may have been lost during the hydrolysis step. The SSF experiments were carried out at 37ºC at which our enzymes had about 50-70% of their optimum activity. This resulted in lower SSF ethanol yields compared to SHF, as reported above. Results with prairie cordgrass were more variable and less conclusive than those with switchgrass and corn stover.

Key Outcomes & Impacts:

- Pretreatment significantly improved glucose and ethanol production for each substrate
- Higher enzyme loadings of 15 FPU/g glucan produced significantly higher glucose and ethanol production than using enzyme loadings of 5 FPU/g glucan for SHF experiments
- 6-month storage of PAKs did not appear to have a significant negative impact on SHF, SSF and thermostable enzyme ethanol yields
- Ethanol yields were 4-5% higher for material with an initial grind size of 2-mm than for material ground to 4-mm or 8-mm
- Densification had no adverse impact on SSF ethanol yields from corn stover or switchgrass
- Higher enzyme loadings of 15 FPU/g glucan produced 15-20% more ethanol than using enzyme loadings of 5 FPU/g glucan
- High thermostable enzyme loadings (15 FPU/g) improved sugar and ethanol yields by 30-50% in comparison to the use of lower thermostable enzyme loadings (5 FPU/g).

Objective 5 - Conduct economic and energy analyses of process to determine optimal and minimal scale
Recipient: Mike Twedt and Chris Saffron
Collaborators: NA

The goal of this project is to estimate the costs associated with pelletizing biomass for use in cellulosic ethanol production. Particularly, information pertaining to multiple off-site pelletizing facilities versus a single on-site facility is of great interest. Multiple off-site pelletizing facilities offer ease of access to suppliers, which theoretically could make the desired biomass more readily available and less expensive to buy. Obvious drawbacks include the added cost of building and operating multiple facilities versus a single one, as well as transportation costs that could be avoided if the biomass were received on-site. The analyses are based around the ComPakCo pelletizing and the AFEX (Ammonia Fiber Expansion) pretreatment processes. The primary benefit of pelletizing is ease of transportation and handling. Pellets can be handled essentially as a fluid, whereas bales of raw biomass are more cumbersome.

A model was generated which was able to calculate the approximate installation and operating costs of a pretreatment facility system which would provide the feedstock to a cellulosic ethanol facility. The pretreatment facility system had the option of subdividing into many off-site pelletizing facilities, ranging from 1 central facility up to 100 individual facilities. The model indicates that a single facility was the most cost-effective way to collect and pretreat biomass. A single facility had a total installation cost of about $60 million, whereas creating 10 facilities (with the same total throughput and processing capabilities of the single facility) had a total installation cost of closer to $70 million (scaled to supply a 50 MGY ethanol production facility).

A process model of AFEX was developed in order to assess the costs and profitability associated with this biomass pretreatment method. This process model includes the cost of the AFEX reactor, the cost of compression needed for ammonia recycle, and the cost of compaction to produce AFEX PAKs. For a 100 dry tonne per day AFEX processing facility, the costs of pretreatment amount to $162 per tonne of AFEX pellets using a pelletizer as described in Hamelinck et al.[1] Using the ComPAKco system studied during this project, the cost of dense AFEX PAKs is $155 per tonne. AFEX with an on-site ComPAKco system has an estimated capital investment of $7.6 MM for a 100 dry tonne per day capacity. Assuming an internal rate of return of 10%, the minimum AFEX PAK selling price amounts to $182 per dry tonne. Future improvements to AFEX, including the partial expansion of ammonia into a second reactor vessel prior to compression, and lower priced ammonia, could significantly reduce costs.

The initial cost of the AFEX system and the cost of replacing lost ammonia make up the largest components of overall facility costs. A sensitivity analysis was performed, which indicates the relative effect of improvements to various variables in the model on the overall facility costs. Again, as the largest costs, changes in ammonia recovery and AFEX system cost will have a larger effect on the overall cost of the system. It is reasonable that as the technology becomes more developed, economies of scale will allow for cheaper installation of the AFEX systems.

Task 5.1 Development of AFEX process model

The AFEX process model has been completed for the reported work. An AFEX system that uses compression to recycle ammonia was modeled in a manner similar to a conventional refrigeration system as ammonia has historical significance as a refrigerant. This system is possible provided that ammonia and water can be aptly separated prior to compression. Figure 5.1.1. depicts the process flow diagram for the modeled system. Mass balances, energy balances, equipment costs, capital investment, operating costs, profitability, and sensitivity worksheets are contained in the Excel Workbook model (provided). Densification was performed by pelletization and by briquetting using the ComPAKco system investigated during the course of this project.

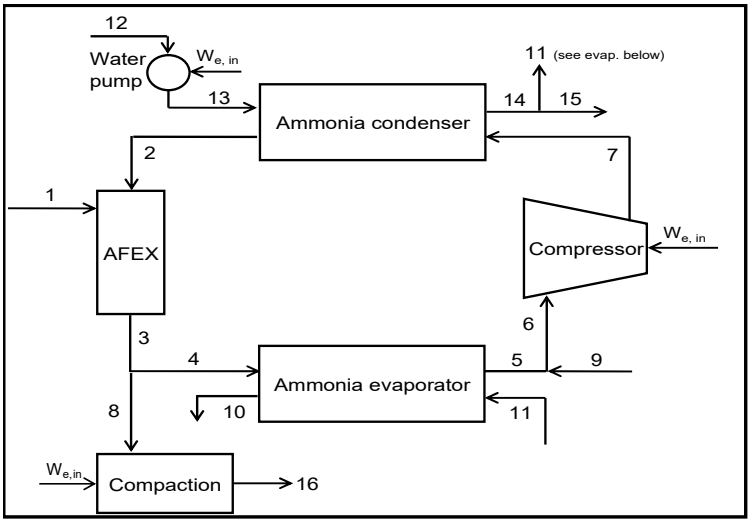

Figure 5.1.1. Process flow diagram for the AFEX-ComPAkco system

Task 5.2 Development of ComPAKco process model

The techno-economic analyses performed in this study centers on developing a model to calculate the approximate installation and operating costs of a biomass pretreatment facility system which would

provide the feedstock to a cellulosic ethanol facility. A large production scale was utilized (base conditions of 50 million gallons per year (MGY) ethanol production facility with 80 gallons of ethanol produced per ton of feedstock (gal/ton), which would require an input feedstock of 625,000 tons per year of biomass). Based on the stated production scale, the material handling, material storage, transportation, building, infrastructure, utilities, and pre-processing systems were determined. The capital and operating costs of these systems were then determined. The specific ComPAKco specifications and costs were obtained through Federal Machine, while the AFEX costs were determined from Task 5.1. The cost metrics were then analyzed to determine the optimum number of pre-processing facilities.

The customary processing method consists of several stages, outlined in Figure 5.2.1. The raw feedstock is brought in by producers (farmers), stored, ground and converted into ethanol.

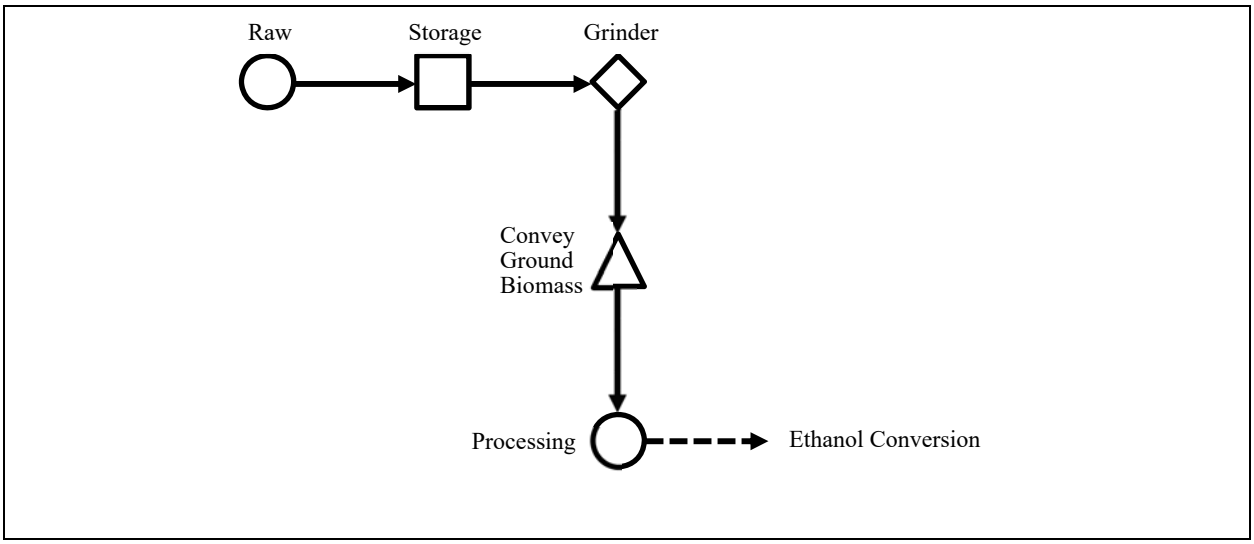

Figure 5.2.1. The "Status Quo"

The goal of this project was to estimate the costs associated with pelletizing and treating biomass for use in cellulosic ethanol production, in addition to determining the optimum number of off-site pelletizing facilities versus a single on-site facility.

Multiple off-site pelletizing facilities offer ease of access to suppliers, which theoretically could make the desired biomass more readily available and less expensive to buy. Obvious drawbacks include the added cost of building and operating multiple facilities versus a single one, as well as transportation costs that could be avoided if the biomass were received on-site. A list of some of the constraints used in the analysis is shown below, and a more thorough explanation of the constraints is given in the next section.

Constraints:

- Feedstock
- Transportation/Handling
- Facility
- Processing
    - ComPakCo
    - AFEX
- Storage
- Grinding

This analysis is based around the pelletizing and pretreatment (AFEX) processes. The ComPakCo pelletizing process, which is currently under development by Federal Machine, aims to eliminate large friction losses found in other pelletizing machines by pressing pellets between intermeshing gear teeth, rather than forcing material through a die.

The new process incorporates the ComPakCo and AFEX equipment into the processing procedure. A flowchart for this process can be seen in Figure 5.2.2. Similarly to the conventional ethanol conversion process, a supplier would need to transport his or her feedstock all the way to the facility in order to sell it. While this does reduce transportation costs borne by the facility, it may drive off potential suppliers and increase feedstock sale price. However, since all of the pelletizing equipment is in one place, the facility would be able to take the most advantage of economies of scale, potentially reducing costs.

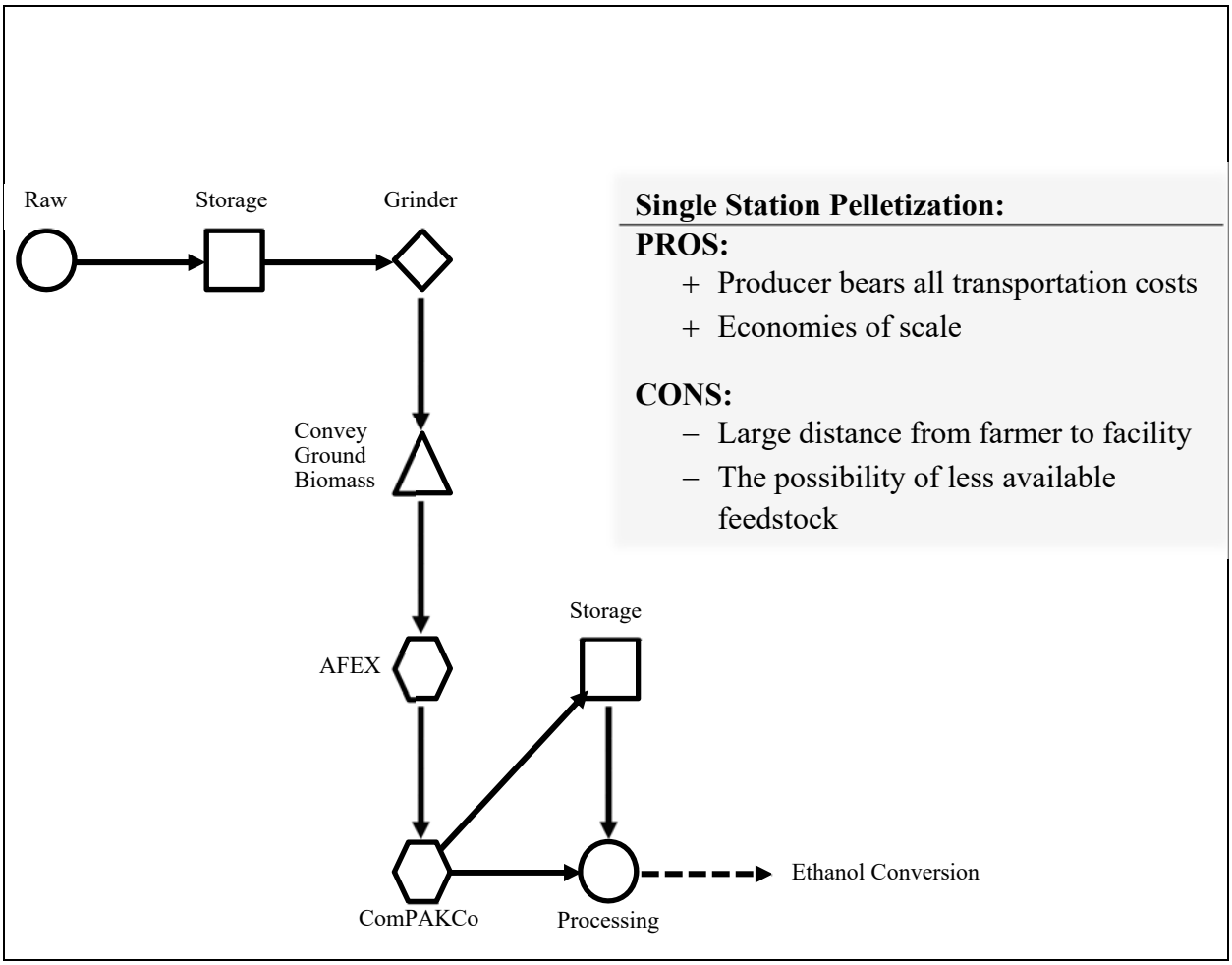

Figure 5.2.2. The Pelletization Process (Single Station)

This study not only analyzes the feasibility and advantageousness of the pelletization process itself: it also investigates the effect of using multiple collection facilities. The pelletization equipment could be located in remote facilities spread out over the same amount of land. By using multiple stations, the feedstock suppliers would have more convenient access to the facility, and more feedstock may be available. However, since the equipment is spread out over several locations, initial and operating costs would increase from the loss of economies of scale.

A table showing all the assumed values during the generation of the model is listed below, in Table 5.2.1:

Table 5.2.1: Assumed Input Values in Base Model

Facility	
Expected Facility Lifetime (years)	20
Plant Size (MGY)	50
Production (gal/ton feedstock)	80
Feedstock Required (ton/yr)	*625,000*
Available Feedstock Density (ton/mi^2)	*320*
Required Growth Area (mi^2)	*1953.13*
Processing time (hr/yr)	8,472
Receiving Time (hr/yr)	3,120
Harvest	
Growing density (ton/acre)	5
% surrounding region utilized	10%
Economics	
Loan Period [n] (years)	20
Annual Effective Interest Rate [i] (%)	10%
Bales	
Geometry: Height (ft)	4
Width (ft)	4
Length (ft)	8
Density (lb/ft^3)	15.625
Facility Land	
Land Amount (acres)	40
Cost of Land ($/acre)	10,000
Bale Storage	
Bale Storage Time (Days)	30
Concrete Pad Thickness (in)	5
Stack Configuration: Height of Row (ft)	24
Depth of Row (Bales)	18
Length (# of Rows of bales)	476
Bale Storage Slack (Extra Concrete)	10%
Concrete Cost ($/yard^3)	$75.00
Pellet Storage	
Output Mass / Input Mass Ratio	1
Pellet Storage Time (Days)	30
Grain Bin Floor Type	Concrete Floor
Grain Bin Size	48 ft Diameter - 48 ft Tall

Transportation	
Pellet Bulk Density (lbf/ft^3)	18.48
Pellet Density Increase	20%
Semi capacity (Pellets) (lbs)	27,238
Semi cost ($/mile)	3.19

Construction	
Economies of Scale Multiplier	10%
Warehouse Construction Cost ($/ft^2)	80
Footprint (ft^2 per ton per hour)	128
Slack (Extra Footprint For Facility)	30%

Processing	
Conveyor Max Length (ft)	1,000
Conveyor Min Length (ft)	250
Conveyor Belt Scaling	95%
Conveyor Cost ($/ft)	$200
Grinder Size (lbs/hr)	60,000
Grinder Cost ($/machine)	$91,000

AFEX	
Ammonia to Biomass Loading (tons/ton)	1
Ammonia Supply (days)	7
Ammonia Recovery	97.0%
Ammonia Cost ($/ton)	670
Natural Gas Cost ($/MMBTU)	$5.00
Heating System Efficiency	75%
Incoming Temperature (F)	60
Outgoing Temperature (F)	212
Specific Heat of Biomass (BTU/lb*F)	0.8
Specific Heat (Cp) of Ammonia (BTU/lb*F)	0.4002

Energy Consumption	
Electric Rate ($/kWh)	0.06
Conveyor Motor Load Scaling Rate	60%
ComPAKCo Machine Load Scaling	55%

The facility was assumed to be sized in a number of gallons produced in output. Similarly, a parameter was specified which sets the number of gallons able to be produced from a ton of (unprocessed) feedstock input. This yields an approximation of the amount of feedstock required for a given size of facility. For instance, a 50 million gallon per year (MGY) facility with a production of 80 gallons per ton feedstock (gal/ton) will require an input feedstock of 625,000 tons annually. Additionally, the operating hours of the

facility are able to be specified in terms of hours per year, and are divided into two categories – processing time and receiving time. The processing time is the number of hours per year that the grinding and processing machines will be running, and is used in calculating the size of machines required to process the input feedstock. For example, a single facility running processing 24 hours per day will only need grinding and processing machines half the size of a facility processing 12 hours per day. The receiving time of a facility outlines the number of hours per year that a facility will accept feedstock from farmers. It controls the amount of labor and equipment required to unload, sort and store the feedstock.

Two parameters are specified regarding harvest: a growing density in tons per acre for the biomass, and a percent of surrounding region able for growing the biomass. With these parameters, a growing density (in tons per square mile of surrounding region) and required growth area can be calculated. The required growth area specifies how far of a "reach" a facility will need to have to collect the required amount of feedstock to meet its production requirements.

For the model to be able to correctly calculate the amount of storage space required to meet an annual processing requirement, information needs to be inputted regarding the geometry and makeup of the bales. The bales can be assumed to be rectangular or cylindrical, and a packed density is set for an average bale (in pounds of feedstock per cubic foot). Additionally, bales are assumed to be stored for a certain amount of time. Since it is unlikely that the perfect amount of bales is arriving at all times, a certain amount of storage is needed to allow the facility to be able to operate without wasted downtime. The amount of time the bales are stored (in days) will likely directly correspond to how often feedstock is going to be received. Next, stacking geometry is inputted: a maximum height of bale stacks as well as a depth of each row of bales (in number of bales). The bales are assumed to be stored in a rectangular configuration on a concrete pad. By selecting a depth of each bale stack, the model calculates how long each storage region will need to be to store bales for the inputted amount of time. Details controlling the concrete pad are also entered: a thickness of the concrete pad (in inches), the amount of slack space assumed to be around the stack of bales (in percentage) as well as a cost per cubic yard of installed concrete. With all of these parameters specified, the model will calculate the number of bales required to be stored, the amount of space required to hold those bales, the size of concrete pad to contain that space, and finally, the cost of that much installed concrete.

Now that storage for the preprocessed biomass material has been specified, the post-processed material needs to be considered. An imputable parameter for the mass ratio of pellet output to feedstock input is specified. This comes from testing, and is a representation taking into account the amount of mass lost in the pelletizing process. With this, an amount of mass of the outputted pellets is calculated. By inputting a pellet bulk density (in pounds per cubic foot, which comes from project test results), the volume of space taken up by the pellets is calculated. Some parameters defining the type of bin used to contain the pellets are user inputted, such as the bin size and floor type, control the cost to store a given amount of pellets. Similarly to the feedstock storage, an (imputable) assumption is made regarding the number of days the pellets will need to be stored. This comes from the difference in rate of pellet production to ethanol processing, and is also affected by the transportation process of pellets to the ethanol facility. The model has two means of calculating grain bin pricing. The first type assumes an installed cost per bushel at a certain level of grain bin size. The second assumes a whole number of installed grain bins. Both numbers are derived from actual grain bin installation cost data, but the first model provides a better comparison within different numbers of facilities and operating hours. The second model correlates a little more logically with the real world, but presents a poorer indication of grain bin costs when comparing different facility configurations, because it assumes a set level of grain bin sizes. Nevertheless, either method can be used, depending on user preferences.

Pellets, once produced, need to get to the central ethanol processing facility. When more than one remote pelletizing facility is built, this requires large scale transportation with semi-trucks. The trucks are

assumed to be grain trucks, with a certain volumetric and weight capacity. For a given inputted pellet bulk density (specified earlier), the model calculates each truck's maximum capacity. In most cases, the truck will reach volumetric capacity before weight capacity. The pellets are assumed to be compressed slightly more under their own weight inside each truck, and the number of trips required to transport the pellets is calculated. The transportation cost (in dollars per mile) is inputted, allowing the model to calculate a cost of transportation.

To approximate the construction costs for a facility structure, an assumption was made about the required footprint of the equipment needed for processing. An increase in footprint size "slack" is added to account for walking space, etc. Then, an imputable parameter for construction costs in dollars per square foot is used to calculate initial facility costs, with a linear scaling factor accounting for economies of scale in costs.

Imputable parameters control the sizing of processing equipment. For a given amount of biomass, the model sizes the appropriate number of grinders and extruders to process the biomass in the required time. Some surrounding equipment is also accounted for in this section, including conveyor belts.

Most of the imputable parameters for this section come from testing. Linear extrapolation is used to calculate the initial costs for a given AFEX machine. Ammonia costs are considered, both initial costs (purchasing all the required ammonia the first year) as well as operating costs (replacing the ammonia lost in the AFEX process). Since the process requires materials to be heated, natural gas consumption is taken into account. By using the specific heat capacities of both biomass and ammonia, the total amount of heat (and therefore, the amount of natural gas) required to increase the temperature of these components to operating conditions is calculated, while accounting for inefficiencies in the heating process. The cost of this amount of natural gas is then computed.

The facility (or facilities) needs personnel to operate/maintain machines, load/unload biomass and manage the facility itself. Imputable parameters outline the number of operators at each level, and account for scaling of personnel when there are multiple facilities (one maintenance team could rotate between facilities, for example). Wages for each level are employee also inputted and likewise scaled.

Since each collection facility will draw materials from the region directly surrounding it, it can be modeled as a circular collection region of a given radius. This radius represents the average maximum distance which a person would be willing to drive to sell materials to the collection facility. These circular regions will, in reality, have some overlap, as a person will likely choose to bring their materials to the most convenient facility, and that isn't always necessarily the facility closest to his or her home. For the analysis, these facilities were assumed to be placed in the most efficient way of packing circles, hexagonal packing, which produces approximately 91% packing efficiency (Wells, D. *The Penguin Dictionary of Curious and Interesting Numbers*; p. 30, 1986). Hexagonal packing means the central facility will be surrounded by facilities in patterns of six. After the central hexagon of six facilities, each subsequent ring of facilities increases by six. That is, the second ring would have 12 facilities, the third, 18, etc.

Constraints centered on the ethanol facility itself included annual production (a typical, early-stage, commercial-scale, corn-based ethanol facility produces roughly 50 million gallons per year, so this value was used) and the amount of ethanol which can be obtained from a given volume of feedstock.

For transportation, the cost of hauling biomass by truck from the Regional Biomass Processing Centers to the ethanol facility was considered. The greatest factor affecting the cost of transportation was whether a single on-site RBPC or multiple off-site RBPC's were used. If the suppliers bring the biomass to a single on-site processing center, then the pellets are already at the facility and no transportation cost is incurred.

If the biomass is processed at off-site processing centers, then the pellets have to be hauled by truck from the processing centers to the ethanol facility.

Some of the equipment used to process the biomass scales linearly. However, some equipment have costs influenced by economies of scale, such as when a single large machine will cost less per unit of throughput than four small machines, even if their combine processing power is equivalent.

The AFEX machine itself scales linearly, but has a 'non-zero-y-intercept'. That is, the equipment can be approximated as having a set 'base' cost, then an additional cost per unit of throughput, which makes up the effect of the economies of scale. The ammonia and biomass need to be heated, which consumes considerable amount of natural gas, but that consumption pales in comparison to the amount of ammonia required for the AFEX process. The amount of ammonia consumed in the AFEX process results in a very significant cost. Figure 5.2.3 shows a breakdown of all annual costs including the annualized capital costs. The AFEX-related costs comprise a significant portion of the costs. However, it is likely that as the AFEX process is refined and becomes more popular these costs could decrease.

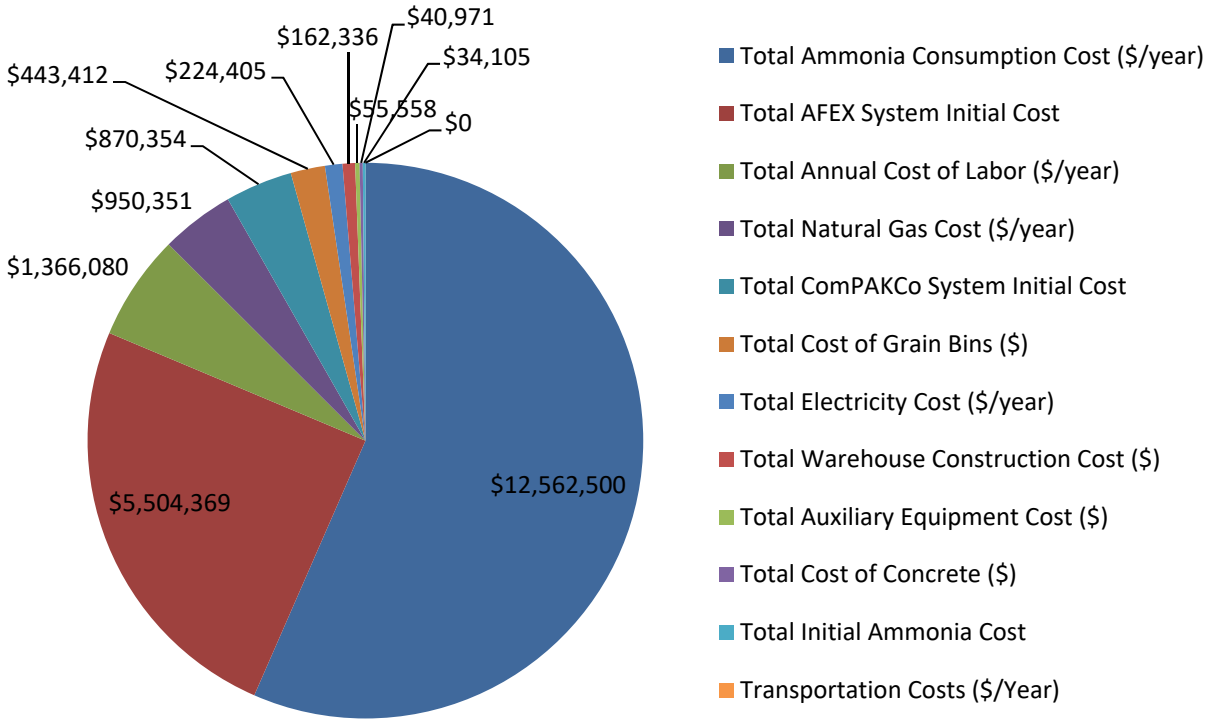

Figure 5.2.3. Distributed Annual Costs Over Facility Lifetime (Interest Included)

Another important observation is the effect of economies of scale. As the number of facilities increases, there is a less efficient return on investment – equipment costs more, more labor is required, and more equipment is necessary to perform the same job. With all variables set at the ideal values, the cost of transporting pellets from any number of off-site pelletizing facilities is substantial. This annual cost can also be seen in Figure 5.2.8. With a single on-site facility, no large-scale transportation would be required.

Due to the facilities being assumed to be arranged in a hexagonal pattern, the effect of adding a facility or two outside of the hexagon represents a larger proportional cost to the total transportation requirements. It is not until that level of the hexagon becomes mostly full that the transportation costs come back down.

At 10 facilities, the transportation of the pelletized biomass has an estimated cost of nearly $2 million. This relatively large cost of transportation is largely due to the fact that biomass is a very inefficient resource to transport. Even when pelletized, the trucks carrying the pellets are not fully loaded. This type of inefficiency becomes even more important when transporting several hundred thousand tons of material. When analyzing the multiple station facility, transportation of feedstock from the remote stations to the central station need to be as efficient as possible to minimize costs and conveyance time. Using fully loaded grain trailers at the best achieved bulk density (as measured in a lab setting), the weight efficiency of the load is as follows:

- Switchgrass
  - PAK's : 59%
  - AFEX Treated PAK: 28%
- Corn Stover
  - PAK's : 42%
  - AFEX Treated PAK: 51%
- Prairie Cordgrass
  - PAK's : 45%
  - AFEX Treated PAK: 24%

Another important factor is ethanol production yield, in terms of gallons of ethanol per ton of feedstock. This addresses both of the major factors in transportation cost - distance and quantity. Extracting 25% more ethanol per ton of feedstock would save a reasonable amount in transportation costs alone, not to mention allowing for smaller, less expensive equipment that would consume less power. Table 5.2.2 shows a breakdown of the added cost per ton of feedstock with the addition of each remote processing facility.

Table 5.2.2. Added Cost of Additional Facilities

Number of Facilities	Price Per Ton Feedstock (During Loan Period)	Added Cost (During Loan Period)	
1	$ 35.47	$ -	0%
2	$ 39.24	$ 3.77	11%
3	$ 42.03	$ 6.56	18%
4	$ 44.07	$ 8.60	24%
5	$ 45.79	$ 10.32	29%
10	$ 52.94	$ 17.47	49%
15	$ 57.14	$ 21.67	61%
20	$ 58.81	$ 23.34	66%
30	$ 69.43	$ 33.96	96%
40	$ 79.66	$ 44.20	125%
50	$ 89.89	$ 54.42	153%
75	$ 116.42	$ 80.95	228%

Task 5.3 Integrate AFEX and ComPAKco process models

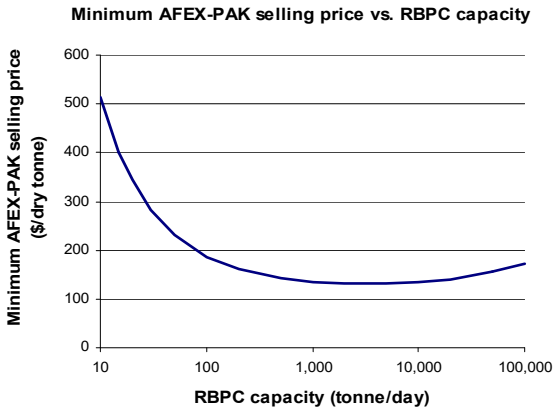

Figure 5.3.1. AFEX-PAK minimum selling price vs. RBPC capacity. Plant capacities between 1,000 and 10,000 tpd exhibit the optimum selling price.

1. The AFEX model was used to generate a plot of profitability vs. the dry biomass processing capacity of the RBPC. The minimum AFEX-PAK selling price was determined by selecting an internal rate of return equal to 10% and by setting the net present value to zero. Figure 5.3.1. contains a plot of selling price vs. plant capacity showing a clear minimum when plotted on a semi-logarithmic scale. Biomass flow rates between 1,000 and 10,000 tonnes per day appear to be optimal in terms of minimum selling price. Small RBPCs are subject to very high fixed costs, such as labor, supervision and overhead. Scales larger than10,000 tonnes per day are subject to high variable costs as the harvest radius increases and the biomass costs climb. At the base case plant of 100 tonnes per day (biomass input or output as no biomass is lost during pretreatment) the cost of AFEX-PAKs are $155 per dry tonne at the RBPC gate. This assumes that biomass costs $57 per dry tonne, ammonia is $770 per tonne, and electricity at $0.10 per kWh. The total capital investment (fixed plus working) is about $8.1 MM dollars, assuming that working capital is 20% of fixed capital and that fixed capital is about three times the equipment cost.

After examining the model predictions, a sensitivity analysis was performed to determine process components that may be subject to improvement. One such component was the compression step of the recycle process. Ammonia compression was responsible for almost $18 per tonne of biomass cost because of electricity consumption and the compressor itself was by far the most expensive equipment item. After identifying the compressor flow as the dominant cost for the selected basis case, a sensitivity model was performed to quantify the effect of varying the amount of ammonia recycled. Figure 5.3.2. shows the dependence of AFEX-PAK minimum selling price, operating costs, compression electricity costs and capital investment on the compressor feed rate. Substantial savings can be realized if the compressor feed is reduced to the fresh ammonia feed rate, which assumes that only ammonia that is lost with the AFEX-PAKs requires compression. Capital investments as low as $3.3 million and selling prices of $138 per tonne are achievable at the 100 tpd scale if the amount of recycled ammonia can be reduced. Technical approaches that can achieve such savings should be pursued as well as less expensive ways of producing plant biomass. The AFEX design reported by MBI International, which requires much lower levels of ammonia recycle, will significantly lower the AFEX pellet or PAK selling price and improve profitability.

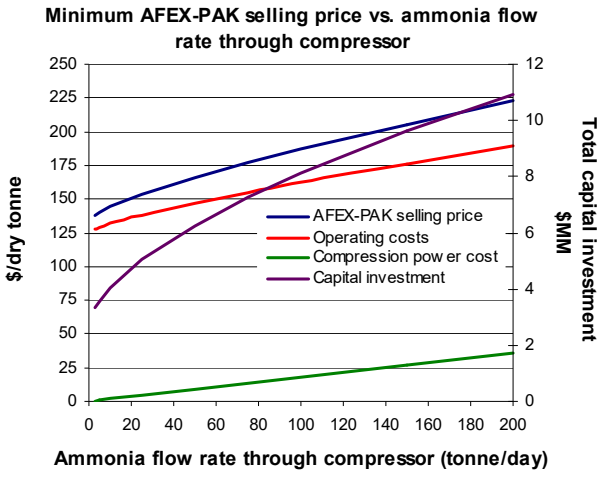

Figure 5.3.2. Sensitivity analysis showing the effect of lower ammonia feed rates to the compressor.

The sensitivity analysis demonstrates the relative significance of each independent variable on the change in the dependent variable. In this case, it also serves to demonstrate the effect of small advancements in the most significant variables of the model. As discussed in the baseline model, the ammonia recovery rate comprises the majority of the operating costs. Small changes in the efficiency of ammonia recovery have drastic changes in the yearly operating costs of the facility: an improvement of 1% (in absolute recovery rate, not relative improvement) produces a savings of about $4 million.

Key Outcomes & Impacts:

- Developed a comprehensive AFEX process model by incorporating energy balance and energy costs
- Developed a comprehensive ComPAKco model by incorporating energy balance and energy costs
- Developed an integrated AFEX and ComPAKco model

Project activities

This has been described above in each objective.

Products developed under the award and technology transfer activities, such as:

a. Publications (list title, year, journal name, volume, issue, and page numbers), conference papers (name of conference; location of conference; date of conference; and conference sponsor), or other public releases or outreaches of results.

Book Chapters

1. Muthukumarappan, K., and C. Karunanithy. 2014. Chapter 23 on 'Lignocellulosic Feedstock Preparation by Size Reduction and Pretreatment' in Biofuel Crops: Production, Physiology and Genetics Edited by B. P. Singh.
2. Karunanithy, C., K. Muthukumarappan, and W. R. Gibbons. 2014. Chapter on 'Advances in Pretreatment Strategies of Biochemical Conversion of Biomass' Bioprocess Engineering of 'Recent Developments in Biotechnology' STUDIUM PRESS LLC, TX.
3. Karunanithy, C. and K. Muthukumarappan. 2013. Thermo-mechanical pretreatment of feedstocks: In Green Biomass Pretreatment for Biofuels Production edited by Dr. Tingyue Gu, Springer-Verlag London Limited., ISBN 978-94-007-6051-6, 31-65.
4. Muthukumarappan, K. 2012. Novel Integration of Preprocessing and Densification of Different Biomass Feedstocks. In: Advanced Biofuels in a Biorefinery Approach. ISBN: 978-87-7903-574-4: 23.
5. Karunanithy, C. and K. Muthukumarappan.2012. Extrusion Pretreatment of Biomass Towards Bioethanol Production. Eds., Lambert Academic Publishing. ISBN: 978-3-8473-4262-5.

Journal Publications

1. Karunanithy, C., K. Muthukumarappan and A. Donepudi. 2013. Moisture sorption characteristics of corn stover and big bluestem. Journal of Renewable Energy. http://dx.doi.org/10.1155/2013/939504.
2. Karunanithy, C., K. Muthukumarappan and A. Donepudi. 2013. Moisture sorption characteristics of switchgrass and prairie cordgrass. Fuel 103: 171-178.

3. Karunanithy, C., Y. Wang, K. Muthukumarappan, and S. Pugalendhi. 2013. Physio-chemical characterization of briquettes made from different feedstocks. Biotechnology Research International: Bioenergy and Biorefinery (Special issue) – DOI:10.1155/2013/165202.
4. Eckard, A. D, K. Muthukumarappan and W. Gibbons. 2013. Enhanced Bioethanol Production from Pretreated Corn Stover via Multi-Positive Effect of Casein Micelles. Bioresource Technology 135(5): 93-102.
5. Zambare, V. P, Zambare, A. V, Muthukumarappan, K. and L. P. Christopher. 2011. Biochemical characterization of thermophilic lignocellulose degrading enzymes and their potential for biomass bioprocessing. International Journal of Energy and Environment 2(1): 99-112.
6. Zambare, V. P, Zambare, A. V, Muthukumarappan, K. and L. P. Christopher. 2011. Potential of thermostable cellulases in the bioprocessing of switchgrass to ethanol. Journal of BioResources 6(2): 2004-2020.

Conference Presentations

1. Sundaram, V., and Muthukumarappan, K. 2014.Effects of biomass blending on sugar yield and pellet hardness of afex treated corn stover and switch grass. To be presented at the 2014 ASABE and CSBE/SCGAB Annual International Meeting, July 13-16, Montreal QC, Canada.

2. Sundaram, V., and Muthukumarappan, K. 2014. Effect of densification and biomass parameters on sugar yield of AFEX pretreated corn stover, prairie cordgrass and switch grass. To be presented at the 2014 ASABE and CSBE/SCGAB Annual International Meeting, July 13-16, Montreal QC, Canada.
3. Sundaram, V., and Muthukumarappan, K. 2014. Influence of AFEX pretreated corn stover and swichgrass ratio levels on the compaction characteristics of pellets. Presented at the 2014 ASABE/CSBE North-Central Intersectional Conference, March 28-29, Brookings, SD.
4. Muthukumarappan, K. 2013. Advanced Biofuels: Challenges and Opportunities. Invited plenary session speaker at the 4th World Gene Convention 2013, November 13-16, Haikou, China, Conference Proceedings: 139.
5. Muthukumarappan, K. 2013. Bioenergy Research at CBRD. Invited Keynote Address at the 2013 International Conference on Energy and Sustainability, October 18-20, Beijing, China, Conference Proceedings: 19.
6. Karki, B., Muthukumarappan, K., Sundaram, V., and Gibbons, W. 2013. Effects of storage conditions on the properties of control, AFEX, and AFEX-PAKed prairie cordgrass samples. Presented at the 2013 ASABE Annual International Meeting, Kansas City, MO.
7. Sundaram, V., and Muthukumarappan, K. 2013. Effect of AFEX treatment on compaction characteristics of biomass. Presented at the 2013 ASABE Annual International Meeting, Kansas City, MO.
8. Pryor, S.W. 2013 Synergies of Biomass Densification and Pretreatment for Biofuel Production, NDSU Agricultural and Biosystems Engineeering Seminar. Fargo, ND Jan 25, 2013
9. Muthukumarappan, K. 2013. Novel Integration of Preprocessing and Densification of Different Biomass Feedstocks. Presented at the 3rd International Conference on Lignocellulosic Ethanol, April 3-6, Madrid, Spain.
10. Muthukumarappan, K. 2012. Novel Characteristics of Pretreated and Densified Biomasses. Invited plenary session speaker at the 2nd Annual World Congress of Bioenergy 2012, April 25-28, Xi'an, China, Conference Proceedings: 125.

11. Muthukumarappan, K. 2012. Novel Integration of Preprocessing and Densification of Different Biomass Feedstocks. Presented at the Advanced Biofuels in a Biorefinery Approach Conference, Feb 28-March 1, Copenhagen, Denmark.
12. Muthukumarappan, K. 2012. Novel Characteristics of Pretreated and Densified Biomasses. Invited plenary session speaker at the 2nd Annual World Congress of Bioenergy 2012, April 25-28, Xi'an, China.
13. Wang, Y., and K. Muthukumarappan. 2012. Moisture adsorption characteristics of control, AFEX and PAKed Corn stover. Presented at the 2012 ASABE Annual International Meeting, July 29-Aug 1, Dallas, TX.
14. Wang, Y., K. Muthukumarappan and C. Karunanithy. 2012. Moisture adsorption characteristics of control, AFEX and PAKed Switchgrass. Presented at the 2012 ASABE Annual International Meeting, July 29-Aug 1, Dallas, TX.
15. Rijal, B., B. Karki, C. Igathinathane, M. Yu, and S.W. Pryor 2012 Interaction of Densification and Pretreatment for the Enzymatic Hydrolysis and Fermentation of Biomass, Paper No. 121338124. ASABE International Meeting. Dallas, TX Jul 29 Aug 1, 2012.
16. Rijal, B., B. Karki and S.W. Pryor 2011. Impact of AFEX Pretreatment and Biomass Densification on Cellulosic Ethanol Production, Paper No. 1111208. ASABE International Meeting. Louisville, KY Aug 7-9, 2011.
17. Muthukumarappan, K. 2011. Novel Integration of Biomass Pretreatment and Densification for Effective Bioethanol Production. Invited plenary session speaker at the 1st Annual World Congress of Bioenergy 2011, April 25-29, Dalian, China.
18. Christopher, L.P., V.P. Zambare, A. Bhalla, K. Muthukumarappan, R.K. Sani. 2011. High-solids extrusion, hydrolysis and fermentation of corn stover to ethanol using a thermophilic Geobacillus strain. Presented at the 33rd Symposium on Biotechnology for fuels and chemicals, May 2-5, Seattle, WA.
19. Wang, Y., C. Karunanithy, K. Muthukumarappan, and S. Pugalendhi. 2011. Physio-chemical characterization of briquettes made from different feedstocks. Presented at 2011 ASABE Annual International Meeting, August 7-10, Louisville, KY.
20. Wang, Y., K. Muthukumarappan, and C. Karunanithy. 2011. Physical and chemical characterization of AFEX-PAKS densified corn stover. Presented at 2011 ASABE Annual International Meeting, August 7-10, Louisville, KY.
21. Wang, Y., K. Muthukumarappan, and C. Karunanithy. 2011. Physical and chemical characterization of AFEX-PAKS densified prairie cord grass. Presented at 2011 ASABE Annual International Meeting, August 7-10, Louisville, KY.
22. Muthukumarappan, K. 2011. Transforming and densifying feedstocks in regional biomass processing center. Presented at the Where there's smoke, there's fuel – A symposium on the thermochemical conversion of biomass to fuels, Aug 2, Oklahoma State University, Stillwater, OK.
23. Muthukumarappan, K and W. Gibbons. 2011. Novel Integration of Biomass Pretreatment and Compaction for Effective Bioethanol Production. Presented at the 2011 Pacific Rim Summit on Industrial Biotechnology and Bioenergy, November 21-23, Kuala Lumpur, Malaysia.
24. Muthukumarappan. 2010. Novel integration of pretreatment and comPAKtion of biomass for bioethanol production. Invited plenary session speaker at 3rd World Congress of Industrial Biotechnology 2010, July 25-27, Dalian, China
25. Muthukumarappan. 2010. Combination of Novel Pretreatments for Effective Bioethanol Production. Invited plenary session speaker at the 2010 International Fuel Ethanol Workshop & Expo, June 14-16, St. Louis, MO.
26. Muthukumarappan. 2010. Integration of Novel Pretreatments for Effective Bioethanol Production. Invited plenary session speaker at the 2010 International Conference on Biomass and Energy Technologies, Aug 20-22, Beijing, China.

27. Muthukumarappan. 2010. Novel Integration of Biomass Pretreatment and Densification for Effective Bioethanol Production. Invited Keynote session speaker at the 2010 International Conference on Biomass and Energy Technologies, Aug 20-22, Beijing, China.
28. Wang, Y., K. Muthukumarappan, and C. Karunanithy. 2010. Physical and chemical characterization of AFEX-PAKS densified switchgrass. Presented at the Pacific Rim Summit on Industrial Biotechnology & Bioenergy, Dec 11-14, Honolulu, HI.

b. Website or other Internet sites that reflect the results of this project.
c. Networks or collaborations fostered.
d. Technologies/techniques.
e. Inventions/patent applications, licensing agreements.
f. Other products, such as data or databases, physical collections, audio or video, software* or Netware, model, educational aid or curricula, instruments, or equipment.

3. Academic

a. Courses developed

Though not directly supported by this grant, three new bioenergy courses were developed at Michigan State University as part of a transcriptable Bioenergy Concentration. This "Concentration" is available to students in the Dept. of Chemical Engineering and Materials Science and the Dept. of Biosystems and Agricultural Engineering at MSU. The courses are CSS/FOR/BE 467, "Biomass Feedstock Production," CHE/BE 468, "Biomass Conversion Engineering," and BE/CHE 469, "Sustainable Bioenergy Systems." Each course has enrolled between 15 and 35 students since their inception in 2009.

b. M.S. students supported

MSU: No M.S. students were required for economic modeling; instead a senior chemical engineering undergraduate student was hired part-time during the project's second fiscal year.

NDSU: Binod Rijal, M.S. in Agricultural and Biosystems Engineering

SDSU: Yijing Wang, M.S. in Agricultural and Biosystems Engineering
Gwen Biersbach, M.S. in Biological Sciences

c. M.S. degrees conferred

NDSU: Binod Rijal, NDSU M.S. in Agricultural and Biosystems Engineering, "Combined Effect of Densification and Pretreatment on Cellulosic Ethanol Production" 2012.

SDSU: Yijing Wang, SDSU MS in Agricultural and Biosystems Engineering, "Physical, flow, and moisture adsorption characterization of afex-paked densified switchgrass, corn stover, and prairie cordgrass, 2012.

Gwen Biersbach, SDSU M.S. in Biological Sciences, "Effects of AFEX Pretreatment, Densification and Storage on Ethanol Yields of Corn Stover, Switchgrass and Prairie Cordgrass" 2013.

d. Ph.D. students supported

SDSU: Vijay Sundaram, Ph.D. in Agricultural and Biosystems Engineering

e. Ph.D. degrees conferred
f. Post-docs supported

1. **For projects involving computer modeling, provide the following information with the final report:**
   a. Model description, key assumptions, version, source, and intended use.

The techno-economic analysis (TEA) was performed upon programming of an Excel spreadsheet model (provided upon request). The basis case for this design assumes a flow rate of 100 dry tonnes of biomass per day. The process flow diagram is constructed in a manner similar to that of a refrigeration system, noting that ammonia has historically been used as a refrigerant. Compaction of the pretreated biomass can occur by either pelletization or compaction using a ComPAKco system. Mass and energy balances were constructed for each process step and these balances are used with equipment and raw material prices to determine capital and operating costs. Biomass delivered cost was determined in a manner consistent with Sokhansanj et. al,[2] i.e. the cultivation, harvesting and transport components were determined individually and then summed. Ammonia is added in a one-to-one ratio with dry biomass to the AFEX reactor. Reactor vessels were sized and designed using Peters and Timmerhaus, "Plant design and economics for chemical engineers."[3] The total reactor volume was determined from assuming a 20 minute residence time and a 4:1 height to diameter ratio. The cylindrical shell thickness was determined upon selection of allowable stress (129 MPa), joint efficiency (1) and corrosion allowance (1 mm/yr). Two ellipsoidal reactor heads were added and the total weight of 316 stainless steel was computed. The cost of steel was then used to determine the total reactor cost assuming a correction factor of 2.8 to correct for high pressure. Instead of one large AFEX reactor, three smaller reactors are assumed to operate in parallel as a contingency in case of malfunction. The ComPAKco equipment was assumed to cost $100K per ton-hour as per a personal communication. Electricity required to operate the ComPAKco system was added at a rate of 0.66 kWh/tonne of biomass processed. Compression operating costs were determined upon energy balance assuming an isentropic compression efficiency of 90% and a motor efficiency of 90%. Compression capital costs were determined based on electrical load and using Peters and Timmerhaus.[3] In order to cool the compressed ammonia stream in preparation for the AFEX reaction, a tube-and-shell heat exchanger is used to generate steam on its shell side. This steam is assigned a value consistent with an equivalent amount of steam created upon combustion of natural gas at $4/million BTU. After AFEX, three storage tanks serve as pulse dampeners so that the compressor can be operated at steady state.

The sum of all equipment costs enter as a line item on the "capital" worksheet to determined total fixed capital investment. Direct costs, such as installation, instrumentation, piping, and indirect costs such as engineering, construction and contingency, are added fixed percentages of the total fixed capital. For the 100 tpd facility, a purchased equipment cost of $2.5 MM results in a total fixed capital of $7.6 MM. The total fixed capital is approximately three times the equipment cost, which is reasonable for such a facility. Working capital is assumed to be 20% of the fixed capital, and therefore the total capital investment amounts to $9.1 MM.

Operating costs are divided into variable costs such as biomass, ammonia and utilities as well as fixed costs such as labor, supervision, maintenance and depreciation. The cost of delivered biomass was found to be $57/tonne, with cultivation, harvesting and transportation being significant cost contributors. Ammonia was found to contribute $23/tonne when 97% is recovered and recycled, implying the need for a 3% fresh ammonia feed. Transferring the spent ammonia from the primary AFEX reactor to a secondary AFEX reactor will avoid much of the compression and greatly reduce electricity costs. Also, the low cost of natural gas should eventually lead to lower cost ammonia and reduced AFEX costs. Fixed costs per unit mass were significant at the smaller scale of 100 tpd. Labor, laboratory (quality assurance and control) and supervision were valued at $25/hr, $30/hr and $35/hr, respectively. Six facility operators were needed

for a 24 hour operation on eight hour shifts. One supervisor and quality assurance engineer are included for a single eight hour shift. Consumables, insurance, taxes and maintenance materials are added as percentages of the total fixed capital investment. Plant overhead was assumed to be 50% of the cost of labor, laboratory and supervision. Total fixed costs were approximately $37.36/tonne AFEX PAK. Depreciation, determined using a 10 year straight-line schedule, added $22/tonne AFEX PAK due to the fixed capital investment. Total operating costs amount to $155/tonne of AFEX PAK, a value that is most sensitive to scale, ammonia price and biomass price. A minimum AFEX PAK selling price of $182/tonne results when assuming a zero salvage value, an internal rate of return of 10% and an annual tax rate of 35%.

A second model was generated in an Excel spreadsheet which is able to calculate the approximate installation and operating costs of a pretreatment facility with a range of off-site pelletizing facilities. The model was utilized to calculate the approximate installation and operating costs of a biomass pretreatment facility system which would provide the material for a cellulosic ethanol facility. A large production scale was utilized (base conditions of 50 million gallons per year (MGY) ethanol production facility with 80 gallons of ethanol produced per ton of feedstock (gal/ton), which would require an input feedstock of 625,000 tons per year of biomass). The model assumptions are outlined in Table 5.2.1 and include conversion rates, utility rates, facility footprint, and equipment metrics. The intended use of the model was to facilitate a technoeconomic analysis to determine the capital and operating costs of the pretreatment systems, in addition to determining the optimum number of off-site pelletizing facilities. The model indicates that a single facility was the most cost-effective way to collect biomass: A single facility had an installation cost of about $60 million, whereas creating 10 facilities (with the same total throughput and processing capabilities of the single facility) had a total installation cost of closer to $70 million.

a. Performance material for the model related to the intended use.
b. Test results to demonstrate the model performance criteria were met (e.g., code verification/validation, sensitivity analyses, history matching with lab or field data, as appropriate).
c. Theory behind the model, expressed in non-mathematical terms.
d. Mathematics to be used, including formulas and calculation methods.
e. Whether or not the theory and mathematical algorithms were peer reviewed, and, if so, will include a summary of the theoretical strengths and weaknesses.
f. Hardware requirements.
g. Documentation (e.g., user's guide, model code).

***Software/Manual (if applicable)**
Content. Unless otherwise specified in the award, the following must be delivered: source code, the executable object code and the minimum support documentation needed by a competent user to understand and use the software and to be able to modify the software in subsequent development efforts.

OUTPUTS (Subsequent Funding):

We submitted the following proposals but they were not funded yet. We will be resubmitting these proposals with preliminary data from this project.

- Production of Long-Chain Alcohol by an Integrated System Comprised of Extractive AFEX and Engineered Microbe, Co-PIs William Gibbons, Ruanbao Zhou, Bruce Dale & Chris Safforn (MSU), NC Sungrant DOT, $390,000 (Jan'12 – Dec'14).
- Second Generation Cellulosic biofuels: An Integrated Approach, Co-PIs POET, Inc, NDSU, ISU, USDA-DOI BRDI, $7,000,000 (July'12-June'16).

Please complete the following table to reflect your project at completion or time of report submission:

ITEM	NUMBER
Abstracts	**20**
***Peer Reviewed Publications**	**11**
Outreach Publications/Web Pages	
***Professional Presentations**	**28**
MS Degrees Conferred	**3**
Ph.D. Degrees Conferred	
MS Students Supported	**3**
Ph.D. Students Supported	**1**
Post-Docs Supported	**1 (SDSMT)**
Undergraduate Students Supported	
Investigators Supported	**1 (SDSU), 1 SDSMT**
Start-Up Jobs Created	
Disclosures	
Patents Filed	
Provisional Patents	
Patents Issued	
License Agreements	
Plant Variety Protection	

Publications/presentations in preparation stage

Back to Table of Contents

Sun Grant Initiative
DOE Final Progress Report

Project Title: In-Field Cubing of Biomass

Project Director/Principal Investigator: Kevin Shinners, Professor, Biological Systems Engineering, University of Wisconsin, Madison, WI.

All Co-Principal/Other Investigators: None

Collaborators: Xuejun Pan, Assistant Professor, Biological Systems Engineering, University of Wisconsin, Madison, WI; William A. Johnson, Manager (retired), Biofuels Development, Alliant Energy, Madison, WI.

Period of Performance: 1 January 2009 - 30 June 2011

Funding Awarded: $159,276

Cost Share Amount: $82,448

Cost Share Sources: Time and effort from PIs and CoPIs; Supplies; Indirect on time and effort and supplies

Executive Summary

One of the many challenges impeding the use of biomass for energy is its inherent low bulk density and the associated high transportation and processing costs. Therefore, the primary goal of this research was to increase the density and improve the handling properties of biomass feedstocks for more efficient energy production, especially in relation to co-firing biomass with coal for electrical or heat generation.

The current system of producing high-density cubes involves first packaging the biomass into large round or square bales which require many handling and processing operations prior to cubing, substantially adding to the cost of cubed biomass. Biomass bales must be deconstructed, size-reduced and then dried prior to cubing in an industrial setting. This research focused on producing cubes at the time of harvest, thereby eliminating many costly operations associated with post-harvest cubing. A mobile in-field cubing machine was modified to create biomass cubes that could be burned simultaneously with coal for electricity or heat generation. Directly creating biomass cubes at harvest eliminates handling and processing bales, thereby reducing the cost of creating energy from co-fired biomass. Cubing produces a feedstock that can be transported and handled with the same equipment currently in place at most coal burning facilities, limiting the capital transition costs necessary to implement co-fire electrical or heat generation.

A test fixture was designed and fabricated to allow experimentation to optimize the cubing process using field constraints but under controlled conditions. The fixture allowed control of the die surface temperature and back pressure, while measuring parameters such as compaction and friction forces. Variables investigated during experimentation included, but were not limited to: crop type, moisture content, back pressure, and amendment type and loading. Laboratory experimental results showed that as the surface temperature of the die block increased, the friction created at the interface between the material and the die decreased. In an in-field cuber, friction is used to create the required back pressure to consolidate the material, so regulating the die temperature to about 50°C could improve the performance of the in-field cuber by increasing consolidation back pressure. However, there would be a corresponding increase in energy required to form cubes. Higher die temperatures also reduced cube density because the higher temperature cubes had a longer cooling period which allowed for more relaxation. However, the elevated die temperatures did improve cube durability in some cases because the glass transition temperature had been exceeded.

Steam conditioning is widely practiced in the formation of pellets and cubes used for animal feed. The temperature and moisture of the steam are used to activate the materials natural binders like starch and protein to improve cube quality. Steam conditioning was found to slightly improve the quality of cubes produced in the test fixture.

Crop moisture above roughly 16 – 17% (w.b.) significantly reduced cube durability and density for reed canarygrass, switchgrass and corn stover cubes formed in the test fixture. It was found that when moisture was 10 to 16% (w.b.), increased moisture resulted in greater wall friction, but as moisture level continued to increase, friction was reduced presumably due to a lubrication effect. Higher moisture cubes also resulted in greater cube relaxation which reduced their density and durability.

Polymer and lignosulfonate binders added in solution were found to have little positive effect on cube quality. Any benefit of the small quantity of binder added was mitigated by the water added by the solution. Calcium oxide (lime) added to the cubing feedstock increased density, cube durability, and die wall friction. Adding lime could be viewed as a benefit or detriment. On one hand, calcium is often added as an emission control additive with some boilers, so adding this

material at cubing would add to feedstock value. On the other hand, logistics of bulk handling of this material in the field will add cost and reduce productivity.

The laboratory test fixture work showed that improved cube properties could be obtained by achieving crop moisture below 16% (w.b.), maintaining die temperature below 50°C, adding lime as an amendment at 1% of DM, and by steam conditioning. The in-field cuber was modified to meet the three machine related requirements. The die ring was cooled with a system that sprayed ambient temperature water on the outer surface of the die ring. A system was developed to apply lime to the material in the mixing/feed chamber located just before the die ring. Finally, a system was installed that injected high-temperature water at high-pressure in the mixing/feed chamber. Although the first two modifications did improve the performance of the in-field cuber, the fraction of material formed into cubes and the durability of the cubes was almost always less than desired. Our target was to achieve better than 90% of the harvested crop as cubes, with unit density of greater than 320 kg DM/m^3 and durability in excess of 75%. Unit density was often greater than 500 kg/m^3 but fraction cubed and especially durability were often less than these targets. The spatial variability of moisture in the windrow made it very difficult to optimize the cuber operating parameters so that a continuous production of cubes could be produced for a sustained period. Much additional research would be needed to develop systems on the in-field cuber which allow consistent and robust production of high-density biomass cubes.

Costs were estimated for harvest, transport to storage, storage, storage losses, and transport to biomass feedstocks to end use destination. Given the estimated large initial investment and the machines relatively low productivity compared to round or square balers, the cost of harvesting perennial grasses or corn stover was estimated to be two to four times that of baling. Cost of storing cubes was also considerably greater than storing bales due to poor space utilization. Although transport costs were somewhat less for cubed biomass, these cost saving did not offset the higher costs of harvest and storage. In-field cubing would produce lower cost biomass only if this physical form were required – for instance when biomass is co-fired with coal in existing power plants.

Project objectives

There were five specific objectives associated with this research project: develop a laboratory cubing test fixture, conduct controlled experiments with the text fixture, modify an in-field cuber based on results of laboratory tests, field evaluate the modified in-field cuber, and estimate the costs of in-field cubing.

Objective 1: A single die test fixture was successfully designed and fabricated (Appendix A). Instrumentation to measure critical cubing parameters such as compression force, piston displacement, cube back pressure, friction force between the cube and die block, and die block temperature were successfully implemented. A system to control die block temperature was developed and utilized. A test fixture to measure cube durability based on ASABE Standards was design, fabricated, and utilized. The performance of the test fixture met expectations.

Objective 2: The test fixture was used for many experiments to optimize the cubing process under the expected constraints for in-field cubing of biomass (Appendix A). Many factorial experiments were conducted which investigated the effect of die temperature, material moisture, back pressure, particle-size, and type and amount of amendment. The most important variables that led to successful formation of quality biomass cubes were, in the order of importance: low material moisture content (< 16% w.b.); die block temperature at or below ~ 50°C; the addition of lime at ~1% of DM as a binding amendment; and steam conditioning. As planned, the results of

experiments provided design direction and constraints for the modifications made to the in-field cuber.

Objective 3: Modification to an existing in-field cuber, which was originally intended for cubing animal forages, were designed and implemented (Appendix A). Modifications included a die cooling system, a system to apply granular binding amendment to the material prior to cubing, a system to apply heated water to the material before cubing, and an improved handling system. The modifications to the in-field cuber were made in a timely fashion and the modifications preformed mechanically as expected.

Objective 4: The modified in-field cuber was evaluated in field experiments using reed canarygrass, switchgrass and corn stover. Experiments were conducted to quantify the improvement in cube quality based on the modifications made to the in-field cuber (Appendix A). The die cooling system and the addition of lime as a binding amendment were successful in improving cube quality. However, the addition of heated water did not have a positive impact. The addition of heated water was intended to improve cube quality by activating the plants natural binders like starch and protein. The quantity of these binders is low in most biomass feedstocks, so even if activation was improved, there may have been insufficient binder quantity to affect an improvement in cube quality. The modified handling system reduced damage to the cubes after formation which improved their durability. Our target was to achieve better than 90% of the harvested crop as cubes (i.e. 10% as chaff), with unit density of greater than 320 kg DM/m^3 and durability in excess of 75%. Although the modifications made to the in-field cuber often resulted in performance improvements compared to the unmodified machine; it was rare that all the performance targets were achieved. The unit density of the cubes formed were often in excess of 500 kg DM/m^3, so that goal was most often attained. The goal of forming better than 90% of the crop into cubes was sometimes met, but often this was an all or nothing proposition. When crop moisture exceeded roughly 16% (w.b.) moisture, the process could abruptly change from successful cubing to no cube formation at all. The process was so highly dependent upon very strict moisture limits that it was not very robust. Finally, the durability of biomass cubes was often well below the target of 75% (Appendix A). Typical biomass crops do not have as many naturally occurring binders as forage crops (i.e. alfalfa), so even when cubes were formed, they did not maintain condition during handling. Although extensive field evaluation was conducted, the modified cuber did not meet our performance goals. Suggestions for further modifications to improve the performance of the in-field cuber are provided in Appendix A.

Objective 5: The cost of forming cubes was estimated using an enterprise budget approach. Costs were derived for harvest, transport to storage, storage, storage losses, and transport to the feedstock's end use destination. Based on productivity of the modified in-field cuber and the power requirements of the machine, an estimate was made for the purchase price and operating costs for an in-field cuber capable of producing 24 ton/h. The in-field biomass cuber was estimated to have a purchase price in excess of $1M. We made this estimate based on current costs of stationary cubing systems and the estimated weight and power of the in-field cuber. Given this investment requirement and the machines relatively low productivity compared to round or square balers, the cost of harvesting perennial grasses or corn stover was estimated to be two to four times that of baling (Appendix A). Cost of storing cubes was also considerably greater than storing bales because of poor utilization of space for cubes piled in commodity sheds. Although transport costs were somewhat less for cubed biomass, these cost saving did not offset the higher costs of harvest and storage. In-field cubing would produce lower cost biomass only if this physical form were required – for instance when biomass is co-fired with coal in existing power plants and the biomass must be densified into cubes having roughly the same physical properties as coal. Our cost estimates would show that in-field cubing is less expensive than the

combined cost of baling plus producing cubes from bales. However, if the physical form of cubes is not required, then baling would be less costly per ton than in-field cubing.

Project activities

Our original hypotheses was that high-density biomass cubes destined for co-fire applications with coal could be more economically produced by forming the cubes in the field at harvest than by baling and cubing after storage. To determine if high-density biomass cubes could be formed in the field, we first designed and fabricated a laboratory test fixture where single cubes of biomass were produced under constraints dictated by field conditions. Many experiments were conducted with the test fixture where it was determined that biomass cubes were most successfully produced when moisture content was less than 16% (w.b.); the die was cooled to about 50°C; lime at 1% of DM was added as a binding amendment; and when steam conditioning was used to improve activation of natural binders. Moisture content of the crop was the most important variable to affect cube quality. Moisture contents greater than approximately 16% (w.b.) reduced friction between the cube and die and caused too much relaxation of the cubes after formation, both of which negatively affected unit density and cube durability.

An in-field cuber was modified to cool the die ring during cube formation and to apply either granular lime or high-pressure heated water or both to the crop material prior to cube formation. Both die ring cooling and addition of lime as a binding amendment helped to improve cube quality. However, adding heated water to the crop material had a negative impact on cube quality. Moisture contents above 16% (w.b.) caused a significant decline in the quality of the cube formed. The spatial variability of moisture in the windrow made it very difficult to optimize the cuber operating parameters so that a continuous production of cubes could be produced for a sustained period.

Costs were estimated for harvest, transport to storage, storage, storage losses, and transport to biomass feedstocks to end use destination. Given the high initial investment and the machines relatively low productivity compared to round or square balers, the cost of harvesting perennial grasses or corn stover was estimated to be two to four times that of baling. Cost of storing cubes was also considerably greater than storing bales. Although transport costs were somewhat less for cubed biomass, these cost saving did not offset the higher costs of harvest and storage. In-field cubing would produce lower cost biomass only if this physical form were required – for instance when biomass is co-fired with coal in existing power plants.

The research conducted for this project has shown that in-field cubing of biomass has several difficult challenges. First, the spatial variability of moisture in the field made it very difficult to optimize the cuber operating parameters so that a continuous production of cubes could be produced for a sustained period. The deployment of moisture sensors and development of a machine control systems that react to changes in moisture might help overcome this challenge, but crop moisture must be readily and consistently dried to near 16% (w.b.) or less for in-field cubing to be a success. Next, the productivity of in-field cubing was low. To produce cubes at sufficient mass-flow-rates to achieve productivity required to harvest biomass in a timely fashion will require massive machines that we estimated will have capital investments in excess of $1M dollars. Finally, the cost to harvest and store cubed biomass was estimated to be considerably greater than bale based systems and the lower in transport costs of high-density cubes could not offset the greater costs of harvest and storage.

Products developed under the award and technology transfer activities, such as:

1. Publications:

a. Hoffman, T. J. 2011. Design and Performance Evaluation of an In-Field Cuber. Master of Science Thesis – Department of Biological Systems Engineering – University of Wisconsin.

2. Outreach:
    a. Shinners, K.J. 2009. Harvesting, transporting and processing biomass on Wisconsin's farms. 49th Annual Wisconsin Public Service Farm Show. April 1st, 2009. Oshkosh, WI.
    b. Shinners, K.J. 2009. Machines and systems for perennial biomass harvest and storage. University of Wisconsin Department of Agronomy Field Day – August 27th, 2009. Arlington, WI.

For projects involving computer modeling, provide the following information with the final report:

Model development was not a component of this research project.

Please complete the following table to reflect your project at completion or time of report submission:

ITEM	NUMBER
Abstracts	
Peer Reviewed Publications	
Outreach Publications/Web Pages	
Professional Presentations	
MS Degrees Conferred	**1**
Ph.D. Degrees Conferred	
MS Students Supported	**1**
Ph.D. Students Supported	
Post-Docs Supported	
Undergraduate Students Supported	**3**
Investigators Supported	
Start-Up Jobs Created	
Disclosures	
Patents Filed	
Provisional Patents	
Patents Issued	
License Agreements	
Plant Variety Protection	

APPENDIX A

DETAILED RESULTS FOR IN-FIELD CUBING OF BIOMASS

DOE AWARD NUMBER DE-FC36-08GO88073

Objective 1 – Development of a Laboratory Test Fixture

A laboratory test fixture was developed that allowed controlled experiments of cube formation using experimental conditions constrained by field conditions (fig. 1). The test fixture consisted of a single die that produced cubes 32 x 32 mm in cross section. The rate of force application, back pressure against the cube, and die temperature were all measured and controlled. Friction force between the die and the cube was also measured. Friction force between the die and the cube is very important because the friction force is the sole parameter that causes back pressure in the die ring of the in-field cuber. If there is insufficient friction force, then consolidation will not occur. Conversely, excess friction force wastes power and fuel.

Figure 1. Single-die test fixture with (a) back-pressure cylinder to control and measure back pressure on cube, (b) temperature controlled die block, (c) load cells to measure friction force, (d) compression plunger with load cell to measure compression force, (e) loading-rate controller, and (f) instrumentation and controls.

The test fixture worked as intended and many statistically designed experiments were conducted that provided direction for modifications to be made to the in-field cuber. Typically 10 replicate cubes were formed for each experimental treatment of a given experiment (fig. 2). Typically three to five experimental conditions were evaluated per experiment, and these experiments could be completed in three to five hours.

Figure 2. After formation the cubes formed in the laboratory test fixture were spaced out to cool and dry. In this experiment there were four experimental treatments considered with 10 replicate cubes per treatment.

Procedures for sample preparations including material rehydration and initial temperature, particle-size distribution, and the addition of such amendments as steam or binding agents were developed. Test procedures for loading of material into the die, controller settings, operation of press and lower hydraulic unit, and extrusion of the formed cube were also developed. Finally, procedures for quantification of cube quality including compressed and relaxed unit density, and cube durability were developed. Details of sample preparation, test procedures and cube quantification can be found in Hoffman (2011). Cube durability was determined following ASABE Standard S269.4 - Cubes, Pellets, and Crumbles - Definitions and Methods for Determining Density, Durability, and Moisture Content (ASABE, 2007). The required tumbling apparatus was fabricated to the specifications designated in the standard (fig. 3).

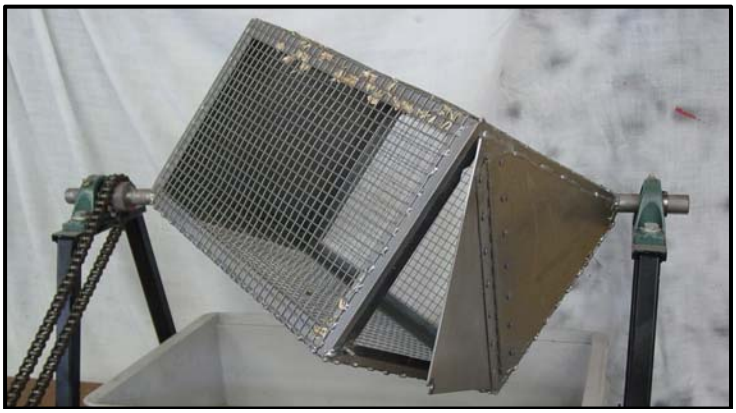

Figure 3. Cube durability test fixture used to tumble 10 cubes for quantification of cube durability based on ASABE Standard S269.4.

Objective 2 –Laboratory Test Results

The laboratory test fixture was used to conduct controlled experiments of cube formation using experimental conditions constrained by field conditions. Our goal was to create cube durability of greater than 75% and unit density of greater than 320 kg DM/m^3. Many different replicated experiments were conducted with the laboratory test fixture. Although the most important results are summarized below, additional information on the full extent of experiments conducted and results can be found in Hoffman (2011).

Moisture content was the most important parameter which affected cube quality because it significantly affected both friction force and cube re-expansion. Unfortunately, control of this parameter in the field is difficult. Moisture content should be below roughly 16% (w.b.) and the drier the better (tables 1 and 2). As the moisture was increased from 10% to 16% (w.b.) the wall friction increased, but at 21% (w.b.) the friction was significantly lower than it was at 16% (w.b.). Results with both switchgrass and reed canarygrass (Hoffman, 2011) showed that moisture content required to maximize friction force should be roughly 16% (w.b.). However, cube unit density and durability both decreased with increasing moisture because the higher moisture cubes tended to have greater re-expansion.

There were differences in friction force and durability of switchgrass and reed canarygrass cubes (tables 1 and 2). Friction force was consistently greater for reed canarygrass compared to switchgrass and friction force is the sole parameter that causes back pressure in the in-field cuber die ring. There are constituent differences between switchgrass and reed canarygrass that makes reed canarygrass more favorable for producing quality cubes. Duncan (2010) reported switchgrass contained 7.5 to 9.9% lignin compared to 6.2 to 7.1% in reed canarygrass. The greater presence of lignin increases the portion of insoluble carbohydrates. Lignin exhibits high stiffness and elasticity leading to an increase in resilience which opposes good particle to particle contact (Thomas et al., 1998). Constituent analyses also showed that switchgrass contained 3.7% to 7.0% protein and reed canarygrass contained 3.6% to 8.4% (Duncan, 2010). Protein acts as a natural binder improving the cube durability and density (Kaliyan and Morey, 2009). It was observed with the in-field cuber that it was much more difficult to create cubes from switchgrass than reed canarygrass, presumably because of this difference in friction and constituent characteristics.

Table 1. Switchgrass cubes were created from material of average particle-size of 5.3 mm, resistance pressure of 110 MPa and compression time of 8 s. Final moisture content for durability test was 10% (w.b.).

Moisture % w.b.	Friction[2] kN	Final Density[2] kg/m^3	Durability[3] %
9.7	13 a	709 a	71 a
13.6	15 b	605 b	62 a
17.3	18 c	419 c	23 b
20.7	14 b	288 d	0 c
LSD[1]	1	11	10

[1] Least significant difference.
[2] Averages with different markers within a column are statistically different at the P=0.05 level.
[3] Averages with different markers within a column are statistically different at the P=0.10 level.

Table 2. Reed canarygrass cubes were created from material of average particle-size of 7.2 mm, resistance pressure of 110 MPa and compression time of 8 s. Final moisture content for durability test was 13% (w.b.).

Moisture % w.b.	Friction[2] kN	Final Density[2] kg/m^3	Durability[3] %
12.5	22 a	649 a	85 a
16.3	28 b	481 b	69 b
19.7	22 a	360 c	39 c
22.9	16 c	272 d	3 d
LSD[1]	1	10	4

[1] Least significant difference.
[2] Averages with different markers within a column are statistically different at the P=0.05 level.
[3] Averages with different markers within a column are statistically different at the P=0.10 level.

Die temperature was another important parameter because it affected friction force and cube re-expansion. When other parameters were similar, a die temperature of 50°C consistently produced cubes that had greater unit density and durability compared to those formed at a die temperature of 150°C (table 3). Friction between the cube and die was also consistently greater at the lower die temperature. Die ring temperatures between roughly 80 and 120°C were measured in initial filed evaluation of the in-field cuber when no die ring cooling was used. Higher die temperatures presumably reduced cube density and durability because the higher temperature cubes had a longer cooling period which allowed for more relaxation.

Table 3. Switchgrass cubes were created from material of average particle-size of 5.3 mm and a compression time of 8 s. Final moisture content for durability test was 10% (w.b.).

Die Temp °C	Resistance MPa	Moisture % w.b.	Friction[1] kN	Final Density[1] kg/m^3	Durability %
150	145	13.5	7 a	430 a	58
50	170	12.9	23 b	607 b	58
150	170	12.9	9 c	417 a	56
50	145	13.1	17 d	630 c	52
50	145	18.7	22 b	327 d	3
150	145	18.8	8 a	201 e	0
150	170	18.7	10 e	192 e	0
50	170	19.1	23 b	304 f	0

[1] Averages with different markers within a column are statistically different at the P=0.05 level.

Many experiments with polymer and lignosulfonate binders added in solution were conducted but these traditional binding agents were found to have little positive effect on cube quality. Any benefit of the small level of binder added was mitigated by the water added by the solution. For instance, carboxymethyl cellulose (CMC) was mixed in solutions at 1% and 2.5% concentrations while polyvinyl acetate (PVAc) was mixed at 1% and 5% concentrations. In all cases 1 g of solution was applied to 40 g DM. The feedstock moisture at cubing was about 7% (w.b.). Increasing the concentration of these binders would have increased the viscosity of the solution to a level that would have made uniform application by spraying onto the feedstock impractical. Increasing the solution application rate to increase the amount of active ingredient would increase feedstock moisture with associated negative consequences.

One amendment that did improve cube quality was calcium oxide (lime). Lime added to the cubing feedstock at ~1% of DM increased unit density, cube durability, and the wall friction (table 4). The addition of lime reduced relaxation by binding with water, and therefore improved cube density and durability. Most importantly, the addition of lime somewhat mitigated the negative effect of moisture greater than 17% (w.b.).

Table 4. Reed canarygrass cubes were formed from material of average particle size of 7.2 mm, at a resistance pressure of 110 MPa, compression time of 8 s. Final moisture content for durability test was 13% (w.b.).

Moisture % w.b.	Calcium Oxide % of DM	Friction[1] kN	Final Density[1] kg/m^3	Durability[2] %
18.7	1.0	35 a	489 a	79 a
21.7	1.0	27 b	390 b	65 b
18.1	0.0	27 b	410 c	51 b
21.6	0.0	20 c	303 d	14 c

[1] Averages with different markers within a column are statistically different at the P=0.05 level.
[2] Averages with different markers within a column are statistically different at the P=0.10 level.

Steam is commonly used to produce feed pellets and cubes because it helps release and activate natural binders, uniformly distributes surface moisture and raises the temperature of the material allowing for more plastic deformation. Although steam is not commonly produced on most agricultural machines, mobile steam application it is not unheard of. Steam from a mobile boiler has been is added to very dry alfalfa hay to rehydrate the leaves to prevent losses (Staheli West Inc., 2011). Steam conditioning did slightly improve cube quality but the improvement was not as great as achieved with die cooling or lime amendment (table 5).

Table 5. Reed canarygrass cubes were created from material of average particle-size of 7.2 mm and compression time of 8 s. The moisture was 12% (w.b.) previous to steam addition and averaged 14% (w.b.) following the addition of steam. Final moisture content for durability test was 9% (w.b.).

Die Temp °C	Back Pressure MPa	Steam Addition Y/N	Friction[1] kN	Final Density[1] kg/m^3	Durability %
150	75	No	17 a	613 a	76
50	75	Yes	37 b	679 b	72
150	75	Yes	16 c	591 c	71
50	55	Yes	30 d	653 d	69
50	75	No	28 e	541 e	68
150	55	No	16 c	585 c	64
50	55	No	30 de	658 d	63
150	55	Yes	15 f	551 e	61

[1] Averages with different markers within a column are statistically different at the P=0.05 level.

Objective 3 – Modification to an In-Field Cuber

Based on the results with the laboratory test fixture three important design modifications were made to the in-field cuber. First, a die ring cooling system was designed and fabricated. Next, a system was developed to apply lime to the crop as an amendment. Finally, a system was added to apply heated water to the crop prior to cubing.

A John Deere model 425 hay cuber was chosen as the base machine for evaluating the potential of creating cubes of biomass at the time of harvest. The machine was manufactured and marketed in the 1960's and 1970's to produce alfalfa cubes in the arid western commercial hay region. Crop entered the machine via a conventional tine pickup that conveyed crop into a two-knife cutterhead. The chopped material was conveyed laterally, by means of flighting on the inner and outer portions of the die-ring mixing/feed drum, toward the die-ring extrusion section of the machine. The die-ring was fixed to the machine frame and an eccentrically mounted press wheel rotated in the inner diameter of the die-ring. The press wheel was constrained to ride in a groove formed by the die-blocks. The flighting on the mixing/feed drum carried material into the groove where the press wheel sheared the material and forced it into the die blocks (fig. 4). With every rotation of the press wheel, more material was forced into the die and the previously compressed material was forced further through the die. The extruded cubes were fractured once they reach the angled shield located around the exterior of the die ring (fig. 4). The cubes were directed into a chain and slat conveyer below the die-ring and conveyed into a trailing wagon for collection (fig. 5).

In previous field testing, external die temperatures were often found to exceed 100°C. The laboratory text fixture results showed that cube quality was improved when die temperature was about 50°C. In order to maintain a lower die temperature, a cooling system was implemented (fig. 6). A circular manifold with eight evenly-spaced nozzles sprayed water on the external surface of the die assembly. Water has a thermal conductivity twenty-four times greater than air. This allowed the heat to be transferred away from the die at a much greater rate than an air stream might have produced. However, cooling in this fashion did require the added challenge of carrying an adequate water supply. The approximate water flow rate used was 11 l/min.

Figure 4. Material forced into the die blocks by press wheel (top two pictures). Formed cubes were fractured against angled shield (bottom left). Cubes transported up conveyor to trailing wagon (bottom right).

Figure 5. John Deere model 425 cuber used to form cubes of reed canarygrass prior to modifications.

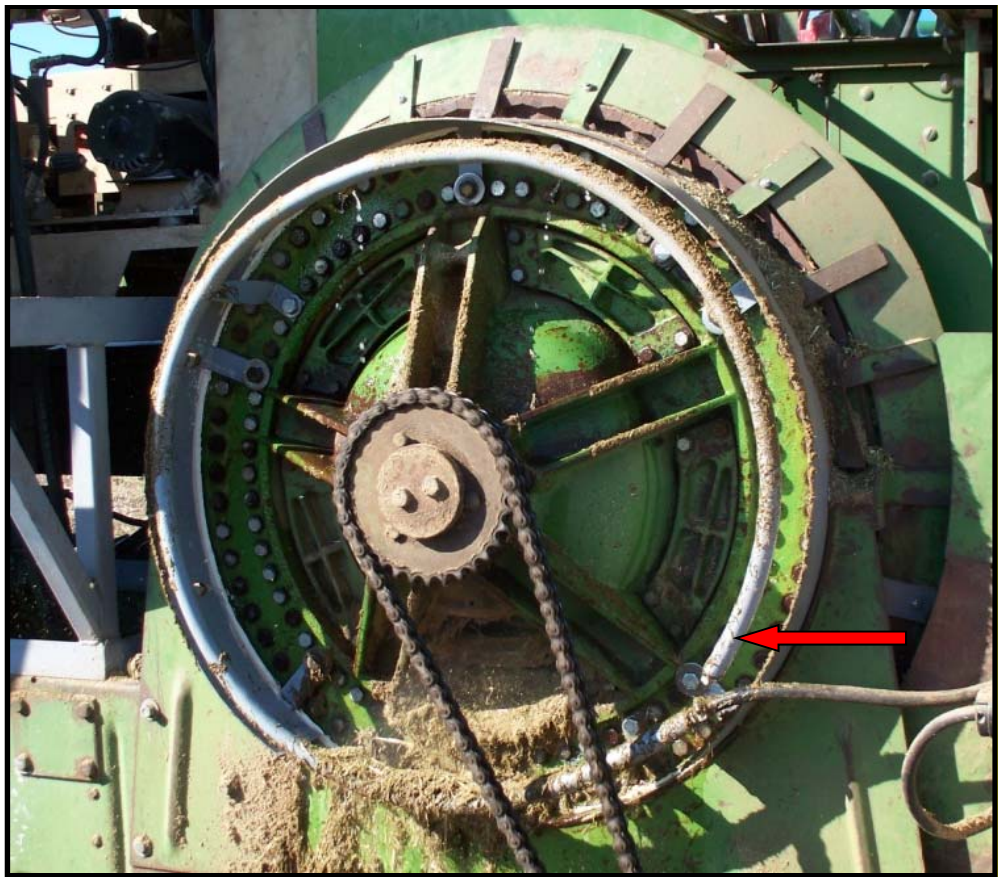

Figure 6. The circular manifold with eight evenly-spaced nozzles was used to sprayed water on the external surface of the die assembly to reduce the operating temperature. Water flow rate was about 11 l/min.

Addition of the lime amendment was achieved through the use of a modified gravity-feed sandblaster. This method was chosen over a fluted wheel and other application methods because it was felt that the turbulence of the compressed air might aid in mixing and distribution of the lime amendment with the crop stream. The air stream only required a small opening to supply the lime to the crop in the die ring mixing/feed drum, limiting required modification to the machine. Also, this method allowed for very small amounts of amendment to be added and dispersed effectively. Lime was applied to crop at the entrance to the die ring mixing/feed drum through a 7.5 mm nozzle. The apparatus required a continuous supply of compressed air when in operation, so a compressor with a 40 liter tank was used to deliver 230 l/min compressed to 620 kPa. A 5.5 kW gas generator was used to produce the required electric power (fig 7).

Figure 7. Modified in-field cuber cubing corn stover. An air compressor (orange arrow) and generator (red arrow) were added to supply dry lime to the die ring mixing/feed drum.

Previous results from the laboratory test fixture had shown the potential benefits of steam conditioning. It was not practical to produce steam on our in-field cuber, so high-pressure water heated to near the boiling point was used as a surrogate to steam. High-pressure and small orifice diameter (0.25 mm) was used to create very small droplet sizes similar to steam. The in-field cuber was modified to apply high-pressure heated water using a Landa SDHW6-3500 steam cleaner (fig. 8). This unit utilized a 19 kW diesel engine to provide 9.5 l/min of flow at 24 MPa. A 495 MJ diesel burner continuously heated the water up to an approximate exit temperature of just under 100°C.

Figure 8. In-field cuber modified to apply heated, high-pressure water to the crop at the feed drum using a modified steam cleaner. Water required for die ring cooling system required use of water tender pulled behind the cube collection wagon**.**

The final modification included installation of tapered dies to increase the back pressure applied to the material. The original dies had a uniform cross section of 32 mm x 32 mm with 3 mm radius corners and a chrome surface finish (fig.8). Tapered aftermarket dies were installed in a few locations in the die ring. These tapered dies were fabricated of hardened steel instead of the more typical chrome surface. Unfortunately the hardened surface caused adhesion at the die-cube interface significantly increasing resistance such that material in some of the dies completely resisted extrusion and plugged the die.

Figure 9. Conventional straight die with chrome plated surface (left) and tapered die with hardened steel surface (right). Material adhered to the hardened surface while the conventional die remained clean.

Objective 4 – Field Evaluation of the Modified In-Field Cuber

In-field cubing performance was quantified by mass fraction of material formed into cubes; cube unit and bulk density; and cube durability. These parameters were determined following ASABE Standard S269.4 - Cubes, Pellets, and Crumbles - Definitions and Methods for Determining Density, Durability, and Moisture Content (ASABE, 2007). Details of sample collection and preparation, test procedures and cube quantification can be found in Hoffman (2011).

Reed canarygrass and corn stover were the predominant crops used during field evaluation. Switchgrass was also used, but this crop rarely resulted in satisfactory in-field cube formation, so there is little data available with this crop. Switchgrass was not readily formed into cubes in the field for several reasons. It had been previously discovered in the laboratory experiments that switchgrass created less frictional resistance than reed canarygrass. Without sufficient friction there cannot be consolidation of the material into a cube. Also, it was observed that the cuber cutterhead was not able to expose as much of the interior portion of the switchgrass stem as it did with reed canarygrass. Exposing interior surfaces is important so that natural binders in the plant are made available.

The die cooling system significantly improved cube quality when used on the in-field cuber (tables 6 and 7). In the second experiment, the flow rate of water was altered to alter the die ring temperature. A system that cooled the entire die ring rather than just the exterior surface might have provided even more

benefit, but it was not possible to do so, given the current configuration of the machine. Ambient temperature water was applied to the windrow to help activate the plants natural binders.

Table 6. Reed canarygrass cubes were formed at an initial moisture of approximately 12% (w.b.) and 2 l/min ambient temperature water applied to windrow, with and without die cooling system active. Final moisture content for durability test was 9% (w.b.).

Cooling yes / no	Cube Fraction %	Bulk Density kg DM/m^3	Unit Density kg DM/m^3	Durability %
yes	81	321	637	40
no	0	167	--[1]	0

[1] Under these conditions no cubes were formed, so no unit density could be quantified.

Table 7. Reed canarygrass cubes were formed at initial moisture of approximately 16% (w.b.) and 2 l/min ambient temperature water applied to windrow with four different levels of die temperature. Final moisture content for durability test was 9% (w.b.).

Die Temperature °C	Unit Density[2] kg DM/m^3	Durability[3] %
50	711 a	67 a
60	554 b	30 b
70	479 c	14 c
80	427 d	1 d
LSD[1]	36	10

[1] Least significant difference.
[2] Averages with different markers within a column are statistically different at the P=0.10 level.
[2] Averages with different markers within a column are statistically different at the P=0.10 level.

Die ring collection position was found to have a significant effect on cube durability and density (table 8). Cubes collected from the top portion of the die ring had almost 50% greater unit density than those cubes collected from the bottom of the die ring. The die ring was configured vertically, so gravity naturally creates a greater volume of material in the lower portion of the mixing/feed drum that supplies the die ring, increasing the mass flow rate of the material through the lower dies and therefore reducing dwell time. This conclusion is supported by results Tabil and Sokhansanj (1996) where die speeds of 501 and 565 rpm were found unsuccessful in pelleting alfalfa, however speeds of 250 and 316 rpm offered significant improvements in durability. The results here suggest that (a) improvements should be sought in the way the die ring is fed so that a more uniform mass flow rate is achieved, and (b) that multiple die

rings should be considered so that productivity is maintained while dwell time is increased. The later modification would of course increase cost and potentially increase energy expenditures.

The addition of lime at 1% of DM improved the cube fraction, final density, and cube durability in the production of reed canarygrass and corn stover cubes (tables 8 and 9). The results of these field experiments were in alignment with results with the laboratory test fixture with both showing significant increases in durability and density with the addition of lime. However, even the cubes formed with lime still resulted in less than desired durability with these feedstock.

Table 8. Reed canarygrass cubes were formed at initial moisture of approximately 12% (w.b.) and 2 l/min ambient temperature water applied to windrow while varying lime addition and cube collection position. Final moisture content for durability test was 11% (w.b.).

Collection Position on Die Ring	Lime Addition % of DM	Cube Fraction % of total mass	Bulk Density kg DM/m^3	Unit Density[2] kg DM/m^3	Durability[2] %
Top	1	na[1]	na[1]	759 a	88 a
Top	0	na[1]	na[1]	725 a	79 b
Bottom	1	91	330	526 b	46 c
Bottom	0	89	319	459 c	22 d

[1] Insufficient cubes were available to perform the cube fraction and bulk density measurements from cubes collected from the top of the die ring.

[2] Averages with different markers within a column are statistically different at the P=0.10 level.

Table 9. Corn stover cubes were formed at initial moisture of approximately 16% (w.b.) and 1 l/min ambient temperature water applied to windrow, with and without lime addition. Final moisture content for durability test was 10% (w.b.).

Lime Addition % of DM	Cube Fraction[2] % of total mass	Unit Density[2] kg DM/m^3	Durability[2] %
1	93 b	507 b	35 b
0	72 a	422 a	22 a
LSD[1]	14	39	9

[1] Least significant difference.
[2] Averages with different markers within a column are statistically different at the P=0.10 level.

The addition of heated water to the mixing/feed drum did not significantly improve cube quality. Although the results were not statistically significant, the addition of heated water prior to cubing reduced the final density of the cubes by 15% (Hoffman, 2011). This is likely due to an increase in moisture content which led to a longer cooling and drying time and a greater level of post-compression relaxation. The pre- and post-cubed moisture was approximately 14% and 16% (w.b.), respectively.

Crop moisture within the field was the most difficult parameter to control and its variability had a major impact on the ability to produce cubes. Moisture in the windrow would vary spatially across the field because of variance in yield, soil conditions, and topography. Excellent quality cubes could be produced at the start of a windrow and by the time the in-field cuber had reached the other end of the field only chaff would exit the die ring. The main reason for this complete loss of performance was moisture content. Table 10 provides an example of material harvested on the same day and field, but in different locations in the field where moisture varied as shown. The results show the complete loss of performance as moisture varied.

Table 10. Reed canarygrass at two different initial moistures and 2 l/min ambient temperature water applied to windrow. Final moisture content for durability test was 9% (w.b.).

Crop Moisture % w.b.	Cube Fraction % of total mass	Unit Density kg DM/m^3	Durability %
13.5	94	528	21
20.0	--[1]	--[1]	--[1]

[1] Cube formation was nonexistent at this moisture.

Objective 5 – Economics of In-Field Cubing

An economic analysis was conducted to evaluate harvest and storage methods and provide a realistic context for the cost of biomass from the producer's and the processor's perspective. Costs associated with baling and cubing both corn stover and perennial grasses (i.e. switchgrass) were estimated. The evaluation compared the economics of cubing biomass feedstocks to round baling with the bales stored outdoors and to large square baling with the bales stored under cover. Our methodology and many of the assumptions for this complex analysis were extensive and are best summarized by referring to Cook, 2011 and Cook and Shinners, 2011.

The harvest analysis was done in two parts, the cost of the machine was analyzed on a cost per unit time basis and the productivity of the machines was analyzed in varying crop and yield environments. The cuber was assumed to be configured as a power assisted trailer with three die rings able to achieve a total of 24 t DM/h when equipped with an 800 hp diesel engine. Retail list price for the cuber was assumed to be just under $1M. This estimate was based on cost of stationary cubers and weight and power of similar mobile equipment. The cuber would be pulled by a small self-propelled forage harvester with roughly 350 hp. The forage harvester would gather and size-reduce the crop and then deliver it to the trailing cuber. There were several reasons for this machine arrangement. First, the self propelled forage harvester can be decoupled for use in other crops, allowing its fixed costs to be diluted over additional operating time. Second, the combined unit has low area productivity while still requiring over 1100 hp between the two units. It was difficult to imagine the capacity of in-field cubing machines being much smaller, and equally difficult to imagine a dedicated harvester with very limiting crop condition requirements that has greater than 1100 hp. Finally, the trailer concept would also open the possibility for other producers to rent the cubing trailer to pull behind their own equipment, again diluting its substantial investment over greater area and time.

The storage scenarios we considered took into consideration the dry matter losses and the value of the dry matter being lost. In so doing, we found that the most expensive method of harvest for agricultural biomass in the Midwest was bales stored uncovered on the field side. In a thermal conversion situation, where the moisture content of the bales is a severe penalty to bale grinding and boiler efficiency, this method of storage will be economically challenged. We developed a novel method to analyze the transportation of biomass that applies a supply curve over the potential supply area, this results in a realistic estimation of the distribution of transportation for each scenario (Cook and Shinners, 2011). For the end user, we also estimated the costs of bale handling and grinding.

The in-field cubing device has relatively low-capacity and therefore low annual usage, so the fixed costs per ton were large. Additionally, the fuel costs per ton were great due to the large power requirements of the combined forage harvester and cuber. Therefore, harvest costs per ton were two to four times that of the bale based systems (table 11 and 12). Current bale density can come close to meeting the legal restrictions on truck weight, so there is not substantial transportation cost benefits for the high-density cubes. Cubes produced in the field would require year round storage in a commodity shed. The cubes would be stored in shallow piles in these sheds, so a substantial volume of the shed would be unoccupied by cubes, which creates a high storage cost despite the high product density. Engineered structures could be built to more efficiently utilize storage space, although building costs would be greater.

The cost of bale deconstruction, drying and cubing corn stover was estimated at roughly $30/ ton DM (Sokhansanj and Turnhollow, 2004). The value would presumably be greater today when inflation is considered. If the costs of converting bales to cubes were roughly $30/ton DM, then our analysis suggests that the costs of the bale-to-cube systems would be 13% to 26% greater than in-field cubing. There are several conclusions of this economic modeling. To the end-user's gate, bales are the lowest

cost per ton, but not necessarily the cheapest at the flame tip. For a boiler that requires a small particle size that is quickly consumed, a bale system is likely the most economical system because there is substantial wasted cost in densification and then subsequent deconstruction of the cubes or pellets. In situations where fuel is consumed over minutes and requires a larger particle-size, e.g. grate boiler, a cube would be preferred. As such this economic analysis suggests that in-field cubing will be more economical than the bale to cube system. However, due to the seemingly strict limitation to moisture content for successful cubing, there is substantial weather related risk, the cost of which we have not considered here.

Table 11. Cost comparison for harvest, storage and transport of perennial grasses in cubes, round bales or square bales. Costs are represented in dollars per dry ton.

Operation	In-Field Cubing	Round Bales – Outdoor Storage	Square Bales – Covered Storage
Harvest	33.1	12.1	16.9
Transport to Storage	7.6	10.6	9.2
Storage	16.5	0.5	1.2
Storage Losses	1.5	19.5	5.0
Transport to End Use	9.6	13.0	10.7
Total	68.3	55.7	42.9

Table 12. Cost comparison for harvest, storage and transport of corn stover in cubes, round bales or square bales. Costs are represented in dollars per dry ton.

Operation	In-Field Cubing	Round Bales – Outdoor Storage	Square Bales – Covered Storage
Harvest	43.5	13.4	11.2
Transport to Storage	3.8	3.2	8.0
Storage	12.5	0.6	1.4
Storage Losses	1.3	6.9	2.4
Transport to End Use	14.2	31.1	28.8
Total	75.3	55.2	51.8

Suggestions for Future Research

One of the major challenges to successful in-field cubing was maintaining back pressure in the dies. Back pressure is created by friction between the material and the die wall. The laboratory experiments showed that wall fraction was influenced by crop type, moisture, particle-size, and die temperature. Additional laboratory research could be done to map the relationship between particle-size, moisture, and die temperature on the wall friction generated for different crops. This would be helpful in determining how "controllable parameters" such as particle-size and die temperature impact the level of friction created depending upon the moisture content of the material. This would result in a peak friction line that could improve the likelihood of high quality cubes. Further experimentation could be done to determine the relationship between the shape of the die and the friction force generated. Tapered dies did show some promise regarding increasing back pressure and these dies should be investigated further albeit with a chrome surface that prevents material from adhering to the die surface.

The most important addition to an in-field cuber would be an on-board moisture sensor. Spatial variability of moisture in the field quickly altered the success of forming quality cubes. It is imperative that the crop moisture by measured on-the-go so that machine parameters such as die ring temperature or amendment application rate can be altered to react to moisture changes.

Particle-size was found to influence density and cube durability; therefore a feedroll and cutterhead assembly comparable to those on current forage harvesters could be implemented to allow for greater variation and control of the TLC. Die ring temperature was found have an important impact on the frictional resistance. A much improved die ring cooling system should be developed that more uniformly cools the die ring. An automated die ring temperature controller should be considered to better optimize its performance. This controller would not only heat the die when cold to eliminate the excessive time required to reach "operating temperature", but it would also cool the die in conditions when the temperature increases above desired values.

An improved system for application of amendments should also be considered to produce a more consistent application of binding amendments on a continuous basis. The mixing/feed drum that meters material to the die ring currently only offers modest agitation of the material; therefore any amendments added to enhance binding may not be well distributed. A larger section for agitation to allow for more thorough mixing and further chemical breakdown of the resilient cell walls could improve cube quality. Currently the mixing/feed drum transports material horizontally into the vertically oriented die ring. The major issue observed with this mechanism was the vertical orientation of the mixing/feed drum and die ring. As a result of gravity, a greater fraction of the material is extruded through the bottom die openings compared to those on the top. This uneven feeding results in varying extrusion rates, cube dwell time, and compaction forces and limits the consistency of the process. A horizontally orientated die ring that is fed more uniformly with a metering device to control the mass flow rate of material into the die openings could improve the consistency and the resulting repeatability of this process. Changes to the handling system could be implemented to transport the cubes more gently to the wagon. The current use of chain-and-slat conveyors is too aggressive and using rubber belt conveyors should be considered. Any modifications which reduce the forces on the cubes during the cooling process would improve cube quality because the cubes are quite ductile as they exit the die ring. A cooling fan could also be implemented into the handling system of the cuber to more quickly reduce the temperature and humidity of the cubes to limit relaxation.

References

ASABE. 2007. Standard S269.4 - Cubes, Pellets, and Crumbles - Definitions and Methods for Determining Density, Durability, and Moisture Content ASABE, St. Joseph, MI.

Cook, D.E. 2011. Whole-plant Corn as a Biomass Feedstock – Harvest, Storage and Economics. Unpublished Master of Science Thesis, Department of Biological Systems Engineering, University of Wisconsin.

Cook, D.E. and K.J. Shinners. 2011. Economics of alternative corn stover logistics systems. ASABE Paper No. 111130. ASABE, St. Joseph, MI.

Duncan, J.A. 2010. A Machine for Harvest Fractionation of Biomass Grasses and Legumes. Unpublished Master of Science Thesis, Department of Biological Systems Engineering, University of Wisconsin.

Hoffman, T.J. 2011. Design and Performance Evaluation of an In-Field Biomass Cuber. Unpublished Master of Science Thesis, Department of Biological Systems Engineering, University of Wisconsin.

Kaliyan, N., and Morey, R. V. 2009. Factors affecting strength and durability of densified biomass products. Biomass and Bioenergy Vol. 33(3): 337-359.

Sokhansanj, S., and A.F. Turnhollow. 2004. Biomass densification – cubing operations and costs for corn stover. Applied Engineering in Agriculture 20(4):495-499.

Staheli West Inc. 2011. DewPoint Information. Retrieved Mar 18, 2011 from Staheli West Inc. http://www.staheliwest.com/dew-simulation.html#anchor_22

Tabil, L. G. and S. Sokhansanj. 1996. Compression and compaction behavior of alfalfa grinds. Part I: Compression behavior. Powder Handling and Processing 8(1):17-23.

Thomas, M., T. van Vliet and A. F. B. van der Poel. 1998. Physical quality of pelleted animal feed: 3. contribution of feedstuff components. Animal Feed Science and Technology 70(1):59-78.

Back to Table of Contents

Sun Grant Initiative
DOE Final Progress Report

Project Title: Landscape Scale Lignocellulosic Biomass Production

Project Director/Principal Investigator: W. Carter Johnson, Distinguished Professor of Ecology, Department of Natural Resource Management, South Dakota State University, Brookings

All Co-Principal/Other Investigators:
David Archer and Scott Kronberg, Agricultural Research Service, Mandan, ND
Arvid Boe, Professor, Department of Plant Science, SDSU, Brookings
David Clay, Professor, Department of Plant Science, SDSU, Brookings
Vance Owens, Professor, Department of Plant Science, SDSU, Brookings
Thomas Schumacher, Department of Plant Science, SDSU, Brookings

Period of Performance: 1 January 2009 - 30 September 2011

Funding Awarded: $400,000

Cost Share Amount: $100,110

Cost Share Sources: Time and effort from PIs and CoPIs; Indirect on time and effort; EcoSun Prairie Farm

Executive Summary

This Prairie Farm project investigated the methods of establishing, managing, and marketing native grassland on former row crop farmland (including CRP land), principally as biofuel feedstock. These included: developing strategic mixtures of perennial grassland species with high economic potential; testing planting methods on upland and lowland (wetland) sites; clipping vegetation to measure biomass production; testing methods of seed collection and haying and producing grass-raised beef; selling grass-based products to test the depth and strength of markets; and determining the overall profitability of grass-based farming after 4 years of work compared to traditional corn and soybean rotation. This research found that restored grassland on tillage land was highly productive; all environmental measures (e.g., soil and water quality) also should have improved. Prairie cordgrass planted in wetland basins and sub-irrigated land was the most productive, followed by switchgrass monocultures and big bluestem mixtures. The most income from grass-based products was earned from native grass seed, primarily from switchgrass, cordgrass, and lowland sedges and wedgegrass. Hay was important to farm income; over 500 tons were sold in 2010-2011. Grass-fed beef was produced in 2011 as a test market at grocery stores, restaurants, and to individual families; income was considerably higher than from stockyard markets. Should markets for cellulosic biofuel feedstock arrive in the next few years, hay income and grass farm profits should rise accordingly. Estimates of potential ethanol yield from our feedstock material ranged from 110-125 gallons/ton of hay. Input costs of grass farming were about one-third of the costs for tillage farms. All in all, grass farm income and profits were considerably lower than those of corn and soybean farms. However, these differences are likely to narrow over the next few years assuming that grain prices will moderate and expertise in marketing grass-based products will improve.

Project Objectives, Outcomes, and Impacts

Objective 1. Develop and test methods/treatments for their effectiveness in renovating degraded CRP into productive swards of native tall grasses for use as biofuel feedstocks, hay, or forage.

Much of the land that has been in the CRP program for 10 or more years has changed in vegetation from that originally planted. The warm season grasses initially drilled in have slowly lost ground to cool season invasive plants such as smooth brome, quack grass, blue grass, and broad-leaved forbs such a Canada thistle. This has occurred because of the absence of burning and the infrequent grazing and haying. Moreover, in eastern South Dakota, pocket gophers have produced hundreds of soil mounds per acre in CRP land that make equipment travel through the field difficult or impossible. As a result, when contracts expire, CRP fields are often not in a condition favorable for profitable agricultural use. Renovation experiments were needed to inform producers of ways to convert degraded CRP to productive perennial grassland once government contracts expire.

We were granted permission in 2008 by the South Dakota Farm Service Agency to conduct renovation experiments on degraded land still enrolled in the CRP program on the EcoSun Prairie Farm. Two fields were renovated: one of about 50 acres (C1) and another of about 15 acres (C2). Both fields were dominated by invasive plants and covered with pocket gopher mounds. Renovation methods tested included: spring burning to remove thick thatch; herbicide use to remove weeds and cool season grasses; disking to level pocket gopher mounds; control of pocket gophers; drilling in warm season grasses; and occasional burning and mowing of the young grass crop.

A range of treatments was tested the first full year of the project (2008). The following methodological sequence was applied to both fields in 2009 and 2010. The most successful sequence was:

Year 1

Spring: burn, Roundup application on regrowth
Summer: light disking of pocket gopher mounds
Fall: Roundup application on regrowth

Year 2

Spring (late): drilling in of 5 species of warm-season grasses (big bluestem, switchgrass, Indiangrass, little bluestem, and side-oats grama
Summer: one mowing
Fall: once warm-season grasses senesce, apply Roundup to control any cool-season regrowth

The treatment cycle took 2 years to complete. However, by the end of the second growing season, a small hay crop (~1 ton/acre) could have been taken from each field or light grazing could have been allowed.

The outcome of this renovation sequence was a well-established sward of warm-season grasses with only small (5%) coverage of undesirable plants. In year 3 (2011), a high quality hay crop was taken off the smaller field (C2) and sold to a cattle producer near Sioux Falls. The crop averaged 2.5 tons of hay per acre. The field was hayed in the early boot stage at the time of high hay quality. Protein content was nearly 9%, and the relative feed value was 65. This field was included in the farm tour conducted in August, 2011 as an example of a successful conversion of degraded CRP into a field with excellent potential for harvestable biomass feedstock production.

This hay, and other mixtures on the Prairie Farm, was tested by the POET ethanol company of Sioux Falls for potential ethanol yield. Our feedstocks produced potential yields of 110-125 gallons of ethanol per ton of hay. These yields are higher than most estimates (90-100) for native, warm-season grasses.

We recommend this method of renovating CRP in our region. A productive sward of grass can be established more quickly than in another method sometimes used. That method is to first till the retired CRP field, crop the field with soybeans for 2 years, and then drill grass into the soybean stubble in year 3. Advantages of this method may be a cleaner field when the grass is drilled, no disking required to remove gopher mounds, and income for 2 years when weeds are being eliminated. Disadvantages are the 4-year wait before the new grass is harvestable and the 2 years of tillage on land that is marginal for agriculture (low bean yields and greater soil erosion).

Objective 2. Conduct field studies to determine the optimal seeding rate for switchgrass across a range of field environments.

The cost of seed is a major expense for producers in the establishment of native grass crops in the northern Great Plains. Ideally, producers would plant just enough seed to quickly obtain a harvestable crop but not too much so that seed would be wasted because more was planted than needed for excellent stand establishment. This experiment was designed to identify optimal seeding rates for switchgrass, the most promising upland native grass for the biofuel industry.

Switchgrass was planted 8 June 2008 at the Prairie Farm at 5.6, 11.2, and 16.8 kg PLS ha^{-1} across three landscape positions. A multi-species mixture of warm-season grasses and forbs was planted at a rate of 11.2 kg PLS ha^{-1} alongside each set of switchgrass plots for biomass production comparisons. Switchgrass stand frequency was determined 9 July 2008, 27 May 2009, and 19 May 2010 using the method of Vogel and Masters (2001; J. Range Mgt. 54:653-655). Biomass yield and tiller density were determined near peak biomass and around a killing frost in autumn by harvesting three 0.19 m^2 quadrats from each plot. Harvest dates were 11 Aug. and 4 Nov. 2009; 25 Aug. and 1 Nov. 2010; and 28 Sep. 2011 (only one harvest was taken in 2011).

Switchgrass frequency was similar across seeding rates in 2008 (establishment year) and increased in subsequent years, particularly at the two higher seeding rates (Fig. 1). The increase in stand frequency was greater as seeding rate increased from 5.6 to 11.2 kg ha^{-1} than from 11.2 to 16.8 kg ha^{-1}. However, even the lowest seeding rate resulted in an average frequency of >50%. Although switchgrass frequency was not affected by seeding rate in 2008, tiller density was lower in the 5 kg ha^{-1} seeding rate compared with the other treatments. Seeding rate did not affect tiller density in subsequent harvests (Fig. 2).

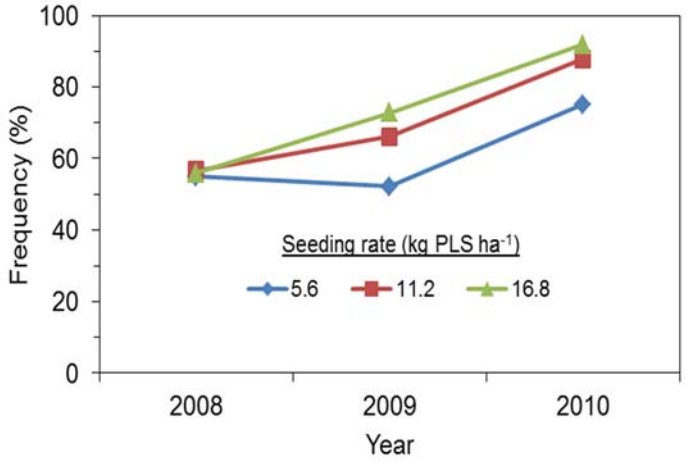

Fig. 1. Effect of switchgrass seeding rate during the establishment year (2008) and two subsequent years (2009-2010).

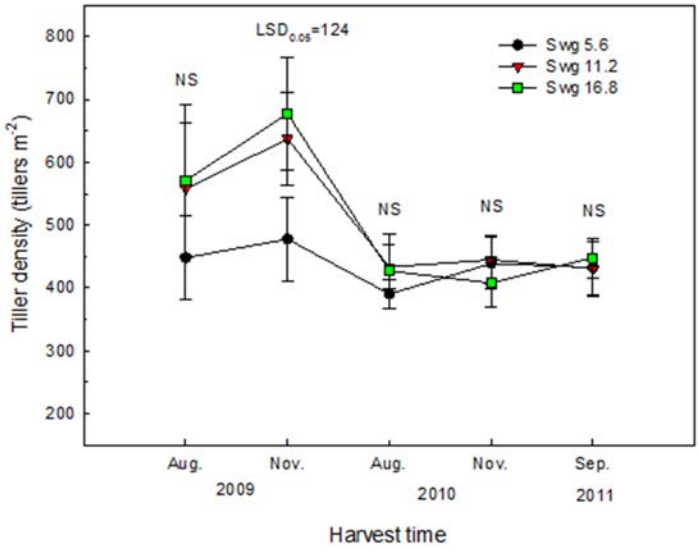

Fig. 2. Effect of switchgrass seeding rate on tiller density at harvest.

Despite the effect of seeding rate on tiller density in the seeding year and on stand frequency the first two years after establishment, switchgrass yield was similar across years and seeding rates (Fig. 3). Apparently, in the year seeded, even the lowest seeding rate provided excellent yields. From a cost standpoint this is extremely important. However, in years with less suitable establishment conditions, a higher rate may be appropriate. We have other on-going projects that parallel this research but were planted in different years and conditions; they will help in making a final seeding rate assessment for this part of South Dakota.

With the exception of the single harvest in 2011, switchgrass always had higher yields than the bluestem-dominated species mixtures. Switchgrass yields, however, appeared to decline more than mixtures did due to lack of rainfall in July and August 2011.

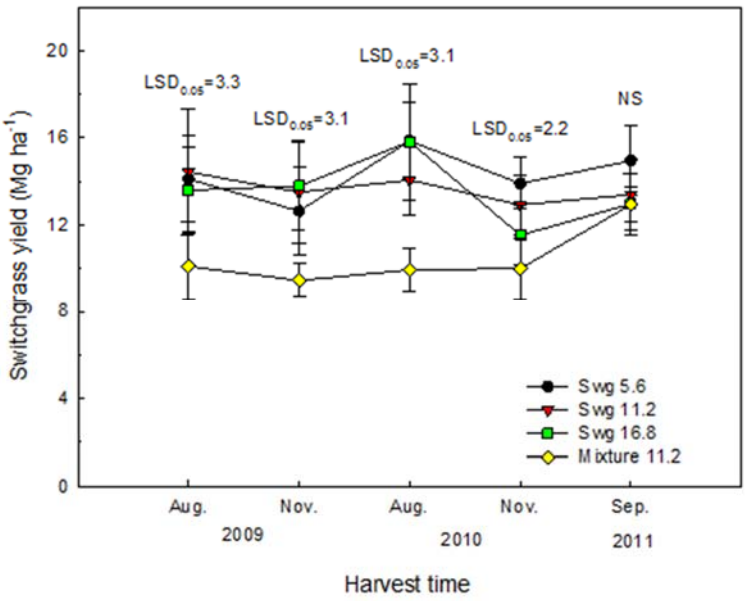

Fig. 3. Switchgrass biomass production at three seeding rates across three years compared with mixture yield at the same harvest date.

Objective 3. Determine the Relationship between Feedstock Production of Vegetation Communities and Monocultures Across Site Environmental Conditions

During the course of this project, numerous large fields and wetlands on the Prairie Farm were planted with a wide range of grassland species with potential as biofuel feedstocks. This provided a unique opportunity to determine: the rate of growth in biomass during the first few years of establishment; which plant mixtures (or monocultures) are the most productive; and how plantings respond to environmental variation, especially across a range of soils and topography.

Biomass at the end of the project (2011) varied by plant composition and age of the planting. Biomass was relatively uniform across fields/wetlands with the same vegetation (Figure 4). For example, the biomass of mature stands of switchgrass (monocultures) plantings clipped at the ground level ranged narrowly from approximately 13-14 Mg/ha across 3 different fields (T1-T6). Bluestem (mixtures) biomass ranged even more narrowly between different plantings (T4, T2). The biomass of prairie cordgrass (monoculture) wetlands ranged more widely from approximately 14-16 Mg/ha. Leaving a stubble height of about 15 cm reduced the harvestable biomass by about 2-3 Mg/ha (Figure 4).

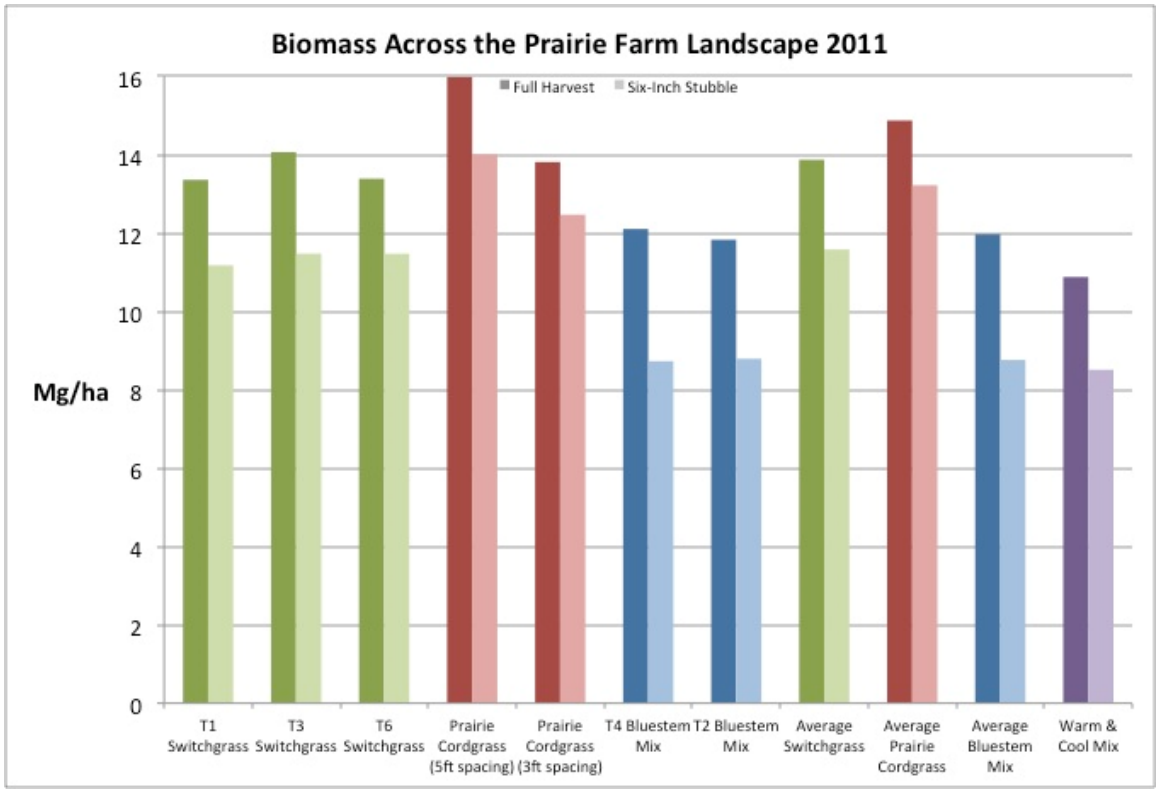

Figure 4. Biomass production of various species and species mixtures at various locations across the farm in 2011.

Highest biomass levels (about 15 Mg/ha) were found in the prairie cordgrass wetlands; switchgrass biomass levels were next highest (about 13.5 Mg/ha). The bluestem mixture produced the lowest biomass levels (about 12.0 Mg/ha) of the warm-season grass fields that had reached maturity. A warm/cool grass planting (mixture), comprised of 30 species of grasses and forbs, produced biomass just below that of the bluestem mixture (about 11 Mg/ha); however, the former was 2 years old and probably had not reached maturity.

Planting age and weather affected biomass levels in 2010 and 2011 (Figure 5). Switchgrass peak biomass dropped between 2010 and 2011, probably due to late summer drought in 2011. In contrast, cordgrass biomass increased sharply during the same period, while the bluestem mix changed little, seemingly unaffected by the dry weather in 2011. Biomass of the warm/cool season mix was sampled only in 2011.

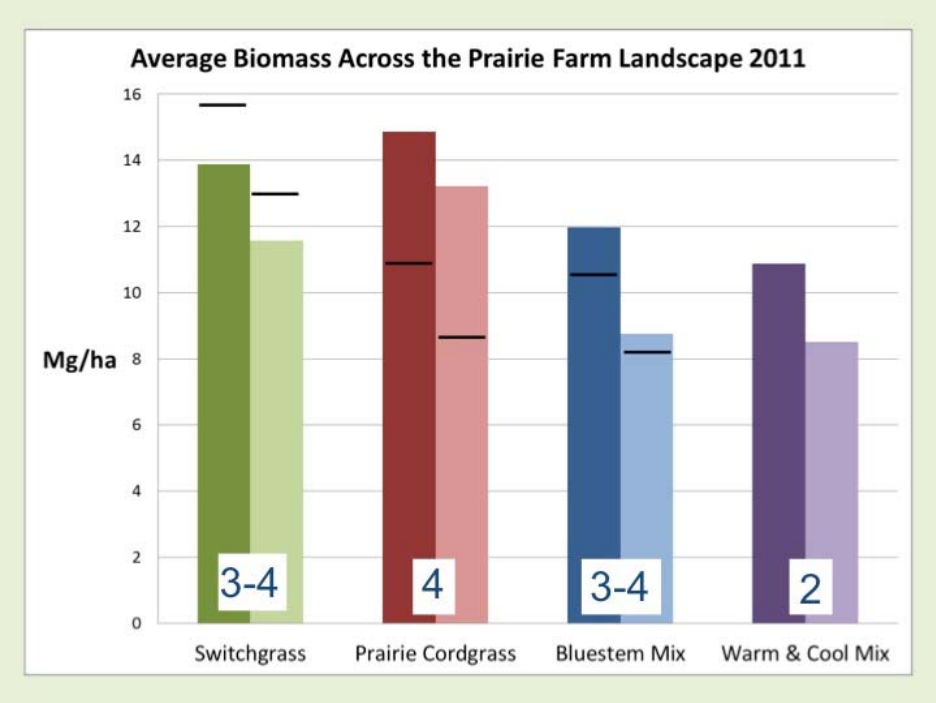

Figure 5. Average biomass production across the farm in 2011 at two cutting heights (dark bars represent a ground-level harvest; light bars represent a cutting height of about 10 cm).

Prairie cordgrass was established in the two temporary water-permanence class wetlands using transplants (plugs) at two spacings (5 foot and 3 foot). The north half of one wetland (T2W1) was planted at the higher density, while the south half was planted with the lower density. The planting pattern was reversed for the other wetland (T2W2). These wetlands were too wet in 2008 to drill in seed using heavy equipment. Hand-planting was the only workable method given the conditions. The upside of transplanting was high survival of plugs (~95% first year survival), even for those planted in standing water. The downside was large spaces among plants that would take several years to fill by tillering from the mother plants.

The cordgrass clipping data from the two wetlands show large increases in biomass each year following planting (Figure 6). Peak biomass may still not have been reached in 2011, four years after planting. Examination of individual sample weights indicated that considerable more biomass may be produced as the stand thickens and occupies empty space among plugs. For example, extrapolating from the best developed, highest biomass sample yielded a stand estimate of 24.1 Mg/ha. The same calculation from the 5 highest samples yielded an estimate of 21.2 Mg/ha. Further infilling of space in the stand may raise the mean biomass; however, genetic differences among plugs and less than optimal environmental conditions in parts of the wetland basin (competition with other wetlands plants that emerged from the seed bank and areas sub-optimal for cordgrass with respect to water depth or depth to groundwater). Clipping in these same two wetlands is planned for 2012 to determine if stand biomass will increase further.

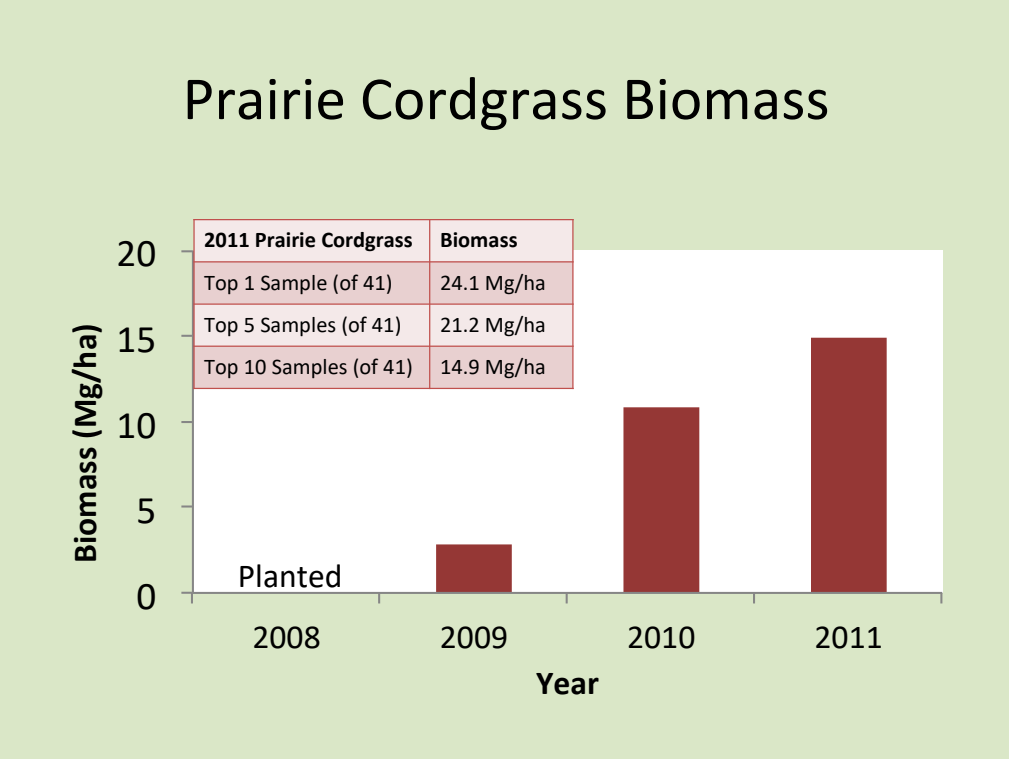

Figure 6. Biomass production of prairie cordgrass in wetlands.

Lastly, clipping data revealed that the biomass of the 3-foot-spaced plugs was higher than the 5-foot-spaced plugs at the end of second year 2 (3.4 vs. 2.0 Mg/ha, resp.). By year 3, however, the biomass of the two wetland halves were statistically indistinguishable. These results indicate that the more widely spaced plants, with lower planting costs, catch up relatively quickly to the densely spaced plants that are more expensive to establish. Since no biomass or seed crop of significance would be harvestable in year 1, the higher biomass and larger seed crop in year 2 would be the only economic benefit of the denser spacing. Seed crop estimates were not made for 2009; biomass of the dense planting weighed 1.5 Mg/ha more (less than one English ton/acre) than that of the sparse planting. At hay prices of $75/ton and a wetland size of about 1 acre, the added income from the denser planting was considerably less than the difference in planting costs, estimated to have been about a thousand dollars. Our recommendation is to plant cordgrass plugs at 5 foot (or greater) spacing to increase profits from the plugging of cordgrass.

Objective 4. Establish Baseline Environmental Conditions and Monitoring Protocol for Soil and Water Quality

Soils (see Appendix I for supplementary material)

Most agricultural soils that have been tilled for decades or centuries are depleted in organic matter and in carbon compared to their natural levels prior to farming. The planting of large areas of cropland to warm-season grassland to provide biofuel feedstock in the future would replenish these materials over time. Few studies, however, are in place to determine how much organic matter and carbon have been lost in the past from farming and how much can be regained by replanting perennial grasses. There may be a time when farmers will be paid through a carbon credit system for storing more carbon in their soils.

In this study and in a related NRCS study on the Prairie Farm, soil quality was measured with soil depth and across topographic positions to determine a baseline or starting point at the transition between row crop and grass farming. After several years of grass farming, soil quality was remeasured in our project to see how quickly these key soil variables were improving. Estimates of how much soil carbon was lost by cultivation and therefore how much could be regained, was made by measuring values at a virgin prairie site (prairie remnant) and at nearby fields farmed for 100 years or more at the EcoSun Prairie Farm (Heimerl. 2011. M. S. thesis, SDSU).

Major soil quality variables (particulate organic matter, soil organic matter, wet aggregate stability, and FDA) were approximately double those in the virgin prairie (Sioux Prairie) than in the cultivated uplands of the Prairie Farm (Figure 7). These much higher levels occurred at all topographic positions in the virgin prairie soils.

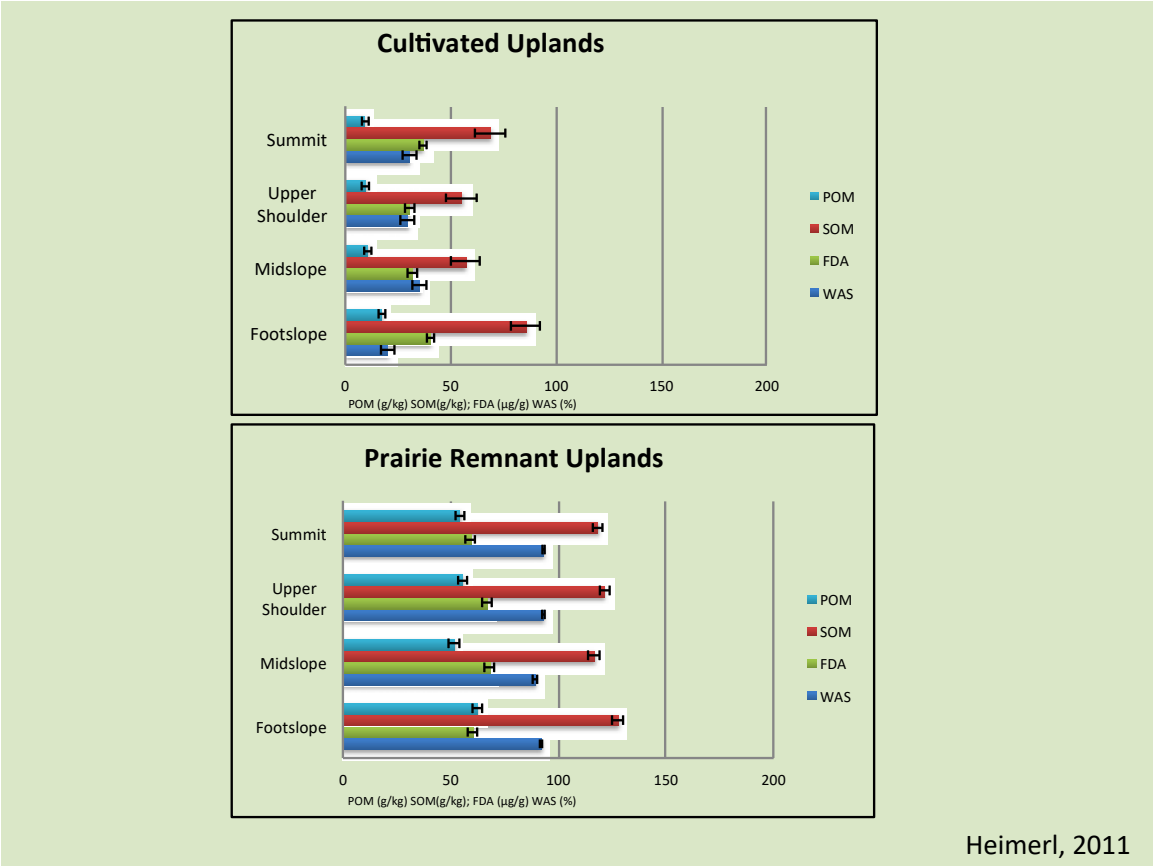

Figure 7. Soil characteristics of cultivated uplands and prairie remnants.

The same soil quality measurements were taken at virgin prairie wetlands and at drained and cultivated wetlands at the Prairie Farm. The differences were even greater, though, between cultivated and natural wetlands than between the upland cultivated and virgin prairie sites (Figure 8). Natural wetlands had soil quality values approximately 2.5 times those of the drained and tilled wetlands.

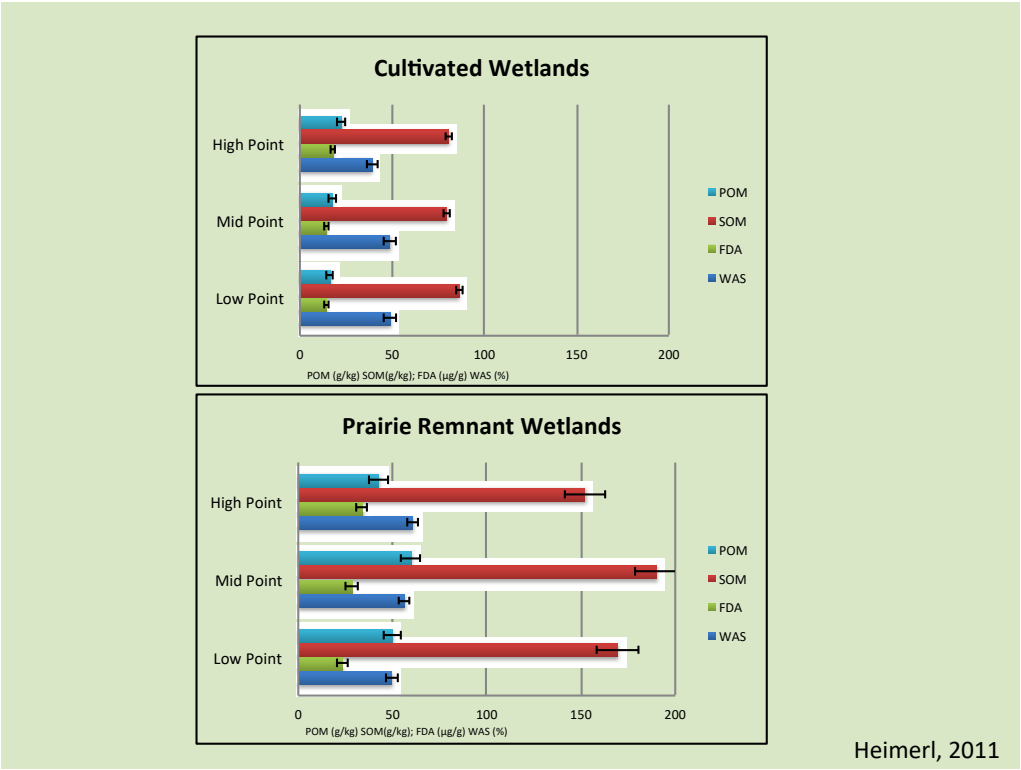

Figure 8. Soil characteristics of cultivated wetlands and prairie wetlands.

Overall, there was an approximate 40% loss of soil organic matter from Prairie Farm tilled soils, based on a comparison with nearby virgin prairie soils in similar topographic positions. The distribution of soil organic matter indicates significant erosion on the Prairie Farm in the past 100 years. Also, there was decreased carbon recycling and structural stability (reduced FDA, lower POM, lower WAS) at the cultivated Prairie Farm site. The effects of tillage were even greater in wetlands than in uplands: a 60% reduction in soil organic matter was observed in cultivated wetlands compared to prairie remnant wetlands. One bottom line is that the cultivated Prairie Farm landscape has significant potential for rehabilitation/restoration.

A controlled and collaborative study was conducted on the Prairie Farm funded by the CIG-NRCS program of USDA (Schumacher et al. 2012. Final Report to the NRCS). Objectives were to determine differences in biomass and soil quality among corn, two types of warm-season grassland, and prairie cordgrass. The experiment was laid out as randomized block with 4 replicates. The comparison with the long-term cultivated sites indicated a 50% reduction in organic matter has occurred since the original prairie was broken 100-120 years ago (Figure 9).

The analysis also demonstrated that soil quality diminished during the past century of cultivating annual crops can slowly be regained over time. For example, particulate and soil organic matter fractions in the top 15 cm were highest in the prairie remnant benchmark (Figure 9). Particulate organic matter (POM) represents a fraction of SOM that is > 0.5 mm in size and represents partially decomposed organic matter. As such this fraction represents a relatively young fraction of SOM and is more sensitive to changes in management practices. A larger component of POM is an indication that over time SOM is beginning to build in the soil.

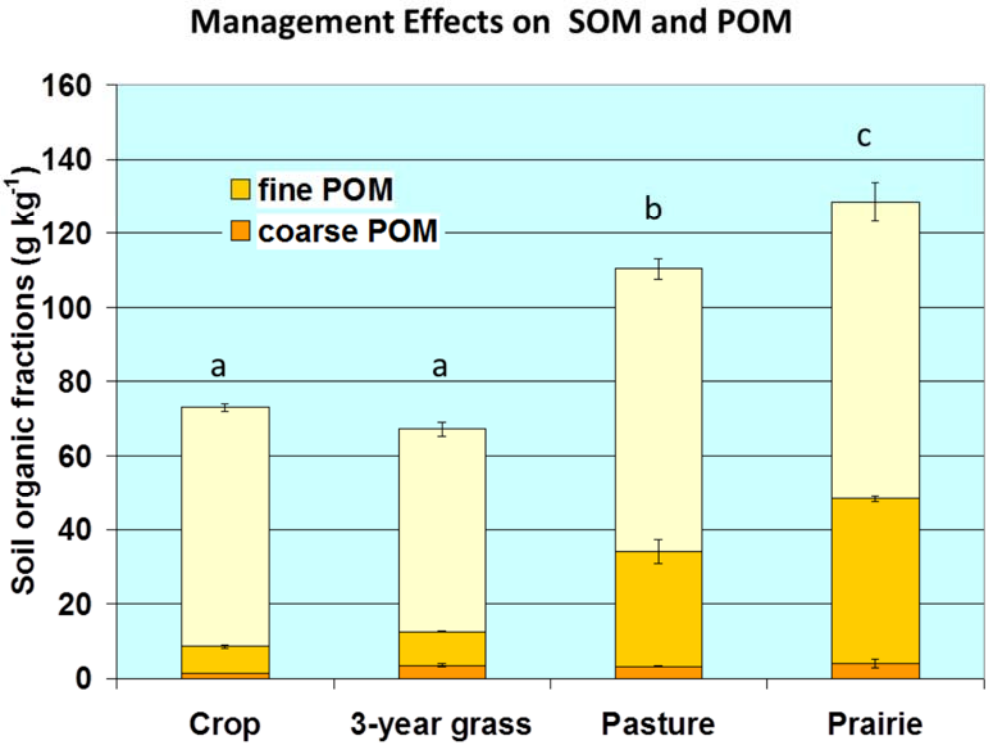

Figure 9. Particulate organic matter fractions of soil organic matter benchmarks for the prairie remnant compared to lont-term cultivated sites. Sample sites were similar in all aspects except for cropping history (LSD P<0.05) (from Heimerl 2011)

Wet aggregate stability, a key soil quality variable, was much higher in the prairie remnant than the cultivated sites (Figure 10). The long-term pasture at the Prairie Farm had similar aggregate stability values. The aggregate stability measurements for the long-term annual cropped land were lower by almost three times compared to the prairie remnant and long term pasture. Interestingly, the switchgrass treatment in the CIG plots showed an increase in wet aggregate stability relative to the corn treatment (representing a history of at least 100 years of annual cropping). This indicates that positive effects of growing switchgrass on degraded soils can be observed in a relatively short time period. A relative difference in aggregate stability between management systems is often the first indication that management is improving soil functions.

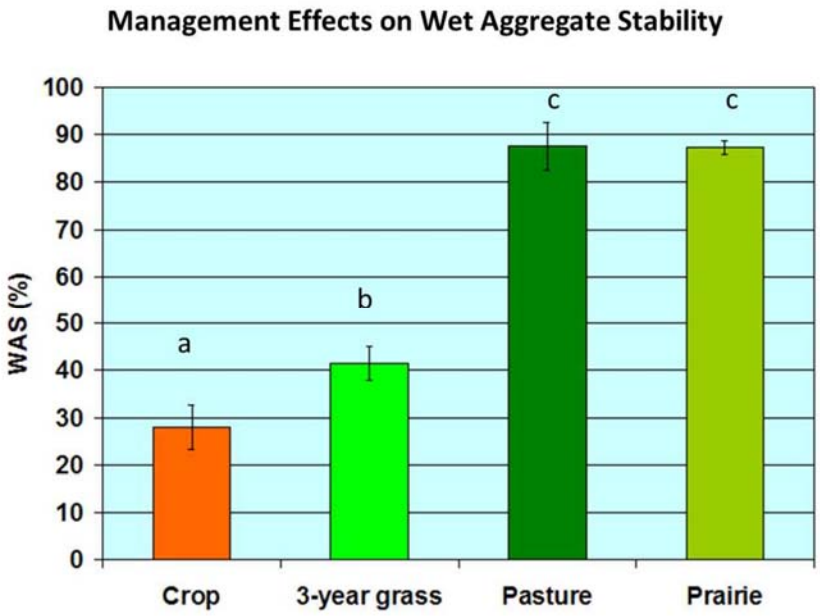

Figure 10. Wet aggregate stability benchmarks for a prairie remnant compared to long-term cropped land with a past history of erosion. Sample sites were similar in all aspects except for cropping history (LSD P<0.05).

Soil Summary

Perennial grass production provided year round cover to all parts of the landscape thus minimizing erosion and sedimentation potential. There is significant room to improve the soil quality of soils in Eastern South Dakota as shown by the 50% loss in soil organic matter that has occurred in the topsoil since settlement and cultivation of the land. This project demonstrated that perennial grasses can slowly improve the soil over time. Although this project had a relatively short time frame a significant improvement was seen in wet aggregate stability, a key indicator of management impacts on soil quality and a predictor of improved potential for increased soil organic matter.

Water volume and quality

Converting row crop fields to perennial grassland will change the water and nutrient budget of farmed landscapes. In theory, percolation of rainwater and snowmelt into soil will increase as soil macropores develop and as the dense vegetation near the soil surface and associated litter slow runoff. With greater percolation, more water will be stored in the ground and released slowly either into surface water systems (wetlands, streams) or into long-term storage in deeper groundwater. More water stored in soil will be present to support plant growth. Overall, water outflow from a farm will be reduced and peaks attenuated compared to that in a tillage system.

The perennial grassland crop with relatively low leaf nutrient content requires less fertilizer than annual crops such as corn and soybeans. Moreover, the deep and fibrous root system of native grassland will quickly sequester available nutrients such as nitrate vulnerable to leaching. The net effect of these properties of a perennial grass system is a tighter nutrient cycle with fewer nutrients lost to stream outflow and to the groundwater.

Environmental monitoring was conducted at the Prairie Farm to track these expected changes in water and nutrients. First, three crest stage gages were installed by the U. S. Geological Survey in 2009. Two of these were placed in streams that flow into the Prairie Farm from the

north. The third was placed in the only stream that leaves the farm and flows to the south. The differences between water volume inflow and outflow would be a measure of water storage in soil on the farm. The U. S. Geological Survey maintained the staff gages and made periodic measurements at a range of flows, from drought to deluge, to develop rating curves to convert a given stage height to flow volume (m^3/sec) for each station. Prairie Farm personnel recorded water levels for each staff gage throughout the growing season months from 2009-present. Water samples also were collected from the 3 streams, and standard analyses were conducted for water quality.

The extremely low gradient of the 2 monitored inflow streams has made it difficult for the USGS to develop useable rating curves. The USGS is still monitoring streamflow to collect more data to increase the chances that reliable curves can be developed. Once acceptable curves are available (expected summer 2012), water volume and quality assessments will be completed. An excellent rating curve has been developed for the steeper gradient outflow stream.

Objective 5. Complete an integrated economic analysis of the potential profitability and sustainability of a grass-based biofuel farm, including the costs of conversion and restoration.

Prairie Farm Economics

Investigation of the productivity and income streams of restored native grassland on former cropland may be important to assist the nascent cellulosic biofuel industry in getting off the ground. This portion of our project addressed several key questions: If producers plant switchgrass and prairie cordgrass in anticipation of the arrival of a cellulosic biofuel market, but that market is delayed, can they depend on other income streams to justify the input and lost opportunity costs? What income streams for grass crops can help to stabilize income for grass farms as prices for biofuel feedstock vary in the future? Can a farm based entirely on perennial grassland make a sustained living for a farm family? These questions are answered in part below to the extent possible with 4 years of data.

A challenge with the economic viability of a grass-based farm is the establishment period, when income from the grass is limited. Figure 11 shows the annual income from grass production and the associated operating expenses paid during the establishment years. Operating expenses did not include labor costs, but included other direct cost including herbicides, fuel, repairs, supplies, as well as depreciation and interest on machinery purchased and fence and water improvements. Seed costs and most wetland earthmoving costs were not included since they were covered by cost-share. Grass was established in phases, so income ramps up a more land generates income. Also, livestock production was added for the first time in 2011. Approximately 24% of the land was still in the establishment phase during 2011, so did not generate any income. As a result, it is expected that grass production income will increase again in 2012.

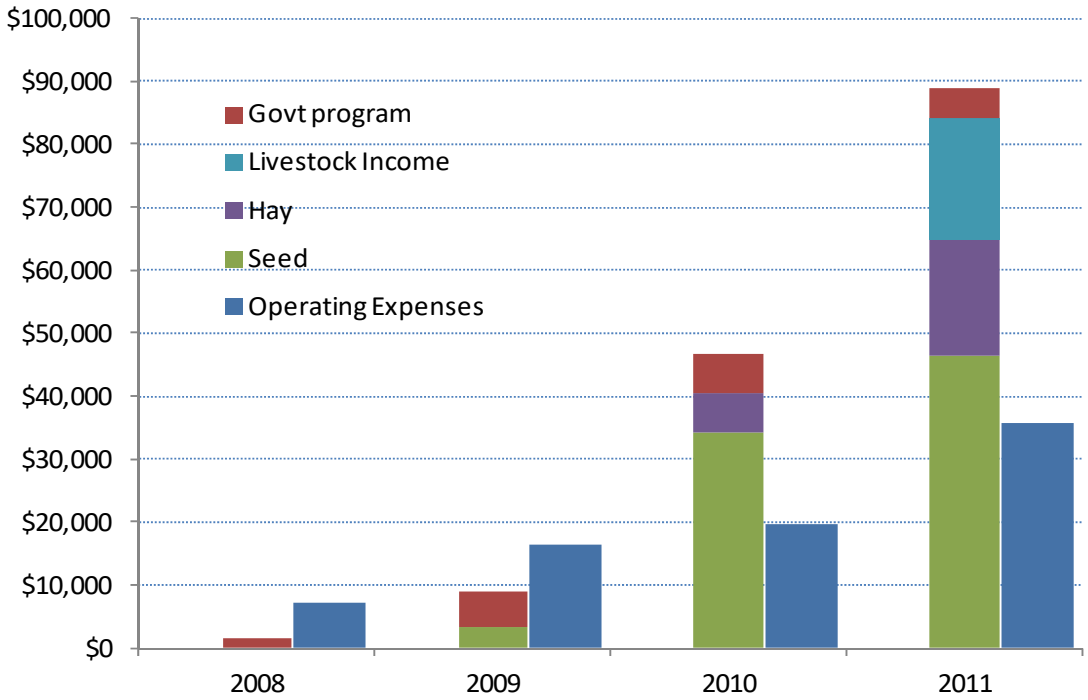

Figure 11. Prairie Farm income and operating expenses for land converted to grass.

Since grass was slowly phased in, the farm was also able to generate income renting the remaining cropland out for crop production. This helped improve the overall net income during the establishment period (Figure 12). However, net income was not sufficient to cover land rent costs in any year. Land rental costs were less in the initial years, since some of the land was in the Conservation Reserve Program (CRP), and the Prairie Farm did not rent that land until it came out of the program.

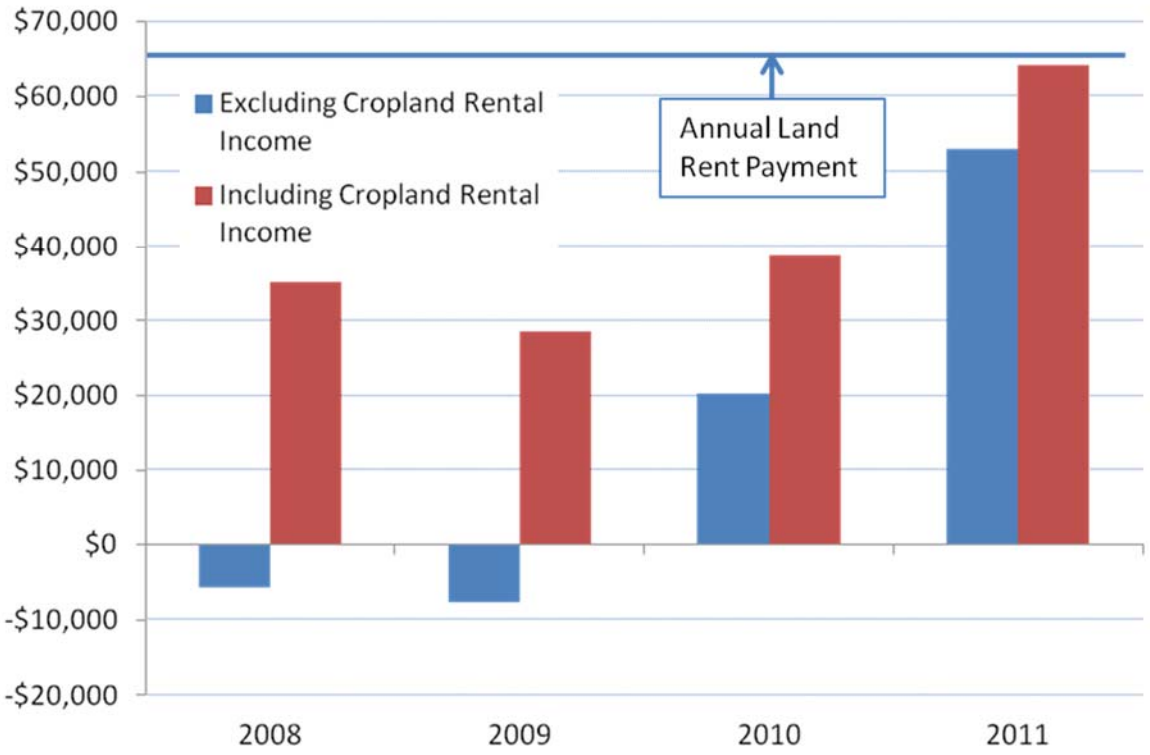

Figure 12. Prairie Farm net income over operating expenses from 2008-2011, with and without cropland rental income.

Gross income for the Prairie Farm was substantially lower than for a typical corn-soybean farm (Figure 13a). Operating expenses for the Prairie Farm were also substantially lower (Figure 13b), but not enough to compensate for the lower gross income. Consequently, net income was lower for the Prairie farm then for a typical corn-soybean farm. Corn-soybean cost and income estimates are from Southwest Minnesota farm business management records (http://www.finbin.umn.edu/), and assumed 400 acres of crop production with half in corn and half in soybean each year. This crop farm scenario is based on the Prairie Farm land base which has 400 tillable acres and assuming that the non-tillable areas did not generate any income.

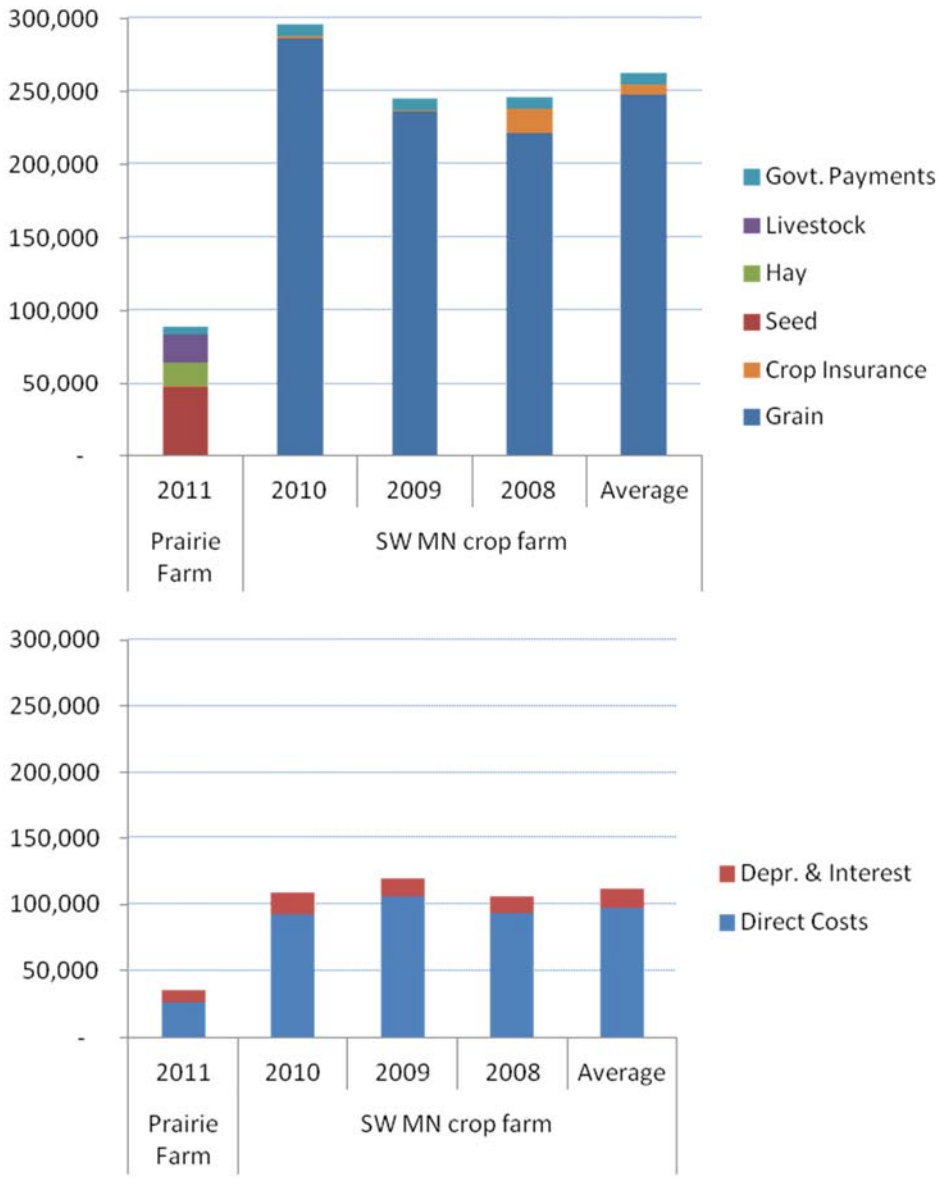

Figure 13. 2011 Prairie Farm and 2008-2010 Southwest Minnesota corn-soybean farm a) gross income and b) operating expenses.

Conclusions

By the fourth year, income and profit was considerably lower on the South Dakota Prairie Farm than on a more productive farm (probably better soils and slightly wetter climate) growing corn and soybeans in SW Minnesota. The profit difference may be narrowed in the future by 2 factors: grain prices and time and experience in marketing grass products. First, grain prices during the period of analysis (2008-2011) were at all-time highs; it is very likely that grain prices will drop as more land is planted to corn and soybeans and as grain buyers, such as those that operate livestock feed lots, look for cheaper alternatives. Second, considerable land on the Prairie Farm was rented but will not generate income until 2012. This includes 55 acres seeded to high diversity prairie in 2010 that is just becoming economically viable for its rare seed crop and use as pasture. Also, about 50 acres of renovated CRP will see its first use as pasture and hayland in

2012. Additionally, the key to profitability on the Prairie Farm is marketing. The grass-fed beef market was only tested in 2011, but will be expanded from 5 to 25-30 animals to be marketed in 2012. Lastly, we expect the cellulosic biofuel market to develop in 1-2 years, an event that should increase hay prices and Prairie Farm profitability. In short, the profitability comparison between these two farms may narrow considerably in the next few years due to the above factors.

Publications/Conference Papers/Public Releases/ Outreach of Results

Documentary Film Production

- Production of privately-funded, documentary feature film "Grass Roots: The Prairie Farm Story" (www.thegrassrootsfilm.com).
- Showings at 5 events: SD Art Museum on SDSU campus (2011); International Conference on Sustainability on SDSU campus (2011); Honors College Sustainability Colloquium on SDSU campus (2011); Dakota Rural Action Annual Meeting, Dahl Arts Center in Rapid City (2011); David Fee Memorial Lecture on SDSU campus (2012).

Popular and Public Press Articles Written About This Project

- "Researchers Evaluate Grass Farming's Potential" in Hay and Forage Grower magazine (written by Loretta Sorenson based on interview with C. Johnson). (2012)
- **"**Remaking Prairie, Re-Greening Agriculture: Creating a Working Farm Growing Native Grass" in Prairie Fire, The Progressive Voice of the Great Plains (written by Peter Carrels; centerfold article describes research and demonstration work on the Prairie Farm)(2011)
- "Taking Grass to the Next Level: Prairie Farm Rooted in Desire to Sustain Land" in Sioux Falls Argus Leader Newspaper (front page) (written by Cody Winchester) (2011)
- "They're Farming a Sea of Grass: Four Ph.D.s Out to Prove Tall-Grass Farming can be Profitable" in Brookings Register (front page) (written by Ryan Woodard) (2011)
- "Second Civitas (Honors) Lecture Features Ecologist" in the Augustana College Mirror (front page) (Promoting lecture by C. Johnson as part of Civitas lecture series) (2011)
- "South Dakota's Best Prairies" in South Dakota Magazine (written by Jerry Wilson) (Prairie Farm project featured) (2011)

Presentations

- Program Review Presentation (C. Johnson), "Landscape-Scale Biomass Production, Economics, and Environmental Quality," North Central Sun Grant Research Center, Indianapolis, IN (2012)
- Contributed Paper (C. Johnson), "South Dakota's Prairie Farm: An Experiment in Ecological and Economic Sustainability," Conference on America's Grasslands: Status, Threats, and Opportunities, Sioux Falls, SD (2011)
- Invited Keynote Address (C. Johnson), "Dakota Grasslands, Wetlands, and Climate Change: Last Nail or Silver Lining?" Annual Meeting of the South Dakota Academy of Science, Oacoma, SD (2011)
- Invited Lecture (C. Johnson),"South Dakota's Prairie Farm, An Experiment in Ecological and Economic Sustainability," Inaugural Civitas (Honors) Lecture Series, Augustana College, Sioux Falls, SD (2011)

- Program Review Presentation (C. Johnson), "Production of Biomass Across Heterogeneous Landscapes," North Central Sun Grant Research Center, Orlando, FL (2011)
- Seminar (C. Johnson),"Biofuel Feedstock Production at the Prairie Farm," NRCS Plant Materials Center, Bismarck, ND (2011)
- Invited Lecture (A. Boe),"South Dakota's Prairie Farm Project—An Experiment in Grassland Farming," Brookings, SD (2011)
- Invited seminar (C. Johnson), "South Dakota's Prairie Farm: An Experiment in Economic and Ecological Sustainability," University of Northern Iowa (sponsored by UNI Tallgrass Prairie Center and the College of Natural Sciences/Humanities and Fine Arts. (2010)
- Invited speaker (C. Johnson), "The Prairie Farm Concept and South Dakota's Alternative Energy Future," Annual Conference of the SD Association of Conservation Districts, Pierre, SD (Alternative Energies Session). (2010)
- Invited banquet speaker (C. Johnson), "Prairie Farm Research," Annual Meeting of the Eastern Dakota Water Districts, Brookings, SD (2010)
- Presenter (C. Johnson), "Research Progress in Biofuel Feedstocks," North Central Sun Grant Research Center 5 X 10 meeting, Brookings, SD (2010)
- Program Review Presentation (C. Johnson), Landscape Scale Lignocellulosic Biomass Production, Economics and Environmental Quality," North Central Sun Grant Research Center, Reno, NV (2010)
- Invited seminar (C. Johnson), "South Dakota's Prairie Farm," Iowa State University Sustainable Agriculture Colloquium, Ames. (2009)
- Invited seminar (C. Johnson), "South Dakota's Prairie Farm," Ecology and Environmental Biology Seminar Series, SDSU, Brookings. (2009)
- Invited seminar (C. Johnson), "South Dakota's Prairie Farm," Plant Science/NCARL Seminar Series, Brookings, SD (2008)

Farm Tours

- Public tour of the Prairie Farm and ongoing Sun Grant funded research sites and results. About 100 attendees were present including producers, state and federal agency representatives, students, professors, NGO reps., and ethanol agency reps. (2010)
- Public tour of the Prairie Farm and active research projects. About 50 attendees were present. (2011)
- Private tour of the Prairie Farm by 40 attendees from America's Grassland Conference in Sioux Falls and 35 attendees from the Land Sustainability Project based in Montevideo, MN (2011)
- Private tour of the Prairie Farm by 4 officials from the POET ethanol company based in Sioux Falls (2011)
- Several dozen small tours were conducted between 2009 and 2011 for individuals from diverse groups interested in the Prairie Farm project. Examples include individuals from congressional offices (senate and house); DOE and DOT agency staff; classes from SDSU; scientists from EROS Data Center; biofuel research from private industry and from other universities; news organizations and many other groups.

Web Sites

- One web site has been active for the past 4 years recording the history of the Prairie Farm and current operations (ecosunprairiefarms.org).
- A second web site (thegrassrootsfilm.com) announces the production of the Grass Roots documentary film and provides downloads and DVD orders.

Appendix I

Physiography of the Prairie Farm

The soils at the Prairie Farm near Colman, SD (96O 50' 37.878" W, 44O 1' 23.139" N; SW1/4, Section 33, T107N, R50W of 5th principle meridian, Moody County, SD) are found in MLRA 102C. MLRA 102C covers about 7.3 million acres in Nebraska, South Dakota, Iowa, and Minnesota and is located in the Dissected Till Plains Section of the Central Lowland Province of the Interior Plains (USDA---NRCS, 2006). The study site area is characterized by glaciated, nearly level to sloping plains and many potholes. The till and drift are strongly calcareous and moderately saline. Where drainage is established the Big Sioux River drains the area to the south. Approximately, 74% of the land in MLRA 102C is used for cropland, 16% for range/pasture land, and 10% is urban, water, forest, and other uses (USDA---NRCS, 2006).

Climate

The area receives about 22.0 inches of precipitation annually with 17.0 inches or 77% falling during the growing season (April---September). Most of the growing season precipitation is associated with high intensity thunderstorms. During the winter the area receives about 30 inches of snow (Kunze, 1989). The precipitation levels have resulted in the leaching of carbonates to a depth of 15 to 40 inches in well-drained soils. The average annual air temperature is 44OF. The average frost---free period (28OF basis with 50% probability) is May 3 to October 7 or 157---day growing season. The average number of growing degree days (50OF basis) during the period of May through September is 2370 (Kunze, 1980).

Soils

The dominant soils in the plots are the Dempster, Talmo, Worthing, Wentworth, and Egan (Soil Survey Staff, 2011). The associated adjacent soil is Baltic. The Wentworth and Egan soils have good productive capability while the Worthing soils do not because of wetness and flooding. The Dempster and Talmo soils have only fair productivity due to shallow/very shallow sandy profiles. See Tables 4a, 4b, and 4c for additional soils information. As a result, the crop productivity index values (a relative ranking from 0 to 100 of soils based on potential for intensive crop production) for the WeB (Wentworth---Egan), DnB (Dempster---Talmo), and Wo (Worthing) are 86, 49, and 32, respectively when compared to the best soils in Moody County. The crop productivity ratings assume: a) adequate management, b) natural weather conditions (no irrigation), c) artificial drainage where needed, d) no frequent flooding in lower lying soils, and e) no land leveling or terracing. The average range production for WeB, DnB, and Wo are 3850, 3300, and 6890 lbs/a respectively with the highest range production values in Moody County at more than 6890 lbs/a (Soil Survey Staff, 2011).

The dominant Great Groups in this site are Haplustolls (Dempster, Egan, Wentworth, and Talmo) and Argiaquolls (Worthing) with a mesic temperature regimes, an ustic or aquic moisture regime, a mixed or smectitic mineraology, fine---silty or fine particle size classes, and mostly superactive cation exchange activity classes. Adjacent soils include the Baltic (Endoaquolls). The Worthing and Baltic soils are hydric soils formed in clayey alluvium. The soils found at the site are mapped in 1.0 million acres in South Dakota, Minnesota, Nebraska, and Iowa (USDA---NRCS, 2011).

References

1. Kunze, B.O. 1989. Soil Survey of Moody County, South Dakota. USDA---SCS. US Government Printing Office. Washington, DC.
2. Soil Survey Staff, Natural Resources Conservation Service, United States Department of Agriculture. Web Soil Survey. Available online at http://websoilsurvey.nrcs.usda.gov/.
3. USDA---NRCS. 2006. Land Resource regions and Major Land Resource Areas of the United States, the Caribbean, and the Pacific Rim. US Department of Agriculture Handbook 296.
4. USDA---NRCS. 2011. Soil Extent Mapping Tool. USDA---NRCS. Available online at http://www.cei.psu.edu/soiltool/semtool.html

Please complete the following table to reflect your project at completion or time of report submission:

ITEM	NUMBER
Abstracts	**15**
Peer Reviewed Publications	**0**
Outreach Publications/Web Pages	**15**
Professional Presentations	**25**
MS Degrees Conferred	**2**
Ph.D. Degrees Conferred	**0**
MS Students Supported	**3**
Ph.D. Students Supported	**0**
Post-Docs Supported	**1**
Undergraduate Students Supported	**10**
Investigators Supported	**7**
Start-Up Jobs Created	**1**
Disclosures	**0**
Patents Filed	**0**
Provisional Patents	**0**
Patents Issued	**0**
License Agreements	**2**
Plant Variety Protection	**0**

Back to Table of Contents

Sun Grant Initiative
DOE Final Progress Report

Project Title: Biofuel Crops in Eastern South Dakota: Establishment, Productivity, Biotic Impact and Multiple Use Potential

Project Director/Principal Investigator:
Paul J. Johnson, Professor of Entomology, Plant Science Department, South Dakota State University, Brookings SD

All Co-Principal/Other Investigators:
Arvid Boe, Professor of Agronomy, Plant Science Department, South Dakota State University, Brookings SD

Collaborators:
Nels Troelstrup, Professor, Natural Resources Department, South Dakota State University, Brookings, SD
Alexander Smart, Professor, Natural Resources Department, South Dakota State University, Brookings, SD
Rocco Morano, South Dakota Game, Fish & Parks Department, Brookings, SD

Period of Performance: 1 October 2010 – 31 December 2013

Funding Awarded: $271,574

Cost Share Amount: $68,001

Costs Share Sources: Time and effort from PIs and CoPIs; Indirect on time and effort

Executive summary

This project emanated from the general background of a federal mandate to reduce the country's reliance on foreign petroleum and increasing biofuels from domestic sources of cellulosic feedstocks, and to produce these on marginal cropland that was suboptimal for conventional grain crops, such as wheat, maize, or soybean. Native perennial grasses grown as feedstock improves environmental quality and provides enhance biological goods and services, such as reduced erosion, carbon sequestration, wildlife habitat, and enhanced non-commercial biological diversity. When native grasses are mixed with native flowering forbs then the additional advantage of pollinator support and conservation applies.

This project was successful in demonstrating that field planting transitions from traditional field crops to grass-dominated biofuels crops is agronomically feasible, a good use of highly marginal land, provides a net increase in animal biodiversity, and provides multiple use potential for land managers. These results provided interpretations and conclusions that provide directly applicable information to producers throughout the northern Great Plains and upper Midwest.

Prior to this study the available information on the production of switchgrass biomass was limited to small plot studies where the plants were grown with optimal conditions on prime land. Here, we attempted to replicate reality conditions on some of the worst marginal lands with shallow cobbly soils that dry quickly and have low fertility due to historical cropping. We demonstrated that without fertilizer or irrigation, and during a drought period, the planting of native grasses and forbs were delayed only one year from a harvestable crop, but provided ecological goods and services beginning the year of planting: reduced erosion, increased water content of the soil, increased and longer retention of snow, and had lower overall pest impact due to increased plant diversity. The lowest rates of biomass production occurred in fields planted with soybean and maize companion, or cover, crops, with switchgrass and alfalfa production depressed due to water and light competition from the companion crops. In contrast, switchgrass with a maize cover under drought conditions was repressed for the first growing season, while maize produced a below par but still profitable crop. By the second growing season both alfalfa the alfalfa was harvestable, while switchgrass accelerated for harvestable biomass in season three.

The public interest is met with the results such that the worst of marginal lands in the northern Great Plans can be used for economically valuable production of biomass based on native grasses and forbs. This combination provides additional environmental benefits in reduced erosion, improved soil and water conditions, drought resistance, enhanced biological diversity, increased pest resistance, and improved support for native bees and other native pollinator insects.

Project objectives

TASK 1: Evaluate establishment rates in nurse crop residue

Nurse crops were used in two plantings: Maize over switchgrass (Table 1) and soybean over alfalfa (Table 2). Both combinations were evaluated in both a normal rainfall season and a drought season. Planting was done in the normal rainfall season. The soybean companion crop produced a meager return, but maize produced a marginal income crop, even in a drought.

Table 1. Maize productivity as a companion crop with switchgrass in 2012

Trait	Mean (SE)
Biomass (kg ha^{-1})	4907.9 (301.7)
Ears ha^{-1}	57,384 (4781.2)
Ears $acre^{-1}$	23,232 (1935.7)
Kg grain ha^{-1}	3269.9 (309.0)
Bushels $acre^{-1}$	52.0 (4.9)
Kg Cobs $hectare^{-1}$	593.7 (51.6)
Harvest index¶	0.36 (0.01)

Table 2. Soybean productivity as companion crop with alfalfa in 2012

Trait	Mean (SE)
Stover biomass (kg ha^{-1})	956 (73)
Grain yield (kg ha^{-1})	812 (47)
Bushels $acre^{-1}$	12.0 (0.7)
Harvest index¶	0.46 (0.009)

TASK 2: Determine relative productivity

The trends in biomass production among the experimental plantings clearly shows that switchgrass and mixed native species plantings provided the larger biomass harvests (Table 3). Switchgrass alone provided the greatest biomass after one year of growth. This was followed by native mix, which was depressed in the 2012 planting because of herbicide application to control weeds, especially Canada thistle (Table 3). The least productive plantings were alfalfa, from the soybean companion planting, and switchgrass from the maize companion planting. However, autumn 2014 samples indicated that native forb recovery from the herbicide contributed substantially to increased biomass accumulation. Furthermore, although maize suppressed switchgrass growth during the first year, the switchgrass recovered in the second year and rapidly gains high productivity (Table 4).

Table 3. Biomass (kg/ha), cover (%) and composition (%) for plant communities planted at Oak Lake. Harvests were in spring of the year following planting.

	2011			2012		
Community	Biomass	Cover‡	Comp†	Biomass	Cover	Comp
Alfalfa	726a	25a	98a	414a	34a	79a
Switch/maize	758a	9b	98a	915b	2.5c	17b
Switch	2078b	17ab	100a	1110b	14b	96a
Mixed	1849b	19a	99a	583a	2.5c	34b

Table 4. Estimates of biomass production from switchgrass in samples from October 2014	
Treatment	Biomass (kg/ha)†
Switchgrass	3910
Switchgrass/corn	5010

TASK 3: Interseeding annual plants into perennial forages.

This trial consisted of planting maize into first and second year established switchgrass, alfalfa, and native mix. Maize performed poorly and failed to complete growth and mature. Multiple reasons are probable but the primary factors were water competition from established plants, shading of seedlings by established plants, and browsing of seedlings by deer.

TASK 4: Survey, define, and assess potential insect pests.

Only two species of insect, one gall midge fly and one moth, were found to be the most persistent and damaging on switchgrass. The gall midge appeared in new fields by the second season of growth, while the moth was not detectable during the project at Oak Lake and required study at the Aurora Farm.

The first primary pest is the switchgrass gall midge, *Chilophaga virgati* Gagné (Diptera: Cecidomyiidae) was discovered as a new species to science shortly before the start of this project, with its basic biology elucidated in this project. During most years this insect is the most important species in terms of readily visible damage, consisting of a malformation of the inflorescence and 100% seed loss, and stunting of the culm, together resulting in upwards of 60% of biomass loss per culm. This gall midge is host to at least three parasitoid wasp species of the families Eulophidae and Platygastridae, all of which are new to science. One of these species was described and named, while the others are under study by collaborators and being prepared for publication. Details on the biology of the gall midge and its parasitoids are being elucidated by a second project derived from this one. The high rate of parasitism by these wasps is a major natural controlling factor in the gall midge's population and can be used to avoid insecticides in switchgrass production fields. This initial study indicates that lowland varieties of switchgrass are more vulnerable to infestation and harbor higher population densities of the gall midge, probably due to the larger diameter of culms. Upland varieties are less vulnerable and harbor smaller populations due to the thinner culms.

The second primary pest is the switchgrass moth, *Blastobasis repartella* (Dietz) (Lepidoptera: Blastobasidae). This little moth was previously described from specimens collected at Denver, Colorado, in 1910 then first recognized as a cultivated switchgrass pest in South Dakota, leading to this project. The caterpillar of this moth feeds on developing buds along the switchgrass rhizome during the winter and moves into and excavates the proaxis in spring and into the lowest nodes and internodes of the culm in early summer. The rhizome feeding destroys upwards of 100% of buds for potential above-ground growth, while the proaxial and culm feeding kills the infested culm while still small. Plant infestation rates vary greatly by site from 10-60%, with per culm per plant infestation rates 7-9%. One parasitoid wasp was discovered, *Bassus difficilis* Muesebeck (Hymenoptera: Braconidae). Parasitism rates are low, <1%, indicating that this wasp is not likely a major natural biocontrol agent.

TASK 5: Establish field use by small mammals.

Small mammal diversity increased due to the diversity of plants. Eleven species of mouse, vole, shrew, weasel, and ground squirrel were found in all plots (Fig. 1). Ten of these species are representative of native small mammal populations and diversity in the general area of the fields. The deer mouse was the single most abundant granivore species in all fields comprising nearly 84% of all captures, followed by the omnivorous short-tailed shrew at 9% of captures. The small predator long-tailed weasel was the most abundant at 2% of captures.

The deer mouse was generally distributed among the experimental fields, but 47% of the captures occurred in switchgrass and native mix fields. This indicates a slight preference for native species habitats. In contrast the short-tailed shrew had only 20% of its captures in native species fields suggesting a preference for unstable habitats that may harbor preferred insect prey.

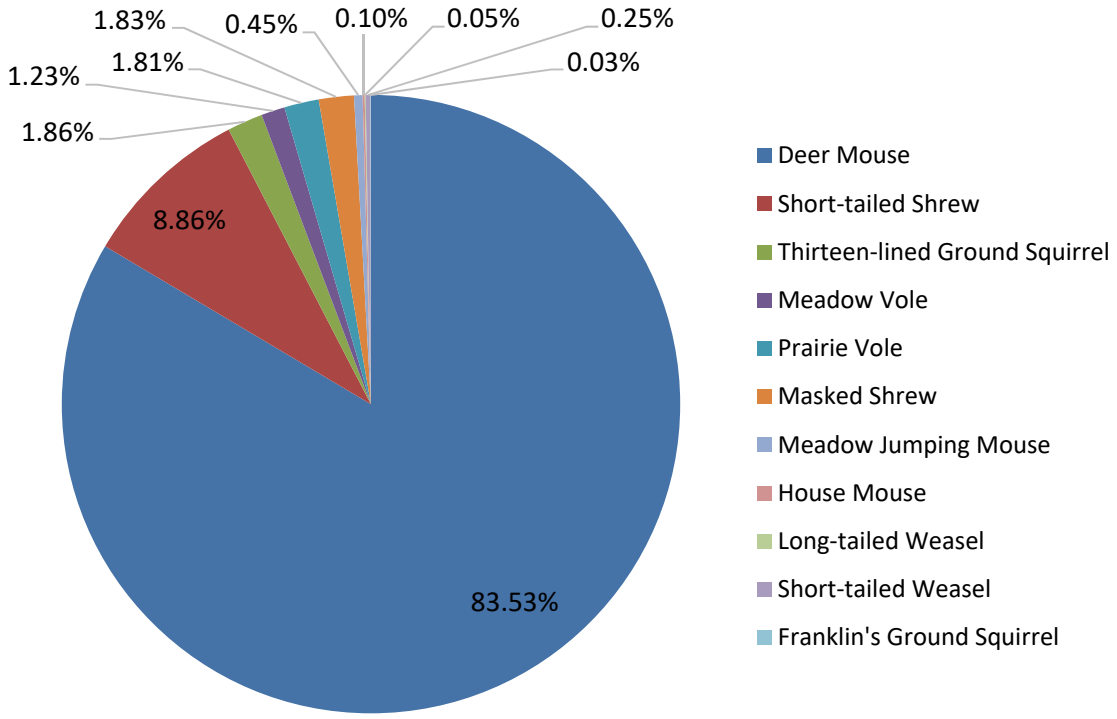

Fig. 1. Eleven species of mouse, vole, shrew, weasel, and ground squirrel found in all plots. Total trap nights = 15,616 with total captures of 4,018 which signifies 25.7% success.

TASK 6: Evaluate field value as anti-predation food for deer.

Whitetail deer residence and transient use estimates showed that plantings of native grass and forbs is highly attractive. Tall stands of native grasses were favorite bedding sites, and browsing evidence on native forbs demonstrated extensive attraction for deer. Alfalfa modified sites are also attractive for browsing, but the preference was focused on plots with mixed native forbs.

TASK 7: Define biodiversity enhancement values.

This aspect of the study focused on measuring relative biodiversity using beetles (Coleoptera), particularly ground beetles, as proxy taxa. Ground beetles are particularly useful due to their frequent use in numerous ecological and agricultural studies. This allows for comparison studies.

A total of 13,691 specimens were recovered representing 98 species. Diversity for all beetles and ground beetles was analyzed for both Shannon and Simpson indices. Figure 2 shows sample graphs for all beetles and ground beetles from 2012. It is clear that the native mix was significantly more biodiverse in all beetles as well as ground beetles. In general, the switchgrass monoculture compared favorably with alfalfa from the soybean companion planting. This similar is likely a combination of the depression of biodiversity in any monoculture, native or not, and the attractiveness of alfalfa to specialized weevils feeding on alfalfa and not present in other habitats. The maize companion planting with switchgrass consistently gave the lowest biodiversity rankings.

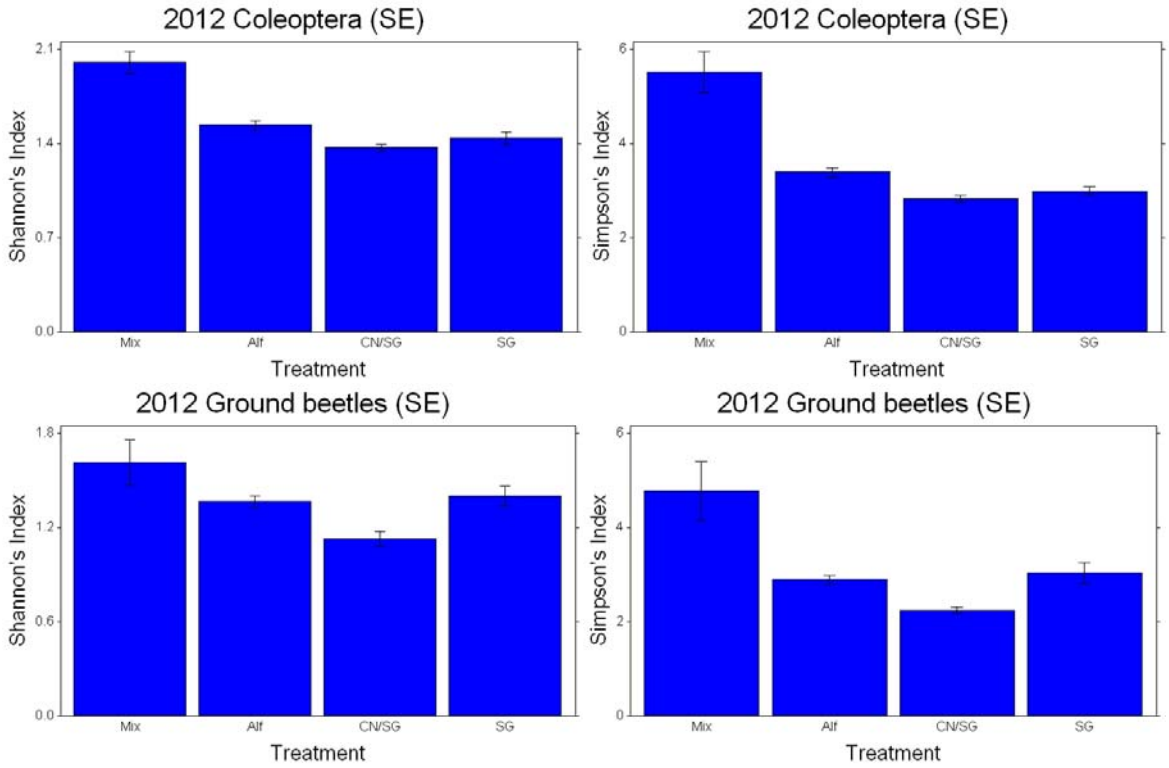

Fig. 2. Shannon's Index and Simpson's Index for all Coleoptera species (top panels) and for ground beetles (bottom panels) in 2012 in field plots with mixed native species (Mix), alfalfa (Alf), corn/switchgrass (CN/SG), and switchgrass (SG).

1. Project activity summary

Primary project activities

1) Establishment and productivity of switchgrass in various mixtures and cover crops on poor soil and multiple site aspects
2) Impact of planting mixtures on biodiversity
   a. Small mammals

b. Ground beetles
c. Biology of primary switchgrass pests
   i. Switchgrass moth
   ii. Switchgrass gall midge
   iii. Occurrence and incidence of associates and secondary potential switchgrass pests

Methodology

1) Establish 3 perennial plant communities for sustainable biofuels
   a. Alfalfa (*Medicago sativa*) seeded with soybean (*Glycine max*) as companion crop
   b. Switchgrass (*Panicum virgatum*)
   c. Native plant mixture composed of 15 species of grasses and forbs
2) Two establishment methods for switchgrass
   a. Seeded alone---the **recommended** method
   b. Seeded with maize (*Zea mays*) as companion crop
3) Companion crop (soybean or maize) provides:
   a. Income from grain in seeding year
   b. 'Some' protection from wind and water erosion
   c. 'Helpful' competition against weeds on marginal land in the seeding year
   d. Competes with seedlings of the perennial biofuel species
4) Replicated in time (2011, 2012, and 2013)
5) Planted with conventional farm equipment
6) Individual plot size was ~ 0.3 hectares
7) Completely randomized design with 3 replications
8) Seeding rates used were recommended for species and region
9) Data collected:
   a. Grain yield of companion crops in the seeding year
   b. Biomass yield of biofuel crops in second and third years (no yield data collected in seeding year)

Problems and departures

Basic operation of the project was compromised by early departure of two of co-PI's. Rupp left after one year and though completed oversight of a graduate research assistant, there was no subsequent continuity of small mammal study. Co-PI Owens also left the project on year 2 due to a change in employment status, but this made only minor adjustments to conduct of the project. Otherwise, there were no significant departures from the original plans of the project. Adjustments to the project timetable occurred in response to weather, only. Specifically, year 2 of the project suffered from a severe growing season drought. The drought suppressed the rate of seedling emergence and plant growth, and reduced the site attractiveness to small mammals and ground beetles during the hottest and driest periods. However, natural adaptations allowed these organisms to take advantage of seasonal climate amelioration as it occurred.

Overall gains of the project are numerous and are summarized here:
Agronomic

1. Switchgrass and native mix plantings establish quickly in drought years and provide economic return by year 2.

2. Co-planted maize or soybean cover crops do not seem to suppress switchgrass establishment in normal years, but crop may not be economically viable in drought years.
3. Biomass productivity is greatest in mixed species biomass plantings.
4. Biodiversity is greatest in mixed species biomass plantings.
5. Switchgrass gall midge present by 2nd year.
6. Switchgrass moth not detectable before 3rd year.
7. Unharvested switchgrass and native mix superior in snow capture and retention, and subsequent soil moisture.
8. Switchgrass and native mix are superior for soil erosion prevention.

Scientific

1. Switchgrass and native mix sustain higher levels of biodiversity.
2. Biology elucidated of *Blastobasis repartella,* switchgrass moth.
3. Biology elucidated o*f Chilophaga virgati,* switchgrass gall midge.
4. Discovery and description of *Platygaster chilophagae,* new species to science
5. Discovery of *Quadrastichus* sp. and *Aprostocetus* sp., as new parasitoids of the gall midge and probable species new to science.
6. Discovery o*f Steneotarsonemus* sp., a new leaf mite species to science

2. Products developed

See table below

3. Academics

a. Courses developed
   None
b. M.S. students supported
   a. Veronica Callez Torrez
   b. Benjamin Carroll
c. M.S. degrees conferred
   a. Veronica Calles Torrez
   b. Benjamin Carroll
d. Ph.D. students supported
   a. none
e. Ph.D. degrees conferred
   a. none
f. Post-docs supported
   a. none

4. Computer modeling

N/A

Outputs table

ITEM	NUMBER	DETAILS (e.g. citations, names, descriptions, varieties, etc.)
Abstracts: include full citation and attach a pdf copy.	3	See attached.
Peer Reviewed Publications: include full citation and attach a pdf copy if available	6	See attached.
Outreach Publications including web pages: include full citation	2	Reitsma, K.D., T.E. Schumacher, V.N. Owens, D.E. Clay, A. Boe, P.J. Johnson. 2012. Switchgrass Management & Production in South Dakota. iGrow Agronomy South Dakota State University, November 2011, 13 p. Johnson, P.J. 2013. Switchgrass Gall Midge Diagnostics http://ncsungrant.sdstate.org/NewsandEvents/Videos.cfm
Professional Presentations: include full citation	16	See attached.
MS Degrees Conferred: include names plus month/year confirmed	2	Veronica Calles Torrez, August 2013 Benjamin Carroll, May 2013
Ph.D. Degrees Conferred: include names plus month/year confirmed		
MS Students Supported: include names	2	Veronica Calles Torrez Benjamin Carroll
Ph.D. Students Supported: include names		
Post-Docs Supported: include names		
Undergraduate Students Supported: include names	5	Krista Hegge Heidi Meyer Emily Gaston Christian McHugh Jeff Augspurger
Investigators Supported: include names		
Jobs Created		

Invention Disclosures		Provide no confidential or enabling information. Just indicate in an invention disclosure has been filed with the employer.
Non-provisional Patent Application(s) Filed		
Provisional Patents Filed		
Patents Filed		
Patents Issued: include full citation		
License Agreements: include description		
Plant Variety Protection: include description		
Subsequent Funding: List proposals funded as a result of this work		Defining Geographic Range and Determining Potential Impact of the Switchgrass Gall Midge Among Best Adated Switchgrass Varieties.
Other: Products, such as data or databases, physical collections, audios or videos, software or Netware, models, educational aids or curricula, instruments, or equipment.		Approximately 17,000 research and voucher insect specimens of new species discovered and target and non-target organisms deposited in the Severin-McDaniel Insect Research Collection.

Back to Table of Contents

Sun Grant Initiative
DOE Final Progress Report

Project Title: Interactions of Biochar/Bio-ash Source/Properties Impacts on Soil Properties, C Sequestration Potential, and Crop Management

Project Directors/Principal Investigators: Douglas Malo and Sharon Clay, Plant Science Department, South Dakota State University, Brookings, SD

All Co-Principal/Other Investigators: Thomas Schumacher, Howard Woodard, David Clay, and Ron Gelderman, Plant Science Department, South Dakota State University, Brookings, SD; H. Lei and James Julson, Agricultural and Biosystems Engineering Department, South Dakota State University, Brookings, SD

Period of Performance: 1 March 2009 - 30 September 2011

Funding Awarded: $78,000

Cost Share Amount: $19,500

Cost Share Sources: Time and effort from PIs and CoPIs

Executive Summary

Biochar is fine-grained highly porous charcoal and is the end product of bio-oil and bio gas production. This grant optimized bio-oil and bio-gas production for selected feedstocks, and tested/characterized biochars produced from a variety of feedstocks (switchgrass, corn stover, and prairie cordgrass. The optimal processing conditions (maximum bio-oil and syngas yield) using a microwave pyrolysis digestion process were obtained using a processing temperature of 650^{O}C with a residence time of 18 minutes for all feed stocks tested. Yields (bio-oil+ bio-gas) for all feedstocks tested were >73% at the optimal conditions. Biochar production averaged about 23 to 27% of the original feedstock. Reaction temperature, residence time, and feedstock were all factors that affected the quantity and composition of the bio-oil produced. Biochars produced from optimal conditions were then tested for selected chemical and herbicide reactions. Feedstock source influenced the carbon to nitrogen ratios of the biochar. The addition of biochar to the soil (10%) reduced the plant available N in the soil, increased phosphorus levels, and increased extractable K values. Biochar additions from the optimal production conditions significantly increased soil salinity when added to the soil (10%). Biochar pH values changed dramatically when processing temperature and time were varied. Highest pH values (very alkaline) were found with 650^{O}C for more than 16 minutes of residence time in the pyrolysis chamber while lowest values (very acidic) were found with temperatures of 550^{O}C. These differences impact biochar suitability as a soil amendment. Herbicide (atrazine [cationic] and 2,4-D [anionic]) sorption studies on selected biochar/bio-ash materials were completed. Biochars differed greatly in their sorption of herbicides. When optimal biochars were added to soil the atrazine sorption significantly increased. The addition of biochars to the soil increased the 2,4-D sorption. These differences significantly impact herbicide application rates for weed control, leaching potentials, and ground water quality. In the microbial studies significant differences (increased growth and diversity) were noted in the soils treated with biochars. The results of this study were used to develop pilot plant production parameters and production of more biochar materials to test in field studies to evaluate the impact of biochar additions on soil quality and productivity (including biochar decomposition rates) in a new USDA-NIFA grant.

Project Objectives/Outcomes

1. Determine the optimal conditions for bio-oil production and testing of the resulting biochar for mineralization stability (breakdown rate) of biochar/bio-ash.
    a. **Task** → Create biochar/bio-ash materials for mineralization study and establish soil mineralization studies with biochar/bio-ash materials generated.
    b. **Accomplishments** →Optimized bio-oil production on feedstocks of corn stover, switchgrass, prairie cordgrass, and ponderosa was completed. A variety of reaction temperatures (550, 600, and 650^{O}C) and residence times (from 8 to 25 minutes) were tested on each feedstock. Maximum bio-oil and biogas (syngas) yield (>73%) was found 650^{O}C with a residence time of 18 minutes for all feedstocks tested. Reaction temperature, feedstock source, and residence time affected the quantity, quality, and composition of bio-oil produced. Preliminary results from the microbial work showed significantly different rates of microbial growth from biochar additions based on feedstock source and optimization conditions.
    c. **Variance** → Only preliminary data on the impacts of biochar additions to soil were obtained. The microbial study extracts were destroyed when the cold temperature room failed late in the study and there was not enough time or biochar material to redo the experiments.

2. Characterize biochar/bio-ash and its impact on selected soil properties.
    a. **Task** → Analyze soil, biochar/bio-ash, and mixtures of soil + biochar/bio-ash. Tests to be run are composition [C, N, and other key nutrients], pH, electrical conductivity, and herbicide sorption/efficacy studies, and other tests as needed. Monitor soil microbial

community changes (e.g., FDA. PCR, and DGGE) when biochar/bio-ash is added to the soil and incubated for selected periods of time.

b. **Accomplishments →** Biochar/bio-ash were characterized for nutrient levels, pH, EC, particle size, SAR, and water holding capacity. There were significant differences in P levels in biochar/bio-ash when compared to soil P levels and also there are differences in when the P comes off in the testing process (more P comes off in the NH_4NO_3 wash when compared to the KCl wash for biochar/bio-ash when compared to soil). Feedstock source influenced the C/N ratios of the biochar (ranging from 35/1 for corn stover to 250/1 for wood chips). The addition of 10% biochar to the soil reduced the plant available N. Phosphorus and potassium levels showed an increase when biochar was added to the soil. Biochar additions from the optimal production conditions significantly increased soil salinity when added to the soil (10% mixture). Biochar additions from the optimal production conditions significantly increased soil salinity (from 1.6 to 2.9 dS/m) when added to the soil (10% mixture). Biochar pH values changed dramatically when processing temperature and time were varied. Highest pH values (pH>8) were found with 650^{O}C for more than 16 minutes of residence time in the pyrolysis chamber while lowest values (pH < 4) were found at reaction temperatures of 550^{O}C at all residence times tested. These pH and salinity differences impact biochar suitability as a soil amendment. Herbicide (atrazine [cationic] and 2,4-D [anionic]) sorption studies on selected biochar/bio-ash materials were completed. Biochars differed greatly in their sorption of herbicides. When optimal biochars were added to soil the atrazine sorption increased by >200% for switchgrass and only 50% for corn stover when compared to soil alone. The addition of optimized pyrolytic biochars to the soil significantly increased the 2,4-D sorption from 300% for corn stover to >800% for switchgrass when compared to soil alone. These differences significantly impact herbicide application rates for weed control, leaching potentials, and ground water quality. Preliminary work on microbial community abundance and diversity were seen in the DGGE tests run on selected biochars during a two month period.

c. **Variance →** With the loss of the microbial extracts/samples as a result of failure in the cold temperature room we were not able to complete the long-term microbial community changes and monitoring part of the project.

3. Determine the influence of biochar/bio-ash on nutrient availability or reduction due to different rates of biochar addition (greenhouse study).
   a. **Task →** Evaluate use as a fertilizer/soil amendment.
   b. **Accomplishments →** Selected biochars were analyzed for C, N, P, and K. Addition of 10% biochar to the soil tested has resulted in soil fertility level changes dependent on the biochar source and the soil used. When switchgrass biochar was added to 8 different soils the amount of NO_3^--N in the soil-biochar mixture (10%) reduced amount of NO_3^-N in the soil from 5 to 30%. Soil test P levels (Olson P) showed an increase from 2 to 25% when switchgrass biochar was added. Extractable K levels also significantly increased when from 5 to 50% with a 10% biochar addition. The range in pH values (4 to 11.5), salinity (1.5 to 3.6 dS/m) of the biochar materials greatly impacts the suitability of these materials as soil amendments or use in riparian areas to trap and hold agrochemical in runoff water.
   c. **Variance →** Because of delays in the manufacture of biochars and the small quantities of biochar produced only limited nutrient testing was completed. A new project concentrating on only one bio-oil process and at a much larger scale will produce adequate quantities of biochar for field and greenhouse testing.

Summary

As energy prices increase and fuel supplies in the United States dwindle, there is a search to replace foreign oil and gas imports. Several different energy production processes are either online or being proposed. Today, ethanol from corn grain is one of the most widely used technologies. However, other production techniques with other starting feedstocks are being developed and researched. One of the techniques that holds great promise is the production of bio-oil and syngas (synthetic natural gas) from different sources of biomass using pyrolysis reactions. Along with syngas and bio-oils, the other byproduct formed is biochar.

Biochar is a form of charcoal produced by heating biomass in the absence of air. Biochar is carbon rich and it is anticipated that its final use will be as a soil/fertilizer amendment. Because biochar is carbon rich, adding it to the soil is also being considered as a form of carbon sequestration in the mitigation of global warming. If the mineralization rate of biochar is slow, then the pyrolysis industry would be considered a carbon-neutral industry or have a very small carbon footprint. This would be very beneficial from both the industry and environmental viewpoints.

There are several unknowns about biochar that need to be explored and assessed in order to understand the effects of biochar on soil processes/quality as well as the soil effects on the life-cycle of biochar. The goal of this 2-year project was to explore selected aspects of biochar/soil interactions in laboratory and greenhouse studies.

This study measured the influence of several microwave pyrolytic conversion processes, which varied temperature and residence time, on pH and EC characteristics of the resulting biochars produced from selected feedstocks (e.g., corn stover, switchgrass, prairie cordgrass, and wood sources). These biochars were used to amend a group of diverse soils and examined the impact of the biochar additions on selected soil properties (e.g., nutrient availability, solution pH, EC, and sorption properties of a weakly cationic herbicide, atrazine, and an anionic herbicide, 2,4-D). Because of differences in the microwave processing parameters of processing time, temperature, and feedstock source there was great variation in the properties of the biochars. As a result of this study the optimum bio-oil and syngas production parameters were identified for the feedstocks tested and this information is being used in a new USDA-NIFA grant.

During the duration of this project there were two problems we encountered. One was the difficulty in obtaining biochar materials in a timely manner because of equipment problems and the need to test the various bio-oil processing parameters before we could begin and only limited amounts of biochar were available to work with in a timely manner. These delays and low output of biochar impacted our ability to complete the greenhouse tests of the biochar on plant growth. The second problem we had was a complete failure of a cold room in a research building for a weekend that resulted in temperatures that made our microbial extracts/results unusable and it was too late in the project to restart. Because of these problems we have partially included these objectives (mineralization of biochar and plant/soil impacts of biochar additions on a field basis) in a new grant that we received from USDA-NIFA that looks at bio-oil production utilizing the optimal conditions identified in this grant. This new grant also looks at three regionally important feedstocks (switchgrass, corn stover, and wood slash/chips).

Publications/Presentations/Grants

1. Krack, K., Clay, S., Hansen, S., Clay, D., and Olson, M. 2009. Switchgrass biochar influence on soil properties and atrazine sorption (published abstract). Weed Science Society of American Annual Meetings. Denver, CO (Feb 2010). https://srm.conference-services.net/reports/template/onetextabstract.xml?xsl=template/onetextabstract.xsl&conferenceID=1756&abstractID=344140 (verified Jan 24. 2010).
2. Malo D.D. and Clay, S.A. (project leaders), Schumacher, T.E., Woodard, H.J., Clay, D.E., Gelderman, R.H., Lei, H. and Julson, J.L. 2010. Interactions of Biochar Source/Properties

Impacts on Soil Properties, C Sequestration Potential, and Crop Management (annual report). Sun Grant Initiative – North Central Center at South Dakota State University Annual Meeting. Jan 2010. Reno, Nevada. http://ncsungrant.sdstate.org/upload/Microsoft-PowerPoint-SDSU-biochar-projects-Presentation-reno_2010-Compatibility-Mode.pdf (verified Jan 24, 2010).

3. Lei, H., S. Ren, and J. Julson. 2009. The effects of reaction temperature and time and particle size of corn stover on microwave pyrolysis. Energy and Fuels. 23, 3254–3261.
4. Awarded new project proposal (USDA-NIFA proposal for Sustainable Bioenergy) with many other researchers on biochar - Optimization of Pyrolytic Bio-oil Production to Maximize Biochar Utility Using Selected Biomass Feedstocks – Schumacher, T.E (PI)., Clay, S.A., Clay, D.E., Chintila, R., Julson, J.L., Gelderman, R.H., Malo, D.D., and Wei, L.. (awarded Dec 2010).
5. Malo D.D. and Clay, S.A. (project leaders), Schumacher, T.E., Woodard, H.J., Clay, D.E., Gelderman, R.H., Julson, J.L., and Wei, L. 2011. Interactions of Biochar Source/Properties Impacts on Soil Properties, C Sequestration Potential, and Crop Management (annual report). Sun Grant Initiative – North Central Center at South Dakota State University Annual Meeting. Jan 2011. Orlando, Florida (verified Jan 24, 2011).
6. Clay, S.A. and D.D. Malo. 2011. The Influence of Biochar Production on Herbicide Sorption Characteristics. Chapter in Herbicides/Book 3. ed. M.N. Hasaneen. Intech Rijeka, Croatia. ISBN 9790953-307-729-0 (accepted for publication/in press).

Please complete the following table to reflect your project at completion or time of report submission:

ITEM	NUMBER
Abstracts	**2**
Peer Reviewed Publications	**2**
Outreach Publications/Web Pages	
Professional Presentations	**3**
MS Degrees Conferred	
Ph.D. Degrees Conferred	
MS Students Supported	**1**
Ph.D. Students Supported	**1**
Post-Docs Supported	
Undergraduate Students Supported	**4**
Investigators Supported	**1**
Start-Up Jobs Created (New Grant received based on this project)	**1 (As a partial result of this study we were successful in obtaining a major grant.)**
Disclosures	
Patents Filed	
Provisional Patents	
Patents Issued	
License Agreements	
Plant Variety Protection	

Back to Table of Contents

Sun Grant Initiative
DOE Final Progress Report

Project Title: South Dakota Wind Resource Assessment Network

Project Director/Principal Investigator: Dr. Dennis Todey, Associate Professor/State Climatologist, Department of Agricultural and Biosystems Engineering, South Dakota State University, Brookings, SD

All Co-Principal/Other Investigators: None

Collaborators: None

Period of Performance: 1 September 2009 - 31 December 2011

Funding Awarded: $119,763

Cost Share Amount: $29,606

Cost Share Sources: Time and effort from PI; Black Hills Power

Executive summary

The SD-WRAN (Wind Resource Assessment Network) was a network developed to place instruments on tall towers around the state to support collection of wind data for wind resource support. The first towers were installed in 2003-04. This was a first of its kind network to collect and archive wind data from towers above a 10 m level and provide data at closer to hub heights. Operation of the WRAN was funded for a two year period to continue data collection from existing towers and establish new towers in the state. The main goal was to provide an open data source for wind information for people of the state and provide feasibility of wind turbine development in various areas of South Dakota. This data was being collected by private entities who usually did not share data.

Fifteen different locations collected data during various times from 2004 to 2011. Because this was a cooperative venture, cooperators collected data for varying times during that period.

Four new stations were established in 2011 in conjunction with Windlogics Inc. from Minnesota through a DOE-funded project with NOAA-ERSL labs in Boulder. The South Dakota component was funded to establish new towers and provide data to Windlogics and NOAA to support detailed wind forecasting.

This project was to continue collection of data, archiving of data and attempts to do error checking on data. The effectiveness of this data collection is straight-forward and easily achieved. The economic feasibility was more difficult. Instrumentation such as these is damaged easily by ice during the winter and requires at least annual visits. The health of the network was largely dependent on cooperators assisting with tower climbers. Money was not included for tower climbing support for installing new towers and to maintain older equipment.

For future work this must be included as part of the project and incorporated in the cost structure.

This project was originally granted to Dr. Michael Ropp of SDSU. It was passed on to Dr. Dennis Todey to continue when Dr. Ropp left the university.

Project objective

Task 1: Operation of WRAN

Much of the basis of the project was maintaining data collection for the WRAN project. We maintained data collection on the original towers into 2011. Towers as part of the WRAN were mainly maintained by other entities including East River Electric. At this point several towers had instruments damaged by two fairly severe winters. Data collected from these was collected and archived daily.

The original plan must have relied on the tower operators to help maintain equipment. This was not the case over the long term and caused degradation of the data over time.

Daily data collection was able to continue. The new data installs (next section) were able to convert from a dial-up modem to data loggers from Campbell Scientific and communicate via cell modem. This was necessary for real-time data collection.

Task 2.0 Commissioning of three new WRAN sites.

Through collaboration with Windlogics and NOAA-ESRL the WRAN was able to establish four new sites. These were at Reliance, Long Valley, Faith and Lowry. Wind speed and direction,

temperature and humidity sensors were installed at 60 and 80 m heights on South Dakota Public Broadcasting towers.

Task 3.0 Assist with WRAN-related research projects

Two minor research pieces occurred related to the WRAN, one an attempt to estimate data using surface based data from established relationships and to support the new wind forecasting project with NOAA. The second is still in process, but has shown the ability to improve short term wind forecasts at hub heights.

The original estimating project utilized wind tower data where nearby surface measurements existed. The technique showed promise on individual sites, but was difficult to duplicate success at other sites.

Task 4.0 Project Management and Reporting

Quarterly reports were delivered to the SDSU Sun Grant office. Annual reporting did occur at the South Dakota Wind Energy Association and at Sun Grant meetings. Reporting at two meetings did not occur because of illness.

Project activities

Dr. Todey inherited the following network for the WRAN operation. The towers included some established with WRAN funds. Others were from cooperators. Data was collected from these towers for varying times from 2004-2011. Data are archived at http://climate.sdstate.edu/wran

Ms. Joanne Anderson, an MS student worked on relating surface wind data to tall tower data using various surface measurements. Initial results showed some promise. These are shown in the next figure for one location located near a surface weather stations where comparisons could occur. Winds estimated from surface data Wcoxbox compared favorably with actual measured wind Wws50. Comparisons here showed promise. But the lack of widespread surface stations across the state to develop relationships and the interaction needed to develop relationships at different locations and times of year limited the use of this technique.

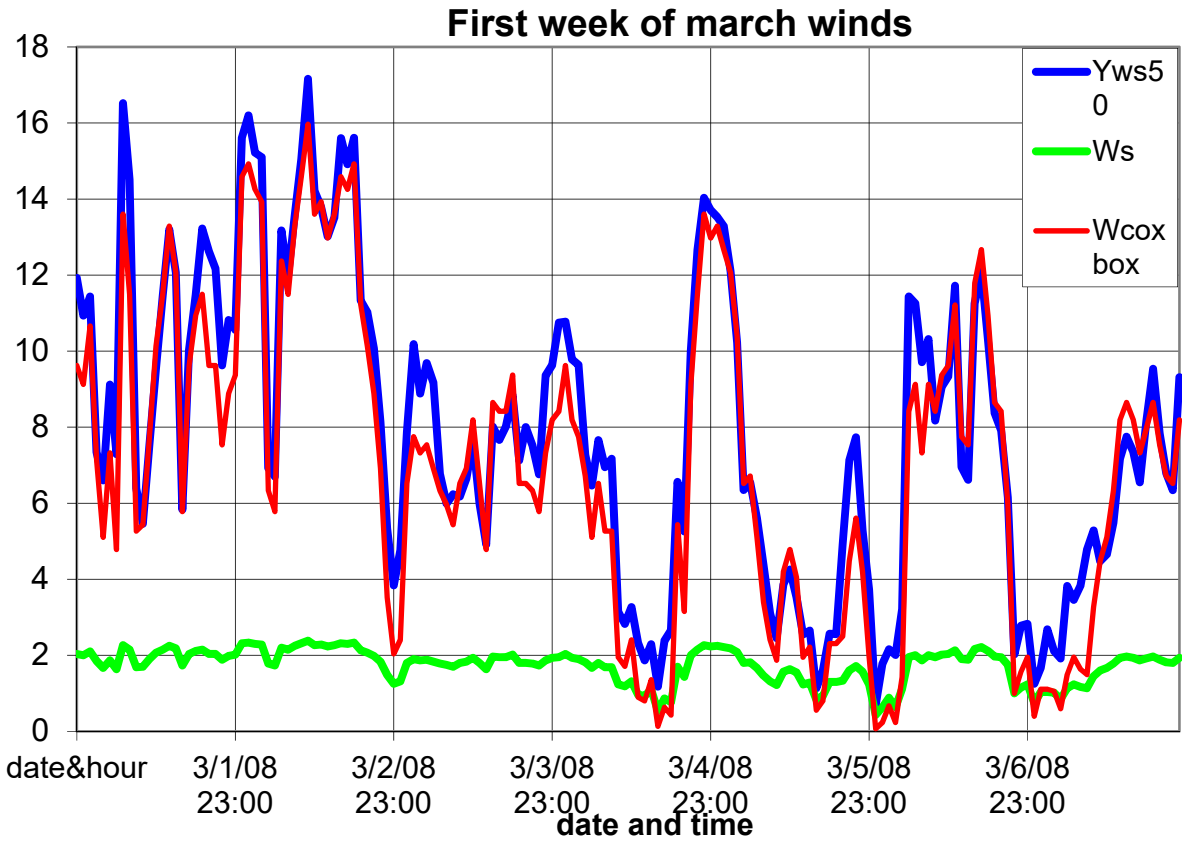

New towers were established at four locations listed below in conjunction with NOAA-ESRL and Windlogics.

TOWN	BASE - AMSL Feet/Meters	TOP - AMSL Feet/Meters	REGISTERED COORDINATES	REGISTERED COORDINATES
			NAD 27	NAD-83
Faith	2615'/797.05m	4311'/1313.99m	45/03/14 102/15/47	45/03/14 102/15/49
Longvalley	3098'/944.27m	3751'/1143.30m	43/25/59 101/33/16	43/25/59 101/33/18
Lowry	2175'/662.94m	3001'/914.70m	45/16/38 99/59/10	45/16/38 99/59/11
Reliance	2059'/627.58m	3385'/1031.75m	43/58/05 99/35/40	43/58/05 99/35/41

Data are collected every hour (which includes data every 10 minutes). These are pushed via SCP to NOAA every hour. Transfer files are around 50K per hour.

Data collection is still occurring and being forwarded to NOAA. The modeling comparisons are also ongoing and showing promise. The following figure shows and example of a wind comparison from SDSU tower data and forecast wind data from the NOAA Rapid Refresh model.

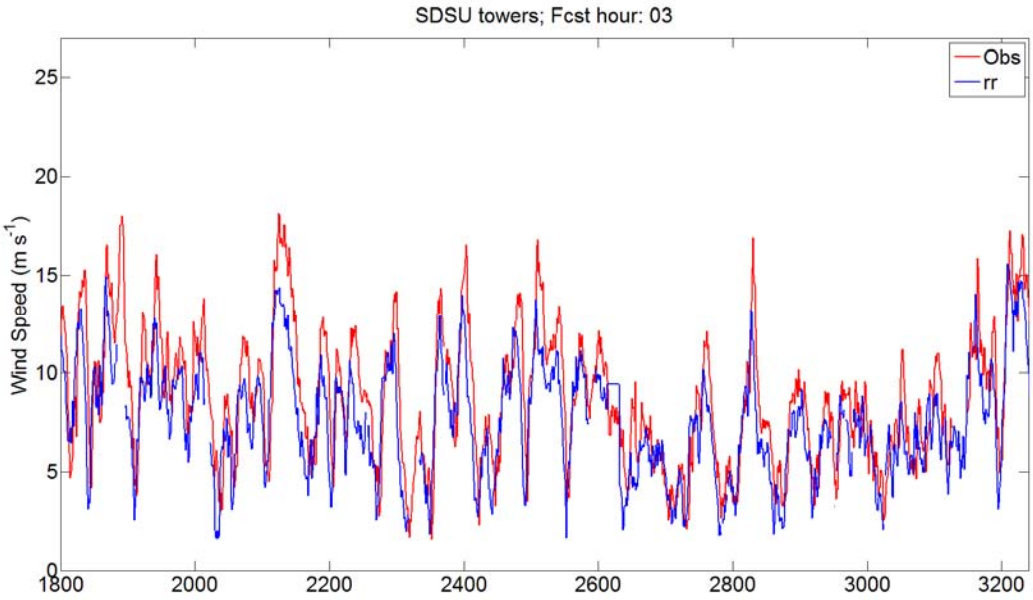

Full results are still pending and could be reported at a future date as an ongoing outcome from the DOE project.

The initial inherited plan which did not have ongoing operational costs included did cause a problem. Damage done to sensors on towers particularly in the winter degraded sensor quality over time. In future projects such as this, annual maintenance visits must be included for data quality to be maintained. Costs will increase because of the tower climber cost. But it is a necessary inclusion for success of data quality.

During the latter part of the project a cooperator who was providing tower climbers (East River Electric) decided to remove instruments and end maintenance. Data was useful, but the overall longevity of thr project was limited because of this.

Products developed under the award:

a. Publications (list title, year, journal name, volume, issue, and page numbers), conference papers (name of conference; location of conference; date of conference; and conference sponsor), or other public releases or outreaches of results.

Conferences

Review of annual trends of atmospheric thermal inversions in South Dakota utilizing NWS radiosonde and WRAN data. South Dakota Academy of Science Annual Meeting, Vermillion, SD 14 April 2012, South Dakota Academy of Science.

South Dakota WRAN Update, South Dakota Wind Energy Association Annual Meeting, Mitchell, SD, 30 November 2010. South Dakota Wind Energy Association.

b. Website or other Internet sites that reflect the results of this project.

Data collected as part of the project were archived on the South Dakota State Climate site. The archive of this data is available at:
http://climate.sdstate.edu/wran

c. Networks or collaborations fostered.

Through this project SDSU and the state climate office developed collaborations with several other universities and companies.

- SDSMT Institute of Atmospheric Science
- NOAA ESRL wind energy modeling group
- Windlogics
- East River Electric (South Dakota)
- Renewable Solutions (renewable energy company)

d. Technologies/techniques.
e. Inventions/patent applications, licensing agreements.

f. Other products, such as data or databases, physical collections, audio or video, software* or Netware, model, educational aid or curricula, instruments, or equipment.

Data collected as part of the project were archived on the South Dakota State Climate site. The archive of this data is available at:
http://climate.sdstate.edu/wran

1. Academic

a. Courses developed
b. M.S. students supported
Ms. Joanne Anderson – degree not completed
c. M.S. degrees conferred
d. Ph.D. students supported
e. Ph.D. degrees conferred
f. Post-docs supported
Three undergraduate students contributed to the computing and equipment deployment of the project.

2. For projects involving computer modeling, provide the following information with the final report: N/A

a. Model description, key assumptions, version, source, and intended use.
b. Performance material for the model related to the intended use.
c. Test results to demonstrate the model performance criteria were met (e.g., code verification/validation, sensitivity analyses, history matching with lab or field data, as appropriate).

d. Theory behind the model, expressed in non-mathematical terms.
e. Mathematics to be used, including formulas and calculation methods.
f. Whether or not the theory and mathematical algorithms were peer reviewed, and, if so, will include a summary of the theoretical strengths and weaknesses.
g. Hardware requirements.
h. Documentation (e.g., user's guide, model code).

***Software/Manual (if applicable)**

Content. Unless otherwise specified in the award, the following must be delivered: source code, the executable object code and the minimum support documentation needed by a competent user to understand and use the software and to be able to modify the software in subsequent development efforts.

Back to Table of Contents

Sun Grant Initiative
DOE Final Progress Report

Project Title: Seed Technologies to Secure Rapid and Complete Switchgrass Establishment

Project Director/Principal Investigator: Brian Baldwin, Professor, Plant Sciences, Department of Plant & Soil Sciences, Mississippi State University, Mississippi State, MS

All Co-Principal/Other Investigators: Vance Owens, Professor of Plant Science, Department of Plant Sciences, SDSU Brookings, SD; Ken Moore, Professor of Agronomy , Department of Crops Sciences Iowa State, Ames, IA; Alan Taylor, Professor of Seed Technology, Department of Horticulture, Cornell @ Geneva, Geneva, NY; John Fike, Associate Professor Crops, Department of Crops and Environmental Soil Sciences, Virginia Tech., Blacksburg, VI.

Collaborators: J. Brett Rushing, RA III, Department of Plant & Soil Sciences, Mississippi State University, Mississippi State, MS; Denise Dulclos, Post-Doc, Department of Horticulture, Cornell University, Ithaca, NY

Period of Performance: 1 July 2010 – 31 December 2012

Funding Awarded: $378,049

Cost Share Amount: $94,512

Cost Share Sources: Time and effort from PIs and CoPIs; Indirect on time and effort

Executive Summary

Switchgrass is a wild grass native to North America that has the potential to be an important raw product for the future production of fuel. To grow enough switchgrass, large tracts of land will need to be planted. However, two issues plague seedling establishment: erratic germination of the seed due to an internal sleeping mechanism of live seed (known as seed dormancy), and slow initial growth of the seedlings makes weed competition a problem. To alleviate these problems, this two year study will look at the causes of seed dormancy and explore seed treatments to awaken the seed, so immediate germination occurs when the seed is planted. To enhance the ability of seedlings to compete after germination, we will treat the seed with a known herbicide antidote. By doing this, only the antidote-treated seed will be able to germinate and grow in a field treated with that herbicide. However, the antidote in large amounts is also toxic to the seedlings, so it must be delivered in a dose that won't kill the switchgrass. Polymer-coating, encapsulating the antidote, may offer a time-released, reliable dose. Both of these methods combine will make switchgrass establishment an easier and more reliable process. Results from these experiments indicate that the seed soak method was easier and more reliable than the polymer coatings. The seed treated with the safener treatment can't be stored for longer than 2½ months before germination declines due to the treatment. Seed dormancy can be ameliorated by breeding for non-dormancy (as in the cultivar, Expresso) or in commercially available seed lots by seed priming. Additionally findings would indicate that switchgrass should be planted on stale seedbed or killed pasture. Attempts to plant on recently tilled ground were less successful. The high level of non-dormancy observed in Expresso switchgrass is due to a natural (selected for) fracturing of the seedcoat as the seed matures.

Project Objectives

Part I – Seed Dormancy. Replicated germination tests will be conducted in the lab at 30°C in the dark. Germination is rapid under these conditions and tests can be completed in 7 days. Seed lot viability will be determined by tetrazoilum testing as routinely used by Seed Testing Laboratories. Cornell's effort in 2010 was focused on two projects: 1) treat four switchgrass varieties with a herbicide safener for the field trials and 2) investigate seed dormancy in four switchgrass varieties. The research was conducted on 4 switchgrass varieties: Trailblazer, Cave in Rock, Kanlow and Alamo.

Seed treatments with herbicide safener

Seed lots were obtained by MSU of the 4 varieties for field trials; information regarding source and quality of seed is included in Table 1. All lots were exposed to a moist chilling treatment (stratification) for 79 days to break dormancy and this was conducted at MSU. Next the stratified seeds were dried and then shipped to Cornell. Prior to seed treatment application, Cornell brushed all seed lots with a Westrup LAH seed conditioning equipment to remove all glumes. The New York State Seed Testing Laboratory conducted purity and germination tests according to standard procedures established by the AOSA (Assoc. Official Seed Analysts). Samples were treated with Thiram 50WP at the labeled rate (8 oz/cwt) to reduce microbial growth in the germination tests.

Table 1. Switchgrass seed information used in the herbicide safeners trial.

Variety	Seed Lot	Source	Germination	Dormancy	Pure live seed
			---------- % ----------		
Trailblazer	SWZ-4050	Sharp Bros.	87	5	92
Cave-in-Rock	02-08	Ernst	79	2	81
Kanlow	FFC6098	Ernst	51	3	54
Alamo	WB-07 MVIA	Ernst	26	1	27

The percent germination and PLS were acceptable for Trailblazer and Cave-in-Rock, while Kanlow and especially Alamo was poor. However, the seed labels stated that the percent PLS for Kanlow and Alamo were 68 and 80%, respectively. There were 2 methods of applying the herbicide safener, Concep III (fluxofenin): 1) coating by seed encrusting at Cornell and 2) controlled hydration at MSU. Film coating was conducted using a lab-scale rotary pan coater (R-6, Germains) and commercial binder (L 1803, Bayer CropSciences) and filler material (MJJ-10, Coating Supply Inc.). The controlled hydration was conducted at MSU by adding a specified amount of liquid to a given weight, so that the seeds imbibed all the water. For both seed treatment methods, Gaucho XT (a formulation of imidacloprid, metalaxyl and tebuconazole) was applied at a labeled rate of 3.4 fl oz/cwt. Fluxofenin was applied in a dosage study at 0, 10, 20 and 40 mg ai/100 g seed. The encrusted, treated seeds were shipped to MSU for distribution to field investigators.

Seed dormancy investigations

Seed dormancy in switchgrass is classified as non-deep, physiological dormancy. There are two components to physiological dormancy: embryo dormancy and the negative effect of seed covering layers on germination. Based on earlier research by Dr. Denise Duclos in Dr. Taylor's lab, the seed-covering layer that has the greatest effect is the pericarp in comparison with the lemma or palea. The pericarp was also the key seed-covering layer in the 4 varieties examined in the project. The primary focus of this report is on embryo dormancy and the effect of temperature and plant hormones on germination and breaking dormancy.

The first objective was to obtain good quality seed lots expressing dormancy for further laboratory investigations on seed dormancy (Table 2). Germination tests were conducted by placing seeds on moist blotters and providing a controlled temperature environment. The first germination test protocol followed the AOSA procedures of 30/15ºC, of 8 hours with light at 30ºC and 16 hours in dark at 15ºC. Preliminary tests were performed on several lots from different sources and germination data on the 4 selected seed lots is shown below. In addition to the 4 seed lots, Expresso, a variety selected for low dormancy by Brian Baldwin at Mississippi State University was tested.

Table 2. Switchgrass seed information used in the seed dormancy trial.

Variety	Seed Lot	Source	Germination	Dormancy	Pure live seed
			---------- % ----------		
Trailblazer	SWZ-4050	Sharp Bros.	79	18	3
Cave-in-Rock	SWR-4024	Sharp Bros.	86	11	3
Kanlow	QP02240	Applewood	60	17	23
Alamo	19-09DN	Ernst	74	14	12
Expresso		Brian Baldwin	91	0	9

The only seed lot that was used for both the field and lab studies was Trailblazer. However, a new sample of Trailblazer was obtained from the seed company that was not stratified. The Expresso lot had exceptional seed quality with no dormancy and 91% germination.

A germination stress test was developed to induce seed dormancy by placing seeds at 30ºC with an 8-hour photoperiod. Several other treatments were also tested by moistening the blotters with solutions of plant hormones (GA and ABA) and the plant growth regulator, fluridone. Gibberellic acid (GA3) is the primary stimulus for germination, while abscisic acid (ABA) blocks germination. Fluridone acts as an ABA biosynthesis inhibitor by blocking an enzyme in the carotenoid biosynthesis pathway. Only data on the promotive effects of GA is summarized below for the 4 varieties (Table 3). Expresso had 87% germination at 30ºC so plant hormones were not tested as the germination was excellent under both optimal and stress conditions.

Table 3. Switchgrass germination trial of four varieties under different temperatures and with or without gibberellic acid (GA).				
	30/15ºC day/night temperature		30ºC constant temperature	
Variety	Control	GA	Control	GA
	---------- % germination ----------			
Trailblazer	75	89	9	61
Cave-in-Rock	77	96	13	53
Kanlow	52	60	6	52
Alamo	71	76	14	59
Average	69	80	10	56

There are two main conclusions from the temperature and plant hormone study. The stress temperature of 30ºC induces dormancy in all seed lots and the mean germination decreased from 69% for the 30/15ºC regime to 10% for the 30ºC constant. GA increased the percent germination under both optimal temperatures and at the stress temperature. The GA concentration used was 2 mM for the Trailblazer and Cave-in-Rock, while 1 mM GA was optimal for Kanlow and Alamo. Trailblazer and Cave-in-Rock are both upland varieties, and Kanlow and Alamo are lowland varieties.

Other research on seed dormancy

The recommended procedure by the AOSA is for light with the 8-hour 30☜C period and dark for the 16 hour 15ºC period. Our research revealed that light is not needed for switchgrass germination. This conclusion was supported that germination results were not significantly different at 30/15ºC or 30ºC with or without light. Seed morphology studies are in progress at the light microscope level.

Shelf-life and Concep III phytoxicity on four switchgrass varieties:

The first objective was to obtain commercial seed lots of Trailblazer, Cave-in-Rock, Kanlow and Alamo for field and laboratory research in 2011. Seed lots were obtained from four companies and germination testing conducted at the New York State Seed Testing Laboratory under the supervision of Dr. Taylor. Germination tests were conducted by placing seeds on moist blotters, and providing a controlled temperature environment. The temperature regime of 30/15˚C with 30˚C for 8 hours with light at and 16 hours in dark at 15˚C was adapted from the AOSA Rules for Testing Seeds. Seed lots of each variety with the greatest percent germination were used for further research. Seeds of each lot were aged at 30˚C and 50% relative humidity to simulate long-term storage. This combination of temperature and relative humidity would deteriorate seed quality in less than a half year, and would be more harsh than seed storage in common storage by a seed company or farmer. Therefore, the time frame of storage is reduced from a few years to several months.

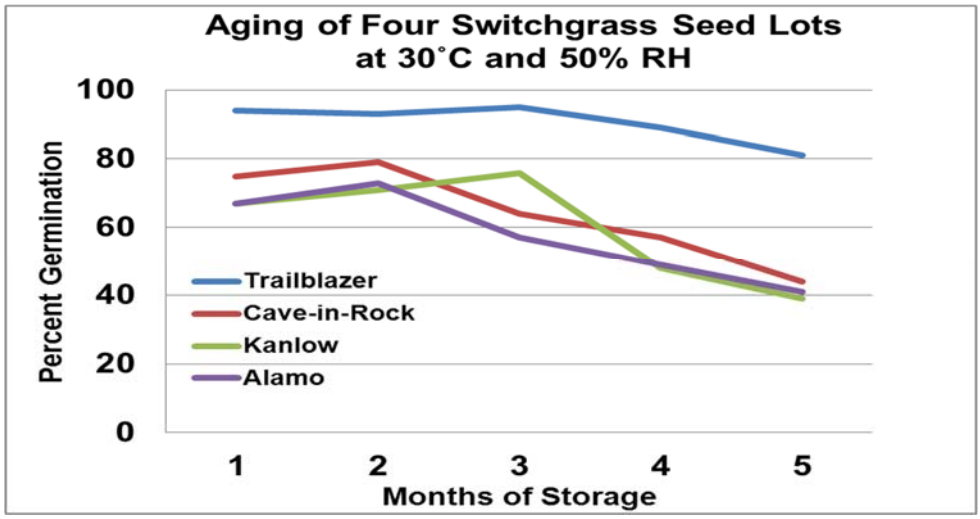

Fig. 1. Effect of storage conditions and time on germination of four switchgrass varieties.

Trailblazer had a higher germination compared to Cave-in-Rock, Kanlow and Alamo. Aging seeds for a 5-month period significantly decreased germination, and the high quality Trailblazer seed lot was more tolerant to aging as illustrated by a smaller percentage point decline in germination compared to the other lots.

Non-aged seeds of each variety were treated with Concep III at 0, 10, 20 and 40 mg active ingredient of fluxofenin per 100 grams of seeds at Cornell using rotary pan seed treatment technology. Mississippi State University treated samples with the same rates of Concep III via a controlled hydration method. Eight treatments of four varieties were aged as described above for five months. Trailblazer had a higher percent germination (main effect) compared with the other varieties. No significant differences were measured between seed treatments. Therefore, there is no evidence of phytotoxicity of Concep III on switchgrass seeds.

Germination of 5-month aged seeds that were treated by two methods (Seed Trt. at Cornell and Controlled Hydration at MSU) and with 4 rates of Concep III.

Develop methods to break switchgrass seed dormancy

Seed dormancy in switchgrass is classified as non-deep, physiological dormancy. There are two components to physiological dormancy: embryo dormancy and the negative effect of seed covering layers on germination. Previous quarterly reports documented several dormancy breaking methods resulting in little or inconsistent efficacy. In an attempt to break embryo dormancy, plant growth regulators termed karrikins, in particular KAR-1 was not effective on switchgrass. Imbibing seeds on blotters with dilute concentration of hydrogen peroxide was ineffective in breaking embryo dormancy. Seed scarification was investigated to alter the seed covering layer integrity and thus break dormancy. Our research revealed that scarification treatments could help overcome dormancy (Table 4). However, there is a very fine line

between treatments being positive (promotional) and negative (harmful). Therefore, the risk/benefit ratio does not appear favorable for commercial use based on our research.

Table 4. Effect of various seed treatments on switchgrass seed dormancy.

		Percent Germination				
Treatment Method	Concep III (mg ai/100 g)	Trailblazer	Cave-in-Rock	Kanlow	Alamo	Treatment Mean
Seed Trt.	0	84	37	37	34	**48 a**
Seed Trt.	10	82	45	47	35	**52 a**
Seed Trt.	20	87	41	47	40	**54 a**
Seed Trt.	40	83	43	45	38	**52 a**
Hydration	0	90	55	32	42	**55 a**
Hydration	10	81	48	41	44	**54 a**
Hydration	20	84	52	29	34	**50 a**
Hydration	40	71	49	29	29	**45 a**
Means		**83 a**	**46 b**	**38 b**	**37 b**	

Our focus was then directed to methods that could be conducted by the seed industry and thus scale-up of the technology would be rapid. Cornell partnered with a California based company, Seed Dynamics that specializes in seed enhancement technologies, in particular seed priming. This company commercially primes lettuce seeds to overcome thermo-dormancy and photo-dormancy.

Kanlow and Cave-in-Rock seeds were primed by Seed Dynamics and returned to Cornell for germination testing. Germination testing was performed under a stressful environment of 28 or 30˚C, a condition that will induce dormancy in switchgrass. Germination was greatly improved in both seed lots with seed priming.

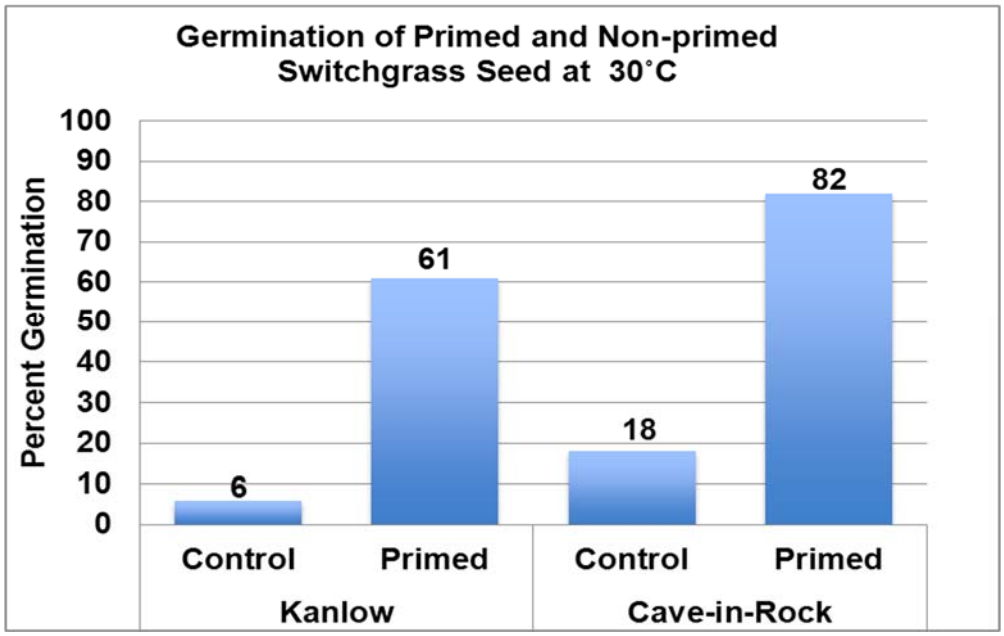

Fig. 2. Germination of Kanlow and Cave-In-Rock switchgrass seed after priming seed by storing at 30ºC.

Part II - Field Testing Safened Seed. There was extreme variance in seedling establishment within the fluxofenin/metolochlor (safener/herbicide, respectively) plots during preliminary testing in 2008 by Rushing (2009). The potential of seed polymer coating as a method to ensure complete and stable coverage of individual seed with fluxofenin was being investigated. Working with Dr. Alan Taylor,

Cornell University at Geneva, this two year evaluation would compare four switchgrass cultivars treated with six fluxofenin treatments (Tables 5 and 6). These tests would be located at Iowa State (Cave-in-Rock; Ken Moore), Mississippi State (Alamo; Brian Baldwin), South Dakota State (Trailblazer; Vance Owens), and Virginia Tech (Kanlow; John Fike) in 2010 -2011. Stratified seed lots of the four cultivars (mentioned above), obtained from Ernst Conservation Seed (Meadville PA), will be planted at each of the four locations. Nine treatments for each cultivar will be evaluated at each location. Emergence, weed control and first and second year yields will be assessed.

Table 5. Treatments for the 2010 and 2011 field trials consisting of controls, rates of safener, fungicide, and location of application.

Treatment	Coating Method	Safener (mg ai/100 g seed)§	Fungicide (g ai/g seed)
1	Polymer brush coating†	no safener/no herbicide	0.19
2	Polymer brush coating	no safener	0.19
3	Polymer brush coating	10	0.19
4	Polymer brush coating	20	0.19
5	Polymer brush coating	40	0.19
6	Seed soak‡	no safener	0.19
7	Seed soak	10	0.19
8	Seed soak	20	0.19
9	Seed soak	40	0.19

†Cornell University, Horticulture Sciences, 630 W. North Street, Geneva, NY 14456

Table 6. Seed characteristics for the lots used in the 2010 and 2011 field trials accessing the antidotal effects of the safener fluxofenim against metolachlor herbicide.

Variety	Commercial Source	2010			
		Origin	Pure Seed	Germination	Dormant
			---------- % ----------		
'Kanlow'	Ernst Seeds†	KS	93.40	66.50	1.75
'Trailblazer'	Sharp Bros. Seed Co.‡	KS	99.96	4.00	93.00
'Cave-in-Rock'	Ernst Seeds	PA	99.28	64.00	23.00
'Alamo'	Ernst Seeds	OK	87.51	10.00	70.00
		2011			
'Kanlow'	Ernst Seeds	NC	89.70	91.00	0.00
'Trailblazer'	Sharp Bros. Seed Co.	KS	99.96	4.00	93.00
'Cave-in-Rock'	Ernst Seeds	PA	99.30	6.00	79.00
'Alamo'	Ernst Seeds	MO	99.54	88.00	5.00

† Ernst Conservation Seeds, 9006 Mercer Pike, Meadville, PA 16335
‡ Sharp Bros. Seed Co., 1005 S. Sycamore, Healy, Kansas 67850

Interaction of year by all treatments made separation of the data by year necessary.

Year 2010 Field Trial

Three of the four sites experienced successful establishment for the 2010 growing season. Extreme flooding following planting at Brookings, SD moved seed and soil outside treatment locations. Crown counts and end of season harvests were not conducted at this location. Broadleaf weed species, specifically Palmer amaranth (*Amaranthus palmeri* S. Watson) were reported problematic later on in the season at Blacksburg, VA once herbicide residual had worn off. Slim amaranth (*Amaranthus hybridus* L.) and horseweed (*Conyza canadensis* L. Cronquist) were problematic at the Ames, IA site. These weeds were eventually controlled using 2,4-D amine. Season long weed control of grasses was experienced at all locations except for control plots. Herbicide residual efficacy and canopy closure provided excellent conditions for switchgrass tillering and maturation.

Significant differences were observed in 2010 by variety (LSD = 5.65). Germination rate did not necessarily correlate with establishment. 'Cave-in-Rock' had the highest number of crowns per plot with 25.42 across all sites and treatments, but had the second highest germination percentage with 64.00% (Table 7).

Table 7. Mean number of crowns per row for each treatment for the 2010 field trial.

Treatment*	Mean Number of Crowns per Row			
	Ames, IA	Blacksburg, VA	Brookings, SD	Starkville, MS
1	34.5 B†	20.1 AB	---‡	30.4 A
2	19.6 C	12.7 B	---	6.2 C
3	19.1 C	12.6 B	---	3.9 C
4	19.2 C	14.6 B	---	3.4 C
5	34.9 B	20.0 AB	---	7.0 C
6	23.8 BC	11.4 B	---	0.6 C
7	53.4 A	33.3 A	---	27.5 AB
8	56.9 A	24.3 AB	---	28.5 AB
9	53.5 A	20.7 AB	---	23.1 B

* Treatment code from Table 2

†Letter following mean number of seedlings denotes differences between means within a column (treatment effects). Means were separated by LSD at $p \leq 0.05$.

‡Brookings, SD site not harvested in 2010 due to extreme flooding following establishment.

End of Season Crown Counts.

Significant differences were experienced for each location (Table 4). For Ames, IA (LSD = 13.991), treatments 7, 8, and 9 (MSU seed soaks with safener and fungicide) had significantly more mean number of crowns per plot for all switchgrass varieties than all other treatments (53.4, 56.9, and 53.5, respectively). For the Starkville, MS location (LSD = 7.206), treatments 1, 8, and 7 had significantly more crowns per row for all switchgrass varieties than all other treatments. The Blacksburg, VA site (LSD = 14.48) was similar to the Ames and Starkville location with treatments 1, 5, 7, 8, and 9 having 20.10, 20.00, 33.30, 24.35, and 20.70 crowns per plot, respectively. In terms of location interaction, the Ames, IA site had the greatest number of crowns per plot across all varieties and treatments with 35.02 crowns per plot.

For safener application comparison, the seed soak outperformed the brush technique by producing significantly more crowns per plot across all treatments, varieties, and locations with 26.47 crowns per plot for the seed soak and 17.74 for the brush technique (LSD = 3.9024).

End of Season Yield.

As with crown counts, significant differences were observed for end of season dry matter yields (Table 8). The treatments with the greatest number of crowns typically had the highest yields. For Ames, IA (LSD = 0.163), treatments 7, 8, and 9 had the greatest tonnage compared to all other treatments (1.29, 1.30, and 1.21 Mg/ha, respectively). At the Starkville, MS site (LSD = 0.4336), treatments 1, 7, 8, and 9 yielded more than all other treatments with 2.21, 2.39, 2.00, and 1.50 Mg/ha, respectively. For the Blacksburg, VA location (LSD = 1.2781), treatments 4, 5, 7, 8, and 9 had greater yields than all other treatments with treatment 7 having the highest yield with 4.16 Mg/ha.

For overall comparison between the two safener techniques, the seed soak was responsible for significantly higher yields across all locations, treatments, and varieties with 1.58 Mg/ha compared to 0.90 Mg/ha for the brush technique (LSD = 0.2173).

Table 8. Mean end of season yield per treatment for the 2010 field trial.

Treatment*	Mean End of Season Yield (Mg/ha)			
	Ames, IA	Blacksburg, VA	Brookings, SD	Starkville, MS
1	0.89 CD†	0.57 B	---‡	2.21 A
2	0.59 D	1.17 B	---	0.36 C
3	0.62 D	0.64 B	---	0.26 C
4	0.67 D	1.77 AB	---	0.33 C
5	0.93 BCD	1.68 AB	---	0.84 BC
6	0.79 D	0.61 B	---	0.03 C
7	1.29 AB	1.08 A	---	2.39 A
8	1.30 A	1.96 AB	---	2.00 A
9	1.21 ABC	1.75 AB	---	1.50 AB
LSD	0.16	1.27	---	0.43

* Treatment code from Table 2

†Letter following mean number of seedlings denotes differences between means within a column (treatment effects). Means were separated by LSD at $p \leq 0.05$.

‡Brookings, SD site not harvested in 2010 due to extreme flooding following establishment.

Year 2011 Field Trial

As with the 2010 season, all sites did not experience successful establishment. The Starkville, MS encountered extremely dry conditions during planting where subsequent irrigation efforts flooded the seed into adjacent plots and herbicide activation was released into control entries. Therefore, replanting was conducted only for treatments 6-9 (seed availability prevented other treatments from being incorporated into the trial) in an adjacent plot and data was collected for only these treatments at the Starkville, MS location. The Brookings, SD site experienced another unseasonably high amount of precipitation following establishment. This allowed for crown counts (prior to harvesting), but not enough biomass had accumulated to justify harvesting the plots.

For the 2010 establishment, significant differences were observed by variety (LSD = 1.6646). ‘Cave-in-Rock’ and ‘Kanlow’ had significantly more crowns per row at all locations over all treatments with 12.29 and 11.42 crowns, respectively. However, the germination percentages for these lots were 6.00% for ‘Cave-in-Rock’ and 91.00% for ‘Kanlow’ (Table 1)

End of Season Crown Counts.

The Ames, IA location (LSD = 3.6628) observed results similar to that of the 2010 season with the top 3 treatments being 7, 8 and 9 (Table 9). However, treatment 9 had significantly more crowns per plot for all switchgrass varieties than all other treatments with 18.81. As previously stated, the Starkville,

MS site (LSD = 7.4719) only recorded data for treatments 6-9. In that case, treatments 7 and 9 had significantly more crowns per plot (24.00 and 31.12, respectively) than the other two treatments. For the Brookings, SD location (LSD = 1.828), treatments 5, 7, 8 and 9 had more crowns per plot than all other treatments with treatment 9 having the most with 6.25. The Blacksburg, VA, like Ames, had results similar to that of the 2010 season. Treatments 1, 5, 7, and 8 had more crowns per plot for all varieties than all other treatments.

To compare safener application methods, the seed soak method had significantly more crowns per plot across all varieties and treatments for all locations with 14.02 versus 7.63 for the brush technique (LSD = 1.1544).

Table 9. Mean number of crowns per row for each treatment for the 2011 field trial.

Treatment*	Mean Number of Crowns per Row			
	Ames, IA	Blacksburg, VA	Brookings, SD	Starkville, MS
1	6.0 C†	18.0 A	2.4 C	---‡
2	5.4 C	10.1 D	3.5 BC	---
3	6.0 C	11.2 CD	3.6 BC	---
4	7.2 C	9.9 D	2.8 C	---
5	7.8 C	14.7 ABC	5.2 AB	---
6	4.5 C	10.3 D	3.1 C	18.5 B
7	12.8 B	13.7 ABCD	6.2 A	24.0 AB
8	15.1 B	17.4 AB	5.6 A	23.8 AB
9	18.8 A	13.2 BCD	5.6 A	31.1 A

* Treatment code from Table 2

†Letter following mean number of seedlings denotes differences between means within a column (treatment effects). Means were separated by LSD at $p \leq 0.05$.

‡Starkville, MS experienced drought during establishment, and due to seed availability, only treatments 6-9 were replanted.

End of Season Yield.

The Ames, IA site (LSD = 0.0459) recorded treatment 9 as having the greatest dry matter yields with 0.43 Mg/ha (Table 10). For the Starkville, MS location (LSD = 0.7885), treatments 7, 8, and 9 were significantly greater in yield than treatment 6 with 5.10, 4.53, and 5.50 Mg/ha, respectively. Blacksburg, VA observed no significant differences in end of season dry matter yields for the 2011 season.
The seed soak method again outcompeted the brush technique for overall yield with the seed soak generating 1.86 Mg/ha, which was significantly more than the brush method with 0.38 Mg/ha.

Table 10. Mean end of season yield per treatment for the 2011 field trial.

Treatment*	Mean End of Season Yield (Mg/ha)			
	Ames, IA	Blacksburg, VA	Brookings, SD	Starkville, MS
1	0.07 C	0.61 A	---‡	---§
2	0.09 C	0.76 A	---	---
3	0.08 C	0.72 A	---	---
4	0.12 C	0.68 A	---	---
5	0.15 C	0.49 A	---	---
6	0.08 C	0.49 A	---	3.51 B
7	0.29 B	0.77 A	---	5.12 AB
8	0.29 B	0.61 A	---	4.53 AB
9	0.43 A	0.68 A	---	5.50 A

* Treatment code from Table 2

†Letter following mean number of seedlings denotes differences between means within a column (treatment effects). Means were separated by LSD at $p \leq 0.05$.

‡Brookings, SD experienced extreme flooding following establishment, therefore lack of biomass accumulation did not justify end of season harvest.

§Starkville, MS experienced drought during establishment, and due to seed availability, only treatments 6-9 were replanted.

Project Activities

Part I – Seed Dormancy

In summary, switchgrass seed quality of commercial seed lots varies tremendously and a standard germination test should be conducted to validate information on the label. Seed testing was conducted at the New York State Seed Testing Laboratory on more than 10 seed lots from four seed companies of the four varieties used in this project in 2011: Trailblazer, Cave-in-Rock, Kanlow and Alamo. Only one seed lot had high seed quality, defined as having germination percentage in the 90's. Therefore, obtaining a high quality switchgrass lot is the exception and not the rule as found in most agronomic and vegetable crop seeds. Therefore, the switchgrass seed industry has the potential to make significant improvements in the future.

Priming is a value-added technology and was demonstrated to break switchgrass dormancy under stress conditions. The enhancement due to seed priming is greatest with high quality seed lots, and seed companies that commercially prime seed would expect a minimum of 85% germination under stress conditions. Our results with priming again emphasizes the need for high quality seed lots to help secure rapid and complete switchgrass establishment.

Part II- Field Testing, Safened Seed

Results from the 2010 and 2011 field trials indicate that overall, the seed soak technique of safener application to switchgrass produced higher number of crowns, and thus higher biomass yields for all varieties at all locations when compared to the brush technique. It is common agricultural knowledge that higher establishment success by the removal of weed competition produces higher yields.

Pre-emergence applications of metolachlor did not cause any injury to developing switchgrass seedlings. The safener provided complete protection against the herbicide. Switchgrass seed protected with safener significantly established and yielded more than unprotected seed. CAS 88485-37-4 at rates of 10 to 40 mg ai/100 g of seed adequately protected switchgrass from the recommended rate of metolachlor, 1.06 kg ai/ha, for fine textured soils. The seed soak method did not adversely affect switchgrass yield, even at the highest level of 40 mg ai/100 g seed (treatment 9; Ellis et al. 1980).

The use of CAS 88485-37-4 (fluxofenim) as a seed safener for switchgrass has proven to be a successful option for establishment. The combination of fluxofenim at the recommended rate (0.4g / kg of seed), metolachlor, and high quality, high germinating seed can be a viable option for switchgrass monocultures. The use of metolachlor in controlling weeds for the first few months of establishment will enable land managers to obtain first year harvests for this biomass crop, which to this point has predominantly been a deterrent to planting.

Products developed under the award

Publications

- Manuscript for Agron J. is complete and going through internal review on the collaborative field effort.

- Rushing, J. Brett. Techniques to aid in establishing switchgrass from seed. M.Sc. Mississippi State Univ. Plant and Soil Sci. Dec. 2009.

- Duclos V.D., D. T. Ray, A. G. Taylor. 2009. Understanding the physiology and mechanisms of seed dormancy in Switchgrass (*Panicum virgatum* L.). Association of the Advancement for Industrial Crops 21st Annual Meeting, Chillán, Chile. p 30.

- Taylor, A. G. 2011. Challenges in seed germination and dormancy for new industrial crops. 23rd Annual meeting of the Association for the Advancement of Industrial Crops. Fargo, ND, September 12, 2011. p 22.

- Rushing, J.B., B. Baldwin and A. Taylor. 2010. Seed safening for use in switchgrass establishment. Seventh Eastern Native Grass Symp. Knoxville, TN. Oct 5-8.

- Rushing, B., B. Baldwin, A. Taylor. 2010. Seed safening for use in switchgrass establishment. MSU Biofuels Conference. Jackson, MS. 11-13 Aug.

Website or other Internet sites that reflect the results of this project.
Networks or collaborations fostered.

- Have increased interaction between researchers in NC region and SE region Boe, Johnson, Owens, with Baldwin, Rushing, respectively. Same for SE and NE region (Baldwin and Taylor, respectively)

- John Fike (Vir. Tec) reports closer ties have developed to SDSU (Owens) and MSU (Baldwin)

Technologies/techniques.

- Safening of switchgrass seed through controlled hydration is a viable and highly successful method of ensuring establishment. A major conclusion is never to plant switchgrass on tilled ground.

1. Academic

a. Courses developed
b. M.S. students supported
- Mitch Holmberg

c. M.S. degrees conferred
- J. Brett Rushing, Miss. State Univ. Dec 2009

d. Ph.D. students supported
- J. Brett Rushing

e. Ph.D. degrees conferred

f. Post-docs supported
- Denise Duclos

2. For projects involving computer modeling, provide the following information with the final report:

- **a.** Model description, key assumptions, version, source, and intended use.
- **b.** Performance material for the model related to the intended use.
- **c.** Test results to demonstrate the model performance criteria were met (e.g., code verification/validation, sensitivity analyses, history matching with lab or field data, as appropriate).
- **d.** Theory behind the model, expressed in non-mathematical terms.
- **e.** Mathematics to be used, including formulas and calculation methods.
- **f.** Whether or not the theory and mathematical algorithms were peer reviewed, and, if so, will include a summary of the theoretical strengths and weaknesses.
- **g.** Hardware requirements.
- **h.** Documentation (e.g., user's guide, model code).

***Software/Manual (if applicable)**

Content. Unless otherwise specified in the award, the following must be delivered: source code, the executable object code and the minimum support documentation needed by a competent user to understand and use the software and to be able to modify the software in subsequent development efforts.

Abstracts		
Peer Reviewed Publications	*2 finished and going to submission*	
Outreach Publications /Web Pages	*1*	
Presentations	*7*	
MS Degrees Conferred	*2*	
Ph.D. Degrees Conferred	*1*	
MS Students Supported	*2*	
Ph.D. Students Supported	0	
Disclosures	0	
Patents Filed	0	
Provisional Patents	0	
Patents Issued	0	
License Agreements	0	
Plant Variety Protection	0	
Investigators Supported	5	
Post-Docs Supported	1	
Graduate Students Supported	4	
Undergraduate Students Supported	7	
Start-Up Jobs Created	0	

Back to Table of Contents

Sun Grant Initiative
DOE Final Progress Report

Project Title: Barley Straw for Fructanosic Ethanol

Project Director/Principal Investigator: Victoria Blake, Research Assistant Professor, Montana State University, Bozeman, MT (until 2010), now Bioinformaticist, USDA-ARS, Western Regional Research Center, Albany, CA
All Co-Principal/Other Investigators: Dr. Thomas Blake, Professor, Montana State University, Bozeman, MT

Collaborators: None

Period of Performance: 1 July 2009 - 31 October 2013

Funding Awarded: $77,868

Cost Share Amount: $79,514

Cost Share Sources: Time and effort from PIs and CoPIs

Executive Summary

In 2007, Dr. Victoria Blake discovered several barley lines that stored fructan, a soluble and fermentable carbohydrate, in their straw at harvest. Two of these produced straw that was approximately 30% fructan on a dry weight basis at harvest, raising the possibility that one could produce a grain crop, then use the straw to produce ethanol. Funding from this project permitted: the evaluation of the productivity of these two lines in Virginia, North Dakota, Montana, Idaho and Oregon; development of a process to extract, concentrate, and ferment into ethanol the fructans from these barley straw sources; perform the initial breeding and genetic analyses needed to create agronomically competitive high straw fructan barley lines.

Actual versus expected accomplishments.

We expected that the two initial lines that produced high fructan straw would be agronomically non-competitive. This turned out to be correct. We did not expect that these lines, when produced under irrigation, would not produce high fructan straw. In relatively low-yield environments, fructan production was stable. As yield levels increased, lodging increased resulting in straw lesions and cracking. We conclude that when straw integrity is compromised, soil microorganisms more easily access the interior of the straw and degrade stored fructans. The most reliable environments in which to produce high fructan straw were the relatively low-yield rainfed environments in central and Southern Montana.

In order to obtain efficient fructan extraction, we learned that we needed to use an approximately 30:1 ratio of water (containing 1% sodium meta-bisulfite to inhibit growth of environmental microorganisms) to straw by weight. Straw needed to be chopped into fragments smaller than 1cm. This extraction resulted in a solution containing approximately 1% fructan. To perform effective fermentation and distillation, this needed to be concentrated ten-fold. We accomplished this by cryoconcentration, partially freezing the solution at -10ºC. Fructans partitioned into the liquid phase, and we were able to effectively recover a 10% fructan solution. We accessed a strain of *Kluyveromyces marxiana* that secreted sufficient fructanase activity to permit fermentation of fructose to ethanol in co-cultivation with a strain of *Saccharomyces cerevesiae*, and we performed multiple 150l fermentations in our small pilot plant. The process was successful, although time, energy and labor-intensive.

Our overall process efficiency (actual ethanol production/theoretical ethanol production) was about 60%. With the original varieties, our best dryland production of 30% ethanol straw resulted in approximately 800Kg recoverable straw per acre. This means that at best we could harvest 240Kg fructan per acre, which has a theoretical yield of 115Kg ethanol per acre. At a process efficiency of 0.6, this results in an estimated ethanol yield of 69Kg/acre. Since a gallon of ethanol weighs about 3Kg, this means that the estimated best ethanol yield would be 23 gallons. At current ethanol prices, this is not a reasonable return on the sort of investment a farmer would require. Also, given the energy costs of harvest and cryoconcentration, it's clear that this is not a green process.

On a more positive note, the high fructan straw trait is highly heritable and our initial analyses discovered four QTL that contribute to the trait. We made crosses between these two landrace accessions, and selected progeny that expressed the high fructan straw trait and provided excellent grain yield. One of these is now being advanced toward release as a feed barley variety, and another is being advanced toward release as a hay variety. The grain of several of these high straw fructan lines was observed to contain relatively high concentrations of β-glucan, and two of these will be considered for release as healthful food barley varieties. These will be public releases and will not be protected under the provisions of the Plant Variety Protection act.

Project activities

During the first year, we grew the USDA barley core collection (1917 lines of spring barley representing barley's global diversity) at the A.H. Post Research Farm near Bozeman, MT, and harvested each line for both straw and grain. Straw was ground, placed in porous nylon bags which were then placed in lingerie bags. These were then manually inserted into the rumens of two rumenally cannulated cows where they were incubated for 48 hours.

Fig. 1. The Barley Core Collection Planted at the A.H. Post Research Farm

The experimental design was a completely randomized block with two reps per cow and two cows. After 48 hours, bags were retrieved, washed, dried and weighed. Large differences were observed among lines. Since the USDA-supported barley CAP project had supported the genotyping of these 1917 lines, we were able to perform an association analysis on these data, and identified six QTL that appeared to contribute to variation in straw digestibility.

Dr. V. Blake became curious regarding the mechanism underlying variation for straw digestibility, and performed a time-course experiment to see how rapidly straw degraded.

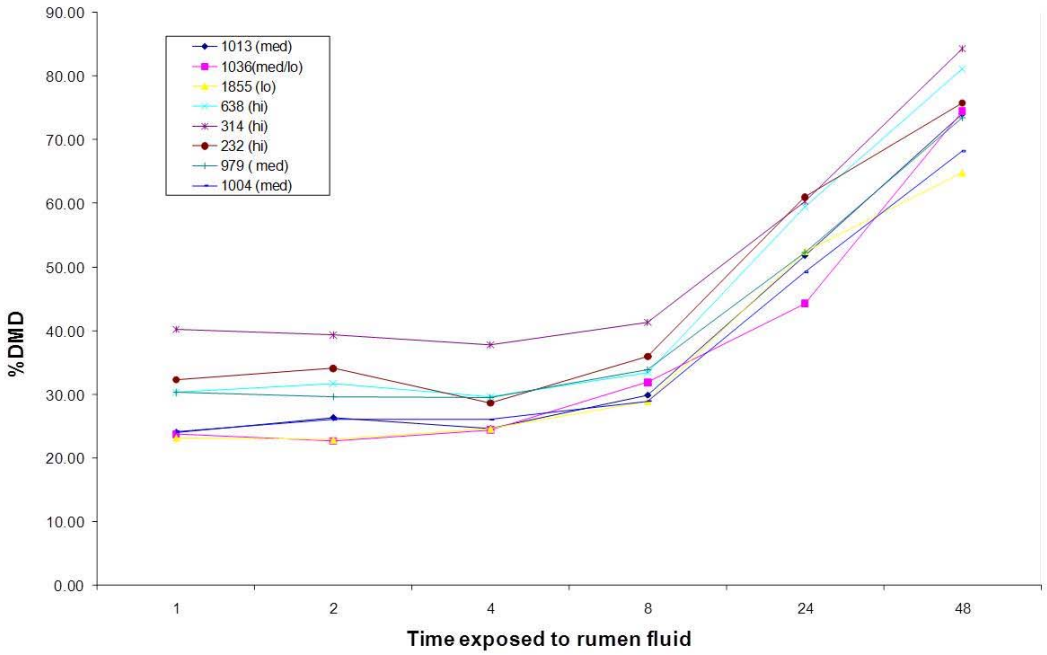

Fig. 2. Timecourse of solubilization of barley straw from core collection lines.

The observation that as much as 40% of straw's dry matter was solubilized within an hour of incubation in rumen fluid suggested that this might represent a significant amount of soluble carbohydrates. We reanalyzed the core collection straw samples for water solubility, and identified lines that produced straw containing 35% water soluble compounds at harvest.

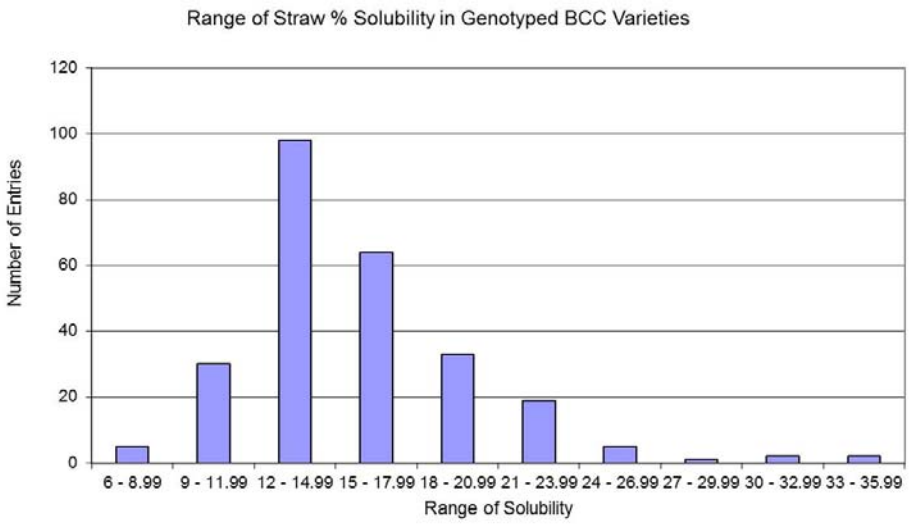

Fig. 3. Straw Solubilities of Barley Core Collection Lines

We hypothesized that the primary soluble compound might be fructan, a highly water-soluble carbohydrate used by barley as a storage carbohydrate early in plant development. We then performed association analysis to see whether we could identify QTL that contributed to this trait.

Table 1. QTL associated with high fructan straw.

QTL	Gene Name	F Value	p Value	Best BLASTX UniProt Hit
qDMD3H	3906-558	25.53	2.20E-06	**Putative sterol-C5(6)-desaturase (*Oryza sativa*)**
qDMD4H	2878-574	26.03	1.82E-06	**Putative transcription factor (*Oryza japonica*)**
qDMD5H	1697-636	17.39	6.93E-05	**IAA1 protein *(Triticum aestivum*l**
qDMD6Ha	5481-1507	19.91	3.49E-05	**Fructan 1-exohydrolase precursor (*Hordeum vulgare*)**
qDMD6Hb	1649-441	18.73	3.89E-05	**Ribosomal protein l35A (*Zea mays*)**

Five QTL with significant impact on straw fructan storage were identified, with one significant genetic marker encoding a fructan exohydrolase. Since this result suggested that the straw fructan storage trait was relatively simple, we initiated selection within populations derived from crosses between high fructan straw lines (HFSL) and well-adapted, high yielding lines. We grew these populations at the A.H. Post research farm in 2010, 2011 and 2012, selecting for high fructan straw and excellent agronomic performance.

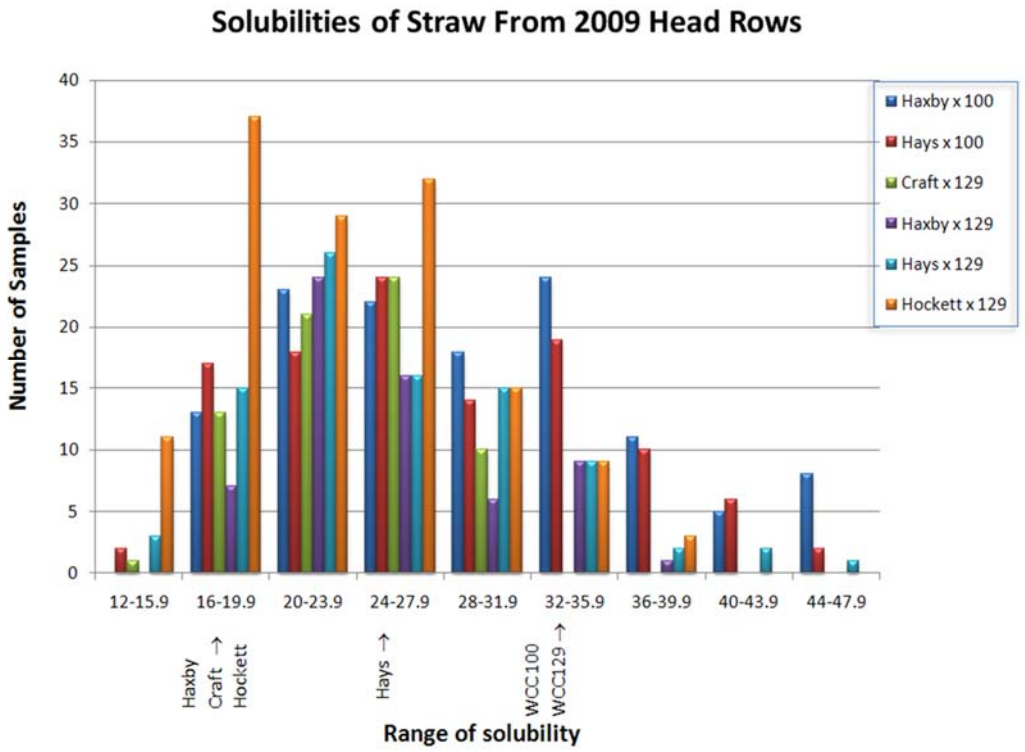

Fig. 4. The Range of Solubilities in Lines derived from Crosses between HSFL WCC 100 and WCC 129 and well-adapted, high yielding cultivars

We were able to recover 22 lines with 35% straw solubles and competitive grain and straw yield.

Products developed under the award

In January, 2014, we will consider several of the lines developed through this project for release to barley producers. We believe that several of these lines will find a place in the upper plains as dual purpose barleys. WCC 100 is a hulless, high grain fiber (10% glucan) barley line that produces grain with a distinctive, nutlike flavor (pers. Comm. T. Blake). Four of these lines incorporate the 'hooded' gene from Hays that converts the awn into a modified leaf. These lines will find use in environments with variable rainfall. In high rainfall years farmers will be able to harvest and market food-grade high fiber hulless barley, and in low rainfall years farmers will be able to harvest high straw fructan hay. Due to reduced funding following the Republican gain of a majority in the House of Representatives, Dr. V. Blake had to leave the MSU barley project in 2010 to return to her former position as USDA bioinformaticist. We are still trying to find the time to publish this work.

Academic

One graduate student was identified to manage much of this project, but he left the project to take a full time position with a local craft brewer.

Please complete the following table to reflect your project at completion or time of report submission:

ITEM	NUMBER
Abstracts	**2**
Peer Reviewed Publications	**0**
Outreach Publications/Web Pages	**0**
Professional Presentations	**2**
MS Degrees Conferred	**0**
Ph.D. Degrees Conferred	**0**
MS Students Supported	**0**
Ph.D. Students Supported	**0**
Post-Docs Supported	**0**
Undergraduate Students Supported	**2**
Investigators Supported	**0**
Start-Up Jobs Created	**0**
Disclosures	**0**
Patents Filed	**0**
Provisional Patents	**0**
Patents Issued	**0**
License Agreements	**0**
Plant Variety Protection	**0**

Back to Table of Contents

Sun Grant Initiative
DOE Final Progress Report

Project Title: Optimization of Biomass Productivity and environmental Sustainability for Cellulosic Feedstocks: Land capability and life cycle analysis

Project Director/Principal Investigator: Sylvie Brouder, Professor of Agronomy, Agronomy Department, Purdue University, West Lafayette, IN

All Co-Principal/Other Investigators: Jeffrey Volenec, Professor of Agronomy, Agronomy Department, Purdue University, West Lafayette, IN; Ronald Turco, Professor of Agronomy, Agronomy Department, Purdue University, West Lafayette, IN; Damian Allen Mendel Bioenergy Seeds/Adjunct Professor of Agronomy, West Lafayette, IN; Benjamin Gramig, Associate Professor of Natural Resource and Environmental Economics, Agricultural Economics Department, Purdue University, West Lafayette, IN; Wallace Tyner, Professor of Agricultural Economics, Agricultural Economics Department, Purdue University, West Lafayette, IN

Collaborators: None

Period of Performance: 1 September 2010 - 30 September 2014

Funding Awarded: $700,000

Cost Share Amount: $175,000

Cost Share Sources: Time and effort from PIs and CoPIs; Indirect on time and effort; Mendel

Executive summary

This was a multifaceted project evaluating the ability of potential bioenergy crops (both annual and perennial) for their ability to produce high biomass yields on land considered 'marginal', determine the quality of the material under various rates of nitrogen fertilizer, and the economic impact of such decisions. The annual cropping systems included four crops (maize as a control, dual-purpose sorghum, sweet sorghum, and photoperiod sensitive sorghum) all of which were fertilized with five different rates of nitrogen. Our perennial systems containted *Miscanthus* x *giganteus*, a novel biomass type switchgrass (Liberty), and a low diversity prairie mix. Additionally, a joint project with Mendel Biotechnology evaluating the ability to seed a novel variety annual of *Miscanthus* x *giganteus* for establishment and understanding the role of fertilization of *Miscanthus* x *giganteus* during its' establishment phase were conducted. Lastly, similar plots at TPAC and ACRE were utilized for greenhouse gas and water analyses to compare to the annuals at that site.

The research adds to a body of knowledge surrounding the use of commercially available or potential bioenergy crops. These studies specifically identify the opportunities and challenges associated with producing a range of bioenergy crops across landscapes which are considered marginal. Specifically, we identified which crops will provide the greatest yields and theoretically the greatest return, the role of fertilization for annual and perennial crops, costs to the environment (through greenhouse gas emission and nitrate leaching), and establishment and transportation costs. The methods involved/employed are commonly used and accepted lab practices for analyzing the composition of the harvested materials.

Objectives

Objective 1: Quantify comparative productivity potentials and environmental impacts of candidate bioenergy systems (*M. giganteus*, switchgrass, native prairie, maize and sorghum) as influenced by land capability including assessment of

a. yield and quality (chemical composition) of feedstocks;
b. crop-specific N use efficiency (NUE) and water use efficiency (WUE);
c. cropping system impact on soil C/N storage and important microbial determinants, and
d. cropping system C/N losses to the atmosphere and surface waters.

Outcomes and Impacts:

a. Yields of stover, grain, and whole plant per plot were captured yearly for the annuals while the whole plant per plot was captured for the perennials studied. Quality analysis was performed on all the stover, grain, and whole plant tissues for structural and non-structural carbohydrates, carbon, nitrogen, phosphorus, potassium, fiber, and ash. There was no deviation for this aspect of the project, but yields were not able to be collected at the same time point at each location each year as mechanical, weather, and plant maturity dictated when the harvests could be completed. The lab/chemical analysis for the 2011-2013 growing seasons are complete however, the 2014 growing season (no cost extension) laboratory/chemical analysis is yet to be completed. Yields for the differing annual biomass crops were in the expected range with the sweet and photoperiod sensitive sorghums having the greatest yields, while the dual purpose and corn were lower yielding. There were location effects, but the sorghums were more resilient/stable across the different environments and yields were less affected compared to maize. The quality components for stover and grain were as expected. The stover NDF, ADF, hemicellulose, and cellulose concentrations were the greatest in maize followed by dual purpose sorghum while the sweet and photoperiod sensitive sorghums contained the least amounts. The stover ADL (lignin) concentration was fairly similar between the annual crops. The grain fiber concentrations were extremely low and similar between maize and the dual and sweet sorghums; however in some years, depending on location, no appreciable grain developed in the sorghums due to their

requirements for a long growing season. This lack of grain, when looking at the plant as a whole was the driving force on the composition of the entire plant as stover production/yield and composition was more consistent. Maize was more reliable at producing grain although the amount was affected by location. The grain yields across all genotypes were the greatest at TPAC while SEPAC had the lowest grain yields. The soluble carbohydrates (sugar and starch) also followed expected outcomes. The stover soluble carbohydrates of sweet sorghum were greater than any of the other annuals while the maize stover contained the least. The starch concentrations of the stover were the lowest in the dual-purpose sorghum with the remaining annuals being similar. Grain, when present, had low sugar with the dual-purpose have the least and maize the greatest concentrations. Starch concentrations were nearly the same for the maize and the sorghums examined. The concentrations of P and K were variable between locations in both grain and stover tissues, but similar trends were observed. Grain K concentrations were the lowest in Maize but similar in the sorghums. Grain P was similar in all the annual crops. Stover K was variable between the crops with dual-purpose sorghum having greater concentrations and sweet sorghum having the lowest concentrations across locations. Stover P was lower than grain P with the maize and photoperiod having higher concentrations than the other sorghums.

The yields of the perennial biomass crops (*Miscanthus* x *giganteus*, switchgrass, and low diversity prairie mix) were variable depending on locations with the greatest yields observed at TPAC and the lowest yields at SEPAC. Yields are primarily linked to the ability of the perennials to become established at a location and establishment can take up to three years. As expected, once established, *Miscanthus* x *giganteus* produced the greatest biomass across all locations followed by switchgrass, then the low diversity prairie. The switchgrass and prairie were less variable in yields while *Miscanthus* x *giganteus* exhibited larger differences between the locations. When evaluating the perennials the fiber concentrations were similar but on average *Miscanthus* x *giganteus* had slightly higher concentrations than switchgrass and the low diversity prairie. The fiber concentrations were greater than the annuals tested at the same locations. Simple sugars were extremely low for the perennials and were similar to the stover samples of dual purpose sorghum and maize but when compared to the whole plant tissue samples of the annuals was much lower due to the perennials lacking grain. The concentrations of P and K were extremely low and lower than in any of the annual crops tested as compared to the whole plant, but more similar to the stover portion of the annuals. Tissue K for *Miscanthus* x *giganteus* was slightly greater when compared to the other perennials across locations while, P was nearly the same.

The implications of this show that if annuals are targeted for use as bioenergy feedstocks utilizing a sorghum has the advantage of producing greater yields that are stable over differing environments. The perennials (*Miscanthus* x *giganteus* and switchgrass) in contrast have the ability to obtain even greater yields on marginal lands with few inputs, but the establishment can be quite difficult depending on location. However, their use will be limited in that these crops will only have one outlet as compared to some of the annuals in that grain could be harvested and sold independently.

b. The NUE of the annuals were calculated for the growing years 2011-2013. The 2014 data have yet to be tabulated. The values calculated for the annuals were variable between the locations as expected and as the nitrogen rate increased the efficiency decreased for all annual crops. Data are available to estimate water use efficiency (WUE) and a new Ph.D. student (Elizabeth Trybula) will be using this data to estimate WUE for specific WQFS biomass treatments. In addition, our capability to estimate WUE has recently improved with the purchase (using Purdue funds) of additional wireless soil moisture sensors that acquire and send soil moisture data in real-time. These new data streams will augment our current data sets to more fully characterize WUE in the near future.

c. An initial soil sampling from each of the sites was collected and evaluated along with soil samples from ACRE and TPAC to determine the microbial populations as well as the amount and types of carbon present in the soils from various cropping systems. A final soil sampling needs to be completed this spring (2015) to try and identify how cropping systems may have changed the soil carbon composition over time. Microbial populations differed between the cropping species with the perennial systems having similar populations of microbes as compared to annual systems. These differing microbial populations can affect the rate and amount of gas the cropping systems contributed to greenhouse gas emissions.
d. In years 2013 and 2014 lysimeters were placed in the annual and perennial systems at TPAC along with static greenhouse gas chambers on plots receiving 0 or 100 kg ha^{-1} nitrogen. Data for both years were collected starting in April going through October/November and removed prior to harvest. Data are currently being analyzed. Preliminarily results display a lower amount of off gassing as well as nitrate leaching in the soil for perennial systems as compared to annuals as expected; however results vary in/across time and across landscape/sites. The main losses are occurring in the spring with little change/loss occurring from June through October/November.

Impacts from the greenhouse gas and water collection data will inform policy about crops targeted as biomass feedstocks for energy conversion on the effects of the crop systems grown on marginal/sensitive lands to N leaching as well as off gassing. From our results annuals pose a greater opportunity/risk to the surrounding environment with their lower ability to capture nitrogen and their greater need for fertilizer inputs.

Objective 2: Compare agronomic performance of seed- versus rhizome-derived *Miscanthus* spp. including characterization of
a. growth, survival and productivity during stand establishment;
b. development, yield and feedstock quality in establishing and established stands, and
c. NUE and a preliminary assessment of contributions of associative N fixation.

Outcomes and Impacts:

a. This particular objective to be performed by Mendel Biotechnology was not completed due to the company closing the station. However, a project that was already underway (Section b of this objective), evaluating the role of nitrogen fertilization on several *Miscanthus* x *giganteus* genotypes during the establishment phase was utilized as a new project to understand the storage of nitrogen (where, how, what form of nitrogen) using a subset of the treatments. We collected whole plants (above- and belowground tissues) from two genotypes and five nitrogen treatments from March through November 2012 from the Buck Creek/Lafayette, IN location. Analysis has been completed on half the samples (July – November) with the remaining samples (March – June) being completed now. Because this was a completely new objective, and due to the number of samples involved, we have yet to fully complete this new objective, but will by the end of February. Thus far it is clear from the data that the rhizomes are the main storage organ for nitrogen. The amount of nitrogen applied is influencing the composition and uptake of N in the tissues by the concentrations observed in the rhizomes, roots, stembases, and shoot tissues although the nitrogen uptake is not directly translating into greater yields in all environments. A clear spike in nitrogen concentration was measured between the August and November sampling dates during the senescence period indicating *Miscanthus* is shuttling nitrogen below ground to the rhizomes for the winter dormancy period. The plant is using soluble protein structures rather than free amino acids as the main way to store nitrogen. This has implications on how *Miscanthus* x *giganteus* is utilizing nitrogen; that it appears to be taking up luxury amounts of nitrogen, as well as the changing nitrogen dynamics in rhizomes throughout the growing season. Currently, this new project is

resulting in the creation of a manuscript that will be submitted once all the analysis are complete.

b. An established stand of Miscanthus at ACRE and 3 establishing stands, one at TPAC and two from Mendel Biotechnology (Schochoh, KY and Lafayette/Buck Creek, IN), were utilized. There was no deviation from the objectives as all sites were harvested and yield data gathered starting in 2011 through 2014 for the ACRE and TPAC sites while the two sites managed by Mendel biotechnology were concluded in 2011 and 2012, respectively. Yields were tabulated and chemical compositions determined as in objective 1. The lab/chemical analysis is not yet complete for the 2014 growing season samples, but are currently being processed from the TPAC and ACRE locations. The Mendel plots have resulted in a manuscript that is in the process of review by the authors and is nearing submission for review at a journal.

c. NUE calculations were made for the two Mendel plots as well as the TPAC site as those studies received variable rates of nitrogen. The NUE values obtained from the Mendel experiments are included in the manuscript from part b above. The NUE was different across the genotypes assessed during the experiment, but the NUE was greater than the annual crops that were assessed in objective 1. The NUE declined as the nitrogen rate increased across all genotypes as expected.

   The implications from this show how nitrogen is being utilized by *Miscanthus* x *giganteus* genotypes in multiple environments. This information further refined our current knowledge regarding the fertilization of *Miscanthus* x *giganteus*. It will inform/aid stakeholders/growers in identifying the appropriate amount of fertilization that is needed both during the establishment phase and for fully mature stands based on different environmental conditions. Additionally, the information will give other researchers a better grasp of nitrogen storage and cycling in *Miscanthus* x *giganteus.*

Objective 3: Complete LCAs to evaluate environmental sustainability of bioenergy crops as compared to liquid petroleum with characterization of conditions under which prospective cellulosic feedstocks are economically viable.

Outcomes and Impacts:

This objective involves two components: (a) Life-cycle assessment (LCA) of the greenhouse gas emissions (GHGs) from stover collection, switchgrass and *Miscanthus* from field through combustion of biofuels, and (b) economic assessment of the cost of farm gate production and conversion at a biochemical or thermochemical biorefinery for each cellulosic feedstock. Each component is discussed below and documented in detail in the attached manuscripts based on the funded research.

a. The LCA was performed using field measurements of biomass yield and nitrous oxide (N_2O) emissions collected from the research plots at Purdue. These data were used to parameterize and calibrate the maize, switchgrass and *Miscanthus* crops in the peer-reviewed biogeochemical model DayCent. DayCent was used to simulate biomass growth, the carbon and nitrogen pools in the soil, and land-atmosphere exchange of the greenhouse gases CO_2, N_2O and CH_4. Parameterization was based on biological measurements taken at different growth stages and harvested yields. All management (tillage, maize residue collection, fertilizer rates, application methods and timing of application, and harvest date) information was modeled according to the experimental plot field logs. Calibration was only performed on a single production parameter, as directed by the model developers at Colorado State University. All crop parameterizations, management files and simulation scenarios were reviewed by the model developers, and preliminary results were presented online using AdobeConnect to ensure that all DayCent modeling was being performed correctly. DayCent was able to explain 93% of the variation in observed yields over all six crops and 79% of the

variation in average daily N_2O emissions over the growing season. All greenhouse gas emissions outside the farm where biomass is grown were calculated using the peer-reviewed GREET model (Argonne National Laboratory). The field-to-wheels life-cycle greenhouse gas emissions of each cellulosic biofuel were compared to conventional unleaded gasoline. The biochemical conversion pathway was found to have higher emissions per energy equivalent (to gasoline) gallon of biofuel than the thermochemical pathway. Corn stover removal has the highest emissions per gallon overall, followed by switchgrass and then *Miscanthus*. There are considerable differences in land emissions from stover removal depending on whether nitrogen removed with crop residue must be replaced with additional fertilizer. Results suggest that corn stover will not achieve the 60% emissions reduction mandate if it is collected using conventional practices studied unless nitrogen does not need to be replaced when crop residue is removed. *Miscanthus* achieves the greatest reduction in emissions relative to gasoline, and it has life cycle emissions per energy equivalent gallon of fuel are more than an order of magnitude lower than corn stover. Switchgrass achieves more modest greenhouse gas reductions, but at lower cost than *Miscanthus*.

b. Farm gate production costs for each crop were calculated based on the management from the Purdue experimental plots and assuming all harvest was performed using conventional forage harvesting equipment. All production budgets are reported in appendices to the attached manuscripts and individual costs with the greatest level of uncertainty and crop yields were simulated as being stochastic. Transportation and conversion costs were not modeled stochastically due to a lack of estimates from which to construct a distribution of costs. Costs of conversion for the biochemical and thermochemical (Fischer-Tropsch liquids) conversion pathways were drawn from the most recent Department of Energy agency reports on each technology based on the minimum feasible scale (plant capacity) in the engineering economic cost studies. Thermochemical pathway was found to be least expensive on a cost per gallon of gasoline equivalent (GGE) basis, but this relies on a very large plant size that requires a much larger upfront capital investment than for a thermochemical plant, which explains in part why the only cellulosic biorefineries built to date use enzymes in a biochemical conversion process. Corn stover has lowest farm gate production cost, even when the cost of nitrogen replacement is included, followed by switchgrass, while *Miscanthus* was the most expensive due to the cost of rhizomes. Including farm gate and conversion costs, the cost for corn stover ranges from $2.36 to $2.63 per GGE depending on the stover removal rate, whether harvested from a corn-soy rotation or continuous corn, and whether or not nitrogen replacement occurs. Switchgrass is estimated to cost $2.91 per GGE and *Miscanthus* is expected to cost over $3.00 per GGE. The ordering of these costs by feedstock is the same for biochemical conversion, but the costs over all the feedstocks range from $3.86 to $4.95 per GGE instead. We also estimate the cost per metric ton of CO_2-equivalent abated relative to gasoline and find carbon abatement costs ranging from $15 to over $60 per Mg CO_2-equivalent using the thermochemical conversion pathway. The biochemical pathway results in carbon abatement costs at least three times higher—more than $191/Mg CO_2- equivalent. This suggests that current conversion technologies using the studied feedstocks are far more costly on a carbon abatement cost basis than other options to clean up greenhouse gas emissions available to society today.

Project Activities

We hypothesized that land capability will influence relative crop feedstock yields and environmental footprints.

The overarching goal of this proposal was to quantify relative productivity and environmental sustainability of candidate species on contrasting soils and landscape positions through field experimentation, data-driven LCA and economic analysis. Comparative assessment

of ecological sustainability encompassed the critical ecosystem services (ES) of soil, air and water quality; project-generated data was used in lifecycle greenhouse gas (GHG) and soil and water resource impacts analysis integrated to consider policy options.

Activities included taking initial soil samples from each site to assess the C concentration at various depths and at specific locations the microbial populations present. Site preparation, which was primarily herbicide application as plots were no-till. Other activities included taking stand counts laboratory analysis of all the samples for structural and non-structural carbohydrates, ash, N, C, P, K and calculations for yield and NUE as well as greenhouse gas emissions and nitrate losses via leaching. Collection of water and greenhouse gas samples began later in the life of the grant (2013 through 2014) as we perfected the experimental systems.

Some issues occurred which did result in some deviations. One deviation was the SEPAC site as it was a very wet heavy clay site. In the second year it was tilled due to the inability for us to fully harvest the site with the machine harvester that resulted in severe rutting. The effects might influence the soil carbon. Also we could not harvest with a machine in autumn; we tried to wait for the ground to freeze however that never took place. Therefore, we had to hand harvest the material in January which affected the quality parameters for that biomass material and its calculated yields. That site had a heavy weed presence prior to the implementation of the experiment. Due to the slow establishment of the perennials our stands were suboptimal and required multiple attempts at getting them established. Even by the end of the experiment stands are still problematic. We also encountered an issue with the establishment of Miscanthus at the NEPAC site due to that site being inherently droughty which was compounded by the severe drought of 2012. Several plants needed to be replaced. The other main deviation was the loss of the Mendel seeding study of *Miscanthus* x *giganteus*. To account for this loss we utilized another experiment to aid in the understanding how nitrogen is used, stored and transported from different tissues.

From these studies it was determined that the experimental sites are critical, but the sorghum's response are more stable across sites and years than the maize control. The TPAC site had the best overall performance of our marginal sites in relation to yield while the SEPAC site preformed the worst. At that location the maize control rarely produced a harvestable crop. A drawback of the sorghums is few are developed for the growing regions tested. These crops currently require a longer growing season which is not always possible, especially in our northern experimental site at NEPAC. Due to the short growing season none of the sorghum's tested dry down in the field like maize and hold appreciable amounts of water. One notable observation over four years of planting maize and sorghum is in the inability to control C4 annual grasses (foxtail, barnyardgrass, crabgrass, ect.). These weeds became increasingly abundant and progressively difficult to control with each passing year and likely began to impact yields. Overall, this experiment added to the overall understanding of how different sorghum crops can produce biomass yields across many of the marginal lands found in Indiana relative to maize, their response to nitrogen fertilization and how the quality of the material is influenced by genotype, location, and fertilization. Our recommendation is that if the sole purpose was for biomass production choosing either a sweet or photoperiod sorghum would be more advantageous than maize.

The perennial crops were evaluated at the same sites (NEPAC, SEPAC, and TPAC), but no differing nitrogen treatments were conducted. One of the main drawbacks is the ability to get these crops established, which took nearly three years to reach peak production at TPAC while the other sites still have not achieved peak production status. This was made evident as each site had particular challenges (weed pressure, droughty or wet soils, and winter kill) to get plants established. Our SEPAC site was the most challenging site and took three attempts at planting switchgrass and the low diversity prairie, while the NEPAC site gave us a challenge with the droughty conditions and winterkill in the *Miscanthus* x *giganteus* plots. Therefore, these crops will take extra care and planning to achieve usable stands. Once established however it was clear

that the yields of switchgrass rivaled the annuals without requiring much fertilizer inputs and that *Miscanthus* x *giganteus* produced significant amounts of biomass surpassing the yields of the annuals.

Greenhouse gas and water samples from a subset of the plots was informative in the release (time of year, duration, amount) of gases and nitrate in the soil. It was clear that the losses in perennials was less than that of the annuals. The majority was lost early in the spring right after fertilization but was influenced by weather events (temperature and rainfall) with subsequent losses being minimal. Additionally, the microbial communities appear to respond to the type of crop being grown and management practices of the soil which likely had an impact on the release of gasses and nitrate leaching.

The LCA used data collected from the various locations and treatments studied which then were utilized in the DayCent and GREET models to better understand the growth, fertilizer usage, and gas emissions along with costs relative to the conversion process for three cellulosic feedstocks (maize stover, switchgrass, and *Miscanthus)*. The DayCent results indicate the thermochemical is superior to the biochemical and of the three crops Miscanthus had the least amount of greenhouse gas emissions. However it was also concluded that *Miscanthus* would be more costly to use at this time than other sources examined for use in current technologies (i.e. biochemical conversion) but results in larger carbon abatement costs, larger than current practices.

Projects developed under the award

Journal Articles/Publications

1. Field-scale potassium and phosphorus fluxes in the bioenergy crop switchgrass: Theoretical energy yields and management implications. 2013. J. Plant Nutr. Soil Sci. 176:387-399.
2. Perennial rhizomatous grasses as bioenergy feedstock in SWAT: parameter development and model improvement. 2014. Glob. Change Biol. Bioenergy DOI: 10.1111/gcbb.12210
3. Farmers' Supply Response, Price of Corn Residue, and Its Economic Viability as an Energy Feedstock. Bioenergy Research. 6(2):797-807, 2013. http://dx.doi.org/10.1007/s12155-013-9300-0
4. Environmental and economic tradeoffs in a watershed when using corn stover for bioenergy. Environmental Science & Technology. 47(4):1787-1791, 2013. http://dx.doi.org/10.1021/es303459h
5. Transition to second generation cellulosic biofuel production systems reveals limited negative impacts on the soil microbial community structure. 2015. Appl. Soil Ecol. (submitted)

Abstracts/conference papers

1. Amer. Soc. Agron. Annu Meeting, San Antonio TX. Oct. 16 to 20, 2011. Woodson, P., S.M. Cunningham, P. Murphy, S.M. Brouder, and J.J. Volenec. Production and quality of switchgrass grown on marginal land.
2. Water for Food Global Conference: Path to Solutions, Lincoln, NE. May 1 – 4, 2011. Brouder, S.M., P. Woodson, L. Bowling, R. Turco and J. Volenec. Yield potential, water and N requirements of non-food biofuels.
3. In Proceedings of the Frontiers in Bioenergy Conference, West Lafayette, IN. May 15 to 18, 2011. Brouder, S.M. P. Woodson, L. Bowling, R. Turco and J. Volenec. Yield potential, water and N requirements of non-food biofuels.
4. Purdue Extended Campus Senior Programs, “All-You-Can-Learn Buffet” Elderhostel Program. West Lafayette, IN. June 14th. Brouder, S.M., R. Turco and J.J. Volenec. Demystifying the promise of bioenergy crops: Environmental impacts and ecological accounting.

5. Global sustainability issues in energy, climate, water, and environment. West Lafayette, Sept. 25 to 28, 2011. IN China-US 2011 Joint Symposium. Brouder, S.M. Comparative agro-ecological performance of perennial and annual biomass systems: metrics and data workflows.
6. Global sustainability issues in energy, climate, water, and environment. West Lafayette, IN, Sept. 25 to 28, 2011. China-US 2011 Joint Symposium. Sajeev E.M., B.M. Gramig and W.E. Tyner. “Validation of the DayCent Model for Bioenergy Feedstocks”
7. Selected Paper for the 2012 Agricultural and Applied Economics Association Annual Meeting in Seattle, WA. Sajeev, E.M., T. Ji, W.E. Tyner, and B.M. Gramig. "Economic Costs and Environmental Performance for Three Cellulosic Biofuel Pathways."
8. ASA-CSSA-SSSA International Meetings, Cincinnati, OH Nov. 3 to 6, 2012. Dierking, R., J. Volenec, and S. Brouder. The Potential of Maize and Sorghum Biomass Grown On Marginal Sites.
9. ASA-CSSA-SSSA International Meetings, Tampa, FL. Nov. 2 to 6, 2013. R.M. Dierking, J. Volenec and P. Murphy. Forage yield and quality of Miscanthus x giganteus subjected to simulated haying/grazing conditions.
10. ASA-CSSA-SSSA International Meetings, Long Beach, CA. Nov. 2-5, 2014. Dierking, R., J. Volenec, S. Brouder, and D. Allen. Miscanthus Yields and Tissue N Concentrations during Establishment with Various N-Rates Grown on Marginal Soils.
11. ASA-CSSA-SSSA International Meetings, San Antonio, TX. Oct. 16 to 19, 2011. Burks, J.L., J.J. Volenec and S.M. Brouder. 2011. Seasonal cycling and partitioning of C and N in perennial bioenergy crops. Abstract ID# 64585.
12. ASA-CSSA-SSSA International Meetings, San Antonio, TX. Oct. 16 to 19, 2011. Smith, D.R., D. Bucholtz, S.M. Brouder, J.J. Volenec, R.F. Turco, and G. Ejeta. 2011. Greenhouse gas emissions from traditional and biofuels cropping systems. Abstract # 64779.
13. In Proceedings of the 6th Frontiers in Bioenergy Conference & US-Brazil Symp. on Sustainable Bioenergy. West Lafayette, IN, May 15 -18 2011. Brouder, S.M., R. Turco, J. Volenec, G. Ejeta, D.R. Smith, L. Bowling, I. Chaubey, B. Gramig. 2011. Nitrogen partitioning and utilization in bioenergy cropping systems.
14. ASA-CSSA-SSSA International Meetings, San Antonio, TX, Oct. 16 to 19, 2011. Woodson, P., S. Cunningham, P. Murphy, S. Brouder, J. Volenec. 2011. Influence of potassium and phosphorus on yield and composition of switchgrass. http://a-c-s.confex.com/crops/2011am/webprogram/Paper65191.html.
15. ASA-CSSA-SSSA International Meetings, San Antonio, TX, Oct. 16 to 19, 2011. Smith, D.R., D. Bucholtz, S. Brouder, J. Volenec, R. Turco, G. Ejeta. 2011. Greenhouse gas emissions from traditional and biofuel cropping systems. http://a-c-s.confex.com/crops /2011am/webprogram/Paper64779.html.
16. ASA-CSSA-SSSA International Meetings, San Antonio, TX, Oct. 16 to 19, 2011. Burks, J.L., J. Volenec, S. Brouder. 2011. Seasonal cycling and partitioning of N, P, and K in perennial bioenergy crops. http://a-c-s.confex. com/crops/2011am /webprogram/Paper64585.html.
17. ASA-CSSA-SSSA International Meetings, Cincinnati, OH, Oct. 21 to 24, 2012. Trybula, E., I. Chaubey, J. Frankenberger, S.M. Brouder, and J.J. Volenec. Quantifying Ecohydrologic Impacts of perennial rhizomatous grasses on tile discharge, a plot level comparison of continuous corn, mixed prairie, upland switchgrass, and Miscanthus x giganteus. Abstract 297-9. http://scisoc.confex.com/scisoc/2012am/webprogram/Paper75175.html
18. ASA-CSSA-SSSA International Meetings, Cincinnati, OH, Oct. 21 to 24, 2012. Long, M., J.J. Volenec, and S. M. Brouder. 2012. Nitrogen impacts on the yield and cell wall composition of contrasting sorghum lines used for biomass. Abstract 383-8.
19. ASA-CSSA-SSSA International Meetings, Cincinnati, OH, Oct. 21 to 24, 2012. Burks, J., S.M. Brouder, and J.J. Volenec. 2012. Seasonal accumulation and partitioning of carbon- and nitrogen-containing compounds in perennial bioenergy crops. Abstract 99-4.

20. ASA-CSSA-SSSA International Meetings, Cincinnati, OH, Oct. 21 to 24, 2012. Turco, R.F., P. Chivenge, J.J. Volenec, and S.M. Brouder. Opening our file cabinets and field notes with meta-analysis: An approach to overcome the soil C sequestration data void. Abstract 179-3.
21. ASA-CSSA-SSSA International Meetings, Tampa, FL. Nov. 2 to 6, 2013. Long, M.K., J.J. Volenec, and S.M. Brouder. Theoretical ethanol yield for potential bioenergy sorghum genotypes of differing compositions. Abstract 373-9. https://scisoc.confex.com/crops/2013am/webprogram/Paper80060.html
22. ASA-CSSA-SSSA International Meetings, Long Beach CA. Nov. 2 to 5, 2014. M.K. Long, J.J. Volenec, and S.M. Brouder. Lignocellulosic theoretical ethanol production of potential bioenergy sorghum genotypes. Poster 284-9. https://scisoc.confex.com/scisoc/2014am/webprogram/Paper87703.html.
23. ASA-CSSA-SSSA International Meetings, Long Beach CA. Nov. 2 to 5, 2014. Orr, M.-J., M. Bischoff Gray, S.M. Cunningham, N. DeArmond, J.J. Volenec, S.M. Brouder, and R.F. Turco. 2014. Comparative analysis of soil properties and greenhouse gas flux responses to nitrogen fertilization in bioenergy production systems. Poster 100-12.
24. Plant Growth, Nutrition and Environment Interactions Conf., University of Veterinary Medicine, Vienna, Austria. Feb 18 to 21, 2012. Volenec J.J. and S.M. Brouder. Nutrient Use in Bioenergy Cropping Systems.

Other Publications

1. Volenec, J.J. and S.M. Brouder. 2010. Water-use efficiency in biomass cropping systems. pp. 18-19. In: Proc. 2nd China-US Workshop on Biotechnology of Bioenergy Plants. Beijing, China. September 19-21.
2. Brouder, S.M., R.F. Turco, and J.J. Volenec. 2010. Nitrogen use efficiency in bioenergy cropping systems. pp. 27-29. In: Proc. 2nd China-US Workshop on Biotechnology of Bioenergy Plants. Beijing, China. September 19-21.
3. Burks, J., J.J. Volenec, and S.M. Brouder. 2010. Nutrient cycling dynamics in perennial bioenergy crops. pp. 24. In: Proc. China-US 2010 Joint Symp. on Energy, Ecosystem, and Environmental Change. Beijing, China. September 22-24.
4. Brouder, S.M., and J.J. Volenec. 2010. Greenhouse gas emissions and pelicans: Ecological accounting in bioenergy cropping systems. pp. 27-29. In: Proc. China-US 2010 Joint Symp. on Energy, Ecosystem, and Environmental Change. Beijing, China. September 22-24.
5. Volenec, J.J., S.M. Brouder, and R.F. Turco. 2010. Agroecological considerations when growing biomass. pp. 39-40. In: Proc. China-US 2010 Joint Symp. on Energy, Ecosystem, and Environmental Change. Beijing, China. September 22-24

a. Website or other Internet sites that reflect the results of this project.
None

b. Networks or collaborations fostered.
Mendel Biotechnology

c. Technologies/techniques.
None

d. Inventions/patent applications, licensing agreements.
None.

e. Other products, such as data or databases, physical collections, audio or video, software* or Netware, model, educational aid or curricula, instruments, or equipment.

All data is or is in the process of being archived for public use using the Purr Database at Purdue University (https://purr.purdue.edu/).

1. **Academic**

   a. Courses developed: 0
   b. M.S. students supported: 2
   c. M.S. degrees conferred: 2
   d. Ph.D. students supported: 3
   e. Ph.D. degrees conferred: 0
   f. Post-docs supported: 1

2. **For projects involving computer modeling, provide the following information with the final report:**

   The peer-reviewed models DAYCENT and GREET used in support of this research are publicly available. The only code modifications made to crop input files in the DAYCENT model are documented in the Supplemental Information at the end of the working manuscripts.

   a. Model description, key assumptions, version, source, and intended use.
   b. Performance material for the model related to the intended use.
   c. Test results to demonstrate the model performance criteria were met (e.g., code verification/validation, sensitivity analyses, history matching with lab or field data, as appropriate).
   d. Theory behind the model, expressed in non-mathematical terms.
   e. Mathematics to be used, including formulas and calculation methods.
   f. Whether or not the theory and mathematical algorithms were peer reviewed, and, if so, will include a summary of the theoretical strengths and weaknesses.
   g. Hardware requirements.
   h. Documentation (e.g., user's guide, model code).

***Software/Manual (if applicable)**
Content. Unless otherwise specified in the award, the following must be delivered: source code, the executable object code and the minimum support documentation needed by a competent user to understand and use the software and to be able to modify the software in subsequent development efforts.

Please complete the following table to reflect your project outputs at completion or at time of report submission. Identify outputs and products developed under the award and any technology transfer activities.

ITEM	NUMBER	DETAILS (e.g. citations, names, descriptions, varieties, etc.)
Abstracts: include full citation and attach a pdf copy.	24	See above
Peer Reviewed Publications: include full citation and attach a pdf copy if available	5	See above

Outreach Publications including web pages: include full citation	0	
Professional Presentations: include full citation	29	Abstracts, and Other Publications See above
MS Degrees Conferred: include names plus month/year confirmed	2	Ji, Tianyun. M.S. in Agricultural Economics. 2012. Thesis: "The Economics of Cellulosic Biofuels: Farm to Fuel Cost Analysis of the Supply Chain." Sajeev, E.M. M.S. in Ecological Science and Engineering. 2012. Thesis: "Greenhouse gas emissions from cellulosic biofuels: A field to wheels analysis."
Ph.D. Degrees Conferred: include names plus month/year confirmed	0	
MS Students Supported: include names	2	Tianyun Ji (AGEC) Sajeev Erangu Purath Mohankumar (AGEC)
Ph.D. Students Supported: include names	3	Long Monique K Orr, Mary-Jane Burks, Jennifer
Post-Docs Supported: include names	1	Ryan Dierking Orr, Mary-Jane Chivenge, Pauline
Undergraduate Students Supported: include names	12	Sarah A Abercrombie, Kyle A Babiak, Thanya D N Cooray Bulathsinhala, Sarah E Estrada, Shelby R Glotzbach, Jason A Kimball, Kelly E Schlotman, Natalie L Shen, Kelsey R Smith, Cameron R Strohla, James G Swanson, Kerri M Swingley
Investigators Supported: include names	4	Sylvie M Brouder, Jeffrey J Volenec, Ronald F Turco Jr., Benjamin M Gramig
Jobs Created	15	Undergraduate, Graduate, and Post-Graduate Employment
Invention Disclosures	0	Provide no confidential or enabling information. Just indicate in an invention disclosure has been filed with the employer.
Non-provisional Patent Application(s) Filed	0	
Provisional Patents Filed	0	
Patents Filed	0	
Patents Issued: include full citation	0	

License Agreements: include description	0	
Plant Variety Protection: include description	0	
Subsequent Funding: List proposals funded as a result of this work	3	DOE. Watershed Scale Optimization to Meet Sustainable Cellulosic Energy Crop Demands in the Midwest USA. I. Chaubey, L.C. Bowling, S.M. Brouder, K.A. Cherkaurer, B.A. Engel, J.R. Frankenberger, R.R. Goforth, B.M. Gramig, P.T. Murphy, J.J. Volenec. 2010-2014. $1,991,177. USDA-AFRI-NIFA Biomass CAP program. Agro-ecosystem Approach to Sustainable Biofuels Production via the Pyrolysis-Biochar Platform. K.J. Moore PI (Iowa State Univ.) and collaborators (Univ. of NE, Purdue, Univ. of MN, Univ. of IL-UC, UW-Madison, USDA-ARS). Total funds: $25 M. Purdue Univ. faculty include: J.J. Volenec (Purdue PD), C.E. Alexander, S.M. Brouder, N.J. Carroll, I. Chaubey, B.J. Erickson, K.D. Johnson, R. Lerner, C.A. Martin, P.T. Murphy, N.J. Olynk, K.S. Orvis, R.F. Turco (listed alphabetically). Sept. 2011 to Aug. 2016. $3.6 M. International Plant Nutrition Institute. Mineral Nutrition and Biomass Production. J.J. Volenec, S.M. Brouder, and R.F. Turco. 2009-2015. $60,000.
Other: Products, such as data or databases, physical collections, audios or videos, software or Netware, models, educational aids or curricula, instruments, or equipment.	0	

Back to Table of Contents

Sun Grant Initiative
DOE Final Progress Report

Project Title: Do Nurse Crops Make *Miscanthus* x *giganteus* Establishment More Sustainable?

Project Director/Principal Investigator: Emily Heaton, Assistant Professor, Dept. of Agronomy, Iowa State University, Ames, IA

All Co-Principal/Other Investigators: Richard Cruse, Professor, Dept. Agronomy, Iowa State University, Ames, IA

Collaborators:
Jeremy Singer, Principal Scientist, BASF, Research Triangle Park, NC
Doug Davenport, District Conservationist, Natural Resource Conservation Service, Creston, IA

Period of Performance: 1 July 2010 - 30 September 2013

Funding Awarded: $180,969

Cost Share Amount: $45,589

Cost Share Sources: Time and effort from PIs and CoPIs; Indirect on time and effort.

1. Executive Summary

This research added to understanding of sustainable feedstock production by assessing the feasibility of establishing the bioenergy crop *Miscanthus* × *giganteus* with nurse crops. Current practice is to plant rhizomes of the sterile *M.* × *giganteus* into bare soil with 24 inches between plants. This planting method is fine on flat lands, but on sloped, marginal lands that are often targeted for bioenergy crops, soil erosion can be severe. In this project, we found that planting *M.* × *giganteus* into living cover (nurse crops) is an effective way to protect the soil during establishment, but comes at a severe yield penalty, reducing *M.* × *giganteus* biomass production by up to 90% in the first year. Through partnership with farmers and government agencies, we found that planting into dead cover, such as winter-killed oats in Iowa, might be a more effective strategy that not only protects the soil but also suppresses weed growth with minimal impact on *M.* × *giganteus* growth. Our findings will directly benefit the public by enabling farmers to protect soil and water resources while also producing abundant, renewable biomass feedstock for low-carbon, domestic energy. This project has produced not only the expected factsheets, presentations and primary data for peer-reviewed journal articles, but as importantly, it enabled new and cross-cutting collaborations between universities (Iowa State, University of Iowa, and University of Missouri), government agencies (DOE, USDA-ARS, NRCS) and stakeholders (farmers, landowners, energy providers).

2. Objectives

Objective 1: Identify nurse crops that a) facilitate *M. x giganteus* establishment and b) improve soil quality and function

Task A: Identify nurse crops that improve *Miscanthus x giganteus* survival and productivity (Ames, IA).

Expected results and impacts

We expected to find that:

- *Survival*: nurse crops insulated *M.* × *giganteus* from lethal winter temperatures, thus improving its winter survival
- *Weeds:* nurse crops suppressed weed growth, thus reducing herbicide requirements
- *Yield:* nurse crops had complimentary water use patterns, thus improving *M.* × *giganteus* yield through greater available soil moisture in dry periods
- *Propagule: Miscanthus* × *giganteus* planting propagule (rhizome or plug) would influence the above responses

Actual results and impacts

Survival: Nurse crops had no clear effect on *M.* × *giganteus* overwinter survival (Fig. 1). Generally, survival was near 100 %, except in 2010, when ~30 % of plugs were lost. This is because the plugs planted in 2010 had been severely heat-stressed during shipment when delayed by a major flood in Tennessee. We learned that plugs are quite tolerant of extreme temperatures

in storage (>100 F), at least for a few days.

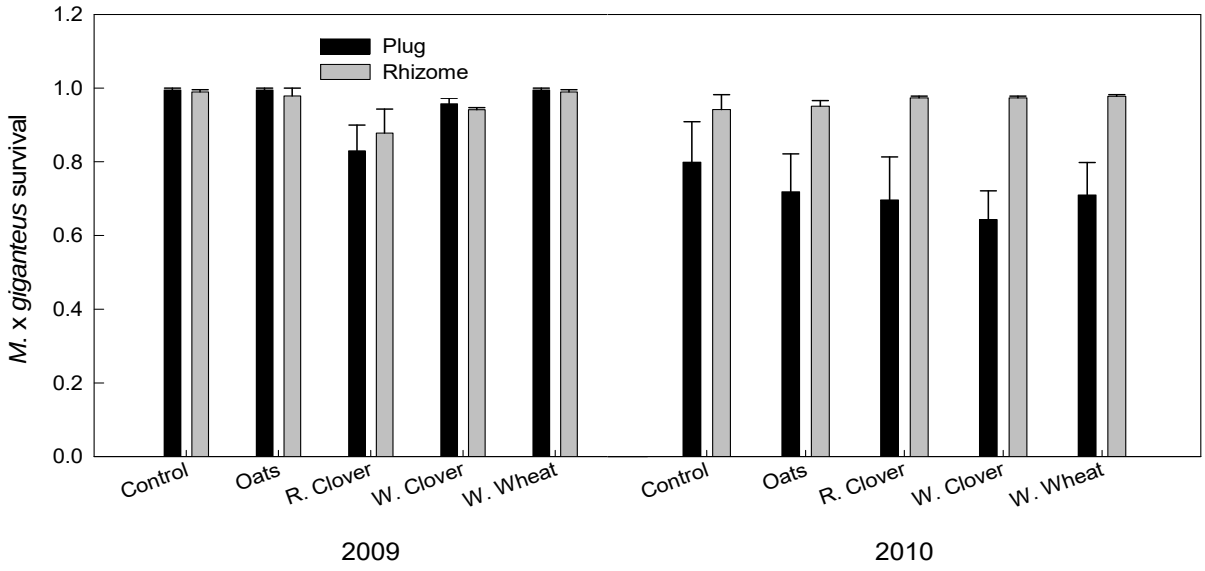

Figure 1. First-winter survival in M. × giganteus planted with four different nurse crops and a weed-free control. Year refers to the year in which the field was planted – both represent 1st year M. × giganteus stands. Propagule only influenced survival in 2010 ($p<0.001$) following damage to plugs during shipment (see Obj. 1 Task A).

Weeds: Nurse crops did suppress weeds, especially when combined with timely herbicide application, allowing fewer applications and/or less mechanical weed control (field cultivation; Fig. 2).

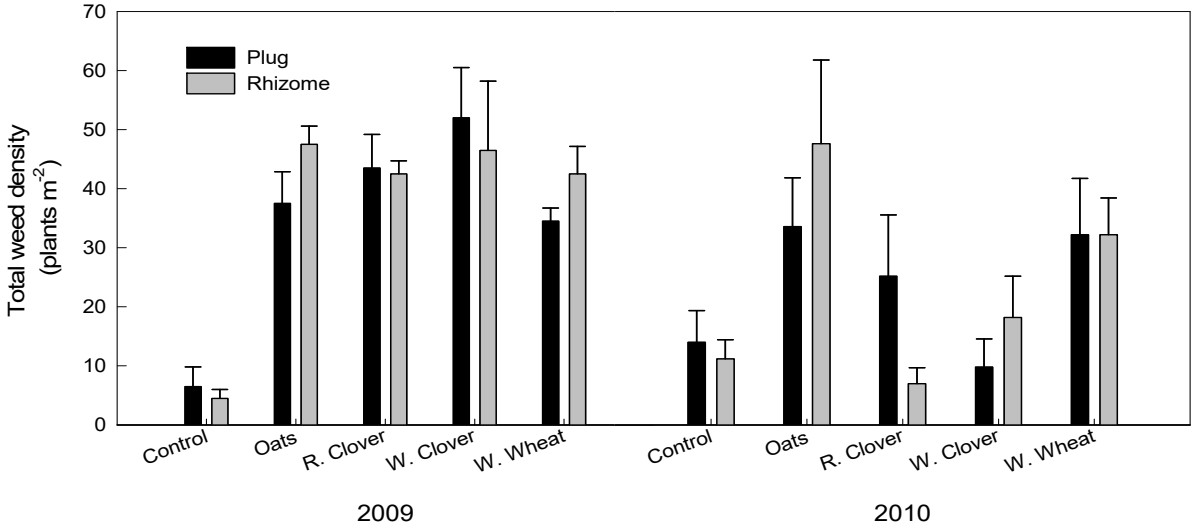

Figure 2. Weed density in M. × giganteus planted with four different nurse crops and a weed-free control. Year refers to the year in which the field was planted – both represent 1st year M. × giganteus stands. Year and cover crop both significantly impacted weed density ($p<0.001$).

- *Yield:* While nurse crop treatments caused differences in available soil moisture (e.g., Fig. 3) those differences did not improve *M.* × *giganteus* yield. In fact, nurse crops dramatically reduced *M.* × *giganteus* yields in the first year after growth (Fig. 4).
- *Propagule:* Generally, propagule type did not affect dependent variables of interest. When a significant propagule effect was found, in plant survival, for example, it was in 2011 and driven by the anomalous plug plants described above. This finding is also supported by complementary research in our group. Stimulated by this project Ph.D. student Nicholas Boersma (graduated 2013) found that propagule type did not influence survival over nine site years (Boersma & Heaton, 2014a), nor did it meaningfully impact plant development or morphology (Boersma & Heaton, 2014b). The fact that planting propagule type doesn't seem to matter to survival and yield is very good news for feedstock producers. Equal performance between plugs and rhizomes means that farmers can plant whichever propagule is most readily available and suitable to their equipment and conditions.

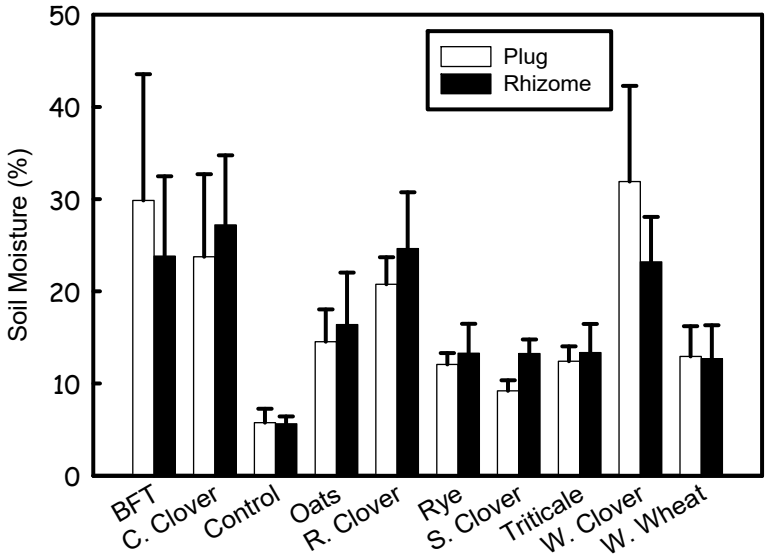

Figure 3. Soil moisture at 10 cm depth below *M.* × *giganteus* planted with four different nurse crops and a weed-free control. Year refers to the year in which the field was planted – both represent 1st year *M.* × *giganteus* stands.

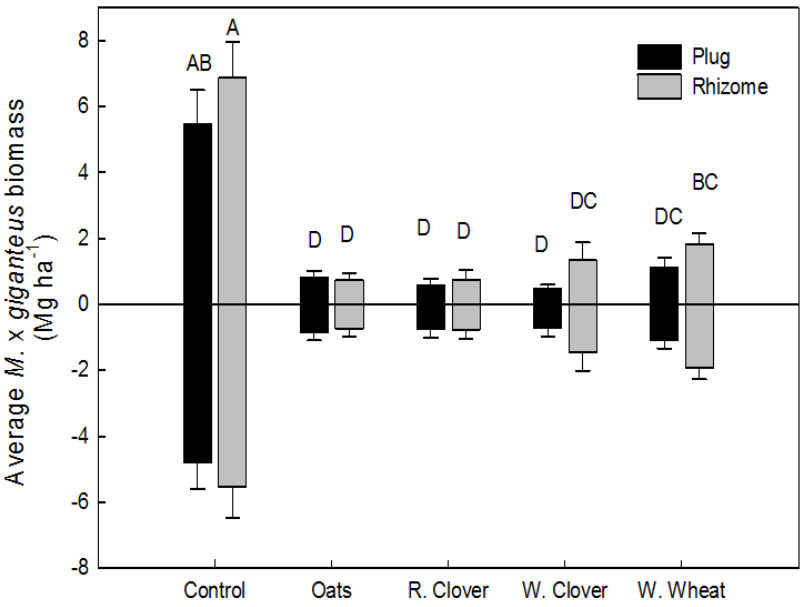

Figure 4. Dry (post-frost) biomass yield of *M.* × *giganteus* planted with four different nurse crops and a weed-free control. Year refers to the year in which the field was planted – both represent 1st year *M.* × *giganteus* stands. Below-ground biomass was excavated to 25 cm. Only nurse crop influenced biomass ($p<0.0001$).

Task B: Quantify preliminary changes in soil surface structure/function during *Miscanthus* x *giganteus* establishment with nurse crops (Ames, IA)

Expected results and impacts

- *Cover:* surface cover will be higher and develop faster under nurse crops than in sole-crop *M.* × *giganteus*.
- *Surface soil organic carbon (SOC):* SOC in the top 2 cm of soil will increase faster under nurse crops than in sole-crop *M.* × *giganteus*.
- *Leaf decomposition: M.* × *giganteus* leaf litter will decompose more slowly than maize (*Zea mays* L.), used as a baseline for agronomic residue.
- *Water infiltration:* water will infiltrate faster under nurse crops than in sole-crop *M.* × *giganteus*.

Actual results and impacts

- *Cover:* surface cover initially was higher under nurse crops than in sole-crop *M.* × *giganteus*, but by mid-season, had been overtaken as competition-free sole-crop plants grew more vigorously than nurse-cropped counterparts.
- *Surface soil organic carbon (SOC):* SOC in the top 2 cm of soil did not change significantly under nurse crops or under sole-crop *M.* × *giganteus*. As establishment is primarily a one to two year process, and cover crops were present for one year, the duration of cover crop biomass was insufficient to allow field measurements that could detect a significant soil organic carbon change. However, wet aggregate stability of the smallest aggregate size monitored improved with cover cropping (Fig. 5). Small aggregates would change the most rapidly as a function of management differences, further suggesting cover crops were having an impact, but duration was insufficient to detect changes in most measurements.

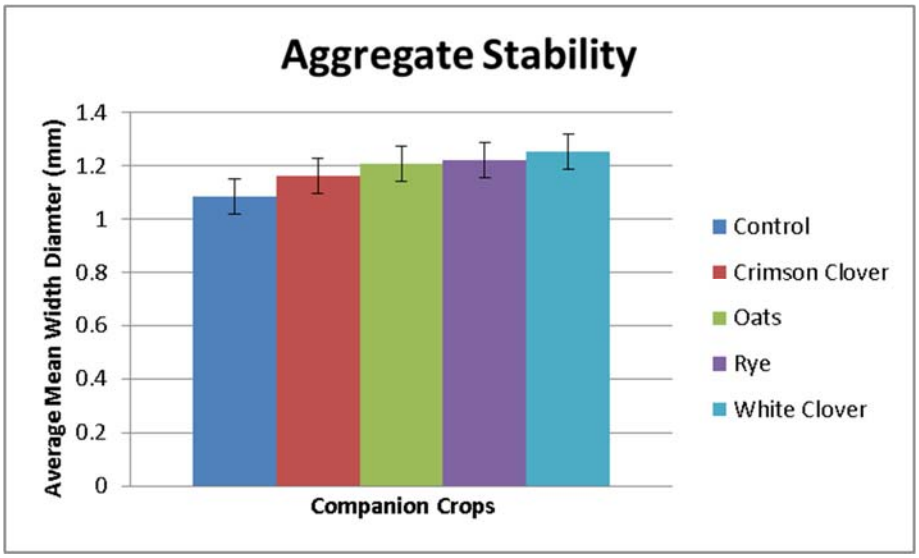

Figure 5. Aggregate size in surface (2 cm) soil under M. × giganteus planted with four different nurse crops and a weed-free control measured in July of the establishment year.

- *Leaf decomposition: M.* × *giganteus* leaf litter did not decompose more slowly than maize (*Zea mays* L.), used as a baseline for agronomic residue.

- *Water infiltration:* water infiltration rates were not significantly different between nurse crops and sole-crop *M.* × *giganteus*. One cycle of cover cropping was insufficient to induce sufficient macropore development and biological activity to significantly influence infiltration rates on these soils.

Objective 2: Raise awareness of *M.* × *giganteus* production potential and best management through outreach activities with stakeholders.

Expected activities and impacts:

- collaborate with ISU and Southwestern Iowa Community College (SWCC) professors and students to collect baseline data (GPS plot locations, soil erosion rates, soil nutrient and carbon content, residue cover, flora and fauna abundance, quality of adjacent water bodies) from prospective biomass plot demonstration sites.
- Analyze information from above and use to make land-use decisions to establish outreach trials on cooperator farms
- Establish companion crops recommended from the research trials (Obj. 1, Task A) at demonstration trial locations. In spring 2011, establish a suite of biomass crops at the demonstration plots.
- Hold field days during 2010 and a symposium over the winter of 2010-2011.

Actual activities and impacts:

- Because of funding delays, the breadth of data collection planned did not occur. Instead, NRCS soil maps and landowner knowledge were used to choose locations for demonstration trials. Further, during the duration of this project, co-PI left the USDA-ARS and co-PI DePoy was transferred within the USDA. Remaining personnel took over their objectives.
- A new trial based on that described in Obj. 1, Task A was established at the SWCC campus in Creston, IA.

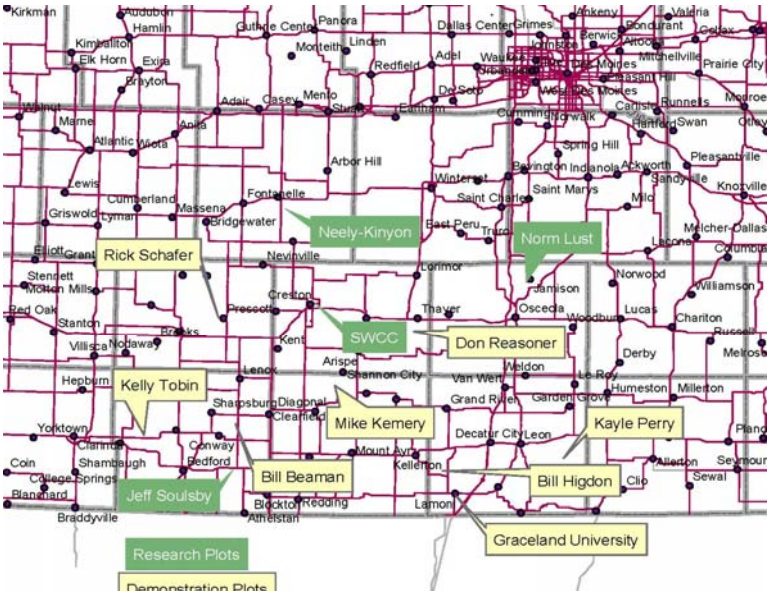

Figure 6. Demonstration trials of a suite of biomass crops including *Miscanthus* x *giganteus*, big bluestem and switchgrass were established without companion crops in southern Iowa during the spring of 2010 and 2011. Trials are conducted with collaborators ranging from community colleges and public farms to private landowners.

Companion crops (winter wheat and red clover) were planted in September, 2010. Only the wheat survived the winter. Plugs and rhizomes of *M.* x *giganteus* were planted into wheat and control plots on May 10, 2011. Separate trials of a suite of biomass crops including *M.* x *giganteus,* big bluestem and switchgrass that did not use companion crops were established on an adjacent plot of land and elsewhere in on-farm trials during the summer of 2011 and harvested in November 2011 (Fig. 6). Extreme drought (2012) and rainfall (2013) did not kill these plots (Fig. 7).

- The one-year extension of this project allowed us to conduct another year of workshops. We conducted one March 19, 2013 in Iowa City, Iowa, and the information from this project is being leveraged forward into the University of Iowa's Biomass Fuel Project (http://sustainability.uiowa.edu), with >200 acres planted for biopower in 2015. The SWCC plots have been used for class teaching and research experience at SWCC in class AGA 114, taught in 2013 by co-PI Davenport.

Figure 7. Co-PI Doug Davenport of the USDA NRCS indicates a plot of Miscanthus for harvest at the Jeff Soulsby farm near Bedford, IA, November, 2011.

3. Project activities

Project activity summary

For project activity details, please see the previous section.

This project enabled some of the first *M.* × *giganteus* work in Iowa, and created lasting partnerships that have supported Miscanthus research and application throughout the region. Results from this work were used to inform *M.* × *giganteus* establishment in Biomass Crop Assistance Program areas in Missouri in 2012 (>1000 acres planted), and then the University of Iowa Biomass Fuel Project, which is planting 2,500 acres for heat and power by 2017. Heaton was a new investigator at the time of this award, and now actively collaborates with the USDA in Columbia MO (co-PI on additional grants with Dr. Newell Kitchen investigated *M.* × *giganteus* on marginal soils in Missouri), as well as with the University of Iowa Biomass Fuel Project (co-PI on multiple submitted grants and presentations).

Problems encountered and departure from planned methodology

a. Funding delays precluded the in-depth data collection planned for site selection of demonstration trials. This has limited our ability to make inferences about the

likelihood that experiences from this project can be directly applied to other similar sites.

b. Budget cuts at the USDA RC&D lead to the departure of collaborator Mark DePoy, who was instrumental in developing on-farm collaborations. Further, USDA funding uncertainty lead to the departure of co-PI Dr. Jeremy Singer, instrumental in crop physiology data collection, who took a position with BASF in 2011. Though challenging, these departures have not significantly impacted the results generated with this funding.

4. Identify products developed under the award and technology transfer activities, such as:

a. Publications (list title, year, journal name, volume, issue, and page numbers), conference papers (name of conference; location of conference; date of conference; and conference sponsor), or other public releases or outreaches of results.

1. Boersma NN, Heaton EA (2014a) Does propagation method affect yield and survival? The potential of Miscanthus × giganteus in Iowa, USA. . *Industrial Crops and Products,* 57, 43-51.
2. Boersma NN, Heaton EA (2014b) Propagation method affects Miscanthus × giganteus developmental morphology. *Industrial Crops and Products,* 57, 59-68.

3. Wilson D.M.* & Heaton E.A. 2013. Giant *Miscanthus* Establishment. Iowa State University Extension publication. https://store.extension.iastate.edu/ItemDetail.aspx?ProductID=14006

4. Wilson D.M.* & Heaton E.A. 2013. Giant *Miscanthus* Eradication. Iowa State University Extension publication. https://store.extension.iastate.edu/ItemDetail.aspx?ProductID=13996

5. Wilson D.M.*, & Heaton E.A. 2013. Giant *Miscanthus* Weed Control. Iowa State University Extension publication. https://store.extension.iastate.edu/ItemDetail.aspx?ProductID=14000

b. Presentations

1. Heaton E.A., Boersma N.N.* Schulte L.A. & Wilson D.* (March 19, 3013) Perennial energy crops in Iowa. 3rd Annual Biomass Workshop. Iowa City, IA. 30 participants.

2. Heaton E.A., Schulte L.A. & Wilson D.* (March 12, 3013) Managing for bioenergy – integrating food and fuel production. Ag Education Day, Emmetsburg, IA, 130 participants.

3. Heaton E.A. (February 28, 2013) Perennial bioenergy crops benefit soil and water. University of Illinois Soil and Water Workshop, Taylorville, IL, 75 participants.

4. Heaton E.A. & Bonin C. (February 20, 2013) Perennials to the rescue! The Dirt on Dirt Soil Health Workshop, Lenox, IA, 78 participants.

5. Heaton E.A., Schulte L.A. & Milster F. 2013. Integrating food and fuel production in the Corn Belt. Kohn Lecture Series, University of Iowa, Iowa City, IA.

6. Heaton E.A. (Oct. 9, 2012) Perennial biomass scavenger hunt. AGA 114 lab, Southwest Iowa Community College, Creston, IA.

7. Heaton E.A. (Oct. 9, 2012) Introduction to biomass crops. AGA 114 lab, Southwest Iowa Community College, Creston, IA.

8. Boersma N. N.* & Heaton E.A. (June 27, 2012) Giant Miscanthus performance in Iowa, Northwest Iowa Research Farm Field Day, Sutherland, IA, 150 participants.

9. Heaton E.A., Berns B.* & Culp, C.* (June 20, 2012) Biomass crops for Iowa overview, Hay and Forage Expo, Boone, IA, 1000 participants.

10. Heaton E.A. (June 18, 2012) Iowa State University Early Outreach Program Intensive Program, Hinds Farm, Ames, IA, 60 participants.

11. Heaton E.A. (June 13, 2012) Ag Energy Workshop, BioCentury Farm, Ames, IA, 75 participants.

12. Heaton E.A. (April 5, 2012) Miscanthus propagation demonstration. In cooperation with Northwest Missouri State University, Hinds Farm, Ames, IA, 25 participants.

13. Heaton E.A., Singer J., Cruse R.M., Boersma N. & Davenport D. 2011. Miscanthus Production Practices: A New Missouri Bioenergy Crop. Special workshop, Columbia, MO.

14. Heaton E.A., Singer J., Cruse R.M., Boersma N. & Davenport D. 2011. Agronomic Issues for Giant Miscanthus. University of Missouri, Special seminar, Columbia, MO.

15. Heaton E.A., Singer J., Cruse R.M. & Davenport D. 2011. Under Cover: Secrets to Using Companion Crops in Establishment of *Miscanthus* × *giganteus.* Biomass & Energy Crops IV, Champaign, IL.

16. Heaton E.A., Singer J., Cruse R.M. & Davenport D. 2011. Under Cover: Secrets to Using Companion Crops in Establishment of *Miscanthus* × *giganteus.* Conservation Districts of Iowa Annual Meeting, Des Moines, IA.

17. Heaton E.A., Singer J., Cruse R., Davenport D. 2010 Under Cover: Secrets to Using Companion Crops in Establishment of *M.* x *giganteus.* In *Abstracts of the 2010 International Meetings* [CD-ROM] ASA-CSSA-SSSA, Madison, WI. ASA/CSSA/SSSA Annual Meeting, Long Beach, CA.

18. Heaton E.A. , Singer J., Dohleman F., Long S.P. 2010. Managing Perennial Monocultures for Ecosystem Services. Ecological Society of America Annual Meeting, Pittsburgh PA, p. 117.

c. Website or other Internet sites that reflect the results of this project.
http://www.agron.iastate.edu/faculty/heaton/
http://sustainability.uiowa.edu

d. Networks or collaborations fostered.
This project enabled multiple collaborations. Though the core PI team has evolved as members changed jobs (see above regarding DePoy and Singer), Heaton has continued to work with Davenport, District Conservationist for Taylor and Adams counties, on extension and outreach. They have also worked together with community college staff at SWCC to team-teach undergraduate lectures in AGA 114.

Miscanthus projects in Iowa and Missouri have been stimulated by this work, leading to the establishment of >1000 acres in MO and expected 2,500 acres in Iowa (200 planted in 2015). Heaton continues to collaborate with both groups, increasing multi-state collaboration and public-private partnerships that are fostering biomass adoption in the central US.

5. Academic

a. Courses developed – None.
b. M.S. students supported – 3 (Joyce Lok, Danielle Wilson, Muhammad Aurang Zaib)
c. M.S. degrees conferred - 2 (Danielle Wilson (2012), Muhammad Aurang Zaib (2012))
d. Ph.D. students supported - 1 (Nicolas Boersma)
e. Ph.D. degrees conferred - 1 (Nicolas Boersma (2013))
f. Post-docs supported – None.

6. For projects involving computer modeling, provide the following information with the final report:

- *Not applicable to this project*

a. Model description, key assumptions, version, source, and intended use.
b. Performance material for the model related to the intended use.
c. Test results to demonstrate the model performance criteria were met (e.g., code verification/validation, sensitivity analyses, history matching with lab or field data, as appropriate).
d. Theory behind the model, expressed in non-mathematical terms.
e. Mathematics to be used, including formulas and calculation methods.
f. Whether or not the theory and mathematical algorithms were peer reviewed, and, if so, will include a summary of the theoretical strengths and weaknesses.
g. Hardware requirements.
h. Documentation (e.g., user's guide, model code).

Please complete to reflect project at completion or time of report submission

ITEM	NUMBER	
Abstracts		
Peer Reviewed Publications	*2, with 1 in preparation*	
Outreach Publications /Web Pages	*4*	
Presentations	*18*	
MS Degrees Conferred	*2 conferred; related but not directly supported*	
Ph.D. Degrees Conferred	*1 Nicholas Boersma (2013) related but not directly supported*	
MS Students Supported	*3: Joyce Lok (in progress), Danielle Wilson (2012), Muhammad Aurang Zaib (2012)*	
Ph.D. Students Supported	*1: Nicolas Boersma (2013)*	
Disclosures	0	
Patents Filed	0	
Provisional Patents	0	
Patents Issued	0	
License Agreements	0	
Plant Variety Protection	0	
Investigators Supported	Emily Heaton, Jeremy Singer, Richard Cruse, Doug Davenport	
Post-Docs Supported	None	
Graduate Students Supported	4 total; See MS and PhD students	
Undergraduate Students Supported	7 total	
Start-Up Jobs Created	0	

Back to Table of Contents

Sun Grant Initiative
DOE Final Report

Project Title: Sustainable Biomass Production on Marginal Lands using a Novel Legume/Grass Mixture

Project Director/Principal Investigator: Vance Owens, Plant Science Department, South Dakota State University, Brookings, SD

All Co-Principal/Other Investigators: Kenneth A. Albrecht, Department of Agronomy, University of Wisconsin-Madison, Madison, WI; DoKyoung Lee, Department of Crop Sciences, University of Illinois, Champaign, IL; Craig Sheaffer, Department of Agronomy and Plant Genetics, University of Minnesota, St. Paul, MN; Senthil Subramanian and Sandeep Kumar, Plant Science Department, South Dakota State University, Brookings, SD

Period of Performance: 1 July 2010 - 31 July 2014

Funding Awarded: $646,021

Cost Share Amount: $162,864

Cost Share Sources: Time and effort from PIs and CoPIs; Indirect on time and effort

Executive Summary

Optimizing the application of N fertilization and proper N management is an important factor for biomass production systems. However, increases in N fertilizer cost and the negative environmental impacts of chemical fertilizers have prompted the use of legumes as a source of N in sustainable biomass production systems. Objectives for this study were to 1) determine N fertilizer replacement value of kura clover (*Trifolium ambiguum* Bieb.) (KC) in a prairie cordgrass (*Spartina pectinata* Link.) (PCG)-kura clover mixed sward compared to monoculture prairie cordgrass fertilized with varying rates of N; and 2) determine fermentable cell wall fractions, N content, mineral composition, and sward composition of prairie cordgrass-kura clover mixtures and prairie cordgrass monocultures over time. Yields varied by location and ranged from 6.4 to 16.6 Mg ha^{-1}. Nitrogen rate, year, and plant spacing affected PCG production at all locations. Yield of PCG with 0 N was equal to or less than the yield of PCG grown with KC at all locations the first two years after establishment; however, there was a N value associated with PCG grown with KC in the third year. In fact, the FNRV of KC ranged from 25 to 82 Kg N ha^{-1} in the third year. Nitrogen application significantly affected mineral composition, cell wall composition and TEY at most locations. PCG and KC mixtures had less desirable mineral concentrations, cell wall compositions and TEY than PCG monocultures. Variability in TEY ha^{-1} was much greater than TEY Mg^{-1} due to yield differences across years and locations. It appears that including a legume such as KC with PCG may provide economic and environmental benefits. However, further evaluation is required to ascertain the specific level of KC to include in such a mixture in order to avoid excessive competition while providing maximum FNRV.

Project Objectives

Objective 1*: Determine N fertilizer replacement value of kura clover in a prairie cordgrass-kura clover mixed sward compared to monoculture prairie cordgrass fertilized with varying rates of N.*

Objective 2: *Determine fermentable cell wall fractions, N content, mineral composition, and sward composition of prairie cordgrass-kura clover mixtures and prairie cordgrass monocultures over time.*

Project Activities by Objective

Objective 1: *Determine N fertilizer replacement value of kura clover in a prairie cordgrass-kura clover mixed sward compared to monoculture prairie cordgrass.*

Due to different environmental conditions, biomass production of PCG varied by location and year (Fig. 1), but the highest yields were generally at the WI location followed by MN, SD, and IL. The low yields at IL are probably a result of using PCG germplasm derived from SD that was not well adapted in IL. DoKyoung Lee (personal communication) has since identified better adapted and higher yielding PCG germplasm (more than 20 Mg ha^{-1}) from that area.

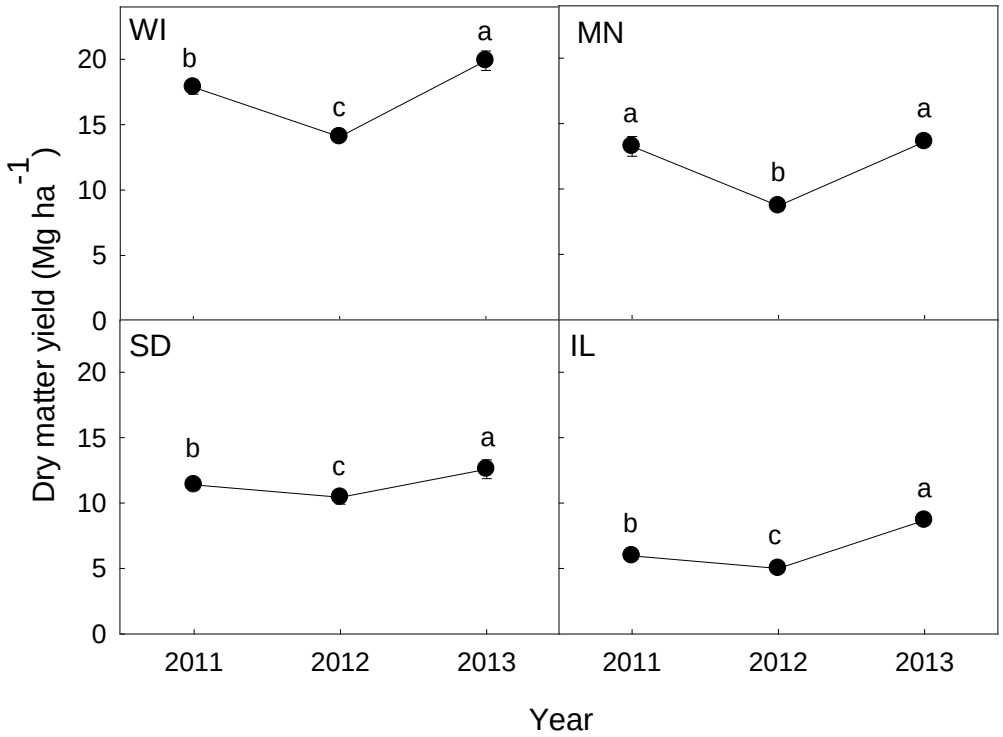

Fig. 1. The effect of year on biomass yield of PCG at each location. Data were averaged across PCG row spacing and N (urea) rates.

A significant year x spacing interaction was observed for PCG yield at each location (Fig. 2). Biomass yield for the first production year in 60-cm plant spacing was higher than that in 90-cm row spacing at all locations in 2011. However, due to the strongly rhizomatous capacity of PCG, biomass yield of PCG in 60- and 90-cm rows was equal at all locations by 2013.

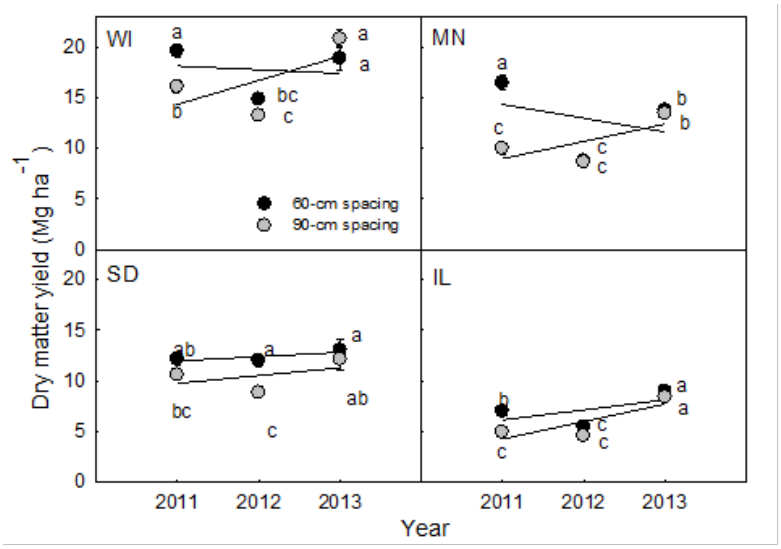

Fig. 2. PCG spacing x year interaction effect on yield of PCG at each location. Data were averaged across N rates.

Yield of PCG monocultures increased with N rate at all locations (Fig. 3). For all locations except IL, PCG yield was highest at either the 150 or 225 kg N ha^{-1}. There was no benefit to N above 75 kg ha^{-1} at IL, however, which was likely due to lower overall PCG yields generally.

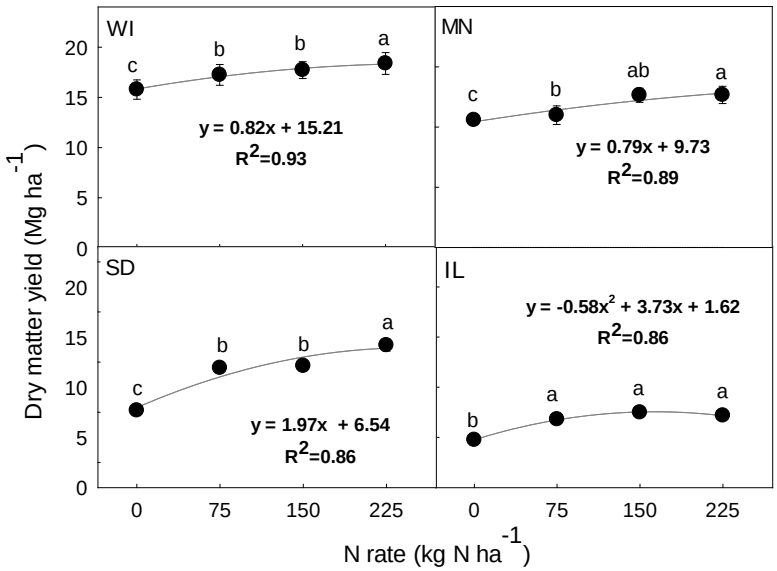

Fig. 3. Nitrogen effect on monoculture PCG yields at four locations. Data are averaged over three years and two plant spacings.

Averaged across plant spacing, biomass yield of PCG monocultures with 0 kg N ha^{-1} tended to be stagnant or decrease over years. In contrast, biomass yield of PCG-KC mixtures generally increased over time at all locations (Fig. 4). In 2011, biomass yield of PCG monoculture with 0 kg N ha^{-1} at each location was greater than that of PCG-KC mixture except for SD, MN which had similar biomass yield between PCG monoculture with 0 kg N ha^{-1} and PCG-KC mixtures. In 2012, biomass yield in both PCG monoculture with 0 kg N ha^{-1} and PCG-KC mixture was the same at MN, SD and IL except for WI. In 2013, biomass production from PCG-KC mixtures was higher than the PCG monoculture with 0 kg N ha^{-1} at all locations (Fig. 4). The FNRV varied among locations in 2013 and it was highest in MN (82 kg ha^{-1}) and lowest in WI (25 kg ha^{-1}).

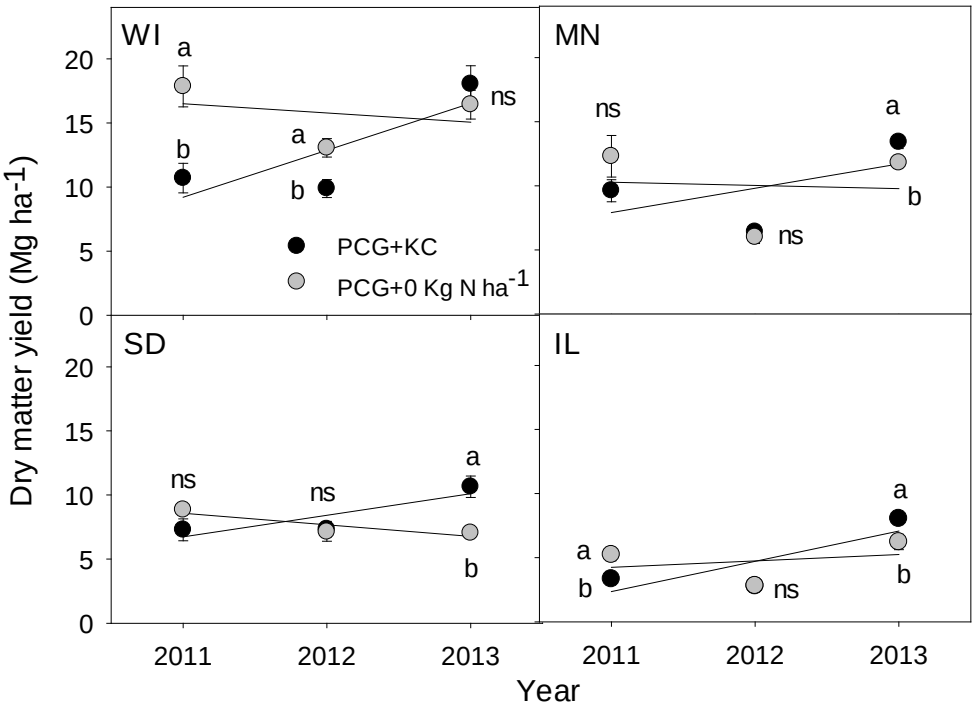

Fig. 4. Biomass yield of PCG monoculture (0 kg N ha^{-1}) and PCG-KC mixtures over three years. Data were averaged across plant row spacing.

Objective 2: *Determine fermentable cell wall fractions, N content, mineral composition, and sward composition of prairie cordgrass-kura clover mixtures and prairie cordgrass monocultures over time.*

Prairie cordgrass biomass at each location was sampled in the fall in 2011, 2012 and 2013. Nitrogen application significantly affected mineral composition, cell wall composition and Theoretical Ethanol Yield (TEY) at most locations. Prairie cordgrass-KC mixtures had less desirable mineral compositions (i.e., generally higher levels of N, P, K, S, and Ca; Table 1) and cell wall compositions (i.e., lower levels 5- and 6-C sugars; Table 2) than PCG monocultures. Also, TEY Mg^{-1} biomass and TEY ha^{-1} was lower for PCG-KC mixtures than that for prairie cordgrass monocultures (Table 3). Most of the differences in TEY ha^{-1} were due primarily to yield variability between PCG and PCG-KC, especially since PCG-KC yields were particularly low in the first two years. We believe this difference will be overcome eventually if KC can provide the type of FNRV seen in the third year of this study; however, more research is required to ascertain this.

Table 1. Mineral composition of prairie cordgrass as affected by N rate. Values are averaged over three years and two plant spacings.

	N	P	K	S	Ca	Mg	Na
	g kg^{-1}						
By N (kg ha^{-1} for urea rate)	WI						
KC†	8.32 a	1.42a	8.13 a	1.13 a	4.21 a	1.61 a	0.081 bc
0	5.45 c	1.08 b	7.08 b	1.02 bc	2.58 b	1.40 b	0.069 c
75	7.20 b	0.80 c	7.38 ab	1.19 a	2.89 b	1.56 ab	0.100 ab
150	7.62 ab	0.81 c	7.51 ab	1.02 bc	3.04 b	1.71 a	0.106a
225	7.83 ab	0.74 c	7.92 ab	0.98 c	3.00 b	1.61 a	0.094 ab
	MN						
KC	7.43 ab	1.80 a	5.93 ab	0.85 a	3.33 a	1.43 a	0.0050 c
0	4.17 d	1.26 b	5.30 b	0.85 a	2.52 b	1.27 b	0.0050 c
75	5.49 c	1.10 c	5.49 b	0.75b	2.48 b	1.25 b	0.0062 bc
150	6.83 b	0.97 cd	5.73 b	0.71 bc	2.60 b	1.31 ab	0.0081 ab
225	7.70 a	0.95 d	6.60 a	0.66 c	2.66 b	1.40 a	0.0087 a
	SD						
KC	2.99 b	0.60 a	4.18	1.22 b	2.03 a	1.78 ab	0.125 bc
0	2.60 b	0.56 ab	4.04	1.01 c	1.79 b	1.41 c	0.081 c
75	2.99 b	0.45 c	4.34 ns	1.21 b	2.18 a	1.61 b	0.125 bc
150	3.13 ab	0.47 bc	4.53	1.49 a	1.99 ab	1.67 ab	0.150 b
225	4.26 a	0.41 c	4.23	1.63 a	1.98 ab	1.83 a	0.231 a
	IL						
KC	4.36 b	1.32 a	2.95 a	0.75 ab	3.54	1.10 a	0.0006
0	3.76 c	1.08 b	2.23 d	0.70 bc	3.23	1.06 ab	0.0000
75	3.76 c	1.01 b	2.49 c	0.67 c	3.28 ns	1.00 b	0.0000 ns
150	4.51 ab	0.88 c	2.69 bc	0.71 bc	3.53	1.06 ab	0.0000
225	4.96 a	0.89 c	2.90 bc	0.78 a	3.57	1.11 a	0.0012

†, Kura clover

Within columns and location, different letters differ significantly at $p \leq 0.05$.

Table 2. Cell wall composition, 5- and 6 C sugars, and theoretical ethanol yields of prairie cordgrass monocultures with added N compared to prairie cordgrass-kura clover mixtures.

	Klason lignin	Cellulose	Hemi-cellulose	Carbohydrate		§TEY	TEY
				5C	6C		
			g kg^{-1}			L Mg^{-1}	L ha^{-1}
By N (kg ha^{-1} for urea rate)				WI			
KC†	165.2	287.7 c	247.7 d	237.9 c	306.8 c	91.4 c	943.5 c
0	164.8	311.3 a	260.0 a	252.7 a	327.0 a	97.5 a	1502.6 ab
75	163.9 ns	301.7 b	254.0 c	245.6 b	318.7 b	94.8 b	1442.0 b
150	166.4	307.2 ab	258.5 ab	249.2 ab	325.2 ab	96.5 ab	1602.7 a
225	165.9	305.9 ab	255.5 bc	247.0 b	322.9 ab	95.8 ab	1596.4 a
				MN			
KC	174.7 c	314.7 c	267.8 b	258.7 c	333.0 b	99.84 c	991.4 c
0	178.9 b	329.1 a	273.4 a	267.2 a	344.8 a	103.2 a	1045.9 c
75	182.3 a	327.2 ab	274.2 a	268.6 a	344.2 a	103.0 a	1226.5 b
150	182.7 a	326.7 ab	273.1 a	263.8 b	345.0 a	102.7 a	1259.0 ab
225	181.4 ab	323.6 b	269.6 b	260.0 c	341.8 b	101.6 b	1356.9 a
				SD			
KC	169.8	306.6 bc	269.0	265.3	318.8 bc	98.6 b	848.5 c
0	172.9	305.1 c	270.2	266.3	317.9 c	98.6 b	768.8 c
75	172.1 ns	310.9 abc	272.5 ns	268.6 ns	323.3 abc	100.0 a	1202.3 b
150	172.1	311.7 ab	270.5	266.4	324.0 ab	99.72 ab	1418.6 b
225	175.9	315.6 a	270.3	265.6	328.5 a	100.3 a	1429.5 a
				IL			
KC	183.2 b	330.7	283.9 ab	276.9 ab	348.5 ab	105.1	497.1 c
0	179.3 c	326.9	285.9 a	279.7 a	344.1 b	104.8	512.9 c
75	182.5 b	326.1 ns	284. 4 a	277.6 a	344.4 ab	104.5 ns	662.1 b
150	185.0 b	327.6	281.1 bc	273.8 bc	346.3 ab	104.1	772.9 a
225	188.2 a	330.2	280.1 c	282.1 c	349.2 a	104.3	724.4 b

†, Kura clover; §TEY, theoretical ethanol yield.
Within columns and location, different letters differ significantly at $p \leq 0.05$.

Publications

Presentations

Owens, V.N., S.U. Kim, S. Subramanian, K.A. Albrecht, D.K. Lee, C. Sheaffer. 2015. Prairie cordgrass (*Spartina pectinata* Link.) yield response to urea N or when grown with kura clover (*Trifolium ambiguum* Bieb.) as a N source. 2015 European Biomass Conf. and Exhibit., Vienna, Austria, 1-4 June 2015.

Kim, S., V. Owens, K. Albrecht, D. Lee, and C. Sheaffer. 2014. Biomass production of prairie cordgrass using urea and kura clover as a source of nitrogen. 20th World Congress of Soil Science, 8-13 June 2014, Jeju, Korea.

Kim, S.U., V.N. Owens, K.A. Albrecht, D.K. Lee, C.C. Sheaffer, and S. Subramanian. 2013. Biomass production of prairie cordgrass using urea and kura clover as a source of nitrogen. ASA-CSSA-SSSA Annual Meetings, 3-6 Nov., Tampa, FL.

Kim, S.U., V.N. Owens, K.A. Albrecht, D.K. Lee, C. Sheaffer, and S. Subramanian. 2013. NC Sun Grant Annual Meeting, Chicago, IL, 26-27 March 2013.

Kim, S.U., V.N. Owens, K.A. Albrecht, D.K. Lee, C. Sheaffer, and S. Subramanian. 2012. Biomass production of prairie cordgrass using kura clover as a source of nitrogen. 2012 National Sun Grant Conference, New Orleans, LA, 2-5 Oct. 2012.

Owens, V.N., S.U. Kim, K.A. Albrecht, D.K. Lee, C.C. Sheaffer, and S. Subramanian. 2012. Sustainable biomass production on marginal lands using a novel legume/grass mixture. 2012 European Biomass Conf. and Exhibit., Milan, Italy, 18-22 June 2012.

Academic

Ph.D. students supported: Sung Un Kim
Ph.D. degrees conferred: Sung Un Kim
Post-docs supported: Chang Oh Hong

Back to Table of Contents

Sun Grant Initiative
DOE Final Progress Report

Project Title: Evaluation of Bioenergy Crop Production on Marginal Land in Wisconsin

Project Director/Principal Investigator: Stephen J. Ventura, Professor, Department of Soil Science and Nelson Institute for Environmental Studies, University of Wisconsin-Madison, Madison WI

All Co-Principal/Other Investigators: Bradford Barham, Department of Agricultural and Applied Economics, Randy Jackson, Department of Agronomy, University of Wisconsin- Madison, Madison WI (original grant included Randal Fortenberry; he left UW).

Period of Performance: 1 July 2010 - 30 September 2014

Funding Awarded: $667,299

Cost Share Amount: $166,528

Cost Share Sources: Time and effort from PIs and CoPIs; Indirect on time and effort

1. Executive Summary

The overall goal of this project was to provide information about costs and benefits of bioenergy crop production from economic and ecological perspectives, with focus on environmental and financial tradeoffs of agricultural activities on marginal lands at a variety of scales. We focused on marginal lands in southwest Wisconsin because these were perceived as a means to avoid "food versus fuels" arguments (to minimize using land capable of producing economically viable yields of food and fiber crops). We evaluated impacts and benefits in environmental and monetary terms because both can have a substantial impact on decision-making.

Specific findings were generated from each of three primary objectives, with implications for two outreach objectives:

- Ecosystem services associated with bioenergy cropping systems on environmentally sensitive land were modeled at regional and watershed scales. Cropping scenarios that converted sensitive lands currently in row crop production to perennial crops such as switchgrass generated substantially greater ecosystem benefits in terms of water quality, soil erosion, greenhouse gas sequestration, and wildlife (pollinator) habitat.

- Based on mail surveys to farmers and non-farming rural land owners in southwest Wisconsin, we were able to construct cost curves that reflected farmers willingness to grow bioenergy crops. In general terms, getting farmers to switch to bioenergy crops would require a substantial subsidy or increase in current market prices, particularly farmers with integrated crop-livestock systems such as dairy operations. Fewer than one-third of farmers would even consider including bioenergy crops in their cropping systems.

- Based on mail surveys and in-person interviews, we identified characteristics of farms and farmers associated with likelihood of adopting bioenergy crops. These included amount of marginal land (slight positive association), type of cropping system (negative for integrated crop-livestock systems), age (younger is more likely) and education of farmer (more educated is more likely), familiarity with bioenergy crops (more familiar is more likely), and non-farm family income (more non-farm income is more likely).

- We generated four distinct options for stimulating bioenergy crop production (demand driven by national markets, public policy/incentives, local or regional facilities, and on- farm use). Interviews with officials, entrepreneurs, farmers, and non-farming land owners indicated that farm gate price was the primary determinant of willingness to adopt bioenergy crops; respondents were mostly indifferent to the type of activity (policy or market demand driver) that would lead to prices competitive with other crops. Both land owners and policy-makers noted that the rapid decline in natural gas prices since the development of this research proposal (circa 2009) has substantially reduced the likelihood of bioenergy crop production in Wisconsin absent substantial incentives or subsidies.

- We worked with state agency staff to develop a manual on safe and sustainable production of bioenergy crops on sensitive landscapes, now adopted and distributed by the Wisconsin Bioenergy Council.

2. Project objectives

Objective 1 - Quantify ecosystem services associated with bioenergy cropping systems on environmentally sensitive land.

From Meehan et al (2013):
Integration of energy crops into agricultural landscapes could promote sustainability if they are placed in ways that foster multiple ecosystem services and mitigate ecosystem disservices from existing crops. We conducted a modeling study to investigate how replacing annual energy crops with perennial energy crops along Wisconsin waterways could affect a variety of provisioning and regulating ecosystem services.

We found that a switch from continuous corn production to perennial-grass production decreased annual income provisioning by 75%, although it increased annual energy provisioning by 33%, decreased annual phosphorous loading to surface water by 29%, increased below-ground carbon sequestration by 30%, decreased annual nitrous oxide emissions by 84%, increased an index of pollinator abundance by an average of 11%, and increased an index of bio-control potential by an average of 6%. We expressed the tradeoffs between income provisioning and other ecosystem services as benefit-cost ratios. Benefit-cost ratios averaged 12.06 GJ of additional net energy, 0.84 kg of avoided

phosphorus pollution, 18.97 Mg of sequestered carbon, and 1.99 kg of avoided nitrous oxide emissions for every $1,000 reduction in income. These ratios varied spatially, from 2- to 70-fold depending on the ecosystem service.

Benefit-cost ratios for different ecosystem services were generally correlated within watersheds, suggesting the presence of hotspots – watersheds where increases in multiple ecosystem services would come at lower-than-average opportunity costs. When assessing the monetary value of ecosystem services relative to existing conservation programs and environmental markets, the overall value of enhanced services associated with adoption of perennial energy crops was far lower than the opportunity cost.

However, when we monetized services using estimates for the social costs of pollution, the value of enhanced services far exceeded the opportunity cost. This disparity between recoverable costs and social value represents a fundamental challenge to expansion of perennial energy crops and sustainable agricultural landscapes.

Objective 2: Construct spatially specific estimates of both economic returns and ecological services for bioenergy crop alternatives;

From Diehl thesis (2014):
Perennial bioenergy crops provide different ecosystem services (food and
fuel production, carbon sequestration, erosion control, nutrient cycling) from those provided by traditional row crops and the delivery of these services varies depending on location (soil type, topography, etc). Strategic placement of perennial bioenergy crops on the landscape can maximize ecosystem services, while minimizing opportunity costs. However, because of social and economic factors, not all land managers are equally willing to convert land to perennial bioenergy crops. We developed a computer program to combine modeled ecosystem service data with survey-derived probabilities of conversion to find target areas where perennial bioenergy crops could provide the highest environmental benefit for the lowest economic cost.

This represented a method of selecting the most likely land to provide benefits, a form of optimization.

Our results suggested locations for biomass crops clustered in areas with high soil organic carbon -- traditional row crops in these locations have the potential to lose a large amount of carbon, whereas perennial biomass crops potentially protect and increase soil organic carbon. When farmer willingness to convert was considered, the suggested locations for biomass crops clustered even further. At current prices for perennial biomass, these energy feedstock crops represent a significant opportunity cost when compared to corn. Hence, to reach target quantities of biomass production, policies that incentivize planting of these crops for their provisioning of ecosystem services are likely necessary. Bioenergy policies should be aimed at the "hotspots" where ecosystem services and farmer willingness converge and the decision support tool offered here should facilitate these landscape configurations.

Objective 3 - Provide dynamic descriptive and behavioral analyses of agricultural land use patterns oriented to biomass production, including productivity and returns to producers

From Mooney and Hunt dissertations (2014):
We assessed farmer and non-farming rural landowner willingness to grow three bioenergy crops – corn stover, switchgrass, and hybrid poplar – in southwestern Wisconsin through a mail-out survey to about 1500 farmers and 1200 landowners.

Details of the farm survey are provided in Mooney et al. (2013); non-farming landowner responses are still being processed, though preliminary results are similar.

From the willingness to pay questions and economic analysis, we developed empirically-grounded supply curves for energy biomass from corn stover and switchgrass. From belief and behavior questions, we characterized farm and non-farm rural landowners who are likely to be early innovators or 'adopters' or bioenergy cropping systems.

Broad findings include:

- even at the highest biomass prices considered, the overall share of farms interested in growing a bioenergy crop is estimated to be below 30%, across farm types and bioenergy crops;

- farmers showed a wide range of variability in terms of the price at which farms first enter bioenergy markets, with large livestock farms and dairy farms being the first to enter the market for all three crops, though these are also generally less responsive to price increases compared to crop farms and small livestock farms;

- farmers are willing to dedicate only a small amount of land to bioenergy crops, 11% of total acreage in our sample, typically in small plots of existing cropland.

Ecological and farming system data were combined in development of a combined biophysical and socioeconomic logistic regression model for identifying and estimating significant drivers of bioenergy feedstock choice for corn stover and switchgrass.

A general logistical choice model was specified to include explanatory variables including biophysical landscape, operation and operator characteristics, environmental attitudes and perspectives, and price points for the proposed bioenergy feedstock. Two models were generated

to estimate the choice drivers for both corn stover and switchgrass because the two feedstocks differ significantly in their operational requirements and land constraints.

Results from mail surveys to revealed that there is a prevalent lack of interest to proposed corn stover or switchgrass feedstock programs, with 65% of farmers stating that they would not enroll in any of the proposed bioenergy feedstock programs. Among those who stated willingness to participate in a proposed corn stover management program, significant ($p < 0.10$) drivers of bioenergy feedstock choice included age, amount of open acreage, percentage of operational acres that are moderate to steeply sloped, having a history of water quality management on farm, and a willingness to make tradeoffs in economic certainty for environmental benefit. Among those who are willing to participate in a proposed switchgrass management program, significant ($p < 0.10$) drivers included raising dairy cattle, age, having an income of $100,000 or greater, percentage of operational acres with marginal characteristics, history of soil quality management on farm, familiarity with switchgrass as a bioenergy feedstock, and an expressed willingness to make tradeoffs in economic certainty for environmental benefits.

Objective 4 - Elicit public policy options for promoting bioenergy crops and evaluate their potential for adoption based on projected behavioral responses from producers

We provided findings to public policy stakeholders, and solicited their input on development of potential scenarios for bioenergy price or market supports.

The gist of the findings provided to policy makers and other bioenergy stake holders is that energy biomass supply from marginal lands is likely to be price inelastic and spatially fragmented. In particular, rural landowners in SW WI would prefer to grow energy biomass crops on existing cropland rather than on non-crop marginal lands.
This outcome suggests that policy prescriptions that seek to limit energy biomass production on marginal lands are not likely to be economically feasible.

Farmers and land owners generally responded to price signals as expected, though as noted above, at low rates. They were generally aware of bioenergy crops, and many participate in other programs related to public support for activities that improve ecosystem services (e.g., USDA Conservation Reserve Program, WI Managed Forest Law, etc.). However, very few were motivated to consider participation in a bioenergy cropping scenario based solely on potential ecosystem benefits such as reduced greenhouse gas generation, improved water quality, or improved wildlife habitat.

Objective 5 - Provide guidance on safe and sustainable production of bioenergy crops on sensitive landscapes

From Ventura et al. (2012):
A working group comprising university and state agency staff created a set of guidelines for sustainable production of nonforest biomass, including crop residue, dedicated bioenergy crops, short-rotation woody crops, and incidental use of biomass from non- cropped open land. The impetus for creating this document is growing interest in use of biomass for energy through combustion or conversion to other forms of fuel. The guidelines provide practical information for producers about site selection, planting, management, and harvesting. They also provide broader discussions of ecosystem service tradeoffs and landscape scale dynamics of bioenergy cropping that will be useful for communities, entrepreneurs, and policy-makers. The guidelines are voluntary, oriented to sustainability, particularly environmental aspects, and based on the

best- available science. They have been adopted by the Wisconsin Bioenergy Council.

3. Project activities

The main project activities were:

1) Multi-county modeling of ecosystem services and net returns under multiple land use scenarios, using INVEST and several add-on models. The major barriers were acquiring sufficiently detailed spatial data to provide watershed and farm-scale estimates. This was accomplished by acquiring, screening, processing, and integrating many data sources. The results were very useful and detailed information about cash and ecosystem service benefits and costs, and opportunity costs associated with potential bioenergy cropping patterns.

2) County-scale optimization modeling of crop income and ecosystem services under bioenergy cropping land use changes with a project-developed tool. The programming involved selecting potential "land use change" cells, based on optimization of results of multiple existing models and indices of ecological and economic benefits. This tool is being incorporated in a "dash board" for decision-makers to understand and evaluate potential land use changes associated with bioenergy cropping scenarios.

3) Farm-scale ecosystem service tradeoffs, using a fine-scale modeling tools including RUSLE-II, SNAP-Plus, and FRAGSTAT. A Quantum-GIS based program was developed to conduct farm-scale analysis of changes on selected farms, associated with adoption of various patterns of bioenergy cropping. The tool was completed and linked with FRAGSTAT (habitat and landscape ecology metrics), and output polygons fed into SNAP-Plus (nutrient analysis model) and RUSLE-II (soil erosion model). However, this process was used only to validate broader scale modeling efforts, not to look at aggregate effects of multiple farm changes in a concentrated area as originally proposed due to insurmountable logistic challenges associated with time and effort at such fine scale.

4) Mail-out surveys went to about 1500 farmers and 1200 non-farming rural land owners to ascertain interest in participation in potential bioenergy crop production. Response rates were about 40% and 35%, and follow up analysis showed no non-response bias, indicating this was an adequate sample to characterize key response variables. The results were used to characterize price points where farmers might be interested in growing bioenergy crops and to understand biophysical variables and farmer/land owner characteristics associated with proclivity to adopt bioenergy crops.

5) "Kitchen table" interviews were conducted with about 50 farmers and non-farming rural land owners to generate more nuanced understanding of response patterns from the surveys. The interviews were not formally analyzed, but were used as anecdotal evidence to bolster findings from the survey process.

6) Project faculty guided development of a manual on safe and sustainable bioenergy crop production now adopted and distributed by state agencies.

4. Products developed under the award:

a. Publications and Presentations

Barham, B., D. Mooney, D. Prager, S. Swinton, T. Skevas, and S. Tanner. Economic "Availability of Private Lands for Bioenergy Crop Production: Looking Towards the Northern Tier." Poster presented at the 8th Annual GLBRC Science Retreat. South Bend, IN, May 20-22, 2014.

Barham, B.L. D.F. Mooney, C. Lian, T. Meehan, R. Jackson, S. Ventura, and N. Hunt. "Supply Prospects for Bioenergy Crop Production on Marginal Land in Southwest Wisconsin." 6th Annual Retreat of the Great Lakes Bioenergy Research Center, Chicago, IL, May 21-23, 2013.

Hull, S., J. Arntzen, K. Bleser, A. Crossley, R. Jackson, E. Lobner, L. Paine, G. Radloff, C. Ribic, D. Sample, J. Vandenbrook, S. Ventura, S. Walling, J. Widholm, and C. Williams. "Wisconsin Sustainable Planting and Harvest Guidelines for Nonforest Biomass." Wisconsin Bioenergy Council, adopted July 2011, 88 pages.

Meehan, T. D., C. Gratton, E. Diehl, N. D. Hunt, D. F. Mooney, S. J. Ventura, B. L.Barham, and R. D.Jackson. 2013. Ecosystem-service tradeoffs associated with switching from annual to perennial energy crops in riparian zones of the US Midwest. PLOS ONE 8:e80093. PDF.

Mooney, D., B. L. Barham, and L. Chang (/201x). "Inelastic and fragmented farm supply response for sustainable biofuel crops: Ex Ante survey evidence from Wisconsin," Applied Economic Perspectives and Policy, (resubmitted 4/2014)

Mooney, D., B. L. Barham, and L. Chang, S. Ventura, N. Hunt, T. Meehan, R. Jackson. (2013). Current Prospects for Bioenergy Crop Production on Marginal Lands: Results from a Farm Survey in Southwestern Wisconsin. University of Wisconsin- Madison, Department of Agricultural and Applied Economics, Staff Paper No. 569, July 2013, 11p.

Mooney, D. E. Barham, B. Barham, T. Meehan, R. Jackson, S. Ventura, N. Hunt. "Economic Responses of Non-Farm Rural Landowners to Bioenergy Cropping Opportunities." Poster presented at the 2014 GLBRC Sustainabilty Retreat. Kellogg Biological Station, Michigan State University, Hickory Corners, MI, February 3-5, 2014.

Mooney, D.F. and B.L. Barham. "What Drives the Adoption of Clean Agricultural Technologies? An Ex Ante Assessment of Sustainable Biofuel Production in Southwestern Wisconsin." Annual Meeting of the Agricultural and Applied Economics Association (AAEA). Washington, DC, August 4-6, 2013.

Mooney, D.F., B.L. Barham and C. Lian. "Sustainable Biofuels, Marginal Agricultural Lands, and Farm Supply Response: Micro-Evidence for Southwest Wisconsin." Annual Meeting of the Agricultural and Applied Economics Association (AAEA). Washington, DC, August 4-6, 2013.

Mooney, D.F., and B.L. Barham. Economic Thresholds, Environmental Stewardship, and Land Use Change: An Empirical Assessment of Farmer Bioenergy Crop Adoption in Wisconsin. 6th Annual Sustainability Conference. Great Lakes Bioenergy Research Center. Kellogg

Biological Station, Hickory Corners, MI, February 17-19, 2013.

Ventura, S., S. Hull, R. Jackson, G. Radloff, D. Sample, S. Walling, and C. Williams (2012) "Guidelines for Sustainable Planting and Harvest of Nonforest Biomass in Wisconsin." Journal of Soil and Water Conservation 67(1):17A-20A

Ventura, S. (2012). "Evaluation of Bioenergy Crop Production on Marginal Land in Wisconsin." Northcentral SunGrant Annual Meeting, January 10-11, 2012, Indianapolis, IN

Ventura, S. (2011). "Mapping Bioenergy Resources at Multiple Scales." Midwest Biomass Conference, November 2-3, 2011, Dubuque, IA.

Ventura, S. (2010). "Biomass Supply: Mapping WI Biofuel Potential." Wisconsin Bioenergy Summit, October 14, 2010, Madison WI.

Ventura, S. (2010). "The Vulnerable Landscapes of Wisconsin." Soil and Water Conservation Society, Wisconsin Chapter, March 11, 2010. Madison WI.

Ventura, S. (2010). "Beyond 'Food vs. Fuels:' Spatial Analysis to Guide Bioenergy Crop Production." Western Michigan University, January 21, 2010. Kalamazoo, MI.

Ventura, S. (2010). "Guidelines and Standards for Bioenergy Crop Production in WI." North Dakota GIS Users Conference, November 2-4, 2009, Grand Forks, ND.

b. Website or other Internet sites that reflect the results of this project.

Many of the environmental models assembled from the literature for use during this project have been incorporated into a web-based decision support tool for evaluating land use change due to bioenergy crop production. The tool can be viewed at http://dss.wei.wisc.edu/ (user name = wei, password = pwd1234).

c. Networks or collaborations fostered.

SunGrant fostered collaboration between ag economists at UW (Barham, Mooney) and Michigan State University (MSU) on survey data collection to understand economic responses to bioenergy cropping opportunities.

d. Other products, such as data or databases, physical collections, audio or video, software* or Netware, model, educational aid or curricula, instruments, or equipment.

We collected several statewide and county-level geospatial datasets for this project, including county level landowner parcel data, statewide CRP data, land cover, and cropland data. Many of these data sets were subsequently cleaned and documented. Data considered in the public domain have been provided to the University of Wisconsin- Madison Map and Airphoto Library archives.

5. Academic

a. Courses developed

b. M.S. students supported

- Herika Kummel – MS Agronomy
- Erica Diehl – MS Environment and Resources
- Maria Lopez Rodrigo – MS Agricultural and Applied Economics

c. M.S. degrees conferred

- Herika Kummel – MS Agronomy
- Erica Diehl – MS Environment and Resources

d. Ph.D. students supported

- Dan Mooney – PhD, Agricultural and Applied Economics
- Natalie Hunt – PhD, Environment and Resources
- Jin Jangik – PhD, Urban and Regional Planning
- Chang Lian - PhD, Agricultural and Applied Economics
- Daniel Prager - PhD, Agricultural and Applied Economics
- Yan Zhang – PhD, Urban and Regional Planning

e. Ph.D. degrees conferred

- Dan Mooney – PhD, Agricultural and Applied Economics
- Natalie Hunt – PhD, Environment and Resources

f. Post-docs supported

- Tim Meehan

g. academic staff

- Tim Meehan, Pam Porter, Elisabeth Graffy

h. Undergraduate Students
- Rob Wills, Elena Barham, Gustavo Bargas

6. For projects involving computer modeling, provide the following information with the final report:

Computer models used in our analyses were all derived from the literature.

Please complete the following table to reflect your project at completion or time of report submission:

ITEM	NUMBER
Abstracts	**11**
Peer Reviewed Publications	**3**
Outreach Publications/Web Pages	**2**
Professional Presentations	**8**
MS Degrees Conferred	**2**
Ph.D. Degrees Conferred	**2**
MS Students Supported	**3**
Ph.D. Students Supported	**6**
Post-Docs Supported	**1**
Undergraduate Students Supported	**2 UW undergrads supported through AAE (Gustavo Vargas, Robert Wills). 3 non---UW undergrads supported through AA in part---**
Investigators Supported	**1 (two months total)**
Start-Up Jobs Created	**0**
Disclosures	**0**
Patents Filed	**0**
Provisional Patents	**0**
Patents Issued	**0**
License Agreements	**0**
Plant Variety Protection	**0**
Subsequent Funding	**Agricultural and Applied Economics received continued funding from Great Lakes Bioenergy Research Center to support additional primary data collection and economic analysis in WI**

Back to Table of Contents

Sun Grant Initiative
DOE Final Progress Report

Project Title: Genetics, Breeding, Agronomy, and Pest Management of Cup Plant (*Silphium perfoliatum*): A Potential New Biomass Crop for the North Central USA

Project Director/Principal Investigator: Arvid Boe, Professor, Plant Science, SDSU, Brookings, SD

All Co-Principal/Other Investigators: Kenneth A. Albrecht, Professor, Agronomy, UW, Madison, WI; Paul J. Johnson, Professor, Plant Science, SDSU, Brookings, SD; Catherine Carter, Professor, Plant Science, SDSU, Brookings, SD; Duane Matthees, Professor, Biochemistry, SDSU, Brookings, SD

Collaborators: Jon Kahler, Biogenetics Services, Brookings, SD

Period of Performance: 1 July 2010 - 30 September 2014

Funding Awarded: $324,183

Cost Share Amount: $81,046

Cost Share Sources: Time and effort from PIs and CoPIs; Indirect on time and effort

Executive summary

Results of the research effectively demonstrated that the experimental methods used resulted in levels of biomass production in SD and WI that would have cup plant economically feasible, in monocultures or in mixtures with perennial native warm-season grasses, compared to other herbaceous perennial biomass production systems such as monocultural switchgrass or monocultural prairie cordgrass. The benefit of this project to the public is that it demonstrated that increasing biodiversity, pollinator habitat, and other ecological services, by including a perennial dicotyledonous species, in biomass feedstock production systems could be achieved without significantly reducing biomass yield. The results also showed adequate genetic variation for biomass and seed related traits to make progress for biomass and seed production in cup plant. New varieties of cup plant will increase biodiversity and environmental sustainability in dedicated biomass production systems on marginal crop land.

Objectives

Objective 1: Determine genetic variation within the genus *Silphium*, isolate genes of interest, and develop molecular markers linked to agronomic traits for cup plant.

Outcomes: Allele frequencies for 198 individual plants within a population composed of 34 half-sib families of cup plant were determined for 27 molecular markers (SSRs) obtained from cultivated sunflower by Jon Kahler, Biogenetics Services, Brookings, SD. A genetic distance analysis indicated considerable genetic variation among and within families for the 198 plants in the population. These molecular data are currently being used in combination with corresponding individual-plant morphological/phenotypic data (i.e., height, crown area, shoots plant^{-1}, mass shoot) for an association mapping analysis, in collaboration with Dr. Jixiang Wu, Plant Science, SDSU. That collaboration will result in the development of a manuscript submitted to a refereed journal during 2015. In addition, DNA extraction protocol for AFLP marker analysis for achene/seed traits, also using markers from sunflower, was developed (T. Mamo. 2014. PhD Dissertation, SDSU).

These results met the expectation for the molecular marker component of the objective, especially since the high resin/terpenoid levels in cup plant tissue impede efficient extraction of DNA useful for molecular studies. However, the genetic-variation- within-the-genus component was not accomplished. The reason being the retirement of Dr. Catherine Carter, who was the lead co-PI for that sub-objective, in 2013. Dr. Carter collected a few samples from natural populations of *S. integrifolium* and *S. laciniatum* in southeastern SD and had intended to obtain samples of several other species from collaborators in the Midwest and Southeast U.S.

Impacts: The impact of the results from this objective are primarily related to the availability of a protocol for efficient extraction of DNA from young cup plant leaves (Mamo 2014) for application by other researchers that are interested in cup plant.

Objective 2: Develop new cultivars of cup plant that are suitable for growing with native warm-season grasses, such as prairie cordgrass and switchgrass, in grass/forb mixtures for biomass feedstock production.

Outcomes: Six out of the 33 half-sib families were identified for among family selection for development of a new ‘first generation’ cultivar of cup plant for biomass production in SD and the northern Great Plains. A different group of six families was identified for among family selection for development of a new cultivar for WI and the Great Lakes Region. However, a Wisconsin population x Arkansas population hybrid developed by co-PI Dr. K.A. Albrecht at the U WI outperformed all of the 33 half-sib families in WI. This indicated, although genetic variation for biomass production occurred among the 33

families in WI, selection would not be expected to increase biomass yield to the level produced by the WI x AR hybrid. Therefore, breeder's seed will be produced from the selected families in SD, but not in WI. The primary criterion for selection is average performance across a 3-year period (2011-2013) that spanned two normal precipitation years (2011 and 2013) and one record-low precipitation year (2012) (Table 1).

Table 1.
Families in the uppermost quartile for biomass yield for 33 half-sib families of cup plant in each of three consecutive years at Brookings, South Dakota.

2011		2012		2013	
Family #	kg ha^{-1}	Family #	kg ha^{-1}	Family #	kg ha^{-1}
18	7,507	3	3,421	31	10,475
3	7,498	11	3,092	5	10,464
7	7,218	7	3,066	7	10,016
23	7,182	23	3,010	12	9973
31	7,138	18	3,008	30	9,664
10	6,966	31	2,741	23	9,600
5	6,921	5	2,641	9	9,216
24	6,741	10	2,326	13	9,195
LSD (0.05)	718		241		2977

Results met expectation for this objective. In the process of identifying superior families for biomass production, data were also collected for morphological traits putatively associated with biomass yield in SD. The experimental design for the nursery that contained the half-sib families enabled the estimation of additive gene effects and calculation of narrow-sense heritability for each trait. That information will be potentially useful in the development of 'second-generation' cultivars developed from among-and-within-family selection. The quantitative genetic analysis of the morphological data is described in Assefa et al. 2015 (in press).

Impacts: The impact of the accomplishment of this objective is associated with the current project's demonstration of cup plant as a high-potential biomass feedstock species on marginal land in the North Central U.S. This research revealed its inherent high biomass production potential and its amenability to conventional genetic improvement strategies and methods. It also called attention to the need for evaluation and breeding of alternative species, other than perennial grasses, for inclusion in herbaceous perennial cellulosic biomass production systems. In the past, native legumes have been suggested as the most logical dicotyledonous species to use in mixtures with native warm-season grasses to increase biodiversity and sustainability due, in part, to their abilities to attract pollinators and fix atmospheric nitrogen. However, no native legumes from the North Central U.S. are adapted to poorly-drained marginal land where cup plant thrives. Dissemination of the findings of this project will bring cup plant to the forefront of dicotyledonous species being considered for new biomass crop development through germplasm collection, selection, and breeding.

Objective 3: Develop best agronomic management practices for sustainable biomass production of cup plant in the North Central U.S.

Outcomes**:** This objective identified, from comparative trials conducted for three years in SD and WI, a superior plant population density for optimizing biomass production in cup plant in the North Central U.S. That population density was 68,900 plants ha^{-1} (Fig. 1 and 2)

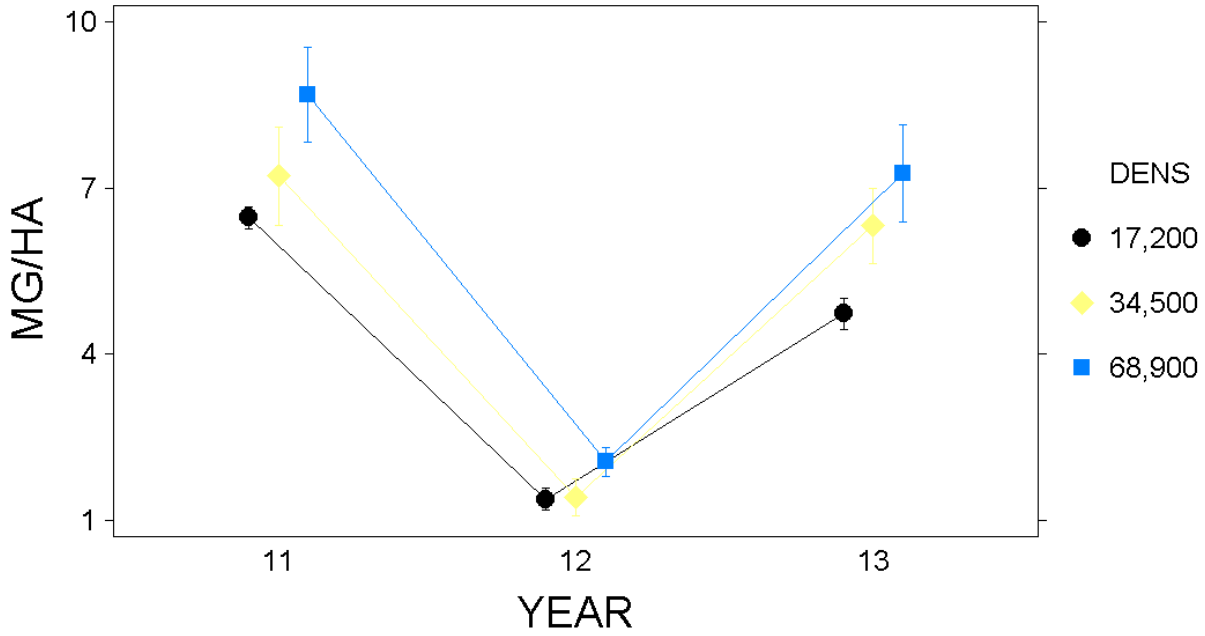

Fig. 1. Response of biomass production to variation in plant population density (DENS=plants ha^{-1}) at Brookings, SD during 2011 through 2013.

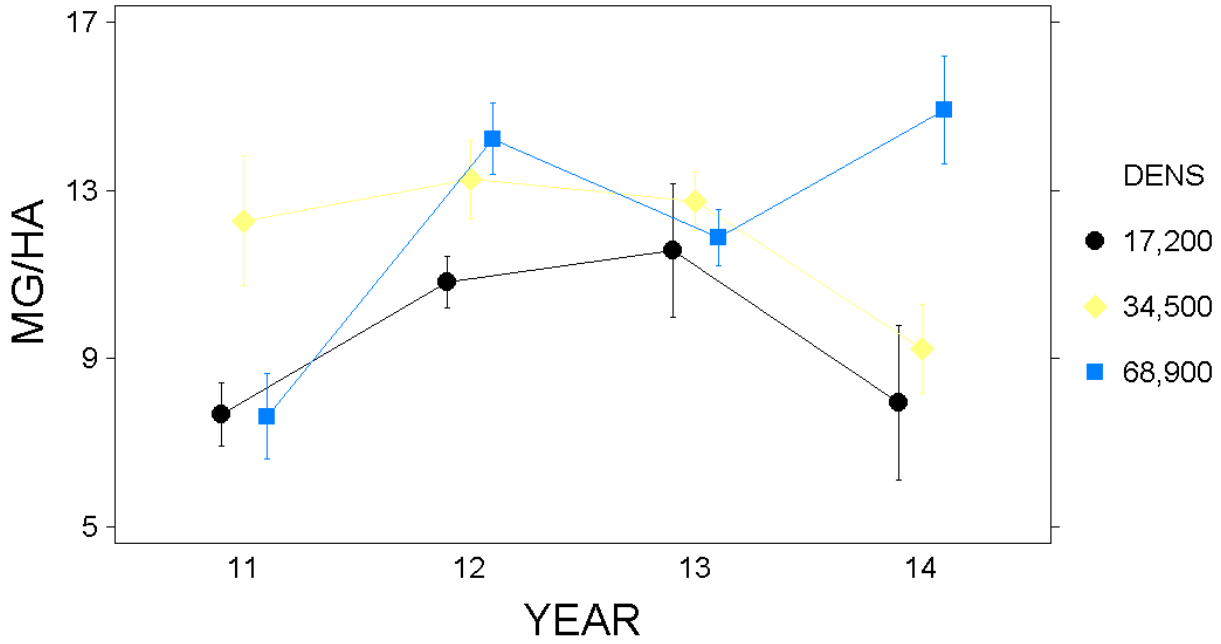

Fig. 2. Response of biomass production to variation in plant population density (DENS=plants ha^{-1}) at Arlington, WI during 2011 through 2013.

This objective also produced several outcomes associated with the relative performances of cup plant, prairie cordgrass, and switchgrass, in monocultures and mixtures, on wet marginal land vs. well-drained cropland in SD and WI. Marginal environments (MRG 1 and 2) were poorly drained crop land sites at foot slope landscape positions; whereas prime environments (PRM 1 and 2) were well drained cropland topographically higher on the same landscape. A highly important outcome of this objective was the demonstration of the effect of land classification on biomass production of cup plant, prairie cordgrass, and switchgrass in WI (Fig. 3). The year 2012 was a severe drought year in both SD and WI. In general, the marginal environments had higher mean biomass yields, averaged across the 6 treatments, than the prime environments at each of the two experimental sites. Also, the cup plant and prairie cordgrass monocultures, and the three mixtures out-yielded the switchgrass monoculture in both marginal environments in WI.

In 2013, a normal precipitation year in WI, biomass yields for the 6 treatments were similar for marginal and prime environments (i.e., MRG 1 and PRM 1) at experimental site 1, with the exception of the switchgrass monoculture, which yielded more at the prime environment compared to the marginal environment. On the other hand, at experimental site 2, all 6 treatments produced more biomass in the marginal environment compared to the prime environment (Fig. 4).

A third important outcome from the monocultures vs. mixtures study in WI was the demonstration of the ability of cup plant to persist and produce large amounts of biomass in 2-way and 3-way mixtures with native warm-season grasses (Fig. 5).

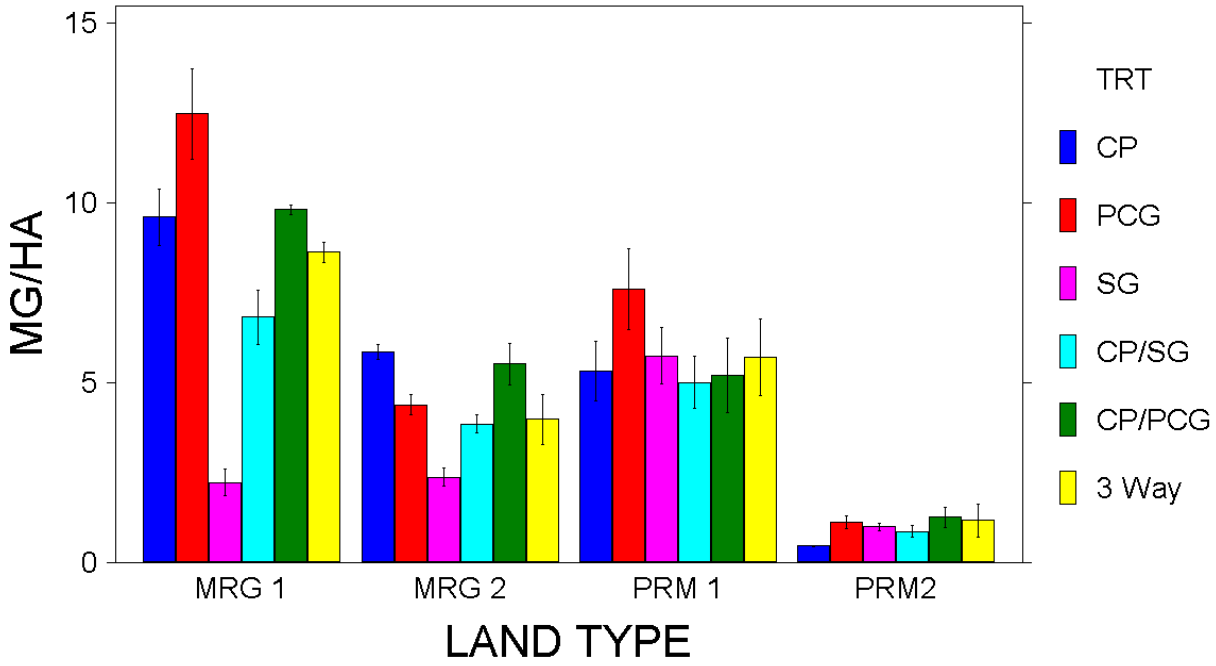

Fig. 3. Biomass production for cup plant, prairie cordgrass, switchgrass and their mixtures on wet marginal (MRG 1 and 2) and prime (PRM 1 and 2) cropland at Arlington, WI during 2012. CP=cup plant monoculture, PCG=prairie cordgrass monoculture, SG=switchgrass monoculture, CP/SG=cup plant-switchgrass mixture (equal number of plants of each species), CP/PCG=cup plant-prairie cordgrass mixture (equal number of plants of each species), 3 Way=cup plant-switchgrass-prairie cordgrass mixture (equal number of plants of each species).

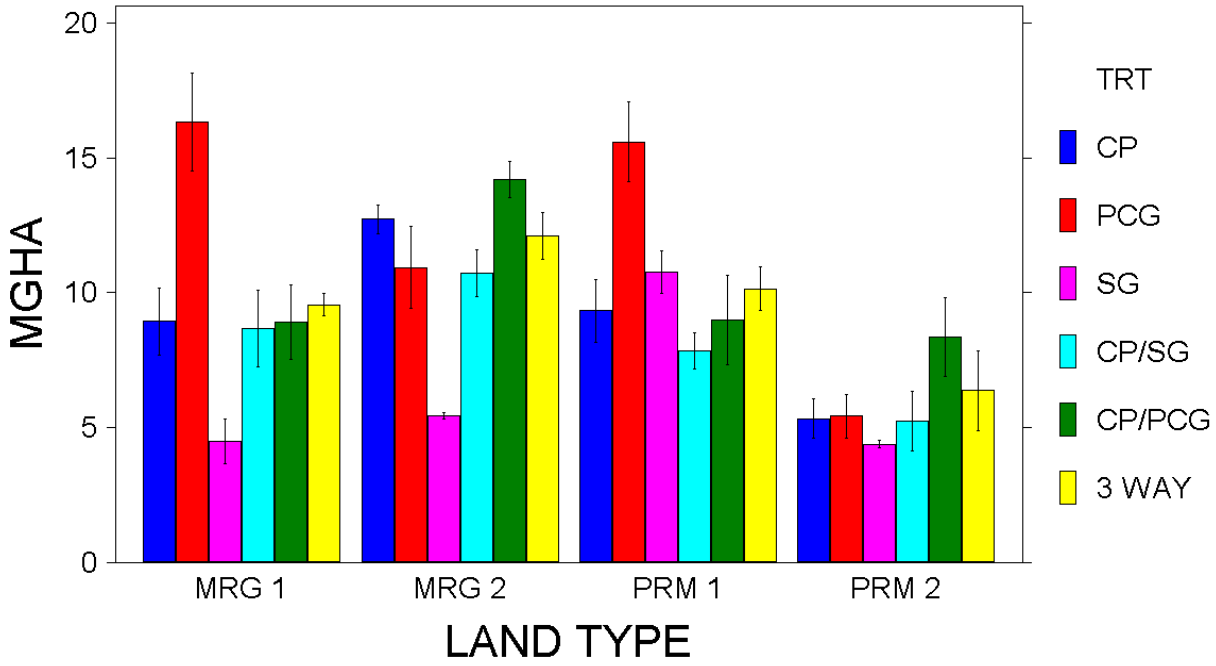

Fig. 4. Biomass production for cup plant, prairie cordgrass, switchgrass and their mixtures on wet marginal (MRG 1 and 2) and prime (PRM 1 and 2) cropland at Arlington, WI during 2013. CP=cup plant monoculture, PCG=prairie cordgrass monoculture, SG=switchgrass monoculture, CP/SG=cup plant-switchgrass mixture (equal number of plants of each species), CP/PCG=cup plant-prairie cordgrass mixture (equal number of plants of each species), 3 Way=cup plant-switchgrass-prairie cordgrass mixture (equal number of plants of each species).

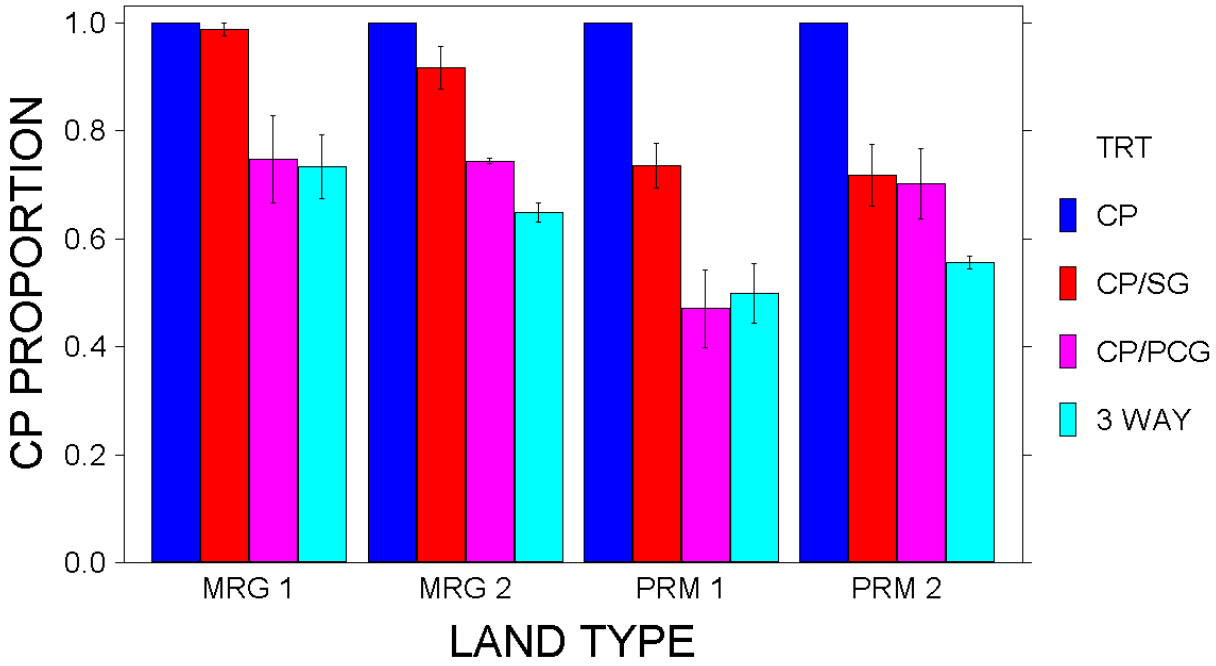

Fig. 5. Cup plant proportion of total biomass in mixtures with prairie cordgrass and switchgrass at Arlington, WI in 2013.

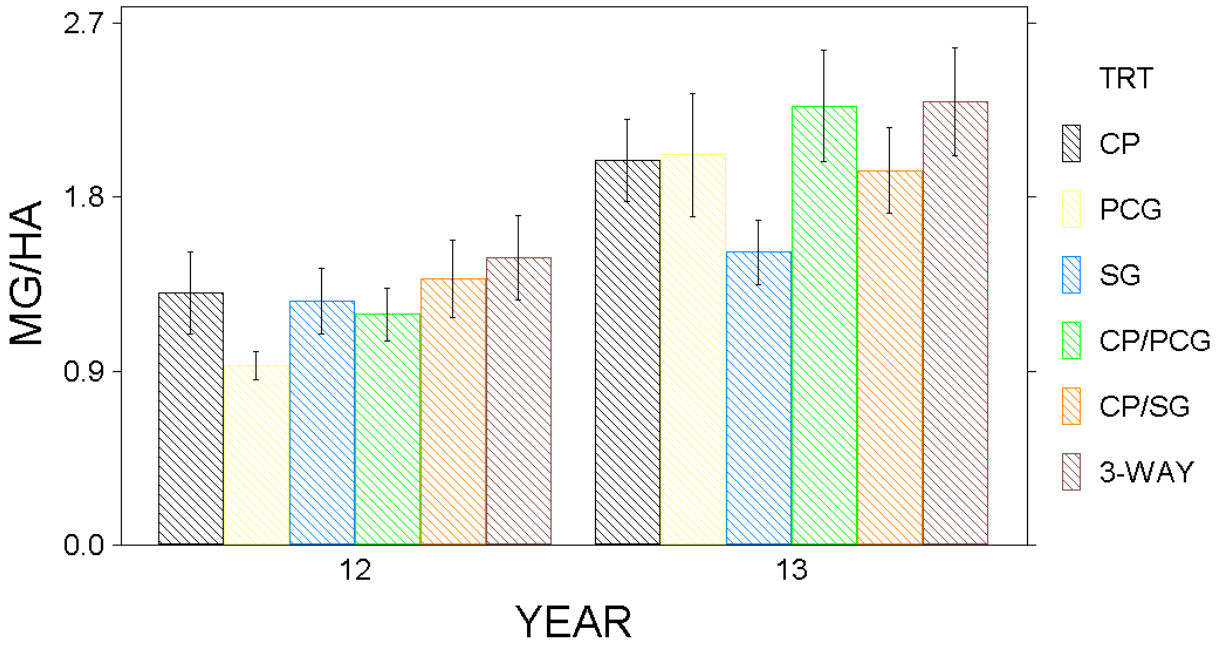

Fig. 6. Biomass production of cup plant, prairie cordgrass, switchgrass and their mixtures at Brookings, SD in 2012 and 2013.

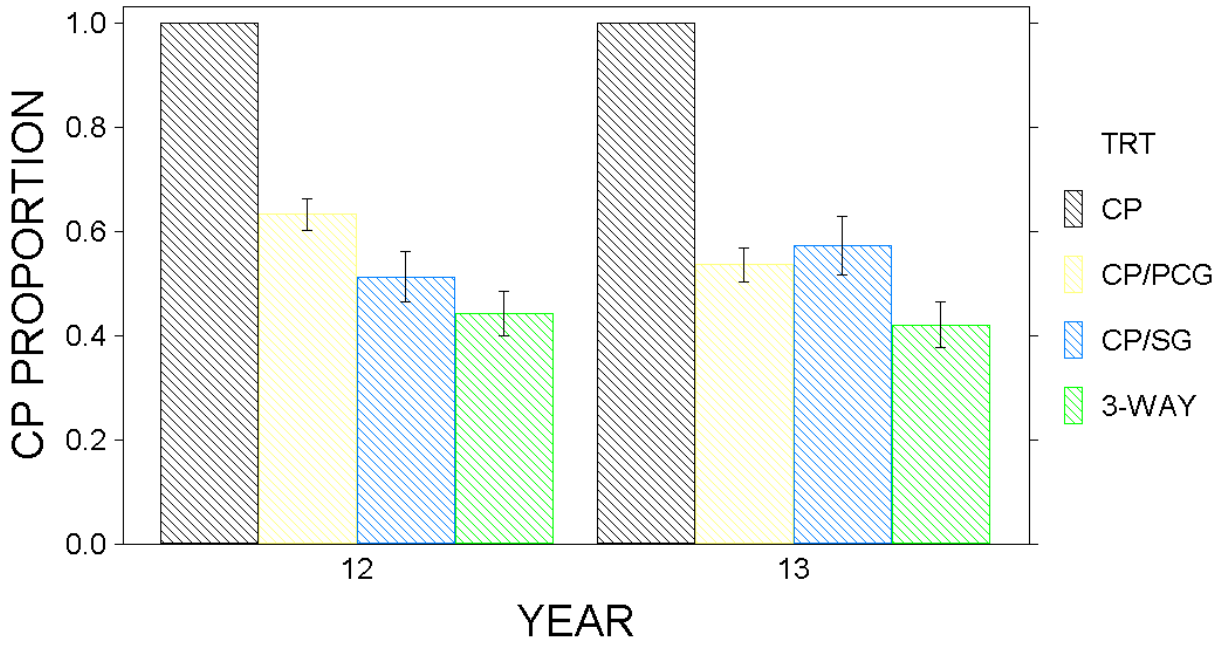

Fig. 7. Cup plant proportion of total biomass in mixtures with prairie cordgrass and switchgrass at Brookings, SD in 2012 and 2013.

In SD, there was a similar outcome regarding biomass production from marginal vs. prime crop land. However, the difference between the two land classes was less than in WI. Nevertheless, marginal land, averaged across treatments, out-produced prime land at both experimental sites. Large differences were found between years for yields of all treatments. Another important outcome was that the mixtures produced as much biomass as the highest yielding monoculture, irrespective of amount of precipitation (Fig. 6). A final outcome from this objective in SD was the proportion of cup plant in the mixtures was similar to that observed for the corresponding treatments in WI, with the notable exception of the cup plant-switchrass mixture, which contained about 50% cup plant in SD compared to >75% cup plant in WI (Fig. 7).

Impacts: The impacts resulting from completion of this objective will have to do with the influence of the present results on future experiments. The new knowledge of effects of plant density on biomass will influence the spacing in future breeding nurseries and agronomic trials. The new knowledge of the compatibility of cup plant in mixtures with native warm-season grasses and the performance of cup plant on marginal vs. prime cropland will influence the design and implementation of future experiments that investigate a 'sculpting the landscape' approach to biomass feedstock production.

Objective 4: Determine the biochemical composition of biomass feedstock of cup plant harvested once annually near the end of the growing season. In addition to feedstock quality, types and concentrations of individual terpenoids will be determined.

Outcomes: An important outcome of completion of this objective was the finding that concentrations of acid detergent fiber, neutral detergent fiber, and acid detergent lignin were influenced by additive genetic variance in the present population of cup plant. This finding was important in that it indicated that progress for either increased or decreased cellulose/hemicellulose or lignin would be expected from among family selection (Mamo 2014).

Impacts: The impact of these results will be realized in the future if and when selection schemes are designed and employed for improving biomass feedstock quality in this or other populations of cup plant.

Objective 5: Determine the life history of the cup plant moth (*Eucosma giganteana*), which can destroy>75% of the floral meristems and severely reduce biomass yields of cup plant in SD and WI.

Outcomes: The life history of the cup plant moth was ascertained (Fig. 8) to include 1) the sites on the plant and duration of oviposition, clutch size, and rate of hatching/egg predation, 2) location of feeding, impact of feeding and behavior of early instars larvae on aerial portions of the plant, 3) time of migration of larvae to underground crowns/buds and feeding sites and behavior, 4) overwintering chambers and duration of larva/pupal stages belowground, 5) survival rate of below ground stages of life history, 6) duration of adult emergence and adult behavior, 7) estimates of meristem infestation and impacts on cup plant growth and development.

Impacts: The giant eucsoma is without question the most detrimental pest to sustainable biomass and seed production from cup plant. The accomplishments of this objective have elucidated its life history and consequently have produced the knowledge necessary for development of management/control strategies.

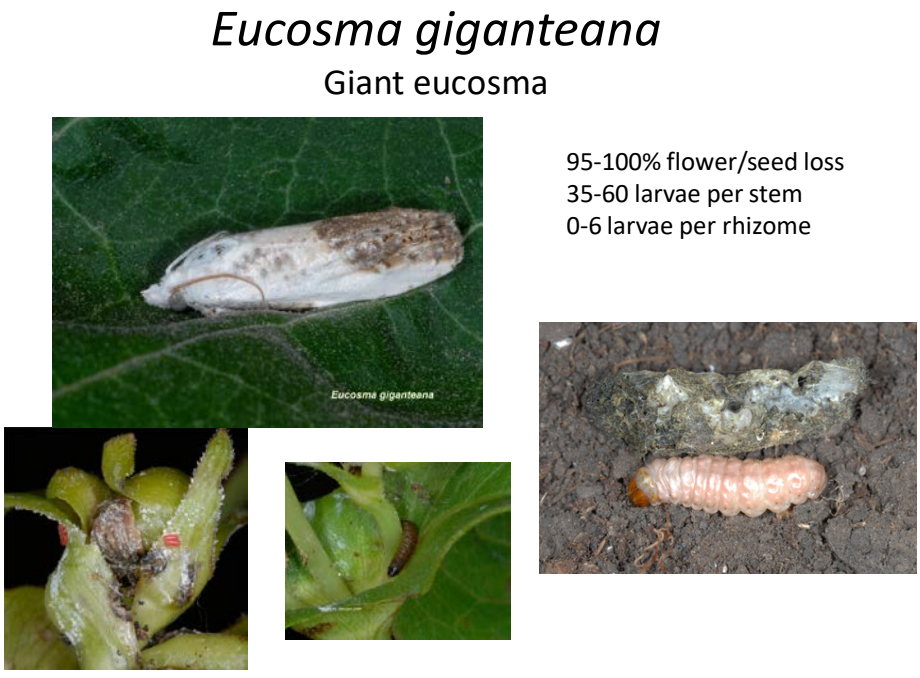

Fig. 8 Life history stages of the giant eucosma (*Eucosma giganteana*) on cup plant in SD.

Summary of Project Activities:

Project activities, hypotheses tested, and approaches/methodologies used were as planned and are described above. The only exceptions where objectives were not met had to do with completion of the: 1)

within-genus molecular genetic variation study, and 2) the terpenoid variation/concentration study. Both activities were dropped due to retirement of original personnel before project completion.

Products developed:

Refereed Journals

Assefa T, Wu J, Albrecht KA, Johnson PJ, Boe A. 2015. Genetic variation for biomass and related morphological traits in cup plant (*Silphium perfoliatum* L.) American Journal of Plant Sciences (in press)

Assefa T, Wu J, Johnson PJ, Boe A. 2015. Genetic variation for achene traits in cup plant (*Silphium perfoliatum* L.) (in review)

Johnson PJ, Albrecht KA, Boe A. 2015. Life history and impact of the giant eucosma (*Eucosma giganteana*) on cup plant (in preparation).

Dissertations:

Mamo T. 2014. Genetics of biomass and biomass-related traits in cup plant (*Silphium perfoliatum* L.). PhD Dissertation, South Dakota State University, Brookings, SD.

Invited Presentations:

Boe A. 2014. Promising new dicots in mixtures with warm-season grasses for bioenergy. 10th Annual Bioenergy Feedstocks Symposium. 24 September. Energy Biosciences Institute, University Illinois, Champaign, IL.

Abstracts:

Johnson PJ, Boe A. 2011. Three interesting insects and the cause of reduced vigor of cup plant (Silphium perfoliatum) in agronomic plantings. Proceedings of the South Dakota Academy of Science. Annual Meeting, Oacoma, SD.

Johnson PJ, Boe A, Albrecht KA, Calles-Torrez, V. 2012. Recent discoveries and development in the entomology of bioenergy crop production. SunGrant Initiative 2012 National Conference: Science for Biomass Feedstock Production and Utilization. 2-5 October. New Orleans, LA.

Boe A, Albrecht KA, Johnson PJ, Owens V, Mamo T, Yang C. 2012. Quantitative genetic analysis of biomass yield, pest resistance, and other agronomic traits in prairie cordgrass and cup plant. SunGrant Initiative 2012 National Conference: Science for Biomass Feedstock Production and Utilization. 2-5 October. New Orleans, LA.

Oral Presentations:

Johnson PJ, Boe A. 2011. Three interesting insects and the cause of reduced vigor of cup plant (Silphium perfoliatum) in agronomic plantings. Proceedings of the South Dakota Academy of Science. Annual Meeting, Oacoma, SD.

Boe A, Albrecht KA, Johnson PJ, Owens V, Mamo T, Yang C. 2012. Quantitative genetic analysis of biomass yield, pest resistance, and other agronomic traits in prairie cordgrass and cup plant. SunGrant Initiative 2012 National Conference: Science for Biomass Feedstock Production and Utilization. 2-5 October. New Orleans, LA.

Johnson PJ, Boe A, Albrecht KA, Calles-Torrez, V. 2012. Recent discoveries and development in the entomology of bioenergy crop production. SunGrant Initiative 2012 National Conference: Science for Biomass Feedstock Production and Utilization. 2-5 October. New Orleans, LA.

Poster: Johnson PJ, Boe A. 2012. Incidence of *Eucosma giganteana* on wild and agronomic populations of *Silphium perfoliatum* in easern South Dakota. Entomological Society of America National Conference, Knoxville, TN.

Academic:

PhD student supported and PhD conferred:

Mamo, Teshale. 2014. South Dakota State University.

ITEM	NUMBER
Abstracts	**3**
Peer Reviewed Publications	**1**
Outreach Publications/Web Pages	
Professional Presentations	**3**
MS Degrees Conferred	
Ph.D. Degrees Conferred	**1**
MS Students Supported	
Ph.D. Students Supported	**1**
Post-Docs Supported	
Undergraduate Students Supported	**1**
Investigators Supported	
Start-Up Jobs Created	
Disclosures	
Patents Filed	
Provisional Patents	
Patents Issued	
License Agreements	
Plant Variety Protection	
Subsequent Funding	

Back to Table of Contents

Sun Grant Initiative

DOE Final Progress Report

Project Title: Biofuel Feedstock Crops in Sub-Irrigated Lowlands

Project Director/Principal Investigator: W. Carter Johnson, Department of Natural Resource Management, South Dakota State University, Brookings, SD

Co-investigators: Tom Schumacher, Arvid Boe, and Vance Owens, Plant Science Department, South Dakota State University, Brookings, SD

Period of Performance: 1 July 2010 - 30 September 2013

Funding Awarded: $180,625

Cost Share Amount: 45,156

Cost Share Sources: Time and effort from PIs and CoPIs; Indirect on time and effort, EcoSun Prairie Farm

Executive Summary

Land considered marginal for crop production holds potential for producing harvestable lignocellulosic biomass suitable for bioenergy production. In the Prairie Pothole region, which includes eastern South Dakota, many farms contain seasonal or temporary wetlands within the boundaries of grain-crop fields. These wetlands are frequently too wet to plant, and if planted, grain crops often fail due to the soils' poor drainage. Wetland restoration can provide ecosystem goods and services in the form of biodiversity, fish and game habitat, flood attenuation, surface and ground water purification, stock watering, and carbon storage. There is a need for solutions that will allow wetlands to provide these valuable ecosystem services while simultaneously providing farmers with economic benefits. Therefore, we evaluated prairie cordgrass (*Spartina pectinata)* as a biomass crop in the restoration of formerly drained shallow wetlands. Cordgrass has high yield potential and is more tolerant of flooding and saline soils than is switchgrass.

We planted cordgrass into soybean stubble in 2010 and evaluated it annually through 2013. We found that an optimum establishment strategy for cordgrass was to transplant into a wetland bottom (maximum water depth > 0.4 m) and drill the higher reaches if seed can be obtained for less than \$138 kg^{-1}. Transplanting would be the optimum establishment strategy over the entire wetland area at higher seed costs. Gradient analysis revealed a zone of maximum prairie cordgrass vigor that shifted downslope to the center of the wetland beginning in 2012, the driest summer on record. Effects of the 2012 drought extended into 2013, when the wetland held much less water despite receiving average precipitation in the spring.

The two commercially available populations of prairie cordgrass seed, Red River and Prairie Farm, were evaluated. Zones of maximum production for the two populations overlapped, and three years after establishment there was no difference in biomass yield of the two populations. In 2012, the zone of maximum vigor ranged from 0.35 m maximum water depth to 0.10 m above the basin rim. This zone yielded 11.1 Mg ha^{-1}. In 2013, yield (6.0 Mg ha^{-1}) was greatest at a maximum water depth of 0.10 to 0.33 m, having declined due to the drought. The most-suited areas for cordgrass production are likely shallow temporary wetlands and seasonal wetlands with short hydroperiods.

Given that prairie cordgrass yields in wetlands were similar to switchgrass yields in the uplands, planting each species in the location where it is best adapted could result in maintenance or increase of field-scale yields in addition to increasing field-scale biodiversity. Alternatively, if the uplands remained in grain production, the wetlands could still be planted to cordgrass and harvested with or without the upland corn stover. Conventional harvesting equipment already present on many farms can be used to harvest the plant's seed and biomass.

We conclude that prairie cordgrass is a high-yielding biomass crop that can be effectively established in temporary or seasonal wetlands of the Prairie Pothole region. Cultivating prairie cordgrass in farm wetlands offers the opportunity to gain income from the sale of biomass (as hay or, potentially, as biofuel feedstock) and seed, while also providing valuable ecosystem services. In conclusion, prairie cordgrass should be considered for revegetation of farm wetlands because of the potential for both income and ecosystem services it can provide.

Project Objectives, Outcomes, and Impacts

1. Introduction

Land considered marginal for crop production holds potential for producing harvestable lignocellulosic biomass suitable for bioenergy production. In the Prairie Pothole region, which includes eastern South Dakota, many farms contain seasonal or temporary wetlands within the boundaries of grain-crop fields. These wetlands are frequently too wet to plant, and if planted, grain crops often fail due to the soils' poor drainage.

Recently, record grain prices have encouraged some farmers to invest in draining wetlands. While expansion of cropland area into lowlands has had short-term economic benefits, losses of ecosystem goods and services in the form of biodiversity, fish and game habitat, flood attenuation, surface and ground water purification, stock watering, and carbon storage have been recognized and in some cases quantified (Galatowitsch 2012). Therefore, there exists a need for solutions that will allow wetlands to provide valuable ecosystem services while simultaneously providing farmers with economic benefits. This type of farming may require the use of new agricultural species and practices for which little information exists.

Prairie cordgrass (*Spartina pectinata*; hereafter cordgrass) was the species chosen for study during the restoration of formerly drained shallow wetlands. Cordgrass is native, vigorously competitive, and often dominant in temporary and seasonal wetlands in the Prairie Pothole Region. Cordgrass has high yield potential; Boe and Lee (2007) found during a 4-yr experiment that cordgrass production exceeded that of switchgrass (*Panicum virgatum*) on well-drained farmland, but cordgrass is more tolerant of flooding and saline soils than is switchgrass. In addition to the biofuel feedstock produced, its seed also has commercial value. The remainder of this report details lessons learned regarding cordgrass management in the course of our research.

2. Methods of Prairie Cordgrass Establishment

It is critical to identify effective methods of establishing cordgrass on low, often wet, ground. Cordgrass may be propagated by seed, or vegetatively by dividing and planting rhizomes. Although transplanting plugs from existing wetlands is effective, it is not practical for large scale plantings. Alternative methods of establishing cordgrass from seed must be found. Much of the following information can also be found in Zilverberg et al. (in review).

The research site was located at the EcoSun Prairie Farm near Colman, SD (44.029, -96.850). The experiment was conducted in a shallow basin (1.4 ha) classified as a temporary wetland (Stewart and Kantrud 1971) that typically fills up to a 50-cm depth with runoff in spring and dries out by mid-summer. Wetland soils included Worthing (fine, montmorillonitic, mesic, Vertic Argiaquolls) in the basin, Chancellor (fine, montmorillonitic, mesic Vertic Argiaquolls) in the swale, and Wakonda (fine-silty, mixed, mesic Aquic Calciustolls) on the ridge surrounding the wetland, as inclusions in the soil association Wentworth-Chancellor-Wakonda silty clay loam with 0 to 2 percent slopes (NRCS 2011). Mean annual precipitation (1981 to 2010) at the Madison, SD weather station was 655 mm, with 495 mm from April to Sept. (NOAA 2013). Four sampling transects oriented northwest, northeast, southwest, and southeast were established in an "X" pattern in the wetland basin (Fig. 2.1). Transects began at the bottom of the basin and extended up the slopes beyond the 50-cm depth contour and into planted upland vegetation dominated by *Andropogon gerardii*. Different slopes in the four directions resulted in different transect lengths (57 to 83 m). Each transect was divided into two contiguous plots that were randomly assigned to planting type: drilling or plugging. Each plot was further divided into 2 subplots, each randomly assigned to a population of cordgrass: Red River or Prairie Farm.

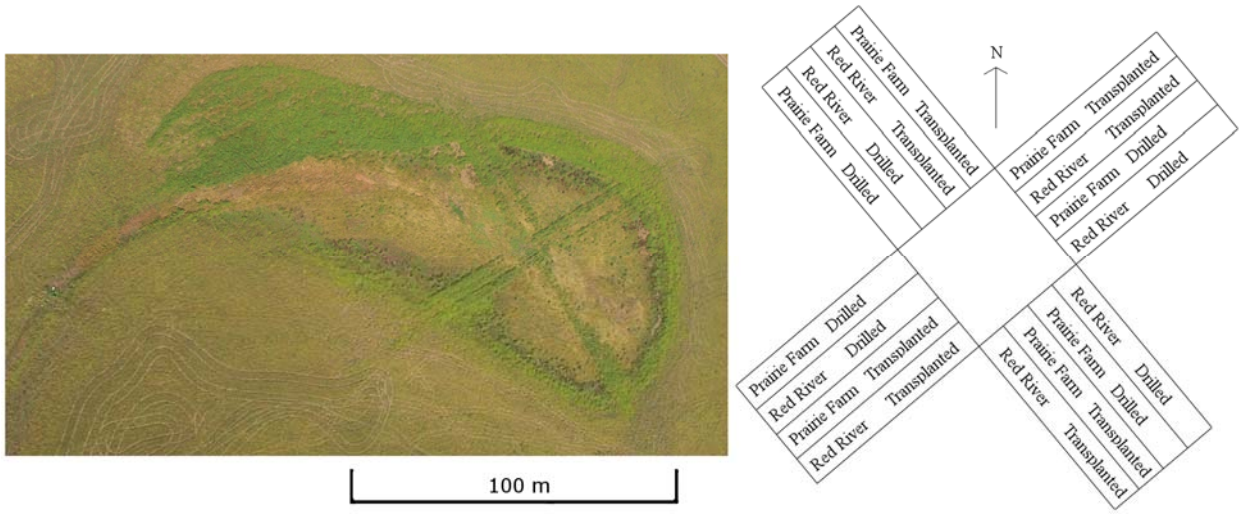

Fig. 2.1 Left, overhead image (to scale) of the experiment in a restored temporary wetland at the EcoSun Prairie Farm. Right, plot diagram showing layout of different treatments (not to scale). Source: Zilverberg et al. (in review).

The wetland had been cultivated for annual crops for a century or more prior to its restoration by this experiment. In the year prior to planting, the field contained soybeans and post-harvest stubble remained at the time of planting cordgrass. Cordgrass plants of both populations were started from seed in conetainers (Stuewe & Sons, Tangent, OR) in a greenhouse in the spring of 2010. Prairie Farm plugs were transplanted to the field on 26 May. Transplanting of Red River was delayed because of poor plant vigor due to growing conditions in the greenhouse, and therefore Red River transplant data were excluded from the analysis.

Each transplant subplot consisted of three rows, with inter- and intra-row plant spacing of 0.9 m. On 22 Apr. 2010, both populations were planted using a 1.6-m wide Truax FLXII-88 grass drill (Truax Company; New Hope, MN) at a rate of 10 kg bulk seed ha^{-1}. Drilled subplots also consisted of three rows, with two rows spaced at 0.8 m and two rows spaced at 0.6 m because of equipment restrictions.

Sampling occurred in autumn of each year after a hard frost, beginning in 2011, the second growing season, and continuing through 2013. Because of erratic establishment in some subplots, we visually determined which row of the three rows of each subplot had the most uniform stand from the center of the wetland to beyond the wetland-upland border, and used that row for all sampling except biomass. Plant height (distance from ground to top of natural leaf blade height), maximum inflorescence height (distance from ground to top of tallest inflorescence), and number of inflorescences were measured or counted within a 1 x 1 m quadrat at 2-m intervals along each transect. Establishment success was defined as at least one cordgrass tiller within a sampling quadrat.

A plant vigor index was created using the following equation:

$$\text{Vigor} = [\ PH/\max(PH) + IH/\max(IH) + NI/\max(NI)\ ] / 3$$

where PH is plant height, max(PH) is the maximum PH of any sample, IH is inflorescence height, max(IH) is the maximum IH of any sample, NI is the number of inflorescences m^{-2}, and max(NI) is the maximum NI of any sample.

Preliminary estimates of biomass were conducted in 2011 and 2012. More thorough biomass sampling was conducted in 2013. For each transect, one point was randomly selected within each ~0.08-m change in elevation from 0 to 0.40 m elevation, and 2 additional points were randomly selected in the

remaining, upper elevations. At each sampling point, all four treatments were sampled by cutting prairie cordgrass at ground level with a rice knife within a 1.5 x 1.0-m quadrat (N = 84). The quadrat was centered on the middle row of each treatment and the quadrat's width ensured that all three rows were sampled. Inter-row and inter-plant spaces had been filled in by new tillers, so that rows were no longer distinct from one another in many locations. Species other than prairie cordgrass were excluded from samples. Other species provided little ground cover except at elevation extremes where prairie cordgrass did not perform well. Biomass samples were weighed in the field. Subsamples were dried and weighed to estimate percentage dry matter. Elevation above the wetland bottom was measured at 2-m intervals along transects using conventional survey equipment.

For the Prairie Farm population, planting technique interacted with relative elevation to influence establishment success. Transplanting plugs was more successful than drilling seed regardless of the elevation; however, this difference was greater near the wetland bottom than on the slopes (Table 2.1). Success on the wetland bottom was less than on the slopes regardless of planting method. Like Prairie Farm, drilled Red River was more successful on higher slopes than on the wetland bottom. Success of both populations and planting techniques increased with time, because established plants expanded vegetatively by rhizomes into unoccupied plots.

Table 2.1 Percentage success of two different planting techniques for two populations of prairie cordgrass, as affected by relative elevation above the wetland bottom. Success was defined as at least one tiller being present within the sampling quadrat. Planting occurred in 2010. Source: Zilverberg et al. (in review).

Population	Planting technique	Relative elevation	Year		
			2011	2012	2013
Prairie Farm	Plug	0 to 0.1 m	65	94	100
Prairie Farm	Drill		0	0	31
Red River	Drill		10	11	15
Prairie Farm	Plug	> 0.1 m	86	96	90
Prairie Farm	Drill		67	74	78
Red River	Drill		57	75	66

The two planting techniques resulted in similar vigor and biomass production except in the wetland center, where drilling was ineffective at establishing plants. Within this region from 0 to 0.1 m elevation from the wetland bottom, the equivalent of 0.4 to 0.5 m maximum water depth, standing water in the center of the wetland either prevented germination or killed small seedlings. In contrast, starting plants in the greenhouse before transplanting to the field was effective along the entire elevational gradient. This technique used less seed but would be more costly at a 0.9-m plant spacing because it required greenhouse access and more labor. However, for seed prices greater than \$138 kg^{-1}, transplanting at a 1.5-m spacing would be less costly than direct seeding, and these two spacing treatments were shown to provide similar biomass yields (Zilverberg et al., in review).

Therefore, an ***optimum establishment strategy*** would be to transplant into the wetland bottom (maximum water depth > 0.4 m) and drill the higher reaches if seed can be obtained for less than \$138 kg^{-1}. Transplanting would be the optimum establishment strategy over the entire wetland area at higher seed costs.

3. Prairie Cordgrass Ecotypes: Performance Across Hydrological Gradients

Optimizing biomass production in wetlands may require selection of plant varieties suited to the particular location and hydrological conditions. However, as noted by Boe *et al.* (2009), there is a lack of gradient studies to determine the optimal topographic and edaphic position for planting and growing cordgrass. Cordgrass is native to most of the U.S., but the Red River population was the only commercially-available cordgrass seed (Jensen 2006) until the Prairie Farm population was released in 2011 by EcoSun Prairie Farms.

Red River was released by the United States Department of Agriculture (USDA) Natural Resources Conservation Service (NRCS) Plant Materials Center in Bismarck, North Dakota and is a composite of plant materials from eastern North Dakota, western Minnesota, and northeastern South Dakota (NRCS 2012). The ***Prairie Farm*** population originated from seed collected from a natural population in the southeastern corner of South Dakota. Details of the methods used to establish and evaluate the two ecotypes across hydrological gradients were provided in the previous section (Section 2.1).

In general, plant vigor at low elevations was similar in 2011 and 2012, but was reduced in 2013 (Fig. 3.1). At high elevations, plant vigor was greatest in 2011. Peak vigor values occurred at lower elevations in 2012 and 2013 than 2011 (Fig. 3.2). Differences between drilled populations were greatest in 2012, when Prairie Farm vigor was greater than Red River. Plant height was correlated with all measured variables, including biomass. Inflorescence density varied much more than plant height or maximum inflorescence height (Table 3.1). All three measurements were affected by elevation x year interactions. Plant height was also affected by a planting x year interaction and a population x year interaction. Maximum inflorescence height also differed by population. Inflorescence density was affected by a population x year interaction.

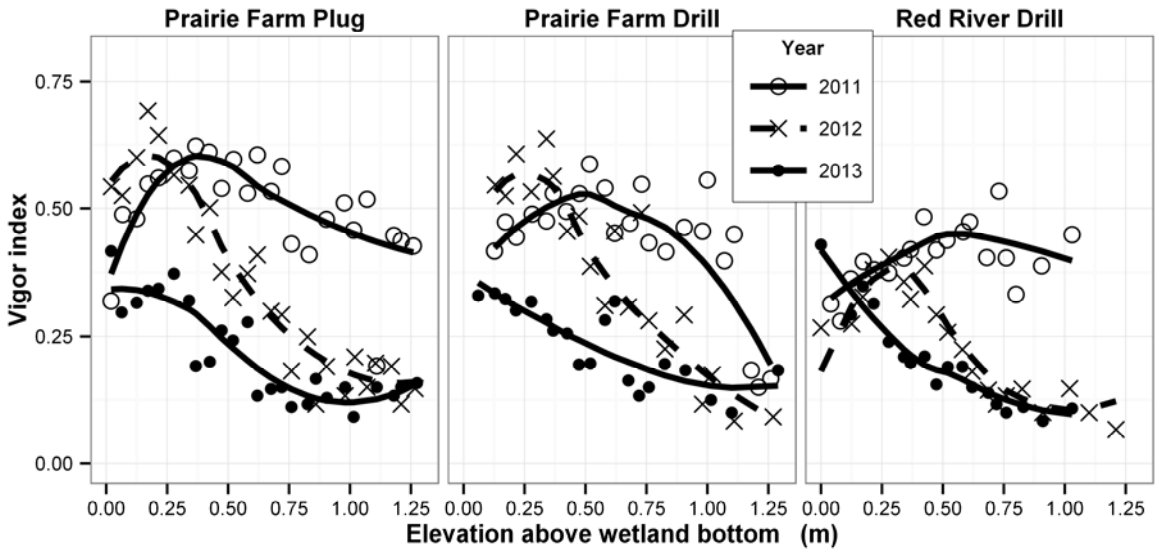

Fig. 3.1 Vigor index of two populations of prairie cordgrass along an elevation gradient, measured in 2011 (solid line with open circles), 2012 (dashed line with exes), and 2013 (solid line with filled circles). The Prairie Farm population was transplanted from greenhouse plugs or drilled. Samples without a plant were removed from the dataset before analysis. Lines were drawn using the second degree local polynomial technique. Before plotting points, values were averaged across transects and elevation ranges of 0.05 m to improve clarity of graphs. Source: Zilverberg et al. (in review).

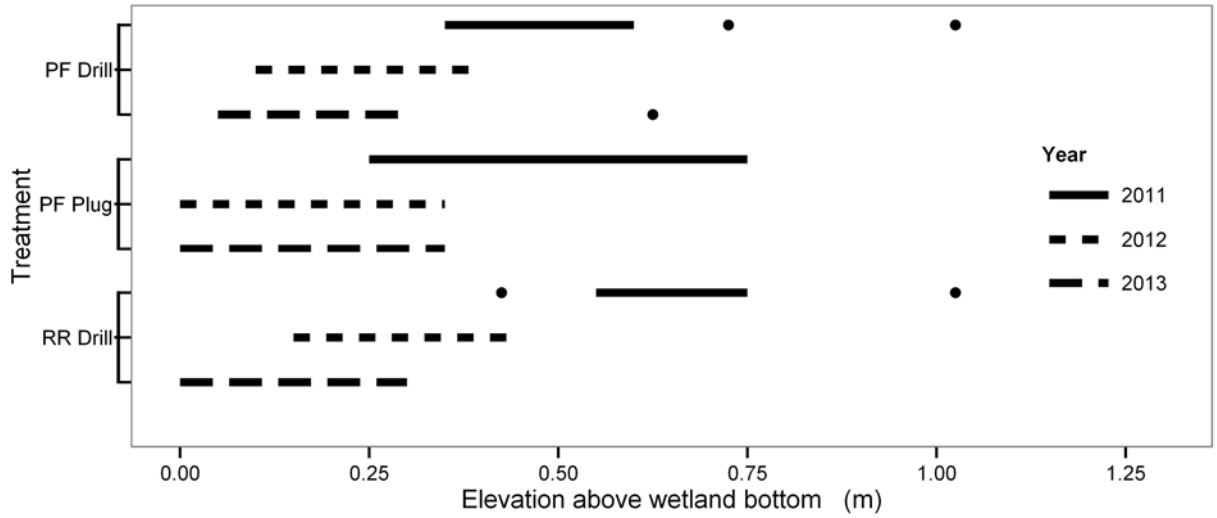

Fig. 3.2 Range of maximum vigor for each combination of population (PF = Prairie Farm; RR = Red River) x planting technique (Drill or Plug), measured in 2011 (solid line), 2012 (short dashed line), and 2013 (long dashed line). Range of maximum vigor was defined as the upper quartile of vigor values, excluding outliers. Outliers are graphically indicated by filled circles. Source: Zilverberg et al. (in review).

Back to Table of Contents

Table 3.1 Descriptive statistics of three plant vigor measurements from two populations of prairie cordgrass planted by drilling or by transplanting plugs. Values are summarized over all years, transects, and elevations. Data were not aggregated by elevation before values in this table were determined. Quadrat size was 1 m^2. Analysis of plant height and inflorescence density excluded quadrats that did not contain at least one tiller. Analysis of maximum inflorescence height further excluded quadrats without at least one inflorescence. Source: Zilverberg et al. (in review).

Population	Planting technique	Plant height (m)					Maximum inflorescence height (m)					Inflorescences (m^{-2})				
		N	Mean	Max	Min	CV	N	Mean	Max	Min	CV	N	Mean	Max	Min	CV
Prairie Farm	Plug	391	1.2	2.0	0.4	0.23	265	2.1	2.8	0.8	0.17	391	8.5	55	0	1.3
Prairie Farm	Drill	288	1.2	1.7	0.3	0.22	189	2.0	2.9	0.7	0.18	288	5.7	41	0	1.4
Red River	Drill	258	0.9	1.5	0.4	0.25	174	1.5	2.2	0.5	0.20	258	5.8	34	0	1.3

Gradient analysis revealed a zone of maximum prairie cordgrass ***vigor*** that ***shifted downslope*** to the center of the wetland beginning in 2012 (Fig. 3.2), the driest summer on record. In 2012, the basin recharged with rainwater early in the spring (326 mm precipitation from Apr.-May) but dried out because little moisture was received from June to Sept. (164 mm). Thus, plants were flooded for less time in the dry summer and probably extended roots deeper to reach groundwater. This was most detrimental to plants in the upper portions of the basin and the upland surrounding the wetland, where vigor decreased more rapidly with increasing elevation than in 2011, when the wetland received normal precipitation. However, the shallow water in 2012 was beneficial for those plants in the basin center, which had presumably been stressed by extended inundation in 2011. Effects of the 2012 drought extended into 2013, when the wetland held much less water despite receiving average precipitation in the spring.

Zones of maximum production for the two populations overlapped. There was ***no difference in biomass yield of the two populations*** ($p = 0.58$) in 2013. In 2012, the zone of maximum vigor ranged from 0.35 m maximum water depth to 0.10 m above the basin rim. This zone yielded 11.1 Mg ha^{-1}. In 2013, yield (6.0 Mg ha^{-1}) was greatest from 0.17 to 0.40 m relative elevation (Table 3.2), which corresponded to a maximum water depth of 0.10 to 0.33 m. Yield declines from 2012 to 2013 were presumably due to the dry summer through winter in 2012 that lowered the water table.

Within our zone of optimal production and after a severe drought, yield was lower than other experiments on good soils (6.4 and 11.7 Mg ha^{-1}; Boe and Lee 2007 and Boe *et al.* 2009) and in natural stands (9 Mg ha^{-1}, Albertson and Weaver 1944). Our yields at the highest elevations, upslope of the temporary wetland in an area dominated by big bluestem (*Andropogon gerardii*), were similar to yields from another experiment on gravelly upland soils (1.4 Mg ha^{-1}; Boe *et al.* 2009). ***The most-suited areas for cordgrass production are likely shallow temporary wetlands and seasonal wetlands with short hydroperiods.***

We observed the Red River population to have a more tussock-like growth form, compared to Prairie Farm, which spread rapidly and obscured the location of the original rows planted. Prairie Farm's natural leaf height (1.2) and inflorescence height (2.0 m) were both greater than Red River (natural leaf height: 0.9 m, inflorescence height: 1.5 m), but the populations did not differ in biomass. The height difference might impact benefits to wildlife because if left unharvested over winter, the taller Prairie Farm population might continue to provide wildlife cover after Red River was buried by deep snow. Population had no effect or an inconsistent effect on inflorescence density and biomass; these factors were more sensitive to effects of year and elevation than population.

Back to Table of Contents

Table 3.2 Biomass production (Mg ha^{-1}) by two populations of prairie cordgrass planted using two techniques at different elevations above the floor of a wetland basin in 2013. Samples were cut at ground level. Within a row, values followed by the same lowercase letter are not different ($p > 0.05$). Values are means of four blocks and two planting techniques (first row) or four blocks and two populations (second row). N = 84. Source: Zilverberg et al. (in review).

Population	Planting technique	Relative elevation						
		< 0.08 m	0.08 to 0.16 m	0.17 to 0.22 m	0.23 to 0.32 m	0.33 to 0.40 m	0.41 to 0.80 m	0.81 to 1.13 m
Prairie Farm	Drill/Plug	1.50 a	4.49 b	6.13 b	5.91 b	6.39 b	1.35 a	0.18 a
Prairie Farm/ Red River	Drill	0.00 a	3.06 b	5.04 c	5.89 c	6.69 c	1.56 ab	0.04 a

4. Harvest Methods

In 2010 and 2011, samples were cut at ground level by hand and the bottom 15 cm were removed and weighed separately. Whole samples averaged 12.9 Mg ha^{-1}, with 1.9 Mg ha^{-1} in the bottom 15 cm. This suggests that harvesting at 15 cm would reduce yields by 15%. In reality, mechanical harvesting is likely to be less efficient than hand harvesting, so losses would probably be greater than 15%.

Therefore, we assessed harvest efficiency with field-scale equipment in 2012. We achieved cordgrass yields of 8.3 Mg ha^{-1} harvested by field-scale equipment to a 12-cm stubble height in the 0.5-ha wetland at the experimental site (Zilverberg *et al.* with editor). This harvest was conducted using a swather and large round baler, conventional haying equipment. The harvest occurred *after* cordgrass had been combined for seed and some biomass consequently removed. In the same year, hand-harvested samples cut at ground level yielded 13.8 Mg ha^{-1}. Thus, removing some biomass during combining, leaving a 12-cm stubble height, and the inefficiencies of mechanized harvest resulted in a 40% reduction in yield.

There is some economic risk associated with harvesting wetlands because a wet autumn could result in standing water that would delay harvest, although this has not been a problem at the experimental site during the past 4 yr. Harvesting on frozen soils or ice is possible, but delaying harvest until soils freeze would lower yields.

5. Integration of Lowland Studies with Previously Funded Upland Studies

The research location was also the site of experiments on upland vegetation and other wetlands. This offered the opportunity to compare results of different vegetation and soil types across the EcoSun Prairie Farm, which contains the heterogeneity typical of eastern South Dakota farms. Other vegetation types evaluated were: three varieties of switchgrass, three different mixtures of prairie plants, and one field planted to seed harvested from a nearby remnant prairie. The fields ranged from 4 to 46 ha in size. In addition, two wetlands of ~ 0.4 ha and numerous smaller wetlands or waterways were planted to prairie cordgrass.

The results of the upland vegetation biomass production are provided in Figure 5.1, with solid dots indicating the yield of cordgrass in its zone of maximum production from the experiment described in sections 2-3. Yield in 2011 was low relative to other fields because cordgrass was not yet fully established. In 2012, though, yield was similar to switchgrass. The trend of low initial yield followed by equaling or exceeding switchgrass yield was also followed by cordgrass planted into a different wetland on the farm, also shown in Figure 5.1 (open squares). Yield of cordgrass in both wetlands declined in 2013, presumably due to a low water table caused by the historic drought of 2012.

Side-by-side comparisons of switchgrass and cordgrass were not available because each species was planted in the topographical position (upland or wetland) to which it was best adapted. Cordgrass is more tolerant of flooded conditions than is switchgrass, but even cordgrass performed poorly in the deepest parts of the experimental wetlands in wet years due to extended inundation. Prior to initiation of the experiment, when the fields were planted to a corn-soybean rotation, these wetlands often experienced crop failures due to poor drainage. Given that ***prairie cordgrass yields in wetlands were similar to switchgrass yields in the uplands***, planting each species in the location where it is best adapted could result in maintenance or increase of field-scale yields in addition to increasing field-scale biodiversity. Alternatively, if the uplands remained in grain production, the wetlands could still be planted to cordgrass and harvested with or without the upland corn stover.

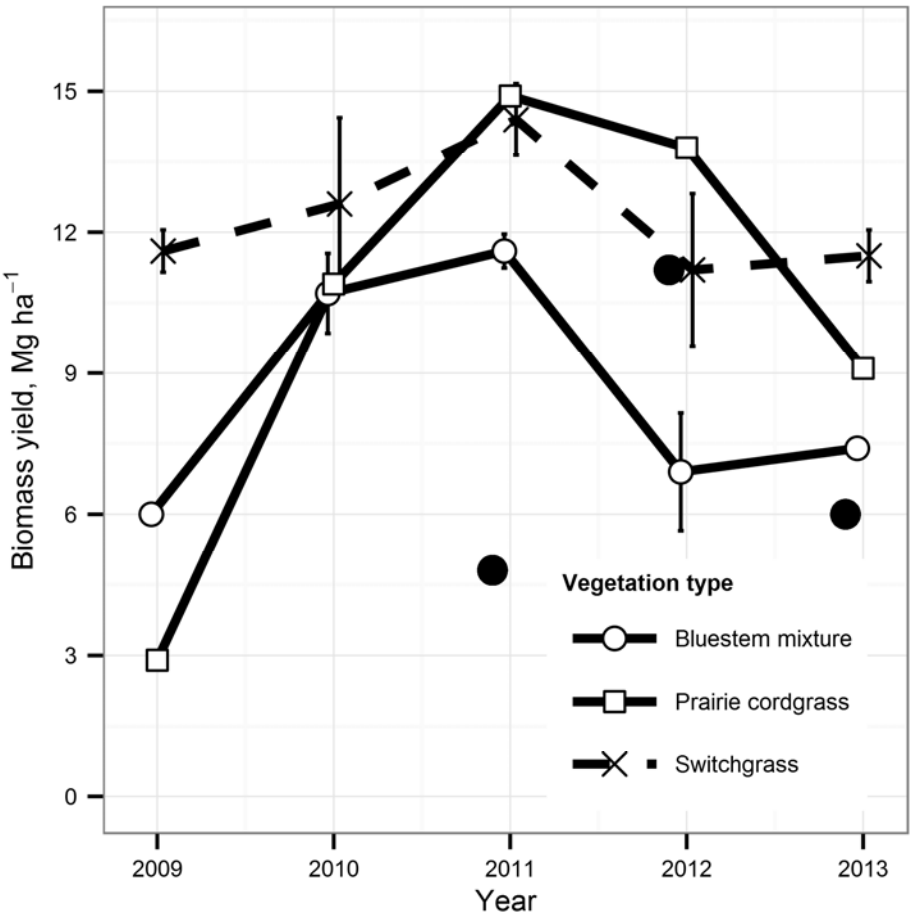

Fig. 5.1 Biomass yield of three vegetation types on the Prairie Farm, harvested by hand at ground level. Each point represents the mean of all established fields in a given year. Vertical lines represent +/- the standard error when more than one field was sampled. Solid dots are the yield of prairie cordgrass in the zone of maximum production in the experimental wetland. In 2011, the experimental wetland was sampled at a 10-cm cutting height; all other years and samples were harvested at ground level. Modified from Zilverberg et al. (with editor).

The 262-ha EcoSun Prairie Farm contained about 30 wetlands. Suppose a farm contained 10 wetlands of ~0.5 ha and each yield 8 Mg ha^{-1}. The resulting yield would be 40 Mg total biomass. This poor quality hay sold at a price of \$100 Mg^{-1} in 2012, for a gross revenue of \$4000, or \$800 ha^{-1}. In 2012, the previously mentioned 0.5-ha wetland also yielded ~60 kg pure live seed ha^{-1}, valued at \$150 kg^{-1}, for a gross seed revenue of \$9000 ha^{-1}. Including this revenue would recover establishment costs with a single harvest. Currently, most cordgrass seed is used for conservation plantings, but the market could expand if cordgrass is used as a biofuel crop.

Farm revenue increased every year as more land came into production and marketing skills improved (Figure 5.2). Wetlands planted to prairie cordgrass were among the most profitable acres on the farm due to their valuable seed and high biomass production. Gross revenue reached US\$138,000 on 221 ha (546 ac) in 2012 despite severe summer drought. A landowner who provided his own labor would have had a ***net income of US $60,000***. Although this was less than what could have been earned at the historically high corn prices from 2010 to 2012, it was more than the median household income (US\$49,415; US Census Bureau 2013) in South Dakota. Many farm families choose to farm because of the lifestyle, and some may be willing to accept a lower income in exchange for a lifestyle that promotes conservation of soil, water, and wildlife while performing animal husbandry. This style of farm may also appeal to landowners who have off-farm income or live elsewhere, but wish to be good stewards of their ancestral land and maintain a place to hunt and recreate.

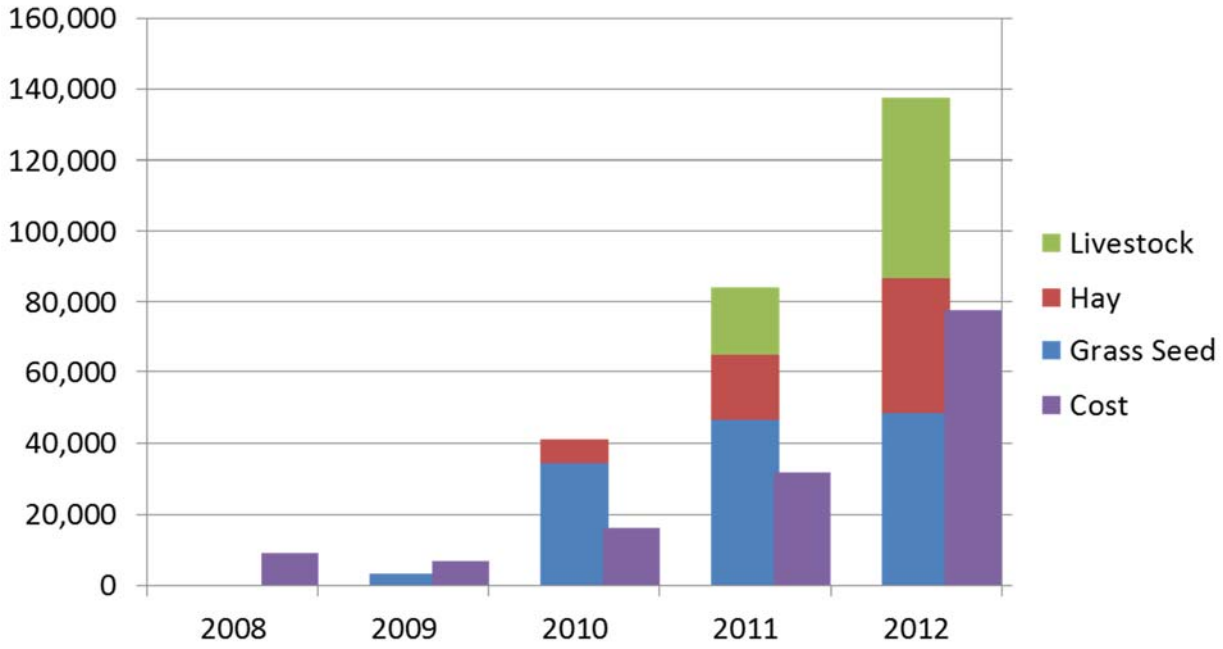

Figure 5.2. Sources of revenue (blue, red and green bars) and operating costs (purple bar) on EcoSun since establishment in 2008. Costs do not include labor or land rental. Source: Archer et al. 2013.

6. Conclusions

Prairie cordgrass is a high-yielding biomass crop that can be effectively established in temporary or seasonal wetlands of the Prairie Pothole region. Cultivating prairie cordgrass in farm wetlands offers the opportunity to gain income from the sale of biomass (as hay or, potentially, as biofuel feedstock) and seed, while also providing valuable ecosystem services in the form of biodiversity, fish and game habitat, flood attenuation, surface and ground water purification, stock watering, and carbon storage.

Prairie cordgrass can be established by direct-drilling of plants into soybean stubble, or by transplanting from plugs started in a greenhouse, but transplanting is more effective than drilling when severe flooding may impact young plants. Yield of prairie cordgrass in wetlands was similar to the yield of switchgrass in nearby uplands. The optimum elevation for prairie cordgrass shifts within a wetland in response to changes in the water table. Conventional harvesting equipment already present on many farms can be used to harvest the plant's seed and biomass. Although the Prairie Farm population of cordgrass was taller than the Red River population and appeared to spread more vigorously by rhizomes, we found no statistical difference in biomass yield between the two populations. In conclusion, prairie cordgrass should be considered for revegetation of farm wetlands because of the potential for both income and ecosystem services it can provide.

Publications/Conference Papers/Public Releases/ Outreach of Results

Publications:

Zilverberg, CJ, WC Johnson, A Boe, V Owens, DW Archer, C Novotny, M Volke, and B Werner. Growing *Spartina pectinata* in previously farmed prairie wetlands for economic and ecological benefits. Wetlands (with editor).

Presentations and farm tours:

Public field Tour of the EcoSun Prairie Farm on August 3, 2012. Research conducted on the farm funded by the Sun Grant Center program was reviewed.

Field Tour of the EcoSun Prairie Farm on July 26, 2013. Research conducted on the farm funded by the Sun Grant Center program was reviewed. This was a focused field tour open to invited stakeholders.

Archer, D.W., W.C. Johnson, C.J. Zilverberg, C. Novotny, T. Schumacher, A. Boe, and S. Kronberg. 2013. Economic Performance of a Corn Belt Grass Farm. Poster presented at the 68th International Annual Conference of the Soil and Water Conservation Society, Reno, Nevada, July 21-24, 2013.

Zilverberg, C.J. *, W.C. Johnson, and D. Archer. Restoring prairie for agricultural production and profit. America's Grasslands Conference, 2013.

Zilverberg, C.J., W.C. Johnson, A. Boe, V. Owens, and D. Archer. 2013. Improving production, resilience, and biodiversity of perennial grass mixtures and monocultures as biofuel feedstocks across environmentally heterogeneous landscapes. Presented at the 2013 North Central Regional Sun Grant Center Annual Meeting. 26-27 Mar., 2013. Chicago, IL.

Johnson, W.C., A. Boe, V. Owens, C. Zilverberg, and C. Novotny. 2013. Biofuel feedstock crops in sub-irrigated lowlands. Presented at the 2013 North Central Regional Sun Grant Center Annual Meeting. 26-27 Mar., 2013. Chicago, IL.

Presentation by W. Carter Johnson on the progress being made at the EcoSun Prairie Farm, "Green Drinks" seminar series, Sioux Falls, SD (July 25, 2011).

Showings of the documentary film by W. Carter Johnson, "*Grass Roots: The Prairie Farm Story*," McCrory Gardens Visitor and Education Center, Brookings, SD, September 15, 2011 (research sponsored by the Sun Grant Center is reviewed in this film) and to a food and nutrition class at SDSU (Dr. Shelly Brandenburger) on November 27, 2011.

Public field Tour of the EcoSun Prairie Farm on August 3, 2011. Research conducted on the farm funded by the Sun Grant Center program was reviewed.

Tours of the EcoSun Prairie Farm by a grassland ecology class (OLLI organization) led by Dr. Larry Tieszen (EROS and Augustana College) on September 20, 2012 and an agricultural economics class from SDSU (Dr. Mike Miller) on October 20, 2013. Sun Grant funded research shown and discussed.

Program Review Presentation (C. Johnson), "Landscape-Scale Biomass Production, Economics, and Environmental Quality," North Central Sun Grant Research Center, Indianapolis, IN (2012)

Contributed Paper (C. Johnson), "South Dakota's Prairie Farm: An Experiment in Ecological and Economic Sustainability," Conference on America's Grasslands: Status, Threats, and Opportunities, Sioux Falls, SD (2011)

Invited Keynote Address (C. Johnson), "Dakota Grasslands, Wetlands, and Climate Change: Last Nail or Silver Lining?" Annual Meeting of the South Dakota Academy of Science, Oacoma, SD (2011)

Invited Lecture (C. Johnson),"South Dakota's Prairie Farm, An Experiment in Ecological and Economic Sustainability," Inaugural Civitas (Honors) Lecture Series, Augustana College, Sioux Falls, SD (2011)

Program Review Presentation (C. Johnson), "Production of Biomass Across Heterogeneous Landscapes," North Central Sun Grant Research Center, Orlando, FL (2011)

Seminar (C. Johnson),"Biofuel Feedstock Production at the Prairie Farm," NRCS Plant Materials Center, Bismarck, ND (2011)

Invited Lecture (A. Boe),"South Dakota's Prairie Farm Project—An Experiment in Grassland Farming," Brookings, SD (2011)

Invited seminar (C. Johnson), "South Dakota's Prairie Farm: An Experiment in Economic and Ecological Sustainability," University of Northern Iowa (sponsored by UNI Tallgrass Prairie Center and the College of Natural Sciences/Humanities and Fine Arts. (2010)
Invited speaker (C. Johnson), "The Prairie Farm Concept and South Dakota's Alternative Energy Future," Annual Conference of the SD Association of Conservation Districts, Pierre, SD (Alternative Energies Session). (2010)
Invited banquet speaker (C. Johnson), "Prairie Farm Research," Annual Meeting of the Eastern Dakota Water Districts, Brookings, SD (2010)
Presenter (C. Johnson), "Research Progress in Biofuel Feedstocks," North Central Sun Grant Research Center 5 X 10 meeting, Brookings, SD (2010)
Program Review Presentation (C. Johnson), Landscape Scale Lignocellulosic Biomass Production, Economics and Environmental Quality," North Central Sun Grant Research Center, Reno, NV (2010)
Invited seminar (C. Johnson), "South Dakota's Prairie Farm," Iowa State University Sustainable Agriculture Colloquium, Ames. (2009)
Invited seminar (C. Johnson), "South Dakota's Prairie Farm," Ecology and Environmental Biology Seminar Series, SDSU, Brookings. (2009)
Invited seminar (C. Johnson), "South Dakota's Prairie Farm," Plant Science/NCARL Seminar Series, Brookings, SD (2008)

Popular and Public Press Articles Written About This Project

- Zilverberg, C. 2013. The Prairie Farm: bringing back grass. Grassroots 15(2):2. March 2013.
- "Researchers Evaluate Grass Farming's Potential" in Hay and Forage Grower magazine (written by Loretta Sorenson based on interview with C. Johnson). (2012)
- **"**Remaking Prairie, Re-Greening Agriculture: Creating a Working Farm Growing Native Grass" in Prairie Fire, The Progressive Voice of the Great Plains (written by Peter Carrels; centerfold article describes research and demonstration work on the Prairie Farm)(2011)
- "Taking Grass to the Next Level: Prairie Farm Rooted in Desire to Sustain Land" in Sioux Falls Argus Leader Newspaper (front page) (written by Cody Winchester) (2011)
- "They're Farming a Sea of Grass: Four Ph.D.s Out to Prove Tall-Grass Farming can be Profitable" in Brookings Register (front page) (written by Ryan Woodard) (2011)
- "Second Civitas (Honors) Lecture Features Ecologist" in the Augustana College Mirror (front page) (Promoting lecture by C. Johnson as part of Civitas lecture series) (2011)
- "South Dakota's Best Prairies" in South Dakota Magazine (written by Jerry Wilson) (Prairie Farm project featured) (2011)
- "The State—And Fate—of Prairie" in Outdoor America (Izaak Walton League of America). 2013 (issue 4): 30-39.

Proposals Submitted/Funded:
Johnson, W. C., A. Boe, V. Owens, and D. Archer. Improving production, resilience, and biodiversity of perennial mixtures and monocultures as biofuel feedstocks across environmentally heterogeneous landscapes. $590,000 for 3 years (funding started in Spring, 2012). (NC Sun Grant Research Center)

References
Albertson FW and Weaver JE (1944) Nature and degree of recovery of grassland from the great drought of 1933 to 1940. Ecological Monographs 14:393-479.

Archer, D.W., W.C. Johnson, C.J. Zilverberg, C. Novotny, T. Schumacher, A. Boe, and S. Kronberg (2013) Economic Performance of a Corn Belt Grass Farm. Poster presented at the 68th International Annual Conference of the Soil and Water Conservation Society, Reno, Nevada, July 21-24, 2013.

Boe A and Lee DK (2007) Genetic variation for biomass production in prairie cordgrass and switchgrass. Crop Science 47:929-934.

Boe A, Owens V, Gonzalez-Hernandez J, Stein J, Lee DK, and Koo BC (2009) Morphology and biomass production of prairie cordgrass on marginal lands. Global Change Biology Bioenergy 1:240-250.

Galatowitsch SM (2012) Ecological restoration. Sinauer Associates, Inc., Sunderland, MA. 630 p.

Jensen NK (2006) Plant guide: prairie cordgrass. United States Department of Agriculture, Natural Resource Conservation Service. Available at: http://plants.usda.gov/plantguide/pdf/pg_sppe.pdf. Accessed: 23 Jan 2013.

NRCS [United States Department of Agriculture Natural Resource Conservation Service] (2011) Custom soil resource report for Moody County, South Dakota. 13 June 2011.

NRCS (2012) Release brochure for Red River natural germplasm prairie cordgrass (Spartina pectinata). Plant Materials Center, Bismarck, ND. Available at: http://www.plant-materials.nrcs.usda.gov/pubs/ndpmcrb11300.pdf. Accessed: 23 Jan 2013.

NOAA [National Oceanic & Atmospheric Administration] (2013) Monthly climatological summary. Available at: http://www.ncdc.noaa.gov/cdo-web/#t=secondTabLink. Accessed: 24 Oct 2013.

Stewart RE and Kantrud HA (1971) Classification of natural ponds and lakes in the glaciated prairie region. U.S. Fish and Wildlife Service, Resource Publication 92.

US Census Bureau (2013) Median household income by state – single-year estimates. http://www.census.gov/hhes/www/income/data/statemedian/.

Zilverberg, C, WC Johnson, D Archer, S Kronberg, T Schumacher, A Boe, and C Novotny. 2014. Profitable prairie restoration: The EcoSun Prairie Farm experiment. Journal of Soil and Water Conservation 69:22A-25A. http://www.jswconline.org/content/69/1/22A.full.pdf+html

Zilverberg, C.J., W.C. Johnson, V. Owens, A. Boe, T. Schumacher, K. Reitsma, C.O. Hong, C. Novotny, M. Volke, and B. Werner. Biomass yield from planted mixtures and monocultures of native prairie vegetation across a heterogeneous farm landscape. Agriculture, Ecosystems, and Environment (with editor).

Zilverberg, CJ, WC Johnson, A Boe, V Owens, DW Archer, C Novotny, M Volke, and B Werner. Growing *Spartina pectinata* in previously farmed prairie wetlands for economic and ecological benefits. Wetlands (with editor).

Back to Table of Contents

Sun Grant Initiative

DOE Final Progress Report

Project Title: Catalytic Fast Pyrolysis of Agricultural and Forest Residues for Aromatic Fuel Additives

Project Director/Principal Investigator: Dr. Lin Wei, Department of Agricultural and Biosystems Engineering, South Dakota State University, Brookings, SD 57007

All Co-Principal/Other Investigators: Dr. James Julson, Professor, Department of Agricultural and Biosystems Engineering, South Dakota State University, Brookings, SD 57007

Collaborators (Cost-Sharing Partners): N/A

Period of Performance: 1 July 2010 - 30 September 2014

Funding Awarded: $329,460

Cost Share Amount: $82,364

Cost Share Sources: Time and effort from PIs and CoPIs; Indirect on time and effort

Executive summary
Lignocellulosic biomass such as cheap, local, and abundant agricultural and forest wastes are not being currently used in the transportation fuel industries. This is primarily because economical processes for their conversion haven't been developed. Although conventional pyrolysis can convert biomass into bio-oil with a yield rate high up to 70%, the quality of bio-oil produced, processing efficiency and economic challenges still remain for its commercialization. A new advanced technology, catalytic fast pyrolysis (CFP), has emerged as the most promising process for lignocellulosic biomass to advanced biofuels in recent years. However, there are very limited reactors currently available meeting the requirement of accurately controling reaction temperature with high heating rate for CFP process. South Dakota State University (SDSU) researchers have developed a proprietary CFP technology to produced quality bio-oils from various biomass feedstocks, which can be upgraded to aromatic hydrocarbon biofuels by combining with a sequential hydrodeoxygenation (HDO) reactor. The biofuels produced were compatible with petroleum-derived hydrocarbons and can be directly dropped in an existing petroleum refinery for further refining to "green" gasoline, diesel, and jet fuel or directly blending with conventional transportation fuels as fuel additives. As parts of the innovative CFP technologies, novel catalysts and their implementations were screened to develop an effective catalyst system. The effects of different catalysts and their implementations on bio-oil yield and quality were investigated during the CFP processing. Instead of noble metals Pt, Pd, or Ru, cheaper transition metals Mo and Cu combined with ZSM-5 were formulated to synthesize new catalysts. Two different catalyst implementation systems, In-situ CFP and Ex-situ CFP, were examined. The results indicated that the SDSU proprietary CFP reactor can convert various biomass feedstocks into bio-oils that can be upgraded into drop-in biofuel using a HDO process with presenting of the catalysts. It was found that the CFP reactor configuration, catalyst and its implementation significantly affect bio-oil yield and quality. There will be a very promising potential to commercialize these technologies to biofuel industry if some minor issues such as gas lacking or condenser cooling efficiency were addressed. Based on the first generation CFP reactor, a second generation of CFP reactor was also designed and fabricated in this project, but its performance examination was not included in this project. In addition to commercial potential of the proprietary CFP reactor and new catalyst systems, the research provides very helpful information for fully understanding the chemical mechanism of CFP–HDO process and the linkages between biomass species, reaction temperature, catalyst systems, and the yield and quality of drop-in biofuels produced. This information is also very useful for biofuel industry and public awareness regarding to sustainable agriculture and advanced biofuels production. Because of helping in domestic biofuel production, the project will eventually benefit national energy security and greenhouse gas (GHG) emission reduction.

BACKBROUND AND OBJECTIVES

As a result of concerning environmental impact, finite resource, and energy security, development of alternatives to fossil fuels has attracted much attention worldwide in recent years. Biomass is the only sustainable alternative to fossil fuels capable of yielding petroleum like products that can be important feedstocks for manufacturing goods ranging from plastics and chemicals to fuel oil, lubricating oil, and hydraulic fluids using existing infrastructures [1 – 7]. Among biomass resources, agricultural and forest residues are the most readily available resources in large quantities at relatively low cost [7 - 9]. These lignocellulosic biomass feedstocks, however, are not being currently used in the transportation fuel industries. This is primarily because economical processes for their conversion haven't been developed. Biomass fast pyrolysis is proven one of the most promising thermochemical technologies to convert cheap, local, and abundant agricultural and forest wastes such as corn stover or sawdust into a useful form [6 - 9].

Pyrolysis is a thermochemical process in which biomass is heated to 400 - 600^{o}C in absence of air decomposing the biomass into three products: solid charcoal (called bio-char), liquid compounds (also called bio-oil), and a gas mixture (so called syngas.) The yield proportions of bio-oil, biochar, and syngas are heavily affected by the feedstock species used, reactor type, and operating conditions. Pyrolysis is a relatively simple, inexpensive, and robust process. The robust nature of pyrolysis technology allows considerable flexibility in the type and quality of the biomass feedstock, product applications, and production scales that may be compatible with existing agriculture and forestry infrastructure [8 – 12]. Generally, crude bio-oil produced from biomass pyrolysis is an unstable acidic combustible liquid containing more than 200 compounds. This crude bio-oil has some undesirable properties including high total acid number, low energy content (~16 MJ/kg), high oxygen content (~40%), high water content (~40%), chemical instability, and not compatible with conventional transportation fuels such as gasoline and diesel. Crude bio-oil must be catalytically upgraded before it can be used for transportation fuels or fuel additives. Various bio-oil upgrading techniques including hydrodeoxygenation (HDO), emulsification, catalytic cracking, etc. are currently under development. HDO is a process removing oxygen from bio-oil in H_2O form by injecting high pressure hydrogen into the reactor coupled with specific catalysts. HDO can elevate bio-oil energy density and quality, but it has to go through multiple steps and needs complicated equipment with the presenting of hydrogen and catalysts, which will significantly increase biofuel production costs. Bio-oils can also be upgraded to diesel for fueling engines or boilers by emulsifying it with a specific surfactant. Although there is no redundant chemical transformation, the high energy consumption and possible corrosion to engines are big concerns for bio-oil emulsification. Another method is to apply acidic catalysts in bio-oil vapor stream for bio-oil quality improvement using catalytic cracking reactions. This technology may offer a cheaper route to convert bio-oil oxygenated components into hydrocarbons. However, multiple step catalytic cracking reactions may result in high coking, low oil yield, and higher costs for reactor complex and catalysts.

Although pyrolysis is an effective process for biomass conversion with up to 70% bio-oil yield, conversion efficiency and economic challenges still remain for its commercialization [6 –22]. To address those issues, a new process called catalytic fast pyrolysis (CFP) has been explored over the last decades. In this process biomass is heated up to 450 – 650^{o}C in the absence of oxygen and presence of catalysts decomposing the biomass to quality bio-oil and small amounts of co-products (bio-char and syngas). CFP combines biomass fast pyrolysis and bio-oil catalytic cracking into one-step in a single reactor. This technology offers a simpler process for the

productions of aromatic fuels or hydrocarbon fuel additives from biomass. A theoretical yield of aromatic fuels or hydrocarbon fuel additives can be up to 150 gallons per dry ton of biomass, depending on feedstock species, reactor types, operating conditions, and catalysts used [12 – 18]. CFP has large potential for converting biomass to bio-oil with better yield and quality, but there are very limited reactors currently available meeting the requirement of accurately controling reaction temperature with high heating rate for CFP process. Conventional fixed-bed reactor can only be run at low heating rate and long residence time; fluidized-bed reactors may provide very high heating transfer efficiency but rely heavily on a large volumetric carrier gas. Auger reactors can minimize inert carrier gas used but they are limited by large scale heat transition. Other reactors like rotatory or vacumm pyrolyzers, their performance still need to be proven [16 – 19, 21 – 26]. To resolve these problems, the goal of this research was to design, construction and instrument a novel CFP system for converting agricultural and forest residues into aromatic fuels or hydrocarbon fuel additives. Corn stover and forest residue were used as feedstocks to test the reactor system. Optimizing operating parameters and evaluating the reactor performance were also carried out. Novel catalysts were screened as parts of the CFP process. The specific objectives of this research were:

1) Design, construct, and instrument an innovative 1 – 3 kg/hr CFP system.
2) Optimize the CFP processing parameters for converting corn stover and sawdust to quality bio-oil, and thus upgrading the bio-oil to aromatic fuels or hydrocarbon fuel additives.
3) Develop an effective catalyst system for the CFP process
4) Evaluate the bio-char produced as a catalyst for the CFP process.
5) Perform a primary technical and economic assessment for the CFP process.

METHODOLOGY

Design and fabrication of a CFP reactor system

To combine biomass fast pyrolysis and bio-oil catalytic cracking in one process, a new novel CFP system was designed by integrating the advantages of conventional pyrolysis reactors (such as fluidized-bed and auger reactors) in one unit and avoiding their limitations. This system can convert solid biomass to aromatic fuel or hydrocarbon fuel additives in one system with shorter residence time. During CFP processing, solid biomass is first decomposed into volatile smaller molecule organics, syngas, and bio-char. Before the volatile organics condense into crude bio-oil, they are led to a proper catalyst bed where they are converted into aromatics/hydrocarbons, carbon monoxide, carbon dioxide, water, and char, and then the mixing streams go through a specific filtration unit and a condenser to separate the different components. Eventually, aromatics or other hydrocarbons are separated from the mixture. A process flow diagram of the CFP system is shown as Figure 1. The new CFP system was constructed to maximize heating rate and heat transfer efficiency without using inert carrier gas using a novel mechanic design that combines the advantages of auger, fluidized-bed, and fixed-bed reactors. Along with the reactor design, a catalyst system was also designed to achieve optimal the heterogeneous catalyst performance. These new designs can utilize the heat generated in the pyrolysis process for bio-oil upgrading reactions, simplify conversion process, shorten reaction time, increase processing rate, and as a result provide more margins for improving economics of the CFP technology.

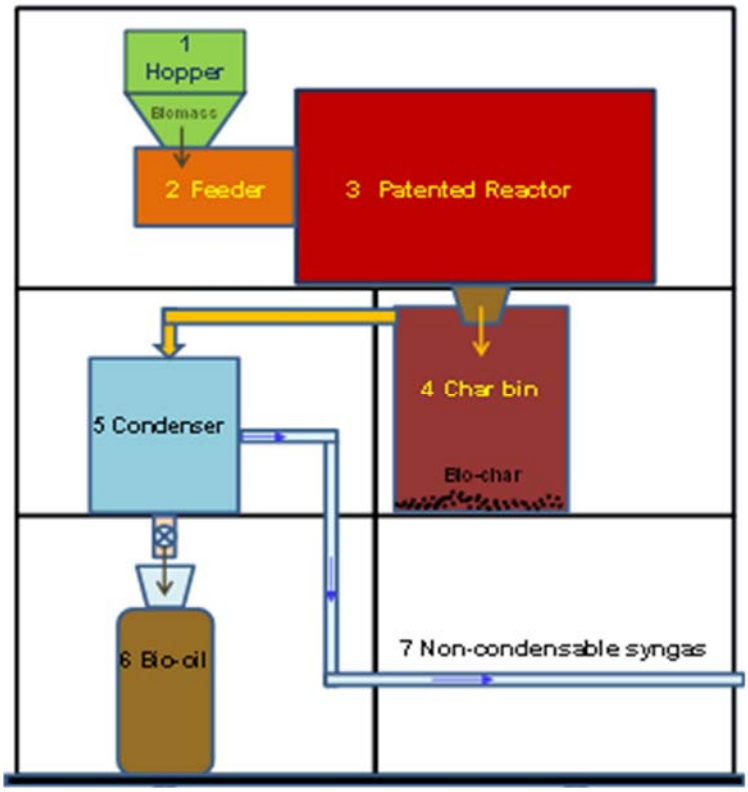

Figure 1. Flowchart of the CFP system

Experimental design

The CFP system was tested by respectively feeding in corn stover and sawdust at different temperatures setting (537°C/1000°F, 648°C/1200°F, and 760°C/1400°F). At the beginning, the reactor was started and the heating trap was pre-heated. After operating temperature was reached, corn stover or sawdust was fed into the reactor. For each test run, 2 kg of feedstock was fed in. During pyrolysis, the bio-oil produced was collected every 20 minutes and then cumulated in a glass bottle for calculating total yield of bio-oil. The yield rate of bio-oil was calculated by total mass of liquid products divided by total mass of feedstock fed in. After finished pyrolysis process, the CFP system was turned off and cooled down. The bio-char cumulated inside the char bin was collected and weighed. The yield rate of bio-char was calculated by the total mass of bio-char divided by total mass of feedstock fed in. Based on mass balance, the syngas yield was calculated by total mass of feedstock fed in minus the yields of bio-oil and bio-char. The test run was duplicated for every feedstock at each temperature. After crude bio-oils were produced, they would be upgraded into hydrocarbons using various approaches such as HDO, catalytic cracking, etc. Different catalysts and implementation systems were also be prepared and tested to develop an effective catalyst system while bio-oils were upgrading. The characterizations of hydrocarbon fuels and catalysts were carried out to examine the performances of the CFP reactor and catalyst system.

Biomass Feedstock

Corn stover and pine sawdust were used as feedstocks in this study. The corn stover was harvested from an agriculture extension farm nearby SDSU after corn harvest, allowed to

dry to about 15 – 20% of MC (moisture content, wet basis) in a swath prior to baling, and then bales stored indoors for about three months. Before hammer milling, corn stover was chopped into small pieces using a knife mill with a 25.4 mm (one inch) screen. The pine sawdust was purchased from local store, in which is produced by the Rushmore Forest Products, Inc. at Rapid City, SD 57745. Both of the corn stover and sawdust were layered on floor and air-dried to about 10 – 12% MC. These dried corn stover and sawdust were ground into powder using a hammer mill (Model M150, Winona Attrition Mill Co. MN) with a 1 mm screen. After the corn stover and sawdust were ground into powder, their moisture content and particle size were determined and the results are showed in Table 1. The analysis of those particle size distributions was also conducted and the results are shown as Figure 2 and 3 respectively.

Table 1. Moisture Content of Feedstock

Feedstock	Corn Stover	Pine Sawdust
Moisture Content (wt %)	6.05	7.15
Particle Size < 1mm (wt %)	87	85

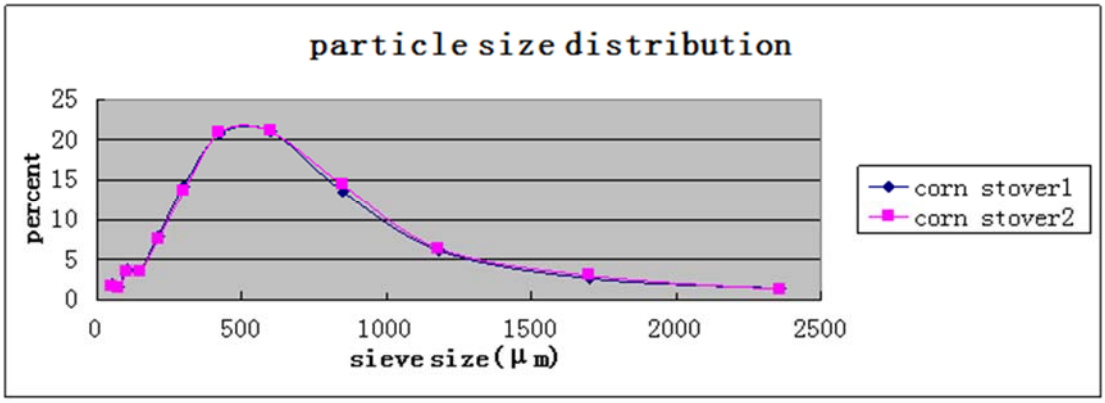

Figure 2. Particle size distribution of the corn stover powder

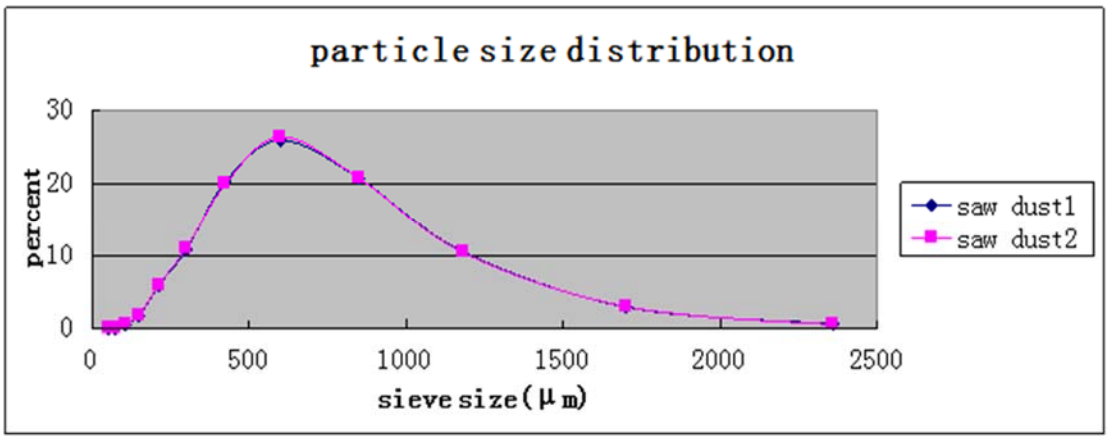

Figure 3. Particle size distribution of the pine sawdust

Bio-oil characterization before and after upgrading

The pH values of bio-oils were measured by a pH meter (AB15, Accumet Company) at room temperature. The instrument was calibrated with liquid calibration standards of pH 4 and 7 prior to the measurement. The viscosity analyzer (REOLOGICA Instruments AB Company Dynamic Viscosity) was used to measure dynamic viscosity at 20 °C. The bio-oil elemental compositions of carbon, hydrogen, nitrogen, and oxygen were determined using a CE-440 Elemental Analyzer. The HHV of samples were determined using a bomb calorimeter (IKA C2000). The moisture contents of samples were measured using a Karl Fischer Titrator V20 (Mettler Toledo Company). Syngas analysis was carried out on a GC (Agilent GC-7890A) equipped with a thermal conductivity detector (TCD) and flame ionization detector (FID). Standard gas mixtures were used for calibration, and argon was used as the carrier gas. GC/MS (Agilent GC-7890A and MSD-5975C) was used to analyze the chemical composition of bio-oil samples. The gas chromatograph was programmed at 60 °C for 1 min, followed by ramp 1 at 3 °C/min to 260 °C and ramp 2 at 5 °C/min to 280 °C. The temperature was held for an additional 10 min after each ramp. The injector temperature was 300 °C, and the injection size was 1 μL. The flow rate of carrier gas (hydrogen) was 1 mL/ min. The compositions were identified through the NIST Mass Spectral Library.

Catalysts preparation

Activated carbon (Norit Company), Alumina oxide (Sasol Inc.) and ZSM-5 (Zeolyst Company) were purchased and used as support materials for the catalyst preparation. These supports were impregnated with a specific loading level of active metals (e.g. Pt, Pd, Ru, Cu, Mo, Ni, Co, etc.) using wet impregnation method and blended with guar gum and boehmite. The catalysts were prepared by pelletizing the mixture into particles with a diameter of 3 mm and the length less than 5 mm. The catalyst pellets were dried at 120˚C for 12hr and calcined at 550℃ for 5hr before use.

Catalysts characterizations

The Brunauer–Emmett–Teller **(**BET) specific surface area and porosity texture of each catalyst were determined by nitrogen adsorption measurements at 77.2 K using an automatic Micromeritics ASAP 2400 apparatus. The catalyst samples were first degassed at 573 K for approximately 6 h and then studied with a static volumetric technique. X-ray crystallography (XRD) was used for phase identification and determination of the relative crystallinity. XRD measurements were carried out using Cu Kα radiation on a RIGAKU SMARTLAB. The X-ray tube was operated at 40 kV and 44 mA and the X-ray pattern was scanned with a step size of crystallite sizes of 0.02° (2θ) from 5 to 50° (2θ) and counting time of 1 s per step.

Catalyst system design and catalysts screening

The outcomes of catalytic reactions depend on not only the catalysts used but also how the catalysts are implemented. An effective catalyst system consists of high active catalysts and reliable implementations. Bio-oil long chain hydrocarbon molecules (tar) produced during pyrolysis can poison HDO catalysts and dramatically reduce their useful life during sequent bio-oil upgrading process. The bio-oils produced by CFP reactions, resulting a higher yield of gasoline and diesel ranged hydrocarbons, reduced tar (long chain hydrocarbons) production and increased functional life of the HDO catalysts. There are two different catalyst implementation systems, In-situ CFP and Ex-situ CFP that can help to convert corn stover or sawdust to quality

bio-oils. Both of these two CFP processes can convert bio-oil long chain hydrocarbon molecules to shorter chain molecules. However, it still remains unclear which approach is better, In-situ CFP or Ex-situ CFP? These two catalyst implementations were tested to screen proper catalysts and examine the catalyst system performance as parts of this project.

In-situ CFP approach is based on a process of biomass directly contacting with hot catalyst (and possibly a heat carrier) in a short residence time in a pyrolysis reactor at ~500°C and atmospheric pressure in the absence of air. As the biomass decomposes due to heating into condensable bio-oil vapors and non-condensable gas, bio-char, and coke, the catalyst acts to partially deoxygenate and stabilize the bio-oil vapor. This bio-oil vapors are catalytically converted to less reactive and shorter molecule compounds than those produced by uncatalyzed fast pyrolysis [3, 6, 8 – 17]. Solid bio-char and catalyst are separated from the bio-oil vapor. This could be done, for example, by hot filtration of the bio-oil vapor product prior to quenching liquid products. The stabilized bio-oil vapor is condensed into liquid bio-oil and exits the reactor. Non-condensable gases are removed from bio-oil by a gas-liquid phase separator. The resulting bio-oil is collected and spontaneously separates into aqueous and oil phases. The oil phase of bio-oil can be hydrotreated (e.g. HDO) in one or more stages. The number of stages and severity will be dependent upon the level of oxygen and oxygenated species in the bio-oil produced. After HDO reaction, the upgraded bio-oil is expected to be a wide-boiling range hydrocarbon mixture that can be distilled into appropriate gasoline and diesel hydrocarbon ranges. The aqueous phases resulting from CFP and HDO may contain up to 40% of the biogenic carbon that can be recycled to the process for maximizing carbon efficiency to get higher biofuel yields [18 – 22]. In an Ex-situ CFP system, biomass is rapidly pyrolyzed into condensable bio-oil vapors, non-condensable gas, and bio-char. The bio-oil vapor is filtrated to remove bio-char and solid particulates, and thus passed through a catalyst bed (either fixed-bed or fluidized-bed) to deoxygenate and stabilize it. The resulting bio-oil vapor is condensed into a liquid and spontaneously phase separates into aqueous and oil phases. Similarly, the oil phase can be hydrotreated (e.g. HDO) to a wide-boiling range hydrocarbon mixture that can be distilled into appropriate gasoline and diesel hydrocarbon ranges. The aqueous phases resulting from CFP and HDO can also be recycled to the process for maximizing carbon efficiency to get higher drop-in fuel product yields.

In order to develop a proper catalyst system, an initial In-situ CFP test was carried out using the first generation CFP reactor with a capacity of processing 2 – 3kg biomass feedstock per hour. The preliminary results indicated that there was no significant improvement in bio-oil yield and quality when biomass to catalyst ratio was greater than 1 in the In-situ CFP process. If biomass to catalyst ratio were less than 1, more than 3kg catalyst per hour would be needed to run the SDSU reactor. Since the catalyst (ZSM-5, pricing about $1400/kg) used was too expensive to run CFP tests at a pilot scale at this stage, two lab scale fixed-bed CFP reactors were used to proof of the concept of converting biomass to quality bio-oils and investigate the effect of catalyst implementation (In-situ CFP or Ex-situ CFP) on bio-oil yield and quality in this project.

A flowchart of the lab scale fixed-bed CFP reactors used for In-situ CFP test for the project is shown as Figure 4. The reactor consists of a carrier gas tank, a reactor vessel, a water bath condenser, and a heating furnace with a temperature controller. The reactor vessel is a cylinder made of steel; its size is 7 inches high and 8 inches diameter. Before a test run, 100 g corn stover mixed with a certain ratio of catalyst was put in the reactor. The sealed reactor was placed in the furnace and connected to the nitrogen tank and condenser with pipe lines. When the test started, the reactor system was purged for about 10 minutes using nitrogen gas. After all air in the reactor

was removed, nitrogen flowing was stopped. The furnace was turned on to raise reactor temperature up to 500°C for pyrolyzing the corn stover with the catalyst presenting. After the CFP reactions reached stable operation, non-condensable gases were sampled and collected in a gas storage bag for composition analysis using a GC (Agilent GC-7890A) equipped with a thermal conductivity detector (TCD) and flame ionization detector (FID). When an In-situ CFP test was done, the reactor system was cooled down. Bio-oil samples were collected from the water bath condenser, weighed, and then sent to analytic labs for characterization. Solid bio-char inside the reactor were collected and weighed to calculate the bio-char and no-condensable gas products' yield rates. The bio-char samples were also characterized. The non-condensable gases' yield was determined by mass balance of biomass feedstock input and the bio-char and bio-oil produced.

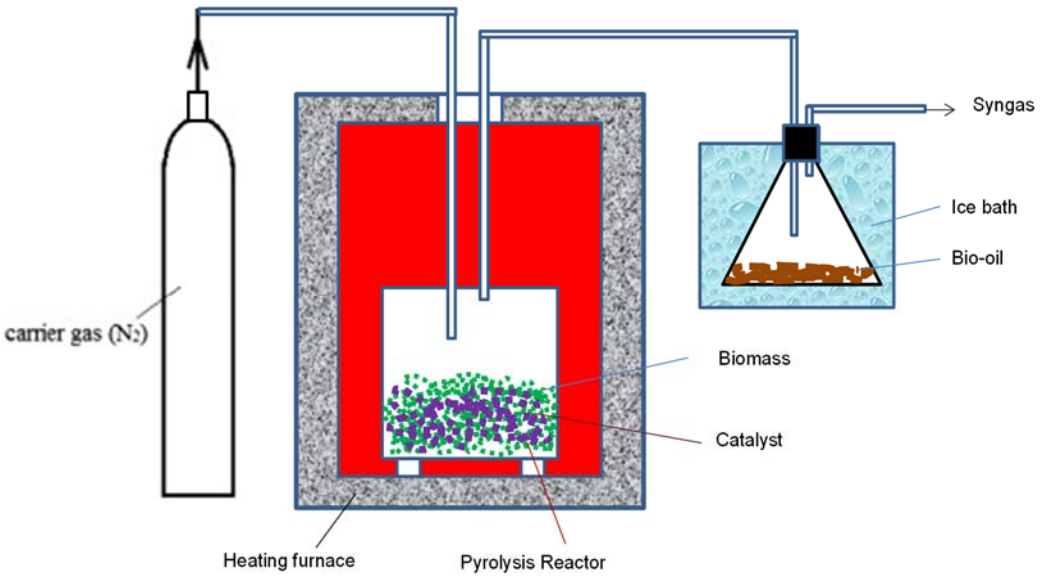

Figure 4. The reactor for biomass and catalyst mixture CFP process

A flowchart of the lab scale coupled fixed-bed CFP reactors used for Ex-situ CFP test in the project is shown as Figure 5. The Ex-situ CFP system is a novel coupled reactor configuration that includes a pyrolysis fixed-bed reactor with 2 inch (50.8 mm) diameter tube, a catalytic fixed-bed reactor with half inch (about 13 mm) diameter tube and a condenser system. Both of the reactors consist of a temperature controlled furnace and a fixed bed tube. During a test run, resulting products went through the condenser to be collected for analysis. The chemical composition of the non-condensable gases was determined using the GC. In each test, 200 g of corn stover was put to the pyrolysis reactor, then 20 g of ZSM-5 was loaded as the catalyst bed. Nitrogen was injected into the system with 10 ml/min flow rate to remove the air for 20 min. The catalytic reactor was heated to a preset temperature (500 °C) at the beginning of the experiment. As the catalytic reactor temperature reached 500 °C, the pyrolysis reactor furnace was turned on to heat up the reactor to 500 °C at a rate of 20 °C/min. When pyrolysis reactor temperature was higher than 200 °C, the corn stover started to be decomposed into condensable bio-oil vapors, non-condensable gas, and bio-char. The pyrolysis reactor temperature was kept at 500 °C for 1 hour to completely pyrolyze all corn stover inside the reactor. The bio-oil vapors went through a filtration set and entered the condenser to be collected as liquid bio-oil. The non-condensable gas

was separated from the bio-oil by a liquid-gas phase separator and existed the condenser. As the pyrolysis reactor was heated up to 500 °C and held stable, the produced non-condensable gases was sampled and collected into a gas bag for later chemical composition analysis. As the Ex-situ CFP test was done, the furnaces were shut off. The system was allowed to cool down for about 2 hours. The Ex-situ CFP test was duplicated for each reaction condition.

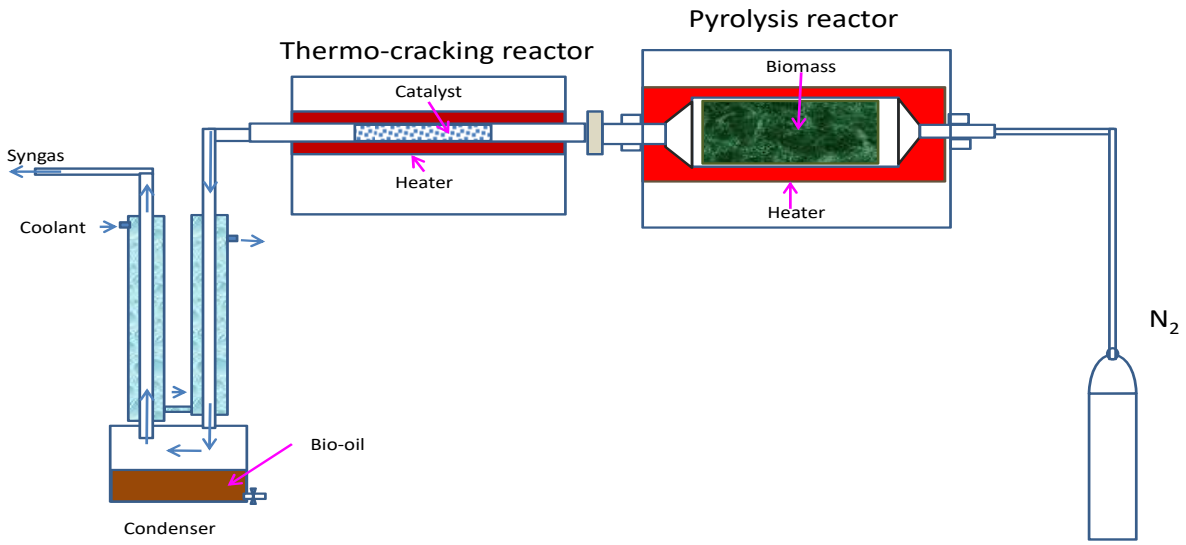

Figure 5. The reactor for CFP process and then followed by bio-oil upgrading process

RESULTS AND DISCOVERINGS

This project originally started on July 1st, 2010 and supposed to be ended up on September 30th, 2012. Based on the project significant progress made, a no cost extension of this project was approved until September 30th, 2014.

Fabrication of a proprietary CFP reactor system ***(This section deleted due to confidentiality)***

(End of Confidential information)

After initial testing and adjustment, the CFP reactor was first tested to examine its performance for pyrolysis of various biomass feedstocks including corn stover, pine sawdust, switchgrass, prairie grass, etc. into bio-oils. The reactor was running well during all test runs. High up to 65% of bio-oil yield was received in the corn stover and sawdust tests. The reactor system temperatures and feedstock feeding rates were easily controlled to the set points. There were no feeding problems or feedstock blockages inside the reactor during pyrolysis, but gas leaks at some connection points was found. These leaks were caused by the gaskets working unstable when the reactor was run too long time at high temperatures. This problem was solved by replacing new high temperature gaskets. Although some improvement is needed, the CFP reactor performance has shown very positive results. All the feedstocks fed into the CFP reactor had

been smoothly pyrolyzed into bio-oil, bio-char, and syngas. The yields of those three products of corn stover and sawdust pyrolysis are showed in Table 2.

Table 2. Average yields of pyrolysis products at different reaction temperatures

	Setting Temp.	537℃	648℃	760℃
	Reaction Temp.	378℃	453℃	558℃
Feedstock	Product Yield	(wt%)	(wt%)	(wt%)
	Bio-oil	41.3	42.7	40.9
	Bio-char	23.4	27.1	24.6
Corn Stover	Syngas	35.3	30.2	34.5
	Bio-oil	47.7	48.5	49.3
	Bio-char	13.2	17.2	14.5
Pine Sawdust	Syngas	39.1	34.3	36.2

Table 2 indicates that the bio-oil yields were relative lower than expected. In contrast, the syngas yields were high. One of reasons may be because of the leaking existing in the reactor system during processing, not all the bio-oil vapors produced were caught into the condenser to be condensed into liquid bio-oil. Although the leaking problem had been found during testing, the reactor was still kept running for examining other functions of the CFP reactor. Another possibility is the condenser was not good enough to condense all the condensable bio-oil vapors into liquid bio-oil since the simple condenser that was made up with a coil tube cooling in ice bath had low cooling efficiency and short retention time. The total loss of bio-oil vapors was estimated at about 10 – 15%, in which had gone with the non-condensable syngas stream. The low bio-oil yields may also be due to the low heat carrier to biomass (H/B) ratios that limited the heating rate of pyrolysis process. According to the average 30 seconds of feedstock retention time inside the reactor, the heating rates were estimated at 706℃/min, 856℃/min, and 1066℃/min for the three setting system temperatures (537℃, 648℃, and 760℃). Those heating rates were not high enough to get optimal bio-oil yields. Table 2 also shows that pyrolysis of pine sawdust yielded more bio-oil than that of corn stover in all operating conditions. This may be because sawdust contains more lignin than corn stover, in which was leading to a higher bio-oil yield.

Another phenomenon is that there was no significant difference in bio-oil yields for both corn stover and sawdust feedstocks when the setting system temperature changed from 537℃ to 760℃, but the bio-char yields at 648℃ were higher than those at two other temperatures (537℃ and 760℃), which resulted in lower syngas yields. This may be because the actual reaction temperatures at the “heat trap” inside the CFP reactor, where the pyrolysis reactions were taking place, were not as high as the setting system temperatures. The actual reaction temperatures were inspected using a thermocouple meter during all the tests. It was found that the actual average reaction temperatures inside the “heat trap” were 378℃, 453℃, and 558℃ respectively (Table 2). Because of the low heating rates and long retention time of bio-oil vapors, the process hasn’t been run in an ideal fast pyrolysis conditions in these tests [24 – 30]. Also, the low reaction temperatures and heating rates resulted in the low bio-oil and high bio-char yields. Some unconverted feedstock particles and char were found in the collected bio-char samples. As an example, the physical properties of bio-oil produced at 453℃ reaction temperature are shown in Table 3. Typical GC/MS profiles of bio-oil chemical composition of corn stover and sawdust

bio-oils are shown as Figure 5 and 6. The testing results (Table 3) shows that the crude bio-oils produced from corn stover and sawdust pyrolysis still have some undesired properties such as high water content and viscosity, low heating value and pH value, etc. Because of reactor leaking issue, ambit air was involved in the pyrolysis reactions that resulted in very high water content in the crude bio-oils. High water content led to low high heating value and viscosity. Before these crude bio-oils can be used for transportation fuels or fuel additives, they must be upgraded into gasoline/diesel ranged hydrocarbons (e.g. aromatics). Different catalysts were prepared to examine their activity, selectivity, lifetime, and regeneration while the crude bio-oils were upgrading using various approaches such as HDO, catalytic cracking, etc. The bio-oil upgrading tests would be very helpful for designing an effective catalyst implementation system for the CFP process development.

Table 3. Properties of bio-oil produced at 453℃ of reaction temperature

Properties	Corn Stover	Pine Sawdust
Density (g/ml)	1.048	1.045
pH	2.7 – 3.5	2.0 – 2.9
Viscosity (cp at 20℃)	3.2	9.8
Moisture Content (wt%)	54.88	47.04
Heating Value (MJ/Kg)	10.19	13.81

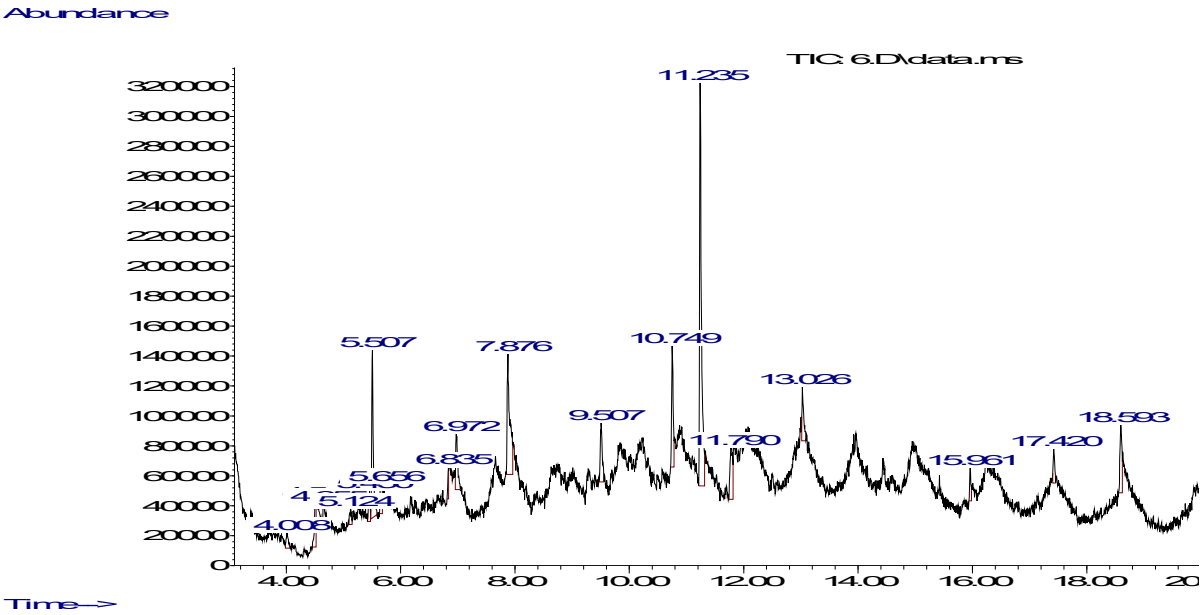

Figure 5. GC/MS profile corn stover bio-oils produced at 453℃of reaction temperature

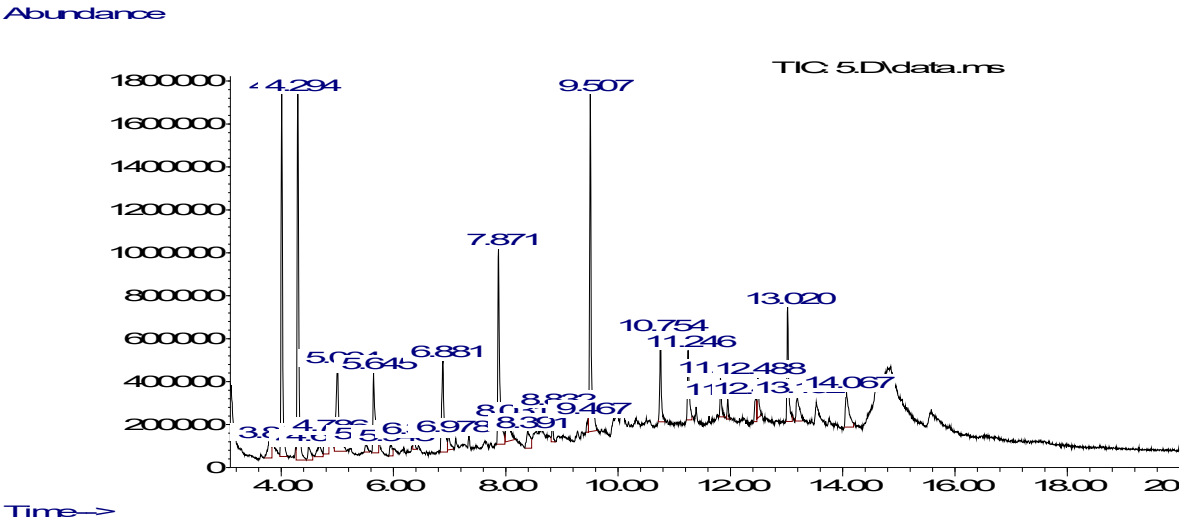

Figure 6. GC/MS profile of sawdust bio-oils produced at 453℃of reaction temperature

Bio-oil upgrading into aromatic hydrocarbons

To explore effective approaches for bio-oil upgrading, after pyrolysis crude bio-oils produced were upgraded using different methods. HDO process was used to upgrade the sawdust bio-oil using a batch reactor (Parr, Model 4575). The bio-oils were individually upgraded using three different catalysts (Ru/C, Ru/ZSM-5 and Ru/Al_2O_3) in the autoclave reactor at high temperature (350℃) and pressure (15.0MPa) under hydrogen atmosphere. The three catalysts prepared were mixed with bio-oil (200g) and then put into the reactor. During upgrading, the reactor was pressurized to 4.8 MPa with hydrogen gas and then heated up to 350˚C at 10℃/min heating. The pressure was raised up to about 15.0MPa at the setting temperature. After HDO process, the reactor was being cooled to room temperature. As the reactor was discharged, upgraded bio-oil samples were collected for analysis. The chemical composition of upgraded bio-oil were determined by a GC/MS. The major compounds were identified by the GC-MS internal library, in which showed the large peaks in the profiles. The function groups of bio-oils were summarized in Table 4. The chemical profiles of the three upgraded bio-oils produced by the HDO process are shown as Figure 7 to 9.

For Ru/C catalyst, alkenes were the main compound with relative content of 11.63%. But in the case of Ru/ZSM-5 catalyst, the relative content of alkenes was only 5.08% and even no alkene was detected in Ru/Al_2O_3 upgraded bio-oil. The content of alkanes was as high as 18.48% in Ru/Al_2O_3 upgraded bio-oil, while no alkane was found in Ru/ZSM-5 upgraded bio-oil. In addition, no alkyne was found in Ru/ZSM-5 upgraded bio-oil. These differences were caused by the differences in surface properties of different catalyst supports. Alkanes were cracked to small molecular chemicals while alkynes were converted to aromatics chemicals on the surface of ZSM-5. In the case of Ru/Al_2O_3 catalyst, the relative amount of aromatics compounds was the smallest among the three upgraded bio-oils, especially for benzenes compounds. These resulted from the surface properties and pore size of alumina. In the presence of water, alumina may change resulting the pore size become smaller, which would limit the formation of large molecular chemicals. Large size pores existed on the surface of activated Carbon and ZSM-5, which would facilitate the formation of aromatics compounds. No alkene was detected in Ru/Al_2O_3 upgraded bio-oil while large amount of alkanes and long chain acids were detected.

These resulted from the hydrogenation of alkenes to alkanes in the presence of hydrogen with Ru/Al_2O_3 catalyst. Though the ketones and aromatics contents in Ru/C upgraded bio-oil were the largest among three bio-oils, the acid content was smallest. Regarding to the performance of these three catalysts, Ru/C catalyst may be the best for bio-oil hydrodeoxygenation.

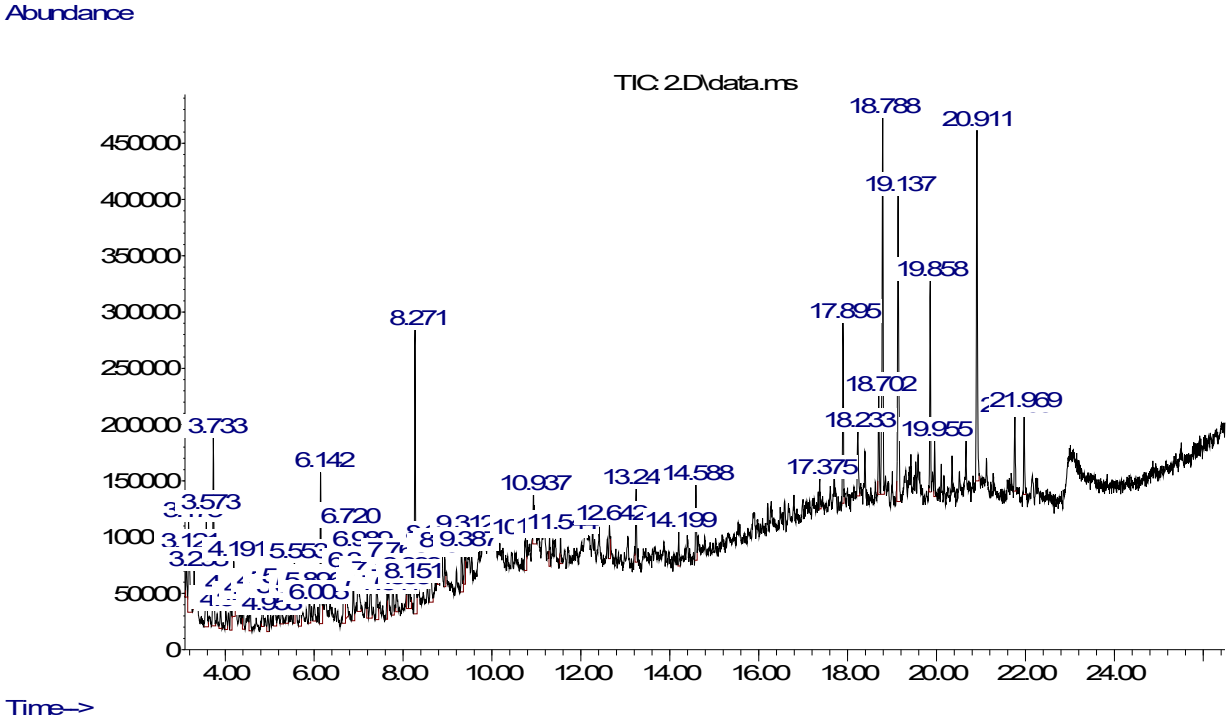

Figure 7. Chemical profile of upgraded bio-oil using Ru/C catalyst

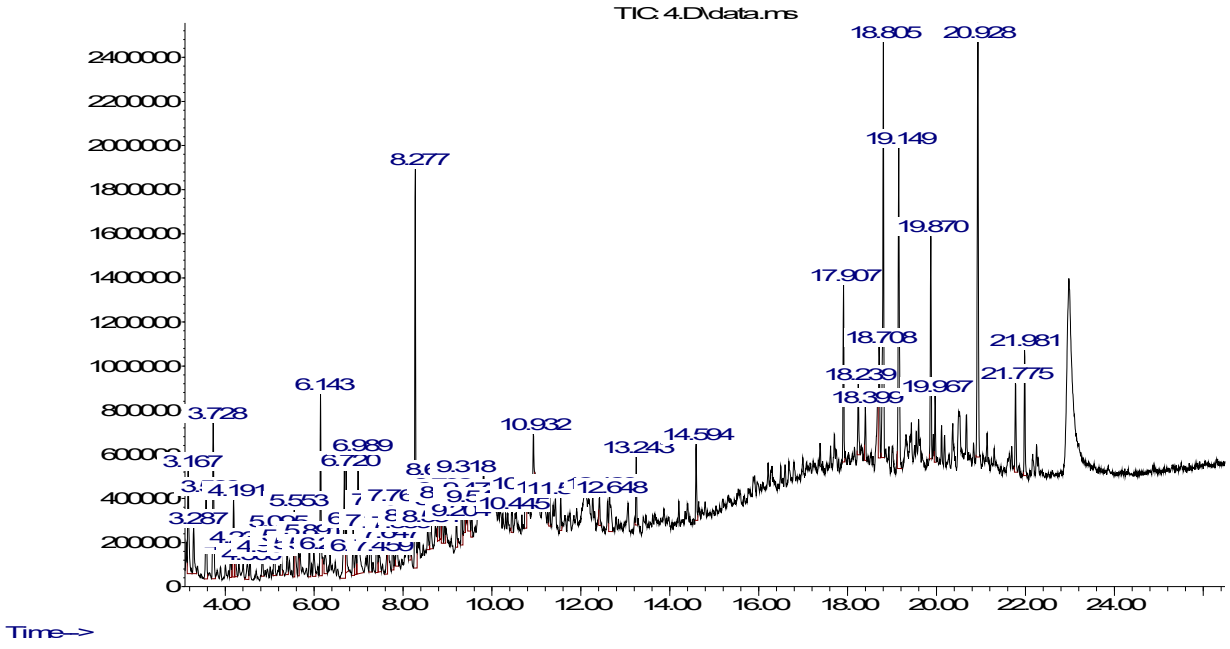

Figure 8. Chemical profile of upgraded bio-oil using Ru/ZSM-5 catalyst

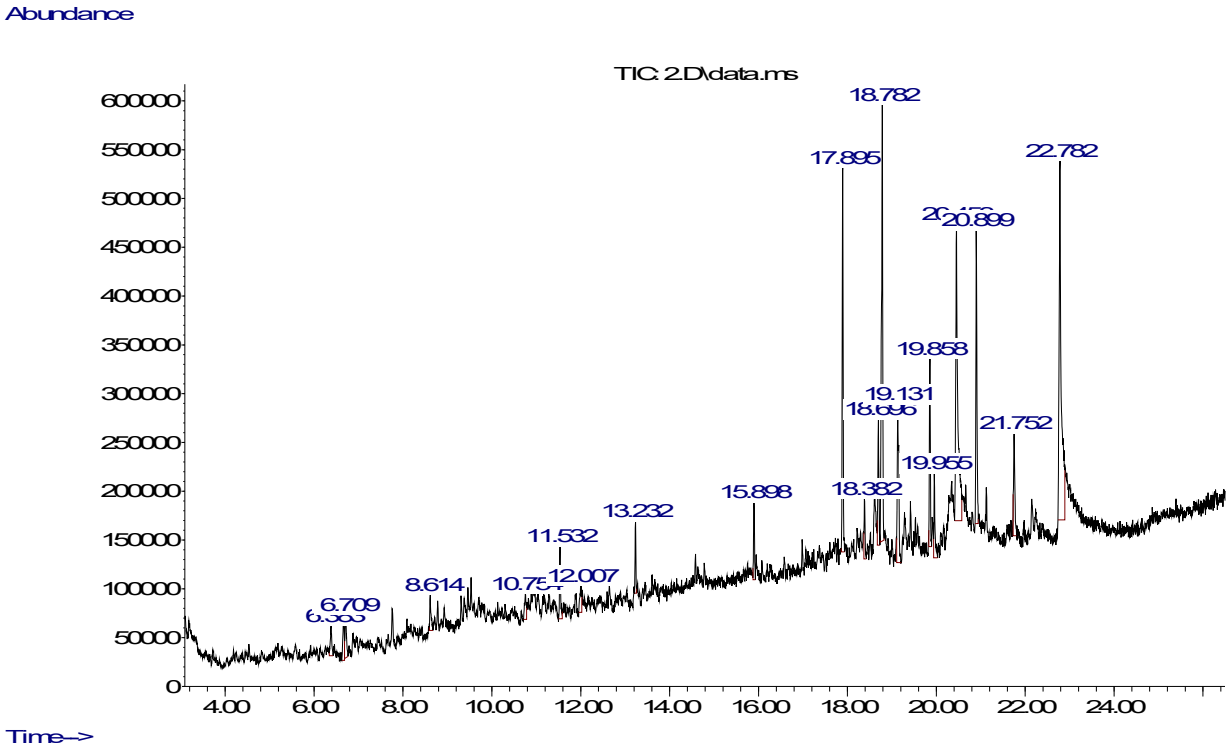

Figure 9. Chemical profile of upgraded bio-oil using Ru/Al_2O_3 catalyst

Table 4 Relative content (area %) of different function groups in the crude sawdust bio-oil and upgraded bio-oils

	Furan	Ketones	Alkenes	Alkanes	Alkynes	Aromatics			Acids	Others
						phenols	benzenes	others		
Raw bio-oil	28.75	21.1	1.16	1.45	0.84	39.05	0	0	3.71	3.90
Ru/C	0	22.19	11.63	3.30	0.85	0	31.85	24.75	1.72	3.71
Ru/ZSM-5	0	12.85	5.08	0	0	0	23.96	29.34	17.52	9.98
Ru/Al_2O_3	0	13.79	0	18.48	2.31	0	10.71	28.42	22.26	4.03

The bio-oil upgrading results showed that there were large differences in chemical compositions between crude bio-oil and upgraded bio-oil. No furan and phenol were detected in the upgraded bio-oils, in which have been hydrogenated and converted to hydrocarbon compounds. Many types of benzene compounds and others aromatics were detected in the upgraded bio-oils. Some organic acids were also found in the upgraded bio-oils. There were also differences among the upgraded bio-oils produced by the three different catalysts.

The high heating value of upgraded bio-oils were shown in Table 5. It is showed that the heating value of upgraded bio-oils was twice more than that of crude bio-oil. It was also found that the three upgrade bio-oils have different heating values due to their different chemical compositions. The Ru/ZSM-5 upgraded bio-oil has the lowest heating value among three upgraded bio-oils

since it has the smallest amounts of alkanes and alkenes (Table 4). The heating value of alkanes and alkenes are higher than those of aromatics because of their higher H/C ratio. [27 - 33]

Table 5 Heating values of the upgraded bio-oils

catalysts	Ru/C	Ru/ZSM-5	Ru/Al_2O_3
Heating value(MJ/kg)	30.5	28.7	30.9

These results indicated that crude bio-oils can be upgraded into aromatic hydrocarbons. The properties of upgraded bio-oil can also be improved after HDO process. The support materials used in catalysts had significant effects on the catalysts' performance. The three catalysts were made by the same noble metal (Ru) using three different support materials (activated carbon, Al_2O_3, and ZSM-5). Compared to other two catalysts, the Ru/C catalyst showed a better performance. Ru/C can be an effective catalyst for bio-oil upgrading since it showed the highest aromatics selectivity and lowest acid selectivity in the HDO process.

The bio-oils were homogeneous at the time of pyrolysis. However, they gradually became two or three phases: water insoluble oil phase, water soluble phase, and some solid sediment, after a few hours or days later. The forming phases may be caused by oxidation or polymerization of the organic compounds in bio-oils. Even though stored in a refrigerator (< 5 ˚C), the oxidation or polymerization reactions were still taking place, in which made the phase separations becoming distinct. The oxidation or re-polymerization will go on as storage time increases. According to Boucher et al.'s report, bio-oil properties such as composition, water content, heating value, pH, and especially viscosity change significantly during storage. A high-viscosity liquid can be formed at the bottom phase, which is defined as heavy bio-oil. A summary of typical heavy bio-oil properties is shown in table 6. In order to understand the linkage between bio-oils, catalysts, and reactor operating conditions, the bio-oil upgrading was carried out for different bio-oil phases using different upgrading methods.

Table 6. Properties of heavy bio-oil at 20°C

Properties	Heavy bio-oil
Density (g/ml)	1.14
Viscosity (cp)	8710
pH	3.00
Moisture content (wt %)	14
HHV (MJ/Kg)	25.09
Oxygen content (wt %)	33.90

A two-stage hydro-treating/cracking experiment was carried out to explore a valid method for improving heavy bio-oil properties in an autoclave reactor under different processing conditions. The heavy bio-oil was put into the autoclave along with a metal-based catalyst with zeolite support. After a heat treatment at 250°C for 4 hours, the heavy bio-oil was subsequently treated with a quick heating of different temperatures in range of 300 – 400°C for about 1 or 2 minutes. The effects of temperatures and catalysts were examined. A property comparison of heavy bio-oil and upgraded bio-oil is shown as Table 7.

Table 7. Properties comparison of heavy bio-oil and upgraded oil

	Heavy bio-oil	Upgraded oil (H250+C400)
Density (g/ml)	1.14	0.97
Viscosity (cp at 20°C)	8710	70
pH (20°C)	3.00	3.77
Moisture content (wt %)	14	2
HHV (MJ/Kg)	25.09	35.60
Oxygen content (wt %)	33.90	9.48

The table 7 results indicate that the upgraded oil properties, such as water content, density, viscosity, pH, high heating value, oxygen content, and chemical compositions were improved significantly. The hydro-treating with catalyst presenting can help to reduce coking formation during bio-oil upgrading. After bio-oil upgrading, a distillation was proceed to isolate pure hydrocarbons from the bio-oil mixture. As an example, the procedure of converting biomass (sawdust) to aromatic hydrocarbons is shown as figure 10. The hydrocarbons produced by this CFP–HDO process can also be called drop-in fuel since it is compatible with petroleum-derived hydrocarbons and can be directly dropped in an existing petroleum refinery for further conversion to "green" gasoline, diesel, and/or jet fuels. The drop-in fuel can also be blended with conventional fuels as fuel additives. A sample of the drop-in fuel produced and its GC/MS profile are shown in Figure 11. This drop-in fuel consists mainly of aromatics and olefins (over 85% of the hydrocarbons in the range of C5 – C15). A comparison of the drop-in fuel and petroleum-derived gasoline is shown in Table 8.

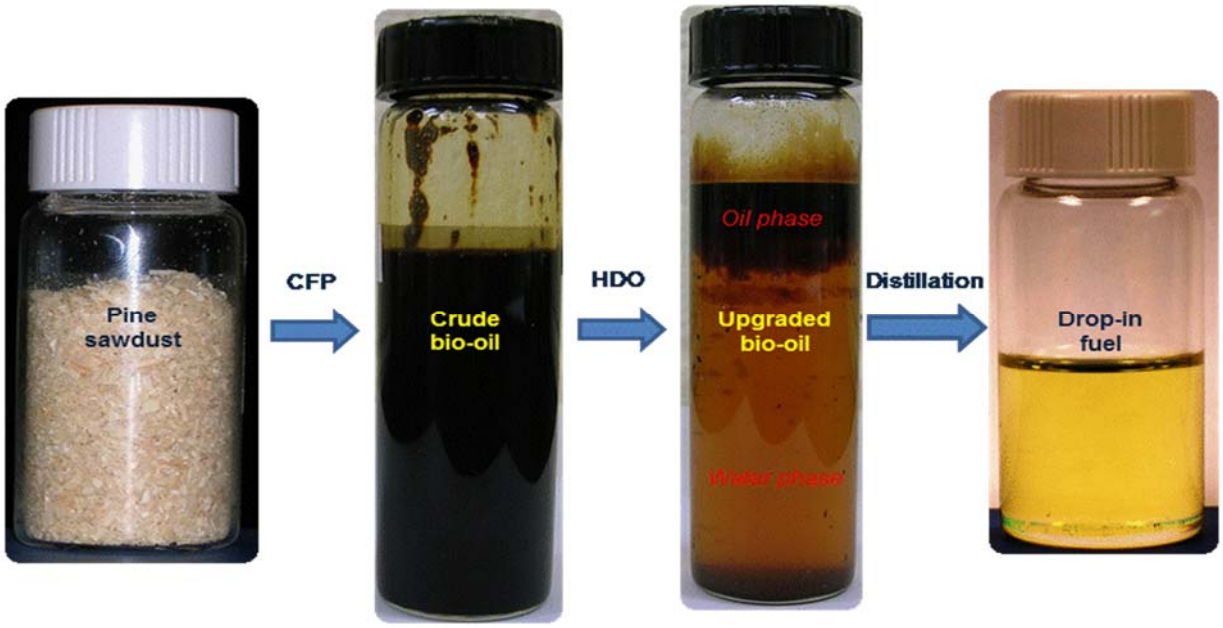

Figure 10. The procedure of converting biomass (sawdust) to aromatic hydrocarbon drop-in fuel

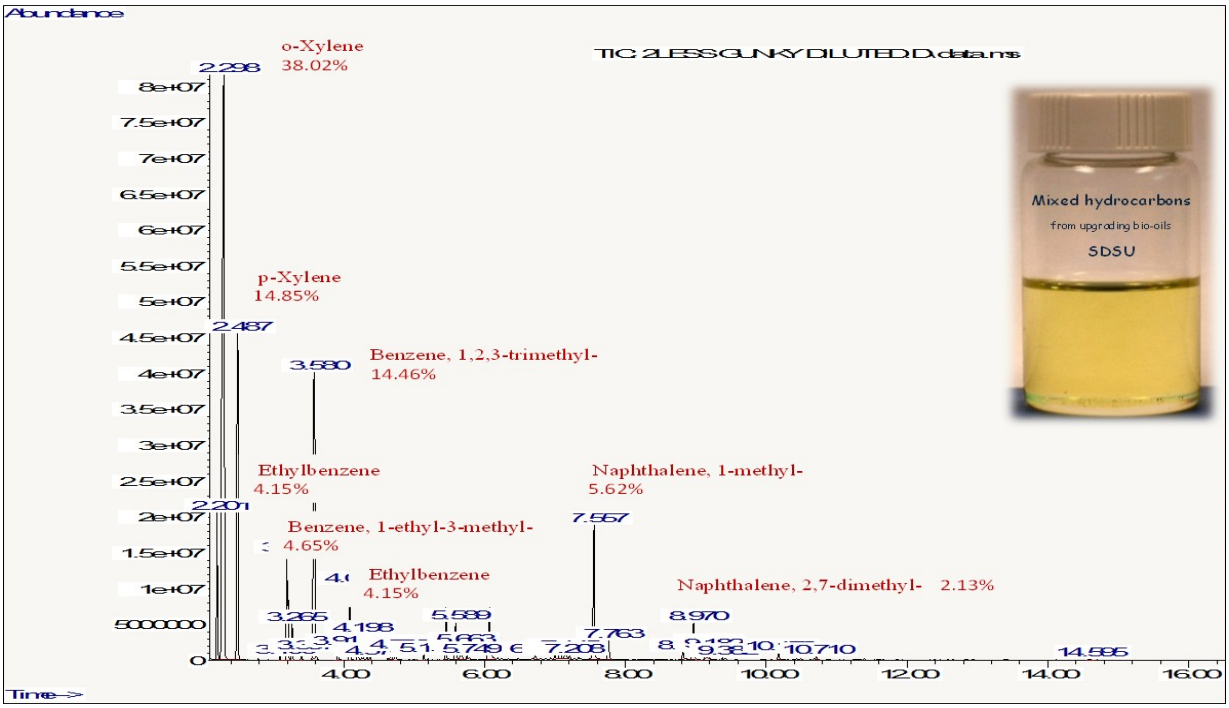

Figure 11. GC-MS profile of the drop-in fuel (hydrocarbons mixture) sample produced from sawdust by the SDSU team and the sample picture.

Table 8. Comparison of advanced biofuel produced from sawdust and petroleum based gasoline

Properties	SDSU drop-in fuels	Gasoline
pH value	5.0 – 5.6	–
Viscosity cSt @20ºC	1.2 – 1.88	0.4 – 0.8
Density, Kg/L	0.8 – 0.85	0.745
Heating value, MJ/kg	41 – 48	43
Carbon content, % w.t.	84.59 – 85.12	85 – 88
Hydrogen content, % w.t.	9.9 – 11.26	12 – 15
Oxygen content, % w.t.	< 0.72	0
Water content, % w.t.	< 0.25	0

Development of effective catalyst systems

Ru (Ruthenium) based catalysts were synthesized by individually impregnating it to the supports: Activated carbon, Alumina oxide, and ZSM-5. After activated the three catalysts, they were tested for bio-oil upgrading using HDO process. The yield and quality of upgraded bio-oils have been described in above sections. The performances of these three catalysts in bio-oil HDO process were examined. The results are listed in Table 9. There were large differences in liquid yield and selectivity of oil phase and water phase for the catalysts. The liquid yield and oil phase selectivity for Ru/C catalyst were as much as 92.40% and 47.25% respectively, which were the highest among three catalysts. In the case of Ru/ZSM-5, liquid yield was higher than that of Ru/Al_2O_3, while the oil phase selectivity was lower than that of Ru/Al_2O_3 catalyst. So the water phase selectivity of Ru/ZSM-5 catalyst was the highest among three catalysts. ZSM-5 was

usually used as cracking catalyst in petroleum refinery process because of high acidity and special pore structure. During Ru/ZSM-5 HDO process, bio-oil may be cracked into small molecular chemicals on the surface of ZSM-5, especially into gas phase chemicals, such as CO, CO_2 and some light hydrocarbons. Therefore, the oil phase selectivity of Ru/ZSM-5 catalyst was the lowest among three catalysts. Activated carbon was used widely as hydrogenation catalyst supports because of low acidity and large pore size. The highest liquid yield and oil phase selectivity may be resulted from less cracking of oil phase or less carbon deposited on catalyst surface. Al_2O_3 was one of common supports for Co-Mo catalysts used in bio-oil hydrotreating, but alumina could be converted to aluminum hydroxide in the presence of water, which may be resulted in catalytic deactivation [11 – 19, 34 - 37]. The oil phase selectivity of Ru/Al_2O_3 catalyst was still higher than that of Ru/ZSM-5, which may be came from different surface activity of Al_2O_3 and ZSM-5.

Table 9. Catalytic performances of Ru catalysts with different supports for bio-oil upgrading

catalysts	Liquid yield (wt%)	Oil phase selectivity (wt%)	Water phase selectivity (wt%)
Ru/C	92.40	47.25	52.75
Ru/ZSM-5	88.69	34.56	65.44
Ru/Al_2O_3	82.84	42.99	57.01

The results shows that these three catalysts made from the same noble metal (Ru) with three different support materials (activated carbon, Al2O3, and ZSM-5) are effective for bio-oil upgrading in HDO process, but the support materials of catalysts had significant effects on the catalysts' performance. The properties of upgraded bio-oil may change when the catalyst supports were different. Compared to other two catalysts, the Ru/C catalyst showed a good performance. Ru/C catalyst may be an effective catalyst for bio-oil upgrading since it showed the highest aromatics selectivity and lowest acid selectivity in the HDO process. Nonetheless, noble metal Ru (over $ 1400 per 100g) is still too expensive for biofuel production, specifically, for industrial scale production. It is necessary to develop more economic and effective catalysts for bio-oil upgrading. Instead of noble metals Pt, Pd, or Ru, cheaper transition metals Mo and Cu combined with ZSM-5 were formulated to synthesize catalysts in this project. Different ratios of Mo-Cu were respectively impregnated into ZSM-5 to formulate 5 different catalysts. The Mo (6%)/HZSM-5, Cu (6%)-Mo (13%)/HZSM-5, Cu (3%)-Mo (3%)/HZSM-5Cu (6%)-Mo (3%)/HZSM-5, Cu (3%)/HZSM-5 catalysts were successfully prepared using impregnation method and shown in Figure 12. Catalyst ZSM-5 without any Mo-Cu impregnated was also prepared and tested as contrast. Integrating with two different catalyst implementation systems: In-situ CFP and Ex-situ CFP, the catalysts' performance were examined. Bio-oils produced from sawdust and corn stover pyrolysis were individually upgraded using the In-situ CFP and Ex-situ CFP reactors with presenting the 6 catalysts.

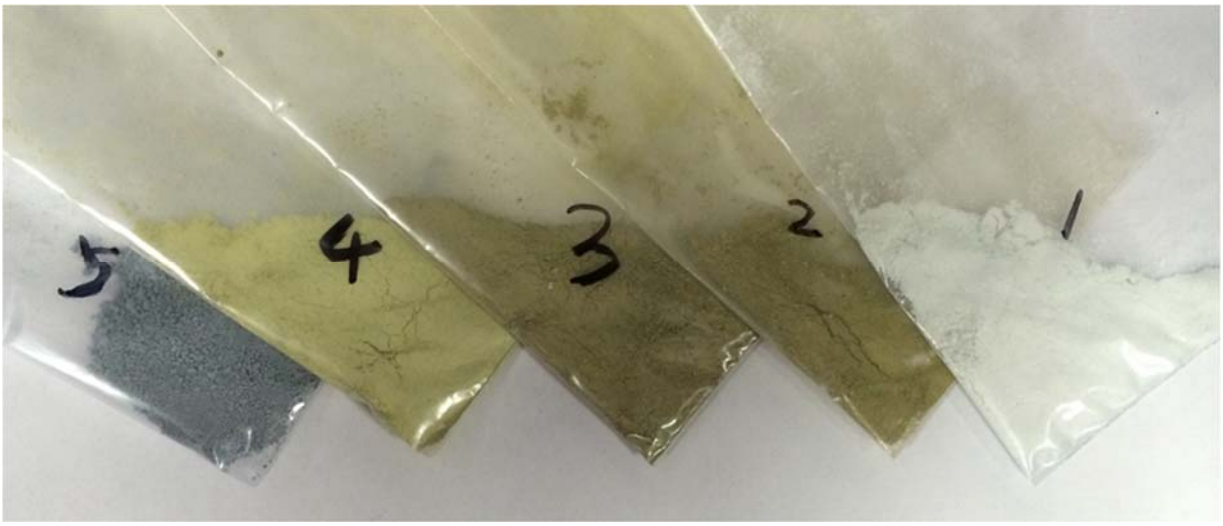

Figure 12. The catalyst samples of Mo (6%)/HZSM-5, Cu (6%)-Mo (13%)/HZSM-5, Cu (3%)-Mo (3%)/HZSM-5Cu (6%)-Mo (3%)/HZSM-5, Cu (3%)/HZSM-5

Effect of biomass to catalyst ratio on In-situ CFP process

An In-situ CFP test of corn stover was carried out to examine the effect of biomass to catalyst ratio on the bio-oil yield and quality. The test was conducted with a 2:1 ratio of biomass to catalyst in the lab scale fixed-bed reactor. As a control, pyrolysis of corn stover without catalyst was also carried out. The proportions of three products of corn stover CFP with/without catalyst is showed in Figure 13. There is no significant difference in the proportion of the three products between corn storver CFP with and without catalyst. This may be because the catalyst was covered or deactivated by the corn stover powder and ash when the biomass was more than catalyst in the mixture, or because there were no enough active sites for the CFP reactions to make the catalyst able to function properly. The composition of syngas produced is shown in Figure 14. The major compounds in syngas were CO and CO_2 with a little of N_2 There was no H_2 or CH_4 detected in the syngas. This result indicated that there was air (oxygen) to be involved in the CFP processing because the ambit air entered into the reaction chamber due to reactor system sealing issue. The small amount of N_2 in the syngas is the residue of carried gas or the ambit air entering into the reactor. Some of physical properties of the bio-oils are listed in Table 10. The energy content was low due to high water content of the bio-oils, 69% for corn stover pyrolysis without catalyst and 73% for corn stover CFP. This also proved that some of corn stover was “burned” (oxidation) with air and generated a large amount of water and CO_2 due to ambit air involving in the reactions if the reactor system had sealing problem. The 4% more water in CFP products came from the deoxygenating reactions due to the catalyst presenting [8, 11 – 12].

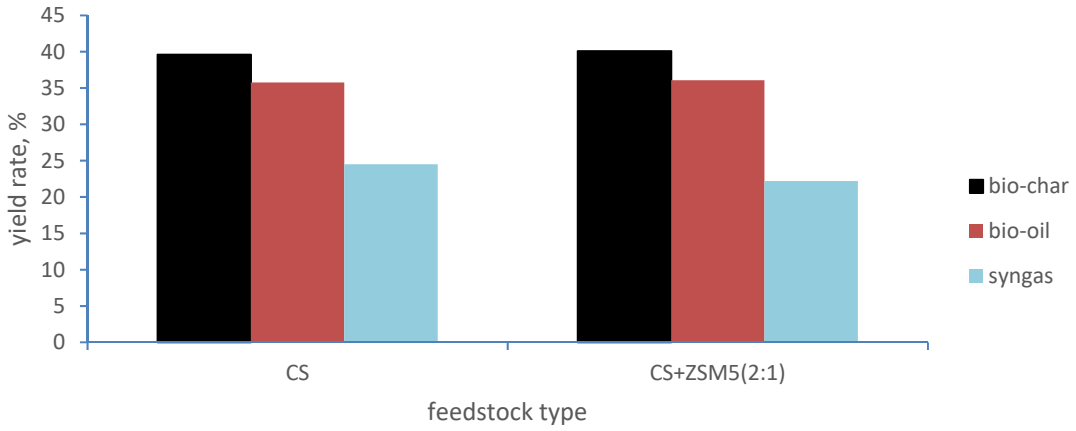

Note: CS = Corn Stover, Catalyst = ZSM5

Figure 13. Proportion of three products of corn stover CFP

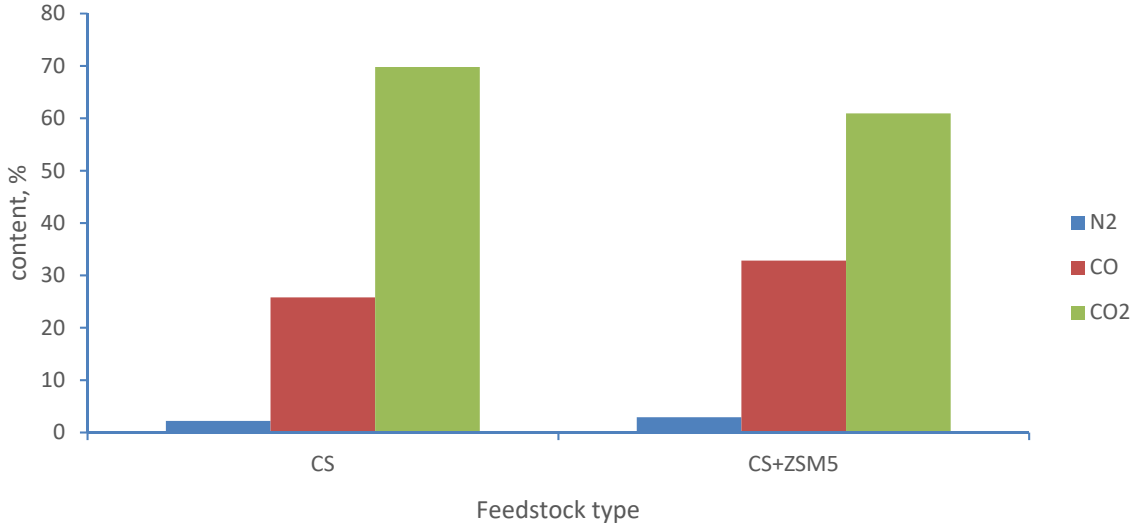

Figure 14. Composition of syngas produced in Corn Stover CFP

Table 10. The physical properties of bio-oil produced from corn storver CFP

Properties	CS	CS+ZSM5
Density(g/ml)	1.09	1.05
MC (%)	69.16	73.06
pH	3.18	3.43
energy content (KJ/g)	6.88	N/A

Note: MC of bio-oil produced from CS+ZSM5 was too high to measure its energy content in our labs.

Effect of catalyst implementation system on biomass CFP process

The effects of catalysts implementation systems on corn stover CFP process was investigated in this project. Two different catalyst implementation systems (In-situ CFP and Ex-situ CFP) for corn stover CFP process were carried out. In the In-situ CFP system, corn stover and catalyst (ZSM5) were mixed with a 2:1 ratio of biomass to catalyst and then pyrolyzed in the lab scale fixed-bed CFP reactor (Figure 4), named CSMC. In the Ex-situ CFP system, corn stover was pyrolyzed first and thus the produced bio-oil vapor went through a catalyst column in the coupled fixed-bed reactor (Figure 5), called CSCC. As control, corn stover was pyrolyzed without catalyst in the coupled fixed-bed reactor, called CS. All the CS, CSMC, and CSCC tests were respectively conducted at three different temperatures, 400, 500, and 600°C, respectively. The CFP product yield rates of the three catalyst implementations at three reaction temperatures are shown in table 11. It was found that catalyst implementation systems and reaction temperatures have significant influence on the three CFP products' (bio-oil, bio-char, and syngas) yield rates. When corn stover pyrolysis reaction temperatures increased, bio-char yield rates decreased while syngas yield rates increased for all of the three catalyst implementation systems. In contrast, the bio-oil yield rates had no significant difference when corn stover was pyrolyzed with CS and CSCC systems at the three reaction temperatures. The bio-oil yield rates increased when reaction temperatures increased if corn stover was pyrolyzed with the CSCM system. The highest bio-oil yield but lowest bio-char yield was obtained when the corn stover CFP process was conducted in the CSMC system at 500 °C. The lowest bio-oil yield but highest bio-char yield was obtained when the CFP process was conducted in the CSCC system at 400 °C. The bio-oil yields were low while syngas yields were high due to low efficiencies of the condenser units used in the CFP process. Some bio-oil vapors escaped with the syngas from the condensers. Another discovering is that the Ex-situ CFP system consumed catalysts 3 times less than that of the In-situ CFP system, but had higher catalysis efficiency and better bio-oil quality.

Table 11. Effects of reaction temperatures and catalyst implementation models on CFP product yields.

Reaction Temp. °C	Reaction model	Bio-oil, %	Biochar,%	Syngas,%
400	CS	28.11	34.38	37.51
	CSCM	25.78	33.37	40.85
	CSCC	14.75	38.64	46.61
500	CS	28.02	30.37	41.61
	CSCM	37.85	27.66	34.49
	CSCC	14.69	38.48	46.82
600	CS	31.82	29.06	39.12
	CSCM	36.18	26.75	37.07
	CSCC	17.07	31.03	51.89

The effects of reaction temperatures on the bio-oils properties are shown in table12. The results indicate that catalyst implementation systems and reaction temperatures have significant effects on bio-oil properties. Corn stover mixed with catalyst in CFP process led to highest pH value and density. The bio-oil densities increased when reaction temperatures increased. Because oxygenation reactions taking place in CFP process can produce more water, the MC of bio-oil

increased for the CSCM and SCCC systems, but these oxygenation reactions were flavor to higher reaction temperatures (500 and 600ºC) [6, 8 – 11, 38 – 43]. There was no significant difference in MC of bio-oils produced from all systems at 400ºC. Catalyst implementation systems and reaction temperatures had no significant influence on bio-oil viscosity.

Table 12. Effect of catalyst implementation system on upgraded bio-oil properties

Reaction Temp.	400ºC				500 °C		600ºC		
Reaction model	CS	CSCM	CSCC	CS	CSCM	CSCC	CS	CSCM	CSCC
pH	3.98	4.03	4.32	3.88	3.93	3.75	3.92	4.22	3.78
Viscosity (Pa*s 10^{-3})	1.93	2.45	1.91	2.00	2.09	1.95	2.43	2.06	1.91
Density (g/mL)	0.90	0.90	0.93	0.91	0.91	0.95	0.92	0.98	0.96
Moisture Content (%)	78.37	73.29	68.87	5.44	77.16	36.93	18.06	43.05	51.86

Catalysts screening for development of effective CFP catalyst system

Based on the test results of In-situ and Ex-situ catalyst implementation systems, the Ex-situ CFP system was found to be better for corn stover conversion to drop-in fuel. These 6 catalysts made from different ratios of Mo-Cu formulate were screened to figure out an effective catalyst system for the CFP process using the coupled fixed-bed reactor. The yield rates of three products (bio-char, bio-oil, and syngas) of corn stover pyrolysized in the Ex-situ reactor are shown as table 13. The results indicated catalysts have significant influences on the bio-oil yield rates. Among the catalysts tested, ratio of Mo-Cu 2:1 showed the best performance with the highest bio-oil yield (29.04 %) and the lowest syngas yields (45.95 %). Compared to literature data of bio- 60-75% oil yields [13 – 19, 36 – 39], this bio-oil yield is low. Again, the low bio-oil yields and high syngas yields were due to low efficiencies of the condenser units used in the CFP process. Some bio-oil vapors escaped with the syngas from the condensers. In order to improve the yield of bio-oils, a more effective condenser system should be designed and used, in which can cool the syngas more efficiently, allowing more bio-oil vapor to be condensed into liquid bio-oils.

Table 13. Yields of bio-char, bio-oil, and syngas of the corn stover CFP using different catalysts.

Catalyst formula	Bio-Char, %	Bio-Oil, %	Syngas, %
No Catalyst	27.03	30.08	42.51
Zeolite	25.47	22.79	51.91
Mo-Cu 1:1	27.28	27.20	45.78
Mo-Cu 0:1	20.84	23.97	55.60
Mo-Cu 1:0	27.48	24.27	48.48
Mo-Cu 1:2	26.53	22.13	51.86
Mo-Cu 2:1	25.69	28.61	45.96

The effects of different catalysts on the bio-oils properties are shown in table 14. The results indicate that catalysts have significant effects on bio-oil properties. Although all upgraded corn stover bio-oil still displayed a high acidity, the catalyst with a ratio of Mo-Cu 2:1 increased the pH value significantly. The bio-oil viscosities decreased when using various catalysts (Figure

17). The catalyst with a ratio of Mo-Cu 0:1 led to the lowest viscosity bio-oil. This is because the high viscosity of bio-oil is attributed to the high molecular weight molecules it contains, which can be broken down by the catalysts, effectively reducing the viscosity of the bio-oil. Bio-oil moisture content and heating value were both affected by the catalysts presenting. Again, more deoxygenating reactions taking place resulted in higher moisture content in the bio-oils because of the catalyst presenting. The bio-oil heating values were affected by the increased moisture contents. The bio-oil produced by the control test without catalyst displayed the highest heating value and lowest moisture content of all tests. Mo-Cu 1:2 had the largest increase in moisture percentage, from 48 wt% to 62 wt%, and the second largest decrease in heating value, from 24.05 MJ/kg to 21.46 MJ/kg. Mo-Cu 2:1 had a slightly lower heating value (21.02 MJ/kg) than Mo-Cu 1:2 but also less water (56 wt%). In the future, the bio-oil should be distilled to reduce the water content to get quality bio-oils with high heating values.

Table 14. Effect of catalysts on the upgraded bio-oils' properties

Catalyst formula	No catalyst	Zeolite	Mo-Cu 1:1	Mo-Cu 1:0	Mo-Cu 0:1	Mo-Cu 1:2	Mo-Cu 2:1
pH	2.82	2.90	3.03	2.98	2.86	3.09	3.23
MC, %	48.07	52.30	57.64	57.12	56.42	62.48	56.75
HHV, MJ/kg	24.05	23.67	21.02	22.40	22.39	21.46	22.23
Viscosity, Pa*s10^{-3}	5.1625	4.28	3.49	3.2125	3.1025	3.3725	3.52

The catalysts used in CFP process also affected elemental composition of the upgraded bio-oils. The carbon, hydrogen, and nitrogen (CHN) contents of bio-oils produced in the tests are listed in Table 15. Compared to the control, every catalyst appears to have reduced the carbon content in the bio-oils, but had varied effects on the hydrogen contents. According to literature, corn stover bio-oil contains about 38.40-47.63 wt% carbon, 4.91-5.48 wt% hydrogen, and 0.84-1.56 wt% nitrogen by weight [22 – 27, 36 – 43]. In this project, the raw corn stover CHN was also analyzed and found to be 45.14 wt% carbon, 7.06 wt% hydrogen, and 0.46 wt% nitrogen. Conversely, the highest achieved carbon and hydrogen contents of the bio-oils in this experiment were 31.97 wt% and 9.09 wt%, respectively. This shows a decrease in carbon content and an increased hydrogen content, most likely caused by high water content in the samples. If ignore measuring errors, water should be removed from the samples to get more accurate bio-oil carbon and hydrogen contents.

Table 15. CHN content (%) of the upgraded bio-oils

Catalyst formula	C	H	N
No Catalyst	30.46	8.49	1.41
Zeolite	19.27	4.97	0.97
Mo-Cu 1:1	18.09	5.01	0.61
Mo-Cu 1:0	17.30	5.37	Un-detected
Mo-Cu 0:1	16.21	5.11	Un-detected
Mo-Cu 1:2	16.51	5.23	Un-detected
Mo-Cu 2:1	11.42	1.18	Un-detected

The 6 catalysts were also tested for pine sawdust pyrolysis using the Ex-situ CFP system. The reaction condition is showed in table 16. In each test, 100 g of sawdust was added into the pyrolysis reactor; 10 g of Cu-Mo/HZSM-5 series catalysts were added sequentially. Nitrogen was filled into the coupled catalytic pyrolysis equipment to remove the air in respectively side with 10 ml/min flow rate for 30 min. The catalytic reactor was heated up to 500 °C at the beginning of the experiment. The nitrogen flow rate was set at 3 ml/min. After that, the pyrolysis reactor furnace was opened and heated at a rate of 20 °C/min to 550 °C. And then, the syngas produced was started to be collected and analyzed. The test was run for 1 hour. The yields of three products produced in the CFP process are listed in table 17.

Table 16. The reaction conditions

Items	Value
Sawdust used in each run / g	100
The temperature of pyrolysis reactor / ℃	550
The temperature of catalytic reactor / ℃	500
The amounts of catalyst used in each run / g	10
Condenser temperature / ℃	-10 ± 2
Running time / hour	1

Table 17. The product distribution of the bio-char, bio-oil and syngas

Catalyst formula	Products, g		
	Bio-oil	Syngas	Bio-char
No catalyst	52.89	22.71	24.40
HZSM-5	45.56	30.46	23.98
Mo(3%)/HZSM-5	50.95	26.1	22.95
Cu(6%)-Mo(3%)/HZSM-5	48.92	27.2	23.88
Cu(3%)-Mo(3%)/HZSM-5	45.62	29.23	25.15
Cu(1.5%)-Mo(3%)/HZSM-5	46.21	28.81	24.98
Cu(3%)/HZSM-5	46.5	29.76	23.74

Table 17 shows that bio-char yields have no big difference in all these experimental tests since all the pyrolysis reactions were occurred at 550 °C. It is clearly illustrated that the yield of syngas increase with the presenting of Cu-Mo/HZSM-5 in the CFP reactions, in which the catalysts are beneficial to produce more smaller molecules of hydrocarbons including C_2-C_4.

The water contents, higher heating values, viscosity and the component of the oil phase of bio-oils are shown in Table 18. These results indicated the properties of upgraded bio-oils. The oil phase of bio-oils has lowest viscosity, high heating value and lowest water content when the Cu (3%)-Mo (3%)/HZSM-5 catalyst was used.

Table 18. The properties of bio-oils

Catalyst formula	Mass / g		Higher heating value KJ/kg		Viscosity 10^{-3}Pa·s		Water content wt%	
	AP	OP	AP	OP	AP	OP	AP	OP
No Catalyst	28.85	24.04	-	24.708	6.23	13.1	84.3	9.4
HZSM-5	31.89	13.67	-	28.542	6.23	13.1	87.2	8.1
Mo(3%)/HZSM-5	38.21	12.74	-	29.777	6.22	7.48	87.7	6.9
Cu(6%)-Mo(3%)/HZSM-5	32.31	16.61	-	26.565	6.24	6.49	89.8	6.5
Cu(3%)-Mo(3%)/HZSM-5	32.06	13.56	-	29.227	6.22	3.49	91.2	4.3
Cu(1.5%)-Mo(3%)/HZSM-5	35.12	11.09	-	24.867	6.29	7.42	90.3	4.5
Cu(3%)/HZSM-5	33.48	13.02	-	25.353	6.25	8.38	87.6	7.4

Note: AP: aqueous phase; OP: oil phase

Characterization of fresh and spent catalysts

The fresh and spent catalysts were characterized using BET, TEM, and XRD approaches. The XRD patterns of fresh ZSM-5 and ZSM-5 used in different temperature conditions in wide angle region of 5-50 are shown in Figure 15. It is found that there is no significant difference in the diffraction pattern of fresh ZSM-5 and ZSM-5 used at different temperatures. No peaks of carbon were observed, indicating carbon crystal was highly dispersed on the ZSM-5 catalyst. It implied that the ZSM-5 crystal was not significantly changed before and after the CFP process tests. This may provide opportunities to regenerate the spent catalysts for longer lifetime and low down drop-in fuel production costs [3, 7 – 17]. In order to further determine whether or not coke was presented inside the catalysts, the XRD patterns of the fresh and used HZSM-5 catalysts in the angle region (5-50°) were measured, and the results are shown in Figure 16. For the fresh catalyst, the two peaks appearing at 23.1° and 23.7° can be found in the XRD patterns. For the used HZSM-5 after P500+C400 treatment, the two peaks appearing at 23.1° and 23.4° can be found in the XRD patterns. However, the two peaks collapse into one at 23.3° for HZSM-5 catalysts after P500+C500 and P500+C600 treatment. The intensities in the angle region (<10°) change for different treatments to HZSM-5 catalyst. The changes in the relative positions and intensities of the peaks in the XRD spectra of the coked ZSM-5 zeolite could be attributed to a displace transformation from monoclinic to orthorhombic caused by deposition of coking within HZSM-5 pores [5, 8 – 12, 19 – 26]. Concentric circles in the TEM (SEAD Pattern) image (Figure 16) indicate that the fresh and used HZSM-5 are polycrystalline.

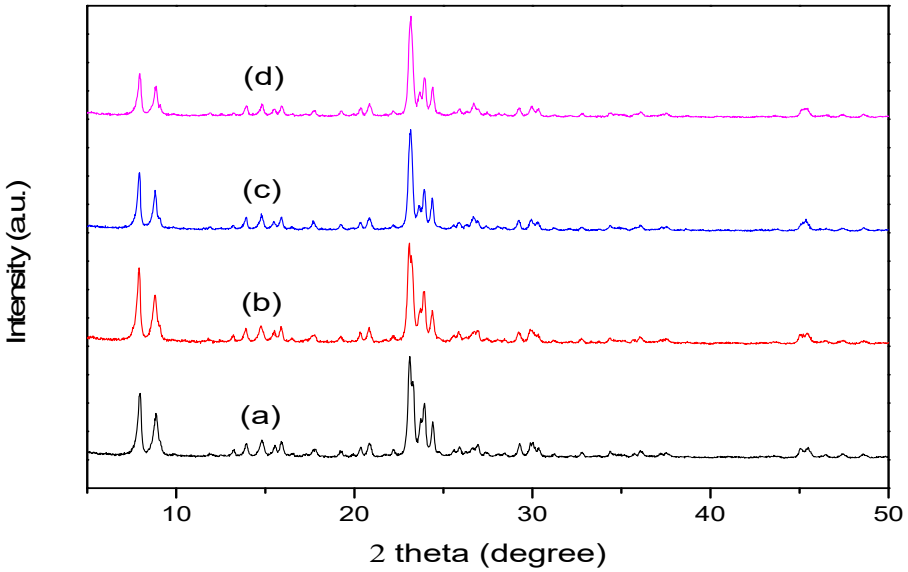

Figure 15. X-ray diffraction patterns of fresh ZSM-5 (a), ZSM-5 after being used in pyrolysis reactor at 500 °C and catalytic reactor at 400 °C (b), ZSM-5 after being used pyrolysis reactor at 500 °C and catalytic reactor at 500 °C (c) and ZSM-5 after being used pyrolysis reactor at 500 °C and catalytic reactor at 600 °C (d)

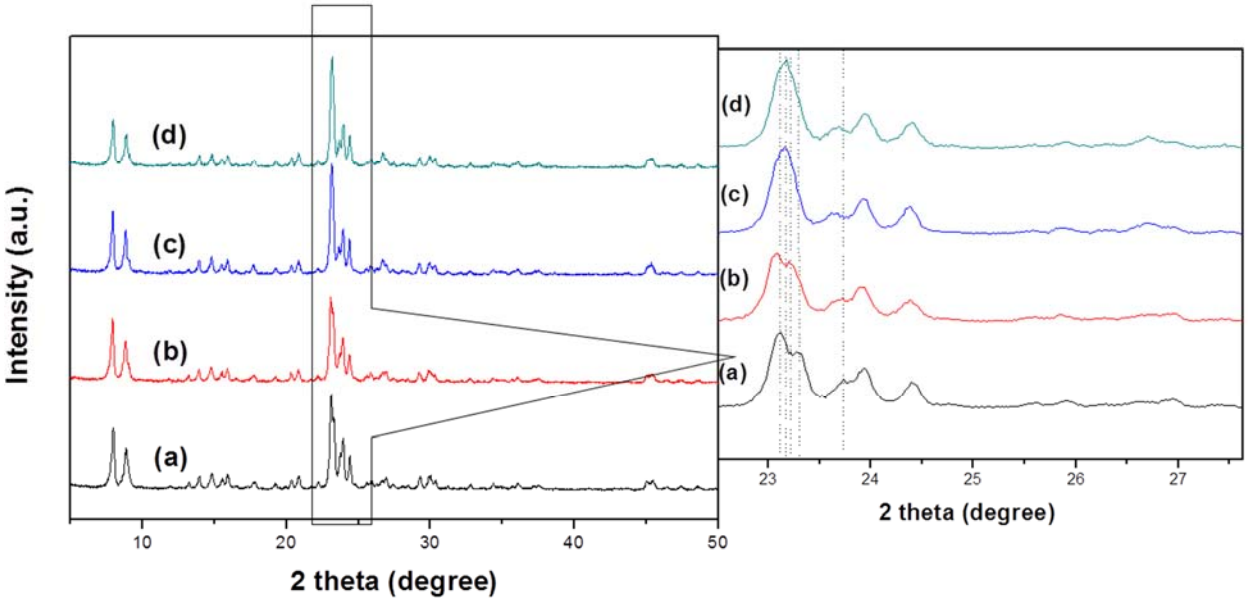

Figure 16. X-ray diffraction patterns of (a) fresh HZSM-5, (b) HZSM-5 after P500+C400 treatment

BET parameters of the catalyst samples are summarized in Table 19. The BET surface area, Langmuir surface area and total pore volume gradually decreased with an increasing catalytic treatment temperature. DFT model simulation results (Fig. 3) indicated that the fresh and used HZSM-5 catalysts contain micropores and mesoporous with a distribution of sizes between 1 and 20 nm. The HZSM-5 catalysts treated by higher temperature have less incremental volume for pore size between 1 and 20 nm. All these results indicates that the higher catalytic temperature is beneficial to the formation of coke in the pores of HZSM-5.

Table 19. BET parameters of the catalyst samples

Sample	Surface area (m^2/g)		Pore volume(cm^3/g)		
	BET	Langmuir	Total[a]	Micropores[b]	Mesopores[c]
Fresh HZSM-5	423.4	506.0	0.343	0.149	0.172
HZSM-5 (P500 + C400)	322.5	389.6	0.330	0.139	0.076
HZSM-5 (P500 + C500)	302.7	366.5	0.317	0.131	0.065
HZSM-5 (P500 + C600)	188.5	229.9	0.271	0.099	0.044

[a] Total pore volume, measured at $P/P_0 = 0.995$.
[b] Micropore volume, derived from NLDFT model.
[c] Mesopore volume, derived from NLDFT model.

The catalysts were also characterized by a TEM. Two typical catalysts TEM images are showed in figure 17. Comparing the TEM image of HZSM-5 with the TEM image of Cu (3%)-Mo (3%)/HZSM-5, we can find there are some black spot on the HZSM-5 interface after loading the copper and molybdenum. As expected, the amount and size of the dark spots, mainly attributed to CuO and MoO_3 as it will be demonstrated afterwards, depends both on the nature of the zeolite and on the CuO and MoO_3 loading. A major number of dark spots are observed for high-copper and molybdenum content catalysts than for the counterpart low-copper content catalysts.

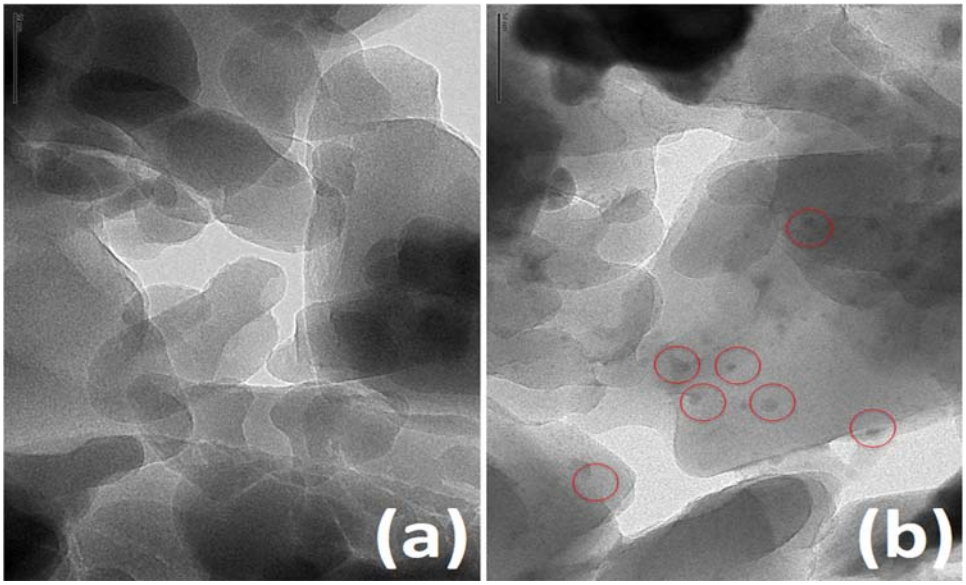

Figure 17. The TEM images of HZSM-5(a) and Cu (3%)-Mo (3%)/HZSM-5 (b)

Fabrication of the second generation CFP reactor system ***(Confidential section deleted)***

(Confidential information ends)

CONCLUSIONS

Based on the results obtained from this study, some conclusions can be drawn:

- The SDSU proprietary CFP reactor can convert various biomass feedstocks into bio-oils that can be upgraded into drop-in fuel using a HDO process with the presenting of catalysts. There will be very promising potential of commercializing these technologies to biofuel industry if some minor issues such as gas lacks and condenser cooling efficiency were addressed.
- Bio-oil yield and quality is significantly affected by air presenting during biomass CFP process. When more air is involved in the CFP reactions, bio-oil moisture content increase while carbon conversion efficiency decreases.
- There are significant differences in bio-oil yields and quality when the same catalysts are applied with different implementation systems in CFP process. Catalysts have better performance in Ex-situ CFP reactor system with less catalyst consumption than that of In-situ CFP reactor system. Catalysts have no significant influence on bio-oil yield and quality if the ratio of biomass to catalyst is greater than 1 during In-situ CFP process, but the ratio can be much higher if the CFP process is conducted in an Ex-situ implementation system.
- ZSM-5 combined with Mo and Cu to formulate multifunctional catalysts have significant effects on bio-oil yield and quality from the CFP process. Different ratios of Mo-Cu impregnated in ZSM-5 support have different effect on bio-oil properties. The catalyst with Mo-Cu 2:1 showed the most promising performance.
- The technologies integrated SDSU proprietary CFP reactor and transition metals (Mo-Cu) catalyst system have promising potential for future commercialization.

LIST OF REFERENCES

1) Jones, S.b., J. L. Male, 2012. Production of Gasoline and Diesel from Biomass via Fast Pyrolysis, Hydrotreating and Hydrocracking: 2011 State of Technology and Projections to 2017. Report No. PNNL – 22133. PNNL, Richland, Washington 99352.
2) Wright, M., R. C. Brown, D.E. Daugaard, and D.D. Hsu, 2010. Techno-Economic Analysis of Biomass Fast Pyrolysis to Transportation Fuels. Technical report, NREL/TP-6A20-46586. Golden, Colorado 80401.
3) Biddy, M., A. Dutta, S. Jones, and Aye Meyer. 2013. In-Situ Catalytic Fast Pyrolysis Technology Pathway. NREL technical report: NREL/TP-5100-58056.
4) Branca, C.; Giudicianni, P.; Di Blasi, C. 2003. GC/MS characterization of liquids generated from low-temperature pyrolysis of wood. *Ind. Eng. Chem. Res. 42*, 3190–3202.
5) Bridgwater, A.V. 1996. Production of high grade fuels and chemicals from catalytic pyrolysis of biomass. *Catal. Today*, *29*, 285–295.
6) Bulushev, D.A.; Ross, J.R.H. 2011. Catalysis for conversion of biomass to fuels via pyrolysis and gasification: A review. *Catal. Today*, *171*, 1–13.

7) U.S. Department of Energy. 2011. U.S. Billion-Ton Update: Biomass Supply for a Bioenergy and Bioproducts Industry. R.D. Perlack and B.J. Stokes (Leads), ORNL/TM-2011/224. Oak Ridge National Laboratory, Oak Ridge, TN. 227p.
8) Hamelinck, C.N., G.V. Hooijdonk, and A.P.C. Faaij. 2005. Ethanol from lignocellulosic biomass: techno-economic performance in short-, middle- and long-term. *Biomass and Bioenergy*. 28: 384-410.
9) Hislop, D. and O. Hall. 1996. Biomass resources for gasification power plant. Report No. ETSU B/M3/00388/31/REP. London: University of London, King College.
10) Cheng, Y.T.; Huber, G.W. 2011. Chemistry of furan conversion into aromatics and olefins over HZSM-5: A model biomass conversion reaction. *ACS Catal. 1*, 611–628.
11) Faix, O.; Meier, D.; Fortmann, I. 1990. Thermal-degradation products of wood: A collection of electron-impact (EI) mass-spectra of monomeric lignin derived products. *Holz als Roh- und Werkstoff. 48*, 351–354.
12) Zhang, Q., Chang J., Wang T., and Xu Y. 2007. Review of biomass pyrolysis oil properties and upgrading research. *Energy Conversion and Management* 48: 87–92.
13) Huber, G., T. R. Carlson, and G. A. Tompsett. 2009. "Aromatic Production from Catalytic Fast Pyrolysis of Biomass-Derived Feedstocks" *Topics in Catalysis* 52 (2009): 241.
14) Zhang, M., and A. Moutsoglou, 2014. Catalytic Fast Pyrolysis of Prairie Cordgrass Lignin and Quantification of Products by Pyrolysis−Gas Chromatography−Mass Spectrometry. Energy & Fuel, dx.doi.org/10.1021/ef401795z.
15) Li, X., S. Lu, Y. Wang, Y. Yu, C. Wang, X. Li, Z. Wang. 2012. Catalytic fast pyrolysis of Kraft lignin with HZSM-5 zeolite for producing aromatic hydrocarbons. Front. Environ. Sci. Eng. 2012, 6(3): 295–303. DOI 10.1007/s11783-012-0410-2.
16) Carlson, T. R., Y. Cheng, J. Jae and G. W. Huber. 2011. Production of green aromatics and olefins by catalytic fast pyrolysis of wood Sawdust. Energy Environ. Sci., 2011, 4, 145.
17) French, R.; Czernik, S. 2010. Catalytic pyrolysis of biomass for biofuels production. *Fuel Process. Technol. 91*, 25–32.
18) Alotaibi, M. A. 2012. Deoxygenation and hydrogenation of biomass-derived molecules over multifunctional catalysts. PhD Dissertation, University of Liverpool, UK.
19) Balat, M.; Balat, M.; Kirtay, E.; Balat, H. 2009. Main routes for the thermo-conversion of biomass into fuels and chemicals. Part 1: Pyrolysis systems. *Energy Convers. Manag. 50*, 3147–3157.
20) Ranzi et al. 2008 Ranzi, E., A. Cuoci, T. Faravelli, A. Frassoldati, G. Migliavacca, S. Pierucci, and S. Sommariva, 2008. Chemical Kinetics of Biomass Pyrolysis. *Energy & Fuels*, *22,* 4292–4300.
21) Zhang, H.; Cheng, Y.T.; Vispute, T.P.; Xiao, R.; Huber, G.W. 2011. Catalytic conversion of biomass-derived feedstocks into olefins and aromatics with ZSM-5: The hydrogen to carbon effective ratio. *Energy Environ. Sci. 4*, 2297–2307.
22) Vispute, T.P.; Zhang, H.; Sanna, A.; Xiao, R.; Huber, G.W. 2010. Renewable chemical commodity feedstocks from integrated catalytic processing of pyrolysis oils. *Science. 330*, 1222–1227.
23) Liska, A., H. Yang, M. Milner, S. Goddard, H. Blanco-Canqui, M. P. Pelton, X. X. Fang, H. Zhu, A. E. Suyker, 2014. Biofuels from crop residue can reduce soil carbon and increase CO_2 emissions. *Nature Climate Change*, Vol. 4, pages, 398–401. DOI: 10.1038/nclimate2187.

24) Environmental Protection Agency. Regulation of Fuels and Fuel Additives: 2012 Renewable Fuel Standards. *Fed. Regist.* 2012, *76*, 1320-1358.
25) Jahirul, M., et al. "Biofuels Production through Biomass Pyrolysis – A Technological Review." Energies. 2012, 5, 4952-5001.
26) Mohan, D., Pittman, C., Steele, P. "Pyrolysis of Wood/Biomass for Bio-oil: A Critical Review." *Energy & Fuels*. 2006, *20*, 848-889.
27) Demirbas, A. *J. Anal. Appl. Pyrolysis*. 2005, *73*, 39-43.
28) Mullen, C, Boateng, A., Goldberg, N., Lima, I., Laird, D., Hicks, K. "Bio-oil and bio-char production from corn cobs and stover by fast pyrolysis." *Nature*. 2009, *34*, 67-74.
29) Green, A., Feng, J. "Systematics of corn stover pyrolysis yields and comparisons of analytical and kinetic representations." *J. Anal. Appl. Pyrolysis*. 2006, *76*, 60-69.
30) Feng, J., YuHong, Q., Green, A. "Analytical model of corn cob Pyroprobe-FTIR data." *Biomass and Bioenergy*. 2006, *30*, 486-492.
31) Aho, A., N. Kumar, K. Eränen, B. Holmbom, M. Hupa, T. Salmi, and D. Y. Murzin. 2008. Pyrolysis of softwood carbohydrates in a fluidized bed reactor. *Int. J. Mol. Sci. 9*: 1665-1675; DOI: 10.3390/ijms9091665.
32) Badger, P.C. 2002. Ethanol from cellulose: a general review, *In* J. Jandick and A. Whipkey, eds. Trends in New Crops and New Uses. ASHS Press, Alexandria, Va.
33) Carlson, T. R., Geoffrey A., Tompsett E., W. C. Conner, and G. W. Huber. 2009. Aromatic production from catalytic fast pyrolysis of biomass-derived feedstocks. *Top Catal.* 52: 241–252. DOI 10.1007/s11244-008-9160-6.
34) Hu, J., Y. Wang, C. Cao, D.C. Elliott, D.J. Stevens, and J.F. White. 2006. Conversion of biomass-derived syngas to alcohols and C2 oxygenates using supported Rh catalysts in a microchannel reactor. *Catalysis Today*. 120: 90-95.
35) Jiang, X. and N. Ellis. 2010. Upgrading bio-oil through emulsification with biodiesel: mixture production. *Energy Fuels*. 24: 1358–1364; DOI:10.1021/ef9010669.
36) Laird, D. A., R. C. Brown, J. E. Amonette, Richland, W. A., and J. Lehmann. 2009. Review of the pyrolysis platform for coproducing bio-oil and biochar. *Biofuels, Bioprod. Bioref.* 3:547–562. DOI: 10.1002/bbb.169.
37) Lehmann, J., J. Gaunt, and M. Rondon. 2006. Biochar sequestration in terrestrial ecosystems: a review. Mitigation and adaptation strategies for global change. 11: 403–427. DOI: 10.1007/s11027-005-9006-5.
38) Liu, S., A. C. Gujar, P. Thomas, H. Toghiani, M. G. White. 2009. Synthesis of gasoline-range hydrocarbons over Mo/HZSM-5 catalysts. *Applied Catalysis A: General*. 357: 18–25.
39) Mullen, C. A., A.A. Boateng, N. M. Goldberg, I. M. Lima, D. A. Laird, and K. B. Hicks. 2006. Bio-oil and bio-char production from corn cobs and stover by fast pyrolysis. *Biomass and Bioenergy.* 34 (1): 67-74.
40) Samolada, M. C., A. Papafotica, I. A. Vasalos. 2000. Catalyst evaluation for catalytic biomass pyrolysis. *Energy Fuels*. 14: 1161– 1167.
41) Walsh, M. E., R. L. Perlack, A. Turhollow, D. T. Ugarte, D. A. Becker, R. L. Graham, S. E. Slinsky, and D. E. Ray, 2000. Biomass feedstock availability in the United States. Oak Ridge, Tenn.: ORNL.

42) Yorgun, S., and Y. E. Simsek. 2008. Catalytic pyrolysis of Miscanthus _ giganteus over activated alumina. *Bioresource Technology*. 99: 8095–8100.

43) Zhang, H., R. Xiao, D. Wang, Z. Zhong, M. Song, Q. Pan, and G. He. 2009. Catalytic fast pyrolysis of biomass in a fluidized bed with fresh and spent fluidized catalytic cracking (FCC) catalysts. *Energy Fuels*. 23: 6199–6206: DOI:10.1021/ef900720m.

ACKNOWLEDGE

Support for this research was provided by a grant from the Northern Central Sun Grant Center with funds provided by the U.S. Department of Energy Bioenergy Technologies Office Award number (DE-FG36-08GO88073).

APPENDIX I

Publications

Peer-reviewed paper:

1) Wangda Qu, Lin Wei, James Julson. An exploration of improving the properties of heavy bio-oil. Energy & Fuels, 2013, 27 (8), pp 4717–4722.
2) Zhongyi Ma**,** Lin Wei, Wangda Qu, James Juson, Qingwei Zhu, Xunzhang Wang, 2013. The effect of support on the catalytic performance for bio-oil upgrading. *Advanced Materials Research.* Vols. 608-609, pp 350-355.

Conference papers and oral presentations:

1) L. Wei, J. Julson. 2014. Catalytic Fast Pyrolysis of Corn Stover to Hydrocarbon drop-in fuels. NC Sun Grant annual meeting, Mar. 27, Minneapolis, MN.
2) L. Wei, Y. Huang, Y. Gao, X. Zhao, and J. Julson. Upgrading pyrolysis bio-oil over ZSM-5 catalyst for advanced biofuel development. July 16 – 21, 2014 ASABE annual meeting, Montreal, Canada
3) L. Wei, K. Muthukumarappan, Z. Gu, and J. Julson. 2013. Catalyst development for biomass conversion to jet fuels. North Dakota/South Dakota Engineering Research Summit, South Dakota State University, April 23, Brookings, SD.
4) Y. Huang, L. Wei, J. Julson, Y. Gao, and X. Zhao. 2014, Upgrading of bio-oil into advanced bio-fuel over Mo/ZSM5 catalysts. ASABE intersection meeting, Mar. 29, Brookings, SD.
5) L. Wei, W. Qu, J. Julson, C. Shi, X. Zhao. 2013. "Experimental study on torrefaction of corn stover, switchgrass, and prairie grass", Paper No. 131585924. ASABE Annual International Meeting, Kansas City, Missouri, July 21 – 24, 2013.
6) Wangda Qu, Zhongyi Ma, Lin Wei, James Julson, 2012. Fast pyrolysis of corn stover and sawdust in a novel reactor, Paper #: 121337678. The 2012 ASABE annual international meeting, July 29, Dallas, TX.
7) Zhongyi Ma, Lin Wei, Wangda Qu, James Julson, 2012. Fast pyrolysis bio-oil upgrading over noble metal catalysts. Paper #: 12134519. The 2012 ASABE annual international meeting, July 29, Dallas, TX**.**
8) Hu, J., F. Yu, Y. Lv, Q. Yuan, J. Wooten, E. P. Columbus, Lin Wei. 2011. Catalytic Conversion of Biomass-derived Syngas to Gasoline Range Hydrocarbons. Paper No. 1110878. Louisville, Kentucky: ASAE Annual International Meeting.
9) Yu, F., Q. Yan, J. Hu, Y. Lu, Lin Wei, J. Wooten, E. Columbus and W. Batchelor. 2010. Mixed Hydrocarbons from Biomass-derived Syngas over Mo/HZSM-5 Catalyst. 9th International Conference on Sustainable Energy Technologies (SET). Shanghai, China. August 24-27.
10) Yu, F., Q. Yan, J. Hu, Lin Wei, E. Columbus and J. Wooten. 2010. Mixed Hydrocarbon Production from Biomass-derived Syngas over a Bi-functional Catalyst. International Symposium on Renewable Feedstock for Biofuel and Bio-based Products. Austin, TX, August 11-13.
11) Hu, J., Yu, F., Lin Wei, Columbus, E., and Batchelor, W. 2010. Preliminary Study of the Conversion of Biomass-derived Syngas to Gasoline-range Hydrocarbons over Mo/HZSM-5. Paper 1008573, ASABE 2010 Annual International Meeting, Pittsburgh, Pennsylvania, June 20-23.

APPENDIX II

Academic outcome

- MS Degrees Conferred: Wangda Qu
- Undergraduate students supported: Brendon Barker, Addison A. Dumke, Kory Alpichi, Zachary DeVaar Crandall
- M.S. students supported: Yijing Wang,
- Ph.D. students supported: Yinbin Huang, Zhongwei Liu, Xianhui Zhao, Shouyun Chen, Dan Liu
- Post-docs supported : Zhongyi Ma, Gao Yang, Chunkai Shi

Please complete the following table to reflect your project at completion or time of report submission:

ITEM	NUMBER
Abstracts	**11**
Peer Reviewed Publications	**2**
Outreach Publications/Web Pages	**2**
Professional Presentations	**12**
MS Degrees Conferred	**1**
Ph.D. Degrees Conferred	
MS Students Supported	**1**
Ph.D. Students Supported	**5**
Post-Docs Supported	**3**
Undergraduate Students Supported	**4**
Investigators Supported	**2**
Start-Up Jobs Created	
Disclosures	**1**
Patents Filed	**1**
Provisional Patents	
Patents Issued	
License Agreements	**1**
Plant Variety Protection	
Subsequent Funding	**5**

Back to Table of Contents

Sun Grant Initiative
DOE Final Progress Report

Project Title: Using Second Generation Biofuel Feedstocks to Improve the Carbon Economy of US Agriculture

Project Director/Principal Investigator: Evan DeLucia, Professor, Plant Biology and Institute for Genomic Biology, University of Illinois, Urbana, IL 61801

All Co-Principal/Other Investigators:
Kristina Anderson-Teixeira, Research Associate, Institute of Genomic Biology, University of Illinois, Urbana, IL 61801
Mark David, Professor, Department of Natural Resources and Environmental Science, University of Illinois, Urbana, IL 61801
Madhu Khanna, Professor, Department of Agricultural and Consumer Economics, University of Illinois, Urbana, IL 61801
Stephen Long, Professor, Institute of Genomic Biology, University of Illinois, Urbana, IL 61801
Thomas Voigt, Professor, Department of Crop Science, University of Illinois, Urbana, IL 61801

Collaborators:
William Parton, Senior Research Scientist, Natural Resource Ecology Laboratory, Colorado State University, Ort Collins, CO 80523
Tara Hudiburg, Assistant Professor, Department of Forest, Rangeland, and Fire Sciences, University of Idaho, Moscow, ID 83844

Period of Performance: 1 December 2011 - 31 March 2015

Funding Awarded: $644,517

Cost Share Amount: $224,172

Cost Share Sources: Time and effort from PIs and CoPIs; Indirect on time and effort

Executive summary

This research relied on a network of experiment plots of two important energy crops – miscanthus and switchgrass – in the eastern US to quantify spatial variation in yield, driven by differences in climate and soil properties. Empirical data on plant productivity and soil properties were then used to parameterize and validate a biogeochemical model – DayCENT – for quantifying the effect of converting current land uses, including row crop agriculture and pasture, to energy crops on the exchange of greenhouse gases with the atmosphere and changes in soil carbon storage. The DayCENT model was then combined with an economic model – BEPAM – to determine the consequence of meeting the Renewable Fuel Standard on land allocation, greenhouse gas exchange, and soil carbon. We predict that meeting the least-cost land allocation for a 32 billion gallon (121 billion liter) renewable fuel mandate in the US, would decrease transportation emissions by 7% when 3.9 million hectares of eastern US land are converted to perennial grasses supplemented with corn, largely because of gasoline displacement and soil carbon storage. If renewable fuel production is accompanied by a cellulosic biofuel tax credit, CO_2 equivalent emissions could be reduced by 12%. We demonstrate that GHG reducing bioenergy landscapes that meet RFS requirements and do not displace food are possible.

Project objectives

This research has two objectives:

Objective 1: Leveraging a unique assemblage of research sites established throughout the central and eastern US; we provide the first side-by-side comparisons for above- and belowground production and changes in SOC for replicate plots of miscanthus and switchgrass. These data provide the first estimates of spatial variation in yield associated with climate and soils for two major energy crops proposed for the central and eastern US.

Progress under Objective 1:

We have concluded collection of yield and soils data for the research sites and are continuing to analyze the results. For *Miscanthus x giganteus*, we determined the effect of three different spring fertilizer treatments (0, 60, and 120 kg N ha^{-1} yr^{-1} as urea) on biomass production, soil organic matter (SOM), and inorganic N leaching in Illinois, Kentucky, Nebraska, New Jersey, and Virginia, along with N_2O and CO_2 emissions at the IL site. There were no significant yield responses to fertilizer treatments, except at the IL site in 2012 (yields in 2012, year 4, varied from 10 to 23.7 Mg ha^{-1} across all sites). Potentially mineralizable N increased across all fertilizer treatments and sites in the 0 – 10 cm soil depth. An increase in permanganate oxidizable carbon (POX-C, labile C) in surface soils occurred at the IL and NJ sites, which were regularly tilled before planting. Decreases in POX-C were observed in the 0 – 10 cm soil depth at the KY and NE sites where highly managed turfgrass was grown prior to planting. Growing *M.* x *giganteus* altered SOM composition in only four years of production by increasing the amount of potentially mineralizable N at every site, regardless of fertilization amount. Nitrogen applications increased N leaching and N_2O emission without increasing biomass production. This suggests that for the initial period (4 yr) of *M.* x *giganteus* production, N application has a detrimental environmental impact without any yield benefits and thus should not be recommended. Further research is needed to define a time when N application to *M.* x *giganteus* results in increased biomass production.

Objective 2: These empirical data then were used to parameterize and validate three process-based models to extrapolate the yield data in space and time, to examine the effect of land use and management change on the soil C stocks and GHG balance for the central and eastern US, and to examine the economic incentives and feedbacks stemming from the wide-scale deployment of low input, perennial biofuel feedstocks on the landscape.

Progress under Objective 2:

We have also completed the modeling activities under objective two. We have a final manuscript under review at Nature Climate change (we are in the process of submitting revisions from the first round of review). We include the abstract here as a summary of our findings: "Sustainable bioenergy for transportation fuel and greenhouse gas (GHGs) reductions may require considerable changes in land use globally. Perennial grasses have been proposed because of their potential to yield substantial biomass on marginal lands without displacing food and reduce GHG emissions by storing soil carbon. Here, we implement an integrated approach to planning bioenergy landscapes by combined spatially-explicit ecosystem and economic modeling to predict a least-cost land allocation for a 32 billion gallon (121 billion liter) renewable fuel mandate in the US. We find that 2022 GHG transportation emissions are decreased by 5% when 4.5 million hectares of eastern US land are converted to perennial grasses supplemented with corn residue to meet cellulosic ethanol requirements, largely because of gasoline displacement and soil carbon storage. If renewable fuel production is accompanied by a cellulosic biofuel tax credit, CO2e emissions could be reduced by 10%, because it induces more cellulosic biofuel and land under perennial grasses than under the mandate alone. While GHG reducing bioenergy landscapes that meet RFS requirements and do not displace food are possible, the reductions in GHG emissions are reduced by at least 50% compared to previous estimates that did not account for economically feasible land allocation.

Project activities

Our research focuses on two plant species, switchgrass and miscanthus, that have high potential as biofuel feedstocks in the central US. Both are high yielding, rhizomatous, C_4 grasses.

1. *Research sites and biomass measurements* - The primary empirical data collected for this research will be above- and belowground biomass and SOC for switchgrass and planted in different locations in the central and eastern US.

2. *Measuring changes in soil organic carbon (SOC)* - Changes in soil organic carbon (SOC) will be determined by measuring total SOC and its isotopic composition pre-planting and after three years from each research site.

3. *Estimating variation in feedstock production, GHG balance and economics with the wide scale deployment of biofuel crops in central and eastern US rain-fed agriculture* - Ultimately, where and how much land is devoted to the production of biofuel crops and the consequent effect on C storage and GHG balance will depend upon their economic value, which is determined by demand, government subsidies, crop productivity and ancillary value associated with carbon sequestration and GHG mitigation. Building on their respective strengths, we will use three different process-based models iteratively to provide an end-to-end analysis of the productivity and ecological and economical sustainability of growing perennial feedstocks on agricultural land.

4. *Productivity of biofuel feedstocks in the central and eastern US* - For our major food and forestry crops it is relatively simple to predict yields empirically from the large temporally and spatially dispersed yield records. For the emerging perennial grass bioenergy feedstocks there are few yield records. We will use WIMOVAC in a stand-alone research effort to quantify climatically induced variation in biomass production for switchgrass and miscanthus.

5. *The GHG balance of the central and eastern US following the deployment of biofuel feedstocks* - Using data including measurements of the accumulation of biomass above- and belowground and changes in SOC from research sites described previously, we will quantify the effect of substituting a portion of row crop agriculture with perennial feedstocks on soil C storage and GHG balance for the entire region of rain-fed agriculture in the central and eastern US using a process-based model, DAYCENT.

6. *Economic value of biofuel crops and carbon storage* - Using measured and simulated data on crop yields and soil carbon storage from DAYCENT, we will use the economic model (BEPAM) to examine economic incentives for growing biofuel feedstocks, the spatial patterns of land allocation to them and the consequences of their deployment on food production and prices.

Deliverables

1. Scholarly publications: (1) Above- and below-ground biomass of switchgrass and miscanthus across widely varying climatic and edaphic conditions in the central and eastern US, (2) Changes in SOC under switchgrass and miscanthus across the central and eastern US, (3) GHG balance of the central and eastern US following the deployment of switchgrass and miscanthus as biofuel feedstocks, (4) Combined economic and GHG analysis of perennial grass biofuel production.

2. Raw data for archival storage: Files containing raw data will be submitted for archival storage with the journals in which manuscripts are published and will be made publicly available upon request.

3. Outreach, including presentations at the Biomass Feedstock Symposium, UIUC, and the Ecological Society of America annual meetings.

Products developed under the award

Manuscripts published, in review, or in preparation:

Davis, M.P., M.B. David, T.B. Voigt, and C.A. Mitchell. 2015. Effect of nitrogen addition on *Miscanthus x giganteus* yield, nitrogen losses, and soil organic matter across five sites. GCB - Bioenergy. doi: 10.1111/gcbb.12217.

Dwivedi, P., W. Wang, T.W. Hudiburg, M. Khanna, D. Jaiswal, S.P. Long, and E.H DeLucia. Cost of Abating Greenhouse Gas Emissions with Cellulosic Ethanol. Environmental Science and Technology 49, 2512-2522. doi: 10.1021/es5052588

Duval BD, Davis SC, Anderson-Teixeira KJ, Keogh C, Parton WJ, Long SP, DeLucia EH. Simulated effects of converting pasture to energy cane for bioenergy: predicting changes to greenhouse gas emissions and soil carbon. PlosOne. Volume 8 (8) E72019.

Hudiburg, T.W., S.C Davis, W.J. Parton, and E.H. DeLucia. Bioenergy crop greenhouse gas mitigation potential under a range of management practices. GCB-Bioenergy. DOI: 10.1111/gcbb.12152

Hudiburg, T.W., Wang, W., Dwivedi, P.,W.J. Parton, , M. Khanna, S. Long, and E.H. DeLucia. Greenhouse gas implications of a 32 billion gallon bioenergy landscape in the US. (In Review, Nature Climate Change)

Masters, M.D., , C.K. Black, I.B. Kantola, K.P. Woli, T. Voigt, M.B. David, and E.H. DeLucia. Soil nutrient removal by four potential bioenergy crops: *Zea mays*, *Panicum virgatum*, *Miscanthus* x *giganteus*, and prairie. (In review, Agriculture, Ecosystems, and Environment)

Oliver, A and M. Khanna. What is the Cost of a Renewable Energy-Based Approach to Greenhouse Gas Mitigation? (In review, Land Economics)

Wang, W., M. Khanna, P. Dwivedi, R. Abt, An Integrated Analysis for Determining Carbon Savings with Transatlantic Trade in Pellets (In Review Environmental Research Letters)

Conference Presentations:

Davis, M., M.B. David, T. Voigt, and C. Mitchell. 2012. Changes in Potential Soil Carbon and Nitrogen Mineralization: A Multistate Analysis of Miscanthus x Giganteus Under Nitrogen Fertilizer Treatments. Presented at the American Society of Agronomy annual meeting, Oct. 21-24, 2012, Cincinnati, Ohio.

DeLucia, E.H. Conversion of Pasture to Energy Cane for Bioenergy is Predicted to Alter Greenhouse Gas Exchange and Soil Carbon. Presented at the 2012 National Sun Grant Conference, New Orleans, LA, October 2012.

DeLucia, E.H. Land use change, bioenergy, and soil organic carbon. Presented at the 20th World Congress of Soil Science, Jeju, South Korea, June 2014. (Invited symposium speaker)

Dwivedi, P. W. Wang, T. Hudiburg, M. Khanna, D. Jaiswal, S. Long, and E.H. DeLucia. Life-cycle carbon intensity and production cost of cellulosic ethanol. Presented at the Energy Biosciences Institute Retreat. July 14 – 17, 2013, Champaign, Illinois.

Hudiburg, T. and E.H. DeLucia. Bioenergy Landscapes of the Future. Presented at the Energy Biosciences Institute Retreat. July 14 – 17, 2013, Champaign, Illinois.

Hudiburg, T. S. Davis, B. Parton, and E.H. DeLucia. Bioenergy crop greenhouse gas mitigation potential under a range of management practices – improved estimates through model-data integration. Presented at the Energy Biosciences Institute Retreat. July 14 – 17, 2013, Champaign, Illinois.

Hudiburg, T., P. Dwivedi, W. Wang, M. Khanna, W. Parton, M. Hartmann, S. Long and E.H. DeLucia. Environmental impacts of a 16 billion gallon bioenergy landscape in the United States. 20th World Soils Congress, Jeju, South Korea, June 2014.

Hudiburg, T., P. Dwivedi, W. Wang, M. Khanna, W. Parton, M. Hartmann, S. Long and E.H. DeLucia. Integrated regional modeling assessment of the environmental and economic potential of perennial grass bioenergy feedstocks. AGU 93, 2013 Fall Meeting, Abstract GC43A-1033, San Francisco, CA.

Hudiburg, T.W., S. Davis, W.J. Parton, K.Anderson-Teixeira, C. Smith, E. DeLucia. Reducing uncertainty of bioenergy crop carbon sequestration strategies using observations from field sites across the central and eastern United States and the DayCent biogeochemical model. Presented at the 4th NACP Investigators Meeting. Feb. 4-7, 2013. Albuquerque, NM.

Jaiswal, D., S.P. Long, W.J. Parton, and M. Hartman. 2012. Two-way Coupling of a Process-Based Crop Growth Model (BioCro) and a Biogeochemistry Model (DayCent) and its Application to an Energy Crop Site in the mid-west USA. Abstract B43F-0482. Presented at the 2012 Fall Meeting of the American Geophysical Union, San Francisco, CA, December 2012.

Kantola, I.B., T.W. Hudiburg, W. Wang, P. Dwivedi, D. Jaiswal, M. Khanna, and E.H. DeLucia. Using Second Generation Biofuel Feedstocks to Improve the Carbon Economy of US Agriculture – Model Validation and Predictions. 2014 NC Region Sun Grant Center Annual Meeting, Minneapolis, MN, March 2014.

Kantola, I.B., T.W. Hudiburg, K.J. Anderson-Teixeira, P. Dwivedi, M. Khanna, and E.H. DeLucia. Second Generation Biofuel Feedstocks and the Carbon Economy of US Agriculture – Soil Carbon. 2015 NC Region Sun Grant Center Annual Meeting. Minneapolis, MN, March 2015.

Khanna, M. "Realizing the Promise of Second Generation Biofuels," Keynote on 2014 Yangling International Agri-Science Forum, North-Western Agricultural and Forestry University, November 4-6, 2014, Yangling, China.

Khanna, M., Achieving the Sustainability Goals of the Bioeconomy: Policy Choices, Advanced Bioeconomy Leadership Conference, Washington DC, March 13, 2015.

Khanna, M., Cost of Abating GHG Emissions with Renewable Fuels: Role of Policy, 8th Berkeley Bioeconomy Conference, University of California, Berkeley, April 1-2, 2015.

Long, S., T. Hudiburg, P. Dwivedi, M. Khanna, E.H. DeLucia, T. Voight, and W. Parton. Spatial and Temporal Variability in Carbon Intensity and Production Cost of Cellulosic Biofuel Feedstocks. Presented at the 2013 NC Region Sun Grant Center Annual Meeting, Chicago, IL, March 2013.

Parton, W. Environmental Impact of Growing Perennial Biofuel Crops on Unproductive Cropland. Presented at the Ecological Society of America Meeting, Portland, OR, August, 2012.

Voigt, T. Establishing and Managing *Miscanthus* x *giganteus* and *Panicum virgatum* Feedstocks in the Temperate U.S. American Chemical Society, Special Session - Biofuels, Bioproducts, and Biomass from Sugar Feedstocks. New Orleans, LA, April, 2013.

Voigt, T. *Miscanthus* x *giganteus* Biomass Feedstock Production and Sustainability Studies in the Eastern U.S. 2012 National Sun Grant Conference: Science for Biomass Feedstock Production and Utilization. New Orleans, LA. October, 2012.

Wang. W., M. Khanna, and P. Dwivedi. Optimal Mix of Feedstock for Biofuels: Implications for Land Use and GHG Emissions. Selected Paper prepared for presentation at the Agricultural & Applied Economics Association's 2013 AAEA & CAES Joint Annual Meeting, Washington, DC, August, 2013

Academic

1. Courses developed: 0
2. M.S. students supported: 2
3. M.S. degrees conferred: 1
4. Ph.D. students supported: 3
5. Ph.D. degrees conferred: 0
6. Post-docs supported: 5

In this research, we combine empirical observations, ecosystem modeling of yield and greenhouse gas (GHG) balance (DayCent[1]), and economic modeling (BEPAM-F[2]) to provide economically feasible bioenergy landscapes under alternative policy scenarios.

The ecosystem model (DayCent) simulates the effects of climate and land use change on carbon and nutrient cycling and has been validated for use in crop ecosystems including perennial grass yield and GHG balance[1,3,4]. The economic model (BEPAM-F) is a multi-market, dynamic, open economy model that integrates the agricultural, forestry, and transportation fuel sectors in the US. The model is extended from BEPAM[5] by adding a forestry sector and allowing for shifts between cropland and forestland based on the net land returns in the two sectors and by including bioenergy crop yields and GHG estimates from DayCent. Market equilibrium is achieved by maximizing the sum of consumers' and producers' surpluses in the agricultural, forestry, and transportation fuel sectors subject to various material balance, technological, land availability, and policy constraints over the 2007-2022 period.

1 Del Grosso, S. J., Mosier, A. R., Parton, W. J. & Ojima, D. S. DAYCENT model analysis of past and contemporary soil N(2)O and net greenhouse gas flux for major crops in the USA. *Soil & Tillage Research* **83**, 9-24, doi:10.1016/j.still.2005.02.007 (2005).

2 Khanna, M., Dhungana, B. & Clifton-Brown, J. Costs of producing miscanthus and switchgrass for bioenergy in Illinois. *Biomass & Bioenergy* **32**, 482-493, doi:10.1016/j.biombioe.2007.11.003 (2008).

3 Campbell, E. E. *et al.* Assessing the Soil Carbon, Biomass Production, and Nitrous Oxide Emission Impact of Corn Stover Management for Bioenergy Feedstock Production Using DAYCENT. *Bioenergy Research* **7**, 491-502, doi:10.1007/s12155-014-9414-z (2014).

4 Hudiburg, T. W., Davis, S. C., Parton, W. & Delucia, E. H. Bioenergy crop greenhouse gas mitigation potential under a range of management practices. *GCB Bioenergy*, n/a-n/a, doi:10.1111/gcbb.12152 (2014).

5 Chen, X., Huang, H., Khanna, M. & Önal, H. Alternative transportation fuel standards: Welfare effects and climate benefits. *Journal of Environmental Economics and Management* **67**, 241-257, doi:http://dx.doi.org/10.1016/j.jeem.2013.09.006 (2014).

DayCENT source code can be found at:

https://www.nrel.colostate.edu/projects/irc/public/Documents/Software/Century5/Reference/html/releasenotesv5.htm

BEPAM source code can be found at:

Chen, X, H. Huang, M. Khanna and H. Onal, "Alternative Fuel Standards: Welfare Effects and Climate Benefits," Journal of Environmental Economics and Management 67: 241–257, 2014

Please complete the following table to reflect your project outputs at completion or at time of report submission. Identify outputs and products developed under the award and any technology transfer activities.

ITEM	NUMBER	DETAILS (e.g. citations, names, descriptions, varieties, etc.)
Abstracts: include full citation and attach a pdf copy.		Publications with abstracts are listed in the conference presentations section above.
Peer Reviewed Publications: include full citation and attach a pdf copy if available		Peer reviewed publications are listed in the manuscripts section above.
Outreach Publications including web pages: include full citation		
Professional Presentations: include full citation		Professional presentations are listed in the professional presentations section above.
MS Degrees Conferred: include names plus month/year confirmed		Morgan Davis, December 2013
Ph.D. Degrees Conferred: include names plus month/year confirmed		
MS Students Supported: include names		Morgan Davis; Robert Paul
Ph.D. Students Supported: include names		Robert Paul, Chris Black, Nicholas DeLucia
Post-Docs Supported: include names		Tara Hudiburg, Ilsa Kantola, WeiWei Wang, Puneet Dwivedi, Kristina Anderson-Teixeira
Undergraduate Students Supported: include names		
Investigators Supported: include names		Evan DeLucia, Madhu Khanna, Stephen Long, Thomas Voigt, Mark David
Jobs Created		
Invention Disclosures		Provide no confidential or enabling information. Just indicate in an invention disclosure has been filed with the employer.
Non-provisional Patent Application(s) Filed		

Provisional Patents Filed		
Patents Filed		
Patents Issued: include full citation		
License Agreements: include description		
Plant Variety Protection: include description		
Subsequent Funding: List proposals funded as a result of this work		
Other: Products, such as data or databases, physical collections, audios or videos, software or Netware, models, educational aids or curricula, instruments, or equipment.		

Back to Table of Contents

Sun Grant Initiative
DOE Final Report

Project Title: Improving production, resilience, and biodiversity of perennial grass mixtures and monocultures as biofuel feedstocks across environmentally heterogeneous landscapes.

Project Director/Principal Investigator: W. Carter Johnson, Department of Natural Resource Management, South Dakota State University, Brookings, SD

Co-Principal Investigators: Arvid Boe, Plant Science Department, South Dakota State University, Brookings, SD; Cody J. Zilverberg, Department of Natural Resource Management, South Dakota State University, Brookings, SD; David Archer, USDA-ARS, Mandan, ND

Period of Performance: 1 December 2011 - 30 September 2015

Funding Awarded: $671,506

Cost Share Amount: $149,138

Cost Share Sources: Time and effort from PIs and CoPIs; Indirect on time and effort

Executive Summary

The primary part of this research dealt with switchgrass (*Panicum virgatum*) monocultures as a leading feedstock choice for producing cellulosic biofuels. However, in natural stands, switchgrass is only dominant in a narrow ecological niche of the Tallgrass Prairie. This suggests that strategically selected monocultures or binary mixtures of species, adapted to particular ecological niches, might outyield switchgrass monocultures while increasing biodiversity at the field and landscape scales. To test this hypothesis, we planted monocultures of switchgrass and three alternative species at each of three landscape positions (shoulderslope, midslope, and footslope) on the EcoSun Prairie Farm near Brookings, SD. Alternative species were also mixed with switchgrass such that they composed 33 or 67% of the total number of plants in each plot. Alternative species at each position included a C_3 grass, a C_4 grass, and a forb. Biomass data were collected in autumn during each of the two consecutive years following the establishment year. At the shoulderslope, the highest-yielding treatments were those containing little bluestem (*Schizachyrium scoparium*; 12.0 Mg ha^{-1}) and those dominated by switchgrass (10.4 Mg ha^{-1}). At the midslope and footslope, there were interactions of year x treatment ($p < 0.05$). In general, the highest-yielding treatments at the midslope were those containing big bluestem (*Andropogon gerardii*; 16.4 Mg ha^{-1}). At the footslope in 2013, the prairie cordgrass (*Spartina pectinata*) monoculture and treatments with at least 67% of the plants being cup plant (*Silphium perfoliatum*) produced the most biomass (24.3 Mg ha^{-1}; $p < 0.05$) but there were few yield differences at the footslope in 2014. This research demonstrated that biomass yield of two- and three-year-old stands of monocultures or binary mixtures of native plant species with switchgrass, when appropriately matched to their natural landscape positions, produced biomass in equal or greater amounts than switchgrass monocultures.

This report also summarizes other work completed at the EcoSun Prairie Farm that was funded by the DOE. The complete report can be downloaded at the following website http://igrow.org/up/resources/07-5001-2015.pdf

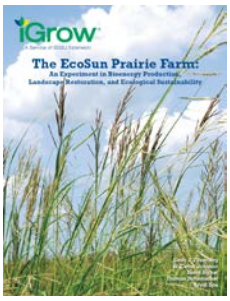

Publications

Zilverberg, C.J., K. Teoh, A. Boe, W.C. Johnson, and V. Owens. 2016. Strategic use of native species on environmental gradients increases diversity and biomass relative to switchgrass monocultures. Agriculture, Ecosystems and Environment 215:110-121.

Book Chapters

Kiniry, J.R., M.N. Meki, T.E. Schumacher, C.J. Zilverberg, F.B. Fritschi, and V.G. Kakani. 2014. Modeling to evaluate and manage water and environmental sustainability of bioenergy

crops in the U.S. in Advances in Agricultural Systems Modeling 5: Practical Applications of Agricultural System Models to Optimize the Use of Limited Water. Ahuja et al., ed. ASA, CSSA, SSSA. pages 139:160.

Outreach Publications

Zilverberg, C.J., W. C. Johnson, D. Archer, T. Schumacher, and A. Boe. 2015. The EcoSun Prairie Farm: An experiment in bioenergy production, landscape restoration, and ecological sustainability. South Dakota State University Cooperative Extension iGrow. http://igrow.org/up/resources/07-5001-2015.pdf

Presentations

Teoh, K.H., C.J. Zilverberg, W.C. Johnson, and A. Boe. 2015. Targeted polycultures as high-yielding bioenergy feedstock. Poster presented at the 68th Society for Range Management Annual Meeting, Sacramento, CA. February 5.

K. Teoh, C.J. Zilverberg, W.C. Johnson, and A. Boe. 2015. High diversity biofuel crops, outperform switchgrass monoculture. Presented to the South Dakota State University Sigma Xi 2015 chapter award competition, Brookings, SD. April 14.

Zilverberg, C.J., K. Teoh, W.C. Johnson, A. Boe, and V. Owens. 2015. Increasing diversity of native biofuel plantings using simple mixtures. Presented at the 68th Society for Range Management Annual Meeting, Sacramento, CA. February 3.

Zilverberg, C.J., W.C. Johnson, A. Boe, V. Owens, D. Archer. 2014. Increasing diversity of biofuel crops. Presented at the 2014 North Central Regional Sun Grant Center Annual Meeting. 27-28 Mar., 2014. Minneapolis, MN.

Johnson, C. 2014. South Dakota's Prairie Farm. SDSU Plant Science GSA "We Talk Science" seminar series, October 21, 2014.

Johnson, C. 2014. How Would Aldo Leopold Farm. Augustana College classroom presentation, October 23, 2014.

Johnson, C. 2014. Profitable Prairie Restoration: the Eco-Sun Prairie Farm Experiment. The Great Lakes Chapter of the Society for Ecological Restoration, University of Minnesota, March 28-29, 2014.

Zilverberg, C.J., W.C. Johnson, and D. Archer. 2013. Restoring prairie for agricultural production and profit. America's Grasslands Conference. Manhattan, KS.

Zilverberg, C.J., W.C. Johnson, A. Boe, V. Owens, and D. Archer. 2013. Improving production, resilience, and biodiversity of perennial grass mixtures and monocultures as biofuel feedstocks across environmentally heterogeneous landscapes. Presented at the 2013 North Page 81 Central Regional Sun Grant Center Annual Meeting. 26-27 Mar., 2013. Chicago, IL.

Academic

M.S. students supported: N. Bourlion
M.S. degrees conferred: N. Bourlion
Post-docs supported: Cody Silverberg and Chang Oh Hong

Back to Table of Contents

Sun Grant Initiative
DOE Final Progress Report

Project Title: Production and Economics of Perennial-based Woody and Herbaceous Biomass Crops under Alley-Cropping Systems

Project Director/Principal Investigator:
Gregg Johnson, Assoc. Professor, Dept. of Agronomy and Plant Genetics, University of Minnesota, St. Paul, MN

All Co-Principal/Other Investigators:
Craig Sheaffer, Professor, Dept. Agronomy and Plant Genetics, University of Minnesota, St. Paul, MN
William Lazarus, Professor, Dept. Applied Economics, University of Minnesota, St. Paul, MN
Dean Current, Research Associate and CINRAM Director, Dept. of Forest Resources, University of Minnesota, St. Paul, MN
Diomy Zamora, Extension Professor in Forestry, University of Minnesota Extension, University of Minnesota, St. Paul, MN

Collaborators:
Gary Wyatt, Extension Professor in Agroforestry, University of Minnesota Extension, University of Minnesota, Mankato, MN.
Bill Berguson, Forestry Program Leader, NRRI, Duluth, MN

Period of Performance: 1 January 2012 - 30 July 2015

Funding Awarded: $515,025

Cost Share Amount: $128,863

Cost Share Sources: Time and effort from PIs and CoPIs; Indirect on time and effort

Executive summary

The emerging bioeconomy presents new opportunities for farmers and other land managers to improve economic return through the integration of perennial biomass crops into the farming enterprise. In particular, agroforestry techniques, such as alley cropping, are being promoted for sustainable bioindustrial feedstock production. However, little is known about appropriate species combinations and long-term production potential of biomass crops in alley cropping systems. We found that perennial biomass alley cropping systems can provide substantial biomass and environmental benefits, but optimal species combinations for maximizing these benefits will depend on local site characteristics. Therefore, more local data (current and future) is needed to help farmers and land managers make decisions on how best to design agroforestry systems that are productive, profitable, and sustainable. We therefore designed a database for storing local production data using standardized forms. This database allowed us to create a web-based enterprise budget for alley-cropping and other perennial-based cropping systems that manages unique users, receives and saves local input and output data. Although this is powerful tool for decision-making, it can be cumbersome to use and interpret, especially for those not familiar with enterprise budgets. Therefore, we design a web-based decision support tool that helps make cropping system decisions in an intuitive and simple format. We created a new decision support tool called 'The Crop Enterprise and Environmental Budgeting Tool (CE^2T)' that is designed to estimate the breakeven price needed to cover the costs of producing biomass from conventional and alternative feedstocks. Moreover, we included a crop model that allows for CE^2T to evaluate environmental components, i.e. carbon, of the cropping system being considered. Through this project, we were able to provide short and long-term economic and production estimates that reflect real-world data linked to local environments.

Project objective, discuss outcomes and impacts including comparing actual versus expected accomplishments.

Objective 1: Determine productivity of woody and herbaceous biomass species in an alley cropping configuration

We found that perennial biomass alley cropping systems can provide substantial biomass and nutrient uptake, but optimal species combinations for maximizing these goods and services will depend on site characteristics. Yield of perennial biomass alley cropping systems was largely dependent on SRWC selection, with NM6 poplar alley systems being more productive than Fish Creek willow alley systems at two of three sites. Herbaceous crop selection influenced overall system yield to a lesser extent, but was an important consideration for maximizing nutrient uptake. Among herbaceous crops, intermediate wheatgrass showed the greatest potential for N, P, and K uptake, though the native polyculture and prairie cordgrass also performed well and are better choices for sites with occasional flooding. These findings can help guide the design of productive buffer systems for waterways in the US Midwest.

Our research also provides a basis for understanding the effects of spatially integrating herbaceous and woody biomass crops into an alley cropping management system. Effects of distance from the tree-crop interface on SRWC and herbaceous crop productivity were not consistent across sites, species, and years. However, general patterns in tree and crop edge effects, as well as declining herbaceous crop yields at Empire, suggest that alley orientation is an important consideration for maximizing long-term yields. Since these systems are likely to be deployed in a variety of configurations to suite on-farm needs, a better understanding of the role of alley orientation and crop edge effects on productivity is required. Future research should focus on optimizing conditions for maximal herbaceous crop yield and longevity; and on further quantifying the environmental and ecological benefits of these systems.

Objective 1a: Evaluate cover crops in short rotation woody biomass cropping systems

We found that winter rye and pennycress cover crops negatively impacted growth of shrub willow 'Fish Creek' during the 2013 growing season. Tilling strips into cover crops resulted in greater stem diameters than in sprayed strips, but this effect did not correspond to greater basal area in tilled versus sprayed plots. Soil moisture was similar among cover crop treatments, but was positively correlated with some willow growth characteristics. Crop ground cover was negatively correlated with willow growth characteristics. Spraying versus tilling strips appeared to conserve soil moisture, especially in August. This could be due to residue cover retained in the strip spray plots, which acted as mulch. These results suggest that suppressive effects of pennycress and winter rye were related to environmental variables other than soil water. Both pennycress and winter rye likely shaded young willow trees, and may have competed for N early in the spring. However, we did not measure these variables.

Overall our results suggest that strip spraying and strip tilling in pennycress and winter rye cover crops had similar effects on willow growth. However, 1 m strips were insufficient in reducing competition between cover crops and shrub willows during the establishment year. Future research should evaluate wider strips and additional cover crops to further examine the potential for successfully integrating cover crops into shrub-willow biomass production systems.

Objective 2: Aggregate production data and refine enterprise budgets for alley-cropping and other perennial-based cropping systems

We established a protocol that integrates data from new and existing field studies on a local basis. To accomplish this task, we worked with colleagues and collaborators to define a minimum data set for both herbaceous and woody perennials and developed standard procedures and forms for obtaining production and environmental data. From this database, we then created a web-based enterprise budget for alley-cropping and other perennial-based cropping systems that manages unique users, receives and saves local input and output data. The budget follows a standard annual crop enterprise budget costs-and-returns format recommended by the American Agricultural Economics Association Task Force on Commodity Costs and Returns. The design of the budget includes high-level summary tables with side-by-side comparisons of key measures on a per-acre and a per-unit basis. For perennial crops, the enterprise budget shows present values of the economic variables summed over the stand life from planting to stump removal which are then converted to annual equivalent cash flows. The annual equivalent cash flows (also referred to as annualized present values) can be compared across crops with different stand lives while still accurately accounting for the time value of money.

Objective 3: Integrate production and economic data into a decision support tool (DST) for biomass cropping systems.

The Crop Enterprise and Environmental Budgeting Tool (CE^2T) was designed to estimate the breakeven price needed to cover the costs of producing biomass from conventional and alternative feedstocks. These include crop residues from corn and energy crops like switchgrass, mixed grasses, shrub willow, hybrid poplar, and agroforestry systems that combine both woody and herbaceous crops. Results from objective 1 were used to provide initial data for the CE^2T. Data for each user account and budget are stored in a relational database management system created specifically for CE^2T. The database is housed on University of Minnesota servers and is built around the MySQL platform. The web-based user interface (http://cropbudget.apec.umn.edu) was built using php, html5 programming languages. Specifically, this tool computes the minimum price per acre of biomass crop that would be needed to cover all the costs of producing the biomass. The tool guides you through describing your farm management practices including alternative future management scenarios. Once complete, a report is generated comparing the economics between your current management practices and future scenarios. The tool also provides an environmental report, comparing changes in soil carbon storage and soil erosion between your current management practices and future scenarios.

Project activities

Alley cropping systems were established at three sites in May 2010 and currently in their third growing season (second year post-coppice in the case of willow and poplar), except for at one site (Fairmont) in which herbaceous crops are in their first growing season due to reestablishment in fall 2011 following crop failure due to weed pressure. Field plots were established in fall 2011 and spring 2012 at the Rosemount Research and Outreach Center in Rosemount, MN and at the Southern Research and Outreach Center in Waseca, MN to evaluate cover crops in a short rotation willow cropping system. In spring 2012, willows were to be planted into fall 2011 seeded cover crops, but planting was be delayed until spring 2013 to better establish perennial covers. In field plots established in spring 2012, cover crops and willows were planted simultaneously.

Willow and poplar plant population, plant height, basal stem area was measured in each plot at all three locations all years of the study. Dry matter yield of herbaceous crops was measured by harvesting herbage following a killing frost. Edge effect was detected for woody species at the Empire site but not at the Granada site. To understand the cause of this finding, a Decagon MPS-2 soil water potential and soil temperature sensors were installed at each site in a transect across the alley to evaluate the effects of shading and proximity to tree rows on herbaceous crop water-use and productivity in May 2013. A Decagon Accupar LP-80 was used to characterize temporal availability of photosynthetically active radiation (PAR) to herbaceous crops across a transect in the alley (i.e. at various distances from the tree rows) as well as to characterize leaf area index (LAI) for each of the woody and herbaceous species. This data will provide insights as to whether competition for growth resources between trees and crops is the cause of reduced yield and lack of edge effects for herbaceous crops.

An existing RDBMS design for biomass production of plantation forests called MiraSilv was identified and is capable of managing information for monoculture or polyculture perennial woody biomass production systems. Although MiraSilv is a good database, we found that it did not meet our goals and would not ultimately allow us to obtain our end goals of a working decision support system. Therefore, development and design of a RDBMS that did meet our needs required programming of a new RDBMS from programs such as MySQL. MySQL is the most widely used RDBMS and is a free open-source program with cross-platform functionality. In addition, tools such as the MySQL Workbench is a visual way in which to design the database. Allowing experts in the production of perennial-based biomass with little knowledge for RDBMS to aid in the design. During this same time period, empirical and process based growth models were reviewed for woody species including minimum datasets. We then designed a draft of the database tables, variables, and structure using MySQL Workbench. We acquired MySQL server space and engineered the draft relational database on the MySQL server.

A crop enterprise budget was modified to combine two different perennial crops (in an alley-cropping configuration) for a combined profitability measure. Data on the pre-harvest costs for the alley cropping system in task 1 was collected and summarized third quarter 2013. Data for the enterprise budgets was updated to mirror current economic conditions. Data tables for cost data were implemented in the database and cost and management data were imported into the database. Database was integrated with online enterprise budget. Data tables for the input data was implemented in the database fourth quarter 2013. Database code was put in a GitHub repository in order to track changes and versions. We also continued updating the database design and data to support the online enterprise budget. Before we could go any further, we needed to wait for the draft completion of the web interface to obtain feedback on standardized forms, database, and minimum dataset from outside reviewers. Therefore, alpha test of draft standardized forms, database, and minimum dataset with UMN data was delayed until next quarter to focus on task 1 and decision support tool.

The database for storing crop productivity information is close to being completed third quarter 2014. Standardized forms are being tested and refined. A draft of the final enterprise budgets is complete. The management information system data related to Task 2.2 is updated to match the needs for research data and to match needs for task 3. Draft enterprise budgets for now complete for alley-cropping and other perennial-based cropping systems. Furthermore, we have alpha tested standardized forms and databases.

Programming also began on a web based enterprise budget to mange users, received and save inputs and output data into a basic enterprise budget second quarter 2013. We also tested the CENTURY model in support of the decision support tool third quarter 2013. Development of a DST has taken more time than originally planned. However, we hired 2 programmers to hasten the develop of a web use interface as well as assist in programming economic calculations and integrating web tool with the database second quarter 2014. Validation of CENTURY model for the decision support tool was expanded to include additional research sites and biomass crops third quarter 2014. A draft CENTRUY schedule and site input file was programmed and tested for compatibility with CENTRUY model during the fourth quarter 2014. We also validated the model for additional sites and biomass crops. The decision support tool was alpha tested first quarter 2015 with a team of students and faculty from the University of Minnesota. Many helpful and productive suggestions were obtained along with identification of software problems. After revising the decision support tool, a beta test was successfully completed second quarter 2015 with users not directly involved in development of the tool.

Products developed under the award

Publications:

Gamble, J.D., G.A. Johnson, D.A. Current, D.L. Wyse, and C.C. Sheaffer. 2015. Productivity and mineral uptake in perennial biomass alley cropping systems in Minnesota. Agron. J. ***Submitted.***

Conference Papers:

Johnson, G., J. Gamble, C. Sheaffer, D. Current, D. Zamora, and G. Wyatt. 2014. Production and economics of perennial woody and herbaceous biomass crops in alley-cropping systems. ASA meetings, Long Beach, CA

Smith, D., D. Current, J. Gamble, G. Johnson, D. Zamora. 2013. Production and economics of perennial-based woody and herbaceous biomass crops including alley-cropping systems. Presented at the 13th North American Agroforestry Conference.

Gamble, J., G. Johnson, C. Sheaffer, D. Current, and D. Wyse. 2013. Establishment and early productivity of perennial biomass alley cropping systems in Minnesota, USA. Presented at the 13th North American Agroforestry Conference.

Gamble, J.D., G. Johnson, C. Sheaffer, D., D. Wyse. 2012. Establishment of Perennial Alley Cropping Systems on Riparian Soils for Bioenergy Feedstock Production. 2012. SunGrant Initiative National Meeting. New Orleans. October 2-5, 2012.

Other Outreach Activities:

Biomass Cropping Systems for Riparian Areas. Walk-n-Talk Field Day sponsored by Rural Advantage. 7/11

Alley Cropping Systems. Walk-n-Talk Field Day sponsored by Rural Advantage. 8/12

Biomass Cropping Systems. NCCC-31 Forage Conference plot tour. 6/12

Website or other Internet sites that reflect the results of this project.

Networks or collaborations fostered.

Technologies/techniques.

Inventions/patent applications, licensing agreements.

Other products, such as data or databases, physical collections, audio or video, software* or Netware, model, educational aid or curricula, instruments, or equipment.

http://cropbudget.apec.umn.edu
https://wiki.umn.edu/CropBudget/UserGuide.

1. **Academic**

   a. Courses developed
   b. M.S. students supported
   c. M.S. degrees conferred
   d. Ph.D. students supported: 2
   e. Ph.D. degrees conferred: Student will defend dissertation December 2015
   f. Post-docs supported

2. **For projects involving computer modeling, provide the following information with the final report:**

   a. Model description, key assumptions, version, source, and intended use.

   The Crop Enterprise and Environmental Budgeting Tool (CE^2T) was designed to estimate the breakeven price needed to cover the costs of producing biomass from conventional and alternative feedstocks. These include crop residues from corn and energy crops like switchgrass, mixed grasses, shrub willow, hybrid poplar, and agroforestry systems that combine both woody and herbaceous crops. Specifically, CE^2T computes the minimum price per acre of biomass crop that would be needed to cover all the costs of producing the biomass using the methods and assumptions of Lazarus (2008) and Lazarus (2011). The tool guides users through describing their farm management practices including alternative future management scenarios. Once complete, a report is generated comparing the economics between current management practices and future scenarios.

   Data for each user account and budget are stored in a relational database management system created specifically for CE^2T. The database is housed on University of Minnesota servers and is built around the MySQL platform. The web-based user interface (http://cropbudget.apec.umn.edu) was built using php, html5 programming languages.

   The tool also provides an environmental report, comparing changes in soil carbon storage between your current management practices and future scenarios. CE^2T utilizes the CENTURY version 4.5 soil organic matter model to estimate changes in soil carbon based on management activities in each user budget. The CENTURY soil organic matter model

version 4.5 is a general process model of the plant-soil system that that simulates plant growth, C, and nutrient dynamics for cropland, grassland, forest, and savanna ecosystems. The model runs on a monthly time step and uses simplified relationships of soil-plant-climate interactions to describe the flow of C and nutrients (N, P, and S) through live plant biomass, plant litter, and organic and inorganic soil C pools. Plant biomass is determined as a function of soil temperature, available water and nutrients. Soil organic matter dynamics are estimated in the top 20 cm of soil and organic matter turnover is determined as a function of temperature, precipitation/potential evapotranspiration, and soil texture. CENTURY also simulates the effects of a wide variety of management practices and ecosystem disturbances including fire, grazing, tillage, herbicide application, and organic matter addition.

A minimum input data set for running CENTURY requires: 1) monthly average precipitation, 2) monthly average maximum and minimum air temperature, 3) soil physical attributes (texture, bulk density, water retention,) 4) plant attributes (lignin, N, S, and P content of plant material) and 5) soil and atmospheric N inputs. Initial soil carbon stocks can be derived from a simulation of several thousand years with site-specific climate and soil data, where selected model parameters are adjusted to measured or referenced soil carbon stocks.

The CENTURY model runs on a University of Minnesota server. User input from CE^2T is used to create the necessary input files to run the CENTURY model. The model then provides output parameters, which are saved to the CE^2T database and used to generate environmental reports for each user budget.

To generate the required outputs for the Environmental reports, two files need to be generated from user input: the site file (<site>.100) and the schedule file (<budget_name>.sch. The "site.100" file contains monthly precipitation and mean monthly minimum and maximum temperatures, as well as soil texture, organic matter, and soil mineral information. Precipitation and temperature data is derived from the user selected weather station (name of table), while soils information is derived from user selected input on the Site and Field forms of the web tool. The function of the schedule file is to detail the management activities for a budget so that CENTURY can accurately simulate plant growth and soil organic matter dynamics. The schedule file is constructed from user input into the web tool for historic management as well as current management from crop budgets.

b. Performance material for the model related to the intended use.

Detailed analysis of the perennial biomass crop budgets used in the CE2T tool can be found in Lazarus (2008) and Lazarus (2011).

The CENTURY model has been successfully used to predict changes in soil organic carbon in a variety of temperate sole crop agroecosystems for annual grain crops, pasture systems, and grasslands (Smith et al., 1997; Bortolon et al., 2011; Cong et al., 2014). However, information is lacking on its application in agroforestry systems (with the exception of Oelbermann and Voroney, 2011) and for perennial biomass crops. Our objective was to evaluate the ability of the CENTURY model to predict the size of biomass and soil C pools following conversion to a short-rotation willow (*Salix* spp.) – C_4 grass alley cropping system.

c. Test results to demonstrate the model performance criteria were met (e.g., code verification/validation, sensitivity analyses, history matching with lab or field data, as appropriate).

Model validation and sensitivity analysis are ongoing as part of manuscript preparation.

d. Theory behind the model, expressed in non-mathematical terms.

The CENTURY model is a general model of plant-soil nutrient cycling that has been used to simulate carbon and nutrient dynamics for different types of ecosystems including grasslands, agricultural lands, forests and savannas. CENTURY is composed of a soil organic matter/ decomposition submodel, a water budget model, a grassland/crop submodel, a forest production submodel, and management and events scheduling functions. It computes the flow of carbon, nitrogen, phosphorus, and sulfur through the model's compartments. The time step is or monthly and the model requires the following driving variables as input:

- Monthly average maximum and minimum air temperature
- Monthly precipitation
- Soil texture
- Plant nitrogen, phosphorus, and sulfur content
- Lignin content of plant material
- Atmospheric and soil nitrogen inputs
- Initial soil carbon, nitrogen (phosphorus and sulfur optional)

The input variables are available for most natural and agricultural ecosystems and can generally be estimated from existing literature. The user can choose to run the model considering only C and N dynamics; or C, N, and P; or C, N, P, and S. The soil organic matter submodel includes three soil organic matter pools (active, slow, and passive) with different potential decomposition rates, above and below ground litter pools and a surface microbial pool which is associated with decomposing surface litter. The simplified water budget model calculates monthly evaporation, transpiration, the water content of the soil layers (0 – 90 cm, 15 cm layers), snow water content, and saturated flow of water between soil layers. As mentioned above, CENTURY contains two plant production submodels; a grassland/crop submodel and a forest production submodel. Both plant production models assume that the monthly maximum plant production is controlled by moisture and temperature, and that maximum plant production rates are decreased if there are insufficient nutrient supplies. The grassland/crop production model simulates plant production for different herbaceous crops and plant communities (e.g. warm or cool season grasslands, wheat, and corn). The forest model simulates the growth of deciduous or evergreen forests in juvenile and mature phases. To simulate a savanna or shrubland, CENTURY uses both of these submodels with some additional code to simulate nutrient competition and shading effects. Disturbances such as fire, harvest, grazing and cultivation can be simulated via the management and events scheduling functions.

Management interventions that can be simulated include:

- Fertilizer additions
- Irrigation
- Grazing
- Fire
- Cultivation

e. Mathematics to be used, including formulas and calculation methods.

All calculations used for generating enterprise budget are described by Lazarus (2008) and Lazarus (2011). Calculations used in the CENTURY 4.5 soil organic matter model are outlined in the CENTURY documentation and also by Parton et al., (1988).

f. Whether or not the theory and mathematical algorithms were peer reviewed, and, if so, will include a summary of the theoretical strengths and weaknesses.

NA

g. Hardware requirements.

The CE^{2}T tool can be used on any computer running a modern web browser (Chrome, Firefox, Safari)

h. Documentation (e.g., user's guide, model code).

The CE^{2}T user's guide can be found online at https://wiki.umn.edu/CropBudget/UserGuide. Development of this user's guide is on-going

Please complete the following table to reflect your project outputs at completion or at time of report submission. Identify outputs and products developed under the award and any technology transfer activities.

ITEM	NUMBER	DETAILS (e.g. citations, names, descriptions, varieties, etc.)
Abstracts: include full citation and attach a pdf copy.	4	Johnson, G., J. Gamble, C. Sheaffer, D. Current, D. Zamora, and G. Wyatt. 2014. Production and economics of perennial woody and herbaceous biomass crops in alley-cropping systems. ASA meetings, Long Beach, CA Smith, D., D. Current, J. Gamble, G. Johnson, D. Zamora. 2013. Production and economics of perennial-based woody and herbaceous biomass crops including alley-cropping systems. Presented at the 13th North American Agroforestry Conference. Gamble, J., G. Johnson, C. Sheaffer, D. Current, and D. Wyse. 2013. Establishment and early productivity of perennial biomass alley cropping systems in Minnesota, USA. Presented at the 13th North American Agroforestry Conference. Gamble, J.D., G. Johnson, C. Sheaffer, D., D. Wyse. 2012. Establishment of Perennial Alley Cropping Systems on Riparian Soils for Bioenergy Feedstock Production. 2012. SunGrant Initiative National Meeting. New Orleans. October 2-5, 2012.

Peer Reviewed Publications: include full citation and attach a pdf copy if available	1	Gamble, J.D., G.A. Johnson, D.A. Current, D.L. Wyse, and C.C. Sheaffer. 2015. Productivity and mineral uptake in perennial biomass alley cropping systems in Minnesota. Agron. J. *Submitted.*
Outreach Publications including web pages: include full citation	1	http://cropbudget.apec.umn.edu
Professional Presentations: include full citation		
MS Degrees Conferred: include names plus month/year confirmed		
Ph.D. Degrees Conferred: include names plus month/year confirmed		
MS Students Supported: include names		
Ph.D. Students Supported: include names	2	Joshua Gamble David Smith
Post-Docs Supported: include names		
Undergraduate Students Supported: include names	2	Airton Serra Leslie Gerberding Adrian Nofzinger (non UMN - UW Eau Claire) Luciane Becchi Anthony Schumacher Daniel Basso Giovana Zucchi Nubia Andrade Kevin Muehlbauer
Investigators Supported: include names	2	Dean Current William Lazarus
Jobs Created		
Invention Disclosures		
Non-provisional Patent Application(s) Filed		
Provisional Patents Filed		
Patents Filed		

Patents Issued: include full citation		
License Agreements: include description		
Plant Variety Protection: include description		
Subsequent Funding: List proposals funded as a result of this work		
Other: Products, such as data or databases, physical collections, audios or videos, software or Netware, models, educational aids or curricula, instruments, or equipment.	1	The Crop Enterprise and Environmental Budgeting Tool (CE^2T) http://cropbudget.apec.umn.edu

Back to Table of Contents

Sun Grant Initiative
DOE Final Progress Report

Project Title: Intensifying the Corn-Soybean Rotation with the Use of Winter Rye Grown for Biomass Energy Production

Project Director/Principal Investigator: Peter Sexton, Plant Science Department, South Dakota State University, Brookings, SD

All Co-Principal/Other Investigators: David Karki, Lon Hall, and Robert Berg, Plant Science Department, Brookings, SD; Michael Miller, Economics Department, South Dakota State University, Brookings, SD

Collaborators: None

Period of Performance: 1 December 2011 - 30 September 2015

Funding Awarded: $248,697

Cost Share Amount: $65,225

Cost Share Sources: Time and effort from PIs and CoPIs; Indirect on time and effort

Executive Summary

A series of agronomic field trials were conducted to evaluate the potential of winter rye as a possible biomass energy crop between corn and soybean grain crops. The goal being to establish a winter rye biomass crop after corn and harvest it the following spring, and then plant soybeans for harvest that fall (three crops in two years). There are several advantages to this approach: it does not displace a grain crop; it adds diversity to the cropping system including a cool-season grass into the corn-soybean rotation; it has environmental benefits of helping to keep the soil covered and rye helps capture nitrate-N so it is less likely to leach into groundwater or streams; it intensifies the production system to allow for biomass harvesting without losing the benefits of returning corn and soybean residue to the soil. Winter rye is very winter hardy, so it will tolerate late planting in the fall better than any other small grain crop. Also it puts on rapid growth early in the spring taking advantage of a time period when the ground is often bare. It is not difficult to establish and is competitive with weeds. Questions which are raised with this system include how to best get the rye established in the fall and impacts of rye production on yield of the following soybean crop.

Project Objectives:

1.) Evaluate the potential biomass production of winter rye when established after corn under varying times of corn maturity. The rye would be harvested for biomass after anthesis (late May / early June) ahead of soybean planting.
2.) Evaluate the effects of this practice on corn and soybean yields.
3.) Estimate the breakeven price matrix for this practice based on biomass production as well as corn and soybean yields and prices.
4.) Compare available winter rye germplasm (including a new variety from SDSU) for potential as biomass crops in this system.

Objective number one was addressed by conducting trials at SDSU research stations looking at establishing rye by aerial seeding at early dent stage, and by direct seeding after harvest, for corn lines ranging in maturity from 75 to 105 days in southeastern South Dakota, and from 75 to 96 days relative maturity in northeastern South Dakota. The idea here was to see if getting the rye in earlier would provide enough of an increase in biomass production to warrant going with an earlier corn line.

Objective number two was met by measuring corn and soybean yields for each treatment in the above experiments, along with a control (no-rye) treatment. We also included a site in Illinois to add another environment to look at impacts of rye production on soybean yields (the Illinois site included trials on rye N response but not different corn maturities to avoid going beyond the resources of our cooperator there).

Objective number three was addressed by working with grower-cooperators to estimate costs and necessary returns to make the system realistically acceptable to farmers. We hoped to use the CROPGRO model to predict yield effects across a range of environments; however, the predicted yield levels from the corn model were not realistic. Data analysis is limited to calculations from observed field values.

Objective four was addressed with rye variety trials conducted in South Dakota and Illinois. The number of lines included was few as there are no active winter rye breeding programs in the country and seed of new experimental lines were only available in very limited quantities.

Results

SDSU Southeast Research Farm. An initial trial was established in the fall of 2011 planting rye after corn raised for silage. The following spring the control plots were seeded to soybeans on May 20. The rye was cut after heading (Fig. 1), hayed off the field, and seeded to soybeans June 6, 2012. The 2012 season at the Southeast Farm was the driest growing season on record for the farm. Soybeans seeded into the control plots had enough moisture for stand establishment and root growth followed moisture down into the soil – these plots yielded about 20 bushels per acre, or 40 % of expected yield. In the rye biomass plots, soil moisture had been depleted by the rye and the soybeans were not able to establish resulting in a virtual crop failure producing less than 5 bu/ac (Table 1).

In the spring of 2012, replicated plots with corn lines ranging in maturity from 75 to 105 days maturity were established at the Southeast Farm. Similar treatments along these lines were repeated in the 2013 and 2014 seasons (Fig. 2 and 3). In all three seasons at Beresford, including the severe drought year of 2012, corn yields dropped sharply as maturity declined below 95 days relative maturity but appeared to be relatively similar at maturities greater than 95 days. This suggests that farmers could go with a slightly earlier line (typical corn maturity for this area is 105 days relative maturity) and not face a significant yield penalty. Rye was broadcast seeded into plots of each of these corn lines at late dough/early dent stage, and also direct seeded after corn harvest in the 2012 and 2013 seasons. Rye biomass was measured the following spring (2013 and 2014, respectively), rye plots were hayed, and soybeans direct seeded into the rye plots and yields compared to no-rye control plots (Table 2).

Fig. 1. Technician Jesse Hall in a plot of rye raised for biomass in 2012. These plots were sampled for dry matter, and then hayed off and seeded to soybeans – which failed to establish due to severe drought conditions.

Table 1. Rye biomass and yield of the following soybean crop in the 2012 season at Beresford, SD. The previous crop in this field was corn raised for silage. Plots were laid out in a randomized complete block design with four replications. There was a severe drought in this season and the soybeans planted into rye stubble did not have enough moisture to establish a good stand, resulting in crop failure.

Treatment	Rye Wt.	Soybean Yield
	(lb/ac)	(bu/ac)
Rye-biomass crop	2770	4.9
No-rye control	----	20.1
Mean		*12.5*
P value		*p<0.05*
CV (%)		*45.2*

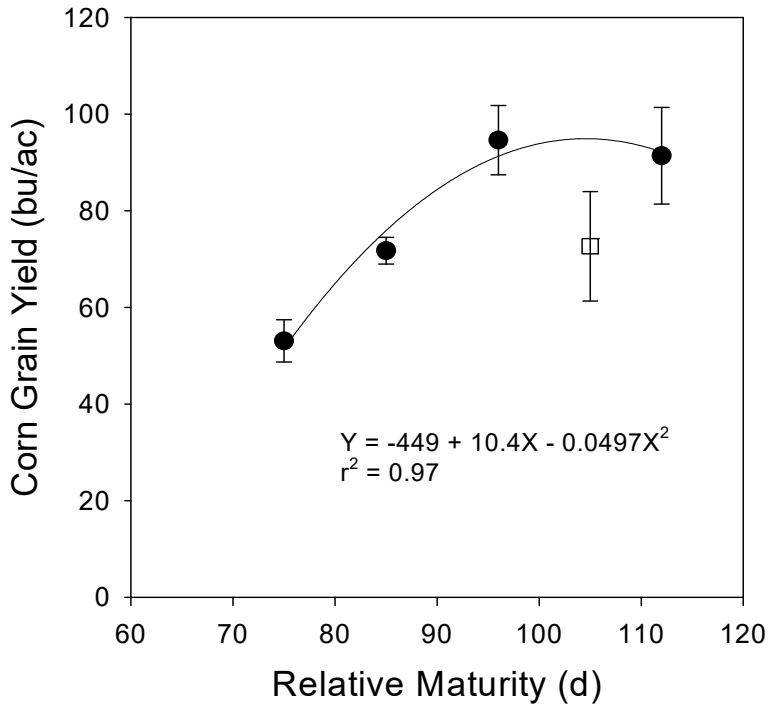

Fig. 2. Yield of corn lines varying maturity at the SDSU Southeast Farm in 2012, which was the driest growing season on record at the farm.

Back to Table of Contents

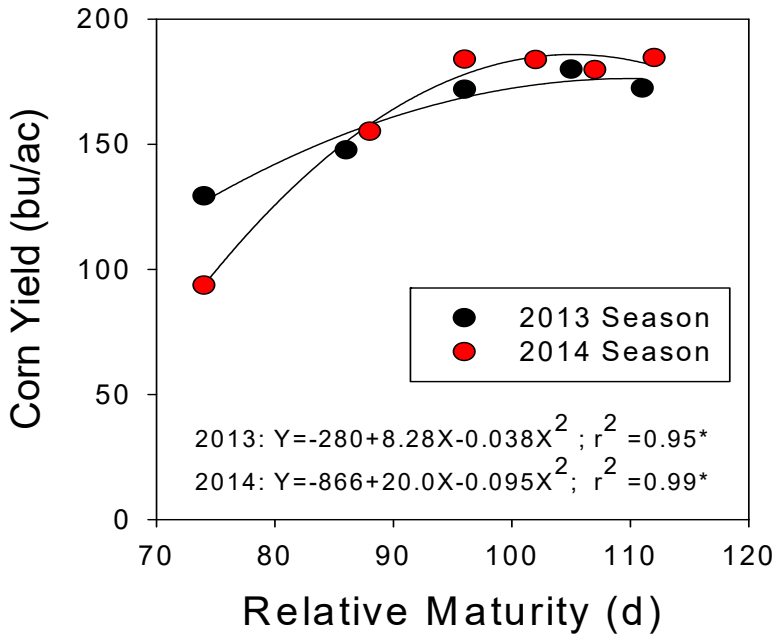

Fig. 3. Yield of corn lines varying maturity at the SDSU Southeast Farm in the 2013 and 2014 growing seasons. Note that yield dropped sharply with maturity less than 95 days.

Reviewing the data in Table 2, there are several points of interest. First is that rye biomass did not benefit from earlier planting with earlier corn lines until we get to the 75 day relative maturity – which would involve a substantial yield penalty for the corn crop (Fig. 2 and 3). Rye biomass was similar planted after corn in the range 85 to 105 days relative maturity, indicating that going from a 105 day line to a 95 day line did not benefit rye biomass production in this environment. (Note there was no significant year by treatment interaction for effects of corn maturity on subsequent rye biomass production and soybean yield; therefore this data was pooled across seasons.) One could speculate that in an irrigated environment, there would be a greater likelihood of benefiting from earlier planting since rye establishment would not be dependent on rainfall at that time of year. In a relatively dry environment, timing of crop establishment is as much dependent on rainfall as much as on planting date. In any case, this data does not support use of an earlier maturing corn line in order to move up the rye planting date in our environment. Rye biomass in drilled plots tended to be about 10 to 15 percent greater than that observed with broadcast seeding.

Looking at soybean yields following rye at Beresford (Table 2), the two seasons tested showed very different results. In 2013, there was no soybean yield penalty from raising a rye biomass crop – treatment effects were not significant and yields average about 46 bu/ac. In 2014, on the other hand, there was a very sharp soybean yield penalty associated with production of a rye biomass crop with soybean yields being less than 10 bu/ac following rye that year. June of 2014 was the wettest month on record at the SDSU Southeast Research Farm. The rye was put down for hay, but didn't get much chance to dry down. Also the field the trial was located in is a relatively lowland area. By the time things dried out enough to get the rye hayed off the field and support traffic, soybean planting was delayed to early July. This resulted in poor soybean yields. If the field had been cut for silage or green-chopped, this could have been avoided – however, putting the field up for dry biomass (hay) involves increased risk of rainfall delaying establishment of the following soybean crop.

Considering the three seasons of data from the Southeast Farm at Beresford, soybean yields following rye suffered severely under both extreme dry (2012 growing season) and wet conditions (June 2014). Under moderate conditions (2013), we were able to gather a rye biomass crop without negatively impacting soybean production.

SDSU Northeast Research Farm. A field experiment that paralleled the ones described above at Beresford, was also run at the SDSU Northeast Research Farm, near Watertown, South Dakota. Corn lines of 75, 85, and 95 days relative maturity were established in the spring of 2012 and rye was seeded by broadcasting seed at late dough/early dent stage and by direct seeding after harvest for each treatment in replicated plots. Rye was harvested in the spring and the plots seeded to soybeans.

Back to Table of Contents

Table 2. Rye biomass and yield of the following soybean crop for rye established after corn lines of varying maturity at the SDSU Southeast Research Farm in Beresford, SD in 2013 and 2014.

Corn Maturity	Rye Seeding	2013 Rye Biomass	2014 Rye Biomass	2013 Soybean Yield	2014 Soybean Yield
		(lb/ac)	(lb/ac)	(bu/ac)	(bu/ac)
75	Control	0	0	45.9	43.2
75	Broadcast	3823	2537	45.8	2.4
75	Drill	4100	3781	45.7	3.9
86	Control	0	0	46.0	58.4
86	Broadcast	3017	1758	46.1	5.4
86	Drill	2850	2423	45.3	9.1
96	Control	0	0	46.3	41.2
96	Broadcast	3141	1719	44.6	3.4
96	Drill	3091	2212	44.9	3.5
105	Control	0	0	46.6	43.6
105	Broadcast	2892	1954	47.1	3.8
105	Drill	3267	2576	46.3	4.3
	Mean	*2181.7*	*1580.0*	*45.9*	*18.5*
	CV (%)	*32*	*39*	*3.0*	*36.0*
	LSD (0.05)	*1139*	*1008*	*NS*	*12.5*

Across Years

Corn Maturity	Rye Biomass[a/]	Soybean Yield
(days)	(lb/ac)	(bu/ac)
75	3524	31.1
86	2530	35.1
96	2540	30.6
105	2720	31.9
Mean	*2829*	*32.2*
CV (%)	*25.3*	*11.5*
LSD (0.05)	*774*	*NS*

Rye Seeding	Rye Biomass[a/]	2013 Soybean Yield	2014 Soybean Yield
	(lb/ac)	(bu/ac)	(bu/ac)
Control	----	46.2	45.5
Drill	3003	45.9	3.6
Broadcast	2643	45.6	5.2
Mean	*2829*	*45.9*	*19.9*
CV (%)	*25.3*	*3.0*	*36.0*
P-value	*<0.10*	*NS*	*12.5*

a/ does not include values from the control (no rye) treatment in the analysis

The rye biomass crop did not have a significant impact on soybean yields in the trial at the SDSU Northeast Research Farm in 2013 (Table 3). There was a trend for slightly lower yield (ca. 4 bu/ac) in soybeans following rye relative to the control plots. Looking at the effect of corn maturity, the earlier maturing lines showed less yield (Fig. 4), indicating that going with an earlier corn line would directly involve yield loss in corn at this location. Rye biomass was not significantly impacted by corn maturity, again indicating that in this environment going with an earlier maturity corn line will cost corn yield and may not benefit rye biomass production. Rye biomass with broadcast seeding was 36 % less than that obtained with direct-seeding with a no-till drill (Table 3).

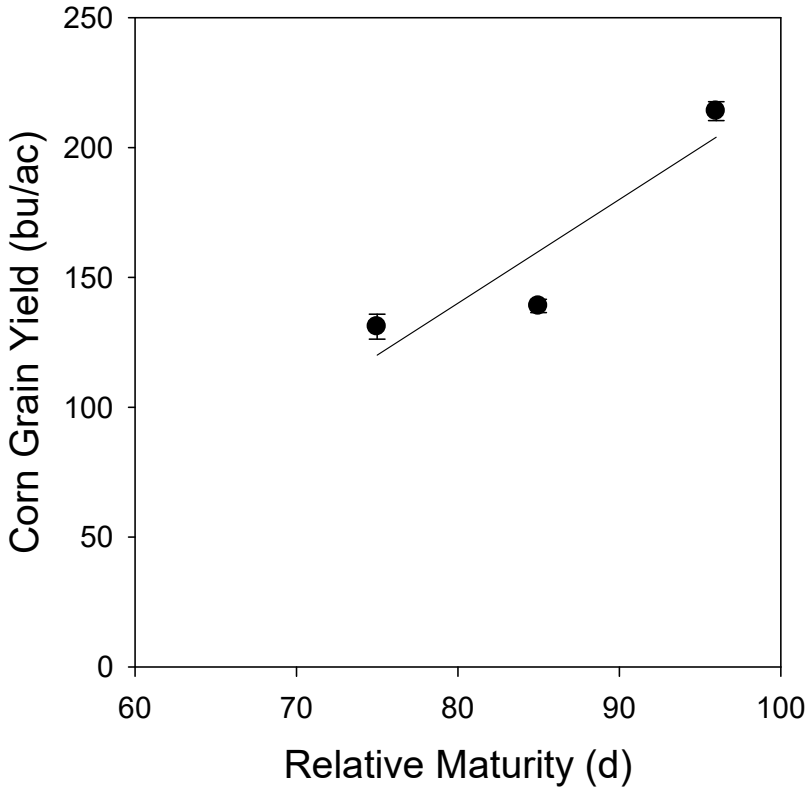

Fig. 4. Yield of corn lines varying maturity at the SDSU Northeast Research Farm in the 2013 growing season. These plots were followed with winter rye broadcast seeded at late dough/early dent stage, and direct seeded after corn harvest.

Table 3. Rye biomass and yield of the following soybean crop for rye established after corn lines of varying maturity at the SDSU Northeast Research Farm near Watertown, SD in 2013.

Corn Maturity	Rye Seeding	Rye Biomass	Soybean Yield
		(lb/ac)	(bu/ac)
75	Control	0	49.3
75	Broadcast	937	39.5
75	Drill	1279	44.1
85	Control	0	49.9
85	Broadcast	689	45.9
85	Drill	1354	45.9
96	Control	0	47.8
96	Broadcast	813	42.4
96	Drill	1188	45.3
	Mean	*696*	*45.8*
	CV (%)	*33.3*	*7.6*
	LSD (0.05)	*401*	*NS*

Corn Maturity	Rye Biomass [a/]	Soybean Yield
	(lb/ac)	(bu/ac)
75	1108	44.9
85	1022	47.3
96	1001	45.2
Mean	*1043*	*45.8*
CV (%)	*26.4*	*7.6*
LSD (0.05)	*NS*	*NS*

Rye Seeding	Rye Biomass[a/]	Soybean Yield
	(lb/ac)	(bu/ac)
Control	-----	49.0
Broadcast	813	43.0
Drill	1274	45.1
Mean	*1043*	*45.8*
CV (%)	*26.4*	*7.6*
LSD (0.05)	*P<0.01*	*2.6*

a/ does not include values from the control (no rye) treatment in the analysis.

Southern Illinois. A series of trials were conducted at Creal Springs, Illinois, in the 2012 through 2014 seasons (actually starting with rye seeding in the fall of 2011). These trials looked at rye biomass response to varying levels of applied N and also at varietal differences. Because of limited seed availability, the first two seasons only had two lines (Rymin and Dacold). In the third season the experimental line '79-8' and a line from Canada, 'Hazlet', were added to the study along with 'Fridge' triticale. In 2012, rye biomass was greater for 'Dacold' than for 'Rymin', and biomass was greater with increased levels of applied N (Table 4). Soybean yields were similar in the control and 'Dacold' plots, but tended to be greater following 'Rymin' than in the other treatments. Overall, it appeared that soybeans did better following rye than in the control plots, but there was a trend for soybean yield to decline as rye biomass production increased (Fig. 5).

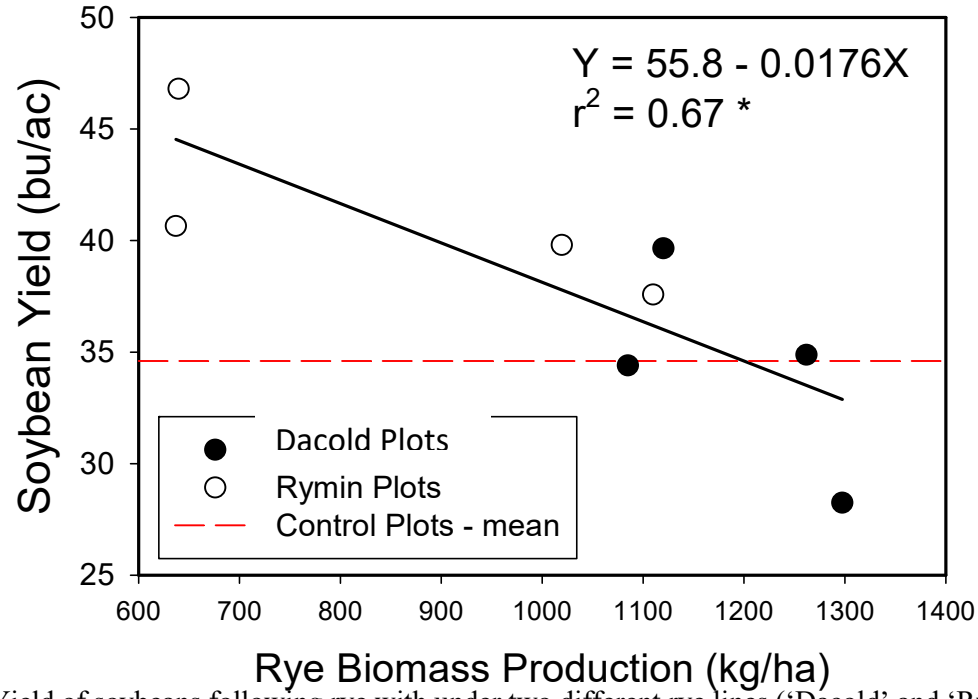

Fig. 5. Yield of soybeans following rye with under two different rye lines ('Dacold' and 'Rymin') and four different levels of applied N. This trial was conducted in Creal Springs, IL in 2012.

In 2013, soybeans seemed to benefit from the rye biomass crop (Table 5); however, the level of rye biomass production was low at Creal Springs. There was no N response observed for rye biomass, and there was no relationship or trend observed between amount of rye biomass produced and soybean yield in this season.

Back to Table of Contents

Table 4. Rye biomass and yield of the following soybean crop for the 2012 season under varying levels of applied N for 'Dacold' and 'Rymin' rye raised in Creal Springs, IL.

Line	N-Rate	Biomass	Soybean Yield
	(lb/ac)	(kg/ha)	(bu/ac)
Rymin	30	640	46.8
Rymin	0	637	40.7
Rymin	60	1020	39.8
Dacold	0	1120	39.7
Rymin	90	1110	37.6
Dacold	60	1262	34.9
control	0	0	34.6
Dacold	30	1085	34.4
Dacold	90	1298	28.3
Mean		*908*	*37.4*
LSD (0.05)		*199*	*8.2*
CV (%)		*15*	*15*

Line	Soybean Yield	Rye Biomass
	(bu/ac)	(lb/ac)
Rymin	41.2	852
Dacold	34.3	1191
control	34.6	0
Mean	*36.7*	*681*
CV (%)	*9.0*	*10.1*
LSD (0.05)	*6*	*119.0*

N Rate	Soybean Yield	Rye Biomass
	(bu/ac)	(lb/ac)
90	32.9	1204
60	37.3	1141
0	40.2	879
30	40.6	862
Mean	*37.8*	*1021*
CV (%)	*15.6*	*13.8*
LSD (0.05)	*NS*	*145*

Table 5. Rye biomass and yield of the following soybean crop for the 2013 season under varying levels of applied N for 'Dacold' and 'Rymin' rye raised in Creal Springs, IL.

LINE	N Rate	Soybean Yield	Rye Biomass
		(bu/ac)	(lb/ac)
VNS (Dacold)	30	56.2	602
Rymin	30	55.4	611
VNS (Dacold)	60	55.0	584
Rymin	60	54.5	714
VNS (Dacold)	90	52.5	691
Rymin	90	51.6	651
Rymin	0	45.4	607
VNS (Dacold)	0	45.4	464
Control	0	43.3	0
Mean		*51.0*	*547*
CV (%)		*6.0*	*19.1*
LSD (0.05)		*4.5*	*152.5*

Line	**Soybean Yield**	**Rye Biomass**
	(bu/ac)	(lb/ac)
Rymin	51.7	646
VNS (Dacold)	52.3	586
Control	43.3	0
Mean	*49.1*	*410*
CV (%)	*19.1*	*14.8*
LSD (0.05)	*4.5*	*105*

N Rate	**Soybean Yield**	**Rye Biomass**
	(bu/ac)	(lb/ac)
30	55.8	607
60	54.7	649
90	52.0	671
0	45.4	535
Mean	*52*	*616*
CV (%)	*3.1*	*12.7*
LSD (0.05)	*2.5*	*NS*

In 2014, there was a significant interaction between level of applied N and genotype evaluated, so lines were compared at each N level. The new line '79-8' performed well at all levels of applied N and showed a biomass response to applied N all the way up to 90 lb N per acre (Table 6). This line averaged over two tons per acre of biomass produced. Rye biomass production did not significantly impact soybean yields in this season at Creal Springs (Table 7); however similar to the 2012 data at this site, there was a trend for decreased soybean yield at higher levels of rye production (Fig. 6).

Table 6. Rye biomass and yield of the following soybean crop for the 2014 season under varying levels of applied N for '79-8', 'Hazlet', VNS ('Dacold'), and 'Fridge' Triticale raised in Creal Springs, IL. There was significant N by genotype interaction in this experiment, so data was analyzed within each level of applied N.

N Rate	Line	Biomass	N Rate	Line	Biomass
(lb/ac)		(lb/ac)	(lb/ac)		(lb/ac)
0	79-8	2767	30	79-8	4247
0	VNS (Dacold)	2537	30	Triticale	3459
0	Rymin	2363	30	VNS (Dacold)	2874
0	Triticale	2109	30	Rymin	2554
0	Hazlet	1260	30	Hazlet	1533
	Mean	*2210*		*Mean*	*2933*
	CV (%)	*32.3*		*CV (%)*	*24.7*
	LSD (0.05)	*NS*		*LSD (0.05)*	*1115*

N Rate	Line	Biomass	N Rate	Line	Biomass
(lb/ac)		(lb/ac)	(lb/ac)		(lb/ac)
60	79-8	4429	90	79-8	5918
60	Triticale	4292	90	Triticale	5828
60	VNS (Dacold)	3381	90	Rymin	3600
60	Rymin	2655	90	VNS (Dacold)	3572
60	Hazlet	1868	90	Hazlet	2063
	Mean	*3325*		*Mean*	*4196*
	CV (%)	*26.6*		*CV (%)*	*19.4*
	LSD (0.05)	*1364*		*LSD (0.05)*	*1252*

Table 7. Soybean yield following different biomass crop genotypes for the 2014 season averaged across levels of applied N for '79-8', 'Hazlet', VNS ('Dacold'), and 'Fridge' Triticale raised in Creal Springs, IL.

Line	Soybean Yield
	(bu/ac)
79-8	23.0
Triticale	27.7
VNS (Dacold)	27.5
Rymin	29.9
Hazlet	34.4
Control	30.7
Mean	*28.9*
CV (%)	*23.4*
LSD (0.05)	*NS*

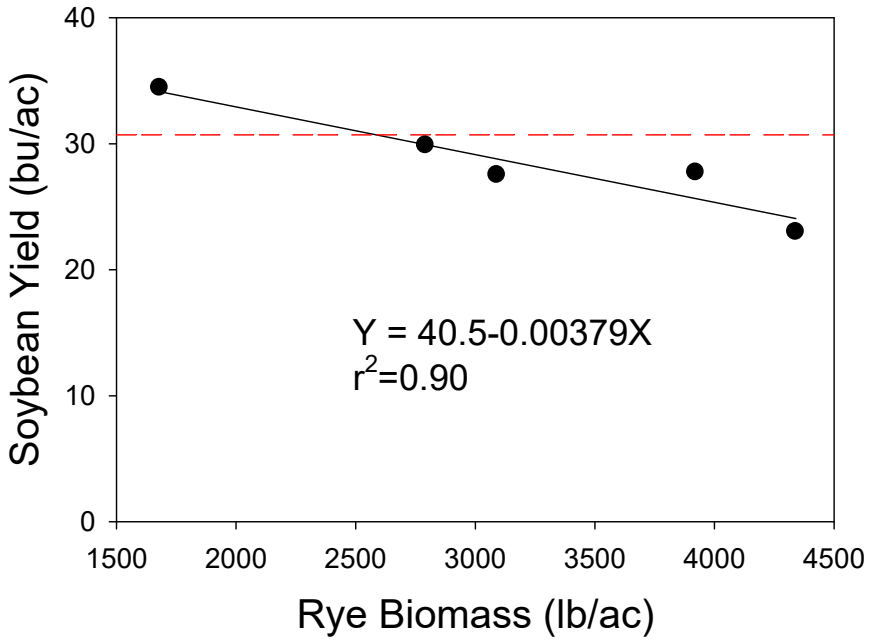

Fig. 6. Plot of average soybean yield versus level of biomass for '79-8', 'Hazlet', VNS ('Dacold'), and 'Rymin' rye, along with 'Fridge' Triticale, raised as previous crops in Creal Springs, IL, in the 2014 season. Each point represents the average biomass value across N levels for that genotype.

South Dakota Variety Trials. Replicated variety evaluations were conducted at Winsor, SD in 2012 (Table 8) and at the SDSU Southeast Research Farm in 2014 (Table 9). While differences were not statistically significant, the new line 79-8 appeared to do well in both trials, producing well over 2.5 tons per acre in both experiments.

Table 8. Biomass from a rye variety trial conducted at Winsor, SD in 2012.

Line	Biomass
79-8	5850
Dacold	5522
Rymin	5247
Mean	*5566*
LSD (0.05)	*NS*
CV (%)	*9.1*

Table 9. Biomass values for several rye and triticale lines evaluated in a variety trial at the SDSU Southeast Research Farm in 2014.

Line	Crop	Biomass
		(lbs/ac)
Dacold	Rye	6827
White rye	Rye	6771
79-8	Rye	6664
Fridge	Triticale	6443
9601	Rye	6060
X83-3HW14	Rye	5853
9606	Rye	5802
Hazlet	Rye	5654
NE42G2T	Triticale	5184
NT01451	Triticale	4753
X83-3PP	Rye	4665
Mean		*5880*
C.V.		*15*
LSD (0.05)		*NS*

Review of agronomic trials. The main points to be drawn from the agronomic data are:

1) Planting an early-season corn line in order to advance the rye planting date cannot be recommended both because of loss in corn yield potential, and the fact that fall soil moisture is inconsistent (i.e. without moisture early planting is of no benefit). Therefore, looking at corn yields, one probably does not want to make anything more than a marginal shift toward earlier corn lines when planning to put in a rye biomass crop.

2) Broadcast seeding rye tended to produce 10 to 35 % less biomass than did direct seeding.

3) Effects of producing a rye biomass crop on yield of the following soybean crop were highly variable depending in large part on soil moisture – both drought, and excessive rainfall in June, resulted in dramatically decreased soybean yields following a rye biomass crop. If these extremes can be avoided, it appears that the rye biomass crop will have minimal effects on the following soybean crop. There was a trend for marginally decreased soybean yield as biomass production increased in two experiments. Planting a rye biomass crop should be avoided in fields or environments where having adequate spring moisture for crop establishment is a concern. The ability to green chop or make silage out of the rye would decrease risk in wetter environments as it would allow for immediate planting of the field to soybeans following rye harvest. To be conservative, the principal investigator would recommend assuming a 3 bushel per acre soybean yield loss with use of a rye biomass crop assuming extreme conditions can be avoided.

4) The new rye line, '79-8' consistently performed well and generally produced over 2 tons per acre of dry matter. This genotype performed the best of the materials tested across a range of N environments in the Illinois trial in 2014. For purposes of economic evaluation, with this line a yield of 1.5 tons per acre would be conservative, and it would be consistent with biomass levels observed in repeated studies with winter rye at the Southeast Research Farm in Beresford.

Costs of Production. On-farm plots with winter rye were run with grower cooperators in Arlington and Beresford to obtain estimates of costs of production. Based on discussions with growers and a review of expenses, we estimate the cost of production to be about $93 per ton. This is a break-even cost assuming land charges will be covered by the soybean crop (and making provision for an average 3 bu/ac yield loss in the soybean crop). If biomass yield were 2 tons per acre, then the cost per ton would be closer to $70 per ton. Based on discussions with growers, the amount of net return per acre needed to get them to change their practices and accept the risks involved, would be between $85 and $125 per acre. Taking a median value, this would mean a net return of $105 per acre should be factored into the cost in order to get some farmers and to buy-in and contract for production. This would raise the projected cost per ton for a processor to $163 per ton. - and even at this point my collaborators told me many farmers would not undertake the changes and risks involved – some people would like to see something closer to $193 per ton as a price so their net return would be close to $150 per acre.

Table 10. Projected costs per acre for production of a rye biomass crop assuming no change in soybean costs of production and a 3 bushel per acre soybean yield loss associated with rye production.

Item	cost per acre
Seed	$25.00
Planting	$15.30
Windrow	$12.50
Baling	$31.25
Moving Bales	$3.30
P&K Replacement	$22.00
Soy yield loss (3 bu/ac)	$29.40
Cost per Acre	$138.75
Yield (tons/ac)	1.50
Cost per ton	$92.50

Projected ethanol yields.

Collected rye samples were weighed and dried for 48 hours at 140F to estimate total biomass per acre. These samples were ground and composited across replications before sending samples to South Dakota Ag. Lab in Brookings, SD for analyses. The values from analyses were used to estimate the theoretical ethanol production using the following approach to estimate ethanol conversion (Borglum, 1980; Personal Communication- William Gibbons, Professor, South Dakota State University; www1.eere.energy.gov):

Hemicellulose (%) = NDF - ADF

Cellulose (%) = ADF - Lignin

Total glucose (%) = (Hemicellulose + Cellulose) x 1.11

Theoretically, 100 g of glucose yields 51 g of ethanol, therefore total glucose values obtained for each rye sample was multiplied by 0.51 conversion factor to estimate the potential ethanol production. For example, 2013 rye sample from Beresford that produced 2985 lbs dry matter per acre (1.5 t) with hemicellulose of 28.1% and cellulose of 31.1% produced 1961 lbs glucose [(28.1+31.1%) x 1.11=65.7% of 2985], thus the estimated ethanol yield would be 152 gal ethanol per acre or 102 gal per ton.

Tables 11 and 12 show estimated ethanol production from rye samples from the plots at the SDSU Southeast Research Farm in Beresford.

In addition to Beresford, SD, biomass samples were collected in 2012 spring for ethanol estimation from similar trials conducted in Winsor, SD and Carbondale, IL. In Winsor among the three rye varieties tested, the ethanol production ranged from 328 gal/ac (79-8, an experimental line from South Dakota) to 290 gal/ac (Dacold). Variety Rymin produced 293 gal/ac in Winsor. In Carbondale, varieties Dacold and Rymin were tested for biomass production under six different nitrogen treatments. When averaged across treatments, Dacold and Rymin produced 66 gal/ac and 49 gal/ac ethanol respectively. Low ethanol yield per acre was due to adverse growing conditions at the time of biomass collection. Assuming a cost of $163 per ton for raw material (i.e. rye biomass hay), and an average conversion value of 90 gal/ton, that would give a raw material cost of $1.81 per gal of ethanol. The range of estimated ethanol conversion values was from 79 to 115 gal/ton, giving a range in estimated raw material costs of $2.06 to $1.42 per gallon assuming a raw material cost of $163 per ton at the farm gate.

Table 11. Total dry biomass and ethanol yield from rye biomass samples collected in spring 2013 in Beresford, SD. The rye seeds in each plot were broadcast or drilled following harvest of various maturity group corn in fall 2012.

Maturity (Day)	Method	Biomass (lb/a)	Ethanol (gal/a)	Ethanol (gal/ton)
75	Broadcast	2892	115	79
75	Drilled	3267	130	79
85	Broadcast	3823	156	82
85	Drilled	4100	168	82
96	Broadcast	3017	120	80
96	Drilled	2850	116	81
105	Broadcast	3141	127	81
105	Drilled	3091	126	81

Table 12. Total dry biomass and ethanol yield from rye biomass samples collected in spring 2014 in Beresford, SD. The rye seeds in each plot were broadcast or drilled following harvest of various maturity group corn in fall 2013.

Maturity (Day)	Method	Biomass (lb/a)	Ethanol (gal/a)	Ethanol (gal/ton)
75	Broadcast	2985	152	102
75	Drilled	4448	240	108
85	Broadcast	2068	104	100
85	Drilled	2851	157	110
96	Broadcast	2022	108	106
96	Drilled	2602	131	101
105	Broadcast	2299	111	96
105	Drilled	3030	155	103

Please complete the following table to reflect your project outputs at completion or at time of report submission. Identify outputs and products developed under the award and any technology transfer activities.

ITEM	NUMBER	DETAILS (e.g. citations, names, descriptions, varieties, etc.)
Abstracts: include full citation and attach a pdf copy.		
Peer Reviewed Publications: include full citation and attach a pdf copy if available	1	In progress
Outreach Publications including web pages: include full citation	3	Karki, D., and L. Hall. 2014. Winter Rye, triticale variety trial. South Dakota State University Agricultural Experiment Station. Southeast Research Farm Annual Progress Report 2013. Pp. 78-80. Karki, D., P. Sexton, J. Hall, and A. Miron. 2013. Observations with a winter rye cover / forage crop grown after corn and ahead of soybeans. South Dakota State University Agricultural Experiment Station. Southeast Research Farm Annual Progress Report 2013. Pp. 41-45. Sexton, P., and L. Hall. 2012. Observations on corn maturity and yield in the 2012 season. South Dakota State University Agricultural Experiment Station. Southeast Research Farm Annual Progress Report 2012. Pp. 14-16. Sexton, P., L. Hall, and A. Miron. 2012. Observations with a winter rye cover / forage crop grown after corn and ahead of soybeans. South Dakota State University Agricultural Experiment Station. Southeast Research Farm Annual Progress Report 2012. Pp. 17-19.
Professional Presentations: include full citation		
MS Degrees Conferred: include names plus month/year confirmed		
Ph.D. Degrees Conferred: include names plus month/year confirmed		
MS Students Supported: include names		
Ph.D. Students Supported: include names		
Post-Docs Supported: include names	1	David Karki (currently working as an extension agronomist)
Undergraduate Students Supported: include names	1	Shaina Sabel
Investigators Supported: include names		
Jobs Created		
Invention Disclosures		Provide no confidential or enabling information. Just indicate in an invention disclosure has been filed with the employer.
Non-provisional Patent Application(s) Filed		
Provisional Patents Filed		

Patents Filed		
Patents Issued: include full citation		
License Agreements: include description		
Plant Variety Protection: include description	1	Development in progress
Subsequent Funding: List proposals funded as a result of this work		
Other: Products, such as data or databases, physical collections, audios or videos, software or Netware, models, educational aids or curricula, instruments, or equipment.	4	Extension presentations made to farm groups

Back to Table of Contents

Sun Grant Initiative
DOE Final Progress Report

Project Title: Beneficial Plant Microbe Interactions and Their Potential Application to Increase Biomass Production and Environmental Sustainability of Prairie Cordgrass

Project Director/Principal Investigator: Dr. Heike Bücking, Professor, Biology and Microbiology Department, South Dakota State University, Brookings, SD)

All Co-Principal/Other Investigators: Dr. Jose Gonzalez, Associate Professor, Plant Science Department, South Dakota State University, Brookings, SD)

Collaborators: No other collaborators

Period of Performance: 1 June 2011 - 31 July 2015

Funding Awarded: $143,763

Cost Share Amount: $35,941

Cost Share Sources: Time and effort from PIs and CoPIs; Indirect on time and effort

Executive Summary

According to the U.S. Department of Energy [1]) an 'ideal' biomass crop should have the following attributes: (1) C_4 photosynthesis with high efficiency; (2) long canopy duration; (3) recycling of nutrients from above ground shoots to roots and rhizomes to reduce required fertilizer inputs; (4) high water acquisition and use efficiency; (5) non-invasive; and (6) high pathogen and pest resistance. However, the capability of plants to fulfill the criteria above, does not only depend on efficient plant traits, but is also the product of interactions between the plant and its microbiome. We studied here the effect of arbuscular mycorrhizal (AM) fungi and other beneficial plant microbes on the biomass potential of prairie cordgrass, a perennial grass species with a wide distribution throughout the continental U.S., and a high biomass potential on marginal lands. We identified the AM fungal species that form interactions with prairie cordgrass and studied their potential to increase the biomass under different input conditions, and we examined genotypic differences of prairie cordgrass in the response to the colonization with AM fungi. The results clearly demonstrate that an efficient AM symbiosis can increase the biomass potential of prairie cordgrass, particularly under low input conditions, and the biomass response is the result of the positive impact of AM fungi on P nutrition. However, there are large genotypic differences in the mycorrhizal responsiveness of prairie cordgrass. The results show that AM fungi can be used as potential biofertilizers and improve the environmental sustainability of bioenergy crop production. The observed genotypic differences indicate that the capability of plants to interact with AM fungi should be integrated as an important trait into breeding programs for bioenergy crops.

Project Objectives

Long term goal of this project is to improve the nutrient efficiency and biomass productivity of prairie cordgrass (PCG), a second generation bioenergy crop with a high biomass potential on marginal lands, and to develop molecular markers for nutrient efficiency and mycorrhizal responsiveness that could facilitate marker assisted selection in breeding programs of prairie cordgrass. The project had four distinct objectives and the outcomes of the different project objective are described below:

Objective 1: To study genotypic differences in the nutrient efficiency of PCG (*Spartina pectinata*) to identify genotypes that are best suited for low input and marginal land growth.

In order to study the genotypic differences in the nutrient efficiency of PCG, we conducted greenhouse experiments, in which the growth potential of seven different genotypes of prairie cordgrass

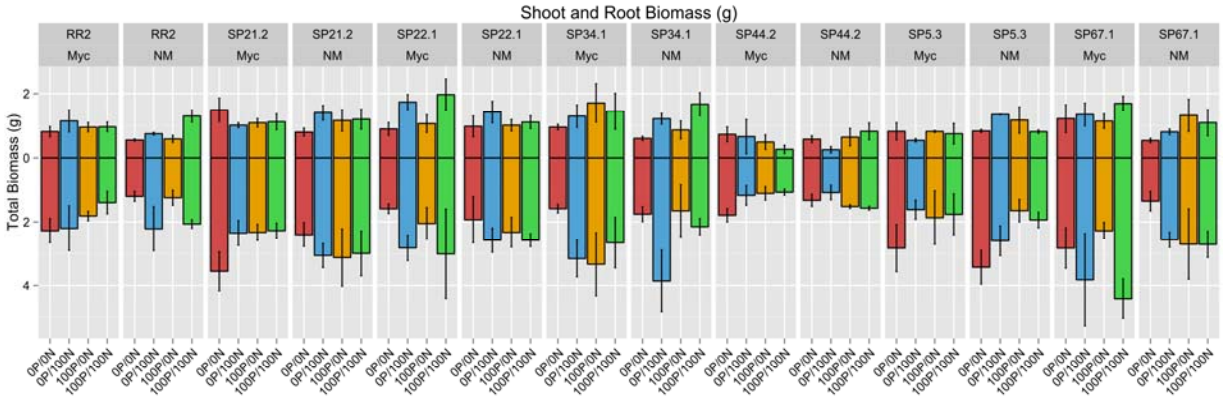

Fig. 1. Genotypic differences in the nutrient efficiency of non-mycorrhizal (NM) and mycorrhizal (Myc) prairie cordgrass plants under different nutrient supply conditions. The plants were grown with no phosphate or nitrogen addition (0P/0N), with low phosphate but high nitrogen addition (0P/100N), with high phosphate but low nitrogen addition (100P/0N), or with high phosphate and high nitrogen additions.

under different nutrient supply conditions and with or without arbuscular mycorrhizal (AM) fungal colonization was tested. The genotypes were selected from a germplasm collection based on Nei and Li coefficients or the analysis of DNA polymorphisms.

The results show that there are high genotypic differences in the biomass potential of prairie cordgrass under low input conditions, in the response to different nutrient supply conditions, in the response to mycorrhizal colonization (see also below), and in the investment in above ground to below ground biomass (Fig. 1). For example, the non-mycorrhizal plants of the genotype SP5.3 show the highest biomass potential under low input conditions, but the growth is not affected by increasing nutrient supply conditions, while SP34.1 produced a significantly lower biomass under low input conditions, but it was able to clearly outperform SP5.3 under higher nutrient supply conditions. While the growth of several genotypes was not affected by different nutrient supply conditions (e.g. SP22.1; SP5.3), the biomass of SP34.1 and of SP67.1 significantly increased when more nutrients became available. The majority of genotypes responded with an increase in shoot versus root growth (reduction in root to shoot ratio) to a higher nutrient availability, while SP44.2 invested under these conditions more resources into root than into shoot growth. The results clearly demonstrate that it is crucial to select suitable genotypes of prairie cordgrass dependent on the soil conditions. Some genotypes are able to develop biomass under low input conditions, but do not respond in growth potential to fertilizer additions, while other genotypes only develop high biomass under high nutrient supply conditions and are able to outperform other genotypes under these conditions.

Objective 2: To identify natural communities of arbuscular mycorrhizal (AM) fungi and diazotrophic bacteria that are associated with PCG to evaluate the effect of indigenous communities of these beneficial plant microbes on biomass production

The mycorrhizal colonization of prairie cordgrass had not been the object of intense investigation at the start of the project, presumably because there was the general belief that AM fungi are not abundant or important under wetland conditions. However, it has now been demonstrated that AM fungi are often abundant in wetlands and may play a more significant role than previously been suggested. We studied the abundance of AM spores and the mycorrhizal colonization of different prairie cordgrass varieties grown on marginal lands in SD and found colonization rates between 53.0% and 72.6% (mean was 60.7%) at all tested sites (26 sites were tested) and under different soil environmental conditions (e.g. nutrient content and moisture).

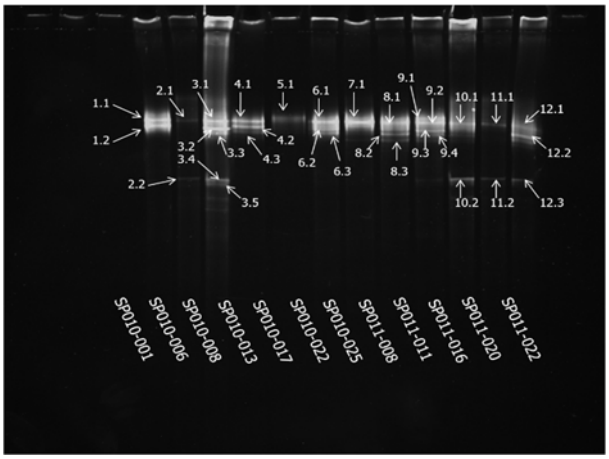

Fig. 2. Denaturing gradient gel electrophoresis (DGGE) of the AM community composition of prairie cordgrass at field sites in SD. After sequencing, the distinct bands were identified as *Glomus intraradices* (e.g. 1.1; now reclassified as *Rhizophagus irregularis*), *Glomus iranicum* (e.g. 3.2), Glomus fasciculatum (11.1), *Glomus hoi* or *Glomus macrocarpum* (9.1), or an unidentified fungal species (5.1).

We used DGGE to identify the fungal species that dominate the AM community of PCG roots in these marginal lands and found that *Glomus intraradices* (now often referred to as *Rhizophagus irregularis*) and other *Glomus* species were among the most dominant fungal species in the AM fungal communities of prairie cordgrass (Fig. 2). We used a similar approach to identify N fixing endophytes in the roots and shoots of prairie cordgrass, and found that N fixing endophytes are regularly associated with prairie cordgrass in the field. Our own studies also demonstrate that the majority of N fixing endophytes have other plant growth promoting capabilities, and reduce for example the growth of fungal pathogens, produce plant hormones such as indole-3- acetic acid, and have P solubilizing ability.

Since metagenomic approaches have now become the technique of choice to identify the microbiome of plants, we collected in May/June of this year prairie cordgrass samples from field sites in South Dakota, Minnesota, Iowa, and Nebraska. We produced amplicons with several primer sets to identify the AM fungal communities (AMV4.5NF/AMDGR; NS31/AML2), the communities of diazotrophs (F2/R6), prokaryotes (F357/R907), and of eukaryotes (ITS1F/ITS4R) that are associated with prairie cordgrass. The analysis of the sequences that we received is still ongoing, but will provide us with the complete microbiome of a high diversity of prairie cordgrass varieties. The metagenome analysis also became necessary, because recent studies indicate that the primers that were used for the DGGE analysis may be biased and amplify more successfully *Glomus* samples.

Objective 3: To evaluate the effect of AM fungi on nutrient efficiency and biomass production of PCG to identify potential candidates that could act as 'biofertilizers' of this bioenergy crop and could further lower the required inputs

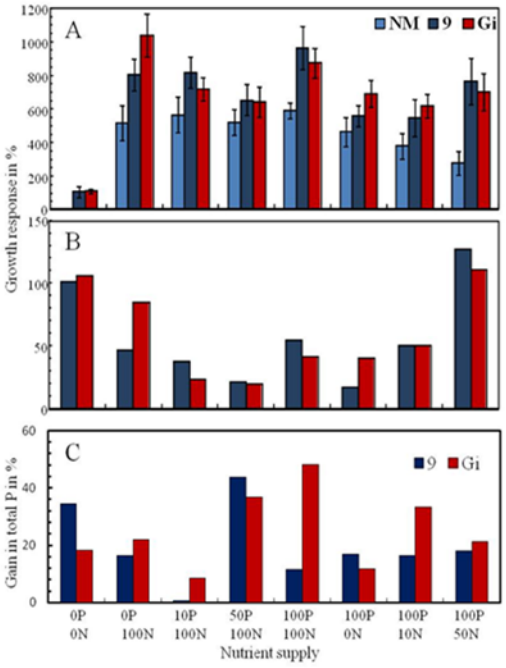

Fig. 3. Effect of two strains of *G. intraradices* on biomass of PCG. A. Growth response in % compared to control without addition of P or N (0P 0N); B. AM responsiveness in % compared to nonmycorrhizal control of each treatment; C. Gain in total P in %.

We conducted greenhouse experiments to examine whether AM fungi are able to increase the nutrient uptake and growth potential of prairie cordgrass. We tested the effect of two different *G. intraradices* (*Rhizophagus irregularis*) strains on biomass parameters under different nutrient supply conditions, and found that the AM symbiosis increased the biomass by more than 100% under low P and N conditions (Fig. 3). The growth of all plants increased when more P and N became available, but even under those conditions the biomass of mycorrhizal plants was between 20% and 100% larger than of comparable non-mycorrhizal controls (Fig. 3B). The P contents in the shoot of mycorrhizal plants were up to 45% higher than in non-mycorrhizal controls (Fig. 3C). The fact that the biomass of mycorrhizal plants also increased when only N was limiting (e.g. 100P 0N, or 100P 10N), suggests that AM fungi may also have also a positive impact on the N supply of PCG. In experiments with multi-compartment systems in which only the fungus had access to ^{33}P or ^{15}N, we were able to confirm that the fungus delivers P and N via its extraradical mycelium to its host plant.

Objective 4: To examine genotypic differences in the symbiotic efficiency and responsiveness of PCG to identify the genotype that can make the most efficient use of indigenous soil microbial communities.

Prairie cordgrass has recently gained interest as a potential alternative to switchgrass, but Web of Science only lists 31 publications for prairie cordgrass in 2010-2014, compared to 1,394 publications for switchgrass or 964 for *Miscanthus*. This clearly demonstrates how far research in this potential bioenergy crop lags behind research in other secondary bioenergy crops, and the lack of genomic resources for this perennial grass slows down the progress that could be made in the genetic improvement of this potential alternative to switchgrass. The significance of mycorrhizal interactions for biomass production and biotic and abiotic stress resistance of plants is long known. Our own preliminary results on prairie cordgrass and the results of other authors for SG clearly demonstrate the positive impact of these interactions on biomass production particularly under low input conditions. However, despite these clearly documented effects on biomass production, conventional breeding programs and most attempts to engineer plants with increased nutrient efficiency have generally ignored the fact that plants under field conditions are associated with arbuscular mycorrhizal (AM) fungi that have a tremendous effect on nutrient and water acquisition, and also change the overall physiology of their host plant. In 2010-2014, only three papers described effects of AM interactions on switchgrass, but for prairie cordgrass no results were published. This is even more important, because molecular breeding programs for switchgrass have already been initiated, but markers that may reflect certain biomass traits under non-mycorrhizal conditions, may not be active under field conditions when the plants will be colonized with ubiquitous AM fungi (see also above).

The need to integrate symbiotic efficiency in breeding programs of bioenergy crops is clearly illustrated by our studies. We compared the biomass potential of seven different prairie cordgrass genotypes and found that there is a high genotypic diversity in the symbiotic efficiency and responsiveness of prairie

cordgrass after AM colonization. For example, while the genotype SP21.2 produced a high biomass under non-mycorrhizal and mycorrhizal conditions, was the performance of SP67.1 very high under mycorrhizal conditions, but very low under non-mycorrhizal conditions. This clearly indicates that in breeding experiments in which the biomass potential of plants is often only considered under non-mycorrhizal conditions, do not reflect the biomass potential of plants in the mycorrhizal stage.

Table 1. Total plant biomass of mycorrhizal and non-mycorrhizal prairie cordgrass genotypes under low input conditions. Different letters indicate statistical significant differences after ANOVA and LSD test.

MYCORRHIZAL – 0P/0N	
GENOTYPE	*TOTAL BIOMASS (g)*
SP21.2	5.04 *a*
SP67.1	4.04 *ab*
SP05.3	3.65 *abc*
RR2	3.09 *bc*
SP34.1	2.54 *bc*
SP44.2	2.52 *bc*
SP22.1	2.49 *c*

NON MYCORRHIZAL – 0P/0N	
GENOTYPE	*TOTAL BIOMASS (g)*
SP5.3	4.26 *a*
SP21.2	3.19 *ab*
SP22.1	2.91 *abc*
SP34.1	2.36 *bc*
SP44.2	1.91 *c*
SP67.1	1.89 *c*
RR2	1.76 *c*

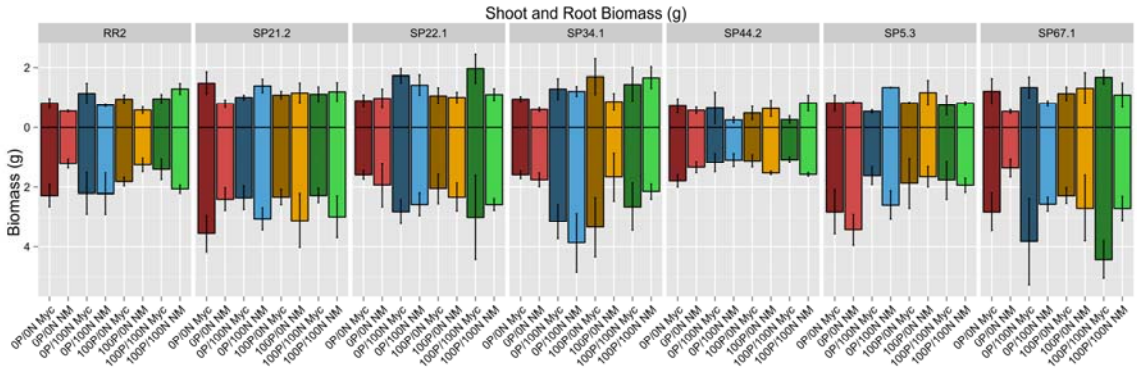

Fig. 4. Genotypic differences in the growth potential of mycorrhizal and non-mycorrhizal prairie cordgrass plants under different nutrient supply conditions. The plants were grown with no phosphate or nitrogen addition (red bars, 0P/0N), with low phosphate but high nitrogen addition (blue bars, 0P/100N), with high phosphate but low nitrogen addition (brown bars, 100P/0N), or with high phosphate and high nitrogen additions (green bars, 100P/100N). The mycorrhizal plants are shown in the darker colors, and the non-mycorrhizal control plants in the lighter colors.

The genotypes also differ in their mycorrhizal responsiveness under different nutrient supply conditions (Fig. 4). While the biomass of SP21.2 was only positively affected by the AM colonization under low input

conditions (mycorrhizal responsiveness was neutral under all other conditions), was the genotype SP22.1 only positively affected under high input conditions. Other genotypes such as SP67.1 and RR2 are generally under all conditions positively affected, while SP44.2 showed a negative mycorrhizal growth response under high nutrient supply conditions. The mycorrhizal responsiveness under low input conditions was highly correlated to the efficiency with which the AM fungus transferred P to the plants, but were independent from the mycorrhizal colonization. In this experiment a positive impact of AM fungi on N nutrition was not found.

In order to identify molecular markers that may be responsible for the genotypic differences in mycorrhizal responsiveness or nutrient efficiency of prairie cordgrass, we conducted experiments to study the transcriptome of mycorrhizal and non-mycorrhizal prairie cordgrass plants under different nutrient supply conditions. These studies are still ongoing and it is anticipated that these studies will be completed in Spring of 2016.

Project Activities

The project activities (a short summary is given above) confirmed our original hypotheses that AM fungi:

- play an important role in the microbiome of prairie cordgrass plants,
- affect the biomass potential of the plants particularly under low input conditions, but
- that there are high genotypic differences in the efficiency with which plants respond to mycorrhizal fungi.

The approaches that were used to study the proposed objectives do not differ significantly from the originally proposed design. However, in addition to the DGGE techniques we originally proposed to identify the microbial communities that are associated with prairie cordgrass, we conducted now a detailed metagenomics analysis of the microbiome of prairie cordgrass. The reason for this additional approach is that metagenomics has now become the technique of choice to study these questions, secondly because DGGE provides only a small overview about a specific group of associated microorganisms, and third recent studies have demonstrated that the DGGE analysis may also have been biased towards a certain group of AM fungi. This is the reason why for the metagenomics analysis now two primer pairs are used.

The originally proposed transcriptome analysis of a relatively small number of mycorrhizal and non-mycorrhizal prairie cordgrass plants has now been extended to a more complete study of the transcriptome of mycorrhizal and non-mycorrhizal prairie cordgrass, switchgrass and *Brachypodium* samples. This was made possible by the successful application for a DOE-JGI sequencing project. The samples had already been submitted to the JGI for sequencing, but the *Brachypodium* samples did not pass the quality test of the JGI. In order to allow the transcriptome analysis of all species under consistent conditions, a repetition of the original experiment was necessary and the RNA extractions and quality checks are currently ongoing and will soon be completed.

Products developed under the award

Two publications are currently in preparation:

- Monier B, Liepold E, Peta V, Gonzalez-Hernandez J, Bücking H. Arbuscular mycorrhizal interactions of *Spartina pectinata* and their impact on biomass production. Currently in preparation for Bioenergy Research.
- Monier B, Peta V, Gonzalez-Hernandez J, Bücking H. The microbiome of Spartina pectinata – future perspectives for an environmental sustainable bioenergy production?

Conference contributions: Oral presentations

- Bücking H, Gonzalez J. 2015. Beneficial plant microbe interactions and their application to increase biomass production and environmental sustainability of prairie cordgrass. North Central Regional Sun Grant Center, Annual meeting, Minneapolis, MN, March 2015
- Bücking H. 2013. Arbuscular mycorrhizal interactions – an important trait for biomass production of bioenergy crops. DOE Symbiosis Conference at Cornell University, May 2013.
- Bücking H, Gonzalez J. 2013. Beneficial plant microbe interactions and their potential application to increase biomass production and environmental sustainability of prairie cordgrass. North Central Regional Sun Grant Center, Annual meeting, Chicago, IL, March 2013.
- Bücking H. 2012. Arbuscular mycorrhizal interactions and their potential application for food and bioenergy crop production. 7th Annual South Dakota Biotechnology Summit & Annual Meeting. South Dakota Biotech Association, Sioux Falls, SD.
- Bücking H, Gonzalez J. 2012. Exploring the transcriptome of perennial grasses in association with beneficial microorganisms to increase biomass production and environmental sustainability of bioenergy production. JGI – Department of Energy User Conference, Walnut Creek, CA, January 2012.
- Bücking H, Gonzalez J. 2011. Beneficial plant microbe interactions and their potential application to increase biomass production and environmental sustainability of prairie cordgrass. North Central Regional Sun Grant Center, Annual meeting, Orlando, FL, January 2011.
- Bücking H, Gonzalez J. 2010. Beneficial plant microbe interactions and their potential application to increase biomass production and environmental sustainability of prairie cordgrass. Presentation at the North Central Regional Sun Grant Center 5 x 10 meeting in Brookings (SD) on December 21, 2010.

Conference contributions: Poster presentations

- Mai W, Cordero-Sepulveda J, Monier B, Peta V, Bücking H. 2015. Identifying the relationship between *Brassica carinata* and diazotrophic endophytes. 2015 South Dakota Undergraduate Research Symposium, Pierre, July 2015.
- Cordero-Sepulveda J. Mai W, Monier B. Peta V, Bücking H. 2015. Optimizing biomass production in *Spartina pectinata* through arbuscular mycorrhizal symbiosis. 2015 South Dakota Undergraduate Research Symposium, Pierre, July 2015.
- Monier B, Gonzalez-Hernandez JL, Bücking H. 2014. Plant microbe interactions increase the biomass potential of the bioenergy crop *Spartina pectinata*. North Central Branch Meeting of the American Society for Microbiology, University of Wisconsin – Superior, October 2014.
- Burch M, Monier B, Bücking H. 2014. Plant microbe interactions increase the biomass potential of the bioenergy crop *Spartina pectinata*. Bioenergy Research Day, Brookings, August 2014.
- Burch M, Monier B, Bücking H. 2014. Plant microbe interactions increase the biomass potential of the bioenergy crop *Spartina pectinata*. 2014 Sanford Summer Research Symposium, Sioux Falls, August 2014.

- Burch M, Monier B, Bücking H. 2014. Plant microbe interactions increase the biomass potential of the bioenergy crop *Spartina pectinata*. 2014 South Dakota Undergraduate Research Symposium, Pierre, July 2014.
- Cat LA, Bushlack S, Monier B, Bücking H. 2013. Mycorrhiza interaction and biofuel crop yield: variation in prairie cordgrass genotypes. Bioenergy Research Day, South Dakota State University, August 2013.
- Liepold E, Sanchez A, Gonzalez-Hernandez J, Bücking H. 2011. The contribution of arbuscular mycorrhizal fungi to biomass production of prairie cordgrass (*Spartina pectinata* L.) under nitrogen and phosphate limitation. Annual meeting of the American Society of Plant Biologists, Minneapolis, August 2011.
- Liepold E, Sanchez A, Gonzalez-Hernandez J, Bücking H. 2011. The contribution of arbuscular mycorrhizal fungi to biomass production of prairie cordgrass (*Spartina pectinata* L.) under nitrogen and phosphate limitation. America´s Grassland meeting, Sioux Falls, August 2011.

a. Website or other Internet sites that reflect the results of this project.

The work on the project contributed to the invitation from the U.S. Department of Energy (10/2013) to participate in a round table discussion to identify research goals for sustainable bioenergy production. A summary of the workshop results were later published in:

- U.S. Department of Energy 2014. Research for sustainability Bioenergy: Linking genomic and Ecosystem Sciences. Workshop report. 1-41

The report is available at: http://genomicscience.energy.gov/sustainability/sustainablebiofuels.pdf
The objectives of this project address several of the research priorities that were identified in this workshop report as relevant for sustainable bioenergy production.
The report for example states: “Improved understanding of the integral association between plants and microbes has led to a paradigm-shifting view of plants as metaorganisms, or holobionts—the combination of host plant and its associated microbes and viruses—rather than as isolated entities. Rarely does plant breeding consider the microbiome a selectable trait (pathogen resistance is a notable exception), yet breeding and managing plants as metaorganisms may benefit both sustainable productivity of bioenergy crops and ecosystem services associated with large-scale bioenergy cropping systems.

b. Networks or collaborations fostered.

The work on the project led to the invitation of the DOE to participate in the workshop and round table discussion described above. During the project we also established collaborations with researchers at the University of Illinois that contributed to two proposals that were submitted to the DOE and that included data that were produced during this project.

c. Technologies/techniques.

Nothing to report.

d. Inventions/patent applications, licensing agreements.

One invention disclosure has been filed with the University.

e. Other products, such as data or databases, physical collections, audio or video, software* or Netware, model, educational aid or curricula, instruments, or equipment.

Nothing to report.

1. **Academic**

a. Courses developed
Nothing to report.

b. M.S. students supported
Two M.S. students were supported by this project. One has successfully completed his graduate program in September of 2013 (Elliot Liepold), and the other M.S. student (Vincent Peta) is still working on the project, and it is anticipated that the student will complete the M.S. program in December 2016.

c. M.S. degrees conferred
The M.S. student Elliot Liepold completed the M.S. program in September of 2013.

d. Ph.D. students supported
One Ph.D. student (Brandon Monier) was supported by this project. It is anticipated that he will defend his Ph.D. thesis in December 2016.
e. Ph.D. degrees conferred
The Ph.D. student who was supported by this project still needs to complete his Ph.D. program, and it is anticipated that the student will defend his thesis in December 2016.

f. Post-docs supported
No post-docs were supported by this project.

2. **For projects involving computer modeling, provide the following information with the final report:** Not applicable.

Table 2. The table reflects the different project outputs at completion or at time of report submission.

ITEM	NUMBER	DETAILS (e.g. citations, names, descriptions, varieties, etc.)
Abstracts: include full citation and attach a pdf copy.	9	• Mai W, Cordero-Sepulveda J, Monier B, Peta V, Bücking H. 2015. Identifying the relationship between *Brassica carinata* and diazotrophic endophytes. 2015 South Dakota Undergraduate Research Symposium, Pierre, July 2015. • Cordero-Sepulveda J. Mai W, Monier B. Peta V, Bücking H. 2015. Optimizing biomass production in *Spartina pectinata* through arbuscular mycorrhizal symbiosis. 2015 South Dakota Undergraduate Research Symposium, Pierre, July 2015. • Monier B, Gonzalez-Hernandez JL, Bücking H. 2014. Plant microbe interactions increase the biomass potential of the bioenergy crop *Spartina pectinata*. North Central Branch Meeting of the American

		Society for Microbiology, University of Wisconsin – Superior, October 2014. • Burch M, Monier B, Bücking H. 2014. Plant microbe interactions increase the biomass potential of the bioenergy crop *Spartina pectinata*. Bioenergy Research Day, Brookings, August 2014. • Burch M, Monier B, Bücking H. 2014. Plant microbe interactions increase the biomass potential of the bioenergy crop *Spartina pectinata*. 2014 Sanford Summer Research Symposium, Sioux Falls, August 2014. • Burch M, Monier B, Bücking H. 2014. Plant microbe interactions increase the biomass potential of the bioenergy crop *Spartina pectinata*. 2014 South Dakota Undergraduate Research Symposium, Pierre, July 2014. • Cat LA, Bushlack S, Monier B, Bücking H. 2013. Mycorrhiza interaction and biofuel crop yield: variation in prairie cordgrass genotypes. Bioenergy Research Day, South Dakota State University, August 2013. • Liepold E, Sanchez A, Gonzalez-Hernandez J, Bücking H. 2011. The contribution of arbuscular mycorrhizal fungi to biomass production of prairie cordgrass (*Spartina pectinata* L.) under nitrogen and phosphate limitation. Annual meeting of the American Society of Plant Biologists, Minneapolis, August 2011. • Liepold E, Sanchez A, Gonzalez-Hernandez J, Bücking H. 2011. The contribution of arbuscular mycorrhizal fungi to biomass production of prairie cordgrass (*Spartina pectinata* L.) under nitrogen and phosphate limitation. America´s Grassland meeting, Sioux Falls, August 2011.
Peer Reviewed Publications: include full citation and attach a pdf copy if available	0	Two manuscripts are currently in preparation
Outreach Publications including web pages: include full citation	1	The work on the project contributed to the invitation by the U.S. Department of Energy (10/2013) to participate in a round table discussion to identify research goals for sustainable bioenergy production. Results of this workshop were later published in: • U.S. Department of Energy 2014. Research for sustainability Bioenergy: Linking genomic and Ecosystem Sciences. Workshop report. 1-41 Available at: http://genomicscience.energy.gov/sustainability/sustainablebiofuels.pdf

Professional Presentations: include full citation	7	• Bücking H, Gonzalez J. 2015. Beneficial plant microbe interactions and their application to increase biomass production and environmental sustainability of prairie cordgrass. North Central Regional Sun Grant Center, Annual meeting, Minneapolis, MN, March 2015 • Bücking H. 2013. Arbuscular mycorrhizal interactions – an important trait for biomass production of bioenergy crops. DOE Symbiosis Conference at Cornell University, May 2013. • Bücking H, Gonzalez J. 2013. Beneficial plant microbe interactions and their potential application to increase biomass production and environmental sustainability of prairie cordgrass. North Central Regional Sun Grant Center, Annual meeting, Chicago, IL, March 2013. • Bücking H. 2012. Arbuscular mycorrhizal interactions and their potential application for food and bioenergy crop production. 7th Annual South Dakota Biotechnology Summit & Annual Meeting. South Dakota Biotech Association, Sioux Falls, SD. • Bücking H, Gonzalez J. 2012. Exploring the transcriptome of perennial grasses in association with beneficial microorganisms to increase biomass production and environmental sustainability of bioenergy production. JGI – Department of Energy User Conference, Walnut Creek, CA, January 2012. • Bücking H, Gonzalez J. 2011. Beneficial plant microbe interactions and their potential application to increase biomass production and environmental sustainability of prairie cordgrass. North Central Regional Sun Grant Center, Annual meeting, Orlando, FL, January 2011. • Bücking H, Gonzalez J. 2010. Beneficial plant microbe interactions and their potential application to increase biomass production and environmental sustainability of prairie cordgrass. Presentation at the North Central Regional Sun Grant Center 5 x 10 meeting in Brookings (SD) on December 21, 2010.
MS Degrees Conferred: include names plus month/year confirmed	1	Elliot Liepold graduated in September 2013
Ph.D. Degrees Conferred: include names plus month/year confirmed	1	One Ph.D. student is still working on the project and will likely defend his thesis in December 2016
MS Students Supported: include names		Elliot Liepold and Vincent Peta

Ph.D. Students Supported: include names	1	Brandon Monier
Post-Docs Supported: include names	0	Nothing to report
Undergraduate Students Supported: include names	7	Jerry Cordera-Sepulveda, Winli Mai, Vincent Peta, Merritt Burch, Linh Anh Cat, Sabrina Larson-Bushlack, Armila Francis (the students were not funded by the project, but contributed to experiments that were conducted for the project)
Investigators Supported: include names	2	Heike Bücking and Jose Gonzalez
Jobs Created	0	Nothing to report
Invention Disclosures	1	One invention disclosure has been filed with the employer.
Subsequent Funding: List proposals funded as a result of this work	1	JGI-DOE. Exploring the transcriptome of perennial grasses in association with beneficial microorganisms to increase biomass production and environmental sustainability of bioenergy production Several subsequent proposals were submitted that included data of this project, but these projects were not funded.
Other: Products, such as data or databases, physical collections, audios or videos, software or Netware, models, educational aids or curricula, instruments, or equipment.	0	Nothing to report

Back to Table of Contents

Sun Grant Initiative
DOE Final Progress Report

Project Title: Develop solid-stem Triticale as a feedstock for biofuel production

Project Director/Principal Investigator: Wanlong Li, Associate professor, Department of Biology and Microbiology, South Dakota State University, Brookings, South Dakota

All Co-Principal/Other Investigators: Yang Yen, Professor, Department of Biology and Microbiology, South Dakota State University, Brookings, South Dakota

Collaborators: Fang Chen, Research professor, Department of Biological Science, University of North Texas, Denton, Texas

Period of Performance: 1 January 2011 - 30 September 2014

Funding Awarded: $141,585

Cost Share Amount: $35,396

Cost Share Sources: Time and effort from PIs and CoPIs; Indirect on time and effort

Executive summary

This project created the first batch of solid-stem winter Triticale lines and demonstrated the great biomass-yielding potential of the solid stem trait, which laid a solid foundation for breeding Triticale for biofuel production in the Corn Belt. The identified high crossable durum and rye lines can be further used for transfer other useful traits into Triticale from its parental species. Since the project start in January of 2011, the results were disseminated through North Central SUNGRANT conferences (Jan 2012, March 2013 and March 2014) and McFadden Symposium (Sept 2014).

Project objectives

Objective 1: Develop 100 solid stem winter Triticale lines.
We developed first batch of solid stem winter Triticale, including 10 primary lines and 68 derived lines. Our results showed that population structure exists in the winter solid-stem durum lines maintained in the National Small Grain Collections, and most of them carry incrossability genes. This is not expected and the difficulty to overcome the incompatibility was underestimated. The rationale for developing "100" lines was to overcome the genetic vulnerability. In this regard, the 10 primary lines and 68 derived lines is enough to fulfill this objective.

Objective 2: Investigate the solid stem effect on biomass yield and quality.
Our results showed that the solid-stem trait greatly increased the bio-mass yield potential but did not significantly reduce lignin content.

Project activities

Objective 1: Over 3,000 crosses (spikes) were made between 41 solid stem durum lines and 18 winter rye cultivars, from which most hybrid seeds died two weeks after pollination and only 10 combinations between seven durum and six rye lines produced fertile Triticale after chromosome doubling, suggesting that these durum and rye lines carry the crossability genes. To improve the fertility of the primary solid-stem Triticale lines, we crossed them with traditional (hollow-stem) Triticale varieties for 68 combinations. In the F2 and F3 populations, solid-stem inherited as a quantitative trait and fertility was increased significantly. They are planted in field for selecting winter hardiness and other traits. The second modification is the method for doubling chromosome numbers. The original approach in Objective 1 for chromosome doubling is to inject colchicine into internodes. This method did not work well for solid stem. So we treated the seedlings at 4-leaf stage (2 tillers). Also, we used embryo rescue protocol to obtain real wheat/rye hybrids.

Objective 2: The original hypothesis is that the wheat solid-stem will greatly enhance the biomass yield and quality of Triticale. Comparison between a pair of solid-stem and hollow-stem Triticale near isogenic lines (NILs) indicated that the linear density of internodes increased by 160% to 190% in the solid-stem line, showing great biomass yielding potential (Fig. 1a). All lignin species in all internode positions showed no significant change between the NILs, indicating the solid-stem gene may did not affect lignin content in the increased biomass (Fig. 1b).

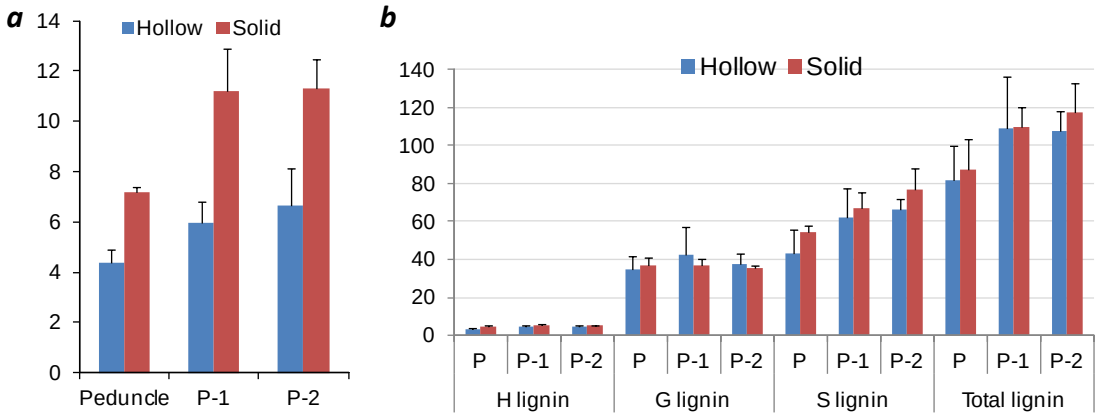

Fig. 1. Density of three top internodes (panel a) and types of lignin in all internode positions (panel b) of hollow- and solid-stemmed triticale.

Products developed under the award:

Publications

a. Website or other Internet sites that reflect the results of this project.
b. Networks or collaborations fostered. Collaboration with Dr. Fang Chen of University of North Texas for determination of lignin content.
c. Technologies/techniques.
d. Inventions/patent applications, licensing agreements. The project created first batch solid-stem winter Triticale.
e. Other products, such as data or databases, physical collections, audio or video, software* or Netware, model, educational aid or curricula, instruments, or equipment.

1. **Academic**

a. Courses developed
b. M.S. students supported: 1
c. M.S. degrees conferred
d. Ph.D. students supported: 1
e. Ph.D. degrees conferred
f. Post-docs supported; 1

2. **For projects involving computer modeling, provide the following information with the final report:**
a. Model description, key assumptions, version, source, and intended use.
b. Performance material for the model related to the intended use.
c. Test results to demonstrate the model performance criteria were met (e.g., code verification/validation, sensitivity analyses, history matching with lab or field data, as appropriate).
d. Theory behind the model, expressed in non-mathematical terms.
e. Mathematics to be used, including formulas and calculation methods.
f. Whether or not the theory and mathematical algorithms were peer reviewed, and, if so, will include a summary of the theoretical strengths and weaknesses.
g. Hardware requirements.
h. Documentation (e.g., user's guide, model code).

***Software/Manual (if applicable)**
Content. Unless otherwise specified in the award, the following must be delivered: source code, the executable object code and the minimum support documentation needed by a competent user to understand and use the software and to be able to modify the software in subsequent development efforts.

Please complete the following table to reflect your project outputs at completion or at time of report submission. Identify outputs and products developed under the award and any technology transfer activities.

ITEM	NUMBER	DETAILS (e.g. citations, names, descriptions, varieties, etc.)
Abstracts: include full citation and attach a pdf copy.	0	
Peer Reviewed Publications: include full citation and attach a pdf copy if available	0	
Outreach Publications including web pages: include full citation	0	
Professional Presentations: include full citation	4	1. Li W, Yen Y. Develop solid-stem triticale as feedstock for biofuel production. North Central Regional Sun Grant Annual conference. Jan 9-11, 2012. Indianapolis, IN. 2. Li W, Yen Y. Develop solid-stem triticale as feedstock for biofuel production. North Central Regional Sun Grant Annual conference. March 21-23, 2013. Chicago, IL. 3. Li W, Yen Y. Develop solid-stem triticale as feedstock for biofuel production. North Central Regional Sun Grant Annual conference. March 25-27, 2014. Minneapolis, MN 4. Li W, Zhu H, Wang W, Wei W, Chen F, Paudel D, Yen Y. Developing solid-stem Triticale as a feedstock for biofuel production. Sept. 22-23, 2014. Brookings, SD
MS Degrees Conferred: include names plus month/year confirmed	0	
Ph.D. Degrees Conferred: include names plus month/year confirmed	0	
MS Students Supported: include names	1	Devendra Paudel worked on projective 2 for measure the linear density of inter nodes
Ph.D. Students Supported: include names	1	Wei Wang worked on Objective for doubling the chromosome number of the durum x rye hybrids
Post-Docs Supported: include names	1	Huilan Zhu worked on Objective for crossing durum and rye
Undergraduate Students Supported: include names	1	Jordyn Ann Gruber worked in greenhouse for harvesting Triticale plants
Investigators Supported: include names	0	

Jobs Created	0	
Invention Disclosures	78	10 primary solid-stem winter Triticale lines and 68 derived solid-stem Triticale lines
Non-provisional Patent Application(s) Filed	0	
Provisional Patents Filed	0	
Patents Filed	0	
Patents Issued: include full citation	0	
License Agreements: include description	0	
Plant Variety Protection: include description	0	
Subsequent Funding: List proposals funded as a result of this work	0	
Other: Products, such as data or databases, physical collections, audios or videos, software or Netware, models, educational aids or curricula, instruments, or equipment.	0	

Back to Table of Contents

Sun Grant Initiative
DOE Final Progress Report

Project Title: Electrophoretic Deposition of Biochar Nanoparticle based Films for Energy Storage

Project Director/Principal Investigator: Qi Hua Fan, Associate Professor, Department of Electrical Engineering and Computer Science, South Dakota State University, Brookings, SD

All Co-Principal/Other Investigators: Dr. Zhengrong Gu, Agricultural and Biosystems Engineering, South Dakota State University, Brookings, SD

Collaborators: N/A

Period of Performance: 1 March 2014 - 28 February 2014

Funding Awarded: $23,878

Cost Share Amount: $5,970

Cost Share Sources: Applied Nanofilms

Executive summary

Energy storage is a critical component in future sustainable energy infrastructure. Among energy storage options, the supercapacitor plays a unique role with a large capacity, fast charge/discharge, and stability. Supercapacitors have the potential to transform transportation; combined with batteries, supercapacitors can make electric cars highly efficient, replacing the current chemical-fuel-based powertrain. Supercapacitors are also effective in mitigating the intermittency of renewable energy sources, such as photovoltaics and wind. Other important applications of supercapacitors include consumer electronic products, agricultural machines, and power tools. State-of-the-art supercapacitors use chemically synthesized carbon nanomaterials, which are expensive and non-sustainable. Alternative low-cost materials are needed to realize efficient energy storage.

Biochar, a byproduct of biomass pyrolysis, recently showed great potential for supercapacitors. This biocarbon material is sustainable, cheap, and environmentally friendly. Conventional approach to fabricating biochar supercapacitors requires high pressure (>5 tons/cm^2) pressing of biochar slurry. The challenge is to accurately control the thickness of the resulted membrane, which in turn determines the capacitance. This proof-of-concept project successfully developed a proprietary electrochemical scheme for efficient deposition of carbon nanoparticles. It addressed the challenge in fabricating high-performance biochar-based supercapacitors or batteries. The outcome is a low-cost and scalable process suitable for depositing biochar nanoparticles into controllable porous film structures. This research led to one patent application (pending) and one invention disclosure that was licensed to a local company Applied NanoFilms, LLC. This project supported one MS student who completed his thesis. One research paper was submitted for publication and another two are under preparation. This research advanced the mission of the Sun Grant Initiative to research, produce, and commercialize renewable, bio-based energy technologies.

Project objective

The objective for this project is to verify the ability of our proprietary electrophoretic deposition scheme to deposit biochar nanoparticle-based films. Through this research, we successfully identified a suitable electrolyte that led to electrophoretic deposition of biochar nanoparticles at high rate of ~200 μm/min. Note that in common supercapacitors, the biochar thickness needed is less than 50 μm.

In addition to successfully completing the proposed research, our team also developed a potentially transformative method to activate biochar. Conventional chemical activation of biochar requires high-temperature baking at over 950°C for over four hours. Our new activation only needs five minutes at temperatures below 150°C. We believe this will be a critical progress that will lead to practical application of biochar supercapacitors. We have filed an invention disclosure and are in contact with a company about technology transfer and further development. We also are preparing an SBIR proposal to seek opportunities to commercialize the novel activation technology.

Project activities

We conducted the following three tasks to achieve our objective:

- Deposit biochar nano-/micro-particle films
- Characterize EPD-fabricated biochar nanoparticle films
- Fabricate and test supercapacitors

The research activities and result obtained are summarized below.

TASK 1:

(1) Planned Activities: *Deposit Biochar Nano-/Micro-particle Films*

Establish electrophoretic deposition (EPD) to deposit biochar nanoparticles onto an electrode substrate. The nanoparticle filmswill be optimized by varying the EPD parameters, such as applied voltage, surface chemistry (via electrolyte solution composition), and electrode spacing. The EPD process optimization will focus on exploring novel electrolytes that allow rapid deposition of dense and closely packed biochar particles with high uniformity and sufficient adhesion. The EPD deposition of different size biochar particles (ranging from a few to hundreds of nanometers) will be studied to identify the effect of particle size on film properties.

(2) Actual Accomplishments:

We identified several biochars that have the potential for supercapacitor applications. Different milling processes were conducted to achieve biochar particles of various sizes. This work was conducted in order to further identify the optimized particle size for charge storage. EPD was established and several electrolytes were tested; an acetone based electrolyte was found to be the most efficient for biochar nanoparticle deposition.

Biochar was grinded for 3 hours prior to the EPD method. Electrophoretic deposition was done using different solvent including acetone, mixture of acetone and ethanol, DI water, Isopropyl alcohol. Good and uniform deposition was observed only with acetone and mixture of acetone and ethanol. The deposition of the biochar was done on aluminum and copper foil as shown in the photograph images in Figure 1.

Figure 1. Photograph image of biochar deposited on copper and aluminum foil.

We worked on activated carbon purchased from kuraray chemical co. ltd. which had the specifications shown in Table 1.

Table 1. Characteristics of activated carbon used in this study.

	Unit	YP-50F
Raw Materials	-	Coconut shell
Surface Area	m2/g	1500 - 1800
pH	-	7 - 10
Moisture Content	wt%	3 Max
Ash Content	wt%	1 Max
Particle Size	μm	5 - 20

Electrophoretic deposition was done using different solvent including acetone, mixture of acetone and ethanol, DI water, Isopropyl alcohol. Good and uniform deposition was found using ethanol, but the adhesion was very poor as shown in figure 2 (a). In the similar solvent the salt was added to see the effect on adhesion, which showed better adhesion and uniform deposition. To confirm the mechanical properties of the nanoparticle films, including scratch test, 100-grid tape test per ASTM standard was performed as shown in figure 2 (b). We added the ethylene glycol to see the effect on adhesion as shown in figure 2(c) but similar result was observed as compared to figure 2(b).

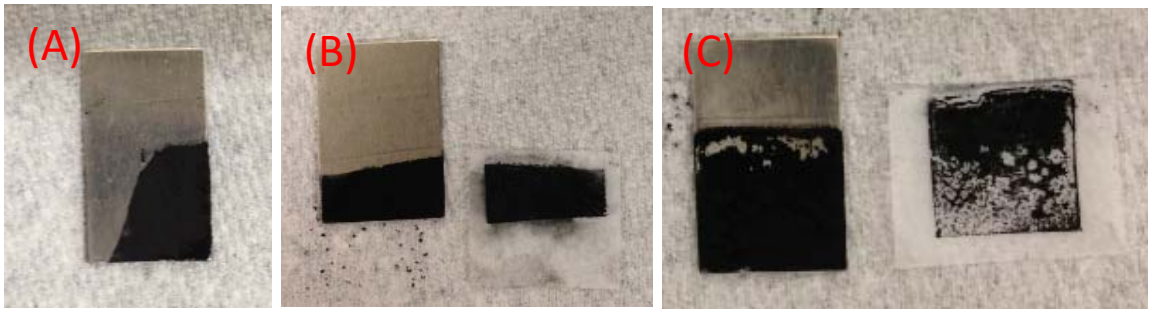

Figure 2. Photograph image of activated carbon deposited on aluminum plate a) ethanol as solvent b) ethanol and salt c) ethanol, salt and ethylene glycol.

TASK 2:

(1) Planned Activities: *Characterize EPD-fabricated BiocharNanoparticle Films*
Multiple advanced tools will be used/developed to characterize the deposited biochar particle films. These tests will help identify optimum particle size and process conditions. The microscopic structure of the nanoparticle films will be characterized with SEM and scanning probe microscopy (SPM). SPM will also determine the surface morphology and surface potential in the nanoscale. Both tools can be used to verify the average nanoparticle diameter. The compositional analysis and structural properties of deposited biochar film will be studied by Raman spectroscopy, Fourier transform infrared spectroscopy, and energy dispersive spectroscopy. We will use various tests to characterize the mechanical properties of the nanoparticle films, including scratch test, 100-grid tape test per ASTM standard, and indentation test. These tests will confirm the durability of the nanoparticle films to be used through the supercapacitor fabrication processes.

(2) Actual Accomplishments:
Figure 3 shows biochar films produced by the EPD method using biochar materials manually grinded for 10 min. It shows that the material is still in large bulk size. Further increasing the milling time is needed.

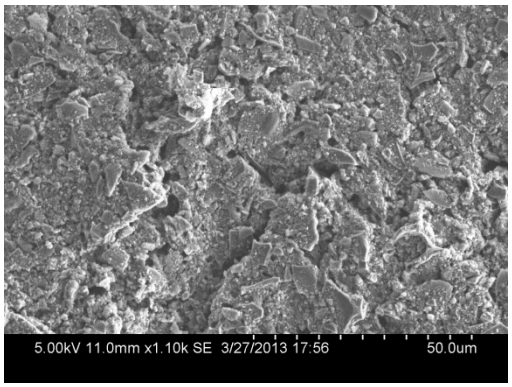

Figure 3. Biochar film deposited by EPD method using biochar grinded for 10 minutes.

Figure 4 shows Raman spectra of two types of biochars in comparison with commercial carbon black purchased from the Sigma Aldrich Company. This result shows that the yellow pine has a similar ratio of ID: IG band spectra.

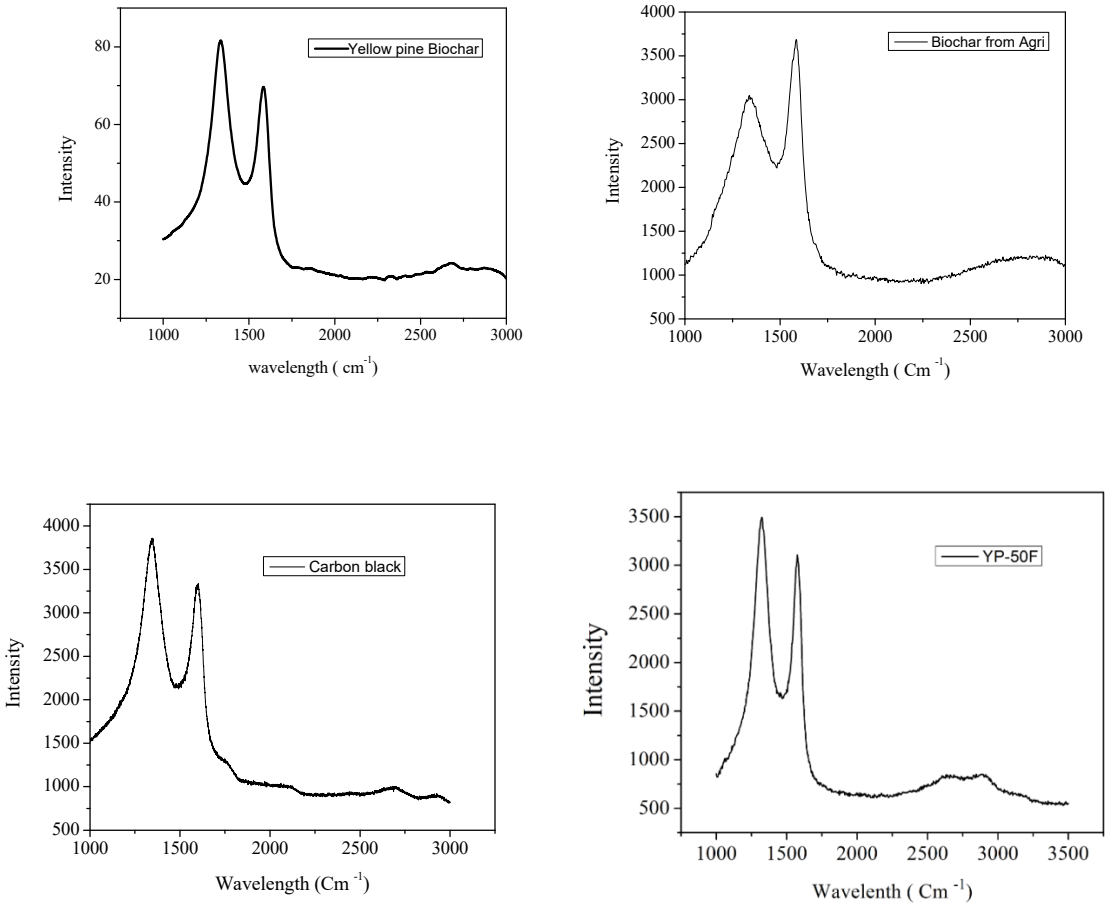

Figure 4. Raman Spectra of EPD deposited biochars and activated carbon and carbon black films.

The SEM was used to characterize the deposited films. Figure 5 shows the SEM image of the biochar sample after manually grinding of 3 hrs. This shows that we have still large chunk and

small particle of biochar. Further increase in milling is required along with the separation of large and small particles is also required.

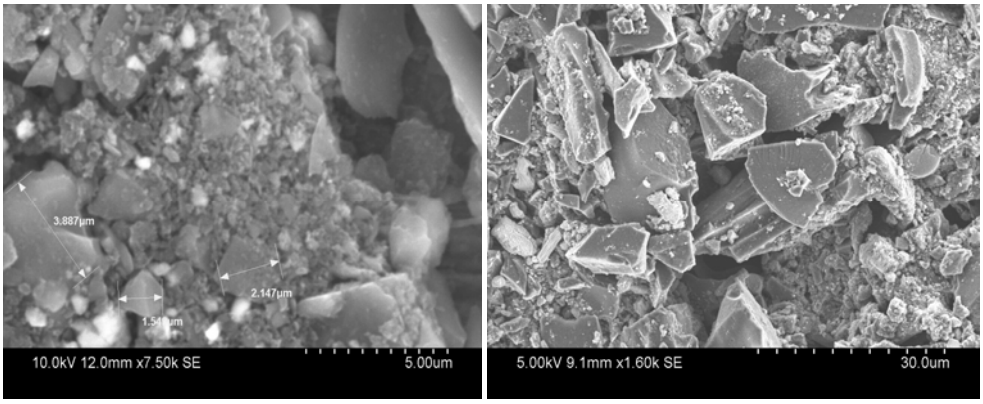

Figure 5. SEM image of biochar a) yellow pine (left) b) biochar from Agriculture Department (right).

EDX was also done to know the chemical composition of the particles present in both the biochar as shown in Figure 6.This shows that the chemical composition of both the biochar had nearly same amount of carbon.

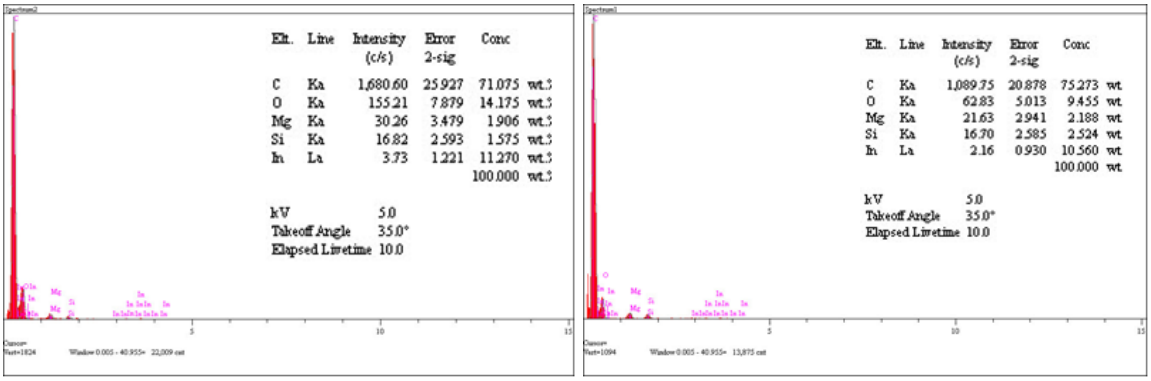

Figure 6. EDX spectra of different yellow pine biochar (left panel) and biochar from Ag and Biosystems Department at SDSU (right panel).

The adhesion to the substrate was found to be weak. Different salts like Mg(NO3)2.6H20 and Tetraoctylammonium bromide will be used to improve the adhesion to the substrate.

The SEM was used to characterize the deposited films. Figure 7 shows the SEM image of the YP-50F sample with ethylene glycol and without ethylene glycol in the presence of salt. This shows with ethylene glycol the particles are agglomerated and covered with some layer of ethylene glycol, which may affect the capacitance behavior of the sample.

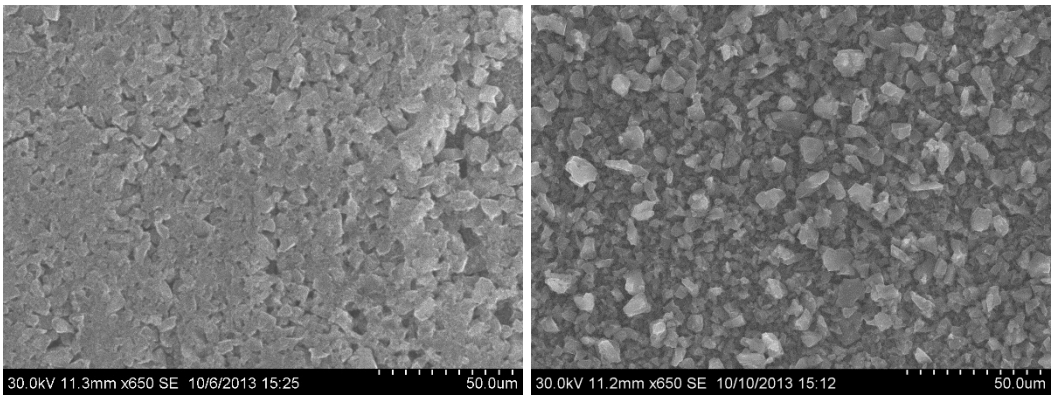

Figure 7: SEM image of YP-50Fa) with ethylene glycol (left) b) without ethylene glycol (right)

Figure 8 shows the cross-section view of YP-50F activated carbon deposited on cupper substrate using EPD. This result show the rapid deposition with the depostion rate of 200 um/ min. EPD is effective way to deposit the film uniformly in short period of time.

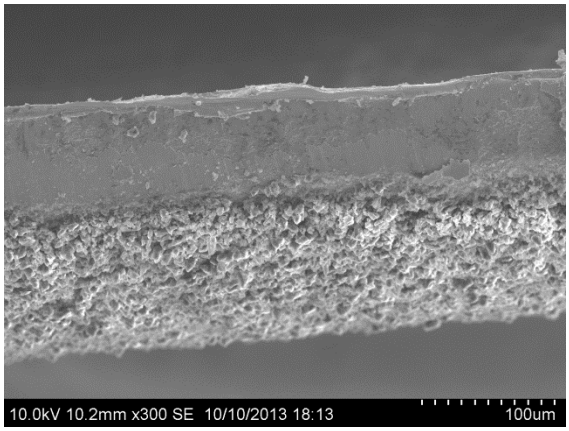

Figure 8: Cross-section view of YP-50F deposited on cupper substrate

EDX was also done to know the chemical composition of the particles present in the EPD film prepared with salt shown in Figure 9.This shows that the chemical composition of carbon is high. The small amount of magnesium is from the salt.

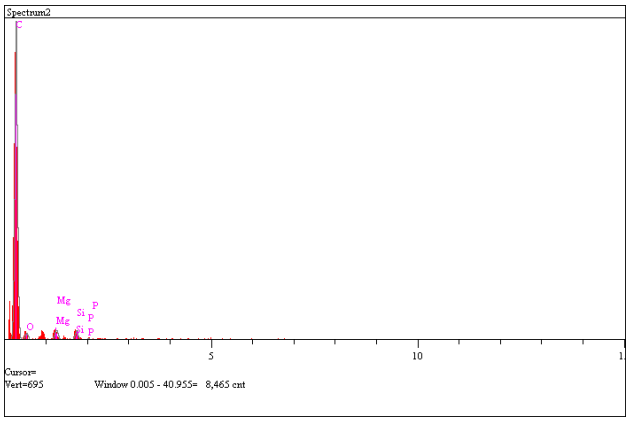

Elt.	Line	Intensity (c/s)	Error 2-sig	Conc	Units	
C	Ka	641.45	16.017	89.500	wt.%	
O	Ka	11.93	2.184	5.461	wt.%	
Mg	Ka	20.06	2.833	2.232	wt.%	
Si	Ka	20.33	2.852	2.541	wt.%	
P	Ka	1.82	0.854	0.267	wt.%	
				100.000	wt.%	Total

Figure 9: EDX spectra of YP-50F activated carbon film

TASK 3:

(1) Planned Activities: *Fabricate and Test Supercapacitors*

The EPD-produced biochar nanoparticle films will be used to fabricate supercapacitors. The prototype device will be tested for electricity storage with different electrolytes. This study will systematically measure the essential characteristics of the biochar supercapacitors, including capacitance, charge time, discharge time, charge/discharge efficiency, internal resistance, cycle life, energy density (Wh/kg), and specific power (W/kg).

(2) Actual Accomplishments:

The samples were tested for the supercapacitor applications. Figure 10 shows the impedance and CV measurement of the supercapacitor. The cell dies out for 40 cycles which show the poor adhesion to the substrate. More focus on the adhesion will be done before the further electrochemical test of the capacitors. Figure 11 shows the CV measurement of purchase activated carbon on different substrate. The carbon, copper substrate has oxidation and reduction peak. The peaks were observed because the copper gets oxidized while doing EPD. The verification was done by a sputtering gold layer of 100nm on copper substrate and the deposition was carried as previously. We would not see any oxidation and reduction peaks as shown in figure 11(right). This suggests that the copper substrate was not appropriate for supercapacitor using EPD method.

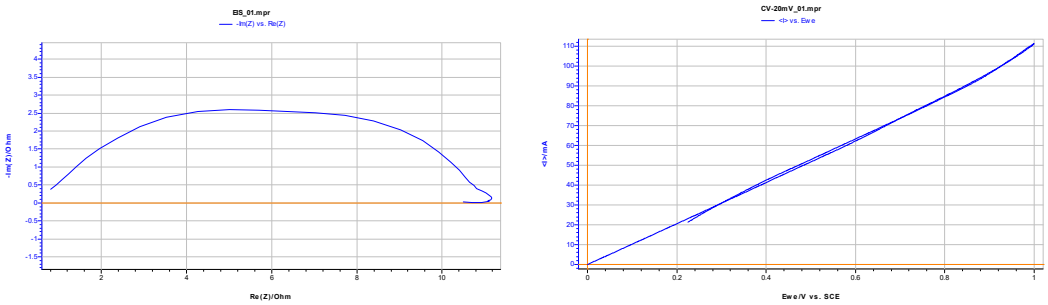

Figure 10: (left) Impedance Spectroscopy (right) CV measurement of Supercapacitor.

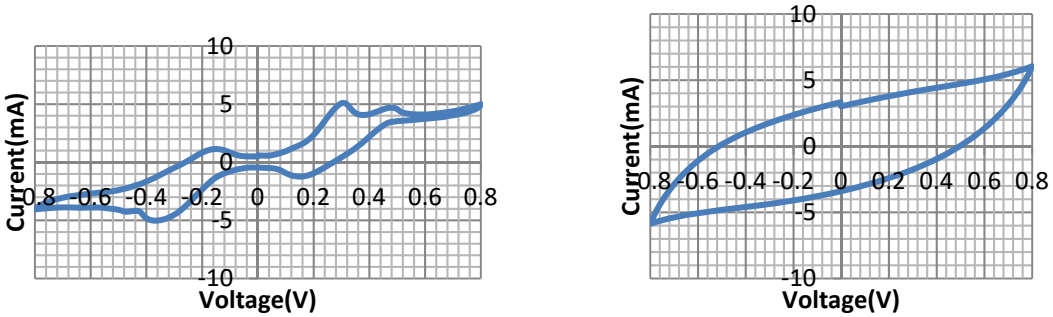

Figure 11: CV measurement for activated carbon (left) copper substrate (right) gold substrate.

The purchased, activated carbon electrode was prepared using both the EPD technique and classical method. Figure 12 shows the CV and EIS measurement for both the case. The CV measurement was done at a scan rate of 10 mV/sec. The specific capacity was found to be 60.8 and 60 F/g for EPD and Classical method respectively. This result shows that EPD can be an efficient method for rapid deposition of uniform carbon particle films as supercapacitor electrode. Since EIS measurement shows the high impedance which may be a major factor in the decrease of capacitance value.

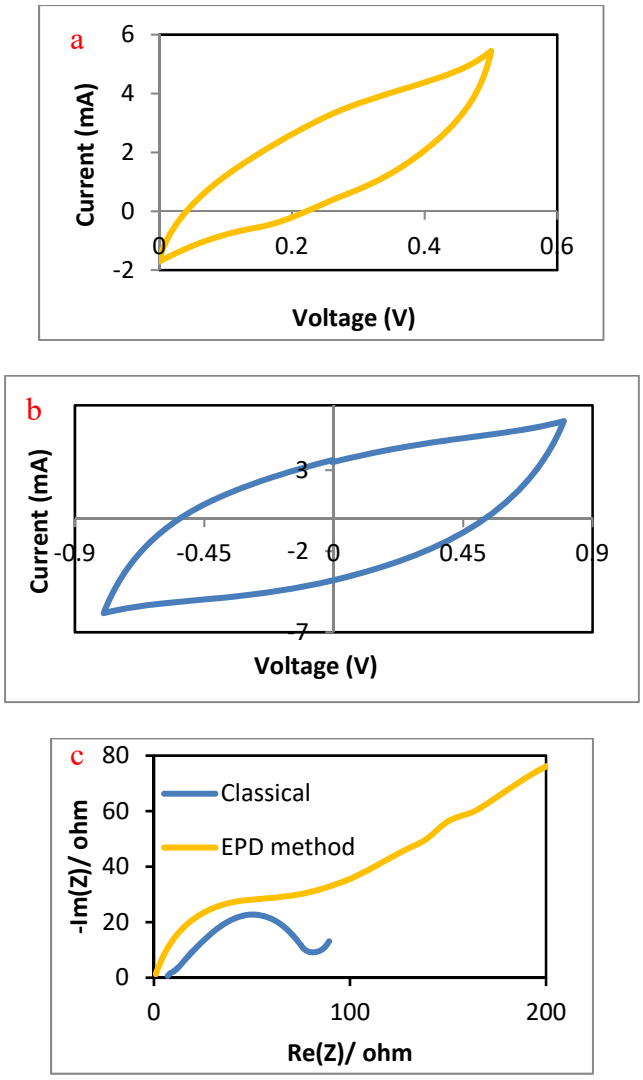

Figure 12: a) CV curve from EPD method b) CV curve from classical method c) EIS measurement.

For high capacitance value the biochar particles must be activated to increase the overall surface area. There are various technique used for activation like chemical, physical, plasma treatment. Plasma treatment is one the most economical and low temperature and environment friendly method. The Plasma treatment increases the surface area and porosity, improvement in wettability, increase in concentration of surface functional groups, decrease in electrical resistance, increase in electro catalytic activity for oxygen reduction. Figure 13 shows Raman spectra before and after plasma treatment. Raman spectra of biochar sample before and after plasma treatment show changed D-band (1320 cm^{-1}) and G-band (1580 cm^{-1}). There is high disordered and imperfect structure in plasma treatment biochar particles.

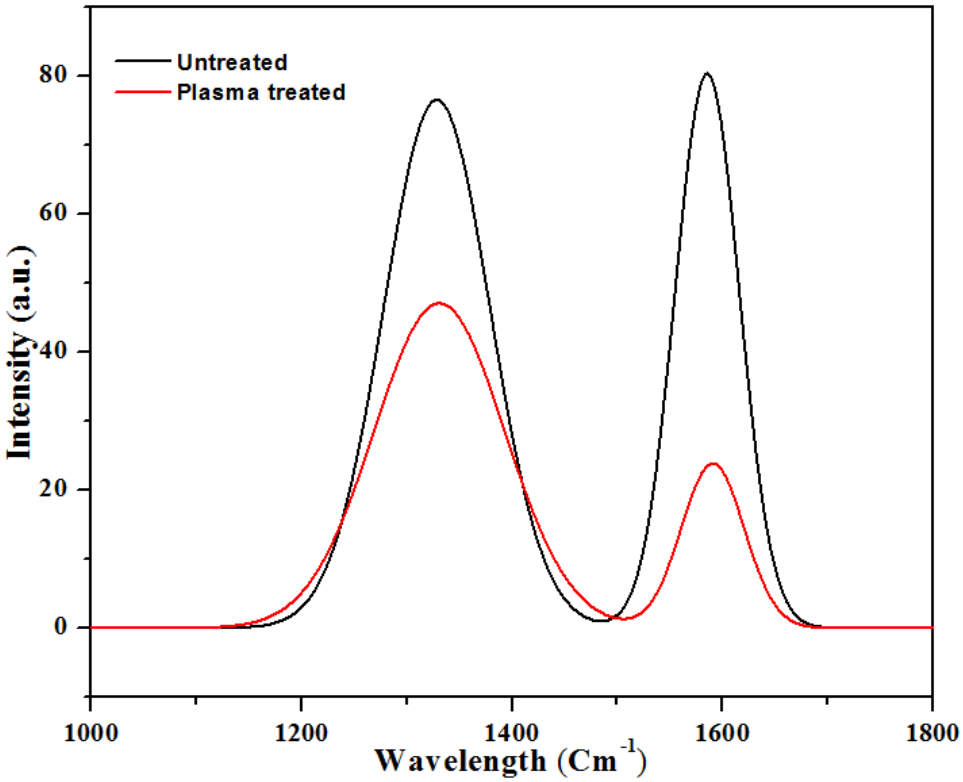

Figure 13: Raman spectra plot

Figure 14 show the SEM and TEM of the biochar particles before and after plasma treatment. From SEM image we would see biochar particles are big chunk with one penetrating over another. After plasma treatment the surface morphology has been changed with shows the large particles breaking down to small one. So plasma acts as etching process to remove the surface impurities and increase the overall surface area. To conform the result further TEM image was done were we found the similar case.

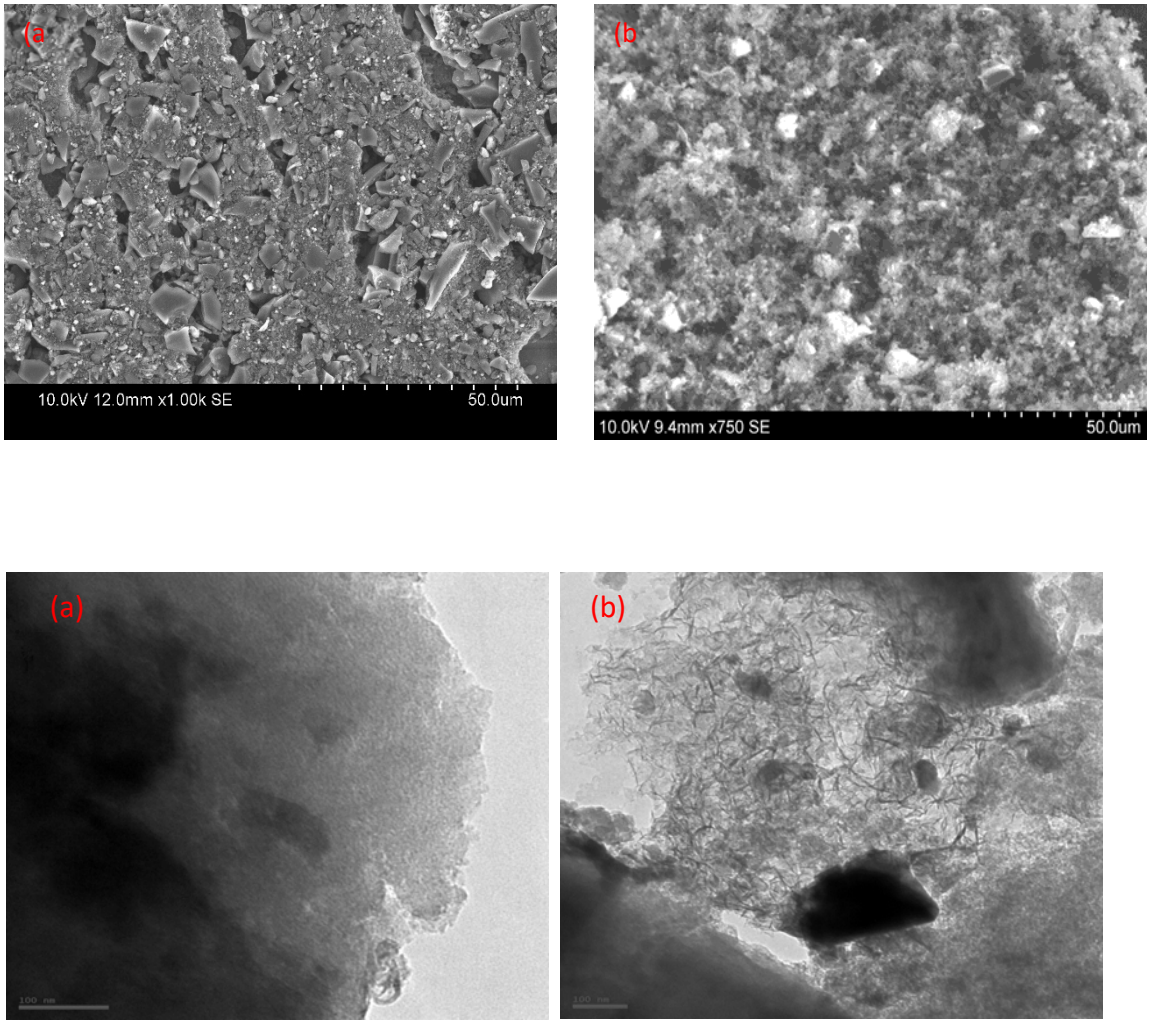

Figure 14: SEM and TEM image of biochar particle before and after plasma treatment.

Figure 15 shows the CV and EIS measurement of biochar supercapacitor for different cases a) untreated b) 2 min plasma treated particles c) 5 min plasma treated particles c) 10 min plasma treated particles d) 30 min plasma treated particles. This showed high improvement in impedance of sueprcapacitor and which was reflected on CV measurement. The capacitance of untreated biochar supercapacitors was found to be 60.4 F/g, while for the plasma treated at different case it was found to be, for 2 min - 80.4 F/g, 5 min - 171.4 F/g,10 min - 106.5 F/g, 30 min - 84.7 F/g. Biochar particles need to be activated to for higher capacitance.

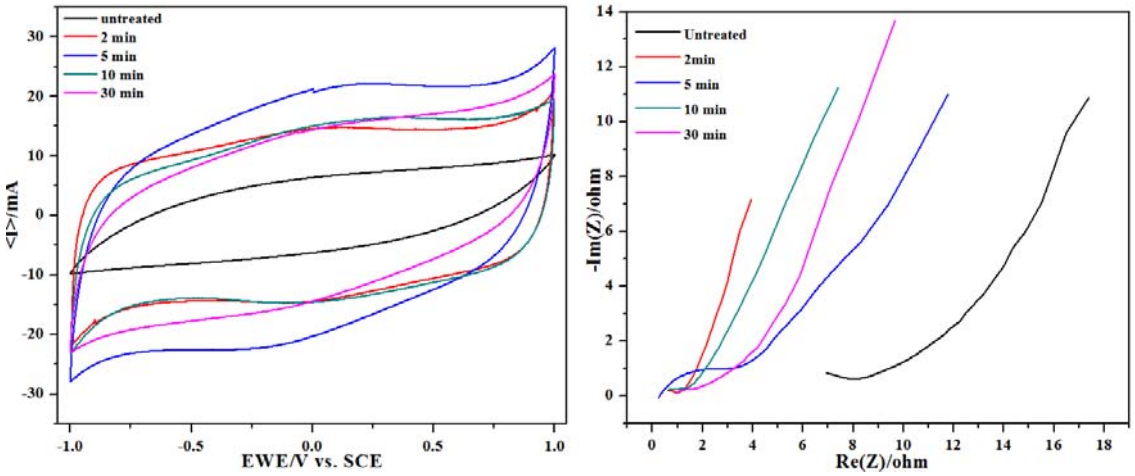

Figure 15: CV and EIS measurement of biochar electrode with and without plasma treatment.

Figure 16 shows the CV and EIS curves for untreated, oxygen plasma (5 min) treated, and chemical treated biochar supercapacitors. The absence of peaks in current within the range -1 to +1 V indicated the absence of reduction and non-faradaic process with considerable resistance to charge transfer (CV curves). The untreated biochar had an elliptical response. The oxygen plasma and chemical treated biochar had a more rectangular response, similar to that of an ideal electric double layer capacitor. The oxygen plasma treated, chemical treated, and untreated biochar-based supercapacitors had resistance of ~ 3.3 Ω, 14.5 Ω, and 8.2 Ω respectively. This indicated that plasma treated biochar supercapacitor had lower real resistance which was attributed to ions more easily entering the micropores. The accumulation of these charges at the electrode/electrolyte interface produced the capacitive behavior.

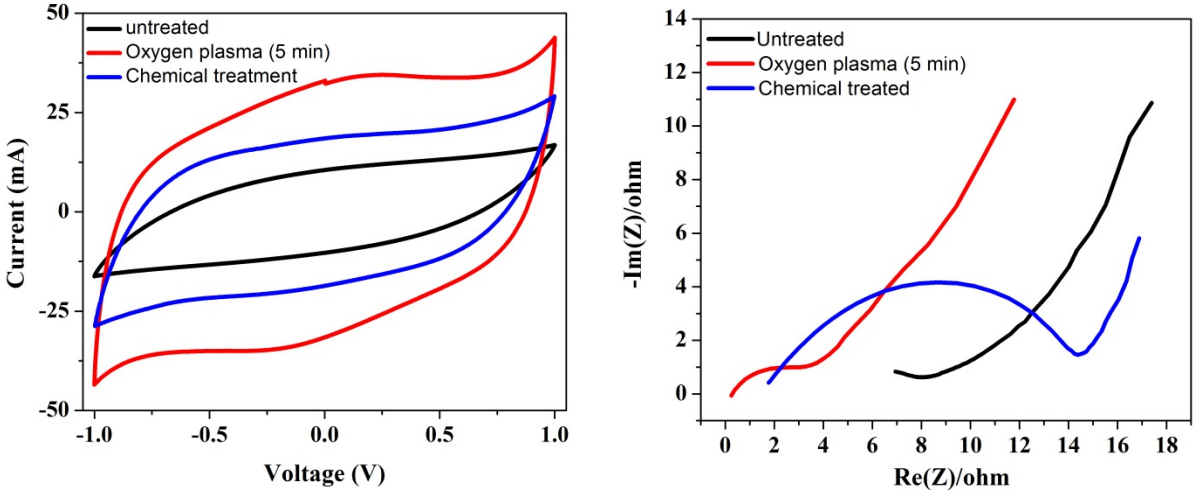

Figure 16: CV and EIS measurement of biochar electrode with and without plasma and chemical treatment.

Figure 17 shows the specific capacitance vs number of charge/discharge cycles for untreated, oxygen plasma, and chemical treated biochar supercapacitor at current density of 160 mA/g. The average specific capacitance was 60.4 F/g, 171.8 F/g, and 99.5 F/g for the untreated, oxygen plasma treated and chemical treated biochar respectively.

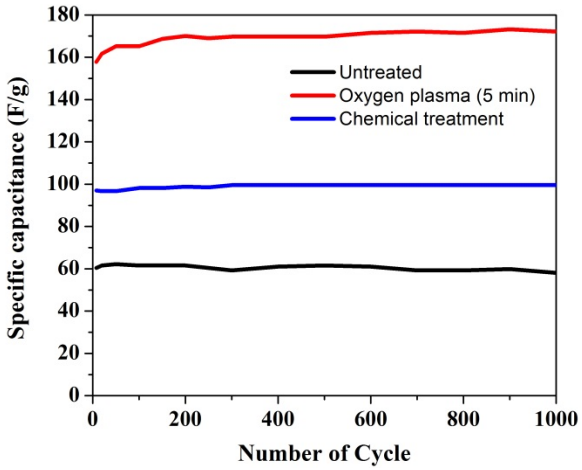

Figure 17: Specific capacitance vs number of charge/discharge cycles for untreated, oxygen plasma, and chemical treated biochar supercapacitors at current density of 160 mA/g.

Products developed under the award

Publications

- M. Dubey, R. Gupta, Z. Gu, Q. Fan, "Plasma Activation of Biochar Nanomaterials for Supercapacitors", J. Power Sources (submitted, 2014)
- R. Gupta, J. Hong, M. Dubey, X. Wang, V. Neto, J. Gracio, Z. Gu, Q. Fan, "Biochar Nanomaterials Activated by Oxygen Plasma for Energy Storage", Proceedings 5th International Conf. on Advanced Nanomaterials, 2-4 July 2014, Aveiro, Portugal
- R. Gupta, M. Dubey, Z. Gu, Q. Fan, "Comparison of Argon and Oxygen Plasma Activation of Biochar for Supercapacitors", Oral presentation, accepted for oral presentation at AIChE Annual Meeting, Nov. 20, 2014 Atlanta, GA
- R. Gupta, Z. Gu, Q. Fan, "High performance plasma treated biochar for supercapacitors", Oral presentation, 2014 ASABE Intersectional Meeting, Mar. 28 – 29, 2014, Brookings, SD
- R. Gupta, Z. Gu, Q. Fan, "Biochar for Energy Storage", GreenWeek poster presentation, May 1, 2014. This is a public education and outreach activity organized by SDSU

Networks or collaborations fostered.

- Established collaboration with the University of Aveiro, national lab PNNL, and the University of Toledo.

Technologies/techniques.

- Developed a novel plasma activation method to efficiently activate biochar.

Inventions/patent applications, licensing agreements.

- Mukul Dubey, Braden Bills, Qi Hua Fan, "Electrophoretic deposition of nanoparticle films for solar cell back reflector and other applications", US patent pending (2014)

- Mukul Dubey, Qi Hua Fan, "Plasma Induced Microporous Structures in Biocarbon", Invention Disclosure, April 8, 2014.

1. Academic

a. Courses developed
b. M.S. students supported: 2
c. M.S. degrees conferred: 1
d. Ph.D. students supported
e. Ph.D. degrees conferred
f. Post-docs supported

Please complete the following table to reflect your project at completion or time of report submission:

ITEM	NUMBER
Abstracts	
Peer Reviewed Publications	**1**
Outreach Publications/Web Pages	
Professional Presentations	**4**
MS Degrees Conferred	**1**
Ph.D. Degrees Conferred	
MS Students Supported	**2**
Ph.D. Students Supported	
Post-Docs Supported	
Undergraduate Students Supported	
Investigators Supported	
Start-Up Jobs Created	
Disclosures	**1**
Patents Filed	**1**
Provisional Patents	
Patents Issued	
License Agreements	**1**
Plant Variety Protection	
Subsequent Funding	

Back to Table of Contents

Sun Grant Initiative
DOE Final Progress Report

Project Title: Developing Gas Stripping - Adsorption/Desorption Separation Processes based on Porous Carbon Adsorbents for Biofuel Purification from Bioreactors

Project Director/Principal Investigator: Zhengrong Gu, Assistant Professor, Dept. of Agricultural & Biosystems Engineering, South Dakota State University, Brookings SD

All Co-Principal/Other Investigators: Muthu K., professor, Dept. of Agricultural & Biosystems Engineering, Gibbons W., professor, Dept. of Microbiology, Zhou R. Asso. professor, Dept. of Microbiology, South Dakota State University, Brookings SD

Period of Performance: 1 April 2013 - 31 June 2014

Funding Awarded: $30,338

Cost Share Amount: $ 7,585

Cost Share Sources: South Dakota Innovation Partners

Executive summary

In this project, viability of the innovative gas-stripping adsorption/desorption separation method was demonstrated. In this project, we have also quantified the dynamic and equilibrium adsorption/desorption capacity and thermo-chemical properties (desorption energy) of ethanol, acetone, and butanol on different renewable carbon adsorbents. An innovative adsorption/desorption characterization system (including Autochem-analyzer and connected on-line GC-MS) was assembled and successfully applied to quantified adsorption/desorption properties of different volatile chemicals on carbon adsorbents.

As a potential recovery method and separation process for achieving commercial production of volatile biofuels, including but not limited to ethanol, acetone, and butanol, the gas-stripping adsorption/desorption separation method showed higher energy efficient and lower cost than membrane pervaporation, adsorption in liquid phase and traditional distillation.

Project objectives

2.1 Equilibrium of adsorption/desorption on hierarchical carbon adsorbents
Adsorption equilibrium, as well as desorption energy of ethanol, butanol and acetone on different carbon adsorbents have been quantified. The desorption energy of all solvents decreased with loading dosage of solvents, while increased with surface area of adsorbents, which indicates the strongest binding happened at 1st layer adsorbed solvent. In addition, surface oxygen functional groups significantly change the desorption energy, more oxygen functional groups resulted in higher desorption energy, which indicated stronger interactions among surface functional oxygen groups and adsorbates (water, butanol and ethanol). (This objective is completed exactly as same as expected).

2.2. Dynamic adsorption/desorption on hierarchical carbon adsorbents
The dynamic adsorption capacity of pure chemicals and mixture of model biofuels (butanol, ethanol and acetone) and water on hierarchical carbon adsorbents have been quantified. Carbon adsorbents, which was developed from renewable biomass and biochar, have demonstrated high selectivity for separating butanol and linalool from water vapors (This objective is completed exactly as same as expected)

2.3 Dynamic adsorption/desorption of real biofuel samples on most promising adsorbents
The gas stripping adsorption/desorption units have been installed on multiple photobioreactors; as well as enabled collaborator, Dr. Zhou and Dr. Gibbons' team to quantify yield and expression level of volatile chemicals. An adsorption/desorption system and standard operation protocols have been developed for our partner (Dr. Deig Sandoval at Oglala Lakota College) in Native American Tribal College. (100% expected objectives have been achieved)

Project activities

Experiments have been performed to obtain baseline adsorption/desorption data for pure chemicals (Ethanol, Acetone, Butanol, and Water). A 50:50 mixture of Acetone and Ethanol was also analyzed using the Auto-Chem II and revealed promising results for initial product separation after a single adsorption /desorption step (Fig. 1).

Desorption heat/energy of pure ethanol, butanol and water has been quantified with DSC analyzer. The desorption energy decreased with loading dosage of solvents, while increased with surface area of adsorbents, which indicates the strongest binding happened at 1st layer adsorbed solvent. In addition, surface oxygen functional groups significantly change the desorption energy, more oxygen functional groups resulted in higher desorption energy, which indicated stronger interactions among surface functional oxygen groups and adsorbates (water, butanol and ethanol). A GC-MS system has been purchased and installed, standard curves of different model biofuels (i.e. ethanol, butanol, and acetone)

has been set up. Further tests of desorption energy and equilibrium adsorption capacity of linalool has been investigated (Table 1 and Figure 2).

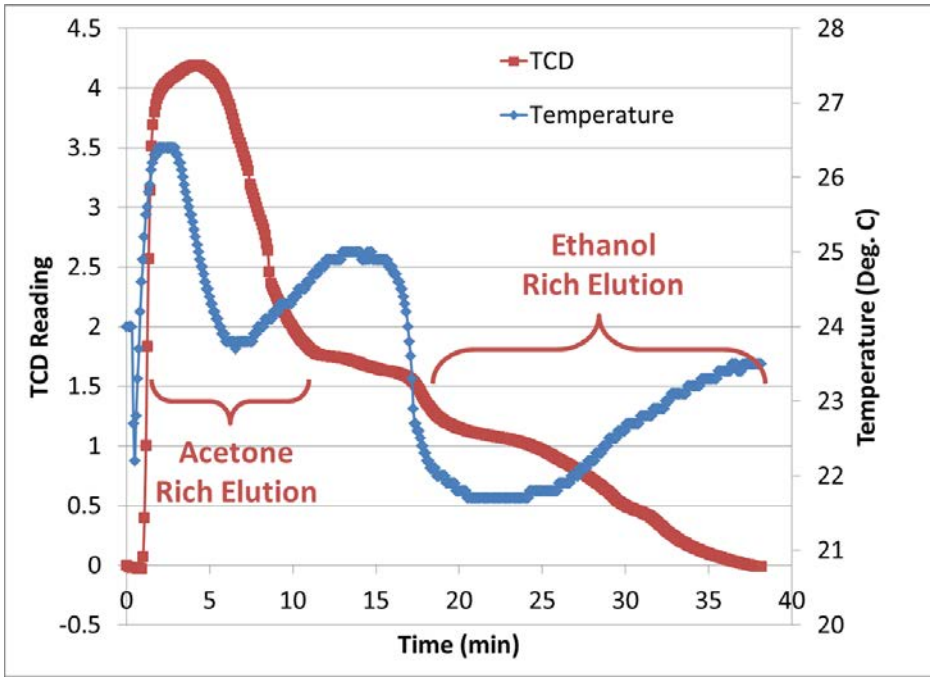

Figure 1 Separation of a 1:1 mixture of acetone and ethanol

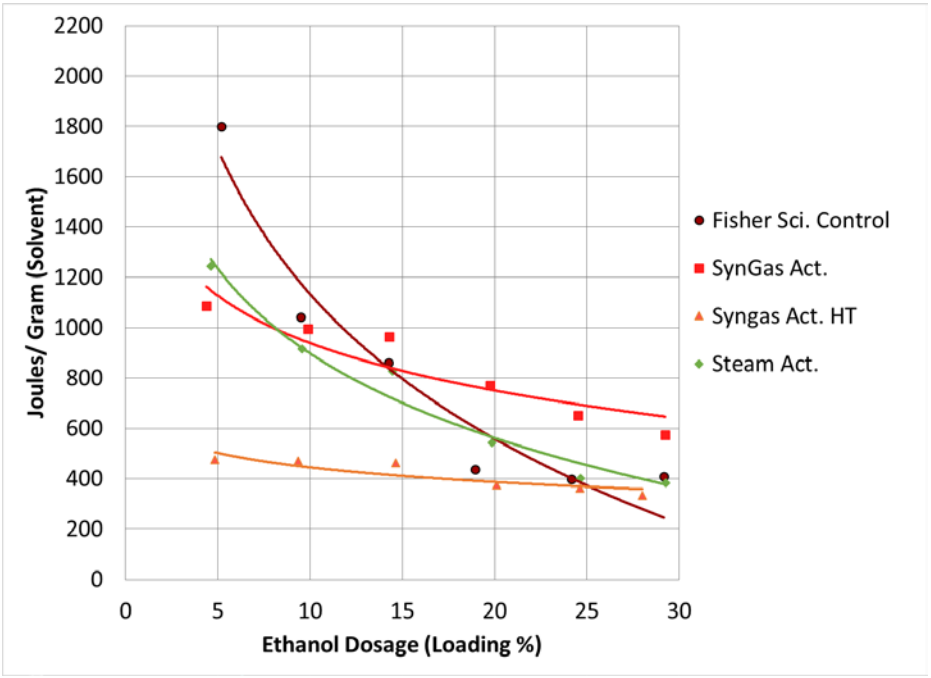

Figure 2 Desorption energy of ethanol (butanol, water and acetone show similar trend, but data was not included in this report)

Table 1. Desorption energy and equilibrium adsorption capacity of linalool			
	BET (M^2/g)	**Vpore (cm^3/g)***	**Oxygen functional group (O mg/g)**
Fisher Sci.	982	0.96	17.9
SynGas Act	847	0.71	12.5
Steam Act	623	0.53	35.7
SynGas Act Heated	620	0.56	5.5

An automatic analysis system has been designed and constructed from Micromatics Autochem Analyzer II and GC-MS. Autochem adsorption analyzer has been modified, by installing an on-line vapor generator, to evaluate dynamic adsorption/desorption of pure chemicals, such as butanol, acetone, ethanol and water. A GC-MS system has been connected with the Autochem system for quantification of chemicals during adsorption and temperature programmed desorption processes. The dynamic adsorption capacity of carbon adsorbents increased with surface area and temperature (30~50 C), while decreased with average pore size (Fig. 3). Dynamic adsorption/desorption of mixture of other model biofuels (butanol, and acetone) and water on hierarchical carbon adsorbents has been characterized with GC-MS connected with autochem-analyzer. Carbon adsorbents, which was developed from renewable biomass and biochar, have demonstrated high selectivity for separating butanol and linalool from water vapors.

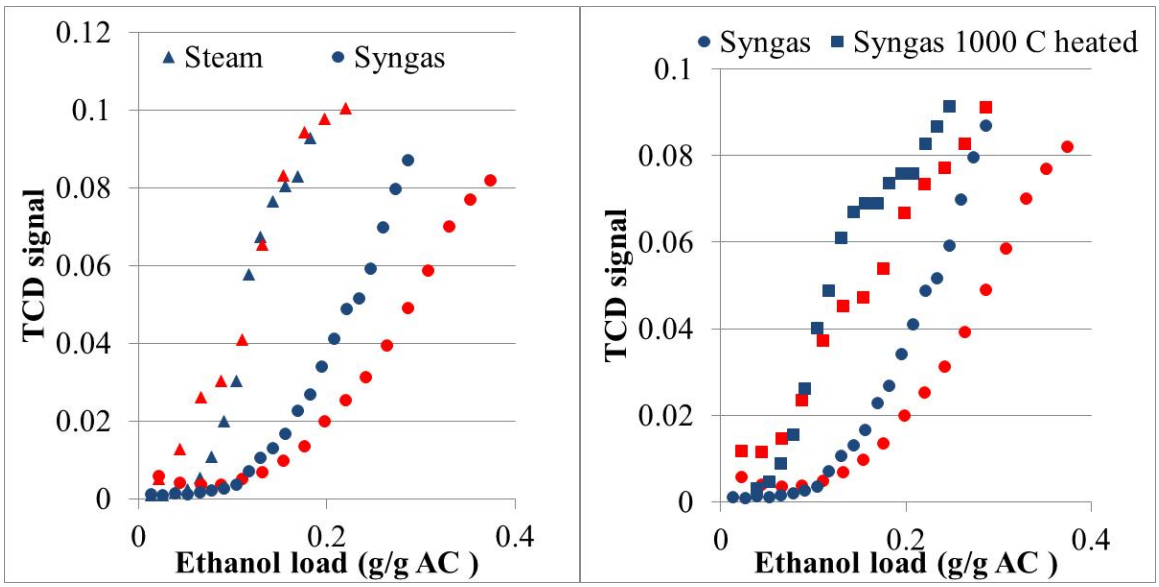

Figure 3 Dynamic adsorption of ethanol
(butanol, water and acetone show similar trend, but data was not included in this report)

Red: 50 C, Blue: 40 C

The gas stripping adsorption/desorption units have been installed on multiple photobioreactors. Polymer resin was used as adsorbents to capture the volatile products, released by transgenic cyanobacterial cultural liquid. This method enable collaborator, Dr. zhou and Dr. Gibbons' team to quantify yield and expression level of volatile chemicals. An adsorption/desorption system and standard operation protocols have been developed for our partner (Dr. Deig Sandoval at Oglala

Lakota College) in Native American Tribal College. All those adsorption units already significantly help collaborators recover their target biofuel products from cyanobaterials culture and improve their research ability in evaluating/quantifying expression level of target products.

Products developed under the award

a. Publications (list title, year, journal name, volume, issue, and page numbers),
b. Conference papers: (name of conference; location of conference; date of conference; and conference sponsor), or other public releases or outreaches of results.

1. Han Vu, Yuhe Cao, Zhengrong Gu, "Recovery of Butanol from Fermentation Using Chemically Modified Activated Carbon as Adsorbent", *REU Students Competition and South Dakota Science Symposium* (Funded by NSF-EpsCor), August 1 and 5th, 2014, Sioux Falls and Brookings SD
2. Yuhe Cao, Xiaomin Wang, Han Vu, Hong Jin, Zhengrong Gu, and Gibbons William, "Gas stripping and Adsorption/desorption separation of volatile alcohol from model solution", *NSF-EpsCor Track II DakotaBiocons annual meeting* (Funded by NSF-EpsCor), July 21, Fargo, ND .
3. J. Polin, X. Wang, J. Bassett, Z. Gu, K. Muthu, and W. Gibbons, Recovery of Butanol and Ethanol From a Photobioreactor Using Bio-Char Based Activated Carbon As Adsorbent, 2014 ASABE Intersectional Meeting, Mar 28-29, 2014, Brookings SD.
4. Gu ZR, Polin J, Muthu R, et al. 2013 "Volatile Product Recovery From a Photobioreactor Using Modified Blue Green Algae Strains and Bio-Char Based Activated Carbon As Adsorbent" AICHE (2013 annual meeting), San Francisco CA, November 6, 2013: 9:35 AM
5. Jacob Bassett, Joseph Polin, Xiaoming Wang, Hong Jin, Zhengrong Gu, "Desorption Thermodynamics of Volatile Organic Compounds from Activated Carbon", REU Students Competition 1st Award Poster (in 20 REU students), August 1,2013, SDSU Brookings

1. Academic

a. M.S. students supported:

Polin, Joe, MS Agricultural Engineering, (2011 Aug-2013 Aug) Pyrolysis and ignition of biomass dusts and physical activation of biochar.

b. M.S. degrees conferred:

Polin, Joe, MS Agricultural Engineering, (2011 Aug-2013 Aug) Pyrolysis and ignition of biomass dusts and physical activation of biochar.

c. Ph.D. students supported

Jin, Hong, PhD Biological science (2011 Aug-2014) Bio-renewable carbon materials for electrical energy storage. Received SDSU Nelson Graduate Award 2013; 5 first author journal articles,

d. Ph.D. degrees conferred

Jin, Hong, PhD Biological science (2011 Aug-2014) Bio-renewable carbon materials for electrical energy storage. Received SDSU Nelson Graduate Award 2013; 5 first author journal articles,

2. For projects involving computer modeling, provide the following information with the final report:

a. Model description, key assumptions, version, source, and intended use.
b. Performance material for the model related to the intended use.

c. Test results to demonstrate the model performance criteria were met (e.g., code verification/validation, sensitivity analyses, history matching with lab or field data, as appropriate).
d. Theory behind the model, expressed in non-mathematical terms.
e. Mathematics to be used, including formulas and calculation methods.
f. Whether or not the theory and mathematical algorithms were peer reviewed, and, if so, will include a summary of the theoretical strengths and weaknesses.
g. Hardware requirements.
h. Documentation (e.g., user's guide, model code).

***Software/Manual (if applicable)**
Content. Unless otherwise specified in the award, the following must be delivered: source code, the executable object code and the minimum support documentation needed by a competent user to understand and use the software and to be able to modify the software in subsequent development efforts.

Please complete the following table to reflect your project at completion or time of report submission:

ITEM	NUMBER
Abstracts	**5**
Peer Reviewed Publications	**2**
MS Degrees Conferred	**1**
Ph.D. Degrees Conferred	**1**
MS Students Supported	**1**
Ph.D. Students Supported	**1**
Start-Up Jobs Created	
Disclosures	
Patents Filed	
Provisional Patents	
Patents Issued	
License Agreements	
Plant Variety Protection	
Subsequent Funding	

Back to Table of Contents

Sun Grant Initiative

DOE Final Progress Report

Award Number: DE-FG36-08GO88073

Recipient: Lin Wei, James Julson

Project Title: Catalytic Fast Pyrolysis Conversion of Corn Stover to Drop-In Quality Hydrocarbons

Project Director/Principal Investigator:

Dr. Lin Wei, assistant professor, Department of Ag. & Bio. System Engineering, South Dakota State University, Brookings, SD 57007

All Co-Principal/Other Investigators:

Dr. James Julson, Professor, Department of Ag. & Bio. System Engineering, South Dakota State University, Brookings, SD 57007

Collaborators (Cost-Sharing Partners):
Ms. Mary Beth Fishback, Director of Operations, Thermo-Ag, LLC. Brookings, SD 57006

Period of Performance: 1 March 2013 – 28 February 2014

Funding Awarded: $52,805

Cost Share Amount: $49,986

Sources of Cost Share: Thermo-Ag, LLC

Executive summary

Catalytic fast pyrolysis (CFP) has emerged as the most promising process for thermochemical conversion of lignocellulosic biomass to advanced biofuels in recent years. South Dakota State University (SDSU) researchers have developed a proprietary CFP technology to produced quality bio-oils from various biomass feedstocks, which can be upgraded to advanced biofuels using a sequential hydrodeoxygenation (HDO) reactor. The biofuels produced were compatible with petroleum-derived hydrocarbons and can be directly dropped in an existing petroleum refinery for further refining to "green" gasoline, diesel, and jet fuel. However, current carbon conversion efficiency and effectiveness of the catalyst systems remain suboptimal. Based on the first generation SDSU proprietary CFP reactor, a second generation of CFP reactor was fabricated in this project. The effects of different catalysts and their implementations on bio-oil yield and quality were investigated for converting corn stover to "drop-in" biofuels using the CFP process. Instead of noble metals Pt, Pd, or Ru, transition metals Mo and Cu combined with ZSM-5 were formulated to synthesize new catalysts. Two different catalyst implementation systems, In-situ CFP and Ex-situ CFP, were examined. Results obtained indicated that CFP reactor configuration, catalyst and its implementation significantly affect bio-oil yield and quality. In addition to commercial potential of the SDSU proprietary CFP reactor and new catalyst systems, this research provide very helpful information for fully understanding the chemical mechanism of CFP–HDO process and the linkages between biomass species, reaction temperature, catalyst systems, and the yield and quality of drop-in biofuels produced. The information is also very useful for renewable biofuel industry and public awareness regarding to sustainable agriculture and advanced biofuels production. Because of helping in domestic biofuel production, the project will eventually benefit national energy security and greenhouse gas (GHG) emission reduction.

BACKBROUND AND OBJECTIVES

Biomass is the only sustainable alternative to fossil fuels capable of yielding petroleum like products that can be important feedstocks for manufacturing goods ranging from plastics and chemicals to fuel oil, lubricating oil, and hydraulic fluids using existing infrastructures [1 – 7]. Fast pyrolysis is one of the most promising thermochemical technologies with the potential to convert cheap, local, and abundant lignocellulosic biomass such as corn stover into a useful form [2 – 6]. When catalyst is integrated with fast pyrolysis, the process is so called catalytic fast pyrolysis (CFP), in which biomass is heated up to 400 – 600^{o}C in the absence of oxygen and presence of catalysts decomposing the biomass to quality bio-oil and small amounts of co-products (bio-char and syngas). The bio-oils produced can be sequentially upgraded into liquid hydrocarbon fuels using a separate hydrodeoxygenation (HDO) reactor. A theoretical yield of hydrocarbon fuels can be up to 150 gallons per dry ton of biomass, depending on feedstock species, reactor types, operating conditions, and catalysts used [2 – 11]. Despite the potential of CFP technologies, effective catalysts and carbon conversion efficiency remaining the biggest challenge [3 – 6, 8, 10].

Our research team at South Dakota State University (SDSU) has conducted an ongoing project to Catalytic Fast Pyrolysis Convert Agricultural and Forest Residues to Aromatic Fuel Additives through funding by DOE (award number: DE-FG36-08G088073/M001). The team has developed a proprietary CFP reactor with a biomass feeding capacity of 1 – 3kg/h, which was capable of converting various biomass to quality bio-oils and upgraded the bio-oils to liquid

hydrocarbon fuels in sequence with a HDO reactor. The hydrocarbon fuel produced by this CFP–HDO process is called drop-in fuel since it is compatible with petroleum-derived hydrocarbons and can be directly dropped in an existing petroleum refinery for further conversion to "green" gasoline, diesel, and/or jet fuels. A comparison of the drop-in fuel and petroleum-derived gasoline is shown in Table 1. A sample of the drop-in fuel produced and its GC/MS analysis are shown in Figure 1. This drop-in fuel consists mainly of aromatics and olefins (over 85% of the hydrocarbons in the range of C5 – C16).

Table 1. Comparison of advanced biofuel produced from sawdust and petroleum based gasoline

Properties	**SDSU drop-in fuels**	**Gasoline**
pH value	5.0 – 5.6	–
Viscosity cSt @20ºC	1.2 – 1.88	0.4 – 0.8
Density, Kg/L	0.8 – 0.85	0.745
Heating value, MJ/kg	41 – 48	43
Carbon content, % w.t.	84.59 – 85.12	85 – 88
Hydrogen content, % w.t.	9.9 – 11.26	12 – 15
Oxygen content, % w.t.	< 0.72	0
Water content, % w.t.	< 0.25	0

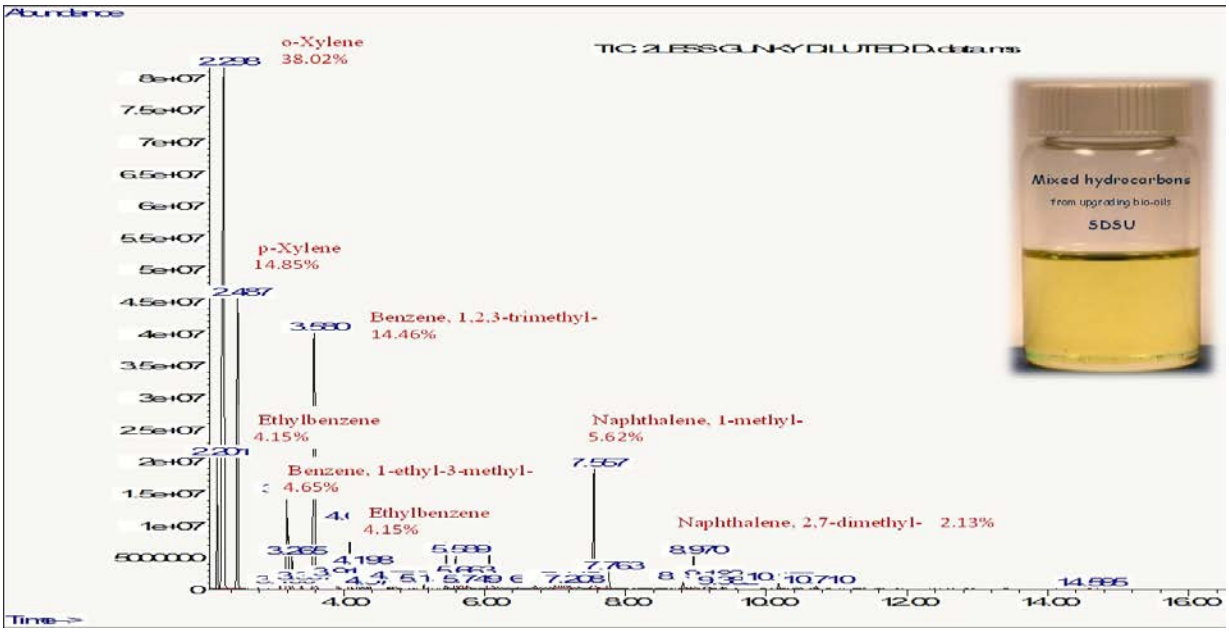

Figure 1. GC-MS profile of the drop-in fuel (hydrocarbons mixture) sample produced from sawdust by the SDSU team and the sample picture.

Although the combined evidence supports the potential of quality, efficiency, and cost-effectiveness of the SDSU process, current carbon conversion efficiency and the catalyst system used remain suboptimal. The original CFP reactor designed by the SDSU team did not include an

air lock at the feedstock entrance port resulting in feeding auger seal inefficiency. Thus more ambient air entered the reactor than is optional. This additional air resulted in low bio-oil yield and quality that significantly influenced the bio-oil upgrading in the sequence HDP reactor for higher drop-in fuel yield and quality. On the other hand, the current high cost noble metal catalysts used were inefficient due to improper catalyst implementation and deactivation. Carbon conversion efficiency of the CFP–HDO process was just about 30% (equivalent to 30 – 40 gallons drop-in fuel per dry ton of biomass), and the production costs was still too high to commercialize the drop-in fuel in market. Thus, there is a critical need to improve the CFP–HDO technologies to an efficient scalable process for the production of drop-in fuels from lignocellulosic biomass. A catalyst systems including effective catalysts and their implementation is the most important component in the CFP–HDO process. The selected catalyst system should be highly active, selective for the production of desired products, resistant to deactivation, readily recycled, and cost competitive. Successfully developing such catalyst system is the key to open the 'door' of commercialization of drop-in fuel production. In the absence of the catalyst system, the promise of a renewable drop-in fuel that is alternative to fossil fuels but does not threaten human or animal food availability will likely remain limited [7 – 11].

The goal of this project is to develop an effective catalyst system and improve the CFP–HDO process for optimization of the decomposition of lignocellulosic biomass to bio-oil that is then upgraded to quality drop-in fuels. The central hypothesis is that integration of effective catalysts coupled with reactor structure modification would effectively improve the catalyst system performance that can increase carbon conversion efficiency and drop-in fuel yield and quality in the CFP–HDO process. To achieve this goal, the specific objectives are to:

1) Eliminate additional air entering the CFP reactor through the biomass feed port to improve bio-oil yield and quality.
2) Develop an effective catalyst system to improve the CFP-HDO process carbon conversion efficiency and production cost.
3) Evaluate the catalyst system performance on bio-oil yield and quality for sequentially upgrading the bio-oil in HDO reactor.
4) Characterize the bio-oils produced for future commercialization of the CFP–HDO process.

The improvement of the CFP–HDO process will likely make possible commercial production of drop-in fuels from biomass. Achieving the specific objectives proposed will provide significant improvement over existing CFP solutions. The proprietary CFP reactor can be integrated with a specific HDO reactor, unique catalyst systems, and accurately controlling reaction conditions into a continuous process. It can provide a favorable environment for decomposing biomass into higher quality bio-oil at higher yield rates while minimizing carbon loss in syngas and bio-char. Properly applying the effective catalyst systems having high selectivity to remove toxic substances or impurities will help the bio-oils when sequentially upgraded resulting in higher yields of drop-in fuels. Thus effectively advancing the technology toward the profitable target: 60% carbon conversion efficiency (equivalent to 70 – 90 gallon of drop-in fuel per dry ton biomass). The research outcomes will help to fully understand the chemical mechanism of CFP–HDO process and the linkages between biomass species, reaction temperature, catalyst systems, and the yield and quality of drop-in fuels produced. Such knowledge is the key for development of a scale up ready CFP–HDO technology and accelerates commercialization of the technology

to renewable energy markets. Because of domestic biofuel production, development of the CFP–HDO technologies is likely to eventually benefit national energy security and GHG emission reduction. Thus, the outcomes are not only expected to fundamentally advance the field of bio-refinery, but also to have simultaneous broad and highly positive societal impact. In addition, information on economic potential, possible environmental impact, and other biomass feedstocks' utilization are likely provided for renewable biofuel industry and public awareness regarding to sustainable agriculture and advanced biofuels production.

APPROACH AND METHODOLOGY

Biomass Feedstock

Corn stover is the largest single source of crop residues available in U.S. [7] The corn stover used as feedstock in this project was harvested from an agriculture extension farm nearby SDSU after corn harvest, allowed to dry to about 15 – 20% of MC (moisture content, wet basis) in a swath prior to baling, and then bales stored indoors for three months. Before hammer milling, corn stover was chopped into small pieces using a knife mill with a 25.4 mm screen. A commercial knife mill (H.C. Davis Sons Mfg. Co., Inc., Bonner Springs, KS) was used for the chopping. After size reduction, the small corn stover pieces were layered on floor and air-dried to about 10 – 12% MC. The dried corn stover pieces was ground into powder using a hammer mill (Model M150, Winona Attrition Mill Co. MN) with a 1 mm screen.

Catalysts preparation

ZSM-5 was purchased from Zeolyst Company. The ZSM-5 was impregnated with a specific loading level of active transition metals (e.g. Cu, Mo, Ni, Co, etc.) using wet impregnation method and blended with guar gum and boehmite. The catalysts were prepared by pelletizing the mixture into particles with a diameter of 3 mm and the length less than 5 mm. The catalyst pellets were dried at 120˚C for 12hr and calcined at 550℃ for 5hr before use.

Catalysts characterizations

The Brunauer–Emmett–Teller **(**BET) specific surface area and porosity texture of each catalyst were determined by nitrogen adsorption measurements at 77.2 K using an automatic Micromeritics ASAP 2400 apparatus. The catalyst samples were first degassed at 573 K for approximately 6 h and then studied with a static volumetric technique. X-ray crystallography (XRD) was used for phase identification and determination of the relative crystallinity. XRD measurements were carried out using Cu Kα radiation on a RIGAKU SMARTLAB. The X-ray tube was operated at 40 kV and 44 mA and the X-ray pattern was scanned with a step size of crystallite sizes of 0.02° (2θ) from 5 to 50° (2θ) and counting time of 1 s per step.

Bio-oil and drop-in fuel characterization

The pH values of bio-oils and drop-in fuels were measured by a pH meter (AB15, Accumet Company) at room temperature. The instrument was calibrated with liquid calibration standards of pH 4 and 7 prior to the measurement. The viscosity analyzer (REOLOGICA Instruments AB Company Dynamic Viscosity) was used to measure dynamic viscosity at 20 ℃. The bio-oil and drop-in fuel elemental compositions of carbon, hydrogen, nitrogen, and oxygen were determined by the CE-440 Elemental Analyzer. The HHV of samples were determined using a bomb calorimeter (IKA C2000). The moisture contents of samples were measured using a Karl Fischer Titrator V20 (Mettler Toledo Company). Syngas analysis was carried out on a GC (Agilent GC-7890A) equipped with a thermal conductivity detector (TCD) and flame ionization detector

(FID). Standard gas mixtures were used for calibration, and argon was used as the carrier gas. GC/MS (Agilent GC-7890A and MSD-5975C) was used to analyze the chemical composition of bio-oil and drop-in fuel samples. The gas chromatograph was programmed at 60 °C for 1 min, followed by ramp 1 at 3 °C/min to 260 °C and ramp 2 at 5 °C/min to 280 °C. The temperature was held for an additional 10 min after each ramp. The injector temperature was 300 °C, and the injection size was 1 μL. The flow rate of carrier gas (hydrogen) was 1 mL/ min. The compositions were identified through the NIST Mass Spectral Library.

Experimental apparatus and procedure ***(this section has been deleted as it contains confidential and proprietary information)***

(End of confidential information)

Results and Discoveries

Effect of catalyst to corn stover ratio on In-situ CFP process

An In-situ CFP test of corn stover was carried out to examine the effect of biomass to catalyst ratio on the bio-oil yield and quality. The test was conducted with a 2:1 ratio of biomass to catalyst in the lab scale fixed-bed reactor. As a control, pyrolysis of corn stover without catalyst was also carried out. The proportions of three products of corn stover CFP with/without catalyst is showed in Figure 6. There is no significant difference in the proportion of the three products between corn storver CFP with and without catalyst. This may be because the catalyst was covered or deactivated by the corn stover powder and ash when the biomass was more than catalyst in the mixture, or because there were no enough active sites for the CFP reactions to make the catalyst able to function properly. The composition of syngas produced is shown in Figure 7. The major compounds in syngas were CO and CO_2 with a little of N_2 There was no H_2 or CH_4 detected in the syngas. This result indicated that there was air (oxygen) to be involved in the CFP processing because the ambit air entered into the reaction chamber due to reactor system sealing issue. The small amount of N_2 in the syngas is the residue of carried gas or the ambit air entering into the reactor. Some of physical properties of the bio-oils are listed in Table 2. The energy content was low due to high water content of the bio-oils, 69% for corn stover pyrolysis without catalyst and 73% for corn stover CFP. This also proved that some of corn stover was “burned” (oxidation) with air and generated a large amount of water and CO_2 due to ambit air involving in the reactions if the reactor system had sealing problem. The 4% more water in CFP products came from the deoxygenating reactions due to the catalyst presenting [8, 11 – 12].

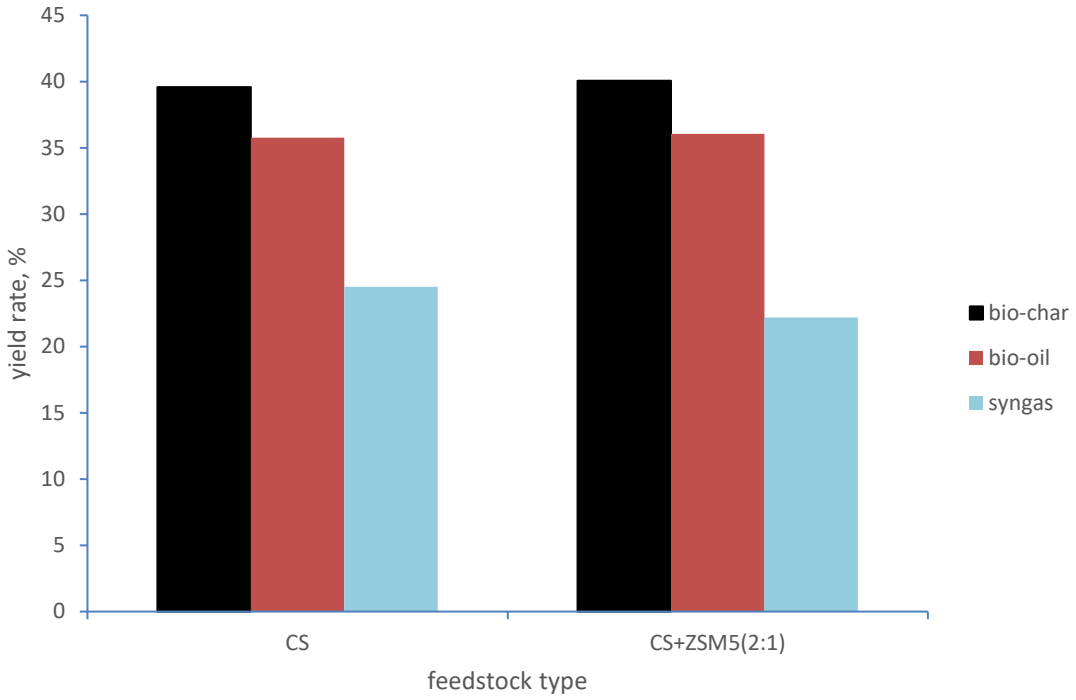

Note: CS = Corn Stover, Catalyst = ZSM5

Figure 6. Proportion of three products of corn stover CFP

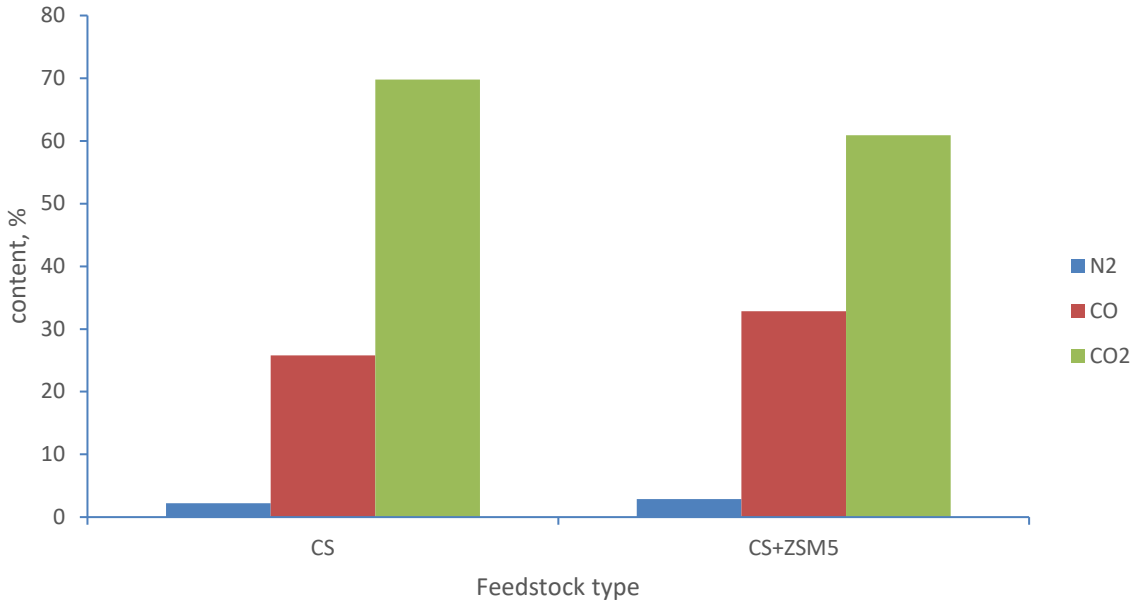

Figure 7. Composition of syngas produced in Corn Stover CFP

Table 2. Some physical properties of bio-oil produced in corn storver CFP

Properties	CS	CS+ZSM5
Density(g/ml)	1.09	1.05
MC (%)	69.16	73.06
pH	3.18	3.43
energy content (KJ/g)	6.88	N/A

Note: MC of bio-oil produced from CS+ZSM5 was too high to measure its energy content in our labs.

Effect of catalyst implementation system on corn stover CFP process

The effects of catalysts implementation systems on corn stover CFP process was investigated in this project. Two different catalyst implementation systems (In-situ CFP and Ex-situ CFP) for corn stover CFP process were carried out. In the In-situ CFP system, corn stover and catalyst (ZSM5) were mixed with a 2:1 ratio of biomass to catalyst and then pyrolyzed in the lab scale fixed-bed CFP reactor (Figure 3), named CSMC. In the Ex-situ CFP system, corn stover was pyrolyzed first and thus the produced bio-oil vapor went through a catalyst column in the coupled fixed-bed reactor (Figure 4), called CSCC. As control, corn stover was pyrolyzed without catalyst in the coupled fixed-bed reactor, called CS. All the CS, CSMC, and CSCC tests were respectively conducted at three different temperatures, 400, 500, and 600°C, respectively. The CFP product yield rates of the three catalyst implementations at three reaction temperatures are shown in Figure 8 – 10. It was found that catalyst implementation systems and reaction temperatures have significant influence on the three CFP products' (bio-oil, bio-char, and syngas) yield rates. When corn stover pyrolysis reaction temperatures increased, bio-char yield rates decreased while syngas yield rates increased for all of the three catalyst implementation systems. In contrast, the bio-oil yield rates had no significant difference when corn stover was pyrolyzed with CS and CSCC systems at the three reaction temperatures. The bio-oil yield rates increased when reaction temperatures increased if corn stover was pyrolyzed with the CSCM system. The highest bio-oil yield but lowest bio-char yield was obtained when the corn stover CFP process was conducted in the CSMC system at 500 °C. The lowest bio-oil yield but highest bio-char yield was obtained when the CFP process was conducted in the CSCC system at 400 °C. The bio-oil yields were low while syngas yields were high due to low efficiencies of the condenser units used in the CFP process. Some bio-oil vapors escaped with the syngas from the condensers. Another discovering is that the Ex-situ CFP system consumed catalysts 3 times less than that of the In-situ CFP system, but had higher catalysis efficiency and better bio-oil quality.

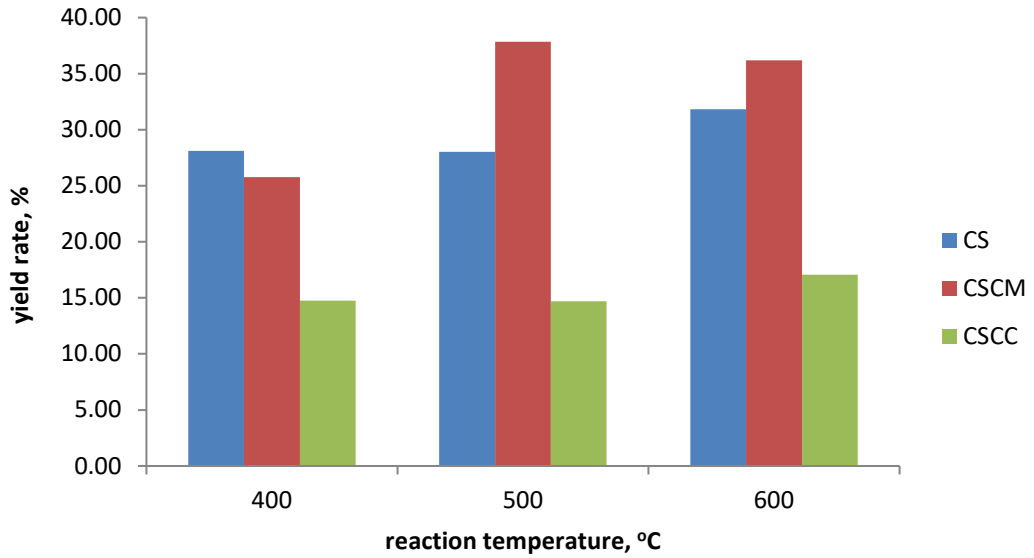

Figure 8. Bio-oil yield rates of different catalyst implementation systems at three temperatures

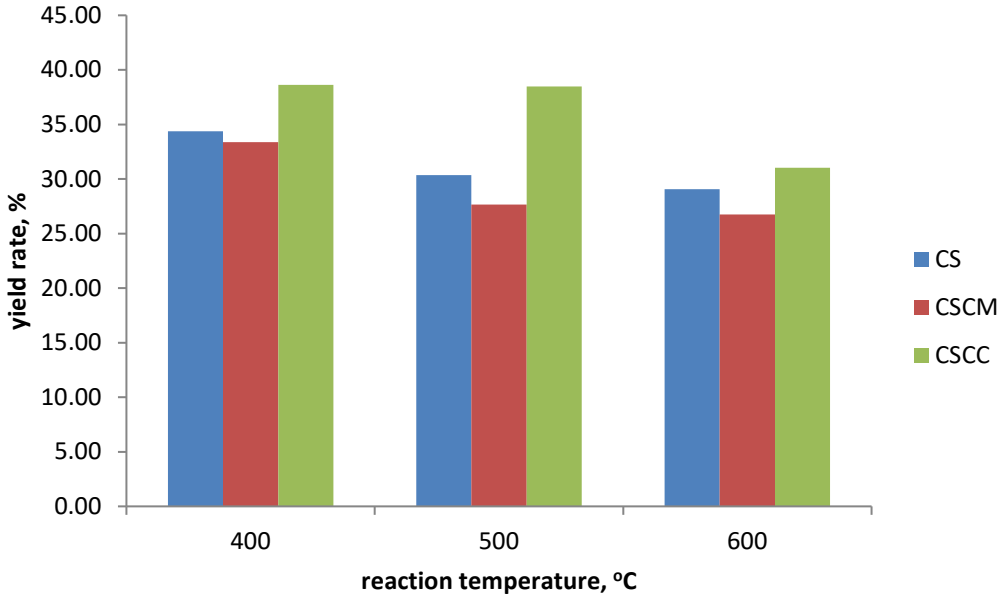

Figure 9. Bio-char yield rates of different catalyst implementation systems at three temperatures

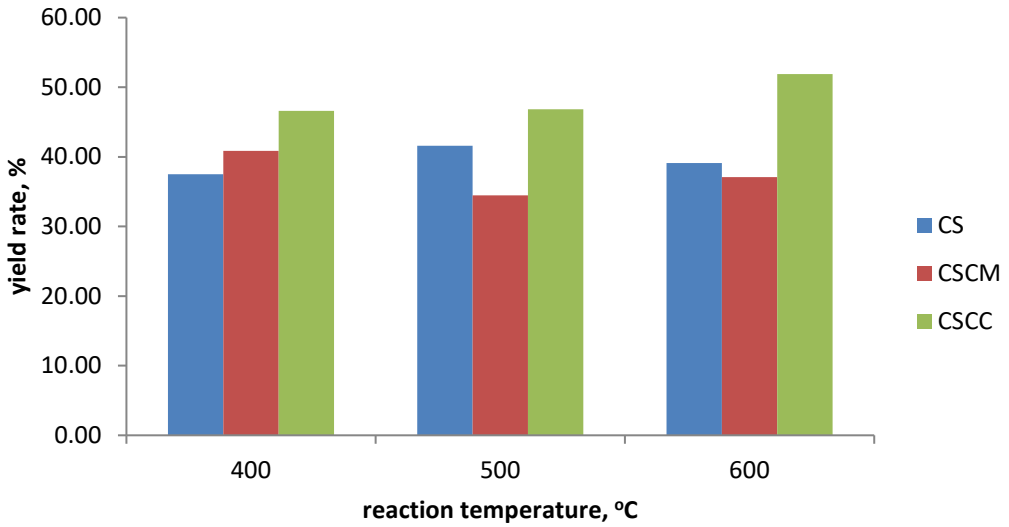

Figure 10. Syngas yield rates of different catalyst implementation systems at three temperatures

The effects of reaction temperatures on the bio-oils properties are shown in Figures 11 – 14. The results indicate that catalyst implementation systems and reaction temperatures have significant effects on bio-oil properties. Corn stover mixed with catalyst in CFP process led to highest pH value and density. The bio-oil densities increased when reaction temperatures increased. Because oxygenation reactions taking place in CFP process can produce more water, the MC of bio-oil increased for the CSCM and SCCC systems, but these oxygenation reactions were flavor to higher reaction temperatures (500 and 600°C) [6, 8 – 11]. There was no significant difference in MC of bio-oils produced from all systems at 400°C. Catalyst implementation systems and reaction temperatures had no significant influence on bio-oil viscosity.

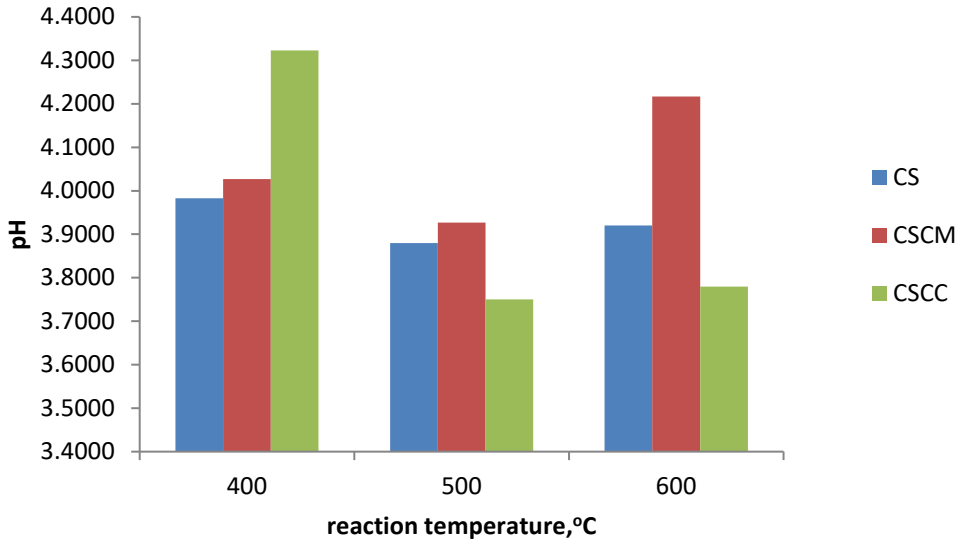

Figure 11. Effects of catalysts and reaction temperatures on bio-oil pH value.

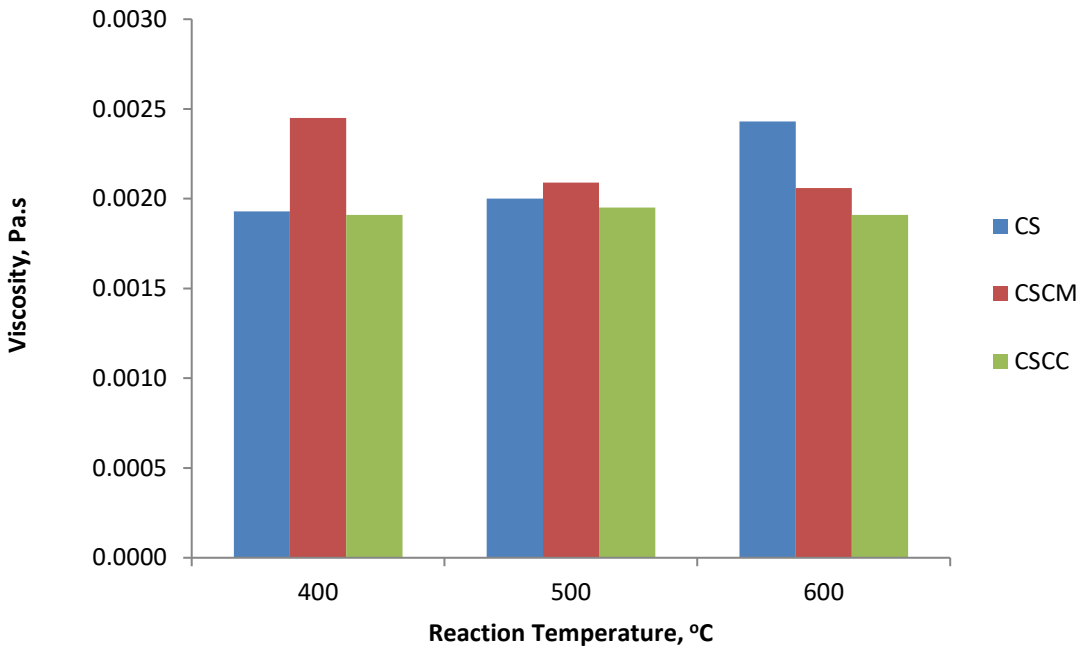

Figure 12. Effects of catalysts and reaction temperatures on bio-oil viscosity.

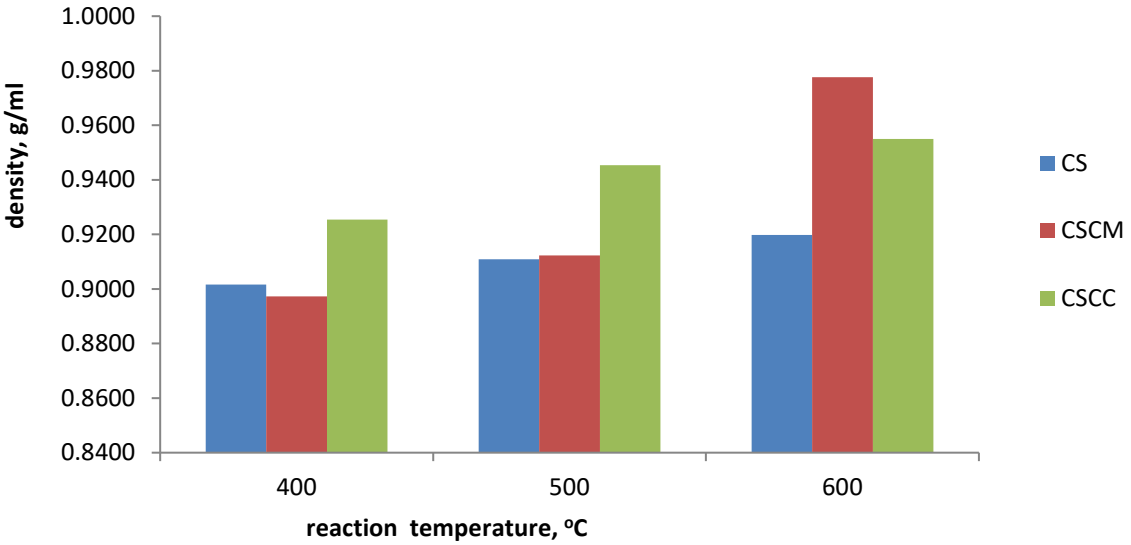

Figure 13. Effects of catalysts and reaction temperatures on bio-oil density

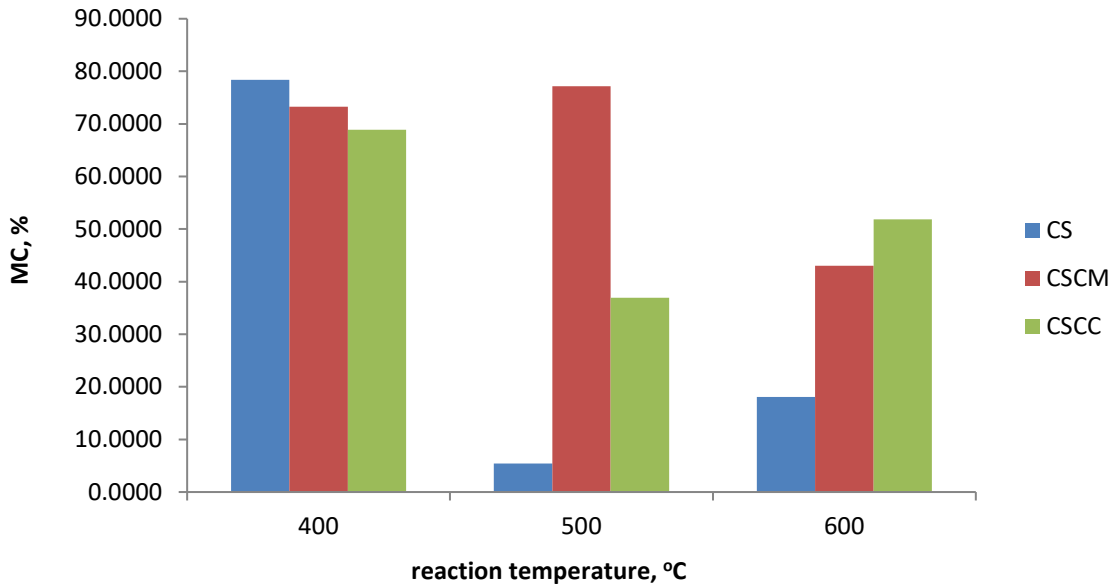

Figure 14. Effects of catalysts and reaction temperatures on bio-oil moisture content.

Catalyst development for CFP process

Instead of noble metals Pt, Pd, or Ru, transition metals Mo and Cu combined with ZSM-5 were used to develop effective catalysts for the CFP process in this projects. Different ratios of Mo-Cu were respectively impregnated into ZSM-5 to formulate 6 different catalysts. Based on the test results of In-situ and Ex-situ catalyst implementation systems, Ex-situ CFP system was found to be better for corn stover conversion to drop-in fuel. These six catalysts were tested to figure out an effective catalyst system for the CFP process using the coupled fixed-bed reactor. The yield rates of three products (bio-char, bio-oil, and syngas) of corn stover pyrolysized in the Ex-situ reactor are shown as Figure 15. The results indicated catalysts have significant influences on the bio-oil yield rates. Among the catalysts tested, ratio of Mo-Cu 2:1 showed the best performance with the highest bio-oil yield (29.04 %) and the lowest syngas yields (45.95 %). Compared to literature data of bio- 60-75% oil yields [13 – 19], this bio-oil yield is low. Again, the low bio-oil yields and high syngas yields were due to low efficiencies of the condenser units used in the CFP process. Some bio-oil vapors escaped with the syngas from the condensers. In order to improve the yield of bio-oils, a more effective condenser system should be designed and implemented that can cool the syngas more efficiently, allowing more bio-oil vapor to be condensed into liquid bio-oils.

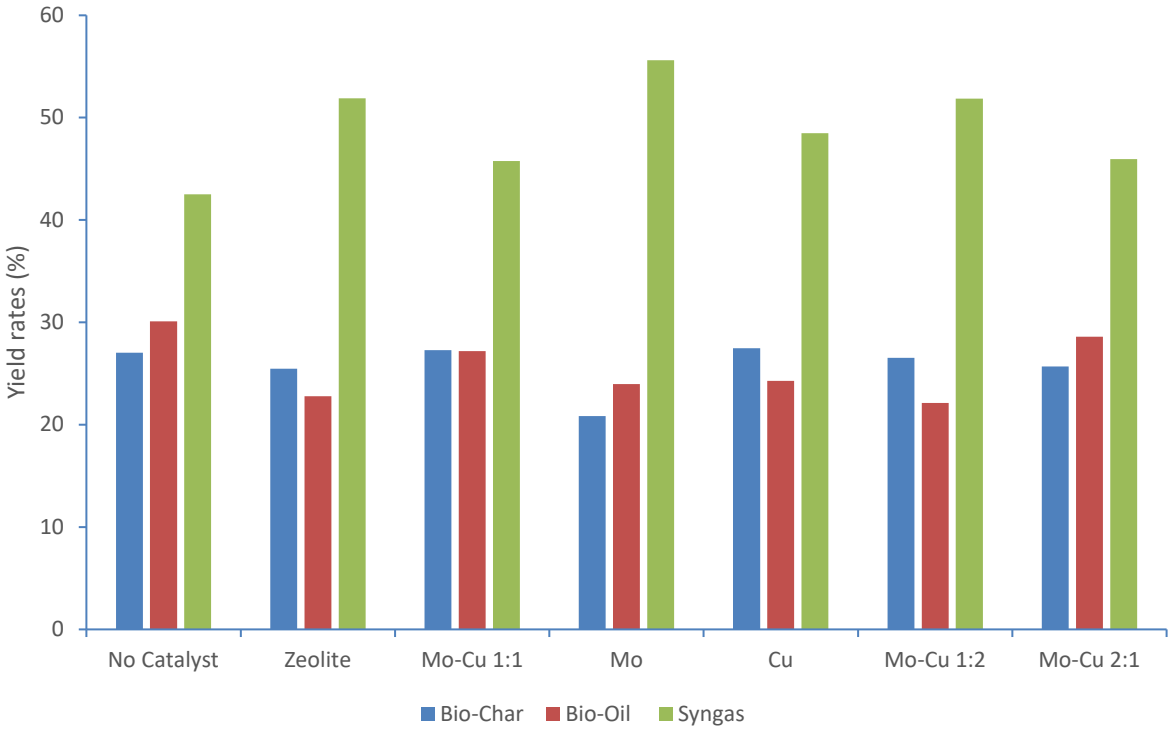

Figure 15. Yields of bio-char, bio-oil, and syngas of the corn stover CFP using different catalysts.

The effects of different catalysts on the bio-oils properties are shown in Figure 16 – 18. The results indicate that catalysts have significant effects on bio-oil properties. Although all upgraded corn stover bio-oil still displayed a high acidity, the catalyst with a ratio of Mo-Cu 2:1 increased the pH value significantly. The bio-oil viscosities decreased when using various catalysts (Figure 17). The catalyst with a ratio of Mo-Cu 0:1 led to the lowest viscosity bio-oil. This is because the high viscosity of bio-oil is attributed to the high molecular weight molecules it contains, which can be broken down by the catalysts, effectively reducing the viscosity of the bio-oil. Bio-oil moisture content and heating value were both affected by the catalysts presenting. Again, more deoxygenating reactions taking place resulted in higher moisture content in the bio-oils because of the catalyst presenting. The bio-oil heating values were affected by the increased moisture contents. The bio-oil produced by the control test without catalyst displayed the highest heating value and lowest moisture content of all tests. Mo-Cu 1:2 had the largest increase in moisture percentage, from 48 wt% to 62 wt%, and the second largest decrease in heating value, from 24.05 MJ/kg to 21.46 MJ/kg. Mo-Cu 2:1 had a slightly lower heating value (21.02 MJ/kg) than Mo-Cu 1:2 but also less water (56 wt%). In the future, the bio-oil should be distilled to reduce the water content to get quality bio-oils with high heating values.

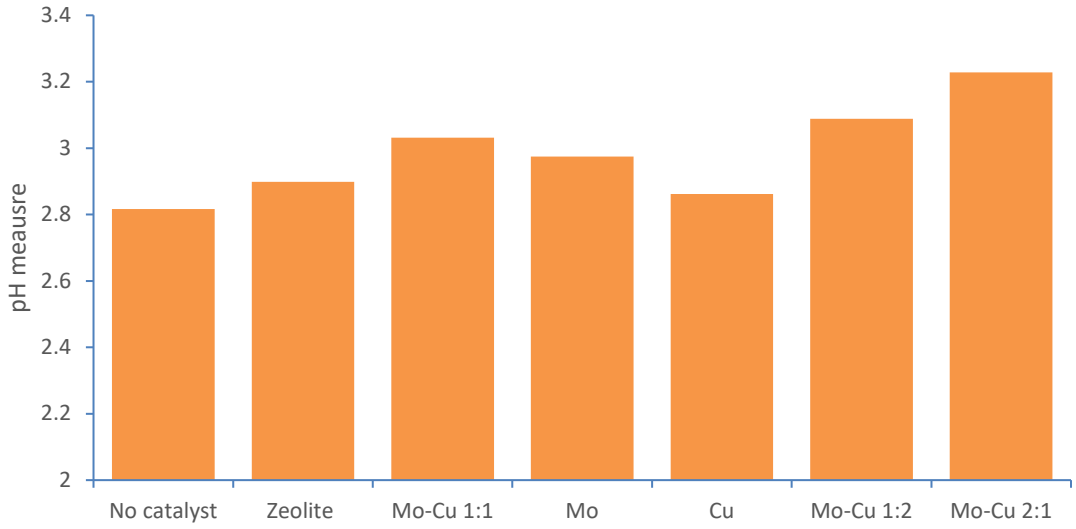

Figure 16. Effect of catalysts on bio-oil pH values.

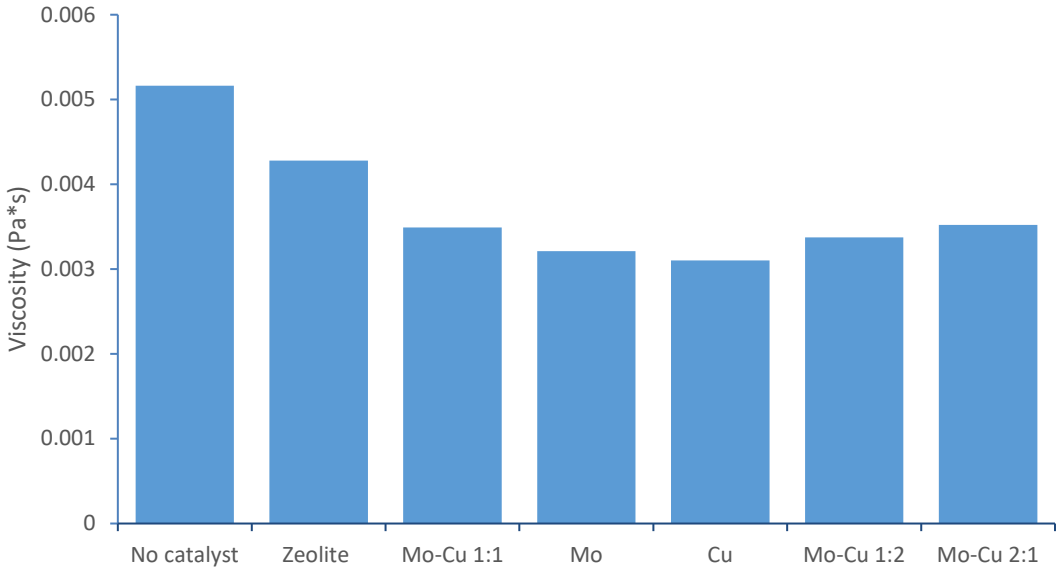

Figure 17. Effect of catalysts on bio-oil viscosity

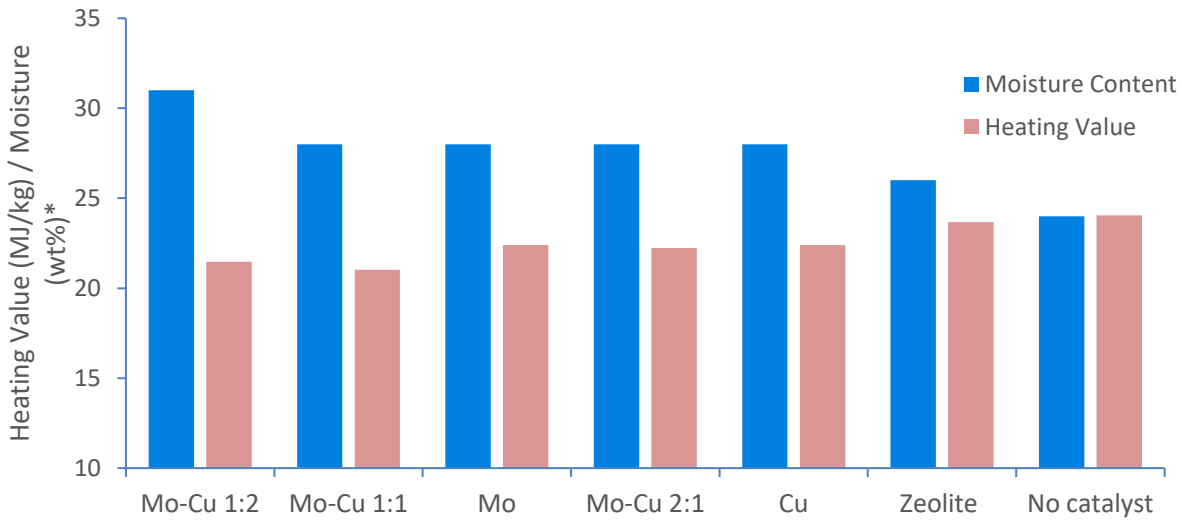

Figure 18. Effect of catalysts on bio-oil heating value and moisture content. *Moisture content was divided by 2 to bring values closer together and show clearer relation between heating value and moisture content

The introduction of a catalysts in CFP process has affected the elemental composition of bio-oils. The carbon, hydrogen, and nitrogen (CHN) contents of bio-oils produced in all tests are listed in Table 3. Compared to the control, every catalyst appears to have reduced the carbon content in the bio-oils, but had varied effects on the hydrogen contents. According to literature, corn stover bio-oil contains about 38.40-47.63 wt% carbon, 4.91-5.48 wt% hydrogen, and 0.84-1.56 wt% nitrogen by weight [22 – 27]. In this project, the raw corn stover CHN was also analyzed and found to be 45.14 wt% carbon, 7.06 wt% hydrogen, and 0.46 wt% nitrogen. Conversely, the highest achieved carbon and hydrogen contents of the bio-oils in this experiment were 31.97 wt% and 9.09 wt%, respectively. This shows a decrease in carbon content and an increased hydrogen content, most likely caused by high water content in the samples. If ignore measuring errors, water should be removed from the samples to get more accurate bio-oil carbon and hydrogen contents.

Table 3 CHN content of bio-oil treated with various catalysts. Nitrogen values of 0 indicate values less than 0.05.

		wt% C	*wt% H*	*wt% N*
No catalyst	Test 1	28.94	8.52	1.37
	Test 2	31.97	8.28	1.62
ZSM-5	Test 1	26.43	8.68	1.25
	Test 2	12.12	1.26	0.70
Mo-Cu 1:1	Test 1	24.97	8.73	0.70
	Test 2	11.22	1.29	0.51
Mo	Test 1	13.02	1.75	0
	Test 2	21.58	8.99	0
Cu	Test 1	21.36	9.05	0
	Test 2	11.06	1.17	0
Mo-Cu 1:2	Test 1	20.41	9.09	0
	Test 2	12.60	1.36	0
Mo-Cu 2:1	Test 1	12.22	1.25	0
	Test 2	10.62	1.12	0

Characterization of fresh and spent catalysts

The fresh and spent catalysts were characterized using BET and XRD approaches. The XRD patterns of fresh ZSM-5 and ZSM-5 used in different temperature conditions in wide angle region of 5-50 are shown in Figure 19. It is found that there is no significant difference in the diffraction pattern of fresh ZSM-5 and ZSM-5 used at different temperatures. No peaks of carbon were observed, indicating carbon crystal was highly dispersed on the ZSM-5 catalyst. It implied ZSM-5 crystal was not significantly changed before and after the CFP process tests. This may provide opportunities to regenerate the spent catalysts for longer useful lifetime and low down drop-in fuel production costs [3, 7, 12, 15 – 17].

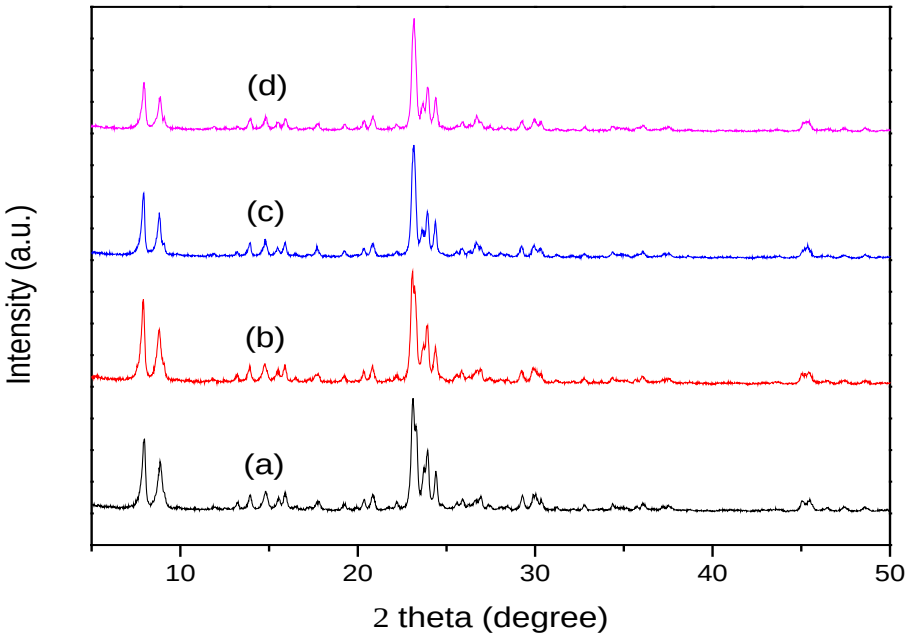

Figure 19. X-ray diffraction patterns of fresh ZSM-5 (a), ZSM-5 after being used in pyrolysis reactor at 500 °C and catalytic reactor at 400 °C (b), ZSM-5 after being used pyrolysis reactor at 500 °C and catalytic reactor at 500 °C (c) and ZSM-5 after being used pyrolysis reactor at 500 °C and catalytic reactor at 600 °C (d)

CONCLUSIONS

Based on the results obtained from this study, some conclusions can be drawn:

- Bio-oil yield and quality is significantly affected by air present in biomass CFP process. When more air is involved in the CFP reactions, bio-oil moisture content increase while carbon conversion efficiency decreases.
- There are significant differences in bio-oil yields and quality when the same catalysts are applied with different implementation systems in CFP process. Catalysts have better performance in Ex-situ fixed-bed reactor system with less catalyst consumption than that of In-situ fixed-bed reactor system. Catalyst has no significant influence on bio-oil yield and quality if the ratio of biomass to catalyst is greater than 1 during In-situ CFP process, but the ratio can be much higher if CFP process is conducted in an Ex-situ implementation system.
- ZSM-5 combined with Mo and Cu to formulate multifunctional catalysts have significant effects on bio-oil yield and quality in CFP process. Different ratios of Mo-Cu impregnated in ZSM-5 have different effect on bio-oil properties. The catalyst with Mo-Cu 2:1 showed the most promising performance in this project.

- The technologies integrated SDSU proprietary CFP reactor and transition metals (Mo-Cu) catalyst system have promising potential for future commercialization to biofuel industry.

LIST OF REFERENCES

1) Jones, S.b., J. L. Male, 2012. Production of Gasoline and Diesel from Biomass via Fast Pyrolysis, Hydrotreating and Hydrocracking: 2011 State of Technology and Projections to 2017. Report No. PNNL – 22133. PNNL, Richland, Washington 99352.
2) Wright, M., R. C. Brown, D.E. Daugaard, and D.D. Hsu, 2010. Techno-Economic Analysis of Biomass Fast Pyrolysis to Transportation Fuels. Technical report, NREL/TP-6A20-46586. Golden, Colorado 80401.
3) Biddy, M., A. Dutta, S. Jones, and Aye Meyer. 2013. In-Situ Catalytic Fast Pyrolysis Technology Pathway. NREL technical report: NREL/TP-5100-58056.
4) Branca, C.; Giudicianni, P.; Di Blasi, C. 2003. GC/MS characterization of liquids generated from low-temperature pyrolysis of wood. *Ind. Eng. Chem. Res. 42*, 3190–3202.
5) Bridgwater, A.V. 1996. Production of high grade fuels and chemicals from catalytic pyrolysis of biomass. *Catal. Today*, *29*, 285–295.
6) Bulushev, D.A.; Ross, J.R.H. 2011. Catalysis for conversion of biomass to fuels via pyrolysis and gasification: A review. *Catal. Today*, *171*, 1–13.
7) U.S. Department of Energy. 2011. U.S. Billion-Ton Update: Biomass Supply for a Bioenergy and Bioproducts Industry. R.D. Perlack and B.J. Stokes (Leads), ORNL/TM-2011/224. Oak Ridge National Laboratory, Oak Ridge, TN. 227p.
8) Cheng, Y.T.; Huber, G.W. 2011. Chemistry of furan conversion into aromatics and olefins over HZSM-5: A model biomass conversion reaction. *ACS Catal. 1*, 611–628.
9) Faix, O.; Meier, D.; Fortmann, I. 1990. Thermal-degradation products of wood: A collection of electron-impact (EI) mass-spectra of monomeric lignin derived products. *Holz als Roh- und Werkstoff***.** *48*, 351–354.
10) Huber, G., T. R. Carlson, and G. A. Tompsett. 2009. "Aromatic Production from Catalytic Fast Pyrolysis of Biomass-Derived Feedstocks" *Topics in Catalysis* 52 (2009): 241.
11) Zhang, M., and A. Moutsoglou, 2014. Catalytic Fast Pyrolysis of Prairie Cordgrass Lignin and Quantification of Products by Pyrolysis−Gas Chromatography−Mass Spectrometry. Energy & Fuel, dx.doi.org/10.1021/ef401795z.
12) Li, X., S. Lu, Y. Wang, Y. Yu, C. Wang, X. Li, Z. Wang. 2012. Catalytic fast pyrolysis of Kraft lignin with HZSM-5 zeolite for producing aromatic hydrocarbons. Front. Environ. Sci. Eng. 2012, 6(3): 295–303. DOI 10.1007/s11783-012-0410-2.
13) Carlson, T. R., Y. Cheng, J. Jae and G. W. Huber. 2011. Production of green aromatics and olefins by catalytic fast pyrolysis of wood Sawdust. Energy Environ. Sci., 2011, 4, 145.
14) French, R.; Czernik, S. 2010. Catalytic pyrolysis of biomass for biofuels production. *Fuel Process. Technol. 91*, 25–32.
15) Alotaibi, M. A. 2012. Deoxygenation and hydrogenation of biomass-derived molecules over multifunctional catalysts. PhD Dissertation, University of Liverpool, UK.
16) Balat, M.; Balat, M.; Kirtay, E.; Balat, H. 2009. Main routes for the thermo-conversion of biomass into fuels and chemicals. Part 1: Pyrolysis systems. *Energy Convers. Manag. 50*, 3147–3157.
17) Ranzi et al. 2008 Ranzi, E., A. Cuoci, T. Faravelli, A. Frassoldati, G. Migliavacca, S. Pierucci, and S. Sommariva, 2008. Chemical Kinetics of Biomass Pyrolysis. *Energy & Fuels*, *22*, 4292–4300.

18) Zhang, H.; Cheng, Y.T.; Vispute, T.P.; Xiao, R.; Huber, G.W. 2011. Catalytic conversion of biomass-derived feedstocks into olefins and aromatics with ZSM-5: The hydrogen to carbon effective ratio. *Energy Environ. Sci. 4*, 2297–2307.
19) Vispute, T.P.; Zhang, H.; Sanna, A.; Xiao, R.; Huber, G.W. 2010. Renewable chemical commodity feedstocks from integrated catalytic processing of pyrolysis oils. *Science. 330*, 1222–1227.
20) Liska, A., H. Yang, M. Milner, S. Goddard, H. Blanco-Canqui, M. P. Pelton, X. X. Fang, H. Zhu, A. E. Suyker, 2014. Biofuels from crop residue can reduce soil carbon and increase CO_2 emissions. *Nature Climate Change*, Vol. 4, pages, 398–401. DOI: 10.1038/nclimate2187.
21) Environmental Protection Agency. Regulation of Fuels and Fuel Additives: 2012 Renewable Fuel Standards. *Fed. Regist.* 2012, *76*, 1320-1358.
22) Jahirul, M., et al. "Biofuels Production through Biomass Pyrolysis – A Technological Review." Energies. 2012, 5, 4952-5001.
23) Mohan, D., Pittman, C., Steele, P. "Pyrolysis of Wood/Biomass for Bio-oil: A Critical Review." *Energy & Fuels*. 2006, *20*, 848-889.
24) Demirbas, A. *J. Anal. Appl. Pyrolysis*. 2005, *73*, 39-43.
25) Mullen, C, Boateng, A., Goldberg, N., Lima, I., Laird, D., Hicks, K. "Bio-oil and bio-char production from corn cobs and stover by fast pyrolysis." *Nature*. 2009, *34*, 67-74.
26) Green, A., Feng, J. "Systematics of corn stover pyrolysis yields and comparisons of analytical and kinetic representations." *J. Anal. Appl. Pyrolysis*. 2006, *76*, 60-69.
27) Feng, J., YuHong, Q., Green, A. "Analytical model of corn cob Pyroprobe-FTIR data." *Biomass and Bioenergy*. 2006, *30*, 486-492.

ACKNOWLEDGEMENTS

This research was supported by funding from the North Central Regional Sun Grant Center at South Dakota State University through a grant provided by the US Department of Energy Bioenergy Technologies Office under award number DE-FG36-08GO88073.

Publications

Peer-reviewed paper:

- Wangda Qu, Lin Wei, James Julson. An exploration of improving the properties of heavy bio-oil. Energy & Fuels, 2013, 27 (8), pp 4717–4722.

Conference papers and oral presentations:

- L. Wei, J. Julson. 2014. Catalytic Fast Pyrolysis of Corn Stover to Hydrocarbon drop-in fuels. NC Sun Grant annual meeting, Mar. 27, Minneapolis, MN.
- L. Wei, Y. Huang, Y. Gao, X. Zhao, and J. Julson. Upgrading pyrolysis bio-oil over ZSM-5 catalyst for advanced biofuel development. July 16 – 21, 2014 ASABE annual meeting, Montreal, Canada
- L. Wei, K. Muthukumarappan, Z. Gu, and J. Julson. 2013. Catalyst development for biomass conversion to jet fuels. North Dakota/South Dakota Engineering Research Summit, South Dakota State University, April 23, Brookings, SD.

- Y. Huang, L. Wei, J. Julson, Y. Gao, and X. Zhao. 2014, Upgrading of bio-oil into advanced bio-fuel over Mo/ZSM5 catalysts. ASABE intersection meeting, Mar. 29, Brookings, SD.

Academic outcomes

- MS Degrees Conferred: Wangda Qu
- Undergraduate students supported: Kory Alpichi, Zachary DeVaar Crandall
- Ph.D. students supported: Yinbin Huang, Zhongwei Liu, Xianhui Zhao, Dan Liu
- Post-docs supported : Gao Yang, Chunkai Shi

Please complete the following table to reflect your project at completion or time of report submission:

ITEM	NUMBER
Abstracts	**4**
Peer Reviewed Publications	**1**
Outreach Publications/Web Pages	
Professional Presentations	**4**
MS Degrees Conferred	**1**
Ph.D. Degrees Conferred	
MS Students Supported	
Ph.D. Students Supported	**4**
Post-Docs Supported	**2**
Undergraduate Students Supported	**2**
Investigators Supported	**2**
Start-Up Jobs Created	
Disclosures	**1**
Patents Filed	**1**
Provisional Patents	
Patents Issued	
License Agreements	**1**
Plant Variety Protection	
Subsequent Funding	**2**

Back to Table of Contents

Sun Grant Initiative
DOE Final Progress Report

Project Title: Plasma Activation of Biochar for Supercapacitors

Project Director/Principal Investigator:
Qi Hua Fan, Associate Professor, Department of Electrical Engineering and Computer Science, South Dakota State University, Brookings, SD

All Co-Principal/Other Investigators:
Dr. Zhengrong Gu, Agricultural and Biosystems Engineering, South Dakota State University, Brookings, SD

Collaborators: N/A

Period of Performance: 1 November 2015 - 31 August 2016

Funding Awarded: $40,000

Cost Share Amount: $10,000

Cost Share Source: Bennet Fellowship Funds (Electrical Engineering Department, South Dakota State University), Wintek

Executive summary

Energy storage is a critical component of the infrastructure needed for sustainable energy. Among energy storage options, supercapacitors play an irreplaceable role due to their large capacity, fast charge/discharge, and stable storage capability. State-of-the-art super-capacitors use chemically synthesized carbon nanomaterials (e.g. carbon nanotubes and graphene), which are very expensive. Biochar, a byproduct of biomass pyrolysis, is environmentally friendly, sustainable, and inexpensive. Several types of biochar recently demonstrated promising potential for supercapacitors with reported specific capacitance comparable to carbon nanotubes. To be used for supercapacitors, biochar must be activated. Activation creates porous nanostructures and promotes the surface energy. Conventional activation requires high-temperature treatment (~960°C) for over two hours followed by chemical washing (to remove the KOH catalyst) and prolonged drying. The total process time is over 70 hours. This energy-intensive and lengthy treatment has become a critical barrier to commercializing biochar supercapacitors.

This project developed a novel plasma activation to efficiently create nanostructured porous biochar suitable for supercapacitors. This research promoted fundamental understanding of plasma-materials interactions. The research results indicated that several plasmas (oxygen and methane) were highly reactive to biochar; (2) the plasmas could selectively etch various carbon phases in biochar and create porous structures with active surfaces; and (3) the chemical and physical reactions between plasma species and biochar occurred at different scales, leading to broad distribution of pore sizes that facilitated electrolyte penetration and charge transport.

The plasma activation technology developed through this project has attractive potential for commercialization because it's highly effective – the plasma activation was completed with only 50 W power in 5 minutes. Therefore, this technology could greatly reduce the costs of supercapacitors. The wide application of renewable energy sources has significant benefits to the public.

1. **For each project objective, discuss outcomes and impacts including comparing actual versus expected accomplishments.**

The objective of this proof-of-concept project is to develop a novel plasma activation to efficiently create nanostructured porous biochar suitable for supercapacitors. This research successfully demonstrated that oxygen and methane plasma were highly efficient in producing activated carbon to meet the needs for energy storage.

Our research has produced strong academic and economic impacts. Our papers published in high-level peer reviewed journals were viewed and downloaded over 1000 times within six months since they were published. Our research was also reported in multiple social medias (such as ScienceDaily, 8/18/2016; American Laboratory News, 8/23/2016; IEEE Engineering360, 9/7/2016). Several companies have contacted the PIs and expressed their interests in collaborating with the team to apply the plasma activation technology to their biochar products. These activities greatly promoted the publics' knowledge on bioenergy and advanced the mission of the Sun Grant Initiative to research, produce, and commercialize renewable, bio-based energy technologies.

P**roject activities**

We conducted the following three tasks to achieve our objective:

- Task 1. Clarify Plasma Reactions and Characterize Activated Biochar.
- Task 2. Optimize Plasma Activation
- Task 3. Fabricate and Test Supercapacitors

The research activities and result obtained are summarized below.

TASK 1: Clarify Plasma Reactions and Characterize Activated Biochar

(1) Planned Activities:

1) Establish an optical emission spectroscopy system for diagnosing plasma. The system will be based on an Ocean Optics USB4000 miniature fiber optic spectrometer that collects plasma emissions. The chemical species and their concentrations will differ based on the nature of plasma–biochar reactions. Analyzing the plasma emission lines will reveal the gas species and related reactions.
2) Use advanced characterization techniques to study the plasma treated biochar..

(2) Actual Accomplishments:

We successfully established a plasma emission spectroscopy system using an Ocean Optics USB2000+ spectrometer (Fig. 1). This system has been used to characterize plasma species during activation of biochar.

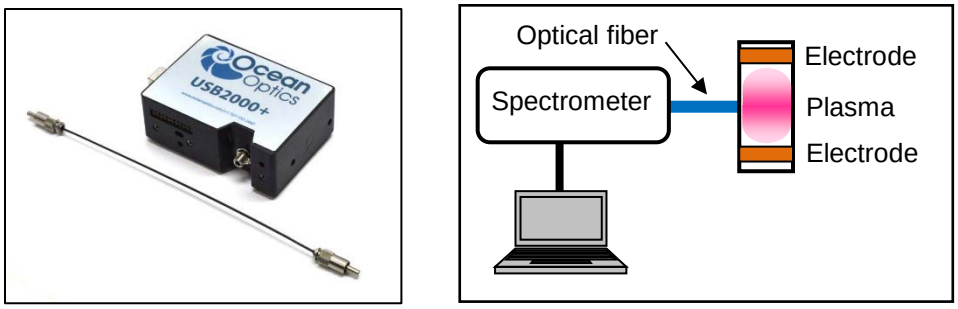

Fig. 1. An Ocean Optics USB spectrometer (left) and the setup of the plasma emission measurement system (right).

Figure 2 is an image of plasma discharge used to treat biochar. Optical emission spectra of plasma with and without biochar are shown in Fig. 3. It can be seen that in addition to the background (red line), new peaks appeared as a result of plasma-biochar interactions.

Fig. 2. An image of plasma discharge. Biochar (black part) is set in the center region.

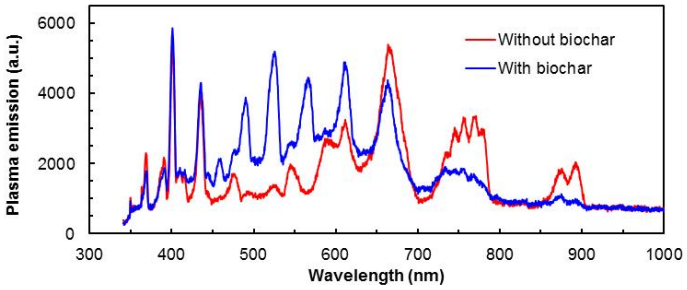

Fig. 3. Optical emission of N2 plasma with/without biochar.

Oxygen plasma was used to treat biochar. Table below shows Brunauer–Emmett–Teller (BET) surface area and pore volume of yellow pine biochar before and after plasma activation. Untreated biochar has low surface area and pore volume (440 m2/g, and 0.455 cm3/g). A 5-minute 50 W plasma treatment leads to 654 m2/g surface area and doubles pore volume, making it suitable for supercapacitors.

Table 1. Surface area, pore volume and average pore size of biochar with and without plasma treatment.

Treatment	BET Surface Area (m^2/g)	Pore Volume (cm^3/g)	Average Pore Size (nm)
Untreated	440	0.455	4.8
Plasma activated	654	0.936	4.9

We used plasma to treat carbon that had graphite structure. After treatment, the graphitic carbon was exfoliated into graphene or multi-layer graphite. X-ray diffraction before plasma treatment showed a characteristic peak of graphite; this peak disappeared after the plasma treatment (Fig. 4). This result indicated that plasma treatment created carbon nanostructures that would greatly promote supercapacitor capacitance.

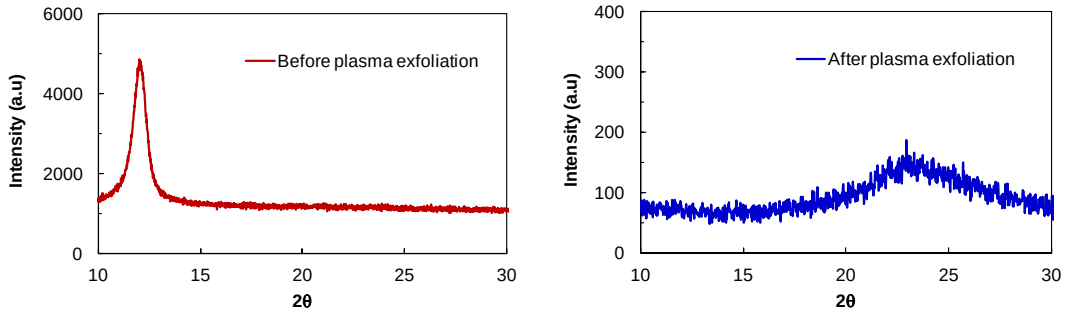

Fig. 4. X-ray diffraction spectra of graphitic carbon before (left) and after (right) plasma activation.

TASK 2: Optimize Plasma Activation

(1) Planned Activities:
Test a variety of source gases for plasma activation of biochar. Three typical gases (O2, H2, and CH4) will be tested and compared.

(2) Actual Accomplishments:
We have tested O2 plasma under various plasma powers (25-100 W). It appeared that 50-75 W was suitable for creating large surface area and good supercapacitor performance. Note that the power density was actually very low because the plasma region was about 100 cm3. This meant that the plasma-biochar interaction was highly efficient and plasma activation was scalable.

We fabricated graphite oxide (GO) and used different plasmas to exfoliate it into graphene. During the exfoliation process, the plasma emission spectra were recorded using an optical spectrometer. The spectra shown in Fig. 5 include the background spectra coming from the process gases (N2, O2, or CH4). After eliminating the background spectra, it was found that there were three common

peaks located at 491.8, 526.8 and 565.9 nm, respectively, for all the three GO samples (GO-N2, GO-O2 and GO-CH4) and O2 plasma background. This result supported the speculation that oxygen was generated during the exfoliation.

The suggested interactions between the plasma and the GO sample are as following. In the dielectric barrier discharge, the GO sample was electrically floating in the plasma. Electrons in the plasma moved faster than ions and led to negative self-bias of the GO samples. Ions attracted by the negative potential bombarded the GO and broke the bonds between the oxygen and carbon. Ion-GO interactions also led to localized rapid increase in the temperature of the GO as a result of kinetic energy transfer. Under the assistance of the ion bombardment, the dissociated oxygen species combined to form oxygen molecules between the GO layers. When the RF power and gas pressure were increased to certain levels (e.g. 70 W and 3 Torr), the thermal expansion of the oxygen gas formed inside the GO led to the separation of the graphite layers and exfoliation occurred. In addition, the exfoliation can be achieved in several seconds once the required energy reached. Moreover, the surface temperature of quartz tube is low enough to be acceptable for hands when taking out samples. In comparison with other methods to prepare graphene, such as CVD, PECVD, thermal solvent, RF dielectric barrier discharge plasma showed low temperature, short time, efficiency, and operable

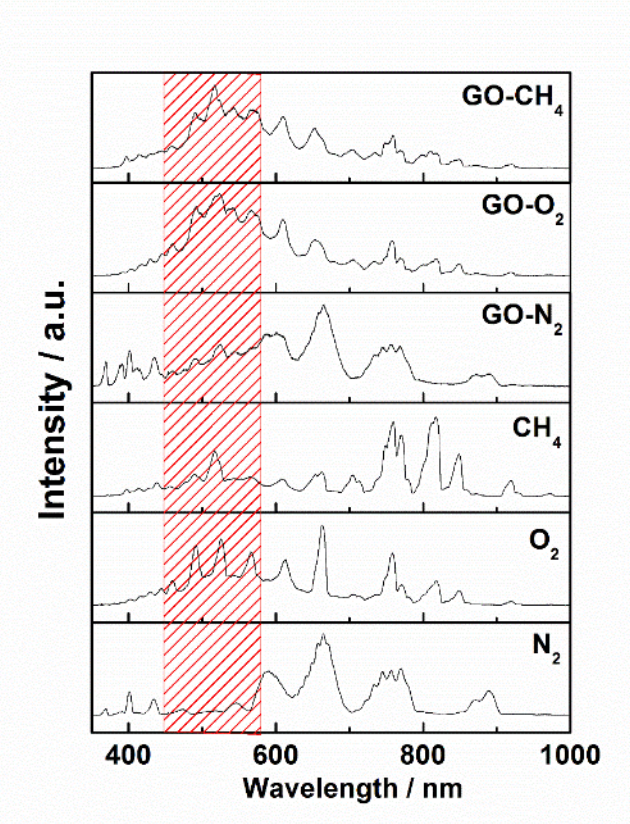

Fig. 5. Optical emission spectra of the background gas plasmas and during the plasma exfoliation of GO. GO-N2, GO-O2 and GO-CH4 mean GO treated with N2, O2, and CH4 plasma, respectively.

Figure 6 shows the Raman spectra of GO-N2, GO-O2 and GO-CH4 in comparison with GO. Two distinct peaks of D-band and G-band located at 1350 cm-1 and 1580 cm-1, respectively, were displayed. The D-band was associated with the A1g mode breathing vibrations of six member sp2 carbon rings, while the G-band was attributed to the first order scattering of the stretching vibration mode E2g observed for the sp2 carbon domain. Generally, the intensity ratio of D-band to G band

(ID/IG) was used to estimate the disorder degree of graphene. The value of ID/IG was 1.24, 1.32, 0.92 and 0.91 for GO, GO-N2, GO-O2 and GO-CH4, respectively. A ID/IG value larger than that of pristine GO implied that more defects were created after the nitrogen plasma treatment. The smaller ID/IG values for GO-O2 and GO-CH4 suggested the removal of oxygen-containing functional groups and partial restoration of the electronic conjugation in graphene sheets by repairing defects. Such a difference most likely arose from the plasma gas during the exfoliation process.

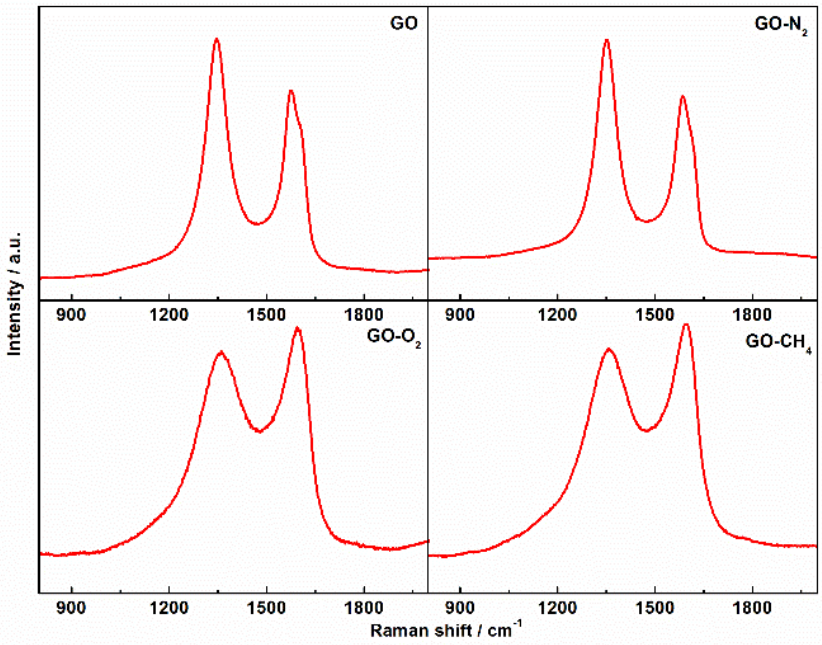

Fig. 6 Raman spectra of GO, GO-N2, GO-O2 and GO-CH4.

TASK 3: Fabricate and Test Supercapacitors

(1) Planned Activities:
Using plasma activated biochar to fabricate supercapacitors.

(2) Actual Accomplishments:
We first selected a commercial biochar YP-50 as baseline for our plasma activation test. YP-50 is a standard biochar made from coconut. The reported specific capacitance for the biochar was about 100 F/g. We fabricated supercapacitors using YP-50. Cyclic voltammetry (CV) and electrochemical impedance spectroscopy were measured on an electrochemical work station (SP-150, BioLogical, France) in 6 mol L-1 KOH electrolyte. Figure 7 shows the CV curve. The electrode mass was M = 6.95 mg, giving a specific capacitance of C = 101.8 f/g, which was in consistence with reported values.

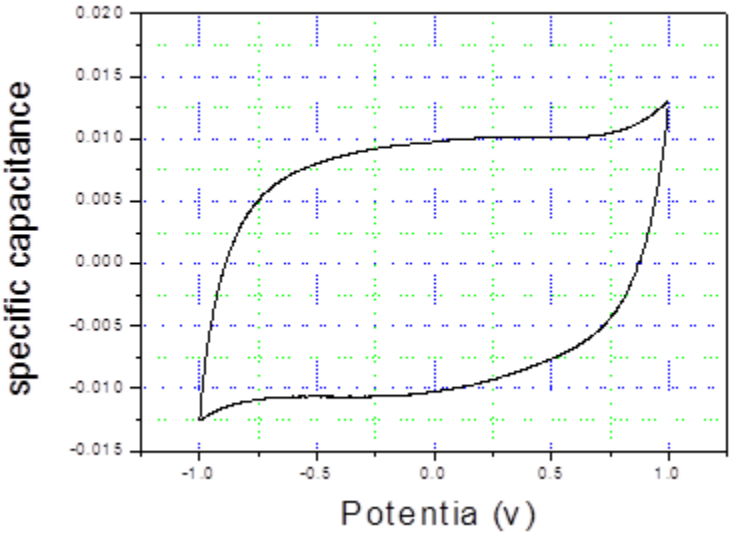

Fig. 7. CV curve of a supercapacitor made of YP-50 without plasma treatment as baseline.

Electrochemical impedance spectroscopy showed in Fig. 8 indicated that the as-fabricated YP-50 electrodes had relatively high resistance (~11 Ohms), which needs to be addressed in the next quarter. We plan to add carbon black that has been known to be effective in reducing the electrode resistance.

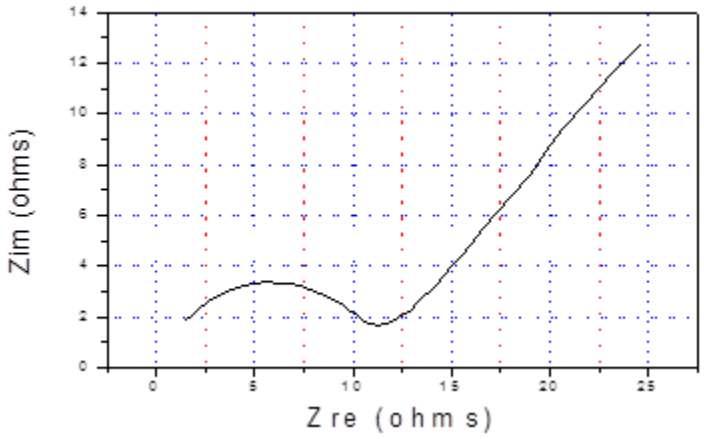

Fig. 8. Electrochemical impedance spectroscopy of supercapacitor electrodes made of YP-50 without plasma treatment as baseline.

We used the plasma activated carbon and fabricated supercapacitors. Figure 9 shows CV curve of a supercapacitor. The capacitance reached >160 F/g. This indicated clearly that the plasma treatment was highly efficient.

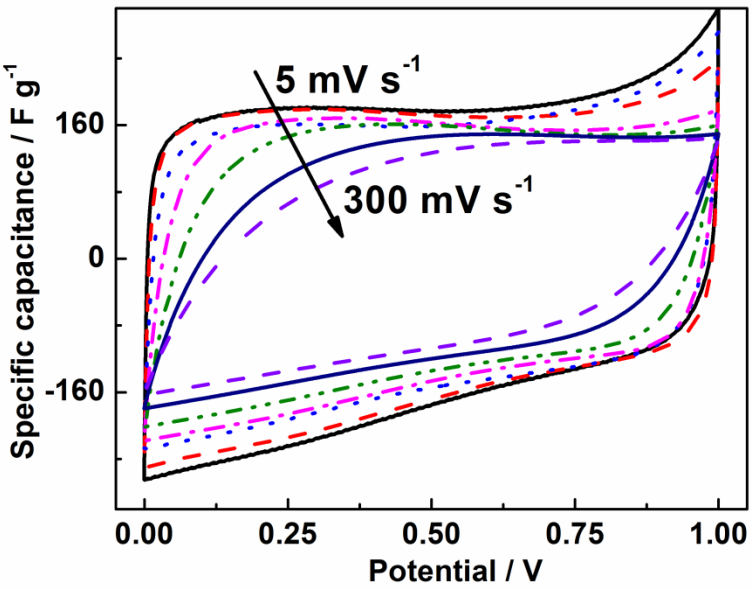

Fig. 9. CV curve of a supercapacitor made of plasma treated carbon.

Products developed under the award:

1. Publications (list title, year, journal name, volume, issue, and page numbers), conference papers (name of conference; location of conference; date of conference; and conference sponsor), or other public releases or outreaches of results.
    a. K. Wang, Y. Cao, X. Wang, M. Castro, B. Luo, Z. Gu, Q. H. Fan, "Rod-shape porous carbon derived from aniline modified lignin for symmetric supercapacitors", J. Power Sources 307, 462-467 (2016).
    b. K. Wang, M. Xu, Z. Gu, P. Ahrenkiel, J. Lee, W. Gibbons, J. Croat, Q.H. Fan, “Pyrrole modified biomass derived hierarchical porous carbon as high performance symmetrical supercapacitor electrodes”, Inter. J. Hydrogen Energy 41, 13109 (2016).
    c. K. Wang, Y. Cao, Z. Gu, P. Ahrenkiel, J. Leed, Q. H. Fan, “Nitrogen-modified biomass-derived cheese-like porous carbon for electric double layer capacitors”, RSC Advances 6, 26738-26744 (2016).
    d. K. Wang, Y. Cao, X. Wang, Q. H. Fan, W. Gibbons, T. Johnson, B. Luo, Z. Gu, “Pyrolytic cyanobacteria derived activated carbon as high performance electrode in symmetric supercapacitor”, Energy 94, 666-671 (2016).
    e. K. Wang, Y. Cao, X. Wang, P. Kharel, W. Gibbons, B. Luo, Z. Gu, Q. H. Fan, “Nickel catalytic graphitized porous carbon as electrode material for high performance supercapacitors”, Energy 101, 9-15 (2016).
    f. R. Gupta, M. Dubey, Z. Gu, Q. H. Fan, “Biochar Nanomaterials Activated by Oxygen Plasma for Supercapacitors”, J. Power Sources 274, 1300 (2015).
    g. K. Wang, Z. R. Gu, Q. H. Fan, “Nitrogen-modified biomass-derived porous carbon for electrical double layer capacitors”, 18th Annual Nanotech Conference, May 22-25, Washington DC (Poster presentation).

    a. Website or other Internet sites that reflect the results of this project.

N/A

b. Networks or collaborations fostered.
   - Established collaboration with the University of Aveiro and national lab PNNL.

c. Technologies/techniques.
   - Developed a novel plasma exfoliation of graphite oxide to fabricate graphene.

d. Inventions/patent applications, licensing agreements.
   - Qi Hua Fan, Mukul, Dubey, Zhengrong Gu, "Method for Plasma Activation of Biochar", US patent application, filed on 6/22/2015 (pending)
   - Lin Wei, Qi Hua Fan, "A novel plasma assisted hydrodeoxygenation process for upgrading pyrolysis bio-oil into hydrocarbons", invention disclosure, filed on 10/17/2016.

e. Other products, such as data or databases, physical collections, audio or video, software* or Netware, model, educational aid or curricula, instruments, or equipment.
   N/A

2. Academic
   a. Courses developed
   b. M.S. students supported: 2
   c. M.S. degrees conferred: 1
   d. Ph.D. students supported: 1
   e. Ph.D. degrees conferred
   f. Post-docs supported

3. For projects involving computer modeling, provide the following information with the final report: N/A
   a. Model description, key assumptions, version, source, and intended use.
   b. Performance material for the model related to the intended use.
   c. Test results to demonstrate the model performance criteria were met (e.g., code verification/validation, sensitivity analyses, history matching with lab or field data, as appropriate).
   d. Theory behind the model, expressed in non-mathematical terms.
   e. Mathematics to be used, including formulas and calculation methods.
   f. Whether or not the theory and mathematical algorithms were peer reviewed, and, if so, will include a summary of the theoretical strengths and weaknesses.
   g. Hardware requirements.
   h. Documentation (e.g., user's guide, model code).

***Software/Manual (if applicable):** N/A
Content. Unless otherwise specified in the award, the following must be delivered: source code, the executable object code and the minimum support documentation needed by a competent user to understand and use the software and to be able to modify the software in subsequent development efforts.

Please complete the following table to reflect your project at completion or time of report submission:

ITEM	NUMBER
Abstracts	
Peer Reviewed Publications	**6**
Outreach Publications/Web Pages	
Professional Presentations	**1**
MS Degrees Conferred	**1**
Ph.D. Degrees Conferred	
MS Students Supported	**2**
Ph.D. Students Supported	**1**
Post-Docs Supported	
Undergraduate Students Supported	
Investigators Supported	
Start-Up Jobs Created	
Disclosures	**1**
Patents Filed	**1**
Provisional Patents	
Patents Issued	
License Agreements	
Plant Variety Protection	
Subsequent Funding	

Back to Table of Contents

Sun Grant Initiative
DOE Final Progress Report

Project Title: Engineering *Aureobasidium pullulans* to produce and secrete poly-lysine and β-glucans

Project Director/Principal Investigator: Jaimie Gibbons (PhD student), Dept. of Biology and Microbiology, South Dakota State University (SDSU), Brookings, SD

All Co-Principal/Other Investigators: Timothy Bruce, (PhD student), Dept. of Natural Resource Management, SDSU, Brookings, SD

William Gibbons, Interim Director of Agricultural Experiment Station, SDSU, Brookings, SD

Collaborators: Prairie Aquatech, Brookings, SD

Period of Performance: 1 January 2016 - 30 June 2016

Funding Awarded: $16,585

Cost Share Amount: $6,146

Cost Share Sources: Prairie AquaTech

Executive Summary
Marine-derived fishmeal (MDFM) is a major source of protein for aquafeeds and agricultural feedstuffs. Overexploitation of MDFM has caused prices to soar above $2000/MT; the subsequently elevated feed prices have placed increased overhead costs upon domestic agricultural producers. Advances in bioprocessing technology have allowed for high-protein plant-based ingredients to enter the agriculture feedstuff industry and replace MDFM at a lower price-point. *Aureobasidium pullulans* and other microbes are able to convert non-utilizable carbohydrates in plant materials into digestible proteins and increase protein content in agricultural feedstuffs. The long-term goal of this project is to manipulate the metabolism of *A. pullulans* to improve the composition and quality of the protein concentrate. Key targets are increasing the levels of lysine and beta-glucans. Plant-based protein sources are low in amino acids such as lysine, and therefore synthetic forms must be added. Beta-glucans are of interest due to their documented immunostimulatory benefits in fish/animals, which may reduce their susceptibility to infectious diseases in confined operations.
In this 6-month project we engineered *A. pullulans* to contain a plasmid directing the production and excretion of poly-lysine peptides. The production of poly-lysine by the engineered *A. pullulans* strain was assessed by Western blotting. Western blots with a protein sample from the engineered strain detected a small amount of poly-lysine. Simultaneously fish feeding trials were conducted with soybean meal that had been bioprocessed with the wildtype *A. pullulans* strain, and supplemented with lysine and beta-glucans (to simulate our final intended product).
A 60-day feeding trial was performed using juvenile rainbow trout (*Oncorhynchus mykiss*) in a biosecure recirculating aquaculture system (RAS). Trout (49.6g starting mass) were fed a 1% body weight ration daily of a fish meal control (FM), a soybean meal control (SBM), a bioprocessed soybean meal (BSBM), a fishmeal diet with 0.1% beta glucans (FM-BG), a soybean diet with 0.1% beta glucans (SBM-BG), and a bioprocessed soybean meal with 0.1% beta glucans (BSBM-BG). Following 32 days of treatment, there was no difference in overall body condition (Fulton's condition factor; P=0.636) or spleen somatic index (SSI; P=0.542). At day 32, the fishmeal control diet demonstrated the specific growth rate (SGR; 2.27) and was different from the MSBM-BG group (1.41; P=0.146). At day 32, treatment fish were challenged with a pathogenic strain of *F. psychrophilum* to assess dietary-related survival and health metrics. No differences were found in total mortality rates (*P*=0.4222), but the negative soybean control diet demonstrated the greatest mortality (7.1±2.9%) over the 28 day pathogen challenge study.

A 20-day digestibility trial was also conducted using juvenile barramundi (*Lates calcarifer*) to evaluate ingredient digestibility using a chromic oxide tracer. Dietary treatments included: a fishmeal reference diet (FM), a bioprocess soy diet (SBM), a bioprocessed soy diet with elevated levels of crystalline lysine (LYS), and a bioprocessed soy diet with 1% inclusion of commercial beta glucans (BG). Fish were fed a reference diets for 10 days, followed by 10 days of treatment diet before fecal matter was extracted and lyophilized. Analyses will be performed for overall protein, lysine (HPLC), and b-glucans (Commercial enzyme kit) digestibility.

Project Objectives

The primary objectives of the project, as enlisted in the proposal, are to:

1. Engineer plasmid for lysine polypeptide production, and insert into *Aureobasidium pullulans*
2. Test lysine production in the modified *A. pullulans* using lab medium
3. Manufacture feed supplemented with commercial β-glucans and/or lysine peptides
4. Evaluate high lysine, β-glucan rich protein feed in trials with rainbow trout

Accomplishments during the funding period are listed by objective below:

Objective 1

- A plasmid for poly-lysine production and excretion was constructed. The plasmid contained a gene encoding poly-lysine attached to an N-terminal signal peptide to direct secretion of poly-lysine from *A. pullulans* through the xylanase transporter. The poly-lysine-encoding gene was under control of the constitutive translation elongation factor promoter (P_{TEF}) from *A. pullulans*. *A. pullulans* was transformed with the poly-lysine encoding plasmid. Two separate biological mutants were verified to contain the poly-lysine plasmid through PCR using plasmid-specific primers.

Objective 2

- Engineered strains of *A. pullulans* containing the poly-lysine plasmid were expected to produce and excrete poly-lysine into the growth medium. To assess poly-lysine production by the engineered strains, the strains were grown in glucose yeast extract medium, and protein samples were prepared from 1-ml samples of growth culture. A faint band the size of the poly-lysine was detected in the medium extract sample by Western blotting. Since the poly-lysine encoding gene was under control of the constitutive P_{TEF} promoter, higher amounts of poly-lysine were expected to be detected through Western blotting. It is possible that lower levels of poly-lysine were detected due to the small sample size and protein purification methods used for Western blotting. Thus, additional Western blots using protein samples prepared from larger growth culture volumes will be performed to verify the presence of poly-lysine and its secretion from the engineered *A. pullulans*. Furthermore, cobalt beads specific for the histidine tag on the poly-lysing polypeptide will be used to purify the protein, allowing for better detection of the protein through Western blotting.

Objective 3

- A short-term digestibility trial using bioprocessed soybean meal with inclusions of lysine and β-glucans was finalized in August. Juvenile barramundi (*Lates calcarifer*) were fed extruded diets containing a chromic oxide tracer to assess the apparent digestibility of supplemented (crystalline) lysine and commercial β-glucans. Bioprocessed soybean meal and a fishmeal control were also included as controls. Treatment groups were fed the fish meal control diet for 10 days before the administration of the trial diets. Following 10 days of treatment diets, fecal matter was collected via hand-stripping and lyophilized. The freeze-dried material is being sent out for final analysis and the chromic oxide tracers will discern apparent digestibility coefficients.

Objective 4

- A 60-day challenge trial was conducted to assess the ability of β-glucans to stimulate the fish immune response. Juvenile rainbow trout (*Oncorhynchus mykiss*) were fed diets supplemented with fish meal (reference diet), defatted soybean meal (negative control), and bioprocessed soybean meal with added commercial β-glucans. Fish were assessed for growth metrics at day 32 and subsequently challenged with *F. psychrophilum* to evaluate innate immune parameters and mortality rates. No differences were found in total mortality rates (P=0.4222), but the negative soybean control diet demonstrated the greatest mortality (7.1±2.9%) over the 28 day pathogen challenge study. Isolated sera samples were analyzed for *F. psychrophilum* specific IgM titers via ELISA, to characterize any treatment influence on antibody generation. These feeding trial results and final innate parameters (i.e. macrophage respiratory burst activity) are currently being analyzed.

Project activities

To construct the poly-lysine-encoding plasmid, P_{TEF} was amplified from *A. pullulans* using gene-specific primers, and cloned to pTOPO 2.1 vector (Invitrogen), creating plasmid pWR2. A DNA sequence encoding 8 consecutive lysines (K8) followed by a poly-histidine (H6) tag was codon optimized for *A. pullulans*. The poly-lysine gene sequence preceded by the XynA signal peptide gene sequence and followed by the hygromycin resistance gene was synthesized as an entire DNA segment by GenScript. The gene poly-lysine gene sequence was then inserted into pWR2 directly following P_{TEF}, creating plasmid pWR4. Plasmid pWR4 was verified by PCR. *A. pullulans* was transformed with pWR4, and mutant colonies, selected for on potato dextrose agar plates containing hygromycin, were verified by PCR.

Two *A. pullulans* mutants verified to contain pWR4 were grown in potato dextrose broth medium with hygromycin (50 µg/ml). Poly-lysine produced by the engineered *A. pullulans* was expected to be present in the growth medium since the poly-lysine polypeptide was attached to an N-terminal XynA signal peptide to direct poly-lysine secretion from the cell via the XynA transporter. To detect poly-lysine production in the engineered mutants, protein was extracted from 1-ml samples of the growth culture. Then, Western blotting was performed to detect poly-lysine using an anti-histidine antibody (since the poly-lysine polypeptide had a poly-histidine tag). Western blotting with medium from the mutant cultures showed a faint band for the poly-lysine peptide. More poly-lysine was expected to be produced by the culture since the poly-lysine gene was under control of the constitutive P_{TEF} promoter. Western blotting methods to detect the poly-lysine polypeptide are being optimized through changing growth culture conditions, specifically allowing the culture to reach a higher OD before protein extraction, and through using cobalt resin beads to purify the protein. Several colonies, each verified by PCR to contain the poly-lysine-encoding plasmid, will be grown and used for protein extraction to verify the presence of poly-lysine. After identifying an *A. pullulans* mutant, which is successfully able to produce poly-lysine in high amounts, the strain will be used in the production process, converting soybean meal to high protein fish meal. The *A. pullulans* mutant will enhance the amino acid content of the feed product by supplying poly-lysine, a limiting amino acid in fish diets.

As for the finfish feeding trials, there were some minor difficulties throughout the experimental duration, mainly with the challenge trial component. A pathogenic strain of *F. psychrophilum*, the causative agent of bacterial coldwater disease (BCWD) in salmonids, had previously been used in juvenile rainbow trout (~10g) and 10-day challenge trial mortality rates of approximately 50% of tank individuals were recorded. For this particular trout cohort (47.9g starting weight) dosages were scaled to compensate for weight differences, but mortality rates were much lower than anticipated. Thus, this experimentation did provide evidence of weight-related reductions in mortality associated with BCWD.

Products developed under the award and technology transfer activities, such as:

Publications: Two publications are anticipated for the finfish feeding trials. One publication (original research manuscript) will present findings from the growth and challenge trial and will be pertinent to a journal such as Aquaculture Research. A second publication (short note or original research manuscript) will present the digestibility findings.

a. Website or other Internet sites that reflect the results of this project. (NA)
b. Networks or collaborations fostered. (NA)
c. Technologies/techniques. (NA)
d. Inventions/patent applications, licensing agreements. (pending)
e. Other products, such as data or databases, physical collections, audio or video, software* or Netware, model, educational aid or curricula, instruments, or equipment. (NA)

5. Academic

a. Courses developed (NA)
b. M.S. students supported (NA)
c. M.S. degrees conferred (NA)
d. Ph.D. students supported (one Ph.D. student)
e. Ph.D. degrees conferred (pending)
f. Post-docs supported (NA)

Please complete the following table to reflect your project outputs at completion or at time of report submission. Identify outputs and products developed under the award and any technology transfer activities.

ITEM	NUMBER	DETAILS (e.g. citations, names, descriptions, varieties, etc.)
Abstracts: include full citation and attach a pdf copy.	0	
Peer Reviewed Publications: include full citation and attach a pdf copy if available	2 pending	Two peer-reviewed publications are anticipated for the finfish feeding trials. These will cover the 60-day growth/challenge trial and digestibility work performed in this period.
Outreach Publications including web pages: include full citation	0	
Professional Presentations: include full citation	0	
MS Degrees Conferred: include names plus month/year confirmed	0	
Ph.D. Degrees Conferred: include names plus month/year confirmed	1 pending	
MS Students Supported: include names	0	
Ph.D. Students Supported: include names	1	Jaimie Gibbons
Post-Docs Supported: include names	0	
Undergraduate Students Supported: include names	0	
Investigators Supported: include names	0	
Jobs Created	0	

Invention Disclosures	1	Invention disclosure has been filed with SDSU for the engineered strain of *A. pullulans*.
Non-provisional Patent Application(s) Filed	0	
Provisional Patents Filed	1	pending
Patents Filed	0	
Patents Issued: include full citation	0	
License Agreements: include description	0	
Plant Variety Protection: include description	0	
Subsequent Funding: List proposals funded as a result of this work	1	United Soybean Board Grant
Other: Products, such as data or databases, physical collections, audios or videos, software or Netware, models, educational aids or curricula, instruments, or equipment.	0	

Back to Table of Contents

Sun Grant Initiative

DOE Final Progress Report

Project Title: Optimize multifunctional catalysts for efficiently converting lignocellulosic biomass to advanced biofuels

Project Director/Principal Investigator: Lin Wei, assistant professor, Agricultural & Biosystems Engineering Department, South Dakota State University, Brookings, SD 57007.

All Co-Principal/Other Investigators: James Julson, Professor, Agricultural & Biosystems Engineering Department, South Dakota State University, Brookings, SD 57007**.**

Collaborators: Mark Luecke, Managing Director and CEO, South Dakota Innovation Partners, Sioux Falls, South Dakota 57104**.**

Period of Performance: 1 November 2015 - 30 April 2016

Funding Awarded: $37,567

Cost Share Amount: $9,330

Cost Share Sources: South Dakota Innovation Partners

Executive summary

Catalytic fast pyrolysis (CFP) has emerged as the most promising process for thermochemical conversion of lignocellulosic biomass to advanced biofuels in recent years. South Dakota State University (SDSU) researchers have developed a proprietary CFP technology to produced quality bio-oils from various biomass feedstocks, which can be upgraded to advanced biofuels using a sequential hydrodeoxygenation (HDO) reactor. The biofuels produced were compatible with petroleum-derived hydrocarbons and can be directly dropped in an existing petroleum refinery for further refining to "green" gasoline, diesel, and jet fuel. However, catalyst deactivations caused by coking, carbon deposition, ammonia or sulfur poisoning in the CFP and bio-oil upgrading processes have become the biggest challenges to increase biomass carbon conversion efficiency. There is a critical need to develop effective multifunctional catalyst systems to improve the CFP technology to an efficient scalable process for the production of hydrocarbon biofuels from biomass. The performance of noble metal catalysts appeared to be better than that of transitional metal catalysts, but the high price of noble metals make them unattractive. The focus of this research is to develop multifunctional catalysts using transition metals (e.g. Zn, Ni, Fe, Mo, and Cu) supported on zeolite (HZSM-5), alumina oxide, and activated carbon. The supported materials (aluminum oxide, activated carbon and ZSM-5) were respectively impregnated with a specific loading level of active transition metals including Fe, Zn, Cu, Mo, Ni, Co and their combinations using wet impregnation method and blended with guar gum and boehmite. The catalysts were prepared by pelletizing the mixture into particles with a diameter of 3 mm and the length less than 5 mm. The catalyst pellets were dried at 120˚C for 12hr and calcined at 550℃ for 5 hours before use. All catalysts were tested in biomass (sawdust and prairie cordgrass) CFP and bio-oil upgrading processes using a two-stage fixed-bed CFP system and a Parr reactor for catalyst screening and optimization. The research results indicate that:

- The yield and quality of bio-oil and upgraded biofuels is significantly affected by the activity and selectivity of catalysts used in biomass CFP process. The better activity and selectivity of catalysts, the better yield and quality of liquid biofuels could be obtained.
- There are significant differences in bio-oil yields and quality when different catalysts were applied in biomass CFP process. Bimetallic Ni-Cu catalysts were more active than single Ni catalysts in hydrodeoxygenation process under mild conditions. The coking (char) yield of Ni-Cu/AC catalyst was lower than Ni/AC catalyst. The combination of Co and Mo supported on Zeolite (HZSM-5) showed favorable to produce higher hydrocarbon biofuel with lower oxygen content.
- Bimetallic Ni-Zn/Al_2O_3 catalysts exhibited higher activity on bio-oil yield and quality, compared to monometallic Ni/Al_2O_3 or Zn/Al_2O_3 catalysts. When an appropriate combination of Ni and Zn loading level, the yield and quality of hydrocarbon in the upgraded bio-oil could be significantly increased while at the same time the undesirable acids, aldehydes and ketones were greatly decreased. 15%Ni-5%Zn/ Al_2O_3 catalyst generated the highest oil phase yield at 44.6% with the highest hydrocarbon content at 50.1%. Physicochemical properties of the upgraded bio-oils such as water content, pH and HHV were also significantly improved.
- All AC supported catalysts increased the hydrocarbon yield in upgraded bio-oil in comparison to raw bio-oil, while the Ni/AC catalysts produced the highest light

hydrocarbons content at 32.6% in upgraded bio-oil. The addition of Fe, Cu and Mo to Ni/AC in- creased the yields of alkyl-phenols, and Ni-Mo/AC generated the upgraded bio-oil with the highest content of alkyl-phenols at 38.41%.

- The technologies integrated SDSU proprietary CFP reactor and the multifunctional catalysts synthesized from transition metals supported on zeolite and activated carbon have promising potential for future commercialization to biofuel industry.

1. BACKBROUND AND OBJECTIVES

Catalytic fast pyrolysis (CFP) is one of the most promising emerging technologies for effectively converting biomass into biofuels and chemicals in the last decades [1 – 5]. This process is generally includes two steps. The first step is that biomass is initially converted into bio-oil vapor. This step is a simultaneous mix of dehydration, depolymerization, re-polymerization, fragmentation, and rearrangement. These reactions result in a bio-oil vapor that contains over 300 individual compounds including a large variety of oxygenates that cause many of the negative properties of bio-oil, such as low heating value, high corrosiveness, high viscosity, and instability. These properties greatly limit the application of bio-oil, particularly as transportation fuels [4, 6 – 9The second step is the produced bio-oil vapor is sequentially upgraded into hydrocarbons or other intermediates that can be directly dropped in an existing petroleum refinery for production of "green" gasoline, diesel, or other industrial chemicals. The purpose of the upgrading step is to remove oxygenated compounds from bio-oil via H_2O and CO_2 formation while at the same time reducing molecular weight and altering chemical structures. The bio-oil upgrading is to conduct either simultaneous or in tandem multiple reactions of catalytic cracking, hydrodeoxygenation (HDO), decarbonylation, decarboxylation, hydrocracking, or hydrogenation in one reactor [10 – 12]. Different catalysts must be used to produce different targeted products. The conversion efficiency of biomass to target products (e.g. hydrocarbons) relies heavily upon the activity, selectivity, and energy efficiency of the catalysts used [10, 13 – 25]. The challenge is to develop active stable catalysts that can deal with a great variety of decomposition intermediates from biomass in the temperature range and complex environment of CFP reactions.

South Dakota State University (SDSU) researchers have developed a proprietary accurate control catalytic fast pyrolysis (ACCFP) technology to convert various biomass feedstocks into quality bio-oils that can be upgraded to hydrocarbon biofuels through a sequent bio-oil upgrading process. A theoretical yield of hydrocarbon biofuels of ACCFP can be as high as 150 gallons per dry ton of biomass, depending on feedstock species, reactor types, operating conditions, and catalysts used [2, 5, 8 – 11]. The SDSU research team has successfully produced quality bio-oils from sawdust and corn stover, and upgraded the bio-oil into hydrocarbon biofuels at 30% of carbon conversion efficiency (equivalent to 30 – 40 gallons of advanced fuel per dry ton of biomass) using a proprietary ACCFP reactor (1 – 3kg/h). The properties of advanced biofuels compared with petroleum-derived gasoline are listed in Table 1. A sample of hydrocarbon biofuel produced by the ACCFP system and its GC/MS analysis are shown in Figure 1. The long-term goal is to develop an efficient ACCFP process that integrates advanced CFP technology with effective catalyst systems to increase biomass conversion efficiency toward the profitable target: 60% carbon conversion efficiency (equivalent to 70 – 90 gallon of drop-in fuel per dry ton biomass). However, catalyst deactivations caused by coking, carbon deposition, ammonia or sulfur poisoning in the ACCFP and bio-oil upgrading processes have become the

biggest challenges to increase biomass carbon conversion efficiency [21 – 26]. Although the preliminary results showed the potential of ACCFP, current catalysts remain suboptimal. Thus, there is a critical need to develop effective multifunctional catalyst systems to improve the ACCFP technologies to an efficient scalable process for the production of hydrocarbon biofuels from biomass. The specific objectives of this research are to:

- Formulate effective low cost multifunctional catalysts based on current SDSU bi-functional catalysts.
- Integrate the multifunctional catalyst with the ACCFP technologies to improve conversion efficiency of biomass to drop-in biofuels.
- Optimize the multifunctional catalyst formulas for maximizing advanced biofuels' yield and quality.

Table 1 Comparison of advanced biofuel produced from sawdust and petroleum based gasoline

Properties	**SDSU Advanced biofuels**	**Gasoline**
pH value	5.0 – 5.6	
Viscosity cSt @20ºC	1.2 – 1.88	0.4 – 0.8
Density, Kg/L	0.8 – 0.85	0.745
Heating value, MJ/kg	41 – 48	43
Carbon content, % w.t.	84.59 – 85.12	85 – 88
Hydrogen content, % w.t.	9.9 – 11.26	12 – 15
Oxygen content, % w.t.	0.4 – 0.72	0
Water content, % w.t.	< 0.2%	0

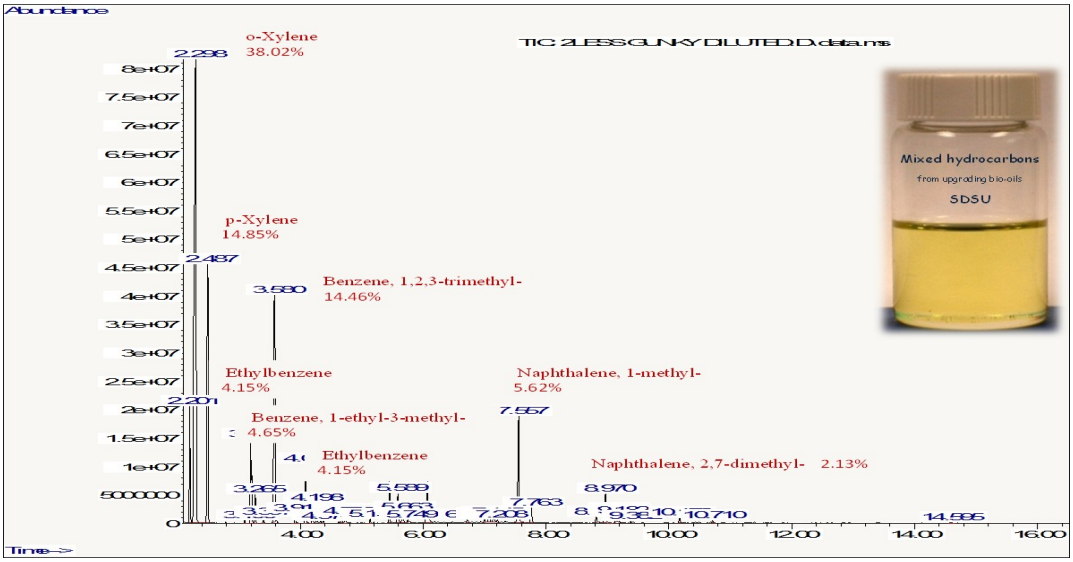

Figure 1: The advanced biofuel (hydrocarbons mixture) sample produced from sawdust by the SDSU team and GC-MS profile of the sample.

Biomass such as forest and crop residues are readily available, annually renewable, and inexpensive [27 – 29]. Replacing petroleum-based fuels and chemicals with biofuels and chemicals produced from biomass minimizes negative impact on the environment and addresses

the challenges of fossil fuel depletion and climate change [30 – 36]. Catalysts are the most important components of ACCFP. The selected catalysts should be highly active, selective to desired products, resistant to deactivation, readily recycled, and cost competitive. Successfully developing such catalysts is the key to open the 'door' for commercialization of advanced biofuel production. In the absence of the catalysts, the promise of a renewable advanced biofuel that does not threaten human or animal food availability will likely remain limited [1 – 11].

2. APPROACH AND METHODOLOGY

2.1 Biomass Feedstock

Prairie cordgrass, corn stover and sawdust were used as feedstocks in this research. Except for sawdust was purchased from a local store, all of other feedstock were harvested from an agriculture extension farm nearby SDSU, allowed to dry to about 15 – 20% of MC (moisture content, wet basis) in a swath prior to baling, and then bales stored indoors for three months. Before hammer milling, the feedstocks were chopped into small pieces using a knife mill with a 25.4 mm screen. A commercial knife mill (H.C. Davis Sons Mfg. Co., Inc., Bonner Springs, KS) was used for the chopping. After size reduction, the small pieces of feedstocks were layered on floor and air-dried to about 10 – 12% MC. The dried feedstock pieces were ground into powder using a hammer mill (Model M150, Winona Attrition Mill Co. MN) with a 1 mm screen.

2.2. Catalysts preparation

Heterogeneous catalysts (simply named catalysts) have achieved great success in petroleum refinery and proved very promising in catalytic fast pyrolysis (CFP) of biomass for the production of hydrocarbon biofuels or other commodity chemicals [3 – 6, 8 – 16]. Various catalysts made from different transition metals (e.g. Fe, Ni, Mo, Zn, Cu, etc.) or noble metals (such as Pt, Pd, Ru, etc.) combined with zeolite (HZSM-5), alumina oxide, or activated carbon have been reported in literatures. The performance of noble metal catalysts appeared to be better than that of transitional metals, but the high price of noble metals make them unattractive. Much attention is attracted to development of transition metal catalyst. Instead of noble metals (e.g. Pt, Pd, or Ru), transition metals (e.g. Zn, Ni, Fe, Mo, and Cu) combined with ZSM-5, alumina oxide, and activated carbon were the focus in this research. As a control, ZSM-5 was also tested in this project.

Activated carbon (AC) was purchased from Norit Company. ZSM-5 was purchased from Zeolyst Company. The activated carbon and ZSM-5 were respectively impregnated with a specific loading level of active transition metals including Fe, Zn, Cu, Mo, Ni, Co and their combinations using wet impregnation method and blended with guar gum and boehmite. The formulas of multifunctional catalyst are summarized in table 2. The catalysts were prepared by pelletizing the mixture into particles with a diameter of 3 mm and the length less than 5 mm. The catalyst pellets were dried at 120˚C for 12hr and calcined at 550□ for 5hr before use.

Table 2. Formulas of multifunctional catalysts made from transition metals supported with zeolite and activated carbon

No.	Support materials	Catalyst formulas
1	HZSM-5	100% HZSM-5
2	HZSM-5	99% HZSM-5 + 1% Ni
3	HZSM-5	94% HZSM-5 + 6% Ni
4	HZSM-5	88% HZSM-5 + 12% Ni
5	HZSM-5	97% HZSM-5 + 3% Mo
6	HZSM-5	91% HZSM-5 + 3% Mo + 6% Cu
7	HZSM-5	94% HZSM-5 + 3% Mo + 3% Cu
8	HZSM-5	95.5% HZSM-5 + 3% Mo + 1.5% Cu
9	HZSM-5	97% HZSM-5 + 3% Cu
10	HZSM-5	97% HZSM-5 + 2% Mo
11	HZSM-5	91% HZSM-5 + 2% Mo + 2% Co
12	HZSM-5	94% HZSM-5 + 2% Mo + 2% Co
13	HZSM-5	95.5% HZSM-5 + 2% Mo + 4% Co
14	HZSM-5	97% HZSM-5 + 4% Mo + 2% Co
15	HZSM-5	97% HZSM-5 + 2% Co
16	Al_2O_3	80%Al_2O_3+ 20%Ni
17	Al_2O_3	80%Al_2O_3+ 15%Ni + 5%Zn
18	Al_2O_3	80%Al_2O_3+ 10% Ni + 10%Zn
19	Al_2O_3	80%Al_2O_3+ 5% Ni + 5%Zn
20	Al_2O_3	80%Al_2O_3+ 20%Zn
21	AC	94%AC + 6%Ni
22	AC	88%AC + 6%Ni + 6%Fe
23	AC	88%AC + 6%Ni + 6%Mo
24	AC	88%AC + 6%Ni + 6%Cu
25	AC	94%AC + 5%Pd + 1%Zn

2.3. Catalysts characterizations

The Brunauer–Emmett–Teller **(**BET) specific surface area and porosity texture of each catalyst were determined by nitrogen adsorption measurements at 77.2 K using an automatic Micromeritics ASAP 2400 apparatus. The catalyst samples were first degassed at 573 K for approximately 6 h and then studied with a static volumetric technique. The surface area, pore size and pore volume of the catalyst were also measured using a Micromeritics TriStar 3000 automated gas adsorption analyzer. Density functional theory (DFT) was utilized to determine the micropore, mesopore and pore size distribution [37 – 40].

Transmission electron microscope (TEM, JEOL JEM-2100 LaB6) was performed with 200 kV of the accelerating voltage. A few micrograms of catalyst samples was dispersed in isopropyl

alcohol (0.5–1.0 mL) and shaked in ultrasonic for about 2 min. Then, a few drops of suspension were dropped on a carbon-coated 200-mesh copper grid and allowed to dry [41].

X-ray crystallography (XRD) was used for phase identification and determination of the relative crystallinity. XRD measurements were carried out using Cu Kα radiation on a RIGAKU SMARTLAB. The X-ray tube was operated at 40 kV and 44 mA and the X-ray pattern was scanned with a step size of crystallite sizes of 0.02° (2θ) from 5 to 50° (2θ) and counting time of 1 s per step. Fourier transform infrared spectroscopy (FT-IR) of the catalysts was performed on a Nicolet 6700 FT-IR spectrometer using KBr pellets.
The surface acidity of catalysts was analyzed using a Micrometrics Autochem II Chemisorption Analyzer with a thermal conductivity detector (TCD). The ammonia temperature-programmed desorption (NH_3-TPD) process was pre-programmed into the analyzer. Due to the use of pure NH_3 and carrier gas (e.g. N_2) for the adsorption and desorption analysis, traditional ammonia-TPD methods have some drawbacks, such as complicated testing procedure, uncertainty on low temperature peaks and the influence of physical adsorption on low temperature peaks. To overcome those drawbacks, a modified ammonia-TPD method was used, with ammonia hydroxide instead of pure NH3 and carrier gas [19 – 21, 26 – 29]. For used catalysts, they were calcined in the air at 600 ºC until the coke was removed completely before the analysis in order not to influence the NH_3 desorption. The ammonia adsorption of the catalyst samples was carried out using a wet impregnation method. A sample of 300 mg was added in ammonium hydroxide (28.0-30.0%) and the mixture was placed in a seal state at room temperature for 3 h. The volume ratio of the sample to ammonium hydroxide was 1:15. Then, the mixture was dried at 60 ºC to remove excess ammonium hydroxide. The dried material was added to the analyzer. Then, helium was purged to remove physically adsorbed impurities such as ammonia, water and CO_2 at 100 ºC with a rate of 60 mL/min. After that, the sample was heated linearly at a rate of 10 ºC/min from 100 ºC to 600 ºC under a constant helium flow of 60 mL/min. The sample was held at 600 ºC for an additional 34 min. During the period of heating from 100 ºC to 600 ºC, ample dilute HCl solu- tion (1.0 mol/L) was used to collect the chemisorbed ammonia by the sample. Finally, NaOH solution (0.1 mol/L) was used to titrate the HCl solution to determine the total acid sites of the sample. For each NH_3-TPD profile, the desorption peak fitting and data analysis was carried out using Lorentzian fitting with Origin8 soft- ware (OriginLab Corporation). The carbon (C) content of used catalysts of metals supported on zeolite was determined using a CE- 440 Elemental Analyzer (Exeter Analytical, Inc.), according to ASTM D4057. The combustion temperature and reduction temperature were 1,040 ºC and 700 ºC, respectively. The purge time and combustion time were 60 s and 90 s, respectively. The fill time was in the range of 20-50 s. The oxygen pressure and helium pressure was 1.72×10^5 Pa (25 psi) and 1.17×10^5Pa (17 psi), respectively. The test of each sample was conducted in duplicate.

2.4. Characterizations of bio-oils and hydrocarbon biofuels

The pH values of bio-oils and drop-in fuels were measured using a pH meter (AB15, Accumet Company) at room temperature. The instrument was calibrated with liquid calibration standards of pH 4 and 7 prior to the measurement. The viscosity analyzer (REOLOGICA Instruments AB Company Dynamic Viscosity) was used to measure dynamic viscosity at 20 °C. The carbon, hydrogen, nitrogen, and oxygen contents of bio-oil and hydrocarbon biofuels were determined using a CE-440 Elemental Analyzer. The HHV of samples were determined using a bomb calorimeter (IKA C2000). The moisture contents of samples were measured using a Karl Fischer

Titrator V20 (Mettler Toledo Company). Syngas analysis was carried out on a GC (Agilent GC-7890A) equipped with a thermal conductivity detector (TCD) and flame ionization detector (FID). Standard gas mixtures were used for calibration, and argon was used as the carrier gas. GC/MS (Agilent GC-7890A and MSD-5975C) was used to analyze the chemical composition of bio-oil and hydrocarbon biofuel samples. The gas chromatograph was programmed at 60 °C for 1 min, followed by ramp 1 at 3 °C/min to 260 °C and ramp 2 at 5 °C/min to 280 °C. The temperature was held for an additional 10 min after each ramp. The injector temperature was 300 °C, and the injection size was 1 μL. The flow rate of carrier gas (hydrogen) was 1 mL/ min. The compositions were identified through the NIST Mass Spectral Library.

2.5. Experimental apparatus and procedure

A two-stage fixed-bed CFP system was fabricated and used for catalyst screening and optimization in the project. The flowchart (a) and picture (b) of this CFP system is shown as Figure 2. This CFP system consists of a pyrolysis fixed-bed reactor with 2-inch diameter tube, a catalytic fixed-bed reactor with half-inch (about 13 mm) diameter tube and a condenser system. Both of the reactors can be heated using controllable temperature furnaces. When a test run started, 100 g of feedstock (e.g. corn stover, switchgrass, prairie cordgrass, or sawdust) was put into the pyrolysis reactor, and 10 g of catalyst was loaded as the bio-oil upgrading catalyst in catalytic reactor. Nitrogen was introduced into the system to remove air with a flow rate of 15 ml/min for 30 min. The catalytic reactor was heated to a designed temperature (300 – 500°C) at the beginning of the experiment. The nitrogen flow rate was set at 5 ml/min when biomass pyrolysis started. Then the pyrolysis reactor furnace was heated at a rate of 25 °C /min to 500 °C. When the pyrolysis reactor reached 500 °C, the reaction pyrolysis gas was collected and analyzed. The pyrolysis reactor temperature was kept at 500°C for 1 – 2 hrs. As the CFP test was done, the furnaces were shut off. The system was allowed to cool down for about 2 hours. The CFP test was duplicated for each reaction conditions.

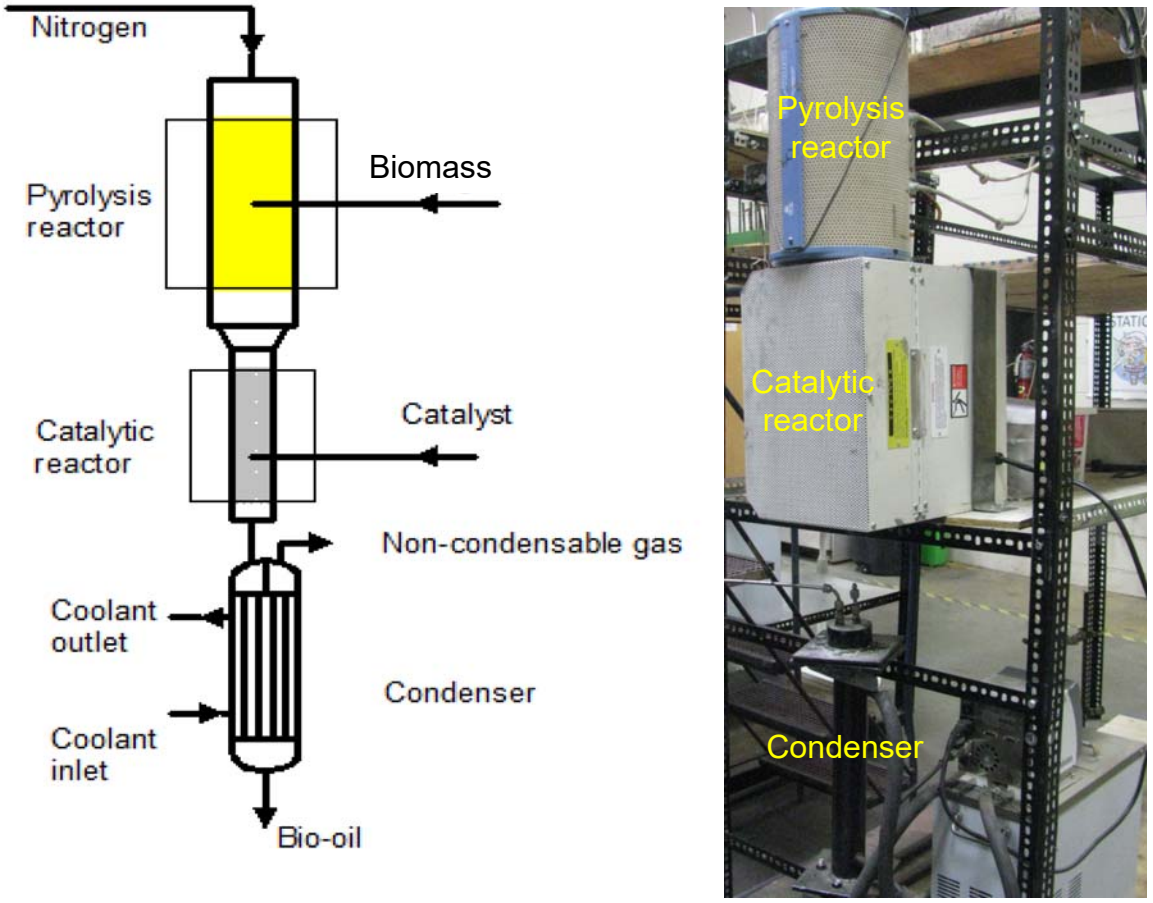

Figure 2. Flowchart of two-stages CFP system (a) and picture of two-stages CFP system (b)

In each test, when pyrolysis reactor temperature was higher than 200 °C, the biomass started to be decomposed into condensable bio-oil vapors, non-condensable gas, and bio-char. The pyrolysis reactor temperature was kept at 500 °C for at least 1 hour to completely pyrolyze all biomass inside the reactor. The bio-oil vapors went through a filtration set and entered the catalytic reactor to upgraded into hydrocarbon biofuels. After catalytic upgrading reactions, the products' stream entered into the condenser to be condensed into liquid biofuel and collected as upgraded bio-oils. The non-condensable gas was separated from the upgraded bio-oils by a liquid-gas phase separator and existed the condenser. As the pyrolysis reactor was heated up to 500 °C and held stable, the produced non-condensable gases was sampled and collected into a gasbag for later chemical composition analysis. Based on the analysis of products produced, effective catalysts were selected and used for optimization tests to figure out optimal combination of catalysts and operation conditions for the best biomass conversion efficiency.

3. RESULTS AND DISCOVERIES

This project was originally to start on September1st, 2015 and ended up on March 30th, 2016. Since the DOE supported funding was actually released to the project on November1st 2015 due to NEPA procedure required, the project was actually started on November 1st 2016 and planed

to complete on April 30th 2016. A no cost extension of this project was approved until July 31st, 2016 since the cost share from the partner, South Dakota Innovation Partner, was delayed.

3.1. Ni supported Zeolite (HZSM-5) Catalysts

The first group of catalysts was synthesized from Ni supported on HZSM-5. These catalysts were tested in catalytic fast pyrolysis of prairie cordgrass (PCG) using the two-stage CFP reactor system. Catalysts characterizations of the catalysts were carried out. Table 3 lists BET surface areas and pore volumes of HZSM-5 and how they are affected by the addition of nickel. There is a large difference in the surface area and pore volume between the HZSM-5 and nickel loaded HZSM-5.The surface area and pore volume decreased when NiO was added to the HZSM-5 supports. This reduction due to pore blocking by metal species dispersed in the channels or by the presence of metal oxide aggregates [28]. This trend is more evident as the nickel loading is increased from 6 to 12%. DFT mode simulation results (Figure 3) show that HZSM-5 and Ni/HZSM-5 mainly contains pores with size distribution between 1 and 20 nm.

Table 3. BET parameters of the different catalysts

Catalyst	Surface area (m^2/g)	Pore volume (cm^3/g)		
	BET	Total[a]	Micropores	Mesopores
HZSM-5	473.33	0.46	0.09	0.25
1%Ni/HZSM-5	451.41	0.44	0.07	0.21
6%Ni/HZSM-5	442.71	0.42	0.06	0.24
12%Ni/HZSM-5	386.16	0.36	0.07	0.16

[a] Total pore volume, measured at P/P_0= 0.995

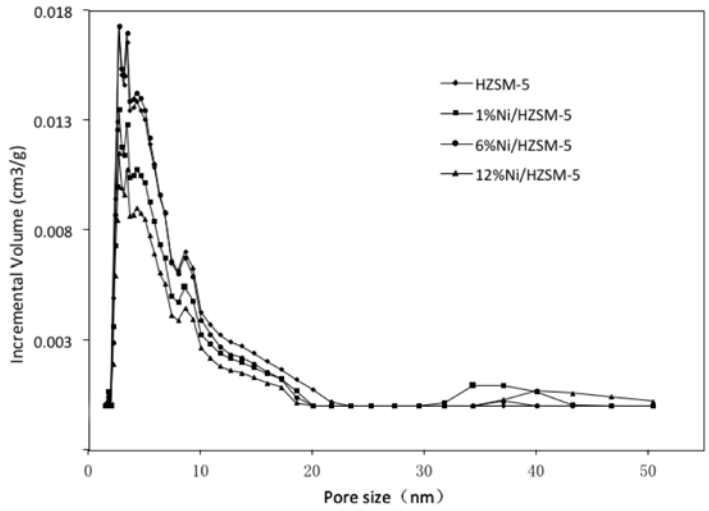

Figure 3. Pore size distribution of HZSM-5 and Ni/HZSM-5 catalysts

The XRD spectras of the fresh and used catalysts in the angle region (5–50°) were measured, and the results are depicted in Figure 4. The similarity of the XRD patterns between fresh HZSM-5 and Ni loaded zeolites indicates that the framework of HZSM-5 was still kept after loading nickel, because the presences of typical peaks of HZSM-5 (23-24°) were still maintained [39 – 47]. The peaks of NiO 37.2°, 43.3° were detected in the diffraction pattern of 6%Ni/HZSM-5

and 12%Ni/HZSM-5, which means crystallinity of NiO was generated on the surface of the catalyst [30 – 36]. However, the peaks of NiO are too small to be shown in diffraction pattern of 1%Ni/HZSM-5, and it indicates that the Ni is presented as much smaller crystal sizes [31 – 37, 48 – 53].

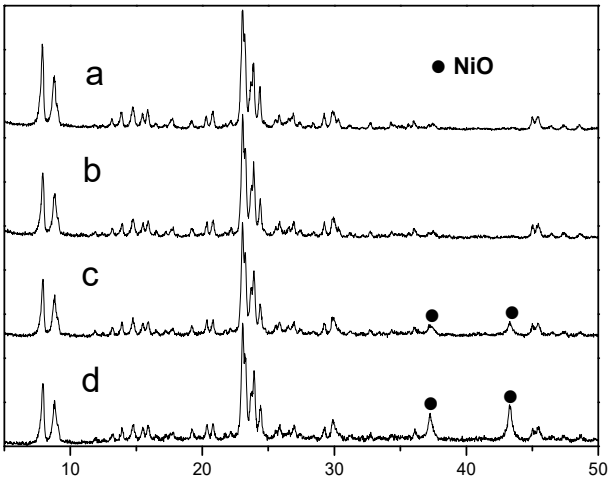

Figure 4. XRD patterns of fresh and used catalysts (a-fresh HZSM-5, b-fresh 1%Ni/HZSM-5, c-fresh 6%Ni/HZSM-5, d-fresh12%Ni/HZSM-5)

Product yields were also determined. The mass balance of different treatments for PCG is presented in Table 4. The bio-char yields of all treatments show no significant difference, because PCG was pyrolyzed at the same condition in the pyrolysis reactor. There is no significant difference in product yields bio-oil and pyrolysis gas among HZSM-5, 1%Ni/HZSM-5, 12% Ni/HZSM-5 and non-catalytic treatment. However, 6%Ni/ HZSM-5 treatment generated the lowest bio-oil yield and highest gas yield. This is probably due to the quick catalyst deactivation that results from serious coke deposition 1.15% over this catalyst [33, 49 – 61].

Table 4 Product yields of different treatments

Treatments	Liquid (wt.%)	Solid(wt.%)		Gas(wt.%)
	Bio-oil	Bio-char	Coke	
No catalyst	29.33	26.07	-	44.60
HZSM-5	24.98	30.59	0.91	43.52
1%Ni/ HZSM-5	25.43	32.73	0.02	41.87
6%Ni/ HZSM-5	18.17	31.46	1.15	49.23
12%Ni/ HZSM-5	29.19	29.79	0.88	40.14

In order to evaluate effect of different Ni/HZSM-5 catalysts on bio-oil compositions, GC-MS was used to analyze bio-oil. During zeolite catalytic upgrading bio-oil vapor stream, various reactions occurred, such as decarbonylation, decarboxylation, dehydration, polymerization, aromatization cracking and hydrodeoxygenation [34 – 35, 62 – 69]. Many organic compounds in bio-oils were produced from those reactions, including hydrocarbons, alcohols, phenols, furans, esters, ethers, aldehydes and ketones.

The detailed effect of HZSM-5 and Ni/HZSM-5 on bio-oil composition was analyzed. The major components in the bio-oil produced by non-catalytic treatment were ketones, phenols, furans,

alcohols and aldehydes. Compared with the components obtained by non-catalyst, the content of furans reduced to some degree in the catalyzed components. Especially the 6%Ni/HZSM-5 and 12%Ni/HZSM-5 obtained bio-oils without furans. In contrast to the non-catalytic treatment, HZSM-5 and 1%Ni/HZSM-5 treatments improved the total percentage of phenols. This indicated that part of pyrolytic lignin was converted into phenolic compounds on the HZSM-5 and 1%Ni/HZSM-5 [36 – 39]. However, no phenols were identified in bio-oils generated by 6%Ni/HZSM-5 and 12%Ni/HZSM-5 treatment, which indicates that more loading Ni to HZSM-5 promote the transformation of phenols to other compounds such as aromatic hydrocarbons, and this is probably due to the decarbonylation and oligomerization [37 – 39, 72 – 79]. The aldehydes can be even removed by catalytic treatment. This may be due to a series of transformations of acetalization, etherification and rearrangement, or by thermal degradation into carbonaceous deposits [38, 56]. Ethers were also decomposed to xxxxx when HZSM-5 presented in the reactions, but it appeared in the Ni/HZSM-5 treatment. Secondary degradation reactions by the catalysts were beneficial for decreasing the ketone content in the bio-oil. The Ni/HZSM-5 catalyst performed well when converting ketones compared to HZSM-5 catalysts. It appears that Ni /HZSM-5 series catalyst had good ability to decrease ketones content in the bio-oil.

The hydrocarbons in the bio-oil are the principal compounds that most researchers have paid attention to. The strong Bronsted acid sites in the HZSM-5 facilitate the formation of aromatics through dehydration, cracking, decarbonylation, decarboxylation and aromatization [39, 69 – 72]. A closer observation of table 3 indicates that the formation of hydrocarbons increased for all catalytic treatments, with HZSM-5 having the most effect. However, the hydrocarbons in the bio-oil obtained by HZSM-5 treatment were mainly heavy compounds (>C15) such as tetradecane, 2,6,10-trimethyl-, hexadecane, 2,6,10,14-tetramethyl- and tricosane, 2-methyl-. All Ni/HZSM-5 treatments seem to increase the formation of gasoline fraction hydrocarbons（C5-C12）in the bio-oil, especially12% Ni/HZSM-5 obtain the highest gasoline hydrocarbons yield at 30.81%. When the NiO was loaded on HZSM-5 support, the framework of HZSM-5 interacted with NiO at channels decreased the Bronsted acid sites, which may lead to obtaining more light hydrocarbons.

Moreover, Ni/HZSM-5 is an efficient catalyst for ethylene, propene and butene oligomerization [22 – 24, 73 – 77]. C_2H_4, C_3H_6 and C_4H_8 were the three components in the vapor from the pyrolysis reactor. Therefore, they can be converted into hydrocarbons over Ni/HZSM-5 catalysts, which is one possible reason for the increase of hydrocarbons.
The syngas produced from non-catalytic and catalytic processes mainly contained hydrogen, carbon dioxide, carbon monoxide, methane and small quantity of C2-C5 light hydrocarbon compounds. Detailed product distributions of all treatments are listed in Table 5. Syngas compositions varied for different treatments. Compared to non-catalytic treatment, both Ni/HZSM-5 and HZSM-5 increased total amount of carbon dioxide and carbon monoxide. This is due to the decarboxylation and decarbonylation reactions that occurred on zeolite catalysts respectively [40 – 46]. H_2 content in various treatment changes slightly. Total content of C_2H_4, C_3H_6 and C_4H_8 in Ni/HZSM-5 treatments decreased compared to non-catalytic and HZSM-5 treatments, this might due to the Ni/HZSM-5's light olefin oligomerization that converts them into liquid hydrocarbons.

Table 5. Syngas distributions of different treatments

Gas (%)	No catalyst	HZSM-5	1%Ni/HZSM-5	6%Ni/HZSM-5	12%Ni/HZSM-5
H_2	7.65	4.78	6.81	7.34	5.35
CO_2	22.37	16.16	45.33	41.97	48.05
CO	18.54	38.85	14.70	23.31	20.64
CH_4	38.44	26.52	25.28	18.33	18.05
C_2H_6	6.46	2.21	3.34	3.03	2.07
C_2H_4	2.61	1.24	1.40	2.20	2.40
C_3H_8	1.35	0.66	0.98	0.90	0.92
C_3H_6	1.79	6.73	1.49	2.48	2.17
C_4H_{10}	0.27	0.91	0.21	0.19	0.18
C_4H_8	0.51	1.91	0.44	0.26	0.17
C_5H_{12}	0.00	0.03	0.01	0.00	0.00

Bio-char is a biomass pyrolysis byproduct along with bio-oil and syngas, and it is a solid material gained from the carbonization of biomass [42, 75 - 78]. The bio-char can be used as solid fuel, soil enhancer or activated carbon [43 – 46, 79 – 82]. Physical properties of bio-chars in all treatments are presented in Table 6. Since all bio-chars were obtained in the same pyrolysis conditions in the pyrolysis reactor, there is no significant difference in their HHV and elemental analysis.

Table 6. Physical properties of different bio-chars

Treatment	No catalyst	HZSM-5	1%Ni/HZSM-5	6%Ni/HZSM-5	12%Ni/HZSM-5
HHV(MJ/Kg)	28.48	26.92	27.94	27.91	29.11
Carbon(wt.%)	74.75	69.42	71.34	73.29	76.26
Hydrogen(wt.%)	2.61	3.18	2.99	3.32	2.86
Nitrogen(wt.%)	3.17	3.14	3.42	3.55	3.64
Rest[b](wt.%)	19.47	24.26	22.25	19.84	17.24

[b] Rest includes oxygen and traces of other elements.

Based on these results, it can be found that Ni/HZSM-5 catalysts could be used for pyrolysis of prairie cordgrass to hydrocarbon biofuels. The loading ratio of Ni to HZSM-5 may affect selectivity and activity of the catalysts prepared. 12%Ni/ HZSM-5 treatment yielded the highest amount of gasoline（C5-C12） hydrocarbons, exhibited an excellent ability to upgrade bio-oil vapor, and showed no significant difference in the properties of bio-char when compared to other treatments in the same pyrolysis conditions.

3.2. Catalysts synthesized from combining Co and Mo supported on Zeolite (HZSM-5)

The second group of catalysts was synthesized from combining Co and Mo supported on HZSM-5. These catalysts were also tested in catalytic fast pyrolysis of prairie cordgrass (PCG) using the two-stage CFP reactor system. Catalysts characterizations of the catalysts were carried out. Table 7 lists BET surface areas and pore volumes of HZSM-5 and how they are affected by the

addition of Co and Mo. The surface area and pore volume decreased when Co and Mo was added to the HZSM-5 supports, this is because of the formation of pore blocking by metal species dispersed in the channels, or by the presence of metal oxide aggregates [16].

Table 7. BET parameters of the different catalyst

Catalyst	Surface area (m^2/g)	Pore Size (nm)	Pore volume (cm^3/g)		
	BET	Average	Total[a]	Micropores	Mesopores
HZSM-5	598.85	4.43	0.66	0.46	0.20
2%Co/HZSM-5	517.59	4.15	0.58	0.37	0.21
2%Mo/HZSM-5	521.06	4.14	0.59	0.39	0.20
2%Mo-2%Co/HZSM-5	495.89	4.59	0.57	0.41	0.16
4%Mo-2%Co/HZSM-5	474.74	4.63	0.55	0.50	0.05
2%Mo-4%Co/HZSM-5	474.98	4.33	0.51	0.33	0.18

[a] Total pore volume, measured at P/P_0= 0.995

The XRD patterns of all catalysts in the angle region (5–80°) are presented in Figure 5. The similarity of the XRD patterns between fresh HZSM-5 and Co or Mo loaded zeolites indicates that the framework of HZSM-5 was still kept after loading Co or Mo, because the presences of typical peaks of HZSM-5 (around 8°, 9°, 23-25°) were still maintained [25, 33, 83 – 85]. However, the crystallite peaks of Co3O4 and MoO3 could not be observed in the XRD patterns of Co or Mo loaded HZSM-5, and it indicates that Co3O4 and MoO3 crystallites are highly dispersed on HZSM-5 surface and/or in its channels [26 – 37].

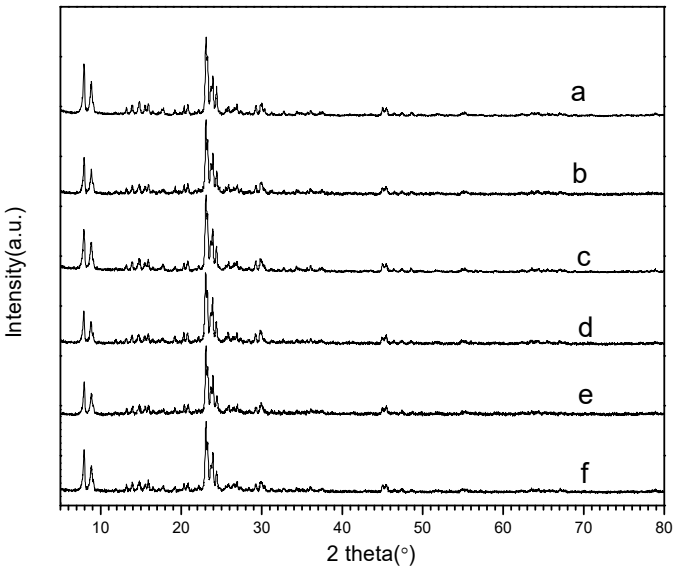

Figure 5. XRD patterns of fresh catalysts (a-HZSM-5, b-2%Co/HZSM-5, c-2%Mo/HZSM-5,d-2%Mo-2%Co/HZSM-5,e-2%Mo-4%Co/HZSM-5,f-4%Mo-2%Co/HZSM-5)

The IR spectra of the parent H-ZSM-5 zeolite and the Co or Mo modified HZSM-5 catalysts are shown in Figure 6. The fresh ZSM-5 exhibited the characteristic peaks of MFI structure at around: 1220 cm^{-1} (external asymmetric stretch); 1100 cm^{-1} (internal asymmetric stretch); 800 cm^{-1} (external symmetric stretch); 550 cm^{-1} (double ring); and 450 cm^{-1} (T-O bending vibration of internal tetrahedral) [20, 82 – 86]. The fresh Co or Mo-loaded HZSM-5 also exhibited the characteristic peaks of MFI structure in the FT-IR spectra, which indicates that the introduction of Co and Mo to HZSM-5 had no significant influence on the framework of the parent HZSM-5. Bands of all catalysts at around 3609 cm^{-1} assigned to strong Bronsted acid sites (Si-OH-Al) were also observed [28, 76 – 79].

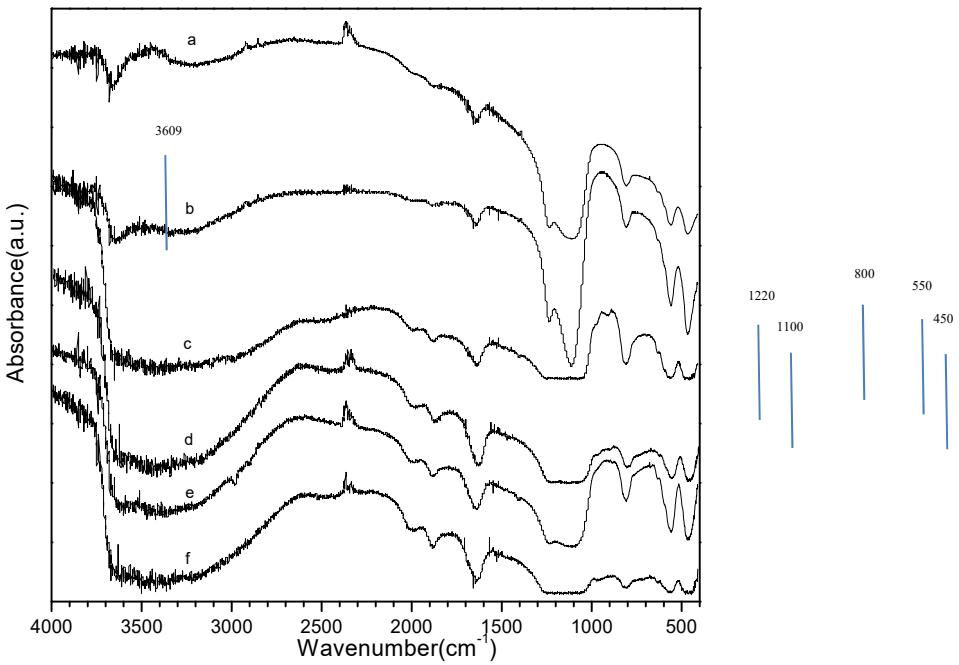

Figure 6. FT-IR spectra of all fresh catalysts (a-HZSM-5; b-2%Co/HZSM-5; c-2%Mo/HZSM-5; d-2%Mo-2%Co/HZSM-5; e-2%Mo-4%Co/HZSM-5; f-4%Mo-2%Co/HZSM-5.

TEM images (50nm) of all fresh catalysts are shown in Figure 7. Fresh HZSM-5 did not show any dark spots because there was no metal loading on it. In addition, there was no dark spot observed for fresh 2%Co/HZSM-5, 2%Mo/HZSM-5 and 2%Mo-2%Co/HZSM-5 catalysts, which confirmed that Co_3O_4 and MoO_3 were well dispersed on the HZSM-5 support. However, fresh 2%Mo-4%Co/HZSM-5 and 4%Mo-2%Co/HZSM-5 showed small dark spots, which were attributed to the presence of Co_3O_4 and MoO_3 aggregation [16].

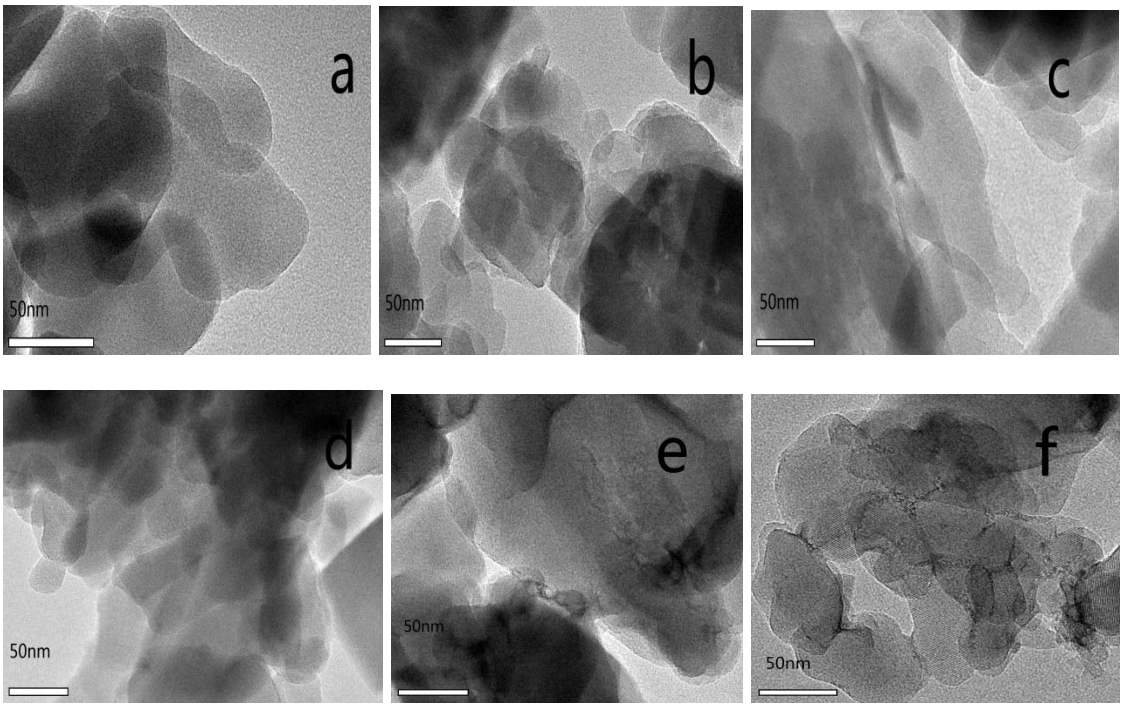

Figure 7.TEM images of all fresh catalysts (a-HZSM-5, b-2%Co/HZSM-5, c-2%Mo/HZSM-5, d-2%Mo-2%Co/HZSM-5,e-2%Mo-4%Co/HZSM-5,f-4%Mo-2%Co/HZSM-5)

Product yields were analyzed in these tests. Three main products (bio-oil, bio-char and non-condensable gas) are generated from the decomposition of cellulose, hemicellulose and lignin in biomass. The mass balances of non-catalytic and catalytic treatments are presented in Table 8. The bio-char yields of all treatments show no significant difference due to the same pyrolysis condition in the first reactor. Compared to non-catalytic treatments, the liquid yield decreased in all catalytic treatments, and this was due to the deoxygenation reaction of bio-oil. Besides, all Co or Mo loading HZSM-5 increased bio-oil yields compared to HZSM-5, and 2%Mo-2%Co/HZSM-5 generated the highest bio-oil yield in all catalytic treatment. This is probably because of the reduced cracking behavior of HZSM-5 caused by the addition of Co and Mo. The catalysts can be deactivated by coke, which is due to the polymerization [29, 72 – 79]. Compared to HZSM-5, the Co-Mo/HZSM-5 decreased the coke yield, and this is consistent with the research results of French, R. [17, 23 – 26, 76].

Table 8. Product yields of different treatments

Treatments	Liquid (wt.%)			Solid(wt.%)		Gas(wt.%)
	Total liquid	Oil phase	Aqueous phase	Bio-char	Coke	
No catalyst	40.38	15.27	25.11	27.33	0.00	32.39
HZSM-5	22.48	9.57	12.91	30.33	0.99	46.20
2 %Co/HZSM-5	26.61	10.31	16.30	28.61	0.33	44.45
2%Mo/HZSM-5	30.79	10.86	19.33	30.08	0.26	38.87
2%Mo-2%Co/HZSM-5	38.23	14.31	23.92	30.06	0.75	30.97
4%Mo-2%Co/HZSM-5	31.62	10.86	20.76	29.81	0.79	37.78
2%Mo-4%Co/HZSM-5	32.57	12.02	20.55	29.91	0.79	36.73

The bio-oil included aqueous phase and oil phase. The aqueous phase mainly contained water, and it was a light yellow liquid. In comparison, the target oil phase was mainly composed of organic compound, and it was dark brown liquid with unpleasant odor. The physicochemical properties of bio-oils generated in different treatment are shown in table 9. It shows properties of the catalytic and non-catalytic bio-oils, including higher heating values (HHV), pH, densities and viscosity and water contents for both aqueous phase and oil phase. The yield of oil phase of the non-catalytic treatment was 40.38%. The catalytic treatments reduced the oil phase. This may be due to the cracking behavior of HZSM-5 and Co-Mo/HZSM-5. The HHV of oil-phase generated by catalysts were higher than the oil phase of non-catalytic treatment. The 4%Mo-2%Co/HZSM-5 generated oil phase with the highest HHV at 26.96MJ/kg. This indicated that Co-Mo/HZSM-5 catalysts can improve the higher heating values of bio-oils. The water content affected the HHV, viscosity, density and acidity of bio-oils. The water content of catalytic bio-oils reduced to less than 9.73% in comparison with the non-catalytic bio-oil (10.80%). The cracking behavior of HZSM-5 and Co-Mo/HZSM-5 led to the formation of lower molecular weight organic compounds, and this resulted in the lower density and viscosity of the catalytic oil phase compared to these properties in the oil phase of non-catalytic oil phase. The pH of oil phase generated by catalytic treatment increased compared with non-catalytic treatment.

Table 9. Properties of different bio-oils

Treatments	HHV(MJ/kg)		Water content (%)		Density(g/ml)		Viscosity(cP)		pH	
	Oil phase	Aqueous phase	Oil phase	Aqueous phase	Oil phase	Aqueous phase	Oil phase	Aqueous phase	Oil phase	Aqueous phase
No catalyst	18.61	5.46	10.80	87.08	1.25	0.91	6.90	2.16	6.03	5.31
HZSM-5	19.45	3.13	9.73	95.16	0.89	0.90	1.87	2.24	6.15	5.28
2 %Co/HZSM-5	19.96	2.36	9.10	89.92	0.90	0.90	1.72	1.56	6.46	6.28
2%Mo/HZSM-5	23.64	2.90	6.74	86.69	0.88	0.90	1.61	1.47	8.07	7.64
2%Mo-2%Co/HZSM-5	22.85	0.84	7.86	85.99	0.79	0.92	1.73	1.55	8.45	8.31
4%Mo-2%Co/HZSM-5	26.96	2.26	5.49	83.70	0.87	0.90	2.26	1.72	8.36	7.52
2%Mo-4%Co/HZSM-5	20.79	2.44	8.92	87.62	0.84	0.90	2.51	1.52	8.64	7.82

In order to evaluate the catalytic effect of different catalysts on product distribution of oil phase, the chemical compositions of all oil phases were analyzed using GC-MS. More than 180 compounds were found in the oil phase (Supporting information, Table S1), and these chemicals originated from the degradation of cellulose, hemicellulose and lignin present in prairie cordgrass. The oil phases produced were classified into different chemical groups, namely phenols, ethers, ketones, esters, aldehydes, furans, alcohols, acids and hydrocarbons.

In the bio-oil of non-catalytic treatment, the PCG bio-oil produced was mainly composed of ketones (22.44%), phenols (20.81%) and alcohols (17.17%), and it also contained undesirable aldehydes (8.25%) and acids (7.55%). The content of hydrocarbons was only 5.32%.

The organic compositions of bio-oil changed significantly after catalytic cracking. After the reaction, the content of phenols increased in all catalytic treatments. Similar results were found by E.F. Iliopoulou [16, 47 – 49] and Bakar, M. S. A., & Titiloye, J. O [30, 58 – 61]. The improvement of phenols was due to the formation of alkyl-phenols such as 2-methyl-phenol and 3, 4-dimethyl-phenol (Supporting information Table S1) that occurred on HZSM-5 and Co-Mo/HZSM-5 catalysts. This is possibly caused by the alkylation-reaction alkylation reactions between phenol and alcohols, and following by cracking, demethoxylation, demethylation and

hydrogenation that generated alkylated phenols [31 – 33]. The bio-oil obtained by HZSM-5 catalyst treatment contained less phenols than the bio-oil produced from Co-Mo /HZSM-5 treatments, which indicated that loading Co and Mo to HZSM-5 benefits in improving the phenol alkyl-reaction performance.

The ketone content in the oil phase of bio-oil decreased in all catalytic treatments, and this is caused by secondary degradation reactions over catalysts. It seemed that the addition of Mo to HZSM-5 significantly helped in reducing the ketone content, especially the 2%Co-2%Mo/HZSM-5 catalyst obtained bio-oil without ketones. The aldehydes content also reduced in all catalytic treatments. The carboxylic acids were eliminated with the use of all catalysts compared to the non-catalytic pyrolysis. The transformation of aldehydes and acids mainly occurs through decarboxylation and dehydration over HZSM-5 and Co-Mo/HZSM-5 catalysts [34]. The contents esters and alcohols in the oil phase of catalytic treatments also decreased compared to non-catalytic treatments. This may be due to the transformation of esters and alcohols to hydrocarbons caused by dehydration, cracking, oligomerization reactions that occurred on HZSM-5 and Co-Mo/HZSM-5 catalysts [32, 37].

Hydrocarbons are the main targeted products that most research focused on. Compared to non-catalytic treatments, the hydrocarbons content increased in all catalytic treatments. This resulted from the thermo-catalytic effects (deoxygenation, cracking, cyclization, aromatization, isomerization and polymerization) of HZSM-5 and Co-Mo/HZSM-5 catalysts. Especially, the 4%Mo-2%Co/HZSM-5 produced the upgraded bio-oil with the highest hydrocarbon content at 41.08%. This is probably due to the aromatization behavior of Mo-HZSM-5 that converted CH4 in the non-condensable gas to hydrocarbons in the bio-oil liquid [36].

Table 10. Chemical composition (relative content %) of compounds in the oil phases

Compounds	**Sand (0P)**	**HZSM-5 (0P)**	**2%Co/HZSM-5 (OP)**	**2%Mo/HZSM-5 (OP)**	**2%Mo-2%Co /HZSM-5 (OP)**	**4%Mo-2%Co /HZSM-5 (OP)**	**2%Mo-4%Co /HZSM-5 (OP)**
Phenols	20.81	24.42	33.45	39.64	57.17	45.80	74.80
Ethers	0	0	1.34	0.83	0.78	0	0
Ketones	22.44	10.15	8.26	0.82	0	0.58	0.54
Aldehydes	8.25	0	0	0	1.39	0	0
Furans	2.77	0	2.01	0	0.54	0	0
Esters	10.31	8.89	6.53	9.99	0.90	8.19	2.10
Alcohols	17.17	14.92	10.04	9.38	1.90	1.51	4.02
Acids	7.55	0	0	0	0	0	0
Hydrocarbons	5.32	24.51	30.33	26.65	36.07	41.08	16.73

Syngas produced in the CFP reactions was also analyzed. The gas distributions of all treatments are listed in Table 11. Compared to non-catalytic treatment, all catalysts increased total amount of carbon dioxide and carbon monoxide. This is due to the decarboxylation and decarbonylation reactions that occurred on zeolite catalysts respectively [36]. CH_4 content in Mo modified HZSM-5 treatments decreased compared to non-catalytic and HZSM-5 treatments, this might

due to the Mo/HZSM-5's role in methane aromatization that converts CH_4 into liquid hydrocarbons.

Table 11. Gas distributions of different treatments

Gas (Vol.%)	Sand	HZSM-5	2%Co/HZSM-5	2%Mo/HZSM-5	2%Mo-2%Co/HZSM-5	4%Mo-2%Co/HZSM-5	2%Mo-4%Co/HZSM-5
H_2	18.34	13.25	11.33	11.34	14.48	14.13	10.43
CO_2	26.44	41.45	40.31	36.33	37.14	31.25	32.94
CO	24.21	19.16	25.47	32.52	27.68	33.64	35.77
CH_4	17.65	14.80	14.60	12.48	10.57	11.91	11.10
C_2H_6	5.31	5.46	3.31	3.00	4.76	3.88	3.80
C_2H_4	3.25	1.63	1.70	1.60	1.56	1.65	1.91
C_3H_8	1.05	1.35	0.74	0.60	1.08	0.85	0.87
C_3H_6	2.55	1.89	1.73	1.50	1.84	1.84	2.17
C_4H_{10}	0.11	0.28	0.13	0.10	0.18	0.27	0.15
C_4H_8	0.75	0.68	0.63	0.50	0.68	0.44	0.81
C_5H_{12}	0.35	0.06	0.03	0.02	0.04	0.14	0.04

Bio-char is a solid material gained from the carbonization of biomass. Physical properties of bio-chars in all treatments are presented in Table 12. Since all bio-chars were obtained in the same pyrolysis conditions in the pyrolysis reactor, there is no significant difference in their HHV and elemental analysis.

Table 12. Physical properties of different bio-chars

Treatment	Sand	HZSM-5	2%Co/HZSM-5	2%Mo/HZSM-5	2%Mo-2%Co/HZSM-5	4%Mo-2%Co/HZSM-5	2%Mo-4%Co/HZSM-5
HHV(MJ/Kg)	26.40	27.06	27.77	26.69	28.07	26.91	27.42
Carbon(wt.%)	69.33	71.40	73.26	73.12	73.04	72.46	72.25
Hydrogen(wt.%)	2.92	3.36	3.25	2.89	3.35	3.48	3.34
Nitrogen(wt.%)	3.51	3.53	3.70	3.58	3.60	3.37	3.28
Oxygen[b](wt.%)	24.24	21.71	19.80	20.42	20.03	20.70	21.14

[b] Calculated by difference.

According to the results of these tests, the catalytic effect of different CoMo loading HZSM-5 on product (bio-oil, bio-char and gas) yields and product distribution were conducted. The results indicated that 4%Mo-2%Co/HZSM-5 treatment yielded the highest amount of hydrocarbons, exhibited an excellent ability to upgrade bio-oil vapor, and showed no significant difference in the properties of bio-char when compared to other treatments in the same pyrolysis conditions.

3.3. Catalysts synthesized from combining Ni and Zn supported on aluminum oxide

The third group of catalysts was synthesized from combining Ni and Zn supported on aluminum oxide. These catalysts were also tested in upgrading sawdust bio-oil processes using a Parr reactor. Catalysts characterizations of the catalysts were carried out. The XRD spectra of Al_2O_3 based catalysts were shown in Figure 8. The diffraction peak characteristics of the Al_2O_3 structure at 25.58°, 35.15°, 37.78°, 43.36°, 52.55°, 57.50°, 61.30°, 66.52°, 68.21°and 77.23° were observed on the XRD patterns of all Al_2O_3 based catalysts according to Joint

Committee on Power Diffraction Standards (JCPDS) file No. 00-046-1212. These peak positions are in accord with the previously reported Al_2O_3 structure studied by Yang et al.[22] It suggested that the crystalline structure of the Al_2O_3 support remained constant after the loading of Ni and/or Zn. Ni/ Al_2O_3 showed NiO phase at peaks of 37.32°, 63.00°, 75.56°and 79.57°according to PDF Card No.1010381. Similar peak positions of NiO was found by Thyssen et al [23, 62 - 66]. Zn/ Al_2O_3 showed ZnO phase at the peak of 32.07°, 36.53°and 81.65° which are consistent with PDF Card No.1011258. Liewhiran et al. also found similar peak positions of ZnO [24, 29, 81 – 86]

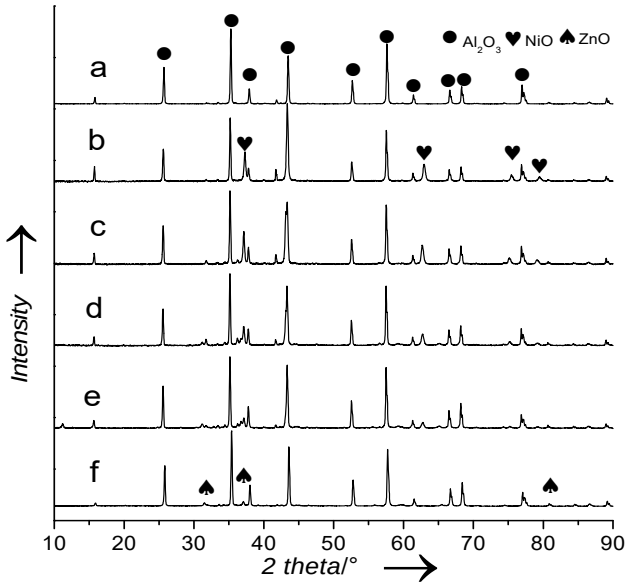

Figure 8. XRD spectra of catalysts: (a) Al_2O_3; (b) 20%Ni/Al_2O_3; (c) 15%Ni-5%Zn/Al_2O_3; (d)10%Ni-10%Zn/Al_2O_3; (e) 5%Ni-15%Zn/Al_2O_3; and 20%Zn/ Al_2O_3.

The TEM images of Al_2O_3 based catalysts are shown in Figure 9. The Al_2O_3 did not show any dark spots since there was no NiO and/or ZnO loading on it. The 20%Ni/Al_2O_3 showed dark spots, which were attributed to the NiO aggregations. The 20%Zn/ Al_2O_3 showed dark spots, which were attributed to the ZnO aggregations. Similar TEM result was found by Kasatkin, et al. that Cu-Zn/Al_2O_3 showed dark particles, which were attributed to copper oxide and/or zinc oxide [25, 42, 78 – 83] The 15%Ni-5%Zn/Al_2O_3, 10%Ni-10%Zn/Al_2O_3 and 5%Ni-15%Zn/Al_2O_3 showed dark spots, which might be attributed to the aggregation of NiO and/or ZnO. The TEM results of Al_2O_3 based catalysts are consistent with the XRD results about the presence of peak phases such as NiO and/or ZnO.

The EDS elemental analysis of fresh and used catalysts is shown in Table 13. The Ni and/or Zn elements were found in Ni and/or Zn loaded Al_2O_3 catalysts, and it confirmed the presence of NiO and/or ZnO. This is in agreement with the existence of XRD peaks of NiO and/or ZnO in catalysts. The bio-oil obtained in HDO process can be separated to two phases: oil phase (targeted biofuel, mainly composed of organic compounds) and aqueous phase (contained main water and a few organic compounds). The yields of bio-oil HDO products (oil phase, aqueous phase, coke and gas) are shown in Table 14. Compared to monometallic catalysts (Ni/Al_2O_3 and Zn/Al_2O_3), bimetallic catalysts such as 15%Ni-5%Zn/ Al_2O_3 and 10%Ni-10%Zn/Al_2O_3 increased the oil phase yields. This change might be due to the promoted hydrodeoxygenation and

hydrogenation reactions of bio-oil over bimetallic catalysts that increased the hydrophobic compounds such as hydrocarbons [26, 63, 79 – 83]. The coke yield decreased in the bimetallic catalysts in comparison with monometallic catalysts, which indicated that bimetallic catalysts might inhibit polymerization and poly-condensation reactions responsible for the coke formation in bio-oil HDO process [27, 49 – 53]. Similar results of the lower coke yields of bimetallic catalysts for bio-oil hydrotreating were confirmed by Ardiyanti et al.[15] In comparison, the 15%Ni-5%Zn/Al_2O_3 catalyst generated the highest oil phase (biofuel) yield at 44.64% and it led to the lowest coke yield at 4.67%.

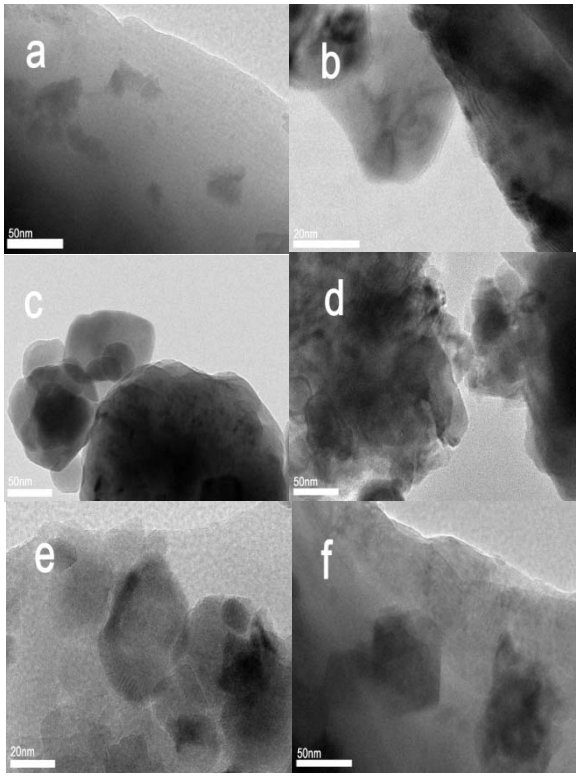

Figure 9. TEM images of catalysts: (a) Al_2O_3; (b) 20%Ni/Al_2O_3; (c) 15%Ni-5%Zn/Al_2O_3; (d)10%Ni-10%Zn/Al_2O_3; (e) 5%Ni-15%Zn/Al_2O_3; and 20%Zn/ Al_2O_3.

The physicochemical properties of upgraded bio-oils (biofuel), such as water content, pH and higher heating values (HHV), were measured and listed in Table 15. The water content of bio-oils has a negative effect on the combustion performance of biofuels in engines [18, 23, 69 – 71] The water content of the oil phase reduced significantly from 26.91% in the raw bio-oil to the figure ranging from 11.48% to 17.53%. This was due to the formation of more hydrophobic products such as hydrocarbons in the oil phase and transferring water to aqueous phase.[28] The HHV of oil phase (ranging from 27.85 MJ kg^{-1} to 30.47 MJ kg^{-1}) also improved greatly in comparison with the raw bio-oil (15.54 MJ kg^{-1}), which was due to its lower water content and higher hydrocarbons content. This indicated that the catalytic HDO process can effectively improve the energy content of the bio-oil samples. Low pH values of bio-oil have a corrosive effect on engine parts. The pH of oil phase (3.31-3.43) is slightly higher than raw bio-oil (3.24), which may result from the transformation of acids to other compounds such as hydrocarbons in the upgraded bio-oils.

Table 13. EDS elemental compositions of Ni-Zn/Al_2O_3 catalysts

Catalysts	Al_2O_3	20%Ni/Al_2O_3	15%Ni-5%Zn/Al_2O_3	10%Ni-10%Zn/Al_2O_3	5%Ni-15%Zn/Al_2O_3	20%Zn/Al_2O_3
Al content [wt.%])	65.99	10.82	44.97	49.17	17.91	52.77
O content [wt.%]	34.01	2.94	31.88	23.59	21.05	30.64
Ni content [wt.%]	0	86.24	18.72	20.47	52.21	0
Zn content [wt.%]	0	0	4.43	6.77	8.83	16.59

Table 14. Product yields of different treatments

Catalysts	Bio-oil			Coke	Gas
	Total [wt.%]	Oil phase [wt.%]	Aqueous phase [wt.%]	Coke [wt.%]	Gas [wt.%]
20%Ni/ Al_2O_3	69.64	39.28	30.36	7.11	23.26
15%Ni-5%Zn/ Al_2O_3	73.08	44.64	28.44	4.67	22.25
10%Ni-10%Zn/ Al_2O_3	76.41	41.88	34.53	5.95	17.63
5%Ni-15%Zn/ Al_2O_3	70.02	34.64	35.38	5.11	24.87
20%Zn/ Al_2O_3	67.25	39.53	27.72	7.49	25.25

Table 15. Physicochemical properties of upgraded bio-oils (oil phase)

Catalysts	20%Ni/Al_2O_3	15%Ni-5%Zn/Al_2O_3	10%Ni-10%Zn/Al_2O_3	5%Ni-15%Zn/Al_2O_3	20%Zn/Al_2O_3
Water content [wt.%]	17.53	14.00	12.98	15.33	11.48
pH	3.41	3.31	3.34	3.43	3.43
HHV[MJ kg^{-1}]	28.47	30.47	30.39	29.37	27.85

In order to determine the activities of different catalysts on the upgraded bio-oil products, the chemical compositions of upgraded bio-oil (OP) were analyzed by GC-MS. The chemical compositions of bio-oils are shown in table 16. Different chemical groups, such as phenols, ethers, ketones, esters, alcohols, furans, aldehydes, acids and hydrocarbons, were determined in the bio-oils. The organic compositions of upgraded bio-oil changed significantly after mild HDO processes over different Ni-Zn/ Al_2O_3 catalysts. The undesirable acids in bio-oil were significantly reduced by all catalysts. The acids may be converted into hydrocarbons via the

decarbonylation, hydrogenation and cracking reaction [29, 41, 69 – 75]. In addition, some carboxylic acids may be transferred from the oil phase to the aqueous phase. The decreasing of acid content is beneficial for refineries to further processing the upgraded HDO bio-oils in terms of reducing corrosion and materials of construction. Ketones that resulted in the low heating value and instability of raw bio-oil were decreased in all catalytic treatments. Ketones were decomposed through decarboxylation to form CO_2 and hydrocarbons [30]. Alcohols were easily transformed to hydrocarbons and phenols in HDO process [6] that led to the decrease of alcohols content in all catalytic treatments. The esters would be cracked into hydrocarbons via the catalytic hydrogenation along with decarboxylation and decarbonylation reactions [29] and this resulted in the decrease of esters in upgraded bio-oils in all catalytic treatments. After the bio-oil HDO reaction, the content of aldehydes and phenols also decreased in all upgraded bio-oil products, possibly because they were transformed into coke-like polymers in the presence of acidic catalyst [31].

Hydrocarbons are the most important compounds that most research focused on. The content of hydrocarbons in oil phase increased in all catalytic treatments. This was due to the HDO reactions (cracking, decarbonylation, decarboxylation, hydrocracking, hydrodeoxygenation and hydrogenation) that converted oxygenated organic compounds to hydrocarbons over Ni-Zn/Al_2O_3 catalysts [26, 81 – 86] Compared to monometallic catalysts, 15%Ni-5%Zn/Al_2O_3 generated the upgraded bio-oil with the highest hydrocarbons content at 50.12%. This might be due to the synergistic effect of Ni and Zn on Al_2O_3 support that promoted HDO performance. After bio-oil HDO reaction, the gas product was collected and analyzed by GC. In order to analyze the HDO reaction, initial, maximum and final pressure of the HDO reactor was also recorded. The initial pressure was the hydrogen pressure used at the beginning of the test. The maximum pressure is the maximum HDO reactor pressure when the bio-oil HDO is running at the targeted temperature. The final temperature is the pressure when the HDO reactor is cooled to room temperature (20°C). The pressure of HDO reactor and compositions of gas are listed in Table 16. As is shown in the table, there are 11 gas compounds detected in the non-condensable gas. The main composition in gas product was unreacted hydrogen, and this indicated that the hydrogen was abundant for bio-oil HDO reactions. Another main gas product is CO_2, which suggested effective decarboxylation of organic acids over Ni-Zn/Al_2O_3 catalysts in bio-oil HDO processes [32]. Light hydrocarbons such as CH_4 and C_2H_6 were formed in each treatment, which was probably due to cracking of organic compounds such as alcohols. The difference between initial and final pressure in the reactor indicated that the hydrogen was consumed in the bio-oil HDO process over Ni-Zn/Al_2O_3 catalysts. Although the initial pressure was the same for all catalyst, the final pressure was lower for 15%Ni-5%Zn/Al_2O_3, 10%Ni-10%Zn/Al_2O_3 and 20%Zn/Al_2O_3 catalysts. This indicated the higher hydrogen consumption for bio-oil HDO reactions in these catalysts. This is helpful for increasing HDO performance for the conversion of oxygenated compounds to hydrocarbons in upgraded bio-oil products. This is consistent with higher hydrocarbons contents in these catalytic treatments. The syngas distributions of different treatments are shown in table 17. The results of these tests can be summarized in these points. 1) The HDO upgrading of pine sawdust raw bio-oil over a series of Ni-Zn/Al_2O_3 catalysts were carried out in the autoclave reactor at 250℃ and 500 psi. The catalytic effects of Ni-Zn/Al2O3 catalysts are evaluated in terms of products (bio-oil and gas) yield and quality. Bimetallic Ni-Zn/Al_2O_3 exhibited higher activity of improving bio-oil yield and quality compared to monometallic Ni/Al_2O_3 or Zn/Al_2O_3 catalyst. 15%Ni-5%Zn/ Al_2O_3 catalyst generated the highest

oil phase yield at 44.64% and it also generated the upgraded bio-oil with the highest hydrocarbon content at 50.12%. Physicochemical properties of upgraded bio-oils such as water content, pH and HHV were significantly improved. The valuable hydrocarbon contents of upgraded bio-oil over Ni-Zn/Al_2O_3 catalysts were significantly increased compared to raw bio-oil, while the undesirable acids, aldehydes and ketones were greatly decreased in upgraded bio-oil in comparison with raw bio-oil.

Table 16. Chemical compositions of different bio-oils (oil phase)

Relative content [%]	Raw bio-oil	20%Ni/Al_2O_3	15%Ni-5%Zn/Al_2O_3	10%Ni-10%Zn/Al_2O_3	5%Ni-15%Zn/Al_2O_3	20%Zn/Al_2O_3
Phenols	21.10	15.48	12.55	19.34	15.46	18.36
Ethers	3.59	1.62	6.21	0.36	0	0.70
Aldehydes	5.40	1.17	0	0.62	0.92	0.48
Ketones	9.77	3.92	0.23	0.28	3.11	4.79
Esters	6.86	3.90	0	3.53	3.72	3.19
Alcohols	5.64	2.18	0.21	1.30	2.23	0.91
Acids	17.62	9.80	6.65	6.39	9.73	6.99
Furans	0.72	0	0	0.35	0	0.23
Hydrocarbons	16.94	38.58	50.12	49.91	39.62	43.86
Others	12.36	23.35	24.03	17.92	25.21	20.49

Table 17. Syngas distributions of different treatment

Catalysts		20%Ni/ Al_2O_3	15%Ni-5%Zn /Al_2O_3	10%Ni-10%Zn /Al_2O_3	5%Ni-15%Zn /Al_2O_3	20%Zn /Al_2O_3
Pressure [psi]	Initial	500	500	500	500	500
	Maximum	1090	1170	1150	1110	1110
	Final	490	470	480	490	480
Gas	H_2	89.77	90.26	89.50	89.71	89.56
composition	CO_2	9.73	9.27	10.02	9.84	9.80
[vol.%]	CO	0.36	0.29	0.31	0.30	0.31
	CH_4	0.11	0.09	0.10	0.09	0.10
	C_2H_6	0.01	0.02	0.02	0.01	0.02
	C_2H_4	0.01	0.00	0.01	0.01	0.02
	C_3H_8	0	0.01	0.00	0.01	0.01
	C_3H_6	0	0.00	0.00	0.00	0.10
	C_4H_{10}	0	0.00	0.00	0.00	0.00
	C_4H_8	0.01	0.04	0.04	0.03	0.08
	C_5H_{12}	0	0.02	0.00	0.00	0.00

3.4. Catalysts synthesized from combining Ni and Cu supported on activated carbon (AC)

The third group of catalysts was synthesized from combining Ni and Zn supported on aluminum oxide. These catalysts were also tested in upgrading PCG bio-oil processes using a Parr reactor. Catalysts characterizations of the catalysts were carried out. The XRD patterns of different metal

loaded AC catalysts are shown in Figure 10. The specific pattern of AC support maintained in all catalysts, since the small sharp peak (26.6°) of graphitic carbon existed in all catalysts [43, 81 – 83]. There are two peaks (44.2°and 51.7°) identified in all metal AC catalysts, corresponding to the presence of metallic Ni particles on the crystalline structure of impregnated catalysts [44, 66 – 69]. In the Ni-Cu/AC catalyst, the existence of Cu particles can be detected from peaks at around 43°and 50°. However, they overlapped the reflection peaks of the metallic Ni phase, which is due to the segregation of some of the metallic Cu particles from the Ni-Cu alloy particles formed after the thermal treatment [44]. The diffraction peaks at 35.5°, 43.1°and 62.6°associated to cubic iron oxide phases (Fe_2O_3) are determined in Ni-Fe/AC catalysts [45, 46]. MoO_2 crystallites along withα-$NiMoO_4$ and β-$NiMoO_4$ mixed phases are identified in Ni-Mo/AC catalysts [43, 46, 57 – 59].

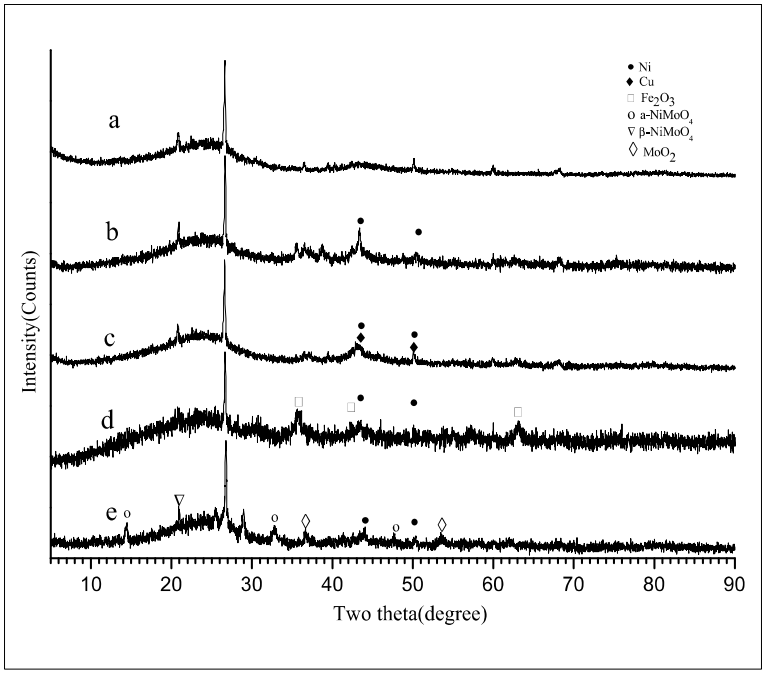

Figure 10. The XRD patterns of different metal loaded AC catalysts

The textural properties of the AC support catalysts with different metals are listed in Table 18. Surface areas of metal loaded AC catalysts are lower than the surface area of the activated carbon. The addition of the metals (Ni, Fe, Mo and Cu) on the AC support resulted in a decrease of the surface area and total pore volumes for all metal loaded catalysts, which is probably due to the filling or blocking of the metal and metal oxides (Ni, Cu, Fe_2O_3, MoO_2,α-$NiMoO_4$ and β-$NiMoO_4$) in the pores of the corresponding AC support [47].

TEM analysis of the catalysts was carried out. Figure 11 shows the bright field high resolution TEM images of catalysts. As seen in Figure 12a, there were no dark spots shown for pure AC, because there was no metal loading on it. However, fresh 6%Ni/AC showed obvious dark spots in Fig. 12b, which was attributed to the presence of Ni particles. As was shown in Fig. 12c, TEM images of Ni-Cu/AC also showed obvious dark spots due to the presence of Ni-Cu alloy particles. Dark spots were also found in the TEM images of Ni-Fe/AC (Fig. 12d), which

indicated the existence of metal Ni or Fe_2O_3. Ni, MoO_2, α-NiMoO4 or β-NiMoO4 crystallites are also detected as dark spots in the TEM images of Ni-Mo/AC (Fig. 12e). The histograms on the particle size distribution were calculated by counting particles appeared in the TEM images of prepared catalysts [48]. The histograms on the particles distributions in the four prepared catalysts are built towards a represented selection of particles (from 711 to 882 depending on the catalyst sample). The histograms in Figure 13 showed the particle size distribution of the four prepared catalyst.

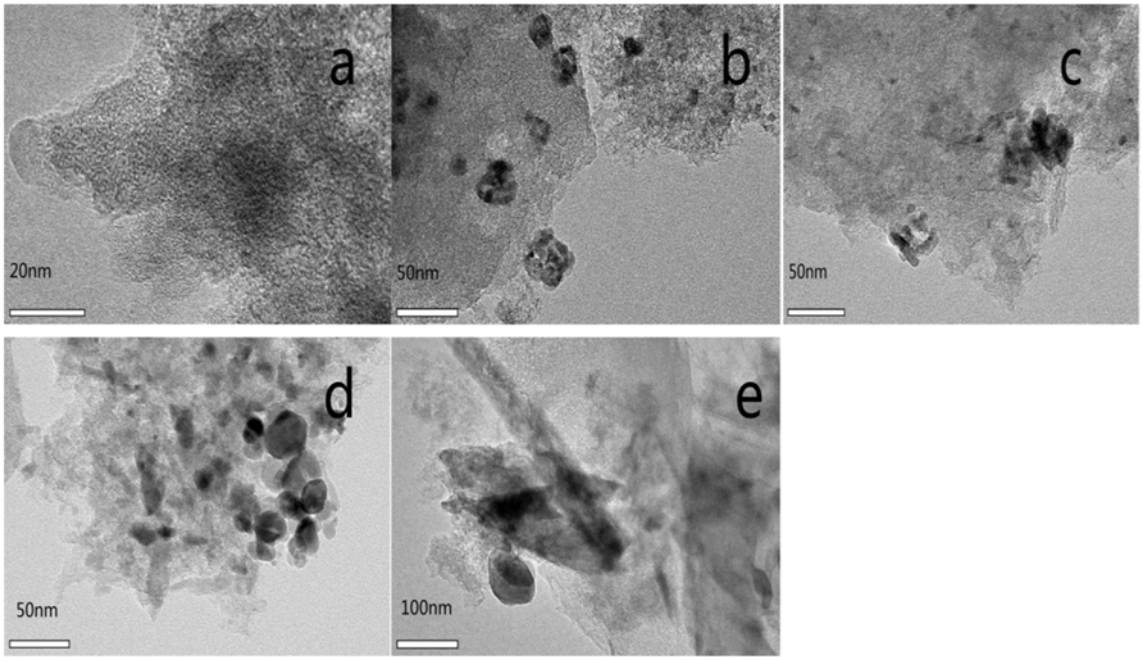

Figure 12. The bright field high-resolution TEM images of the catalysts

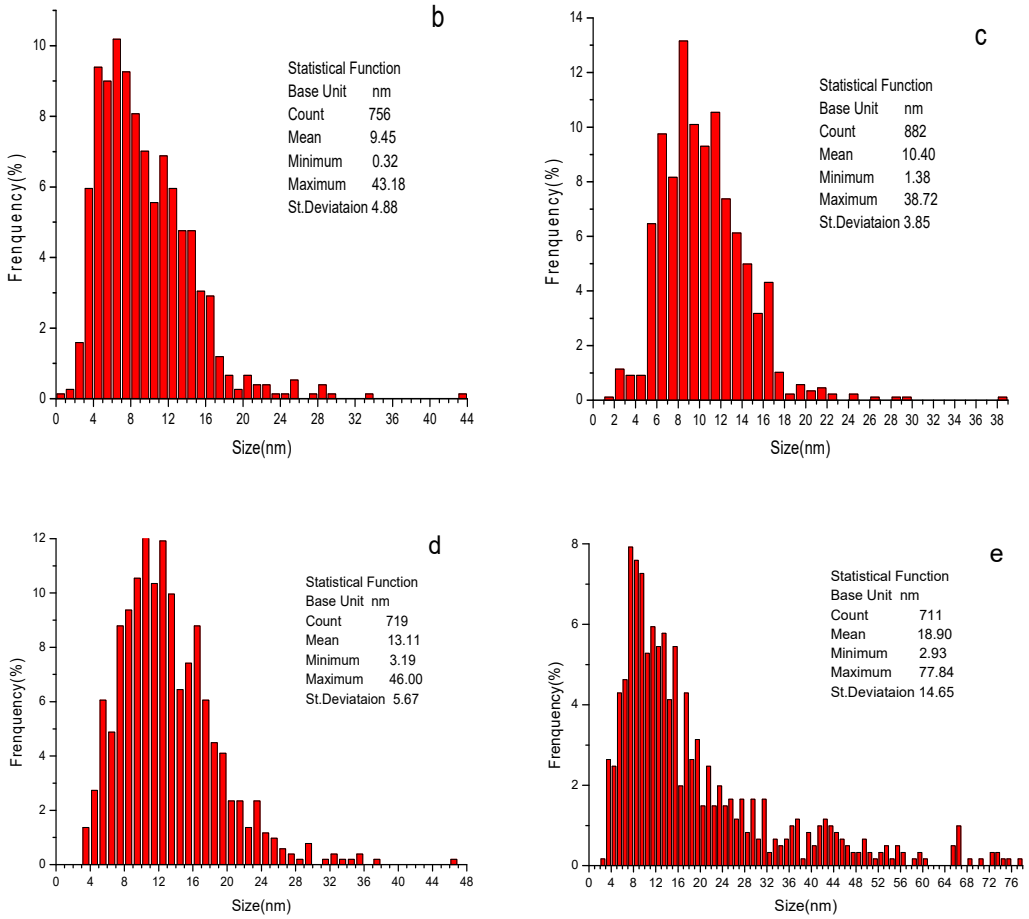

Figure 13. The histograms of metal particle size distribution based on TEM images for the following catalysts: b-6%Ni/AC, c-6%Ni-6%Cu/AC, d-6%Ni-6%Fe/AC and e-6%Ni-6%Mo/AC.

The sample b (6%Ni/AC) has a narrow size distribution with a maximum at 6–7 nm, also there are a very few large particles or agglomerates with size above 28 nm. The sample c (6%Ni-6%Cu/AC) also has a narrow size distribution with a maximum at 8–9 nm, there are also a very few large particles or aggregates with size above 28 nm. The sample d (6%Ni-6%Fe/AC) has a wide size distribution with a maximum at 10–11 nm, and there are some large particles or aggregates with size above 36 nm. The sample e (6%Ni-6%Mo/AC) has a wide size distribution with a maximum at 8–9 nm, and there are a very few large particles or aggregates with size above 72 nm.

The metal dispersions, D (%) were calculated as the number of metal atoms at the surface divided by the total number of metal atoms in the catalyst sample [49-50]. The dispersion are calculated according the following equation: dispersion (D (%)) = number of metal atoms on surface / total number of metal atoms = [(surface area)/(cross section area of metal atom)] / [(volume of sphere)/(metal atom volume in space lattice)] = 3/r×(metal atom volume in space lattice / cross section area of metal atom), where r is the radius of metal particle [51, 78 – 81]. The average metal particle size and metal dispersion are shown in the Table 19.

Table 19. Average metal particle size and dispersion of prepared catalysts

Catalyst	Average metal particle size (nm)	Metal dispersion (%)
b (6%Ni/AC)	9.45	10.64
c (6%Ni-6%Cu/AC)	10.40	9.82
d (6%Ni-6%Fe/AC)	13.11	7.68
e (6%Ni-6%Mo/AC)	18.90	5.60

The dispersion of the prepared catalysts was varying in a range of 5.60–10.46%. Compared to b-6%Ni/AC, the addition of Cu, Fe and Mo reduced the metal dispersion of c-6%Ni-6%Cu/AC, d-6%Ni-6%Fe/AC and e-6%Ni-6%Mo/AC. This might be due to the larger particle size of bimetallic catalyst, which resulted from the aggregations of metal particles on the surface of the bimetallic catalysts [52]. Similar result was found by Duvenhage DJ et al [53-58]. The aggregations which were responsible for the low metal dispersion of bimetallic catalysts were also found as larger dark spots appeared in the TEM images of the four prepared catalysts (Figure 12).

The yield of the bio-oil HDO products (aqueous phase, oil phase, char and gas), based on the weight of the raw bio-oil, are shown in Table 20. Compared with Ni/AC treatment, the Ni-Fe/AC catalyst obtained the lowest oil phase yield and char yield, and produced the highest gas yield. This trend may result from the further decomposition of organic compounds in the liquid phase due to the addition of Fe, such as deoxygenation to form carbon dioxide in the gas (20.01% in further gas analysis). The addition of Mo to Ni/AC generated the higher oil phase yield and lower char yield, and it indicated that Ni-Mo/AC slightly reduced the formation of polyaromatic species due to the polymerization and polycondensation reaction, which result in the lower char forming (8.78%) [59]. The addition of Cu also improved the HDO effect of Ni/AC in terms of increasing oil phase yield and decreasing char yield. The aqueous phase yield of all treatments is similar at around 50%, this might be the result of the de-moisturization of the organic compound in the oil phase to the aqueous phase with high water content (around 90%) [60].

Table 20

Mass balance of upgrading products from different catalytic treatments

Treatments	Bio-oil		Char	Gas
	Oil phase (wt%)	Aqueous phase (wt%)	Char (wt%)	Gas (wt%)
Ni/AC	20.17	51.35	8.86	19.63
Ni-Fe/AC	17.35	51.34	3.09	28.24
Ni-Cu/AC	21.57	51.62	4.80	22.02
Ni-Mo/AC	21.91	49.37	8.78	19.96

The physicochemical properties of different upgraded bio-oils, such as water content, pH, elemental compositions and higher heating values, are measured and listed in Table 21. The water content of the oil phase reduced significantly from 48.91% in the raw bio-oil to the figure ranging from 6.12% to 11.98% through hydrodeoxygenation and transferring water to aqueous phase. The HHV of the oil phase (ranging from 29.65 MJ/kg to 31.61 MJ/kg) also improved greatly in comparison with the raw bio-oil (11.33MJ/kg), which is due to its much lower water

and oxygen content. The pH of oil phase is slightly higher than raw bio-oil, which may result from the transformation of acids to esters in the upgraded products.

Table 21
Physicochemical properties of different upgrading bio-oils

Treatments	Ni/AC	Ni-Fe/AC	Ni-Cu/AC	Ni-Mo/AC
Water content (wt%)	8.10 ± 0.77	11.98 ± 1.10	6.12 ± 0.33	6.52 ± 1.30
pH	3.63 ± 0.06	3.48 ± 0.03	3.13 ± 0.01	3.50 ± 0.01
Carbon (wt%)	65.13 ± 0.23	67.64 ± 0.98	64.29 ± 1.19	66.55 ± 1.94
Hydrogen (wt%)	8.28 ± 0.36	9.30 ± 0.84	8.54 ± 1.14	8.72 ± 0.88
Nirogen (wt%)	1.55 ± 0.20	1.36 ± 0.02	1.29 ± 0.06	1.35 ± 0.04
Oxygen[a] (wt%)	25.04 ± 0.79	21.70 ± 0.15	25.88 ± 0.01	23.38 ± 1.09
HHV (MJ/kg)	29.65 ± 0.32	31.61 ± 1.17	31.50 ± 1.37	31.58 ± 1.08
DOD	63.60 ± 1.15	68.46 ± 0.23	62.39 ± 0.02	66.02 ± 1.59

[a] Calculated by difference.

Compared to the carbon and oxygen contents in raw bio-oil (20.01% and 68.81% separately), the carbon content in the upgraded bio-oil (64.29-67.64%) increased significantly, while the oxygen content deceased to only 21.70-25.88%. This was mainly caused by the hydrodeoxygenation and decarboxylation reactions of oxygenated compounds that remove oxygen in the form of H_2O and CO_2, which were then transferred to aqueous phase and gas respectively. The decrease of oxygen levels also lead to the high degree of deoxygenation (DOD), which ranged from 62.39% to 68.46%. This DOD is comparable to the DOD of noble Pt/C catalysts (64%) for the HDO of bio-oil [23]. One of the major objectives for this study was to explore the effects of different catalysts on the distribution of organic compounds in the upgraded liquid products. Therefore, the chemical compositions of upgraded bio-oil (OP) are determined by GC-MS. The various components present in the original bio-oil were also analyzed for comparison. The main chemical compounds of raw bio-oil and upgraded bio-oils, as analyzed by GC-MS, are shown in Table 22. The compositions were classified into different categories: phenols, ethers, ketones, esters, alcohols, acids and hydrocarbons. In raw PCG bio-oil, the type and proportion of organic components are in agreement with those reported by others [61]. The PCG bio-oil produced was rich in phenols (55.88%), and it also contained undesirable carboxylic acids (3.05%) and ketones (8.55%). The content of hydrocarbons was only 8.78%. The organic compositions of upgraded bio-oil changed significantly after mild HDO processes over different AC supported catalysts. After the reaction, the content of phenols increased in all catalytic treatments except Ni/AC. The improvement of phenols is due to the formation of alkyl-phenols such as 2-methyl-phenol and 3, 4-dimethyl-phenol. The Ni/AC was not very active for the hydrogenation of phenol ring, therefore most of the phenol rings were maintained in all treatments [62]. The addition of Fe, Cu and Mo to Ni/AC might promote the alkylation reactions between phenol and alcohols or light olefins, and then the following reactions of demethoxylation, demethylation and hydrogenation lead to the generation of phenolic derivatives such as alkyl-phenols [60]. By comparison, the Ni-Mo/AC generated the upgraded bio-oil with the highest alkyl-phenol content at 38.41%. The alkyl-phenols have been found to possess high blending octane numbers. Therefore, it might have potential to be an excellent gasoline blendstock [63].

Table 23

Chemical composition analysis of upgraded bio-oils (OP) by GC–MS

Compounds relative content (%)	Raw bio-oil	Ni/AC	Ni-Fe/AC	Ni-Cu/AC	Ni-Mo/AC
Phenols	55.88	54.65	71.28	65.98	69.99
Alkyl-phenols[a]	0	0.86	33.84	31.46	38.41
Ethers	2.83	0	0.29	0	2.00
Ketones	8.55	0.68	0.63	0.36	1.87
Esters	3.98	0	0.36	0	2.61
Alcohols	7.49	3.2	1.67	5.72	3.40
Acids	3.05	0.43	0	0	0.46
Hydrocarbons[b]	8.78	39.42	24.98	26.60	16.37
Light hydrocarbons (C6–C12)	6.32	32.63	23.01	24.62	13.80
Heavy hydrocarbons (C13–C35)	2.46	6.79	1.97	1.98	2.57

[a] Alkyl-phenols are included in phenols.
[b] Sum of light hydrocarbons and heavy hydrocarbons.

The undesirable acids in bio-oil are significantly reduced by all HDO processes over different AC supported catalysts. The acids may be converted into relatively stable esters through decarbonylation, dehydroxylation and ring opening [60]. In addition, some carboxylic acids may be transferred from the oil phase to the aqueous phase [9]. Acids even disappeared totally in Ni-Fe/AC and Ni-Cu/AC treatments. The decreasing of acid content is beneficial for refineries to further processing the upgraded HDO bio-oils in terms of reducing corrosion and materials of construction.
Ketones, which are responsible for the low heating value and instability of raw bio-oil, were also reduced in all HDO processes. Micromolecule ketones were decomposed through decarboxylation to form CO_2 and hydrocarbons, while macromolecule ketones were transferred to other ketones [9]. Alcohols were easily transformed to hydrocarbons and phenol derivatives by HDO, which leads to the decrease of alcohol content in all catalytic treatments.
The content of hydrocarbons in oil phase increased because of the HDO effect of oxygenated organic compounds in all catalytic treatments, and Ni/AC generated the upgraded bio-oil with the highest hydrocarbon content at 39.42%. The lower yield of hydrocarbons over Ni-Fe/AC, Ni-Cu/AC and Ni-Mo/AC catalysts might results from the competition reaction to form phenolic derivatives, which reduced the proportion of alcohols that can be used to produce hydrocarbons. The alkylation reactions between phenol and light olefins also consumed partial hydrocarbons. However, the main proportion of hydrocarbons is still light hydrocarbons (C6-C12), which has the potential to be utilized as gasoline additives.

Gas analysis of the non-condensable gas (NCG, also named syngas) produced in the tests were performed using a GC. The composition of non-condensable gas (NCG) provides valuable information on the types of reactions that occurred in the HDO processes. The compositions of syngas are listed in Table 23. As is shown in the table, there are 10 gas compounds detected in the non-condensable gas. As expected, the main component is hydrogen, which was the unreacted hydrogen that fed into the autoclave at the beginning of the experiment. The presence of unreacted hydrogen also indicates that the reactions were not conducted under hydrogen starvation conditions. The second highest composition of gas is always CO_2, which suggested effective decarboxylation of such as ketones and esters followed by water gas shift or disproportionation (Boudouard reaction) over the AC supported catalysts in all bio-oil HDO processes [63]. For each case, small amount of CH_4 were formed as well, which was probably as result of the demethylation of phenolic derivatives [9]. Some light hydrocarbons (C2-C5) were also produced, and this might

Table 24

NCG distributions of different treatments

Gas (vol%)	Ni/AC	Ni-Fe/AC	Ni-Cu/AC	Ni-Mo/AC
H_2	75.29	61.16	70.58	68.08
CO_2	9.86	20.01	11.70	12.73
CH_4	1.97	3.46	3.78	4.27
C_2H_6	0.72	1.45	1.66	1.55
C_2H_4	7.12	0.08	0.09	0.09
C_3H_8	1.59	5.84	5.40	5.80
C_3H_6	2.81	7.63	6.39	7.05
C_4H_{10}	0.54	0.22	0.30	0.25
C_4H_8	0.01	0.11	0.07	0.13
C_5H_{12}	0.09	0.04	0.03	0.05

Ni based catalyst was very active in the hydrogenation reactions [64]. However, monometallic Ni-based catalyst showed higher coking levels in HDO process [65]. In this study, the char (coking) yield of the Ni/AC treatment was 8.86%. Compared to the monometallic Ni catalysts, the addition of a second metal such as Mo, Fe and Cu can reduce the coke formation and increase catalyst activity. Bimetallic Ni–Cu catalysts are found to be more active than single Ni catalysts in HDO under mild conditions [66]. The char (coking) yield of Ni-Cu/AC catalyst (4.80%) was lower than Ni/AC catalyst (8.86%). The possible reason might be that the copper addition facilitates reduction of nickel oxide and decreases the coke formation on Ni catalysts [67].

In Ni-Fe bimetallic catalysts, the addition of Fe can promote the C=O hydrogenation and inhibit the C-C breaking [68-69], which might result in the higher yield of phenols in Ni-Fe/AC treatment (compared to Ni/AC). The Ni-Fe/AC treatment also led to lower char (coking) yield (3.09%) than Ni/AC treatment (8.86%). Bimetallic Ni-Mo catalyst was a highly active and stable [70]. The Ni-Mo/AC catalysts can promote C-O activation while inhibiting the C-C breaking [15], which might result in the higher DOD of Ni-Mo treatment (66.02%) than the Ni/AC treatment (63.06%).

The HDO upgrading of PCG raw bio-oil over different metal AC catalysts under mild conditions were carried out in the autoclave reactor. The effects of the different catalysts are evaluated in terms of organic liquid product yield and selectivity towards alkyl phenols and hydrocarbons. The results show that all catalysts had significant improvements on the physicochemical properties (water content, pH, oxygen content, higher heating value and chemical compositions) of the upgraded PCG bio-oil. All AC supported catalysts increased the hydrocarbon yield in upgraded bio-oil in comparison to raw bio-oil, while the Ni/AC catalysts produced the highest light hydrocarbons content at 32.63% in upgraded bio-oil. The addition of Fe, Cu and Mo to Ni/AC increased the yields of alkyl-phenols, and Ni-Mo/AC generated the upgraded bio-oil with the highest content of alkyl-phenols at 38.41%.

3.5. CFP technology commercialization

The SDSU proprietary ACCFP technology has been licensed to the Thermo-Ag LLC, a start-up South Dakota limited liability company under the umbrella of South Dakota Innovation Partners for biofuel development, scale-up and commercialization. This technology has gained interest

from a number of industry partners, one of which is International Guangxi Yongkai Industrial Group, LTD. The company CEO, Mr. Kepin Lai, has visited the research lab on SDSU campus and the Thermo-Ag LLC. Negotiations with Mr. Lai to supply capital for pilot plant construction are ongoing and appear favorable. The new research results indicated that multifunctional catalysts synthesized from transition metals could improve bio-oil yield and quality. Compared to noble metal catalyst, the transition metal catalysts showed compatible activity and selectivity but the costs were much lower. There is very promising potential to commercialize these technologies to biofuel industry.

4. CONCLUSIONS

Based on the results obtained from this study, some conclusions can be drawn:

- The yield and quality of bio-oil and upgraded biofuels is significantly affected by the activity and selectivity of catalysts used in biomass CFP process. The better activity and selectivity of catalysts, the better yield and quality of liquid biofuels could be obtained.
- There are significant differences in bio-oil yields and quality when different catalysts were applied in CFP process. Bimetallic Ni-Cu catalysts were more active than single Ni catalysts in hydrodeoxygenation process under mild conditions. The coking (char) yield of Ni-Cu/AC catalyst was lower than Ni/AC catalyst. The combination of Co and Mo supported on Zeolite (HZSM-5) showed favorable to produce higher hydrocarbon biofuel and lower oxygen content.
- Bimetallic Ni-Zn/Al_2O_3 catalysts exhibited higher activity on bio-oil yield and quality compared to monometallic Ni/Al_2O_3 or Zn/Al_2O_3 catalysts. When an appropriate combination of Ni and Zn loading level, the yield and quality of hydrocarbon in the upgraded bio-oil could be significantly increased while at the same time the undesirable acids, aldehydes and ketones were greatly decreased. 15%Ni-5%Zn/ Al_2O_3 catalyst generated the highest oil phase yield at 44.64% with the highest hydrocarbon content at 50.12%. Physicochemical properties of the upgraded bio-oils such as water content, pH and HHV were also significantly improved.
- All AC supported catalysts increased the hydrocarbon yield in upgraded bio-oil in comparison to raw bio-oil, while the Ni/AC catalysts produced the highest light hydrocarbons content at 32.63% in upgraded bio-oil. The addition of Fe, Cu and Mo to Ni/AC in- creased the yields of alkyl-phenols, and Ni-Mo/AC generated the upgraded bio-oil with the highest content of alkyl-phenols at 38.41%.
- The technologies integrated SDSU proprietary CFP reactor and the multifunctional catalysts synthesized from transition metals supported on zeolite and activated carbon have promising potential for future commercialization to biofuel industry.

LIST OF REFERENCES

[1] Mohr SH, Wang J, Ellem G, Ward J, Giurco D. Projection of world fossil fuels by country. Fuel 2015;141:120–35.

[2] Srokol Z, Bouche AG, van Estrik A, Strik RC, Maschmeyer T, Peters JA. Hydro- thermal upgrading of biomass to biofuel; studies on some monosaccharide model compounds. Carbohydr Res 2004;339:1717–26.

[3] Ranzi E, Cuoci A, Faravelli T, Frassoldati A, Migliavacca G, Pierucci S, et al. Chemical kinetics of biomass pyrolysis. Energy Fuels 2008;22:4292–300.

[4] Cheng S, Wei L, Zhao X, Huang Y, Raynie D, Qiu C, et al. Directly catalytic upgrading bio-oil vapor produced by prairie cordgrass pyrolysis over Ni/HZSM-5 using a two stage reactor. AIMS Energy 2015;3:227–40.

[5] Zhang Q, Chang J, Wang T, Xu Y. Review of biomass pyrolysis oil properties and upgrading research. Energy Convers 2007;48:87–92.

[6] Shemfe MB, Gu S, Ranganathan P. Techno-economic performance analysis of biofuel production and miniature electric power generation from biomass fast pyrolysis and bio-oil upgrading. Fuel 2015;143:361–72.

7] Zhang X, Wang T, Ma L, Zhang Q, Jiang T. Hydrotreatment of bio-oil over Ni- based catalyst. Bioresour Technol 2013;127:306–11.

[8] Popov A, Kondratieva E, Mariey L, Goupil JM, El Fallah J, Gilson JP, et al. Bio-oil hydrodeoxygenation: adsorption of phenolic compounds on sulfided (Co) Mo catalysts. J Catal 2013;297:176–86.

[9] Xu X, Zhang C, Liu Y, Zhai Y, Zhang R. Two-step catalytic hydrodeoxygenation of fast pyrolysis oil to hydrocarbon liquid fuels. Chemosphere 2013;93(4):652–60.

[10] He Z, Wang X. Hydrodeoxygenation of model compounds and catalytic systems for pyrolysis bio-oils upgrading. Catal Sustain Energy 2012;1:28–52.

[11] Zhao C, He J, Lemonidou AA, Li X, Lercher JA. Aqueous-phase hydrodeoxy- genation of bio-derived phenols to cycloalkanes. J Catal 2011;280:8–16.

[12] Gutierrez A, Kaila RK, Honkela ML, Slioor R, Krause AOI. Hydrodeoxygenation of guaiacol on noble metal catalysts. Catal Today 2009;147:239–46.

[13] Centeno A, Maggi R, Delmon B. Use of noble metals in hydrodeoxygenation reactions. Stud Surf Sci Catal 1999;127:77–84.

[14] Chen L, Zhu Y, Zheng H, Zhang C, Zhang B, Li Y. Aqueous-phase hydrodeox- ygenation of carboxylic acids to alcohols or alkanes over supported Ru catalysts. J Mol Catal A Chem 2011;351:217–27.

[15] Yang YN, Zhang HK, En-jing L, Zhang CH, Ren J. Effect of Fe, Mo promoters on acetic acid hydrodeoxygenation performance of nickel-based catalyst. J Mol Catal (China) 2011;25:30–6.

[16] Yakovlev VA, Khromova SA, Sherstyuk OV, Dundich VO, Ermakov DY, Novopashina V, et al. Development of new catalytic systems for upgraded bio-fuels production from bio-crude-oil and biodiesel. Catal Today 2009;144: 362–6.

[17] Furimsky E, Catalytic hydrodeoxygenation. Appl Catal A 2000;199:147–90.

[18] Zhang X, Wang T, Ma L, Zhang Q, Yu Y, Liu Q. Characterization and catalytic properties of Ni and NiCu catalysts supported on ZrO_2–SiO_2 for guaiacol hydrodeoxygenation. Catal Commun 2013;33:15–9.

[19] Olcese RN, Bettahar M, Petitjean D, Malaman B, Giovanella F, Dufour A. Gas- phase

over Fe/SiO_2 catalyst. Appl Catal B 2012;115:63–73.

[20] Romero Y, Richard F, Brunet S. Hydrodeoxygenation of 2-ethylphenol as a model compound of bio-crude over sulfided Mo-based catalysts: promoting effect and reaction mechanism. Appl Catal B 2010;98:213–23.

[21] Duchet JC, van Oers EM, de Beer VHJ, Prins R. Carbon-supported sulfide catalysts. J Catal 1983;80:386–402.

[22] Figueiredo JL, Pereira MFR. The role of surface chemistry in catalysis with carbons. Catal Today 2010;150:2–7.

[23] Stakheev AY, Kustov LM. Effects of the support on the morphology and electronic properties of supported metal clusters: modern concepts and progress in 1990s. Appl Catal A 1999;188:3–35.

[24] Venderbosch RH, Ardiyanti AR, Wildschut J, Oasmaa A, Heeres HJ. Stabilization of biomass-derived pyrolysis oils. J Chem Technol Biotechnol 2010;85:674–86.

[25] Laurent E, Delmon B. Influence of water in the deactivation of a sulfided NiMo/ g-Al_2O_3 catalyst during hydrodeoxygenation. J Catal 1994;146:281–91.

[26] Elliott DC. Historical developments in hydroprocessing bio-oils. Energy Fuels 2007;21:1792–815.

[27] Furimsky E. Catalytic hydrodeoxygenation. Appl Catal A 2000;199:147–90.

[28] Echeandia S, Arias PL, Barrio VL, Pawelec B, Fierro JLG. Synergy effect in the HDO of phenol over Ni–W catalysts supported on active carbon: effect of tungsten precursors. Appl Catal B 2010;101:1–12.

[29] De S, Saha B, Luque R. Hydrodeoxygenation processes: advances on catalytic transformations of biomass-derived platform chemicals into hydrocarbon fuels. Bioresour Technol 2015;178:108–18.

[30] Angın D, Ko¨se TE, Selengil U. Production and characterization of activated carbon prepared from safflower seed cake biochar and its ability to absorb reactive dyestuff. Appl Surf Sci 2013;280:705–10.

[31] Mortensen PM, Grunwaldt JD, Jensen PA, Knudsen KG, Jensen AD. A review of catalytic upgrading of bio-oil to engine fuels. Appl Catal A 2011;407:1–19.

[32] Saidi M, Samimi F, Karimipourfard D, Nimmanwudipong T, Gates BC, Rahim- pour MR. Upgrading of lignin-derived bio-oils by catalytic hydrodeoxygenation. Energy Environ Sci 2014;7:103–29.

[33] Dutta S, Wu KCW, Saha B. Emerging strategies for breaking the 3D amorphous network of lignin. Catal Sci Technol 2014;4:3785–99.

[34] Elkasabi Y, Mullen CA, Pighinelli AL, Boateng AA. Hydrodeoxygenation of fast- pyrolysis bio-oils from various feedstocks using carbon-supported catalysts. Fuel Process Technol 2014;123:11–8.

[35] Wang X, Meng L, Wu F, Jiang Y, Wang L, Mu X. Efficient conversion of microcrystalline cellulose to 1,2-alkanediols over supported Ni catalysts. Green Chem

2012;14:758–65.

[36] Ji N, Zhang T, Zheng M, Wang A, Wang H, Wang X, et al. Catalytic conversion of cellulose into ethylene glycol over supported carbide catalysts. Catal Today 2009;147:77–85.

[37] Gai XK, Arano H, Lu P, Mao JW, Yoneyama Y, Lu CX, et al. Catalytic bitumen cracking in sub- and supercritical water. Fuel Process Technol 2016;142:315–8.

[38] Zhao X, Wei L, Cheng S, Julson J. Optimization of catalytic cracking process for upgrading camelina oil to hydrocarbon biofuel. Ind Crops Prod 2015;77:516–26.

[39] Zhao X, Wei L, Cheng S, Cao Y, Julson J, Gu Z. Catalytic cracking of carinata oil for hydrocarbon biofuel over fresh and regenerated Zn/Na-ZSM-5. Appl Catal A 2015;507:44–55.

[40] Cheng S, Wei L, Zhao X. Develop bifunctional Ni/HZSM-5 catalyst for convert- ing prairie cordgrass to hydrocarbon biofuel. Energy Sources A 2015. http:// dx.doi.org/10.1080/15567036.2015.1065298.

[41] Zhao X, Wei L, Cheng S, Huang Y, Yu Y, Julson J. Catalytic cracking of camelina oil for hydrocarbon biofuel over ZSM-5-Zn catalyst. Fuel Process Technol 2015;139:117–26.

[42] Cheng S, Wei L, Zhao X, Kadis E, Julson J. Conversion of prairie cordgrass to hydrocarbon biofuel over Co-Mo/HZSM-5 using a two-stage reactor system. Energy Technol 2016. http://dx.doi.org/10.1002/ente.201500452.

[43] E.Reyhanitash, M.Tymchyshyn, Z.Yuan, K.Albion, G.van Rossum, C. C. Xu, *Fuel* 2016,*179*, 45-51.

[44] J.Wildschut, I.Melián-Cabrera, H. J. Heeres, *Appl. Catal., B* 2010, *99,* 298-306.

[45] S.Cheng, L.Wei, X.Zhao, Y.Huang, D.Raynie, C.Qiu, J. Kiratu, Y.Yu, *AIMS Energy* 2015, *3*, 227-240.

[47] C. A. Fisk, T. Morgan, Y. Ji, M. Crocker, C. Crofcheck, S. A. Lewis, *Appl. Catal., A* 2009, *358*, 150-156.

[48] Z.Tang, Q. Lu, Y. Zhang, X. Zhu, Q. Guo, *Ind. Eng. Chem. Res.* 2009, *48*, 6923-6929.

[49] S. Cheng, L. Wei, X. Zhao, E. Kadis, Y. Cao, J. Julson, Z. Gu, *New Biotechnol.* 2016,*33*, 440-448.

[50] J. Wildschut, F. H. Mahfud, R. H. Venderbosch, H. J.Heeres, *Ind. Eng. Chem. Res.* 2009, *48*, 10324-10334.

[51] C. Zhao, J. He, A. A. Lemonidou, X. Li, J. A. Lercher, *J. Catal.* 2011, *280*, 8-16.

[52] F.de Miguel Mercader, M. J. Groeneveld, S. R. Kersten, C. Geantet, G.Toussaint, N. W. Way, C.J. Schaverien, K. J. Hogendoorn, *Energy Environ. Sci.* 2011,*4*, 985-997.

[53] Jones, S.b., J. L. Male, 2012. Production of Gasoline and Diesel from Biomass via Fast Pyrolysis, Hydrotreating and Hydrocracking: 2011 State of Technology and Projections to 2017. Report No. PNNL – 22133. PNNL, Richland, Washington 99352.

[54] Wright, M., R. C. Brown, D.E. Daugaard, and D.D. Hsu, 2010. Techno-Economic Analysis of Biomass Fast Pyrolysis to Transportation Fuels. Technical report, NREL/TP-6A20-46586. Golden, Colorado 80401.

[55] French, R.; Czernik, S. 2010. Catalytic pyrolysis of biomass for biofuels production. *Fuel Process. Technol. 91*, 25–32.

[56] Biddy, M., A. Dutta, S. Jones, and Aye Meyer. 2013. In-Situ Catalytic Fast Pyrolysis Technology Pathway. NREL technical report: NREL/TP-5100-58056.

[57] Branca, C.; Giudicianni, P.; Di Blasi, C. 2003. GC/MS characterization of liquids generated from low-temperature pyrolysis of wood. *Ind. Eng. Chem. Res. 42*, 3190–3202.

[58] Bridgwater, A.V. 1996. Production of high grade fuels and chemicals from catalytic pyrolysis of biomass. *Catal. Today*, *29*, 285–295.

[59] [52] Bulushev, D.A.; Ross, J.R.H. 2011. Catalysis for conversion of biomass to fuels via pyrolysis and gasification: A review. *Catal. Today*, *171*, 1–13.

[60] R.Gunawan, X. Li, C. Lievens, M. Gholizadeh, W. Chaiwat, X. Hu,D. Mourant, J. Bromly, C. Z. Li, *Fuel*, 2013,*111*, 709-717.

[61] A. Popov, E. Kondratieva, L. Mariey, J. M.Goupil, J. El Fallah, J. P. Gilson,A. Travert, F. Maugé, *J. Catal.* 2013, *297*,176-186.

[62] N. Joshi, A. Lawal, *Chem. Eng. Sci.* 2012, *74*, 1-8.

[63] Z. He, X. Wang, *Catal. Sustainable Energy* 2012, *1*, 28-52.

[64] Y. Xu, T. Wang, L. Ma, Q. Zhang, W. Liang, *Appl. Energy*, 2010,*87*, 2886-2891.

[65] A. R. Ardiyanti, S. A. Khromova, R. H. Venderbosch, V. A.Yakovlev, H. J.Heeres, *Appl. Catal., B* 2012, *117*, 105-117.

[66] S. Leng, X. Wang, X. He, L. Liu, Y. E. Liu, X. Zhong,G. Zhuang, J. G. Wang, *Catal. Commun.* 2013, *41*, 34-37.

[67] X. Zhao, L.Wei, S. Cheng, Y.Cao, J.Julson, Z. Gu, *Appl. Catal., A* 2015,507, 44-55.

[68] X. Zhao, L. Wei, S. Cheng, J. Julson, *Ind. Crops Prod.* 2015,*77*, 516-526.

[69] X. Zhao, L.Wei, S. Cheng, Y. Huang, Y.Yu, J. Julson, *Fuel Process. Technol.* 2015, *139*, 117-126.

[70] Y. Qian, S. Liang, T. Wang, Z. Wang, W. Xie, X. Xu, *Catal. Commun.* 2011, *12*, 851-853.

[21] X. Zhao, L.Wei, S. Cheng, E. Kadis, Y. Cao, E. Boakye, Z. Gu, J. Julson, *Appl. Catal., B.* 2016,*196*, 41–49.

[72] Z.Yang, J. Yu, C. Li, Y. Zhong, W. Xuan, Z. Ren,Q.Wang, Y. Dai, H. Wang, *Cryst. Res. Technol.* 2015, *50*, 645-653.

[73] V. V.Thyssen, T. A. Maia, E. M. Assaf, *J. Braz. Chem. Soc.* 2015, *26*, 22-31.

[74] C. Liewhiran, S. Phanichphant, *Sensors*, 2007, *7*, 1159-1184.

[75] I. Kasatkin, P. Kurr, B. Kniep, A. Trunschke , R. Schlögl, *Angew. Chem.* 2007, *119*, 7465-7468.

[76] P. M. Mortensen, J. D. Grunwaldt, P. A. Jensen, K. G. Knudsen, A. D.Jensen, *Appl. Catal., A* 2011, *407,* 1-19.

[77] R. Nava, B. Pawelec, P.Castaño, M. C. Álvarez-Galván, C. V. Loricera, J. L. G.Fierro, *Appl. Catal., B* 2009, *92*, 154-167.

[78] T.Yang, Y.Jie, B. Li, X. Kai, Z.Yan, R. Li, *Fuel Process. Technol.* 2016, *148*, 19-27.

[79] R. O. Idem, S. P. Katikaneni, N. N. Bakhshi, *Energy Fuels*, 1996,*10*, 1150-1162.

[80] X. Xu, C. Zhang, Y. Liu, Y. Zhai, R. Zhang, *Chemosphere*, 2013,*93*, 652-660.

[81] X. Zhang, T. Wang, L. Ma, Q. Zhang, T. Jiang, *Bioresour. Technol.* 2013, *127*, 306-311.

[82] S.Wang, Z. Guo, Q. Cai, L.Guo, *Biomass Bioenergy*, 2012,*45*, 138-143.

[83] Y. Huang, L.Wei, X. Zhao, S. Cheng, J. Julson, Y. Cao, Z. Gu, *Energy Convers. Manage.* 2016, *115*, 8-16.

[84] L.Wei, Y. Gao, W. Qu, X. Zhao, S. Cheng, *Trans. ASABE*, 2016,*59*,717-726.

[85] X. Zhao, L.Wei, S. Cheng, J. Julson, G. Anderson, K. Muthukumarappan, C.Qiu, *J. Renewable Sustainable Energy* 2016, *8*, 013109.

[86] S.Cheng, L.Wei, X. Zhao, E. Kadis, J. Julson, *Energy Technology* 2016, http://dx.doi.org/10.1002/ente.201500452.

ACKNOWLEDGEMENTS

This research was supported by funding from the North Central Regional Sun Grant Center at South Dakota State University through a grant provided by the US Department of Energy Bioenergy Technologies Office under award number DE-FG36-08GO88073. South Dakota Innovation Partners also provided financial support for this project.

APPENDIX I

Publications

Peer-reviewed paper:

1. Yinbin Huang, **Lin Wei***, Xianhui Zhao, Shouyun Cheng, James Julson, Yuhe Cao, Zhengrong Gu. 2016. Upgrading pine sawdust pyrolysis oil to green biofuels by HDO over zinc-assisted Pd/C catalyst. *Energy Conversion and Management*, 115 (2016) 8–16.
2. Shouyun Cheng, **Lin Wei***, Xianhui Zhao, Ethan Kadis, Yuhe Cao, James Julson and Zhengrong Gu. 2016. Hydrodeoxygenation of prairie cordgrass bio-oil over Ni based activated carbon synergistic catalysts combined with different metals. *New Biotechnology*, Volume 33, Number 4, pp 440 – 448.
3. Cheng, S., **Lin Wei***, Zhao X. Develop Bifunctional Ni/HZSM-5 Catalyst for Converting Prairie Cordgrass to Hydrocarbon Biofuel. Energy Sources, Part A http://dx.doi.org/10.1080/15567036.2015.1065298.
4. Cheng, S., **Lin Wei***, Zhao X, Kadis E, Julson J. Converting prairie cordgrass to hydrocarbon biofuel over Co-Mo/HZSM-5 using a two-stage reactor system. Energy Technol. http://dx.doi.org/ 10.1002/ente.201500452.
5. S. Cheng, **Lin Wei*,** X. Zhao, Y. Huang, D. Raynie, C. Qiu, J. Kiratu, and Y. Yu. 2015. Directly catalytic upgrading bio-oil vapor produced by prairie cordgrass pyrolysis over Ni/HZSM-5 using a two stage reactor. *AIMS Energy,* Volume 3, Issue 2, 227-240. DOI: 10.3934/energy.2015.2.227.

Conference papers and oral presentations:

1. Shouyun Cheng, **Lin Wei** * James Julson, 2016. Effect of Co-Mo/HZSM-5 on ex-situ catalytic fast pyrolysis of different biomass feedstocks. Paper Number: 2456383. DOI: 10.13031/aim.202456383. The ASABE Annual International Meeting, July 17 – 20th, 2016,Orlando, Florida.
2. Shouyun Cheng, **Lin Wei** * James Julson, 2016. Ex-situ catalytic fast pyrolysis of pine sawdust over two different catalysts. Paper Number: 2456386. DOI: 10.13031/aim.202456386. The ASABE Annual International Meeting, July 17 – 20th, 2016,Orlando, Florida.

APPENDIX II

Academic outcome

- MS Degrees Conferred: Yinbin Huang
- PhD Degrees Conferred: Xianhui Zhao
- Undergraduate students supported: Fletch Corbin
- Ph.D. students supported: Shouyun Cheng
- Post-docs supported:

Please complete the following table to reflect your project at completion or time of report submission:

ITEM	NUMBER
Abstracts	**2**
Peer Reviewed Publications	**5**
Outreach Publications/Web Pages	
Professional Presentations	**2**
MS Degrees Conferred	**1**
Ph.D. Degrees Conferred	**1**
MS Students Supported	
Ph.D. Students Supported	**1**
Post-Docs Supported	
Undergraduate Students Supported	**1**
Investigators Supported	
Start-Up Jobs Created	
Disclosures	
Patents Filed	
Provisional Patents	
Patents Issued	
License Agreements	
Plant Variety Protection	
Subsequent Funding	**1**

Back to Table of Contents

Request for Applications

2008 Biomass Feedstock Logistics

North Central Sun Grant Center
Regional Competitive Grants Program

All 5 Sun Grant Regions Eligible

Pre-Proposal Due: July 23, 2008

The Sun Grant Initiative

World-wide energy demand is increasing. America's consumption of oil and dependency on imported oil to satisfy its needs continue to grow. Agriculture and forestry can reduce America's reliance on imported petroleum by providing domestic feedstocks for the manufacture of biobased products, fuels, and power. The Sun Grant Initiative was authorized by Congress in 2004 as a national network of land grant universities partnering with U.S. federal agencies to build a biobased economy. The authorizing legislation establishes the mission of the Sun Grant Initiative as:

1. to enhance national energy security through the development, distribution, and implementation of biobased energy technologies;
2. to promote diversification in, and the environmental sustainability of, agricultural production in the United States through biobased energy and product technologies;
3. to promote economic diversification in rural areas of the United States through biobased energy and product technologies; and
4. to enhance the efficiency of bioenergy and biomass research and development programs through improved coordination and collaboration between federal agencies and the nation's land-grant colleges and universities.

Five land-grant universities serve as regional Sun Grant centers for the land-grant network. The Sun Grant Regional Centers are located at South Dakota State University (North Central), Oklahoma State University (South Central), the University of Tennessee (South East), Cornell University (North East), and Oregon State University (West). These regional centers are charged with making significant advances in biobased industries and emphasizing research, extension, and educational programs on renewable energy technology. Such activities are to promote the development of biobased industries in rural communities. These Sun Grant Centers will facilitate ongoing and proposed federally funded research, extension and education programs in their respective regions. These programs will embrace the multi-state, multi-function, multi-disciplinary integrated approach that is at the heart of the land-grant mission and methodology for developing science-based solutions to national challenges.

Current Regional Grant Program

The North Central Sun Grant Center expects to receive funding from the U.S. Department of Energy (DOE) Energy Efficiency and Renewable Energy's Office of Biomass Programs. Through these DOE funds the NC-SGC Regional Competitive Grants Program will have approximately $3 M to distribute for research projects related to biomass feedstock logistics. These funds will be released through an application process (Request for Applications, RFA) describe below. We seek both large (up to $700,000) and small (up to $80,000) project applications for projects 2 to 3 years in duration. **Funding of all proposals is subject to availability/receipt of federal funds.**

Eligibility for Current RFA

Principal investigators must be employed by an eligible institution (described below). Principal investigators and key personnel must demonstrate competency to implement and complete a

comprehensive research project, provide fiscal accountability, prepare project reports and demonstrate a willingness to share information with researchers and other interested parties.

All institutions with land-grant status (1862, 1890, and 1994) are eligible to submit an application. Other individuals, businesses, non-profit entities or educational institutions may participate through partnership with a land-grant institution. Partnerships among universities, industries, national laboratories, and other appropriate groups are strongly encouraged.

Required Cost Share

Successful applicants must provide a 20% cost share. For example, if the total project cost is $100,000, then the NC Sun Grant Center will provide $80,000 and $20,000 must be provided as cost share. Grantees may provide funds through in-kind contributions including faculty salaries, facilities, or from state, local, non-profit or private funds. No federal funds may be used as cost share.

Priority Areas for this RFA

The priority area for this request, as identified by the North Central Sun Grant Center and the U.S. Department of Energy, is biomass feedstock logistics directly relevant to future biomass utilization in the North Central Sun Grant Region. Feedstock logistics is being defined to include biomass harvesting, handling (field operations), transportation, storage (including degradation & transformations), and densification. Biomass feedstocks of interest for this RFA include woody and herbaceous crops suitable for commercial production in the North Central Sun Grant Region and herbaceous crop residues (for example corn and small grain crop residues) produced in the NC Region. Forest residues will not be considered in this request. Each proposal should include a component on economics.

Application Process and Requirements

Pre-Proposal: (Submission Deadline July 23, 2008) a pre-proposal is required and should be submitted using the online proposal submission system located on the NC Sun Grant website at http://ncsungrant.sdstate.org. You must register as a "user" if you had not done so for previous NC Sun Grant applications. Users from Sun Grant regions outside the North Central Region will have to register as a new user even if they have previously registered on their home Sun Grant Regional WEBNIBUS system. Please follow the instruction available on the site. Pre-proposals should contain: (12,000 character limit)

1. A descriptive title for the proposed project
2. What problems or opportunities are to be addressed and why it is important
3. The names of key personnel and their institutions
4. A brief statement of the proposed project objectives and a general description of the research methods to be used
5. An outline of deliverables and potential impacts of the work
6. An estimate of total project cost

Pre-proposals submitted by July 23 will be screened and those selected will be asked to submit a full application by the to-be-determined application deadline.

Full Application: Investigators invited to submit a full application will be requested to do so via an online system located on the North Central Sun Grant website at http://ncsungrant.sdstate.org. Proposal submission instructions are available on the site. Details on the application materials are as follows:

1. Proposal Summary: Complete information as requested by the proposal submission system.
2. Project Narrative: This section will be uploaded into the online system as an Adobe pdf file. The Project Narrative should use 12 point Times New Roman font, single spaced and 1 inch margins. The Project Narrative should include the following sections and information:

   a. Non-technical abstract: A short (250 words or less) non-technical abstract. This abstract will be for a general audience and will be used in public descriptions of the Sun Grant research portfolio.

   b. Description of Proposed Project - 20 page limit and must include:

   Introduction: A clear statement of the long-term goal(s) and supporting objectives or research questions of the proposed project should be included. Summarize the body of knowledge or other past activities that substantiate the need for the proposed project. Describe ongoing or recently completed significant activities related to the proposed project including the work of key project personnel. Preliminary data/information pertinent to the proposed research should be included in this section. All works cited should be referenced.

   Rationale and Significance: Concisely present the rationale behind the proposed research. The specific relationship of the project's objectives to one or more of the Sun Grant's goals should be explicit. Any novel ideas or contributions that the proposed project offers should also be discussed in this section.

   Approach: The activities proposed or problems being addressed must be clearly stated and the approaches being applied clearly described. Specifically, this section must include:
   - A description of the activities proposed and their sequence
   - Methods to be used in carrying out the proposed project, including the feasibility of the methods
   - Expected outcomes
   - Means by which results will be analyzed, assessed, or interpreted
   - How results or products will be used
   - Pitfalls that may be encountered
   - Limitations to proposed procedures; and
   - A full explanation of any materials, procedures, situations, or activities related to the project that may be hazardous to personnel, along with an outline or precautions to be exercised to avoid or mitigate the effects of such hazards

   Deliverables: Clearly articulate the expected outcomes and products of the proposed research.

   Key Personnel: Clearly describe the roles and responsibilities of the project director, co-directors, and/or collaborator(s).

   Facilities and Equipment: Facilities and Equipment needed for execution of the proposal should be described here.

Literature Cited. All work cited should be referenced in this section of the application. All references to works cited should be complete, and should conform to an acceptable journal format. References should be listed in numerical order corresponding to their appearance in the text. References can be uploaded into the system as a separate pdf file under file attachments if necessary.

3. Collaborative Agreements *(include as separate attachments under file attachments).* If it will be necessary to enter into formal consulting or collaborative arrangements with others, such arrangements should be fully explained and justified. If the consultant(s) or collaborator(s) are known at the time of application, a vitae or resume should be provided in the key personnel section. In addition, evidence (e.g., letter of support) should be provided that the collaborators involved have agreed to render these services. These documents are to be uploaded into the proposal system as pdf attachments. The applicant also will be required to provide additional information on consultants and collaborators in the budget portion of the application.

4. Budget: The requested budget for the project will be entered through a series of sheets provided by the online system. The budget program will calculate a cumulative budget page and a breakdown for each year of the project. Please follow the on-screen instructions. The budget sheets will include items such as:
   - Salaries and wages for all senior personnel, post-doctoral research associates, graduate students, secretarial and technical workers, etc.
   - Costs of fringe benefits
   - Nonexpendable items with an itemized list and cost for each item
   - Materials and supplies
   - Travel
   - Publication costs
   - Computer costs
   - Any other direct costs, with an explanation
   - Indirect costs
   - Cost share
   - Total costs

5. Budget Justification —All budget categories for which support is requested must be completed in this section.

Indirect Costs: Institutions are allowed to charge indirect costs at their standard federal negotiated rate. Please attach your institutions rate schedule in the file attachment section.

Program Preferences

Applications must meet the minimum requirements of eligibility and 20% (of total project costs) non-federal cost-share to be considered. Applications with multi-state partnerships and a cost-share commitment greater than the required 20% are highly encouraged. The application ranking process will allocate points based on these factors. Scientific merit and regional relevance, however, will have a greater influence on ranking.

Proposal Review Information

The following criteria will be used to evaluate the submissions:

1. Scientific Merit of the Application for Research (50%)
   a. Novelty, innovation, uniqueness, and originality
   b. Conceptual adequacy of the research, as applicable
   c. Clarity and delineation of objectives
   d. Adequacy of the description of the undertaking and suitability and feasibility of methodology
   e. Demonstration of feasibility through preliminary data
   f. Probability of success of project
2. Qualifications of Project Personnel, Adequacy of Facilities, and Project Management (25%)
   a. Qualifications of applicant (individual or team) to conduct the proposed project
   b. Demonstrated awareness of previous and alternative approaches to the problem identified in the application
   c. Institutional experience and competence in subject area
   d. Adequacy of available or obtainable support personnel, facilities, and instrumentation
   e. Planning and administration of the proposed project, including: time allocated for systematic attainment of objectives, project administration and maintenance, and dissemination of information for multi-institutional projects over the duration of the project
   f. Level of partnership and collaborative efforts with other educational institutions, non-profits, small business, and/or industry
3. Project Relevance (25%)
   Documentation that the proposed research is directed toward biomass feedstock logistics and the specific priority areas identified for this program and stated preferences.

Final selection will include consideration of topic area balance in the final research portfolio. Research portfolio balance will only be used as a deciding factor when proposals of equal merit are under consideration.

Award Administration

Program Management: Administration of the program will be handled by the North Central Sun Grant Center. The NC-SGC Director and Advisory Committee are responsible for selection of the awards and determination of funding priorities for the region. Contracts and payments for the awards will be written and distributed from South Dakota State University. Reports and reviews will be collected and maintained by North Central Sun Grant Center at South Dakota State University.

Award Notification: Notification of awards will come from the North Central Sun Grant Center. Notification is expected to be made by the end of September 2008.

Reporting Requirements: A quarterly report of progress must be submitted by each funded project to be considered for continuation of funding. Successful applicants will be given detailed guidelines for reporting.

It is also important to disseminate information from NC-SGC funded projects. At least one Experiment Station or Extension bulletin is required for all funded projects and at least one peer-reviewed article is expected. Investigators must acknowledge US-DOE and the NC-SGC in related publications and presentations. If available, PIs will also be invited to present research findings during the North Central Sun Grant Center's Regional Conference.

Continuation of Funding: Continuation of funding beyond the first year will be determined by first year performance, as well as continued funding from the United States Department of Energy.

Contact Person:

For questions on proposal development and submission or general information on the North Central Sun Grant Center:

James J. Doolittle, Ph.D.
Director and Professor
North Central Sun Grant Center
South Dakota State University
815 Medary Avenue, Suite 210
Brookings, SD 57006
605-696-7870
James.doolittle@sdstate.edu

Back to Table of Contents

Request for Applications

2009 Sustainable Biomass Feedstock Production Systems

North Central Sun Grant Center
Competitive Grants Program

All Sun Grant Regions Eligible

Pre-Proposal Due: August 1, 2009

Back to Table of Contents

The Sun Grant Initiative

World-wide energy demand is increasing. America's consumption of oil and dependency on imported oil to satisfy its needs continue to grow. Agriculture and forestry can reduce America's reliance on imported petroleum by providing domestic feedstocks for the manufacture of biobased products, fuels, and power. The Sun Grant Initiative was authorized by Congress in 2008 as a national network of land grant universities partnering with U.S. federal agencies to build a biobased economy. The mission of the Sun Grant Initiative is:

1. to enhance national energy security through the development, distribution, and implementation of biobased energy technologies;
2. to promote diversification in, and the environmental sustainability of, agricultural production in the United States through biobased energy and product technologies;
3. to promote economic diversification in rural areas of the United States through biobased energy and product technologies; and
4. to enhance the efficiency of bioenergy and biomass research and development programs through improved coordination and collaboration between federal agencies and the nation's land-grant colleges and universities.

Five land-grant universities serve as regional Sun Grant centers for the land-grant network. The Sun Grant Regional Centers are located at South Dakota State University (North Central), Oklahoma State University (South Central), the University of Tennessee (South East), Cornell University (North East), and Oregon State University (West). These regional centers are charged with making significant advances in biobased industries and emphasizing research, extension, and educational programs on renewable energy technology. Such activities are to promote the development of biobased industries in rural communities. These Sun Grant Centers will facilitate ongoing and proposed federally funded research, extension and education programs in their respective regions. These programs will embrace the multi-state, multi-function, multi-disciplinary integrated approach that is at the heart of the land-grant mission and methodology for developing science-based solutions to national challenges.

Current Regional Grant Program

The North Central Sun Grant Center expects to receive funding from the U.S. Department of Energy (DOE) Energy Efficiency and Renewable Energy's Office of Biomass Programs. Through these DOE funds the NC-SGC Regional Competitive Grants Program will have approximately $2.5 M to distribute for research projects related to sustainable biomass feedstock production systems. These funds will be released through an application process (Request for Applications, RFA) describe below. We seek both large (≈ $700,000) and small (≈ $80,000) project applications for projects 2 to 3 years in duration. **Funding of all proposals is subject to availability/receipt of federal funds.**

Eligibility for Current RFA

Principal investigators must be employed by an eligible institution (described below). Principal investigators and key personnel must demonstrate competency to implement and complete a comprehensive research project, provide fiscal accountability, prepare project reports and demonstrate a willingness to share information with researchers and other interested parties.

All institutions with land-grant status (1862, 1890, and 1994) are eligible to submit an application. Other individuals, businesses, non-profit entities or educational institutions may participate through collaboration with a land-grant institution. Collaborations among universities, industries, national laboratories, and other appropriate groups are strongly encouraged.

Required Cost Share

Successful applicants must provide a 20% non-federal cost share. For example, if the total project cost is $100,000, then the NC Sun Grant Center will provide $80,000 and $20,000 must be provided as cost share. Grantees may provide funds through in-kind contributions including faculty salaries, facilities, or from state, local, non-profit or private funds. No federal funds may be used as cost share.

Priority Areas for this RFA

The priority area for this request, as identified by the North Central Sun Grant Center and the U.S. Department of Energy, is sustainable biomass feedstock production systems directly relevant to future biomass utilization in the North Central Sun Grant Region. A sustainable feedstock production system is being defined to include biomass crop development, production, and systems/life-cycle analysis. Biomass feedstocks of interest for this RFA include woody and herbaceous crops suitable for commercial production in the North Central Sun Grant Region and annual crop residues (for example corn and small grain crop residues) produced in the NC Region.

Application Process and Requirements

Pre-Proposal: (Submission Deadline August 1, 2009) a pre-proposal is required and should be submitted using the online proposal submission system located on the NC Sun Grant website at http://ncsungrant.sdstate.org. You must register as a "user" if you had not done so for previous NC Sun Grant applications. Users from Sun Grant regions other than the North Central Region will have to register as a new user on the NC WEBNIBUS even if they have previously registered on their home Regional Sun Grant WEBNIBUS system. Please follow the instruction available on the site. There are 4 parts to the Pre-Proposal/Letter of intent submission:

1. PI Biosketch
2. Senior Personnel
3. Title Page
   This includes project collaborators, an estimate of requested funds and an estimate of cost-share
4. Narrative (12,000 character limit)
   - What problems or opportunities are to be addressed and why they are important
   - A brief statement of the proposed project objectives and a general description of the research methods to be used
   - An outline of deliverables and potential impacts of the work

Pre-proposals submitted by the August 1, 2009 deadline will be screened and those selected will be asked to submit a full application by the to-be-determined application deadline.

Full Application: Investigators invited to submit a full application will be requested to do so via an online system located on the North Central Sun Grant website at http://ncsungrant.sdstate.org. Proposal submission instructions are available on the site. There are 12 parts to a full proposal submission:

1. PI Biosketch (from pre-proposal, can be updated)
2. Senor Personnel (from pre-proposal, can be updated)
3. Title Page (from pre-proposal, can be updated)
4. Proposal Sign-Off Sheet

   Completed and certified by PI, Co-PI's and Official University Approver
5. Proposal Summary

   DO NOT include proprietary information in summary. Note character limitations in each section. Appropriate information may be cut and pasted from full narrative.
6. Pre-Proposal Narrative (from pre-proposal, can be updated)
7. Full Proposal Narrative

   This is an uploaded document in Adobe pdf format. The Project Narrative should use 12 point Times New Roman font, single spaced and 1 inch margins. The Project Narrative should include the following sections and information:

   a. Non-technical abstract: A short (250 words or less) non-technical abstract. This abstract will be for a general audience and will be used in public descriptions of the Sun Grant research portfolio.

   b. Description of Proposed Project - 20 page limit and must include:

   Introduction: A clear statement of the long-term goal(s) and supporting objectives or research questions of the proposed project should be included. Summarize the body of knowledge or other past activities that substantiate the need for the proposed project. Describe ongoing or recently completed significant activities related to the proposed project including the work of key project personnel. Preliminary data/information pertinent to the proposed research should be included in this section. All work cited should be referenced.

   Rationale and Significance: Concisely present the rationale behind the proposed research. The specific relationship of the project's objectives to one or more of the Sun Grant's goals should be explicit. Any novel ideas or contributions that the proposed project offers should also be discussed in this section.

   Approach: The activities proposed or problems being addressed must be clearly stated and the approaches being applied clearly described. Specifically, this section must include:
   - A description of the activities proposed and their sequence
   - Methods to be used in carrying out the proposed project, including the feasibility of the methods
   - Expected outcomes
   - Means by which results will be analyzed, assessed, or interpreted
   - How results or products will be used

- Obstacles that may be encountered
- Limitations to proposed procedures; and
- A full explanation of any materials, procedures, situations, or activities related to the project that may be hazardous to personnel, along with an outline or precautions to be exercised to avoid or mitigate the effects of such hazards

Deliverables: Clearly articulate the expected outcomes and products of the proposed research.

Key Personnel: Clearly describe the roles and responsibilities of the project director, co-directors, and/or collaborator(s).

Facilities and Equipment: Facilities and Equipment needed for execution of the proposal should be described here.

Literature Cited. All work cited should be referenced in this section of the application. All references to work cited should be complete, and should conform to an acceptable journal format. References should be listed in numerical order corresponding to their appearance in the text. References can be uploaded into the system as a separate pdf file under file attachments if necessary.

8. Budget Forms

The requested budget for the project will be entered through a series of sheets provided by the online system. The budget program will calculate a cumulative budget page and a breakdown for each year of the project. Please follow the on-screen instructions.

9. Budget Justification

10. Suggested Reviewers (encouraged but not required)

11. File Attachments

Other pertinent documentation such as

- Letters of support/commitment

- Institution's indirect rate schedule:

Institutions are allowed to charge indirect costs at their standard federal negotiated rate

- Collaborative Agreements

If it will be necessary to enter into formal consulting or collaborative arrangements with others, such arrangements should be fully explained and justified. If the consultant(s) or collaborator(s) are known at the time of application, a vitae or resume should be provided in the key personnel section. In addition, evidence (e.g., letter of support) should be provided that the collaborators involved have agreed to render these services. These documents are to be uploaded into the proposal system as pdf attachments. The applicant also will be required to provide additional information on consultants and collaborators in the budget portion of the application.

12. Proposal Certification

Official University Representative makes final submission after review and approval. No edits can be made after final approval and submission. The University Official is added by PI under "Manage Approvers". A unique log-in is sent to the approver for each proposal.

Program Preferences

Te be considered all applications must meet the minimum requirements of eligibility and 20% (of total project costs) non-federal cost-share to be considered. Applications with multi-state partnerships and a cost-share commitment greater than the required 20% are encouraged. The application ranking process will allocate points based on these factors. Scientific merit and regional relevance, however, will have a greater influence on ranking.

Proposal Review Information

The following criteria will be used to evaluate full-proposal submissions:

1. Scientific Merit of the Application for Research (50%)
   a. Novelty, innovation, uniqueness, and originality
   b. Conceptual adequacy of the research, as applicable
   c. Clarity and delineation of objectives
   d. Adequacy of the description of the undertaking and suitability and feasibility of methodology
   e. Demonstration of feasibility through preliminary data
   f. Probability of success of project
2. Qualifications of Project Personnel, Adequacy of Facilities, and Project Management (25%)
   a. Qualifications of applicant (individual or team) to conduct the proposed project
   b. Demonstrated awareness of previous and alternative approaches to the problem identified in the application
   c. Institutional experience and competence in subject area
   d. Adequacy of available or obtainable support personnel, facilities, and instrumentation
   e. Planning and administration of the proposed project, including: time allocated for systematic attainment of objectives, project administration and maintenance, and dissemination of information for multi-institutional projects over the duration of the project
   f. Level of partnership and collaborative efforts with other educational institutions, non-profits, small business, and/or industry
3. Project Relevance (25%)
   Documentation that the proposed research is directed toward sustainable biomass feedstock production and the specific priority areas identified for this program and stated preferences.

Final selection will include consideration of topic area balance in the final research portfolio. Research portfolio balance will only be used as a deciding factor when proposals of equal merit are under consideration.

Award Administration

Program Management: Administration of the program will be handled by the North Central Sun Grant Center. The NC-SGC Director and Advisory Committee are responsible for selection

of the awards and determination of funding priorities for the region. Top ranking proposals will undergo a scientific merit review. Contracts and payments for the awards will be written and distributed from South Dakota State University. Reports and reviews will be collected and maintained by North Central Sun Grant Center at South Dakota State University.

Award Notification: Notification of awards will come from the North Central Sun Grant Center. Notification is expected to be made by the end of November 2009.

Reporting Requirements: A quarterly report of progress must be submitted by each funded project to be considered for continuation of funding. Successful applicants will be given detailed guidelines for reporting.

It is also important to disseminate information from NC-SGC funded projects. At least one Experiment Station or Extension publication is required for all funded projects and at least one peer-reviewed article is expected. Investigators must acknowledge US-DOE and the NC-SGC in related publications and presentations. Funded projects are required to present research findings during the North Central Sun Grant Center's Regional Conference or the National Sun Grant Conference.

Continuation of Funding: Continuation of funding beyond the first year will be determined by first year performance, as well as continued funding from the United States Department of Energy.

Contact Person:

For questions on proposal development and submission or general information on the North Central Sun Grant Center:

James J. Doolittle, Ph.D.
Director and Professor
North Central Sun Grant Center
South Dakota State University
815 Medary Avenue, Suite 210
Brookings, SD 57006
605-696-7870
James.doolittle@sdstate.edu

Back to Table of Contents

Request for Applications

2010

Optimizing Lignocellulosic Feedstock Production Across a Landscape: Production, Economic, and Environmental Feasibility

North Central Sun Grant Center
Competitive Grants Program

Pre-Proposal Due: August 16, 2010

The Sun Grant Initiative

As world-wide energy demands increase, America's oil consumption and dependency on imported oil continues to grow. Agriculture and forestry can reduce America's reliance on imported petroleum by providing domestic feedstocks for the manufacture of biobased products, fuels, and power. The Sun Grant Initiative, authorized by Congress in 2004 and reauthorized in 2008, is a national network of land-grant universities partnering with U.S. federal agencies to build a biobased economy. The mission of the Sun Grant Initiative is to:

1. enhance national energy security through the development, distribution, and implementation of biobased energy technologies;
2. promote diversification in, and the environmental sustainability of, agricultural production in the United States through biobased energy and product technologies;
3. promote economic diversification in rural areas of the United States through biobased energy and product technologies; and
4. enhance the efficiency of bioenergy and biomass research and development programs through improved coordination and collaboration between federal agencies and the nation's land-grant colleges and universities.

Five land-grant universities serve as regional Sun Grant centers. The Sun Grant Regional Centers are located at South Dakota State University (North Central), Oklahoma State University (South Central), the University of Tennessee (South East), Cornell University (North East), and Oregon State University (West). The Sun Grant Centers will facilitate ongoing and proposed federally funded research, extension and education programs in their respective regions to promote the development of biobased industries in rural communities. These regional centers are also charged with making significant advances in biobased industries while embracing the multi-state, multi-function, multi-disciplinary integrated approach that is at the heart of the land-grant mission and methodology for developing science-based solutions to national challenges.

Current Regional Grant Program

The North Central Sun Grant Center (NC-SGC) expects to receive funding from the U.S. Department of Energy (DOE) Energy Efficiency and Renewable Energy's Office of Biomass Programs. Through these DOE funds, the NC-SGC Regional Competitive Grants Program will have approximately $2M to distribute for research projects related to optimizing lignocellulosic feedstock production systems across a landscape. These funds will be released through an application process (Request for Applications, RFA) described below. We seek both large (≈ $700,000) and small (≈ $80,000) project applications for projects 2 to 3 years in duration. **Funding of all proposals is subject to availability and/or receipt of federal funds.**

Eligibility for Current RFA

Principal investigators must be employed by an eligible institution (described below). Principal investigators and key personnel must demonstrate competency to implement and complete a comprehensive research project, provide fiscal accountability, prepare project reports and demonstrate a willingness to share information with researchers and other interested parties.

Only institutions with land grant status (1862, 1890, and 1994) in states within the region of the North Central Sun Grant Center are eligible to submit an application. The states within

the NC Sun Grant region include Illinois, Indiana, Iowa, Minnesota, Montana, Nebraska, North Dakota, South Dakota, Wisconsin, and Wyoming. Other individuals, businesses, non-profit entities or educational institutions may participate through partnership with a land-grant institution in the North Central region. Partnerships among universities, industries, national laboratories, and other appropriate groups are strongly encouraged.

Required Cost Share

Successful applicants must provide a 20% non-federal cost share. For example, if the total project cost is $100,000, then the NC Sun Grant Center will provide $80,000 and $20,000 must be provided as cost share. Grantees may provide cash funds or provide in-kind contributions including faculty salaries, facilities, or from state, local, non-profit or private funds. No federal funds may be used as cost share.

Priority Areas for this RFA

The priority area for this request, as identified by the North Central Sun Grant Center and the U.S. Department of Energy, is production systems that optimize biomass feedstock yield and economic return across a diverse landscape in the North Central Sun Grant Region while minimizing negative effects on the environment and food/feed production. Biomass feedstocks of interest for this RFA include woody and herbaceous crops suitable for commercial production in the North Central Sun Grant Region and annual crop residues (for example corn and small grain crop residues) produced in the NC Region.

Application Process and Requirements

Pre-Proposal (Submission Deadline August 16, 2010): a pre-proposal is required and should be submitted using the online proposal submission system located on the NC Sun Grant website at http://ncsungrant.sdstate.org. You must register as a "user" if you have not done so for previous NC Sun Grant applications. Please follow the instructions available on the site. There are 4 parts to the Pre-Proposal/Letter of Intent submission:

1. PI Biosketch
2. Senior Personnel
3. Title Page
   This includes project collaborators, an estimate of requested funds and an estimate of cost-share
4. Narrative (12,000 character limit)
   - What problems or opportunities are to be addressed and why they are important
   - A brief statement of the proposed project objectives and a general description of the research methods to be used
   - An outline of deliverables and potential impacts of the work

Pre-proposals submitted by the August 16, 2010 deadline will be screened and those selected will be asked to submit a full application by the to-be-determined application deadline.

Full Application: Investigators invited to submit a full application will be requested to do so via the online system located on the North Central Sun Grant website at

http://ncsungrant.sdstate.org. Proposal submission instructions are available on the site. A full proposal submission requires 12 parts:

1. PI Biosketch (from pre-proposal, can be updated)
2. Senor Personnel (from pre-proposal, can be updated)
3. Title Page (from pre-proposal, can be updated)
4. Proposal Sign-Off Sheet

   Completed and certified by PI, Co-PI's and Official University Approver
5. Proposal Summary

   DO NOT include proprietary information in the summary. Note character limitations in each section. Appropriate information may be cut and pasted from the full narrative.
6. Pre-Proposal Narrative (from pre-proposal, can be updated)
7. Full Proposal Narrative

   This is a document uploaded in pdf format. The Project Narrative should use 12 point Times New Roman font, single spaced and 1 inch margins. The Project Narrative should include the following sections and information:

   a. Non-technical abstract: A short (250 words or less) non-technical abstract. This abstract will be for a general audience and will be used in public descriptions of the Sun Grant research portfolio.

   b. Description of Proposed Project - 20 page limit and must include:

   Introduction: A clear statement of the long-term goal(s) and supporting objectives or research questions of the proposed project. Summarize the body of knowledge or other past activities that substantiate the need for the proposed project. Describe ongoing or recently completed significant activities related to the proposed project including the work of key project personnel. Preliminary data/information pertinent to the proposed research should be included in this section. All work cited should be referenced.

   Rationale and Significance: Concisely present the rationale behind the proposed research. The specific relationship of the project's objectives to one or more of the Sun Grant's goals should be explicit. Any novel ideas or contributions that the proposed project offers should also be discussed in this section.

   Approach: The activities proposed or problems being addressed must be clearly stated and the approaches being applied clearly described. Specifically, this section must include:
   - A description of the activities proposed and their sequence
   - Methods to be used in carrying out the proposed project, including the feasibility of the methods
   - Expected outcomes
   - Means by which results will be analyzed, assessed, or interpreted
   - How results or products will be used
   - Obstacles that may be encountered
   - Limitations to proposed procedures; and

- A full explanation of any materials, procedures, situations, or activities related to the project that may be hazardous to personnel, along with an outline or precautions to be exercised to avoid or mitigate the effects of such hazards

Deliverables: Clearly articulate the expected outcomes and products of the proposed research.

Key Personnel: Clearly describe the roles and responsibilities of the project director, co-directors, and/or collaborator(s).

Facilities and Equipment: Facilities and Equipment needed for execution of the proposal should be described here.

Literature Cited. All work cited should be referenced in this section of the application. All references to work cited should be complete, and should conform to an acceptable journal format. References should be listed in numerical order corresponding to their appearance in the text. References can be uploaded into the system as a separate pdf file under file attachments if necessary.

8. Budget Forms

The requested budget for the project will be entered through a series of sheets provided by the online system. The budget program will calculate a cumulative budget page and a breakdown for each year of the project. Please follow the on-screen instructions.

9. Budget Justification

10. Suggested Reviewers (encouraged but not required)

11. File Attachments

Other pertinent documentation such as

- Letters of support/commitment

- Institution's indirect rate schedule:

Institutions are allowed to charge indirect costs at their standard federal negotiated rate

- Collaborative Agreements

If it will be necessary to enter into formal consulting or collaborative arrangements with others, such arrangements should be fully explained and justified. If the consultant(s) or collaborator(s) are known at the time of application, a vitae or resume should be provided in the key personnel section. In addition, evidence (e.g., letter of support) should be provided that the collaborators involved have agreed to render these services. These documents are to be uploaded into the proposal system as pdf attachments. The applicant also will be required to provide additional information on consultants and collaborators in the budget portion of the application.

12. Proposal Certification

Official University Representative makes final submission after review and approval. No edits can be made after final approval and submission. The University Official is added by PI under "Manage Approvers". A unique log-in is sent to the approver for each proposal.

Program Preferences

To be considered, all applications must meet the minimum requirements of eligibility and 20% (of total project costs) non-federal cost-share. Applications with multi-state partnerships and a cost-share commitment greater than the required 20% are encouraged. **The application ranking process will allocate points based on these factors. Scientific merit and regional relevance, however, will have a greater influence on rank.**

Proposal Review Information

The following criteria will be used to evaluate full-proposal submissions:

1. Scientific Merit of the Application for Research (50%)
   a. Novelty, innovation, uniqueness, and originality
   b. Conceptual adequacy of the research, as applicable
   c. Clarity and delineation of objectives
   d. Adequacy of the description of the undertaking and suitability and feasibility of methodology
   e. Demonstration of feasibility through preliminary data
   f. Probability of success of project
2. Qualifications of Project Personnel, Adequacy of Facilities, and Project Management (25%)
   a. Qualifications of applicant (individual or team) to conduct the proposed project
   b. Demonstrated awareness of previous and alternative approaches to the problem identified in the application
   c. Institutional experience and competence in subject area
   d. Adequacy of available or obtainable support personnel, facilities, and instrumentation
   e. Planning and administration of the proposed project, including: time allocated for systematic attainment of objectives, project administration and maintenance, and dissemination of information for multi-institutional projects over the duration of the project
   f. Level of partnership and collaborative efforts with other educational institutions, non-profits, small business, and/or industry
3. Project Relevance (25%)
   Documentation that the proposed research is directed toward sustainable biomass feedstock production and the specific priority areas identified for this program and stated preferences.

Final selection will include consideration of topic area balance in the final research portfolio. Research portfolio balance will only be used as a deciding factor when proposals of equal merit are under consideration.

Award Administration

Program Management: Administration of the program will be handled by the North Central Sun Grant Center. The NC-SGC Director and Advisory Committee are responsible for selection of the awards and determination of funding priorities for the region. Top ranking proposals will undergo a scientific merit review. Contracts and payments for the awards will be written and

distributed from South Dakota State University. Reports and reviews will be collected and maintained by North Central Sun Grant Center at South Dakota State University.

Award Notification: Notification of awards will come from the North Central Sun Grant Center. Notification is expected to be made by the end of November 2010.

Reporting Requirements: A quarterly progress report must be submitted by each funded project to be considered for continuation of funding. Successful applicants will be given detailed guidelines for reporting.

It is also important to disseminate information from NC-SGC funded projects. At least one Experiment Station or Extension publication is required for all funded projects and at least one peer-reviewed article is expected. Investigators must acknowledge US-DOE and the NC-SGC in related publications and presentations. Funded projects are required to present research findings during the North Central Sun Grant Center's Regional Conference or the National Sun Grant Conference.

Continuation of Funding: Continuation of funding beyond the first year will be determined by first year performance and continued funding from the United States Department of Energy.

Contact Person:

For questions on proposal development and submission or general information on the North Central Sun Grant Center, contact:

James J. Doolittle, Ph.D.
Director and Professor
North Central Sun Grant Center
South Dakota State University
815 Medary Avenue, Suite 210
Brookings, SD 57006
605-696-7870
James.doolittle@sdstate.edu

Request for Proposals
North Central Sun Grant Center and Technology Transfer Office Proof of Concept Grants

Background and Purpose

The North Central Sun Grant Center and the SDSU Technology Transfer Office (TTO) are soliciting applications that promote knowledge-based economic development in science and technology.

The purpose of the program is to advance commercialization of inventions developed through SDSU research and that meet the mission of the Sun Grant Initiative. Specifically, through research, production and commercialization of renewable, biobased energy technologies, the Sun Grant Initiative aims to:

- Enhance national energy security
- Provide opportunities for rural economic development in America's traditional agricultural communities
- Promote environmentally sustainable and diversified production opportunities for agricultural and forestry resources
- Encourage further bioenergy research collaboration between government agencies and land-grant colleges and universities

Funds are available for projects that have advanced beyond basic or curiosity-driven research to applied research, but need funding for early stage data to show commercial potential.

Available Funds

Total available funds are approximately $150,000. Awards for at least one major project ($40,000 - $60,000) and several smaller projects are anticipated.

Indirect Charges

SDSU negotiated indirect charges apply to all submitted projects.

Project Duration

Successful projects will be funded for six (6) months and must be completed within this timeframe. *No extensions, including no-cost extensions, will be allowed for these grants.*

Project Requirements

1. Project principal investigators must be current SDSU employees who have properly filed an invention disclosure to the TTO.
2. Projects must advance economic development through commercialization of an invention(s) discovered and developed through SDSU research.
3. A minimum of 20% cash match (no in-kind allowed) of total direct costs is required for each project. The cash match must be from a source other than federal, state, or SDSU

funds (e.g. private investment fund or industry partner). Match above the 20% is encouraged and any fund source, including in-kind, may be used for this.

4. Awarded funds must be expended by the end date of 31 August 2013 and budgeted accordingly. Unspent funds remaining after the end date will be de-obligated and returned to the North Central Sun Grant Center.

Project Preferences: Proposals with written interest from commercial/industry partners are preferred for this request.

Selection Criteria—Proposals will be ranked using the following criteria ranked from lowest (1) to highest (5) priority.

1. Level of IP protection (e.g. invention disclosure filed, patent application filed etc.).
2. Level of interest and support from commercial partner(s)
3. Level of support from the Department Head and the Dean
4. Potential for creating ***new*** jobs in South Dakota.
5. Potential for creating a ***new*** business in South Dakota

Proposal Requirements

Proposals should not exceed 2,000 words and should be prepared using the following format: 1.5 line spacing, font size of 12 using Times New Roman, 1-inch margins on all sides. Proposals must include the following sections:

A. **Cover Page:** Proposal title; Principle Investigator name, position, and department/college; percent effort for PI; other personnel involved and their respective responsibilities; names and spaces for authorizing signatures of the respective department heads and deans.

Note: This section is not included in the 2,000 word limit.

B. **Summary:** Provide a succinct and rational synopsis of the proposed work, including objectives, methodology, expected outputs, and relevance (about 200 words).

C. **Introduction:** List and briefly describe the objectives. Briefly review the current status of the proposed work and include any pertinent IP status, commercial interest, and preliminary data. It is not necessary to include an exhaustive literature review.

D. **Experimental Plan:** Clearly and succinctly describe the experiments or investigations in the sequence they will be performed. Include adequate, but not excessive, detail on techniques, protocols, and data analysis procedures. List and briefly describe projected outputs/outcomes.

E. **Impact Plan:** Include a summary of the commercialization plan and the expected impact on local economic development and new job creation.

F. **Timeline:** Include a 6-month timeline and Gantt chart that presents key events and activities of the project.

G. **Literature Cited:** Include key literature for the project. This section should be single spaced using Times New Roman 10 point font in the following format:

Lemus R., E.C. Brummer, C.L. Burras, K.J. Moore, M.F. Barker, and N.E. Molstad. 2008. Effects of nitrogen fertilization on biomass yield and quality of large fields of established switchgrass in southern IA, USA. Biomass and Bioenergy 32:1187–1194.

Note: This section is not included in the 2,000 word limit.

H. **Vita:** One page vita for each participant. *(This section is not included in the 2,000 word limit.)*

I. **Supplementary Proposal Information** *(This section is not included in the 2,000 word limit.)*

   i. **Budget:** Include a budget justification for items other than salary, wages, and benefits (e.g. supply, travel). Equipment (non-expendable items above $5,000) is not allowed.

   ii. **Letters of Support:** Include letters of support from the Department Head, Dean, and commercial or industry partners.

   iii. **Statements:** Proposals dealing with human subjects, biosafety or animal management issues must complete the appropriate IRB, IBC, and/or IACUC procedures.

Project Reporting Requirements
Awarded projects will be required to submit a mid-term report and a final project report to the North Central Sun Grant Center.

Submitting Proposals
Proposals should be routed using the SDSU online routing form which can be found at the following website: https://appsrvsp.sdstate.edu/sdsufunding_routing. Please select the US Department of Energy as the sponsoring organization.

Proposals must be submitted electronically to Dr. Vance Owens at the North Central Sun Grant Center no later than **15 January 2013 at 5:00PM CDT.** Email address is vance.owens@sdstate.edu. Any other form of submission will not be accepted.

Proposals should be sent as attachments in both MS Word and Adobe Acrobat formats. Please include "NCSG-TTO Proof of Concept Proposal" in the subject line.

Notification of Award
Award notifications will be sent by **15 February 2013** with a projected start date of 1 March 2013 and completion date of 31 August 2013.

For More Information
For more information, contact the grant program directors:

Vance Owens
North Central Sun Grant Center
815 Medary Avenue, Ste. 301
Brookings, SD 57006

Campus Mail Box: FND 525
Telephone: 605-696-7870
Email: vance.owens@sdstate.edu

Will Aylor
Technology Transfer Office
815 Medary Avenue, Ste. 301
Brookings, SD 57006

Campus Mail Box: FND 525
Telephone: 605-696-7872
Email: william.aylor@sdstate.edu

Non-Discrimination Policy

It is the policy of South Dakota State University to not discriminate on the basis of race, color, creed, religion, national origin, ancestry, citizenship, age, gender, sexual orientation, disability, or Vietnam Era Veteran status in the offering of benefits, services, and educational and employment opportunities.

Principal investigator understands and agrees to be responsible in following and abiding by the university's non-discrimination and other relevant policies in the conduct of research program funded from this program.

Back to Table of Contents

Request for Proposals

North Central Regional Sun Grant Center and the Office of Technology Transfer & Commercialization Proof of Concept Grants

Important Dates

Proposals submission deadline: 22 May 2015 by 5:00 pm central time
Award notification: 26 June 2015

Background and Purpose

The North Central Regional Sun Grant Center (NCRSGC) and the Office of Technology Transfer & Commercialization (OTTC) at South Dakota State University are soliciting applications that promote knowledge-based economic development in science and technology. The purpose of the program is to advance commercialization of inventions developed through SDSU research and that meet the mission of the Sun Grant Initiative. Specifically, through research, production, and commercialization of renewable, biobased energy technologies, the Sun Grant Initiative aims to:

- Enhance national energy security
- Provide opportunities for rural economic development in America's traditional agricultural communities
- Promote environmentally sustainable and diversified production opportunities for agricultural and forestry resources
- Encourage further bioenergy research collaboration between government agencies and land-grant colleges and universities

Funds are available for projects that have advanced beyond basic or curiosity-driven research to applied research, but need funding for early stage data to demonstrate commercial potential.

Available Funds

There is approximately $100,000 in available funding for this request. We anticipate making two to three awards depending on submitted proposals.

Indirect Charges

Full SDSU negotiated indirect charges apply to all submitted projects.

Project Duration

Successful projects will be funded for six (6) months and must be completed within the allotted timeframe. *No-cost extensions will not be allowed for these grants.*

Project Requirements

1. Project principal investigators (PIs) must be current SDSU employees who have properly filed an invention disclosure with the OTTC or will file an invention disclosure based on the plans for these funds.
2. Projects must advance economic development through commercialization of an invention(s) discovered and developed through SDSU research.
3. Successful applicants must provide 20% non-federal cash match (no in-kind match allowed for the first 20%) based on total project costs. For example, if the total project cost is $50,000, then the NCRSGC will provide $40,000 and $10,000 must be provided as cash match. Cash match must be from a source other than federal, state, or SDSU funds (i.e., appropriate sources of cash match include private investment funds or industry partners). Match above the 20% is encouraged and any fund source, including in-kind, may be used for this.
4. Awarded funds must be expended by the end of the six-month project. Unspent funds remaining after the end date will be de-obligated and returned to the NCRSGC.

Project Preferences: Proposals with written interest from commercial/industry partners are preferred for this request.

Selection Criteria—Proposals will be evaluated using criteria 1-5 listed below. The potential to create new jobs and/or a new business in South Dakota is of particular interest in this program.

1. Level of IP protection (e.g. invention disclosure or patent application filed or with intent to file)
2. Level of interest and support from commercial partner(s)
3. Level of support from the Department Head and the Dean of the College
4. Potential for creating ***new*** jobs in South Dakota.
5. Potential for creating a ***new*** business in South Dakota

Proposal Requirements

Proposals should not exceed 2,000 words and should be prepared using the following format: 1) line spacing of 1.5, 2) Times New Roman 12 point font, and 3) 1-inch margins on all sides. Proposals must include sections A-K listed below; however, sections A (Cover Page), F (Timeline), G (Literature Cited), H (Curriculum Vitae), I (Budget), J (Letters of Support), and K (Regulatory Statements) are not included in the 2,000 word limit.

A. **Cover Page:** Proposal title; Principle Investigator name, position, and department/college; percent effort for PI; other personnel involved and their respective responsibilities and percent effort; names and spaces for authorizing signatures of the respective Department Heads and Deans.

B. **Summary:** Provide a succinct and rational synopsis of the proposed work, including objectives, methodology, expected outputs, and relevance (about 200 words).

C. **Introduction:** List and briefly describe the objectives. Briefly review the current status of the proposed work and include any pertinent IP status, commercial interest, and preliminary data. It is not necessary to include an exhaustive literature review.

D. **Experimental Plan:** Clearly and succinctly describe the experiments or investigations in the sequence they will be performed. Include adequate, but not excessive, detail on techniques, protocols, and data analysis procedures. Describe projected outputs/outcomes.

E. **Impact Plan:** Include a summary of the commercialization plan and the expected impact on local economic development and new job creation.

F. **Timeline:** Include a 6-month timeline or Gantt chart that presents key events and activities of the project.

G. **Literature Cited:** Include key literature for the project. This section should be single spaced using Times New Roman 10 point font.

H. **Curriculum Vitae:** Include a one page CV for each participant.

I. **Budget:** Include a detailed budget and budget justification for expenses associated with the project. Expenses for equipment (non-expendable items above $5,000) and foreign travel (includes Canada and Mexico) are not allowed.

J. **Letters of Support:** Include letters of support from the Department Head, Dean, and commercial or industry partners.

K. **Regulatory Statements:** Proposals dealing with human subjects, recombinant DNA, or animal management issues must complete appropriate IRB, IBC, and/or IACUC procedures.

Project Reporting Requirements

Project PIs will be required to submit a mid-term report (approximately half way through project) and final project report (within 30 days of project completion) to the NCRSGC. PIs will also be expected to present project results and outcomes at the NCRSGC annual meeting.

Submitting Proposals

Proposals should be routed using the SDSU online routing form which can be found at the Office of Research Assurance & Sponsored Programs website: http://www.sdstate.edu/research/orsp/index.cfm. Please select the US Department of Energy as the sponsoring organization.

Proposals must be submitted electronically to Vance Owens (vance.owens@sdstate.edu) at the NCRSGC by **5:00 PM CDT on 22 May 2015.** No other form of submission will be accepted. Proposals should be sent as attachments in both MS Word and Adobe Acrobat formats. Please include "NCRSGC-OTTC Proof of Concept Proposal" in the subject line.

Notification of Award

Award notifications will be sent to PIs by **26 June 2015**. Following award notification, PIs must complete appropriate DOE NEPA forms and receive final approval for their project. The start date for each project will be determined pending DOE approval.

For More Information
For more information, contact the grant program directors:

Vance Owens
North Central Regional Sun Grant Center
Administration Bldg. 200, Box 2201
Telephone: 605-688-5476
Email: vance.owens@sdstate.edu

Will Aylor
Office of Tech. Transfer and
Commercialization
Administration Bldg. 200, Box 2201
Telephone: 605-688-4752
Email: william.aylor@sdstate.edu

Non-Discrimination Policy
It is the policy of South Dakota State University to not discriminate on the basis of race, color, creed, religion, national origin, ancestry, citizenship, age, gender, sexual orientation, disability, or Vietnam Era Veteran status in the offering of benefits, services, and educational and employment opportunities.

Principal investigator understands and agrees to be responsible in following and abiding by the university's non-discrimination and other relevant policies in the conduct of research program funded from this program.